

Role of Dams and Reservoirs in a Successful Energy Transition

Robert M. Boes
Patrice Droz
Raphaël Leroy



CRC Press
Taylor & Francis Group

ROLE OF DAMS AND RESERVOIRS IN A SUCCESSFUL ENERGY TRANSITION

Today, new and unexpected challenges arise for Europe's large array of existing dams, and fresh perspectives on the development of new projects for supporting Europe's energy transition have emerged. In this context, the 12th ICOLD European Club Symposium has been held in September 2023, in Interlaken, Switzerland. The overarching Symposium theme was on the "Role of dams and reservoirs in a successful energy transition". The articles gathered in the present book of proceedings cover the various themes developed during the Symposium:

- Dams and reservoirs for hydropower
- Dams and reservoirs for climate change adaptation
- Impact mitigation of dams and reservoirs
- How to deal with ageing dams

In conjunction with the Symposium, the 75th anniversary of the Swiss Committee on Dams offered an excellent opportunity to not only draw from the retrospective of Switzerland's extensive history of dam development, but to also reveal perspectives on the new role of dams for a reliable and affordable energy transition. These aspects are illustrated by several articles covering the various activities, challenges, and concerns of the dam community.



Taylor & Francis

Taylor & Francis Group

<http://taylorandfrancis.com>

PROCEEDINGS OF THE 12TH ICOLD EUROPEAN CLUB SYMPOSIUM 2023 (ECS 2023,
INTERLAKEN, SWITZERLAND, 5-8 SEPTEMBER 2023)

Role of Dams and Reservoirs in a Successful Energy Transition

Edited by

R.M. Boes, P. Droz & R. Leroy

Swiss Committee on Dams



CRC Press

Taylor & Francis Group

Boca Raton London New York

CRC Press is an imprint of the
Taylor & Francis Group, an **informa** business

A BALKEMA BOOK

Front Cover Image: David Birri

First published 2023
by CRC Press/Balkema
4 Park Square, Milton Park, Abingdon, Oxon, OX14 4RN

and by CRC Press/Balkema
2385 NW Executive Center Drive, Suite 320, Boca Raton FL 33431

CRC Press/Balkema is an imprint of the Taylor & Francis Group, an informa business

© 2023 selection and editorial matter, R.M. Boes, P. Droz & R. Leroy; individual chapters, the contributors

Typeset by Integra Software Services Pvt. Ltd., Pondicherry, India

The right of R.M. Boes, P. Droz & R. Leroy to be identified as the author of the editorial material, and of the authors for their individual chapters, has been asserted in accordance with sections 77 and 78 of the Copyright, Designs and Patents Act 1988.

All rights reserved. No part of this book may be reprinted or reproduced or utilised in any form or by any electronic, mechanical, or other means, now known or hereafter invented, including photocopying and recording, or in any information storage or retrieval system, without permission in writing from the publishers.

Although all care is taken to ensure integrity and the quality of this publication and the information herein, no responsibility is assumed by the publishers nor the author for any damage to the property or persons as a result of operation or use of this publication and/or the information contained herein.

British Library Cataloguing-in-Publication Data
A catalogue record for this book is available from the British Library

Library of Congress Cataloging-in-Publication Data
A catalog record has been requested for this book

ISBN: 978-1-032-57668-8 (hbk)
ISBN: 978-1-032-57671-8 (pbk)
ISBN: 978-1-032-44042-0 (ebk)
DOI: 10.1201/9781003440420

Table of contents

Role of dams and reservoirs in a successful energy transition	xiii
12 th ICOLD European Club Symposium 75 th Anniversary of the Swiss Committee on Dams Interlaken, Switzerland, 5-8 September	xv
Members of the 12 th ICOLD European Club Symposium Scientific Committee	xvii
Sponsors of the 12 th ICOLD European Club Symposium and 75 th anniversary of the Swiss committee on Dams	xix
Keynotes	
Past, present and future role of Dams in Switzerland <i>R. M. Boes & A. Balestra</i>	3
Swiss dams: Overview of historical development <i>H. Pougatsch & A.J. Schleiss</i>	18
Outstanding past Swiss dam engineers <i>W.H. Hager</i>	32
Water resources optimisation – A Swiss experience <i>R. Leroy</i>	39
Dam heightening in Switzerland <i>A. Wohnlich, A. Fankhauser & B. Feuz</i>	48
Swiss dam engineering in the world <i>P. Droz</i>	60
Dam surveillance in Switzerland: A constant development <i>H. Pougatsch & I. Fern</i>	72
Contributions of geodesy to the safety of dams in Switzerland <i>A. Wiget, B. Sievers & F. Walser</i>	80
Swiss contribution to geology and dams <i>A. Jonneret, T. Bussard & G. Schaeren</i>	89
Dams and photovoltaic plants – The Swiss experience <i>E. Rossetti, D. Maggetti & A. Balestra</i>	100
The importance of young professionals for dam engineering in Switzerland <i>S. Vorlet & V. Favero</i>	107
Theme A: Dams and reservoirs for hydropower	
How to win an international competition on sustainable sediment management <i>L. Gehrmann, T. Gross & M. Detering</i>	113

Specialist grouting works in the renewal of Ritom HPP, Switzerland <i>A. Heizmann & G. Lilliu</i>	121
Wave return walls within the adapted freeboard design at dams <i>M. Heß & D. Carstensen</i>	129
PV plant - New potentials in Vau i Dejes HPP, Albania <i>A. Jovani & F. Shaha</i>	137
Drini River Cascade - Unique in Europe <i>A. Jovani, E. Verdho, E. Kacurri & E. Qosja</i>	141
Photovoltaics and hydropower – Potential study at Alpine reservoirs in Switzerland <i>G. Maddalena, B. Hohermuth, F.M. Evers, R.M. Boes & A. Kahl</i>	150
Photovoltaic on dams – Engineering challenges <i>D. Maggetti, F. Maugliani, A. Korell & A. Balestra</i>	161
Vianden pumped storage plant - large-scale shear tests on rockfill material of the upper reservoir ring-dam <i>Ch. Meyer & K. Thermann</i>	169
Capacity building of dam wardens <i>A. Mico, N.-V. Bretz, O. Sarrasin & J. Fluixa-Sanmartin</i>	177
Collection and dissemination of knowledge on dams of Italy <i>S. Munari</i>	183
Flood control across hydropower dams: The value of safety <i>C. Ntemiroglou, G.-K. Sakki & A. Efstratiadis</i>	187
Blasting excavation close to fresh Roller Compacted Concrete, in RCC Dam construction sites <i>P. Ruffato & R. Folchi</i>	199
Swiss dam safety regulation: Framework, recent changes and future perspectives <i>M.V. Schwager, A. Askarinejad, B. Friedli, P.W. Oberender, A.J. Pachoud & L. Pfister</i>	209
Châtelard basin storage expansion by making use of a spoil area <i>H. Stahl, B. Müller, Ch. Hirt & B. Romero</i>	220
An application of sophisticated FEM and simplified methods to the seismic response analysis of an asphalt-concrete core rockfill dam <i>A.D. Tzenkov, D.S. Kisliakov & M.V. Schwager</i>	229
Trift Arch Dam – an opportunity for hydropower generation due to a retreating glacier <i>A.D. Tzenkov, O. Vallotton & A. Mellal</i>	240
Fulfilling pumped storage plants requirements with advanced geomembrane technology <i>G. Vaschetti & M. Scarella</i>	250
Ritom HPP – Unforeseen challenges during the inclined shaft excavation <i>R. Zanoli & S. Massignani</i>	258
 <i>Theme B: Dams and reservoirs for climate change adaptation</i>	
CRHyME (Climatic Rainfall Hydrogeological Modelling Experiment): A versatile geo-hydrological model for dam siltation evaluation <i>A. Abbate & L. Mancusi</i>	267

Electronic monitoring of natural hazards prone reservoir regions and catchment areas of Alpine dams <i>M. Carrel, S. Stähly, J. Gassner & S. Wahlen</i>	277
Role of water storage reservoirs management and flood mitigation in climate change conditions <i>T. Dašić</i>	286
XFLEX HYDRO: Extending operation flexibility at EDF-Hydro Grand Maison PSP <i>J.-L. Drommi, B. Joly, D. Aelbrecht, C. Nicolet, C. Landry, C. Münch & J. Decaix</i>	294
Additional water and electricity storage in the Swiss Alps: From studies of potential towards implementation <i>J. Fauriel, J. Filliez, D. Felix & R.M. Boes</i>	303
Guidelines for modelling dam safety adaptation to climate change <i>J. Fluixa-Sanmartin, A. Morales-Torres & I. Escuder-Bueno</i>	312
Upgrade of the Perlenbach Dam in Germany – A multi-purpose sustainability project <i>R. Haselsteiner, B. Ersoy & L. Werner</i>	322
PKW Spillways: An innovative, resilient and flexible solution from run-off river dams in plains to large dams in mountains suitable for climate change <i>F. Laugier, M. Ho Ta Khanh & J. Vermeulen</i>	329
Enhancing dam safety through contractual strategies <i>M. Lino, S. Giraud, L. Canale & B. Geisseler</i>	338
Risk management for the Lago Bianco reservoir in case of a rupture of the Cambrena glacier <i>J. Maier, R. Baumann, H. Stahl & T. Menouillard</i>	347
Inclinometer monitoring of a dam during hot weather <i>N. Manzini, S. Van Gorp & Y. Jobard</i>	357
Multipurpose dams – A European perspective <i>A. Palmieri, D. Maggetti & A. Balestra</i>	367
How to evaluate arch dam's behaviour under increased thermal load such as heat waves and extreme cold <i>E. Robbe, L. Suchier, A. Simon & T. Guilloteau</i>	377
Importance of hydropower reservoirs and dams in Europe to mitigate the energy crisis and to serve as a catalyst and enabler for the Green Deal <i>A.J. Schleiss, J.-J. Fry & M. Morris</i>	386
From energy producer to water manager: A research-industry collaboration <i>X. Schröder, E. Reynard & S. Nahrath</i>	394
The use of motor vessels on the reservoirs in Slovenia: A case study on the Sava River <i>N. Smolar-Žvanut, M. Centa, I. Kavčič & N. Kodre</i>	402
Re-operationalization of dams to adapt to climate change in Romania <i>D. Stematiu & A. Abdulamit</i>	409
Design values for dams exceeded: Lessons learnt from the flood event 2021 in Germany <i>S. Wolf, E. Klopries, H. Schüttrumpf, D. Carstensen, R. Gronsfeld & C. Fischer</i>	418
 Theme C: Impact mitigation of dams and reservoirs	
New Poutès dam (France): Innovative retrofitting to reconcile environment and hydropower <i>T. Barbier, S. Lecuna & P. Meunier</i>	431

Effects of water releases and sediment supply on a residual flow reach <i>C. Blanck, R. Schroff & G. De Cesare</i>	440
Bedrock scour prediction downstream of high head dams due to developed rectangular jets plunging into shallow pools <i>A. Bosman & G.R. Basson</i>	450
Fish passes on the Rhine River – Major structures at EDF Hydro plants to restore fish continuity <i>G. Brousse, R. Thevenet & A. Vermeille</i>	460
Efficiency evaluation and simulation of sediment bypass tunnel operation: Case study solis reservoir <i>S. Dahal, M.R. Maddahi, I. Albayrak, F.M. Evers, D.F. Vetsch, L. Stern & R.M. Boes</i>	469
Reduction of riverbed clogging related to sediment flushing <i>R. Dubuis & G. De Cesare</i>	479
Norwegian sediment handling technologies - recent developments and experiences from projects <i>T. Jacobsen</i>	487
Study on the sedimentation process in Boštanj reservoir, Slovenia <i>M. Klun, A. Kryžanowski, A. Vidmar, S. Rusjan & A. Hribar</i>	494
Submerged wood detection in a dam reservoir with a narrow multi-beam echo sounder <i>T. Koshiba, S. Takata, K. Murakami & T. Sumi</i>	503
HYPOS – Sediment management from space <i>M. Leite Ribeiro, M. Launay, K. Schenk, F. von Trentini, M. Bresciani, E. Matta, A. Bartosova & D. Gustafsson</i>	511
Comprehensive assessment of sediment replenishment and downstream hydro-geomorphology, case study in the Naka River, Japan and the Buëch River, France <i>J. Lin, S.A. Kantoush & T. Sumi</i>	518
Experimental modeling of fine sediment routing: SEDMIX device with thrusters <i>M. Marshall, A. Amini & G. De Cesare</i>	526
Dynamic environmental flows using hydrodynamic-based solutions for sustainable hydropower <i>S. Martel, P. Saharei, G. De Cesare & P. Perona</i>	532
Improving fish protection and downstream movement at the Maigrauge Dam (Switzerland) using an electric barrier <i>A. Moldenhauer-Roth, D. Lambert, M. Müller, I. Albayrak & G. Lauener</i>	540
Assessment of the hydromorphological effectiveness of sediment augmentation measures downstream of dams <i>C. Mörtl & G. De Cesare</i>	548
Revitalization of the Salanfe river (Valais, Switzerland): A multi-faced project <i>M. Perroud, C. Gabbud, P. Bianco, J. Rombaldoni & V. Degen</i>	558
Storage tunnels to mitigate hydropeaking <i>W. Richter & G. Zenz</i>	566
Can hydropeaking by small hydropower plants affect fish microhabitat use? <i>J.M. Santos, R. Leite, M.J. Costa, F.N. Godinho, M.M. Portela, A.N. Pinheiro & I. Boavida</i>	574

The Cimia dam in Sicily. A relevant case of rehabilitation <i>L. Serra, G. Gatto & E. Costantini</i>	582
Assessing the carbon footprint of pumped storage hydropower – a case study <i>R.M. Taylor, V. Chanudet, J.-L. Drommi & D. Aelbrecht</i>	590
Exploring the efficacy of reservoir fine sediment management measures through numerical simulations <i>S. Vorlet, M. Marshall, A. Amini & G. De Cesare</i>	600
Theme D: How to deal with ageing dams Dam safety	
Ageing dams in Switzerland: Feedbacks of several case studies <i>N.J. Adam, J. Filliez & J. Fauriel</i>	613
Geological hazard evaluation for the dams constructed at Drin valley <i>S. Allkja, A. Malaj & K. Petriti</i>	622
Galens arch dam strengthening works <i>F. Andrian, N. Ulrich, P. Agresti & Y. Fournié</i>	632
Design concept for sustainable cut-off walls made of highly deformable filling materials <i>K. Beckhaus, J. Kayser, F. Kleist, J. Quarg-Vonscheidt & D. Alós Shepherd</i>	641
Digitalization for a targeted and efficient dam management <i>F. Besseghini, C. Gianora, M. Katterbach & R. Stucchi</i>	651
Digital cloud-based platform to predict rock scour at high-head dams <i>E.F.R. Bollaert</i>	659
Sharing elements of EDF feedback on the operation and maintenance of pendulums <i>P. Bourgey, T. Guilloteau & J. Sausse</i>	669
Lifetime analysis of the Sta. Maria arch dam behaviour <i>M. Bühlmann, S. Malla & R. Senti</i>	678
Effect of invert roughness on smooth spillway chute flow <i>M. Bürgler, D.F. Vetsch, R.M. Boes, B. Hohermuth & D. Valero</i>	687
Nonlinear deterministic model for a double-curvature arch dam <i>E. Catalano & R. Stucchi</i>	696
Breach analysis of the Lozorno II. Dam <i>E. Cheresova, T. Mészáros & M. Mrva</i>	703
Dam safety and surveillance: Return of experience from the perspective of the Swiss Federal authorities <i>M. Côté, R.M. Gunn & T. Menouillard</i>	713
Failures and incidents in Greek dams <i>G.T. Dounias, S.L. Lazaridou & Z.R. Papachatzaki</i>	724
A dam-foundation seismic interaction analysis method: Development and first case studies <i>G. Faggiani & P. Masarati</i>	734
Concrete swelling: Studies and pragmatic results. Case study of Cleuson dam <i>J. Fauriel, A. Abati, M. Côté & R. Berthod</i>	745
The safety assessment of buttress, hollow gravity and multiple arch/slab dams. The contribution of numerical modeling <i>A. Frigerio, M. Colombo, G. Mazzà, F. Rogledi & A. Terret</i>	753

Rehabilitation and upgrade of old small dams <i>B. Gander</i>	763
Experimental investigation of the overtopping failure of a zoned embankment dam <i>M.C. Halso, F.M. Evers, D.F. Vetsch & R.M. Boes</i>	768
Reconstruction of hydrographs of the maximum annual flood event at dam site <i>F. Santoro, F. Pianigiani, A. Bonafè, L. Ruggeri, D. Feliziani, M. Maestri, F. Piras, F. Sainati, P. Claps & A. Brath</i>	778
Experiences from inspections and controls on ageing penstocks of hydropower plants <i>A. Kager & R. Sadei</i>	783
Instable rock cliff at Steinwasser water intake: Immediate and safety measures <i>A. Koch & D. Bürki</i>	791
Emergency preparedness planning in Greek dams <i>S.L. Lazaridou, G.T. Dounias, S.C. Sakellariou, A.E. Kotsonis, G.P. Kastranta & M.V. Psychogiou</i>	801
Seismic analysis of old embankment dams: Qualification of the Fr-Jp method <i>N. Lebrun, M. Jellouli & J.-J. Fry</i>	810
Obturation solutions for dry works on underwater installations <i>M. Leon</i>	820
The decommissioning of dams in Italy: The state of the art <i>P. Manni & G. Mazzà</i>	827
Rehabilitation of the Pavana Dam in Tuscany (IT) Advantages from the use of building information modelling in the design of a complex hydraulic project <i>F. Maugliani, A. Piazza, D. Longo, G. Raimondi, R. Sanfilippo & A. Parisi</i>	837
Potential Failure Mode Analysis (PFMA) to deal with ageing and climate change affecting dams <i>P. Méan & T. Bryant</i>	846
GRIMONIT (GroundRiskMonitor) – an early warning system for difficult measurement conditions <i>E. Meier, I. Gutiérrez & M. Büchel</i>	855
Arch dams: A new methodology to analyse the sliding stability between the dam and the foundation <i>X. Molin, C. Jouy, S. Delmas, P. Anthinac, G. Milesi & C. Noret</i>	863
Spitallamm Arch Dam – Challenges faced for replacing the existing Old Dam <i>E.A. Odermatt & A. Wohnlich</i>	871
Concrete dams upgrading using IV-RCC <i>F. Ortega</i>	881
The driving force of AAR – An in-situ proof <i>B. Otto & R. Senti</i>	889
Effects of wall roughness on low-level outlet performance <i>S. Pagliara, B. Hohermuth, S. Felder & R.M. Boes</i>	898
Safety of embankment dams in the case of upgrading the existing tailings storage facilities <i>L. Petkovski, F. Panovska & S. Mitovski</i>	908
First rehabilitation measures of the Biópio dam, Angola <i>C.J.C. Pontes & P. Afonso</i>	918

Dams in Angola, reconstruction of the Matala dam <i>C.J.C. Pontes & P. Portugal</i>	923
Estimation of settlement in earth and rockfill dams using artificial intelligence technique <i>M. Rashidi, K. Salimi & S. Abbaszadeh</i>	927
Structural health monitoring of large dams using GNSS and HSCT-FE models. Swelling effect detection <i>M. Rodrigues, J.N. Lima, S. Oliveira & J. Proença</i>	937
Dynamic behavior of exposed geomembrane systems in pressure waterways <i>S. Vorlet, R.P. Seixas & G. De Cesare</i>	946
The Rigoso project. Two old masonry dams to be recovered <i>L. Serra, G. Gatto, F. Bisci, M. Rebuschi, F. Fornari & L. Dal Canto</i>	956
Numerical modelling of the Pian Telessio dam affected by AAR <i>R. Stucchi & E. Catalano</i>	964
Flood protection levees – from an existing portfolio of old structures to safe and reliable protection systems <i>R. Tourment, A. Rushworth, J. Simm, R. Slomp, M. Barker, D. Bouma & N. Vroman</i>	972
Software tool for progressive dam breach outflow estimation <i>D.F. Vetsch, M.C. Halso, L. Seidelmann & R.M. Boes</i>	981
Ageing and life-span of dams <i>M. Wieland</i>	989
Hongrin arch dams – Rehabilitation works of the central artificial gravity abutment <i>A. Wohnlich & R. Leroy</i>	996
Dealing with aging dams on the Drava River in Slovenia <i>P. Žvanut</i>	1005
Author index	1011



Taylor & Francis

Taylor & Francis Group

<http://taylorandfrancis.com>

Role of dams and reservoirs in a successful energy transition

The Swiss Committee on Dams is proud to host the 12th ICOLD European Club Symposium in Interlaken, Switzerland. The overarching Symposium theme is on the “Role of dams and reservoirs in a successful energy transition”.

At the global scale, hydropower is by far the most important renewable energy source, accounting for one sixth of electricity generation. In Switzerland, this share amounts to almost 60%. The recent past has impressively demonstrated the importance of a reliable electricity supply for modern societies. Energy is more than electricity, but the role of electricity among the many energy carriers is and will be ever increasing, not least in the light of replacing fossil fuels with CO₂-free alternatives. A recent Swiss study on nationwide risks has shown a scenario of large-scale shortage of electricity to feature the highest risk to the Swiss society, with an annual probability of occurrence of about 3% and a damage potential of several hundred billion Swiss francs. To ensure flexible storage capacity availability at all times and to limit the likelihood of a blackout in the winter 2022/23, planned refurbishment works at Swiss storage reservoirs were postponed by two years.

But dam reservoirs offer more than water for hydroelectric energy. They have also an important retention effect during floods and contribute to protect downstream infrastructure and settlements from inundations. Worldwide, irrigation and water supply are among the widespread purposes of artificial reservoirs, and even in Switzerland, a country with high annual precipitation and known to be the “Water tower of Europe”, droughts increase in frequency and extent. Therefore, new reservoirs will feature multiple uses, from storage for hydropower over flood protection to water supply for domestic, industrial and agricultural use, and even artificial snow production. With 50% of European glacier ice volume located in Switzerland, the rapid glacier retreat following the substantial atmospheric warming in the Alps results in the formation of periglacial lakes forming at depressions formerly covered by glacier ice. In an attempt to adapt to climate change, new dam projects at such sites aim at artificially creating water storage to at least partly compensate for the natural water storage loss from glacier melt, which, amongst others, will lead to larger flood peaks in the downstream valleys.

The 12th ICOLD European Club Symposium coincides with the 75th anniversary of the Swiss Committee on Dams (SCD). Based on a loose union of five Swiss dam engineers, the predecessor of SCD, the Swiss Dam Commission, had been established in 1928, in the same year as the International Commission on large dams (ICOLD). On December 20, 1948, Henri Gicot chaired the founding assembly of the SCD. It comprised 68 members, many of them from construction and machine industry as well as electric utilities. With more than 300 members nowadays, of which 80 institutional members, the SCD is a private association representing the Swiss dam community within ICOLD. The Committee’s main objective is to promote dam engineering including planning, construction, operation, maintenance and monitoring. To achieve this goal, SCD unites experts and specialists from various dam technology branches offering them a platform to share experiences, publish technical papers and organize symposia and workshops related to dam engineering.

We are convinced that dam and reservoir engineering keeps being vital for society and will have an important future. Several new dam projects are presently under study in Switzerland and in Europe. But in parallel, the important legacy of our predecessors requests attentive

surveillance and innovative solutions to ensure the safety of a large fleet of ageing dams. In addition, climate change as well as the necessity for a better protection of ecosystems and biodiversity are challenges which dam engineers have to take up. Hence, attracting young engineers is thus an important goal of the dam community, and the ICOLD European Club Symposium is a perfect event to network and draw the attention of a broader public to the role of dams and reservoirs.

Robert Boes
President of the
Swiss Committee on Dams

Patrice Droz
Chair of the ECS2023
Organizing Committee

Raphaël Leroy
Vice-President of the
Swiss Committee on Dams

Themes of the 12th ICOLD European Club Symposium

Theme A: Dams and reservoirs for hydropower

- Opportunity for energy generation and storage
- Large-scale storage reservoirs
- Pumped storage reservoirs
- New energy potential (PV, ...)
- Efficiency increase of existing schemes

Theme B: Dams and reservoirs for climate change adaptation

- Balancing extreme hydrological conditions (floods, droughts)
- Protection against floods
- Protection against other natural hazards (mass movements, glacier lake outburst floods, ...)
- Irrigation and water supply
- Multipurpose dams

Theme C: Impact mitigation of dams and reservoirs

- Environmental flows
- Sediment continuum
- Fish passage
- Hydropeaking
- Greenhouse gas emissions

Theme D: How to deal with ageing dams

- Dam safety
- Upgrade and refurbishment
- Extension and renewal
- Incorporating new purposes
- Decommissioning

12th ICOLD European Club Symposium 75th Anniversary of the Swiss Committee on Dams Interlaken, Switzerland, 5-8 September

The 12th ICOLD European Club Symposium will take place in Interlaken, Switzerland on September 5th to 8th, 2023. It is an opportunity for the European members, to focus and discuss on the role of dams and the challenges that arise to adapt effectively to all changes imposed by the energy crisis, climate induced impacts, legislative evolution and ageing of dams, following the themes of the Symposium.

This event will also provide us with the opportunity of a second Board Meeting of the ICOLD European Club within the same year, to discuss additional issues in more detail.

The Symposium will also be the occasion for several European Working Groups to meet and exchange on their works regarding specific technical subjects related to penstocks and pressure shafts, internal erosion in embankment dams, dikes and levees as well as dams and earthquakes.

The Swiss Committee on Dams, founding member of the Club and one of the most active among the European Committees, is excellently committed to the organization of the Symposium, also providing several workshops and a unique opportunity for a technical visit to Spitalamm Dam construction site. Furthermore, it is important to mention that it has actively involved Swiss Committee on Dams Young Professionals in multiple organizing procedures.

The Symposium in Interlaken will also give the opportunity to celebrate the 75th anniversary of the Swiss Committee on Dams. This event will give an excellent opportunity to not only draw from the retrospective of Switzerland's extensive history of dam development, but to also reveal perspectives on the new role of dams for a safer energy transition.

Strong representation, from all member countries and sectors in dam engineering, by participating in the 12th ICOLD European Club Symposium, is highly important for the advancement and to strengthen the collaboration of the European dam community.

It is a great privilege to present the proceedings of the Symposium and I would like to congratulate the Swiss Committee on Dams and all those who contributed to this final selection.

Sera Lazaridou
President of the ICOLD European Club



Taylor & Francis

Taylor & Francis Group

<http://taylorandfrancis.com>

Members of the 12th ICOLD European Club Symposium Scientific Committee

Aufleger Markus	Austria
Balestra Andrea	Switzerland
Balissat Marc	Switzerland
Baumer Andrea	Switzerland
Boes Robert	Switzerland
Carstensen Dirk	Germany
Conrad Marco	Switzerland
De Cesare Giovanni	Switzerland
Droz Patrice	Switzerland
Ehlers Stefan	Switzerland
Epicum Sébastien	Belgium
Favero Valentina	Switzerland
Fielding Mark	Ireland
Fry Jean-Jacques	France
Gunn Russel	Switzerland
Humar Nina	Slovenia
Jovani Arjan	Albania
Leroy Raphaël	Switzerland
Mazzà Guido	Italy
Mouvet Laurent	Switzerland
Otto Bastian	Switzerland
Petkovski Ljupcho	North Macedonia
Pinheiro Antonio	Portugal
Ruggeri Giovanni	Italy
Schleiss Anton	Switzerland
Sliwinski Piotr	Poland
Wieland Martin	Switzerland
Yang James	Sweden



Taylor & Francis

Taylor & Francis Group

<http://taylorandfrancis.com>

Sponsors of the 12th ICOLD European Club Symposium and 75th anniversary of the Swiss committee on Dams

Main Event Partner Sponsors



Silver Sponsors



Bronze Sponsors





Taylor & Francis

Taylor & Francis Group

<http://taylorandfrancis.com>

Keynotes



Taylor & Francis

Taylor & Francis Group

<http://taylorandfrancis.com>

Past, present and future role of Dams in Switzerland

R.M. Boes

ETH Zürich, Laboratory of Hydraulics, Hydrology and Glaciology, President Swiss Committee on Dams

A. Balestra

Lombardi Engineering Ltd., Secretary and Treasurer Swiss Committee on Dams

ABSTRACT: Switzerland is considered the water tower of Europe because of its topographically, and hydrologically favourable conditions with abundant water resources. The headwaters of Europe's major rivers Rhine and Rhône as well as relevant tributaries to the Danube and Po rivers, namely Inn and Ticino, respectively, are in the Swiss Alps. In lack of other major natural resources to generate electricity, the country has therefore been greatly exploiting its water resources since an early stage through the construction of storage hydropower schemes with regulating dams, now accounting for a good half of Switzerland's total annual hydropower production.

Although most of the Swiss dams were built for hydropower generation, they also increasingly provide considerable benefits as multipurpose reservoirs in terms of storage for natural hazards protection as well as agricultural, domestic, industrial and recreational scopes.

It is expected that the importance of hydropower storage on various time scales will continue to increase in the context of the envisaged renewable energy transition. Meanwhile, previously glaciated areas also offer sites for new multipurpose reservoirs. The expected challenges for Swiss dam engineering will be more and more interdisciplinary: operation and maintenance of ageing dams and hydropower plants, climate change adaptation, environmental compatibility and the increasing pressure for multipurpose exploitation of the water resources impose a comprehensive understanding and a participatory approach involving all stakeholders.

1 INTRODUCTION

Switzerland is a country rich in water, and dams are primarily used to store water for the generation of electricity. Larger dams were built as early as the 19th century, so that by 1928, at the time of the founding of the *International Commission on Large Dams (ICOLD)*, there was already extensive national expert knowledge on dam engineering. This manifested itself in the Swiss Commission on Dams, also founded in 1928, which initially consisted of five experts who were also internationally connected and recognised. Nevertheless, it took until 1948 for the Swiss National Committee on Large Dams to be founded - later known as Swiss Committee on Dams, whose 75th anniversary is celebrated in 2023.

This article provides an overview of dams in Switzerland as the largest man-made structures, including the country's natural conditions, and highlights the importance of dams and reservoirs for water resources and energy management. The article concludes with an outlook on current challenges and on the importance of dams in Switzerland in the future.

2 FUNCTION AND PURPOSE OF DAMS

Dams, barrages and appurtenant structures are collectively referred to as dams. As the name suggests, they dam a valley considerably above the highest flood level of the natural stream. ICOLD defines a dam as “large” if its height is at least 15 m from lowest foundation to crest or a dam between 5 and 15 m with a storage volume of at least 3 Mm³.

Reservoirs impounded by dams serve worldwide to store water in times of abundant inflow for periods of low inflows. In many warm and arid countries, dry periods without precipitation result in low runoffs in the watercourses, which can be compensated by releasing previously stored water from reservoirs. Occasionally, even over-year or multi-annual storage is sought, i.e. excess water of one or several wet year(s) is stored to compensate for lower precipitation and runoffs in (a) dry year(s). In the Alpine region, runoffs occur mainly in spring and summer because of precipitation in the form of rain, the melting of snow from the winter precipitation and the melting of glaciers. On the other hand, water demand for electricity production is particularly high in winter and must be compensated for by means of seasonal storage.

Dams serve worldwide a variety of purposes, primarily agricultural irrigation, hydropower, domestic and industrial water supply, low-water recharge, inland navigation and flood control. In Switzerland the focus is on hydropower utilisation, with an inherent flood protection effect.

3 SWISS DAM INFRASTRUCTURE

3.1 *Temporal development and dam types*

The oldest reservoir dam under federal supervision is the 14.5 m high earthfill dam of the Wenigerweiher on the outskirts of the city of St Gallen. It was built in 1822 to supply water and energy to nearby industrial plants and is still in operation, although kept solely for ecological reasons to maintain an amphibian spawning site of national importance (Hager, 2023).

Between 1869 and 1872, Europe’s first concrete gravity dam, Maigrange, was built at Péroilles just south of the city of Fribourg. Nearby, 50 years later, a 55 m high double curvature arch dam was built at Montsalvens, again a European premiere. This dam type later became the second most widespread of large dams in Switzerland (Figure 1). Initially, preference was given to gravity dams, such as the 110 m high gravity dam Schräh in the Wägital, completed in 1924 and considered the world’s highest dam until 1929. In the years of the Great Depression and during the Second World War, some material-saving buttress dams were built, such as the Lucendro dam on the Gotthard Pass. More information on the main phases of Swiss dam development is given by Pougatsch & Schleiss (2023).

The economic upswing after the Second World War called for more hydropower, which led to a vigorous construction of dams in Switzerland: In the short period from 1950 to 1970, around 90 large dams were built (Figure 1). This corresponds to almost half of all large Swiss dams existing today. The Grande Dixence dam, which at 285 m is still the highest concrete gravity dam in the world, was also built during these years. From the 1980s onwards, the construction of large new dams in Switzerland slowed down, while the construction of small dams with other purposes than hydropower, mainly for flood retention, continued (Schwager et al., 2023). Given their knowledge and experience, Swiss engineers have been and continue to be involved in numerous dam projects abroad (Droz, 2023). In doing so, they keep pace with the constantly growing level of experience, which in turn benefits the optimal monitoring and adaptation of domestic dams and sets the basis for new Swiss dam development and refurbishment projects.

Today, there are 200 large dams in Switzerland according to the ICOLD definition (Figure 1). More than 220 dams, weirs and corresponding reservoirs are under the overall supervision of the Swiss federal authority (Schwager et al., 2023). These essentially include dams which either have a storage height of more than 10 m, or a storage height of at least 5 m and a storage volume of at least 50'000 m³. The relevant storage height is defined as the

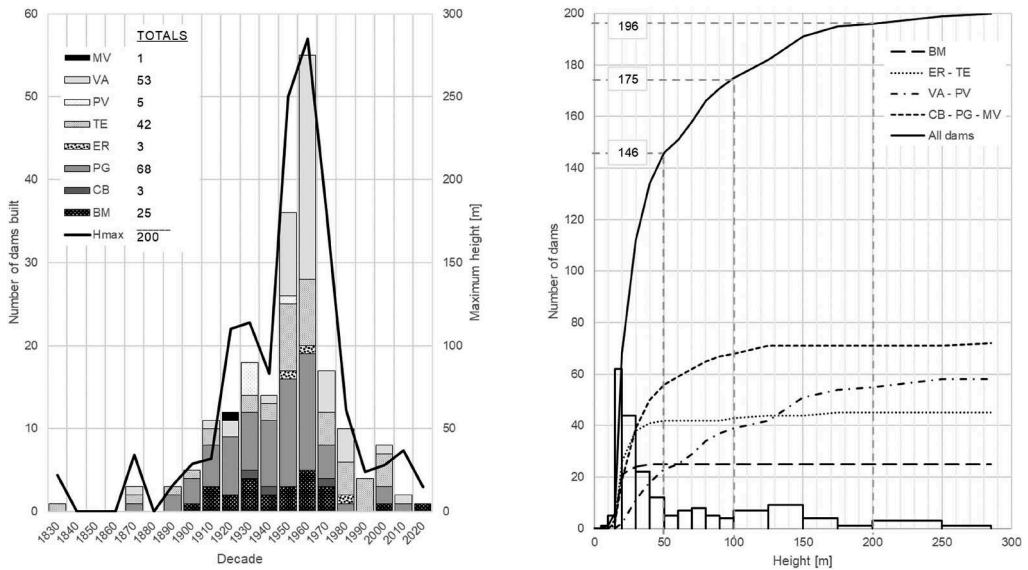


Figure 1. Development of large dams in Switzerland by type (left) and by maximum height above foundation (right); classification according to ICOLD: BM = barrage, CB = buttress dam, ER = rockfill dam, MV = multiple arch dam, PG = gravity dam, PV = arch gravity dam, TE= earthfill dam, VA= arch dam (own representation).

vertical distance between the full supply level and a lower reference level, the latter corresponding to the low water level or the ground elevation. Most large Swiss dams are located in the Alps (Figure 2).

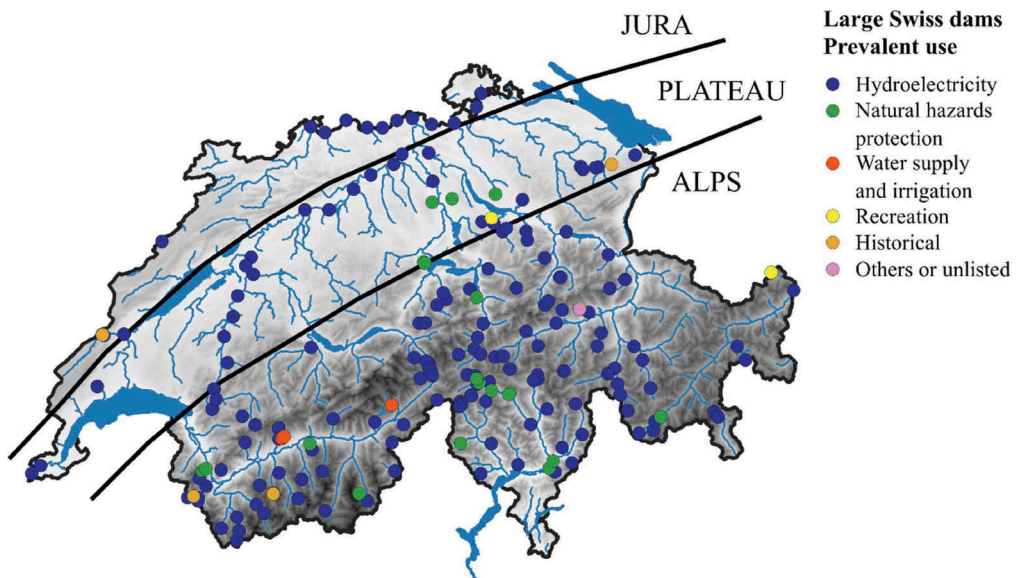


Figure 2. Spatial distribution and purposes of large dams in Switzerland (own representation).

Although well-maintained dam structures can fulfil their functions for decades, dam ageing nevertheless makes great and increasing demands on monitoring, maintenance, and operation. Negative phenomena that occur or are noticed only after a long operation time are, for

example, concrete decay processes such as swelling (SCD, 2017a). The maintenance of the existing dam fleet is a demanding challenge for the specialists involved and is often technically supported by the Swiss federal institutes of technology in Zürich and Lausanne as well as other higher education institutions. As of 2023, 165 out of 200 Swiss large dams are older than 50 years, while the average age of the large Swiss dams is 70 years (Figure 3).

The demand for new dams has declined sharply since the millennium change but has recently been the subject of intense discussion again (Felix et al., 2022; Fauriel et al., 2023), see also sections 6.1 and 6.2. Heightening of existing dams is one way to increase the storage volume for winter energy production. In the past, for example, the Mauvoisin (Canton Valais) and Luzzone (Canton Ticino) arch dams were raised by 13.5 and 17 m, respectively, for this purpose (Schenk & Feuz, 1992; Baumer, 2012). An overview of the dam heightening experience of Swiss engineers is provided by Wohnlich et al. (2023).

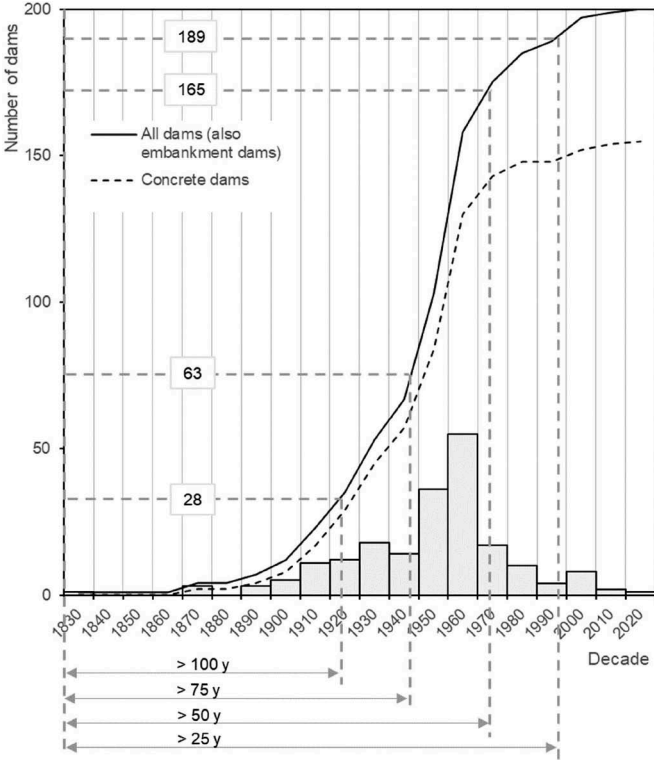


Figure 3. Development of large dams in Switzerland by age (own representation).

3.2 Dams for hydropower

Thanks to the favourable natural conditions regarding topography, hydrology and geology, the hydropower potential in Switzerland has been intensively exploited since the first power plant for electricity production in 1878 in St. Moritz (St. Moritz Energie 2023) until today. There are more than 650 run-of-river, storage, and pumped-storage power plants with installed capacities ranging from 300 kW to the 1'269 MW of the Bieudron hydropower plant (HPP). Their annual production is nominally around 36 TWh/a, which corresponds to about 57% of the country's electricity demand. In an international comparison, Switzerland has by far the highest hydropower generation per unit land area.

The following two main types of HPPs are distinguished in Switzerland:

- Low-head (below 30 m), run-of-river HPPs on the major rivers,
- High-head (200-2'200 m) HPPs with storage dams mostly of medium to large height, generating in one, two or three stages on Alpine tributaries.

Between these two predominant groups, the medium head (30-200 m) range is only sparsely represented in Switzerland, although the corresponding type of HPP is very common worldwide and also constitutes the largest HPPs, i.e. on water-rich streams with relatively high dams, and a powerhouse located nearby. The corresponding reservoirs are characterized by a small to medium capacity inflow ratio (e.g. smaller 0.25), that still allows the HPP to be operated largely independent of fluctuations in inflow with only moderate fluctuations in reservoir water level to meet demand.

The technical potential for hydropower development in Switzerland is often quantified as being exploited by around 90%, so that the potential for further expansion by construction of new schemes is rather low. Current efforts focus on maintaining and optimizing the capacity and efficiency of existing HPPs and related dams. In the future, the value of hydropower is expected to lie even more in storage on various time scales (short-term to seasonal) and the provision of great flexibility for load absorption and short-term generation by means of pumped storage (Boes et al., 2021). Pumped-storage power plants (PSPs) can be used either for electricity production or for pumping operation over the same gross head. No energy is generated in this cyclic process, as the availability of energy is only shifted over time. However, PSPs are of great value in large-scale electricity grids, as they allow to store excess energy in the form of water that can be released to generate electricity within tens of seconds to minutes, with a cyclic or round-trip efficiency of 70 to 80 %. Swiss PSPs are typically designed to store excess natural inflows in seasonal, high-head reservoirs. On the other hand, some storage HPPs also feature pumps to transfer water from lower-lying stream intakes to a reservoir. The largest Swiss storage scheme at Grande Dixence in the Canton of Valais comprises four large-scale pumping stations (Leroy, 2023).

3.3 *Dams for other purposes*

Alongside hydropower, the large seasonal reservoirs in the Alps contribute considerably to flood retention and hence downstream flood protection. However, important for the protection of the population from natural hazard in various regions of Switzerland are also sediment retention and flood retention dams. In addition, numerous small reservoirs (ponds) have been created in the Alps in recent decades, which serve for artificial snowmaking on ski slopes. Especially in the Canton of Valais there are several reservoirs serving for irrigation and water supply. Finally, reservoirs that no longer serve a purpose of economic relevance have ecological and recreational functions nowadays (Figure 2), so that dam removal has not yet been a topic for large Swiss dams. On the contrary, a few mostly small reservoirs impounded by dams are kept in function to preserve habitats that have established in the course of time, as exemplified by the Wenigerweiher in St Gallen (see section 3.1).

4 WATER TOWER SWITZERLAND

4.1 *Topography and relief*

With an area of 41'285 km², Switzerland is one of the smaller countries in Europe. The total extension in east-west direction is about 350 km, and in north-south direction about 220 km. Switzerland is very mountainous by nature and can be divided into three major landscape areas, which show great differences: the Jura, the densely populated Plateau and the Alps (Figure 2). Around 60 % of the country's area belongs to the Alps, 30 % to the Plateau, and 10 % to the Jura. Switzerland has more than 3350 peaks above 2'000 m a.s.l. The sixteen highest peaks in Switzerland are all in the Valais Alps and the highest peak is the Dufourspitze (4'634 m a.s.l.) in the Monte Rosa massif close to Zermatt.

4.2 Climatic regions and Hydrology

The Alps form an important climate and water divide in Central Europe with additional Alpine and intra-Alpine weather effects, so that several weather situations prevail in Switzerland despite its small size, providing a great variability in precipitation distribution (Figure 4). North of the Alps, there is a temperate, Central European climate mostly dominated by oceanic winds, whereas south of the Alps it tends to be more Mediterranean.

The mean annual precipitation is about 1400 mm (reference period 1981 to 2010). In Alpine regions, the mean precipitation is higher, e.g. 1750 mm per year, depending on the elevation. In the Plateau and the Jura, the amount is about 1000 to 1500 mm per year. Precipitation in Switzerland is about twice as high in summer as in winter. Around 32 % of Switzerland's annual precipitation evaporates, with the remaining 68 % flowing abroad as runoff (Viviroli & Weingartner, 2004).

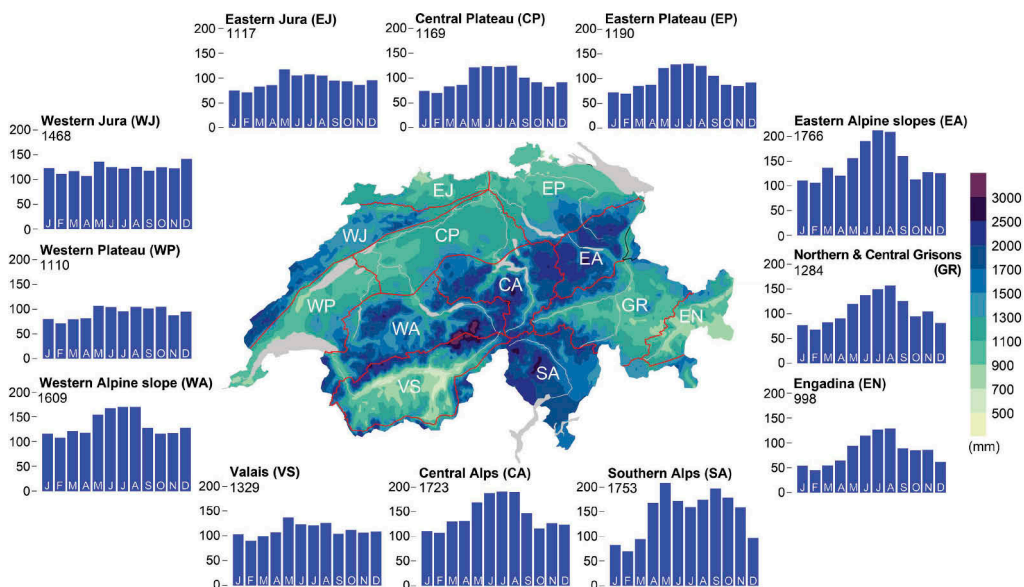


Figure 4. Annual mean precipitation and monthly sums [mm] of the measurement series 1981 to 2010 for the twelve Swiss climate regions; the annual means are indicated in the upper left corners of each barplot (Source: adapted from CH2018, 2018).

4.3 Glaciers

Swiss Alps are significantly shaped by numerous glaciers. The largest and longest Alpine glacier is the Great Aletsch Glacier, followed by the Gorner Glacier (by area). The Swiss glaciers reached their last peak during the Little Ice Age, which lasted from the beginning of the 15th to the middle of the 19th century. Since the end of the Little Ice Age, a clear retreat of the glaciers has also been observed in Switzerland, as almost worldwide. This glacier retreat has intensified in recent decades. Between 1920 and 2019, the ice volume of all glaciers in the Swiss Alps decreased by about half to 51 km³, of which 38% alone occurred between 1980 and 2019 (Zekolari et al., 2019).

4.4 Climate change impacts

Due to the global temperature increase, the runoff distribution over the year is changing and the amount of stored water in snow and glacier ice will further decrease, thus affecting the

multipurpose exploitation of the resource. Figure 5 shows for typical catchments and discharge regimes how seasonal runoffs will change over the course of the year until the middle and end of the century, provided that no climate protection measures are taken, and emissions and warming continue to increase (emission scenario RCP8.5).

By the end of the century, an average increase in winter runoff of around 10 % is expected with climate protection actions (RCP2.6) and around 30 % without such actions (RCP8.5) (Brunner et al. 2019). Winter runoffs increase particularly strongly in today's nival, i.e. snow-melt-dominated regimes (see e.g. Figure 5, Plessur). The smallest changes in winter runoffs are expected in catchments in the Plateau, where snow cover already contributes little to runoff, and in very high catchments (Figure 5, Rosegbach), where most precipitation will continue to fall in the form of snow in the future due to low winter temperatures (Mülchi et al. 2021).

By the end of the century, the summer scenarios show an average decrease in runoff of around 10 % with climate protection actions and 40 % without. Responsible for this decrease are reduced summer precipitation, higher evaporation and the reduction of glacier and snow melt water. Areas of all altitudes and regions are affected by declining summer runoff. There will also be a decrease in summer runoffs in areas that are still glaciated today (Figure 5, Rosegbach).

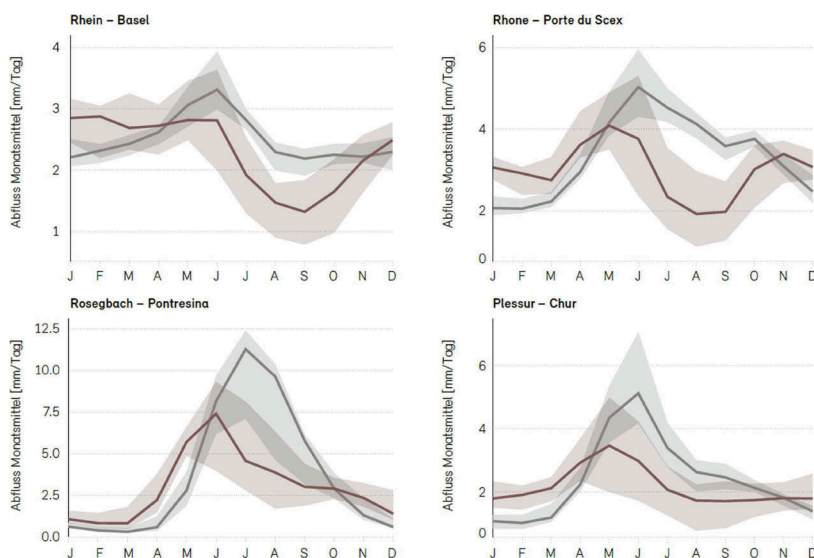


Figure 5. Change in mean monthly runoffs in characteristic catchments with median (line) and uncertainty range (fill) for the reference period (1981 - 2010) (grey) and the scenario without climate protection actions (RCP8.5) by the end of the century (2085, brown line and fill) (Source: adapted from FOEN, 2021).

5 SYSTEMIC RELEVANCE OF SWISS DAMS FOR BALANCING WATER RESOURCES

5.1 Swiss electricity system

Water resources in Switzerland are abundant, but the runoff regimes are subject to large seasonal fluctuations, particularly in small catchments at high altitude. In winter, the runoff is lower than in summer while the electricity demand is higher (55 % of the annual demand in the decade 2013 to 2022). To counteract this imbalance, seasonal hydropower storage systems play a relevant role.

For rivers with small catchments in the side valleys of the Central Alps, the balancing of power generation in summer and winter requires a storage volume of typically 30-40 % of the

annual runoff, depending on the degree of glacier coverage in the catchments. For the rivers of the main valleys, this share is significantly lower, but in absolute terms very large storage volumes would be required. In this respect, the natural sub-Alpine between the Alps and the Plateau have an important balancing function, partially decoupling the catchment areas above and below thanks to their retention effect.

In the large hydropower reservoirs in Switzerland, a considerable part of the natural inflows is transferred from the summer to the winter half-year (1st October to 31st March), so that today the storage power plants generate half of their annual production in the summer and half in the winter half-year, whereas the inflows are distributed over these two half-years at a ratio of about 4:1.

The ratio of electricity production of storage and run-of-river HPPs in Switzerland is approximately 53 %: 47 %, while globally it is around 33 %: 67 %. Almost 90 % of the total storage capacity of Swiss hydropower reservoirs of around 9 TWh is provided by reservoirs with volumes above 20 Mm³ Figure 6). This storage capacity represents a valuable reserve that renews itself every year and that increases the security of electricity supply, especially in the winter half-year. The water stored in the reservoirs until late summer is sufficient to cover around 25 % of the country's total electricity demand in the winter half-year.

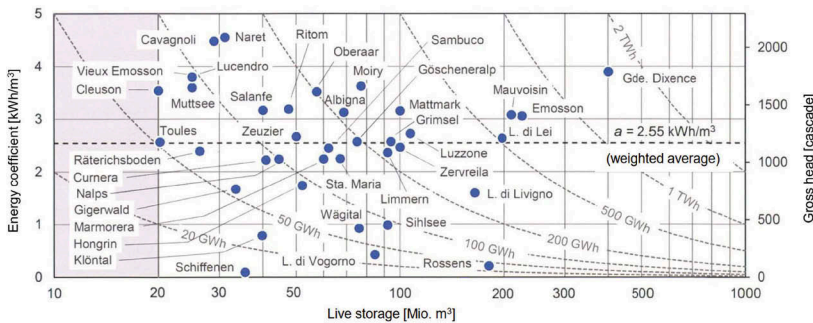


Figure 6. Storable electric energy (dashed curves), average exploitable gross head (of the HPP cascade if applicable) and corresponding energy coefficient of Swiss reservoirs above 20 Mm³ as a function of their live storage volume (adapted from Felix et al., 2020).

5.2 Flood risk management

Natural and artificial lakes can significantly contribute to prevent downstream flood damage through their water retention effect. Every lake has a retention effect because inflow is always delayed and attenuated, even when fully filled. For dams and weirs, this depends on the capacity and mode of operation of the spillway, i.e. the lake outflow. The larger the lake area, the greater the attenuation effect. Thus, flood risk management is increasingly considered in the operation of the relevant Swiss reservoir dams, retention basins and regulated natural lakes.

After the 1993 flood in Valais, the spillway of the Mattmark reservoir was converted in such a way that the uppermost 2 m of the reservoir with a volume of 3.6 Mm³ serve exclusively for flood retention, which the canton of Valais has at its disposal (Biedermann et al., 1996; Sander & Haefliger, 2002).

The Sihl valley in the cantons of Schwyz and Zurich has experienced no major flooding since the construction of a hydropower dam on the Sihl river some 40 km upstream of the city of Zurich in the 1930s. The Sihl reservoir (Sihlsee) regulates almost half of the Sihl catchment area at the Zurich gauging station. In the city of Zurich the damage potential in the event of extreme flooding of the Sihl, largely exceeding the retention effect of the Sihlsee, has been estimated at up to 6.7 billion CHF. The consequential costs of disruptions in energy supply, telecommunications, and transport would exceed the material damage several times. The Canton of Zurich is therefore implementing a comprehensive plan to improve flood protection around the Limmat and the Sihl rivers as well as for the natural Lake Zurich, whose level can be artificially lowered before an incoming flood. Several immediate measures have already been

implemented, including specific structural measures at critical infrastructure, optimisation of emergency planning and emergency organisation, improvements to flood forecasting including anticipatory regulation of Lake Zurich and of the hydropower reservoir Sihlsee, the largest in Switzerland by area, where an overflow of 1 m on the spillway means an additional water retention of about 10 Mm³. In addition, since 2017, a driftwood retention structure in the Sihl river prevents blockages caused by large floating debris at critical points downstream, including the culverts under the Zurich main train station. As a long-term solution to protect the lower Sihl valley and the city of Zurich from extreme flooding of the Sihl, a flood diversion tunnel is under construction to partly transfer flood peaks from the Sihl river (between the Sihlsee and the city of Zurich) into Lake Zurich (AWEL, 2017; FOEN, 2020).

6 OUTLOOK ON DAMS AND RESERVOIRS IN SWITZERLAND

6.1 *Dams and reservoirs to ensure security and flexibility of electric energy supply*

Storage hydropower from the Swiss Alps contributes significantly to the stability of the national and European electricity grids and is key to the envisaged energy transition to renewables. Hydropower plays a central role in the Swiss energy strategy, especially for the security of the electricity supply in the seasonal balancing. Both hydropower production and storage capacity are to be increased in the coming years and decades. This can generally be achieved through new constructions, expansions and extensions as well as renewal and rehabilitation of existing installations. Since the economically feasible hydropower potential in Switzerland is already exploited to a high degree, the focus is on energy storage in large hydropower reservoirs and a further flexibilization between electricity generation and consumption by means of pumped storage power plants.

By 2040, at least 2 TWh of additional electricity storage capacity should be available from hydropower. To this end, a participatory process has been initiated by the Federal Department of the Environment, Transport, Energy and Communications (DETEC), the so-called “Hydropower Round Table”. It was aimed at developing a common understanding between project developers, responsible authorities and other stakeholders of the challenges facing hydropower in the context of the Energy Strategy 2050, the net-zero climate target, security of supply and the preservation of biodiversity. In this process, 33 potential projects, for which the Swiss Federal Office of Energy (SFOE) had obtained brief descriptions and key figures from the project developers, were screened regarding biodiversity, landscape and energy. The projects with the lowest expected specific impacts on biodiversity and landscape per GWh of additional annual storage capacity received the highest scores. To achieve the target of +2 TWh/winter of additional electricity production, 15 projects with the highest scores were finally listed (SFOE, 2021).

The list includes 11 reservoir enlargements through moderate heightening of dams (H) and other adaptation measures, two new reservoirs in the glaciated high mountains (N) and two expansions of existing facilities (N). The two new reservoirs and the two extensions are expected to contribute around 1 TWh/winter, like the 11 dam heightening projects. The total expected additional electricity storage of 2 TWh/winter results mainly from additional production shifting from summer to winter and to a lesser extent from additional production. The projects are further described in Fauriel et al. (2023), including a comparison to recent studies by ETH Zurich (Ehrbar et al., 2018, 2019; Felix et al., 2020; Boes et al., 2021). Accordingly, the construction of a few new dams and the heightening of several existing dams are expected until 2040 or 2050. Thanks to load bearing reserves, the heightening of existing Swiss dams by a certain percentage of their initial maximum height (e.g. 10 %) is often technically feasible by raising the dam on or near its crest only, i.e. the top of the structure itself, without major structural adaptations like a change of dam type. The reserves stem from intentional overdesign of many Swiss dams designed after 1943 following the experiences of the bombing of German dams by the Allies in the second World War.

The Swiss Energy Strategy 2050 poses several technological challenges, which can only be met by adoption of interdisciplinary solutions. Among these, solar energy will play a key role, and installations in Alpine contexts are confirmed to be more and more competitive thanks to their

increased efficiency and to a balanced production profile over the year. Thus, the installation of photovoltaic panels on dams and on their corresponding reservoirs is a solution to be considered because of the following advantages: (i) use of existing hydropower infrastructure for installation and grid connection, (ii) reduced impact on the landscape, (iii) speed of realization, and (iv) production pattern that matches well in combination with the flexibility of storage hydropower. An overview of photovoltaic installations on dam faces and reservoirs in Switzerland is provided by Maddalena et al. (2022), Rossetti et al. (2023) and Maggetti et al. (2023).

6.2 Multi-purpose dams and reservoirs

To date, only a few Swiss reservoirs are explicitly managed as multi-purpose facilities and only a few concessions are linked to further water-related services (Palmieri et al., 2023). With climate change, however, the pressure on water resources will increase due to other usage demands (section 4.4). With regard to the irrigation function, it must be taken into account that most of Switzerland's Alpine reservoirs are located too far away from agricultural areas (Kellner & Weingartner, 2018) and are many times smaller compared to natural lakes (e.g. Grimsel Lake compared to Lakes of Brienz and Thun).

Multi-purpose use of reservoirs creates synergies and is expected to increase public acceptance. For some of the new reservoirs from the list of the Round Table Hydropower, other uses besides hydropower are discussed and planned. For example, the Gorner Lake is to fulfil an essential flood protection function for Zermatt and the Mattertal and shall additionally serve the water supply for irrigation, drinking water, snow production, firefighting, etc. (Fauriel et al., 2023).

The most advanced new multipurpose reservoir project in the Swiss Alps is the Trift dam in the Bernese Oberland, currently in the licensing procedure. Where 75 years ago, at the time of the founding of the Swiss Committee on Dams, the tongue of the Trift glacier was located, a proglacial lake has formed since about the turn of the millennium. The storage volume of this natural lake is to be increased to about 85 Mm³ with a new arch dam (Figure 7). From a water management perspective, such a reservoir can partially replace the storage function of the glacier by temporarily storing the runoff and releasing it to downstream users in a delayed manner or at times of increased demand (geo7 AG, 2017; Kellner & Weingartner, 2018).



Figure 7. Trift glacier (Canton Berne) 1948 (left), 2008 with proglacial lake (centre) and visualisation of the planned arch dam with reservoir (right) (photos: Kraftwerke Oberhasli AG).

6.3 Dam and reservoir adaptation measures due to climate change

As the climate changes, the variability of runoff increases (Annandale et al., 2016; Palmieri et al., 2023). Annual runoff volumes are also affected by this, as dry and wet years tend to increase in severity (section 4.4). The need for dams and the storage volumes of the corresponding reservoirs to balance water supply and demand will thus increase, especially in

regions where natural storage such as from glaciers is declining or diminishing. At the same time, there is still contradictory discussion among experts as to whether sediment input into reservoirs will increase or decrease. While sediment availability tends to increase on the one hand, a decreasing sediment transport capacity is to be expected with decreasing summer run-offs on the other hand.

Impacts of climate change with possible adaptation measures are reported in Table 1.

Table 1. Impacts of climate change with possible adaptation measures.

Impacts	Possible adaptation measures
Increase in magnitude of extreme floods	Capacity increase of spillways, if necessary, including consideration of increased risks of clogging with a trend towards increasing volumes of floating debris (SCD, 2017b; Schmocker & Boes, 2018).
Increasing need for flood protection for downstream dwellers	Adaptation of reservoir management and/or the outlet devices, if necessary (see examples of Sihlsee and Mattmark in section 5.2).
Changes in inflow volumes and water demands in the region of a dam	Adaptation of reservoir management, and conversion into a multi-purpose facility
Intensification of sediment input into reservoirs	Effective reservoir sediment management for sustainable operation, heightening of power water intakes and outlets on dams if necessary.
Possibly more frequent and more intense gravitational natural disasters in the area of dams, e.g. mass slides into reservoirs and danger of impulse waves (Evers et al., 2018, 2022).	Increased monitoring of the reservoir slopes, investigation of the effects of impulse waves, disposition for short-term partial drawdowns, if necessary.
Changed displacement behaviour of concrete dams due to higher ambient temperatures	Predictive assessment by analytical investigations and modelling; if necessary intensified dam monitoring

6.4 Dam and reservoir adaptation measures due to new ecological requirements

The European Water Framework Directive and national legislation place new requirements on transverse structures such as weirs and dams in terms of ecology. In Switzerland, the revised Waters Protection Act entered into force in 2011, which imposes various new or stricter requirements on HPPs. With regard to dams used for hydropower, these are, in particular:

- Reestablishment or improvement of fish migration, both upstream and downstream,
- Reestablishment or improvement of bedload passage and/or bedload management,
- Measures to mitigate hydropeaking effects on the watercourse downstream of storage HPPs.

The Swiss cantons have identified the need for action in strategic planning, and the implementation of the measures for so-called “hydropower rehabilitation” is to take place by 2030. Consideration is given to whether the measures are technically and financially feasible, i.e. whether they have a reasonable cost-benefit ratio. The upstream and/or downstream fish passage must be rehabilitated at around 700 facilities (Dönni et al., 2017), whereby not all of them are considered dams. Sediment passage is to be improved at up to 200 HPPs (Bammatter et al., 2015). While these two aspects apply mainly to low-head facilities on the larger valley watercourses (Boes et al., 2017), hydropeaking countermeasures are to be implemented at around 100 storage power plants, mainly in the Swiss Alpine region (Bammatter et al., 2015).

Rehabilitation of existing HPPs will generate high costs for owners or concessionaires. First and foremost, structural adjustments are planned, but operational measures may also be used, for example temporary drawdown of a reservoir water level to increase the passage of sediment and driftwood during a flood. The HPP operators are compensated by the national grid operator (Swissgrid) for the necessary rehabilitation measures. Eligible non-recurring cost elements are, for example, planning and project costs, acquisition costs for land or buildings, construction costs, costs for new control technology, outage costs and revenue losses due to reduced production.

In the recent past, these requirements have already led to the construction or renovation of ancillary facilities such as upstream and downstream fishways (Meyer et al., 2016), to sediment management measures on dams (Schleiss et al., 2016; Boes et al., 2017) and to new compensation basins for hydropeaking (Schweizer et al., 2021). Examples include a fish lift at the Maigrage dam in the city of Fribourg, the compensation basin of the Oberhasli power plants in Innertkirchen (Figure 8) and sediment replenishment below the Rossens dam on the Sarine river. There, gravel is deposited on the riverbank below the dam and eroded and transported downstream by means of so-called artificial floods, which are generated by discharge through bottom outlets (Figure 9), see also Friedl et al. (2017).

Many efforts will still have to be made to meet the requirements of the revised Swiss Waters Protection Act. From today's perspective, this will go far beyond the target year of 2030. Among others, new solutions will have to be found, which have been the subject of intensive research projects for years. One example is the protection of fish at large HPPs and water intakes with design discharges well above 100 m³/s, for which there is still no generally recognised technological state of the art (Rutschmann et al., 2022). The use of synergies is another approach to restoring or improving the watercourse continuum for both sediment and aquatic organisms at transverse structures (Foldvik et al., 2022).



Figure 8. Innertkirchen hydropeaking compensation basin (Canton Berne) of Kraftwerke Oberhasli KWO (photo: KWO AG).



Figure 9. Artificial flood at the Rossens dam (Canton Fribourg) of Groupe E (photo: Ecohydrology Research Group, ZHAW).

ACKNOWLEDGEMENTS

The authors cordially thank Dr. David Felix, AquaSed GmbH, for his careful proofreading and valuable inputs.

REFERENCES

- Annandale, G.W., Morris, G.L., Karki, P. (2016). Extending the Life of Reservoirs: Sustainable Sediment Management for Dams and Run-of-River Hydropower. *Directions in Development*. Washington, DC: World Bank. doi: 10.1596/978-1-4648-0838-8.
- AWEL (ed.) (2017). Hochwasserschutz Sihl, Zürichsee und Limmat (Flood protection Sihl, Lake Zurich and Limmat). Amt für Abfall, Wasser, Energie und Luft (AWEL), Abteilung Wasserbau. Available at: <https://www.zh.ch/de/planen-bauen/wasserbau/wasserbauprojekte/hochwasserschutz-sihl-zuerich-see-limmat.html> (accessed May 29th, 2023; in German)
- Bammatter, L., Baumgartner, M., Greuter, L., Haertel-Borer, S., Huber Gysi, M., Nitsche, M., Thomas, G. (2015). Renaturierung der Schweizer Gewässer: Die Sanierungspläne der Kantone ab 2015 ('Restoration of Swiss watercourses: rehabilitation plans of the Cantons from 2015'). Federal Office for the Environment FOEN, Water Department, Ittigen, Switzerland.
- Baumer, A. (2012). Innalzamento diga Luzzzone: uno sguardo su 15 anni d'esercizio (Luzzzone dam heightening: glance of 15 years of development). *Wasser Energie Luft* 104 (3):204–208 (in Italian).
- Biedermann, R., Pougatsch, H., Darbre, G., Raboud, P.-B., Fux, C., Hagin, B., Sander, B. (1996). Speicherkraftwerke und Hochwasserschutz ('Storage hydropower plants and flood protection'). *Wasser Energie Luft* 88(10): 220–265 (in German and French).
- Boes, R., Hohermuth, B., Giardini, D. (eds.), Avellan, F., Boes, R., Burlando, P., Evers, F., Farinotti, D., Felix, D., Hohermuth, B., Manso, P., Münch-Aligné, C., Schmid, M., Stähli, M., Weigt, H. (2021). Swiss Potential for Hydropower Generation and Storage, Synthesis Report, ETH Zurich, <https://doi.org/10.3929/ethz-b-000517823>.
- Boes, R.M., Albayrak, I., Friedl, F., Rachely, C., Schmocker, L., Vetsch, D., Weitbrecht, V. (2017). Geschiebedurchgängigkeit an Wasserkraftanlagen ('Bedload continuity at hydropower plants'). *Aqua viva* 59(2): 23–27, <http://www.aquaviva.ch/aktuell/zeitschrift> (in German).
- Brunner M., Björnsen Gurung A., Zappa M., Zekollari H., Farinotti D., Stähli M. (2019). Present and Future Water Scarcity in Switzerland: Potential for Alleviation through Reservoirs and Lakes. *Science of The Total Environment*, 666: 1033–1047. DOI: 10.1016/j.scitotenv.2019.02.169.
- CH2018 (2018). CH2018 – Climate Scenarios for Switzerland, *Technical Report*, National Centre for Climate Services, Zurich, 271 p.
- Dönni, W., Spalinger, L., Knutti, A. (2017). Erhaltung und Förderung der Wanderfische in der Schweiz – Zielarten, Einzugsgebiete, Aufgaben ('Keeping and fostering migratory fish in Switzerland – target species, catchment areas, tasks'). Study on behalf of the Feral Office for the Environment, 53 pages.
- Droz, P. (2023). Swiss dam engineering in the world. *Proc. ICOLD European Club Symposium "Role of dams and reservoirs in a successful energy transition"* (Boes, R.M., Droz, P. & Leroy, R., eds.), Taylor & Francis, London.
- Ehrbar, D., Schmocker, L., Vetsch, D., and Boes, R. (2018). Hydropower Potential in the Periglacial Environment of Switzerland under Climate Change. *Sustainability* 10.8: 2794. DOI: 10.3390/su10082794.
- Ehrbar, D., Schmocker, L., Vetsch, D., Boes, R. 2019. Wasserkraftpotenzial in Gletscherrückzugsgebieten der Schweiz ('Hydropower potential in regions of retreating glaciers in Switzerland'). *Wasser Energie Luft*, 111(4): 205–212 (in German).
- Evers, F.M., Schmocker, L., Fuchs, H., Schwegler, B., Fankhauser, A.U., Boes, R.M. (2018). Landslide generated impulse waves: assessment and mitigation of hydraulic hazards. *Proc. 26th ICOLD Congress*, Vienna, Austria, Q.102-R.40: 679–694.
- Evers, F., Boes, R.M. (2022). Slide-induced impulse waves in the context of periglacial hydropower development. *Proc. 27th ICOLD Congress*, Marseille, France, Q.106-R.36: 59–69
- Fauriel, J., Filliez, J., Felix, D., Boes, R.M. (2023). Additional water and electricity storage in the Swiss Alps: from studies of potential towards implementation. *Proc. ICOLD European Club Symposium "Role of dams and reservoirs in a successful energy transition"* (Boes, R.M., Droz, P. & Leroy, R., eds.), Taylor & Francis, London.
- Felix, D., Müller-Hagmann, M., Boes, R. (2020). Ausbaupotential der bestehenden Speicherseen in der Schweiz ('Potential of extending existing storage lakes in Switzerland'). *Wasser Energie Luft*, 112(1): 1–10 (in German).

- Felix, D., Ehrbar, D., Fauriel, J., Schmocker, L., Vetsch, D.F., Farinotti, D., Boes, R.M. (2022). Potentials for increasing the water and electricity storage in the Swiss Alps. *Proc. 27th ICOLD Congress*, Marseille, France, Q.107-R.24: 367–387.
- FOEN (ed.) (2020). Regulierung Zürichsee (‘Regulation of Lake Zurich’), Fact Sheet. Available at: <https://www.zh.ch/de/umwelt-tiere/wasser-gewaesser/hochwasserschutz/hochwasserrueckhalt-seeregulierung.html> (accessed May 29th, 2023; in German)
- FOEN (ed.) (2021). Auswirkungen des Klimawandels auf die Schweizer Gewässer. Hydrologie, Gewässerökologie und Wasserwirtschaft (‘Impacts of climate change on Swiss watercourses. Hydrology, stream ecology and water resources management’). Federal Office for the Environment FOEN, Bern. *Umwelt-Wissen 2101*: 134 p.
- Foldvik, A., Silva, A.T., Albayrak, I., Schwarzwälder, K., Boes, R.M., Ruther, N. (2022). Combining Fish Passage and Sediment Bypassing: A Conceptual Solution for Increased Sustainability of Dams and Reservoirs. *Water* 14(12), 1977, <https://doi.org/10.3390/w14121977>.
- Friedl, F.; Battisacco, E.; Vonwiller, L.; Fink, S.; Vetsch, D.F.; Weitbrecht, V.; Franca, M.J.; Scheidegger, C.; Boes, R.; Schleiss, A. (2017): Geschiebeschüttungen und Ufererosion (‘Bedload replenishment and bank erosion’). In: *Geschiebe- und Habitatsdynamik. Merkblatt-Sammlung Wasserbau und Ökologie*. Federal Office for the Environment FOEN, Bern: Bulletin 7 (in German, French and Italian).
- geo7 AG (2017): Multifunktionsspeicher im Oberhasli (‘Multi-purpose reservoirs in the Oberhasli’). Report on behalf of Wasser und Abfall (AWA) des Kantons Bern. Bern, Switzerland.
- Hager, W.H. (2023). Outstanding past Swiss dam engineers. *Proc. ICOLD European Club Symposium “Role of dams and reservoirs in a successful energy transition”* (Boes, R.M., Droz, P. & Leroy, R., eds.), Taylor & Francis, London.
- Kellner, E., Weingartner, R. (2018). Chancen und Herausforderungen von Mehrzweckspeichern als Anpassung an den Klimawandel (‘Chances and challenges of multi-purpose reservoirs as an adaptation to climate change’). *Wasser Energie Luft*, 110(2): 101–107 (in German).
- Leroy, R. (2023). Water resources optimisation – a Swiss experience. *Proc. ICOLD European Club Symposium “Role of dams and reservoirs in a successful energy transition”* (Boes, R.M., Droz, P. & Leroy, R., eds.), Taylor & Francis, London.
- Maddalena, G., Hohermuth, B., Evers, F.M., Boes, R., Kahl, A., (2022). Photovoltaik und Wasserkraftspeicher in der Schweiz-Synergien und Potenzial. *Wasser, Energie, Luft* 114(3): 153–160 (in German).
- Maggetti, D., Maugliani, F., Korell, A., Balestra, A. (2023). Photovoltaic on dams – Engineering challenges *Proc. ICOLD European Club Symposium “Role of dams and reservoirs in a successful energy transition”* (Boes, R.M., Droz, P. & Leroy, R., eds.), Taylor & Francis, London.
- Meyer, M., Schweizer, S., Andrey, E., Fankhauser, A., Schläppi, S., Müller, W., Flück, M. (2016). Der Fischlift am Gadmerwasser im Berner Oberland, Schweiz (‘The fish lift on the Gadmerwasser in the Bernese Oberland, Switzerland’). *WasserWirtschaft* 106 (2/3):42–48 (in German).
- Muelchi, R., Rössler, O., Schwanbeck, J., Weingartner, R., Martius, O. (2021). River runoff in Switzerland in a changing climate – runoff regime changes and their time of emergence. *Hydrology and Earth System Sciences*, 25(6): 3071–3086.
- Palmieri, A., Maggetti, D., Balestra, A. (2023). Multipurpose dams – A European perspective. *Proc. ICOLD European Club Symposium “Role of dams and reservoirs in a successful energy transition”* (Boes, R.M., Droz, P. & Leroy, R., eds.), Taylor & Francis, London.
- Pougatsch, H., Schleiss, A.J. (2023). Swiss dams: overview of historical development. *Proc. ICOLD European Club Symposium “Role of dams and reservoirs in a successful energy transition”* (Boes, R.M., Droz, P. & Leroy, R., eds.), Taylor & Francis, London.
- Rossetti, E., Maggetti, D., Balestra, A. (2023). Dams and photovoltaic plants – The Swiss experience. *Proc. ICOLD European Club Symposium “Role of dams and reservoirs in a successful energy transition”* (Boes, R.M., Droz, P. & Leroy, R., eds.), Taylor & Francis, London.
- Rutschmann, P., Kampa, E., Wolter, C., Albayrak, I., David, L., Stoltz, U., Schletterer, M. (eds.) (2022). *Novel Developments for Sustainable Hydropower*, Springer, Cham: 91–98, <https://link.springer.com/book/10.1007/978-3-030-99138-8>.
- Sander, B., Haefliger, P. (2002). Umbau der Stauanlage Mattmark für den Hochwasserschutz: Schlüsselereignisse und -aktionen, welche die Zeit seit dem Hochwasser von 1993 bis heute prägten (‘Conversion of the Mattmark dam for flood protection: key events and actions that have marked the period since the flood of 1993 until today’). *TEC 21*, 128 (36):20–26 (in German).
- SCD (2017a). Concrete swelling of dams in Switzerland. *Report of the Swiss Committee on Dams*, https://www.swissdams.ch/fr/publications/publications-csb/2017_Concrete%20swelling.pdf, 78 p.
- SCD (2017b). Floating debris at reservoir dam spillways. *Report of the Swiss Committee on Dams*, https://www.swissdams.ch/fr/publications/publications-csb/2017_Floating%20debris.pdf, 78 p.

- Schenk, T., Feuz, B., 1992. Die Erhöhung der Staumauer Mauvoisin ('The heightening of Mauvoisin dam'). *Wasser Energie Luft*, 84(10): 245–248 (in German).
- Schleiss, A. J., Franca, M.J., Juez, C., De Cesare, G. (2016). Reservoir sedimentation. *Journal of Hydraulic Research*, 54:6, 595–614, DOI: 10.1080/00221686.2016.1225320
- Schmocker, L.; Boes, R. (2018). Schwemmgut an Hochwasserentlastungsanlagen (HWE) von Talsperren ('Floating debris at reservoir dam spillways'). *Wasser, Energie, Luft* 110(2): 91–98 (in German).
- Schwager, M., Askarinejad, A., Friedli, B., Oberender, P. W., Pachoud, A. J., Pfister, L. (2023). Swiss dam safety regulation: Framework, recent changes and future perspectives. *Proc. ICOLD European Club Symposium "Role of dams and reservoirs in a successful energy transition"* (Boes, R.M., Droz, P. & Leroy, R., eds.), Taylor & Francis, London.
- Schweizer, S., Lundsgaard-Hansen, L., Meyer, M., Schläppi, S., Berger, B., Baumgartner, J., Greter, R., Büsser, P., Flück, M., Schwendemann, K. (2021). Die Schwall-Sunk-Sanierung der Hasliaare: Erste Erfahrungen nach Inbetriebnahme und ökologische Wirkungskontrolle ('The hydropeaking remediation of the Hasliaare: First experiences after commissioning and ecological impact monitoring'). *Wasser Energie Luft*, 113(1): 1–8 (in German).
- Schweizerisches Baublatt (1990). Staumauer des Stausees von Mauvoisin VS wird erhöht ('Dam of the Mauvoisin reservoir VS is raised'). 57/58: 2–4 (in German).
- SFOE (2021). Press release Round Table Hydropower. Swiss Federal Office of Energy SFOE, <https://www.admin.ch/gov/de/start/dokumentation/medienmitteilungen.msg-id-86432.html> (in German)
- St. Moritz Energie (2023). Geschichte und Pioniergeist ('History and pioneer spirit'). <https://www.stmoritz-energie.ch/en/about-us/portrait/history-pioneer-spirit.html>; accessed on 29 May 2023.
- Viviroli, D., Weingartner, R. (2004). Hydrologische Bedeutung des Europäischen Alpenraumes ('Hydrological significance of the European Alpine region'). In: Federal Office for the Environment FOEN (ed.): *Hydrologischer Atlas der Schweiz*. ISBN 978-3-9520262-0-5.
- Wohnlich, A., Fankhauser, A., Feuz, B. (2023). Dam heightening in Switzerland. *Proc. ICOLD European Club Symposium "Role of dams and reservoirs in a successful energy transition"* (Boes, R.M., Droz, P. & Leroy, R., eds.), Taylor & Francis, London.
- Zekollari, H., Huss, M., Farinotti, D. (2019). Modelling the future evolution of glaciers in the European Alps under the EURO-CORDEX RCM ensemble. *The Cryosphere*, 13(4), 1125–1146.

Swiss dams: Overview of historical development

H. Pougatsch

Geneva, Switzerland

A.J. Schleiss

Ecole polytechnique fédérale de Lausanne (EPFL), Lausanne, Switzerland

ABSTRACT: With more than 220 large dams in operation, compared to its surface of some 41'000 km², Switzerland has a very large fleet. They were erected to meet various economic and protection needs. Their main assignments concern the storage of water for later use, mainly hydropower, and the protection of property, particularly against floods. It is from the 19th century with the growth of the population and the industrial development that the marked beginning of the construction of large dams. This paper describes, over time, the various stages of this development, the main period of which is between 1950 and 1970. Guaranteeing the safety of these storage schemes at all times is essential. A concept based on three pillars (structural safety, monitoring and maintenance, emergency plan) was developed. Periodic safety assessments have led to the undertaking of maintenance and rehabilitation works for several storage schemes. In the future, the monitoring and uprating of existing structures will remain an important task. New projects with the purpose to increase storage for the winter critical season are also planned and are partly already integrated into an expansion process, in particular to meet actual needs for a safe and low carbon energy transition. Of course, research and development remain specific objectives to maintain the competences of dam engineering not only in Switzerland but also for the participation to worldwide development of dams and reservoirs.

1 INTRODUCTION

The oldest dam structures still in use date from the nineteenth century. During the twentieth century, the country's economic development and ensuing energy needs had an influence on the rate of construction of dams associated with quite remarkable hydroelectric projects. While Switzerland today has many large dams, this is due to the driving force of eminent engineers who played pioneering roles: F.L. Ritter, H. Juillard, F. Meyer-Peter, H. E. Gruner, Alfred Stucky, Henri Gicot, Giovanni Lombardi. The most active period of dam building occurred between 1950 and 1970 (Figure 1). There are more than 220 dams in Switzerland under the jurisdiction of the Confederation of which 87% are designed to produce hydropower. Other uses include the storing of water for irrigation, supply of drinking water, and the production of artificial snow (3%), biotopes and leisure activities (3%), as well as protective structures for controlling flooding events and retaining sediment (7%). Among these dams, 56% are concrete dams (which can be further split into 54% gravity dams, 41% arch dams, and 5% multiple arch and buttress dams), 31% embankment dams (earth or rockfill), and 13% gated weirs. Twenty-five dams have a height greater than 100 m and four of these are taller than 200 m. The most impressive dams are in the Alps. Finally, it is important to note the existence of several hundred dams and weirs of more modest dimensions and of various types and uses.

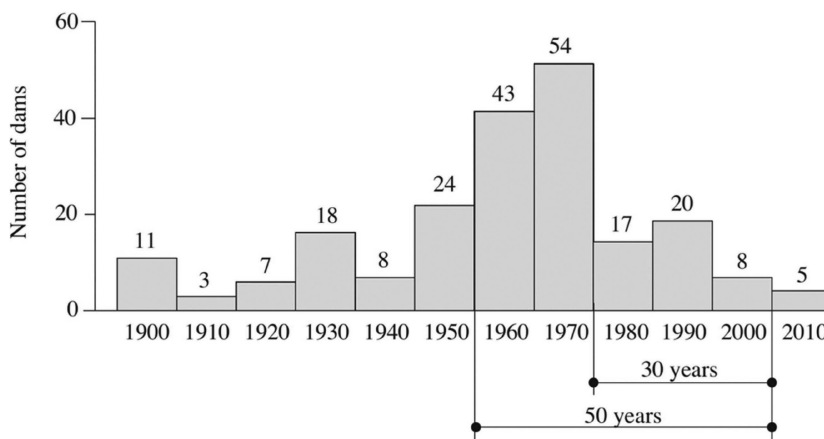


Figure 1. The age structure of large dams in Switzerland.

2 MAIN STAGES IN THE CONSTRUCTION OF DAMS

The growth in population and industrial development of the twelfth century led to the appearance of the first water storage structures in Switzerland (Sinniger, 1985). These installations were modestly for the use of hydropower. Only some of these structures still exist today. The industrial revolution in the eighteenth and nineteenth centuries brought about great economic growth, in particular due to the development of hydroelectric schemes in which turbines gradually replaced water wheels. From 1869 to 1872, Guillaume Ritter (1835–1912) built the Péroles hydropower scheme on the Sarine River upstream of Fribourg. The slightly curved gravity dam (height 21 m, crest length 195 m) was at the time the largest dam in Switzerland. Its trapezoidal section includes two inclined faces. Its construction in concrete was also an innovation in Europe. Interesting rehabilitation works across the whole dam structure were carried out from 2000 to 2004.

In the late nineteenth and early twentieth centuries, many embankment dams were built (Figure 2). At that time, techniques for earthworks were based on empirical criteria far removed from the later science of soil mechanics. The failure of a small, five-meter dike in 1877 encouraged engineer Friedrich de Salis (1828–1901) to undertake a detailed study of the dam break wave, which was most probably the first calculation of its kind. Some of the more remarkable constructions include the Günsen saddle embankment (SG/1900/H = 19 m) and the Klöntal embankment (GL/1910/H = 30 m), which was designed to raise the water level of a natural lake. During this same period, many gravity dams were also built, most often using traditional masonry techniques, including dams at Buchholz (SG/1892/H = 19 m), List (SG/1908/H = 29 m), Muslen (SG/1908/H = 29 m), and at the Bernina Pass (GR/1911/H = 15 and 26 m). Substantial rehabilitation works were carried out on the dams at the Bernina Pass in the late twentieth and early twenty-first centuries.

Due to increasing energy needs, from 1914 attention turned to the construction of water-storage reservoirs, in particular water issuing from summer snowmelt and glacier melt, and to guarantee the production of energy in winter when demand for electricity rises. This transfer of energy necessitated the availability of large reservoirs and therefore the construction of large dams.

The construction of the Montsalvens dam (FR/1920/H = 55 m) marks the beginning of a new period of dam development. It was the first double-curvature arch dam in Europe and was designed by Heinrich E. Gruner (1873–1947). Static calculations were based on a trial-load method devised by Hugo F. L. Ritter (1883–1956), which was then developed by Alfred Stucky (1892–1969) and Henri Gicot (1897–1982), who were both working with H. E. Gruner.

The Swiss Commission on Dams was founded on 2 October 1928 by six renowned scholars and practitioners in the construction of dams namely H. Eggenberger, H. E. Gruner, A. Kaech, E. Meyer-Peter, M. Ritter, A. Stucky, A. Zwygart and W. Schurter. Somewhat later the renown

experts J. Bolomey, O. Frey-Bär, H. Gicot, H. Juillard, M. Lugeon, E. Martz, M. Roš, and M. Roš. jun. joined the commission. According to its statutes, the aim of the commission was to “deal with problems related to dams and to collect information and knowledge about these constructions and their operation.” In the beginning, the Commission dealt with issues brought up in conferences held by the International Commission on Large Dams (ICOLD), founded in 1928. It later went on to establish guidelines for the construction and maintenance of Swiss dams. In addition, it set itself the task of carefully examining the results of observations carried out on dams. In 1948 the Swiss Commission on Large Dams became the Swiss National Committee on Large Dams (SNCOLD) and in 1999, the Swiss Committee on Dams (SwissCoD).

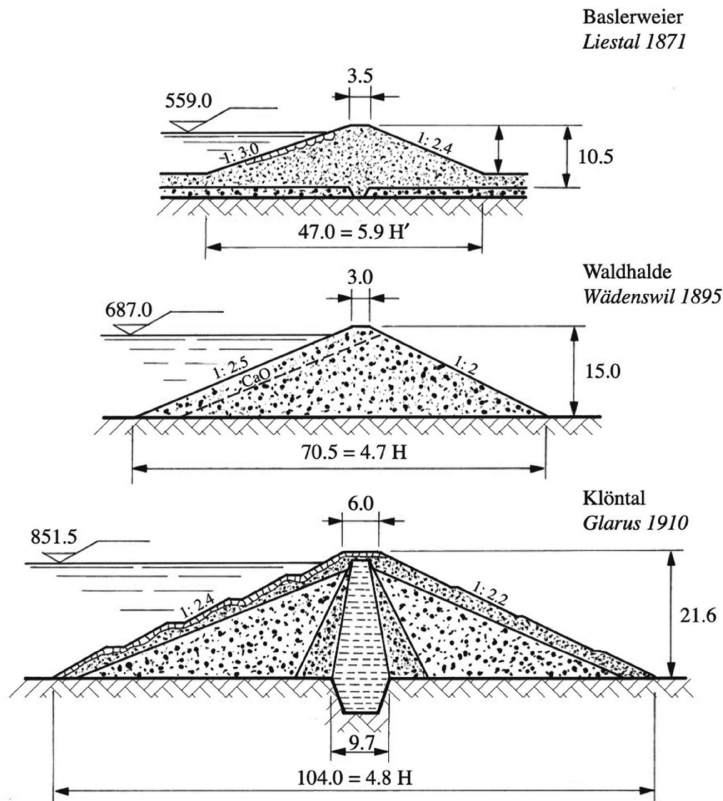


Figure 2. Examples of embankment dams built in the late nineteenth and early twentieth centuries (from Schnitter, 1985).

In the 1930s, the global economic crisis slowed the rise in the consumption of electricity, as well as the need for new hydropower schemes, and, as a result, the construction of dams. However, it was at this time that the Dixence dam was built (VS/1935/H = 87 m), based on a project by Alfred Stucky. This buttress dam has a volume of 421'000 m³ and until the end of the Second World War was the highest dam of its type in the world. Construction of the Verbois dam (GE/1943/H = 34 m) and the buttress dam at Lucendro (TI/1947/H = 73 m) began during the Second World War.

After the bombing of German gravity dams by the English air force in May 1943, the Federal authorities stipulated that horizontal buttress struts had to be added to the already completed Lucendro buttress dam, as well as major reinforcement to the Cleuson dam (VS/H = 87 m) built between 1947 and 1950. Thereafter, only very narrow hollows were to be admitted, as is the case for the dams at Räterichsboden (BE/1950/H = 94 m) and Oberaar (BE/1953/H = 100 m).

During the Second World War, a sharp increase in the consumption of electricity was observed, which continued in the post-war context. Hydroelectric schemes, of which large

dams were the centerpiece, were constructed to respond to this demand for additional energy. In 1945 the construction of the Rossens arch dam began (FR/1947/H = 83 m). From 1950 and throughout the 1970s, dam construction boomed, and more than one hundred dams were commissioned. The construction of the 237-meter-high Mauvoisin arch dam (Figure 3) heightened to 250 m in 1991 and the 285-meter-high Grande Dixence gravity dam (Figure 4) began in 1951. Commissioned in 1957 and 1961 respectively, these two dams are still today among the highest operating dams in the world. Thanks to the skills of renowned experts and engineers from high-level consultancy firms, many impressive arch dams were erected.



Figure 3. The Mauvoisin arch dam (H = 250 m).

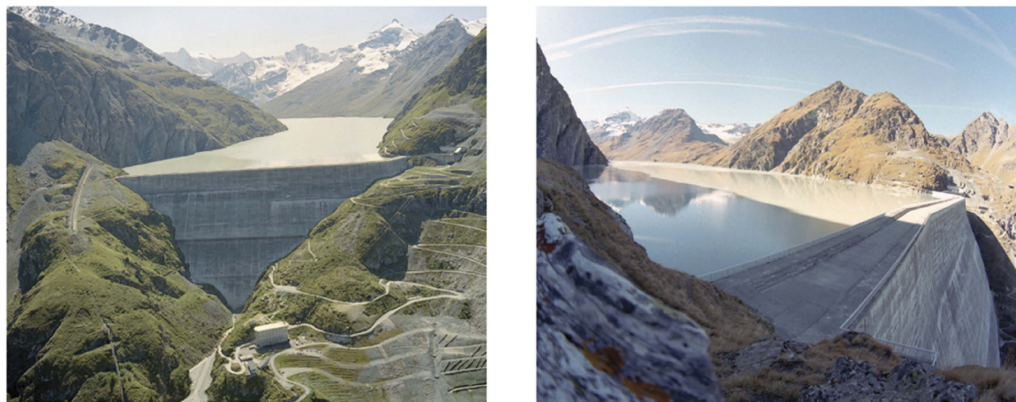


Figure 4. The Grande Dixence gravity dam (H = 285 m).

In the design of arch dams, the traditional circular arches were replaced by parabolic or elliptic arches in order to ensure a better orientation of the pressure of the arches against the rock foundation and abutments. Among the structures with a height greater than 100 m, the following dams can be listed: Emosson (VS/1974/H = 180 m), Zeuzier (VS/1957/H = 156 m), Curnera (GR/1966/H = 155 m), Zervreilla (GR/1957/H = 151 m), Moiry (VS/1958/H = 148 m), Limmern (GR/1963/H = 146 m), Punt dal Gall (GR/1968/H = 130 m), Nalps (GR/1962/H = 127 m), and Gebidem (VS/1967/H = 122 m). The twin-arch dams at Lake Hongrin (VD/1969/H = 125 and 90 m) should also be noted, whose double arches joined by a common, central abutment, give the structure a distinctive look (Figure 5). After the Grande Dixence and Mauvoisin dams, the 200 m barrier was broken, notably by the arch dams of Luzzzone (TI/1963/1997/H = 225 m) and Contra (TI/1965/H = 220 m) (Figure 6) in Ticino. The latter was designed by Giovanni Lombardi (1926–2017).

Utilizing primarily the core scientific and rational developments established by Karl Terzaghi, the founder of soil mechanics, the construction of several embankment dams was



Figure 5. The double-arch Hongrin dam ($H = 125/90$ m).

undertaken. In addition, on the initiative of Eugen Meyer-Peter (1883–1969), the ETHZ created an institute for foundation engineering and soil mechanics, whose research has proven to be of great use. The embankments at Marmorera (Castiletto), (GR/1954/ $H = 91$ m), Göschenalp (UR/1960/ $H = 155$ m), and Mattmark (VS/1967/ $H = 120$ m) are the largest embankment dams built in Switzerland (Figure 7).



Figure 6. The Contra arch dam ($H = 220$ m).

From 1980, new constructions integrated into hydroelectric schemes became less common. The largest are the structures in Solis (GR/1986/ $H = 61$ m) and Pigniu (GR/1989/ $H = 53$ m). However, to better operational conditions and ensure improved energy transfer, the arch dam at Mauvoisin (VS) was raised by 13.5 m to reach a height of 250 m in 1991 and the dam at Luzzone (TI) by 17 m to reach 225 m in 1997. Two pumped-storage projects have been launched. The first is the scheme at Limmern (GL); here, the construction of the Mutsee gravity dam (GL /2015/ $H = 35$) has raised the level of a natural lake, situated at an altitude of 2,500 meters above sea level, by 28 m. During construction of the Nant-de-Drance pumped-storage hydropower plant (VS), the Vieux-Emosson Dam, built in 1955, was raised by 21.5 m to reach a height of 76.5 m, which has doubled the storage capacity of the reservoir.

Furthermore, several structures with heights between 7 and 30 m have been built to protect against natural events such as floods and avalanches. In the late 1990s, reservoirs created to store water with the aim of producing artificial snow began to appear.

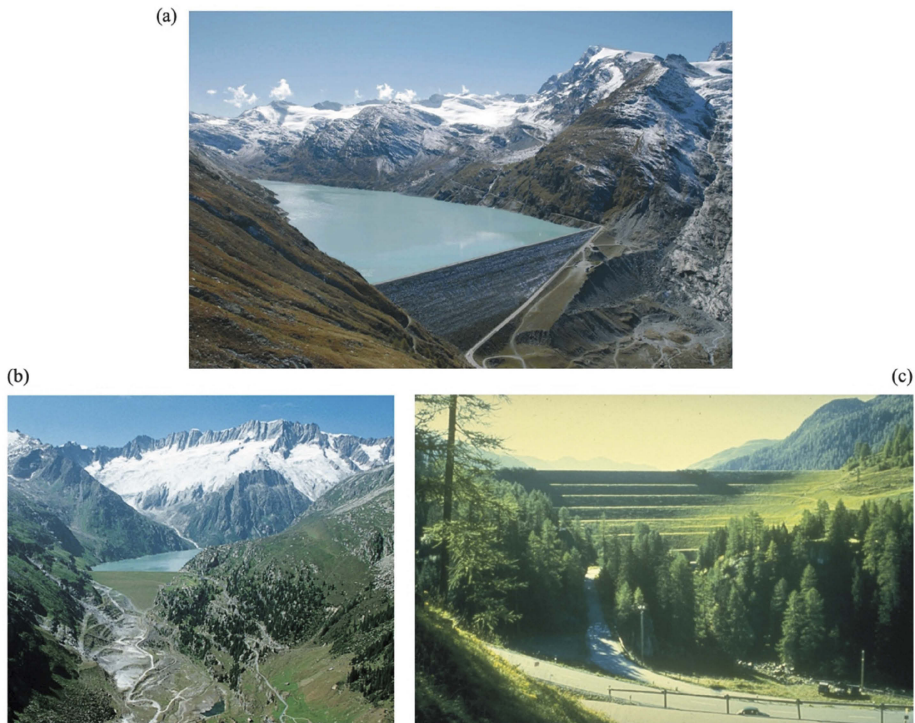


Figure 7. The largest embankment dams in Switzerland: (a) Mattmark (H = 120 m), (b) Göscheneralp (H = 155 m), and (c) Marmorera (Castiletto) (H = 91 m).

3 REINFORCEMENT AND REHABILITATION WORKS

On a different note, from the early 1980s, attention turned toward old dam structures of all sizes whose safety had to be reassessed on the basis of modern standards and technological advances. Depending on the results obtained, it may be necessary to rehabilitate all or some of the structure elements in order to guarantee its safe operation for many more years. Of course, there are many reasons why the strengthening and rehabilitation of a dam are necessary. Often, the structure no longer meets the latest stability criteria. The accepted hypotheses for load on the structure from the initial project may have to be revised. These hypotheses may concern the weight itself, the distribution of uplift or the induced effects that may occur during an earthquake. New operational conditions, such as, for example, new flooding levels, a large accumulation of upstream sediment, or the installation of downstream rockfill may also have an impact on load. Several different types of rehabilitation works are possible and may sometimes be combined. Possible interventions reinforcement and rehabilitation interventions are:

- Dam heightening
- Complete rehabilitation of all structures
- Treatment of facing
 - Laying membrane
 - Asphalt facing
 - Concrete cover, gunite
- Rehabilitation of dam body (concrete, embankments)
 - Grouting
 - Sealing

- Reinforcement of downstream toe
- Foundation treatment
 - Grouting
 - Drainage
- Flood safety
 - Modification of the spillway
 - Modification of the crest
 - Creation of a parapet wall
- Drawdown of the reservoir
 - Transformation of the bottom outlet
 - Implementation of a new bottom outlet

In the case of the Mairgrauze dam (FR/H = 22 m), commissioned in 1872, the rehabilitation project was designed to improve safety in case of flooding by uprating the spillway, improving the dam's structural safety with the installation of prestressed rock anchors, and optimizing operating conditions with the modification of water intakes. Furthermore, the monitoring system was modernized. And last but not least, a ladder including a lift was constructed for fish to migrate upstream past the dam and a series of channels and pools were added for downstream migration. These works were carried out from 2000 to 2004. When the stress and stability assessment demonstrate that safety conditions are not being met, drawing down the reservoir or reinforcing the dam becomes inevitable. For the Gübsensee dam (SG/1900/H = 24/17 m), the chosen solution was to install post-stressed cables. As for the concrete dams at Muslen (SG/1908/H = 29 m) and List (SG/1908/H = 29 m), their upstream and downstream faces were covered with a concrete shell while the height of the crest was also raised in order to increase the volume of the reservoir and thus optimize hydropower generation.

Remedial work may become necessary if the material at the core of the dam has suffered from major internal damage, due, for example, to swelling caused by an alkali-aggregate reaction (AAR), which can significantly impact concrete characteristics. To limit the development of this type of swelling, the upstream face of the Illsee dam (VS/1923–43/H = 25 m) was lined with a PCV geomembrane, and the Lago Bianco Sud dam (GR/1912–42/H = 26 m) was lined with a membrane comprising a synthetic liquid applied in successive layers. At the Illsee dam, the system put in place did not prevent water penetration via the foundation and thus did not slow the swelling phenomenon. Concrete drying measures were also taken without success. Vertical sawing cuts into the concrete are still to be done in order to relieve the stresses in the dam. After being commissioned in 1952, monitoring of the behavior of the Serra arch dam (VS/1952–2010/H = 25.7 m) was principally carried out through geodetic measurements and leveling. Concrete in the Serra dam, affected by an alkali-granulate reaction (AAR) leading to the swelling of the concrete, resulted in irreversible upstream deformation, accompanied by an uplift to the dam and diffuse cracking. Rehabilitation of the structure was necessary, as the gradual deterioration in its conditions of use and safety had been highlighted. The rehabilitation solution that was chosen consisted in building a new dam downstream of the original one (Figure 8). The partial and necessary demolition of the downstream toe of the old dam enabled a new and more favorable geometry to be determined. From a structural point of view, the Serra dam is close to a double-curved arch dam (SwissCoD, 2017b).

In the 1930s, the designers and builders of the Spitallamm dam (BE/1932/H = 114 m) did pioneering work. The dam near the Grimsel pass is one of the first large arch-gravity dams. The Seeuferegg gravity dam (BE/1932/H = 42 m) was built at the same time as the Spitallamm dam. These two dam walls created the reservoir of Lake Grimsel. In the 1960s, detailed examinations and checks revealed that the Spitallamm dam had a vertical crack in its core. In fact, the crown and the concrete of the downstream face of the Spitallamm dam had started to separate from the rest of the dam. Initially, it was decided to carry out the necessary rehabilitation work as part of the possible raising of the two Grimsel dams. Due to a possible alkali-aggregate reaction, the operator decided not to rehabilitate the dam and, in the fall of 2015, started the planning work for a new dam. In June 2019, the construction of a new double-



Figure 8. Serra Dam during reconstruction: new arch dam in front of the old dam before its partial demolishing.



Figure 9. Spitallamm dam under construction in front of the existing arch-gravity dam (Courtesy A. Schleiss, 2022).

curved arch dam located immediately in front of the old dam began. The old Spitallamm dam will be left as it is and will subsequently be submerged (Figure 9).

In cases of significant deterioration due mainly to frost, both faces must be treated. For example, around 1983, after damaged zones had been scored, the surface of the upstream face of the Schräh dam was covered with lightly reinforced shotcrete to a depth of 8 to 12 cm. In another example, wet shotcrete was applied across practically the whole surface of the upstream face of the Cleuson dam between 1995 and 1998. The affected area had previously been stripped by hydro-demolition. The bond between the base concrete and the sprayed concrete was guaranteed by a grid with mushroom-shaped anchoring bolts made of 12-mm-diameter reinforced steel placed at 4 bolts per m^2 .

After severe flooding in 1978 in Ticino and the blockage of the spillway channels at the Palagnedra dam (TI/1952/H = 72 m) by the massive piling up of driftwood (Figure 10) (Swiss-CoD, 2017a), the supervisory authority reviewed general safety criteria in cases of flood and asked for an investigation into the safety requirements to be carried out. It is important to note that in the Alps, floods can strike with devastating speed. For many dams, spillways or crests had to be modified, or a large parapet wall had to be added so as to provide increased retention capacity.

Studies have shown that during major flooding events, reservoirs attached to hydroelectric schemes contribute substantially to the reduction of peak flooding levels, due to their capacity for retaining water, even though that is not their primary function. In order to increase



Figure 10. Blocked passes at the Palagnedra dam (TI) during the flood on August 7, 1978.

protective measures against flooding events downstream of a dam, without having to restrict production of hydroelectric power, one option is to transform a single operation into a multipurpose operation. The idea is to create an additional volume in the upper part of the reservoir that can be used hold a specific volume of water in cases of flood. Such a project was completed in 2001 for the Mattmark embankment dam by adapting the side weir spillway. Other proposals are also being considered.

In Switzerland, the general rule is that all dams must be equipped with a bottom outlet to empty the reservoir in cases of abnormal dam behavior or lower the water level for maintenance to be carried out. Due to insufficient capacity or obsolete equipment, some structures had to be completely transformed or a new bottom outlet had to be created. For example, a gallery was drilled into the foot of the Schräh dam (SZ/1924/H = 111 m). To ensure compliance, a bottom outlet was created in the Illsee dam (VS/1924-43/H = 25 m) by utilizing a gallery that had originally been used to lower the level of the natural lake at the time the dam was being built. In other cases, gates have simply been replaced or a new gate added.

Geodetic measurements carried out between 1921 and 1937 had already highlighted weak plastic movement perpendicular to the bed of the downstream section of the left-bank abutment of the Montsalvens dam (FR/1920/H = 52 m). As this movement continued, additional monitoring devices (pendulum, extensometers) were installed in 1969 in order to ensure more systematic reporting of the behavior of the downstream zone. Analyses carried out later showed that the state of equilibrium was situated at the limit of elastic behavior. Strengthening works were decided on out of a fear that the deformations would only continue to intensify or that a rockfall would be caused by a seismic shock. Works on the left abutment were designed with two objectives in mind; firstly, bolts sealed with cement grout were applied to a concrete sprayed surface to protect the valley flanks against the risk of rock fall, and secondly, reinforced bars sealed completely into the rock with cement grout were designed to increase resistance to shearing along bedding planes. At the Pfaffensprung dam (UR/1921/H = 32 m), it was not known how long existing anchors would hold downstream of the left bank abutment, so it was decided that additional prestressed anchors would be installed with a system that enabled their tension to be controlled at all times.

4 DEALING WITH RESERVOIR ISSUES

4.1 *Reservoir surroundings*

It is of the utmost importance to monitor the behavior of banks and slopes, as instabilities can occur, sometimes without any direct connection to activity at the reservoir. For example, upstream of the Mauvoisin dam, a crack was observed in a mountain road running alongside the reservoir. Snowmelt had saturated scree in the area, which had slipped in sections of differing depths. A monitoring system (geodetic measurements, inclinometric measurements from boreholes) was set up, and a limited water level was set while the zone was still unstable. Similarly, experts inspected several glaciers in order to ensure that large sections of material did

not break off and end up in the reservoir. With progressing climate change, it has to be expected that the risk of instabilities of reservoir bank and slopes will increase.

4.2 *Sedimentation*

Due to climate change and its consequences (glacier retreat, the zero-degree line and permafrost levels rising in altitude, increased precipitation), an increase in the arrival of solid materials into alpine lakes must be expected. Solid materials issuing from soil erosion are transported toward water reservoirs in watercourses by bed load or suspended load. Whether this material settles in a particular place or spreads out into the reservoir depends on its size. This deposited sediment has a direct impact on the operation of the overall storage scheme, as well as on the safety of the dam. With regard to operation, this will above all be manifested in a loss of usable storage capacity. According to estimations, at a global level this reservoir volume loss is between 1 and 2% per year. Based on an analysis of 19 reservoirs (Beyer, Portner, and Schleiss, 2000), it is in the order of 0.2% for alpine storage schemes in Switzerland. The siltation of reservoirs can affect the lifetime of a dam. With regard to safety issues, there is a considerable risk of water intakes and bottom outlets in particular being obstructed. These situations must be avoided. For bottom outlets to remain operational at all times, a free space directly upstream of the discharge system must be guaranteed. For various reasons, it is vital that an appropriate amount of this deposited sediment be periodically removed. Several means for limiting the arrival of sediment into reservoirs already exist (settling basins, diversion galleries, sand traps, etc.). Sediment by-pass tunnels are successfully in operation at several dams (Palagnedra, Pfaffensprung, Rempfen, Runcahez, Solis) with more than 100 years of experience at Pfaffensprung dam (Boes, 2015). In many cases (Gebidem, Rempfen, Palagnedra, Luzzone, etc.), a program of periodic flushing takes place in accordance with a predefined schedule. The legal basis regarding the protection of water establishes the terms relative to the flushing and emptying of reservoirs.

Specifically, it is important to ensure that as far as is possible flora and fauna in the river downstream are not harmed during these operations. Furthermore, except in extraordinary events, permits are issued by the relevant cantonal authorities, some of which have established regulatory requirements. In the future, designers and operators will be required to take effective measures for preventing reservoir sedimentation. In alpine reservoirs, turbidity currents that form during floods are responsible for the transportation of considerable amounts of fine particles of sediment along the reservoir. Turbidity currents, which are like underwater avalanches, also erode sediment that has already been deposited, bringing it nearer to the dam itself where it is more likely to block the entrance to bottom outlets or water intakes (Schleiss and Oehy, 2002; Oehy and Schleiss, 2003). The increase in reservoir sedimentation can force operators to undertake substantial work in order for these structures to retain their primary functions. For example, at the Mauvoisin dam, the water intake had to be raised by 38 m and the bottom outlet by 36 m by building new intakes and gate chambers. Many other cases also exist.

Fine sediment, principally transported along the bottom of the reservoir by turbidity currents, can contribute to more than 80% of sedimentation in alpine reservoirs. In addition to controlling turbidity currents in reservoirs through the use of obstacles (Oehy and Schleiss, 2003), the deposit of fine material in the vicinity of the dam can be avoided by venting it through bottom outlets. This approach is economically and environmentally beneficial. Artificial flood releases combined with sediment replenishment downstream of dams can work together with this venting of fine sediment and restore, as well as dynamize, bedload transport in the river downstream (Döring et al., 2018). Another promising option for the management of fine sediment is by using water jet installations in the reservoir near the dam to ensure its suspension before evacuating it at controlled concentrations through the powerhouse intake (Jenzer, Althaus et al., 2011).

5 BRIEF REMINDER OF THE LEGAL BASES

As regards the safety of dams, the Swiss supervisory authority has two goals. Firstly, that of ensuring the safety of the dam and therefore that of the population, and secondly, of ensuring

the safety of the operation itself. From a historical point of view, the June 22, 1877 Water Regulation Act amended in 1950 outlines the provisions relating to dam safety. It stipulates in one of its primary articles that concerning dams the Federal Council must take all necessary measures to prevent, insofar as is possible, any danger and damage that may result from their means of construction, their inadequate maintenance, or from acts of war. Currently, the legislative basis includes an act on dams (WRFA, 2010) in effect since 2013, accompanied by an ordinance (WRFO, 2012). In addition to the terms relating to their safety, the act introduces the notion of civil liability due to the risks.

In terms of scope, the act (WRFA, 2010) specifies that the liability applies:

- To dams whose water level H above the low-water level of the watercourse or the thalweg (reservoir height) is at least 10 m, or
- If this water level is at least 5 m, for those whose reservoir capacity is higher than $50,000 \text{ m}^3$
- To dams of smaller dimensions, if they represent a specific potential risk for people and property; otherwise they are exempt.

6 MEASURES TO GUARANTEE PUBLIC SAFETY

Following the bombing of German gravity dams located in the Ruhr valley by the English air force during the nights of May 16 and 17, 1943, Swiss military and civil authorities were concerned about the vulnerability of dams to acts of war or sabotage. An initial measure introduced in June 1943 was to suspend a cable above dams as a means of protection against airplanes. In September 1943 the Federal Council, who had worked quickly on the legislation, announced an ordinance whose provisions covered active and passive dam protection measures against destruction in times of war, the use of reservoirs, and the lowering of their level, as well as the installation of an alarm system. It was decided that sirens would initially be installed in the near zone—the area subject to flooding 20 minutes after destruction of the dam. A list of dams that had to be equipped with the alarm system was published in late November 1943.

In 1945 the Bannalp (NW/1937/H = 32 m) and Klöntal (GL/1910/H = 30 m) embankment dams were the first to be fitted with the flood wave alert system. The regulation concerning dams that came into effect in July 1957 gave a legal basis to the recommendation that alarm systems should be installed. However, this system still needed to be improved, and a technical committee was mandated to establish the terms of reference for a new system. A more concrete definition of the flood wave alert system was introduced in the 1957 version of the regulation concerning dams. For the first time, the near zone identified was extended to 2 hours and a far zone was designated. The alarm systems for each zone are different. In addition, it was decided that the flood alert system would also be used in peace time and extended to all other possible hazards to dam safety. The introduction of degrees of preparation and the definition of criteria for the triggering of the flood alert system were also new elements.

7 LOOKING TO THE FUTURE

The saga of the construction of large dams in Switzerland is now practically over, as the technically most interesting sites are mostly exploited. The most recent major dam project in Switzerland was the heightening between 1995 and 1997 of the Luzzzone arch dam, built in the early 1960s and whose height was increased from 208 to 225 m. Another large-scale project concerning the raising of the Grimsel reservoir level by 23 m (Spitallamm and Seeuferegg dams) is under study and should come to fruition.

In order to support the energy transition defined by the 2050 energy strategy, the Swiss government organized a round table in 2021, including civil society, to define projects with the objective of ensuring the security of energy supply in winter while preserving biodiversity and the landscape. With the aim of increasing the flexible production of storage facilities in winter

by at least 2000 GWh until 2040, the participants agreed on a list of 15 priority projects. This list includes three new dams in valleys freed up by the retreat of the glaciers (Figure 11), e.g. the future Trift dam, and the rest are extensions of existing facilities, including dam heightening.



Figure 11. Photomontage of the future 180 m high Trift dam, which uses the already freed valley by glacier retreat. Above: with empty lake with glacier position today. Below: with full lake (Curtesy KWO).

These last examples show that the field of dams remains attractive for designers, builders and operators. Indeed, by the diversity of its assignments, it offers interesting perspectives not only for projects of transformation or modernization of existing works, but also for new projects. It is also a question of ensuring the good health of the existing works.

With the aging of structures and equipment, some problems must be examined, such as the evolution of mass concretes (long-term creep, alkali-aggregate reaction) or the behavior of foundations (development of under-pressures, preservation of networks of drainage).

In the short term, the monitoring and maintenance of dams of all sizes remain essential tasks in order to guarantee their safety. While the organization of these activities for large and medium structures has been in place for many decades, that of small structures still needs to be regulated. With regard to hydroelectric developments, the future of hydraulic power is part of the framework of sustainable development. Several socio-economic and ecological parameters will influence operators in their future investments, namely the opening of the market, the evolution of supply and demand, electricity prices and construction costs, hydraulic royalties and politics.

First of all, many concessions are coming to an end. When renewing them, assessing the safety of structures that are sometimes dilapidated is a necessary phase which in most cases leads to having to consider major reinforcement and rehabilitation work, or even the replacement of the electromechanical equipment of the landfill structures. Other measures can be taken before this deadline to proceed with the modernization and optimization of existing installations. The idea of raising a dam to increase the capacity of its accumulation basin is a realistic option. Pumped storage projects are back in the news. They have the advantages of storing hydraulic energy and recovering the basic energy of non-adjustable power stations

(thermal, solar, wind) produced outside consumption hours. Some thirty potential sites were assessed during the 1970s. Today, efforts are being made to combine this type of structure with existing storage facilities by equipping them with new water supply systems and increasing the retention capacity. For example, the Nant de Drance pumped storage project, which operation started in 2022, uses the difference in level between the Emosson (VS / 1974/H = 180 m) and Vieux Emosson (VS / 1974/2017/H = 76.5 m) reservoirs.

Although the majority of reservoirs were created with a view to producing hydraulic energy, the construction of water storage basins for the production of artificial snow developed strongly towards the end of the 1990s. These structures are generally located outside the river, on a flat area or on the side of a hill; much of the artificial basin can be made by excavation. Given the local conditions and the availability of materials, the use of an embankment dam is frequent. There is no doubt that ski lift operators will still continue to use this means to guarantee the snow cover of the slopes as well as possible. Finally, hydraulic development can also promote the creation of biotopes and recreational areas.

Every year natural disasters (floods, avalanches, debris flows) cause substantial damage and result in considerable costs. The increased need for safety will lead to the design and construction of new protection systems including flood retention works and anti-avalanche dikes. Some protective measures will be revisited, improved, or completed. In Switzerland, reservoirs for existing hydroelectric schemes are generally speaking single-purpose reservoirs. They can be converted into multipurpose reservoirs by setting aside a clearly specified storage volume for retaining water during floods. This solution has already been implemented in certain cases and others may well follow. Various solutions are possible for maintaining the available capacity of reservoirs when necessary, including dam heightening, creating a supplementary connected reservoir, or by adding a seasonal pumped-storage system. It is possible to refer to a flood forecasting model so as to better manage reservoirs. The canton of Valais has taken this approach and developed the Minerve project, which simulates the overall hydraulic behavior of catchment areas and hydropower schemes in Valais. The model is designed to help cantonal officials make decisions (Garcia Hernandez et al., 2011, 2014; Jordan et al., 2008; Raboud et al., 2001).

Ongoing research and development over many years has led to technological advances. Various problems have been tackled such as safety under dynamic loading during earthquakes, extreme flood events, the long-term behavior of dams, and the behavior of foundations. Of course, these issues have not yet been fully resolved. Problems related to safety and the overall behavior of dams continue to occupy researchers in such domains as the behavior of overtopped dams, the long-term behavior of facing and drainage, and reservoir sedimentation. The development of data collection and methods for analysis and data measurement continue to be used in the monitoring of dams. And finally, new and increasingly applied construction methods, such as roller compacted concrete (RCC) and cemented soils, are the focus of specific studies. Swiss expertise in the field of dams is recognized internationally and can thus be employed elsewhere in the world. Global demand for the construction of hydraulic schemes and dams in particular is high and will continue to grow. Logically, the strategy which should be implemented is one that looks outward (Schleiss, 1999). Swiss industry and engineering are capable of achieving this vision thanks to more than one hundred years of experience in hydraulic construction and the international renown garnered since the 1960s by the construction of over 180 large dams outside of Switzerland.

ABBREVIATIONS OF SWISS CANTONS

ZH Zurich, GL Glarus, AR Appenzel Outer-Rhodes, VD Vaud, BE Bern, ZG Zug, AI Appenzel Inner-Rhodes, VS Valais, LU Lucerne, FR Fribourg, SG St. Gallen, NE Neuchâtel, UR Uri, SO Solothurn, GR Grisons, GE Geneva, SZ Schwyz, BS Basel, AG Aargau, JU Jura, OW Obwalden, BL Basel District, TG Thurgau, NW Nidwalden, SH Schaffhausen, TI Ticino.

ACKNOWLEDGEMENT

This contribution is essentially based on Chapter 2.2 and 2.3.2 of the book *Design, Safety and Operation of Dams* by Schleiss A. et Pougatsch H., 2022, EPFL Press, Presse polytechnique et universitaire romande. <https://www.epflpress.org/produit/1407/9782889154852/design-safety-and-operation-of-dams>.

Most of the dam pictures have been published in the calendars “Dams in Switzerland” issued yearly since 2005 by the Swiss Committee on Dams.

REFERENCES

- Beyer Portner N., Schleiss A., 2000. Bodenerosion in alpinen Einzugsgebieten in der Schweiz. *Wasserwirtschaft* 90(2),88–92.
- R. M. Boes (ed.), 2015. Proc. 1st Int. Workshop on Sediment Bypass Tunnels Zurich. VAW Mitteilung 232, Versuchsanstalt für Wasserbau, Hydrologie und Glaziologie, ETH Zurich, Zürich, 258 pages.
- Döring M., Tonolla D., Robinson CH. T., Schleiss A., Stähly S., Gufler CH., Geilhausen M. et Di Cugno N., 2018. Künstliches Hochwasser an der Saane – Eine Massnahme zum nachhaltigen Auenmanagement. *wasser, energie, luft – eau, énergie, air*, 110. Jahrgang, Heft 2, 119–127.
- García Hernández J., Schleiss A. J. et Boillat J.-L., 2011. Decision Support System for the hydropower plants management: the MINERVE project. *Dams and Reservoirs under Changing Challenges – Schleiss & Boes (Eds)*, Taylor & Francis Group, London, 459–468. ISBN 978-0-415-68267-1.
- García Hernández J., Claude A., Paredes Arquiola J., Roquier B. et Boillat J.-L., 2014. Integrated flood forecasting and management system in a complex catchment area in the Alps – Implementation of the MINERVE project in the Canton of Valais. *Swiss Competences in River Engineering and Restoration*, Schleiss, Speerli & Pfammatter Eds, 87–97. Taylor & Francis Group, London, ISBN 978-1-138-02676-6, doi:10.1201/b17134-12.
- Jenzer Althaus J., De Cesare G. et Schleiss A. J., 2011. Entlandung von Stauseen über Triebwasserfassungen durch Aufwirbeln der Feinsedimente mit Wasserstrahlen. *wasser, energie, luft – eau, énergie, air*, 103. Jahrgang, Heft 2, 105–112.
- Jordan F., García Hernández J., Dubois J. et Boillat J.-L., 2008. Minerve – Modélisation des intempéries de nature extrême du Rhône valaisan et de leurs effets. Communication n° 38 du Laboratoire de constructions hydrauliques, LCH-EPFL, Ed. A. Schleiss, Lausanne.
- Oehy Ch. et Schleiss A., 2003. Beherrschung von Trübeströmen in Stauseen mit Hindernissen, Gitter, Wasserstrahl- und Luftblasenschleier. *wasser, energie, luft – eau, énergie, air*, 95. Jahrgang, Heft 5/6, 143–152.
- Raboud P.-B., Dubois J., Boillat J.-L., Costa S. et Pitteloud P.-Y., 2001. Projet Minerve – Modélisation de la contribution des bassins d’accumulation lors des crues en Valais. *wasser, energie, luft – eau, énergie, air*, 93e année, cahiers 11/12, 313–317.
- SwissCoD, 2017a. Swiss Committee on Dams, Floating debris at reservoir dam spillways. Report of the Swiss Committee on Dams on the state of floating debris issues at dam spillways. Working group on floating debris at dam spillways, November 2017.
- SwissCoD, 2017b. Swiss Committee on Dams, Concrete swelling of dams in Switzerland. Report of the Swiss Committee on Dams on the state of concrete swelling in Swiss Dams. AAR Working Group. May 2017.
- Schleiss A. et Oehy Ch., 2002. Verlandung von Stauseen und Nachhaltigkeit. *wasser, energie, luft – eau, énergie, air*, 94. Jahrgang, Heft 7/8, 227–234.
- Schleiss A., 1999. Constructions hydrauliques. Facteur clé de la prospérité économique et du développement durable au XXIe siècle, IAS n° 11, 9 juin 1999, 198–205.
- Schnitter, N.J., 1985. Le développement de la technique des barrages en Suisse. Comité national suisse des grands barrages, Barrages suisses – Surveillance et entretien, publié à l’occasion du 15e Congrès international des grands barrages, Lausanne 1985, 11–23.
- Sinniger, R., 1985. L’histoire des barrages. EP FL, Polyrama, 1985, 2–5.
- WRFA, 2010. Water Retaining Federal Act (in French, German, Italian). RS 721.101 of 1st October 2010 (State in 1st January 2013).
- WRFO, 1998. Water retaining Federal Ordinance (in French, German, Italian). December 7, 1998.
- WRFO, 2012. Water retaining Federal Ordinance (in French, German, Italian). RS 721.101.1 of October 17, 2012 (state in 1st April 2018).

Outstanding past Swiss dam engineers

Willi H. Hager

VAW, ETH Zurich, Zürich, Switzerland

ABSTRACT: Switzerland is a country rich in waterpower, yet without hardly any other resources. The electricity production, therefore, was based on hydropower a long time ago. To store energy, dams are key structures for hydropower schemes. For both low and high head dams these were provided by keen engineers who oversaw the activities relating to dam construction. This paper highlights five selected engineers having significantly contributed to Swiss dam engineering. Of relevance is of course their role within the Swiss National Committee on Large Dams.

RÉSUMÉ: La Suisse est un pays riche en énergie hydraulique, mais sans pratiquement aucune autre ressource. La production d'électricité était donc basée sur l'énergie hydraulique il y a longtemps. Pour stocker l'énergie, les barrages sont des structures clés pour les projets hydro-électriques. Pour les barrages à basse et haute chute, ils ont été fournis par des ingénieurs passionnés qui ont supervisé les activités liées à la construction de barrages. Cet article met en lumière cinq ingénieurs sélectionnés qui ont contribué de manière significative à l'ingénierie des barrages suisses. Leur rôle au sein du Comité national suisse des grands barrages est bien sûr pertinent.

1 INTRODUCTION

Although hydropower remains the largest renewable electricity technology by capacity and generation, the current capacity growth trends are insufficient to place it on the trajectory under the Net Zero Scenario. Reaching about 5 700 TWh of annual electricity generation by 2030 will require a 3% average annual generation growth between 2021 and 2030, which appears additionally challenging when considering the accelerating disturbances to the water availability caused by the climate change and an ageing fleet of hydropower plants. On the capacity side, an average of 50 GW of new hydropower plants needs to be connected to the grid annually until 2030, which is more than twice the average of the past five years. Much greater efforts, especially in developing and emerging markets, will be globally required to achieve that pace of growth.

Thanks to its topography, geology and high levels of annual rainfall, Switzerland has ideal conditions for the utilization of hydropower. Starting in 1892 with the first plant for electricity generation installed in St. Moritz, hydropower underwent an initial period of expansion, and between 1945 and 1970 it experienced a genuine boom during which numerous new power plants and low-head dams were commissioned in the Swiss Plateau, together with large-scale storage plants and reservoir dams in the Alps.

Based on the estimated mean production level, hydropower still accounted for almost 90% of domestic electricity production in 1970, but this figure fell to around 60% by 1985 following the commissioning of Switzerland's nuclear power plants, and is now around 57%. Hydropower therefore remains Switzerland's most important domestic source of renewable energy.

Today there are nearly 700 hydropower plants in Switzerland having a capacity of at least 300 kW, producing an average of around 37,260 GWh/y, 48% of which is supplied both by run-of-river power plants, and by storage power plants, whereas 4% by pumped storage power plants (from natural inflow only). 63% of hydroelectricity are generated in the

mountain cantons of Uri, Grisons, Ticino, and Valais, while Aargau and Bern also generate significant quantities. 11% of Switzerland's hydropower generation comes from facilities located on water bodies along the country's borders. The hydropower market is worth around 1,8 billion Swiss francs and is therefore an important segment of Switzerland's energy industry (Bundesamt für Energie 2021). Figure 1 shows a top view of the beautiful Hongrin Dam and its Veytaux emergence structure located on the shores of Lake Geneva.



Figure 1. (up) Hongrin Dam in Canton of Vaud, (down) Veytaux I emergency outlet into Lake Geneva
<https://www.alpiq.ch/energieerzeugung/wasserkraftwerke/pumpspeicherkraftwerke/hongrin-leman>;
<https://www.raonline.ch/pages/edu/nw3/power01a4a7.html>.

This paper deals with engineers at the heart of the early dam engineering knowhow in Switzerland. Five selected portraits are provided who mostly have a close relation to the Swiss National Committee on Large Dams. In addition to the main projects realized, their input to the Swiss engineering organizations is provided, and their roles as technical and human leaders is highlighted.

2 THE SWISS COMMITTEE ON DAMS

The Swiss National Committee on Large Dams (SNCOLD) is a private association representing the Swiss dam community within the International Commission on Large Dams (ICOLD). The committee's objective is to promote construction, operation, maintenance and monitoring of hydraulic structures and their environment. To achieve this goal, it unites specialists from various branches of dam technology offering them a platform to discuss experiences, publish technical papers and organize symposia and workshops related to dam engineering.

Based on a loose union of five Swiss dam engineers, the Swiss Dam Commission was established in 1928. On December 20, 1948, Henri Gicot chaired the founding assembly of the SNCOLD. It comprised 68 members, many of them from industry and

electric utilities. During the 1950s, important dams were built, among which Grande Dixence (PG), Mauvoisin (VA), Moiry (VA), Göschenalp (ER), Valle di Lei (VA), Albigna (PG), Luzzone (VA) or Malvaglia (VA). Typical topics of discussion were then the vulnerability under military attacks or frost resistance of mass concrete.

Switzerland counts some 1200 dams, of which most are small, however. About 225 dams are under the direct supervision of the Swiss Federal Office of Energy in view of their dimensions and the potential dangers they may include. 162 dams meet the criteria for large dams established by the International Commission on Large Dams (ICOLD).

Based on the number of dams under federal supervision, the dam density in Switzerland is more than 5 dams per 1000 km². Most of these dams are key elements of major hydropower schemes. 80% of the dams are in mountainous regions. The construction of the schemes was vital for the development of these economically less favorable areas.

Dam construction in Switzerland has a long tradition. The oldest dam under federal supervision is the 15 m high Wenigerweiher embankment in the city of St Gallen. It was constructed in 1822 for the energy supply of nearby industry and currently is still impounded and in use, serving ecological purposes nowadays by creating an amphibian spawning area of national importance. Most of the dams taken into service in the 19th century were located close to cities because it was either prior to the invention of electricity or then difficult to transfer electricity over long distances. An example is the Maigrauge Dam, a roughly 20 m high gravity dam built in 1872 on the Sarine River slightly upstream of Fribourg city. The dam is currently also still in operation for hydropower use and has greatly contributed to the economic development and the prosperity of the city.

The first dams in the Alps were built starting from 1900. This includes the 112 m high Schräh Dam commissioned in 1924, then being the highest dam worldwide. The real start of Swiss dam development initiated after WWII, however. 86 large dams were commissioned between 1947 and 1970, four of which being higher than 200 m:

- Mauvoisin Arch Dam (1957), 237 m high, raised to 250 m in 1990;
- Grand Dixence Dam (1961), 285 m high, still the highest gravity dam worldwide;
- Luzzone Arch Dam (1963), 208 m high, raised to 225 m in 1998;
- Contra Arch Dam (1965), 220 m high.

The large Swiss dams are mainly concrete structures; only the Göschenalp Dam (155 m) and the Mattmark Dam (117 m) are rockfill dams higher than 100 m, followed by the 91 m high Marmorera earthfill dam.

Some 90% of the technically feasible hydropower potential is currently in operation. The remaining 10% is difficult to achieve for economic reasons and because of increased conflicts of interests. One of the major challenges of current dam engineering in Switzerland is to cope with aging of the large fleet of existing dams at the highest level of safety. The Swiss Committee on Dams (2011) portrays the main Swiss dams including the name, the owner, the dam purpose, the type of foundation, various technical data, a short history, and further technical specifications of interest. Each dam is also described with a plan view and a cross-section, plus its location in Switzerland, and a full-page photo.

The main purpose of this paper is the presentation of five outstanding past Swiss dam engineers, who have greatly contributed to the technical development of Swiss dams and its electricity potential. These personalities include:

- Guillaume Ritter, hydraulic engineer and designer of the first concrete dam in Europe at Maigrauge on the Sarine River
- Heinrich Eduard Gruner as a pioneer in dam engineering, realizing together with Alfred Stucky the Montsalvens Dam as the first arch dam of Europe
- Alfred Stucky, professor of hydraulic engineering at the Ecole Polytechnique Universitaire de Lausanne (EPUL) and founder of its hydraulic laboratory, with publications for the design of dams
- Henri Gicot, designer of many arch dams and the first dams with either parabolic or elliptic arches

- Giovanni Lombardi introducing the Lombardi slenderness coefficient characterizing an arch dam, and criteria for dam cracking.

3 PORTRAITS OF SWISS DAM ENGINEERS

3.1 *Guillaume Ritter*

Ritter was born in Neuchâtel in 1835 to Alsatian parents; he died in Monruz near Neuchâtel in 1912 (Anonymous 1913; Walter, 1977; Vischer 2001). After basic schooling in Neuchâtel, he entered *Ecole Centrale des Arts et Manufactures* in Paris, graduating in 1856 with a diploma as *Ingénieur constructeur* (civil engineer). Subsequently, he devoted himself in Neuchâtel specifically to projects of urban water supply and industrial hydropower. One of the extraordinary projects dealt in 1872 with the hydroelectric power plant on Sarine River near Maigrauge (German: Magerau).

Ritter was considered an enthusiastic and inspiring innovator. The plant near Maigrauge was the second major Swiss power plant after that on the Rhine in Schaffhausen. It supplied Fribourg with a network of rope transmissions and a pressurized water network. Electrification did not take place until 1891-1895. With a height of 21 m, a crown length of 195 m and a dam capacity of 1 million m³, the Sarine Dam was a novelty in Switzerland. Ritter was the first in Europe to use concrete as a building material, after it had been used for the first time for American dams just a few years earlier. His financially and technically most complex proposal did not get beyond the planning and acquisition stage. It was the water supply of Paris from Lake Neuchâtel, involving a 37 km base tunnel under the Swiss Jura and a 470 km long pipeline. Ritter expected construction to begin in 1900, the need of 400 million Swiss francs in investment costs by financing until the year 2000.



3.2 *Heinrich Eduard Gruner*

He was born in 1873 in Basel, passing away there in 1947. His family was a true engineering household. He obtained the civil engineering diploma from ETH Zurich, undertook then study tours to Saxony, England, and the USA, starting his engineering career in 1914 at his father's office. His first project involved the Laufenburg Power Plant on the Rhine River upstream of Basel, where he headed the local works. He there collected his first practical experiences, applying these later to similar projects including the Eglisau and the Ryburg-Schwörstadt low-head dams, both also located on the Rhine River (Hager 2003).

He and his collaborator Alfred Stucky designed around 1920 the first Swiss arch dam at Montsalvens in Canton Fribourg, of 55 m height. Gruner also realized the importance of the scientific hydraulic modelling, being one of the financial supporters of the ETH Hydraulic Laboratory taken into service in 1930 under its director Prof. Eugen Meyer-Peter (Hager et al. 2021). Later, Gruner's main activities were in Iran, improving there the irrigation techniques, and in Egypt as a member of the Commission for the second Aswan Dam. He was in addition

the first Swiss delegate of ICOLD. Gruner was awarded the honorary doctorate from ETH Zurich in 1930, and was since 1925 a member of the American Society of Civil Engineers (ASCE). Mommsen (1962) gives a detailed and historically interesting account of the Gruner engineering family.



3.3 Alfred Stucky

He was born in 1892 in La Chaux-de-Fonds (NE) and passed away in Lausanne (VD) in 1969. Stucky was a true expert in hydraulic engineering during the golden age of hydropower. After having graduated at ETH Zurich in 1915, he joined the engineering office of Gruner in Basel. In parallel, he submitted to ETH Zurich in 1920 a PhD thesis on arch dams. He was appointed hydraulic engineering professor at EPUL in 1926. He founded the EPUL Hydraulic Laboratory in 1928 and initiated his private engineering office in parallel to his commitment at EPUL. Stucky further acted as EPUL president from 1940 to 1963, when retiring from EPUL and concentrating on consulting work until his passing (Hager 2003).

Stucky's career was threefold as hydraulic engineer, researcher in dam engineering and as the organizer of the engineering school. Based on his PhD, he initiated the design of arch dams in Switzerland. He was an expert of the Italian Gleno Dam disaster of 1923 (Stucky 1924). Stucky also investigated sea wave forces on vertical walls in his laboratory, based on his international expertise. In 1936, his interest into surge tanks started, culminating in a text book (Stucky 1962).



He was in addition largely involved in the Grande Dixence Dam, currently still the largest gravity dam worldwide. He also was for 20 years president of the technical journal *Bulletin Technique de la Suisse Romande*. He was awarded the honorary doctorate degree from ETH Zurich in 1955, among many other distinctions for his outstanding engineering career.

3.4 Henri Gicot

He was born in 1897 in Le Landeron (NE) passing away in 1982 in Fribourg. After having completed his civil engineering studies at ETH Zurich in 1919, he joined as previously did

Stucky the engineering office Gruner in Basel. From 1927 to 1971, he owned his engineering office in Fribourg. In addition, Gicot was the president of the SNCOLD from 1948 to 1961, and from 1953 to 1967 a member of the ETH Board. He was in addition an expert of the World Bank active in Asia and South America.

Gicot became internationally known as a dam engineer for the Rossens Dam built on Sarine River from 1944 to 1948. He was in addition also responsible for the Montsalvens Dam close to Broc (FR) built on the Sarine River from 1919 to 1921, the Gebidem Dam below the Aletsch Glacier from 1949 to 1950, the Delcommune Dam in the Belgian Congo from 1950 to 1952, the Vieux Emosson Dam from 1954 to 1955, Zeuzier Dam from 1955 to 1957, Schiffenen Dam from 1960 to 1964, and the beautiful Hongrin Dam built from 1964 to 1968 (Figure 1). He was awarded the honorary doctorate degrees from the University of Fribourg in 1962, and of ETH Zurich in 1968 (Schnitter 1982).



3.5 *Giovanni Lombardi*

He was born in 1926 in Lugano (TI), passing away in 2017 in Monte Carlo, Monaco. Lombardi was an internationally renowned civil engineer who was an outstanding expert in tunnel and dam projects. He graduated in 1948 from ETH Zurich as a civil engineer obtaining in 1952 the PhD title with a work on slender arch dams. He founded in 1955 with G. Gellera the engineering office Giovanni Lombardi PhD Consulting Engineers in Lugano, from 1989 a stock corporation and renamed in Lombardi AG Consulting Engineers in Minusio (TI).

His firm's projects included numerous tunnels, such as the Gotthard Road tunnel or the Gotthard Base Tunnel. Other projects were dams in the Verzasca Valley in 1965, also known as Contra Dam, and in the Valle Morobbia (Lago di Carmenta), dams in Austria (Kops, Kölnbrein), Italy (Ridracoli Dam in Emilia-Romagna, Flumendosa Dam in Sardinia) or in Mexico (210 m high Zimapan Dam). He was a member of the commission to investigate the subsidence that occurred in 1978 at Zeusier Dam, caused by the neighboring construction of an exploratory tunnel for a road tunnel in which water ingress occurred, draining the groundwater in the surroundings. From 1979 to 1985 he was president of the Swiss Committee on Dams. He was the first Swiss president of ICOLD from 1985 to 1988. In 2008 he received the Swiss Award, a prize for outstanding Swiss personalities. He holds honorary doctorates from EPFL (1986) and the *Politecnico di Milano* (2004).



4 CONCLUSIONS AND OUTLOOK

Switzerland's history of modern reservoir dams is 200 years old. Starting from small embankments, mainly low-head hydropower dams along rivers were erected in the 19th century. These were located close to industries because the transmission of electricity remained a problem until the end of the century. Switzerland, a country without notable treasures of the soil, had to concentrate early on energy obtained from hydropower. As an example, most trains were driven from WWI with electricity, or the so-called white coal, given the absence of conventional black coal. The large dams were erected after WWII, with dams reaching nearly a height of 300 m. This intense phase of dam construction activity came to its end around 1970, given that most of the favorable dam sites had been used.

Switzerland had and still has many outstanding dam engineers, who explored the possibilities to construct appropriate dam structures to supply electricity and protect against floods. While the focus was on Switzerland until the 1980s, it has since then shifted to dam engineering worldwide (Droz 2023), enlarging the scope of the dam purposes also to irrigation and water supply. Still today, some 50% of the electricity consumed in Switzerland originates from hydropower. The present paper presents five selected individuals having greatly contributed to Swiss dam engineering. They represent all major parts of the country and have been active both in their homeland and internationally. A short review of their education is provided, along with the main projects of their professional activity. In addition, important other occupations are presented, such as in national or international committees, particularly within the Swiss National Committee on Large Dams, who has reached its 75th anniversary. It is also noted that the Swiss dam engineering will have an active role in the future, given its relevance for water resources management and society, not least in view of climate change adaptation and new demand for multipurpose reservoirs (Boes & Balestra 2023).

ACKNOWLEDGEMENT

The author would like to acknowledge the interest of his colleague Prof. Dr. Robert M. Boes, Director VAW, in the present work, by adding suitable comments.

REFERENCES

- Anonymous. 1913. Guillaume Ritter. *Verhandlungen der schweizerischen naturforschenden Gesellschaft*, 96: 28–33 (in French).
- Boes, R.M., Balestra, A. 2023. Dams in Switzerland. Proc. ICOLD European Club Symposium *Role of dams and reservoirs in a successful energy transition* (Boes, R.M., Droz, P. & Leroy, R., eds.). Taylor & Francis, London.
- Bundesamt für Energie 2021. *Wasserkraft Schweiz: Statistik 2021* <https://www.bfe.admin.ch/bfe/de/home/news-und-medien/medienmitteilungen/mm-test.msg-id-88652.html>.
- Droz, P. 2023. Swiss dam engineering in the world. Proc. ICOLD European Club Symposium “Role of dams and reservoirs in a successful energy transition” (Boes, R.M., Droz, P. & Leroy, R., eds.), Taylor & Francis, London.
- Hager, W.H. 2003. *Hydraulicians in Europe 1800-2000*. IAHR: Delft, the Netherlands.
- Hager, W.H., Schleiss, A.J., Boes, R.M. & Pfister, M. 2021. *Hydraulic engineering of dams*. CRC-Press, Taylor & Francis Group: Boca Raton, London, New York.
- Mommsen, K. 1962. *Drei Generationen Bauingenieure* (The generations of civil engineers). Schwabe: Basel (in German).
- Schnitter, G. 1982. Henri Gicot. *Wasser, Energie, Luft*, 74(9): 255 (in German).
- Stucky, A. 1924. La rupture du barrage du Gleno (Dam break of Gleno Dam). *Bulletin Technique de la Suisse Romande*, 50(6): 65–71; 50(7): 79-82; 50(9): 107-108 (in French).
- Stucky, A. 1962. *Druckwasserschlässer von Wasserkraftanlagen* (Surge tanks of hydropower plants). Springer: Berlin (in German).
- Swiss Committee on Dams 2011. *Dams in Switzerland: Source for worldwide Swiss dam engineering*. Buag: Baden-Dättwil (in German).
- Walter, F. 1977. Ritter Guillaume. *Encyclopédie du Canton de Fribourg*, 2, 497. Office du livre: Fribourg (in French).
- Vischer, D.L. 2001. *Wasserbauer und Hydrauliker der Schweiz* (Swiss hydraulic engineers and hydraulicians). Verbandsschrift 63. Schweizerischer Wasserwirtschaftsverband, Baden (in German).

Water resources optimisation – A Swiss experience

R. Leroy

Alpiq SA; Swisscod - Swiss Committee on dams

ABSTRACT: Historically, during the 20th century and up to the present day, water management has evolved significantly. During this period, much progress has been made for better understanding the importance of water as a vital resource and in implementing appropriate measures for its management and arbitration. During the 20th century, hydraulic infrastructures such as dams and reservoirs were built to store and distribute water more efficiently. Climate change and overexploitation of resources make water management an increasingly complex issue.

RÉSUMÉ: Depuis toujours, durant le 20e siècle et jusqu'à nos jours, la gestion de l'eau a évolué de manière significative. Au cours de ces périodes, de nombreux progrès ont été réalisés dans la compréhension de l'importance de l'eau en tant que ressource précieuse et dans la mise en place de mesures pour sa gestion et son arbitrage. Au cours du 20e siècle, des infrastructures hydrauliques, telles que les barrages, les réservoirs ont été construites pour stocker et distribuer l'eau de manière plus efficace. Les changements climatiques et la surexploitation des ressources font de la gestion de l'eau un enjeu toujours plus complexe.

1 INTRODUCTION

Switzerland, a country of mountains, streams, rivers and lakes, possesses the most beautiful, the most priceless of all riches: blue gold! A precious reserve of life and energy in the heart of Europe. Due to its altitude and the Alpine foothills, more than two thirds of the precipitations are retained in winter in solid form. In spring and summer, snow and ice turn into liquid. From time immemorial, man has tried to tame these streams of life. He has fought against water and its overflow. Above all, he has fought for water and its benefits. The history of the Alpine cantons bears witness to these struggles. It is the patient work of damming up the rivers, the extraordinary network of irrigation systems and bisses and the mastery of this energy.

Water management is an important issue. While ensuring long-term sustainability, an integrated approach allows for equitable management and sharing of water resources between competing uses such as hydropower generation, irrigation, flood protection, drinking water supply and protection of aquatic ecosystems.

The last century was the epic of dam construction. The titanic struggle in the heart of the mountains to capture and store the most incredible energy: hydroelectricity. A clean, renewable, ecological energy. The production of hydroelectric energy in Switzerland is very important, as it represents nearly 60% of the country's electricity production. Storage dams are one of the key facilities, as they allow water to be stored for later use, whether for hydroelectric production, to support low-water flows, or to regulate river flows. The large Swiss dams, such as the Maggia scheme, the Grimsel scheme, the Mattmark embankment dam, the Grande Dixence dam or the Emosson dam, are examples of dams that contribute and will continue to contribute significantly to electricity production in Switzerland.

At all times, when it has been a question in the past of catching and transferring water, today of making a better use of water in a difficult energy context, and tomorrow, considering the predicted climate changes and the necessary arbitration between the various stakeholders, resource management and optimisation have been, are and will be the challenges, both on the technical and societal aspects.

2 CASE STUDIES

Water...the original element without which no form of life is possible.
Water... Silent and calm, slumbering in the reservoirs.
Water... Wild and tumultuous, raging through the turbines.
Water... an inexhaustible source of energy

2.1 *Grande Dixence*

One of the most striking episodes in the conquest of this “white coal” is without doubt the construction of the Grande Dixence complex. This pharaonic construction site is a jewel of ingenuity and human courage to develop a unique glacial basin of 350 km².



Figure 1. Grande Dixence gravity dam.

Since the end of the Second World War, Switzerland has needed energy to meet the demands of its industrial development. In 1945, the Swiss Federal Water Board drew up a comprehensive inventory of the country’s hydroelectric potential. Analysing the possibilities in the Rhone basin, the experts came to the conclusion that there were still a number of valleys that could be exploited under economically attractive conditions. The Val des Dix soon emerged as the site with the greatest development potential. This high valley had the ideal geological and topographical conditions to become a giant reservoir. No human settlements were affected; the only agricultural land was highland pasture, and above all, the predicted storage capacity was enormous: 400 million m³.

Geologists, hydrologists, topographers and engineers set out to solve two major problems. On the one hand, to enlarge the existing lake with the Dixence complex built some fifteen years earlier. On the other hand, to create a catchment network capable of collecting water from the neighbouring valleys of Mattertal, Ferpècle and Arolla. More than three thousand men fought this battle until the beginning of the 1960s. A daring and avant-garde project which today contributes to the well-being of the community.

However, although the sight of this gravity dam, the highest in the world, is impressive, it is only the tip of the iceberg. The particularity of Grande Dixence scheme, and the genius of its

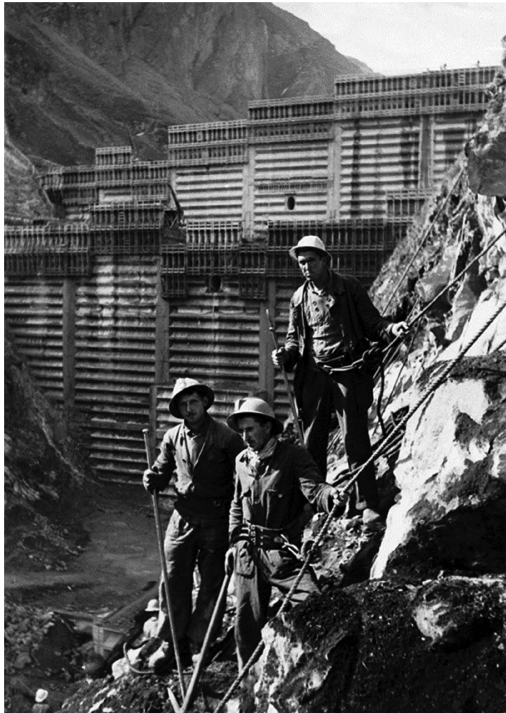


Figure 2. Grande Dixence dam under construction.



Figure 3. Grande Dixence dam under construction.

designers, is that it is able to collect the water from 35 glaciers, from the confines of the Zermatt valley to the Hérens valley. To bring all this water to the Val des Dix, men had to drill

the rock before excavating it to create the 75 water intakes and water transfer gallery network of around 100 kilometres with a gradient of 2 ‰ along its length. Some important glaciers such as Ferpècle, Arolla, Z'Mutt and Gorner are located lower than the level of the main collector at an altitude of 2 400 metres. Thus, 4 pumping stations are needed to transfer water in the main reservoir.

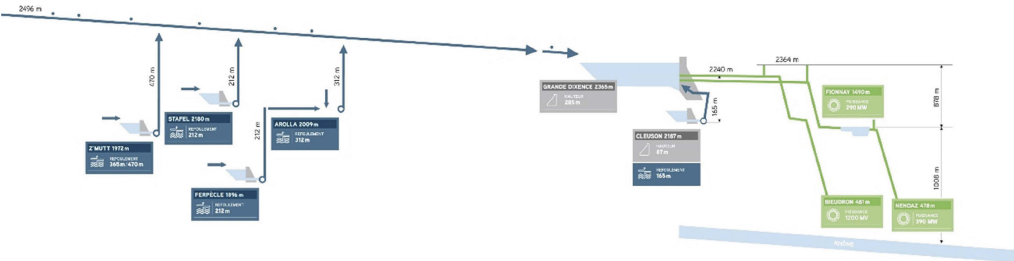


Figure 4. Grande Dixence scheme - longitudinal profile.

Collecting, pumping, and bringing the water from 35 glaciers to the Val des Dix, in order to use it for power generation, has been a difficult and hazardous task. In recognition of the commitment of previous generations, the real challenge is nowadays to carefully manage this source of energy and to fully exploit its value. It is a question of finding the best possible match between the constraints of the installation, the power demands, and the market prices. At first sight, the problem is simple: fill the Lac des Dix with as much water as possible during the limited period of glacial and snowmelt. But in reality, it is a headache: it is necessary to take into account the capacity of the water transfer galleries, but above all of the main collector, to integrate the variations in the flows of the water intakes, to monitor the meteorological forecasts and the forecasts of short, medium and long term power demand, to carry out the pumping of the water collected in the neighbouring valleys during the favourable hours, without forgetting to return large quantities of water for ecological, tourist and contractual reasons.

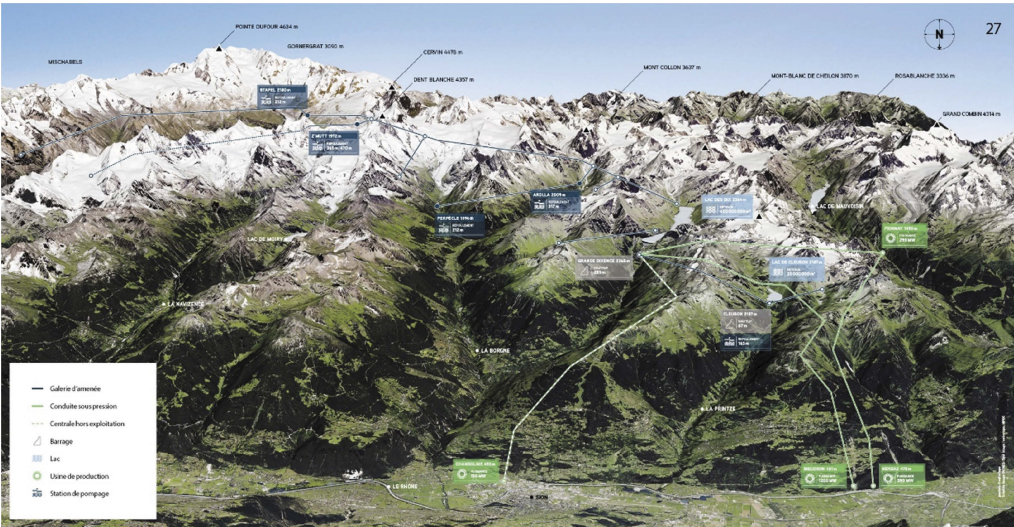


Figure 5. Grande Dixence scheme- 3D view.

The hydro-scheme is there to provide high quality energy to supply the market at peak times. The level of storage in the scheme must be optimised for maximum availability before periods of high demand. To achieve a satisfactory balance, the optimisation of the summer

pumped storage energy must be done in relation to the energy produced in the winter by integrating a multitude of parameters. All the data collected allows for optimised management of the inflows and outflows required to fill the reservoir. The challenge of this high-precision management is crucial: one million cubic metres of water lost represents more than four million kWh of energy in winter. The adaptability of the scheme and its development to the changing contexts is to be noted. The Cleuson-Dixence development with the Bieudron 1200 MW power station corresponds to a quest for power and stabilisation of the power grid.

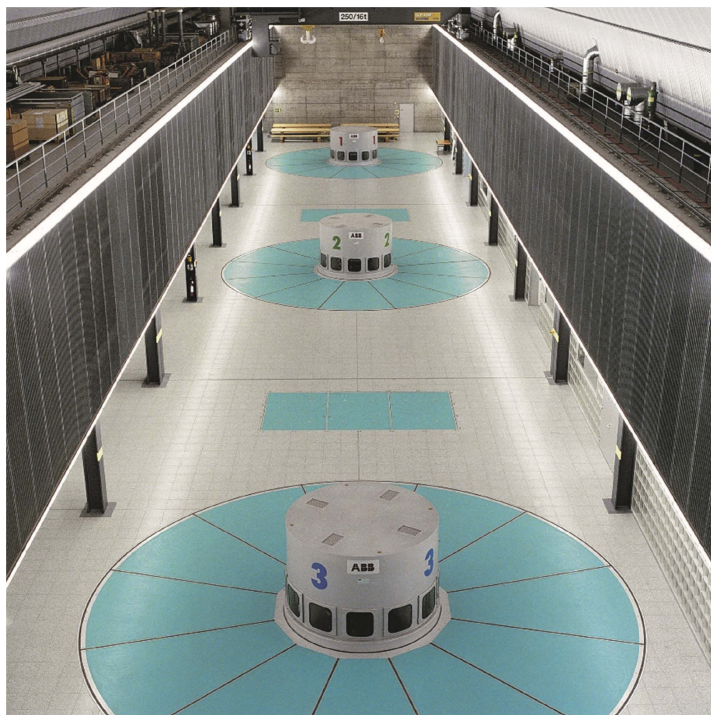


Figure 6. Bieudron 1200 MW powerplant.

Climate change increases the multiple threats to water availability. The spatial and temporal pattern of precipitation and water availability is changing. The frequency, intensity and severity of extreme weather events are likely to increase. Glaciers are melting and natural water storage is diminishing. In view of this, the project to build a new reservoir, the Gornerli reservoir in the upper Zermatt valley, is intended to secure the valley by reducing flooding and providing a new strategic winter reserve.

2.2 Emosson

At the beginning of the 20th century, engineers had already noticed that the Emosson site was suitable for the construction of a large hydraulic reservoir, but because of the limited natural water inflows and the impossibility, at the time, of collecting water via long galleries and of carrying out large-scale pumping, the project was not developed until 1953. The preliminary project to use the waters of the Drance d'Entremont, the Drance de Ferret, the Trient and the Eau Noire to fill this new retention structure in the Barberine region was launched and discussions were held to obtain the necessary concessions to carry out this work. At that time, Electro-Watt, which was responsible for the construction of the Mauvoisin scheme and was awarded the Mattmark water concession in February 1954, abandoned the "Grand Emosson" project.

Motor Columbus SA d'Entreprises Electriques de Baden founded the company "Usines hydro-électriques d'Emosson SA" in 1954, which became "Electricité d'Emosson SA" in 1967. The



Figure 7. Gorner glacier valley - view from above.



Figure 8. Photomontage of the future Gornerli dam.

acquisition of the local community concessions and the extension of the project into French territory took place at the same time and led to the admission of Electricité de France into the company in 1955. It took many years to get the administrative apparatus of both countries up and running and to get the project underway. The project's interest in the highly sought-after peak energy quality was undisputed. At the same time as the project was being studied, discussions were initiated with the Swiss Federal Railways (SBB), whose previously used Barberine reservoir would be flooded. France and Switzerland decided to change the border



Figure 9. Emosson dam under construction.

line. The wall of the Emosson dam would have been cut in the middle by the Franco-Swiss border, leaving its right side on French soil and the rest of the structure in Switzerland, while the Châtelard-Vallorcine hydroelectric power station would have been entirely in Swiss territory. The agreement of August 23, 1963 made it possible to rectify the Franco-Swiss border so that the project could be carried out in accordance with the respective interests of the two States. France and Switzerland proceeded to an “exchange of territory of equal area” which placed the wall of the Emosson dam entirely in Switzerland and, symmetrically, the Châtelard-Vallorcine hydroelectric power station entirely in France. Works began in 1967 and the plant was commissioned in 1975. The constructions, more than 65% of which are in Switzerland and 35% in France, constitute an indivisible entity. The authorities of the two countries, meeting in the permanent supervisory commission, are also very diligent in dealing with the problems that arise due to the existence of national borders in the middle of the installations and the different legislation between the two countries.



Figure 10. Emosson dam.

The Franco-Swiss Emosson scheme drains water from the French valleys of the Arve and Eau Noire and Swiss water from the Val Ferret and the Trient Valley. The South Collector, 8.55 km long, collects water from the Lognan, Argentière and Tour glaciers, which flows towards the dam gravitationally, via a siphon. The West Collector, 7.95 km long, collects the water from the Bérard and Tré-les-Eaux valleys at an altitude of 1 990 m above sea level and conveys it directly into the dam’s reservoir. The East Collector collects water from La Fouly at an altitude of 1 550 m above sea level. The water comes from the Val Ferret, the Saleinaz and Trient glaciers and various other torrents. The gallery is 18.3 km long. This water flows into the Esserts basin. It is either turbiné in Vallorcine or pumped into the Emosson reservoir.



Figure 11. Emosson scheme - 3D view.



Figure 12. Nant de Drance PSP – heightening of the Vieux-Emosson dam – upper reservoir.

Dam heightening in Switzerland

A. Wohnlich
Gruner Stucky SA

A. Fankhauser
Kraftwerke Oberhasli AG

B. Feuz
Independent Engineer

ABSTRACT: Raising the height of existing dams is becoming an increasingly topical issue in Switzerland. This particular construction method offers a number of environmental, technical and economic advantages, which are presented in this article. Swiss engineers have been raising their dams for more than a century, and the article describes the various structures involved. Finally, a perspective on future dam heightening is offered considering the climate and energy issues prevailing at the start of the 21st century.

1 INTRODUCTION

The technology of dam heightening is not recent. In fact, the first known heightening of a dam in Switzerland during the modern era of dam construction (from the end of the 19th century) dates back to 1910 (Maigrange dam, canton of Fribourg). Throughout the 20th century and into the 21st century, no less than a dozen dams have been raised in Switzerland. Most of these were concrete dams, and the vast majority were gravity dams.

This article begins by outlining the advantages of raising dams and the main issues involved in this challenging work. The main aim is to increase the storage volume of the reservoir. However, this is not always the only objective, as will be shown below.

The various heightened dams are presented, highlighting the characteristics and specific features of each structure. The first part of the publication presents mainly and chronologically heightened gravity dams, all of which are of moderate size. The second part of the publication deals with the more recent and much larger scale raising of arch dams. Over the past 30 years, three major arch dams have been raised in Switzerland: Mauvoisin, Luzzzone and Vieux Emosson dams.

Swiss know-how in the field of dam heightening has also been exported: Swiss engineering has had the opportunity to make its mark from time to time, as will be recalled in a dedicated section.

Finally, considering the tense geopolitical situation prevailing in Switzerland and Europe at the start of the 21st century, which has direct repercussions on the energy sector, as well as the effects of global climate change, a perspective is offered in conclusion, showing that the interest in raising existing dams is likely to continue over the coming decades.

2 INTEREST OF DAM HEIGHTENING

The main purpose of raising a dam is to create additional storage volume in the reservoir. The possibility of having a greater storage volume offers major economic advantages to the operator of the structure, in the form of increased flexibility in the management of its hydroelectric

scheme (optimization of productive hours, as well as transfer of part of the summer production to the winter).

Considering the shape of a valley used as a reservoir, the storage volume is generally always significantly higher at the top of the dam than in the talweg. Each additional metre of height therefore contributes more to the volume stored than the levels below.

In contrast, when considering the shape of concrete dams, it can be seen that the greatest dam thickness is close to the foundations, and that as the dam rises, it becomes thinner. The volume of concrete required to raise a dam is therefore relatively small compared with the additional volume of water stored in the upper levels. In principle, this twofold geometric advantage makes dam heightening projects economically attractive.

In addition, the environmental issues involved in raising a dam are normally reduced compared with building a new dam on a greenfield site. When a dam is raised, the site has already been constructed for many years and public acceptance is easier, as the impact on the environment and on the landscape is reduced.

What's more, in most cases (most heightening works are carried out on the top of the structure itself, or on its downstream side, only rarely on its upstream side), a heightening project can be carried out without emptying the existing reservoir and therefore without any loss of operation, which is a key economic factor for the operator of the hydroelectric scheme.

Finally, it should be noted that raising a dam is generally only possible if it can take advantage of 'generous' dimensioning at the time the dam was designed, developments in science (better knowledge of construction materials, characteristics of rock foundations, etc.), and progress in design tools (more recent and sophisticated calculation methods).

3 HISTORICAL REVIEW

The review presented below spans the whole of the 20th century up to the 2020s. The main group of heightened dams described first below concerns only relatively modest-sized gravity dams, between 10 m and 40 m high. This is clearly the type of structure that has been most widely considered for raising during the 20th century.

A second group of gravity dams is dealt with separately. These are two dams (Muslen and List) for which raising the water level was not the primary aim but was subordinate to the objective of strengthening the structure. As part of such a safety project, it turned out that it was also possible to take advantage of major reinforcement work to raise the dam.

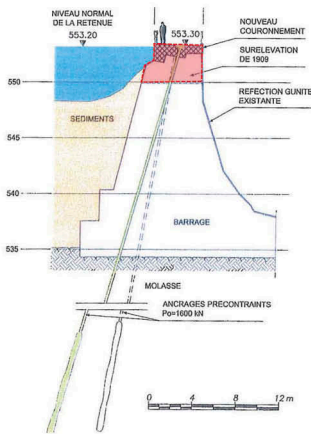
Finally, a third group of dams is discussed next. These are two relatively high structures (Salanfe and Les Toules), between 50 m and 90 m, which were raised very shortly after the construction of the initial dam, and for which the raising was designed from the outset. The reason for the two-stage construction was the operator's intention to bring its hydroelectric scheme into service as soon as possible. For various reasons, the hydraulic circuit and the hydroelectric powerplant were operational earlier than the dam, and the most economical way of commissioning the scheme as quickly as possible was to build a small retaining structure sufficient to supply the water intake, and then to plan the subsequent construction of the dam to its full height in a second phase.

The presentation and description of the three large arch dams raised between 1990 and 2020 is addressed separately in Chapter 4.

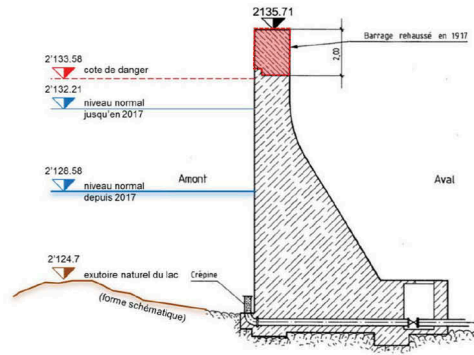
3.1 *Gravity dams*

The structures described below are presented by date of heightening.

Maigrage dam (Figure 1, left) is one of the oldest dams in Switzerland. It was built in 1870-72 and heightened in 1909-10, probably because of the rapid silting up of the reservoir. It should be noted that the prestressed anchors (1600 kN/2 m) shown in the cross-section in Figure 1 were added in 2000-03 to ensure that the structure complies with stability requirements (structural safety). Relatively high tensile stresses could develop at the heel of the dam, particularly in the event of exceptional loads such as the safety flood or an earthquake.



Maigrage Dam (Fribourg)
 Construction 1870-1872 H=19 m
 Heightening 1909-10 H=21.7 m (+2.7 m)



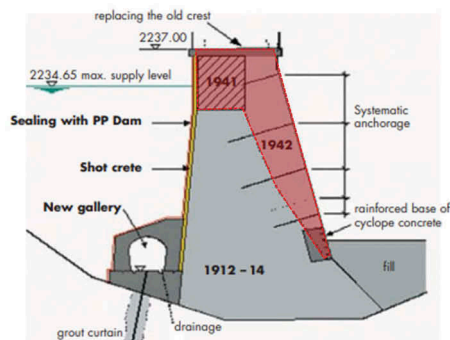
Fully Dam (Valais)
 Construction 1914-15 H=9 m
 Heightening 1917 H=11 m (+2 m)

Figure 1. Maigrage dam and fully dam.

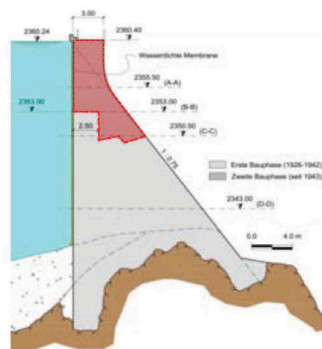
Fully dam (Figure 1, right) was built in 1914-15 and raised by 2 m in 1917. The dam axis is not straight, but curved in plan, which probably generates a three-dimensional effect and explains how the raised section can be stable. It should be noted, however, that the dam has been operated at a lower water level for several decades.

Lago Bianco South dam (Figure 2, left), built at the beginning of the 20th century, was raised by 4 m in 1941-42. The dam axis also has a curvature in plan, which in reality makes it an arch-gravity dam. Over time, the concrete of the raised section was found to suffer from the alkali-aggregate reaction (AAR), resulting in vertical cracking and increased deformation. The raised section was rehabilitated in 2000-01.

It should also be noted that as part of the development of the pumped-storage project, a new raising of 3.5 m was studied in 2011-12. However, this project has not yet been implemented.

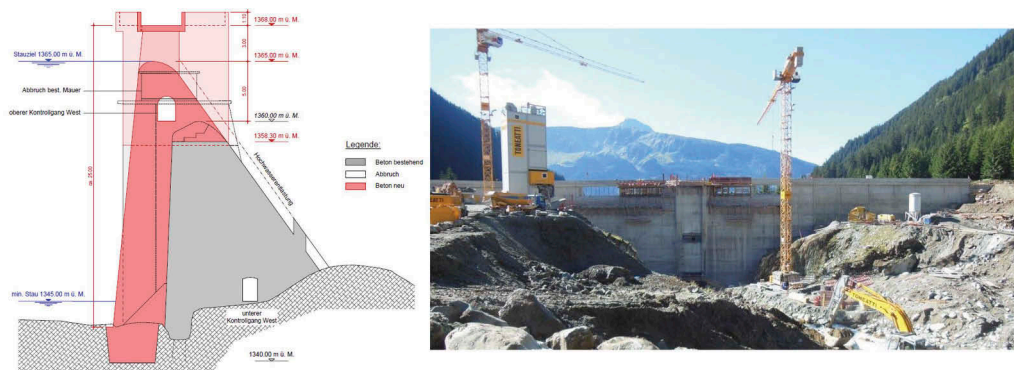


Lago Bianco South Dam (Grisons)
 Construction 1912-1914 H=22 m
 Heightening 1941-42 H=26 m (+4 m)



Raised by 7 m in the early 1940s, Illsee dam, built in 1926-27, is shown in Figure 2, right. Like the other two dams described above, Illsee dam axis is curved in plan in its main section, where it crosses the talweg. Over the years, the structure has been found to suffer from AAR, leading to significant and irreversible deformation and cracking. In addition, the dam did not meet modern safety requirements, having been designed without regard to seismic loading. Considerable rehabilitation works were carried out in 2012-13 (concrete sawing to relax the bank-bank stresses caused by the RAG, installation of vertical prestressed anchors, and reconstruction of the dam crest).

Barcuns dam, built in 1947 and shown in Figure 3, is the gravity dam that was most recently raised in Switzerland, that is in 2013-14. Its 5 m heightening is remarkable in that it was carried out on its upstream face, unlike all the dams described above. This solution is constraining because it requires the reservoir to be emptied. It was possible to implement it at Barcuns because the entire hydraulic circuit and hydroelectric power station were rehabilitated simultaneously. The facility was shut down for around two years to carry out this work.



Barcuns Dam (Grisons)
 Construction 1947 H=31.8 m
 Heightening 2013-14 H=36.8 m (+5 m)

Figure 3. Barcuns dam, with view from upstream of the dam heightening works.

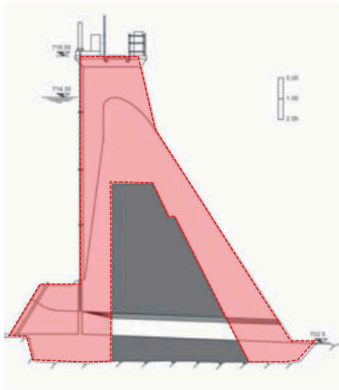
3.2 Compliance with safety standards

In Switzerland, two dams are known to have been raised to improve their safety. These are List and Muslen gravity dams, both of which were reinforced and raised in 1982. The respective cross-sections are shown in Figure 4 below. During the 1970s, the safety requirements for dams were updated and these two dams did not meet the overturning criterion, thus generating high tensile stresses on the upstream face. When they were designed in the beginning of the 20th century, uplift pressure was not considered in dam design, nor were exceptional load cases (floods, earthquakes). In addition, the spillways on the two dams had insufficient capacity.

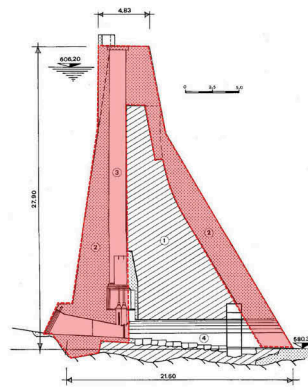
Faced with the need for major reinforcement work, the owners of these two facilities took the opportunity to raise their respective dams, resulting in the concrete covering of the old dam, which is no longer visible or accessible.

3.3 Early commissioning of the scheme

The two dams presented in this section are special cases of heightening. These dams were raised immediately after the construction of the initial dam, which was considerably reduced in size. The aim of this two-stage construction was to enable the hydraulic circuit to be commissioned ahead of time and to start producing hydroelectric power, without having to wait for the final size of the dam to be built.

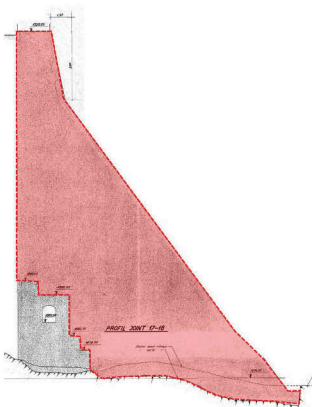


List Dam (Appenzell Rh.-Ext.)
 Construction 1900-1901 H=13.5 m
 Heightening 1982 H=16.5 m (+3 m)



Muslen Dam (St-Gall)
 Construction 1909 H=23 m
 Heightening 1982 H=28 m (+5 m)

Figure 4. List dam and Muslen dam.



Salanfe Dam (Valais)
 Construction 1947-1950 H=14.5 m
 Heightening 1951-1953 H=52 m (+37.5 m)



Figure 5. Salanfe dam. On the right, photo of the first stage dam, H=14.5 m.

Salanfe dam is the first example shown in Figure 5 above. The first stage of the dam was built in 1947-50, with the second stage following in 1951-53. Miéville hydroelectric power plant, almost 1500 m lower down on the Rhône Valley, came into service in 1951.

This dam also suffered from AAR, which led to concrete sawing work on the structure in 2012-13 to release the compressive stresses generated by the reaction. The dam crest was also refurbished during this work.

The second case discussed in this section is that of les Toules arch dam, illustrated in Figure 6 below. Construction in two stages enabled Pallazuit power station to be commissioned in 1958 but was also made necessary by the road to the Grand-St-Bernard pass, which runs along the right bank of the valley and had to be raised some fifty metres before the reservoir could be impounded.

It can be seen that the first structure is a single-curvature arch dam, while the second is a double-curvature arch dam. The joint between both structures proved particularly difficult to manage. Added to this was the very wide shape of the valley, which is not very suitable for an arch dam (ratio of crest length to height > 5) and geological conditions which are not very homogeneous, particularly on the left bank, it was necessary to reinforce this dam by adding concrete strengthening on both downstream banks. This work took place in years 2008-11.

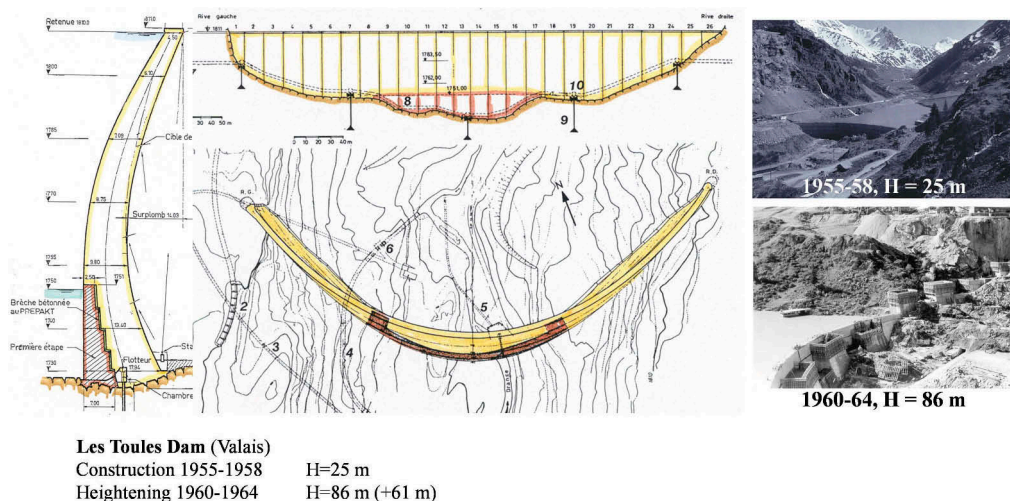


Figure 6. Les Toules dam. On the right, photos of the two stages of construction. It should be noted that this dam was further reinforced between 2008 and 2011 on its downstream face, using around 60000 m³ of concrete. This is not shown on the figure above.

4 RECENT DAM HEIGHTENING

Three of Switzerland's major arch dams have been raised since the 1990s. They are Mauvoisin, Luzzzone and Vieux Emosson dams.

There are only two ways of raising an arch dam:

- Either by propagating the shape of the upstream and downstream faces upwards. This is naturally the most natural and simple method. However, it is not always feasible, depending on the shape of the two faces. Mauvoisin and Luzzzone dams were raised using this method.
- Or by modifying the shape of the arch. This method is considerably more complicated and costly than the previous one, as it involves partially deconstructing the existing arch dam before raising it. This is the case with Vieux Emosson dam.

4.1 *Mauvoisin dam*

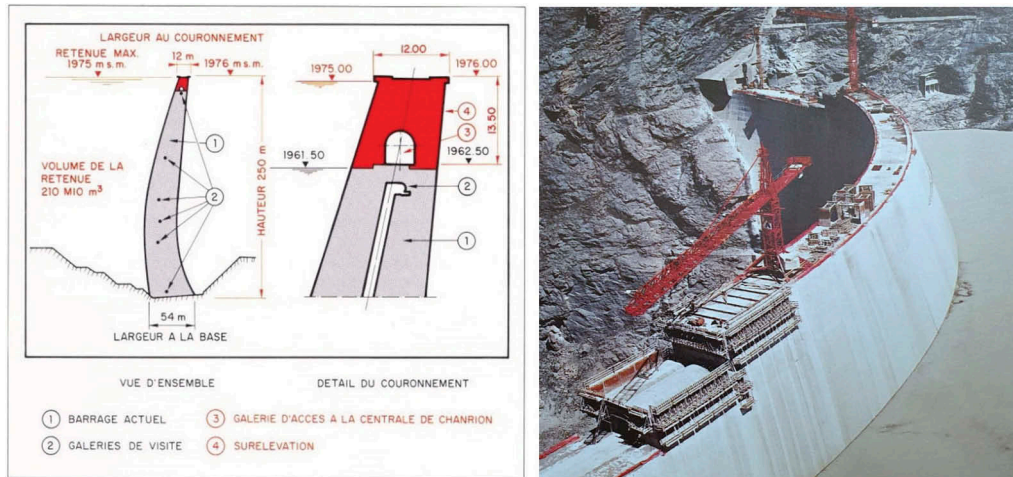
The purpose of raising Mauvoisin dam is to transfer energy from summer to winter. Energy production in summer exceeds demand, while energy production in winter is insufficient to cover the country's needs. Thanks to the favourable hydrological conditions in the Haut Val de Bagnes, the operator (Forces Motrices de Mauvoisin) had the opportunity to increase winter energy production by 100 million KWh while reducing summer production by the same amount. This could be achieved by increasing the storage capacity of Mauvoisin reservoir by around 30 million m³.

With a height of 236.5 m, Mauvoisin arch dam was the highest dam in operation in Europe in 1989. It had a crest length of 520 m and a crest width of 14 m at 1962.5 m asl. The dam was

raised by constructing an additional arch in the extension of the original dam faces. The width of the raised dam crest at an altitude of 1976 m asl is 12 m, incl. a 6.6 m wide road. A gallery 5 m wide and 5.5 m high, located in the raised section, provides access to the underground hydraulic power station located upstream of Mauvoisin scheme. The volume of concrete used is 80 000 m³, representing 4% of the volume of concrete used in the original dam.

The heightening has a crest length of 540 m and consists of 28 blocks that are concreted between the vertical joints of the dam. Each block, approximately 18 m long and 13.5 m high, is concreted in 5 lifts of 2.7 m each. The volume of each lift varies between 400 m³ and 650 m³ of concrete.

Ancillary work on the surface spillway, the mid-level outlet gate and the surge tank near Fionnay power station was carried out in parallel with the main work on the dam.



Mauvoisin Dam (Valais)
 Construction 1951-1957 H=236.5 m
 Heightening 1989-1991 H=250 m (+13.5 m)

Figure 7. Mauvoisin dam. Right, picture of the heightening job site (1990).

Work was carried out over three summer periods (April to October) from 1989 to 1991. Site installations began in April 1989. The batching plant, cement silos and crushing plant for preparing concrete aggregates were located at the foot of the dam, close to the large stockpile of materials left over from the construction of the dam. The cement was transported by train to Le Châble, and then by truck to the silos.

Concreting works were carried out from September 1989 to August 1991, using one crane (capacity 150 mt) in the first year and two cranes placed on the blocks already built, in 1990. By spring 1991, all that remained to be done was the concreting of the new dam crest. The joints between dam blocks were grouted between the end of May and the beginning of July 1991.

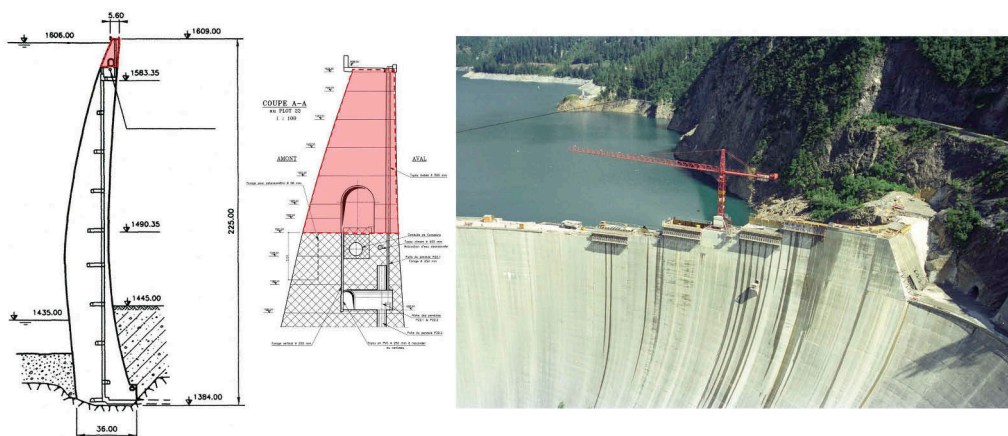
The raised dam was impounded in summer 1991, reaching its maximum level of 1975 m asl at the end of September. The dam behaviour was as expected by the design engineers.

4.2 Luzzone dam

Luzzone arch dam was built between 1959 and 1963. With a height of 208 m, a crest length of 550 m, a thickness of 36 m at the base and 10 m at the crest, the volume of concrete for this dam amounted to 1.32 million m³ before heightening. The seasonal storage basin had a capacity of 87 million m³ and is the main reservoir of the Blenio power plant. However, given the growing demand for energy in winter and the fact that the summer inflow of

127 million m³ far exceeded the reservoir storage capacity, it became interesting to increase the storage volume.

A project to raise the dam by 17 m was designed and work began in 1995. Since 1999, the dam is 225 m high, has a concrete volume of 1.40 million m³ and a storage capacity of 107 million m³ (85% of average summer inflows), see Figure 8.



Luzzone Dam (Tessin)
 Construction 1959-1963 H=208 m
 Heightening 1995-1998 H=225 m (+17 m)

Figure 8. Luzzone dam. Right, picture of the heightening job site (1995), showing detail of the left bank abutment.

As shown above for Mauvoisin arch dam, the technical concept of the heightening involves the upward propagation of the geometric definition of the upstream and downstream faces. An additional arch was therefore added to the dam, bringing the width at the new crest to 5.6 m. The abutment on the left bank of the heightening is special. To save concrete, the raised section ends on an artificial abutment in the shape of a gravity dam (see Figure 8, photo right) and in order to have the compression forces of the arch diving down into the existing section, the bloc joints near the artificial abutment were only partially grouted. To maintain access to a mountain pasture upstream of Luzzone reservoir during and after the heightening work, a road gallery was integrated into the raised dam section.

Concreting was carried out using a crane placed halfway up the raising, which moved as the work progressed from the left bank to the right bank. As with the original dam, the aggregates came from a moraine quarrel located in a side valley a few kilometres away. The batching plant was located on the right bank of the dam and produced a total of 80 000 m³ of dam concrete, with a binder content of 250 kg/m³ and a maximum size aggregate of 63 mm. The binder contained 80% Portland cement and 20% fly ash, making it possible to give up artificial cooling of the concrete (post-cooling).

In parallel with the concrete work on the dam, the spillway and surge tank were raised and a new access gallery to the mountain pasture upstream of the reservoir was excavated.

The heightened dam has been in service since 1999, behaving satisfactorily and in line with its design.

4.3 *Vieux Emosson dam*

Vieux Emosson dam is located in Canton of Valais, close to the border with France. The raising of the dam is a key element of the vast Nant de Drance pumped-storage scheme, which came into operation in 2022. This dam serves as an upper reservoir, and the raising of the

dam allowed more than doubling the active storage capacity (from 11.2 million m³ to 24.6 million m³), giving the pumped-storage scheme greater flexibility.

The dam was built in the 1950s by Swiss Federal Railways. The cross-section of the dam corresponds to a 62 000 m³ concrete gravity dam, which was actually a single-curvature arch dam. The heightening consists of a double-curvature arch dam with horizontal and vertical sections formed by parabolic segments. Geometric constraints due to the shape of the valley and the first dam meant that the upper part of the latter had to be demolished and removed (17 000 m³ of concrete), before the raising could be built (65 000 m³ of concrete) and the transition made from the initial single-curvature to the double-curvature of the raising. The total volume of concrete for the raised structure amounts to 110 000 m³. The heightening concept is shown below in Figure 9.

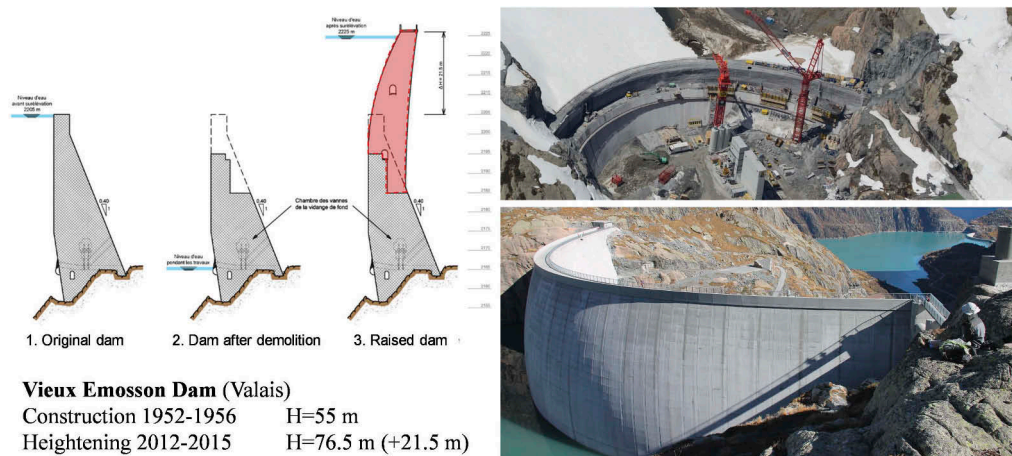


Figure 9. Vieux Emosson dam. Right, photos of the heightening work.

On the right bank, the first dam is just above the surface of the rock mass. On this bank, the crest of the raised dam is clearly above the rock mass. For this reason, a wing wall had to be built at the end of the arch. Its function is to close off the reservoir and house the spillway, which is a free flow ungated spillway.

The reservoir was empty from the start of the demolition work until the raising of the vault was completed. During this period, the spillway gates remained open and were being refurbished. However, at least one valve always remained operational so that the flow could be managed in the event of flooding.

The demolition of the upper part of the first dam was a critical point and a major challenge for the project. Initially, blasting was planned to demolish the dam concrete over a height of around 20 m. However, this technology proved unsuitable. The demolished surfaces had discontinuous and rugged shapes and the allowable shaking limits were difficult to comply with. Finally, the efficiency of demolition by blasting was low. Following this observation, the contractor gave up the method and switched to demolition of the concrete by using road-type machines (planer machines) that travelled back and forth over the crest. Milling machines were used to demolish the concrete that the large planers could not reach. This demolition method proved to be far more efficient than blasting, while limiting the problem of vibrations generated by blasting. The demolition work lasted from mid-June to the end of October 2012.

Concreting took place over two summer seasons (April to October), in 2013 and 2014. The concrete aggregates were produced lower in the valley and transported by truck to the toe of the dam, where the batching plant was located. The concrete was transported onto the dam using two tower cranes, also installed downstream of the dam.

In spring 2015, the dam blocs were grouted in two stages over the raised height. The dam was then commissioned over the following years to the satisfaction of the design engineer and the supervisory authorities.

5 DAM HEIGHTENING ABROAD

Swiss engineering know-how in the field of (large) dams is widely recognised throughout the world and has historically been exported well throughout the 20th century and into the early 21st century. There are many examples, and some of the most daring projects, to be found in numerous references and publications on the matter.

The same is certainly true for the very specific field of dam heightening. Although this type of work is more recent and its applications still rarer, Swiss engineering firms have had a few opportunities to demonstrate their capacity for innovation and their technical expertise in various countries. Some outstanding examples are described briefly below.

In the early 2000s, the raising of the Ekbatan buttress dam in Iran, built between 1959 and 1963, was designed and dimensioned by Swiss engineers. The project involved raising the dam by 25 m, from 54 m to 79 m. The project was built and successfully commissioned in the early 2010s.

In Angola, the Cambambe double-curvature arch dam on the Kwanza River, 180 km east of the capital Luanda, was raised between 2012 and 2018 (Figure 10). The design, execution project and supervision of the works were carried out by Swiss engineering firms. Particularly slender, and located in a spectacular natural landscape, the heightening project has given rise to a number of publications. In particular, the construction of the elevation had to be planned according to the flow of the river, continuously spilling over the existing dam.

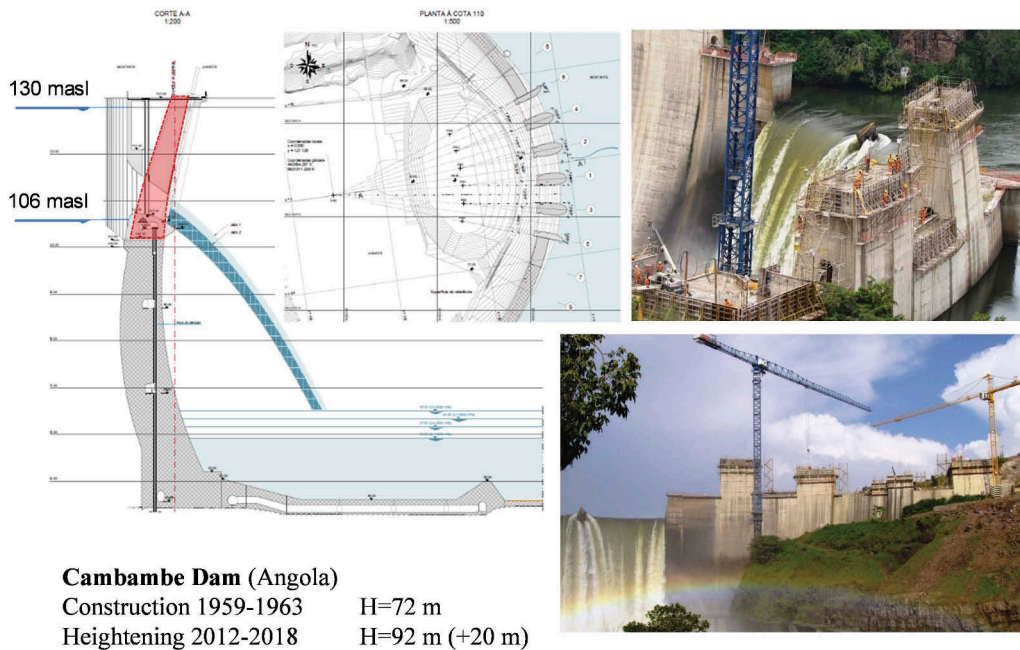


Figure 10. Cambambe dam. Right, photos of the heightening works.

Finally, there is the Limberg arch dam in Austria, near Kaprun/Zell am See, whose initial height of 120 m will be raised to 129 m. Studies are ongoing and work is scheduled to begin in the coming years. A Swiss engineering firm is in charge of the design and production of the construction project.

6 CONCLUSIONS AND FUTURE PROSPECTS

6.1 *Retrospective*

Dams have been raised in Switzerland for over a century. Twelve examples have been listed and described in this paper. The size of the structures raised varies greatly, ranging from around ten metres for the most modest to over 200 m high for Luzzone and Mauvoisin arch dams.

The many advantages of such challenging projects have been highlighted, both from an environmental and an economic point of view. Generally speaking, the gain of a relatively large additional water storage volume compared with the often moderate scale of the heightening work and its impact on the environment and landscape makes raising a dam economically attractive.

The review showed that, in Switzerland, the majority of projects involve raising the height of concrete dams; however, there are also heightening projects for embankment dams. Work to raise Plans Mayens embankment dam in Crans-Montana is scheduled for 2023-2025.

Given the diversity of each dam in its natural environment and the unique nature of each facility, each raising project requires the implementation of specific solutions tailored to the site and the problems encountered, as it has been amply demonstrated throughout this retrospective. The range of technical solutions deployed over the last century demonstrates the expertise of Swiss engineering in this field, which has also been exported.

6.2 *Future prospects*

In the current geopolitical and energy context (growing population, rising electricity consumption, political determination to move away from nuclear power, heavy dependence on fossil fuels such as gas and oil, unstable political situation in Europe, climate crisis, strong development of solar and wind energy), the need to create energy storage facilities for the winter is becoming increasingly obvious. Only hydroelectric schemes with their reservoir dams can offer the possibility of transferring water reserves (i.e. energy) from summer to winter, with the reservoirs acting as huge rechargeable batteries.

In this context and under the leadership of the Swiss government, the various stakeholders in the field of hydropower (cantons, universities, environmental and landscape protection associations, electricity companies) have come together in 2020-2021 in a round table to develop a common approach to the challenges facing hydropower in the context of the 2050 energy strategy, the zero-emissions climate target, security of energy supply and the preservation of biodiversity. The round table identified 15 hydroelectric storage power plant projects that, based on current knowledge, are the most promising in terms of energy production and whose implementation would have the least impact on biodiversity and the landscape. Their implementation would make it possible to achieve a cumulative additional adjustable winter production of 2 TWh by 2040. The list of these 15 projects is indicative and not exhaustive. The projects are eligible for investment grants of up to 60%.

Of the 15 projects highlighted by the round table in December 2021, at least 10 involve heightening of existing dams. The context is therefore very favourable for several dams to be raised in the coming years and decades, and numerous studies are under way in Switzerland.

6.3 *Final remark*

There is no official directory of heightened dams in Switzerland. As far as possible, this paper aims to present an exhaustive list of raised dams in this country. However, it cannot be ruled out that some dams may have escaped the authors' attention.

This research would not have been possible without the active collaboration of several operators (Alpiq, Axpo, Groupe E, KWO) and engineering firms (Afry, Gruner Stucky, Lombardi), as well as the supervisory authority (SFOE) and the ETHZ, all of whom contributed to this work by sharing the information and data in their possession. Our sincere thanks to all of them.

REFERENCES

- Amman E. 1985. La transformation des barrages de Muslen et de List. *Commission Internationale des Grands Barrages, Quinzième Congrès des Grands Barrages, Lausanne*: Q59, R23, 381-394.
- Dams in Switzerland, Source for Worldwide Swiss Dam Engineering. 2011. *Swiss Committee on Dams*. Baden-Dättwil: buag
- Felix, D., Müller-Hagmann, M. & Boes, R. 2020. Ausbaupotenzial der bestehenden Speicherseen in der Schweiz. *Wasser, Energie, Luft – Eau, Energie, Air, Heft 1*: 1–10
- Feuz, B. & Schenk, Th. 1992. Die Erhöhung der Staumauer Mauvoisin. *Wasser, Energie, Luft – Eau, Energie, Air, Heft 10*: 245–248
- Feuz, B. 1994. Raising of the Mauvoisin Dam. *Structural Engineering International, International Association for Bridge and Structural Engineering, 2/94*: 103–104
- Golliard, D., Lazaro, P., Demont, J.-B. & Favez, B. 2001. Travaux de réhabilitation de l'aménagement de l'Oelberg-Maigrauge, Fribourg. *Wasser, Energie, Luft – Eau, Energie, Air, Heft 3/4*: 63–70
- Kressig, D. 2012. Realisierung Sanierung Talsperre Illsee. *Schweizerischer Wasserwirtschaftsverband, Fachtagung Wasserkraft*, Luzern.
- Leite Ribeiro, M., Vallotton, O. & Wohnlich, A. 2022. Two Recent Cases of Arch Dam Raising, Lessons Learnt and Innovation. *Commission Internationale des Grands Barrages, Vingt-Septième Congrès des Grands Barrages, Marseille*: Q104c
- Vallotton, O. 2012. Surélévation du barrage de Vieux Emosson. *Wasser, Energie, Luft – Eau, Energie, Air, Heft 3/4*: 209–215
- Vallotton, O. 2015. Surélévation du barrage de Vieux Emosson. *Commission Internationale des Grands Barrages, Vingt-Cinquième Congrès des Grands Barrages, Stavanger*: Q99
- Wohnlich, A. 2012. Surélévation du barrage-voûte de Cambambe, Angola. *Wasser, Energie, Luft – Eau, Energie, Air, Heft 3/4*: 216–219
- Wohnlich, A. 2021. Barrage des Toules – Faiblesses structurelles, confortement du barrage. *Comité Suisse des Barrages, Journées d'études CSB*, Crans-Montana.

Swiss dam engineering in the world

Patrice Droz

Swiss Committee on Dams

ABSTRACT: Swiss dam engineers and contractors have always demonstrated a great interest in exporting their know-how and expertise in the domain of dams and hydropower. The article presents an overview of the most recent international projects.

RÉSUMÉ: Les ingénieurs et entreprises suisses ont depuis longtemps montré un intérêt à exporter leur savoir-faire et leur expérience à l'étranger dans le domaine des barrages et des aménagements hydroélectriques. Cet article présente un tour d'horizon des activités récentes hors de Suisse dans le domaine.

1 INTRODUCTION

The development of dams and hydropower in Switzerland started at the end of the 19th century, taking advantage of the topography of the country as well as its water resources. The development of hydropower encouraged the industrialization of the country as well as its electric railway system. But progressively, with their know-how gained in the Alps, Swiss engineers and contractors exported their experience abroad, firstly to Europe and then worldwide.

As the Swiss Committee on Dams is celebrating its 75th anniversary, it should be of interest to briefly describe some of the recent international projects in which Swiss engineering consulting firms and experts, contractors and research laboratories have been involved. Of course, an exhaustive treatment is not the aim of the present paper: a selection has been made by the author, taking into account the importance of the project, the difficulties encountered in the completion of the projects, and the specific techniques used, and solutions selected.

2 DEVELOPMENT OF NEW DAM PROJECTS

2.1 *Europe*

The 690 MW capacity, 600 m gross head Kárahnjúkar hydroelectric scheme (Iceland), harnesses water from two glacial rivers originating in the large Vatnajökull Glacier, stored behind the 198 m high Kárahnjúkar concrete-faced rockfill dam (CFRD). Difficult tunnel conditions due to large groundwater inflows and to locally unstable rock conditions were encountered during the excavation of the headrace tunnel. The resulting delays required acceleration of the filling, pressurizing and commissioning of the headrace tunnel. This was achieved by filling the headrace tunnel in two stages. First the penstocks and the lower section of the tunnel were filled using the groundwater inflow, and water stored in the lower tunnel behind a temporary cofferdam in the tunnel was used to commence the wet testing of several turbine units while finishing work continued in the upper section of the tunnel. Following completion of the tunnel finishing work, the remainder of the tunnel was filled and pressurized in a second stage (Kaelin 2009). The dam body is also located on a fault, which required the construction of a joint in the toe wall and the concrete face. Model studies on that project were conducted at both hydraulic laboratories of the Swiss Federal Institutes of Technology in Lausanne (Bollaert 2003) and Zurich (Berchtold and Pfister 2011).

The Neikotski dam is under construction in Northern Bulgaria, it is part of a water supply project. The maximum height of the dam is 47.2 m; the crest is 200 m long, and the embankment volume is approx. 300,000 m³. The asphalt core rockfill dam (ACRD) is founded on rock. The asphalt-concrete core is vertical, located in the central section of the dam. It starts from the top of a grouting gallery which is embedded in the rock foundation. During the design phase, a comparison was made of seismic horizontal displacements obtained from a dynamic analysis and by two simplified analytic methods. In this case the results of the dynamic analysis and the simplified analysis were almost the same. However, the dynamic analysis using the finite element method provides much more information on the seismic behaviour of the dam (Tzenkov 2023).

Devoll Hydropower Project is located about 70 km southeast of the Albanian capital Tirana and consists of two hydropower plants, Banja and Moglice. The hydropower plants will have a total installed capacity of 256 MW and a mean annual production of about 703 GWh, increasing the Albanian electricity production by about 17 per cent. The lower one (Banja) was commissioned in 2016. The construction of the Moglice HPP began in 2014 with an installed capacity of 184 MW. The 167 m high dam is an ACRD with a crest length of 370 m and is one of the highest of its type in the world (Tirunas 2018).

2.2 Middle East

The recent development of hydropower projects and the construction of numerous large dams in Turkey offered the opportunity to Swiss consulting firms to be part of the design and construction of a couple of very significant dams in Anatolia.

The Deriner dam is a double curvature arch dam located on the Çoruh River in Northeastern Turkey. With a height of 249 m and a concrete volume of 3.5 Mm³, it is currently the second highest dam in Turkey. The installed capacity of the powerhouse is 670 MW, with four Francis turbines, and its annual power generation amounts to 2118 GWh, accounting for approximately 1.1% of the total energy production in Turkey and roughly 6% of Turkey's hydropower generation capacity. State Hydraulics Works (DSI) of Turkey owns the project. Swiss consulting firms were part of the project either on the owner side (Wieland et al. 2008) or the Turkish contractor side (Müller 2009). The construction works started in 2000 and the dam was commissioned in 2012. The flood evacuation system is particularly impressive with two gated overflow spillways at the left and right abutments of the dam with a total capacity of 2,225 m³/s and eight mid-level bottom outlets with a total discharge capacity of 7,000 m³/s. The total volume of excavated material amounted to 8.7 Mm³, and for the stabilization of the abutments more than 2,000 2 MN post-tensioned anchors were installed (Figure 1).



Figure 1. Upstream view of Deriner dam and rock stabilization of abutments.

The Ilisu Dam & Hydroelectric Power Plant (1,200 MW) is located on the Tigris River in the Southeast of Turkey close to the border with Iraq (Figure 2). The power plant is composed of a 135 m high and 2,289 m long CFRD, a gravity dam section, a spillway, power intakes

and power tunnels with a maximum diameter of 13 m, a powerhouse (6 Francis turbines with an installed capacity of 1200 MW), a tailrace channel and three river diversion tunnels ($\text{\O}12$ m), one of them acting as bottom outlet. The construction was finished in 2020 (IM 2023, Stucky Gruner 2023).



Figure 2. Ilisu dam, powerhouse and spillway.

2.3 Central Asia

Rogun dam is under construction in Tajikistan and will be completed in stages until 2030. The dam is a 325 m high earth core rockfill dam (ECRD). Extensive studies were carried out in order to assess its impacts on the riparian countries in terms of water resources (Pöyry 2014). At present several Swiss consulting firms as well as contractors are taking an active part in the detailed design and the construction of the dam. The dam is located in a highly seismic region in the Pamir Mountains and an active fault passes through the footprint of the dam parallel to the dam axis. Further challenges are the difficult geological conditions with rock salt formations and the high sediment content of the Vakhsh River.

During the construction of the Sangtuda 2 HPP in Tajikistan, severe water inflows occurred within the excavation of the run-of-river type powerplant. A specific support was provided for understanding the particular hydrogeological conditions, which led to the drainage of a regional karst aquifer, and for designing appropriate mitigation measures (Ghader et Busard 2013). A pumping of around 10 m³/s allowed the successful completion of the project.

Rudbar Lorestan is an earth core rockfill dam with a height of 156 m. It is located in a narrow canyon in the seismically very active Zagros Mountain Range in the west of Iran. The dam is subjected to multiple seismic hazards including ground shaking, movements along multi-directional discontinuities and faults in the dam footprint. Due to the presence of these discontinuities and secondary faults, the originally planned concrete gravity dam with a slip joint across the main fault was replaced by a conservatively designed earth core rockfill dam. The worst-case earthquake scenario is a magnitude 7.5 earthquake at a distance of 1.5 km from the dam site causing a horizontal peak acceleration of 0.75 g and maximal movements along faults in the dam footprint of 1.5 m. A large freeboard was provided to cope with seismic deformations of the dam body and the run-up of impulse waves caused by mass movements into the reservoir. The first reservoir impounding started in 2017 (Wieland 2019).

2.4 Southeast Asia

The Xayaburi Hydroelectric Power Project (Figure 3) is a run-of-river hydropower plant located in the mainstream of the Mekong River, in Lao PDR, approximately 100 km downstream of the city of Luang Prabang. The scheme includes a navigation lock, spillway and intermediate block, and the main powerhouse with an installed capacity of 1,285 MW.

The project also comprises state-of-the-art fish passing facilities for upstream and downstream migration. The project was commissioned in 2019 (Morier-Genoud 2019).

At present the 1460 MW Luang Prabang run-of-river power plant, located about 30 km upstream of Luang Prabang in Laos, is under construction in which Swiss dam consultants are involved.

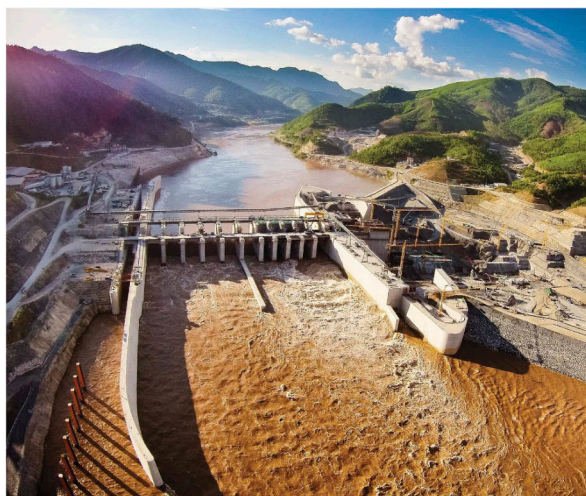


Figure 3. View of Xayaburi dam.

Nam Ou VI, located along a tributary of the Mekong River in Laos, is an 88 m high rockfill dam with an upstream geomembrane. The composite PVC geomembrane, installed using an innovative design, is now increasingly adopted to construct rockfill dams, which allows the construction of embankment dams at lower costs. At Nam Ou VI the geomembrane system was installed in three stages (Scuero et al. 2016).

Son La and Lai Chau are RCC dams located in Vietnam. The highlight of those projects is the use of “pond ash” i.e. fly ash that went into a waste lagoon as a slurry as nobody in Vietnam had any use for such material. Son La was the first RCC dam globally that made use of such material as a major cementitious material in the mix. Lai Chau again used it, as well as other large RCC dams in Vietnam and later also in Laos. Both projects were completed ahead of schedule (Conrad et al. 2010, Conrad et al. 2014).

2.5 Africa

Worth mentioning are the design and construction supervision of a number of irrigation, water supply and flood protection dams in North Africa by various Swiss consulting firms. Swiss consultants also served as members of panels of experts for different dams in Africa and have advised on the formation of the Dam Safety Directorate in Ethiopia, the country with the largest number of dams under construction in Africa. In the past decade, a number of hydraulic model studies on African dam projects have been performed at the hydraulic laboratories of the Swiss Federal Institutes of Technology in Lausanne (Stojnic et al. 2018) and Zurich (e.g. Arnold et al. 2018). Water resources management studies are also worth to mention (Gamito de Saldanha Calado Matos and Schleiss 2017).

2.6 Americas

The Toachi-Pilatón hydroelectric power plant uses the water from the homonym Rivers, in the North-West of Ecuador. The power plant has an installed capacity of 255 MW and is connected to the 59 m high Toachi concrete gravity dam. Construction was completed in 2015 (Lombardi 2023).

The Cerro del Águila HPP is located in the Peruvian Andes about 270 km from the capital Lima. This new scheme on the Mantaro River includes an 88 m high RCC arch-gravity dam, a 5.7 km long headrace tunnel, a 242 m high pressure shaft, an underground powerhouse with an installed capacity of 510 MW, and a 1.9 km long tailrace tunnel. A gated crest spillway with a discharge capacity of 7,000 m³/s is integrated in the dam body as well as 6 bottom outlets with a total capacity of 5,000 m³/s. At the dam toe, a 3 MW power plant makes use of the ecological flow. Construction was completed in 2016 (Lombardi 2023).

2.7 Oceania

It is worth mentioning that physical model tests of the power intakes and surge chamber system of the Snowy 2.0 pump-storage scheme, presently under construction in Australia, were carried out at the hydraulic laboratory of EPF Lausanne (PL-LCH EPFL 2023).

3 DAM REHABILITATION

3.1 Aging

The Enguri dam (Figure 4), located in the western part of Georgia, is a 272 m high arch dam and until recently was the highest arch dam in the world. The dam was completed in 1984, several years after the power production at reduced head started (the units were commissioned in 1978-80). Treatment of the dam foundation and other works continued until 1988, the first year in which the reservoir was allowed to be filled to its maximum level.

After independence from the former Soviet Union the dam suffered due to the lack of maintenance and political unrest. Among the major parts of the scheme affected were the dam hydro-mechanical works particularly the drainage system, electro-mechanical elements and the low-level outlets of the dam, all contributing to poor reliability and safety in operation of the scheme.



Figure 4. Enguri arch dam, Georgia.

An expert mission was then organized by a group of Swiss and French Engineers aimed at defining a rehabilitation program (Quigley et al. 2006), which consisted mainly of:

- General safety assessment and identification of the status of the monitoring equipment for the dam;
- Assessment of the feasibility of the rehabilitation of the entire project; and
- Definition of the scope of the work required for the dam body, pressure tunnel and powerhouse.

The first phase of the rehabilitation works extended until 2006.

Within the grid of Montenegro the Hydro Power Plant Piva plays an important role. It has been in operation since 1976 and needed to be rehabilitated. The plant is located in the north-western part of Montenegro, close to the border with Bosnia and Herzegovina. The high storage capacity of the basin guarantees a high plant utilisation factor, even during dry years. The 220 m high arch dam, also known as Mratinje Dam, is one of the highest arch dams in Europe. The hydro-mechanical and electrical-equipment as well as the civil structures, including the dam, intake and outlet structure needed rehabilitation and modernisation in order to extend their economic lifespan (Obermoser 2009). Based on a detailed investigation, short-term rehabilitation measures related to the dam were identified, including rock support in unlined galleries, improvement of the dam grout curtain and modernization of the dam monitoring system. The observed damage to the dam concrete were minor and could be addressed as part of regular maintenance.

The Studena dam in Bulgaria is a 55 m high buttress dam in a seismically active region. The dam, composed of 25 blocks, is used for water supply, hydropower generation, and flood protection. Heavy deterioration of the concrete face required complete rehabilitation. As the water supply could not be interrupted, rehabilitation works had to be performed, mostly underwater. A new watertight synthetic facing covers the upstream face of the dam. A major challenge was the repair of the upstream face because of its complicated geometry with complex intersecting concave corners requiring special fixation of the membrane and the very low temperatures during the construction work (Scuero et al. 2019).

The Kariba Dam is a 128 m high arch dam that was constructed between 1955 and 1959 across the Zambezi River that borders Zambia and Zimbabwe. The six centrally located submerged sluices form the spillway with a combined discharge capacity of 9,000 m³/s. Prolonged spillages with a total volume of 511.1 km³ through the floodgates from January 1962 to June 1981 resulted in an 80 m deep scour hole in the plunge pool immediately downstream of the dam (Figure 5).

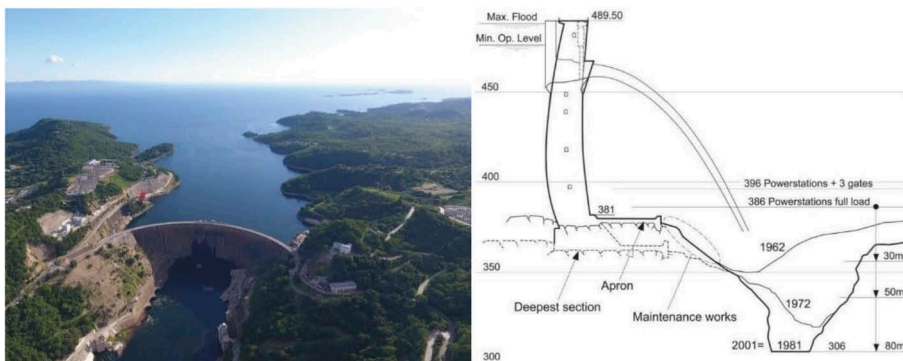


Figure 5. Kariba arch dam and the evolution of scouring close to the dam toe.

Numerical modelling and hydraulic model tests were carried out in order to define the geometry of the reshaping of the plunge pool to avoid further scouring (Stojnic et al. 2018). The remedial works are presently in progress (Mellal et al. 2023). In addition, the hydromechanical equipment of the 6 spillways, threatened by the development of alkali-aggregate reaction in the dam concrete, is being refurbished.

3.2 Alkali-aggregate reaction

The Chambon dam in France is an excellent example of how geomembrane systems can contribute to the extension of the lifespan of a dam. This 137 m high concrete gravity dam, completed in 1935, is affected by alkali-aggregate reaction (AAR). A series of slot cuttings were made and a drained exposed PVC geomembrane system was installed in 1994 to provide waterproofing

protection at the upstream face. In 2013, the owner decided to carry out new slot cutting, and to strengthen the dam by means of an upstream system of tendons and carbon bands, which required removing the geomembrane system. The same geomembrane system was installed again. Rehabilitation works were successfully completed in 2014 (Scuero et al. 2016).

The Pian Telesio dam is an arch gravity dam completed in 1955 in Northern Italy. With a height of 80 m and a crest length of 515 m the dam impounds a reservoir with a capacity of 24 Mm³. The dam thickness ranges from 5.7 m at the crest to a maximum of 35 m at its base. After approximately 20 years of operation the dam showed an upstream drift of up to 60 mm at the central pendulum in 2008. It was concluded that the permanent displacements were caused by the concrete expansion due to AAR. Rehabilitation works required the cutting of 16 vertical slots with a depth of 21 to 39 m, using a diamond wire saw (Amberg et al. 2009). Further analyses are still performed in order to assess the time-dependent decrease of the dam safety (Stucchi et al. 2023).

The Kainji dam is located on the river Niger in Nigeria. The plant suffers from AAR, especially the spillway structure, since a few years after its commissioning in 1968. The mass concrete structures on both sides of the spillway apply a thrust on the spillway structure. The mechanism is in general confirmed by monitoring results and visual observations. To mitigate the negative effect of AAR, rehabilitation works were carried out in 1996/97, comprising slot cutting for relief of compressive stresses, drilling of drainage holes and installation of additional monitoring instruments. Thanks to the previous rehabilitation works, there is sufficient evidence to conclude that the spillway can safely be operated within the coming years. Rehabilitation and upgrading of the monitoring instruments and improvement of the surveillance procedures are on the way (Ehlers et al. 2023).

3.3 *Seismic resistance*

The Fontanaluccia dam is a 40 m high and almost 100-year-old structure constituted by a central multiple-arch masonry dam body with the spillway and two side cyclopean concrete gravity dam sections. The dam is located in a narrow valley in the Italian Apennine region, a moderate-to-high seismic area. Following the release of new guidelines on the seismic safety assessment of dams in Italy in 2019, a re-assessment of the seismic safety of the dam was carried out. The results of the dynamic analyses showed that the multiple arch section is vulnerable to the earthquake action in the cross-canyon direction, which required seismic strengthening of the dam. A retrofit program was developed to enable the dam to remain in operation during the remedial works. (Abati et al. 2023).

3.4 *Dam heightening*

The Cambambe arch dam on the Kuanza River in Angola, was built from 1959 to 1963. From its initial conception, the dam was planned to be heightened in a later stage. However, for different reasons these works did not start until 2010. The initial arch dam was 72 m high, with a crest length of 250 m. The heightening of the dam was planned to be 20 m leading to a final dam height of 92 m. The heightening works (Figure 6) were completed in 2020 and took place at the same time as the rehabilitation of the existing power plant and the construction of a new open-air power plant. The management of the flood release during the construction of the dam-heightening required proper timing of the works (Wohnlich et al. 2012).

3.5 *Sediment bypass tunnels to counter reservoir sedimentation*

Nanhua reservoir in Taiwan suffers from large and ongoing sedimentation, threatening its sustainable operation. A large sediment bypass tunnel to route sediment from turbidity currents past the dam was planned and built, which was cross-checked by experts from the hydraulic laboratory of ETH Zurich (Boes et al. 2018). Similarly, the refurbishment of an existing sediment bypass tunnel with granite pavers at the Mud Mountain dam in the US Pacific Northwest was profiting from Swiss research and development performed at ETH Zurich (Auel et al. 2018), gaining an American engineering award. Another sedimentation model study



Figure 6. Heightening of Cambambe dam in Angola.

with settling pond and bypass tunnel was conducted at the ETH Zurich laboratory for a new reservoirs dam in Pakistan (Beck et al. 2016, Boes et al. 2019).

4 DAM SAFETY

4.1 *Post-seismic inspections*

The 106 m high Sefid Rud buttress dam, located in the Alborz Mountains in Iran, was completed in 1962. The dam was designed to withstand a peak ground acceleration (PGA) of 0.25 g. The dam was damaged by the magnitude 7.4 Manjil earthquake of the 21 June 1990, during which the nearby cities of Manjil and Rudbar were destroyed. The horizontal component of the PGA was estimated as 0.7 g. The main shock was followed by several strong aftershocks with magnitudes up to 6.0. The top portion of the dam was damaged. A large crack along the horizontal lift joint about 18m below the dam crest was observed on the upstream face of the dam involving all buttresses. In one buttress a wedge was created on the downstream face by a system of horizontal and inclined cracks along construction joints, which was displaced by about 30 mm. Spalling of concrete along the vertical block joints were also noticed as well as leakage through some of the cracks. Detailed inspection (Wieland et al. 2003) led to rehabilitation works including epoxy grouting and post-tensioned rock anchors.

On January 12, 2010, a magnitude 7.0 earthquake caused extensive damage and loss of lives in Haiti. The Péligre dam located about 60 km from the epicenter, was inspected in March 2010 (Droz et al. 2010). In the absence of appropriate monitoring instrumentation, only a thorough visual inspection could be made. No signs of structural damage were visible. However, because of the relatively large epicentral distance the level of ground shaking at the dam was rather low.

4.2 *Dam monitoring instrumentation and survey*

The Inga 1 (Figure 7) and 2 hydropower schemes are located on the Congo River, approximately 150 km southwest of Kinshasa. Both dams are of the buttress type and have shown irreversible movements downstream for decades. Unfortunately, the monitoring instrumentation of the dams, which was installed at the time of the construction, in the 1970s for Inga 1 and in the 1980s for Inga 2, appears to be incomplete, in poor condition, obsolete or inadequate to follow up the evolution of the deformations, in particular due to AAR, and to assess the safety of the dams regularly. In view of these problems a project, financed by the World Bank, was implemented (Droz et al. 2019):

- To improve the quality of the surveillance of the structures by restoring and enhancing the monitoring system of the dams and of the hydro plants as well as installing an adequate geodetic network; and
- To carry out the necessary investigations and studies to determine the causes of the irreversible movements observed in most of the structures of both Inga 1 and 2.



Figure 7. Inga 1 dam, DR Congo.

The Sardar Sarovar Dam is a concrete gravity dam built on the Narmada River in India. The dam was built to provide water and electricity to four Indian states. The gravity dam is 136 m high with a crest length of 1300 m. Almost 400 sensors were installed around 1994. The rehabilitation project was organized in 5 steps. In 2021 (step 1), functional tests of the existing instruments were carried out. Then, the system was upgraded from manual to semi-automatic by installing multiplexer boxes. In 2022, after the partial rehabilitation of the existing shafts (step 2), 3 new 76 m long direct pendulums were installed (step 3) with an automatic acquisition system for measuring the horizontal deformations of the dam. The commissioning of the complete automatic plumb-lines is planned for 2023 (step 4). By switching from manual and semi-automatic to fully automatic monitoring (step 5), the dam owner benefits from a quicker and safer monitoring of the dam (Ballarin et al. 2023).

Many of the dams in Sri Lanka are ageing and suffer from various structural deficiencies and shortcomings in their operation and maintenance procedures. To overcome these inadequacies, the Dam Safety and Water Resources Project (DSWRPP) was initiated in August 2008, with the assistance of World Bank financing. Besides rehabilitation of 32 major dam structures that show signs of deterioration, improvement of the monitoring data acquisition and analysis was performed (Sorgenfrei et al. 2011).

The installation of a monitoring system on and around the Usay dam remains an exceptional project. Lake Sarez in the Pamir Mountains in Tajikistan was formed in 1911 when a massive earthquake triggered a rockslide that buried the village of Usay under a 650 m high mass of rock and ice debris, which dammed the Murghab River. The resulting 60 km long lake containing over 17 km³ of water was created by the Usay landslide dam, the highest dam in the world. Owing to its huge mass, the level of knowledge of the Usay dam (Figure 8) is reduced to hypothesis based on observations and analysis of a few parameters gathered in the past, in particular the seepage rate evolution through the natural embankment. In order to reduce the risk related to Lake Sarez, a modern monitoring system and an early warning system were installed in 2006. The monitoring system covers an unstable slope, located some 4 km upstream of the dam, which, if it would fail, would create impulse waves that could threaten the stability of the dam or, at least, modify its seepage regime (Droz et al. 2006 and 2008).



Figure 8. Usoy landslide dam storing Lake Sarez in Tajikistan.

4.3 *Emergency preparedness plans*

Besides a safe design and construction of high quality as well as appropriate maintenance, monitoring and surveillance, the third pillar on which lays the safety of dams is the preparedness in case of emergency which enables to cope with residual risks. Recently, Emergency Preparedness Plans (EPP) have been elaborated for 20 dams in Turkey.

At present, the EPPs of Rogun dam (under construction), of Nurek dam a 305 m high ECRD located directly downstream Rogun and completed in 1980, and of Kariba dam (both under rehabilitation), are under elaboration.

4.4 *Capacity building*

A dam safety project incorporating five dams along the Drin and Mat Rivers was carried out in the northern part of Albania. One of the components of the project was the refurbishment and upgrading of the monitoring instrumentation for all five dams. The goal was to implement a durable modern monitoring system. The new instruments will help to improve the long-term safety of the dams. The safety, however, can only be improved if the installations are properly maintained, the instruments are frequently read, and the values are immediately evaluated and regularly analysed by specialized engineers. Hence training was the most important component for the sustainability of this investment. The instrument and software installations were completed with a comprehensive training program for both dam wardens and specialized engineers in charge for the data analysis and reporting (Stahl et al., 2013).

The Dam Safety Enhancement Program (DaSEP) was set in 2010. DaSEP aimed at improving the dam safety procedures of the thousands of dams under the responsibility of the Chinese Ministry of Water Resources (Méan et al. 2012). The various missions of Swiss experts and the training of Chinese counterparts in China and in Switzerland resulted in the modification of the legal dam safety regulatory framework in China, including, for example, the obligation to prepare annual safety reports and define clearly roles and responsibilities for small and medium size dams.

In the wake of the failure of the Xepian-Xenamnoy saddle dam in Laos in 2018 (Schleiss et al. 2019), a nationwide dam safety inspection was launched. The synthesis report of the main findings of the various inspections pointed out the necessity to improve the dam safety organization and procedures in Lao PDR including technical (Droz et al. 2022) and institutional (Darbre et al. 2022) aspects. This Swiss Agency for Development and Cooperation project is in progress and has already given fruitful results with the membership of Laos as full member of the ICOLD community, the modification of the Dam Safety Law, and the creation of a department specifically in charge of dam safety.

5 CONCLUSIONS AND PERSPECTIVES

After a long period of dam construction in Switzerland, owners, consulting firms and contractors, like their European colleagues, are facing aging problems of these dams, which on average are 75 years old. Coping with the aging problem requires rehabilitation works and the development of new solutions. The know-how gained may be used in other projects worldwide, including new dam projects, dam safety assessment, dam rehabilitation, as well as dam heightening and capacity building. Nowadays, due to climate change issues and increasing energy demand, new projects are under development in Switzerland.

ACKNOWLEDGMENTS

The preparation of this paper would not have been possible without the support of the following consulting firms, contractors, organisations and research institutes: AFRY, BG, Carpi, EPFL (PL-LCH), ETH Zurich (VAW), Gruner Stucky, Norbert Géologues, Helvetas, Huggenberger, IM Maggia, Lombardi, Rittmeyer and Walö.

REFERENCES

- Abati, A., Gatto Frezza, G. A., Sparnacci, R. 2023. Seismic safety assessment of an old multiple arch gravity dam. *Symposium "Management for Safe Dams" - 91st Annual ICOLD Meeting – Gothenburg*.
- Amberg, F., Bremen, R., Brizzo, N. 2009. Rehabilitation of the Pian Telesio dam (IT) affected by AAR-reaction. *23rd ICOLD Congress, Brasilia, Q. 90*.
- Arnold, R., Bezzi, A., Lais, A., Boes, R.M. (2018). Intake structure design of entirely steel-lined pressure conduits crossing an RCC dam. *Proc. Hydro 2018 Conference*, Gdansk, Poland: Paper 04.02. Aqua~Media International, Wallington, UK.
- Auel, C., Thene, J.R., Carroll, J., Holmes, C., Boes, R.M. (2018). Rehabilitation of the Mud Mountain bypass tunnel invert. *Proc. 26th ICOLD Congress*, Vienna, Austria, Q.100-R.4: 51–71.
- Ballarin, A., Gardenghi, R., 2023, Huggenberger Communication.
- Beck, C., Lutz, N., Lais, A., Vetsch, D., Boes, R.B. (2016). Patrinid Hydropower Project, Pakistan Physical model investigations on the optimization of the sediment management concept. *Proc. Hydro 2016 Conference*, Montreux, Switzerland: Paper 26.08.
- Berchtold, Th., Pfister, M. (2011). Kárahnjúkar Dam spillway, Iceland: Swiss contribution to reduce dynamic plunge pool pressures generated by a high-velocity jet. in: *Dams in Switzerland*. Swiss Committee on Dams, pp. 315–320, ISBN 978-3-85545-158-6, Switzerland.
- Boes, R.M.; Beck, C.; Lutz, N.; Lais, A.; Albayrak, I. (2017). Hydraulics of water, air-water and sediment flow in downstream-controlled sediment bypass tunnels. In *Proc. 2nd Intl. Workshop on Sediment Bypass Tunnels* (Sumi, T., ed.), paper FP11, Kyoto University, Kyoto, Japan.
- Boes, R.M., Müller-Hagmann, M., Albayrak, I., Müller, B., Caspescha, L., Flepp, A., Jacobs, F., Auel, C. (2018). Sediment bypass tunnels: Swiss experience with bypass efficiency and abrasion-resistant invert materials. *Proc. 26th ICOLD Congress*, Vienna, Austria, Q.100-R.40: 625–638.
- Bollaert, E., Tomasson, G. G., Gisiger J.-P., Schleiss, A. 2003. The Karahnjúkar hydroelectric project: transient analysis of the waterways system. *Wasser Energie Luft, Heft 3, 2003*.
- Conrad, M., Dunstan, M.R.H., Morris, D., Pham Viet An, 2010. The Son La RCC dam – Testing in-situ properties, *Hydro Asia 2010*.
- Conrad, M., Morris, D., Nguyen Phan Hung 2014. The RCC dam for the Lai Chau HPP- RCC full scale trials and challenges in the construction of the RCC dam, *Hydro Asia 2014*.
- Darbre, G., Droz, P., Malaykham B. 2022. Institutional organization for dam safety in Lao PDR, *ICOLD Q105/R1, June 2022*, Marseille.
- Droz, P., Darbre, G., Malaykham, B. 2022. Emergency dam safety inspections in Lao PDR, *ICOLD Q105/R38, June 2022*, Marseille.
- Droz, P., Fumagali, A., Novali, F., Young, B. 2008. GPS and INSAR technologies: a joint approach for the safety of lake Sarez, *4th Canadian Conference on Geohazards, Université Laval, mai 2008*.
- Droz, P., Hegetschweiler, D 2010. Inspection du barrage de Péligré suite au séisme du 12 janvier 2010 en Haïti, *Eau Energie Air (WEL)*, 3–2010.
- Droz, P., Spacic-Gril, L. 2006. Lake Sarez Risk Mitigation Project: a global risk analysis, *Q86 – R75, 22nd ICOLD Conference on Large Dams, 2006, Barcelona*.

- Droz, P., Wohnlich, A. 2019. Rehabilitation of the monitoring system of Inga 1 and 2 dams, *Hydropower & Dams, Issue 2*, 2019.
- Ehlers, S., Goltz, M., 2023. The development of Alkali Aggregate Reaction (AAR) at the Kainji spillway structure after 50 years of operation, *Hydro Africa, Uganda*.
- Gamito de Saldanha Calado Matos, J. P., Schleiss, A. 2017. A free and state-of-the-art probabilistic flow forecasting tool designed for Africa. *Proceedings of Int. Conference Africa 2017, Marrakech, Morocco*.
- Ghader, S., Bussard., T. 2013. The study of drainage and water pumping of spillway and hydropower plant foundation in Sangtuda 2 project. Tajikistan. *1st Iranian Conference on Geotechnical Engineering, 22–23 October 2013. University of Mohaghegh, Ardabil, Iran IM, 2023, web site*.
- Kaelin, J., Olafsson, S., Leifsson, P.S. 2009. Filling and pressurizing the headrace tunnel at Karahnjúkar in Iceland. *Hydro2009, Lyon, France*.
- Lombardi, 2023, *web site*.
- Méan, P., Droz P., Cai, Y., Sheng, J 2012. Dam Safety Enhancement Program: A Cooperation Project between Switzerland and China, *Int. Symposium on dams for a changing world, ICOLD, Kyoto*.
- Mellal, A., Chibvura, C., Mhlanga, S. Z., Nkweendenda A, Munodawafa, M. C., Quigley, B.M., Arigoni, A. 2023. Use of computational modelling for prediction and follow up of dam behaviour during plunge pool reshaping of the Kariba Dam. *Symposium “Management for Safe Dams” - 91st Annual ICOLD Meeting – Gothenburg 13–14 June 2023*.
- Morier-Genoud, G. 2019. Fish pass design on the Mekong River – Challenges and lessons learned from Xayaburi HPP, *SHF Conference HydroES 2019, Grenoble, France, January 2019*.
- Obermoser, H., Pješčić, S., Conrad, M., 2009. Focused Rehabilitation of the Piva HPP in Montenegro, *Conference Hydro 2009, Lyon, France*.
- PL-LCH EPFL 2023, *Personal communication*.
- Pöyry 2014, <https://www.worldbank.org/en/country/tajikistan/brief/final-reports-related-to-the-proposed-rogun-hpp>.
- Quigley B., Matcharadze G. 2006. Upgrading and Refurbishment of Enguri Dam and Hydro Power Plant in Georgia, *HYDRO 2006, Porto Carras, Greece*.
- Schleiss, A., Tournier, J.-P., Chraïbi, A. 2019. XPXN-Saddle Dam D failure - IEP Final Report, *ICOLD annual meeting, Ottawa, 2019*.
- Scuero, A., Vaschetti, G., Machado do Vale, J. 2016. A unique case: new works at Chambon dam. *International Symposium on “Appropriate technology to ensure proper Development, Operation and Maintenance of Dams in Developing Countries”, Johannesburg, South Africa*.
- Scuero, A. Vaschetti, G. 2019. Underwater technologies for rehabilitation of dams: Studena case history. *ICOLD annual meeting, Ottawa, 2019*.
- Scuero, A. Vaschetti, G. J. Cowland, J., Cai, B., Xuan, L. 2016. Nam Ou VI: Geomembrane Face Rock-fill Dam in Laos. *Proceedings of Asia 2016, Vientiane, Lao PDR, 2016*.
- Sorgenfrei, A., Friedrich, M. 2011. Dam Safety and Operational Efficiency Improvements in Sri Lanka, *ICOLD 70th Annual meeting, Lucerne, Switzerland, June 2011*.
- Stahl, H., Celo, M. 2013. Refurbishment and Upgrading of the Monitoring Instrumentation for Fierza and Ulza Dams in Albania, *Proc. ICOLD European Club Symposium held in Venice, Italy, Paper B18*.
- Stojnic, I., Ylla, C., Amini A., De Cesare, G., Bollaert, E.F.R., Mhlanga, S.Z., Mazidza, D.Z., Schleiss, A.J. 2018. Kariba plunge pool rehabilitation, *HYDRO 2018 proceedings, Gdansk, Poland*.
- Stucchi, R., Catalano, E., 2023. Numerical modelling of the Pian Telesio dam affected by AAR. *Proc. 12th ICOLD European Club Symposium “Role of dams and reservoirs in a successful energy transition”, Interlaken, Switzerland (Boes, R.M., Droz, P. & Leroy, R., eds.)*, Taylor & Francis, London.
- Stucky Gruner, 2023, *web site*.
- Tirunas, D., Aspen, B.V. 2018. The Moglice Hydropower Project, Albania – Construction Design Experience. *Proc. of HYDRO 2018, Gdansk, 15.-17.10.2018. Int. J. on Hydropower and Dams*.
- Tzenkov, A.D., Kisiakov, D.S., Schwager, M. 2023. An application of sophisticated FEM and simplified methods to the seismic response analysis of an asphalt-concrete core rockfill dam. *Proc. 12th ICOLD European Club Symposium “Role of dams and reservoirs in a successful energy transition”, Interlaken, Switzerland (Boes, R.M., Droz, P. & Leroy, R., eds.)*, Taylor & Francis, London.
- Wieland, M., Aemmer, M. and Ruoss, R. 2008. Designs Aspects of Deriner Dam. *Int. Water Power & Dam Construction, Volume 60 Number 7, pp 19–23*.
- Wieland, M., Brenner, R.P., Sommer, P. 2003. Earthquake resiliency of large concrete dams: damage, repair, and strengthening concepts, *ICOLD Conference, Montreal, 2003*.
- Wieland, M., Roshanomid, H. 2019. Seismic design aspects and first reservoir impounding of Rudbar Lorestan rockfill dam. *Proc. Symposium on Sustainable and Safe Dams around the World, ICOLD 2019 Annual Meeting, Ottawa, Canada, June 9–14, 2019*.

Dam surveillance in Switzerland: A constant development

Henri Pougatsch

Civil engineer EPF, Formerly Commissioner for Dam Safety Water and Geology

Isabelle Fern

Civil engineer EPFL, Head of hydraulic team, Lombardi SA Ingénieurs Conseils, Fribourg, Switzerland

ABSTRACT: The main purpose of this article is to recall the essential elements that govern the installation of a monitoring system whose purpose is to follow-up the behavior of water retention structures. It describes the past, the present and the future of this type of installation.

RÉSUMÉ: Le propos principal de cet article est de rappeler les éléments essentiels qui régissent l'installation d'un dispositif d'auscultation dont le but est d'assurer le suivi du comportement des ouvrages d'accumulation. Il fait état du passé, du présent et du futur de ce type d'installation.

1 INTRODUCTION

In the 1920s, Switzerland undertook many constructions of large dams. Specific monitoring systems were developed to gather data of the dams and its surroundings to assess their behaviours, guarantee safety and improve the design of new ones. The Montsalvens dam, in Canton of Fri-bourg, with a height of $H=55\text{m}$, was the first to be equipped with monitoring instruments. Using triangulation and leveling (Figure 1), clinometers and thermometers at different points, it was possible to assess the deformations for different levels of restraint and thermal stresses. The purpose of these measurements was to confirm the correctness of the calculation assumptions. The Federal Office of Topography was responsible for the triangulation and leveling measurements. In 1932, a pendulum reading system, developed by Juillard, was installed at the Spitalamm dam (Canton of Bern). This instrument became an essential monitoring device for Swiss dams and around the world.

Gradually, the monitoring of dams became predominant and the requirements for this mode of monitoring evolved. It resulted in increased precision and simplification of measurements. In addition, the computer processing of the data allowed a powerful analysis. Given the importance attributed to the monitoring device, adaptations have been made periodically in relation to the knowledge acquired and the new requirements.

2 LEGAL REQUIREMENTS

With the intensification of the construction of dams, the Swiss authorities deemed useful to complete the legislation, which was limited at that time to article 3bis of the federal law on the water police of June 1877, which also applied to dams. When it was drafted, the overriding importance of dam monitoring was recognized. An article of this regulation specifies that installations adapted to the dimensions of the structure will be fitted with so that it is possible

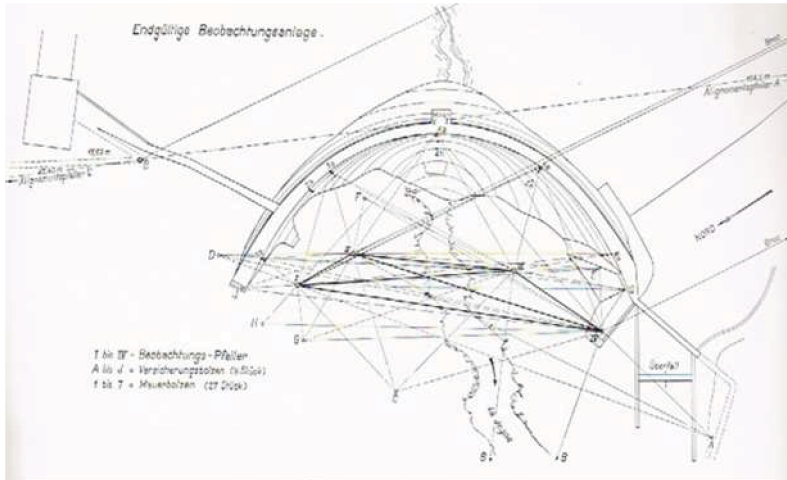


Figure 1. Montsalvens dam Map of the network of trigonometric and alignment measurements (after CSGB 1946).

to measure both the loads which apply on the structure (causes) and the various parameters which characterize the behavior of a restraint (consequences). These measures should already be undertaken during the construction of the structure. Mention is also made of the importance of performing measurements regularly and interpreting them without delay. It is also requested to compile a dam file and keep it up to date. Over time, this regulation has undergone various modifications and improvements. Currently, the legislative aspect is regulated by the federal law on accumulation works (WRFA, 2010. RS 721.102 of October 1, 2010) and its ordinance (WRFO. 2012. RS721.101.1 of October 17, 2012). These were supplemented in 2002 by Regulations which govern the methods of application of the ordinance and in particular provide information on the safety concept. It is based on three pillars which are: structural safety, monitoring and maintenance and emergency plan (Figure 2). It should be noted that the first pillar minimizes the risk while the other two minimize the residual risk.

Monitoring involves setting up a strict organization to monitor the behavior of storage structures and their foundations. It calls on the operator's staff, engineers and experts in the field of dams. They must ensure in all circumstances that the structure and its foundations behave appropriately and, if necessary, propose any useful measure to remedy any potential threat. It should be noted that during the life of the dam, even unpredictable phenomena may occur. Three essential tasks are carried out according to a precise program: a) visual checks, b) direct measurements from monitoring instrument, and c) operating checks of moving parts, instrumentation and means communications.

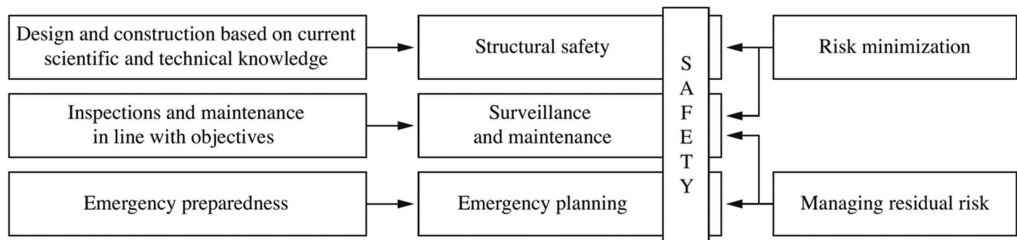


Figure 2. Diagram of the safety concept in effect for dam structures in Switzerland based on the three pillars (from SFOE, 2015a).

3 OBJECTIVES OF THE MONITORING SYSTEM

The measurement system has several purposes. First, to run checks during construction and first impounding; for this reason, such system will already be planned as part of the project. Checks are carried out during operation in order to detect any anomalies in behavior in time. Secondly, it permits gaining knowledge on the behavior of the dam and improve the design of new ones.

4 PRINCIPLE AND CONCEPT

The monitoring system must permit to measure the external loads which apply to the structure, especially the hydrostatic load (water and ice) and sediment pressure, the temperature of the water and the air and any seismic loads. The various parameters which characterize the behavior of a retaining structure, namely the deformations undergone by the foundations and the body of the dam, the leaks and percolations through the dam and the foundations, the thermal state, the uplift pressure in the dam foundations as well as the pore water pressures and possibly the saturation lines in the dykes (Table 3).

Concrete dam	Embankment dam	Foundations
Structural deformation	Deformation in the dam body	Deformation Abutment movements
Local movements (cracks, joints)	Specific movements (connection with a concrete structure)	Specific movement (cracks, diaclases)
Dam body temperature	Dam body temperature to detect seepage (possible)	
Uplift (at the concrete-foundation interface and in the rock)	Pore pressure in embankment dam body and piezometric level	Pore pressure Deep body uplift pressure Piezometric level Groundwater level
Seepage and drainage flow	Seepage and drainage flow	Seepage and drainage flow, resurgence (springs)
Chemical analysis of seepage water Turbidity (possible)	Chemical analysis of seepage water Turbidity	Chemical analysis of seepage water Turbidity

Figure 3. Significant parameters measured using monitoring instrumentation (after Schleiss and Pougatsch, 2011).

The monitoring instrumentation project will be adapted to the particularities and the importance of the accumulation structure. In addition, it will be taken into account that the dam and its foundations constitute a whole, so it must make it possible to clearly distinguish the behavior of the dam from that of its foundations and its surroundings. There is no rule to define the number of measuring devices needed to ensure satisfactory monitoring of behavior; it is preferable to have a limited number of reliable instruments, which also facilitates the interpretation of the measurements. To deal with breakdowns or failures, it is recommended to provide redundant measurements of certain parameters (i.e., the measurement of deformations). It should also be noted that a monitoring instrument is not a fixed system. Indeed, it is good to examine periodically if it still satisfies the requirements and the needs; if necessary, it is supplemented, adapted or modernized. Even if the instruments offered are more and more numerous and are constantly evolving, it should however be noted that the parameters to be measured remain the same. Table 4 shows by way of example the different equipment and types of measurement in use for the monitoring of concrete dams and their surroundings.

Type of measurements	Equipment
Structural deformation	Direct pendulum Inverted pendulum Inclinometer Extensometer Fiber-optic sensor and cable Geodesy Geodetic survey (terrestrial measurements and GPS) Leveling Polygonal Vertical line of sight Simple angular measurements Alignment
Local movements (cracks, joints)	Jointmeter Micrometer Fiber-optic sensor and cable Dilatometer Deformeter
Dam body temperature	Normal thermometer Electronic thermometer Fiber-optic sensor and cable
Uplift at the concrete-foundation interface	Manometer Pressure cell
Leaks, seepage, and drainage flow	Weir, venturi Volumetric measurements
Chemical analysis of seepage water	
Tension of anchors (in the body of the dam, in the foundation)	Load cell (hydraulic or electrical system)

Figure 4. Equipment and types of measurement of a concrete dam.

5 REQUIRED QUALITY OF THE INSTRUMENTATION AND EXPECTED EVOLUTION

The choice of measuring devices depends on the parameters to be observed, the construction method of the structure and the installation possibilities. The choice must be adapted to each specific case. Priority must be given to instruments meeting the following criteria (CSB, 2005, 2006): simple and robust,

- precise and reliable,
- durable,
- easy to read,
- insensitive to environmental conditions; provided that they are not integrated into the body of the structure, they will be accessible and replaceable.

To deal with breakdowns or failures, it is recommended to provide redundant measurements of certain parameters (for example, the measurement of deformations). Regarding the reliability of measuring devices, the failure rate is highly variable and depends on the type of instrument. It should also be noted that the longevity of the instruments is less than the life-span of the dam. In general, suitable monitoring of deformations requires an extensive (Figure 5) and spatial (Figure 6) measuring device, which makes it possible, using geodesy,

to collect information on the altimetric and planimetric displacements of selected points. The control or measurement points are located on the crest and in the galleries, on the facings or on the embankments as well as on the ground (surroundings of the dam). As part of the routine monitoring of a low or medium-height structure, we are often limited to monitoring the movements of points located at the crest level. Sometimes a faulty instrument needs to be replaced. It is therefore recommended to have suitable reserve instruments (CSB, 2013a).

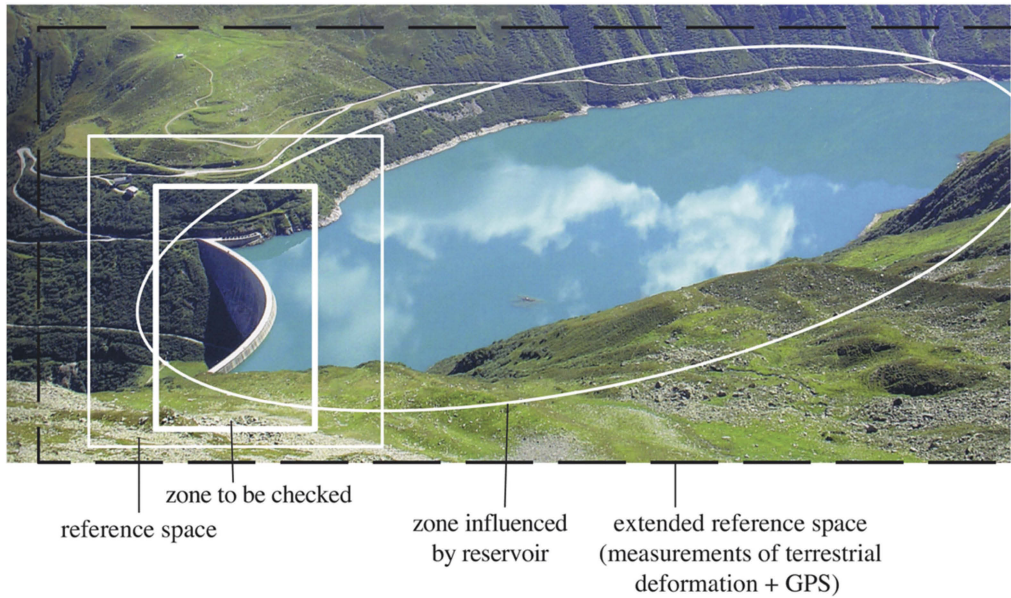


Figure 5. Extended reference space (terrestrial deformation measurements + GPS) (after Schleiss and Pougatsch, 2011).

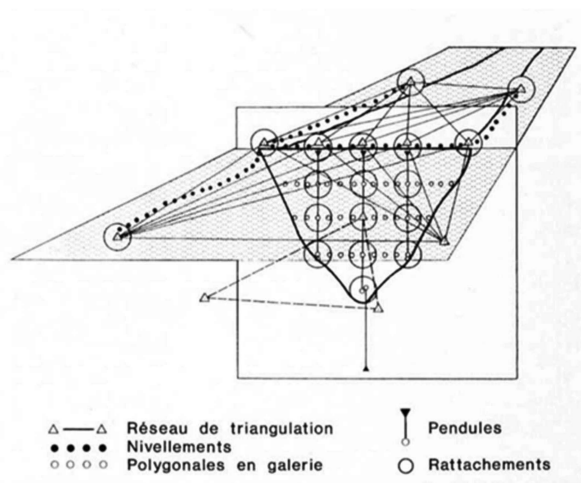


Figure 6. Diagram of a spatial measurement network (after Biedermann, 1997).

6 ANALYSIS OF RESULTS AND PREDICTION OF BEHAVIOR

In order to adequately interpret the behavior of a dam, it is possible to rely on mathematical models which determine the expected response under the effect of the applied loads. Interpretive models allow checking the plausibility of the measurements and to identify any irreversible behavior. The two main families of models used are on the one hand statistical and on the other hand deterministic. The latter are particularly useful in the case of the interpretation of the displacements of concrete structures whose reaction is mainly influenced by the level of the reservoir as well as the thermal state.

The overall monitoring process for an accumulation structure is illustrated in Figure 7.

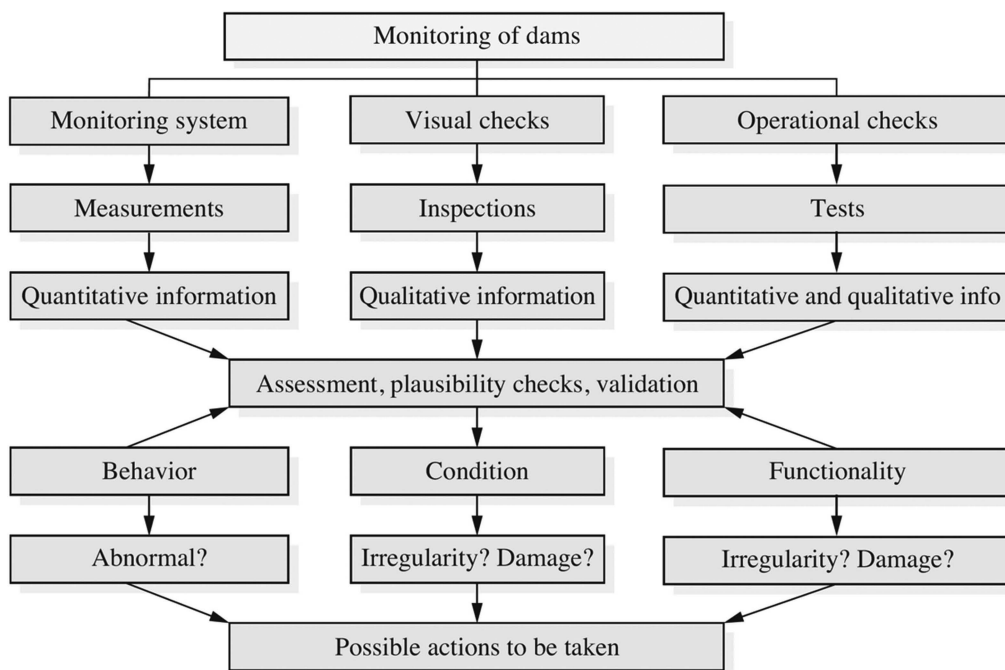


Figure 7. Process for monitoring an accumulation structure (Schleiss and Pougatsch, 2011).

7 THE MAIN RECENT DEVELOPMENTS IN INSTRUMENTATION AND THEIR APPLICATIONS

7.1 Strain and temperature measurements

a) Fiber-optic sensors and cables In the context of new measurement technology, it should be noted that fiber-optics have been used in measuring instruments in dams since the 1990s, primarily as (CSB, 2005a):

- A device in which the optical fiber is itself the measuring instrument (such as the extensometer)
- A device in which various phenomena are measured along the fiber-optic cable.
- A device in which the optical fiber provides a means for transporting data (pressure, temperature, difference in length)

b) 3D measurements of deformation in a borehole.

The borehole micrometer is a mobile measuring device that enables measurement in successive 1-meter sections of, for example, differential variations in length along the borehole. This instrument is equipped with an inclinometer that determines displacement in 3 orthogonal directions along a vertical borehole (CSB, 2005a).

7.2 Displacement measurements

GPS (Global Positioning System)

Space measurements by satellite (accurate distance measurements between orbits and sensor)

7.3 Various surveys

a) Ground Survey Aperture Radar (GBInSAR)

Photogrammetry method using ground station images

b) Ground Penetrating Radar (GPR)

Detect changes in properties of near-surface ground layers, localization of defects or voids in concrete structures

7.4 Observation of surfaces

a) Face observation using a drone A hi-res photographic recording of the downstream face of the dam can be produced by using a drone, which can then form part of an inspection report. This type of inspection was used for the Zeuzier dam in Switzerland in 2016.

b) Laser scanning Laser scanning and digital imagery Accurate distance measurements using laser with high spatial resolution on surfaces (3D geometry of dam). This type of measurement was used for the St-Barthélémy dam A in Switzerland.

8 AUTOMATION AND TRANSMISSION OF MEASUREMENTS

Following the developments of electronics and data processing, the possibilities and the interest of the automation of the monitoring instrumentation increased. They allow a direct link with the user. Such devices consist of means of measurement (measuring devices), means of data transmission, automatic means of acquisition and storage of data (databases) and means of processing and presentation of data (analysis of measurement results, drawing up graphics and writing reports - Stucchi, Crapp R., Fern I., 2022).

REFERENCES

- Publications of the Swiss Committee on Dams - SDC (formerly Comité Suisse des Grands Barrages – CSGB or Comité National Suisse des Grands Barrages - CNSGB).
- CSGB, 1946. Mesures Observation et Essais sur les Grands Barrages Suisses 1919–1945.
- CNSGB, 1964. Comportement des Grands Barrages suisses.
- CNSGB, 1985. Barrages suisses - Surveillance et entretien. *published during the ICOLD 15th International Congress, Lausanne, Switzerland.*
- CNSGB, 1993. L'informatique dans la surveillance des barrages, saisie et traitement des me-sures. *Groupe de travail pour l'observation des barrages.*
- CNSGB, 1997a. Surveillance de l'état des barrages et check-lists pour les contrôles visuels. *Groupe de travail pour l'observation des barrages.*
- CNSGB, 1997b. Mesures de déformations géodésiques et photogrammétriques pour la surveillance des barrages, 82 pages. *Groupe de travail pour l'observation des barrages.*
- CSB, 2003. Méthodes d'analyse pour la prédiction et le contrôle du comportement des barrages. *Wasser, Energie, Luft - Eau, Énergie, Air, 95^e année. cahiers 3/4, 74-98.*
- CSB. 2005. Dispositif d'auscultation des barrages. Concept, fiabilité et redondance. *Groupe de travail pour l'observation des barrages.*
- CSB. 2006. Dispositif d'auscultation des barrages. Projet, fiabilité et redondance. *Groupe de travail pour l'observation des barrages. Wasser, Energie, Luft - Eau, Énergie, Air, 98^e année, cahier 2, 144-180.*
- CSB. 2013a. Géodésie pour la surveillance des ouvrages d'accumulation. *Groupe de travail pour l'observation des barrages.*

- CSB, 2013b. Instruments de mesures - contrôles et calibrages, *Groupe de travail pour l'observation des barrages* Legislative acts and Regulations.
- WRFA, 2010. Water Retaining Federal Act (in French, German, Italian). RS 721.101 of 1st October 2010 (State in 1st January 2013).
- WRFO, 2012. Water retaining Federal Ordinance (in French, German, Italian). RS 721.101.1 of October 17, 2012 (state in 1st April 2018).
- SFOE, 2015a. Directives sur la sécurité des barrages. PartieA: Généralités. Richtlinie über die Sicherheit der Stauanlagen. Teil A: Allgemeines. In French, German. Articles in Swiss technical journals and Congresses.
- Biedermann R., 1987. Anforderung an die Messeinrichtungen von Talsperren. *Wasser, Energie, Luft - Eau, Énergie, Air*, 79. Jahrgang, Heft 112, 10-11.
- Biedermann R., 1997. Concept de sécurité pour les ouvrages d'accumulation: évolution du concept suisse depuis 1980. *Wasser, Energie, Luft - Eau, Énergie, Air*, 89e année, cahier 314, 63-72.
- Bischof R. et al., 2000. 205 dams in Switzerland for the welfare of the population. *20th International ICOLD Congress, Q.77 - R.64. Beijing 2000, 997-1018.*
- Darbre, G. R. , Pougatsch, H. 1993. L'équipement de barrages dans le cadre du réseau national d'accélérographie. *Wasser, Energie, Luft - Eau, Énergie, Air*, 85e année, cahiers 11112, 368-373.
- Deinum Ph. J. 1987. Versuchsinstallation des Sperry-Tilt Sensing Systems zum Erfassen der Durchbiegung der Bogenmauer Emosson. *Wasser, Energie, Luft - Eau, Énergie, Air*, 79. Jahrgang, Heft 112, 17-19.
- Egger K., 1982. Geodätische Deformationsmessungen. Eine zeitgemässe Vorstellung. *Wasser, Energie, Luft - Eau, Énergie, Air*, 74. Jahrgang, Heft 112, 1-4.
- Gicot H., 1976. Une méthode d'analyse des déformations des barrages. *12th International ICOLD Congress, Mexico, Vol. IV, communication C1, 787-790.*
- Lombardi G., 1992. L'informatique dans l'auscultation des barrages. *Wasser, Energie, Luft - Eau, Énergie, Air*, 84e année, cahiers 112, 2-8.
- Lombardi G., 2001. Sécurité des barrages - Auscultation. Interprétation des mesures. *Commentaires généraux, 25 pages.*
- Pougatsch H., 2002. Surveillance des ouvrages d'accumulation. Conception générale du dispositif d'auscultation. *Wasser, Energie, Luft - Eau Énergie, Air*, 94e année, cahiers 9110, 267-271.
- Sinniger R., 1987. Observation des versants d'une retenue. *Wasser, Energie, Luft - Eau, Énergie, Air*, 79. Jahrgang, Heft 9. 209-210.
- Sinniger R., 1985. L'histoire des barrages. *EPFL, Polyrama, 1985, 2-5.*
- Schleiss A. et Pougatsch H., 2011. Les barrages. Du projet à la mise en service. *EPFL Press. Traité de génie civil, Vol 17. Presse polytechnique et universitaire romande.*
- Stucchi R., Crapp R., Fern I., Development of a Software as a Service platform for dam monitoring, *Hydro 2022, Strasbourg, France.*

Contributions of geodesy to the safety of dams in Switzerland

A. Wiget

Former Head of Geodesy, Federal Office of Topography, Swisstopo, Wabern, Switzerland

B. Sievers

Prof. em., University of Applied Sciences and Arts Northwestern, Switzerland

F. Walser

Senior Engineer and Member of the Board at Schneider Ingenieure AG, Chur, Switzerland

ABSTRACT: Geodetic deformation measurements have been used successfully in Switzerland for over 100 years to survey and monitor dams. They make it possible to determine any displacements and deformations of the dams as well as the surrounding terrain with high precision and reliability in relation to an absolute reference frame. Combined with other instruments for deformation measurements, geodetic methods contribute considerably to the determination of dam behaviour and to the assessment of exceptional situations or behavioural anomalies of dams and thus to their safety.

This article specifies the tasks and requirements of dam surveys. Established methods of geodesy, their evaluation as well as recent instrumental developments are described and possible methodological and technological developments are pointed out.

The article published in German in the journal «Wasser Energie Luft» 3-2023 as well as other publications by the working group on dam surveying of the Society for the History of Geodesy in Switzerland (GGGS) can be accessed on the website of the GGGS (www.gggs.ch > Virtuelles Museum > E-Expo Schweizer Talsperrenvermessung). Also available are an extensive bibliography of relevant technical publications beginning in 1920 and a picture gallery from different time-epochs categorized in 17 topics.

RÉSUMÉ: Les mesures géodésiques de déformation sont utilisées avec succès en Suisse pour la surveillance des barrages depuis plus de 100 ans. Elles permettent de déterminer avec une grande précision et fiabilité, par rapport à un cadre de référence absolu, les éventuels déplacements et les déformations des barrages ainsi que du terrain environnant. Associées à d'autres dispositifs de mesure de déformations les méthodes géodésiques contribuent de manière décisive à la détermination du comportement des barrages et à l'évaluation des situations exceptionnelles ou des anomalies de comportement des ouvrages d'accumulation, et donc à leur sécurité.

Cet article explique les tâches et les exigences des levés de barrages. Les méthodes éprouvées de la géodésie, leur évaluation ainsi que les développements instrumentaux récents sont décrits et les développements méthodologiques et technologiques possibles sont soulignés.

L'article publié en allemand dans la revue « Eau énergie air » 3-2023 ainsi que d'autres publications du groupe de travail sur la mensuration des barrages de la Société pour l'histoire de la géodésie en Suisse (SHGS) sont disponibles sur le site web de la SHGS (www.gggs.ch > Virtuelles Museum > E-Expo Schweizer Talsperrenvermessung). On y trouve également une vaste bibliographie de publications spécialisées depuis 1920 et une galerie d'images sur 17 thèmes couvrant toutes les époques.

1 TASKS AND REQUIREMENTS OF DAM SURVEYS

According to the “Directive on the Safety of Water Retaining Facilities” issued by the Swiss Federal Office of Energy, geodetic measurements are an integral part of dam surveillance. Used in combination with other means and instruments for detecting deformation, they contribute to:

- the determination of the behaviour of dams (as part of the ongoing assessment of the impacts and conditions of the structure);
- rapid assessment in case of extraordinary situations or following an extraordinary occurrence;
- clarification of causes of anomalous behaviour detected by other measurement instruments.

Geodetic measurements can be used as a stand-alone method to determine the deformation and displacement behaviour of dams and reservoirs and their surroundings. However, they are usually used in conjunction with other measurement systems, such as pendulum systems, to determine changes in the position and height of selected points on a dam, thus providing redundancy in the overall monitoring concept. The control points included may be located on the crest and at different elevations at the airside surface (downstream face) of the dam; and, if accessible through galleries, within the structure (e.g. reference points of pendulum measurements or of traverses in the galleries), on the banks and in rock formations in the immediate vicinity, as well as in the wider environment of the dam outside its pressure zone. Finally, critical terrain features such as landslide slopes or glaciers in the danger zone of the dam can also be monitored. The magnitude of the accuracy requirements can be summarised as follows:

Table 1. Accuracy requirements for dam surveys.

Objects of the survey	arch or gravity dam (VA or PG) (concrete dam)	earth or rock fill dam (TE or ER) (embankment dam)	environment, critical terrain zones (e.g. landslides)
Deformations	mm	mm	mm
Horizontal	0.5 – 1	2 – 5	5 – 10
Vertical	0.1 – 0.2	0.5 – 5	5 – 10

The Subgroup Geodesy of the Working Group on Dam observations of the Swiss Committee on Dams has developed detailed recommendations for the use of geodetic deformation measurements at dams (Schweizerisches Talsperrenkomitee STK/CSB, Arbeitsgruppe Talsperrenbeobachtung 2013). Long-term reliable deformation measurements with millimetre accuracy are a complex and challenging field of application for engineering geodesy; and the observations are time consuming. They must be carried out and evaluated by specialists with the necessary competence and experience, using high quality and tested instruments (Walser 2014). Furthermore, in addition to civil engineering knowledge of the possible dam behaviour, an understanding of geological and geotechnical aspects is required. Geodesy provides the basis for determining the deformations and displacements of the dam in combination with the control procedures and measurement methods of the dam operators, such as the visual inspections, clinometer, extensometer and pendulum measurements, which monitor the geometric behaviour of the structure itself. The results are used by the civil engineering and geology experts to judge the slide safety of the dam and to verify its stability. As part of the dam safety inspection, geodetic measurements are usually carried out at least every five years. The reports of the geodetic deformation measurements are therefore kept as part of the file collection on the dam facility.

2 PROVEN METHODS AND INSTRUMENTS OF GEODESY

Geodetic deformation measurements on dams have a history of more than 100 years in Switzerland (Wiget et al. 2021, Wiget 2022). The oldest method of monitoring dams is geometric alignment. Starting from a stable pillar assumed to be fixed, a vertical plane is established by aiming

the alignment instrument at a reference mark (target). Using the instrument's telescope, the horizontal deviations of the alignment points on the crest of the dam (signalled by alignment target marks or by means of a measuring rod) are measured from this vertical plane.

The accuracy and reliability of alignment observations were limited by refraction phenomena and uncontrolled stations or pillars (assumed to be fixed). On the occasion of the construction of the *Montsalvens* dam (canton FR) in 1921, which was the first double arch (horizontally and vertically curved) dam in Europe, engineers of the Swiss Federal Office of Topography (swisstopo) proposed the application of trigonometric methods used in national surveying: direction and angle measurements (triangulation) and precision levelling. For this purpose, theodolites were used for repeated bearing intersections (forward intersections, see Figure 1) from (at least) two observation pillars outside the dam to target control points on the crest and on the downstream airside surface of the dam, in combination with more distant reference points ("fixed points"). To determine the grid scale, the distance between the observation pillars had to be measured. In addition to the horizontal position observations, the target points could also be monitored vertically by means of height angle measurements. The first measurements were made at Montsalvens in January 1921, before the initial filling of the reservoir, and in November 1921, when the lake was full.

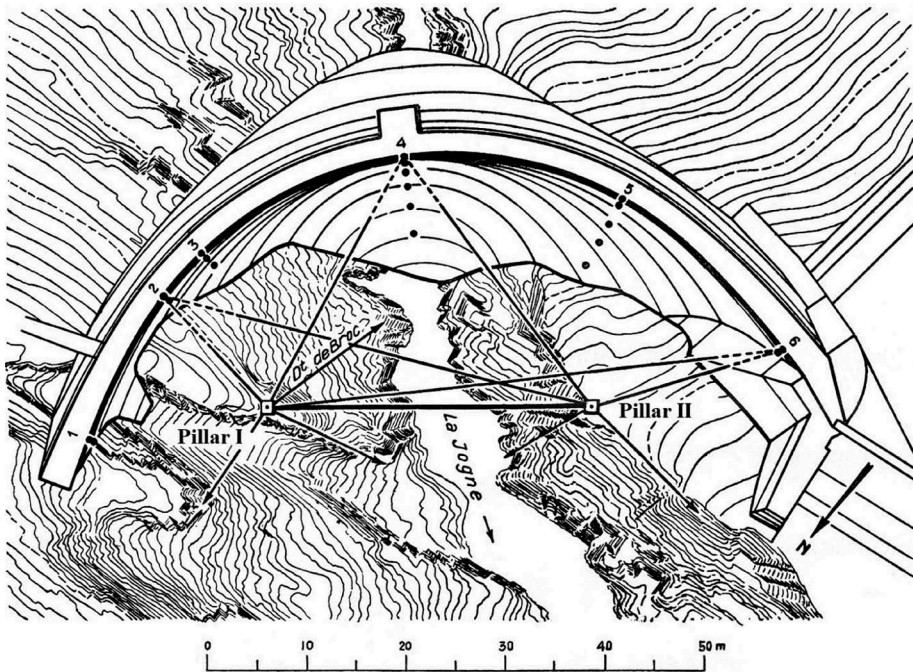


Figure 1. Forward intersections using angle measurements at Montsalvens dam, 1921.

Geodetic deformation measurements were also used at the *Pfaffensprung* dam (canton UR) as early as 1922. In order to be able to measure dam deformations and movements in real time during filling or emptying of the reservoir, all points were measured simultaneously by two observers from two pillars by means of forward intersections.

During the first epoch of Swiss dam construction until the middle of the 20th century, swisstopo was the only institution in Switzerland to carry out geodetic deformation measurements on dams. With the upswing in Swiss dam construction from 1950 onwards, the geodetic methods of dam monitoring were further developed and taught at the Swiss Federal Institutes of Technology in Zurich and Lausanne (ETHZ and EPFL). As a result, engineers from private surveying offices were increasingly commissioned to carry out this work, which eventually also became essential due to the large number of objects to be monitored.

Geodesy has been used for surveillance of all major dams in Switzerland from the very beginning. The methods, of course, have been continuously improved and adapted to technological developments. The measurement networks have been extended and the number of well-founded observation pillars has been increased, partly because of the increasing size of the dams, but also in order to be able to better monitor the stability of the pillars and reference points. Therefore, some of the observation pillars are located up-stream and down-stream of the dam, outside the zone of load influence (pressure bulb). Measurements are taken from the ‘fixed’ to the ‘moving’ and give ‘absolute’ displacements in relation to the chosen reference frames. Whereas in the early days the focus was on short-term differential movements between two epochs, today’s measurements are designed for long-term studies.

In addition to the trigonometric measurements already mentioned, precision levellings are measured in order to monitor the changes in height (subsidence, rise) of the dams or of individual parts of the structure, as well as the foundation and the banks in their vicinity, which are also of great interest (Figure 2). The levellings provide even higher accuracies than trigonometric height differences. They usually run from reference points on one side of the valley over the crest to the other side, but are also measured in the galleries within the dam. Whenever possible, the height reference points are located in stable areas that are not subject to the pressure effects and load influences of the reservoir’s varying water volumes, and if necessary in geologically stable areas further away.



Figure 2. Precise levelling in the vicinity of Contra dam (canton TI).

Today, the “classical” methods (trigonometry and levelling) still form the backbone of geodetic deformation measurements on dams. However, the geodetic methods have undergone continuous development in terms of measuring stations (e.g. pillars and target bolts) and instrumentation (theodolites, levelling instruments, forced centring, etc.). Since the 1970s, developments in electronics and instrumentation have contributed to a significant increase in the accuracy of geodetic deformation measurements. The biggest step forward was the development of electro-optical distance measuring devices. Previously, distances were measured between the survey pillars by precision invar subtense bars. In polygonal traverses over the

dam crest and in galleries invar wires are still used today. Since 1973, electro-optical distance-measuring instruments of the highest accuracy class have been on the market (e.g. Kern Mekometer ME3000 and ME5000). These allowed distances to be measured in the sub-millimetre range in the immediate vicinity or inside the dam, and in the millimetre range over several kilometres in the outer extended network, provided that the representative meteorological parameters are carefully recorded. These instruments were convincing not only because of their high measurement accuracy, but also because of the relatively short measuring time of a few minutes. Today, modern electronic total stations, i.e. theodolites with built-in distance meters, provide similar accuracies with even shorter survey times.

The introduction of electronics brought further important innovations to geodetic instruments: Automatic levelling of the instruments, considering the inclination of the vertical axis; electronic readings of the circle of the theodolites or total stations; automated reading of the staff for digital levels; support of the data acquisition and preprocessing on site by means of external software; digital recording of measurement data on internal or external data carriers, etc. Thanks to developments such as motorisation and automatic reflector alignment, the latest generation of instruments allow faster and more convenient measurements, which in turn can have a positive effect on accuracy. They also enable automated measurement systems for continuous monitoring of dams and their surroundings, known as geodetic monitoring systems (see Geomonitoring in chapter 4).

Since the late 1980s, terrestrial measurements have been supplemented by GPS measurements, today known as GNSS measurements, incorporating all available Global Navigation Satellite Systems. As these do not require line-of-sight between the stations or points to be measured, the external measurement networks can be extended to more distant reference points in geologically stable zones, unaffected by the water retaining facility and its load influences. Thus, long-term displacements of the dam and the surrounding area can be monitored in the well controlled three-dimensional reference frames in the range of a few millimetres.

Especially for large dams, geodetic measurements are used in combination with other measurement systems such as pendulum measuring systems, extensometers, joint meters or deformation meters, etc. These usually provide relative displacements and deformations, whereas geodesy measures absolute displacements in position and height with respect to the above-mentioned reference frames. For the interpretation of the behaviour of the dam and its surroundings, an optimal linking of the so-called “inner” and “outer” measuring systems is therefore essential. The analysis must take into account the local position as well as the temporal execution of the measurements (time, frequency), with careful registration of the respective environmental conditions such as water level or air and concrete temperatures. For example, pendulum system reference points (set plates and suspension or anchor points) should be connected directly or indirectly to the geodetic measurement network. Finally, geophysical and geotechnical instruments such as sliding micrometers or deformation meters, borehole extensometers, etc. can also be linked carefully and precisely to the geodetic network.

Table 2. Advantages and qualities of geodetic deformation measurements.

-
- Geodetic measurement methods are very adaptable, from the installation of the network, the instrumentation, signalisation and execution of the measurements, to the evaluation; they can be well adapted to the different types of dams and local conditions.
 - Geodesy makes it possible to determine the absolute deformations and displacements of dams and their surroundings in relation to the immediate and wider environment and, if the measurement networks are extended accordingly, also to regional or national reference frames in geologically stable or well-studied areas.
 - Movements of dams can be recorded even if they are not associated with changes in slope, strain or stress.
 - Measurements are made in one, two or three dimensions (horizontal and vertical) and deformations can be analysed accordingly.
 - Short-term (elastic) changes, e.g. during the initial accumulation of the reservoir, can be determined as well as long-term phenomena (e.g. subsidence, rise due to concrete changes) or permanent deformations and trends in the measurement series over decades, even with changed methodology and renewed instrumentation.
-

3 EVALUATION AND DEFORMATION ANALYSIS

The goal of geodetic deformation measurements is to monitor and record the kinematic behaviour of dams, its foundation and surrounding by taking “snapshots” of its geometry at different time epochs, calculating changes of control points in position and height together with their corresponding accuracy, and describing the differences or movements in an appropriate way. The kinematics to be studied may vary. For example, relatively short-term movements or reversible deformations of the dam in the context of filling or emptying of the reservoir may be of interest, or the long-term stability of the dam over decades may be to be investigated. The questions to be answered also influence the conditions under which the measurements must be carried out and how they are evaluated.

The first trigonometric measurements were evaluated “by hand” using relatively simple functional models or graphical methods. Today, digital recording or on-line data transfer to the analysis software in the case of automatic measuring systems and electronic data processing allow faster and less error-prone evaluation of geodetic measurements and the adjustment of extensive measurement networks. This and the subsequent deformation analysis can be roughly divided into the following phases:

- 1) Verification of the measurements carried out by specific processing of the raw measurements according to the measurement procedures (directions, angles, distances, levelling, GNSS), taking into account calibration values, meteorological conditions as well as geometric corrections such as instrument heights, etc.; modelling and correction of systematic error influences; determination of stochastic key figures for parametric estimation.
- 2) Network adjustment of all measurements of an epoch to calculate the epoch-specific geometry (coordinates, heights) of the permanently marked control points on the structure and in the terrain; “fixed point analysis”: i.e. testing of fixed point hypotheses and reasonable selection of fixed points in the chosen reference frame. The calculated coordinates and heights of the control points, as well as their accuracy, refer to the selected fixed points.
- 3) Overall adjustment of all measurements and point calculations over several epochs or adjustment of all previous measurement epochs, considering the above mentioned fixed point analysis (the aim is to achieve a spatial reference frame as uniform as possible in the long term); calculation of the epoch-specific coordinates and heights in all epochs in relation to the selected reference points, considering their accuracies.
In addition to point coordinates and heights, the adjustment provides a great deal of additional information which is important for assessing the quality of the measurements and for analysing displacements and deformations (see also Table 3):
 - Accuracy in the form of empirical standard deviations and confidence ellipses: The values are “absolute” with respect to the fixed points, but “relative” between the determined points in the same epoch or in different measurement epochs;
 - Information on the geometric reliability of the coordinates and heights;
 - Estimation of the achieved overall accuracy of the different types of observations (so-called variance component estimation).
- 4) Deformation analysis: Calculation of the position and height differences of the control points over one or more periods (difference between two epochs), including their accuracy and reliability; i.e. calculation of short-term differences, displacements or deformations, e.g. between the last two measurement epochs, as well as comparison and determination of long-term trends over all epochs; reporting of relative accuracies compared to the selected reference points as well as between the measurement epochs; clarification of the significance of the changes for the selected confidence level (e.g. 95% or 99%) for the detection of real displacements.
- 5) The measurements carried out (including measurement programme, personnel, instruments and measurement conditions), the evaluation procedure, the fixed point analysis and the results of the deformation analysis are documented in a technical report as part of the long-term monitoring of the dams. The results are presented in clear tables and descriptive graphs and are evaluated from a geodetic point of view (including choice of control points, significance, special conditions before and during the measurements) as a basis for the technical assessment by the experts (Figure 3).

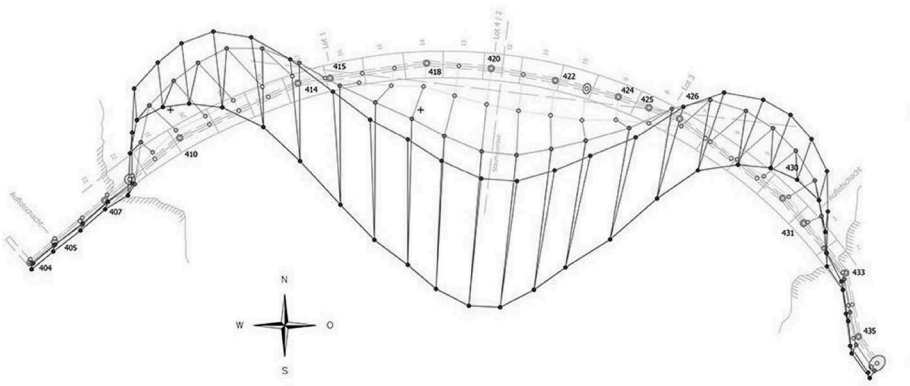


Figure 3. Horizontal displacements over four epochs.

Table 3. Quality features of the evaluation of geodetic deformation measurements and results.

-
- Adjustment of the precisely collected and recorded measurements using high quality functional (physical) models and considering verified stochastic parameters of the measurement methods used.
 - Determination of the coordinates and heights of the control points on the dam, inside the structure and in the surrounding area to be investigated, with high precision (relative accuracy) as well as absolute accuracy with respect to the reference points, which can be located at almost any distance from the structure, defining the reference frame.
 - Optimal combination with other measurement methods to determine displacements and deformations of the dam and surrounding terrain with respect to the reference frame.
 - Controlled high reliability of all results.
-

4 MODERN METHODS AND OUTLOOK ON POSSIBLE FUTURE TECHNOLOGICAL DEVELOPMENTS

The methods described so far enable surveying of discrete individual points (control points) at periodic intervals and comparing them with previous surveys. Differential, irregular movements in space and time between the surveyed points are usually not determined; they can be interpolated if necessary.

But with today's instruments and software tools, automated, continuous monitoring of the position and height of dams and their surroundings is possible. For permanent monitoring with high accuracy requirements and temporally dense sampling rates, geodetic monitoring systems (so-called geomonitoring) are increasingly being used. A well-known example was the monitoring of the dams above the Gotthard Base Tunnel during its construction. Such geomonitoring applications are conceivable, for example, for monitoring critical terrain zones like slopes and unstable parts of the valley that could damage the dam structure or its auxiliary works directly or indirectly by falling into the reservoir. Dams of pumped storage power plants, which are additionally or increasingly stressed by more frequent and rapid changes in lake levels, are particularly suitable to be automatically and permanently monitored by monitoring systems. Temporary monitoring systems are installed especially when work or construction has to be carried out on, under or in the vicinity of the dam that can endanger its safety.

The monitoring systems can be composed of several different sensors, such as total stations, digital levels, GNSS receivers, electronic inclinometers and hydrostatic levelling, CCD sensors, inertial measurement units (IMU), extensometers, temperature and pressure sensors or other modern measurement methods, which will be mentioned below (TLS, In-SAR, FOS, etc.). The software systems for control, evaluation, analysis and alarms are integrated into the monitoring system. The results are determined in real time, broadcasted or made available for viewing via web browser; alarms and error messages are transmitted at critical moments.

New techniques for area and time continuous measurements of deformations are laser scanning and radar interferometry. They shall be briefly described:

Terrestrial laser scanning (TLS): The scanner measures the dam surface in a freely definable geometric point grid (in horizontal and vertical direction) in three dimensions without contact, providing oblique distances, intensity and possibly RGB colour values (Barras 2014). The rapid measurement of large numbers of points (up to 1 million points/second) is less precise (a few mm to cm) than the conventional, highly redundant but time-consuming multi-point determination (sub-millimetre to mm). However, the mentioned accuracies of the laser beam can practically only be determined one-dimensionally in the direction of the laser beam. In addition, the georeferencing and modelling of the point cloud is a challenge. In the future, but probably for some time to come, TLS will increasingly be used in combination with traditional geodetic methods.

Terrestrial and satellite radar interferometry: In the case of high risk potential, terrestrial radar interferometry (ground-based interferometric synthetic aperture radar, GB-InSAR) can monitor surface deformations at dams or in their vicinity, quickly over a wide area or, if necessary, continuously with millimetre precision (Jacquemart & Meier 2014). The range of the sensor is up to 4 km, the area covered is over 5 km². Movements can be detected in the millimetre range, under favourable conditions even in the sub-millimetre range, but only in the direction of the axis of the radar beam (line-of-sight LOS). By using several GB-InSAR sensors at different stations, 3D displacements can be determined. So far, the method has only been used experimentally in the vicinity of Swiss dams.

Interferometric Synthetic Aperture Radar (InSAR) from satellites can be used to monitor the surface of entire valleys or countries. The areas that can be measured and the periodicity result from the illumination zones of the satellite passes. In Switzerland, for example, subsidence in salt mining areas, landslides, block glaciers and permafrost areas are studied. The accuracy of the average displacement rates is better than 1 mm/year in the LOS direction and better than 4 mm/year for individual measurements.

Table 4. Other methods related to or combined with geodesy.

-
- Close-range photogrammetry: High quality photographs, if necessary with overlaps for stereographic evaluation, to document and interpret cracks and other surface changes. Today, drones (unmanned air vehicles UAV) are also used as sensor carriers (Figure 4). Accuracies are in the centimetre range. This area of application is currently developing rapidly and it can be assumed that the use of artificial intelligence will lead to major increases in productivity.
 - Deformation Camera: Automatically analyses sequential high-resolution imagery and uses sophisticated image processing techniques to determine two-dimensional deformations of unstable slopes, rock faces or rock glaciers to an accuracy of a few centimetres.
 - Monitoring of deformations in dams using integrated fibre optics with integrated sensor systems (FOS) to determine changes in length, e.g. in block joints, with an accuracy of a few micrometres.
 - Rockfall radar: Detects rockfall events in all weather conditions, including darkness, and alerts within seconds.
 - Digital geotechnical sensors for sub-millimetre fracture measurements (extensometers, telejointmeters, etc.).
 - Motion sensors, piezoelectric sensors or MEMS (Micro-Electro-Mechanical Systems).
 - Digital level measurements.
-

High-precision, long-term reliable deformation measurements are an exciting, complex and highly demanding field of application for engineering geodesy. Geodetic monitoring of dams will remain an important pillar in the safety concept of dams, mainly because of its “absolute” results.



Figure 4. UAV for close range photogrammetry of dam surface.

Table 5. Possible future developments.

-
- Measurement systems with increased networking and integration of geodetic, geotechnical and other, possibly new, sensors (meteorological, inertial, tide gauges, etc.).
 - A transition from periodic measurements to continuous time series at selected, permanently installed monitoring stations, thanks to lower sensor prices even in large numbers.
 - Integration of the geodetic dam monitoring networks by means of GNSS into the “absolute”, well-monitored and long-term stable reference frame of the national survey for inter-regional comparisons, e.g. in case of earthquakes.
 - Evaluation and analysis tools with advanced algorithms, i.e. more complex adjustment methods, near real-time 3D time series and strain analysis, trend derivation, cloud services, artificial intelligence, deep learning.
 - Use of new Internet of Things technologies for networking and remote control of autonomous multi-sensor systems (machine-to-machine communication via 5G, IPv6).
 - Terrestrial positioning systems using pseudolites (pseudo-satellites, i.e. locally mounted microwave transmitters), analogous to Ground Based Augmentation Systems (GBAS) in aviation.
 - Technologies from indoor navigation methods.
 - Modern representation methods and graphic tools such as augmented and virtual reality for simulating deformation processes or predicting future object states.
-

REFERENCES

- Barras, V. 2014. Lasergrammétrie terrestre – une Solution pour l’Auscultation Surfaceute. *Wasser Energie Luft* 106(2): 112–115.
- Jacquemart, M. & Meier, L. 2014. Deformationsmessungen an Talsperren und in deren alpiner Umgebung mittels Radarinterferometrie. *Wasser Energie Luft* 106(2): 105–111.
- Schweizerisches Talsperrenkomitee STK/CSB, Arbeitsgruppe Talsperrenbeobachtung 2013. Geodäsie für die Überwachung von Stauanlagen. See also publications and contributions to CSB/STK symposia 2014 and 2022. <https://www.swissdams.ch/de/publications/journees-d-etudes>.
- Walser, F. 2014. Geodäsie für die Talsperrenüberwachung. *Wasser Energie Luft* 106(2): 101–104.
- Wiget, A., Sievers, B., Huser, R. & Federer U. 2021. Beiträge der Geodäsie zur Talsperrensicherheit – Zum 100-jährigen Jubiläum der Talsperrenvermessungen in der Schweiz. *Geomatik-Schweiz* 119 (7/8):170–177 in German, 178-185 in French.
- Wiget, A. 2022. Hundert Jahre Talsperrenvermessungen in der Schweiz. *Wasser Energie Luft* 114(1): 39–42.

Swiss contribution to geology and dams

A. Jonneret, T. Bussard & G. Schaeren

Norbert SA, Switzerland

ABSTRACT: Geology is a key factor in the site selection, design, construction and safety of dams. This article summarizes the different geological aspects that must be considered at the various stages of a dam's life. The foundations and abutments, integral parts of a dam, are then discussed. Among other things, they must ensure the stability of the structure, control and limit water seepage and pressure build up below the dam, resist internal erosion and not deteriorate during the life of the structure. The geology of the reservoir and of the catchment area is also an essential aspect to consider in the design and surveillance of dams. In particular, the stability of the slopes must be studied in order to assess the associated hazards (propagation of unstable masses and creation of an impulse wave, blockage of emergency organs, etc.). Targeted investigations, necessary during the design of the dam, monitoring of excavations during construction and a detailed surveillance plan for the life of the structure must be put in place in order to identify any abnormal evolution and, if necessary, to define appropriate mitigation measures. It is essential that the geological model is communicated in a clear and pragmatic way to the various project stakeholders.

RÉSUMÉ: La géologie est un facteur clé pour l'implantation, la conception, la construction et la sécurité des barrages. Cet article résume les différents aspects géologiques qui doivent être pris en compte aux différentes étapes de la vie d'un barrage. Les fondations et les appuis, parties intégrantes d'un barrage, doivent notamment assurer la stabilité de l'ouvrage, contrôler et limiter les infiltrations d'eau et les sous-pressions sous le barrage, résister à l'érosion interne et ne pas se dégrader pendant la durée de vie de l'ouvrage. La géologie du réservoir et du bassin versant est également un aspect essentiel à prendre en compte dans la conception et la surveillance des barrages. En particulier, la stabilité des pentes doit être étudiée afin d'évaluer les dangers associés (propagation de masses instables et création d'une vague d'impulsion, blocage des organes d'urgence, etc.). Des investigations ciblées, nécessaires lors de la conception du barrage, un suivi des excavations pendant la construction et un plan de surveillance détaillé pour la durée de vie de l'ouvrage doivent être mis en place dans le but d'identifier toute évolution anormale et de définir, le cas échéant, des mesures de mitigation appropriées. Il est essentiel que le modèle géologique soit transmis de façon claire et pragmatique aux différents acteurs liés à l'ouvrage.

1 INTRODUCTION

Dams are complex structures that require careful design, construction, and surveillance to ensure their long-term stability and safety. Statistics (ICOLD, 1995) indicate that most dam failures occur in newly built dams with approximately 70% of dam failures happening within the first ten years. When it comes to concrete dams, foundation problems are the leading cause of failure, with internal erosion and insufficient shear strength contributing equally (each 21%) to failures. On the other hand, embankment dams face different challenges, with overtopping being the most common cause of failure, accounting for 49% of cases. Internal

erosion within the dam body follows closely at 28%, while foundation erosion accounts for 17% of failures in this type of dam. These statistics emphasize that the geology is a sensitive issue, and that the foundation is to be considered as an integral component of the dam. Consequently, appropriate assessment and monitoring should be conducted not only for the dam foundation but also for the slope stability of the reservoir and above the dam crest to mitigate risks including the potential generation of impulse waves.

To this effect, the Swiss Directive on Dam Safety provides a comprehensive set of guidelines and regulations aimed at ensuring the safety of dams in Switzerland. It is based on three elements: structural safety, surveillance & maintenance and emergency response plan. It is enforced by continuous surveillance, yearly detailed report and five yearly comprehensive reports carried out by two experienced independent experts including a civil engineer and a geologist (Swiss Federal Office of Energy SFOE, 2015).

This paper will therefore review the main geological aspects which have to be taken into consideration throughout the life span of a dam to ensure its long-term safety.

Establishing and updating a geological model is the thread that runs through the various geological studies and assessments from feasibility to long-term surveillance. To this end, the importance of a sound geological investigation, construction supervision and geotechnical monitoring will be discussed. An overview of the main geological and hydrogeological aspects that may affect a dam foundation and its reservoir is given.

2 GEOLOGICAL MODEL FROM FEASIBILITY STAGE TO DAM SURVEILLANCE

As it has been shown in the previous chapter, the geological aspects have an essential impact on dam design and safety. It is therefore important to review the best practice to ensure that all these essential aspects have been considered from the feasibility study stages throughout the entire life span of the dam. A description of the various geological related tasks which need to be carried out at various stages of a project is provided below.

2.1 *Feasibility studies*

During the prefeasibility stage of dam projects, a thorough evaluation is conducted considering various selection criteria such as cost, socio-economic and environmental consideration as well as geographic and geological aspects. These include the topography, the geology of the foundations, the tectonic setting, the availability of construction materials, the watertightness of the reservoir, and natural hazards both at the dam site and around the reservoir. In general, several options of dam sites are assessed at this early stage in order to determine the most suitable site.

The geological assessment should begin with a desk study, which involves reviewing existing geological and geotechnical data available for the foreseen site. This includes geological maps, geological reports, previous drilling or exploration data, seismic activity records, and any other relevant geological information. This will be followed by geological mapping of the site and its surrounding area in order to identify rock types, structural features (faults, folds, fractures), and any potential geological hazards. Preliminary geological and hydrogeological investigations are then conducted to assess the depth of bedrock, its weathering, the extent in depth of decompression, the engineering properties of the soils and rocks at the site, the orientation, nature and geotechnical characteristics of discontinuities and the hydrogeological conditions at the future dam site. This typically involves a geophysical campaign, pitting and trenching, drilling cored boreholes, carrying out in situ tests such as Lugeon water tests and collecting samples for laboratory testing. The investigation can also be complemented by a detailed assessment of the topography and rock slopes by photogrammetry and LiDAR measurements.

A site-specific seismic hazard assessment is conducted in collaboration with specialists which involves studying historical seismic data, analysing fault lines, assessing the potential for ground shaking, topographic and site amplification, liquefaction, landslides, or other seismic hazards that could affect the dam's stability including reservoir-triggered seismicity

(RTS). In addition, the behaviour of the foundation in case of an earthquake must be assessed to ensure that failure leading to uncontrolled water flow due to earthquake loads can be excluded.

Finally, an assessment of the geological hazards, such as landslides, rockfalls, or other geological events that could affect the dam's structural safety and operation are assessed.

Based on the findings of the geological investigation, a comprehensive report is prepared. The report includes a summary of the geological and geotechnical conditions, potential geological hazards, design considerations and recommendations for further studies. This report therefore includes the first geological model which will be tested and updated by additional studies at later stages of the project development.

Figure 1 is an example of a geological cross section compiled for the feasibility study of the new Fah dam in Switzerland.

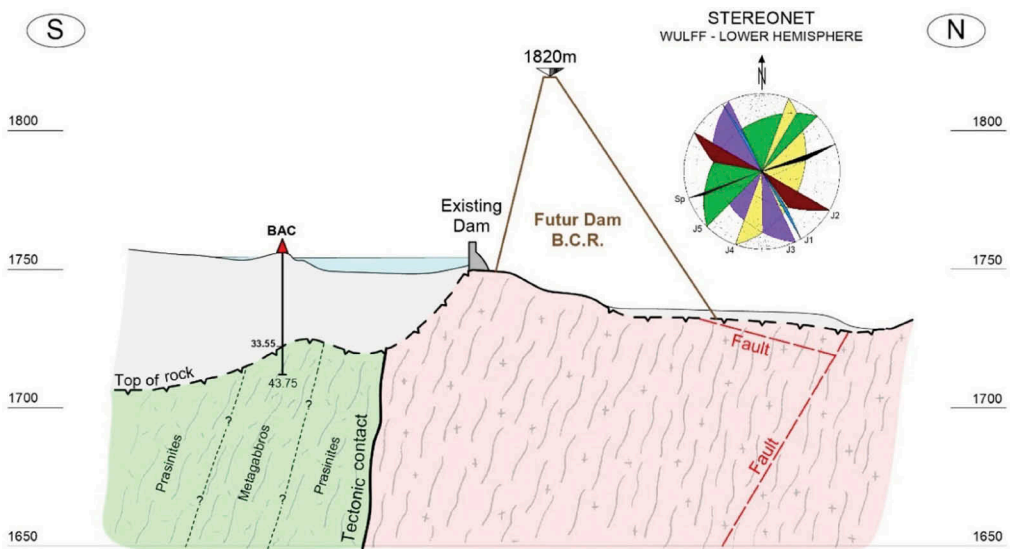


Figure 1. Illustration of an interpretative geological cross section (RCC-BCR dam project in Switzerland).

2.2 Design stage

Once the site of the dam has been defined and the design is ongoing, it is essential that an update of the geological model is carried out to ensure that all geological aspects which could have an impact on the design of the dam and its appurtenant structure have been reviewed. At this stage, additional detailed geological mapping and complementary investigation whether geophysical or by the means of boreholes and possibly exploratory galleries will be required. Good collaboration and interaction with the engineer responsible for the design are essential. The geological model will then be updated and will include all the assumptions made for the design. At this stage a 3D geological model is a very effective tool that can be used by the engineer for design as illustrated in Figure 2. The successful project should identify geological hazards and, if necessary, mitigate the potential effects that hazards could bring on the construction and operation of the dams and reservoirs. It is therefore essential that the engineers develop a clear understanding of the geological model delivered by geologists (World Bank, 2021).

2.3 Construction

Geological follow-up of the construction phase is essential to control that the geological model developed during the design phase is adequate. Any unexpected geological conditions

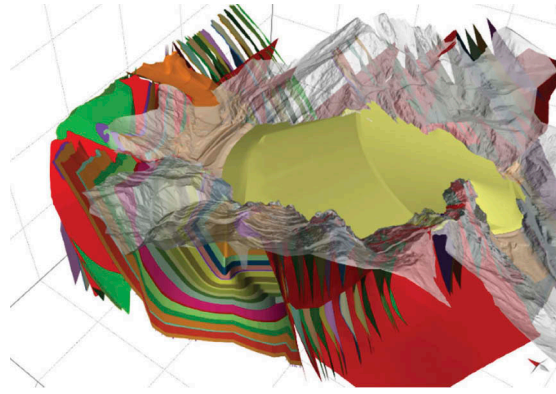


Figure 2. Illustration of a 3D Geological model prepared for the design of a large dam (in yellow) in Central Asia. It includes all the geological mappings (underground and surface), geophysics, boreholes and in situ tests as well as the dam and appended structures.

encountered during excavation should be promptly assessed, and appropriate measures taken to address them whether by additional treatment of a zone or adaptation of the design.

In addition, a detailed mapping of all the dam and appurtenant structures' excavations should be carried out together with records of geological observations and of mitigation measures which might have been taken. Not only will it provide the basis on which the geological model can be updated but it will also form a comprehensive record of the geological conditions encountered during construction. These as-built records are essential in assessing the cause of any abnormal behaviour that might be observed during the life of the dam.

An example of geological mapping during Les Toules dam reinforcement works is given in Figure 3. This geological follow up during construction provided as built drawings and allowed the verification of the geological model.

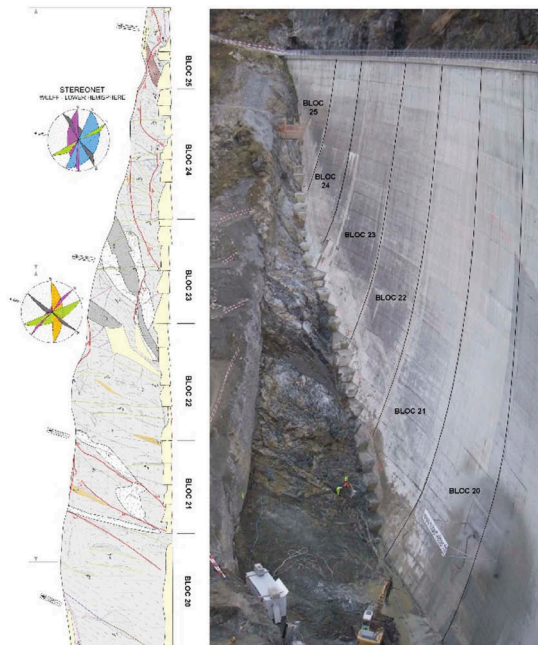


Figure 3. Geological as-built mapping during reinforcement works at Les Toules dam - Switzerland.

3 GEOLOGY AND HYDROGEOLOGY OF FOUNDATIONS

The foundations and abutments of a dam are crucial components that play a significant role in the stability and safety of the structure. Several geological aspects need to be considered during the design and construction of the structure.

3.1 Geological characteristics of the foundations

The rock-matrix's composition and degree of weathering are essential factors to consider since the dam foundations need to support the weight and load distribution. Indeed, different rock types have distinct mechanical and physical properties. The composition, grain size, and mineralogy of the rock affect its strength, permeability, and durability, which are crucial geotechnical parameters. The weathering and alteration will also play a significant role in the quality of the rock mass. Generally, the weathered material will be removed from the foundation, but specific mitigation measures must be taken in case of localised deep-seated alteration.

In addition to the rock matrix, discontinuities, such as joints, faults or bedding planes, can have a significant impact on the geomechanical properties and stability of dam abutments and foundations. Discontinuities are natural planes of weakness in the rock mass, and their orientation determines how they interact with the applied loads and the overall stability of the dam structure. Analysis of discontinuities including their orientation, roughness, alteration, persistence, spacing and infill is essential to assess the geotechnical parameters to take into account in dam stability calculations.

An example of a potential problem due to discontinuities is shown in Figure 5. During the course of a geological study carried out as part of the heightening by 20 m of a dam in Africa, a specific study was performed with regards to the potential risk of sliding of some part of the rock mass due to the thrust from the dam and water pressure. The analysis requested a detailed assessment of the joint properties, in particular a subhorizontal fault system parallel to the bedding plane with low shear resistance. The result was then used to design a satisfactory dam upgrade.

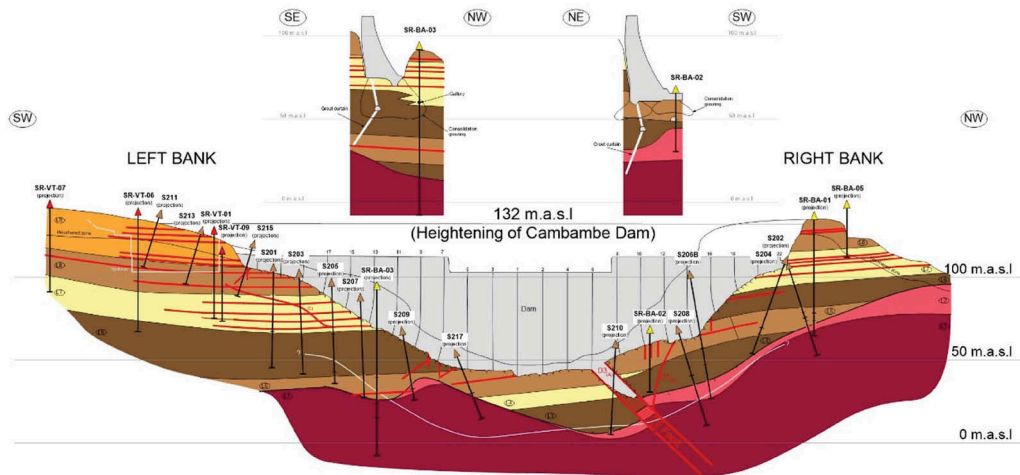


Figure 5. Geological cross-sections of the dam foundation and illustration of subhorizontal faults (red lines) in both abutments which present unfavourable conditions in combination with vertical joint sets - Africa.

It is not only the quality of the foundation that is important, but also the homogeneity of its geotechnical characteristics. The rock mass heterogeneity can significantly influence the behaviour of dam foundations, affecting factors such as shear strength, permeability and

deformation patterns. This can be illustrated by the example of Les Toules dam in Switzerland, where the permanent deformations were significantly higher on the left bank, indicating that the rock mass was almost twice as deformable as on the right bank. This was due to the presence of a rock compartment on the left bank with geomechanical characteristics significantly inferior to those of the remaining of the foundation (Figure 6). This meant that requirements regarding seismic safety could not be met. Consequently, significant works had to be undertaken to reinforce the dam.

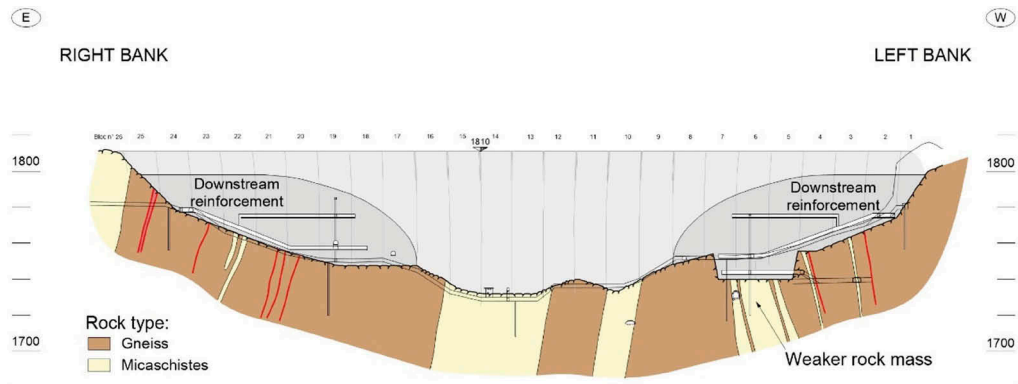


Figure 6. Les Toules, Switzerland - Geological cross section along the dam showing the heterogeneity of the foundations.

Another aspect where the rock mass quality plays an important role is regarding scouring which refers to the erosion and removal of rock caused by the flow of water. Scouring generally occurs during extreme events such as floods. It is a significant concern as it can undermine the stability of the dam or some dam organs. Factors influencing the scouring include the channel morphology, the water flow conditions, the reservoir sedimentation and the sediment characteristics and, of course, the rock mass properties which can be characterised by an erodibility index (Annandale, 1995).

A famous example is the case of Kariba dam in Zambia-Zimbabwe where an 85 m deep plunge pool scouring developed immediately downstream of the dam due to prolonged spillages during the first 20 years after construction (Michael, 2006). The chosen treatment measure was to reshape the plunge pool to avoid further scouring (Figure 7). The ongoing mitigation work requested the preliminary construction of a downstream cofferdam to isolate the reshaping works.



Figure 7. Kariba Dam, Zambia/Zimbabwe - View of the plunge pool (March 2023) and computer-generated view of the reshaped excavation (Razel Bec, 2016).

3.2 Water pressure and possible seepage through the foundation

High water pressure below the dam and/or seepage through the dam foundation are very sensitive issues since they could lead to unfavourable conditions in terms of dam safety in addition to the potential negative impact with regards to the loss of water. The well-known dam failures of (1) Malpasset dam in 1959 and (2) Teton dam in 1976 respectively illustrate these two problematics related to the hydraulic conditions within the foundation:

1. High hydraulic head combined with unfavourable orientations of joint sets may lead to unstable wedges below the dam or within its abutments. It is therefore crucial to identify and to assess the joint sets in order to determine if unfavourable geological structures prevail, and to properly design a grout curtain and drainage system to prevent unacceptable load conditions. If necessary, additional treatment of the upstream toe of the dam can be carried out.
2. Concentrated leaks within the rock mass at the base of the core may lead to the development of a continuous conduit at the base of the core and unacceptable erosion conditions. A systematic treatment of joints, an appropriate cut-off foundation (including filters) and appropriate core materials (low erodibility) are therefore essential.

Figure 8 illustrates some seepage located downstream of the Hongrin North Dam, on the right abutment. The water discharge was low but the installed piezometers confirmed water pressure up to 4 bars. Stability calculations of the rock mass have been performed and indicated that a significant improvement in term of safety factor can be achieved via a proper drainage of the rock mass, i.e. a reduction of the water pressure (Koliji et al, 2011a and 2011b; Bussard et al, 2015). A targeted and phased action plan has been implemented (Leroy et al, 2016) and rehabilitation works of the local defect of the grout curtain as well as additional drainage have been carried out in 2018 (Bussard & Wohnlich, 2018). The new conditions led to the drying up of the water outflow illustrated on Figure 10. The results indicate a significant decrease of the hydraulic head within the downstream right bank (general decrease of 70%) and a similar decrease of the seepage water discharge (decrease of 70%) which confirm a satisfying improvement in terms of slope stability.

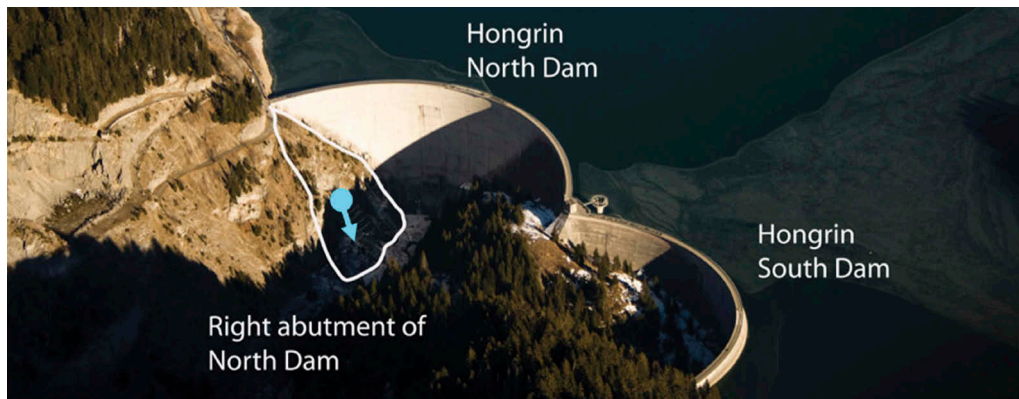


Figure 8. Hongrin dams, Switzerland – The seepage that developed within the right abutment immediately after the reservoir impounding has been treated in 2018.

A numerical model is recommended to assess the likely hydraulic head distribution below the dam and potential seepage conditions. The model will assist in the appropriate design of the grout curtain and drainage system, as well as the installation of an adapted monitoring system.

Finally, the presence of soluble rocks within the dam foundation could be a critical issue, particularly in the case of extremely to highly soluble rock (halite, anhydrite and gypsum),

which may evolve significantly during the life span of the dam (active development of karsts). Such types of rock should be clearly identified during the investigation phases in order to precisely determine the site conditions and if appropriate mitigation measures can be implemented or not. In case of less soluble rocks (carbonate: limestone, dolomite), there is a risk that existing cavities and conduits prevail within the foundation and abutments and could lead to potential seepage, including a risk of wash-out of infilling materials during the reservoir impounding.

4 GEOLOGY OF THE RESERVOIR AND CATCHMENT AREA

The geology of a dam reservoir and its catchment area plays a significant role not only regarding water leakage and therefore the long-term economic viability of the dam and its potential for sedimentation, but also in terms of the integrity and stability of the structure which can be threatened by natural hazards.

4.1 *Reservoir watertightness*

The presence of permeable features within the reservoir contour may lead to some leakage if they are connected to possible resurgence points located at a lower elevation than the reservoir water level.

The permeable features may consist of permeable formations, in particular soluble rocks or coarse and porous loose deposits, and possibly fault zones. The assessment of the risk of leakage requests a detailed analysis of the local and regional hydrogeological conditions. The implementation of mitigation measures could be an option (Figure 9) and a dedicated surveillance plan is recommended along the sensitive sections.



Figure 9. Example of a reservoir slope reshaping and a geomembrane lining installation for preventing water leakage in karst and fissured rock formations (Middle East).

4.2 *Natural hazards*

Dams are often located in mountainous areas which are prone to natural hazards such as landslides, debris flows and avalanches. If close to the structure, these hazards can damage the dam itself or essential dam structures, such as spillways, or compromise their functionality which can lead to overtopping of the dam.

Furthermore, the impact of natural hazards on a reservoir even far from the dam also needs to be addressed as it can have dramatic consequences. A famous example is the Vajont dam disaster in Italy which happened on 9 October 1963. The disaster was triggered by a massive landslide on Monte Toc, a mountain adjacent to the dam. An estimated 270 million cubic metres of rock and soil fell into the reservoir at high-speed creating a large wave that overtopped the dam. The Vajont Dam disaster is a tragic reminder of the potential impact of landslides on dam safety and the importance of thorough geological assessments, monitoring systems and emergency preparedness in areas prone to such hazards.

A sound assessment of the hazards around the reservoir must therefore be carried out by means of desk and in situ studies, analysis and computer modelling using state of the art softwares. Studies should encompass hazard identification and characterization, vulnerability assessment and risk analysis (Figure 10). Recommendations regarding mitigation strategies, monitoring and early warning systems should be made so that dam owners can effectively assess and manage natural hazards around the dam reservoir, therefore safeguarding the structure, downstream communities and the environment from potential risks.

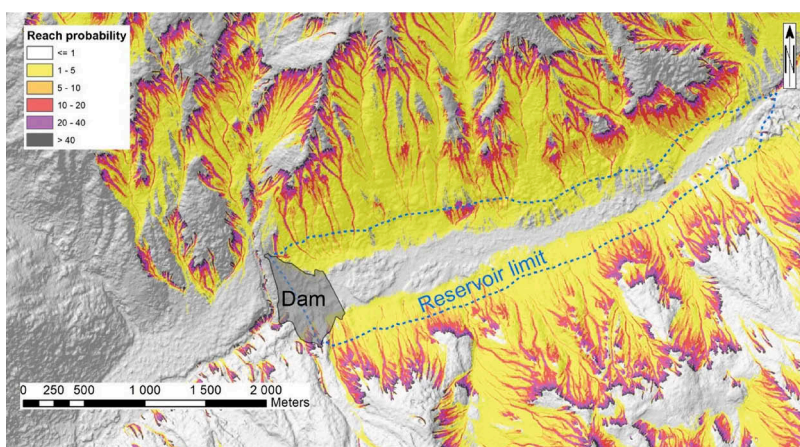


Figure 10. Example of an assessment of rock fall reach probability for a dam's reservoir project in Georgia.

With potentially the same tragic consequences as large landslides, Glacial Lake Outburst Floods (GLOFs) can have significant impacts on dam safety. GLOFs occur when a glacial lake dammed by a glacier or moraine fails, releasing a large volume of water downstream. These events can result in catastrophic flooding, with devastating consequences for dams located downstream. In the past few decades, the progressively warming climate has caused the volume of the glacial lakes to expand rapidly over the world increasing the risk. If a dam is in the path of the floodwaters, it may be overwhelmed by the excessive flow, potentially leading to structural damage or even complete failure.

In addition, the high-velocity floodwaters associated with a GLOF can cause erosion and scouring of the dam's foundation and surrounding areas. This erosion can weaken the dam's structure, compromise its stability, and undermine its foundation. Furthermore, GLOFs can transport substantial amounts of debris, including trees, rocks, and ice. This debris can accumulate at the dam site, potentially blocking water flow and obstructing spillways.

To mitigate the hazards posed by GLOFs, various measures such as remote sensing, early warning systems, monitoring of glacial lakes, reinforced dam designs, and emergency preparedness plans must be implemented (Weicai, 2022).

Climate Change is also degrading the permafrost conditions in mountainous areas. Such effects are already visible and have notable impacts in the Himalayan mountain belt. For instance, a debris flow of around 4 mio m³ occurred in Barcem in 2015 (Pamir mountain, Tajikistan) during heat wave conditions. The deposits dammed the Gunt valley and the upstream area was flooded almost to the Pamir 1 HPP. Reflection is in progress for building a derivation structure

(bypass) for preventing a potential flooding of the powerplant during a next event. Disaster Risk Reduction and resilience strategy are necessary in the present changing environment.

5 CONCLUSIONS

In conclusion, geological studies play a crucial role in ensuring the safety and integrity of dams. The complexity of geological conditions at dam sites necessitates a thorough understanding of the underlying rock and/or soil properties, structural geology, and potential geological hazards.

Geological studies enable the selection of suitable dam sites, taking into account factors such as foundation conditions, seepage control and natural hazards. They also provide valuable insights for the design of dam foundations and structures considering the strength, permeability and deformation characteristics of the underlying geology.

Ultimately, the importance of geological studies for dam safety cannot be overstated. By integrating geological data by means of a geological model into the design, construction, and ongoing monitoring of dams, informed decisions can be made to mitigate risks.

By integrating geological knowledge and expertise into dam engineering practices, we can ensure the long-term safety.

ACKNOWLEDGMENTS

The authors would like to thank the Swiss Dam Owners for their trust and continued collaboration over the years, and Gruner Stucky for their frequent requests for our geological expertise on projects around the world.

REFERENCES

- Annadale, G.W. 1995. Erodibility, *Journal of Hydraulic Research*, 33:4, 471–494.
- Bussard, T., Wohnlich, A., Leroy, R. 2015. Monitoring of the Hongrin arch dams in Switzerland, water leakage and stability of the foundation issues. Colloque CFBR (Comité Français des Barrages et Réservoirs): Fondations des barrages: caractérisation, traitements, surveillance, réhabilitation. 8-9 April 2015. Chambéry, France.
- Bussard, T., Wohnlich, A. 2018. Ouvrages de l’Hongrin. Travaux d’entretien 2018. Comité Suisse des Barrages. Interaction entre barrages et foundation. 20 August 2018. Montreux, Switzerland
- Droz, P., Wohnlich, A. 2019. Rehabilitation of the monitoring system of Inga 1 and 2 dams, *Hydropower & Dams, Issue 2*, 2019
- Fern, I., Jonneret, A., Kolly, J.C. 2019. Travaux de confortement de l’appui rive gauche du barrage de Lessoc, *Wasser Energie Luft – 111. Jahrgang*, 2019, Heft 3.
- ICOLD. 1995. Dam Failure Statistical Analysis. Bulletin 99
- Koliji, A., Bussard, T., Wohnlich, A., Leroy, R. 2011. Abutment stability assessment at the Hongrin arch dam. *Hydropower & Dams. Issue Three*, 2011.
- Koliji, A., Bussard, T., Wohnlich, A., Zhao, J. 2011. Abutment stability assessment at the Hongrin arch dam using 3D distinct element method. 12th ISRM Congress. 16-21 October 2011. Beijing, China.
- Leroy, R., Bussard, T., Wohnlich, A. 2016. Hongrin Dam – Long Term Serviceability of the Right Bank. HYDRO 2016. International Conference and exhibition. 10-12 October 2016. Montreux, Switzerland
- Michael, F.G., Annadale, G.W., 2006. Kariba Dam Plunge Pool Scour, International Conference on Scour & Erosion, November 2006.
- Razel Bec, 2016, Kariba Dam, Plunge pool reshaping, method statement (not published)
- Swiss Federal Office of Energy SFOE. 2015. Directive on the Safety of Water Retaining Facilities
- Weicai W., Taigang Z., Tandong Y., Baosheng A., 2022, Monitoring and early warning system of Cirenmaco glacial lake in the central Himalayas, *International Journal of Disaster Risk Reduction*, Volume 73, 15 April 2022, 102914.
- World Bank. 2021. Good Practice Note on Dam Safety – Technical Note 2: Geotechnical Risk

Dams and photovoltaic plants – The Swiss experience

E. Rossetti, D. Maggetti & A. Balestra

Lombardi Engineering Ltd., Switzerland

ABSTRACT: Nowadays, energy transition is an increasingly frequent theme addressed by many actors belonging to a variety of sectors, from private institutions to governmental ones. Commonly, the main objective is to promote the transition from fossil fuels to renewable energy sources. This challenge is addressed in many ways, also depending on the administrative boundaries considered, and range from more local solutions to continental and global ones.

For example, in Switzerland, in 2017, the Swiss electorate accepted the revised Federal Energy Act (known as Energy Strategy 2050). This amendment promotes the energy transition, setting the basis for increasing the sustainability and efficiency of energy generation.

In this context, exploiting solar energy as a renewable resource plays an important role. However, the generic topographic limitations can represent an important restriction for the spreading of such installations. With a production pattern that fits well together with the flexibility of hydropower, innovative solutions, such as the possibility of placing photovoltaic (PV) panels on the downstream face of dams (dam mounted photovoltaics, DMPV) or over large reservoirs (floating photovoltaic, FPV), can represent a turning point to promote solar energy production.

In this article, such pioneering solutions are exploited, with a special look at the Swiss Alpine area. The authors also reported four examples of PV panels installation in such geographic region, which emphasizes the importance and the potential of these solutions to promote the diffusion of solar energy production.

1 INTRODUCTION

Switzerland, in 2017, adopted the new energy law known as the Energy Strategy 2050 (in the following ES2050). This law imposes a progressive transition from nuclear and fossil fuels by promoting renewable energy sources. Therefore, the question arises of replacing these energy vectors by building new solar, wind and hydroelectric plants and exploiting any other renewable production methods.

These include the possibility of building photovoltaic systems on almost any kind of surface, ranging from simple roofs and house facades to large industrial areas, car parks, motorways, and Alpine solar fields. The goals of the ES2050 are very ambitious and stimulate technological progress and research. For photovoltaics, the aim is to increase from the current 2.9 TWh/y of energy produced (2021) to a future 34 TWh/y. Photovoltaic installations are growing in number at a rapid pace, however, large areas are required to achieve the goals of the ES2050. Some good opportunities can be found at altitude, where certain advantageous aspects can positively influence photovoltaic production. A solar module in the mountains is expected to produce more than the same one in the lowlands and, above all, transfers most of its production to the winter (even more than +50% compared to the lowlands), which is the time of year when electricity is most required; these offsets can be reduced with Alpine photovoltaic systems. This positive effect is due to reduced blurring of the air (clouds and fog),

a less filtering atmosphere, higher efficiency of the panels at low temperatures and the Albedo effect. The latter consists of the increased exposure of the panels due to the reflection of snow, which increases the amount of solar energy reaching the surface covered by the installations.

2 DMPV AND FPV INSTALLATIONS

This article deals with solar energy by discussing two types of photovoltaic systems with a particular focus on the Swiss context. The first concerns the installation of panels on dam walls (Dam Mounted Photovoltaics, DMPV), while the second involves the construction of floating platforms on Alpine lakes (Floating Photovoltaics, FPV).

As far as the DMPV installations are concerned, the favourable aspects are mainly the simplicity of the installation on a concrete structure and the reduced environmental impact, by taking advantage of an already anthropogenic and available area. On the other hand, there are some limitations, such as the exposure of the dam depending on its position and orientation, the slope of the downstream wall which is not very adaptable, and the shape of the dam (curvature).

Due to the larger possible plant area on the reservoir compared to the wall/dam surface, FPV plants have a larger potential energy production than DMPV plants. Furthermore, the alignment of FPV systems can be chosen at will and is not dictated by the dam. On the other hand, the impact of a DMPV on the landscape is lower and the installation effort is lower, which makes implementation easier.

3 POSSIBLE EVALUATION METHODOLOGY OF THE SWISS POTENTIAL

As part of two Master's theses at ETH Zurich, an evaluation method was developed and the potential and suitability of FPV and DMPV systems for 23 of the largest reservoirs and dams in Switzerland was examined (Rytz, 2020; Maddalena, 2021). Two evaluation matrices were developed, one for FPV and one for DMPV systems, which were divided into three main categories: "Acceptance", "Energy and Potential" and "Economics". The weighting was determined at the discretion of the authors and was based on potential studies on hydropower expansion (Ehrbar et al., 2019; Felix et al., 2020). The estimated potential production for the studied dams and reservoirs, ranges for FPVs from 350 to 450 GWh/y and for DMPVs from 11.5 to 14.5 GWh/y. Applying the method to all storage facilities in Switzerland, it is estimated that the potential could be between 500-1000 GWh/a for FPV and 15-20 GWh/a for DMPV (Maddalena et al., 2022).

4 CASE STUDIES

4.1 *FPV installation on the Lac des Toules*

On the Lac des Toules, in the canton of Valais, a prototype Alpine FPV installation was placed in 2019. The platform, located at 1810 m a.s.l., consists of 35 floating elements carrying 2'240 m² array of bifacial panels and a resulting installed capacity of some 426 kW_p, expected to produce about 800 MWh/y (Romande Energie, 2019).

Purpose of this installation, which precedes the large-scale installation, was to verify the technical and financial feasibility of the project. Pilot tests between 2013 and 2019 suggested a 50% increase in power generation compared to plateau levels. From this data, the annual yield was estimated at 1'800 kWh per installed kW_p. The actual result averaged 1'400 kWh, representing an increment of only 30% (Romande Energie, 2023). This difference can be explained by the fact that the floating plant was designed to maximize winter production and greater panel slope at the expense of the total energy production; for technical reasons it was also located further south and therefore closer

to the mountains than the ground-based structure tested during the feasibility studies, resulting in additional shade, leading to up to one hour of lost sunshine exposure per day. In addition, snow – and especially drifting snow – caused a few days of downtime each year and damaged approximately ten of the photovoltaic (PV) panels.

The prototype is currently being adapted to prevent snow accumulation by installation of windbreakers. Several technical challenges have also been faced: it has been necessary to anchor the FPV to the bottom of the reservoir, thus allowing the structure of being theoretically able to withstand wind gusts of up to 120 km/h, ice layers of up to 60 cm and temperatures from -25 to 30 °C.

The experience gained during the prototype phase will enable Romande Energie to develop a more efficient large-scale installation. In the future, this plant is expected to be enlarged; indeed, developer's ambition is to add floating elements to reach a production of about 22 GWh/y (which should be the maximum potential available for that reservoir, i.e., enough for 6'200 households).



Figure 1. Pilot FPV plant on Lac des Toules (© Romande Energie).

4.2 DMPV installation on the Mutsee dam

On the Mutsee dam, in the canton of Glarus, a pioneering DMPV plant with a total power output of 2.2 MW has been installed between 2021 and 2022 by the companies Axpo and IWB. Its expected production of approximately 3.3 GWh/y (the annual demand of 950 households). This amount of annual energy is produced at 2500 m a.s.l. by about 5000 panels mounted on a dam surface of about 10'000 m². Approximately 50% of the production is generated in winter due to the favorable conditions caused by the altitude. Investment costs are about CHF 8 million (Heierli, 2022; Maggetti et al, 2023) and are mainly referable to the high logistic costs.



Figure 2. DMPV plant on the Muttssee dam (© AlpinSolar).

4.3 DMPV installation on the Albigna dam

Another example can be found in Albigna, in the canton of Grisons, where ewz (Elektrizitätswerk der Stadt Zürich) installed in summer 2020 a DMPV plant on 670 m of the dam's upstream face for 410 kWp capacity. The plant, located at 2165 m a.s.l., exploits the reflection of the sun's rays on the lake (in addition to the direct incidence) to amplify the energy production and manages to balance the energy between summer and winter, which in total is worth about 500 MWh/y (the annual needs of 210 households). Investment cost are about CHF 700'000 (ewz, 2020).

During the construction and operation of the plant, various synergies were taken in account:

- The grid connection at the Albigna dam was already in place.
- Most of the installation work was carried out by ewz employees, who have already initiated the pilot project.
- The year-round availability of own staff also simplifies any maintenance work.



Figure 3. DMPV plant on the Albigna dam (© ewz).

4.4 DMPV installation on the Valle di Lei dam

Very similar to the Albigna plant is the one on Valle di Lei arch dam in Grisons, also from ewz. Put in service in September 2022, the plant, which is also located on the upstream crest of the dam, is 550 m long and lies at an altitude of slightly less than 2000 m a.s.l., allowing it to have an increased efficiency of around 25% compared to the Plateau. The installed power of the plant is 343 kWp for a production of about 380 MWh/y (annual consumption of 110 households). Investment cost are about CHF 800'000 (ewz, 2022).



Figure 4. DMPV plant on the Valle di Lei dam (© ewz).

5 IMPLICATIONS FOR DAM SAFETY – THE MUTTSEE EXPERIENCE

With regard to the safety of the Muttsee dam, the supervisory authority (dams section, SFOE) formulated several requirements that had to be fulfilled:

- **Stability:** Verification of stability due to the changes in concrete temperatures caused by the placement of the solar modules over the entire area. In fact, the dam wall experiences a different temperature distribution due to the covering with solar panels. With an FE analysis, it could be proven that this temperature changes only result in a very insignificant change in the behaviour of the dam in the form of additional valley-side deformations of < 2mm. These minor, additional deformations do not affect the stability of the dam.
- **Flood safety:** Verification of flood safety by installing the solar modules in the spillway. The generously selected distance of the solar panels from the spillway crest (approx. 7 m) ensures that the function of the spillway is always guaranteed, and that no interference takes place due to the solar panels.
- **Anchorage in the airside parament:** Specification of the number and detailed design, the maximum forces introduced as well as the representation of the anchorage system of the supporting structure. With a specification of the anchorage used and an anchor depth that is not critical for the barrier, this verification could be provided without any problems.

- Visual inspection: Showing with a walk-on concept how the visual inspection can be carried out quickly and easily under the solar modules. A walkway between the airside parapet and the solar panels (1.5 m distance) allows visual inspection of the concrete surface at any time. Furthermore, the individual block joints were kept free by a gap of 0.5 m between the panel blocks.
- Existing measuring equipment: Evidence that the monitoring of the Muttssee barrier is not affected by the construction or operation of the solar power plant. It was checked and proven that all visors for geodetic measurement remain free and that other measuring equipment is not restricted in its function by the PV plant.

6 OVERVIEW AND OUTLOOK

6.1 Overview

In the following Table 1, an overview of the by-now existing Swiss FPV/DMPV-plants is given and comparison is made with a reference Swiss Plateau rooftop installation in the city of Zürich computed with an internet-based tool (EnergieSchweiz, 2022).

Table 1. Overview of Swiss FPV and DMPV plants.

PV-Plant name	Les Toules	AlpinSolar Muttssee	Albigna Solar	Lago di Lei Solar	Reference PV-plant in Zürich
Type	FPV	DMPV	DMPV	DMPV	Rooftop
Commissioning	2019	2022	2020	2022	-
Elevation [m asl]	1'810	2'474	2'165	2'000	500
Surface [m ²]	2'240	10'000			
Capacity [kWp]	About 400	2'184	410	343	150
Expected annual generation [MWh/yr]	530	3'300	500	380	150
Specific yield [kWh/kWp]	1'400	1'500	1'200	1'100	1'000
Investment cost [million CHF]	Pilot project, not directly comparable	About 8	0.7	0.8	0.2
Specific cost [CHF/Wp]		3.70	1.70	2.30	1.40

As a comparison, the average worldwide total investment cost of an FPV system in 2018 varied between US\$0.8/Wp and 1.2/Wp, depending on the system's size and location. The CAPEX of large-scale but relatively uncomplicated FPV projects (around 50 MWp) was in the range of US\$0.7-\$0.8/Wp in the third and fourth quarters of 2018, depending on the location and the type of modules involved (World Bank Group, ESMAP and SERIS. 2019).

6.2 Outlook

The ES2050 targets of 34 TWh/a from PV remain ambitious, especially because in 2021, photovoltaics in Switzerland had an installed capacity of about 3.6 GW that produced 2.9 TWh. This would therefore be more than a tenfold increase of current production in 29 years. However, a very positive trend for the photovoltaic sector can be seen from 2019 onwards, as each year the installed capacity increased by around 40% compared to the previous year (+43% between 2020 and 2021).

The ES2050 poses several technological challenges, which can only be met with interdisciplinary solutions. Among these, solar energy will play a key role, and installations in Alpine contexts are confirmed to be interesting and increasingly competitive. The installation of

photovoltaic panels on dams and in their corresponding reservoirs is a solution to be considered, especially because of the reduced impact on the landscape, the speed of installation and deployment (especially for DMPVs) and the possibility of balancing production between summer and winter.

DMPVs are likely to be the exception, but hydropower plants have considerable potential for new alpine PV plants due to their existing infrastructure.

To assess the suitability of the two discussed PV variants in Switzerland, a methodology has been proposed and the potential was assessed. With in-depth multi-criteria analyses, one should recognize the best alternatives and proceed further.

Some Swiss case histories exist and useful lessons can already be drawn for further installations.

ACKNOWLEDGEMENTS

The authors acknowledge the inputs regarding Mutsee dam safety provided by Rico Senti from Axpo Power AG.

REFERENCES

- Ehrbar, D.; Schmocker, L.; Vetsch, D.; Boes, R. (2019). Wasserkraftpotenzial in Gletscherrückzugsgebieten der Schweiz. *Wasser Energie Luft* 111(4): 205–212.
- EnergieSchweiz (2022). Simulation von Energiesystemen mit dem Tachion-Simulation-Framework, Benutzerdokumentation, Oktober 2022. Available at: <https://www.energieschweiz.ch/tools/solarrechner/> (accessed: May 29th, 2023)
- Foen Hrsg. (2022) Energy strategy 2050. Available at: <https://www.uvek.admin.ch/uvek/en/home/energy/energy-strategy-2050.html> (Accessed: May 26th, 2023).
- Ewz (2020), Albigna Solar – Erste hochalpine Solar-Grossanlage, Factsheet, Available at: <https://www.ewz.ch/de/ueber-ewz/newsroom/medienmitteilungen/Solar-Albigna-produziert-ab-September.html> (accessed: May 29th, 2023)
- Ewz (2022), Lago di Lei Solar – Hochalpine Solargrossanlage auf der Staumauer Valle di Lei, Factsheet, Available at: <https://www.ewz.ch/de/ueber-ewz/newsroom/medienmitteilungen/LagodiLei-Solar.html> (accessed: May 29th, 2023)
- Felix, D., Müller-Hagmann, M., Boes, R. (2020) Ausbaupotential der bestehenden Speicherseen in der Schweiz; *Wasser, Energie, Luft* 112(1): 1–10.
- Heierli, C., 2022, A new Swiss partnership. *Waterpower Magazine*, November 2022: 16–17
- Romande Energie (2019). Le premier parc solaire flottant en milieu alpin est en service; Communiqué de presse du 16.12.2019, Available at: <https://www.solaireflottant-lestoules.ch/> (accessed, May 29th, 2023)
- Romande Energie (2023). First ever high-altitude solar farm delivers initial findings; Press release 27.04.2023, Available at: <https://www.solaireflottant-lestoules.ch/> (accessed, May 29th, 2023)
- Rytz, S. (2021). Photovoltaics and hydropower reservoirs in Switzerland – Synergies and potential. *Master Thesis*, Laboratory of Hydraulics, Hydrology and Glaciology (VAW), ETH Zürich.
- Maddalena, G., Hohermuth, B., Evers, F.M., Boes, R., Kahl, A., (2022). Photovoltaik und Wasserkraftspeicher in der Schweiz-Synergien und Potenzial. *Wasser, Energie, Luft* 114(3): 153–160 (in German).
- Maggetti, D., Maugliani, F., Korell, A. Balestra, A., (2023). Photovoltaic on dams – Engineering challenges. *Proc. ICOLD European Club Symposium “Role of dams and reservoirs in a successful energy transition”* (Boes, R.M., Droz, P. & Leroy, R., eds.), Taylor & Francis, London.
- Rytz, S. (2021) Photovoltaics and hydropower reservoirs in Switzerland – Synergies and potential. *Master Thesis*, Laboratory of Hydraulics, Hydrology and Glaciology (VAW), ETH Zürich.
- World Bank Group, ESMAP and SERIS. 2019. Where Sun Meets Water: Floating Solar Handbook for Practitioners. Washington, DC: World Bank. Available at: <https://www.worldbank.org/en/topic/energy/publication/where-sun-meets-water> (accessed, May 29th, 2023)

The importance of young professionals for dam engineering in Switzerland

Samuel Vorlet

Hydraulic Constructions Platform (PL-LCH), Ecole Polytechnique Fédérale de Lausanne (EPFL), Switzerland

Valentina Favero

Dam supervision section, Swiss Federal Office of Energy (SFOE), Switzerland

ABSTRACT: In Switzerland, hydropower is the main energy source and contributes to about 58.3% of the total production. The 2050 energy strategy aims to increase this share in the coming decades. This increase is a challenge for hydropower plants. The maintenance and rehabilitation of these facilities is therefore of paramount importance for their structural integrity and resilience, to guarantee a reliable and optimized operation in the medium and long term. Tomorrow's engineers will have a key role to play, and the great level of expertise acquired over the past decades in Switzerland must be maintained and transferred to the new generations of engineers. In fact, most of the dams in Switzerland have been constructed between the 50's and the 70's allowing a great level of expertise to be developed among dam engineers. The Young Professionals Group of the Swiss Committee on Dams, founded in 2019 and presented in this paper, has the role to ensure the knowledge transfer between generations.

1 INTRODUCTION

Decarbonization is a major challenge with a direct impact on energy strategies. It promotes the reduction of greenhouse gas emissions and the transition to renewable energy production in order to promote sustainability. In this context, hydropower is set to play a major role in the coming decades, due to its historical importance and its storage capacity, which enables operation reliability and compliance to complex grid requirements. In Switzerland, hydropower is the main source of energy, contributing to around 58.3% of the total domestic production (BFE 2022). The 2050 energy strategy aims to increase this share over the coming decades. This increase is a challenge for hydropower schemes, and maintenance and rehabilitation of these facilities are therefore of paramount importance for their structural integrity and resilience, to ensure reliable and optimized operation in the medium and long term. Tomorrow's engineers will therefore play a crucial role, and the level of expertise acquired over the decades in Switzerland must be maintained and passed on to the next generation of engineers. Indeed, most of dams in Switzerland were built between the 50s and the 70s, allowing a great level of expertise to be developed among dam engineers. This article briefly introduces the current situation of the next generation of dam engineers in Switzerland, presenting the importance of hydropower in Switzerland and the intergenerational transfer of knowledge. In addition, the recent creation of the Young Professionals group of the Swiss Dams Committee is presented as an example of how to encourage exchanges and knowledge transfer between different generations.

2 THE IMPORTANCE OF HYDROPOWER IN SWITZERLAND

Dams and hydraulic systems in Switzerland are an integral part of the country's history and geography. With most of its territory covered by the Alps, Switzerland is crossed by numerous rivers and has a dense network of Alpine reservoirs. In this favorable framework, hydropower has played an essential role in the country's energy, environmental and economic development. Over the course of the 20th century, Switzerland developed its considerable hydropower potential by building more than 200 large dams and numerous ancillary structures, enabling it to become a leader in hydropower production and contributing to its energy independence and sustainability.

Dams play an essential role in regulating water flows and inflows to optimize hydropower production. Reservoirs also manage and store water resources from precipitation and snowmelt, ensuring flood protection and drinking water supplies. Engineers have made an essential contribution to the design and optimization of these structures, and to the management of their operations. They have played an essential role in ensuring the proper operation of dams over the years, combining resource management with environmental protection.

Dam safety in Switzerland includes structural safety, monitoring, and maintenance, as well as an emergency plan to control the residual risk. The supervision of the structures is guaranteed by four levels of supervision including various levels of expertise (SDC 2015): the dam warden (level 1), an experienced professional (civil engineer) (level 2), confirmed experts (civil engineer and geologist) (level 3) and the supervisory authority (level 4). These different levels of supervision are essential to ensure optimum monitoring and maintenance of dams and reservoirs.

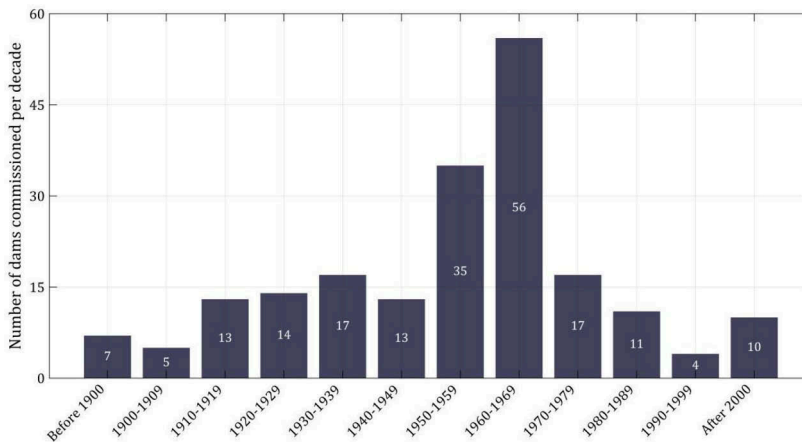


Figure 1. Number of dams commissioned per decade in Switzerland, according to Swiss Committee on Dams (SCD).

Although the construction of dams had already begun in Switzerland, it was between the 50s and 70s that almost half of all large dams were built, thanks to the favorable economic situation. During this period, more than 90 dams were built, and considerable experience was gained. This experience has led to the development of a high level of expertise in dam planification, design and construction, which is now internationally recognized. Yet, the number of dams commissioned in Switzerland strongly reduced in the following decades.

Today, experienced engineers often have the role of senior expert (level 3) and have an important wealth of technical knowledge. However, as most of them reach the end of their careers, it is essential to maintain an adequate level of expertise by investing in the education of future engineers and ensuring the transfer of knowledge to new generations, in order to guarantee the future competences.

3 YOUNG PROFESSIONALS GROUP OF THE SWISS COMMITTEE ON DAMS

The Young Professionals group of the Swiss Committee on Dams (SCD) was officially created at the General Assembly in Bern in 2019, with the aim of encouraging the participation and involvement of young professionals in the national committee, composed of Switzerland's leading experts in the field of dams, and promoting the transfer of knowledge to new generations of engineers. The creation of the group provides an opportunity for young professionals to meet and share experiences, and to promote the transfer of knowledge to the younger generation through meetings, seminars, conferences, technical visits, and exchanges organized with senior engineers and experts. It also promotes exchanges with other groups of young professionals in Europe and worldwide. SCD members under the age of 36 are members of the Young Professionals Group. Currently, the Young Professionals group has 42 members, including 10 women, from all over Switzerland. Members are mainly employed by engineering firms, operators, research and education institutions, or government.

The group meets officially four times a year. A core group of 4 to 5 people who meet monthly has also been set up to organize and manage the group on a more regular basis. The group is active within the SCD, since a representative of its members can participate in the various meetings of the main Working Groups, in order to promote knowledge transfer. Since its creation, the group has organized various activities in line with its objectives: various technical visits, guided by experienced engineers; visits to research facilities in Switzerland, enabling exchanges with industry professionals, in particular the Laboratory for Hydraulics, Hydrology and Glaciology (VAW) at the Swiss Federal Institute of Technology in Zurich (ETHZ); various meetings and conferences with recognized experts, notably in partnership with Hydro-Québec and the Swiss Federal Office of Energy (SFOE), among others. The group also works closely with the Young Professionals groups of other national committees, mainly in neighboring countries, and with the International Commission on Large Dams (ICOLD).

The creation of the Young Professionals group has made it possible, through the various activities carried out by the group, to foster the integration and participation of its members in the activities of the SCD, and to promote exchanges between Young Professionals and more experienced engineers, thereby promoting the transfer of knowledge. Passing on the experience gained by dam engineers to new generations in Switzerland is essential and is promoted by the group, which represents an example of how to encourage exchanges between people from the same profession, helping to prepare the next generation of engineers in the field of dams and hydraulics in Switzerland.

4 CONCLUSION

In a context of energy transition, the role of dams is essential to ensure a reliable and optimized energy supply in Switzerland in the medium and long term. Tomorrow's engineers will play an essential role in ensuring the operation, maintenance and rehabilitation of these structures, and the level of expertise acquired over the past decades in Switzerland needs to be passed on to new generations of engineers. This article briefly describes the current situation of the next generation of dam engineers in Switzerland, highlighting the importance of hydropower and intergenerational knowledge transfer in the dam sector. In addition, the recent creation of the Young Professionals group of the Swiss Dams Committee was presented as an example of how to encourage exchanges and knowledge transfer between different generations in Switzerland.

REFERENCES

- BFE 2022. Stand der Wasserkraftnutzung in der Schweiz am 31. Dezember 2022. *Bundesamt für Energie, Sektion Wasserkraft, Ittigen, Switzerland*; 2023 Apr. Report No.: 11375.
- SDC 2015. Role and duties of Dam Wardens. *Working Group on Dam observations. Wasser Energie Luft. 2015;107.*



Taylor & Francis

Taylor & Francis Group

<http://taylorandfrancis.com>

Theme A: Dams and reservoirs for hydropower



Taylor & Francis

Taylor & Francis Group

<http://taylorandfrancis.com>

How to win an international competition on sustainable sediment management

L. Gehrman & T. Gross

Hülskens Sediments GmbH, Wesel, Deutschland

M. Detering

D-Sediments GmbH, Werne, Deutschland

ABSTRACT: The winning idea of the 2022 Guardians of the Reservoir Challenge, the Continuous Sediment Transfer, has shown great potential as an effective way to restore or maintain the functionality of reservoirs capacity and restore ecological conditions in downstream aquatic systems. The competition was organized by the Bureau of Reclamation (BoR) and United States Army Corps of Engineering (USACE) and had three stages: submitting an idea, developing a concept, and demonstrating the technology in a field test. The winning idea, which was selected by a technical jury, was Continuous Sediment Transfer, a near-natural method for autonomous restoring and maintaining reservoir volume and restoring sediment conditions in the tailwater.

The team's technology, the SediMover, was used to remobilize the sediment inside the reservoir and transfer it to the tailwater. Its modularity allows for adaptation to almost every situation, including difficult situations such as flood events and dry falls or quantitative limitations in sediment transfer. The team successfully demonstrated the process in a field test, which was presented in a demonstration video, a presentation, and a written essay. The technology is expected to undercut the cost of applying conventional dredging methods for reservoirs, thus saving reservoir operators money. Nevertheless, the new technology can be combined with conventional dredging technology and other equipment. After the pilot application in the competition, the team already has three larger commercial projects in preparation in Germany.

In addition to the practical need for application, the team aims for a broad and scalable application of the developed technologies. The judicious application of autonomous dredging will not only ensure cost-effective remediation of reservoirs and ensure their future operation but will also restore sediment continuity in rivers in a naturalistic manner. The benefits are not limited to the immediate downstream sections of the river but extend far downstream to river deltas and coastal regions, preventing further erosion damage. In this way, ecological benefits are achieved at no additional cost.

Moreover, the team is participating in developing guidelines for sediment management in reservoirs and researching the combination of sediment methane gas harvesting with the continuous sediment transfer, using different autonomous vessel types. The team is also working to adapt the technology to harvest methane generated inside the sediment to combat greenhouse gas emissions. Furthermore, a smaller version of the SediMover, the MiniMover, has been developed for use in tributaries, limited spaces of reservoirs or shoreline areas.

The Continuous Sediment Transfer process conducted with autonomous vessels shows great potential as it combines ecological benefits with economic benefits to combat a global problem. Reservoir operators and the government will have to invest significant sums in the coming years to ensure water supply in several regions of the USA and in Europe. Therefore, the automation achieved by the technology will ensure that it is able to undercut the cost of applying conventional dredging methods for reservoirs, thus saving reservoir operators money. The team's technology is expected to have good prospects as it offers both ecological and economic benefits.

1 THE COMPETITION - GUARDIANS OF THE RESERVOIR CHALLENGE

The well-organized Guardians of the Reservoir Challenge was conducted in three stages, spanning a total of two years. The goal was to reduce the number of participants from stage to stage and to determine a winner at the end. In the first stage, all registered teams were invited to submit innovative concepts that addressed the given challenge. The contributing panel of USA, reservoir and sedimentation experts selected the top five teams that advanced to the second round.

The focus of the second phase was to demonstrate the applicability of the specific concepts. The hosts expected technical results and significant progress in the solutions. To support the problem solvers, technical contacts were provided at both United States Army Corps of Engineering (USACE) and Bureau of Reclamation (BoR), and consulting services were offered by FedTech, an organization that focuses on strategic development support that may be relevant to several areas of the USA government.

From these five teams, another panel of experts selected three teams to advance to the third and final phase. In this phase, a pilot demonstration was expected, if possible on a real scale and under realistic operating conditions. Again, progress was expected from each participating team. The competition was conducted during the Covid 19 pandemic, which caused a significant amount of extra work, especially in the field trials. The winner was selected based on a comprehensive report, video documentation of the field tests, and a presentation and questioning by the final jury. The jury then decided on the winner, who is represented by the authors.

2 APPROACH TO WINNING

The competition guide included an overview of the main problem and many sediment-related aspects. It was aimed at participants inside and outside the reservoir scene. As we have been intensively involved in solving sediment issues for many years, we were able to benefit from the knowledge gained during this time.

Against this background, it was and is our goal not only to win the competition, but also to put the results into practice across a broad operational, ecological, technical, and economic spectrum. Therefore, the equipment must be easy to install without interrupting the operation of the reservoir, environmentally friendly by finding a reasonable path for the sediment, and cost-efficient through autonomous operation.

2.1 Essential features

Our innovative idea is to restore a near-natural, continuous sediment transfer in an existing reservoir to maintain (or restore) its functionality and restore the morphological and ecological conditions of the downstream system. One or more specially designed modular sediment transfer vessels (Figure 1), named SediMover®, will remobilize the accumulated sediment upstream

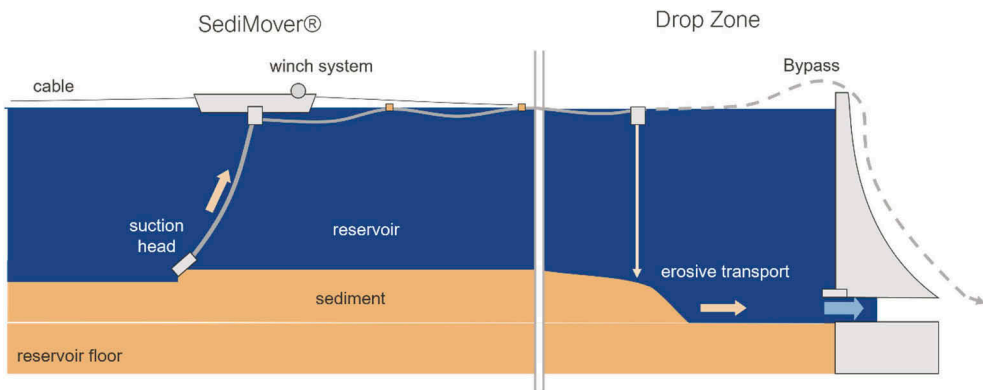


Figure 1. Principle continuous sediment transfer.

of the dam and transport it to the downstream section of the river via (a) dam outlets/turbines or (b) above the dam or (c) onshore for further processing (not shown here).

The continuous sediment transfer technology is an automated system that allows 24/7 operation. It is equipped with a mass flow meter and a density meter to measure and monitor sediment transfer, and GPS for position determination. The operating pattern is controlled and automatically adjusted to changing conditions. The equipment is modular and can be adapted to a project-specific configuration to increase the efficiency of the plant. Unlike conventional methods, this new concept considers the reservoir and retained sediments as part of a river system to restore sediment equilibrium. Operation occurs in conjunction with reservoir operations, hydropower generation, water withdrawal, or recreation, without interference, even during installation. The vessel moves over a predefined reservoir area.

It is positioned by a winch system (Figure 2). Power is usually supplied to the vessel and its equipment via a cable connection on the shore of the reservoir. Positioning cable anchor points are usually located on the shore but may also be established within the reservoir if a section of the reservoir needs to be kept clear for vessel traffic/ navigation or to overcome the large width of the reservoir.



Figure 2. SediMover with visible cable connection to anchor points.

The maximum particle size that can be transferred can be selected with an actual maximum of 100 mm, depending on the suction device and pump type. Smaller particle limits can be applied with larger particles remaining on the bottom of the reservoir or being separated from/inside the running transfer line. This is important in the case of an optional turbine diffuser, where we recommend not exceeding 40 mm. The maximum transferable particle size is also adaptable to the turbine type. Kaplan turbines, for example, are relatively abrasion-resistant compared to Pelton turbines, partly due to different drop heights and applications. However, smaller particle limits such as 3 mm can be applied if needed. Since large particles typically account for less than 1 to 2% of all sediment and are generally found in the upstream inflow zone of the reservoir, this sediment fraction can be excavated and placed downstream using conventional dredging equipment.

The choice of the recommended suction head depends on the distribution of particle size, compactness of sediment, water depth, and presence of sediment. We have developed mechanical sediment removal units, high pressure jets, or a combination of both. A hydraulically driven screw cutter head mechanically crushes the sediment. The rotating screw conveys the sediment into the centred suction hose. Alternatively, a high-pressure water jet suction head can be used for concentrated sediment remobilization of heavy cohesive sediments at relatively sensitive sites. In addition, a combination of the two systems is possible by attaching the jet system to a screw cutter. The system allows water level changes of ± 5 to 10 m within one hour, depending on the type of suction head.

Unlike conventional dredging equipment, the suction units do not focus on always gaining a smooth basin bottom, such as is required in harbor basins. Instead, the focus is on robust operation in sediments containing a certain level of obstacles (debris, stones, etc.) without stopping the operation and on optimizing fully automatic sediment transfer.

The standard transfer capacity for marine pumps is approximately 1 - 3 km, depending on the type selected. However, to extend the range or increase the capacity, booster pumps can be used, which can be placed on shore or on floating platforms. Delivery length and head are limited only by economic constraints, not by physical constraints. In practice, our tests have already overcome a 15 m high dam; even overcoming a 60 m high dam (at actual water level) is not a problem from a hydraulic standpoint.

No major equipment failures have occurred to date; however, sediment transfer rates are reduced when sediment is very hard. Another problem is flood events where the equipment must be secured to the shore for safety reasons, which requires a reasonable response time. We have solved this so far by involving local contractors with short response times. By selecting appropriate equipment and a sufficient number of units, continuous sediment transfer can be scaled to any size to achieve the required size of the project. The modular design of the equipment and the fully controlled and adjustable operating process allow applicability to virtually any type of reservoir.

As demonstrated by the Phase 3 demonstration, the equipment can be installed quickly and typically requires no interruption to reservoir use or power generation and does not interfere with recreational use or navigation. The amount of sediment transferred, and other parameters are documented in terms of solids transferred and total media (Figure 3).

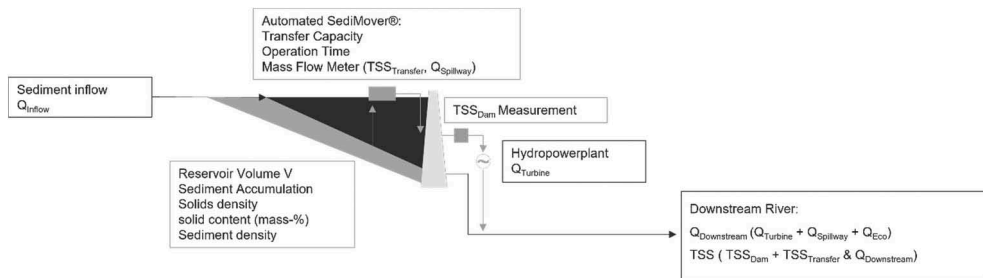


Figure 3. Continuous sediment transfer solution process overview and parameter measured.

2.2 Development and field tests

Unlike other competing teams, we were already beyond model scale or lab testing at the beginning of the competition. Instead, we were heading straight for real-scale pilot applications. In phase 2 of the competition, we had already successfully completed two pilot projects (Figure 4a and b). The two projects had different requirements for the sediment removal operation and reservoir characteristics, so it was necessary to modify the equipment and the mode of operation. This gave us the opportunity to gain a lot of experience with project implementation and operation under different conditions. Between the projects, we integrated some improvements of the experiences from the first pilot projects. The final demonstration projects removed more than 25,000 m³ of sediment accumulation by relocating sediment to the downstream portion of the river in a nearly natural manner that met project requirements and operator needs. By demonstrating functionality in operational scenarios, we rated our sediment transfer system with a TRL 8 technology status improvement.

Having already successfully transferred 25,000 tons (solid mass) of sediment through the SediMover® in two consecutive test projects during Phase 2, in Phase 3 proper we focused on:

- Installation work improvements,
- technology demonstration and
- Video documentation.



Figure 4. Field test SediMover in 1st and 2nd reservoir.

With a team of six (four craftsmen and two engineers), the entire on-site installation, including unloading, placement of ground anchors, pipe/hose and cable connections, power supply, installation of the hose float, data access, and commissioning of the system took less than six hours (Figure 5). The first sediment was transferred the same day.



Figure 5. (a-d). a) installation works; b) start of system; c) initial outflow; d) inside of tube.

No sound meter was used during the demonstration, but as with the previous pilot projects, the SediMover®'s noise emissions were imperceptible in a natural environment, even under full load from more than 30 m away.

2.3 Findings and technical approvals

We encountered significant operational problems, especially during the first pilot application (Figure 6):

- frequent flooding with strong currents
- frequent drying of reservoirs and SediMover (reservoir is emptied without prior information for flood control)
- very shallow sections
- debris (car parts, branches, machines, carpets, ...)

- plant growth
- power limitations due to poor local electricity network
- difficult access to the reservoir (truck access only through a quarry)
- The transfer line had to be longer than planned and required a booster pump to reach the planned capacity
- remote location/long journey
- Covid-19, with strict lockdowns and travel restrictions.



Figure 6. a) SediMover during dryfall; b) SediMover in shallow water among strong underwater plant growth.

We are proud that despite all these additional challenges, we were able to successfully complete the first pilot application, albeit with a lower sediment transfer than planned. During the prototype competition and field testing, we made several improvements to the SediMover. We also further improved the ease of installation and maintenance. Overall, however, the concept and technology developed proved to be adequate.

3 ACCOMPANYING WORK

3.1 *Development of guidelines*

One thing is to develop an applicable technology for sediment management. However, this should be accompanied by an appropriate framework and other aspects to enable easy implementation and handling by operators and authorities. In many countries, including the USA, there were no guidelines for environmental compliance and technical sizing of sediment transfer from reservoirs. Based on our previous work in sediment solutions, we were asked to participate in the development of several sediment management guidelines.

In cooperation with authorities and environmental agencies, two important guidelines were developed. DWA M-513-1 deals with general sediment criteria including permissible contamination. DWA M-513-3 focuses on the application at reservoirs and on sediment application, including a near-natural sediment transfer and its operational design. Since the sediment characteristics and hydraulic aspects do not differ in general worldwide, the developed recommendations can also be useful in other regions. We have also provided input to the ICOLD Sedimentation Technical Committee, which is in the process of publishing a guidance document.

3.2 *Sediment cleaning*

Since the developed technology can usually be combined with conventional equipment or new inventions, we have also started to develop additional technical options. One problem at water bodies near or downstream of industrial sites, harbors, marinas, or shipyards is contaminated sediments that can harm the environment. Treating sediments is usually very costly. Therefore, we are developing a cost-efficient sediment treatment process for certain pollutants. Analyses have shown that we are able to improve the ecotoxic load (OECD Guidelines for Testing of Chemicals 2013) in sediment from aquatic ecotoxicity level VI (“very high toxic

contamination”) to ecotoxicity levels I and II (“non-critical contamination”), so that the cleaned sediment can be relocated or used elsewhere. Continuous sediment transfer is particularly advantageous for this purification process because it allows for a steady supply of sediment, good process stability, and high plant efficiency, rather than batch feeding as in conventional dredging.

3.3 Combating greenhouse gas emissions

As mentioned in the introduction, methane emissions from reservoirs are among the most important greenhouse gas emissions worldwide because they are generated in the sediment. Methane and other climate-relevant gases are produced in anoxic reservoir sediments during biodegradation processes. Sediment movement, such as dredging, can release large amounts of the stored gas, which has a global warming potential 80 times higher than CO₂ (based on 20 years, IPCC 2014). Aquatic ecosystems are thought to account for up to 53% of global methane emissions, including reservoirs at about 6% (Rosentreter et al. 2021).

We have developed technology to harvest methane during sediment transfer. This not only eliminates the greenhouse effect of the captured methane, but even enables its energetic use, since the methane fractions in the captured gas were between 55 and 90%. We succeeded in operating conventional mobile power generators only with sediment gas.

During the competition, our patent application was successfully converted into a valid patent, which has now been granted by the USA Patent Office as Patent No. US 11 041 280. Additional applications involving methane harvesting are pending.

3.4 Additional vessel series

In addition to improving our existing system, we developed an additional, simplified sediment transport vessel in Phase 2 (Figure 7). This smaller, lighter, and less expensive vessel (Mini-Mover) is suitable for areas with limited space and shallow waters such as forebays, ponds, and tributary or shoreline areas of reservoirs. The MiniMover has an approximate length of only 4.5 m, a height of 2 m and a width of 2.85 m. This makes transport and installation quick and easy.



Figure 7. MiniMover a) under construction; b) during field test and operation.

Like the original technology line, it consists of a modular system that can be adapted to different requirements. Further developments and improvements of the MiniMover (such as an appropriate graphical user interface) are still in progress, but the general system is already operating successfully in a forebay of a drinking water reservoir in Germany (Figure 7b). In this installation, the MiniMover overcomes a transfer length of more than 1,1 km to the downstream section without an additional booster pump. Measurement data from a downstream in-stalled turbidity sensor is integrated into the automated control system, allowing for a controlled and balanced transfer of sediment to the river.

4 PERSPECTIVE ON APPLICATION, ENVIRONMENT AND BUSINESS POTENTIAL

From the beginning, our goal was not limited to competition, but we aimed for a broad and scalable application of the developed technologies. The practical need for application is obvious. Reservoir operators and the government will have to invest significant sums in the coming years to ensure water supply in several regions of the USA and in Europe.

From a commercial point of view, this in turn offers a suitable business perspective for a deep application of the developed and patented technologies with significant business volume. The automation achieved will ensure that our technology is able to undercut the cost of applying conventional dredging methods for reservoirs, thus saving reservoir operators money. Nevertheless, the new technology can be combined with conventional dredging technology and other equipment. After the pilot application in the competition, we already have three larger commercial projects in preparation in Germany.

The judicious application of autonomous dredging will not only ensure cost-effective remediation of reservoirs and ensure their future operation but will also restore sediment continuity in rivers in a naturalistic manner. The benefits are not limited to the immediate downstream sections of the river but extend far downstream to river deltas and coastal regions, preventing further erosion damage. In this way, ecological benefits are achieved at no additional cost.

5 CONCLUSION

In conclusion, the Continuous Sediment Transfer, executed by autonomous vessels called Sedi-Mover, has been declared the winning idea of the Guardians of the Reservoir Challenge conducted by the Bureau of Reclamation and United States Army Corps of Engineering in 2022. This near-natural method is an effective way to restore or maintain the functionality of reservoirs capacity and restore ecological conditions in downstream aquatic systems.

The SediMover is used to remobilize the sediment inside the reservoir and transfer it to the tail-water. Its modularity allows for adaptation to almost every situation, including difficult situations such as flood events and dry falls or quantitative limitations in sediment transfer. With our equipment, more than 25,000 m³ of sediment have been relocated so far without any major failures.

The team successfully demonstrated the process in a field test, which was presented in a demonstration video, a presentation, and a written essay.

The team is also working in cooperation to develop guidelines for sediment transport and sustainable sediment management of reservoirs.

Additionally, research is being conducted on adapting the technology to harvest methane generated inside the sediment to combat greenhouse gas emissions. Furthermore, a smaller version of the SediMover, the MiniMover, has been developed for use in tributaries, limited spaces of reservoirs or shoreline areas.

The continuous sediment transfer process conducted with autonomous vessels shows great potential as it combines ecological benefits with economic benefits to combat a global problem.

REFERENCES

- Rosentreter, J.A. & Borges, A.V. & Deemer, B.R. et al. 2021. Half of global methane emissions come from highly variable aquatic ecosystem sources. *Nat. Geosci.* 14: 225–230.
- IPCC 2014. Climate Change 2014: Synthesis Report. Contribution of Working Groups I, II and III to the Fifth Assessment Report of the Intergovernmental Panel on Climate Change [Core Writing Team, R.K. Pachauri and L.A. Meyer (eds.)].
- IOECD 2013. Test No. 236: Fish Embryo Acute Toxicity (FET) Test, *OECD Guidelines for the Testing of Chemicals*, Section 2. Paris: OECD Publishing.

Specialist grouting works in the renewal of Ritom HPP, Switzerland

A. Heizmann

Renesco GmbH, Lörrach, Germany

G. Lilliu

Renesco Holding AG, Chiasso, Switzerland

ABSTRACT: This paper presents an approach to grouting in a highly water bearing ground, by means of a hybrid grout. A cement suspension is mixed with a variable ratio of polyurethane and depending on the pressure development during grouting, the percentage of cement suspension and polyurethane are correspondingly adjusted. Both the selection of the cement type, of the ratio water/cement and of the polyurethane system potentially allow for a wide range of application. The method was first applied in 2019, during excavation of the new headrace tunnel at Ritom HPP, in Switzerland. An unexpected strong water inflow in a highly fractured rock mass called for the selection of a suitable grouting technique to seal the rock without being washed out. Hybrid grouting proved to be very efficient in stopping the water inflow, and economical. Following the application at Ritom HPP, a laboratory test campaign was conducted to study the short- and long-term properties of the hybrid grout. The effect of adding polyurethane is to significantly reduce the setting time. It also affects some of the mechanical properties, e.g. compressive strength and Young's modulus. Additional laboratory testing aimed to optimize the grout design with respect to specific applications, and large-scale projects will help to refine and further improve the efficiency of the hybrid approach.

1 INTRODUCTION

Cement suspensions and polyurethane resins (PU) are the preferred materials for achieving consolidation and sealing in pre-excavation grouting. Grouting technology has for a long time been challenged by the idea of combining the two materials so to benefit of the advantages of both. The main difficulty to put this idea into practice was that a special grouting equipment and grouting control system were required. The grouting equipment must consist of different mixers and pumps that work in parallel. The control system must adapt the grouting process to the real conditions that are encountered, so to optimize the use of material and the timing. The concept of hybrid grouting developed in this paper is that the cement suspension is the prevailing component of the grout, and PU is added only when needed.

This method was applied in a large-scale project for the first time in 2019, during the excavation of the headrace tunnel in the renewal project of Ritom HPP, in Switzerland. Heavy water inflow made necessary to stop the excavation. The two options of cement and chemical grouting were considered. The engineer had a consolidated experience in cement grouting, and less experience in chemical grouting. On the other side, the specialist grout contractor saw the opportunity to test the newly developed hybrid grouting method. Finally, based on a cost/benefit comparison, the decision was taken to perform hybrid grouting. The hybrid grout consisted of a cement suspension made of an early high-strength Portland cement, CEM I 52.5 R,

with water/cement=0.6, and a fast-reacting, solvent-free, low-viscosity bi-component PU resin. Tests were conducted at site, adding different quantities of PU, and it was concluded that an addition of PU of 20% in weight was the optimum.

After Ritom HPP, hybrid grouting was also applied during excavation of a traffic tunnel in soil, which showed that hybrid grouting can be efficient also in the case of a granular medium. Following these large-scale applications, a series of laboratory tests was conducted to investigate the short- and long-term properties of hybrid grouts with different additions of PU.

The concept of hybrid grouting and the findings from the experimental campaign are summarized in this paper.

2 RITOM HPP

2.1 *Background and renewal project*

Ritom HPP in Canton Ticino, Switzerland, was constructed in 1917 for producing energy for the Gotthard railway line. The components of this 44 MW HPP are: the intake and valve chamber at Ritom lake, a 1030 m long headrace tunnel, surge shaft, valve chamber, and exposed penstocks with a length of approximately 1400 m that convey the water to the four Pelton turbines in the Piotta powerhouse. The maximum head is 850 m. In 2010, the owner of Ritom HPP, the Swiss Federal Railways (SBB), signed an agreement with Canton Ticino and its owned Azienda Elettrica Ticinese (AET), with the scope to construct and operate a new HPP. The project is of strategic importance because it satisfies the increasing demand of energy due to the growth of passenger and freight trains and makes hydroelectric production more efficient. The new HPP will be owned and operated by a new entity, Ritom SA, a company 75% owned by SBB and 25% by Canton Ticino.

The renewal project involves connection of Ritom HPP (SBB) to Stalvedro HPP (AET). The new Ritom HPP will have two turbines, and one pump. The pump can pump water from the lake that feeds Stalvedro HPP into the Ritom Lake, thereby improving current energy production and achieving safe and optimized storage utilization. A re-regulating reservoir with a volume of 100,000 m³ at the outlet of Ritom and Stalvedro HPPs will reduce hydropeaking in the Ticino River (Bronzetti et al. 2022). Construction started in 2018 and is expected to be completed in 2024.

One of the components of the new powerplant is the headrace tunnel connecting the valve chamber with the powerplant. This tunnel consists of three sections: the lower section, excavated by drilling and blasting, has a cross section of 20 m² and a slope of 2%; the mid- and the upper sections, excavated with a TBM, have a diameter of 3.23 m and a slope of 42% and 92% respectively.

2.2 *Grouting works in the headrace tunnel*

During excavation of the lower section of the headrace tunnel, an unexpected water inflow of 135 l/s (Figure 1) made necessary to stop immediately the excavation. Exploratory boreholes showed a weathered rock with fissures of different openings. It was decided that blasting operation could be resumed only after sealing the highly water-bearing rock areas by means of grouting. Hybrid grouting was selected as the most efficient method. A cost-time analysis based on a test-phase where a pure cement suspension and a PU resin were used, showed that in this specific project hybrid grouting could cut costs and time by approximately 50%.

As a first step, a concrete plug was created at the excavation front so to stop immediately the water inflow. This allowed to perform the post-grouting in the already excavated section, in dry conditions. Eight injection screens were created, each consisting of 18 boreholes with a length of 20 m, and 5 m overlapping between the boreholes of two consecutive screens. The injections were carried out in two stages, with packers placed at 10 and 5 m. Next, pre-excavation grouting was executed, with the scope of sealing and consolidating the rock while advancing with the excavation. In the pre-excavation grouting, up to 71 boreholes were drilled

along the perimeter and in the middle of the excavation front, depending on the feedback from exploratory boreholes. Like the post-excavation grouting, the boreholes had a length of 20 m and an overlapping of 5 m. When necessary, primary, secondary, and tertiary injections were performed.

Hybrid grouting showed quite successful, since the water inflow after the treatment reduced to 5 l/s. Furthermore, the important water inflow that was experienced at each sequent excavation stage, gave evidence that the treatment in the previous excavation stage was localized as intended.



Figure 1. New headrace tunnel excavated at Ritom HPP. (Left) Water inflow. (Right) Discontinuities in the rock efficiently sealed with the hybrid grout.

3 HYBRID GROUTING

3.1 Background

Important water inflow during excavation of underground structures may have serious consequences on the economy of the project, or even become a hazard for the structure and its surroundings. Efficient and reliable control of water ingress by means of grouting, without explosion of costs, is a challenge. The ideal grout should have low viscosity, to permit fast penetration rate, and instant setting at pre-defined controllable time intervals. It should have adequate strength if consolidation is also a scope of the grouting; it should not shrink and be durable if the intended result is permanent. Toxicity and price are other critical aspects. Grout materials can be designed to meet some of these requirements, but there is not the “ideal” grout that meets all the requirements. Usually, the choice is between cement suspensions, a large variety of chemical grouts, or hybrid grouts.

In general, cement suspensions are superior to chemical grouts in terms of mechanical performance, they are more readily available and less expensive. The properties of a cement suspension can be adjusted varying the type and granulometry of cement, the ratio water/cement, and using additives or admixtures. Cement grouts can reach their technical limits in presence of flowing water, especially when the water is in pressure. A major problem of pumping cement suspensions into voids filled with water is that curing is delayed, and the grout can be washed out. In this case, the benefit of using a cheaper material is cancelled by the dispersion of the grout out of the section to be treated.

Chemical grouts are superior to cement suspensions in terms of penetration capacity and controllability of the setting time. Their higher costs can be justified in emergency cases when grouting must provide a fast and efficient solution. Hydrophobic PU is commonly used when flowing water becomes critical for the grouting process. The characteristic of PU is that the volume increases after the reaction. The foaming factor affects the final mechanical properties and depends on the specific pressure and temperature conditions. A high foaming factor entails a softer and weaker material. High temperatures can accelerate the reaction, to the critical situation when the reaction occurs ahead of the borehole, with possible damage to the grouting equipment. Depending on the size of the voids where the reaction is taking place, foaming can also bring to build-up an undesired, excessive pressure. It is comprehensible that, more than ever, the grout specialist contractor, and the synergy with the material supplier play an important role on the result of the grouting works.

A hybrid grout, obtained adding PU to the cement suspension, can combine advantages of both components. The hydrophobic PU withstands the water in pressure and fills the large fissures, so reducing the water inflow, while the cement suspension fills the remaining fissures without being washed out. The concept of hybrid grouting is not new. Hybrid grouting in the sense of staged process has been quite common in the past. Adding PU to a cement suspension is also not new. The real novelty of the hybrid grouting applied in the renewal project of Ritom HPP, is that addition of PU is adapted to the real needs while the grouting process is ongoing. This can be done fully automatically, or by the operator. All data of the grouting process, such as the consumption of PU and of cement suspension, the injection pressure and injection times, are recorded. The correct mixing ratio of the two PU components is monitored by corresponding measurements. Possible deviations are communicated to the pump operator.

Hybrid grouting has several advantages: it stops the water inflow and consolidate the ground in one continuous grouting process; there is no useless spread of grout, since the grout process is limited only to the region where indeed needed; since the cement suspension is the largest fraction of the hybrid grout, costs are lower than pure PU grouting. Depending on the specific project conditions, the overall costs are even lower than pure cement grouting, as the injection time is enormously reduced.

Table 1 summarizes and compares the performance of cement, PU, and hybrid grouting. The symbols -, 0, + and ++ indicate an increasingly good performance.

Table 1. Qualitative comparison among cement, PU, and hybrid grouts.

	Cement	PU	Hybrid
Washout resistance	-	+	+
Fast setting time of the grout material → reduction of waiting times	-	++	+
Adjustment of the properties of the grout material during grouting	0	+	++
Reduction of material losses due to the adjustment of the grout properties from borehole to borehole	-	0	+
Economic efficiency			
overall system	0	0	++
material costs	++	0	+

An important aspect of using chemical grouts is the potential danger to the operators and to the environment. Chemicals should be handled with care; therefore, respect of safety regulations at the job site is of utmost importance. Concerning impact on the environment, in general the manufacturer should provide proof that the discharge of substances into water bodies or ground is harmless. Since chemicals in the hybrid grout make up only a small part of the total mixture, its environmental impact is correspondingly smaller than a grout made 100% of resin.

3.2 Equipment and grouting process

Two mixing processes are required to produce the hybrid grout. Water and cement, in the due proportions, are mixed in the cement mixing plant and injected by a pump into the injection hose. The two components of the polyurethane, A and B, are injected by another pump into separate hoses, mixed and injected into the injection hose only ahead of the borehole. The whole process is controlled by a software, which also measures and records the relevant grouting data: pressure, flow rate of the cement grout and of the polyurethane, and the cumulative volume of grout. These data can be included into a BIM as-built model. The layout of the equipment for producing the hybrid grout is shown in Figure 2.

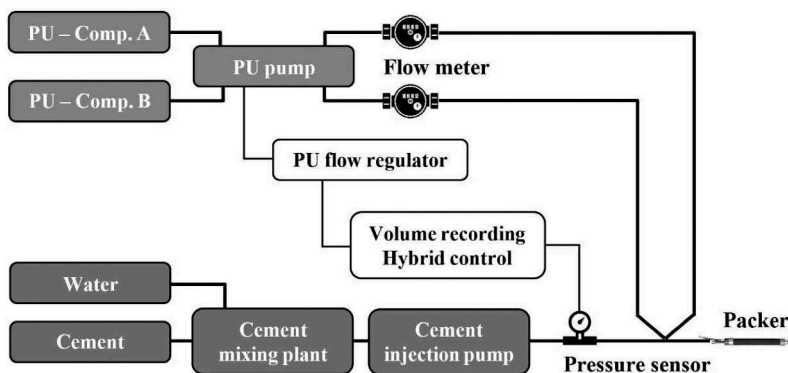


Figure 2. Equipment for hybrid grouting.

The grouting process starts with injecting a pure cement suspension. The cement suspension fills the fissures around the borehole if these are small. In this case the pressure measured by the pressure sensor shows an important increase. In case of large fissures, the increase in pressure is limited and PU is added, in a predefined ratio in weight. Such ratio may vary within the same grouting process, depending on the need. The addition of PU can be done automatically or manually; in case of manual addition, the operator gives to the software the command of adding PU. The addition of PU shortens the setting time, and the highly viscous grout fills the large fissures, without being washed out, so stopping the water inflow. The addition of polyurethane stops when the pressure reaches a maximum, pre-defined value, and the flow rate of the cement suspension falls under

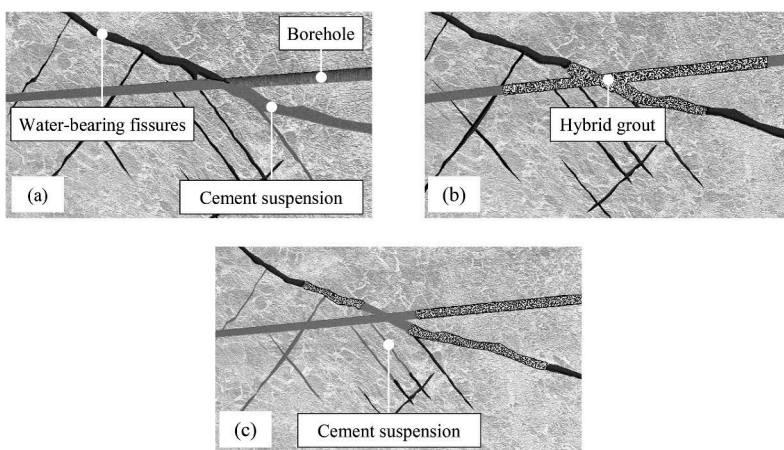


Figure 3. Grouting sequence. (a) Washing out of the cement suspension in large fissures. (b) Injection of the hybrid grout in large fissures. (c) Large fissures are sealed; small fissures are filled with the cement suspension.

a certain limit. Then, the grouting process continues only with the cement suspension, which fills the remaining small fissures, until stabilization of the pressure. Figure 3 shows the injection sequence.

4 GROUT PROPERTIES

After the application at Ritom HPP, hybrid grouting was also applied in another large-scale project, of a tunnel excavation in soil. In both projects, the main scope of the grouting was to stop water inflow during the excavation. The question is if hybrid grouting can serve also as a permanent solution and can have a wider range of applicability, such as foundation grouting of dams, etc. To better understand the short- and long-term properties of the hybrid grout, laboratory tests were conducted in 2020/2021 (Bronzetti et al. 2023). The lack of experience with similar laboratory tests, and the difficulty to construct the specimens because of the fast reaction of the PU were a real challenge in the planning of the test campaign. While performing the tests it also appeared that results were influenced by the procedure with which the specimens were prepared. All this required some adaptation and optimization of the test procedure. All the difficulties reflect in the results, which show some scatter and are sometimes of difficult interpretation.

The components of the grout tested in the laboratory are like those used at Ritom HPP, namely a cement suspension made of a Portland CEM I 52,5 R, with water/cement=0.6, and a fast-reacting, solvent-free, low-viscosity PU resin. The quantity of PU added to the cement suspension varies in the range 0% to 40%. The scope of the laboratory tests was to quantify the properties of the grout in the liquid phase and in the hardened phase. The properties in the hardened phase include compressive and flexural tensile strength, splitting strength, Young's modulus tests and shrinkage.

4.1 *Viscosity*

Penetration of the grout into fissures and voids depends on the size of the largest cement particle and the viscosity. The results of the viscosity tests, which were conducted with a rotational viscometer, show that for a PU content of 10-20%, the reaction time is up to 30 and 15 minutes, respectively. The reaction time reduces to 4 and 2 minutes when the content of PU increases to 30% and 40%, respectively. The fast reaction time is a major advantage in practice, especially when there is an important water inflow.

4.2 *Mechanical properties of the hardened grout*

The compressive strength was determined according to the European norm DIN EN 196-1 on specimens of different age (24 hours, 72 hours, 28 days, 56 days, and 91 days). The test results show that an addition of 10% PU causes an important reduction of the compressive strength. This reduction can be as much as 70% at the early age of 24 hours, while it is limited to 30%-40% when the material matures. If the quantity of PU increases to 20%, the compressive strength further decreases, although less remarkably. After the limit of 20%, the compressive strength remains practically unchanged (Figure 4).

The tensile splitting strength, determined after 28 days according to the European norm DIN EN 12390-6, remains practically unchanged and does not depend on the quantity of PU (Figure 5).

The Young's modulus was determined according to DIN EN 12390-13. The tests were conducted at an age of approximately 90 days so that the results can be considered representative of the long-term behavior. As for the compressive strength, indeed the addition of 10%-20% PU causes a decrease of the Young's modulus, however such decrease is less remarkable when the quantity of PU increases up to 30%-40% (Figure 6).

4.3 *Shrinkage behavior*

Shrinkage was measured with the shrinkage device type C according to the European norm DIN 52450. The results of the tests show that the specimens shrink less when PU is added to the cement suspension (Figure 7). This is an advantage especially for sealing applications.

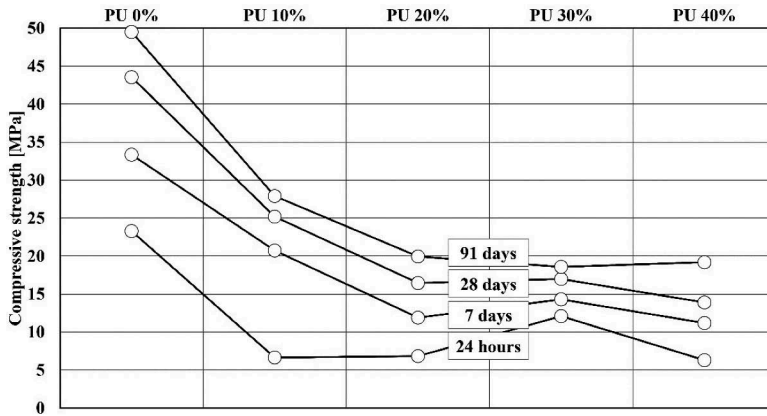


Figure 4. Compressive strength at different ages and for different PU contents.

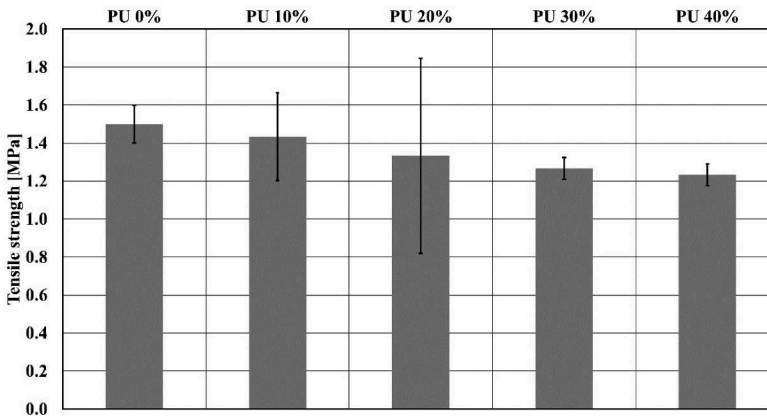


Figure 5. Splitting tensile strength at different ages and for different PU contents.

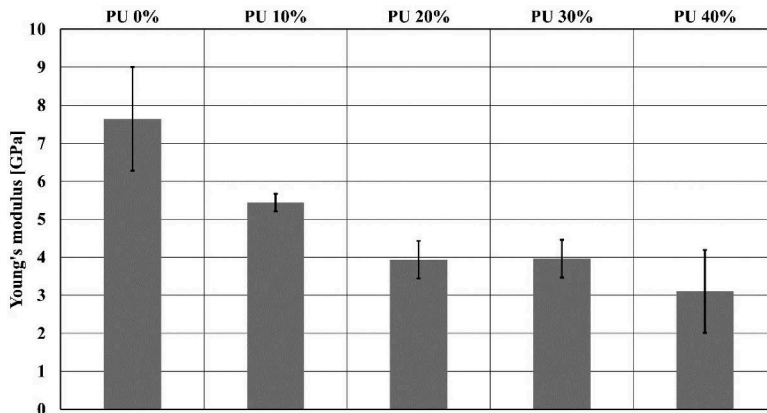


Figure 6. Young's modulus at different ages and for different PU contents.

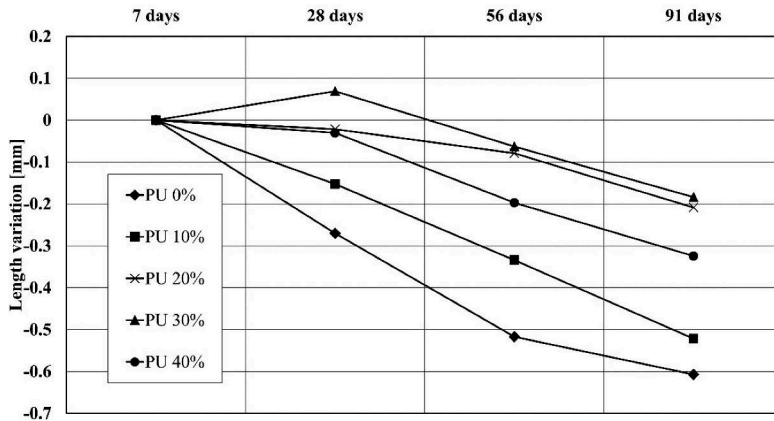


Figure 7. Variation of the length of the specimens, with respect to the length measured at an age of 7 days, for different PU contents.

5 CONCLUSIONS

Excavation of the new headrace tunnel in the renewal project of Ritom HPP, in Switzerland, was the opportunity for applying for the first time a hybrid grouting approach in a large-scale project. In this approach, the grout is basically a cement suspension, with addition of polyurethane. In this manner, advantages of the two components of the grout, such as economy and controllable setting times, are combined. The grouting process is computer-steered, and addition of the polyurethane is controlled automatically, or manually by the operator. A major achievement with hybrid grouting is to limit grouting only to the intended section, so preventing useless spread of material, which can be critical in presence of flowing water. The great flexibility in the material design possibly allows for a wider range of applications. To better investigate this point, laboratory tests were performed with the scope of determining short- and long-term properties of hybrid grouts with different contents of polyurethane. The main findings are that addition of polyurethane reduces the setting times to a few minutes, but also has the effect to reduce some of the mechanical properties of the hardened grout. Due to the fast reaction of the polyurethane, construction of the specimens was quite complex. Execution of the laboratory tests was made complex also by the lack of previous experience in this type of testing. More laboratory testing is necessary, especially with the aim of optimizing the grout design with respect to specific applications. Finally, more large-scale projects of different types are necessary to refine and improve the current hybrid grouting process.

REFERENCES

- Bronzetti D. et al. 2023. Hybrid injections – Laboratory testing and field experience during tunnel excavation. Proc. 6th International Conference on Grouting & Deep Mixing, New Orleans 15–18 January 2023.
- Ritz, M. et al. 2022. Ritom power plant renewal with new inclined pressure shaft. *Proc. ITA-AITES World Tunnel Congress, WTC2022 and 48th General Assembly*, Copenhagen 2–8 September 2022.

Wave return walls within the adapted freeboard design at dams

Max Heß & Dirk Carstensen

*Institute of Hydraulic Engineering and Water Resources Management, Technische Hochschule Nürnberg
Georg Simon Ohm, Nuremberg, Germany*

ABSTRACT: Optimizing freeboard at dams, became more and more relevant for operators of dams due to climate change, the assurance of flood retention, or the adjustment of the design water levels. The wave run-up represents the dominant portion of the freeboard at reservoirs and therefore deserves the most attention regarding optimizations. With the usage of wave deflection structures the safety of overtopping can significantly be increased. In contrast to coastal engineering overtopping as a result of the wave run-up with or without wave return walls in the adapted freeboard design at dams is generally not tolerated (zero overtopping). However existing design approaches for wave deflectors are currently always based on the overtopping rate, which therefore is greater than zero.

As part of independent investigations a hydrodynamic numerical model had been developed, calibrated and validated by using data obtained from physical hydraulic model tests. Based on performed simulations the general understanding of the redirection process of the wave run-up surge had been studied. Furthermore a data set, that specifies the required wave deflector size and the forces acting on the deflector at maximum (optimal) capacity utilization without overtopping was developed and used to build a dimensioning concept depending on the boundary conditions mentioned.

1 INTRODUCTION

Considering climate change, ensuring the flood retention area or because of adjustments of the design water levels at reservoirs, the optimization of the freeboard at dams is becoming increasingly important for operators of dams. The freeboard at dams R_C can be defined as the vertical distance between the dam crest and the maximum design-pool elevation. According to the recommendations for dams by the German Institute for Standardization (DIN 19700-11) the freeboard design in Germany generally consists of four parts: wind surge h_{wind} , wave run-up h_{run-up} , if needed ice surge h_{ice} , as well as a safety margin h_{safety} (see Equation 1).

$$R_C = h_{wind} + h_{run-up} + h_{safety} (+h_{ice}) \quad (1)$$

Through analytical calculations these formula components are usually determined with sufficient accuracy. The wind surge component is mostly dependent on the water surface area, which is limited at reservoirs, and on the water depth, which is mostly high, hence the wind surge is only a few centimeters. Furthermore, the safety margin more or less represents a fixed value, which is determined, among other things, with regard to the existing remaining risks. In Contrast, the wave run-up height has a decisive influence on the composition of the freeboard as it depends on local shore conditions, and wind-induced wave loads which are determined by sea state forecasting methods.

Reservoirs and dams are built based on available data and forecasts to last for several centuries. Changes in the planned use of a reservoir or due to climate change can lead to a freeboard deficit

at barrier structures. In general, two procedures can be followed to reassess the freeboard. On the one hand, since an analytical calculation only represents an estimation, an exact determination of the freeboard components can be carried out by the means of thorough, individual investigations, using physical or numerical model experiments. With the acquired results, the analytically obtained values can be corrected - at best in favor of the required freeboard. On the other hand, the wave run-up surge can be turned away from the dam crest with the usage of appropriate crest elements, so-called wave deflectors or wave return walls, and thus wave overflow can be reduced or fully prevented. Designing geometric dimensions and determination of wave loads on wave deflectors for the intended use at dam embankments or crests using analytical methods is only possible to a limited extent. Currently, available design approaches are always based on the assumption of the wave run-up on an infinitely long embankment extending beyond the crest of the structure and the associated wave overflow. Examples of such design approaches are the scientific work of Van Doorslaer (2015) or Pohl (1990), which both developed calculation methods based on model tests and field measurements. In coastal engineering the overflow of waves at barrier structures, the so-called overtopping, is usually tolerated to a certain extent and justifies the use of the existing design approaches. However, the overtopping is fundamentally dangerous and in the context of the freeboard design at dams at inland areas it is basically not permitted. This principle is also reflected in the safety margin according to the German Institute for Standardization. A design concept for wave deflectors at an optimal capacity utilization but without planned overtopping currently represents a deficit in the adjusted freeboard design at dams.

In addition to the execution of physical model tests for the precise determination of the wave run-up heights or wave loads for the design of crest elements, the hydrodynamic numerical (HN) simulation represents a promising alternative with today's available high performance computers. Independent investigations were carried out to verify the predictability of numerical methods relating to the wave run-up process as a result of the breaking of waves at embankments as well as the deflection of the run-up surge. Therefore, physical model tests had been carried out in order to measure significant hydraulic parameters. The collected data was then used to develop a well calibrated and validated numerical model. Furthermore, the established numerical models were applied to analyze the flow behavior, especially during the process of run-up surge redirection using wave deflectors. Finally, the results were used to develop a dimensioning chart through which the required wave deflectors size as well as the expected occurring forces can be easily determined.

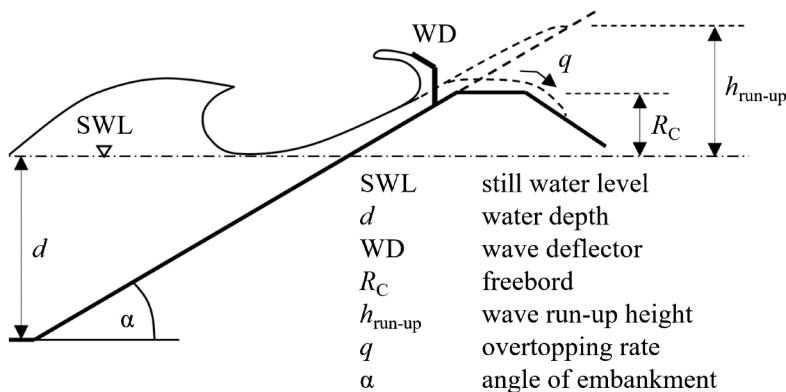


Figure 1. Sketch of the flow process in the context of wave run-up, overtopping and deflection.

2 BASICS OF THE HYDRAULIC PROCESSES

If waves reach the shore, their energy is basically converted into run-up, reflection and dissipation energy and, among other things, this results in a more or less distinctive run-up surge. Initially, the surge contains a large part of kinetic energy, which is dissipated with the distance covered on the embankment and decisively gets converted into potential energy. At the

moment, when the surge has dissipated all its kinetic energy, the maximum wave run-up height has been reached on a theoretical infinitely long embankment and the backflow of the water due to the downhill-slope force begins. If the available free space up to the crest of a dam is not sufficient, the wave tongue bends onto the approximately horizontal crest and thus can cause a more or less pronounced overflow of the air-side embankment. Crest elements for wave deflection can reduce or avoid the overflow volume by changing the direction of the run-up surge and deflecting the flow back into the reservoir. The processes described are outlined in Figure 1.

Depending on the characteristic of the breaking of waves, the hydraulic processes described generally result in an unsteady, non-uniform flow under the influence of frictional forces, turbulence and air entrainment. These complex boundary conditions lead to the conclusion that hydraulic model experiments are usually necessary for the analysis of the processes described. However, a mathematical description can be given using the equations for the conservation of mass, momentum and energy, which can nowadays usually be solved with sufficient accuracy using numerical methods.

3 NUMERICAL METHODS

The open source CFD library OpenFOAM can be used to solve the conservation equations for describing continuum flows. Due to the possibility of reviewing the source code without restrictions and expanding it if necessary, OpenFOAM represents a suitable platform for scientific investigations. The Volume-Of-Fluid method `interFoam` and `interIsoFoam` had been used to analyze the hydrodynamic processes of wave run-up events and the deflection of the surge. These solvers use the incompressible momentum equations, the continuity equation and an additional equation for the phase fraction, which can define the transition between the air and the water phase. Detailed information of the mathematical models implemented in the solution methods can be found in the work of Damián (2012) or Roenby et al. (2017).

Due to the generally limited availability of computational resources, it is fundamentally necessary to model turbulent structures in the flow for larger model areas. Detached Eddy Simulation (DES) turbulence models, which are combinations of the Large Eddy Simulation (LES) method and the Reynolds-Averaged Navier-Stokes (RANS) equations, are well suited for this purpose. With these models, the turbulent structures in the free flow are either directly numerically calculated or get modeled in dependency on the local grid size (LES method). Further, a complete RANS modeling takes place in the vicinity of object surfaces (walls), which generally corresponds to a temporal averaging of the turbulent fluctuations in this area. With the used DES turbulence model based on Menter's $k-\omega$ -SST model (Menter, 1994), equations for the turbulent kinetic energy k and the turbulent dissipation rate ω need to be solved within the numerical solution procedure. Based on these, the required eddy viscosity, which is needed to solve the discretized continuum equations, is being calculated.

4 CALIBRATION OF THE NUMERICAL MODEL

To provide a substantiated data basis for the calibration of the numerical models, a test setup was built and experiments were carried out at the laboratory of the Institute of Hydraulic Engineering and Water Resources Management at Technische Hochschule Nürnberg. In addition to a customized wave generator, an embankment with an adjustable incline were installed in an existing test flume. Furthermore, various types of wave deflectors could be installed at the embankment. The recording of relevant parameters, such as wave shield positions, water depths, wave run-up heights or forces acting on wave deflectors, was carried out using various modified measurement devices. The hydrodynamic numerical models were set up in accordance to the test setup at hand. A movable boundary wall was implemented via a dynamic calculation grid and thus made it possible to change its position according to the

wave shield in the context of the physical model tests. As a result, the boundary conditions for the experiments could be precisely reproduced with the numerical model and allowed a direct comparison of the wave profiles and the resulting flow behavior at the embankment.

The numerical model was developed and refined over several test series and experiments. Initially measurement data on the simple propagation of waves along the test flume served to check the numerical boundary conditions and enabled the adjustment of basic simulation parameters. As already described by other authors, it could be shown that the differencing and interpolation schemes used as well as the Courant criterion can have a significant influence on the stability of the calculations and on the propagation of the waves. In addition, the grid size at the water surface represents an important criterion with regard to the stability of the shape of the waves. The statement by Larsen et al. (2018) that a grid resolution of approximately 20 cells in relation to the wave height should be maintained for a realistic depiction of the wave profiles could be confirmed. Further test procedures, which included wave trains containing only a small number of waves, allowed the detailed recording of the waves breaking when reaching the embankment as well as each individual run-up surge. Data from these experiments were also used to calibrate the numerical models, as significantly higher requirements regarding the grid resolution at the embankment were needed for depicting these processes with the numerical models. Depending on the nature of the breaking of the waves, air entrainment and increased turbulence are to be expected, which requires the use of corresponding model approaches. At the beginning of each simulation, the flow conditions were stationary and therefore there was no turbulence. With the use of turbulence models, this means that the initialization values for the turbulent transport variables are theoretically set to zero. Depending on the solution method, the general production of turbulent viscosity can thereby fail, and the turbulence model is actually not working properly. An adequate estimation of the initialization values for the turbulent transport parameters, in the application at hand the turbulent kinetic energy and the turbulent dissipation rate, is therefore an important part of the calibration.

Furthermore, the spatial discretization, particularly on the surface of the embankment, is decisively influencing the formation of the wave run-up surge and thus the resulting run-up height. With a sufficiently fine mesh at no-slip surfaces, the flow behavior in the boundary layer can be fully resolved. However, for larger model areas, this is generally not feasible since the required number of cells would be too high. This is why so-called wall functions were developed and are applied in these cases. Wall functions model the flow at the boundary layer using the knowledge of the universal law of the wall, which means that there are still certain requirements for the local grid size. Assuming a fully developed turbulent boundary layer, the common recommendation of positioning the cell center closest to the wall in the log-law region can usually be achieved with the use of flat cell shapes (layers). In addition, there is a dependency on the free stream velocity, which is varying over time and space in a run-up surge. This is why an adapted spatial discretization together with the unsteady flow conditions is difficult to implement and makes a case-specific calibration and validation indispensable.

5 CONCLUSIONS ON THE NUMERICAL MODELLING

Among others, the calibrated numerical models had been validated using large scale wave run-up test results gained at the Large Wave Flume (Großer Wellenkanal, GWK) at Coastal Research Center Hanover. This data showed good agreement with the results of corresponding numerical simulations and thus allowed a good transferability of the models for large scales. As a result of the thorough calibration and validation, recommendations regarding the numerical modeling of the wave run-up and the wave deflection could be formulated. The most important numerical model settings are, firstly, the initialization values for the turbulent field variables of the turbulence models, secondly, the use of an adequate spacial discretization especially at the waver surface as well as at the surf zone and, thirdly, the limitation the time step size via the Courant criterion (recommendation: $Co \leq 0.3$).

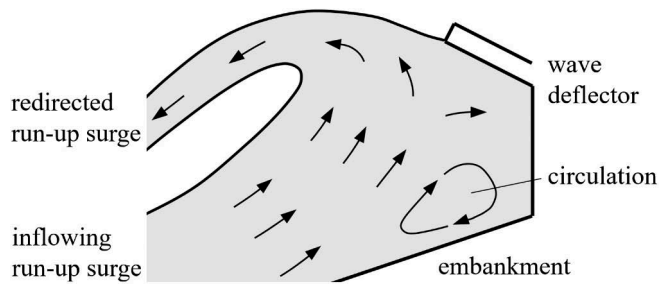


Figure 2. Sketch of the flow behavior at the wave deflector near its maximum capacity utilization.

With the performed hydrodynamic numerical calculations, the process of the wave run-up surge deflection had been analyzed. According to this, the general development of a circulation at the foot of the wave deflector could be proven during the surge deflection, which intensity showed a dependence on the capacity utilization of the deflector. In general, this condition causes a shift of the deflecting effect in the direction of the inflowing surge and thus influences the condition of the resulting surge when exiting the wave deflector. Furthermore, the latter influences the potential of overtopping. Figure 2 shows an example of a wave deflector, consisting of a vertical wall with a cantilevered deflector directed towards the water-side, and a sketch of the flow behavior during the deflection of the run-up surge near the maximum capacity utilization.

6 ZERO OVERTOPPING DESIGN APPROACH FOR WAVE DEFLECTORS

Existing design concepts for wave deflectors are generally adapted for coastal engineering applications. With these, certain amounts of overtopping rates are usually tolerated at wave deflectors, which is why existing dimensioning approaches are generally based on the specification of overflow rates. This procedure is only useful to a limited extent for the design of wave deflectors on dams at inland areas, since the overflow of such structures is normally an exclusion criterion. Considering the fact that there is a current deficit in design concepts for wave deflectors without intended overtopping, appropriate simulations were carried out with the established numerical models to gather data for a new design approach.

Due to the variety of structural design opportunities for wave deflectors, the development of one universally valid all-encompassing dimensioning approach is improbable. Consequently, numerical investigations were limited to a deflector type consisting of a vertical wall with a cantilevered deflector directed towards the water-side. Among other things, such a construction can be considered favorable from an economic point of view due to its simple structural realization. With the variation of the boundary conditions for each numerical simulation (compare system sketch in Figure 4), consisting of

- the wave parameters in deep water (wave length L_0 and wave height H_0),
- the inclination of the embankment α or $1:n$,
- the position of the wave deflector on the embankment above the still water level h_U and
- the total height of the wave deflector through which the flow passes H_U ,

the hydraulic effectiveness of the wave deflector was evaluated according to the respective conditions. In general, the process of the wave surge deflection could be classified into four categories, depending on the run-up surge dimension. Figure 3 sketches this subdivision. Accordingly, in categories 1 and 2, the run-up surge gets completely deflected without any overtopping. In category 3, the backflow of the surge, as a result of the collapse of the insufficiently deflected run-up surge, already leads to a certain overflow over the deflector. Category 4 finally represents a clear overflow of the deflector already during the ongoing inflow process. As part of further simulations to develop a data set, that specifies the required wave deflector height at maximum (optimal) capacity utilization depending on the boundary conditions mentioned, the overtopping of the deflector was defined as a termination criterion.

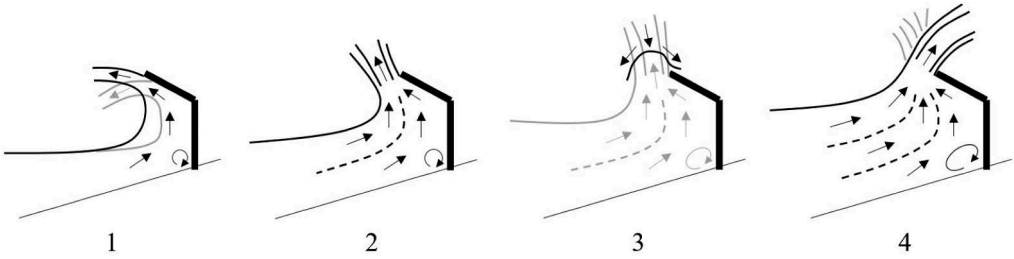


Figure 3. Schematic sketch of the four categories in wave run-up surge deflection processes depending on the inflow condition at the wave deflector.

The parameters of the data sets were evaluated in dimensionless form and with the help of regression analyses. In general, approximately linear correlations could be shown between the required height of a wave deflector and its positioning on the embankment in relation to the wave parameters and the embankment inclination. The dimensionless wave deflector height H_U^* can be determined on the basis of the dimensionless position of the wave deflector on the embankment above the still water level h_U^* as a function of the wave steepness H_0/L_0 according to Equation 2.

$$H_U^* = A \cdot h_U^* + B \quad (2)$$

The parameters A and B in Equation 2 represent functions of the wave steepness and vary with the slope of the embankment. With the help of the derived equations, diagrams with function lines of selected wave steepnesses were created as a dimensioning approach for various embankment inclinations.

Additionally, the horizontal and vertical forces acting on the deflection structure as well as the resulting moment at the base of the wave deflector had been calculated within the numerical simulations and the maximum design loads for each constellation were extracted. Using regression analyzes, these data had been edited, and graphical design sheets were produced in dependence of the wave deflector height. With this, the decisive loads to be expected as a consequence of the deflection at maximum capacity utilization can be transferred directly to the structural design and planning.

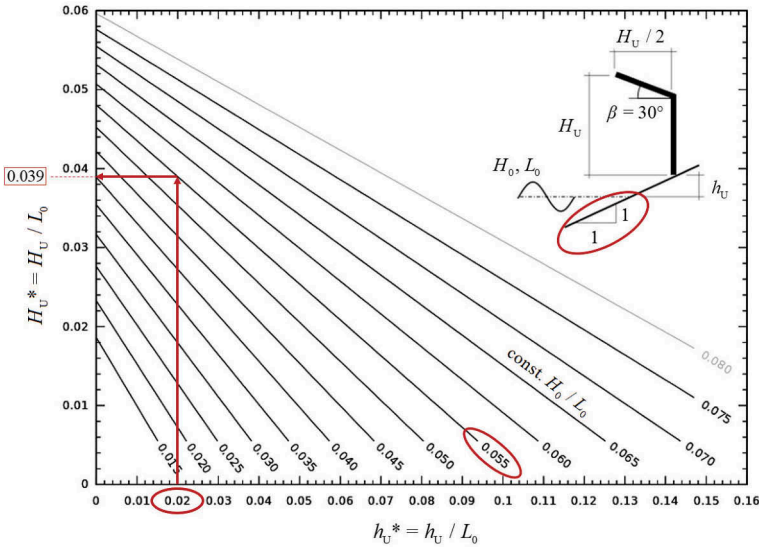


Figure 4. Application example: Dimensioning diagram for a slope inclination of $1 : n = 1 : 1$ to estimate the required wave deflector height H_U , respectively H_U^* , at maximum capacity utilization. (Heß, 2022).

Figure 4 and 5, which are referred to in Section 8 as part of an application example, show the structure of these diagrams for a set of specific boundary conditions.

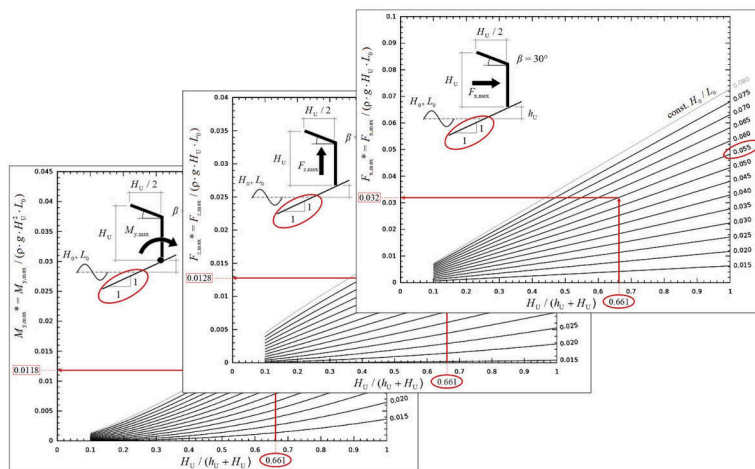


Figure 5. Application example: Dimensioning diagrams for a slope inclination of $1 : n = 1 : 1$ to estimate the maximum horizontal and vertical forces $F_{x,max}$ and $F_{z,max}$ as well as the maximum moment acting at the base of the wave deflector $M_{y,max}$ at maximum capacity utilization.

7 CONCLUSIONS ON THE DESIGN APPROACH

With the developed design concept for wave deflectors on dams, applied to a vertical wall with a cantilevered deflector, the required wave deflector height and the loads to be expected can be estimated depending on the positioning of the wave deflector, the embankment inclination and the wave parameters. In contrast to the existing design approaches, the dimensioning is not based on the overtopping rate as a result of an overflow event, but on the parameters of the structure at maximum capacity utilization without overtopping. Conceptualized specifically for the use in the adapted freeboard design at dams at inland areas, where the wave overtopping is usually not tolerated, the developed dimensioning concept can be utilized. To guarantee the reliability and usability of the concept for practical applications, it can be advisable to confirm the determined parameters by means of corresponding field or model tests until this procedure becomes a recognized rule of technology. Likewise, the consideration of safety factors to minimize the residual risk of overtopping in practical operation can be expedient.

8 APPLICATION EXAMPLE

After analyzing historical wind data measurements and relevant fetch lengths, along with considering new design water levels at an existing reservoir, it was determined that the established dam structure can no longer guarantee the required freeboard. The assessment report indicates that a wind surge of $h_{wind} = 0.03$ m and a wave run-up height of $h_{run-up} = 2.7$ m (calculated according to EurOtop, 2018) can be expected at the dam. The latter is based on the wave parameters of $H_0 = 0.825$ m and $L_0 = 15.0$ m, respectively. Furthermore, the probability of a relevant flood event together with ice coverage at the reservoir is very low, and therefore the ice surge can be neglected. Without taking into account the safety margin, the required freeboard amounts to $R_{C,req} = h_{wind} + h_{run-up} = 2.73$ m, as per Equation 1. In comparison, the present freeboard together with the new design water level is only $R_{C,pres} = 0.33$ m.

To eliminate this deficit, wave deflectors will be installed on the crest of the dam as part of an adjusted freeboard design. The proposed verification process includes the following steps:

1. Determination of the vertical distance between the design water level and the foot of the wave deflector:

$$h_U = R_{(C,pres)} \cdot h_{wind} = 0.3 \text{ m}$$

2. Determination of the dimensionless parameters h_U^* and H_0/L_0 :

$$h_U^* = h_U/L_0 = 0.02$$

$$H_0/L_0 = 0.055$$

3. Based on the inclination of the embankment, which is $1:n = 1:1$, the required dimensioning diagram is selected from the collection. This diagram is then used to estimate the dimensionless wave deflector height - see Figure 4.

$$\rightarrow H_U^* = H_U/L_0 = 0.039$$

To prevent overtopping at the dam, a wave deflector with a height of $H_U = 0.039 \cdot L_0 = 0.585 \text{ m}$ must be installed on the water-side crest of the dam. The geometric design of the deflector is shown in the sketch at the upper right corner of Figure 4. When calculating the resulting freeboard (without the safety margin), the wave run-up height h_{run-up} is replaced by the sum of the wave deflector parameters H_U and h_U , which yields $R_{C,new} = h_{wind} + H_U + h_U = 0.915 \text{ m}$.

In analogy to step 3 and based again on the wave steepness and on the ratio of $H_U/(h_U + H_U)$, which in this example amounts to 0.661 and includes the wave deflector height received, the horizontal and vertical forces as well as the moment acting at the base of the wave deflector at maximum capacity utilization can be assessed. To comprehensively demonstrate the design procedure, Figure 5 shows the determination of these parameters with the corresponding diagrams. On closer examination of the horizontal force component, this leads to a dimensionless horizontal force of $F_{x,max}^* = F_{x,max}/(\rho \cdot g \cdot H_0 \cdot L_0) = 0.0319$. By rearranging this formula and substituting the given values, with the density of water $\rho = 1000 \text{ kg/m}^3$ and the gravity acceleration $g = 9.81 \text{ m/s}^2$, a maximum horizontal force on the wave deflector of approximately $F_{x,max} = 3.9 \text{ kN}$ is to be expected. Likewise, vertical force components up to $F_{z,max} = 1.6 \text{ kN}$ and moments acting at the base of the wave deflector up to $M_{y,max} = 1.2 \text{ kNm}$ may occur during the redirection processes at maximum capacity utilization.

REFERENCES

- Damián, S.M. 2012. Description and utilization of interfoam multiphase solver. *Technical report; International Center for Computational Methods in Engineering*.
- EurOtop. 2018. Manual on Wave Overtopping of Sea Defences and Related Structures. An overtopping manual largely based on European research, but for worldwide application. Van der Meer, J.W., Allsop, N.W.H., Bruce, T., DeRouck, J., Kortenhaus, A., Pullen, T., Schüttrumpf, H., Troch, P. & Zanuttigh, B.
- Heß, M. 2022. Wellenumlenker in der Freibordbemessung an Stauanlagen. *WasserWirtschaft*, 9/2022: 28–32.
- Jacobsen, N. G., Fuhrman, D. R., & Fredsoe, J. 2011. A Wave Generation Toolbox for the Open-Source CFD Library: OpenFOAM. *International Journal for Numerical Methods in Fluids*, 70: 1073–1088.
- Larsen, B.E., Fuhrman, D.R., & Roenby, J. 2018. Performance of interFoam on the simulation of progressive waves. *Coastal Engineering Journal*, 61(3): 380–400.
- Menter, F.R. 1994. Two-Equation Eddy-Viscosity Turbulence Models for Engineering Applications. *AIAA Journal*, 32(8): 1598–1605.
- Pohl, R. 1990. Die Berechnung der auf- und überlaufvermindernden Wirkung von Wellenumlenkern im Staudambau. *Dresdner Wasserbauliche Mitteilungen*, Heft 3.
- Roenby, J., Larsen, B.E., Bredmose, H. & Jasak, H. 2017. A new Volume-of-Fluid Methode in OpenFOAM. *MARINE. 7th International Conference on Computational Methods in Marine Engineering*.
- Van Doorslaer, K., De Rouck, J., Audenaert, S., & Duquet, V. 2015. Crest modifications to reduce wave overtopping of non-breaking waves over a smooth dike slope. *Coastal Engineering*, 101: 69–88.

PV plant - New potentials in Vau i Dejes HPP, Albania

A. Jovani

Albanian National Committee on Large Dams (ALBCOLD), Tirana, Albania

F. Shaha

Albanian Young Engineers Forum, Tirana, Albania

ABSTRACT: This paper provides the information and results on the implementation of a photovoltaic (PV) plant on the Qyrmaq Dam of Vau i Dejes Hydropower plant (HPP) in Albania. Qyrmaq Dam is 54 meters high and has a dam crest length of 514 meters. This composite dam consists of a rock-fill dam with a clay core and a concrete gravity dam. The concrete gravity dam includes the power water intake and spillway systems, with a total capacity of 3900 m³/s. The main purpose of the implementation of this project is the production of energy through the use of solar energy using the surface of the downstream face of Qyrmaq Dam. The project is an attempt to implement new technology in this field as well as the possibility of installing PV plants in other dams in the future. Albania is a country rich in water and sunlight, with a hydrographic catchment area covering 43700 km². Approximately 35% of the average water inflow is used for hydro energy. Moreover, Albania experiences over 300 sunny days per year. For 3 years, the Albanian Government has started the implementation of a strategy for installation of PV plants with capacity of 400 MW in some areas of our country. Till now, 3% of the energy is produced by them. Furthermore, the synthesis will give the requirements of ALBCOLD for installation of PV plant on large dams.

1 INTRODUCTION

Qyrmaq Dam is 54 m high and has a crest length of 514 m. The dam consists of a rock fill dam section with a clay core, and a concrete gravity dam section with the power intake and spillway. It was completed in 1971. The following five monitoring systems are installed:

- Geodetic monitoring system: 18 concrete monuments, 8 geodetic reference points, 16 leveling points, and 4 pillars.
- Seismic monitoring system: 3 strong motion accelerometer.
- Hydro-meteorological monitoring system: 2 hydrometric stations for water level measurements and 2 meteorological stations.
- Hydraulic monitoring system: 5 flow measurement instruments to monitor seepage through the rock-fill dam.
- Hydro-geological monitoring system: 9 piezometers.

A photo-voltaic (PV) plant has been installed on the downstream face of the embankment dam. The surface where the solar panels are installed is about 32,000 m².

The PV plant is conceived as a PV park with panels mounted on metallic construction installed on the ground. The PV park has been treated as a system connected to the energy network which includes numerous arrays of panels and directly connected to the medium voltage network located near Vau i Dejes Hydro power plant (HPP).

The PV panels are installed in 3 main areas according to a well-defined scheme that makes possible not only the high efficiency production of energy but the future monitoring of the dam through the instruments installed in it. A total of 10,640 photovoltaic panels of the SPR-P3 type has been installed there, which have a total capacity of 5.14 MW have been installed. After an optimization process of the PV system, the designers have decided to select mono-crystalline PV panels with 72 cells and high performance. The efficiency of the PV panels is 20%.

2 MAIN REQUIREMENT TO BE SOLVED DURING THE DESIGN PHASE

The project has addressed the main tasks as follows:

- Evaluation the current state of the area where the PV plant will be installed
- Evaluation of solar radiation in the project area
- Selection of the technology for photovoltaic elements
- Dimensions of PV panels and power transmission cables
- The method of installation of the solar panels and determining the yield of the PV plant
- Assessment and mitigation of the impact on the environment
- Connection to the energy system
- Sizing the supporting structures for the PV panels
- Static and dynamic calculations of supporting structures of PV panels closely related to the stability of the dam rockfill material
- Determining the control and monitoring systems for the photovoltaic system including automatic operation through a SCADA system
- Establishing protective measures against over-currents over-voltage and against fire
- Determining the technical specifications for civil works and the main elements of the plant
- Analysis and evaluation of seismic impact corrosion in assembly structures snow and flood impacts on the assembly structure
- Analysis and evaluation of the new conditions regarding the removal and drainage of surface waters in the dam area.

The installation method for PV panels has taken into consideration additional requirements from Albanian National Committee on Large Dams (ALBCOLD) for:

- Checking of structural safety of the Qyrdaq dam,
- Continuation of the dam monitoring and control of all monitoring instruments,
- Continuation of access to the existing dam monitoring instruments.

In order to minimize the impact of the PV plant on the dam, the normal distance between rows of panels, the ventilation and passage spaces between sub-areas, the placement angles of PV panels, the orientations of the panels, the monitoring system installed on the dam, the easiest possibility to move in the areas between main rows, and the use of lighter materials were taken into consideration.

3 DAM SAFETY ANALYSIS AND STRUCTURAL SAFETY

During the project preparation phase, a safety analysis of the dam was carried out, which consisted in:

- Analysing the stresses on the dam body from the applied loads (photovoltaic panels + their b/a foundation), with normal water level (operation case).
- Analysing the stresses on the dam body from applied loads (photovoltaic panels + their b/a foundation), with maximum water level (emergency case).
- Evaluating the sliding plans and factors of safety.

The purpose of these analyses was to analyze the effect the PV panels static loads together with their supporting elements on the body of the dam in the most unfavorable transverse



Figure 1. Views of PV Plant on the downstream face of Qyrsaqi Dam.

section determined. In addition, these analyses aimed at evaluating the dam behaviour and structural safety after 50 years of operation, during which two strong earthquakes had hit the area of this dam (1979 and 2019).

The analysis was based on the design standards such as Eurocode 1, 2, 3, 7, 8, respectively for loads, concrete structures, metal construction, geotechnical works, and structures in seismic areas.

Based on the predetermined scheme, the photovoltaic panels will be mounted on the body of rock-fill dam by fixing them with metal profiles on reinforced concrete bases in the form of foundation beams.

The self-weight of the PV panels, metal construction for panel placement, and foundations were distributed on the loading surface per m^2 according to the spacing of the foundations. The weight of the metal construction and the photovoltaic panels was determined based on available materials and references from similar construction.

For the analysis of the stability, stress state, and deformations, the engineering Finite Element software PLAXIS 2D was used in plane stress conditions.

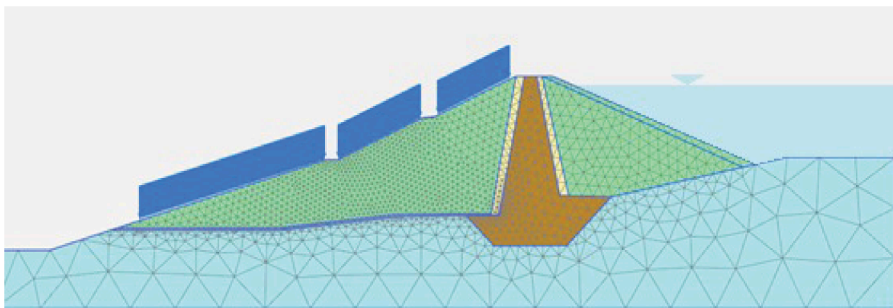


Figure 2. Mathematical model for additional load of PV plant on Qyrsaqi Dam.

The stability of the downstream slope of the dam has been analyzed considering a saturation line between the upstream face of the dam and the filter and drainage layer under the downstream shell. The results show that the installation of these panels does not impact the stability of the dam and the safety reliability index of the dam is within the limits specified by technical standards, the safety reliability index being determined based on the average safety factor and a standard deviation indicator.

4 CONCLUSIONS AND RECOMMENDATIONS OF ALBCOLD

Based on design studies and on the dam safety analysis, it can be concluded that:

- PV installations on rock-fill dams may complicate visual inspections, and therefore, measures should be taken to ensure that visual inspections can still be carried out effectively.
- PV installation impact on the stability and the behaviour of the dam must be studied through static model. Nevertheless, the effects from the installation of the PV panels on the dam can be negligible.

- The resistance of the PV installation system must be checked in case of earthquake according to the national rules.
- An additional risk is that the PV installations on dams can burn, which could damage fasteners, mounting structures, and monitoring instruments installed. Proper fire protection devices should be put in place to mitigate this risk.

Based on these conclusions, ALBCOLD has provided the following recommendations:

- The surveillance, monitoring, and maintenance of the rock-fill dam must not be hindered by the photovoltaic installation, and visual inspections should still be possible as before the installation of the panels. Unrestricted checks should also be carried out after exceptional events such as earthquakes and floods.
- Geodetic measurement has been adapted in particular with higher pillars and easy access between PV panels
- The dam operator should continue to implement control and monitoring measures for the photovoltaic installation for dam safety purposes, including geodetic surveys.
- Lightning protection should be installed to protect the photovoltaic panels and associated equipment from lightning strikes.
- The photovoltaic panels should be properly grounded to mitigate electrical risks.
- The emergency switch of the inverter should be easily accessible to the dam operator and fire department for quick response in case of emergencies.

The installation of the PV plant on the Qyrdaq dam has been carried out in compliance with all technical conditions related to dam safety. This initiative by Albanian Power Corporation to produce electricity using photovoltaic technology in otherwise unusable areas is a positive step towards further expanding renewable energy generation.

The development of the PV project on the Qyrdaq dam presents a significant opportunity that can improve network and energy supply security. Considering the average annual consumption of a household in the country, the PV plant would be sufficient to supply clean energy to approximately 1,900 households. This indicates the potential of renewable energy projects, such as PV installations, to contribute to meeting energy demands, reducing reliance on fossil fuels, and promoting sustainability and environmental conservation.

The Qyrdaq dam photovoltaic power generation demonstrates the potential for utilizing existing infrastructure, such as dams, for solar energy projects, which can maximize the efficient use of resources and contribute to a more sustainable energy mix.

REFERENCES

- ALBCOLD & TCA, 2022, Main Dams in Albania, Tirana, Albania.
- ERE, 2022, Annual Report on Energy Sector in Albania, Albania.
- Bezati, G.J., Shaha, F., Limani, L. 2021. Study of Analysis for Dam Stability and Structural Analyses after PV panels installation on Qyrdaq Dam, Albania.
- EN 50110, 2013, General Requirements for Electric installations.
- EN 50539 Part 11, 2013, Requirement and Tests for SPD of Photovoltaic installation.
- IEC 60364, Electric Installation with low tension.
- IEC 62053, Electric energy measurement instruments.
- EUROCODE Publications 1,2,3,7,8.

Drini River Cascade - Unique in Europe

A. Jovani

Albanian National Committee of Large Dams, Tirana, Albania

E. Verdhó, E. Kacurri & E. Qosja

Albanian Power Corporation, Tirana, Albania

ABSTRACT: This paper delves into the fascinating Drini River Cascade, a cascade of six large reservoirs and five Hydro power plants (HPPs), that serves Albania and North Macedonia. The Drini River Cascade is a unique and remarkable engineering feat in Europe, boasting a total water capacity of 4.3 billion m³, and remarkable infrastructure. It features the tallest rockfill dam with clay core in Europe - the Fierza HPP dam, which stands at a staggering height of 166.5 m, and the largest Hydro power plant (HPP) with Hydro-matrix turbines-the Ashta 1 HPP and Ashta 2 HPP, with a total capacity of 53 MW.

Drini River flow from Ohrid Lake in Struga town of North Macedonia and Zhleb Mountain near of Peja town of Kosovo. They receives many relatively long tributaries. White Drin reaches the town of Kukes in Albania where it meet the Black Drin and forms the Drin River which flow into the Adriatic sea. At 335 km long, the Drin is the longest river of Albania of which 285 km passes across Albania and the remainder through Kosova and North Macedonia.

The Drini River Cascade's ability to harness the power of water for energy production is un-matched in Albania, with over 70% of the country's energy being generated by the cascade's HPPs. Moreover, the cascade's versatility is its strength, as it provides an array of services including hydro power production, water transport, aquaculture, tourism, flood protection, and even solar energy production.

The Drini River Cascade's future looks bright, with plans underway to construct a new HPP and expand its solar energy production capabilities.

In conclusion, this paper provides a comprehensive overview of the Drini River Cascade, highlighting its engineering marvels, remarkable energy production capabilities, and versatile applications, as well as its future prospects for dam safety improvement, expansion and new development.

1 INTRODUCTION

This presentation provides a general overview of the dams and reservoirs in the Drini River Cascade, including the history of the construction of the main large dams, current monitoring and management of the dams and reservoirs, efforts to improve operations, and measures planned for the future to increase energy potential and dams safety.

Due to historical and economic conditions, Albania began designing and constructing large dams after World War II. The modern history of large dams in Albania began in 1951 with the preparation of several sketches and schemes for the exploitation of the Drini, Mati, and Vjosa rivers for the purpose of hydro-power production and irrigation.

In 1952, work began on the construction of the Ulza HPP dam, which was the first dam built in Albania. In November 1957, the gates were closed, and the filling of the Ulza HPP reservoir with a total volume of 240 million m³ of water began.

To prepare for future construction of large dams, the National Institute of Research and Design was established in 1957 at the Construction Ministry, which served as the basis for the Institute of Hydro Technical Studies and Designs No.3 (ISP No.3) and the Institute for Studies and Design of Irrigation and Drainage Systems (ISPVKU). These institutes were supported by the Directorate of Geology and Geodesy established in 1961, the Hydro-meteorology Institute established in 1962, and the Hydraulic Research Center established in 1968.

The main task of the designers and engineers at ISP No.3 was to study and design the large dams and facilities for the hydro power plants in the Drini River Cascade. This task was one of the biggest challenges at the time, as it aimed to make use of the hydro power potential of the Drini River, which was the greatest asset of the country.

Until 1960, preliminary studies for the exploitation of the Drini River showed that the most feasible option was to build dams no higher than 60 m due to technical, economic, and logistical limitations. However, this approach turned out to be uneconomical and did not allow for the creation of large reservoirs, which were necessary for the complete annual regulation of the river inflows and optimal management for electricity production throughout the year.

In 1961, a feasibility study began, and in 1963, the Albanian Government approved the feasibility study on energy utilization of the Drini River. This study was conducted with professionalism, competence, and knowledge by Prof. Petrit Radovicka, who was also the first Chairman of the Albanian National Committee of Large Dams in 1964.

From the beginning of the study on the exploitation of the hydro power potential of the Drini River, it was accepted that large reservoirs needed to be created, which required the design and construction of very high dams with a height of 60-167 m. At the time, only 10 dams with a height over 160 m had been built in Europe in 1962, and this idea was challenging to conceive and implement in Albania.

The height, type of dams, conditions of operation, maximum flow during the winter, the water reservoirs they created and the multiply purpose of their operation, the solar energy production and the installed power capacities and the dynamic of exploitation of Hydro power plants make this river cascade to be unique cascade in Europe.

The design of this cascade has started 60 years ago. Till now, there are constructed 9 large dams with height 21 m to 166.5 m and 8 HPPs with total power capacity of 1520 MW and average energy production of 5 million MWH per year.

Three largest HPP and six large dams of this cascade in Albania are constructed from 1966 to 1986. Their capacity is 1350 MW and the projected total water volume of 3 main reservoirs is 3.7 billion m³.

From 2021, there has started the preparation of new feasibility study for Skavica HPP on the Black Drini (main tributary of Drini River) that is last part of the approved energy utilization scheme.

In the North Macedonian side, there are Spillje HPP and Globocica HPP with total power capacity of 110 MW and total water volume of reservoirs is 580 million m³. At September 2012, there has started the energy production from new Ashta 1 HPP and Ashta 2 HPP with total capacity 53 MW and annual energy production of 240000 MWH.

However, relying on the achievements of science and technology in the world for the construction of large dams and the professionalism, determination, and belief in the technical-scientific values of Albanian designers and engineers, it became possible to successfully solve all the problems that arose during the design and construction of these dams, creating the largest cascade in the country.

Based on the approved study, the technical potential of the Drini River in Albania would be exploited through the construction of 7 hydro power plants with a total power of about 1600 MW. These HPPs would use 5 reservoirs with an area of about 200 km² created by 7 large dams. During the study of the exploitation scheme of the Drini River, various problems related to the geological conditions of the area, the type of dam, construction materials, and the time of their construction were taken into account.

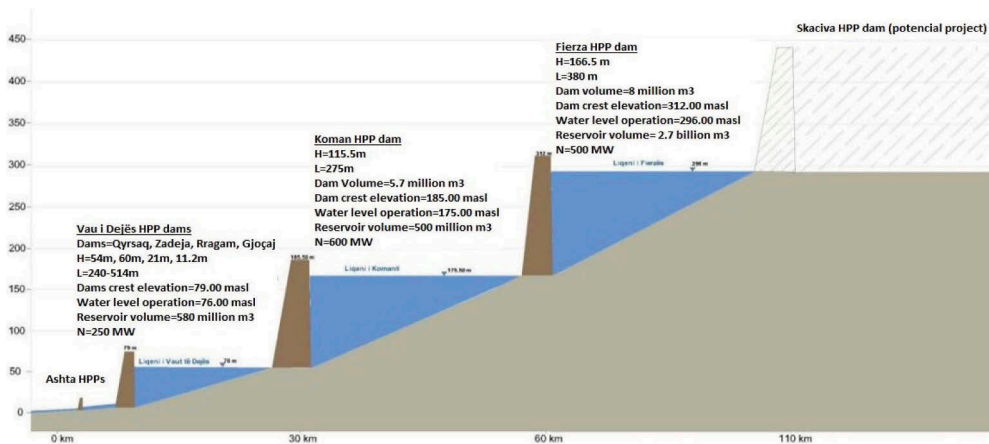


Figure 1. Hydro-power exploitation scheme of drini river cascade.

2 GENERAL OVERVIEW ON THE DAMS AND RESERVOIRS

Below is a general overview of main dams and reservoirs of Drini River Cascade regarding the main data, actual conditions, monitoring and safety:

2.1 Fierza HPP Dam

This is a rock-fill dam with a clay core, measuring 166.5 m in height and 380 m in length at the crest. The dam body has a volume of 8 million m³, and is one of the three tallest rock-fill dams with clay core in Europe.

In November 1971, construction of the dam for Fierza HPP dam began. To produce filling material for the dam, 11 mass explosions were carried out using explosives, providing approximately 500000 m³ of stones with each explosion. Excavators with a capacity of 2-4 m³ were used for loading the filling materials, and self-unloading trucks with a capacity of 20-32 tons were used for transport. The grout curtain placed on the dam axis was built up to 100 m deep in the riverbed and up to 300 m at the shoulders of the dam. A total of 80000 m of boring and cementing were carried out, fulfilling the high technical requirements with a percolating rate of 0.015 m/day.

On the left side of the dam are all the facilities for the hydro power plant, while on the right side are the water spillway systems with a total capacity of 2670 m³/s.

In February 1978, the gates were closed, and the creation of the Fierza HPP reservoir began with a projected water volume of 2.7 billion m³.

2.2 Komani HPP Dam

This is a concrete faced rock-fill dam. In 1980, construction began for the Komani HPP dam, which measures 115.5 m in height and 275 m in length at the crest, with a discharge capacity of 3,600 m³/s and a dam body volume of 5.7 million m³. It was the first Concrete faced rock-fill dam (CFRD) in Albania, and at that time, the tallest in Europe.

The construction area for the dam, spillways, and water intake tunnels consists of limestone slab and layers, flint stone, interlaced with silica and stratification with high properties of strength and resilience.

The main challenges in the design and construction of this dam and its sub-facilities were the application of new technologies in the grout curtain, concrete face screen, construction of large tunnels, and construction of the reinforced concrete screen.

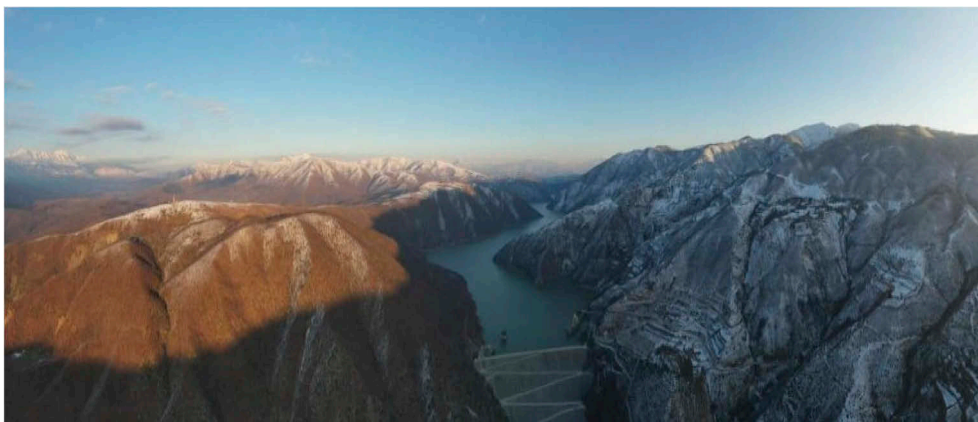


Figure 2. View of Fierza HPP Dam and reservoir.

On the right side of the dam are all the facilities for the hydro power plant, including the water intake, equilibrium tower and a spillway tunnel with capacity of 1800 m³/s, while on the left side is a water spillway tunnel with capacity of 1800 m³/s.

In 1986, the gates were closed, and the creation of the Komani HPP reservoir began with a projected water volume of approximately 500 million m³.



Figure 3. View of Komani HPP Dam and reservoir.

2.3 Vau i Dejes HPP Dams

Based on technical and economic conditions and possibilities, the construction of the dams in the Drini River Cascade began in January 1967 with the construction of the hydro-technical complex of Vau i Dejes HPP. This complex includes:

- Zadeja Dam, which is a rock-fill dam with a clay core, with a height of 60 m, a dam crest length of 387 m, and a body volume of 3.1 million m³. On the left side of this dam, there is a spillway system consisting of two spillway gates and a discharge tunnel that is 322 m long and 11 m high. The current discharge capacity of this tunnel is 2100 m³/s.
- Qyrsaqi Dam, which is 54 m high and has a dam crest length of 514 m. This dam consists of two parts: the first part is a rock-fill dam with a clay core, and the second part is

a gravity concrete dam. The concrete dam also includes the water intake and spillway systems, with a total capacity of 3900 m³/s.

- Rragami Dam, which is a rock-fill dam with a clay core, with a height of 21 m and a dam crest length of 240 m.
- Gjocaj Dam, which has a height of 11.2 m and a dam crest length of 295 m. This dam includes an intake system with a capacity of about 8 m³/s to supply a main irrigation canal from the dam to the upper part of the Shkodra district.



Figure 4. View of Zadeja Dam and Rragami Dam in Vau i Dejes HPP.

In August 1971, the gates were closed and the creation of the Vau i Dejes HPP reservoir began with a projected water volume of 580 million m³.

The construction of this complex served as a good learning experience and professional training for workers, specialists, and engineers. The mechanization of the work reached an unprecedented level and was one of the most advanced at that time. The equipment and machinery used had a capacity of about 700000 horsepower. The maximum daily excavation intensity reached up to 8500 m³/day, filling with rocks and stones reached up to 13000 m³/day, and concrete production reached up to 1300 m³/day.

3 MONITORING AND MANAGEMENT OF DAMS AND RESERVOIRS

Based on a study of dam safety investments at the Drin River Cascade, monitoring of all the dams had many problems.

At Fierza HPP dam, all pressure piezometers were out of function, and seepage measurement instruments were installed but not recorded since 1987. Monitoring equipment for water level measurement was installed, but data transfer was manual. Monitoring of two main landslides (Porava landslide with a volume of 22 million m³ and Gropaj landslide with a volume of 4 million m³) was problematic, and no seismic monitoring system was installed.

At Komani HPP dam, all pressure piezometers were out of function, and seepage measurement instruments were installed but not recorded since 1987. Leakage in downstream of the dam was not measured for 20 years. Monitoring equipment for water level measurement was installed, but data transfer was manual. A monitoring system for measurements of pressure and slope of the upstream concrete lining was installed by a French company, but only 20% of the monitoring system was functioning. No seismic monitoring system was installed.

At Vau i Dejes HPP dams, nine piezometers had monitored the water level until 2007. According to the monitoring system design, a monitoring system was foreseen for measurement of pore pressure as well as for inclination by the hydro-static tube balance system. The existing instrumentation for pore pressure monitoring was located in the basement of the cabinet in front of the dam, and they had been observed until 2008. Seepage measurement instruments were installed, but not recorded since 1987. Monitoring equipment for water level measurement was installed, but data transfer was manual.

exploitation of the dams in the Drini River Cascade, and integrate the management of the cascade. These comprehensive studies have yielded relevant conclusions and suggested ways to improve cascade management, reduce risk, increase dam safety, and modernize monitoring and management systems.

On 2015, KESH launched a project on risk governance implementation for a cascade system in Drini river. In this project was developed a risk analyses process.

This analyses has been programmed in a way that, following best international practices, puts the focus on three main goals:

- Providing robust and defensible practical results for risk assessment
- Reinforcing dam safety decision making
- Creating the proper dynamics for knowledge transfer and capacity building

Also, on 2017, KESH launched a project on safe flood management of Drini River Cascade. The overall objective of this assignment was to carry out the engineering services that will permit the implementation of flood management of Drini River Cascade.

The following main tasks were carried out within this project was:

- Update of hydrological model and verification of PMP and PMF;
- Bathymetrical and terrestrial survey of three main reservoirs of Drini River Cascade;
- Update of flood routing and PMF analyses and determination of design flow;
- Assessment of current conditions of existing spillways;
- Identification and assessment of alternative flood control measures;
- Computation of reservoir water levels under PMF conditions;
- Numerical and physical model tests for the preferred spillway alternatives.

In order to develop current reservoir elevation-volume curves, bathymetric and topographic survey of the three reservoirs were performed. Calculations were performed related to the rate of sedimentation of the reservoirs and calibrated with available data. By means of the sedimentation model the available live storage volumes in 50 years from today were projected. The reduction of storage capacity was especially notable at Fierza HPP reservoir, where approx. 2.3 billion m³ are available today and 1.75 billion m³ are expected in 2065.

Drini River Cascade is a reservoir operation and flood routing model, which has been specifically tailored for the performance of flood routing and reservoir operation studies in the Drini River Cascade. Based on the hydrological modeling of Drini river catchment area and applying the KESH operation rules that are approved 35 years ago for three reservoirs, flood routing and reservoir operation studies were carried out. The results of modeling show that in order to render the Drini River Cascade safe for the event of a PMF, Fierza HPP dam and Komani HPP dam require additional spillway capacity with total capacity of 2 280 m³/s and 3 600 m³/s.

Main results of the computations are that flooding of the Fierza HPP and Komani HPP power stations cannot be avoided during a PMF event. In both cases, the expected PMF water level in the tailrace exceeds significantly the maximum allowable tail water level at the power stations.

After the above analyses, Consultants proposed main risk reduction measures as follows:

- ✓ Rehabilitation of Spillway No.3 in Fierza HPP dam;
- ✓ New Operation Rules for Drini River Cascade;
- ✓ High maintenance program for all spillways currently used;
- ✓ New additional Spillway in Fierza HPP;
- ✓ New Additional Spillway in Komani HPP;
- ✓ Rehabilitation of bottom outlet in Qyrsaqi dam.

5 NEW SOLUTIONS FOR INCREASING OF ENERGY PRODUCTION

In 2021, the Albanian Power Corporation (KESH) began preparing a detailed design for the installation of a photovoltaic (PV) plant on the surface of the Qyrsaqi dam.

This project involves constructing and installing a photovoltaic plant on the lower part of the Qyrsaqi dam in Vau i Dejes HPP. It is the first project developed by KESH using new generation sources from renewable sources, and it is also the first project in Albania where a PV plant is installed on the surface of a dam.

The PV plant was commissioned in February 2022. The construction of this plant is meant to diversify KESH's production portfolio from renewable energy sources. In the future, KESH plans to install a floating PV plant on the Vau i Dejes HPP Reservoir, with a capacity of 12 MW in the first phase and an extension of this capacity up to 100 MW in the future.

Diversification of electricity generation sources from renewable sources other than hydro, as well as the policy for building with zero-zero energy, is one of the commitments undertaken by the Albanian government. The model proposed by KESH is not only part of decarbonisation policy but is also a suitable model for promoting these commitments as viable and affordable ventures that offer secure return on investment. There is great potential for the development of similar projects if existing structures are referred to.

The PV plant is installed on the Qyrsaqi dam, respecting all technical conditions related to dam safety. Currently, KESH produces electricity from hydro sources, and such an initiative is positive in view of the further extension of this technology even in similar unusable areas.

The development of this project is an indicator of the real opportunity for investments with an impact on improving the indicators of network security and energy supply security. Referring to the average annual consumption of a household in our country, the energy provided for annual production by the PV Plant in question would be sufficient to supply clean energy to 1900 households.



Figure 6. Photovoltaic plant on Qyrsaqi Dam of Vau i Dejes HPP.

6 CONCLUSIONS

After studying and evaluating the current condition of the large dams in the Drini River Cascade, their monitoring and maintenance, as well as their safety assessments and the risks from the dams in the urban areas below them, experts have concluded the following:

- All large dams in the Drini River Cascade are very important for the economy of Albania. There is a possibility to increase energy production through the installation of PV plants and floating PV plants and integrated flow management.
- The dam operator must develop a risk governance implementation program for the Drini River Cascade. This program should include the operation of a modern alarm system plan and an emergency preparedness plan.
- The dam operator must develop a new operation rule focused on increasing dam safety and integrated flow management of the cascade.
- The dam operator must continue to analyze the sedimentation process in the three reservoirs and take measures to reduce it.
- The monitoring systems of all dams should be modernized and provide real-time information in accordance with ALBCOLD recommendations and technical standards.
- Asset evaluation and management for all large dams and reservoirs of the Drini River Cascade.
- Increase building capacity for monitoring all dams and collecting monitoring data.
- There is necessary to construct the new additional spillways in the Fierza HPP dam with a capacity of 2280 m³/s and the new additional spillways in the Komani HPP dam with a capacity of 3600 m³/s.

REFERENCES

- ALBCOLD & TCA, Albania, 2022. *Main Dams in Albania*, Tirana, Albania.
- ALBCOLD, 2022. *Annual Report on large dams in Albania for 2021*, Tirana, Albania.
- ERE, 2022. *Annual Report on Energy Sector in Albania for 2021*, Tirana, Albania.
- Fichtner GmbH-Germany, 2017. *Safe Flood Management of the Drini River Cascade*, Albania.
- GNF-Spain, 2015. *Risk Governance Implementation for the Drini River Cascade*, Albania.
- GIZ-Germany, 2014. *Development and Application of a Hydrological model for the Drin-Buna basin*, Albania.
- POYRY-Switzerland, 2009. *Feasibility Study for Dam Safety Investments at the Drini River Cascade*, Albania.
- Musliu Emin, 1999. *Hydroenergy Sector in Albania during 1949-1999*, Tirana, Albania.

Photovoltaics and hydropower – Potential study at Alpine reservoirs in Switzerland

G. Maddalena

beffa tognacca, Claro, Switzerland
Laboratorium^{3D}, Biasca, Switzerland

B. Hohermuth, F.M. Evers & R.M. Boes

Laboratory of Hydraulics, Hydrology and Glaciology (VAW), ETH Zurich, Zürich, Switzerland

A. Kahl

SUNWELL, Lausanne, Switzerland

ABSTRACT: Photovoltaics (PV) play a major role in Switzerland's energy transition. Compared to conventional installations in urbanized areas, PV at high altitudes may yield a 30% increase in power generation due to stronger solar irradiation and lower module temperatures as well as a considerably higher production share in winter. Numerous Swiss hydropower reservoirs are situated above 1,000m.a.s.l. and already offer a good accessibility and grid connection. Therefore, they could provide an ideal base infrastructure for the installation of PV. The two main options for PV operation at reservoirs include modules mounted to the dam structure and modules floating on the reservoir.

This study investigates 23 selected Swiss hydropower reservoirs with 26 dams at elevations between 1,200 and 2,500m a.s.l. regarding their power production potential. The developed work-flow comprises a GIS analysis including inter-daily as well as seasonal shading effects. The resulting electricity production from solar radiation impinging on a PV module installed at a given orientation and tilt are simulated using the software SUNWELL. For validation, the simulated electricity production at selected sites is compared to planned or recently installed PV plants. The study ranks the investigated sites according to a multicriteria assessment matrix considering *societal acceptance*, *energy yield* and *economic feasibility*. The estimated total electricity production at the investigated sites amounts to 11.5 to 14.5 GWh/a for dam-mounted PV and 370 to 490 GWh/a for floating PV. The developed work-flow may also be applied to assess other promising PV installation sites.

1 INTRODUCTION

With the objective of a climate-neutral Switzerland by 2050, the Swiss Energy Perspectives 2050+ (EP 2050+) envisage a massive expansion of energy production from photovoltaics (PV) from around 2TWh/a in 2019 to 34 TWh/a in 2050. The intermittent, weather-dependent electricity production of PV plants poses challenges for grid stability and supply security, especially in the winter half-year. One possible solution to mitigate these problems is to combine several types of generation with different production patterns. The characteristics of PV and hydropower complement each other very well in this respect; on the one hand, storage hydropower is flexible and can counterbalance irregular power output from PV, while on the other hand PV production allows for conserving water impounded in storage reservoirs during periods of high solar irradiation. This enables a stable, weather-independent energy supply (An et al., 2015). In the case of pumped storage, the storage reservoir can act as a battery and absorb excess energy produced by the PV system, for example at midday, and release it back to the grid in the evening hours (Lee et al., 2020).



Figure 1. Left: FPV plant on Lac des Toules on 16 October 2021 (photo by Christian David, Wikimedia Commons, CC BY-SA 4.0), right: DMPV plant under construction at Lago di Lei on 28 July 2022 (photo by GF-wmch, Wikimedia Commons, CC BY-SA 4.0).

Table 1. Overview of investigated dams and reservoirs; elevation, (maximum) dam height, and crest length from swissdams.ch; module areas for FPV and DMPV from GIS analysis with Ground Cover Ratios (GCR) of scenario *full year 60°*.

Dam/ Reservoir	Canton	Elevation [m a.s.l.]	Dam height [m]	Crest length [m]	Module area FPV [m ²]	Module area DMPV [m ²]
Albigna	GR	2,165	115	759	47,100	2,030
Emosson	VS	1,930	180	554	110,200	15,300
Gelmer	BE	1,850	35	370	21,700	9,670
Göscheneralp	UR	1,797	155	540	-	-
Grande Dixence	VS	2,364	285	695	223,900	1,030
Hongrin North	VD	1,257	123	325	151,800	720
Hongrin South	VD		95	272		860
Lago Bianco North	GR	2,237	13	290	150,200	560
Lago Bianco South	GR		26	190		830
Les Toules	VS	1,811	86	460	27,400	640
Limmern	GL	1,859	146	370	-	-
Luzzzone	TI	1,609	225	510	27,600	480
Marmorera	GR	1,684	91	400	128,000	1,010
Mattmark	VS	2,196	117	780	150,100	1,820
Mauvoisin	VS	1,976	250	520	15,900	130
Moiry	VS	2,250	148	610	104,000	1,240
Muttsee	GL	2,476	37	1,025	54,400	9,530
Oberaar	BE	2,298	104	526	9,500	450
Piora	TI	1,851	27	309	110,100	1,450
Punt dal Gall	GR ^a	1,805	130	540	163,400	1,280
Salanfe	VS	1,925	52	617	25,500	10,530
Santa Maria	GR	1,910	117	560	247,000	1,350
Seeuferegg ^b	BE	1,912	42	336	3,200	860
Spitallamm ^b	BE	1,911	114	258		-
Lago di Lei	GR ^a	1,934	138	635	169,100	1,570
Zervreila	GR	1,864	151	504	83,500	790

^a major parts of the reservoir lake are located in Italy

^bSeeuferegg and Spitallamm dams both impound Grimsensee reservoir

Alpine PV systems not only produce higher total annual yields than systems on the Central Plateau (Kahl et al., 2019). They also deliver up to 50% of their production in the winter half-year (and thus about twice as much as in lower regions). This is due to the cloud- and fog-free conditions in winter, a thinner atmosphere, the albedo effect of snow, and higher efficiency at

low temperatures (Osman & Alibaba, 2015). Alpine PV systems can thus contribute to closing the looming winter electricity gap (Kahl et al., 2019). Since large-scale, ground-mounted projects in the Alps that are currently debated in Switzerland, e.g. Gondosolar, meet a lot of public opposition, it is worth taking a closer look at the potential of PV systems on existing Alpine infrastructure including water reservoirs. There are two options for the combination of hydropower and PV: floating photovoltaics (FPV) are plants on the water surface, while dam-mounted photovoltaics (DMPV) are PV plants directly attached to the dam structure.

Both arrangements have advantages and disadvantages. Due to the larger potential plant area on the reservoir's water surface compared to the dam surface, FPV plants have a larger potential energy production than DMPV plants. The global potential for floating photovoltaic plants is estimated to be in the order of magnitude of all currently installed fossil thermal power plants (Almeida et al., 2022). Furthermore, the orientation of FPV plants can be adjusted flexibly and is not constraint by the dam orientation and inclination. On the other hand, the impact of a DPMV on the landscape is lower and less effort is necessary for its installation, which facilitates an easier and faster implementation. In Switzerland, there are four projects that have already been implemented: a FPV system on Lac des Toules in the canton of Valais by Romande Energie, and three DMPV systems: Albigna dam and Lago di Lei in the Canton of Grisons, both by ewz, as well as Mutsee in the Canton of Glarus by Axpo and IWB (Figure 1). This study investigates 23 selected hydropower reservoirs with 26 dams in Switzerland at elevations between 1,200 and 2,500m a.s.l. (Table 1) regarding their power production potential of DMPV and FPV.

2 METHODS

Two assessment matrices were developed, one for FPV and one for DMPV systems, each including three main categories: *societal acceptance*, *energy yield*, and *economic feasibility*. Several sub-criteria were defined in each main category. While the weighting of the individual criteria was defined at the discretion of the authors, a sensitivity analysis has shown that the influence of the weighting on the ranking of the sites is small.

Table 2. Assessment matrix for FPV installations.

Main category	Weight [%]	Subcategory	Weight [%]
Societal acceptance	30	Conservation area	15
		Glare	5
		Impact landscape	10
Energy yield	40	Available area	14
		Normalized production	14
		Winter production share	9
		Evaporation	3
Economic feasibility	30 + 10	Grid access	9
		Water level variation	5
		Wind	5
		Snow	3
		Ice	3
		Driftwood	1
		Subsidies (Bonus)	10

Table 2 shows the criteria and weightings of the assessment matrix for FPV installations. The DMPV matrix is structured similarly, but the criteria *impact on the landscape*, *evaporation* and *driftwood* were not taken into account. Overall, the *energy yield* category was given a higher weighting in order to meet the expansion targets of PV in Switzerland until 2050. For this main category, the suitable area and the resulting production had to be determined.

The suitable areas were determined with a GIS analysis, taking into account three criteria:

1. A suitable area should have solar radiation during more than 85% of the time between 09:31 and 15:30, i.e. not be shaded. This time period contains approximately 75% of the daily

radiant energy, and shading outside this time is consequently less important. The representative monthly shading or solar radiation was determined based on the digital terrain model swissALTI3D (Federal Office of Topography) with the *Area Solar Radiation* tool of ArcGIS Pro for the 21st day of each month of a year, generating twelve shading grids with a spatial resolution of 30m. The solar radiation was determined by adding up the twelve monthly grids and the solar radiation. By adding the twelve monthly grids and dividing by the total number of annual hours considered, the percentage of sunshine duration can be calculated.

2. To avoid structural stress and potential damage to the floating substructure, it was assumed that FPV installations should not run aground and consequently come to rest within the smallest reservoir area at the lowest water level that occurs during normal operation. For this criterion, the minimum lake area was extracted from high-frequency orthophotos by Planet Labs Inc.
3. To prevent excessive grid connection costs, the installation of PV modules was only planned within 2 km of the nearest suitable grid connection. As no detailed information was available, possible connection points were estimated from topographic maps (e.g. warden's house at dams, restaurants).

These three criteria lead to a restriction of the reservoir and dam surfaces within which a possible FPV and DMPV installation was drawn. For DMPV, it was additionally considered that areas sensitive in terms of dam safety, e.g. spillways, are not covered with PV modules.

In the context of the Swiss EP 2050+, production in winter is of central importance for closing winter electricity gaps. Alpine PV systems can make a contribution (Kahl et al., 2019). Therefore, the GIS analysis described under 1) was additionally carried out for the winter months only, in order to identify areas that are not shaded for more than 85% of the desired time for the six months from October to March.

The energy production of the PV modules was determined using the software SUNWELL (Kahl et al., 2019). SUNWELL is a satellite data-based model that calculates the energy production of PV modules taking into account the local topography and the time-varying surface reflection (albedo). The radiation products used were provided by MeteoSwiss and are based on data from the SEVIRI sensors (Meteosat Second Generation, Schmetz et al., 2002). In SUNWELL, the user can, on the one hand, compute the energy production depending on a given orientation (tilt angle and azimuth) and, on the other hand, have the orientation optimised for maximum production in a user-defined time period (Kahl et al., 2019). In the context of this study, three scenarios were considered for calculating the optimal orientation of the PV modules: The main scenario (*full year 60°* scenario) was to optimise production over the entire year. In this scenario, the tilt angle of the PV modules was limited to at least 60° to reduce snow accumulation and production losses in winter. As a second scenario, the specific production (kWh/m²) was optimised over the winter months from October to March (*winter half-year 60°* scenario). In the third scenario, optimisation was carried out over the entire year and the restriction on the tilt angle was removed (*full year* scenario). Without appropriate maintenance, heavy snowfall in this scenario could substantially reduce effective production in winter. In all scenarios, the available surface area on which PV modules can be installed remains the same as in the *full year 60°* scenario. However, depending on the tilt angle of the modules, the effective module area changes.

3 SELECTED CASE STUDIES: LUZZONE & SANTA MARIA RESERVOIRS

Figure 2 shows the result of the GIS analysis using the example of Lago di Luzzone. The location of the FPV system was determined taking into account the following three conditions: 1) within the yellow-orange bands corresponding to solar irradiation for at least 85% of the time considered; 2) within the minimum surface of the reservoir (dashed purple) and 3) within 2 km (red circle) of a possible connection point with the electricity grid (green pentagon, in this case the mountain station of a cable car). In this example, the front two-thirds of the lake are in the shade for more than 85% of the year, and even more in the winter months. The dam itself lies almost entirely in the heavily shaded area. In the zones with high irradiation duration, the usable area is additionally limited by the minimum lake area at low water levels; here the minimum operation water level. The restriction of less than 2 km distance to the grid connection point limits the area

even further. With just under 28,000m² FPV, or 480m² DMPV module area, the production expectation is in the lower third of all plants studied.

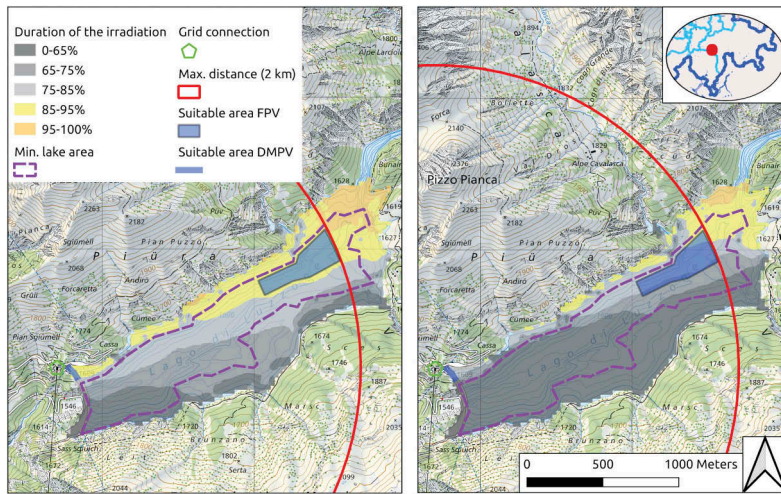


Figure 2. GIS analysis of Luzzone reservoir with duration of solar irradiation from (left) January to December and (right) October to March (background map: Federal Office of Topography).

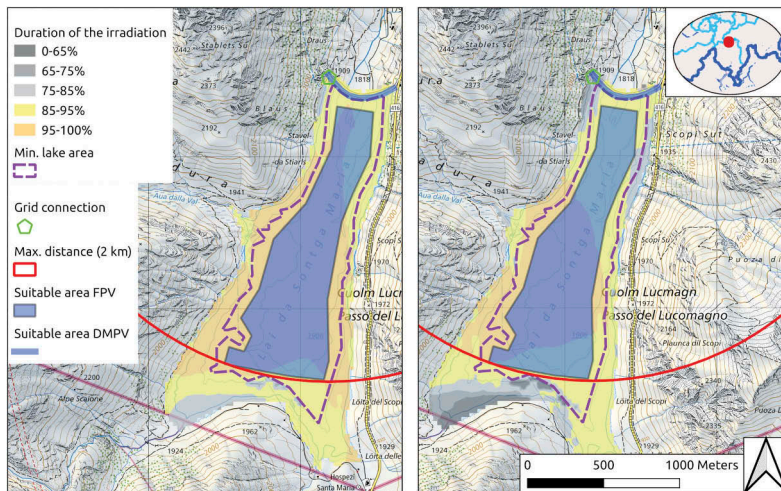


Figure 3. GIS analysis of Santa Maria reservoir with duration of solar irradiation from (left) January to December and (right) October to March (background map: Federal Office of Topography).

The site with the highest overall production potential is the Santa Maria reservoir immediately south of the Lukmanier Pass (Figure 3). At this location, 55 to 65 GWh/a could be generated with FPV and around 300 MWh/a with DMPV. Due to its location on the north-south oriented pass, the horizon line is very low and the possible sunshine hours correspondingly long – especially in the winter half-year. More than half of the reservoir surface is irradiated during more than 95% of the time between 9:30 and 15:30 over the entire year, and about one third of the reservoir in the winter half-year. Due to the Lukmanier Pass national road, the high-voltage line across the lake and a cell phone tower, the additional landscape impact of the PV plants is assessed as low. However, directly adjacent to the lake is a wetland inventoried in the national ecological network (REN: *réseau écologique national*) and an area included in the Federal Inventory of Landscapes and Natural Monuments of National Importance

(BLN: *Bundesinventar der Landschaften und Naturdenkmäler von nationaler Bedeutung*), so that the overall assessment of the category *societal acceptance* is 1 point out of a maximum of 1.5 for FPV, or 0.9 out of a maximum of 1.3 for DMPV. To assess the extent of the impact by the PV plants on the inventoried and protected areas, more detailed investigations are required. In the category *energy yield*, it can be seen that the rating for DMPV in particular is relatively low, despite the optimal orientation of the arch dam to the south. The reason for this is that the PV modules can only be installed above the water on the upstream face of the dam and the available area for DMPV is small. In the category *economic feasibility*, this site receives a bonus of 0.5 points, since the plant is located in the Canton of Grisons and might benefit from a cantonal subsidy for PV plants with high expected winter production.

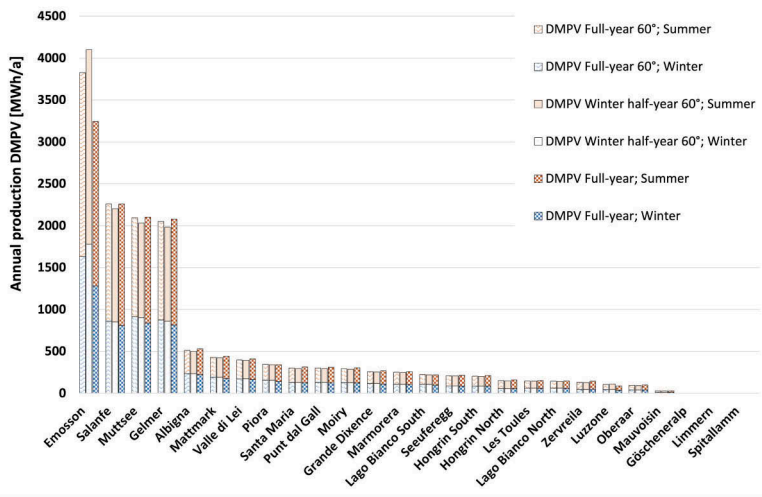


Figure 4. Annual production DMPV.

4 PRODUCTION POTENTIAL & RANKING

Figures 4 and 5 show the potential energy production for DMPV and FPV plants according to the three scenarios investigated: *full year 60°*, *winter half-year 60°*, and *full year*. Three columns are therefore shown for each site, each divided into summer and winter production, i.e. April to September and October to March, respectively. The annual production corresponds to the product of specific yield in kWh/(am²) and the determined suitable area.

The production potential for FPV plants is substantially higher than for DMPV plants due to the larger available areas. In addition, the possible optimisation by SUNWELL can also have an influence: for FPV systems, the azimuth alignment of the PV modules was optimised, whereas for DMPV the azimuth is determined by the alignment of the dam. As expected, the largest annual production is achieved in the *full year* scenario. In the case of FPV, which are located on the horizontal lake surfaces, a flatter tilt angle is advantageous for overall production. The production losses due to the restriction of the tilt angle to 60° are between 10 and 15%. However, note that a flatter tilt angle could lead to losses due to snow accumulation, which have not been taken into account in the model calculation. Furthermore, with less inclined modules, a considerable part of the production is shifted to the summer months at the expense of valuable winter electricity. The optimal orientation of the PV modules is therefore highly site-specific. When considering the winter and summer half-years separately, it is apparent that the winter production in the *winter half-year 60°* scenario is lower than in the other two scenarios, although SUNWELL has optimised the orientation of the PV modules so that the specific energy production per square meter of module surface [kWh/(am²)] is maximum in winter. The reason for this is that due to the steeper tilt angle of the PV modules, the distance

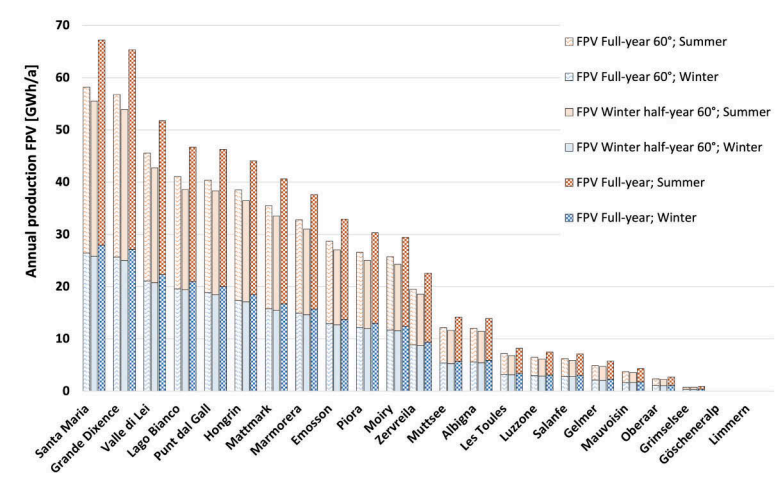


Figure 5. Annual production FPV.

between the PV modules must be increased; the so-called Ground Cover Ratio (GCR), i.e. the proportion of the usable area without mutual shading between two rows of modules, becomes smaller. The specific yield increase in winter due to steeper tilt angles cannot compensate for the loss of area due to the smaller GCR. Accordingly, the *winter half-year 60°* scenario shows no advantages for FPV systems from the perspective of total production. However, the production per square meter of module surface is greater – especially in winter – than in the *full year 60°* scenario. From an economic point of view, this is advantageous because it shortens the payback period. Which variant makes more sense and whether inter-row shading should be allowed at times must be investigated in more detailed, site-specific studies.

Among the DMPV plants, four sites have a particularly higher annual production. At these four sites, the PV plant can be arranged at the downstream face of the dam due to its orientation, which means that more surface area is available than with an upstream, i.e. waterside, arrangement. Especially at Emosson, the possible energy production for *winter half-year 60°* is higher than in the other two scenarios. The reason for this is again the GCR: in the case of DMPVs mounted on the steeply inclined to vertical dams (or even overhanging, i.e. featuring a negative tilt angle to the vertical), a steeper angle leads to a larger GCR and thus to a larger module area. This difference is more pronounced for arch dams such as Emosson than for gravity dams such as Salanfè, Muttsee, or Gelmer. If, in practical implementation, the

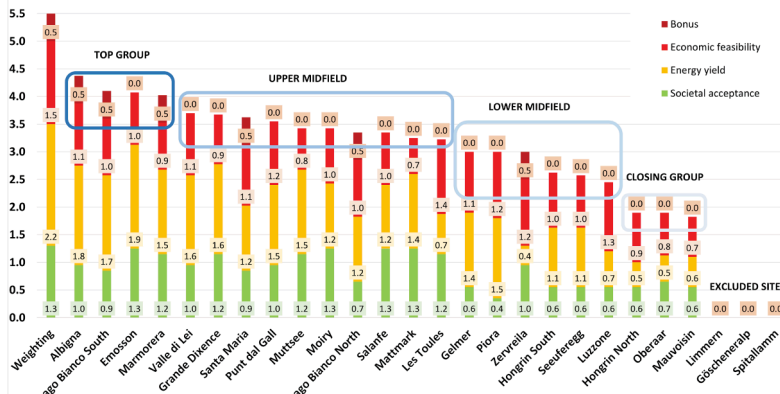


Figure 6. DMPV ranking based on the assessment matrix.

modules are installed as a closed surface at the angle of the dam faces, this consideration would, however, become obsolete. In this case, lower production numbers can then be expected due to the suboptimal tilt angles.

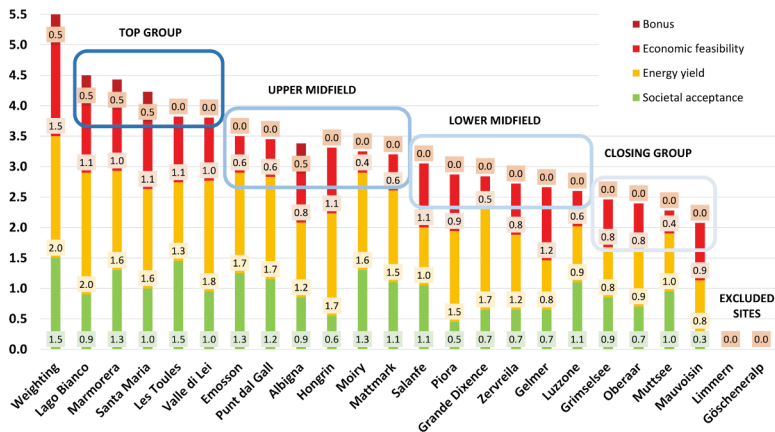


Figure 7. FPV ranking based on the assessment matrix.

Applying the assessment matrices to all the sites studied results in the rankings for DMPV and FPV shown in Figures 6 and 7. The columns for the respective sites are divided according to the three main categories of the assessment matrix to visualize the strengths and weaknesses of each site. For further discussion, the sites were divided into five groups: *top group*, *upper mid-field*, *lower mid-field*, *closing group* and *excluded sites*. The *top group* sites are the most promising and further feasibility studies are recommended. *Upper mid-field* sites should also be considered in light of the EP 2050+ targets for PV installation. The sites in the *lower mid-field* might still warrant further investigation, provided that the negative aspects are justifiable (e.g. interference with protected areas). In addition, it must be further clarified whether the existing production potential is sufficient for economic implementation. Sites in the *closing group* have a low potential and further studies on them would therefore be of lower priority. For the excluded sites, the GIS analysis has already shown that the solar radiation is not sufficient for further pursuit.

5 DISCUSSION

In order to assess the reliability of the applied method, a comparison was made with the four existing PV plants Albigna, Muttsee, Lago di Lei, and Les Toules. Albigna is a DMPV plant in Val Bregaglia/Bergell in the Canton of Grisons which has been in operation since summer 2020. There are PV modules on the upstream dam face above the reservoir level over a length of 670m and the expected electricity production is 500 MWh/a according to the operator ewz. In the first year, a total production of 527 MWh was reported. These data show good agreement with the results of this study. The possible length of the PV modules of 755m estimated with the GIS analysis is 13% higher, but the production agrees well with 502 to 530 MWh/a (Figure 4). The rating also matches well, as Albigna scores the highest of all DMPV plants in the matrix, with good ratings in all categories (Figure 6).

Another DMPV plant was built in summer 2021 at Muttsee in the Canton of Glarus. It was preliminarily commissioned on 8 October 2021, although construction of the full 10,000 m² was completed in summer 2022 only. This large area of PV modules is possible despite the low dam height (37 m) due to the installation on the the dam's downstream face and the over one kilometer long dam. The expected production of 3.3 GWh/a estimated by the operators is higher than the 2 GWh/a estimated in this work (Figure 4). On the one hand, this is due to the larger PV module area; in this study, the area of the spillway was deliberately kept free, whereas it was covered in the project. In addition, it is assumed that this difference could also be partly due to an

overestimation by the manufacturer or to inaccurate parameter entries in the SUNWELL model. For example, the efficiency of the Muttsee plant and its bifaciality were not yet known at the time of the study. Bifaciality describes the possibility or efficiency of electricity production from the back of the modules; compared to monofacial PV modules, 5 to 30% higher yields are possible. The assessment matrix places Muttsee in the upper midfield and would recommend implementation of the plant, which is obviously in line with the operators' assessment. It is noticeable that the economic feasibility of the site was assessed rather poorly compared to the top group; due to the location at around 2500ma.s.l. and the associated increased installation effort. The reported estimated investment costs of around 3.6 CHF/Wp are also more than twice as high as for Albigna with 1.7 CHF/Wp, thereby confirming the assessment methodology of economic feasibility.

At Lago di Lei, a 550m long and 1795m² large DMPV plant with an annual production of 380 MWh/a expected by the operator ewz was installed on the dam's upstream face above the reservoir level in 2022. In the assessment method, a somewhat shorter system length of approximately 520m was determined for this site, which also means that the total module area estimated at 1570m² is smaller than actually built. The computed annual production of 400 MWh/a (Figure 4) is only 5% larger than the value expected by the operator. In the evaluation, the site is in the upper midfield and close to the top group (Figure 6).

The FPV demonstration project at Lac des Toules has 2,000m² of module surface on a little over 6,000m² of base area on the water surface, with a production expectation of 0.8GWh/a. However, the operator Romande Energie is planning to expand the plant to 35% of the lake surface, which would correspond to a base area of around 210,000m², with an expected production of 22 GWh/a, i.e. 105 kWh/(am²). In the context of this work, a much smaller FPV plant with a base area of 78,400 m² yielding 7.2 GWh/a was proposed (91 kWh/(am^{2full-year 60° scenario limits the tilt angle of the modules to 60°, while the demonstration plant features a flatter angle of only 30°. Without this restriction, i.e. as in the *full-year* scenario, SUNWELL calculates an angle of 43° and a production of 8.2GWh/a, i.e. 105 kWh/(am²). For simplicity, all modules were modelled as monofacial, but the installed modules at Lac des Toules are again bifacial, which can explain the remaining production difference. Despite the small area and the low production expectation, the assessment matrix places Les Toules in the top group (Figure 7). This is mainly due to the full score in the category *societal acceptance*. Due to already existing infrastructure in the landscape surrounding Les Toules (Great St Bernard pass road, extra-high voltage power line), few additional negative impacts are to be expected. Based on reported data, the investment costs for the FPV demonstrator plant were estimated to 5.2 CHF/Wp and therefore higher than for the DMPV plants Albigna and Muttsee.}

For FPV, an additional benefit other than the PV production is the reduction in evaporation, increasing hydropower production. While this is very relevant on the global scale, particularly for large FPV areas on arid reservoirs, its effect is likely not so pronounced for Alpine reservoirs where evaporation is relatively low. However, this has not been quantified here and constitutes an additional non-negligible positive effect in terms of total energy yield and economical feasibility of hybrid FPV-hydropower systems.

6 CONCLUSIONS

In addition to developing a general assessment work-flow, the aim of this study was to estimate the potential of PV systems on storage lakes in Switzerland. Based on the *full year 60°* scenario and by excluding the *closing group*, a range for the possible annual production potential may be estimated. The lower limit of the production estimation corresponds to the sum of the production of the plants in the *top group* and the *upper midfield*. The upper limit additionally includes the plants in the *lower midfield*. This results in 370 to 490 GWh/a for FPV and 11.5 to 14.5 GWh/a

for DMPV. This means that the calculated figures for FPV are only 1.1% to 1.5% and for DMPV even only 0.04% to 0.05% of the 32 TWh/a increase planned by the Swiss EP 2050+. Although the overall contribution of the investigated 23 reservoir sites to Switzerland-wide annual electricity production appears to be comparatively small, the following points should be noted:

- The high importance of electricity generation in the winter months may become a central point in the evaluation of future investments in the energy sector. The targeted promotion of plants with steeply inclined modules on Switzerland's Central Plateau is a step in this direction.
- With different weather conditions on the Central Plateau and in the Alps, the production profiles may complement each other, i.e. Alpine PV plants often produce when it is cloudy on the Central Plateau, and vice versa. In combination with wind power plants, this balancing effect could be further enhanced (Dujardin et al., 2021). In this way, the grid can be relieved and overcapacities avoided.
- PV systems on existing infrastructure like hydropower reservoirs have a smaller additional impact on the mountain landscape and natural resources compared to large-scale systems on open spaces (e.g. Gondosolar).
- This analysis covers 23 selected reservoir sites. These include most of the largest reservoirs in Switzerland, but not all. Reservoirs with large areas that might be important for FPV, such as Lake Sihl or Lake Wägital, were not investigated here due to their lower elevation. The same applies to DMPV, especially at reservoirs where a south-facing, downstream installation would be possible, such as the Sella or Robiei dams.
- The assessment and production estimates are based on simplifications and assumptions. The assumption that FPV plants are not allowed to land dry leads to a substantial reduction in the suitable area at many sites. Using the example of Les Toules, it was shown that the production potential may be increased if the landing of PV floats is possible. The distance to the nearest grid connection is associated with great uncertainty and currently also severely limits the available area at certain locations. In addition, all modules were modelled as monofacial; the use of bifacial modules could increase production by 5 to 30% and should be considered in the context of further economic feasibility studies.

A detailed consideration of the economic efficiency in the sense of an investment calculation goes beyond the objectives of this study. In addition, there are some technical aspects, e.g. in connection with dam safety, that need to be further investigated. In this study, ice and driftwood were taken into account for the evaluation of FPV systems, but it was assumed that the FPV modules can be prevented from breaking loose by technical means. Dam safety must always be the top priority for both FPV and DMPV installations. Even during extreme floods, for example, the FPV modules must not be allowed to break loose, which could lead to a blockage at the weir structure of the spillway. Likewise, geodetic monitoring of the dams must continue to be possible even with DMPV modules mounted on the dam. Another simplification is the assumed availability of FPV mooring systems that may adjust to large water level variations of storage reservoirs.

The potential identified in this study is not inconsiderable when compared to Switzerland's current annual PV production of around 2 TWh/a and the assessment provides a prioritisation for more detailed feasibility studies. Moreover, the developed work-flow (or parts thereof) can be applied to reservoirs in mountainous regions world-wide.

REFERENCES

- Almeida, R.M., Schmitt, R., Grodsky, S.M., Flecker, A.S., Gomes, C.P., Zhao, L., Liu, H., Barros, N., Kelman, R. & McIntyre, P.B. 2022. Floating solar power could help fight climate change – let's get it right. *Nature* 606: 246–249.
- An, Y., Fang, W., Ming, B. & Huang, Q. 2015. Theories and methodology of complementary hydro/photovoltaic operation: Applications to short term scheduling. *Journal of Renewable and Sustainable Energy* 7(6): 063133.
- Dujardin, J., Kahl, A. & Lehning, M. 2021. Synergistic optimization of renewable energy installations through evolution strategy. *Environmental Research Letters* 16: 064016.

- Kahl, A., Dujardin, J. & Lehning, M. 2019. The bright side of PV production in snow covered mountains. *Proceedings of the National Academy of Sciences* 116(4): 1162–1167.
- Lee, N., Grunwald, U., Rosenlieb, E., Mirlitz, H., Aznar, A., Spencer, R. & Cox, S. 2020. Hybrid floating solar photovoltaics hydropower systems: Benefits and global assessment of technical potential. *Renewable Energy* 162: 1415–1427.
- Osman, M. M. & Alibaba, H. Z. 2015. Comparative Studies on Integration of Photovoltaic in Hot and Cold Climate. *Scientific Research Journal* 3(4): 48–60.
- Schmetz, J., Pili, P., Tjemkes, S., Just, D., Kerkmann, J., Rota, S. & Ratier, A. 2002. An introduction to Meteosat Second Generation (MSG). *Bulletin of the American Meteorological Society* 83(7): 977–992.

Photovoltaic on dams – Engineering challenges

D. Maggetti, F. Maugliani, A. Korell & A. Balestra

Lombardi Engineering Ltd., Switzerland

ABSTRACT: The installation of photovoltaic (PV) systems on dams is a pioneering initiative and an exciting interdisciplinary challenge.

The performance of a photovoltaic system strongly depends on its location, altitude, and exposure. Many existing dams offer a downstream surface of large extension suitable for the installation of a high-power PV plant; in the case of southward-oriented dams (located in the northern hemisphere) the conditions of incident solar radiation are optimal and therefore potentially capable of high efficiency.

The installation on existing structures of PV plants is particularly interesting due to the simplified authorization process: PV technology is broadly accepted in public opinion and in the case of installation on dams presents limited, or no dam safety issues.

A further advantage of these types of installations is the connection to the existing power-lines of the dam and to the nearby located hydropower plant, already connected to the distribution grid. No major additional works for the connection of the PV plant are thus required.

The design of PV plants on dams must match the characteristics of the existing structures as well as O&M requirements of PV plants: specific structural and access solutions must be developed.

Some of the authors were involved since the first ideas until the final commissioning in 2022 of the by-now largest Alpine PV power plant on the downstream face of Muttsee concrete dam, Glarus, Switzerland. At an elevation of 2'474 m a.s.l. and with a surface of 10'000 m², the plant shows a peak capacity of 2.2 MW with an expected annual yield of 3.3 GWh, mostly in Winter months.

RÉSUMÉ: L'installation de systèmes photovoltaïques (PV) sur les barrages est une initiative pionnière et un défi interdisciplinaire passionnant.

La performance d'un système photovoltaïque dépend fortement de son emplacement, de son altitude et de son exposition. De nombreux barrages existants offrent une surface aval de grande extension adaptée à l'installation d'une centrale photovoltaïque de grande puissance; dans le cas des barrages orientés vers le sud (situés dans l'hémisphère nord), les conditions de rayonnement solaire incident sont optimales et donc potentiellement capables d'un rendement élevé.

L'installation de centrales photovoltaïques sur des structures existantes est particulièrement intéressante grâce au processus d'autorisation simplifié. La technologie photovoltaïque est largement acceptée par l'opinion publique et, dans le cas d'une installation sur un barrage, elle ne pose que peu ou pas de problèmes de sécurité.

Un autre avantage de ce type d'installation est la connexion aux lignes électriques existantes du barrage et à la centrale hydroélectrique située à proximité, déjà connectée au réseau de distribution. Il n'est donc pas nécessaire d'effectuer des travaux supplémentaires importants pour le raccordement de l'installation photovoltaïque.

La conception des centrales photovoltaïques sur les barrages doit correspondre aux caractéristiques des structures existantes ainsi qu'aux exigences d'exploitation et de maintenance des centrales photovoltaïques: des solutions structurelles et d'accès spécifiques doivent être développées.

Certains des auteurs ont été impliqués depuis les premières idées jusqu'à la mise en service finale en 2022 de la plus grande centrale photovoltaïque alpine sur la face aval du barrage en béton de Muttsee, à Glaris, en Suisse. À une altitude de 2'474 m et avec une surface de 10'000 m², la centrale a une capacité de pointe de 2,2 MW avec un rendement annuel prévu de 3,3 GWh, principalement pendant les mois d'hiver.

1 INTRODUCTION

Dam purposes, which set them being one of the most significant civil engineering works, are already multiple. Among them, some of the most relevant are surely: generation of hydroelectric power and energy storage, water supply (domestic or industrial), irrigation, flood mitigation and managing stream flows, recreation and tourism, and navigation.

In recent years, the observation of the large extensions offered by dams on their downstream surface, has induced in some visionary designers the idea of the suitability of these surfaces to high power PV installations.

This uncommon technical installation offers some remarkable opportunities and several benefits. First, these solutions avoid the installation of new generation capacity by avoiding the subtraction of large lots to agricultural and forest use. In addition, the exploitation of an already existing industrial infrastructure, such as a dam, generally leads to the perception of higher environmental compatibility, favoring local social acceptance. In this case, the minor landscape modifications generally require a shorter authorization process. Moreover, the technical installation of large PV plants can generally benefit from existing infrastructures (existing medium voltage and high voltage lines for grid connection, roads, and support buildings for the construction yard, existing on-site O&M organization, and so on), thus increasing the efficiency and the sustainability of a project. In addition, other factors, such as the southward orientation, the downstream slope, the high altitude (with higher Albedo offered by the snow cover of the surrounding during the Winter season), and the absence of mist and smog effects, can generally enhance the whole efficiency. Therefore, in general, mountain installations offer optimal conditions for energy production from PV systems.

The possibility to fully exploit these advantages may also depend on the dam typology. Indeed, concrete gravity and embankment dams are generally more favorable for PV installations, while arch and buttress dams are usually less suitable to host such systems (Kougias et al. 2015).

However, the installation's technical design must consider the possible constraints introduced by the existing structures, with reference to the existing functional access architecture and spillway hydraulics, and to the requirements of dam safety control and operation. An example of these constraints will be reported more in detail in this paper, with reference to the case study presented, which is the Mutsee gravity dam.

2 ALPINE PHOTOVOLTAIC INSTALLATION

Since the case study presented in this article is a PV system installed on a dam located in the Alpine area, the main factors affecting the efficiency and design of installations located in such an area are reported in this paragraph.

2.1 *Geographical and morphological aspects*

Dam exposure is a very important aspect; indeed, the southward orientation of the downstream surface is an important plus. In addition, azimuth orientations between -30° and $+30^\circ$ are optimal, but acceptable until -45° and $+45^\circ$.

Moreover, the Alpine sites frequently offer elevations above fog and mist limits, with a clean atmosphere and seasonal lower temperatures with a consequent coolant effect on the panels, resulting in improved efficiency throughout all the seasonal cycles (particularly during Winter).

In addition, also the valley morphology must be considered. A wide, rounded, amphitheater-like, glacial high valley reduces the shadow effect of the mountain slopes on the PV plants, thus elongating the exposure time to the sunlight of the system.

2.2 *System architecture*

The optimal slope for PV systems at the latitude of the Alpine area is around $31-32^\circ$, while the slope of the downstream face of gravity dams is generally around 55° or more. However, the inclination angles higher than the optimal ones reduce the performance of the system only to

a limited extent, while they offer a self-cleaning effect on the panels from snow. The snow accumulation at the dam base on the lower part of the PV plants can be avoided by raising the elevation of the bottom layer of the panels from the dam foundation.

The dam's preexisting, structural, hydraulic, and architectural functional parts are usually not an obstacle to the construction and exploitation of the PV plant, hence requiring only some minor conditioning of the design.

Furthermore, the height span of the dam requires a specific design of lifting devices for installation and O&M access paths, the last to be architecturally integrated with existing accesses and PV panel supports.

2.3 *Climatic aspects*

The white surface of the snow, present on the slopes surrounding the Alpine PV dam installations for many months over a year, offers a very high Albedo effect with a correspondent effect on the improvement of the energy performance of the PV panels. With respect to this aspect, Figure 2 shows a comparison between the monthly performance of PV installations in the Swiss Plateau and of Alpine installations.

2.4 *Environmental aspects*

The exploitation of existing infrastructures is appreciable for the reduced land use and limited environmental impact.

The installation of a PV plant on a dam is totally new and not explicitly foreseen in existing national environmental, urbanistic, and construction frameworks nor in dam guidelines. However, the permitting process is generally facilitated by the general perception of a favorable integration of technologies, without additional land use. An issue that may arise in some cases is the color modification from dam concrete grey to a uniform dark surface of the PV panels.

2.5 *Chances*

New PV plants generally profit from the pre-existing energy grid and ancillary infrastructures, thus avoiding additional costs due to an eventual grid expansion or for the design of new temporary support facilities. Therefore, this frequently results in the creation of an efficient hybrid system, which can be even more effective in the case of pumped-storage dams by foreseeing the use of PV production to cover off-peak periods.

2.6 *Structural and dam safety-related aspects*

Generally, the loads applied by the new PV installation on existing structures (including the PV panels, supports, new pathways, cableways, and electrical parts) are only a very small fraction of the total weight of the dam, so the general behavior of the structure is not altered by the installation itself. However, a critical point is the connection between the existing dam body and the lightweight supports of the panel, especially when a seismic design is required.

The design of the support structures must reduce as much as possible interferences with the existing structure to limit emerging dam safety issues. Visual controls of the downstream surface must remain possible at any time, access to internal parts has to be granted, and existing control systems must remain functional with no or slight adaptation.

3 CASE STUDY

3.1 *AlpinSolar photovoltaic plant on Muttssee dam*

The Muttssee dam (Figure 1) was built between the years 2012 and 2015 to expand an existing natural lake already exploited for hydropower production to a 23 mio m³ reservoir for the 1 GW "Linthal 2015" pumped-storage hydropower plant. This gravity dam is in the Glarus

Alps (Switzerland) and, being situated at 2'474 m a.s.l., is the highest reservoir in Europe. The 35 m high dam consists of 68 concrete blocks 15 m long and two final elements 17 m long, for a total length of about 1'050 m, making it the longest dam in Switzerland. The downstream face is inclined 51° at the bottom and 90° at the crest.



Figure 1. Muttssee dam before installation of the PV system¹.

The dam layout, as well as its orientation and its altitude, have been evaluated as suitable for the installation of a PV system on its downstream face.

Indeed, the favorable factors are multiple:

- The dam is perfectly south-southeast to south-southwest oriented; therefore, the sun exposure is significant throughout the whole year.
- The large slopes of the downstream face allow snow to slide off the surface on its own, preventing also possible ice-related problems.
- The low temperatures correspond to an increased efficiency of the PV panels.
- The high altitude is also favorable for the “Albedo effect” since the reflection of the light is significant on snow-covered surfaces.
- The structure is above the usual fog elevation on the Swiss midland.
- Part of the existing infrastructures (e.g., 16 kV grid connection, small expansion of the existing technical building) could be used for the installation.

The advantages result in an expected increase in the productivity of solar modules per unit area, with respect to what is recorded in the Swiss Plateau, equal to 50%. This is even more strengthened during Winter, when the productivity is expected to increase by three times. The advantages in the production, with respect to midlands PV systems are summarized in Figure 2, using data adapted from ZHAW (University of Applied Sciences Wädenswil, Switzerland).

1. <https://www.axpo.com/ch/de/magazin/erneuerbare-energien/ab-in-die-hoehe.html>

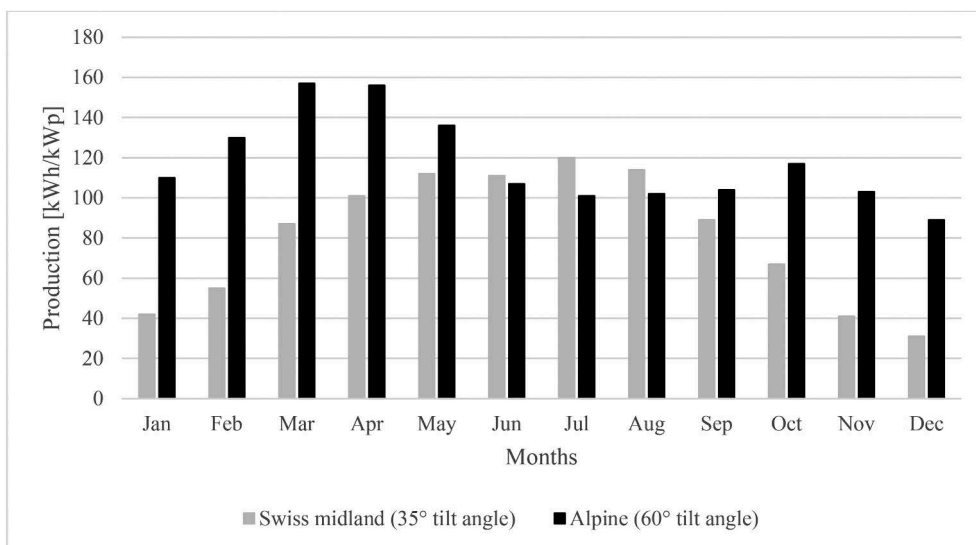


Figure 2. Annual production profile of Alpine and Midland PV systems.
(Source: ZHAW).

However, despite the several benefits coming from installing a PV system, in this context, various challenges were addressed for the realization of the project. First, the return on investment is a crucial problem that was faced by the investors of the dam since these types of solutions are still not very diffuse and the absence of specific regulation must be considered as a risk. In addition, the extreme weather conditions of the site posed additional challenges, related both to the construction and the operation phases of the project. These challenges are related to the accessibility of the construction site, the delivery of construction materials, and the impossibility of working during the Winter months due to the large amount of snow. Furthermore, the high thermal variability and the need for periodic cleaning and maintenance work require careful consideration to be given to the support and accessibility structures of the PV system itself. Moreover, dam stability, as well as flood safety, are also aspects that must be carefully evaluated. Specifically, the verification of stability is necessary due to the changes in concrete temperatures caused by the area-wide placement of the solar panels (while the added weight given by the panels themselves can be considered negligible with respect to the weight of the dam body), while flood safety must be considered in relation to the fact that the PV panels are installed in the area of the spillway. Finally, also the COVID-19 pandemic created some problems related to delays in the delivery of some materials.

The problem of accessibility was solved by using helicopters for workers and material transportation. Instead, the installation of the PV system in-site was done by accessing with ropes to the dam face and fitting aluminum rails, which are almost not affected by temperature variations (Figure 3). In addition, the designed generous distance between the solar panels and the spillway edge (approximately 7 m) ensures that the function of the spillway is always guaranteed and that the solar panels do not interfere with it. Moreover, a spacing between the bottom of the downstream face of the dam and the solar panels of about 5 m was ensured to avoid possible malfunctions due to snow accumulation. Finally, an accurate Finite Element (FE) analysis demonstrated that temperature change in the concrete surface results in only a very insignificant change in the behavior of the dam in the form of additional valleyward deformations of a few millimeters, thus not affecting the dam stability.



Figure 3. Construction phase of the PV system on the Muttssee dam².

A further aspect that was addressed is to allow the periodic monitoring activities required by such an imponent structure. The visual inspection of the concrete surface is allowed at any time by the walkway between the airside parament and the solar panels (1.5 m distance). Furthermore, the individual block joints were kept free by a gap of 0.5 m between the panel blocks. In addition, it was also checked and proven that all sights for the geodetic measurement remain free and that other measuring equipment is not restricted in its function by the PV plant.

The project was completed in August 2022, after the installation of 4'116 modules of 460 and 756 modules of 385Wp each, corresponding to a total installed capacity around 2.2 MW and a surface area around 10'000 m². The expected annual production is equal to 3.3 GWh.

The production of electricity already started in October 2021 exploiting the PV panels installed up to that time. Figure 4 (generated by adapting data from Axpø) shows the monthly percentage of power production (over the total production of one year) for both the new Muttssee PV system (2022) and the average of the Swiss PV plants (2017-2019). The profiles highlight how the Muttssee PV plant produced, during its first year of exploitation, up to five times more electricity in the Winter months than average plants on the Swiss Plateau, and therefore substantially confirm the predictions of Figure 2.

This project is not the sole in Switzerland but is surely the most significant in terms of dimensions and impact. Overall, the positive implications of such pioneer projects, in addition to the intrinsic energy-related aspects, have already been appreciated following the introduction, which occurred in September 2022, by the Swiss government of “Urgent measures for the short-term provision of reliable power supply in Winter”. These amendments to the Energy Act guarantee additional grants and simplified approval processes which will surely result in an important short-term impulse for Alpine plant installations. The new regulations will be in force until the end of 2025 or until a total annual production of 2 TWh has been

2. <https://www.axpo.com/no/en/energy-knowledge/pioneer-project-in-the-swiss-alps.html>

reached, but it is expected that they will pose the foundations for a continuously increased interest in innovative solutions such as those of the Muttsee dam PV system project.

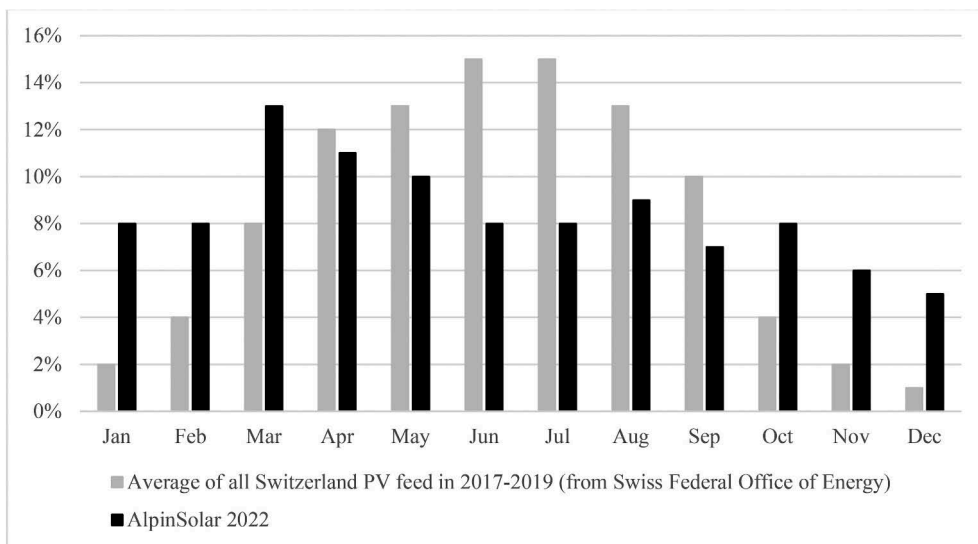


Figure 4. Comparison between the average monthly production of energy of Switzerland PV plants and those corresponding to the Muttsee PV plant³.



Figure 5. Muttsee dam with the installed PV system⁴.

3. <https://www.axpo.com/ch/de/ueber-uns/magazin.detail.html/magazin/erneuerbare-energien/Fuer-mehr-Win-terstrom.html>

4. Courtesy AlpinSolar AG

4 CONCLUSIONS

Dams, being already existing structures and part of industrial power plants, offer interesting possibilities for the deployment of a new generation of high-power PV plants.

The new integration model has special features making it environmentally friendly and moreover acceptable, making the authorization process generally easier and with a high success rate.

The pioneering solar projects, such as the one presented of the Mutsee dam, will definitely exploit the real potential of using dams for the hybrid installation of PV plants, ultimately defining the real benefits of this type of installation against the specific technical issues coming from the intrinsic hydraulic and structural functionality of the original support.

Surely, these experiences will provoke the consideration and set up of reglementary references both from the structural and environmental points of view, at national and European levels, as already occurred in Switzerland with the recent introduction of specific amendments to the Energy Act.

In the future, it is important to have a continuous exchange of information from lessons learned for this type of unconventional and innovatory installations, where dam engineering and PV engineering need to match and mediate existing and new technical requirements: only an in-depth analysis of a wide spread of cases can support the share of the required experience for the set and completion of this type of innovative project.

The defying technical design task must analyze and make compliant the features and special needs of the existing hydraulic and structural installation with the standard optimization requirements of the younger PV technology, matching all the needs of safe installation, cost-effectiveness, and serviceability.

ACKNOWLEDGEMENTS

The authors acknowledge the inputs regarding Mutsee dam safety provided by Rico Senti from Axpo Power AG.

REFERENCES

- Ab in die höhe!* (2021) Axpo. Available at: <https://www.axpo.com/ch/de/magazin/erneuerbare-energien/ab-in-die-hoehe.html> (Accessed: 17 May 2023).
- Alpenstrom Davos (no date) ZHAW Institut für Umwelt und Natürliche Ressourcen IUNR. Available at: <https://www.zhaw.ch/de/lsfm/institute-zentren/iunr/oekotechnologien-energiesysteme/erneuerbare-energien/solarenergie/alpenstrom-davos/> (Accessed: April 14, 2023).
- Heierli, C., (2022) "A new Swiss partnership.", Waterpower Magazine.
- Kougias, I., Bódis, K., Jäger-Waldau, A., Monforti-Ferrario, F., Szabó, S., (2015) Exploiting existing dams for solar PV system installations. *Progress in photovoltaics: research and applications*. 24:229–239.
- Müller, U., Marclay, R., Dunn, J., Hohberg, J.M., Hase, M., (2013) The Linth-Limmern hydro-power plant – Design and construction of a large pumped storage scheme. *World Tunnel Congress 2013 Geneva*.
- Schranz, J. (21.01.2021) Pioneer project above the fog line, Axpo. Available at: <https://www.axpo.com/no/en/about-us/magazine.detail.html/magazine/renewable-energy/pioneer-project-above-the-fog-line.html> (Accessed: April 14, 2023).
- Schranz, J. (13.04.2023) Für Mehr Winterstrom, axpo. Available at: <https://www.axpo.com/ch/de/ueberuns/magazin.detail.html/magazin/erneuerbare-energien/Fuer-mehr-Winterstrom.html> (Accessed: April 25, 2023).
- The largest alpine solar plant in Switzerland (no date) Axpo. Available at: <https://www.axpo.com/no/en/energy-knowledge/pioneer-project-in-the-swiss-alps.html> (Accessed: April 14, 2023).
- The largest alpine solar plant - Mutsee, Switzerland (21.06.2022) INNOTECH. Available at: <https://www.innotech-safety.com/en/news/current-topics/detailpage/the-largest-alpine-solar-plant-mutsee-switzerland> (Accessed: April 14, 2023).

Vianden pumped storage plant - large-scale shear tests on rockfill material of the upper reservoir ring-dam

Ch. Meyer & K. Thermann

Tractebel Engineering, Bad Vilbel, Germany

ABSTRACT: Located on the Our River on Luxembourg’s eastern border with Germany, the Vianden pumped storage power plant was commissioned in 1964. The plant has a two-section upper basin, which was built on the summit plateau of the Nikolausberg mountain. The ring dam enclosing the upper basin is designed as a rockfill dam with an asphalt surface sealing. In the context of a routine safety review of the ring dam, in 2021 large-scale triaxial shear tests were carried out on the existing dam fill material. The aim of the tests was to verify the shear parameters adopted for the design considering an operating period of almost 60 years with regard to the stability calculations to be carried out. The paper describes the tests carried out and presents the results in the specific setting of the investigation program, which was performed as a basis for the safety review. The test results are also put into perspective of the frequently used approach for rockfill dams from Leps (1970) with a stress-dependent friction angle for different material qualities.

1 INTRODUCTION

The Société Electrique de l’Our (SEO) operates the Vianden pumped storage power plant on the eastern border of Luxembourg with Germany on the River Our. The plant was commissioned in 1964 with 9 units and was extended in 1970 and 2014 by 2 additional units to a current total of 11 units. Today, the plant provides a total capacity of 1290 MW in turbine mode and 1040 MW in pump mode.

The lower basin of the plant is located in the Our river valley and is impounded by the Lohmuehle dam, which is located directly north of the town of Vianden. It stretches over a length of about 8 km and provides a storage volume of 11.3 million cubic meters. The upper basin takes advantage of the topographically favorable situation on the summit plateau of the Nikolausberg. The two-section upper basin is enclosed by a 14 m to 35 m high rockfill ring dam with an asphalt surface sealing. The two sections of the upper basin have a combined capacity of 7.7 million cubic meters and an active volume of 7.3 million cubic meters.

For this project, the regulations of DIN 19700 apply to the planning, construction, operation, and monitoring of dams. Part 14 of DIN 19700 in particular is applicable to pumped storage reservoirs. According to the provisions of DIN 19700, a review of the up-to-dateness and conformity of the safety-relevant documents of existing dams (so called “in-depth review”) must be carried out at appropriate intervals. With the new installation of unit 11, not only the capacity of the plant but also its working capacity was increased by extending the usable reservoirs in the upper and lower basin by 500,000 m³ each. For this purpose, the crest of the ring dam of the upper basin was raised by 0.50 m and additional wave protection elements were added. This structural modification was taken as an incentive to carry out an “in-depth review” of dam stability in 2015. This study was based exclusively on values taken from existing design documents. Subsequent to this investigation, the geotechnical conditions were again verified by investigations and laboratory tests (including large-scale triaxial shear tests). On this basis, the “in-depth review” of dam stability was again revised in 2021.

2 SITUATION

2.1 *Upper basin*

Figure 1 Shows the upper basin with its two sections (upper basin I and II) with their ring dam in an aerial photograph.



Figure 1. Aerial Photo of the Two-Section Upper Basin (Source: www.geoportail.lu).

The ring dam has a varying height of the dam foundation surface along the dam axis, which is an essential feature for distinguishing the characteristic dam cross-sections used in the stability analysis. This arises from the former topography and geology of the hilltop, which was removed to create the upper basin. Depending on the resulting excavation profiles, the bottom of the basin is therefore either below or at the level of the dam foundation surface.

2.2 *Geological conditions*

The project area is located in the Ardennes, which in the area under consideration is composed of Lower Devonian rocks. As it is characteristic for this area, the tectonic structures strike from NE-SW while the dip of the layers is quite shallow.

The bed of the Our River has carved into a series of clay- and siltstones. The gray to dark gray rock may locally also contain a higher content of fine sand, which is also noticeable in alternating layers of clayey and silty material intercalated with layers of silty sand. Accordingly, the Nikolausberg, where the upper basin is located, is also made up of clay- and siltstones. The overburden material resulting from the removal of the hilltop was crushed and homogenized during the construction process and used as embankment fill material for the ring dam.

2.3 *Characterization of the dam fill material*

The ring dam in general consists of excavated material. This is the clay stone, which was obtained by ripping up the rock in place. The geotechnical investigations carried out latest at the upper basin confirm that the dam is built up mainly with a rather homogeneous fill material. The composition (grain size distribution) varies depending on the source rock used in each case, but the main fill can in general be described as crushed stone (cobbles) with an average content of fines (silt and clay) of less than 15%. Coarse fractions are predominately gravel-like fractions and cobbles.

The dam fill material was mechanically compacted during placement. The achievable degree of compaction was determined by laboratory tests. Overall, an average dry specific weight of 22.5 kN/m³ can be considered as a representative value for the dam fill.

The shear strength of the embankment fill material was determined during construction mainly by triaxial tests at the universities of Karlsruhe (Prof. Leussink) and Darmstadt (Prof. Breth). The results of the historical triaxial shear tests are summarized in Table 1.

As the fill material is proven to be well compacted, based on the historical results of the triaxial shear tests and also considering Leps (1970), the 2015 stability analysis was based on a friction angle of $\phi = 43^\circ$ and a cohesion of $c = 0 \text{ kN/m}^2$.

Table 1. Results of historical triaxial shear tests.

Source	Breth (1963)	Leussink (1960) Loose	Leussink (1960) Compacted
Dry Density γ_d [kN/m^3]	20.5	17.9/19.3	21.4/21.0
Max grain size d_{max} [mm]	70	100	100
Friction Angle ϕ [$^\circ$]	39	40	43
Cohesion c [kN/m^2]	50	0	0

3 TRIAXIAL SHEAR TEST

3.1 Sample material

In the period between 2018 and 2020, geotechnical investigations were carried out in the area of the upper basin in order to check the input parameters for the stability analysis. In this context, it was also decided to investigate the shear parameters of the dam fill material by means of an exemplary laboratory test. The investigations were intended to clarify whether there were any indications of a change in the shear parameters of the dam fill material associated with the operation of the plant, which would have to be taken into account in the stability review.

To carry out the triaxial test, a representative sample for the entire ring dam with a total weight of around 5,000 kg was required. This corresponds to around 2.2 to 2.3 m^3 of material. For logistical reasons, the sampling location was arranged in the area of one of the access ramps to the dam crest. Sampling was carried out on 30.03.2021 using a hydraulic excavator with backhoe (cutting width = 600 mm). The sample was obtained starting from the main access ramp to Upper Basin I in the northern area of the basin. The sample was taken from the upper part of the dam fill. The overburden (protective layer with more fines) was excluded from the sampling.



Figure 2. Sample collection for the triaxial tests.

For logistical reasons, the sample material was distributed among 5 transport containers with an individual weight of up to max. 1,000 kg.

3.2 Laboratory test setup

For the determination of representative shear parameters of the embankment fill material, the in-situ grain size distribution (in particular the maximum grain size) must be taken into account as a decisive boundary condition. In order to be able to investigate a sample that is as representative as possible, a test with a diameter as large as possible should therefore be aimed at.

At the Karlsruhe Institute of Technology (KIT), a triaxial cell for specimens with a diameter of 80 cm is available for this purpose. Samples with a maximum grain size of 100 mm (single components up to 125 mm are still within the tolerance range) can be tested in this device. Considering expected grainsize distribution of the Vianden sample material, components with a diameter > 100 mm present in the sample had to be sorted out before the test. This procedure was considered acceptable in agreement with the laboratory to be able to achieve representative shear parameters for the dam fill material with the triaxial cell available at KIT.

The homogenized sample material taken from the transport containers was placed in layers in the cylinder and was carefully compacted. Dry densities between 2.18 and 2.21 g/cm³ were achieved for the placed material. This is in the range of the target compaction which corresponds to the values documented during construction.



Figure 3. Preparation of the specimen at KIT (KIT 2021).

Three tests were carried out on three parts of the same sample material. The tests were carried out with different lateral confining pressures of 0.1/ 0.2/ 0.3 MPa to simulate different depths of incorporation. The lateral pressure was applied hydraulically through a diaphragm enclosing the specimen (see Figure 4, left), and the lateral strain was not limited during the test. During the tests, the lateral pressure was kept constant and the axial pressure was continuously increased so that a constant deformation rate of 0.05%/min was achieved. An axial deformation of 12% was



Figure 4. Left: Sample ready for testing inside the membrane Right: Sample before closing the apparatus (KIT 2021).

defined as the termination criterion. After completion of the tests, the grain size distribution was determined again to gain information on the effects of the test on the specimen material.

3.3 Results

The particle size distribution of the homogenized sample material supplied was determined before the start of the tests. After each test, the particle size distribution of the sheared sample was determined and compared with the initial distribution curve.

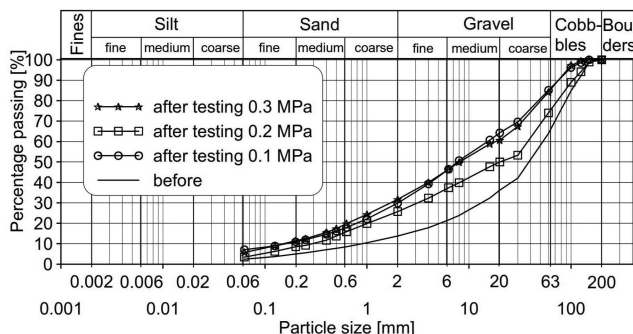


Figure 5. Grain size distribution before and after the tests (KIT 2021).

From the results shown in Figure 5 it can be concluded, that in connection with the shearing of the specimen, a fragmentation of the coarser components must have occurred. This is resulting in particular in a reduction of the coarse gravel components and the cobble components. The curves of the tests carried out at 0.1 MPa and 0.3 MPa have a similar path, but the curve of the 0.2 MPa test runs slightly below these two. The cause for this cannot be read from the test data.

The results of the triaxial tests are given in Figures below. Figure 6 shows the deviator stress (q) versus the axial strain (ϵ_1). Tests show similar stiffness until reaching about 0.5 % strain. After this point test results differ. While the tests with the lower horizontal confining stress ($\sigma_3 = 0.1$ MPa and $\sigma_3 = 0.2$ MPa) show a gentle maximum, the test with the highest horizontal stress ($\sigma_3 = 0.3$ MPa) does not show any significant peaking behavior.

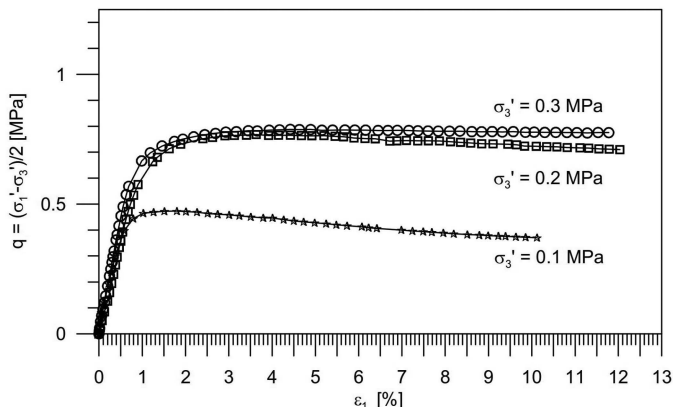


Figure 6. Test results showing deviator stress (q) vs. axial strain (ϵ_1) (KIT 2021).

The volumetric change (ϵ_v) versus the axial strain (ϵ_1) resulting from the tests is shown in Figure 7. From this figure it can be seen, that at the beginning of each shear phase a reduction in volume can be noticed for all specimens. This volumetric change is comparable to an oedometric deformation (contractive behavior). At a later stage of the test, when the axial strain reaches about 0.5 % to 1 %, the samples show a dilative behavior where the volume of the

sample again starts increasing. The sample volume at the end of the test is always noticed to be larger than at the beginning of the test.

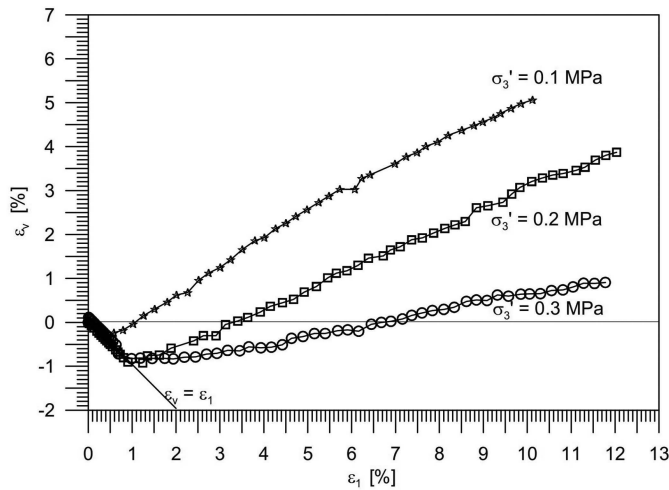


Figure 7. Test results showing volumetric change (ϵ_v) versus the axial strain (ϵ_1) (KIT 2021).

The Mohr's circles resulting from the three tests are given in Figure 8.

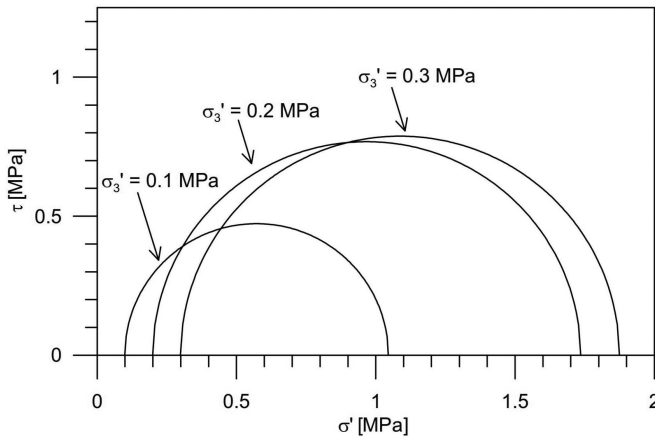


Figure 8. Mohr's Circles resulting from the tests (KIT 2021).

The friction angles listed in Table 2 were determined from the Mohr's circles shown above in Figure 8 in a linear relationship from the slope of the tangent line of the respective stress circle passing through the origin. This approach seems to be justified for the investigated material, since stresses in the rockfill material under consideration are predominantly worked off via grain-to-grain contacts and it thus behaves like a non-binding material. When considering the friction angles shown in Table 2, it is noticeable that smaller friction angles result

Table 2. Results of triaxial shear tests (KIT 2021).

Test No.	Horizontal Stress σ_3 [MPa]	Deviator Stress q [MPa]	Friction angle ϕ
1	0.1	0.472	55°
2	0.2	0.765	52°
3	0.3	0.787	46°

with increasing stress. This development is characteristic for sample material of rockfill dams and is documented accordingly in literature (e.g. Leps 1970).

4 INTERPRETATION

The evaluation of numerous triaxial tests carried out by Leps (1970) showed that the effective friction angle ϕ of rockfill material is non-linear. According to Leps (1970), the magnitude of the friction angle of the rockfill depends on the backfill height (stress). This correlation was also observed in the triaxial tests carried out in 2021 (see Table 2).

The empirical, non-linear development of the effective friction angle is shown according to Leps (1970) as a function of the stress for different material grades in Figure 9. The results of the current triaxial tests carried out at KIT have been plotted as colored (red) dots in the diagram.

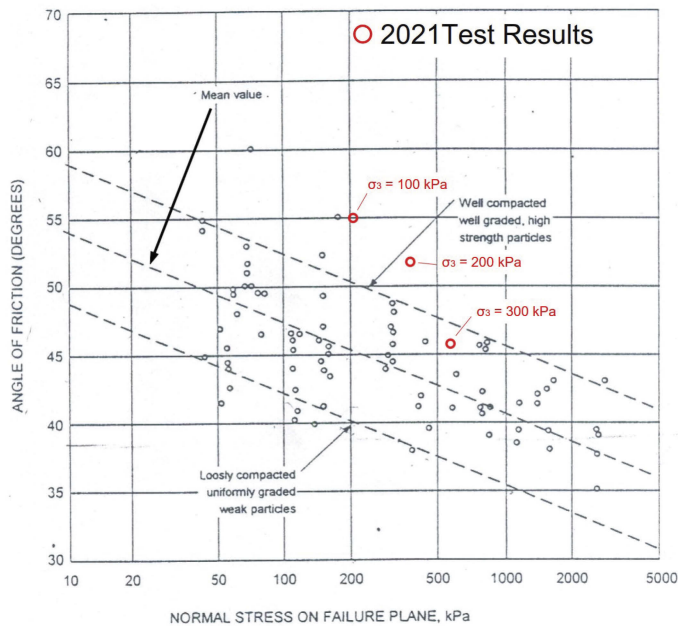


Figure 9. Shear strength for rockfill according to Leps (1970) Red dots: Results of the 2021 triaxial tests (modified from Leps 1970).

Figure 9 shows that the 2021 test results obtained for the tests run with 100 kPa and 200 kPa horizontal stress are situated above the line for well compacted rockfill material determined by Leps (1970). The value for the test at a horizontal stress of 300 kPa is below the line for well graded and well compacted material. Following the relationship described by Leps (1970), a higher value for the friction angle should have been expected for the test at 300 kPa lateral pressure. The lower friction angle determined in the third test could be explained by the fact that at this load level, a higher degree of fracturing occurred during this test and that the behavior of this sample is changed regarding the shear parameters. On this basis, the test carried out therefore only allows statements to be made about the friction angle in the load range investigated. An extrapolation of the value based on the relationship described by Leps (1970) does not seem appropriate on this basis.

The results of the historical triaxial shear tests are shown in Figure 10 in combination with the non-linear shear strength derived according to Leps (1970). This was done under the justified assumption, that the cohesion can be assumed to be $c' = 0 \text{ kN/m}^2$ for this type of rockfill

material. In this context, the graph was supplemented by the results of the triaxial shear tests carried out in 2021.

From the historical test results shown, no comparable fracture phenomena in the grain structure can be identified as derived from the results of current shear tests.

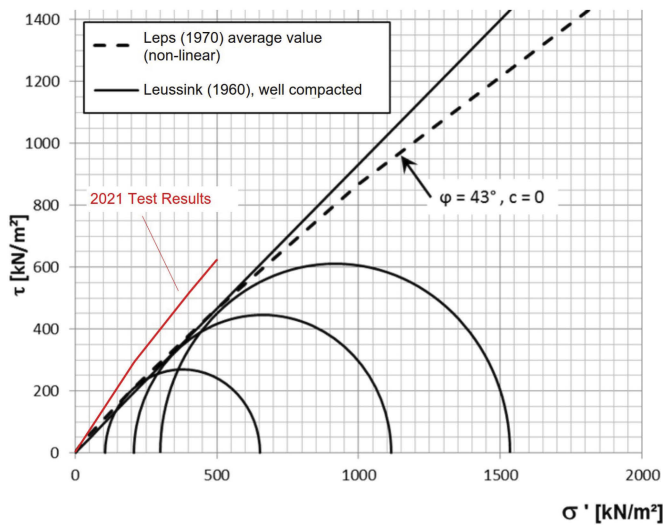


Figure 10. Results of shear tests according to Leussink (1960) combined with Leps (1970) and results of shear tests from 2021 (modified from IHS 2006).

5 CONCLUSIONS

For the stress range up to 500 kN/m², the friction angle determined by testing in 2021 is higher than the value used as a basis for the 2015 stability analysis. This value was based on Leussink (1960) and Leps (1970). The triaxial tests carried out at KIT in 2021 allows the conclusion that a friction angle of $\varphi = 43^\circ$ and a cohesion $c = 0$ kN/m² can still be considered as applicable, rather indicating that the shear parameters used so far are more on the conservative and safe side. Irrespective of this, it must of course be taken into account, that the test material comes from one sample location only. A certain variability of particle size distribution is an intrinsic feature of rock fill material which consequently results also in a certain variability of the shear parameters. Nevertheless, such tests are still considered as essential since they provide, in combination with the other available information, a sound basis for the assessment of the stability of the ring dam of the upper reservoir in Vianden.

On a more general level, it should be noted that the relationship between overburden stress and friction angle that have been documented by Leps (1970) are on a qualitative level confirmed by the results of the triaxial shear tests presented in this paper.

REFERENCES

- Leussink, H. 1960. *Pumpspeicherkraftwerk Vianden in Luxemburg: Bodenmechanisches Gutachten über den Damm des Oberbeckens*. Karlsruhe: Institut für Boden- und Felsmechanik der Universität Karlsruhe.
- Leps, T.M. 1970. Review of Shearing Strength of Rockfill. *ASCE*, 96(4), 1159–1170.
- Breth, H. 1963. Die boden- und felsmechanischen Untersuchungen für das Pumpspeicherkraftwerk Vianden. *Wasserwirtschaft*, 53(7).
- KIT - Karlsruhe Institute of Technology. 2021. Report on laboratory tests on the rockfill of the upper reservoir of the Vianden pumped-storage power plant. – not published
- IHS - Ingenieurbüro Heitfeld-Schetelig GmbH. 2006. Stellungnahme zu den bodenmechanischen Kennwerten der Steinschüttung des Oberbecken-Ringdammes beim Pumpspeicherkraftwerk Vianden – not published

Capacity building of dam wardens

A. Mico, N.-V. Bretz, O. Sarrasin & J. Fluixa-Sanmartin
HYDRO Exploitation, Sion, Switzerland

ABSTRACT: Dam wardens are responsible for carrying out measurements and visual inspections of dams. Their duties constitute the foundation of the four-level structure of Swiss dam surveillance. HYDRO Exploitation SA has been providing services in the operation and maintenance of hydropower plants since 2003. It employs approximately 40 dam wardens and periodically organizes technical training courses for them. These trainings offer a useful tool for new and experienced dam wardens to better apprehend their role in the dam's safety management. During these so-called capacity building events, dam wardens are also taught practical aspects on site, which represent an excellent opportunity to share experiences and improve their know-how.

1 CONTEXT

In Switzerland, dam safety monitoring is organized in 4 levels according to the Swiss Federal Act on Water Retaining Facilities (WRFA, 2010) and the Federal Ordinance on Water Retaining Facilities (WRFO, 2022):

- Level 1 is carried out directly by the dam wardens, who are the first to detect anomalies thanks to their knowledge of the structure and the monitoring equipment.
- Level 2 is carried out by engineers, who evaluate the dam operators' measurements, analyze the dam's structural behavior and its conditions.
- Level 3 is ensured by external experts, namely a civil engineer and a geologist, who conduct a thorough safety review of storage facilities every five years. Those experts are appointed by the Swiss Federal Office of Energy (SFOE)
- Level 4 is ensured by the SFOE or the competent cantonal supervisory authority, depending on the size of the infrastructure.

Thanks to their almost daily presence on a dam and its surroundings, dam operators can be called the “eyes” of the engineers: as they know the structure best, in all its nooks and crannies, a structure that ultimately becomes “their” dam.

Since its creation in 2003, HYDRO Exploitation has brought together some forty dam operators within its operating staff. These agents come from a variety of backgrounds, with different training such as mechanics, electricians, masons or others, and work on storage structures of different types, sizes and locations; they usually learn their function as dam operators from colleagues already active in the field. The experienced professionals (level 2 of the above-mentioned surveillance scale) therefore felt the need to offer a specific training course. The goals were to enhance the value of the profession of the dam operators and make them aware of the importance of their role in the monitoring of dams.

In order to standardize the level of knowledge among dam operators, HYDRO Exploitation has been organizing a training course for dam operators every four years since 2007, with its experienced professionals and dam operators. At the beginning, this training was exclusively aimed for its own staff and; since 2015, it has been open to all dam wardens in

Switzerland with one session for French-speakers and one for German-speakers. About 40 dam wardens currently attend each session.

2 THE FIGURE OF THE DAM WARDEN

2.1 *Roles and duties*

For level 1 monitoring, the dam operator must regularly inspect the dam and its surroundings in detail at least once a month. The scope of their monitoring is not limited to the dam, but spans the reservoir, water intakes, galleries or access roads. Measurements made by the dam operator are numerous and varied, including for example:

- Upstream-downstream and left-right bank movements, using direct or inverted pendulums.
- Pressures and uplift pressures using manometers.
- Infiltration flows, by means of volumetric gauges.
- Opening of joints and cracks.
- Temperatures of the concrete.
- In addition, the dam operator tests the operation of the drain valves.

In the context of monitoring and surveillance of dams, it is essential to have skilled staff with direct and immediate access to the facilities. Thanks to their closeness to the structure, dam wardens know “their” dam best. They frequently perform inspections of the dam and its surroundings, which allows them to have an overall view of its condition. In addition, the dam wardens are the main users of the measuring devices, so they are aware of their possible drifts and malfunctions.

Thus, the dam guards are the best positioned to provide valuable information, which is directly extracted from the data of the measurements taken, on the state of the dam to qualified professionals (level 2). The level 2 engineer is not able to access the dam as frequently: he must thus rely on the feedback from the dam wardens. The goal is to define a control program that clearly specifies what must be checked and measured, and at which frequency. These priorities are subjected to changes depending on the facility and past observations.

The Swiss Committee on Dams (SCD, 2015) lists the main tasks assigned to dam wardens:

- Performing visual inspections of the dam, its associated structures and surroundings on a regular basis. These inspections are important as they provide information on the condition and evolution of the structure that measurement instruments cannot provide (e.g., presence of saltpeter in the concrete, rockfalls reaching the structure, etc.).
- Performing periodic control measurements and collaborate in the organization of measurement activities of external specialists (e.g. geodetic measurements).
- Performing preliminary assessments of measured values (based on known or calculated theoretical estimates).
- Maintaining measurement devices in good condition, as well as reviewing and proposing improvements to measurement and monitoring equipment.
- Post-processing and analyzing the readings from the measuring devices and, if necessary, entering them into the centralized database.
- Controlling the operation of the relief and outlet works.
- Accompanying the qualified professional in his dam control visits, as well as the supervising authority and the experts in the five-yearly inspection.
- In general, carrying out activities related to their competencies in masonry, electricity, mechanics, etc. that are needed for the correct functioning of the dam installations.

2.2 *Background and capabilities*

Knowing what to report and which faults are relevant is a key element which implies that dam warden is required to meet certain capabilities, in order to successfully complete their duties.

First and foremost, he must know which dangers lie at or in the vicinity of the dam and how to use the required safety equipment. Working conditions are sometimes harsh and for certain dangers, such as snow avalanches, mountain guides are mandated to provide support.

Then basic knowledge of dam breaching, construction or civil engineering helps him to better focus on observations that could otherwise be overlooked.

Once the warden has figured out that, the surveillance level 2 is a trustworthy partner who will help him and that his work can help giving precise and relevant indications to other parties, communication will be easier.

The warden is also asked to understand functioning of the instrumentation and to perform basic maintenance on it. He should also be able to determine whether an instrument should be sent to the manufacturer for further maintenance. He should know the operating range of the instruments (temperature, humidity) and how to react, should a deviation occur.

With the deployment of telemetry systems, he should finally learn how to provide basic first level support on such equipment in order to troubleshoot any communication losses.

3 TRAINING FOR DAM WARDENS

3.1 Objectives and approach

Technical capacity of all participants is required to ensure long term sustainability of critical infrastructures such as dams and hydropower plants. In order to ensure that the staff in charge of the surveillance of these facilities assumes its role in their management, several trainings have been organized by HYDRO Exploitation. These trainings aim at increasing the level of knowledge and the use of adapted tools to improve the management of dams and their safety.

The approach followed for the design of these trainings relies on a 5-stage process, as shown in Figure 1. This consists on:

1. Defining the strategy of the training.
2. Adapting the approach based on staff needs.
3. Implementing the capacity building actions at the training level.
4. Assessing the results of the training based on the participants feedback.
5. Incorporating feedback to improve the content and organization for future trainings.

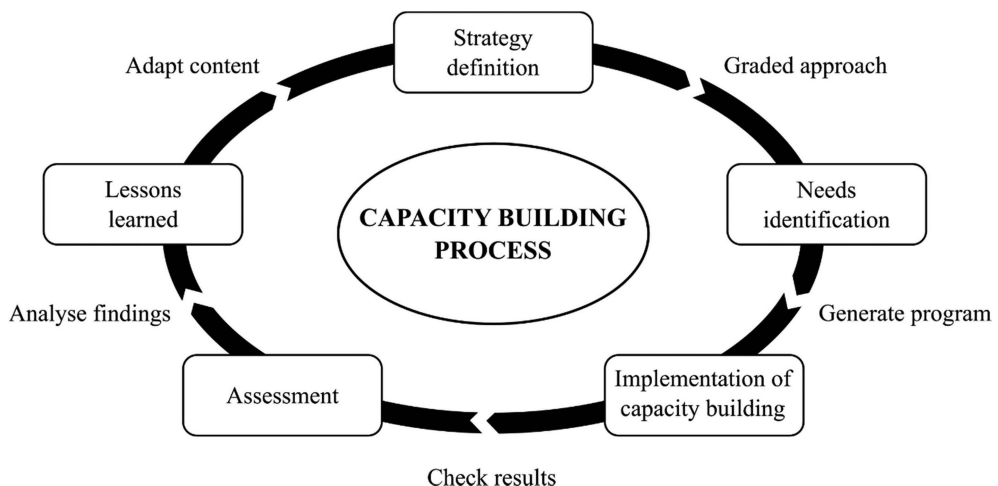


Figure 1. Planning and implementation process for capacity building (source: WFEO, 2010).

3.2 Training course program

The three-part training course taught by the engineers from HYDRO Exploitation spans two half-days (about 3 hours each): one focusing on the theoretical aspects and the other tackling the practical ones. The practical part usually takes place on a dam site, which is highly appreciated by the attendees. At the end of the training, the participants receive a USB key with all the documentation presented during the different lectures.

The course content can evolve and be tailored upon request to the needs of participants. At the end of the training, participants are asked to fill out a survey, which helps improving this content.

Furthermore, guest speakers from outside HYDRO Exploitation are often invited to present specific areas such as monitoring instruments, geology or the organization of civil protection.

3.2.1 Theoretical aspects

First, a basic theoretical training for new and experienced dam wardens is provided. The content of this part focuses on:

- The Swiss legal framework, in particular the WRFA and the WRFO.
- Duties of the dam warden.
- Review of the directives established by the SFOE's Dams Supervision Division.
- Measures and controls (what is measured and how instrumentation works).
- Controls after an earthquake.
- Internal (engineer) and external (geologist) visual inspection.



Figure 2. Participants to the 2019 training at the Grande Dixence dam.

3.2.2 Practical aspects

The practical part offers a tour in and around a dam. Along this tour, several stations are organized in which groups of participants practice for about 20 minutes on different topics such as:

- Pendulum and rocmeter measurements.
- Flow and pressure.
- Visual inspection and geological observation.
- Geodetic measurements.
- Crack monitoring.



Figure 3. Visit to the Grande Dixence dam during the 2019 training. Participants train here on a coordiscope.

3.3 Continuous training

Staff turnover (a significant part of current wardens will retire in the coming years), occasional changes in the legislative framework and new problems encountered, pose a thrilling challenge to the profession and plead for continuous training.

In the interest of openness and mutual trust, knowledge is often passed on directly from those with the most experience within an operating group. The organization of continuous training, through supervised coaching and on-site learning, facilitates this transmission between generations to the new wardens.

3.4 Timeline of past workshops

Two internal training courses took place in 2007 and 2011. Given their success, HYDRO Exploitation opened them in 2015 to external dam operators at the suggestion of the SFOE. Several trainings have been taught since (Table 1). The next training is scheduled for 2023 and is open to staff members from all Swiss dams.

Table 1. Past trainings organized by HYDRO Exploitation.

Year	Place	Dam visited	No. attendees
2007	Bourg-St-Pierre	Les Toules	25
2011	Le Bleusy, Nendaz	Cleuson	17 (FR) + 12 (DE)
2015	Naters	Gebidem	39 (FR) + 37 (DE)
2019	Hérémenche	Grande Dixence	36 (FR) + 27 (DE)
2020	Hérémenche	Grande Dixence	23 (FR)*
2021	Bitsch	-	7 (DE)*
2023	Grimentz	Moiry	still open

* Internal course due to health situation at that time

4 LESSONS LEARNED AND PERSPECTIVES

A summary of the main findings of the HYDRO Exploitation teaching staff after the six trainings already taught is presented below:

- Dam wardens are skilled and thorough professionals with diverse background, training and experience.
- It is important to make participants feel useful and actively participating in all activities.
- A focus should be put on the participants needs.
- Training does not end after the course. A training program that spans several years and involves a practical transfer of knowledge is essential.
- A positive aspect identified by the courses participants is the privileged contact between dam wardens, which allows them to share their experiences.
- During the 2-day training, it is enriching to include talks or experiences other than those of the company's lecturer.
- In order to make the experience as satisfactory as possible, it is important to take into account beforehand organizational aspects such as transportation, accommodation, audio-visual equipment, etc.
- Combining theoretical and practical contents in the training is fundamental.

The quality and content of the courses is continuously evaluated and improved. HYDRO Exploitation now offers a high-quality open course to new and experienced professionals that is useful for both dam owners and dam wardens. This is practically the only training in Switzerland specifically addressed to dam wardens that continues to be taught on a 2- to 4-year basis.

REFERENCES

- Federal Assembly of the Swiss Confederation. 2010. *Water Retaining Facilities Act (WRFA)*. 1 October 2010 (Status as of 1 January 2013), <https://www.fedlex.admin.ch/eli/cc/2012/703/en>.
- Federal Assembly of the Swiss Confederation. 2022. *Water Retaining Facilities Ordinance (WRFO)*. 23 November 2022 (Status as of 1 January 2023), <https://www.fedlex.admin.ch/eli/cc/2022/821/fr>.
- SCD (Swiss Committee on Dams). 2015. Role and duties of Dam Wardens. Level 1 surveillance of water retaining facilities. *Wasser, Energie, Luft* 107(2).
- WFEO Committee on Engineering Capacity Building. 2010. Guidebook for Capacity Building in the Engineering Environment. World Federation of Engineering Organizations.

Collection and dissemination of knowledge on dams of Italy

S. Munari

Enel Green Power – ITCOLD, Turin, Italy

ABSTRACT: The knowledge documented in technical literature about a specific dam is a valuable source of information when dealing with the control and assessment of the dam. It is therefore essential to keep the knowledge acquired in the past. ITCOLD, through a specific working group, since several years has promoted the collection and dissemination of articles and memories concerning the dams in operation in Italy, through an ITCOLD Bulletin dedicated to this subject. A first edition of the Bulletin was published in 2012 up to the last update of 2019 in which the number of 2000 collected memories broke through. With the latest update of the bulletin, the reader's experience has been made more usable, making it easier to search and download the article of interest. In the coming years, ITCOLD will continue this path of disseminating knowledge on dams and in this sense the creation of an internal online library of indexes will only help this purpose. This article therefore intends to describe the results achieved by the ITCOLD working group in recent years and sets the objectives for the near future.

RÉSUMÉ: Les connaissances documentées dans la littérature technique sur un barrage spécifique sont une source précieuse d'informations lorsqu'il s'agit du contrôle et de l'évaluation du barrage. Il est donc essentiel de conserver les connaissances acquises dans le passé. ITCOLD, à travers un groupe de travail spécifique, promeut depuis plusieurs années la collecte et la diffusion d'articles et de mémoires concernant les barrages en exploitation en Italie, à travers un Bulletin ITCOLD dédié à ce sujet. Une première édition du Bulletin a été publiée en 2012 jusqu'à la dernière mise à jour de 2019 dans laquelle le nombre de 2000 documents techniques collectés a percé. Avec la dernière mise à jour du bulletin, l'expérience du lecteur a été rendue plus utilisable, ce qui facilite la recherche et le téléchargement de l'article qui l'intéresse. Dans les années à venir, ITCOLD poursuivra cette voie de diffusion des connaissances sur les barrages et en ce sens la création d'une bibliothèque interne en ligne d'index ne fera que contribuer à cet objectif. Cet article entend donc décrire les résultats obtenus par le groupe de travail ITCOLD ces dernières années et en fixe les objectifs pour le futur proche.

1 THE IMPORTANCE OF HISTORICAL MEMORY

People has always caught experiences from the past in order to better understand the present and the future: recent history can give us the ability to grasp signs and similarities with events that have already occurred. Working on memory means extending the boundaries and building the foundations of the future on history, and this is even more true in technical areas such as in the case of dams, highly engineered works built since ancient times and with a very long service life spanning over the professional activity of various generations.

And it is precisely because of the passing of the years that historical archives, very often forgotten, become at risk of disappearing: to safeguard this historical heritage, starting from 2009 a working group of the Italian Committee on Large Dams (ITCOLD) surveyed the publications and technical articles concerning the existing dams in Italy to provide a consultation tool in the activity of reconnaissance, supervision, verification and intervention. The survey included publications in international, national and local journals, proceedings of congresses

and meetings, and any other form with which utilities, designers, companies have decided to make specific studies and information accessible.

2 THE FIRST CENSUS OF 2009

The first census of the memories was carried out in 2009 and collected a total of 1764 articles for the about 530 dams located in the Italian territory (Figure 1). This work, very onerous from a man work point of view, made it possible to create a reference for researching scientific material concerning these structures, highlighting how most of the memoirs were published during the periods of construction, therefore in the years after the two world wars.

Furthermore, the current Italian ageing of the dams is leading to carry out studies, analyses, monitoring and structural and hydraulic improvement works and consequently a new cycle of scientific publications has been establishing itself since the 2000s (Figure 2).

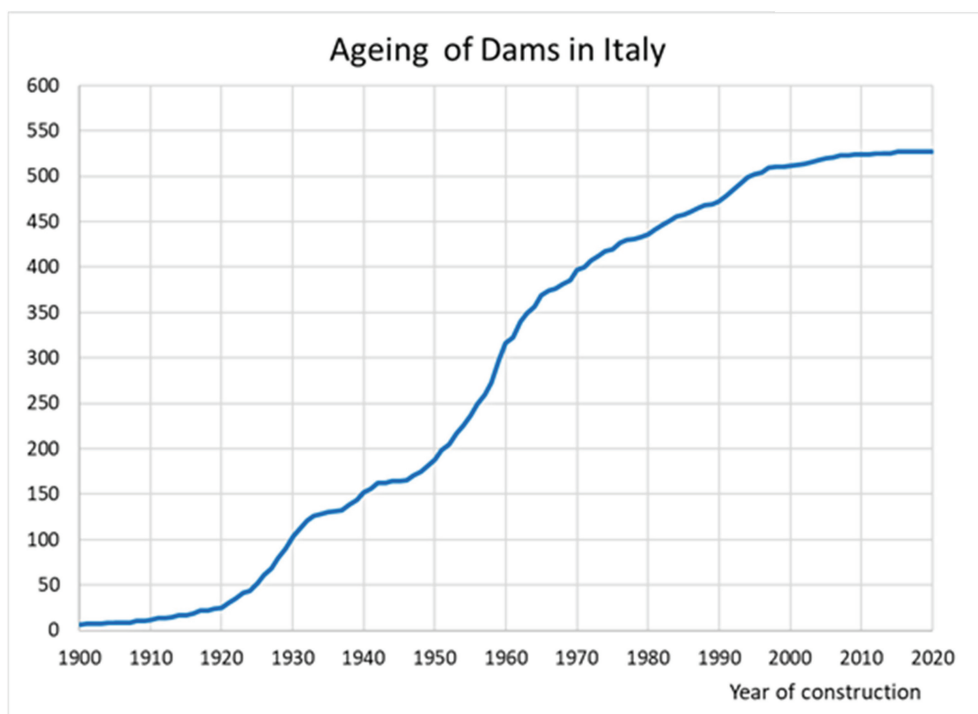


Figure 1. Ageing of dams in Italy by year of construction.

Table 1. Number of memos subdivided by groups of years.

Years	1891-1910	1911-1930	1931-1950	1951-1970	1971-1990	1991-2009
Nr. Memos	8	167	223	652	287	427

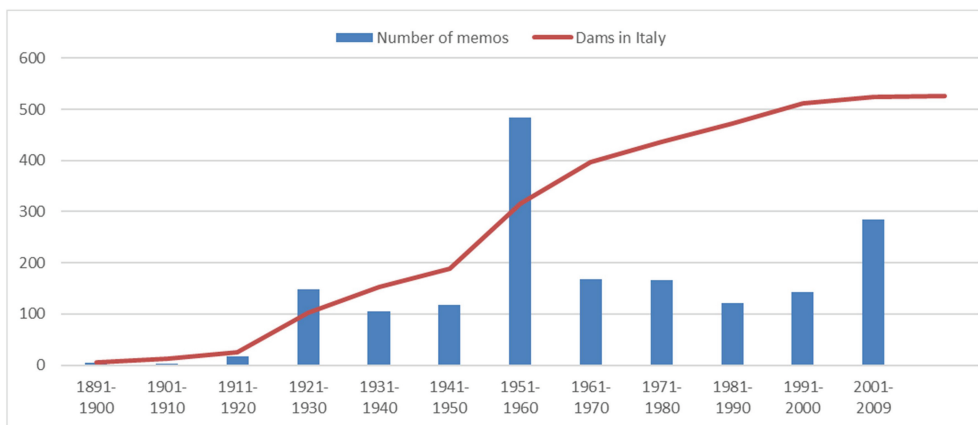


Figure 2. Distribution of memos in first census by years.

3 THE FOLLOWING UPDATES

To keep the bulletin updated, three updates have been issued over the years: in 2014 and 2016 (Calvi), and in 2019 (Munari). The updates were prepared with the contribution of the ITCOLD Young Engineers Forum (YEF).

With the continuous searching of new publications and through a better interface and cataloging, it was possible to reach the number of 2076 papers, with an increase of about 20% compared to the first edition (Figure 3).

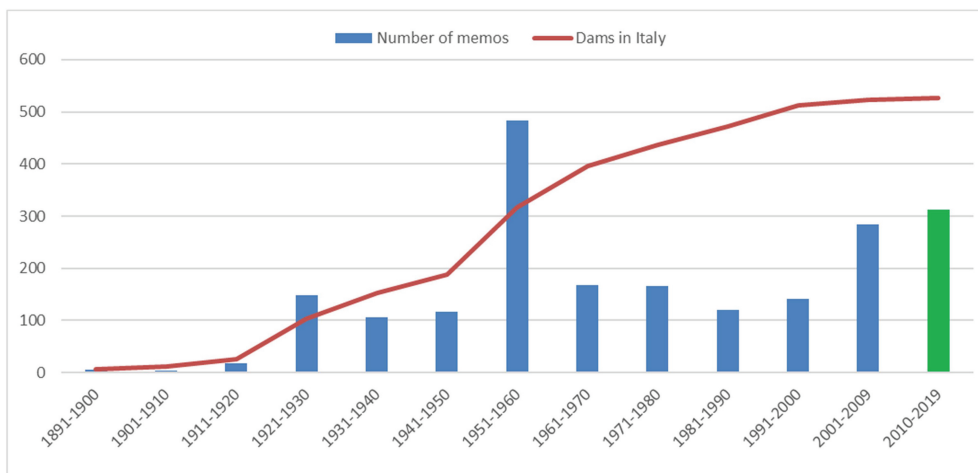


Figure 3. Distribution of memos after the last census (2019).

The cataloging also made it possible to highlight the main topic of the memos (Figure 4): a large part concerns the monographs of the dams, which mainly describe the construction and the characteristics of civil structures and connected power plants. Two other highly studied topics concern geology - geotechnics and the seismic behavior of structures.

Overall, articles concerning 371 dams were found in the bulletin and in subsequent updates, around 70% of the dams present in Italy: on average there are 5.5 articles for each dam.

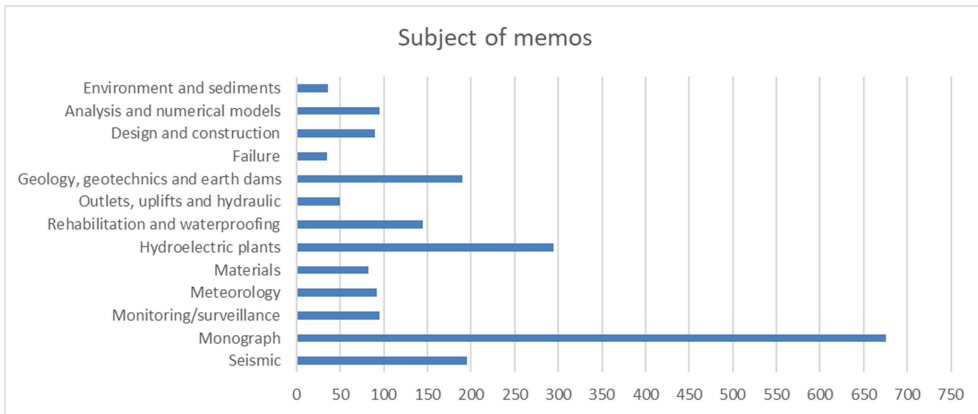


Figure 4. Distribution of memos for main argument.

4 CONCLUSIONS

ITCOLD as a cultural and scientific association always promote activity for effective studies of all the problems associated with dams.

Undoubtedly the continuous census and updating of the published articles concerning these structures makes a fundamental contribution in facilitating their analysis and study.

In parallel with this activity, ITCOLD has completed the digitalization of the indexes of its internal library in Rome with the aim of facilitating the user's searching of the article or study of interest. Stimulating interaction and collaboration between the association and the users them- selves is one of the basic elements of the association's vitality.



Figure 5. First page of the last update of the bulletin.

REFERENCES

- Jappelli, R. & Angelucci, C. 2009. Rassegna bibliografica della letteratura italiana sulle dighe di ritenuta. Roma
Munari, S. 2019. Bibliografia delle dighe italiane. Raccolta dei riferimenti bibliografici di memorie concernenti dighe italiane pubblicate su riviste o in atti di congressi/simposi/seminari. Roma

Flood control across hydropower dams: The value of safety

Christina Ntemiroglou, Georgia-Konstantina Sakki & Andreas Efstratiadis

Department of Water Resources and Environmental Engineering, National Technical University of Athens, Greece

ABSTRACT: Hydropower reservoirs inherently serving as major flood protection infrastructures, are commonly occupied with gated spillways, to increase both their storage capacity and head. From an operational viewpoint, during severe flood events, this feature raises challenging conflicts with respect to combined management of turbines and gates. From the perception of safety, a fully conservative policy that aims to diminish the possibility of dam overtopping, imposes to operate the turbines in their maximum capacity and, simultaneously, opening the gates to allow uncontrolled flow over the spillway. Yet, this practice may have negative economic impacts from three aspects. First, significant amounts of water that could be stored for generating energy and also fulfilling other uses, are lost. Second, the activation of turbines may be in contrast with the associated hydropower scheduling (e.g., generation of firm energy only during peak hours, when the market value of electricity is high). Last, the flood wave through the spillway may cause unnecessary damages to downstream areas. In this vein, this paper aims to reveal the problem of ensuring a best-compromise equilibrium between the overall objective of maximizing the benefits from hydropower production and minimizing flood risk. In order to explore the multiple methodological and practical challenges from a real-world perspective, we take as example one of the largest hydroelectric dams of Greece, i.e., Pournari at Arachthos River, Epirus (useful storage 310 hm³, power capacity 300 MW). Interestingly, this dam is located just upstream of the city of Arta, thus its control is absolutely crucial for about 25 000 residents. Based on historical flood events, as well as hypothetical floods (e.g., used within spillway design), we seek for a generic flood management policy, to fulfil the two aforementioned objectives. The proposed policy is contrasted with established rules and actual manipulations by the dam operators.

1 INTRODUCTION

According to recent statistical data by ICOLD, there exist more than 12100 large dams worldwide for hydropower generation. In particular, in the European Union, the majority of large dams (39%) are hydroelectric, while the share of hydropower over the total renewable electricity generation exceeds 40% (Wagner et al., 2019). By definition, all reservoirs, apart from their main water uses, they also contribute to the reduction of flood risk to downstream areas, since even under full storage conditions, inflow floods are attenuated. In about one third of large dams globally, particularly the hydroelectric ones, the spillway system also comprises control gates. This feature provides flexibility to the operators, since they allow to exploit the surplus inflows in order to increase both the storage and the head. On the other hand, the gate management turns to a quite complex task, since decisions are taken under pressure and highly uncertain conditions. Yet, a wrong policy may have significantly negative aspects, either in terms of economy or safety.

More specifically, the conflict between safety and economy arises from the controversial role of spillway gates. For instance, an unnecessary or too early open of gates during an

incoming flood event may result to quite important losses of potential hydropower production. On the other hand, a too late open may cause significant flood damages downstream, and under extreme conditions also put the dam itself under the risk of overtopping. We underline that in the case of hydroelectric reservoirs, the overall flood management also includes the emergent activation of turbines to release the surplus water, which may be in contrast with the associated hydropower scheduling (Efstratiadis et al., 2021).

The real-time gate management during flood events is recognized as a multiobjective problem of major complexity. This is typically expressed through multistage opening rules, by taking advantage of real time monitoring data and, occasionally, some kind of flood forecasting inputs (e.g., Sordo-Ward et al., 2017; Nematzadeh and Hassanzade, 2021; Albo-Salich and Mays, 2021; Soriano et al., 2022; Salehi et al., 2022). Their definition is addressed either through simulation or optimization. Common simulation-based tools are the so-called Volumetric Evaluation Method (Giron, 1988) and its variants, e.g., the K-Method (Sordo-Ward et al. 2017). All these are based on specific assumptions about the reservoir management and do not employ optimization.

On the other hand, optimization methods aim at determining suitable flood control policies (e.g., Bagis and Karaboga, 2004; Karaboga et al., 2008). These mainly account for safety criteria to ensure minimal risk of dam overtopping and flood damages across downstream areas. Yet, only few methods highlight the impacts of flood routing to hydropower production, which is the main economic scope of hydroelectric reservoirs (Zargar et al., 2016; Liu et al., 2017). Furthermore, in most of literature approaches, the optimization does not explicitly incorporate the management of turbines (e.g., Jordan et al., 2012), since emphasis is given to the spillway gates.

Key issue is the definition of flood conditions for optimizing the operational rules. The typical case is to use either a set of historical flood events (e.g., Malekmohammadi et al., 2009; Jordan et al., 2012; Feng and Liu, 2014; Nematzadeh and Hassanzade, 2021; Liu et al., 2017) or empirically-defined flood hydrographs that correspond to specific return periods (e.g., Salehi et al., 2022). These may range from medium-frequency events (e.g., few decades) up to extreme ones that are used in the hydrological design of spillways, also including the so-called Probable Maximum Flood. There also exist some cases where a mixing of historical and empirical hydrographs is applied (e.g., Chou and Wu, 2015; Zargar et al., 2016; Amirkhani et al., 2016).

There are also few attempts that make use of synthetic inflows that are derived through stochastic approaches. For instance, the flood events by Bianucci et al. (2015) have been obtained by coupling the RainSimV3 synthetic rainfall time series model with a deterministic hydrological model. Soriano et al. (2022) use a cascade of three models. First, they generated long time series of precipitation data at the sub-daily scale, which are inputs to a continuous hydrological simulation model. Finally, the sample of annual maximum hydrographs have been considered as inflow hydrographs to a reservoir simulation model that employed the VEM.

In this research, we develop a more comprehensive simulation-optimization context that seeks for an equilibrium between safety and economy across a wide range of flood events. The decision variables are expressed in terms of a small set of characteristic reservoir stage values, which are mapped to spillway gates opening and turbine activation. On the other hand, the objective function accounts for the amount of potentially energy loss due to water releases through the spillway (economy criterion) and the distance of the maximum flood level from the dam crest and other crucial levels, such as the top of gates (safety criterion).

As a proof of concept, we investigate the flood control policy of Pournari dam, at Arachthos River, Epirus. The combined hydropower production and flood management problem is highly challenging, since the dam is located just upstream an urban area, i.e., Arta. Taking as example a number of historical and synthetic flood events, we optimize its operational rules and contrast them with the running ones.

2 STUDY AREA

2.1 *Brief description and characteristic quantities*

In order to explore the multiple methodological and practical challenges of the spillway gate control problem from a real-world perspective, we take as example one of the largest hydroelectric system of Greece, i.e., Pournari, at Arachthos River, Epirus. The system was established in 1980 and operates by the Public Power Corporation (PPC). The location of the dam, just upstream the city of Arta, is shown in Figure 1. The drainage area upstream of the dam is 1794 km², with average altitude +854.0 m and average slope 25% (Koutsoyiannis et al., 2010). The mean annual inflow during years 1981-2021 is 50 m³/s (1580 hm³).

Pournari complex comprises an earthfill dam with central clay core, of 107 m height and maximum length of 580 m, that creates a reservoir area of up to 20.6 km². The spillway control is made by three arched gates of 12.5 m width and 12.5 m height each one (total width 37.5 m), and total outflow capacity of 6100 m³/s. The gross storage capacity at the spillway crest level (+107.5 m) is 505 hm³, yet it reaches 885 hm³ at the maximum level of +120.0 m. According to the design study of the system, the maximum flood level is at +125.5 m, namely 1.5 m lower than the top of the dam (+127.0 m).

The hydropower station is equipped with three Francis-type turbines of total power capacity 300 MW, that produce 437 GWh, on mean annual basis. The reservoir produces peak energy, and operates four hours per day, on average. Yet, during the summer period, the turbines are operating up to eight hours. Since their discharge capacity is 500 m³/s, the total discharge that can be conveyed through the spillway and the turbines is up to 6600 m³/s.

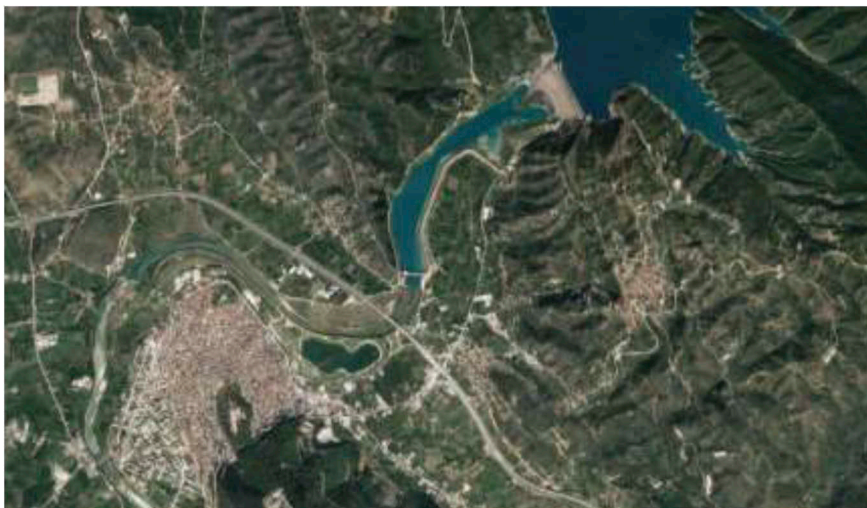


Figure 1. Location of Pournari Dam, just upstream of the city of Arta (Source: Google Earth).

2.2 *The flood management challenge*

In general, the overall flood management policy of the large Greek dams operated by the PPC focuses on three objectives, i.e., protection of river side areas, safety of hydroelectric installations, and maximization of hydropower generation (Leris, 2008). Their implementation in practice is based on the expertise of each dam staff and empirical manipulations that are made in real time.

The case of Pournari dam is the most challenging, since this is located just upstream of an urban area, namely the city of Arta. In this vein, its flood control is absolutely crucial for the

safety of 25 000 residents, as well as the protection of the historical stone bridge of 17th century, which is a worldwide recognized heritage monument. Currently, the sole specific constraint is an alarm stage at +118.0 m, which implies the full opening of the three gates. We remark that formerly, this stage was higher, namely at +120.0 m (top of gates). Yet, this rule was abandoned because it was too difficult and highly uncertain, and thus risky, to open the gates under such strong hydrostatic pressure, while the time of reaction in case of malfunction would be extremely limited. As result of this more conservative policy, the system losses a retention capacity of about 40 hm³ (i.e., storage difference between +118.0 to +120.0 m), which corresponds to a potential energy loss of up to 8.2 GWh (about 2% of mean annual energy production).

2.3 The disastrous flood events of 2005 and 2015

The floods of December of 2005 and January 2015 are of significant interest, since they are considered as two of the most disastrous events during the lifetime of the dam. Their evolution, as well as the evolution of the reservoir level, are shown in Figures 3 and 4. The accumulated inflows during the two events were estimated at 222 and 262 hm³, respectively, and the associated peak flows are estimated up to about 1700 and 2100 m³/s, respectively (Roilos, 2018).

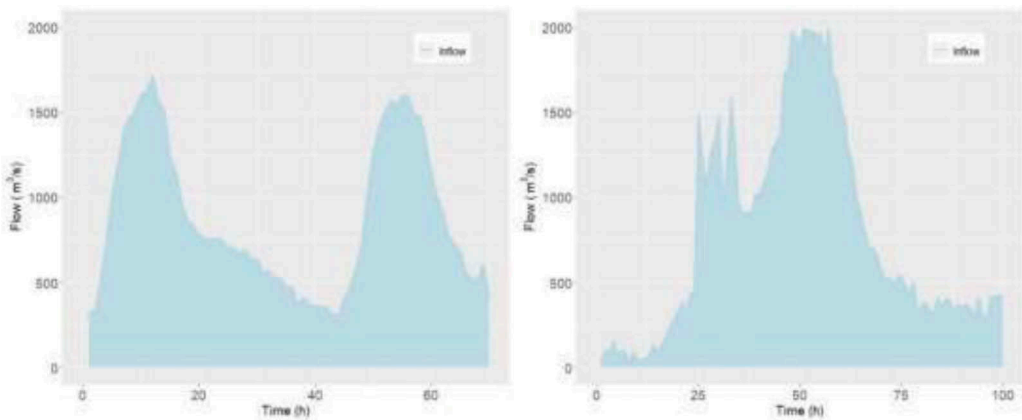


Figure 2. Evolution of inflows during the flood events of 2005 (left) and 2015 (right).

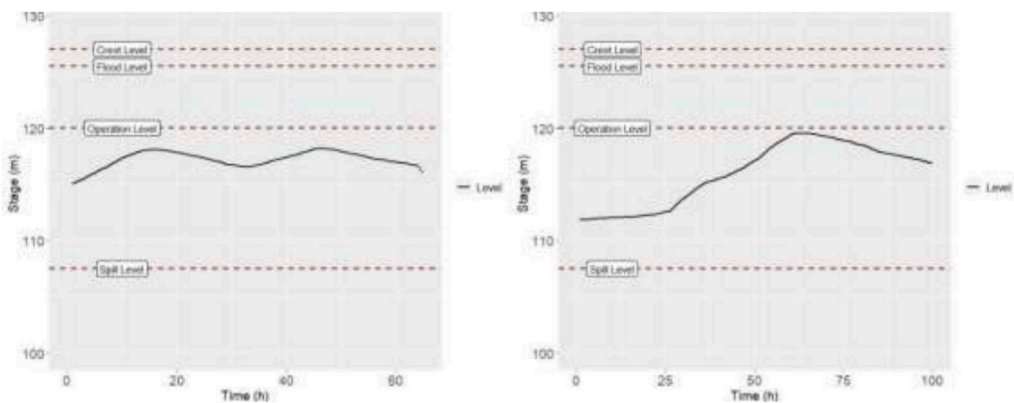


Figure 3. Evolution of reservoir level during the flood events of 2005 (left) and 2015 (right).

The first event lasted from 28/12/2005 to 1/1/2006, and initiated when the reservoir was at a quite high level of 115.5 m. As shown in Figure 3, left, the inflow hydrograph exhibited two almost equal peaks within a 40 hours interval. We remark that double peak floods are particularly difficult to handle, and rarely only accounted for in the design context (Gioia, 2016). The afternoon of 27/12/2005, by facing a sharp increase of the reservoir level by 20 cm per hour, the dam operators adopted a quite conservative policy. In particular, when the reservoir level reached +118 m, they partially opened the spillway gates to release 300 m³/s (800 m³/s in total, also considering other 500 m³/s from the turbines). Grace to this manipulation, they ensured the safety of the dam and its installations, besides the unexpected arrival of a subsequent, equally extreme, event (Leris, 2008). On the other hand, from a power production perspective, the adopted policy was clearly sub-optimal, as the estimated loss of energy was up to 7.5 GWh.

The second flood event lasted from 30/1/2015 to 2/2/2015 and produced an even higher flood peak (2050 m³/s) and flood volume, as well. Although the reservoir level at the beginning of the flood was quite lower than in 2005 (113.0 m, in contrast to 115.5 m), and although the operators opened the gates at the emergent level of +118.0 m, the flood eventually reached +119.5 m, thus close to the top of the gates.

3 METHODOLOGY

3.1 *Input data, governing equations and assumptions*

Let a hydroelectric reservoir, the spillway control system of which comprises n_G similar gates of height h_g , which are installed over an ogee-type crest, at elevation z_c . The reservoir's geometry is described through a power-type storage-elevation function, i.e.:

$$s = \kappa(z - z_0)^\lambda \quad (1)$$

where z is the reservoir level, z_0 is a datum level (e.g., minimum pool level or river bed elevation) and κ, λ are constants. On the other hand, the energy production is expressed as:

$$E = \psi r (z - z_p) \quad (2)$$

where r is the water release through the turbines (for convenience, we apply lowercase letters for water volumes and capital ones for fluxes), z_p is the power station level (penstock outlet), and is the so-called specific energy, which is defined as follows:

$$\psi = \rho g \eta h_n / (z - z_d) \quad (3)$$

where ρ is the water density (1000 kg/m³), g is the acceleration of gravity (9.81 m/s²), η is the electromechanical system's efficiency (overall efficiency across turbines, generators and transformers), and h_n is the net head, namely the available hydraulic energy at the turbines (i.e., gross head minus friction and minor losses across the conveyance system). In the generic case, ψ is a nonlinear function of head and discharge, but under some premise (e.g., turbine operation close to its nominal capacity) it can be handled as approximately constant. Its theoretical maximum is 0.2725 GWh/hm⁴, and refers to an ideal hydropower system of unit efficiency and zero hydraulic losses (Efstratiadis et al., 2021).

The discharge capacity, which depends on the gross head, $z - z_d$, and the properties of the conveyance system (length, diameter, roughness, etc.), can be also approximated as:

$$U = \alpha(z - z_d)^\beta \quad (4)$$

where α and β are constants.

Finally, by considering fully open gates, the discharge over the spillway crest is given by:

$$Q = c \sqrt{2g} L h^{3/2} \quad (5)$$

where g is the acceleration of gravity, c is a discharge coefficient, which accounts for energy losses, and depends on the ogee shape and the head, L is the effective length of the spillway crest, and h is the upstream energy head above the spillway crest. If the top of the ogee is at elevation z_s , the head is estimated by:

$$h = z - z_s + V^2/2g \quad (6)$$

where v is the flow velocity at the entrance section, which is function of q . The combination of (5) and (6), as well as the nonlinearity of term c , which is typically expressed by means of empirically-derived nomographs (US Bureau of Reclamation, 1987), results into to quite complex numerical problem. This can be significantly simplified by writing the theoretical formula (5) as:

$$Q = c^* \sqrt{2g} L (z - z_s)^\zeta \quad (7)$$

where c^* is an equivalent discharge coefficient, which may be assumed approximately constant, and ζ is a shape parameter that exceeds the theoretical value of $3/2$, thus allowing to omit from the head function (6) the kinetic energy term, $V^2/2g$. Under this premise, the discharge over the ogee is explicitly expressed as function of the actual level, z .

If the gates are partially only opened, the discharge calculations become even more complex. In order to facilitate computations, this case is not examined here.

3.2 Simulation model

We consider the reservoir operation during a flood event, which is represented by a sequence of given inflows i_t . If n is the length of simulation, the reservoir dynamics is described through the water balance equation, written in the discretized form:

$$s_t = s_{t-1} + i_t - r_t - w_t \quad (8)$$

where r_t are the controlled releases through the turbines, w_t are the spill losses, and s_t is the reservoir storage at the end of time step t (all quantities are given in volume terms).

Starting from a given initial level z_0 , which corresponds to a storage value, s_0 , through eq. (1), the estimation of the unknown outputs r_t and w_t can be explicitly employed, by expressing the turbine and spillway control policies by means of parametric operational rules.

In particular, the turbine control is associated with two different operational modes, hereafter referred to as *normal* and *emergent*, which are determined through two characteristic level thresholds, z_{e_0} and z_{e_c} . During the rise of the flood, if the pool level exceeds the first threshold, i.e., $z > z_{e_0}$, the system is set under emergent operation conditions, and thus the power station is forced to operate in its maximum capacity. In contrast, during the recession of the flood, when the level falls below the second threshold, thus $z < z_{e_c}$, the system returns to its normal operation.

Under normal conditions, the release policy follows a standard energy production schedule, by means of energy production targets, e_t^* , during the time period n . In the case of dams providing peak hydropower, target energy is set to zero, except for few hours per day. We highlight that the power production scheduling is independent of the flood control policy, since it is specified a priori, on the basis of the strategic management of the hydropower system. Hence, the targets e_t^* are inputs to simulation and not parameters to optimize, as made with thresholds, z_{e_0} and z_{e_c} .

Regarding the gate control, provided that the system comprises n_G gates, we introduce three thresholds, which are symbolized z_o^k , denoting a progressive opening of gates, and a generic threshold z_c for determining the closure of all gates. In particular, during the rising of the flood, each time the reservoir level exceeds the associated threshold z_o^k , the gates are appropriately manipulated to release a specific percentage, a_k , of the corresponding spillway capacity, which is estimated by the analytical formula (5) or its approximative expression (7). Under this premise, the outflow through the spillway at level z , where $z_o^k \geq z > z_o^{k+1}$, is given by:

$$w = a_k Q(z) \Delta t \quad (9)$$

We remark when the pool level exceeds the upper threshold $z_o^{n_G}$, all gates are opened, to allow operating the spillway at its full capacity, thus under free flow conditions ($a_{n_G} = 1$). Next, during the recession of the flood, when the pool level falls below, all gates are closed.

At the beginning of each time step, t , the model updates the reservoir level, z_t , thus determining whether the system is under normal or emergent conditions, and also estimates the turbine and spillway capacity, through eqs. (4) and (7), respectively. In the first case, all gates are closed, thus $w_t = 0$, while the water released through the turbines is adapted to fulfill the energy target, e_t^* , by applying eq. (2). If the system is under emergent conditions, the full capacity of turbines is used, and thus the water releases are set equal to $r_t = U \Delta t$, where Δt is the time interval of computations. Besides, and according to both the state of the flood (rising or falling) and the value of z_t with respect to associated thresholds, the model recognizes the state of the system, in order to employ the appropriate control of gates, namely progressive opening or closing.

3.3 Performance metrics

As already discussed, the flood control of hydroelectric reservoirs is subject to two conflicting criteria, namely safety and economy. The first one refers to two aspects, the safety of the dam, per se, and the safety of the floodplains downstream of the dam, which may be put in danger according to the intensity and duration of flows released through the spillway. The dam safety criterion is quantified by determining a set of characteristic elevation thresholds, and compute their distance from the maximum level reached during the flood event, as derived through the simulation model. These may include the dam crest elevation, the maximum flood level, as specified within the spillway design study, the top of the gates, etc. On the other hand, the floodplain safety criterion can be expressed in dimensionless terms, as the ratio of the maximum value of outflow to the discharge capacity of the spillway system.

Regarding the economy criterion, this also involves two aspects. The first is the deviation from the normal power generation scheduling, due to the operation of their turbines in their full capacity whenever the pool level exceeds the emergency threshold, z_{e_o} , thus the production of secondary instead of firm energy. The market value of secondary energy is lower than the firm one, which is some kind of long-term economic loss for the system. The unnecessary generation of surplus energy can be introduced within the economy metric by means of a small penalty term. Yet, the most important impact to its economic performance refers to the direct loss of water, and thus hydropower, due to the opening of gates. This quantity can be easily estimated, by computing the potential energy that would be produced by the overflowing water, i.e.:

$$E_{L,t} = \psi w_t (z_t - z_p) \quad (10)$$

In order to provide an overall performance measure that ensures good equilibrium among the various safety criteria as well as the two economy-related criteria, it is essential to assign suitable weighting coefficients to the corresponding distance and energy metrics. The derived metric can be next set as the objective function of a global optimization problem, as discussed hereafter.

3.4 Optimization

The extraction of generic flood management rules, which are efficient across different conditions, both in terms of safety and economy, imposes to configure the optimization problem in a scenario-based context. In this vein, we must use as inputs a number of inflow data sets, and seek for an overall optimal policy, which maximizes the average performance measure across all scenarios. Crucial modelling decisions involve: (a) the formulation of inflow scenarios, either based on observed flood events or synthetically generated, (b) the assignment of the initial condition of the system, i.e., the reservoir level at the beginning of the flood, and (c) the definition of the normal operation scheduling of turbines (e.g., activation during peak demand hours). In order to simulate the system under a wide range of potential states, the optimization problem should run for combined scenarios of inflows, initial levels and hydro-power production schedules.

An alternative option is to determine different rules according to the initial state of the system, which is an absolutely crucial input (cf. Gabriel-Martin *et al.*, 2019). In this respect, the optimized turbine and gate management are adapted to the reservoir level at the beginning of the flood event. Apparently, the higher is this level, the more conservative is expected to be the associate rule.

Regardless of the formulation of the objective function and the state scenarios, the underlying optimization problem comprises a set of parameters, i.e.: (a) the two turbine control thresholds, z_{e_o} and z_{e_s} , (b) the n_G gate opening thresholds, z_o^k , (c) the $n_G - 1$ spillway capacity ratios, a_k (we remind that at threshold, $z_o^{n_G}$, this ratio is by definition unit), and (d) the closing threshold for all gates, z_c . In this vein, the total number of parameters to optimize is $2(n_G + 1)$.

For convenience, the turbine operation in their full capacity is employed by priority with respect to gate opening, while the upper threshold $z_o^{n_G}$ cannot exceed the top level of the gates. Therefore, the level thresholds are forced to satisfy the sequence $z_{e_o} < z_o^1 < \dots < z_o^{n_G} < z_c + h_g$ and $z_o^{n_G} > z_c > z_{e_s}$, while for the flow ratios we set $a_1 < \dots < a_{n_G-1} < 1$.

4 CASE STUDY

4.1 Problem setup

The proposed framework is applied to determine an optimal flood control policy of Arachthos dam. In this context, we run the optimization problem against four characteristic synthetic input hydrographs that correspond to return periods of 5, 10, 50 and 100 years (Figure 5). The data were retrieved from the flood engineering study by Koutsoyiannis *et al.* (2010), also involving: (a) the derivation of areal intensity-duration-frequency (also referred to as ombrian) curves over the upstream catchment, based on a comprehensive statistical analysis of observed rainfall maxima, (b) the construction of 48-hours design storm events for the aforementioned return periods, by applying the worst profile approach, and (c) the implementation of the NRCS-CN method to transform rainfall to flood runoff, (d) the routing of the derived runoff of the upstream area to the dam site, through the unit hydrograph theory, and (e) the addition of a constant baseflow, which is also considered as increasing function of return period.

The power plant scheduling imposes to release a constant discharge equal to nominal capacity of turbines (500 m³/s), during peak electricity demand hours. Two time-blocks are considered, i.e., from 8:00 to 12:00 am and from 18:00 pm to 22:00 pm. Following the rationale of section 3.4, we formulate a large number of scenarios, by means of randomly selected input hydrographs with random time arrivals, and under random initial level values. We remark that the assignment of random time arrivals becomes essential, since the power production policy refers to specific intraday periods. Regarding initial levels, these range from the ogee crest elevation (+107.5 m) up to +118.0 m, which is the alarm stage imposed by the operator of the dam (see section 2.2).

The formulation of the optimization problem follows the principles of section 3.4. Since the dam is equipped with three gates ($n_G = 3$), the number of control variables to optimize is 8.

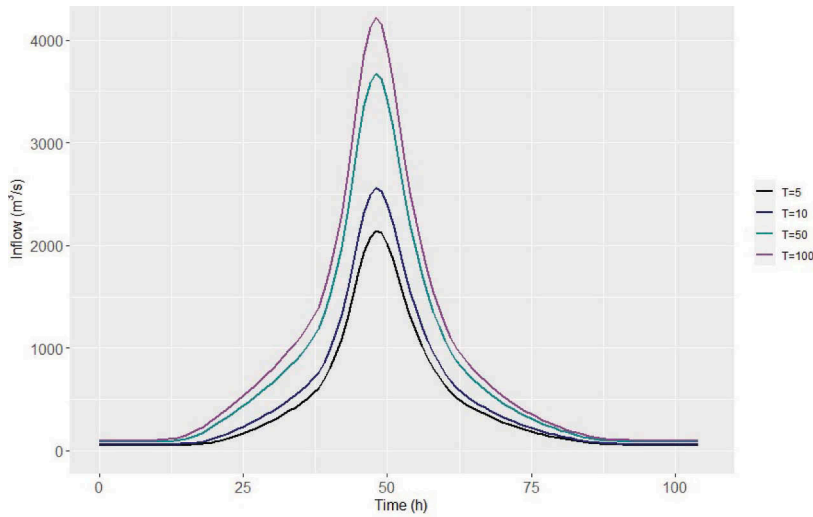


Figure 4. Input hydrographs for four characteristic return periods ($T = 5, 10, 50$ and 100 years).

4.2 Optimized flood management policy

The optimized management policy of the major flood control components of the dam (turbines and spillway gates) is expressed in terms of six characteristic level thresholds and two ratios, i.e.:

- If the reservoir level exceeds $z_{e_0} = 117.84$ m, the turbines are forced to operate in the maximum capacity, thus releasing $500 \text{ m}^3/\text{s}$ in continuous time, while at the same elevation threshold ($z_o^1 = z_{e_0}$) the gates are manipulated to release $a_1 = 3.3\%$ of the associated discharge capacity of the spillway system.
- If the level further rises up to $z_o^2 = 118.45$ m, the outflow ratio through the spillway increases to $a_2 = 17.7\%$.
- The three gates are fully opened, thus establishing free flow conditions through the spillway, at level $z_o^3 = 119.20$ m.
- Provided that the evolution of the flood event is clearly under recession, the three gates are closed when the level falls lower than $z_c = 117.65$ m.
- The power generation system returns to its normal operational policy when the level is further decreased to $z_{e_c} = 116.70$ m.

We remark that the activation level of $+117.84$ m is very close to the legal threshold of 118.0 m, which has been empirically established by the PCC. Yet, at this threshold the dam operator is forced to open all gates to operate the spillway in its full capacity, while our rule only considers a quite limited water release through the spillway, in order to save energy.

4.3 Evaluation of optimized rules with respect to historical flood events

In order to evaluate the optimized management policy in practice, and contrast it with the real-time manipulations by the dam operator in the field, we reconstruct the inflow events of 2005 and 2015 (section 2.3) and run the associated simulation model, by starting from the same initial level. The theoretical evolution of the reservoir stage compared to the real evolution as demonstrated in Figure 4. Summary information is also provided in Table 1.

This analysis further reveals the effectiveness and efficiency of the proposed policy. This allowed to release less water from the spillway, thus retaining significantly larger amounts of potential energy in the reservoir, and also causing less severe damages downstream. Focusing to the more severe event of 2015, our rules would result to a slightly higher maximum stage, while the risk of dam overtopping would remain negligible.

Table 1. Actual vs. simulated data by considering the flood events of 2005 and 2015.

	Flood 2005	Flood 2015
Pool level at the beginning of the flood (m)	115.06	111.83
Maximum observed inflow (m ³ /s)	1712	2095
Maximum observed level (m)	116.79	119.55
Maximum simulated level (m)	118.21	119.66
Actual loss of energy (GWh)	12.0	6.4
Theoretical loss of energy (GWh)	3.3	1.0

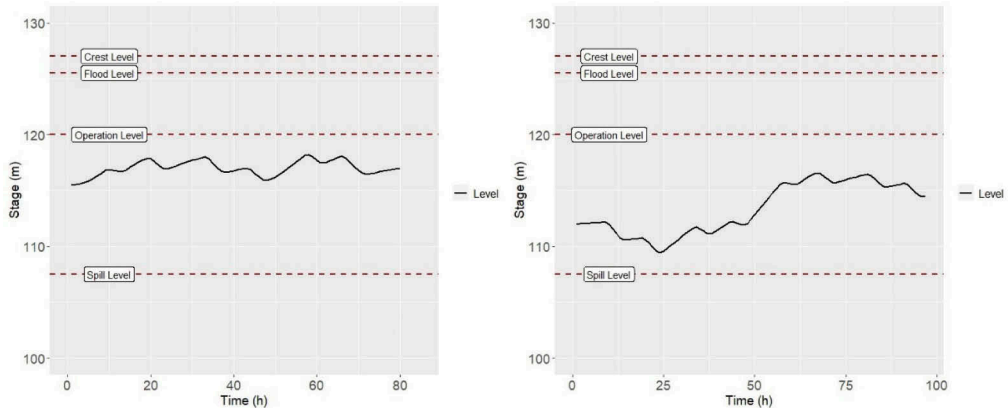


Figure 5. Simulated evolution of reservoir level, driven by the inflow hydrographs of 2005 (left) and 2015 (right), and by applying the optimized flood control policy.

5 CONCLUSIONS

The optimal operation of hydroelectric dams that are equipped with gated spillways, during severe flood events, is a challenging problem, which is subject to the highly conflicting criteria of economy and safety. In this vein, we developed a generic simulation-optimization method that allows for establishing simple yet effective rules, for the conjunctive control of turbines and gates.

The control rules are expressed in terms of a small number of level thresholds and discharge capacity ratios. In order to ensure generality, the methodology is tailored in a scenario-based context, namely by formalizing a global optimization problem driven with a wide spectrum of potential states of the system, i.e., inflow hydrographs, arriving at random time stamps, and under varying pool level conditions. This accounts for the multiple aspects of the real-world management problem, namely the safety of the dam per se, and the downstream areas, as well, and the potential loss of energy due to water release through the spillway.

The effectiveness of the proposed context has been demonstrated in the case of Pournari dam, which is the most crucial of the country, in terms of flood risk awareness. Fruitful conclusions were obtained by contrasting the derived policy with its real-time implementation during the two most severe events of the time life of the dam so far. In fact, this would save quite large amounts of energy, also being marginally only riskier.

In terms of practical implementation, a strong advantage of the proposed operational policy is its simplicity. Actually, the sole external information to the dam staff is the reservoir stage, which is an easily measured quantity that can be manually retrieved through conventional instruments.

Potential improvements are twofold. First, the optimization may run with a large number of stochastically-generated flood events instead of few deterministically-derived hydrographs corresponding to specific return periods. We remark that the common engineering practice for producing “design” floods results to hydrographs of specific bell-type shape, as shown in Figure 5, while in reality a hydrograph shape is irregular (cf. Figure 3). This will make the method much more generic, since the less the number of scenarios examined and the more specific is the hydrograph shape, the more dependent are the optimized rules to the model inputs.

Second, the information provided to the dam operator could be substantially enhanced by also accounting for real-time monitoring data over the upstream river basin, as well as short-term hydrometeorological forecasting products (provided that the time response of the basin is large enough to take advantage of such information). This will allow to adapt the operational policy to the running conditions, thus ensuring an even better equilibrium between economy and safety.

ACKNOWLEDGMENTS

The authors would like to reveal their appreciation and gratitude to the respected reviewers and handling editors for their constructive comments.

REFERENCES

- Ahmed, E. S. M. S., & Mays, L. W. 2013. Model for determining real-time optimal dam releases during flooding conditions. *Natural Hazards* 65(3): 1849–1861.
- Albo-Salih, H., & Mays, L. 2021. Testing of an optimization-simulation model for real-time flood operation of river-reservoir systems. *Water* 13(9): 1207.
- Amirkhani, M., Bozorg-Haddad, O., Azarnivand, A., & Loáiciga, H. A. 2017. Multiobjective optimal operation of gated spillways. *Journal of Irrigation and Drainage Engineering* 143(2).
- Bagis, A., & Karaboga, D. 2004. Artificial neural networks and fuzzy logic based control of spillway gates of dams. *Hydrological Processes* 18(13): 2485–2501.
- Bianucci, P., Sordo-Ward, Á., Moralo, J., & Garrote, L. 2015. Probabilistic-multiobjective comparison of user-defined operating rules. Case study: Hydropower dam in Spain. *Water* 7(3): 956–974.
- Chou, F. N. F., & Wu, C. W. 2015. Stage-wise optimizing operating rules for flood control in a multi-purpose reservoir. *Journal of Hydrology* 521: 245–260.
- Efstratiadis, A., Tsoukalas, I., & Koutsoyiannis, D. 2021. Generalized storage-reliability-yield framework for hydroelectric reservoirs. *Hydrological Sciences Journal* 66(4): 580–599.
- Feng, M., & Liu, P. 2014. Spillways scheduling for flood control of Three Gorges reservoir using mixed integer linear programming model. *Mathematical Problems in Engineering* 921767.
- Gabriel-Martin, I., Sordo-Ward, A., Garrote, L., & Granados, I. 2019. Hydrological risk analysis of dams: The influence of initial reservoir level conditions. *Water* 11(3): 461.
- Gioia, A. 2016. Reservoir routing on double-peak design flood. *Water* 8(12): 553.
- Girón, F. 1988. The evacuation of floods during the operation of reservoirs. *Transactions Sixteenth International Congress on Large Dams* 75(4): 1261–1283. ICOLD. San Francisco, CA, USA.
- Jordan, F. M., Boillat, J. L., & Schleiss, A. J. 2012. Optimization of the flood protection effect of a hydropower multi-reservoir system. *International Journal of River Basin Management* 10(1): 65–72.
- Karaboga, D., Bagis, A., & Haktanir, T. 2008. Controlling spillway gates of dams by using fuzzy logic controller with optimum rule number. *Applied Software Computing Journal* 8(1): 232–238.
- Koutsoyiannis, D., Markonis, Y., Koukouvinos, A., & Mamassis, N. 2010. Hydrological study of Arachthos floods. *Delineation of the Arachthos river bed in the town of Arta*, ADK Consulting Engineers, YDROTEK, V. Mouzos, 272 p. (<https://www.itia.ntua.gr/950/>).
- Leris, G. 2008. Dealing with floods of PPC’s dams on Acheloos, Arachthos and Nestos river. *First Hellenic Conference on Large Dams*, Larisa, Hellenic Commission on Large Dams, Technical Chamber of Greece. (<http://portal.tee.gr/portal/page/portal/teelar/EKDILWSEIS/damConference/eisigiseis/8.1.pdf>)
- Liu, X., Chen, L., Zhu, Y., Singh, V. P., Qu, G., & Guo, X. 2017. Multi-objective reservoir operation during flood season considering spillway optimization. *Journal of Hydrology* 552: 554–563.
- Malekmohammadi, B., Zahraie, B., & Kerachian, R. 2010. A real-time operation optimization model for flood management in river-reservoir systems. *Natural Hazards* 53(3): 459–482.

- Nematzadeh, R., & Hassanzadeh, Y. 2021. A novel method to plan short-term operation rule for gated spillways during flood. *Arabian Journal of Geosciences* 14: 2812.
- Roilos, C. 2018. Dealing with flood events at hydroelectric plant areas in Western Greece. ALTER Project Meeting (<https://alter-project.eu/trainings/>).
- Salehi, F., Najarchi, M., Najafizadeh, M. M., & Hezaveh, M. M. 2022. Multistage models for flood control by gated spillway: Application to Karkheh dam. *Water* 14(5): 709.
- Sordo-Ward, A., Gabriel-Martin, I., Bianucci, P., & Garrote, L. 2017. A parametric flood control method for dams with gate-controlled spillways. *Water* 9(4): 237.
- Soriano, E., Petroselli, A., de Luca, D. L., Apollonio, C., Grimaldi, S., & Mediero, L. (n.d.). Assessment of the impact of climate change on hydrological safety of dams with gated spillways. Proceedings of the 39th IAHR World Congress, 19–24 June 2022, Granada, Spain.
- US Bureau of Reclamation 1987. *Design of Small Dams*. U.S. Dept. of the Interior, Washington, DC.
- Wagner, B., Hauer, C., & Habersack, H. 2019. Current hydropower developments in Europe. *Current Opinion in Environmental Sustainability* 37: 41–49. Elsevier.
- Zargar, M., Samani, H. M. V., & Hghighi, A. 2016. Optimization of gated spillways operation for flood risk management in multi-reservoir systems. *Natural Hazards* 82: 299–320.

Blasting excavation close to fresh Roller Compacted Concrete, in RCC Dam construction sites

P. Ruffato

Civil Engineer, Webuild, Milano, Italy

R. Folchi

Nitrex Srl, Lonato, Brascia, Italy

ABSTRACT: RCC dam construction is a long process which takes years to be completed, and requires precise planning and a tight sequence of activities. Due to planning constraints, RCC placement is to start before the completion of the dam foundation blasting excavation. The purpose of this paper is to demonstrate the possibility to perform blast excavation while in the same foundation area RCC is under placing at a distance in the order of 50m or less to the blasting, and compacted by vibrating rollers. The vibrations generated by rollers at different levels into the RCC were measured and compared with vibrations generated by the nearby excavations executed with explosive. It is assumed that controlled blasting excavation is safe in the vicinity of fresh RCC, if the induced vibrations are in the same order as those generated by rollers during the compaction operations. Laboratory tests on fresh RCC that sensed the reduced vibrations compared to those on RCC that did not, confirm that its material properties are not affected by the controlled blasting. The outcome of this work and added value on an RCC dam construction lies in allowing the excavation of a part of the dam foundations to be completed while RCC concrete placement is already in progress in the other part of the foundation.

1 INTRODUCTION

The excavation of a dam foundation is a long process which is usually performed by drilling and blasting method. Tight time constraints compel the contractor to perform more activities at the same time and to start concrete or roller compacted concrete (RCC) placement before excavation of the foundation is completed.

The present article is inspired by the works performed in a dam excavation in Indochina.

Blasting forms vibration waves (see Figure 2) that can damage and even stop the hardening of RCC (see Figure 1). An RCC dam is a monolithic barrier provided that all the layers are adequately connected to one another and above all to the Dam foundation rock. This study investigates a procedure to start the RCC placement while excavation by explosive still continues without producing dangerous vibrations into the fresh RCC.

The guideline of this paper will be to analyze the situations that are usually tolerated by Projects Specifications, namely the vibrations produced into the RCC during normal construction activities by operating machines (especially vibrating compactors). As long as the blasting vibrations are below the level generated by the compacting rollers on the fresh and recently placed RCC, the excavation works will not be a cause for concern for the RCC performance.

Symbols and terminology

PPVo = accepted limit of vibrations on RCC

PPV_b = vibration induced by the blasting for excavation
PPV_r = vibration induced by the vibrating roller
BL.0 = quantity of explosive giving the level of vibrations PPV_o
n.del.0 = number of delays applied to a blasting, giving the level of vibrations PPV_o
n.blast = n.del.0 = number of single blasting (one per delay), required for the desired rock excavation

2 USE OF RCC IN DAM CONSTRUCTION

In massive dam construction, RCC may be preferable to rock-fill or earth-fill dams due to the following reasons:

- A considerably smaller volume is required;
- The exploitation of the rock source is reduced and causes a lower environmental impact, as a result of a lower total volume of required aggregates;
- The dam face protection is faster and cheaper using the grout enriched RCC (GERCC) technology;
- The execution time is shorter due to reduced volume, to the tested GERCC execution system and to the RCC industrialized process of execution.

2.1 *Dam foundations and RCC placement*

With the exception of some structures with earth-fill big body, almost all dams are based on competent solid rock; consequently foundations must be excavated by explosive, with a constrained and short excavation schedule. The phases of the foundation construction are the following:

1. First side dam foundation excavated with explosive and no constraints (no RCC being placed)
2. Concrete levelling and RCC placement in the first side, while the foundation is excavated with blasting in the other side.
3. The second side blasting excavation is completed while RCC continues in the first side abutment.
4. RCC placement proceeds in the first abutment and starts in the second side as well.

This article focuses on the blasting excavation during phases 2, 3, as was done during RCC placement in a dam Project in Indochina in the years 2018-2019, which had never been done before in any other RCC dam Project.

With reference to blasting dam excavation (see Section 5) and blasting monitoring (Sections 2.3 and 3), the accepted limit of vibrations on RCC (PPV_o) must be defined. Never was the blasting executed near fresh RCC structures before the case described in this paper, hence no reference limit was available. Nevertheless, on the strength of laboratory experience about the effects of vibrations on concrete, such a limit is supposed to be PPV_o=15 to 20mm/s.

RCC is placed on the Dam body and remains in “hot” status (i.e. no physical connection RCC-rock foundation or RCC-RCC has been established yet) until the setting time begins, which occurs around 8 to 11 hours after mixing.

At the setting time, the “warm” status starts. RCC creates and consolidates its internal physical links to other RCC particles and to the rock foundation, via chemical reaction of the cement and fly-ash (images 2 and 3 in Figure 1).

The good connection between RCC and foundation rock (and also RCC layer N to layer N+1), makes the dam body monolithic with the foundation, therefore no water penetrates under the dam (also thanks to the curtain grouting) and the stability of the dam is granted.

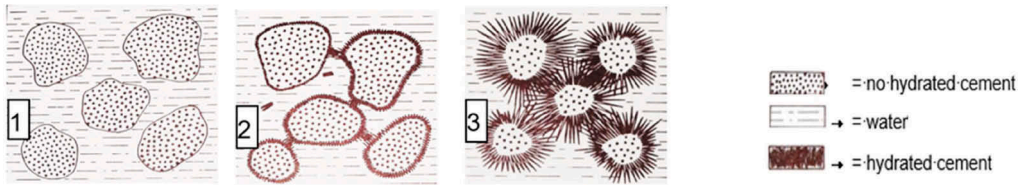


Figure 1. Bonds formation during curing.

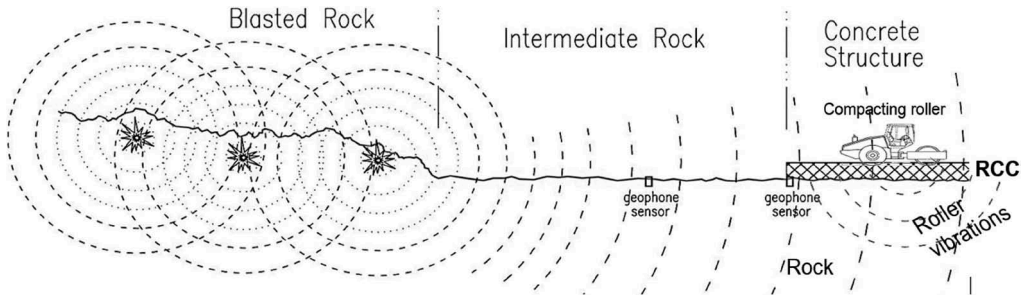


Figure 2. Blasting vibration propagation.

If forces or excessive vibrations disturb the RCC in this status of vulnerability, the needles (see images 2, 3 in Figure 1) are broken and link creation is interrupted, so needle links are lost.

In the case study, the blast vibrations are so low and imperceptible to the rock and RCC that the links under creation in warm status (vulnerable status) do not break and the controlled blasting and the RCC placement may continue in parallel (see Figure 2 above).

RCC (in “hot”, “warm” or other status) perceives the vibrations created by the equipment working in the dam (tippers for transport, dozers for spreading, rollers for RCC compaction, etc. . .)

The first factor used to determine the maximum vibration (damage criteria) that the “warm” status can tolerate without breaking the links as described above is the vibration given by the action of the compacting roller (see Figure 2) which is accepted as a normal operation on the RCC.

2.2 Assumed damage criteria vibration limit

The blasting vibration limit PPV_b must be compared to the vibrations induced by the vibrating roller (PPV_r). PPV_b must be not greater than PPV_r and both PPV_b and PPV_r must be not greater than PPV_o.

In lack of specific reference from international norms or from previous works, the following was assumed:

- A 30m safety belt must be kept from the blasted area to the freshly-placed RCC, in order to avoid the creation of cracks in the RCC-rock interface and RCC layer to layer, and to avoid the extension of pre-existing cracks in the foundation rock where levelling is already placed.
- A safe top limit of Peak Particle Velocity (PPV) must be kept in the green RCC, at the limit of the safety belt. The assumed limit in green RCC was PPV=PPV_o, as fixed in Section 2.1 above.

In order to define the damage criteria (see Sections 3 and 4), tests were executed on a real RCC dam scale mock up, far from the dam (out of the excavation blasting effect) on a similar foundation rock (see Section 3), with placing procedures and equipment equal to the RCC

activity on site, instrumented with geophones at rock-concrete interface and in the RCC layers interfaces (see Figure 4 and 5). In the mock up, vibrations are induced into the RCC by:

1. RCC operation. Vibrations induced by a 12 tons roller (equal to the real case, see PPVr at page 2) with layers of fresh concrete placed one above the other in sequence (as in the dam), therefore with every new layer placed above a “warm” joint.
2. Blasting detonating cord (see Figure 4 scheme, 1st and 2nd shot line) to simulate the real case of dam blast excavation on site close to the RCC.

Induced vibrations were analyzed and decay curve computed to quantify the PPV in spots other than that of the transducers position. This gave evidence of vibration induced in the rock bed and in the body of the dam throughout the RCC placement stages and at various distances from the source. Concrete samples were cored before (sample s.1) and after (sample s.2) firing the trial blasting (1st and 2nd shot line).

The uniaxial crushing tests on samples cored in the RCC which received the blasting waves (s.2) and in the RCC which did not (s.1), prove that these vibrations reduced neither adhesion or mechanical connection between layers at foundation level, nor concrete resistance (see Table 3). Based on this, PPV₀ was assumed as threshold for safe vibrations induced into the RCC.

Damage criteria were approved by the client and implemented in the construction method, therefore controlled blasting on one bank continued while RCC was placed at the other bank (30m far and more).

2.3 Blasting vibrations

Pressure waves propagation (Figure 3 and Figure 4) generates vibrations in the blasted rock, including the concrete structures in direct contact with it.

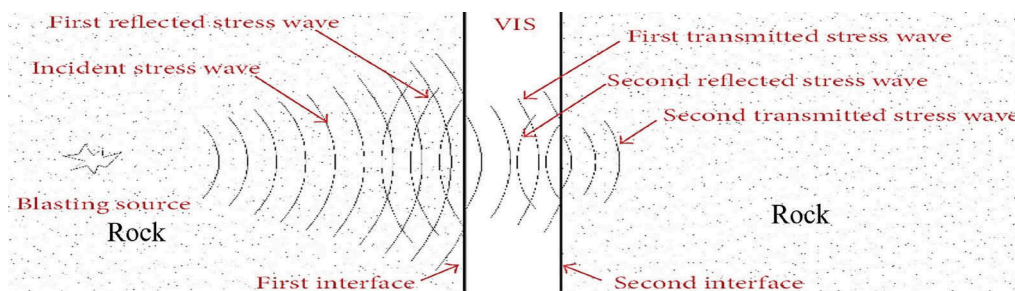


Figure 3. Blasting vibration propagation at interfaces.

Vibrations may have effects on the RCC or on the link between RCC and foundation rock. Coring of the contact RCC/foundation rock, allow to check the quality and integrity of the RCC/rock bonding and continuity. The coring of the RCC-Rock foundation interface before (see A in Table 3) and after (see B in Table 3), the controlled blasting in the RCC trial embankment (Table 3), and laboratory tests on the cores, revealed that blasting vibrations under the limit mentioned in Section 2.2, did not induce any damage in the RCC or in the RCC-Rock interface.

3 BLASTING TEST ON RCC SAMPLE

The RCC test area is located close to the quarry, based on a rock platform of lithological characteristics similar to the dam foundation and is approximately 10m x 5m in size. The first blast line is located 3m far and half meter more is the second line, in the same direction (see Figure 4).

Two sensors are located at level 0, simulating the RCC-Rock connection (TVT1, TVT3) and a third one is at level 1 (TVT2), simulating the RCC-RCC connection.

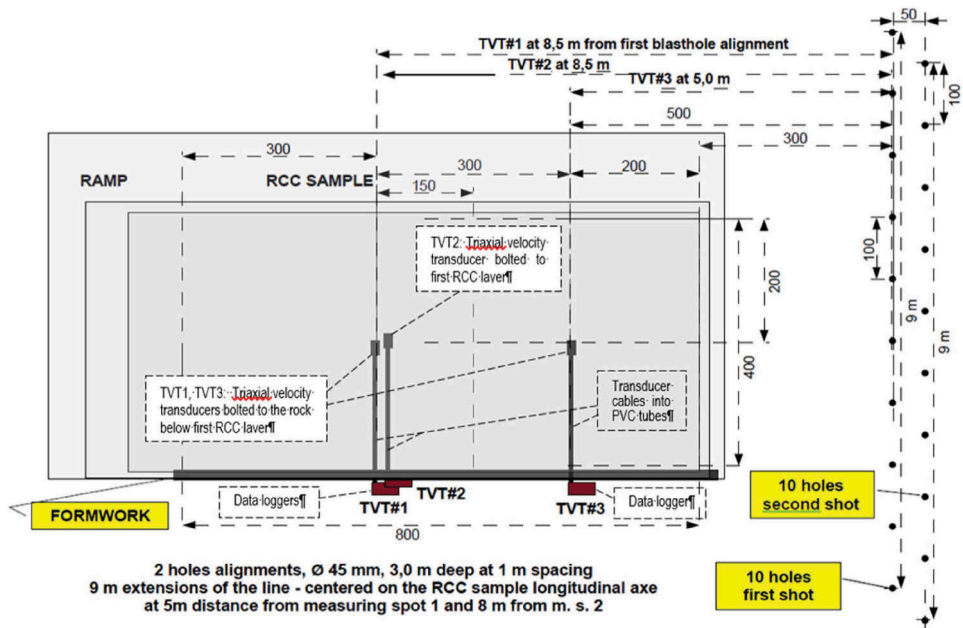


Figure 4. Vibration monitoring set up and blasting holes.

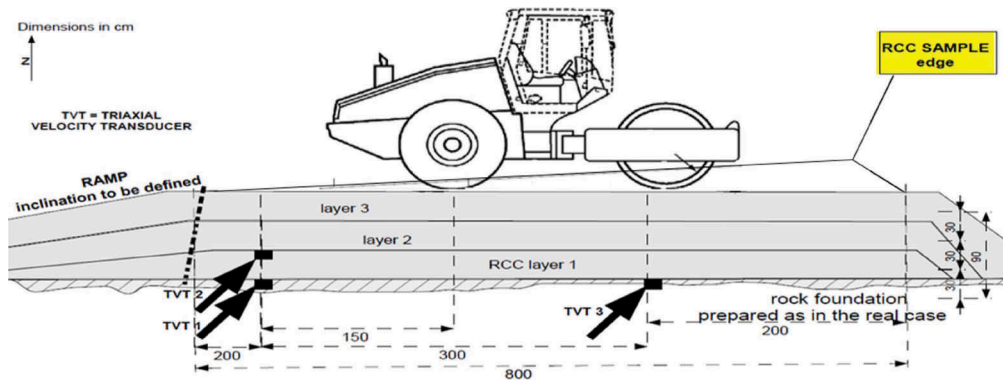


Figure 5. Embankment layers under roller and sensors positions.

3.1 RCC dam sample structure and construction sequence

The purpose of the full scale trial executed far from the dam area (see Table 1) was:

- To define the blasting criteria to excavate a Dam bank as the RCC is placed on the other bank.
- To measure the roller compactor vibrations and the blast induced vibrations.
- To measure the strength of RCC affected by the blast induced vibrations and of the same RCC before blasting, to define the damage criteria as per Section 2.2 above.

The measurements defined above focus on:

- amplitudes, frequencies and situations close to the vibration limit PPV_o defined in 2.2;
- ultimate resistance of concrete in the mentioned situations;
- RCC DAM rock foundation boundary effects and adhesion

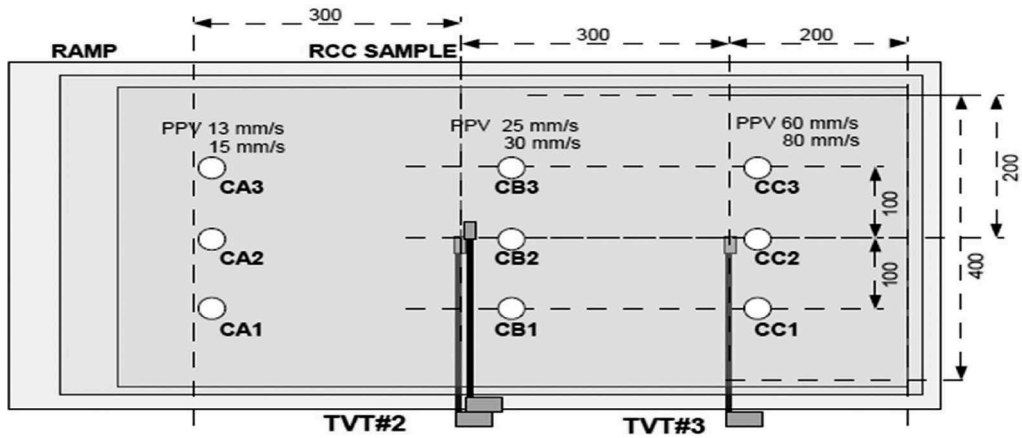


Figure 6. Core samples position in Trial embankment.

Table 1. RCC trial embankment test planning.

Date	time	activity description
14-nov-18		test platform area preparation + sensor placement
15-nov-18		drilling for test charge placement in lines A and B
16-nov-18		RCC placement start and test organization
16-nov-18	12:00 PM	concrete levelling and GERCC
16-nov-18	4:00 PM	RCC 1st layer placement
16-nov-18	7:00 PM	RCC 2nd layer placement
16-nov-18	10:00 PM	RCC 3rd layer placement
17-nov-18	8:00 AM	blasting the second shot line (10 holes) test data recording
17-nov-18	8:55 AM	blasting the first shot line (10 holes) test data recording

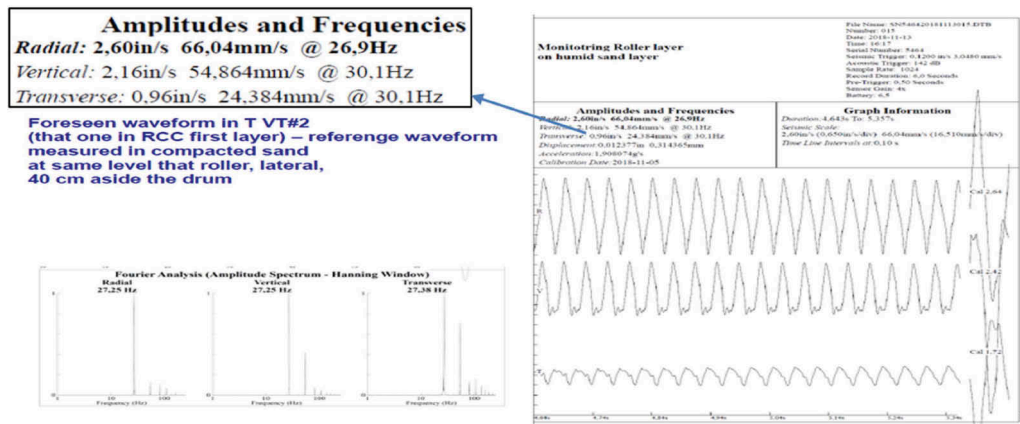


Figure 7. RCC Trial embank. 2nd layer placement, PPV produced by roller and induced in RCC (1hr after end of first layer).

ROLLER: RCC layers are compacted by the 12t roller to 30cm thickness. The vibrations read in TVT#2 (layer1-layer2) are 50mm/s with roller passing on layer2, and 20mm/s with roller passing on layer3.

Vibration Report

Event Name: V4AJ058024-111718-080317
 Recording Date: 17-11-2018 Recording Time: 08:03:17

Project Information
 Project: Company name – Project name
 Operator: Operator name
 Monitoring Location: RCC Blasting Control
 Blast Location: Quarry
Total charge (Kg): Rock Volume (m³):
 Powder Factor: Blast to sensor distance (m): 5m

Peak Measurements			
	Vertical	Transverse	Radial
PPV (mm/s)	11.635	4.416	15.527
Freq. (Hz)	85.3	170.7	102.4
Time (ms)	22	16	17
PPA (g)	0.64	0.48	1.02
PPD (mm)	0.02171	0.00412	0.02413
PVS (mm/s)	16.157 @ 17.6ms		
PSPL (PA)	8.25 (112.307 dB)@18.6ms		
PSPL Freq	2Hz		
Sensor Test	Passed	Passed	Passed

Figure 8. RCC Trail embank. 1st detonating cord blasting – order of magnitude of PPV (see Figure 5 for position of detonating cord position in RCC test block.

Table 2. Roller vibrations reading.

Roller on RCC layer n.	PPV vibration reading (mm/s)		
	TVT#1	TVT#2	TVT#3
1	15		15
2	5	50	5
3	3	20	3

BLASTING: 10 to 11 hours after the RCC placement, 1st and 2nd shot holes lines are blasted (Figure 4) as a controlled blasting performed by detonating cord. Vibrations read by the transducers are:

Vibration produced by roller passage on the RCC layers: 50mm/s

Vibration produced by controlled blasting on the RCC embankment: 15.53mm/s (see Figure 8)

Vibration produced by controlled blasting on Site RCC: 10.1mm/s - 17.56mm/s (see Figure 9)

3.2 Resistance parameters of the RCC being impacted by vibration

Coring of the contact RCC-rock were performed to check the quality/integrity of the rock bonding and continuity. Coring of RCC to check the strength of material as indicated in Table 3. Strength tests were performed on the corings, on RCC before the controlled blasting (test 0) at 7, 28, 90, 180 days, and on RCC after the controlled blasting (affected by relevant vibrations - test 1) at 28 and 90 days.

4 ADDITIONAL CONSIDERATIONS ABOUT THE ANALYSIS

Bearing in mind that construction operations must produce no dangerous vibrations, the damage criteria refer to the relevant PPV induced. A prudent analytical approach is recommended because;

- The approach has low statistical accuracy in the correlations owing to few recorded data.
- Accuracy in assessing thickness of the layers is low.
- The geometry of the model minimizes boundary effects but does not describe the physical phenomena in the field with sufficient precision.

We considered the PPV measured on site (see Figure 10a) or even 150% of it (17.5mm/s x 1.5), hence 26 mm/s for blast induced vibration. Thus the PPV during the controlled blasting in the real model (Figure 7- 80mm/s) has a safety factor of 3 in vibration amplitude (80/26 ≈ 3) and of 16 in distance of occurrence on the 0.9 m (= 14/0.9), with 14 m the distance at which a PPV of 26 mm/s from Roller would be sensed, considering the decay curve of PPV [mm/s] (77 x R [m]^{0.40}).

As a reference, considering the (Kolsky 1963) formula ($\sigma_p = \rho * C_p * PPV$), a conservative density of 2.4 t/m³ and velocity of compression waves in the range of 3.80 mm/s are expected.

Additionally, a stress of 0,24 MPa (2.4 t/m³/9.81 m/s² x 3,500 m/s x 24 mm/s x 10⁻³) associated to the 26 mm/s PPV should be expected and as well as 7 microstrain: (((26 mm/s x 10⁻³)/3800 m/s) x 10⁶).

A continuous seismic monitoring on the RCC DAM under construction will give evidence that the above given PPV safe limit is not exceeded. Considering the doubling of the PPV at interface Rock/RCC, for the first layer placements, when the seismic monitoring has to be executed in the rock at the foot of the half dam, a safety PPV of 13 mm/s should be considered in the blasting pattern design.

5 BLASTING AND RCC EXECUTION ON SITE

The RCC structure and physical properties are not negatively affected by the vibrations if those are not greater than the vibrations transmitted by the action of the compacting vibrating roller (PPV_r) and not greater than the assumed RCC damage criteria (PPV_o).

The mentioned value (Section 2.2) is a maximum limit, assumed with a sufficient degree of safety (with reference to the vulnerability defined in Section 2.1). The vibration target value has been therefore assumed to be around 80% of PPV_o = 8-12mm/s (in order to be sure to respect the limit PPV_o = 10-15mm/s).

The damage criteria could be fine-tuned, and less conservative values could be adopted in the future.

5.1 *Level of vibrations expected in the RCC foundation area.*

A blast trial should be performed in an area close to the dam foundation, on a similar foundation material, before starting the RCC placement, in order to verify the level of the vibrations produced at a distance D by a blasting expected to be performed for the excavation after the first RCC placement. The trial should make it possible to calibrate the blasting (BL.0) and the number of delays (n.del.0), in order to induce at the distance D a level of vibrations not greater than PPV_o.

Should it be difficult to reduce vibrations under PPV_o, even with many delays, the total quantity of explosive and total volume of blast rock should be reduced (by keeping the same blasting factor) until PPV_o is achieved.

The number of delays required for the blasting is equal to the total quantity of explosive for the excavation, divided by the Maximum Weight of explosive per delay. If the further blasting in the excavation area is managed in this way, the maximum expected vibrations will be under PPV_o.

In the example in Figure 10, the specific charge is the average 0.3 kg/c.m., total explosive quantity is BL.0=640kg and delays used are n.del.0=20, therefore the charge blast at a single moment is 640kg/20 = 32kg (18kg emulsion + 14kg ANFO). This can be reduced by limiting the total volume of rock blast. If necessary, it is possible to perform two blasts, one a few minutes after the other, halving the rock volume and the quantity of explosive in the two blasts, in order to make two detonations with the same global result as the one single total blast.

In the two detonations, 16kg of explosive (9kg emulsion + 7kg ANFO) would be blasted at a single moment multiplied by 20 moments (thanks to the N=20 delays). Impact of vibrations on the existing RCC would be in this way under control as per any requirement.

5.2 *Control of the blasting effects in the RCC on site*

At the moment of placement of the RCC in the dam foundation, a RCC trial embankment should be executed in an area out of the reach of the blasting waves and on similar foundation

Vibration Report

EventName: V22B275528-102018-122150
 Recording Time: 12:21:50
 Recording Date: 10-20-18
 Project: C
 Operator:
 Monitor Location: Right Bank EL 134
 Blast Location: Main RCC Dam Right Abutment EL 137-134
 Total Charge(kg): 640
 Rock Volume(cu.m): 2120
 Powder Factor: 0.3
 Blast to Sensor Distance: 30



	Peak Measurements		
	Vertical	Transverse	Radial
PPV (mm/s)	13.804	17.559	12.590
Freq. (Hz)	21.3	20.5	26.9
Time (ms)	84	185	88
PPA (g)	0.19	0.23	0.22
PPD (mm)	0.10314	0.13632	0.07449
PVS (mm/s)	19.622 @ 185.5ms		
PSPL (PA)	201.57 (140.070 dB)@105.5ms		
PSPL Freq	4.3Hz		
Sensor Test	Passed	Passed	Passed

EventName: V4AJ058024-102218-122938
 Recording Time: 12:29:38
 Recording Date: 10-22-18
 Project: C
 Operator:
 Monitor Location: Right Bank EL 134
 Blast Location: Main RCC DAM Right Abutment EL 134-131
 Total Charge(kg.): 480
 Rock Volume(cu.m.): 1650
 Powder Factor: 0.3
 Blast to Sensor Distance(m.): 30

	Peak Measurements		
	Vertical	Transverse	Radial
PPV (mm/s)	6.324	3.725	10.133
Freq. (Hz)	13.5	14.2	10.4
Time (ms)	325	295	343
PPA (g)	0.05	0.03	0.07
PPD (mm)	0.07456	0.04175	0.15507
PVS (mm/s)	10.920 @ 347.7ms		
PSPL (PA)	203.19 (140.140 dB)@107.4ms		
PSPL Freq	51.2Hz		
Sensor Test	Passed	Passed	Passed

Figure 9. PPV produced by blasting in an abutment and induced in the RCC in opposite abutment, 30m far.

Structure: RIGHT BANK			Date: 19/10/2018	
Location: RIGHT BANK			Drawing n.:	

Item	DESCRIPTION	UNIT	Theory	Actual
1	DRILL PATTERN			
-	Hole diameter	mm	76	
-	Bench Height	m	3	
-	Burden	m	2,2	
-	Spacing	m	2,2	
-	Stemming	m		
-	Volume / Hole	m ³		
-	Number of holes	no.	146	
-	Numb.of holes (ANFO)	no.		
-	Total Volume	m ³	2120	
2	CHARGE			
-	Emulsion Hole	kg		
-	Total Emulsion (435)	kg	360	
-	Anfo / Hole	kg		
-	Total Anfo	kg	280	
-	Weight of charge	kg	640	
-	Specific charge	=	0,30	

EXAMPLE OF FIELD FORM, FILLED
 DURING WORK ON SITE

Item	DESCRIPTION	UNIT	Theory	Actual
3	DETONATOR			
-	No.1 (L=5m)	pcs	4	
-	No.2 (L=5m)	pcs	4	
-	No.3 (L=5m)	pcs	4	
-	No.4 (L=5m)	pcs	4	
-	No.5 (L=5m)	pcs	4	
-	No.6 (L=5m)	pcs	4	
-	No.7 (L=5m)	pcs	4	
-	No.8 (L=5m)	pcs	4	
-	No.9 (L=5m)	pcs	4	
-	No.10 (L=5m)	pcs	4	
-	No.11 (L=5m)	pcs	4	
-	No.12 (L=5m)	pcs	4	
-	No.13 (L=5m)	pcs	4	
-	No.14 (L=5m)	pcs	4	
-	No.15 (L=5m)	pcs	4	
-	No.16 (L=5m)	pcs	4	
-	No.17 (L=5m)	pcs	4	
-	No.18 (L=5m)	pcs	4	
-	No.19 (L=5m)	pcs	4	
-	No.20 (L=5m)	pcs	4	
-	Electric detonator #0 (L=3m)	pcs		
	Detonating cord	m		
	Connecting wire	m		

Figure 10. Example of 20 delays used to reduce the charge blast at a single moment and relevant vibrations.

rock, in order to keep under control the strength and characteristics of the RCC not affected by vibrations, to compare it with the RCC strength in the real dam foundation (vibration-affected) at any time. RCC core samples should be collected in the trial embankment and in the RCC foundation after the first blasting as well, and they should be tested for RCC strength and physical detailed inspection (test 0).

Table 3 shows that the strength of vibration-affected samples (B) is similar to that of the core samples taken in the no-vibration affected area (A).

As a result, the controlled blasting can be applied for excavation as far as the produced vibration is not above PPV₀, and cross checking as in Table 3 must be performed at regular intervals, at least every 2 days.

Table 3. Compressive strength of RCC samples.

Description	RCC parameters	Density (ton/m ³)	Compressive strength (MPa)			
			7 days	28 days	90 days	180 days
Samples taken at moment of RCC placing in Dam area (no vibration affected)	A	2.330	3.1	4.9	11	13.4
		2.300	3.05	4.95	12.5	14.1
Samples taken from RCC coring after the dam foundation excav.blasting (controlled blasting vibration affected)	B	2.287		4.65	11.4	
		2.297		4.75	10.9	
		2.267		5.1	10.2	

6 CONCLUSIONS

RCC dams are erected by compacting numbers of layers. RCC reaches its final physical status after having been cured for several hours. During this period no stressing actions should be applied to the recently placed layers.

Blasting excavation produces vibration waves that may disrupt the correct maturation of the RCC. But if a controlled blasting produces vibrations under the level normally tolerated during normal construction activities, the excavation with explosive for the completion of excavation works can be performed in parallel to RCC dam erection, with great benefit to the planning of the works and considerable economic advantage for the project.

ACKNOWLEDGMENTS

Many thanks for the encouragement and support in drafting the article and for participation in the proofreading and suggestions in the finalization phase must be given to Camillo Tena-glia, Bruno Ferraro and Ruggero Gallera.

Many thanks are due to all the colleagues who cooperated with high competence and passion for the swift and successful completion of the RCC dam sample and testing.

Many thanks to Mr. Arnaldo Di Virgilio, production manager of the project where this system was applied in 2017-2018.

REFERENCES

- Forbes, B., 1999. Grout Enriched RCC: a history and future. *Water Power & Dam construction*
- Warren, T., 2011. Taking advantage of RCC. *Water Power and Dam Construction*
- Kwan A.K.H., Lee P.K.K. 1998. A study of the effects of blasting vibration on green concrete”, GEO REPORT No. 102, Civil Engineering Dep., The government of the Hong Kong, 1998.
- DIN 4150-1, “Erschütterungen im Bauwesen - Teil 1: Vorermittlung von Schwingungsgrößen”, 2001.
- DIN 4150-3, “Erschütterungen im Bauwesen - Teil 3: Einwirkungen im bauliche Anlagen”, 2016.
- Dowding C. H., 1985. Blast vibration monitoring and control. Prentice Hall, INC., Englewood Cliff, NJ
- Folchi R. 1992. Abbattimento controllato con esplosivi: la fratturazione indotta oltre il profilo finale di scavo”, *Rivista Italiana di geotecnica*, vol. 4.
- Harris C. M., 1995. Shock and vibration handbook, McGraw Hill, 1995.
- Kolsky H. 1963. Stress waves in solids, *Dover Publication on Physics*
- Oriard L. 1999. The effects of Vibrations and Environmental Forces – a guide for the investigation of structures, ISEE
- Swiss Norm SN 640 312 a “Vibrations effect on constructions”

Swiss dam safety regulation: Framework, recent changes and future perspectives

M.V. Schwager, A. Askarinejad, B. Friedli, P.W. Oberender, A.J. Pachoud & L. Pfister
Swiss Federal Office of Energy, Bern, Switzerland

ABSTRACT: This paper outlines the current structure and evolution of the Swiss dam safety regulation and provides insights into the underlying reasoning and research. The structure of the Swiss regulatory framework is based on three pillars: structural safety requirements, surveillance and emergency planning. Emphasis is given to recent changes of the regulations due to ongoing advancements in the field of dam safety and related fields, reflecting the dynamic nature of the regulations. In particular, four different challenges are discussed. They relate to updating the requirements following the latest change of the Swiss national seismic hazard model, dealing with uncertainties regarding flood safety, preparing for future influence of dam ageing and accounting for particularities of natural hazard protection dams. Conclusions are drawn how to address the discussed challenges in the framework of potential future changes in the dam safety regulation.

1 INTRODUCTION

1.1 Dams in Switzerland

There are 225 large dams and around 200 small dams in Switzerland under supervision (SFOE, 2015a). The majority of large dams, were constructed from the 1940s until the 1970s for the purpose of hydropower generation (see Figure 1), which covers about 57% of Swiss electricity consumption. In the recent decades, an increasing number of mostly small dams were built to protect against natural hazards (such as floods, debris flows, etc.).

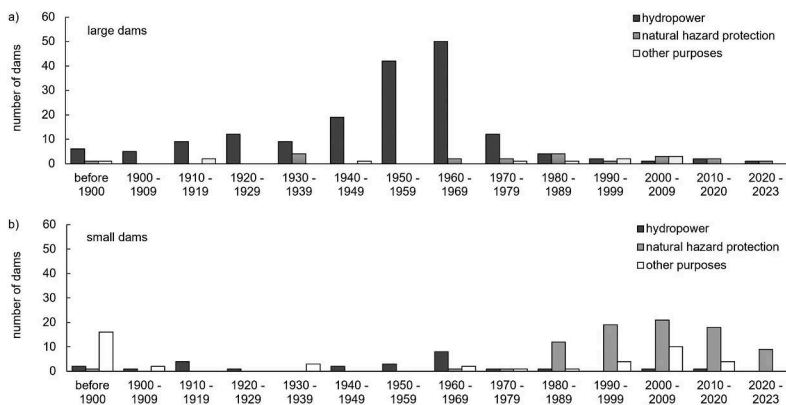


Figure 1. Year of construction and today's purpose of the dams under supervision in Switzerland: a) large dams, b) small dams.

Since Switzerland is densely populated also in the mountain areas, a rupture of a dam would threaten a large number of people. Some of the large dams may affect up to 60'000

people¹ in case of catastrophic dam failure. On average, 5'000 people are at risk downstream of a large dam. For small dams, the number of people potentially at risk is estimated to be on average around ten times smaller. Due to the potential consequences, dam safety is considered a crucial component of civil protection. A return of experience from the dam safety authority perspective is given in Côté et al. (2023).

1.2 Dam safety regulation in Switzerland

The first federal legal act addressing dam safety in Switzerland was established in 1943 by a decision of the Federal Council (Swiss Confederation, 1943) as a reaction to the failures of Möhne and Edersee dams in Germany due to war actions four months before. The first law addressing the issue of dam safety went into force in 1953 (Swiss Confederation, 1953). It has been replaced in 2013 by the current legislation (Swiss Confederation, 2010).

There is a federal ordinance detailing the law and outlining the three major pillars of the Swiss dam safety concept, that are: (i) structural safety, (ii) surveillance and maintenance as well as (iii) emergency concept (see Art. 5, 6 and 7 in Swiss Confederation, 2022). This ordinance has recently been revised particularly emphasizing the pillar of structural safety by outlining the general requirements in respect to normal, extraordinary and extreme load cases (see Art. 5).

In addition to the ordinance, a directive in five parts (A-E) has been established detailing the ordinance and providing methods and specific requirements for all three pillars (i)-(iii) of the dam safety concept (SFOE 2014, 2015a, 2015b, 2015c, 2017a, 2017b, 2021). The specific requirements are different for the three different classes of dams, which are defined by the volume and the corresponding storage height of the reservoir. The so-called class I and class II dams are large dams under federal supervision, whereas the class III dams are small dams mainly under cantonal supervision. Thus, the technical safety requirements are depending on the amount of water and on the height of water body stored in the reservoir. Latter criteria are supposed to work as an approximation of the potential consequences. However, they cannot be considered to be entirely risk-based in a strict sense.

1.3 Current challenges

The dam safety regulation is subject to continuous evaluation and further improvement. Fundamental developments such as the change in state-of-the art procedures and methods to ensure dam safety, additional knowledge about the exposure of dams to specific hazards, significant change in type or condition of the supervised dam portfolio and change in the general safety demand by the society may require a revision of specific safety requirements.

Several challenges related to fundamental developments are currently considered to be asking for future revisions of safety requirements. Four of these challenges, listed hereinafter, are discussed in this paper.

- The latest update of the seismic hazard model led already to revision of the respective dam safety requirements (SFOE, 2021). However, detailed technical recommendations regarding the methods to be used for the seismic safety assessments are partially yet to be formulated. Section 2 provides an overview of the change in the seismic hazard as well as future perspectives in respect to the consequent revision of the seismic safety assessments.
- Large uncertainties about the exposure of dams to floods as well as latest developments regarding the state-of-the-art in hydro-meteorological modelling are asking for a comprehensive revision of the entire set of requirements regarding flood safety. Section 3 discusses the different uncertainties to be addressed as well as potential paths to be followed.

1. People are considered to be at risk when living within the area potentially inundated within two hours after a catastrophic entire failure of a dam.

- Progressive ageing of dams is going to have a potential major influence on dam safety for the next decades in Switzerland (Figure 1). Section 4 outlines the future challenges related to ageing of dams.
- More recently constructed dams are often serving the purpose of protection against natural hazards (Figure 1). Since the dam safety regulation has been developed mainly for dams serving for hydropower generation, adopted requirements for natural hazard dams are recommended to be elaborated (see Section 5).

2 CHALLENGES REGARDING SEISMIC SAFETY

2.1 *Concept of seismic safety of dams in Switzerland*

As Switzerland is a seismically active region, medium to large earthquakes pose a constant threat to people and the built environment. Therefore, the seismic safety of dams must be in focus in the design of new dams and in the safety assessment of existing dams.

With an average age of about 72 years, Switzerland has one of the worldwide oldest portfolios of large dams (Figure 1). Many dams were not designed for earthquake loading or at least not for modern day seismic demands. The Swiss legislation requires the same level of (seismic) safety for new as for existing dams. Hence, the seismic safety of dams in Switzerland must be reassessed in case the seismic hazard is updated or improved safety assessment methods become available. Since seismology and earthquake engineering are relatively young fields of research the knowledge is progressing fast. Thus, a regular review of seismic safety assessments is necessary.

By law, the mandate of the Swiss federal dam safety authority is limited to the protection of society. Therefore, seismic safety assessments are considering the Safety Evaluation Earthquake (SEE) only. Dam owners have to prove that an uncontrolled discharge of water can be avoided. Seismic safety assessments with respect to Operating Base Earthquakes (OBE) are not required.

2.2 *Evolution of seismic safety requirements before 2003*

Formally, no seismic load was considered before the 1950s. Since then, the common practice was to design dams with a quasi-static force according to a horizontal acceleration of 0.1 g (e.g., Schleiss and Pougatsch, 2022). After 1980, some large dams were designed using a hazard developed by Säegger and Mayer-Rosa (1978) for Switzerland, but no uniform requirements for seismic design existed. The seismic safety of structures and infrastructure has become a focus of Swiss federal policy in the late 1990s and early 2000s.

2.3 *Evolution of seismic safety requirements from 2003 until 2021*

In 2003, the Federal Office for Water and Geology issued the first directive (FOWG 2003) that included national consistent requirements for the seismic safety assessment of dams. FOWG (2003) defined the earthquake hazard in three parts:

- Reference acceleration (SA(T=0s)) based on the seismic hazard from Säegger and Mayer-Rosa (1978) which only used data from reconstructed historical seismic events.
- Response spectra from Eurocode (EC) 8 pre-standard (SIA, 1997a) and the Swiss EC8 national annex (SIA, 1997b) for three different site classes, to account for site amplification.
- Synthetic acceleration time histories generated to match the entire response spectrum.

In contrast to FOWG (2003), the Swiss building standards SIA 261 (2004), published one year later, adopted a novel national seismic hazard model developed by the Swiss Seismological Service (SED, Giardini et al., 2004). In general, this hazard predicted higher accelerations in most regions. In Figure 2a the differences of the two hazard specifications are shown for areas with low (city of Bern) and high seismicity (city of Sion). Additionally, Figure 2a

shows the hazard for the nuclear power plant of Mühleberg near Bern, which has been developed by SSHAC² level 4 projects: (i) PEGASOS (NAGRA, 2004), (ii) PRP (Swissnuclear, 2013) and (iii) PRP-SED (ENSI, 2016). For the same annual exceedance probability (AEP), the hazard for the nuclear power plants is found to be similar to SIA 261 (2004). However, it is higher compared to requirements for dams.

This fact has also been addressed by the Swiss committee on dams (Brenner et al. 2010, Annex 5), stating that in some regions of Switzerland the seismic hazard for dams with intended annual exceedance probability (AEP) of 10^{-4} /yr just reaches the level of the seismic hazard for buildings with an AEP of 10^{-3} /yr. The report raised the question whether the hazard for dams was sufficiently well determined and concluded that the next revision of the dam safety directive should incorporate the latest hazard.

The spectral site response given in FOWG (2003) predicted lower accelerations for soft soil sites than for stiff sites. Modern site classifications, however, which were incorporated into SIA 261 (2004) and Eurocode 4 (2004), use higher amplifications the softer the site. Already before 2003, publications showed that this FOWG (2003) definition does not reflect the real phenomenon (e.g., Wenk, 2000; Dobry et al., 2000).

In 2010 these facts were already known. At this stage, about 20% of the dams had been seismically assessed (see Figure 2a). Still, it was decided to keep the 2003 issued hazard and to incorporate a new hazard in a future revision of the directive. Today, more than 95% of the large dams in Switzerland have been assessed by the dam owners with respect to the 2003 hazard.

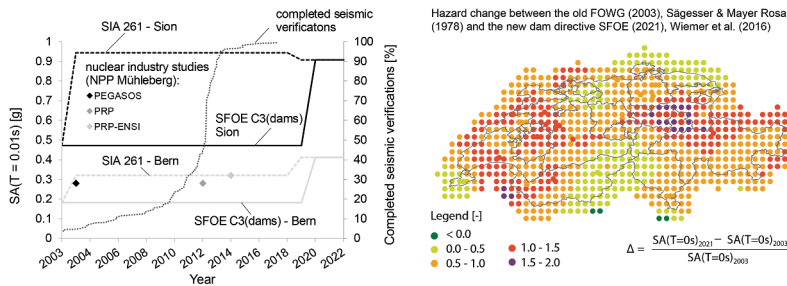


Figure 2. Left: Evolution of the seismic hazard for dams ($AEP=10^{-4}$ /yr, site class $A_{Dam,2003}$ with $vs_{30} > 400$ m/s) at two different sites (Sion and Bern) and comparison with the hazard according to SIA 261 ($AEP=10^{-4}$ /yr, site class $A_{SIA261,2004}$ estimated according to Wenk and Fäh, 2012) as well as the hazard for the nuclear power plant Mühleberg (close to Bern, $AEP=10^{-4}$ /yr). The dotted line shows the evolution of the completed seismic safety assessments. Right: Change of the spectral amplification $SA(T=0s)$, from FOWG (2003) to SFOE (2021), $AEP = 10^{-4}$ /yr, for the site class A ($vs_{30} > 800$ m/s).

2.4 Evolution of seismic safety requirements after 2021 and future challenges

In 2016, the dam safety directive was revised but without changing the underlying hazard. In 2015, the Swiss Seismological Service (SED) published a revised seismic hazard for Switzerland (SuiHaz15, Wiemer et al., 2016). This hazard compares well to the one published by SED in 2004 (Giardini et al., 2004).

Subsequently, the dam safety directive was again partially revised (SFOE, 2021) and the revised hazard by SED was introduced as reference hazard together with modern site amplification spectra. These are consistent with the also revised building standard SIA 261 (2020). It can be stated that a consistent hazard now applies to all types of civil structures in Switzerland (Figure 2a).

Additionally, contrasting the SIA 261 (2020), for stiff rock sites ($vs_{30} > 1100$ m/s), a new site class “R” is introduced. This aims to reflect the better foundation conditions at many dam

2. For details on SSHAC levels see Budnitz et al., 1997 and ENSI, 2012.

sites (Oberender et al. 2021). In addition, the directive also allows performing site-specific spectral amplification studies. Both, the use of site class R and site studies are conditional to a comprehensive quantitative assessment of the foundation of a dam. This follows the regulatory philosophy that reduced uncertainty due to in depth investigations may allow for less conservative model assumptions (e.g., site specific spectral acceleration may be less conservative than response spectra of normative site classes).

Further work is on the way to provide requirements for the selection of acceleration time histories that better reflect the seismic hazard compared the synthetic ones used in the past. The new acceleration time histories aim to account for the disaggregated hazard. The new motions will not reproduce the entire response spectrum but only the spectral accelerations that are relevant for the dam to be assessed. This aims to reduce exaggerated conservatism in particular with respect to irreversible behavior of dams.

Based on experiences from past seismic safety assessments, SFOE initiated a number of research projects for particular challenges such as the seismic behavior of (i) permanent landslides along reservoir flanks (e.g., Kohler et al. 2022) or (ii) bituminous linings on embankment dams.

Since the publication of the new directive in 2021, a comprehensive review of the change in seismic hazard for all dams under federal supervision confirmed the expected increase of the hazard (in terms of spectral acceleration) for about 75% of the dams (Friedli, 2023), see also Figure 2b. For these dams, revised seismic safety assessments will be requested by the authorities.

Simultaneously with the incorporation of the new hazard, SFOE also aims to have the seismic safety assessments updated according to the state-of-the-art (e.g., accounting for foundation mass and radiation of energy at the model boundaries; consideration of nonlinear behavior of material, block and dam-foundation joints, etc.). Currently, SFOE is working on a manual on state-of-the-art seismic modelling of dams, in particular regarding the assumptions for non-linear FEM analyses. It is intended to support dam owners and their engineers in the choice of methods and assumptions as well as in their documentation.

3 CHALLENGES REGARDING FLOOD SAFETY

3.1 *Uncertainties and perspectives in hydro-meteorological modelling*

Current dam safety regulations (SFOE 2017b) require a design flood corresponding to a return period of 1'000 years and a safety check flood determined either by multiplying the design flood hydrograph by a factor of 1.5 or by estimating the probable maximum flood based on probable maximum precipitation amounts (Hertig et al. 2007). The determination of such extreme flood events is undeniably prone to large uncertainties and exhibits various challenges. Particularly the pronounced natural variability of precipitation as well as catchment-specific effects in extreme runoff generation contribute to the uncertainty of extreme flood estimation. As most dams are located in remote Alpine areas often without direct or nearby discharge and precipitation measurements, data availability also proves to be a major challenge. Although this has improved in the past with more and longer measurement series, better instrumentation at dam sites and new data products covering Switzerland (FOEN 2007, Fukutome et al. 2018), there is still limited data available for many dam catchments.

Considerable improvements can also be seen regarding the methodology of flood estimation. Early design flood analyses were usually restricted to empirical formulas or frequency analyses of a few years of local runoff measurements. Today, complex numerical models representing various aspects of the hydrological cycle and a better data basis are available. However, as a large number of flood analyses for dams has not been kept up to date, flood estimates are based on vastly different approaches, reflecting previous states of the art. This heterogeneity of underlying data and methods makes flood estimates difficult to evaluate and compare. In addition to that, the effects of climate change have become obvious in recent decades. Results from the Hydro-CH2018 report (FOEN 2021) show a clear tendency towards an increase in floods in Switzerland by the end of the century, although regional changes are subject to strong uncertainty (Ruiz-Villanueva and Molnar 2020). Addressing these changes in the regulatory framework of dam safety is a challenging task.

The directive for flood safety assessments (SFOE 2017b) aims at reducing uncertainties or – if not possible – ensuring that estimates are on the conservative side, even in a changing future climate. For example, the use of multiple approaches for extreme flood estimation is prescribed, as well as a number of intended safety margins (e.g., initial conditions, runoff coefficients) in relation to data availability and method complexity. A systematic comparison of flood safety assessments by the SFOE in recent years has revealed, that design flood estimates are on average, as expected, higher than values obtained from the extreme value statistics provided by the Federal Office for the Environment (Baumgartner et al. 2013), extrapolated to a corresponding return period of 1'000 years (Figure 3). Furthermore, the design flood estimates show a large spread of values even for similar catchments. This is to a substantial part the result of the aforementioned heterogeneity in flood estimation approaches and data availability.

In this context, the SFOE has undertaken great efforts over the past years to provide a homogeneous flood data basis for Swiss dam catchments. Within the scope of the EXAR project (Andres et al., 2021; Viviroli et al., 2022), a state-of-the-art model chain has been developed using precipitation data generated by a weather generator that is fed to hydrological models to simulate 300'000 years of hourly runoff at each dam site along the middle and lower Aare catchment. These long-term simulations allow for determining floods of different return periods based on a frequency-analysis. The chosen approach has the advantage that return periods of precipitation and runoff are decoupled, while other important factors for flood generation, such as soil saturation and snow cover, are continuously modelled. Furthermore, temporal evolution and flood volumes can also be analysed. Currently, a successor project aims at adapting and applying this approach to all Swiss dam catchments.

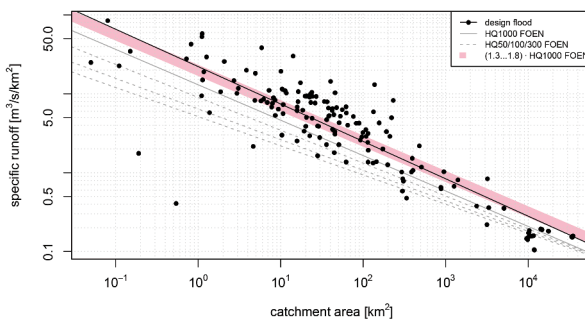


Figure 3. Specific runoff vs. catchment area for design flood estimates of dams under federal supervision (black dots). Indicated as lines are log-linear fits between area and runoff of dam design floods (solid black), as well as estimated fits from extreme value statistics of the FOEN hydrometric network for different return periods (solid grey, dashed grey). The red shaded area shows the range between 1.3 and 1.8 times the value of the 1'000-year flood based on FOEN frequency analyses overlapping with the log-linear fit of the dam design flood values.

3.2 Uncertainties and perspectives in dam safety assessment against floods

Besides the hydro-meteorological modelling to determine flood peak values and hydrographs, flood safety assessments of dams are subjected to further major uncertainties. These are, in particular, related to the hazard evaluation of potential driftwood clogging of flood release structures (STK, 2017), the estimation of the needed safety freeboard (Section 3.3) as well as the danger level (Section 3.4) potentially being above the crest or parapet level for concrete dams. A future revision of the respective directive (SFOE, 2017b) aims to account for as well as reduce these uncertainties.

3.3 Safety freeboard

The directive (SFOE, 2017b) defines the safety freeboard as “the distance from the danger level to the maximum water level that can arise in an extraordinary situation”, and specifies minimum

required lump values as a function of dam height and type. Putting aside particular risks such as impulse waves, preventing wind-induced waves overtopping is amongst the main objectives of the safety freeboard, and is particularly crucial for erodible dams. However, it has been observed that adequate data for reliable wave and overtopping prediction are often lacking and that sometimes practitioners rely upon outdated methods (Pullen et al., 2018). For example, the wind input parameters pose a great challenge at most dams, as sustained velocities for various return periods and durations may be required. The load cases to be considered as well as the correlation between extreme rainfall and wind during compound events is also an open question.

An attempt to systematically assess and compare existing wind-induced wave overtopping methods is currently ongoing by SFOE, based on available manuals/guidelines to estimate wave overtopping in reservoirs (e.g., ICOLD, 1992; USBR, 1992; DVWK, 1997) including the latest overtopping methods from EurOtop II (2018).

3.4 *Influence of the scour potential on the danger level determination*

The danger level corresponds to “the water level above which the water retaining facility is endangered” (SFOE, 2017b). For the overtopping of a dam to be allowed for the safe passage of extreme floods, its stability under overflow should be demonstrated, i.e., substantiating that there is no or negligible scour/erosion potential due to that overflow. The assessments submitted to SFOE often refer to qualitative geological assessments and expert geologist judgement, often ignoring the multiphysics of the scour phenomena.

The factor “duration” in case of overtopping, i.e., the required time for potential scour to endanger the dam stability, may be of utmost importance for Alpine dams as extreme flood hydrographs for those reservoirs may only induce overtopping during peaks of the order of hours. This often raises the question whether a critical scour depth for dam stability would be reached or not. However, evaluating the rate of scour remains a challenge in practice.

There is a large spectrum of scour assessment methods. The widely applied empirical methods (see, e.g., Castillo & Carrillo, 2017) and comparative methods based on erodibility indexes (Annandale, 1995; Pells et al. 2017) do not explicitly include the evolution of scour in time. Alternatively, the Comprehensive Scour Model (Bollaert and Schleiss, 2005) allows for estimating the evolution of scour over time through a chain of physically based models.

Current efforts by SFOE are aiming to rationalize future requirements for determining the danger level accounting for scour potential.

4 CHALLENGES WITH RESPECT TO AGEING

4.1 *Ageing factors on dam safety*

Damaging effects due to ageing do not only lead to higher, recurring maintenance costs, but can also significantly affect the safety of dams. For this reason, the ageing of dams is also of great relevance to the dam safety authority. Some of the most important ageing effects concerning the safety of dams are: (i) chemical attacks in concrete causing swelling (e.g., alkali-aggregate reaction or internal sulphate attack), (ii) damage of concrete faces due to freezing and thawing cycles, (iii) clogging of drainage systems, (iv) degradation of grout curtains, (v) damage of sealing systems at dam faces and joints, (vi) shrinkage cracks caused by drying of earth dams and (vii) reinforcement corrosion in appurtenant structures and in a few reinforced concrete dams.

4.2 *Alkali aggregate reaction in concrete*

The alkali aggregate reaction (AAR) occurs when certain aggregates in concrete react with the alkali pore solution present in the concrete, causing expansion and cracking. Concrete dams which have been built without much knowledge about the reactivity of aggregates form the majority of large Swiss dams. The Swiss Committee on Dams assumes that 35-45% of the concrete dams are affected (Amberg et al., 2017) but recent findings indicate that there could be even more.

In the past, understanding the chemical and micromechanical processes of AAR (e.g., Lee-mann & Griffa, 2013; Ben Haha, 2006) as well as its diagnosis in structures were at the focus

of research. Also, possible modelling approaches have been published (e.g., Cuba Ramos, 2019; Souma, 2021). However, no comprehensive framework is yet established that allows to reliably determine the effects of AAR on the safety of dams. In order to build such a framework, the following questions need to be answered:

- How does a concrete with AAR behave under environmental conditions (e.g., influence of temperature, moisture, alkali content in concrete, stresses and creep in concrete)?
- How can the behaviour of a dam with AAR be predicted on the basis of model calculations?
- How does the evolution of damage due to AAR affect the safety of the entire dam (e.g., how is the resistance of a dam against static and seismic loading affected by AAR)?

In order to answer these questions, SFOE is initiating research on the topics of (i) concrete behaviour under environmental conditions (SFOE is funding a project at the Swiss Federal Laboratories for Materials Science and Technology EMPA to study the expansion of concrete blocks at different exposure sites), (ii) development of a constitutive model to be implemented in boundary value problems, (iii) development of a methodology for the calibration of this model via laboratory tests and measured behaviour of dams and (iv) investigation of safety affecting damage mechanisms. It is planned to also evaluate the above-mentioned aspects in detailed analyses of a few well instrumented case studies of dams and to build an up-to-date database of the affected dams. Note, that the possible mitigation measures for AAR (e.g., saw-cutting to reduce stresses, Droz et al., 2012) are limited, their effectiveness is not fully understood and they can usually only postpone more damage.

4.3 Future assessment of dam safety affected by ageing

Decisions on the safety of aged dams can result in major rehabilitation measures or even decommissioning with significant costs for dam owners. SFOE aims to develop clear and applicable guidelines for dealing with ageing processes in dams to ensure proportionality of measures. Such guidelines are important to help the safety authority in its decision-making, but also to give the dam owners a legal and planning framework.

5 CHALLENGES WITH RESPECT TO NATURAL HAZARD PROTECTION DAMS

By law (Swiss Confederation, 2010), a retaining or dam structure is an installation designed to retain water, debris, sediment, ice or snow permanently or temporarily. Therefore, natural hazard protection dams (NHPD) are also subject to the legislation in case they fulfil the size criteria or have a particular risk potential in case of collapse of the retaining facility (Swiss Confederation, 2022).

About 50 new NHPDs have been constructed in Switzerland since the year 2000 and been subjected to the water retaining facility act. Although most of them are categorized as small dams this number amounts to about 70% of all newly built dams in the country in the past two decades (Figure 1). With the predicted increase of extreme weather events due to climate change it is expected that the number of these dams continues to grow in the future (FOEN, 2020). However, it should be noted that despite similar appearance, there is a series of fundamental differences between NHPDs and the “conventional” water retaining dams, as summarized in Table 1.

Table 1. Comparison of NHPDs and “conventional” water retaining structures.

	Natural hazard protection dams	Conventional water retaining dams
Purpose	Civil and infrastructure protection	Usage (mainly for energy production)
How often is the reservoir impounded?	Seldom (Return period of 100-300 a)	Most of the year
Duration of impoundment	Hours to days (for case of debris and snow: weeks to months)	Months or permanently
Reservoir fill material	Water, snow, debris, rock	Water

In spite of the fundamental differences between the two types of dams, the current directives of the SFOE on safety of dams treats NHPDs very similarly to the “conventional” water retaining facilities. This potentially leads to unproportionate safety requirements for natural hazard protection dams. Hence, there are needs to revisit and, where necessary, to add or modify safety regulations for this specific type of dams. Some of the aspects that require further research and potentially updates of the dam safety regulations in Switzerland are as follows:

- Specific load cases and load combinations for NHPDs (e.g., avalanche impact forces)
- Determination of the downstream inundation zone in case of (partial) failure (e.g., breach mechanisms, remobilization of retained debris, vulnerability of downstream objects)
- Specific monitoring and maintenance concepts
- Emergency planning

Based on the aforementioned considerations, new concepts of safety requirements and condition assessment are necessary to be developed. Due to the nature of the natural hazards a risk-based approach is considered to be the most appropriate and reliable option to develop a proportionate safety assessment concept for the specific case of the natural hazard protection dams.

6 CONCLUSIONS

For dam owners and engineers, changes in the state-of-the-art, in specific hazards, in the conditions of the dams or in the safety demand by society pose continuous challenges. Also, from the dam safety authority perspective, a significant effort is needed to keep the normative requirements in accordance with the evolution of knowledge and safety demand. The authority needs to actively monitor and follow current developments to keep regulations up to date and to build up the competences internally to be able to provide guidance to dam owners and engineers in case of changing safety requirements.

In the previous sections, four different challenges and their potential future implications on the Swiss dam safety regulations have been discussed. Whereas a revision of existing directives is foreseen to address the challenges regarding flood safety and natural hazard protection dams, the already released new seismic safety directive requires further supporting documentation to ensure its technically sound implementation. To address the challenge with respect to progressive ageing of dams, a scientifically based framework is to be developed to gain the necessary knowledge to provide future ageing specific safety regulations.

In Switzerland, any action and change in regulation by the dam safety authority must be “proportionate to the ends sought” (Swiss Confederation, 1999, Art. 5.2; Swiss Confederation 2010 Art. 5). This conflict of objectives between the safety of people downstream and the economic benefit of the society poses a challenge for the authority. To resolve this challenge, general safety targets are to be developed based on legal, technical, economical and even ethical and sociological considerations. This requires from the dam safety authority to foster a continuous dialogue with all stakeholders including the public and its representatives.

REFERENCES

- Amberg, F., Droz, P., Leroy, R., Maier, J., Otto, B., Bremen, R. 2017. *Concrete swelling of dams in Switzerland*. Swiss Committee on Dams, Switzerland.
- Andres, N., Steeb, N., Badoux, A., Hegg, C. (eds.) 2021. *Extremhochwasser an der Aare: Hauptbericht Projekt EXAR: Methodik und Resultate*. WSL Berichte, 104, Birmensdorf, Switzerland.
- Annandale, G.W. 1995. Erodibility. *Journal of Hydraulic Research* 33(4):471–494.
- Baumgartner, E., Boldi, M.-O., Kan, C., Schick, S. 2013. Hochwasserstatistik am BAFU – Diskussion eines neuen Methodensets. *Wasser Energie Luft*, 105(2):103–110.
- Ben Haha, M. 2006. *Mechanical Effects of Alkali Reaction in Concrete Studied by SEM-Image Analysis*, PhD Thesis, EPFL, Lausanne, Switzerland.
- Bollaert, E.F.R. & Schleiss, A.J. 2005. Physically based model for evaluation of rock scour due to high-velocity jet impact. *Journal of Hydraulic Engineering* 131(3):153–165.

- Budnitz, R.J., Apostolakis, G., Boore, D.M., Cluff, L.S., Coppersmith, K.J., Cornell, C.A., Morris, P.A. 1997. *Recommendations for Probabilistic Seismic Hazard Analysis*, NUREG/CR-6372, Vol 1, Washington, USA.
- Castillo, L.G. & Carrillo, J.M. 2017. Comparison of methods to estimate the scour downstream of a ski jump. *International Journal of Multiphase Flow* 92 (June):171–180.
- Chopra, A.K. 2020. *Earthquake Engineering for Concrete Dams – Analysis, Design and Evaluation*. Wiley Blackwell. Berkeley, California, USA.
- Cuba Ramos, A.I. 2019. *Multi-Scale Modeling of the Alkali-Silica Reaction in Concrete*, PhD Thesis, EPFL, Lausanne, Switzerland.
- Dobry, R., Borchardt, R.D., Crouse, C.B., Idriss, I.M., Joyner, W.B., Martin, G.R., Power, M.S., Rinne, E.E., Seed, R.B. 2000. New Site Coefficients and Site Classification System Used in Recent Building Seismic Code Provisions. *Earthquake Spectra* 16(1): 41–67.
- Côté, M., Gunn, R.M., Menouillard, T. 2023. Dam Safety and Surveillance: Return of experience from the perspective of the Swiss Federal Authorities. In *Proc. of the 12th ICOLD European Club Symp.* (Boes et al., eds.), Interlaken, Switzerland, 5-8 September 2023.
- Droz, P., Seignol, J.F., Leroy, R., Boldea, L. 2012. Strategy for the rehabilitation of Salanfe Dam. In *14th International Conference on Alkali-Aggregate Reaction (ICAAAR)*, Austin, Texas.
- Duvernay, B. 2008. Earthquake Risk Mitigation in Switzerland – Successes, Failures and Challenges in a Country of moderate Seismicity. In *14th World Conf. on Earthquake Engineering*. Beijing, China.
- Deutscher Verband für Wasserwirtschaft und Kulturbau DVWK (ed.). 1997. Freibordbemessung an Stauanlagen. In *Merkbblätter zur Wasserwirtschaft* 246/1997, Bonn, Germany.
- ENSI 2012. PEGASOS: SSHAC-Verfahren für genaue Erdbebenwerte. (accessed 21. 03.2023) <https://www.ensi.ch/de/2012/07/11/pegasos-sshac-verfahren-fuer-genaue-erdbebenwerte>.
- ENSI 2016. Neubestimmung der Erdbebengefährdung an den Kernkraftwerkstandorten in der Schweiz, ENSI-AN-9657 <https://www.ensi.ch/en/documents/pegasos-updated-seismic-hazard-assumptions-for-swiss-npps/> (accessed 21.03.2023).
- EuroTop II (Van der Meer, J.W., et al.) 2018. *Manual on wave overtopping of sea defences and related structures - An overtopping manual largely based on European research, but for worldwide application*.
- European Committee for Standard. (ed.). 2004. *Eurocode 8: Design of structures for earthquake resistance - Part 1: General rules, seismic actions and rules for buildings*, EN 1998-1-1:2004, Brussels, Belgium.
- Federal Office for the Environment FOEN (ed.) 2007. *Hydrological Atlas of Switzerland*, Switzerland.
- Federal Office for the Environment FOEN (ed.) 2021. *Effects of climate change on Swiss water bodies. Hydrology, water ecology and water management*. Environmental Studies, 2101.
- Federal Office for Water and Geology FOWG (ed.) 2003. *Directive on the Safety of Water Retaining Facilities, Basisdokument zum Nachweis der Erdbebensicherheit. Version 1.2*, Biel, Switzerland.
- Friedli, B. 2023. Auswirkungen der neuen Erdbebengefährdung auf die Stauanlagen unter Bundesaufsicht (Presentation). *Informationsveranstaltung vom 27. Januar. 2023*, (<https://www.bfe.admin.ch/bfe/de/home/versorgung/aufsicht-und-sicherheit/talsperren.html>, last accessed 21.03.2023).
- Fukutome, S., Schindler, A., Capobianco A. 2018. *MeteoSwiss extreme value analyses: User manual and documentation*. Technical Report MeteoSwiss, 255, 3rd Edition.
- Giardini D., Wiemer S., Fäh D., et al. 2004. *Seismic Hazard Assessment of Switzerland*, Available at: http://www.seismo.ethz.ch/prod/haz_map/hazard_report
- Hertig, J.-A., Fallot, J.-M., Brena, A. 2007. *Etablissement des cartes de précipitations extrêmes pour la Suisse, Méthode d'utilisation des cartes de PMP pour l'obtention de la PMF, Projet Cruex*.
- ICOLD 1993. *Embankment dams upstream slope protection – Review and recommendations*. Bulletin 91.
- Kohler, M., Stoecklin, A., Puzrin, A.M. 2022. A MPM framework for large deformation seismic response analysis. *Canadian Geotechnical Journal* 59(6).
- Leemann, A. & Griffla, M. 2013. *Diagnosis of alkali-aggregate reaction in dams*, Swiss Federal Laboratories for Material Science and Technology EMPA, Dübendorf, Switzerland.
- NAGRA 2004. Probabilistic Seismic Hazards Analysis for Swiss Nuclear Power Plant Sites (PEGASOS Project)/prepared for Unterausschuss Kernenergie der Überlandwerke, final report.
- Oberender, P. W., Panduri, R., Schwager, M.V. 2021. *Erläuterung zur neuen Erdbebengefährdung für Stauanlagen in der Schweiz und zur Teilrevision der Richtlinie Teil C3*. <https://www.bfe.admin.ch/bfe/de/home/versorgung/aufsicht-und-sicherheit/talsperren.html> (accessed: 21.03.2022).
- Pells, S.E., Douglas, K., Pells, P.J.N., Fell, R., Peirson, W.L. 2017. Rock mass erodibility. *Journal of Hydraulic Engineering* 143(5):06016031.
- Pullen, T., Allsop, W., Silva, E., Goff, C., Williamson, T. 2018. Wave and overtopping predictions on reservoirs and inland waterways. In *Proceedings of the 3rd International Conference on Protection against Overtopping*, UK, 6-8 June 2018.

- Ruiz-Villanueva, V. and Molnar, P. (eds.) 2020. *Past, current, and future changes in floods in Switzerland. Hydro-CH2018 project*. Commissioned by Fed. Office for the Environment (FOEN), Bern, Switzerland.
- Sägesser, R., Mayer-Rosa, D. 1978. Erdbebengefährdung in der Schweiz. *Schweiz. Bauz.* 7, Switzerland.
- Schleiss, A.J. & Pougatsch, H. 2022. *Design, Safety and Operation of Dams*. EPFL Press, Switzerland.
- SIA (ed.) 1997a. Norm SIA V160.811, Eurocode 8 – *Auslegung von Bauwerken gegen Erdbeben Teil 1-1. Europäische Vornorm ENV 1998-1-1*. SIA, Zürich.
- SIA (ed.) 1997b. Norm SIA 460.000. *Nationale Anwendungsdokumente zu den Europäischen Vornormen für den Konstruktiven Ingenieurbau (Eurocodes)*. SIA, Zürich.
- SIA (ed.) 2004. Norm SIA 261:2004 – *Einwirkungen auf Tragwerke*, SIA, Zurich, Switzerland.
- SIA (ed.) 2020. Norm SIA 261:2020 – *Einwirkungen auf Tragwerke*, SIA, Zurich, Switzerland.
- Souma, V.E. (ed.) 2021. *Diagnosis & Prognosis of AAR Affected Structures, State of the Art Report of the RILEM Technical Committee 259-ISR*.
- STK 2017. *Schwemmgut an Hochwasserentlastungsanlagen (HWE) von Talsperren*. Schweizerisches Talsperrenkomitee.
- Swiss Confederation 1943. *Bundesratsbeschluss vom 7. September 1943 über den Schutz schweizerischer Stauanlagen (AS 1952 1052)*.
- Swiss Confederation 1953. *Bundesgesetz vom 27. März 1953 über die Ergänzung des Bundesgesetzes betreffend die Wasserbaupolizei (AS 1953 950)*.
- Swiss Confederation 2010. *Federal Act on Water Retaining Facilities of 1 October 2010 (CC 721.101)*.
- Swiss Confederation 1999. *Federal Constitution of the Swiss Confederation of 18 April 1999 (CC 101)*.
- Swiss Confederation 2022. *Water Retaining Facilities Ordinance of 23 November 2022 (CC 721.101.1)*.
- Swiss Federal Office of Energy SFOE (ed.) 2014, 2015a 2015b, 2015c, 2017a, 2017b, 2021. *Directive on the Safety of Water Retaining Facilities, Part A: Introduction (2015a), Part B: Particular risk potential as subordination criterion (2014), Part C1: Design and construction (2017a), Part C2: Flood safety and lowering the reservoir water level (2017b), Part C3: Earthquake safety (2021), Part D: Commissioning and operation (2015b), Part E: Emergency plan (2015c)*. Bern, Switzerland.
- Swissnuclear (2013). *Probabilistic Seismic Hazard Analysis for Swiss Nuclear Power Plant Sites - PEGASOS Refinement Project*. Final Report, Vol. 1-5.
- USBR (ed.) 1992. *Freeboard criteria and guidelines for computing freeboard allowances for storage dams*. ACER (Assistant Commissioner - Engineering and Research) Technical Memorandum no. 2, Revised 1992 (1981). U.S. Department of the Interior, Bureau of Reclamation, Denver Colorado, USA.
- Viviroli, D., Sikorska-Senoner, A.E., Evin, G., Staudinger, M., et al. 2022. Comprehensive space-time hydrometeorological simulations for estimating very rare floods at multiple sites in a large river basin. *Natural Hazards and Earth System Sciences* 22(9):2891–2920.
- Wenk T., Fäh D. 2012. Seismic Microzonation of the Basel Area. *15th World Conf. on Earthquake Engineering*, Lisbon, Portugal.
- Wiemer, S., Danciu, L., Edwards, B., Marti, M., Fäh, D., Hiemer, S., Woessner, J., Cauzzi, C., Kästli, P., Kremer, K. 2016. *Seismic Hazard Model 2015 for Switzerland (SUIhaz2015)*. SED at ETH Zurich, Zurich, Switzerland.
- Wieland, M. 2016. Safety Aspects of Sustainable Storage Dams and Earthquake Safety of Existing Dams. *Engineering* 2(3): 325–331.

Châtelard basin storage expansion by making use of a spoil area

H. Stahl

AFRY Switzerland Ltd., Zürich, Switzerland

B. Müller & Ch. Hirt

Swiss Federal Railways, Zollikofen, Switzerland

B. Romero

AFRY Switzerland Ltd., Lausanne, Switzerland

ABSTRACT: The compensation reservoir Châtelard is an asphalt lined basin owned and operated by the Swiss Federal Railways. It is located in a narrow valley that has been partly filled to the downstream by a spoil area of tunnel muck derived from the construction of Nant de Drance pump storage scheme. The area between the asphalt lined embankment dam and the spoil area provided good opportunity to increase the storage volume of the basin. The Swiss Federal Railways took a brave decision for the alternative with the greatest increase of storage volume but also maximum impact on the existing scheme. With the chosen alternative, the active storage volume was doubled from 200'000 m³ to 394'000 m³.

The spoil area was not originally planned to serve as a water retaining structure and efforts needed to be made to investigate its properties and analyze its stability under static and dynamic loads as well as post-earthquake state with ruptured surface sealing. It was concluded that the original grade of the spoil area slopes of 1:1.5 (v:h) is too steep to meet the required factors of safety for a water retaining dam and an additional embankment to flatten the slope to 1:2.5 (v:h) was planned and implemented. In agreement with the supervising authorities, a fiber-optic deformation measurement system was included within the asphalt sealing of the new dam in order to monitor closely the embankment for settlements and the asphalt sealing for unacceptable strains during first impounding. The monitoring system was enhanced with geodetic measurements, piezometers within the embankment and a drainage system beneath the asphalt sealing.

The project implementation started in April 2021 and first impounding took place in February and March 2022. The first full impounding resulted in strains of 250 microstrains (0.025% or 0.25 mm on 1 m) in different areas of the new dam. Only along the plinth between the asphalt surface sealing and the rock cliff strains of up to 1'500 microstrains (1.5 mm on 1 m) were observed. All in all, the deformations observed with the fiber optic cables remained small and well distributed (no abrupt changes), indicating no deformation critical to watertightness. Three weeks after first full impounding, the geodetic measurements showed a maximum horizontal displacement of the five measuring points located on the new dam of 3.5 mm and a maximum settlement of 6.8 mm. After 9 months of operation, the horizontal deformation is still of the same order of magnitude and the settlements only increased slightly to 8.8 mm. These values confirm an appropriate compaction of the spoil deposit and the new earthworks embankment with flattened slope. Also, the piezometric pressures and drainage water quantities confirmed a satisfactory behavior during first impounding. After 9 months of normal operation the behavior is still fully up to expectation.

With this project, the Federal Railways facilitated a considerable increase in the efficiency of the existing scheme and improved its capability for flexible energy storage and just in time generation according to the ever-changing demands.

1 INTRODUCTION

After construction of the Nant de Drance pump-storage scheme, the area between the asphalt lined embankment dam of the Châtelard compensation basin and the spoil area built from the tunnel muck of the pump-storage scheme provided good opportunity to increase the storage volume of the basin. At feasibility and preliminary design stage carried out between 2014 and 2017, several alternatives were studied. The Swiss Federal Railways as the project owner, in times with low energy prices, took a brave decision for the alternative with the greatest increase of storage volume but also maximum impact on the existing scheme. With the chosen alternative, the active storage volume was doubled from 200'000 m³ to 394'000 m³. After going through the tender and building permit procedure, construction started in April 2021. First impounding took place in February and March 2022.

With this project, the Federal Railways took the opportunity to facilitate a considerable increase in efficiency of the existing scheme and improved its capability for energy storage and just in time generation according to the ever-changing demands.

2 BACKGROUND

The Châtelard compensation basin is part of the Barberine hydropower scheme, owned and operated by the Swiss Federal Railways. The Barberine hydro power scheme is in the western Swiss Alps, near the border with France and was built in its original form in the beginning of the 1920's, when the Swiss Federal Railways started with the electrification of its engines. The head reservoir of the hydro power scheme was extended in the 1970's with the construction of the Emosson dam. At the same time, the discharge capacity from the new Emosson reservoir to the Châtelard power station and the capacity of the power station itself were increased, whereas the discharge capacity of the free surface flow gallery towards the Les Marécottes basin and the lower power station at Vernayaz was left unchanged. Therefore, a compensation basin became necessary. With the extension of the power plant, a pump was installed, and provisions were made for a second pump to allow for a pump storage operation between the Châtelard and Emosson reservoirs.

Between 2008 and 2022, the 900 MW Nant de Drance pump storage scheme was built between the Emosson and Vieux-Emosson reservoirs. The main access tunnel to the powerhouse cavern starts just next to the Châtelard compensation basin. Large parts of the muck of the 18 km of underground galleries within the Nant de Drance plant were deposited in the narrow valley where the Châtelard compensation basin is located. The area between asphalt lined embankment dam of the basin and the spoil area provided good opportunity to double the storage volume of the basin.

3 THE EXTENSION PROJECT

3.1 *General description*

The asphalt lined embankment dam of the original basin was completely removed, and the basin extended towards the spoil area that serves as the new dam. The eastern edge of the basin is bounded by a 40 m high rocky cliff, while an embankment serves as a boundary to the west, see Figure 1.

The waterproofing element of the basin is an asphalt concrete lining that covers the base and slopes. The rock face on the eastern bank of the reservoir is lined with shotcrete to improve watertightness over the reservoir area. During the project execution, the lining of the existing part has been rehabilitated. The maximum depth of the reservoir is 26.0 m (1090.0 to 1116.0 m asl.).

The ancillary structures of the existing reservoir, such as the inlet structures for the power station and the intermediate catchment area, the water intake to the pumps and free-surface flow gallery to the Les Marécottes basin and the access ramp to the bottom of the reservoir,

remained unchanged. This also applies to the spillway and the bottom outlet, whose capacity was checked for the enlarged basin volume and updated hydrology and found to conform with the current regulations.

With the removal of the embankment of the original dam, access to the spillway and bottom outlet gate chamber was interrupted. Therefore, a new access extending the road south of the basin to the top of the spillway platform was constructed in the form of a footbridge anchored in the rocky cliff.

Finally, an access tunnel built for the construction of Nant de Drance scheme, which leads to the basin extension, with elevation below the level of impounding, required plugging.



Figure 1. Châtelard compensation basin - original part (left side) and enlarged part (right side).

3.2 Spoil area as dam

The spoil area was not originally planned to serve as a water retaining structure. It was nonetheless designed as foundation for the substation of the Nant de Drance plant. Accordingly, it was compacted to an M_E value of 50 MPa to minimize the settlements and at an early stage regular levelling measurements were undertaken to monitor the settlement of the fill around the substation and close to the new dam face, which confirmed a good compaction of the fill.

To obtain the commissioning license from the supervising authorities, the same requirements as for a new built dam had to be fulfilled. This included stability calculations for static and seismic load cases. To determine the material parameters of the in-situ material, a first investigation program was initiated in September 2018 comprising field and laboratory testing.

The field testing included: Three vertical core drillings through the spoil area and the underlying alluvium, torrential deposits, scree materials and moraine down to the rock. During the drilling process, SPT tests were carried out. Where the nature of the ground allowed, pocket penetrometer tests were carried out on the core samples.

The laboratory testing comprised; water content, density, Atterberg limits and grain size analysis (sieving and hydrometry) on nine bulk samples taken from the drill boxes.

The results revealed that the compacted spoil consists of coarse, angular, sandy, slightly silty gravel, with some pebbles and occasional blocks. The fill can be classified as “silty gravel with sand”. It is compact (SPT tests: 46 strokes/30 cm) to a very dense degree (SPT have reached refusal). The characteristic geotechnical parameters derived are; unit weight of 21.0 to 22.5 kN/m³, mean friction angle of 35° with zero cohesion, elastic modulus between 60 and 90 MPa and a hydraulic conductivity between 2*10⁻³ to 10⁻⁷ m/s.

The three boreholes were equipped with piezometric tubes. The pre-impounding measurements confirmed that the water table is lower than the invert of the extended basin and indicated the presence of underground water circulation at the rock head interface along the sides of the valley.

On this basis, stability calculations of the existing slope of the compacted spoil area towards the extended basin were executed and it was found that, despite the favorable characteristics derived from the investigations, its slope of 1:1.5 (v:h) was too steep to meet the applicable safety factors for a water retaining dam. The critical loading case was seismic, with a peak acceleration at the crest level of more than 1.0 g. In a next step, an embankment to flatten the slope was investigated, see Figure 2. It was found that with a slope of 1:2.5 (v:h) an MCE earthquake with a return period of 5'000 years still results in deformation (few decimeters, depending on the reservoir level), which was considered to be acceptable. However, a rupture of the surface sealing in the event of the MCE could not be excluded.

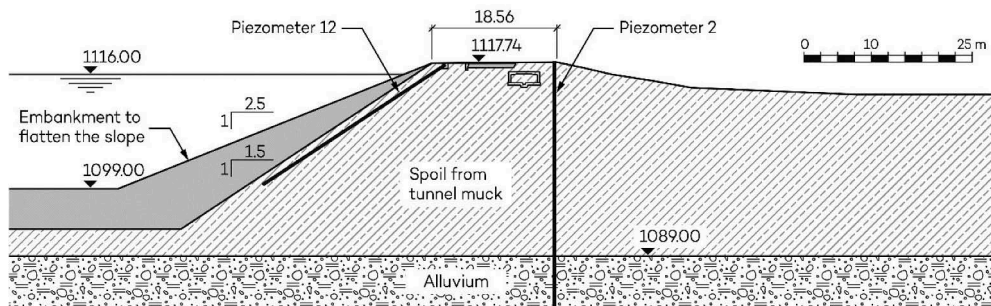


Figure 2. Châtelard compensation basin – typical section through the spoil area and flattened slope.

For this reason, in a next step, the potential for internal erosion in the unlikely event of a surface sealing rupture was investigated using the diagram of Wan & Fell (2008). The result is that the existing material is in the stable zone of the diagram, with the sole exception of one sample taken in one of the bore holes. This sample was taken at an elevation where the dam is about 300 m wide. It was therefore considered that the seepage gradient at this level is too low to initiate internal erosion.

In this context, the saturation of the dam body following the rupture of the surface sealing was also studied. The main findings are that, despite conservative assumptions, a steady state condition within the dam body will only be reached after some 24 hours, whereas the reservoir can be lowered to an uncritical level by opening the bottom outlet within less than an hour. Within this short time, the saturation of the dam body will not reach a level that influences neither the upstream, nor downstream slip circles.

Samples taken from the drillings were also used to evaluate the liquefaction potential of the available material, which allowed to exclude any risk thereof. In addition, the piezometer readings continued to confirm that the fill is not saturated, which also excludes the risk of liquefaction.

To further assess the behavior of the existing material under seismic loading, a second investigation campaign was launched in late 2020, with the aim of estimating the possible maximum settlement at the dam crest resulting from a post seismic settlement (or consolidation) caused by rearranging of the contained particles (sand, gravel) from its actual compaction to the maximum possible compaction. In the course of this investigation campaign, two more drillings in the existing material were executed closer to the basin slope to confirm the homogeneity of the fill material and thus confirm the earlier results on design parameters, internal erosion and liquefaction potential. The laboratory results indicated that the in-situ density is already close to the maximum density. Considering the maximum height of fill material of 40 m, the maximum possible settlement was estimated to be in the order of 1.4 m. Another estimation following Bureau (1997) together with the estimated vertical deformation of the sliding body concluded a maximum vertical displacement of the crest of 0.95 m. Both obtained values are less than the available freeboard of 1.5 m.

Despite the crest width of between 20 and 80 m and the very gentle slope on the downstream side, stability analysis was also carried out for this side of the dam.

The embankment to flatten the existing slope from 1:1.5 to 1 to 2.5 (v:h) was designed with the same parameters as derived from the existing fill. The filling material was sourced from the demolition of the original embankment dam of the basin, which was constructed in the 1970s with tunnel muck from the excavations made for the Emosson scheme. The source of the material is thus pretty much the same as the source of the material of the existing spoil area. Samples taken from the original dam confirmed the same granulometry. Proctor tests were executed on the material to obtain the optimum water content and density after compaction and a testing program was set up to control the key parameters during execution of the works, including a trial embankment to be executed before filling of the dam part could start.

With these investigations, analysis and conclusions, the supervising authorities finally consented to flatten the slope of the spoil area and to upgrade it to a water retaining dam, but with strict conditions for the monitoring during first impounding.

3.3 *Monitoring instrumentation of the new dam and basin*

The extended section of the basin is equipped with a drainage system connected to the drainage system of the original basin and including flow measurement. The instrumentation also includes piezometers in the embankment, an extension of the geodetic measurement system and fiber-optic cables in the waterproofing of the new dam to measure deformations in the asphalt lining. The measuring array is augmented with instruments for the reservoir water level, precipitation, and ambient temperature.

The drainage system of the enlarged section, as for the original section, consists of two separate pipes, one for the left and one for the right side, as well as fishbone drains beneath the invert. In the enlarged part of the basin, two new measuring points are installed separately for the left and right pipes. The automatic flow meters (electromagnetic system) are located in a new measuring chamber, see Figure 3. When the basin is empty, a watertight and accessible shaft gives access to the measuring chamber. Downstream of the measuring chamber, the pipes are connected to the corresponding pipes of the original basin. The total drainage water quantities are measured, as before, separately for the left and right side in the bottom outlet gate chamber. Two triangular weirs with manual and pressure probe level measurement are available. The flow rates of the original basin are determined by subtraction of the flow rates measured for the extended basin from the total flow rates.

The three piezometers installed during the design stage of the project were completed with additional piezometers in the same cross section drilled inclined in the sloped embankment (see Figures 2 and 3). All six piezometers reach below the invert of the basin and are equipped with a pressure gauge for permanent measurement.

The geodetic measurement system of the original basin was completed with 12 planimetric and altimetric measurement points along the basin rim, five of which are on the new dam, as shown in Figure 3. Three fixed points are added to enable their measurement. The measuring

network also includes points further away from the dam face on the spoil fill, in particular around the substation, and on the spillway structure.

In agreement with the supervisory authorities, a fiber-optic deformation measurement system was included in the asphalt sealing of the new dam. This system replaces the inclinometers foreseen in an earlier stage of the project. The cables were installed in three loops, one horizontal and two vertical, see the Figures 3 and 4.

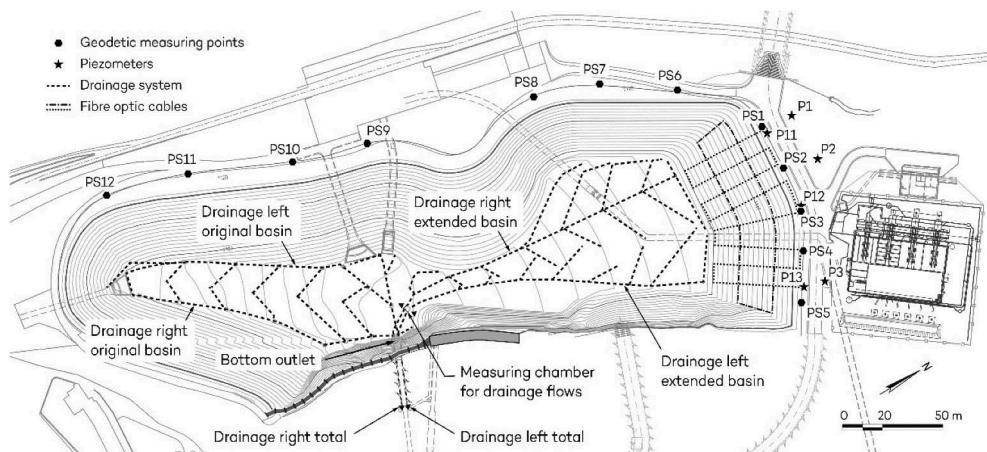


Figure 3. Layout of monitoring instrumentation.

The cable in one of the vertical loops was found to be broken some time after installation. Measurement remained possible from one side only, which reduces the precision indicated by the provider to be 50 microstrains (0.005%) for the closed loop and 200 microstrains (0.02%) for the cable with open end. In laboratory tests of the bituminous sealing, an elongation of 2% was maintained without cracking. This value is not a limit value, but if the strain remains below this value, cracking of the waterproofing should not be expected. It is concluded that the method is sufficiently accurate for this assessment, even after the breaking of a cable.

Measurements were carried out during the first impoundment to detect possible cracking of the sealing asphalt layer caused by settlement of the dam. In the operational phase, measurements are only planned after a strong earthquake to exclude cracking of the asphalt, without having to empty the basin. It is considered, however, that a sliding body rupturing the surface sealing would be visible at the dam crest and a drawdown of the basin will give faster and a clearer picture of the actual situation as compared to calling the provider of the system to carry out a measurement.

4 MONITORING RESULTS

This chapter describes the monitoring results collected during the first impounding and first months of operation.

4.1 Drainage system

The total drainage water quantities from the left side remained low during the filling process. Within 2 days after first complete filling however, it increased to almost 10 l/s. The flow meter of the enlarged part of the basin indicated that most of this flow came from the enlarged part on the cliff side, while the contribution of the drainage from the original part was small. In addition, the flow from the rock side of the enlarged basin showed a clear correlation with the fluctuation of the reservoir water level. It can be assumed that the reservoir water found a way through the shotcrete of the cliff and/or the access tunnel (in the 60 m long unplugged stretch

connected to the basin). A further increase to between 14 and 16 l/s was observed on 24 March 2022, 10 days after first full impounding.

After emptying the reservoir, a crack was found halfway up the dam in the plinth concrete between the asphalt and the rocky cliff. The crack ran through the plinth concrete and extended between the plinth and the shotcrete. The length of the crack was several meters, with a maximum opening at the surface of about 1 cm. This crack probably developed on the day of the increase of the flow. It was repaired and sealed before refilling the basin.

The total drainage water quantities from the right side rose with the half-filling of the reservoir and then continued to rise with the full filling. The maximum value reached was about 4 l/s. It can be assumed that most of this flow comes from the drain along the cliff of the original basin. In this area, the plinth between the asphalt and the cliff was not refurbished over the full length.

In early May 2022, the basin went into normal operation. Since then, the reservoir level fluctuates between its maximum at 1'116 m asl and an intermediate level. The sealing of the crack proved very successful and the seepage through the shotcrete and rock reduced due to clogging. The drainage water quantity from the extended basin part is below the measuring capability of the flow meters (a filling rate of 10% is required for accurate measurements) and the drainage water quantities from the original part of the basin remained significantly lower than the flows measured before the rehabilitation of this part.

On various occasions, the reservoir was kept without in- or outflow for between 34 and 120 h. The lost reservoir volume could then be compared to the measured drainage discharge. It revealed that in addition to the discharge measured, a considerable amount of water is lost without passing through the drainage system. It can be assumed that this is seepage through the shotcrete of the cliff and/or the 60 m long stretch of the plugged gallery connected to the basin. With time, a reduction in this unmeasured loss is observed. This could be explained by a clogging of the seepage joints.

4.2 *Piezometers*

For the vertical piezometers P1, P2 and P3, which are located at a certain distance from the dam face, no influence of the reservoir level was noticed during impounding. The measured values corresponded to the values measured in 2021 during construction when the reservoir was still empty.

Of the inclined piezometers P11, P12 and P13, located in the sloped embankment (see Figure 2), only P12 and P13 showed a reaction. The water table in these piezometers rose with the filling, first and more pronounced in P13, which is located closer to the rock cliff. In P12, located in the middle of the dam between the two abutments, the water table remained at the bottom of the basin. For P13, the measurements indicated, at some distance to the surface sealing, an increase to level 1'103.80, i.e. 5 m above the bottom of the basin.

As with the drainage on the cliff side of the enlarged basin, the water table in piezometer P13 reacted to the level of the reservoir. It increased significantly on 24 March 2022. This confirms that by this date the crack in the plinth may have developed. The water table in the piezometer dropped with the lowering of the reservoir and this more pronounced when the level of the reservoir passed the area of the crack in the plinth concrete, which was found later.

Since start of the normal operation of the reservoir, pressures in piezometers P1, P2, P3 and P11 remain unchanged. After sealing of the crack in the plinth, the pressures in P12 and P13 are considerably lower, especially in P12, where an almost constant low pressure is observed. The water table in P13 is to a certain extent still influenced by the reservoir level through seepage into the rock cliff, that find their way into the embankment.

4.3 *Geodetic measurement system*

During the impounding process, the following four measuring campaigns were executed: zero reading at empty reservoir and subsequent measurements at mid-level, after full impounding and 3 weeks after full impounding.

In this last measuring campaign and for the 12 points around the basin, the horizontal deformations compared to the zero state were between 1.0 and 5.3 mm, which is evaluated to be a very small deformation. In general, the points have moved away from the basin. This also applies to the five points on the new dam, where the deformations were between 1.0 and 3.5 mm only.

In the vertical direction (levelling), the 12 points around the basin have settled between 0.7 and 7.0 mm compared to the zero state. The five points on the new dam settled between 1.4 and 6.8 mm. These settlements are not significant in view of the available freeboard.

In January 2023, after 9 months of operation, the horizontal displacement of the measuring points along the basin rim is with a maximum of 5.1 mm still very small and hardly significant (the 95% reliability index is 2.9 mm in planimetry). The maximum displacement of the five points on the new dam is 3.2 mm and thus even smaller. In vertical direction, the greatest settlement is evaluated to be 10.6 mm and 8.8 mm on the new dam. The values confirm an appropriate compaction of the spoil area and abutting flattened embankment slope.

4.4 Fiber optic cables

The fiber optic cables were measured in two measuring campaigns, first during the filling from the embankment toe to mid-level (1'108 m asl) and then from mid-level to full impounding. The first series comprised measurements every 20 minutes for 66 hours, the second series comprised measurements every 20 minutes for 120 hours.



Figure 4. Layout of fiber-optic deformation measurement system.

The first measurement campaign showed significant strains in the course of day and night above the water level and almost constant strains in the already inundated asphalt. The strains were attributed to temperature changes. Thus, no significant temperature compensated strains were observed, i.e. the hydrostatic load on the asphalt sealing and embankment caused strains in the asphalt that were below the measurable strains, i.e. below 50 and 200 microstrains respectively. The full impounding caused strains of 250 microstrains (0.025% or 0.25 mm on 1 m) in different areas, which again confirms a good compaction. Only along the plinth between the asphalt and the rock cliff strains of up to 1'500 microstrains (1.5 mm on 1 m)

were observed. The largest deformations are observed at about 1'105 to 1'108 m s.m., i.e. in the area of the crack observed after emptying the basin. The deformation occurred with the reservoir filling as a result of the additional hydrostatic load. It seems that the compaction of the dam was inhomogeneous in this area close to the plinth. According to the drainage and piezometer measurements, it is considered that the crack developed only after the fiber optic measurements were completed.

In summary, the deformations observed with the fiber optic cables are small and well distributed (no abrupt changes). They are probably due to compaction inhomogeneities and not at all critical for watertightness.

5 SUMMARY AND CONCLUSION

After construction of the Nant de Drance pump-storage scheme, the area between the asphalt lined embankment dam of the Châtelard compensation basin and the spoil area built up with the tunnel muck of the pump-storage scheme provided good opportunity to increase the storage volume of the basin. The Swiss Federal Railways as the project owner, took a brave decision for the alternative with the greatest increase of storage volume but also maximum impact on the existing scheme. With the chosen alternative, the active storage volume was doubled from 200'000 m³ to 394'000 m³.

The spoil area was not originally planned to serve as a water retaining structure and efforts needed to be made to investigate its properties and analyze its stability under static and dynamic loads as well as post-seismic state with ruptured surface sealing. It was concluded that the original slope of the spoil area of 1:1.5 (v:h) is too steep to meet the applicable safety factors for a water retaining dam and an embankment to flatten the slope to 1:2.5 (v:h) was planned and implemented. In agreement with the supervisory authorities, a fiber-optic deformation measurement system was included in the asphalt sealing of the new dam in order to monitor closely the embankment for settlements and the asphalt sealing for unacceptable strains during first impounding. The monitoring system was completed with geodetic measurements, piezometers within the embankment and a drainage system under the asphalt sealing.

The project implementation started in April 2021 and first impounding took place in February and March 2022. The measuring results of the piezometric pressures, drainage water quantities, deformation of the asphalt sealing measured with fiber optic cables and deformation of the basin rim measured with geodetic means confirmed a satisfactory behavior during first impounding. After 9 months of normal operation the behavior is still fully up to expectation.

REFERENCES

- Wan, C.F. & Fell, R. 2008. Assessing the potential of internal instability and suffusion in embankment dams and their foundations, *Journal of Geotechnical and Geoenvironmental Engineering*, Vol.134, Issue 3
- Bureau, G. 1997. Evaluation Methods and Acceptability of Seismic Deformations in Embankment Dams. 29th International Congress on Large Dams (ICOLD), Florence, Italy

An application of sophisticated FEM and simplified methods to the seismic response analysis of an asphalt-concrete core rockfill dam

A.D. Tzenkov

Gruner Stucky Ltd, Renens, Switzerland

D.S. Kisliakov

University of Architecture, Civil Engineering and Geodesy, Sofia, Bulgaria

M.V. Schwager

Swiss Federal Office of Energy SFOE, Bern, Switzerland

ABSTRACT: Despite the intensive development of sophisticated dynamic analysis methods and their implementation in the field of dam engineering over the last decades, some well-established simplified methods are still widely used for a rapid evaluation of the most important response parameters of an embankment dam under earthquake excitation. The present work deals with the application of a sophisticated FEM analysis and two simplified methods to the analysis of the seismic response of a rockfill dam with asphalt-concrete core (ACRD) in Bulgaria. The results of the two approaches are compared and conclusions are drawn as to the applicability of the simplified methods used for a typical ACRD.

1 INTRODUCTION

The construction of large new dams, as well as the verification of existing ones, require performing studies aimed at defining the dam safety in terms of local and global stability of the structure. These studies involve comprehensive field and laboratory investigations, definition of material parameters and performing advanced static and seismic numerical analysis. The behaviour of rockfill dams can be reasonably well approximated by means of elasto-plastic models associated to the material of the dam shells, which requires nonlinear numerical approach. Due to the static and seismic loads, some plastic strains might occur and propagate in the dam body. In case of strong ground motions, the amount of these plastic strains and the associated permanent deformations strongly depend not only on the peak ground accelerations, but also on the time history of the accelerations of the dam foundation caused by the seismic excitations. It is therefore necessary to perform site-specific studies to define properly the relevant seismic input necessary for the numerical analysis. The differences of the structural response obtained by using site-specific and synthetic time histories may be significant, depending on the size of the dam and the severity of the seismic impact investigated.

On the other hand, some simplified methods are widely used which may allow for a preliminary design or verification. These methods have proven over the years their ability to define the most important response parameters of embankment dams subjected to strong ground movements.

The aim of the present work is to compare the characteristic horizontal displacements near the crest of a typical ACRD obtained by a sophisticated numerical analysis on the one hand and by two simplified methods on the other hand in order to conclude on the applicability of the latter.

2 DESCRIPTION OF THE INVESTIGATED DAM

The investigated dam is under construction in North Bulgaria and, together with its appurtenant structures, is part of a potable water supply project for a town at approximately 7.5 km downstream and the nearby villages. The maximum height of the dam is 47.15 m; its crest is 200 m long, and its total embankment volume is approximately 300 000 cubic meters.

The dam is founded on rock. The asphalt-concrete core is vertical, and it is in the central section of the dam. The asphalt-concrete core starts from the top of a grouting gallery which is embedded in the rock foundation.

According to the Bulgarian code for design of hydraulic structures, BCA (1983), the dam class is III. The latter corresponds to embankment dams of height from 15 m to 50 m founded on rock. However, the design code allows to increase the dam class should an eventual damage or failure of the dam can pose danger to human life and/or cause catastrophic consequences to settlements and/or infrastructure. Having in mind that the height of the dam is close to the 50 m upper limit of Class III, as well as that several settlements are located downstream, the class of the dam has been modified accordingly. Therefore, the dam and its appurtenant structures have been designed considering Class II design criteria.

Figure 1 gives a cross section at the highest dam profile. The zones in the dam body are as follows: Zone 1 is coarse rockfill from limestone quarry with maximum diameter 600 mm, which is compacted in 800 mm thick layers; Zone 2 is fine rockfill from limestone quarry scalped at 300 mm, compacted in layers of 400 mm; Zone 3 is an one-metre thick transition zone of well-graded gravel and sand of 0-60 mm diameter that is built simultaneously with the core; Zone 4 is the asphalt-concrete core built in layers of 200 mm; Zone 5 is a rip-rap of rock blocks obtained from limestone quarry of sizes greater than 400 mm; and Zone 6 is a rockfill lining of well-graded material with diameter of 400mm.

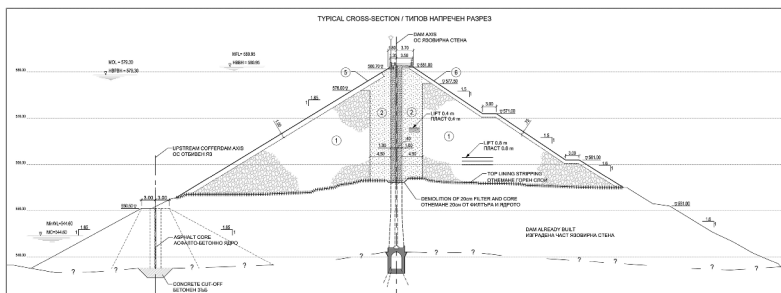


Figure 1. Typical cross section.

3 FINITE ELEMENT METHOD ANALYSIS

The first part of the current study consists in performing a finite-element method (FEM) analysis of the dam static and seismic behaviour. The ultimate objective is to enable comparing the calculated by means of the FEM analysis residual seismic displacements of the dam against the respective displacements obtained by means of simplified methods.

The behaviour of embankment fills is in general elastoplastic and is characterised by dependency of the stress levels. The Hardening Soil model enables simulating relatively well the behaviour of frictional materials like gravel and sand. It is based on an elasto-plastic formulation and can capture the basic properties of soil materials, which are namely pressure-dependency of stiffness, plastic shear yielding with hardening and dilatancy, as well as irreversible volumetric pre-consolidation. This leads to the so-called Double Hardening model. Its yield surfaces are shown in Figure 2. In addition, the model optionally allows the consideration of nonlinearity at small strains. The theoretical formulation of the model is described in Schanz et al. (1999); its parameters are calibrated based on triaxial shear and oedometer tests (see Section 4).

The behaviour of asphaltic-concrete is in general visco-elasto-plastic as well as strongly temperature dependent. While the elasto-plastic part of the behaviour is accounted for by the material model used itself, the rate and temperature dependence are implicitly accounted for by deriving the model parameters for the actual rate and temperature conditions. The parameters are calibrated based on triaxial shear tests performed on samples obtained from the already constructed part of the core (see Section 4).

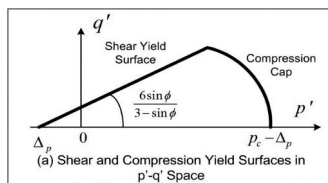


Figure 2. Graphical representation of the Double Hardening model yield surfaces.

It is assumed that the rock of the dam foundation, as well as the reinforced concrete of the grouting gallery respond linear-elastically to external loading. This assumption is based on the properties of these materials, their conditions of work and their location.

The nonlinear and nonelastic behaviour of the structures depends on their loading history. Therefore, the present analysis is performed taking into consideration the sequence of the dam construction and impoundment of the dam reservoir.

The seismic impacts are considered for conditions with dam reservoir full to Maximum Operating Level (MOL). Due to the nonlinear behaviour of the dam-foundation system, the seismic analyses are conducted in the time-domain by direct integration of the dynamic equilibrium equations in each time step. The viscous damping of the forced vibrations is modelled by means of the Rayleigh method.

The analysis is performed on a 2D finite element model of the dam-reservoir-foundation system by means of the Rocscience RS2 software package, Version 11. The analysis is carried out in the assumption of drained conditions.

3.1 Material parameters

3.1.1 Rockfill and Transition Zone materials

3.1.1.1 Static properties

The material behaviour of the Rockfill and the Transition Zone under static conditions has been investigated performing large-scale laboratory tests on the two fill materials. For this purpose, the grain size distribution of the Rockfill is scalped to 250 mm.

The shear strength is obtained from direct shear tests performed in shear boxes with dimensions of 1700 x 1700 x 1000 mm for the Rockfill and 800 x 800 x 1000 mm for the Transition Zone material. The tests were conducted both in dry and saturated conditions. Figure 3 shows the friction angles measured for different levels of normal stress applied. The friction angle is found to be higher for lower stress levels as well as for dry conditions compared to saturated ones. The difference in shear strength between dry and saturated conditions is considered in the analyses by applying two different friction angles. However, the change in friction angle due to different overburden stress is not taken into account in the analyses. The considered friction angles are derived for the (effective) stress level of 20 m of overburden which is assumed to be representative for the entire dam body. Thus, the angle of internal friction is obtained to be 45.5° and 43° for the Rockfill in dry (i.e. before impounding) and saturated conditions (i.e. after impounding) respectively. For the Transition Zone material, the angle of internal friction remains equal to 40.5° for both dry and saturated conditions since the decrease in friction angle due to the wetting of the material is entirely compensated by the increase in friction angle due to the lower effective stress level in saturated conditions.

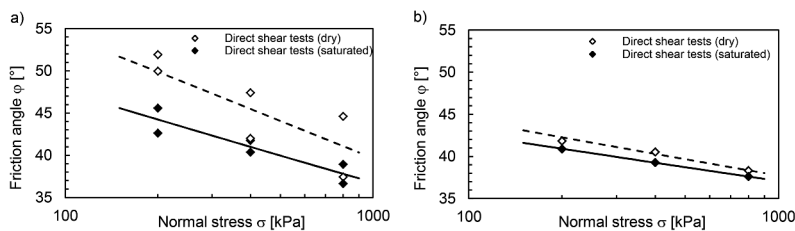


Figure 3. Friction angle depending on the level of normal stress: a) Rockfill, b) Transition Zone.

The so-called Hardening-Soil constitutive model is assumed to be appropriate for the fill materials. Its further parameters describing the deviatoric behaviour are estimated based on the results of the direct shear tests in comparison with triaxial shear tests performed on similar fill materials of another dam. The reference secant modulus E_{ref}^{50} , the failure ratio R_f and the dilatancy angle ψ are given in Table 1.

The stiffness of the fill materials is obtained from oedometer tests performed in the same shear boxes as the ones used for the direct shear tests. The parameters governing the volumetric behaviour of the Hardening-Soil model (i.e., the reference oedometer modulus E_{ref}^{oed} , the reference unload-reload modulus E_{ref}^{ur} and the exponent m) are calibrated on the change in volume measured in the oedometer tests (see Table 1). In addition, the Poisson's ratio is assumed to be equal to 0.25.

The density of the embankment materials is considered according to the in-situ measurements performed on the fill during construction. The porosity is calculated knowing the solid particle density which has been determined in the laboratory (see Table 1).

3.1.1.2 Dynamic properties

The maximum dynamic shear modulus of the fill materials is assumed to be depending on the effective mean stress p' :

$$G_0 = G_{ref}^0 \left(\frac{p'}{p'_{ref}} \right)^{\bar{m}} \quad (1)$$

where the reference maximum shear modulus G_{ref}^0 and the exponent \bar{m} are calibrated against relationships provided in Kokusho and Esashi (1981). The latter relationships giving the shear modulus as a function of the void ratio for crushed rock and round gravel are assumed to be representative for the Rockfill and the Transition Zone respectively.

As long the dynamic shear modulus is higher than the shear modulus given by the Hardening-Soil model for static conditions, its decay with shear strain is considered according to Hardin and Drnevich (1972).

$$G/G_0 = \frac{1}{1 + a \frac{\gamma}{\gamma_{0.7}}} \quad (2)$$

assuming $\gamma_{0.7}$ (i.e. the shear strain where $G \approx 0.7 G_0$) equal to 0.01% and a being equal to 0.385.

Since the constitutive model used allows for plastic work, a viscous damping ratio of only 0.5% is considered in order to address dissipation at small strains and potential rate effects.

3.1.2 Asphalt-concrete

3.1.2.1 Laboratory tests

The material behaviour of the asphalt concrete has been investigated performing triaxial shear tests on cylindrical samples (100 x 200 mm) taken from the already constructed part of the core of the dam. The samples containing 5.7% of B50 bitumen are tested at 5°C applying an axial strain rate of 2%/h and a confining pressure of 500 kPa. Figure 4 shows the measured deviatoric stress and volumetric strain during shearing.

Table 1. Material parameters of the Rockfill and the Transition Zone.

Parameters	Dimensions	Rockfill	Transition Zone
E_{ref}^{50}	[MPa]	35	22
E_{ref}^{oed}	[MPa]	30	18
E_{ref}^{ur}	[MPa]	240	150
p_{ref}	[MPa]	0.1	0.1
m	[-]	0.35	0.40
ν	[-]	0.25	0.25
c	[MPa]	0	0
φ	[°]	45.5/43.0	40.5/40.5
ψ	[°]	3	0
R_f	[-]	0.9	0.9
G_{ref}^0	[MPa]	410	250
\bar{m}	[-]	0.55	0.60
$\gamma_{0.7}$	[-]	0.0001	0.0001
a	[-]	0.385	0.385
ρ_d	[kg/m ³]	2000	1800
n	[-]	0.25	0.33

The constitutive behaviour of asphalt concrete is visco-elasto-plastic as well as strongly temperature dependent. Several assumptions are made in order to reduce the complexity of the constitutive behaviour for the analyses. Firstly, the temperature dependency is neglected since the temperature of 5°C at which the laboratory testing has been performed is assumed to be appropriate or even conservative for the dam site. Secondly, the viscous behaviour is not taken into account by the constitutive model itself. However, the parameters of the model considered for the static and the dynamic analyses are chosen differently taking into account the prevailing strain rates.

Therefore, the remaining purely elasto-plastic constitutive behaviour is aimed to be taken into account by a rather simple model, being aware of the major influence of the strain rate and the temperature not taken into account by the model itself. As a consequence, features such as the stress-dependency of stiffness and volumetric yielding (of the almost incompressible asphalt concrete material) are ignored since they are of relatively minor influence.

The elasto-plastic constitutive model assumed to be appropriate is including linear elasticity, the Mohr-Coulomb failure criterion, frictional strain hardening with the hardening rule after Duncan-Chang and a non-associated flow rule. Its parameters are calibrated against the triaxial shear tests performed (see Figure 4). The angle of friction is found to be 46.5° after assuming the cohesion to be equal to 250 kPa. The dilatancy angle is obtained to be 11.5°. The Young's modulus, the secant modulus and the failure ratio are found to be 180 MPa, 90 MPa and 0.9 respectively. In addition, the Poisson's ratio is assumed to 0.46 according to Wang and Höeg (2016).

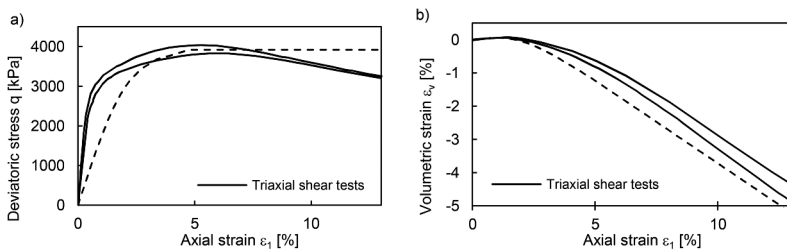


Figure 4. Comparison of the results of triaxial shear tests performed on asphalt concrete samples against finite element calculations: a) deviatoric stress for the applied axial strain, b) volumetric strain for the applied axial strain.

3.1.2.2 Static properties

The strain rates in the asphalt core during the construction and impounding process are expected to be around four orders of magnitude lower than the strain rate at which the laboratory tests have been performed. Due to the viscous component of the asphalt concrete stiffness, the core is supposed to be considerably softer during construction and impounding than measured in the laboratory. In order to account for the influence of the different strain rates, the stiffness parameters (i.e., the Young's modulus E and the secant modulus E_{50}) are divided by a factor of 3. This correction factor is estimated based on the data provided by Wang and Höeg (2016) taking into account that below a certain low strain rate no further reduction in modulus is observed. The correction factor applied is confirmed by tests performed at different strain rates on core samples of another dam.

The shear strength and the plastic flow are supposed not to be affected by different strain rates. The resulting material parameters considered for the static analysis are given in Table 2.

3.1.2.3 Dynamic properties

The strain rates in the asphalt core during an earthquake are expected to be around three to four orders of magnitude higher than the strain rate at which the laboratory tests have been performed. Therefore, the core is supposed to be considerably stiffer when subjected to seismic excitation than measured in the laboratory. The dynamic stiffness is estimated based on the results of cyclic triaxial shear test performed at 5°C on samples with a comparable content of a similar bitumen provided by Feizi-Khankandi et al. (2008). The correction factor to be applied on the stiffness parameters (i.e., the Young's modulus E and the secant modulus E_{50}) is found to be around 30.

The material parameters considered for the dynamic analysis are given in Table 2.

Table 2. Material parameters of the asphalt concrete.

Parameters	Units	Static properties	Dynamic properties
E	[MPa]	60	5'400
E_{50}	[MPa]	30	2'700
ν	[-]	0.46	0.46
c	[MPa]	0.25	0.25
φ	[°]	46.5	46.5
ψ	[°]	11.5	11.5
R_f	[-]	0.9	0.9
ρ_d	[kg/m ³]	2430	2430
n	[-]	0.025	0.025

3.1.3 Foundation

The foundation is composed of rock (conglomerate), which is assumed homogeneous, isotropic and with linear elastic constitutive behaviour. The values for unit weight, Young's modulus and the Poisson's ratio are assumed to be 26 kN/m³ 1 500 MPa and 0.33 respectively.

3.2 Definition of the acceleration time-histories

The analyses of the developed dam model under earthquake excitation were performed in the time-domain using two sets of acceleration time-histories for the horizontal and vertical components, as described in more detail below.

The first of these sets is a synthetic one generated with respect to a given target response spectrum. The PGA of the horizontal excitation component is 0.15g. The vertical component was scaled so that the PGA is 2/3 of the horizontal component PGA.

Since the dam site is located in Northern Bulgaria, the second set of input acceleration time-histories was taken from a real record set from Vrancea which represents the most decisive source for this part of Bulgaria. Both the horizontal and the vertical components were scaled

to the above PGA values. Since this set is used for comparison purposes, the response spectra of these recordings naturally differ significantly from the aforementioned design response spectrum used in generating the artificial acceleration time-histories.

3.2.1 Artificially generated acceleration time-histories

As already mentioned above, the seismic excitation on the dam is represented in one of the FEM models for the seismic input by two synthetic acceleration time-histories compatible with the given response spectrum. One of the acceleration time-history is applied in the horizontal direction and the other one is applied in the vertical direction.

The acceleration time-histories for the two spatial components have been taken from the database of the Swiss Federal Office of Energy, BWG (2003), which is also responsible for dam safety. These synthetic acceleration time-histories conform to the following requirements:

- The time length of stationary part of the acceleration time-histories is:

$$T_3 = 10 + 50 \cdot \left(\frac{a_h}{g} - 1 \right) \quad (3)$$

where $T_{3,min} = 10$ sec

- The difference between the given target response spectrum and the one of the generated synthetic accelerograms may not be larger than 10%; moreover, the resulting response spectrum of a generated accelerogram shall always be above the target one in the dominating range of eigenfrequencies of the particular structure considered.

The Arias intensity of the artificially generated excitation horizontal component is 0.54 m/s.

3.2.2 Site-specific acceleration time-histories

As mentioned above, the set of acceleration records used here represents the records of the real Vrancea earthquake of 4th March 1977, 19:21, IZIIS (1977), since the source of the Vrancea mountain in Romania has a decisive influence on the seismological situation in Northern Bulgaria.

The total length of the record for all the components is 43.4 sec. The maximum horizontal PGA was 0.44403 m/s². For the comparison purposes of the analysis performed here, scaling of the input signals were necessary so that the maximum horizontal PGA becomes 0.15g. Thus, a scale factor of 3.31396 was applied to all component records. It is emphasised that the record for the vertical earthquake component was scaled by the same factor without considering certain ratio (e.g., 2/3) between the maximum PGA of the vertical and horizontal records. The Arias intensity of the site-specific excitation horizontal component is 0.55 m/s.

3.3 FEM Model

The analyses are performed on a two-dimensional FEM model of the dam – foundation – reservoir system. The dam geometry shown in Figure 1 is slightly simplified by assuming a horizontal foundation surface at the location of the typical section. The grouting gallery at the bottom of the core, as well as the retaining walls at the dam crest are neglected. The modelled part of the foundation extends 50 m in depth and 100 m upstream and downstream from the respective dam toes. The FEM mesh consists of 3200 quadrilateral elements with eight nodes, the maximum size of which corresponds to the specifics of the model and the purposes of this study.

As already stated, due to the nonlinear response of the dam-foundation system to the external loads, the analyses are performed by modelling, in a realistic way, the history of loading. After defining the initial state of the foundation, the static loads from the self-weight of the dam fill are introduced in nine further steps. The loads due to groundwater flow and hydrostatic pressure are next modelled by simulating the dam impoundment to MOL in nine consecutive stages. At each stage of impounding the analysis is performed in two uncoupled steps. In the first step, a steady-state seepage analysis is performed in order to determine the pore-water pressure field. In the second step, the calculated pore-water pressures are used in mechanical analysis to define the dam-foundation system's displacements, strains and stresses. At the end, the strong ground motions due to earthquake impact are specified.

Different mechanical boundary conditions are applied in the static and dynamic analyses.

In the static analyses, kinematic constraints are set in the direction perpendicular to the vertical and lower boundaries of the rock foundation.

The dynamic boundary conditions consist of transmitting boundaries along the vertical extremities and absorbing boundaries along the bottom of the modelled part of the rock foundation. The foundation base is specified as compliant base and the drift correction option of RS2 is also used. The seismic input is specified as horizontal and vertical velocity time-histories which are applied to the bottom of the modelled part of the rock foundation. The velocity time-histories are defined by deconvolving the provided outcrop acceleration time-histories. The mesh of finite elements and the dynamic boundary conditions are given in Figure 5.

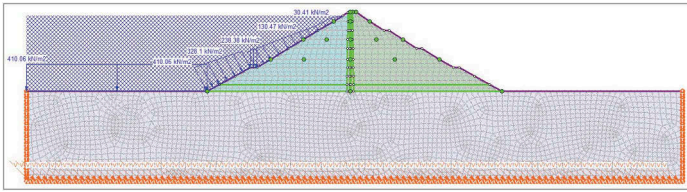


Figure 5. FEM model and dynamic boundary conditions in the seismic analysis.

3.4 FEM analysis results

3.4.1 Static analysis results

Figures 6 and 7 show the end-of-construction (EoC) and the end-of-impoundment (EoI) horizontal and vertical displacement contours. The maximum settlements due to the construction process occur in the central part of the dam body and amount to 0.13 m. At the end of the impoundment, the horizontal displacements increase in the central zone of the dam body and reach 0.06 m, which is caused by the effect of the impervious core. At the same time, upstream from the core the settlements increase to 0.16 m.

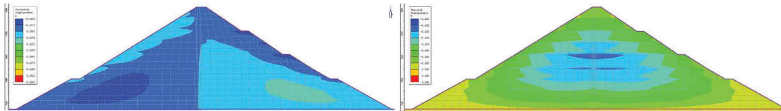


Figure 6. End-of-construction horizontal and vertical displacements, m.

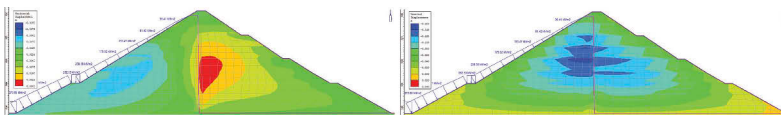


Figure 7. End-of-impoundment horizontal and vertical displacements, m.

Figures 8 and 9 show the EoC and the EoI horizontal and vertical effective stress contours. The EoC vertical stress contours run parallel to the dam outer contour, i.e., to the polygon formed by the upstream face, the crest and the downstream face of the dam. Due to the impounding, the horizontal and the vertical effective stress reduce in the upstream shell, which is coupled with a significant increase of the horizontal stresses in the downstream shell.

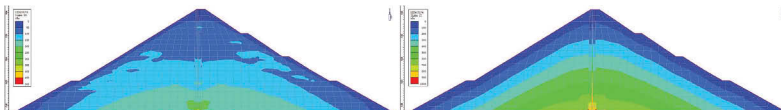


Figure 8. End-of-construction horizontal (on the left) and vertical (on the right) effective stresses, kPa.

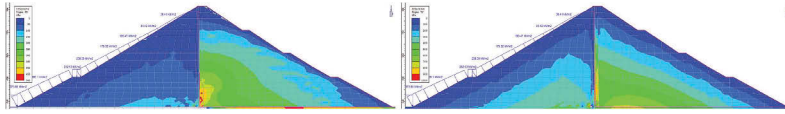


Figure 9. End-of-impoundment horizontal (on the left) and vertical (on the right) effective stresses, kPa.

3.4.2 Dynamic analysis results

For the two types of seismic input studied, i.e., artificially generated and site-specific acceleration time-histories, the maximum horizontal dynamic displacements occur on the downstream slope, at a level about 10 meters below the crest, while the maximum vertical dynamic displacements occur in the upstream shell, in a zone also 10 meters below the crest, but midway between the upstream slope and the core. Figures 10 and 11 show the time-histories of the dynamic displacements at these locations for both types of seismic input (the results for the artificially generated acceleration time-histories are shown in the figures on the left). As can be seen in these figures, in terms of displacements, the seismic response of the dam to the artificially generated seismic input is significantly higher than that to the site-specific input. The maximum permanent horizontal and vertical displacements at the end of the strong ground motions are, approximately, 6 cm and 16 cm for the former versus 3 cm and 8 cm for the latter, respectively. That is, the artificially generated input gives a maximum permanent displacement twice as high as the site-specific input.

The maximum shear strains in the dam body at the end of the earthquake are compared in Figure 12. They reach 2.2‰ for the artificially generated seismic input and 1.5‰ for the site-specific seismic input. This comparison of maximum shear strains confirms the observation that the dam response is significantly higher for the artificially generated acceleration time histories.

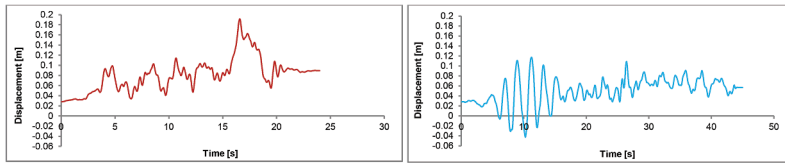


Figure 10. Time-history of the horizontal displacements in critical zones near the dam crest.

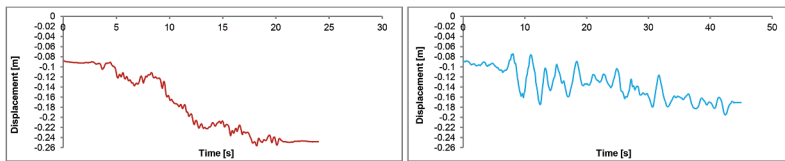


Figure 11. Time-history of the vertical displacements in critical zones near the dam crest.

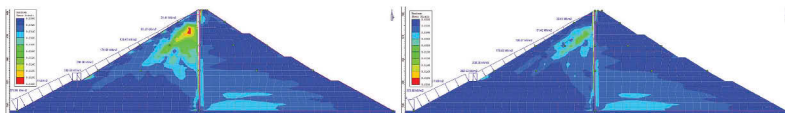


Figure 12. Contours of the maximum shear strains.

4 ESTIMATION OF DEFORMATIONS USING SIMPLIFIED METHODS

For comparison purpose, the earthquake-induced deformations are estimated by using two simplified methods which do not require finite element modelling. The shear deformations are calculated applying the decoupled method of Makdisi and Seed (1978) and the coupled method of Bray and Travasarou (2007). Both methods are based on correlations which allow estimating the amount of

shear deformations depending on the so-called critical (or yield) seismic coefficient k_y , the spectral accelerations S_a for different eigenmodes and the earthquake magnitude M .

The critical seismic coefficient is derived by means of a slope stability analysis. To keep the results of the different methods comparable to each other, the friction angles, the densities and the geometry assumed are the same as the ones used for the FEM analyses. The determinant mechanism is found to form around 5 m under the upstream surface and ranging from the crest to the upstream berm. It is noteworthy that the location of the critical mechanism coincides with the major shear strains calculated in the FEM analysis (see Figure 12). The critical horizontal seismic coefficient is obtained to be 0.12 when applying also a vertical seismic coefficient of $k_v=2/3*k_y=0.08$.

The spectral accelerations for different eigenmodes are derived considering soil class A and a damping ratio of 5% according to the relevant code (BCA, 1985). The fundamental period of the dam is estimated to be 0.33s based on the analytical solution by Sarma (1979) assuming the small strain stiffnesses as given in Section 3.1.1.2. The corresponding spectral acceleration S_{a1} is obtained to be 0.26g, which is the same also for the second and the third eigenmode due to the plateau in the response spectrum. The spectral acceleration for the period of $1.5*S_{a1}$ is equal to 0.19g.

The determinant magnitude M is assumed to be 7.5 since earthquakes such as the Vrancea earthquake of 1977 are considered to contribute mainly to the local seismic hazard.

Based on these assumptions, the methods after Makdisi and Seed (1978) and Bray and Travarou (2007) result in median estimates for the shear displacements of 6 cm and 2 cm respectively. The estimate after Makdisi and Seed (1978) is found to be very close to the horizontal displacements obtained in the finite element analysis at the crest level (see Table 3).

Table 3. Comparison of horizontal displacements calculated by different methods.

Method	Makdisi & Seed (1978)	Bray & Travarou (2007)	FE analysis with synthetic accelerations	FE analysis with recorded accelerations
Displacements	6 cm	2 cm	6 cm	3 cm
Range	1 cm – 15 cm	1 cm – 3 cm	-	-
Type of range	min – max	84% – 16% exc.	-	-

Furthermore, the estimate after Bray and Travarou (2007) is found to be quite lower than the estimate after Makdisi and Seed (1978). A respective comparison by Rathje and Bray (1999) suggests that this difference is due to the coupled and respectively uncoupled nature of the two approaches. For an uncoupled approach, it is assumed that the seismic response is not affected by the sliding response and the related loss in stiffness, whereas a coupled approach accounts for this interaction. For the case under study (with ratios in between the fundamental period of the dam and the mean periods of the applied acceleration time series of 0.8 and 0.3 and with a ratio in between the critical acceleration and the maximum acceleration of around 0.44), a decoupled approach such as the one by Makdisi and Seed (1978) is indeed expected to result in higher displacements (Rathje and Bray, 1999). However, it should be noted that it could also be the opposite for different cases with different ratios.

5 CONCLUSION

This study presents a comparison of the results for the characteristic seismic horizontal displacements of a typical ACRD obtained by the FEM method on the one hand and by two simplified methods on the other hand.

It is shown that if the coupled approach is applied to both the FEM analysis and the simplified calculation, the results of both methods are almost identical for analysis with site-specific seismic input. On the other hand, the uncoupled simplified calculations and the coupled FEM analysis with synthetic acceleration input yield higher seismic response of the investigated dam.

In conclusion, the simplified methods allow for a quick estimate of certain seismic response parameters to be used at a preliminary design/verification stage. However, the FEM analysis yields much more comprehensive information on the seismic behaviour of ACRD.

REFERENCES

- BCA 1985. *Bulgarian norms for design of hydraulic structures*.
- Bray, J.D. & Travasarou, T. 2007. Simplified procedure for estimating earthquake-induced deviatoric slope displacements. *Journal of geotechnical and geoenvironmental engineering* 133(4): 381–392.
- Bundesamt für Wasser und Geologie BWG (2003). *Beschleunigungszeitverläufe in Übereinstimmung mit der BWG Richtlinie zur Erdbebensicherheit von Stauanlagen*.
- Feizi-Khankandi, S., Mirghasemi, A. A., Ghalandarzadeh, A. & Hoeg, K. 2008. Cyclic triaxial tests on asphalt concrete as a water barrier for embankment dams. *Soils and Foundations* 48(3): 319–332.
- Hardin, B.O. & Drnevich, V.P. 1972. Shear modulus and damping in soils: Design equations and curves. *J. Soil Mech. Found. Div. ASCE* 98(7): 667–692.
- IZIIS, Skopje, 1977. *Publication no. 55*.
- Kokusho, T. & Esashi, Y. 1981. Cyclic triaxial test on sands and coarse materials. *Proceedings of the 10th international conference on soil mechanics and foundation engineering, Stockholm, 15-19 June 1981*. Balkema, Rotterdam.
- Mahabadi, S.G., Roosta, R.M., Seismic analysis and design of asphaltic concrete core embankment dams, *Hydropower & Dams*, Issue Six, 2002, pp.75–78.
- Makdisi, F.I., & Seed, H.B. 1978. Simplified procedure for estimating dam and embankment earthquake-induced deformations. *Journal of the Geotechnical Engineering Division* 104(7): 849–867.
- Rathje, E.M., & Bray, J.D. 1999. An examination of simplified earthquake-induced displacement procedures for earth structures. *Canadian Geotechnical Journal* 36(1): 72–87.
- Schanz, T., Vermeer, P.A. & Bonnier P.G. 1999. The hardening soil model: Formulation and verification. *Beyond 2000 in Computational Geotechnics*. Balkema, Rotterdam.
- Valstad, T., Selnes, P.B., Nadim, F., Aspen, B., Seismic response of a rockfill dam with an asphaltic concrete core, *Water Power & Dam Construction*, April 1991, pp.22–27
- Wang, W. & Höeg, K. 2016. Simplified material model for analysis of asphalt core in embankment dams. *Construction and Building Materials* 124: 199–207.

Trift Arch Dam – an opportunity for hydropower generation due to a retreating glacier

A.D. Tzenkov, O. Vallotton & A. Mellal
Gruner Stucky Ltd, Renens, Switzerland

ABSTRACT: This article presents the concept for construction of an arch dam at the former downstream end of the retreating Trift Glacier in Switzerland. It describes the context of the project, the approach adopted for defining and optimising the shape of the arch dam, as well as the static and dynamic structural analyses carried out to verify the dam safety.

1 INTRODUCTION

1.1 *Glacier retreat*

With global warming, the melting of the Swiss glaciers has various effects on the operation of hydropower plants. Some are negative, such as the increase in erodible surfaces or the collapse of moraines, which can lead to an increase in sediments. Others are positive for hydropower production, as the melting of glaciers temporarily increases the water supply. The disappearance of glaciers also creates new surfaces, some of which may be suitable for new developments. The rapid retreat of the Trift Glacier in the Gadmertal in the Bernese Oberland created in 1998 a new natural lake at the entrance to a narrow gorge at an altitude of 1650 m.

An analysis of the national topographic maps speaks for itself. In 150 years, the retreat of the glacier front by almost 4 km is spectacular, see Figure 1. Perhaps even more impressive is that 150 years ago the thickness of the glacier at the site of today's new natural lake was over 300 m.

The retreat of the glacier even seems to be accelerating, since less than 50 years ago, the thickness of the ice above the future lake was still 150 m and the glacier was reaching the gorge.

1.2 *New hydropower development*

Today, the combination of a narrow gorge and a significant widening of the valley upstream offers an ideal opportunity for the creation of a new 85 million m³ reservoir. This reservoir will not only collect water from its own catchment area, in particular meltwater from the Trift Glacier, but also, via new aqueducts, from the neighbouring valleys. The water from this reservoir will be turbinised in a new hydroelectric power plant with a hydraulic head of 425 m. The installed capacity of this plant will be 80 MW and the expected electrical production is 145 GWh/year. After the hydropower plant, the water will be conveyed to the existing, highly complex KWO scheme (see Figure 2) in order to utilise other potential, resulting in overall capacity to produce 215 GWh in the winter period.

To minimise the impact of the new facility on the landscape, KWO has chosen to build the new hydroelectric plant underground. All accesses to the plant and to the dam will also be underground. Finally, only the dam will be visible.

1.3 *Trift dam*

The site of the Trift Dam came into being only a few years ago as a result of the melting of the glacier of the same name. The construction of this retention structure combined with a new power station, all connected to the existing KWO hydropower scheme, will make it possible to

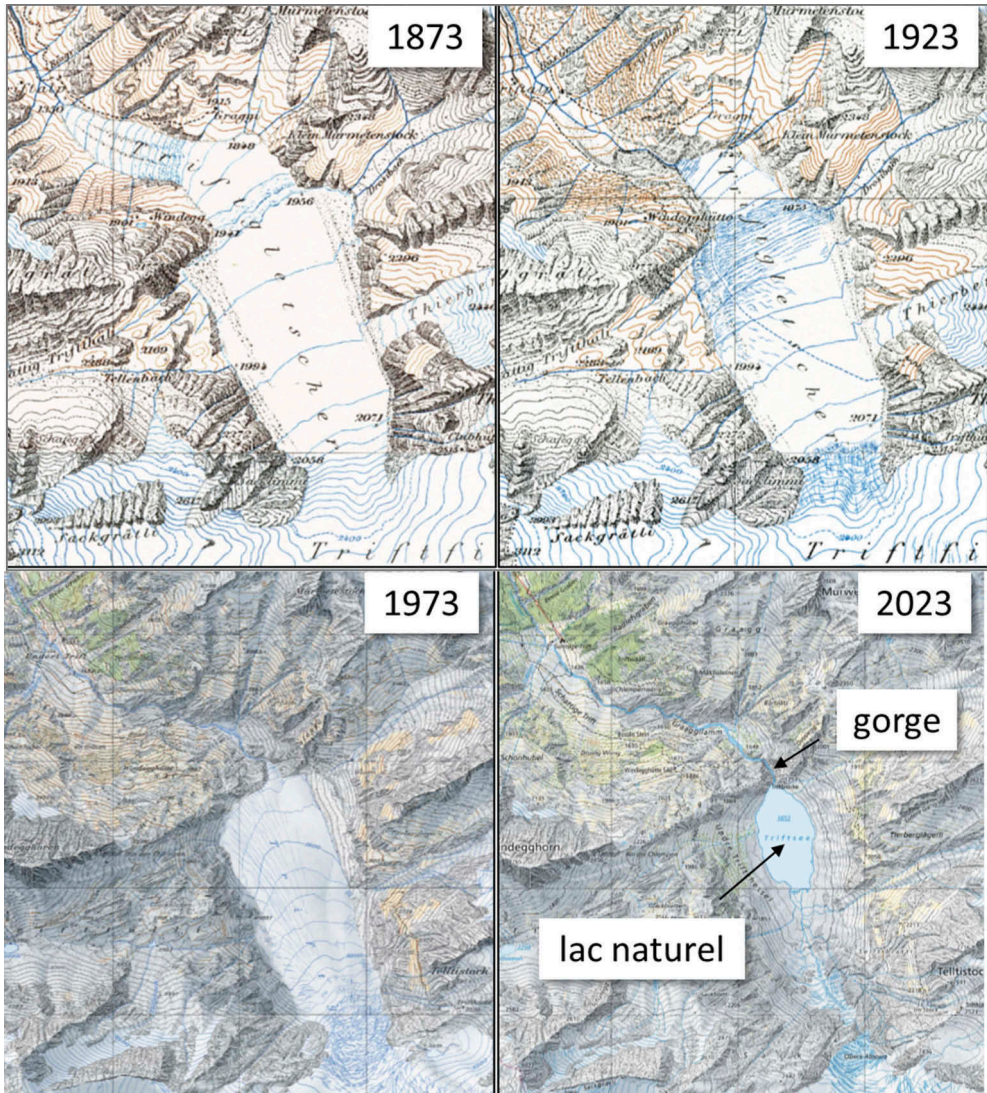


Figure 1. Development of the Trift glacier retreat and appearance of the natural lake (© swisstopo).

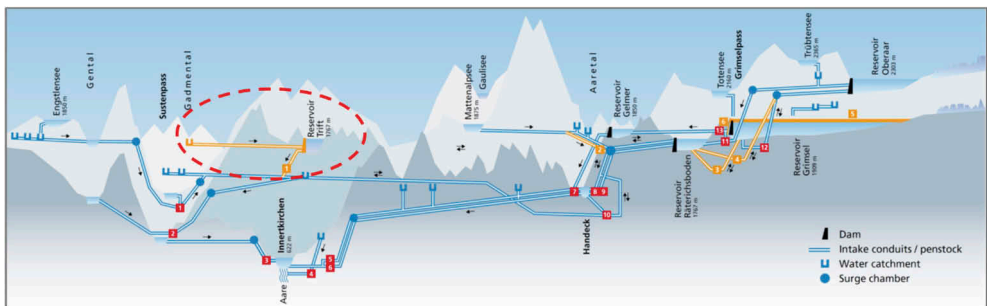


Figure 2. Schematic longitudinal profile of the KWO development with the new Trift branch circled in red (© KWO).

produce more electricity from non-fossil fuels. It will also offer a significant potential for winter production, which is currently in great demand in Switzerland.

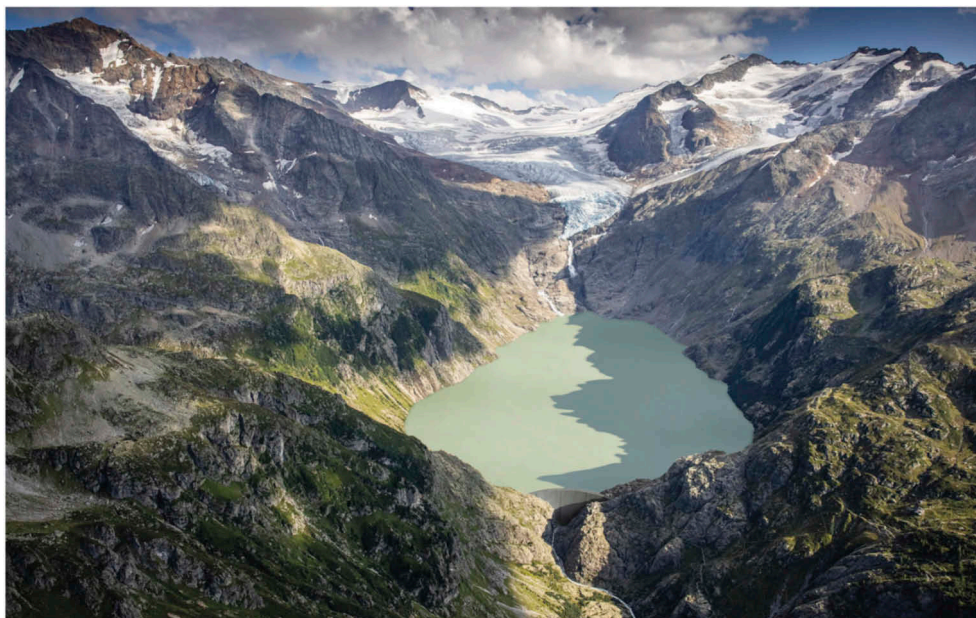


Figure 3. Photomontage of the Trift dam and reservoir (© KWO).

2 DEFINITION OF THE DAM LOCATION AND SHAPE

2.1 *Definition of the dam location*

In view of the identified topographical and geological conditions, it has been decided that the best location of the planned Trift Dam is at the rock sill of the current lake, i.e., at the transition between the latter and the downstream valley. At this location, the site is V-shaped, relatively narrow, slightly asymmetrical, with steep abutments and composed of solid rock. Such conditions predefine to a large extent a double-curvature arch dam as the optimal dam type to be implemented.

Placing the dam at this location, and not upstream from the lake sill, allows avoiding excavating the largely water-saturated sediments of the lake. On the other hand, the possible dam sites downstream from the sill are significantly wider. Hence the selected location provides for an optimal dam height and concrete volume, good topographical conditions, and sound rock foundation.

2.2 *Preliminary definition of the dam shape*

The shape of the planned double-curvature arch dam has been defined with horizontal parabolas. An iterative shape optimisation procedure has been followed using in-house computer-aided design tools especially developed for arch dam applications.

The following criteria for a successful shape definition have been applied:

- A favourable distribution of the compressive stresses is to be provided and the maximum compressive stress shall not be higher than one third of the compressive strength of concrete.
- Vertical tensile stresses at the lowest point of the concrete-rock interface are to be avoided for the basic load combination of self-weight and hydrostatic pressure at full reservoir. Horizontal tensile stresses at the upstream face of the arch abutments and at the downstream face of the arch cantilevers are to be kept as low as possible.

- The upstream overhangs of the lateral cantilevers are to be controlled to avoid tensile stress during construction, as well as to minimise the upward component of the hydrostatic forces.
- The downstream overhangs of the central cantilevers are to be controlled to avoid tensile stress during construction.
- Smooth dam profiles are to be provided.
- The optimisation of the dam shape seeks reasonably low concrete volume.

Based on the design criteria and constraints presented above, the precise geometry of the chosen parabolic arch dam is defined for the crown cantilever profile, the main parabolas and the dam footprint.

The main characteristics of the dam, considering the excavation on the banks, are as follows:

- Dam height: 125 m.
- Crest length and crest width: 350 m and 5.40 m, respectively.
- Dam base width: 17.44 m.
- Maximum arch width at the abutments: 19.7 m.
- Upstream face and downstream face areas: 20'500 m² and 19'580 m², respectively.
- Total volume of the dam: 243'750 m³.
- Slenderness coefficient: 13.8 .

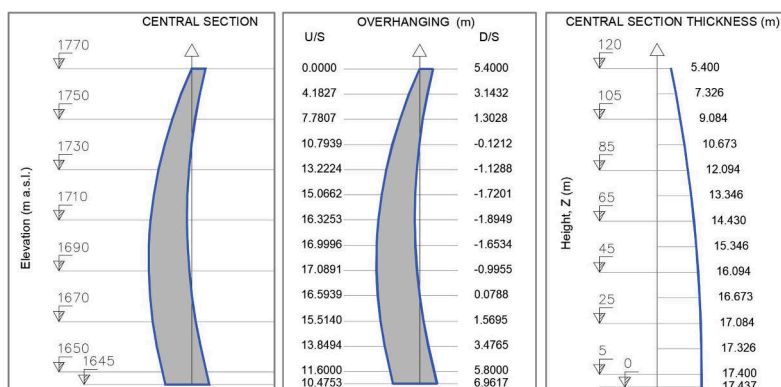


Figure 4. Geometrical definition of the arch dam central section (preliminary).

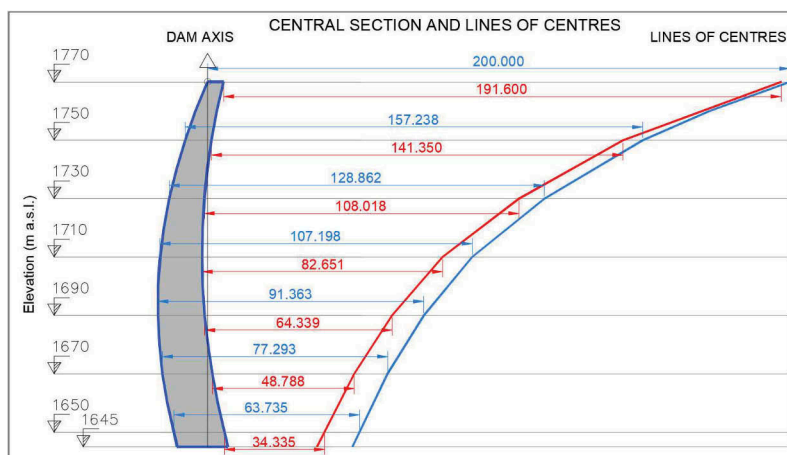


Figure 5. Geometrical definition of the lines of centres (preliminary).

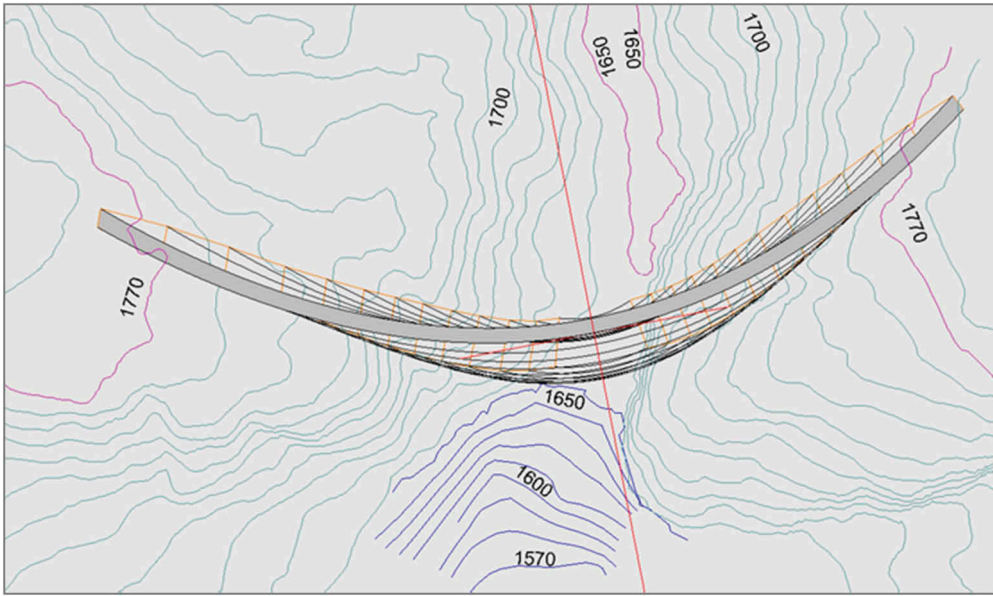


Figure 6. Plan view (preliminary).

3 FEM ANALYSIS AND STRUCTURAL DESIGN

The calculations have been carried out in accordance with international practice, the recommendations of the ICOLD/CIGB and the guidelines of the Swiss Federal Office of Energy (BFE 2016, BFE 2017). Trift Dam must meet the requirements set by the SFOE for a Class I concrete dam.

The FEM analysis has been performed by means of the software program Z-SOIL, in the assumption of linear-elastic behaviour of the dam-foundation system. The foundation material has been assumed massless and isotropic. An attempt has been made to model the topographic conditions as realistically as possible.

3.1 Material parameters

The adopted material parameters are given in Table 1.

Table 1. Material parameters.

Material	Young's Modulus	Poisson's Ratio	Unit Weight	Thermal Expansion	Thermal Conductivity	Volumetric Heat Capacity
	E [GPa]	ν [-]	γ [kN/m ³]	α [1/°C]	k [kJ/(m d°C)]	c [kJ/(m ³ °C)]
Concrete	25	0.25	24.5	0.87E-5	241.9	2180
Rock	30	0.25	0.00	1.00E-5	259.2	2160

3.2 Load cases and load combinations

The following load cases have been considered:

- Self-weight (construction stages)
- Hydrostatic pressure
- Thermal gradients (seasonal temperature variations)
- Earthquake

A constant value of 8°C is assumed when grouting the block joints and is used as the thermal reference condition for the calculation of the thermal gradient. The temperature gradients within the dam and its foundation are determined with respect to an initial state for four characteristic states (TC1, TC2, TSU and TWI) occurring at different times. The estimated time points are as follows (see also Figure 7):

- TC1: Temperatures at Full Supply Level (1767 m a.s.l.) (September).
- TC2: Temperatures at Minimum Operating Level (1660 m a.s.l.) (April).
- TSU: Maximum summer temperatures (July).
- TWI: Minimum winter temperatures (January).

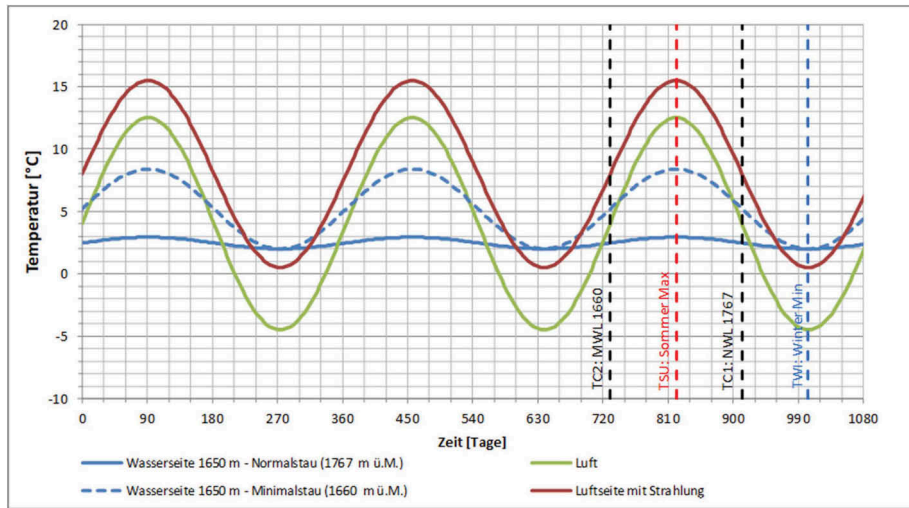


Figure 7. Temperature cycles acting on the upstream and downstream dam faces.

The seismic impact has been defined following the directives of SFOE, as follows:

- Earthquake return period: 10 000 years (Safety Evaluation Earthquake, SEE).
- Peak ground accelerations at the dam site:
horizontal: 0.29 g
vertical: 0.19 g
- Three series of stochastically independent synthetic acceleration time-histories compatible with the local response spectrum.

The investigated load combinations and the corresponding factors of safety with respect to the maximum compressive and tensile stresses are shown in Figure 8.

3.3 FEM model

The static and dynamic behaviour of the planned Trift Dam has been investigated on a 3D FEM model of the dam-foundation system, see Figure 9. The FEM model is built with hexahedral and tetrahedral elements with linear interpolation of the shape functions. The dam-reservoir interaction is represented by Westergaard added masses (Westergaard 1931) at the upstream face nodal points. The viscous damping of the dam-foundation system is simulated by means of the Rayleigh method by setting the proportionality constants so as to give a modal damping ratio of 5% in the first and the nineteenth vibration modes. A time step of 0.01 seconds is used in the α -method of Hughes, Hilbert and Taylor (Hughes 1987) with $\alpha = -0.3$ for direct integration of the equations of motion of the system. A criterion of 0.01 is set for displacement and force convergence.

Load Case		Self-Weight	Hydrostatic Pressure		Thermal Loading				Earth-quake 10 000 Years	Safety Factor	
Load Combination			FSL	MinWL	TC ₁	TC ₂	TSU	TWI		Com- pression	Tension
Static Usual	SU0	✓	✓							3.0	2.0
	SU1	✓	✓		✓					3.0	2.0
	SU2	✓		✓		✓				3.0	2.0
Static Unusual	SUN1	✓	✓				✓			2.0	1.5
	SUN2	✓		✓				✓		2.0	1.5
	SUN3	✓	✓					✓		2.0	1.5
	SUN4	✓		✓			✓			2.0	1.5
Dynamic Extreme	DE1	✓	✓		✓				✓	1.5	1

Figure 8. Investigated load combinations and required local safety factors.

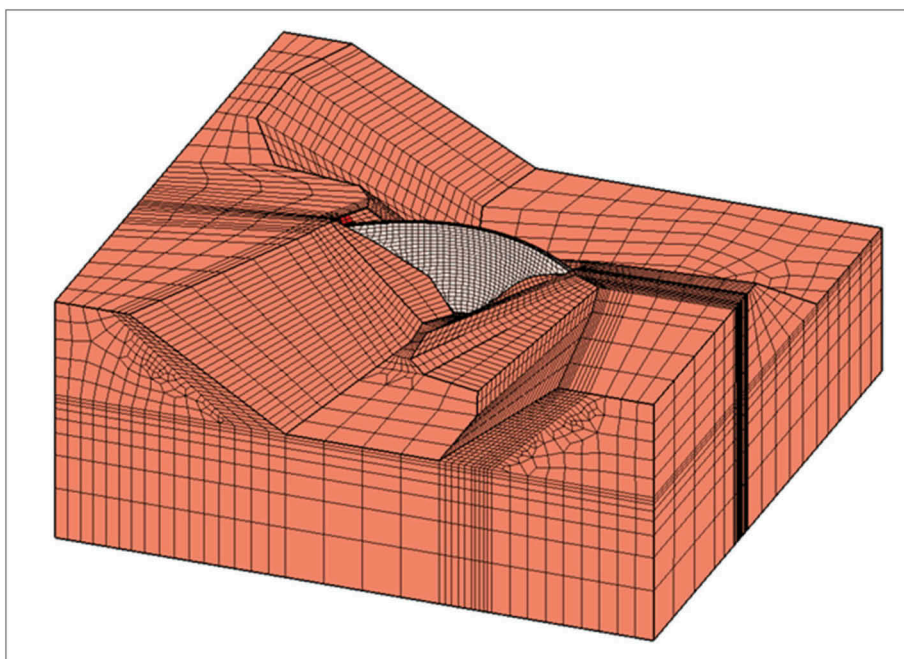


Figure 9. Finite element model of the dam-foundation system.

3.4 Static and dynamic analyses

The deformed shape of the dam for Load Combination SU1 is given in Figure 10. The maximum displacements are at the crest of the dam and reach 3.5 cm.

The principal compressive stresses for Load Combination SU1 on the upstream and downstream faces of the dam are shown in Figures 11 and 12 respectively. Note that compressive

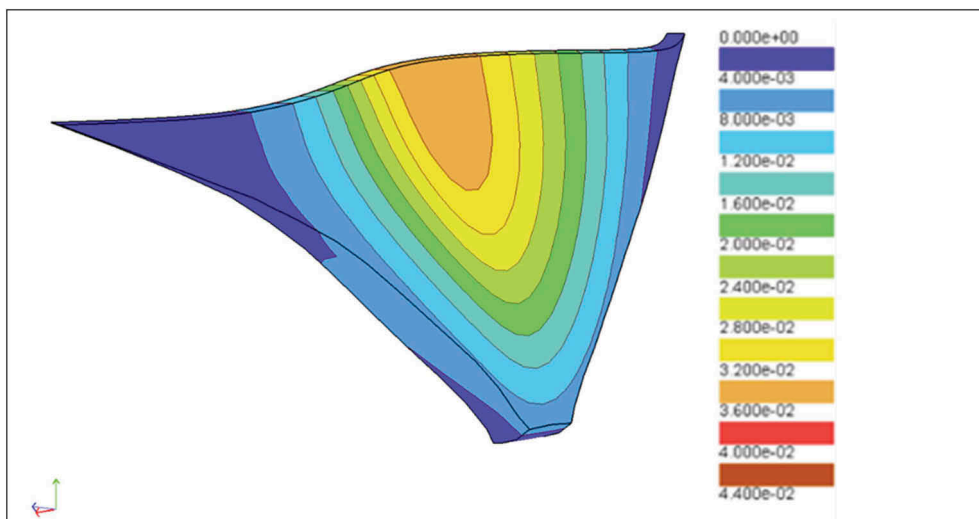


Figure 10. Deformed shape and displacements [m] of the dam for SU1.

stresses are negative, while tensile stresses are positive. The maximum compressive stresses on the upstream side are in the middle part and reach 5 MPa, while on the downstream face they attain 9 MPa in a very limited area at the lower third part of the dam, close to the dam-foundation interface.

The values of the maximum accelerations in the dam body obtained from the time-history dynamic analysis are given in Table 2. The accelerations in the cross-valley direction attain 0.7 g, which corresponds to a dynamic amplification of 2.4 times the horizontal component of the PGA (0.29 g). The peak vertical acceleration is 0.94 g, i.e., 4.9 times the vertical component of the PGA (0.19 g). The maximum dynamic amplification is obtained for the along-valley accelerations at the dam crest, which reach 3.1 g. This compares well with the natural frequencies of the dam-reservoir-foundation system, whose mass is activated mainly in the along-valley direction.

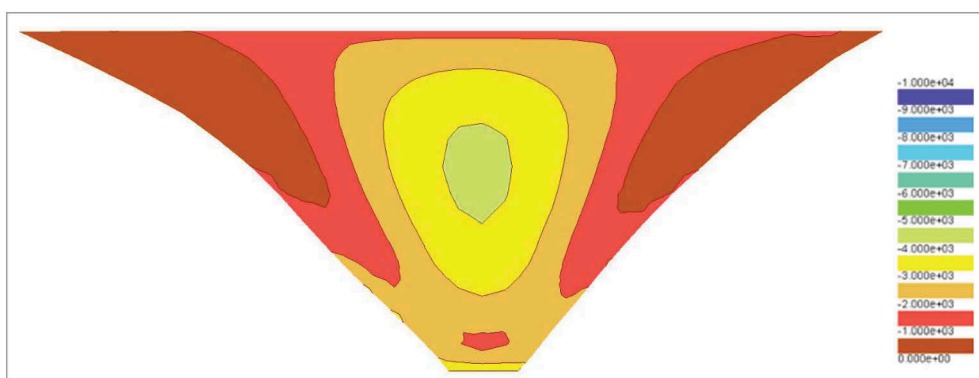


Figure 11. Principal compressive stresses [kPa] on the upstream face of the dam for SU1.

The envelopes of the maximum values of the compressive stresses for Load Combination DE1 with Series 2 of acceleration time histories are given in Figures 13 and 14 for the upstream and the downstream faces of the dam, respectively.

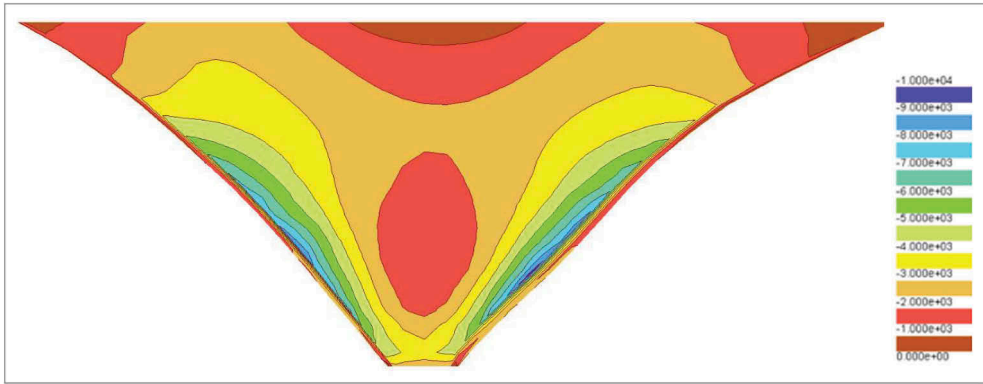


Figure 12. Principal compressive stresses [kPa] on the downstream face of the dam for SU1.

Table 2. Accelerations [g] at the crown cantilever crest.

Load combination	Cross-valley		Vertical		Along-valley	
	min	max	min	max	min	max
DE1 with Series 1	-0.53	0.59	-0.66	0.65	-2.86	2.98
DE1 with Series 2	-0.68	0.70	-0.77	0.77	-3.09	2.97
DE1 with Series 3	-0.58	0.56	-0.94	0.78	-2.77	2.97

On the upstream face, the maximum compressive stresses in case of SEE occur in the middle of the crest and extend approximately 25 m downward. On the downstream face, they are found near the dam-foundation interface in the lower part of the dam. However, the peaks of the principal compressive stresses never exceed 15 MPa, which is below the dynamic compressive strength of the concrete.

The envelopes of the maximum values of the tensile stresses on the downstream face of the dam for Load Combination DE1 and Series 2 of the seismic input are given in Figure 15. The maximum tensile stresses are calculated for a zone near the crest of the dam's central cantilevers. However, these stresses are in the arch direction, and will cause opening and subsequent closing of the contraction (block) joints. Since the latter are equipped with waterstops, no uncontrolled release of water will occur.

There are two other zones on the downstream side where the tensile stresses have high values. They are located in the upper left and right parts, about 25 to 30 metres below the crown. Their peaks are 4.4 MPa in the left zone and 4.7 MPa in the right zone. These tensile stresses have a horizontal and a vertical component. The vertical components, which can lead to cracking in the mass concrete, reach just under 2.5 MPa, which is less than the dynamic tensile strength of concrete and, therefore, will not lead to crack initiation and propagation.

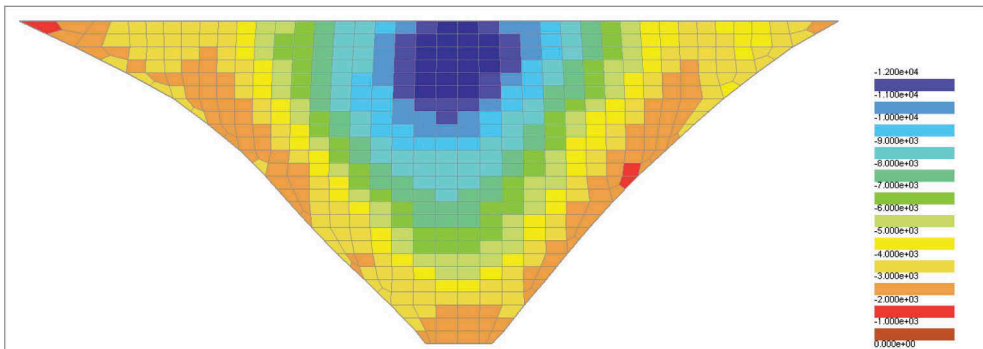


Figure 13. Principal compressive stresses [kPa] envelopes on the upstream face for DE1 with Series 2.

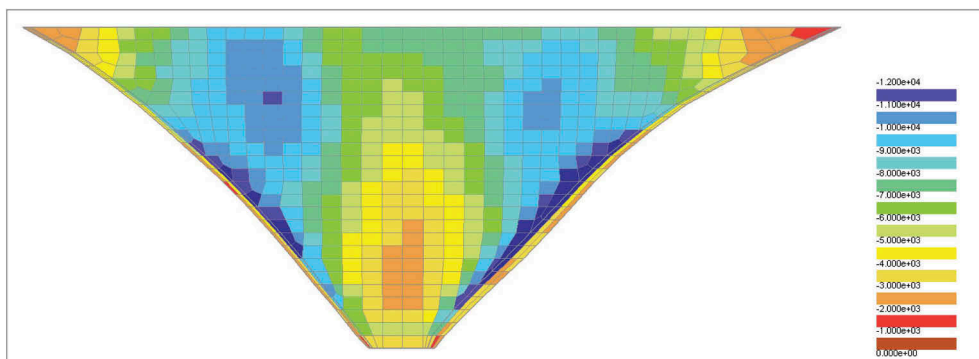


Figure 14. Principal compressive stresses [kPa] envelopes on the downstream face for DE1 with Series 2.

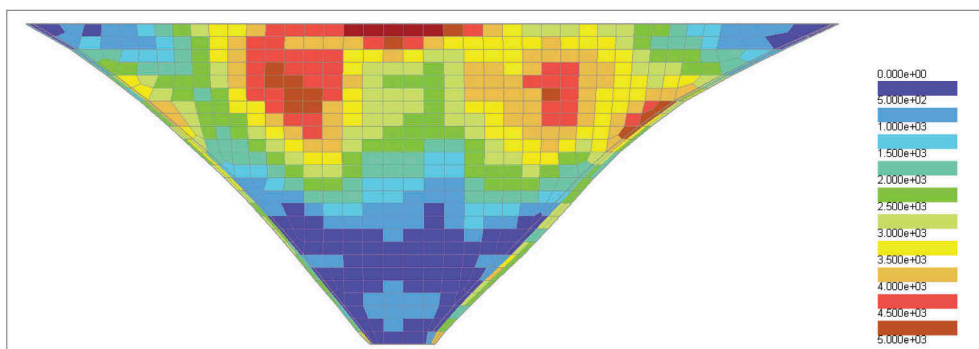


Figure 15. Principal tensile stresses [kPa] envelopes on the downstream face for DE1 with Series 2.

The results from the static and dynamic analysis of the dam show that the dam shape has been successfully defined and optimised and that the dam can withstand without suffering major damage the extreme load conditions in case of a 10,000-year earthquake.

4 CONCLUSIONS

The melting of glaciers in the Alps offers certain opportunities for hydroelectric development. This is the case with the Trift Glacier, whose retreat has created a new natural lake just upstream from the beginning of a narrow gorge. This article describes the conceptual design of a 125 m high arch dam that will create a reservoir with a total capacity of 80 million m³ for hydropower generation. The paper presents the main aspects of the preliminary definition of the dam location and geometry, as well as the results of the static and dynamic numerical analysis performed to verify the structural safety of the dam. It is concluded that the dam is feasible and that its safety is guaranteed for usual, unusual and extreme load conditions.

REFERENCES

- Bundesamt für Energie BFE, 2017. Richtlinie über die Sicherheit der Stauanlagen, Teil C1: Planung und Bau.
- Bundesamt für Energie BFE, 2016. Richtlinie über die Sicherheit der Stauanlagen, Teil C3: Erdbebensicherheit.
- Hughes, T., 1987. The Finite Element Method – Linear Static and Dynamic Finite Element Analysis. Prentice-Hall, Inc.
- Westergaard, H.W., 1933. Water pressures on dams during earthquakes. *American Society of Civil Engineers (ASCE), Proceedings*.

Fulfilling pumped storage plants requirements with advanced geomembrane technology

G. Vaschetti & M. Scarella
Carpi Tech, Balerna, Switzerland

ABSTRACT: The construction of pumped storage plants is increasing due to the need of providing grid balance as wind and solar production increases. Pumped storage plants are demanding structures, due to the continuous variations of the water level that result in repeated loading and unloading conditions impacting on all the components of the plant. In particular, since the upper and lower reservoirs are often formed by excavating the natural slopes and by earthen or rock embankments, it is important to ensure that possible settlements and differential displacements will not affect the watertightness and will not cause uncontrolled water seepage. Waterproofing the reservoirs with conventional liners, such as concrete or bituminous concrete, has shown some drawbacks. The rigid liners demonstrated a poor capability to accommodate settlements, to provide efficient joint sealing, and to preserve the dimensional stability under temperature variations. As a consequence, the rigid liners often need maintenance, which in some cases implies outage of the plant and revenue losses. Geomembrane liners are characterised by outstanding endurance properties and are considered an efficient and durable alternative to more rigid liners, especially when important settlements are expected. Geomembrane liners provide a quicker installation, an early exploitation of the plant, and in case of accidental damage the possibility to be easily repaired, even underwater, without impacting on the plant operation. The 18 Water Saving Basins of the Third Set of Locks of the Panama Canal expansion project can be considered the first geomembrane application in new pumped storage plants, since they have an average of 5 to 6 fill/empty cycles/day. In this project, several anchorage systems were used to retain the exposed geomembrane liner stable and taut to the surface of the basins under daily varying water levels and against wind uplift. The paper discusses the design, characteristics and advantages of advanced exposed geomembrane systems in recent new projects. At Kokhav Hayarden pumped storage project in Israel, completed in 2022, the anchorage system consists of heat-seaming the geomembrane liner to geomembrane anchor bands embedded in vertical trenches. The connection to the concrete structures (water intakes) consists of a mechanical anchorage designed to accept large settlements and differential displacements. At Abdelmoumen pumped storage project in Morocco, completed in 2023, the concept of heat-seaming the geomembrane liner to geomembrane anchor bands was maintained, while a specific construction method was defined to conform to different embankment materials and subgrade preparation. The liner is a lacquered geomembrane, intended to enhance durability in an environment with particularly high UV radiation. At Pinnapuram pumped storage project in India, currently on-going, the geomembrane liner will be installed on three large embankment dams in the lower reservoir and a 6.6 km long continuous embankment dam in the upper reservoir. The anchorage on the dam face will be obtained by geomembrane anchor bands embedded in vertical trenches and created into a bedding layer of porous concrete.

1 INTRODUCTION

In recent times, following the increased consciousness of the need to protect the environment, the construction of wind and solar plants has increased. The intermittent nature of wind and

solar calls for energy storage. Among available storage technologies of different nature, the pumped storage plants are among the best options in terms of technical maturity, reliability, and environmental sustainability. Pumped storage plants can store large amounts of renewable energy and make it available to the grid almost instantaneously by releasing the water stored in the upper reservoir to the lower reservoir through the generating units. During hours of low demand, the excess of energy produced by wind or solar plants can be used to pump water from the lower reservoir to the upper reservoir. The revenues of the plant come from selling energy at peak demand, when prices are higher, and using low-cost off-peak energy to run the pumps.

The efficiency of pumped storage plants depends on several factors, among which conversion losses, loss of water due to evaporation, impact of seasonal and long-term climate changes. Water can also be lost, however, through deficiencies in the waterproofing liners of the reservoirs. Pumped storage plants can be built re-using existing lakes and dams, or by constructing new reservoirs either excavated or/and harnessed by new embankments, mostly made of earth and rock. Accordingly, a lining system is commonly required to assure the watertightness at the reservoirs. In pumped storage plants, the requirements for the waterproofing liners are particularly demanding, since the continuous variations in the water level result in repeated loading and unloading conditions, which can increase the potential for settlements and differential movements. If the waterproofing liners are not capable to accommodate such situations, water leakage can occur through localized damages, decreasing the efficiency of the system, and possibly affecting the safety of the plants.

Traditional waterproofing liners for pumped storage reservoirs are concrete or bituminous concrete. Concrete liners may show cracking under large settlements. Secondly, the performance of the embedded waterstops of the concrete joints is not always as expected, either because of inadequate installation or excessive deformations. Bituminous concrete may show construction issues on steep slopes, and critical behaviours in maintaining the watertightness at the connection with rigid appurtenance structures. Concrete and bituminous concrete are sensitive to weather conditions during placement and during the service life (e.g., freeze/thaw cycles), and require routine maintenance, which may turn into long outage periods with a consistent loss of revenue. Minimising the outages for pumped storage plants is in fact of paramount importance to grant the overall profitability of the project. Accordingly, the selection of a waterproofing liner with minimal or no maintenance is a key factor.

Geomembrane liners have the advantage of having an outstanding elongation capacity, which allows to accept large settlements and differential displacements while preserving the watertightness and the mechanical properties. This characteristic makes the geomembrane liners the preferred option to comply with demanding surface irregularities under repeated cycles of water pressure loading. All components of a geomembrane system are prefabricated in a factory, under controlled and documented conditions. During installation, the properties of the geomembrane system (watertightness, junctions, and perimeter seals) are controlled 100% and are not affected by climatic or curing conditions. Geomembrane liners can be formulated for long durability and no maintenance, to provide low lifetime costs. In general, the lifetime costs and not the initial capital costs should be the aspect to consider when selecting a waterproofing liner. Additionally, the fast installation of the geomembrane liners allows exploiting the scheme earlier, further lowering lifetime costs and increasing the project revenues. Typically, geomembrane liners can be integrated with a dedicated monitoring system and can be also repaired underwater, so that any accidental damage can be remediated without putting the entire scheme out of operation.

The cyclic variations of the water level in pumped storage projects pose a challenge also for the geomembrane liner installed in exposed position. The geomembrane liner may be cyclically exposed to UV radiation and wind uplift during the reservoir operation. The exposure to UV requires the selection of polymeric materials with enhanced durability. The exposure to strong winds may also demand for a capable anchorage to prevent the adverse consequences of the uplift, particularly along the reservoir slopes, which are the areas with the higher wind uplift pressure. Furthermore, the design of the anchorage shall be particularly suitable in preventing/minimising the formation of wrinkles and folds in the geomembrane liner. The stress

concentrations in correspondence of wrinkles and folds may be amplified by the cyclic variations in water pressure created by fill-empty cycles. Experience has shown that flexible geomembranes thermally bonded at fabrication to a non-woven geotextile are to be preferred because the geotextile can effectively increase the resistance to puncturing, the dimensional stability, the resistance to tear.

In the case histories discussed in this paper the geomembrane liner consists of a SIBELON[®] CNT geocomposite, comprising a flexible geomembrane, formulated with a special compound of plasticised polyvinylchloride, thermally bonded to a non-woven, needle punched, polypropylene geotextile.

2 A PARTICULAR PUMPED STORAGE SCHEME IN PANAMA

The 18 Water Saving Basins of the Third Set of Locks of the Panama Canal expansion project, which started operation in 2016, can be considered the first new pumped storage scheme where an exposed geomembrane liner was selected to minimise water losses. The basins feed water to the navigation locks, designed to accommodate the post-Panamax ships, which have a tripled transport capacity as compared to the previous ships. There are two lock complexes, one on the Pacific side and one on the Atlantic side; each lock is provided with 3 chambers, and each chamber is fed by 3 water saving basins for a total of 18 basins. By means of an ingenious system, the water used for the locks is moved by gravity in and out of the basins, allowing reusing 60% of the water in each ship transit. The navigation system requires each basin to be filled and emptied 5 to 6 times per day, which practically make it comparable to a pumped storage plant, whilst with a much more demanding operation.

To ensure the long-term watertightness of the basins an exposed geomembrane liner was selected as alternative to the original design, which involved the construction of a concrete cover. The selection of an exposed geomembrane liner allowed to eliminate the risk of damaging the geomembrane during casting of the concrete cover and to conduct a detailed inspection at any time, with possibility of easier and cheaper repairs (if needed). The strategic importance of the Panama Canal required the selection of a geomembrane liner assuring a functional life of 100 years. To comply with the durability required by the project, the selected geomembrane liner is a SIBELON[®] CNT 4400 geocomposite, made of a 3.0 mm flexible PVC geomembrane thermally bonded to a non-woven, needle punched, 500 g/m² polypropylene geotextile.

The different geology at the Pacific and Atlantic sides, the characteristics of the subgrade, and the inclination of the slopes of the basins, required the design of different anchorage systems for the geomembrane liner. In the bottom of the basins, made of compacted granular material, the anchorage consists of tensioning trenches (Figure 1). The technical solution is based on the installation of the geomembrane liner into trenches backfilled with concrete (patented by Carpi).



Figure 1. Panama Canal Expansion Water Saving Basins. Anchorage by tensioning trenches on the invert. These trenches avoid the formation of loose areas and folds in the geomembrane, which is crucial in these basins with several daily water level fluctuations, and thus ensure the longevity of the system.

In the slopes of the basins made of a 2H/1V excavation, the anchorage consists of mechanical point anchors or geomembrane bands embedded in trenches backfilled with concrete, while at increasing inclination 1H/1V and 1H/4V, the anchorage consists of stainless-steel profiles fastened into a shotcrete layer (Figure 2).



Figure 2. Panama Canal Expansion Water Saving Basins. Anchorage at points (at left) and by with tensioning profiles secured with deep anchors or chemical anchors, depending on the conditions of the subgrade.

More information on the anchorage system and on the durability analysis of the geomembrane liner can be found in a detailed case history already published (Machado do Vale, J. et al., 2018). The installation of a geomembrane surface $> 590,000 \text{ m}^2$ was completed in less than one year, in challenging weather conditions, site and operation constraints, fulfilling all contract requirements and passing all tests on completion. The project was open to ship transit on June 26, 2016. Since then, the exposed geomembrane system has gone through some 13,500 cycles of filling and emptying, equivalent to more than 36 years of operation with 1 cycle per day.

3 NEW PUMPED STORAGE SCHEMES: RECENT CASE HISTORIES

3.1 *Kokhav Hayarden, Israel*

When in operation, Kokhav Hayarden, with an installed capacity of 344 MW, will be the largest pumped storage project in Israel. The project comprises an upper and a lower reservoir, with a total capacity of approximately $3,000,000 \text{ m}^3$ each. The upper reservoir is partly excavated in river deposits of clay and a clay-gravel mixture, and partly formed by a compacted earthfill embankment. The inclination of the slopes is 3.5H:1V, the water fluctuation is around 22 m. The lower reservoir is formed by a continuous compacted earthfill embankment, composed of river deposits of clay and a mixture of silty clay and gravel. The inclination of the slope is 3H:1V, the water fluctuation is around 21 m.

The original design foresaw waterproofing both reservoirs with an exposed high-density polyethylene (HDPE) geomembrane liner. After a detailed review of the project, in order to provide higher performance in respect to possible large settlements of the subgrade, a different waterproofing liner was evaluated. The geomembrane liner selected is a SIBELON[®] CNT 3100 geocomposite, made of a 2.0 mm flexible PVC geomembrane thermally bonded to a non-woven, needle punched, 500 g/m^2 polypropylene geotextile. In addition, in order to increase the resistance of the anchorage system for the geomembrane liner, a specific technical solution was developed, which consists of anchor bands of SIBELON[®] CNT 2300 geocomposite, embedded into vertical trenches placed at regular spacing and ballasted with compacted granular material, to which the waterproofing liner is anchored by heat-seaming. The trench spacing is different in the top and bottom parts of the slopes (Figure 3), in function of the local suction effect of the wind. Details have been discussed in recent literature (Vaschetti et al., 2022). The anchorage system is complemented by a mechanical fixation at the base of the parapet wall along the reservoir crest, made watertight against rainfall and wave run-up. In the reservoir bottom, the permanent presence of a water cushion of about 1 m depth allows to reduce the anchorage requirements, providing an effective ballast.

To avoid backpressures when the water level in the reservoir drops, a drainage layer was placed under the geomembrane liner on the slopes. The drainage consists of a synthetic geocomposite, made of a high transmissivity drainage geonet bonded to a filter geotextile and placed directly on the soil excavation or embankment material. In the bottom, the drainage layer consists of selected gravel. The drained water is discharged through a network of perforated pipes.

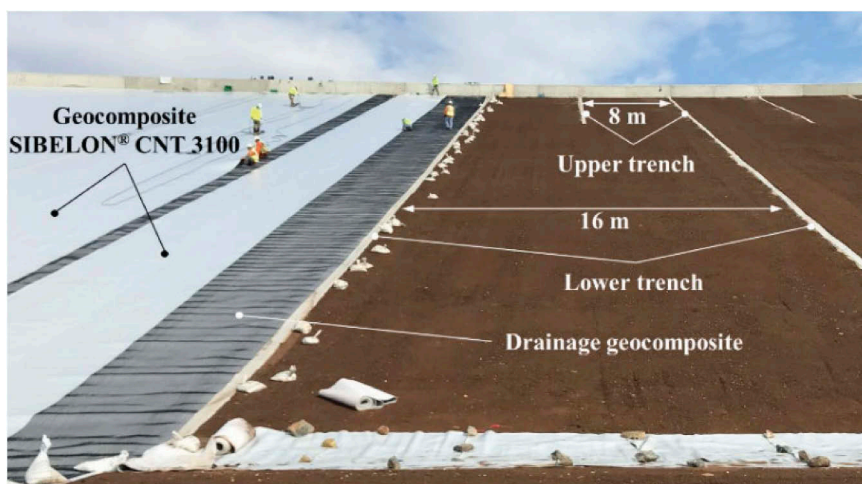


Figure 3. Kokhav Hayarden pumped storage plant. From left to right, the vertical geomembrane anchor bands at different spacing in the top and bottom of the slopes, the drainage geocomposite, and the waterproofing liner.

In order to optimise installation time and to decrease potential material waste in the curvilinear shape of the reservoirs, a precise scheme for the arrangement and sequential installation of the geodrain and geocomposite sheets was developed. The adjacent geomembrane sheets laid over the drainage layer are seamed to the anchor bands, adjacent sheets are watertight joined by heat-seaming, and then mechanically anchored at the parapet wall. A watertight mechanical seal around the concrete structures (intakes) ensures that no water may leak under the geomembrane liner. The joints of the intake structures have been treated with Carpi patented external waterstops system. The installation of the geomembrane system in the lower reservoir started on July 21, 2021, and was completed on September 29, 2022. The lower reservoir started filling of water in January 2023. Installation of the geomembrane system in the upper reservoir started on July 20, 2020, and was completed on December 17, 2022. Impounding has not started yet. In total, about 433,000 m² of exposed geomembrane liner have been installed.

3.2 Abdelmoumen, Morocco

Abdelmoumen pumped storage project, with an installed capacity of 350 MW, is located in Morocco on the River Issen. The project comprises two reservoirs storing 1,300,000 m³ of water, connected by a 3 km-long waterway and a powerhouse hosting two reversible pump-turbines. The plant is designed to operate in turbine mode when electricity is at peak by exploiting the 500 m head between the reservoirs, and in pumping mode when surplus electricity is available. Both reservoirs are harnessed by embankments made of compacted granular material, with a slope inclination 2H:1V and a water level fluctuation 20 m.

The project foresaw an exposed geomembrane system to waterproof both reservoirs. The conditions at site posed additional challenges: a particularly intense UV radiation, requiring a liner tailored for long durability in such climate, the steepness of the embankments, requiring a higher stability, and the potential for large settlements under the effect of cyclic loading, requiring a flexible and performant geomembrane liner.

The selected geomembrane liner is a SIBELON[®] CNT 4400 L geocomposite, made of a 3.0 mm flexible PVC geomembrane thermally bonded to a non-woven, needle punched, 500 g/m²



Figure 4. Kokhav Hayarden pumped storage plant. At left, start of impounding at lower reservoir, at right, waterproofing works completed at the upper reservoir.

polypropylene geotextile. The geomembrane includes a surface lacquered treatment (L), designed to enhance the service life of the material under intense UV radiation, when compared to a non-treated geomembrane liner of the same thickness. The anchorage system for the geomembrane liner is based on the concept of embedding geomembrane anchor strips inside the embankment during construction. An additional band of geomembrane heat-seamed to the wings creates a continuous vertical anchorage lines, distributing the stresses at placement and during operation. The spacing of the vertical anchorage lines on the slopes is 8.0 m, measured along the reservoir crest. Considering the possibility of a complete depletion of the reservoirs, a specific anchorage system is provided in the bottom, which consists of longitudinal trenches backfilled with concrete at 16 meters spacing (Figure 5).

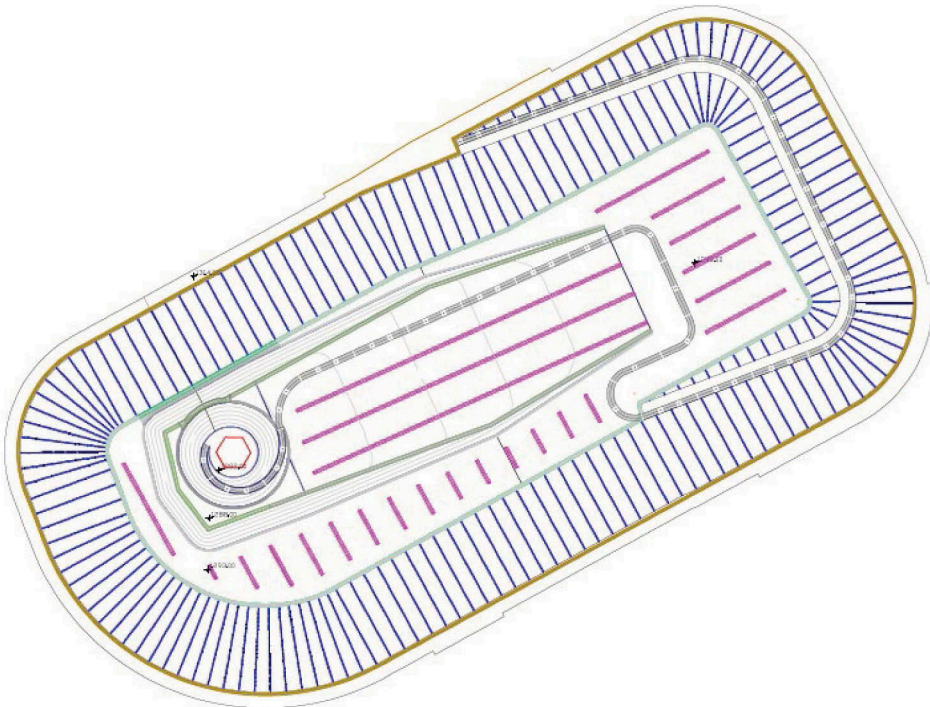


Figure 5. Abdelmoumen pumped storage plant. Layout of the face anchorage system at upper reservoir.

A particular procedure was developed to embed the geomembrane anchor strips in the embankments, which allowed a good compaction of the subgrade material and, at the same time, an effective anchorage and confinement. The result is the formation of a stable slope of compacted material, or structural fill.



Figure 6. Abdelmoumen pumped storage plant. At left, the geomembrane anchor wings embedded in the embankment, and the geomembrane anchor band heat-seamed unto the wings. At right, the geomembrane liner under installation on the slopes.

At the lower reservoir, installation of the geomembrane anchor strips started in April 2021, and within August 2022 the geomembrane system was completed. At the upper reservoir, installation of the geomembrane anchor strips started in May 2022, and within January 2023 the geomembrane system was completed. In total, about 195,500 m² of exposed geomembrane liner have been installed. Both reservoirs are now impounding (Figure 7).



Figure 7. Abdelmoumen pumped storage plant with both reservoirs impounding.

3.3 Pinnapuram, India

Pinnapuram pumped storage plant is part of the 1,680 MW Pinnapuram Integrated Renewable Energy pumped storage project, with solar, wind and pumped hydro storage components, which is under construction in the state of Andrah Pradesh. Pinnapuram is a first-of-its-kind pumped storage project to be developed by an independent power producer in India. The upper

reservoir will be harnessed by a 6.5 km long rockfill dam, forming a continuous embankment ring with a nearly rectangular-shaped perimeter with a maximum height of about 40 m. The lower reservoir will be harnessed by three separate rockfill dams connecting existing natural slopes, with a total crest length of about 3.3 km and maximum height of about 46 m.

The original design of the lining system for the rockfill dams foresaw a bituminous concrete sealing system, which was eventually replaced by an exposed geomembrane system after a positive technical and economic assessment. The anchorage system for the geomembrane liner consists of anchor bands embedded in vertical trenches to which the geomembrane liner is connected by heat-seaming. The selected geomembrane liner is a SIBELON® CNT 4400 geocomposite, made of a 3.0 mm flexible PVC geomembrane thermally bonded to a non-woven, needle punched, 500 g/m² polypropylene geotextile. The earth works for the construction of the embankments are currently ongoing and the installation of the geomembrane liner will start in mid-2023 and will account for a surface of some 400,000 m² of geomembrane liner.



Figure 8. Pinnapuram pumped storage plant. At left, the rectangular upper reservoir under construction; in the background the intake structure of the penstocks leading to the downstream channel conveying water to the lower reservoir can be seen. At right, raising of one of the three dams forming the lower reservoir, with the plinth in the foreground.

4 CONCLUSIONS

Geomembrane systems are now an established waterproofing technology for pumped storage plants. In particular an exposed geomembrane system made of a flexible PVC geomembrane liner can provide an efficient durable water barrier, which can be installed in shorter times and is also a more sustainable system than traditional liners.

REFERENCES

- Machado do Vale, J., Vaschetti, G., Scuero, A., & Lilliu, G. 2018. A geomembrane liner at the Panama Canal Expansion Project: 18 Water Saving Basins. *Proc. 3rd intern. Dam World Conference, Foz do Iguaçu 18-21 September 2018*.
- Vaschetti, G., Tronel, F., & Scuero, A. 2022. Geomembranes in new pumped storage schemes: two ongoing innovative projects. *Proc. Hydro 2022 - Roles of Hydro in the Global Recovery, Strasbourg, 25-27 April 2022*.

Ritom HPP – Unforeseen challenges during the inclined shaft excavation

R. Zanolli & S. Massignani

Marti Tunnel AG, Moosseedorf, Switzerland

ABSTRACT: The Ritom hydropower plant is located in Switzerland south of the Gotthard massif. Ritom SA, a partner company of the Swiss Federal Railways (75%) and the Canton of Ticino (25%), represented by Azienda Elettrica Ticinese, holds the hydroelectric concession until 2094. The capacity of the over 100-year-old power plant is increased and converted into a pumped storage plant by building a new steel-lined headrace tunnel. The sub-horizontal section (length = 750 m, cross-section = 18.4 m²), excavated in granite by drilling and blasting, encountered a highly fractured section with high water inflows requiring special grouting measures. The following inclined pressure shaft (length = 1.4 km, Outer Diameter = 3.23 m) was excavated by an open hard rock tunnel boring machine specifically configured for this project. The excavation of the shaft with gradients of 42% in the lower section and 90% in the upper section has proven to be one of the biggest challenges of the entire project. This paper focuses on the unforeseen geological challenges encountered during the inclined shaft excavation, and the TBM configurations that allowed them to be safely overcome.

1 INTRODUCTION

The existing Ritom hydropower plant, located in Switzerland south of the Gotthard massif, was built in the 1920s by the Swiss Federal Railways (SBB). The headrace system links lake Ritom, at an altitude of about 1850 masl, and the powerhouse in Piotta, located at about 1000 masl. The existing plant consists of the power intake and valve chamber at Ritom reservoir, an approx. 900 m long headrace tunnel, surge tank, valve chamber and two exposed penstocks to the Piotta powerhouse with a length of approx. 1400 m (Figure 1). The four horizontal Pelton turbines with a single-phase synchronous generator have an output capacity of around 40 MW.

After almost 100 years in operation, a major refurbishment was necessary in order to extend the lifetime of the plant. After the new operating license was granted, Ritom SA, a partner company of the Swiss Federal Railways (75%) and the Canton of Ticino (25%), represented by Azienda Elettrica Ticinese, awarded the main construction works to the “Marti-Ferrari Ritom” joint venture (Marti Tunnel AG (lead), Mancini & Marti SA, Ennio Ferrari SA).

The new scheme was developed according to the requirements of both the railway and the public transmission grids in order to optimize the use of existing hydropower resources in the Leventina Valley. The railway and the public grids, which operate with different frequencies of 16.7 Hz and 50 Hz, need to be linked through frequency converters at some points to provide system stability. Such an interconnection was created at the new Ritom plant. To enhance the benefits of this interconnection and the regulation capacity, the plant will be converted into a pumped-storage facility. The water to be pumped to the Ritom lake is supplied by the existing Stalvedro HPP, owned by Azienda Elettrica Ticinese, and its reservoir located in Airolo (Figure 2).

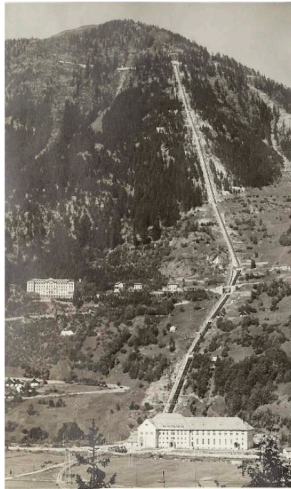


Figure 1. Ritom HPP a few years after construction.

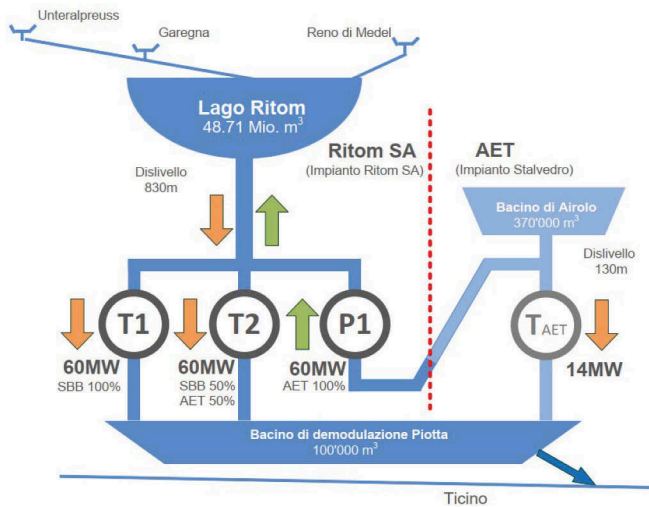


Figure 2. Hydraulic scheme of Ritom HPP and upstream Stalvedro HPP.

The existing headrace tunnel and the penstocks will be decommissioned and replaced by an underground headrace system including a new intake in the Ritom lake, a short headrace tunnel (length = 130 m), a valve chamber accessed by a 50 m high vertical shaft, an inclined pressure shaft (total length of 1.4 km; 816 m with a gradient of 90% and 565 m with a gradient of 42%, excavation diameter = 3.23 m, steel lining diameter = 2.10 m), a high-pressure tunnel (length = 750 m, excavation cross section = 18.4 m², steel lining diameter = 2.00 m), and a manifold with three branches (steel lining diameter = 1.40 m) linking the main headrace tunnel to the main units in the new outdoor powerhouse. These consist of two Pelton generating units (60 MW each, one unit connected to the 16.7 Hz grid and the other unit connected to the 50 Hz grid) and a 60 MW pump linked to the 50 Hz grid.

From a geological point of view, the project is located in the front part of the Lucomagno Penninic tectonic strata, close to the allochthonous sediments covering the Gotthard massif. The relevant rock formations for construction are of pre-Alpine age and show high

metamorphism. The main lithotypes are orthogneiss, paraschistgneiss and, subordinately, amphibolites (Figure 3).

The fracturing degree of the rock mass is notable down to about 250 m depth. The alignment of the headrace system was selected, on the one hand, to avoid tunneling the lower part of the inclined shaft within the fractured surficial layer and, on the other hand, to limit the depth because of the higher water pressure on the steel lining.

The rock mass is traversed by kachyritic bands, i.e., fault zones with a thickness between a few cm and approximately 1 m, filled with completely fractured material. These bands constituted a major challenge for the design and operation of the TBM.

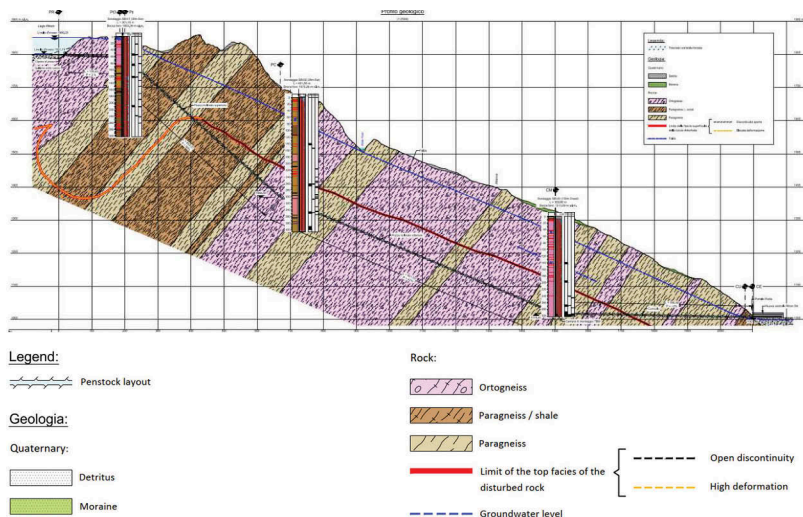


Figure 3. Geological section of the new headrace tunnel.

Before launching the TBM, due to the difficult geological and hydrogeological conditions encountered in the sub-horizontal portion of the waterway and the possibility to cross similar conditions along the shaft, additional investigation boreholes were realized from the surface and from the cavern to identify in advance the presence of possible weak rock zones combined with high water permeabilities and to characterize these conditions. As a result, the project alignment was modified during construction (before the TBM launching) to mitigate geological risks.

2 THE TUNNEL BORING MACHINE

The excavation of the inclined tunnel was planned with a hard rock TBM (Gripper). The nominal diameter of the excavation is 3.2 m, for the subsequent installation of a 2.2 m diameter inner lining. The M-2378 machine, a tailor-made TBM manufactured specifically for the project by Herrenknecht AG, was used for this excavation (Figure 4, Table 1).

Like a common Gripper-TBM, before each stroke the machine is braced against the previous excavated tunnel using laterally extendible hydraulic cylinders. In addition to the main gripper unit, the Ritom tunnel boring machine was equipped with two additional gripper units that were mounted on the backfall locking system, so that the machine could always be secured while moving forward or backward by a minimum of two gripper units. Furthermore, in the case of a failure of the hydraulic system, a mechanical self-locking system allowed to automatically increase the gripping force of the gripper units in the backfall locking system. Each of the three gripper units can carry the entire weight of the TBM on its own. This double backfall locking system, applied for the first time on a TBM of this diameter and in an inclined shaft, ensures maximum work safety at every stage of excavation.

The construction of the cutter head also met the highest safety standards. With the back-loading system, the disc cutters could be replaced in the protected area from inside the cutter head. This means that workers no longer had to work in front of the excavation face and were therefore no longer exposed to possible rockfalls. The so-called backloading system is a common standard for bigger boring machines used for horizontal tunnel excavations, but in this case, applied to an inclined shaft TBM, it represents a novelty.



Figure 4. Pre-assembled TBM at the Herrenknecht factory.

The machine was equipped with two bolting machines, one just behind the cutter head and the second one after the backfall locking system, as well as a shotcrete machine. Other support measures like steel arches (liner plates) and wire meshes had to be mounted by hand by the staff. The TBM and back-up gantries were assembled in the cavern at the foot of the assembly pit.

Table 1. Main features of the TBM M-2378.

Total length	98 m
Total weight	305 ton
Excavation diameter	3.230 m
Number of disc cutters	23 pcs. 14" each
Max. torque	1'300 kNm
Stroke length	1.20 m
Max. thrust force	5'700 kN
Max. gripping force TBM	25'736 kN
Max. gripping force backfall locking system	23'200 kN
Number of back-up gantries	7 pcs

3 CHALLENGES

On 6th July 2021 at 9 a.m., at tunnel meter 451 the TBM crossed what immediately appeared to be an important passage of fault gouge (kachyritic bands, Figure 5). As described before, additional geognostic probe drilling from the surface, from the TBM assembly cavern at the inclined shaft foot, and from the top of the penstock had been

carried out. A few hundred meters of the inclined shaft remained uncovered anyway by probing parallel to the excavation axis. This is the case with tunnel meter 451, where unfortunately the geological scenario encountered was therefore not foreseen. Fragile detensioning phenomena, later observed and documented in the section preceding the disturbed zone, had anticipated the approach to the zone. After having unsuccessfully removed about 10 m³ of material and attempted to empty the head by spinning it without thrust, work was suspended.



Figure 5. Cutter head at the fault gouge at tunnel meter 451.10.

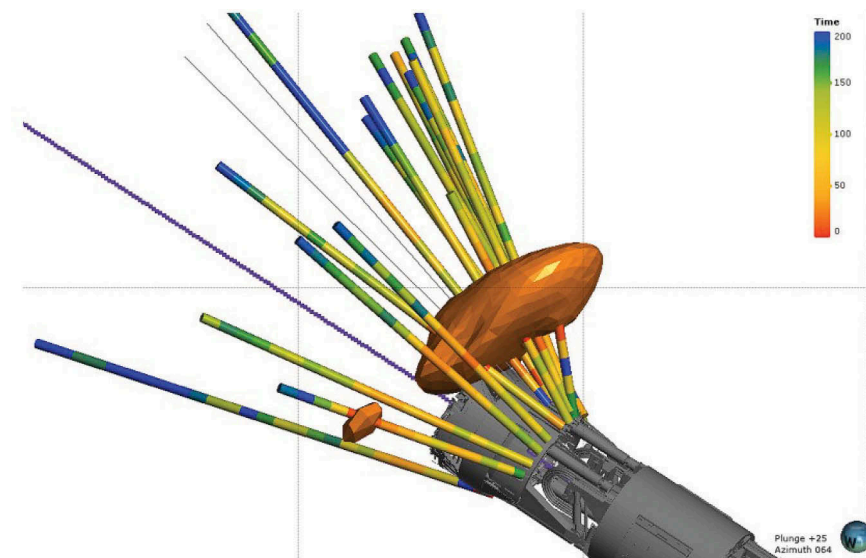


Figure 6. Core holes for post-injections.

As a first measure, it was decided to drill a destruction borehole, performed by hand in the crown area (Figure 7). The material was found to be completely non-cohesive, and it was not possible to continue beyond 3.8 m. Two further boreholes with an inner diameter of 150 mm were drilled, one in the crown area and one in the tunnel floor level. In both cases, a liner was partially used to push the hole as far as possible and to locate the end of the disturbed zone. Soundings showed that the fault gouge lens was about 2.2 m thick, but, more importantly, it was followed by strongly altered rock mass. The advancement of the TBM had effectively removed the footing and support from the altered rock mass ahead, resulting in a landslide and in an over-excavation both in the crown above the cutterhead

of the machine and at the front. The presence of fault gouge passages was expected, but the combination with the following altered geology made it impossible to continue the excavation without further measures. The TBM used in this project was not equipped for either probe-drilling or injection work, as neither scenario had been foreseen. With the same hand down-the-hole (DTH) drill used for exploration, 16 core holes with an inner diameter of 124 mm, distributed over a 150-degree arc, were drilled by hand into excavation direction, in the maximum available upper L1* area of the TBM (Figure 6). Self-drilling R38/19 anchors with hoses to perform ground post-injections were then inserted into the pre-drilled holes.



Figure 7. Destruction boreholes by hand behind the cutter head.

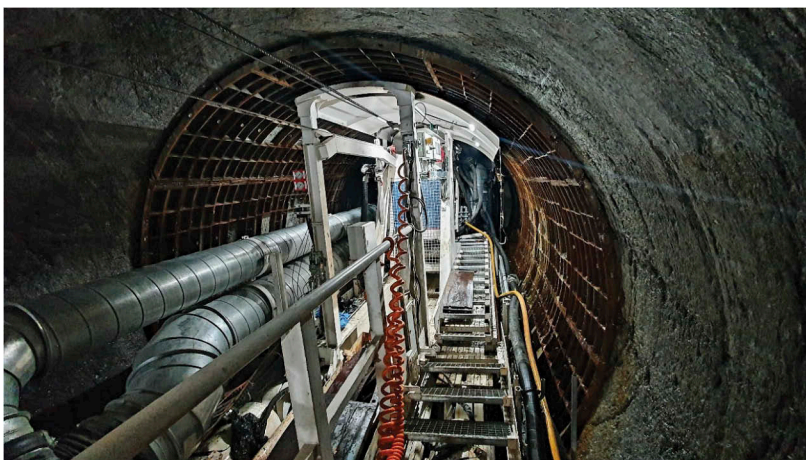


Figure 8. Excavation profile secured with liner plates.

Overall, almost 13 tons of cement mixture were injected at low pressure, through this previously described setup, stabilizing and strengthening the ground in front of the TBM and probably partially filling the void left by the collapse in the crown area. It was then possible to resume the excavation on 6th August 2021, exactly one month after the work had stopped. During the first few meters of excavation, the use of water inside the cutterhead had to be carefully avoided so as not to compromise the stability of the obtained material. Directly above the head of the TBM, the profile was then secured with hand-sprayed dry shotcrete, as the profile became reachable. The securing was then completed just behind the cutter head (L1*) with the installation of liner plates (Figure 8), specially developed for this project, between tunnel meter 446 and tunnel meter 456.

The disturbed area remained in principle dry during the entire securing operation. Water ingress in combination with fault gouge (kachyritic bands) would have made it even more difficult, if not impossible, for the work to continue as it did.

4 CONCLUSIONS

The prompt reaction of the excavation team on the TBM when the machine entered the disturbed area made it possible to reduce the overhead collapse and did not affect the implementation of the safety measures then adopted. The experienced team played a key role.

The design of the TBM, even though no probe drilling or injection equipment had been planned and were required, meant that in the few meters behind the cutter head (L1*) it was possible to install a hand-held drill capable of covering an arc of 150 degrees.

Limited space and passageways meant that all materials and equipment had to be transported by hand.

Knowing this, the areas suspected of being unstable based on the clients probe drilling findings were then explored by drilling probe holes from the inside of the TBM, with the contractors self-developed hand-held probe drilling device, up to the end of the tunnel excavation. This further reduced the risk of unforeseen events with far worse financial and timing consequences.

REFERENCES

- Bronzetti, D., Cippà, F., Müller, U., Sangalli, G., Zanolì, R. 2022. The peculiarities of the construction of the inclined shaft for the new Ritom pumped storage hydropower plant. *Tunneling Asia 2022, Mumbai, India, June 27–28, 2022*.
- Marti AG. 2023. Pumped-Storage Plant Project - Tunneling under extreme conditions. *YouTube, uploaded by Marti Gruppe, 18 January 2023*, <https://www.youtube.com/watch?v=6AV2NcyX7p>.
- Müller, U. & Ritz, M. 2019. Modernisation and Upgrading of Ritom Hydropower Plant, *Swiss Tunnel Congress 2019. Lucerne*.
- Zanolì, R. & Massignani, S. 2022. Rinnovo Centrale Idroelettrica Ritom – Le sfide inattese dello scavo del pozzo forzato, *Swiss Tunnel Congress 2022. Lucerne*.
- Ritz, M., Sangalli, G., Ullrich, M., Müller, U., Bronzetti, D., Grosso, N. & Massignani, S. 2022. Ritom power plant renewal with new inclined pressure shaft, *World Tunnel Congress 2022. Copenhagen*.
- Renescio GmbH and Lombardi Consulting Engineers Ltd. 2023. Hybrid injections – Laboratory testing and field experience during tunnel excavation, *6th International Conference on Grouting and Deep Mixing, New Orleans, Louisiana, January 15–18, 2023*.

Theme B: Dams and reservoirs for climate change adaptation



Taylor & Francis

Taylor & Francis Group

<http://taylorandfrancis.com>

CRHyME (Climatic Rainfall Hydrogeological Modelling Experiment): A versatile geo-hydrological model for dam siltation evaluation

Andrea Abbate & Leonardo Mancusi
RSE Ricerca Sistema Energetico, Milano

ABSTRACT: Dams and reservoirs represent a strategic infrastructure from an energetic viewpoint and their future operativity maintenance is a challenge. Since they interact directly with the surrounding environment, they may encounter siltation problems which undermine the proper functionality. A physical quantification of geo-hydrological processes at the basin scale is a necessary task that hydropower stakeholders require for maintaining the infrastructure functionality. This is particularly true under the projected future climate change scenario where extreme events intensification is expected with high confidence.

The new model concept called CRHyME (Climatic Rainfall Hydrogeological Modelling Experiment) is here presented. This model represents an extended version of the classical spatially distributed rainfall-runoff models. CRHyME model has been written in Python language and it aims to model the effect of geo-hydrological processes occurring at a watershed scale. Knowing the location of a reservoir, the model can quantify the flood and sediment income from the upstream catchment, reconstruct past events or deal with future climate projection.

The CRHyME model, although it is already operational, is continuously updated in order to improve its performance and expand its possible use. Remarkable results have been obtained for the study case of the Valtellina catchment in the Alpine region (northern Lombardy, Italy) where six reservoir siltation ratios have been estimated. CRHyME was also applied considering three different climatic models from the EURO-CORDEX program. The results have highlighted a probable intensification of the geo-hydrological processes across the Alps leading to possible aggravation of reservoir siltation.

1 INTRODUCTION

Geo-hydrological hazards are complex and heterogeneous phenomena, so a great deal of effort has been made in the past to try and interpret their dynamics and triggering factors (Gariano and Guzzetti 2016). There are many studies concerning mass wasting dynamics in the literature based both on laboratory and field experiments (Iverson 2000, Brambilla *et al.* 2020, Abbate *et al.* 2021), which individuate rainfall as the main triggering factor for this type of phenomenon.

Geo-hydrological hazards may have serious effects on existing infrastructures (Albano *et al.* 2017, E. Ciapessoni *et al.* 2022), especially across developed countries where they are capillary diffused across the entire landscape. In this regard, dams and reservoirs represent a strategic infrastructure from an energetic viewpoint and their future operativity maintenance is a challenge (ITCOLD 2009, 2016). Their interaction with the surrounding environment is direct since they are in correspondence with rivers and watershed basins where the geo-hydrological process generally occurs. Beyond the production of hydropower energy, dams and reservoirs have a crucial role in balancing extreme hydrological conditions protecting downstream areas from flash flood events and against mass wasting hazards (Dixon *et al.* 1989). It is recognized worldwide that flood lamination operated by reservoirs is a good strategy for preventing potential flooding downstream

thanks to the smoothing of the hydrological peak and it represents a mitigation measure implemented by the Civil Protection for reducing flood risk (Kreibich *et al.* 2017).

Dams and reservoirs represent a disconnection of the river flow. Even if the water flow could be maintained thanks to the release of the minimum vital flux, sediment connectivity cannot be assured properly (ITCOLD 2009). As a result, dams may block the sediment flux leading to siltation problems for reservoirs (ITCOLD 2009, 2016). Siltation is a perpetual process that cannot be stopped or controlled at all since is embedded in the natural geo-hydrological cycle (Brambilla *et al.* 2020) and it is a result of two types of solid transport processes occurring simultaneously: bedload and fine (or suspended) (Vetsch *et al.* 2018).

In Italy, but also in other countries, several reservoirs are encountering siltation problems (ITCOLD 2009, 2016). In some cases, strategies of maintenance are necessary to keep the functionality of the hydraulic structures of the dams (spillways, drains etc.) and to try to reduce the amount of sediment stored flushing activities or periodic cleaning are planned (ITCOLD 2009, 2016). The sediment removal operations are regulated since the sludge represents a special waste that must be disposed of according to national regulations (ITCOLD 2009). Moreover, the cost of this type of operation is not affordable from an economical viewpoint (de Trinchiera and Otterpohl 2018). Thus, dam manager companies are interested to retrieve quantitative estimations of the actual and future tendency of the siltation process in their reservoir. This goal could be reached in principle using different techniques: direct-indirect measurements and numerical modelling of the geo-hydrological processes in the upstream basin. For a complete characterization of the degree of siltation of the reservoirs, a combination of these approaches is generally carried out (ITCOLD 2009, 2016, Brambilla *et al.* 2020). In fact, through direct and indirect measurements it is possible to analyse the local sedimentological dynamics in the upstream river basin, identifying potential critical situations such as the presence of areas subject to localized erosion or the presence of instability. The latter can accelerate the process of siltation as they represent natural sources of potentially mobilizable material that can be transported to the reservoir (Adamo *et al.* 2021). Numerical modelling, on the other hand, has multiple advantages regarding the characterization of the erosion phenomenon, allowing one to carry out the siltation speed evaluation both on past events and considering future projections.

In this work, the potentiality of a new physically-based geo-hydrological model called CRHyME (Climatic Rainfall Hydrogeological Modelling Experiment) is tested for assessing reservoir siltation. CRHyME is an extension of a classical rainfall-runoff hydrological model where also geo-morphological dynamic aspects are taken into account. From the analysis of the literature (Roo *et al.* 1996, Bemporad *et al.* 1997, Sutanudjaja *et al.* 2018), rarely the two aspects have been jointly analysed. A lot of hydrological models adopted worldwide, are interested mainly in flood propagation and water balance assessment (Sutanudjaja *et al.* 2018). One of their main limitations is that they are rather advanced in the hydrological part, proposing a very detailed description of the hydrological cycle while geo-hydrological hazards interaction is barely taken into account (Shobe *et al.* 2017, Strauch *et al.* 2018). CRHyME is written in a Python language program implementing the PCRaster libraries (Karssenbergh *et al.* 2010). The PCRaster Python framework offers a series of standard functions prepared for hydrological processing on calculation grids that schematize a territory (Roo *et al.* 1996). These permit a higher versatility of the CRHyME model for implementing and investigating specific geo-hydrological processes such as reservoir siltation.

Starting from these considerations this paper presents the main features of the CRHyME model applied to the reservoir siltation problem. Constitutive equations of erosion and solid transport are reported in the Material and Method section. In the Result section, the case study of Valtellina, Sondrio Province (Italy), selected for the calibration and validation of the new model, is presented. Moreover, climate change scenarios are applied to the model routine for investigating possible siltation long-term effects in the future. The main outcomes of CRHyME applications are extensively commented in the Discussion and Conclusions sections.

2 METHODS AND MODELS

CRHyME's engine is based on PCRaster libraries (Karssenbergh *et al.* 2010) which is a collection of open-source software targeted at the development and deployment of spatio-

temporal environmental models. Thanks to PCRaster libraries, the most innovative part of the code includes the physical relations that describe how the hydrological assessment can influence and potentially trigger the geo-hydrological hazards occurring at the basin scale. Since we are interested in modelling reservoir siltation, we present here the theory behind the erosion and solid transport dynamics implemented in the code. For further details about the whole structure of the CRHyME model see (Abbate and Mancusi 2021a, 2021b, Abbate 2022).

2.1 Erosion production and bed-load solid transport evaluation

To assess erosion, empirical models including USLE and its evolution RUSLE (Panagos *et al.* 2015) have been considered in the past decade thanks to their simplicity and their implementation affordability. In this context, also physically based models have been tested in the laboratory field, but, since they faithfully adhere to the physics of erosion, they have demonstrated not always able to glimpse the global behaviour at the basin scale since some processes and feedbacks are still unknown. Gavrilovic's method or Erosion Potential Method (EPM) (Milanesi *et al.* 2015), initially developed in southern ex-Yugoslavia and then successfully applied also in Switzerland and Italy, is a semi-quantitative method capable of giving an estimate of erosion and sediment production in a basin (Globevnik *et al.* 2003, Milanesi *et al.* 2015). Equation 3 represents the synthesis of Gavrilovic's method. The average annual volume of eroded material G , expressed in m^3/yr , is a product of W_s and R , which are respectively the average annual production of sediment due to surface erosion, expressed in m^3/yr Equation 1, and the retention coefficient, adimensional in Equation 2, which considers the possible re-sedimentation of the eroded material across the watershed.

$$W_s = \pi H \tau_G Z^3 A \quad (1)$$

$$R = \frac{\sqrt{OD}(l + l_{lat})}{(l + 10)A} \quad (2)$$

$$G = W_s R \quad (3)$$

The terms that appear in the equations are τ_G temperature coefficient $^{\circ}C$, H average annual precipitation value mm/yr , Z erosion coefficient $[-]$, A basin area km^2 , O perimeter of the basin km , D average height of the basin km , l length of the main watercourse km , l_{lat} the total length of the lateral tributaries km . The values of Z are obtained from experimental tables reported in the appendix and are generally correlated to the land use characteristics and geological maps. The Gavrilovic method was developed to work with annual data of mean precipitation and temperature. Since with CRHyME continuous daily simulations were conducted, the method has been simply temporally downscaled substituting P and T yearly coefficients with the daily precipitation and temperature.

Gavrilovic method defines W_s as the source of available sediment that can be routed through the watershed until the outlet is reached. In CRHyME, the first calculation considers a pure Transport Limited (TL) bed load transport, where the solid discharge is expressed as a power-law function of the river channel slope and liquid discharge (Vetsch *et al.* 2018). A second calculation is a Erosion Limited (EL) bed load transport. The latter recalls the kinematic model adopted for clear water routing assuming that the velocity of sediment transport, when the critical value of incipient motion has overcome (Figure 1), is in function of the water flow (Vetsch *et al.* 2018).

According to (Lamb and Venditti 2016, Pearson *et al.* 2017), the spatial distribution of D_{50} , the mean diameter of granulometric curve of terrain sediments, is the most uncertain parameter that has been found to sharply modify the effective sediment transport routing and the watershed sediment yield. In CRHyME have been implemented empirical *slope*- D_{50} relations for assessing the effective production of the bed-load transport (Figure 1). These relations simulate the functions proposed by (Berg 1995), varying the two power-law coefficients.

2.2 Reservoir siltation measurements

With the CRHyME model, some monitoring points in correspondence with the reservoir could be defined. Simply knowing the location of the dam in geographical coordinates (latitude and

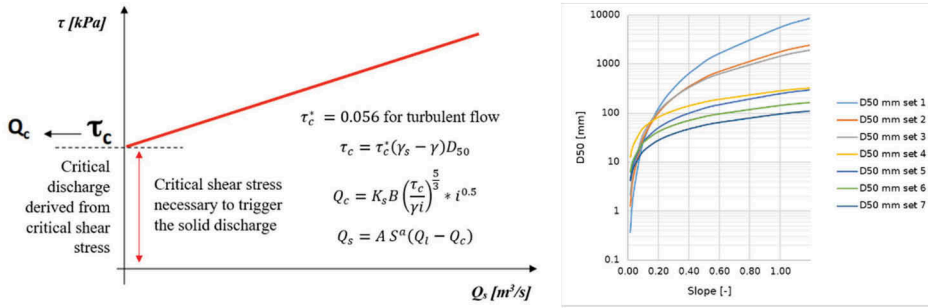


Figure 1. Left) evaluation of the incipient motion condition for solid transport where the critical liquid discharge Q_c are a function of the local granulometry through the parameter D_{50} ; right) $slope$ - D_{50} relationships.

longitude) the model can pick up at that point all the variables we are interested in, e.g. the liquid and solid discharge. Knowing the duration of the simulation is possible to convert discharges into volumes and aggregate them seasonally or yearly to evaluate the possible sediment siltation rates in the area. In the calibration and validation phases, the yearly based sediment yield rate measured at reservoirs, expressed in m^3/yr has been considered as a reference for the CRHyME ranking and compared to the one available in the literature. Since managing operations were not completely described or reported in the references (ITCOLD 2009, 2016) we have neglected them, considering the maximum value of siltation that occurred.

3 RESULTS

The case study used for the calibration and validation of the CRHyME model concerns the dramatic geo-hydrological episode triggered by rather intense and prolonged rainfalls that happened in the Valtellina basin of the Adda river. The Valtellina valley (Figure 2) is comprised of the northern part of the Lombardy region and similar episodes iteratively hit the area in July 1987, November 2000 and November 2002 causing extensive damage across the entire province (Rappelli 2008, Abbate *et al.* 2021). During these events, several dams and reservoirs experienced significant siltation due to large sediment discharge triggered by the heavy rainfalls (Rappelli 2008, ITCOLD 2016).

Table 1. Simulation settings for calibration and validation of the new model CRHyME in the Valtellina case study.

	Starting Date	Ending Date	Rainfall Dataset used
Calibration	01/09/2015	31/08/2018	ARPA
Validation	01/09/2018	31/12/2021	ARPA

The CRHyME model was calibrated and validated considering a long-term simulation (LT) (Table 1). The calibration for Valtellina has been carried out for three years comprised between 1 September 2015 and 31 August 2018. A period of 2-3 years is necessary to rise the model to a realistic “initial condition”. A redistribution of the erodible material according to the Gavrilovic model is also necessary for the correct reproduction of sediment transport. Then, a subsequent validation period started on 1 September 2018 up to 31 December 2021. The meteorological dataset containing rainfall and temperature data was provided by ARPA Lombardia (Regional Agency for the Protection of the Environment), considering for this type of simulation a timestep of 1 day (ARPA Lombardia 2022).

3.1 Model calibration and validation

The calibration of the solid routing in CRHyME has followed a different strategy. The bed-load sediment transport has been evaluated using the Gavrilovic model and checked in

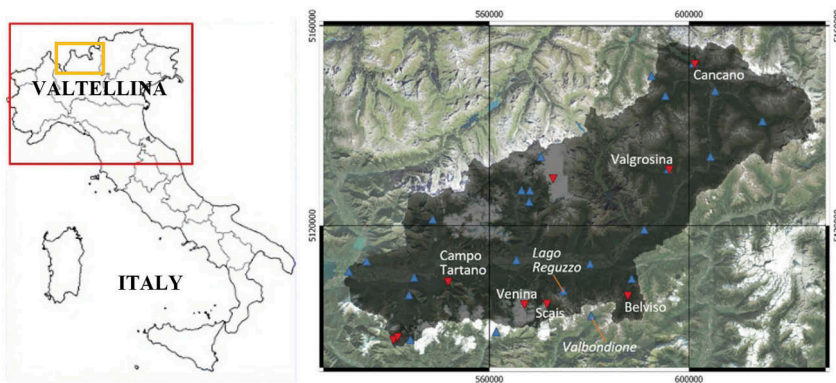


Figure 2. Valtellina case study area. Blue triangles are rain gauge stations while red triangles are hydro-power reservoirs.

correspondence with the three hydropower reservoirs of Campo Tartano, Valgrosina and Cancano (Table 2). For each reservoir, a literature survey has been conducted to estimate the sediment accumulation inside (ITCOLD 2009, 2016). The calibration parameter of the sediment yield is mainly represented by the D_{50} diameter that in our case has been expressed as a power-law continuous function of the slope. The calibration procedure consisted of several runs of the model during the calibration and validation periods, testing the *slope- D_{50}* equations proposed in Figure 1. After some attempts were found that the set n°6 was sufficiently representative of the Valtellina area. In fact, in correspondence with each reservoir, the total solid transited during the calibration and validation period was in accordance with the reference values reported for the three reservoirs (Table 2).

Table 2. Comparison between the sediment yield measured (Reference) and simulated by CRHyME for the Campo Tartano, Valgrosina and Cancano dams, during the period 2015-2019.

Sediment Yield	Campo Tartano Dam	Valgrosina Dam	Cancano Dam
Reference	38'037 m ³ /yr	33'600 m ³ /yr	21'450 m ³ /yr
Simulated 2015-2019	33'604 m ³ /yr	34'324 m ³ /yr	18'893 m ³ /yr

For the three examined reservoirs, the physical representation of the sediment transport evolution across the catchments is quite consistent with the measurements. Another confirmation can be also highlighted for the other three reservoirs of Venina, Scais and Belviso (Figure 4) are situated in correspondence with the left flank of the Valtellina watershed, across the Orobie Alps. All of them are similar to the Tartano reservoir in highlighting the Vaia storm as the most intense of the entire period, giving a sharp volume increase due to the huge amount of water discharge produced by the event (Abbate *et al.* 2021). Rainfall amounts recorded by the local ARPA stations were significant: the rain gauges of Lago Reguzzo and Valbondione have recorded amounts comprised of between 200 and 500 mm (Figure 3). These rain gauges are in the same area as Venina, Scais and Belviso dams. For the Belviso reservoir, the intense rainfall events have produced a huge amount of sediments that have increased sensible annual sediment yield estimation. Looking at Table 3, the simulated sediment yields with and without Vaia storm contribution are reported.

3.2 Future projections of solid discharge and volume

This section reports the results of the climate simulations conducted with CRHyME using the data produced by the EURO-CORDEX project (scenario RCP 8.5) and applied to the Adda basin for the Valtellina case study. These models come from the EURO-CORDEX project (Jacob *et al.* 2014), under climate scenario RCP 8.5, and have been applied to the Adda basin

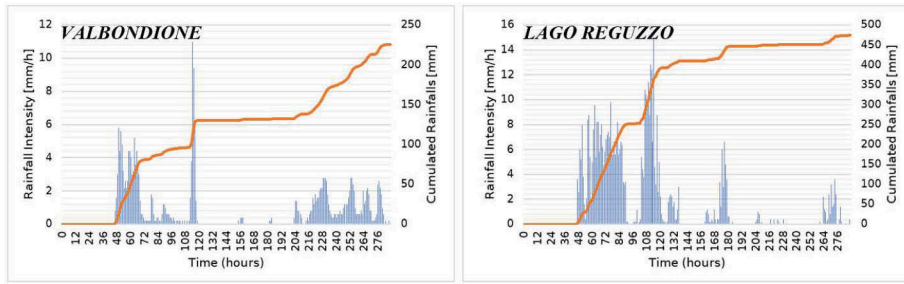


Figure 3. Rain gauge series of rainfall intensity (blue) and cumulated rainfall (orange) recorded by Lago Reguzzo station and Valbondione station during the Vaia storm. The hours are counted since 25 October 2018 at 00:00.

Table 3. Comparison between the sediment yield measured and simulated by CRHyME for the Venina, Scais and Belviso dams, during the period 2015-2019.

Sediment Yield	Venina Dam	Scais Dam	Belviso Dam
Reference	6'370 m ³ /yr	20'430 m ³ /yr	23'440 m ³ /yr
Simulated	12'128 m ³ /yr	26'422 m ³ /yr	37'338 m ³ /yr
Simulated without VAIA Storm (2018) contribute	8'913 m ³ /yr	19'877 m ³ /yr	23'910 m ³ /yr

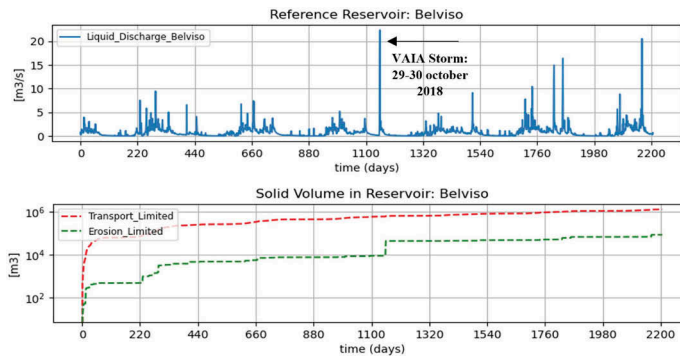


Figure 4. CRHyME simulations of water discharge, solid transport, and volume at Belviso Dam. For sediment yield production, both transport-limited (TL) and erosion-limited (EL) conditions have been tested. It can be noticed the important contribution of the Vaia storm in October 2018 to the eroded volume in EL condition.

for the Valtellina case study (Table 4). The climatic data were considered as the drivers for the CRHyME models to retrieve possible future tendencies of geo-hydrological variables.

Table 4. EURO-CORDEX Climatic models considered for CRHyME.

Id	Name	EURO-CORDEX Climatic Model
2	<i>mod2</i>	CLMcom_EC-EARTH_CCLM
3	<i>mod3</i>	CLMcom_MPI-ESM-LR_CCLM
4	<i>mod4</i>	CLMcom_CNRM-CM5_CCLM

For the EURO-CORDEX models analysed (e.g. *mod2*, *mod3* and *mod4*), CRHyME was run both for the historical data, from 01-01-1986 to 31-12-2005, and then for the future projection, from 01-01-2006 to 01-01-2075. The result's plots are organized as follows: the data

series for the three climatic models are shown against the LOWESS interpolator (LOcally WEighted Scatterplot Smoothing) (Moran 1984), implemented for highlighting the possible future tendency. Four variables have been reported: Maximum daily Precipitation (Max_Prec) in mm/day , Maximum Discharge (Q_max) in m^3/s , Maximum Sediment Discharge (Q_max_s) in m^3/s and Sediment Yield (Sed_Yield) in m^3/yr (Figure 5).

For the Mean Precipitation (not shown) no particular trends are highlighted by LOWESS. It can be appreciated that a slight bias exists among the three models where $mod2$ is drier than $mod3$ and $mod4$ which is the wettest. For the Maximum Precipitation (Max_P), the LOWESS interpolator shows a slight increase in the mean, especially for the periods 2006-2025 and 2026-2045. On the contrary, for the second half of the century, a decrease is expected, especially for $mod4$. Moreover, the outliers are projected to increase with respect to the reference period with high confidence. For the Maximum Discharge, a less clear trend concerning the mean is here shown by LOWESS. A rather flat tendency is reported in the graphs especially for the $mod3$ while for the others, a slight increase is expected during the period 2026-2045. Outliers are also suspected to increase sharply during the 21st century. For the Sediment Yield can be appreciated by LOWESS graphs, a rather flat trend is reported with slight or no significant variation in mean. The anomalous data will increase in the future with higher uncertainty.

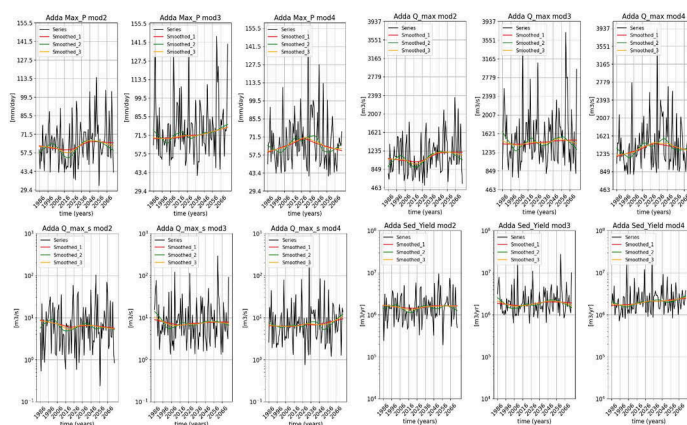


Figure 5. Climate Change simulated with EURO-CORDEX $mod2$, $mod3$ and $mod4$ for the geo-hydrological variables of Max_P (maximum daily precipitation), Q_max (maximum daily discharge), Q_max_s (maximum daily discharge) and Sed_Yield (average annual sediment yield). In black is depicted the series while the LOWESS interpolator is shown in colour (red, yellow, and green) with different values of the hyperparameters.

4 DISCUSSION

In this work, an application of the new model CRHyME has been described addressing the topic of dam siltation. A quantitative description of the siltation processes is rather complicated even though on-site measurements are provided periodically (Adamo *et al.* 2021). Moreover, each reservoir has a sediment dynamic that makes it difficult into defining a robust methodology for its assessment and prevision (de Trinchiera and Otterpohl 2018). Erosion and solid transport phenomena are processes that have been studied in literature closing relating to hydrological simulations (Vetsch *et al.* 2018). In this framework, the new CRHyME model represents a possible solution and a useful and versatile tool where the theory of erosion and sediment transport dynamics has been extensively implemented and fully coupled with hydrology.

Looking at the simulation results, the model has correctly reproduced the siltation ratio of the analysed reservoirs of the Valtellina catchment. Tartano, Valgrosina and Cancano dams have been considered in the study thanks to the availability of historical data coming from bathymetries conducted in the past by reservoir managers (ITCOLD 2009, 2016). As can be appreciated in Table 2, the errors committed by CRHyME are negligible with respect to the references, with

differences around 10-20%. Even though the period of the simulation was rather short (only six years), the results are appreciable and significant, bearing in mind that the simulation timestep was about 1 day. This fact highlights the robustness of the methodology implemented for reproducing erosion and sediment routing jointly with the stability of the code in reproducing long simulations with coarse timestep. In the second set of Belviso, Venina and Scais reservoirs, we have highlighted another interesting aspect: the contribution of a single extreme event to siltation and sediment routing. Looking at Table 3, the simulated sediment yields were rather overestimated with respect to the reference. So that, the contribution of the Vaia Storm occurred in late October 2018 was glimpsed and then removed from the mean calculation. As a result, the corrected sediment yields were now better in accordance with respect to the mean references. This fact represents a typical situation that occurs in mountain reservoirs where sediment yields and therefore siltation ratios may change abruptly in the function of the amount of precipitation and rainfall-runoff dynamics that originates inside a catchment (Vetsch *et al.* 2018, Adamo *et al.* 2021). In our experience, that evidence only emerged during the most intense event of 2018 but in principle could be detected in others.

CRHyME has been also driven by EURO-CORDEX climate change models showing possible future tendencies of the critical variables related to reservoir siltation. This task has been completed correctly by the model, carrying out almost 90 yrs (1986-2075) of simulation. As could be appreciated, the yearly mean of sediment yield is not supposed to have huge modifications in the long term, but outliers have been suspected to increase by the end of the century. This data is supported by recent IPCC Assessment Reports (Arias *et al.* 2021) where are states that the frequency of extreme events will probably increase. Since this signal has been detected both in *Prec*, *Max_Prec* and *Q_max* future series is logical to find this evidence also in *Sed_Yield*: these variables are physically correlated in geo-hydrological processes. These results could be interpreted in this way: in the next future, a possible acceleration of the geo-hydrological will occur influencing siltation not in average rates but rather in short-term rates *Q_max_s*, like already experimented during the recent Vaia event of 2018.

Erosion and solid transport quantification cannot be treated deterministically if some key data are not available or tuned indirectly from the others. The lack of free-available monitoring data, i.e. dam bathymetry or direct measurement of erosion and solid transport discharges, poses some difficulties. These processes depend on granulometry composition, in terms of D_{50} , which is uncertain since field data are very scarce, and affordable reference databases are still not available (Hengl *et al.* 2017). In the recent literature, some simplified models dealing with sediment erosion and transport have been proposed to fulfil the need to quantify these processes more expeditiously (Tangi *et al.* 2019, Bizzi *et al.* 2021). One of their main worth points is the possibility to include statistical analysis on inputs and to make Montecarlo iterations extending a deterministic simulation to probabilistic scenarios. However, these models suffer from the same problem as the distributed ones: the scarcity of reference data. The former is necessary to select the most representative simulation among the others bearing in mind that some aspects of the erosion-transport interactions remain unknown. Anyhow, the efforts conducted in this study with the creation of CRHyME move in the direction of a better investigation around the geo-hydrological hazard which is an open research frontier.

5 CONCLUSION

Reservoir siltation represents a current problem for dam manager companies which are interested to preserve the capacity and the operativity of their reservoirs, strategies are needed for estimating the current siltation state and to give projections for the next future. The new model CRHyME represents a novelty in the panorama of the classical spatially distributed hydrological model, trying to couple together erosion and sediment routing processes with the hydrological part, extending the applicability to classical rainfall series and climate change scenarios. The application of CRHyME to the Valtellina case study has reached good performances in reconstructing the siltation rates in correspondence with six reservoirs located in the area. Moreover, the importance of the extreme event of Vaia that occurred in 2018 has

been highlighted with respect to the siltation dynamics and sediment yield estimations. Then an application using the EURO-CORDEX climate change scenario has shown the versatility of the model for carrying out long simulations, depicting also a possible acceleration of the geo-hydrological processes in the next decades.

ACKNOWLEDGMENTS

“This work has been financed by the Research Fund for the Italian Electrical System under the Three-Year Research Plan 2022-2024 (DM MITE n. 337, 15.09.2022), in compliance with the Decree of April 16th, 2018”.

REFERENCES

- Abbate, A., 2022. Hydrogeological hazards evaluation under climate change scenarios: an application of the CRHyME model (Climatic Rainfall Hydrogeological Modelling Experiment). Milano: Politecnico di Milano.
- Abbate, A. and Mancusi, L., 2021a. Manuale del modello CRHyME (Climate Rainfall Hydrogeological Modelling Experiment). Milano: RSE Report RdS 21012462.
- Abbate, A. and Mancusi, L., 2021b. Strumenti per la mappatura delle minacce idrogeologiche per il sistema energetico e incidenza dei cambiamenti climatici. Milano: RSE Report RdS 21010317.
- Abbate, A., Papini, M., and Longoni, L., 2021. Analysis of meteorological parameters triggering rainfall-induced landslide: a review of 70 years in Valtellina. *Nat. Hazards Earth Syst. Sci.*, 21 (7), 2041–2058.
- Adamo, N., Al-Ansari, N., Sissakian, V., Laue, J., and Knutsson, S., 2021. Dam safety: Sediments and debris problems. *Journal of Earth Sciences and Geotechnical Engineering*, 11 (1), 27–63.
- Albano, R., Mancusi, L., and Abbate, A., 2017. Improving flood risk analysis for effectively supporting the implementation of flood risk management plans: The case study of “Serio” Valley. *Environmental Science & Policy*, 75, 158–172.
- Arias, P., Bellouin, N., Coppola, E., Jones, R., Krinner, G., Marotzke, J., Naik, V., Palmer, M., Plattner, G.-K., Rogelj, J., Rojas, M., Sillmann, J., Storelvmo, T., Thorne, P., Trewin, B., Rao, K., Adhikary, B., Allan, R., Armour, K., and Zickfeld, K., 2021. IPCC AR6 WGI Technical Summary.
- ARPA Lombardia, 2022. Rete Monitoraggio ARPA Lombardia [online]. Available from: www.arpalombardia.it/stiti/arpalombardia/meteo.
- Bemporad, G.A., Alterach, J., Amighetti, F.F., Peviani, M., and Saccardo, I., 1997. A distributed approach for sediment yield evaluation in Alpine regions. *Journal of Hydrology*, 197, 370–392.
- Berg, J.H., 1995. Prediction of Alluvial Channel Pattern of Perennial Rivers. *Geomorphology*, 12, 259–279.
- Bizzi, S., Tangi, M., Schmitt, R.J.P., Pitlick, J., Piégay, H., and Castelletti, A.F., 2021. Sediment transport at the network scale and its link to channel morphology in the braided Vjosa River system. *Earth Surface Processes and Landforms*, 46 (14), 2946–2962.
- Brambilla, D., Papini, M., Ivanov, V.I., Bonaventura, L., Abbate, A., and Longoni, L., 2020. Sediment Yield in Mountain Basins, Analysis, and Management: The SMART-SED Project. In: M. De Maio and A.K. Tiwari, eds. *Applied Geology: Approaches to Future Resource Management*. Cham: Springer International Publishing, 43–59.
- Dixon, J.A., Talbot, L.M., and Le Moigne, G.J.M., 1989. Dams and the Environment. World Bank technical paper, 110.
- E. Ciapessoni, D. Cirio, A. Pitto, L. Mancusi, and A. Abbate, 2022. Modeling the vulnerability of power system components to debris flows for power systems resilience analyses. In: 2022 17th International Conference on Probabilistic Methods Applied to Power Systems (PMAPS). Presented at the 2022 17th International Conference on Probabilistic Methods Applied to Power Systems (PMAPS), 1–6.
- Gariano, S.L. and Guzzetti, F., 2016. Landslides in a changing climate. *Earth-Science Reviews*, 162, 227–252.
- Globevnik, L., Holjevč, D., Petkovaek, G., and Rubinj, J., 2003. 145. Applicability of the Gavrilovic Method in Erosion Calculation Using Spatial Data Manipulation Techniques. *Tunnelling and Underground Space Technology*, 14.
- Hengl, T., Mendes de Jesus, J., Heuvelink, G.B.M., Ruiperez Gonzalez, M., Kilibarda, M., Blagotić, A., Shangquan, W., Wright, M.N., Geng, X., Bauer-Marschallinger, B., Guevara, M.A., Vargas, R., MacMillan, R.A., Batjes, N.H., Leenaars, J.G.B., Ribeiro, E., Wheeler, I., Mantel, S., and

- Kempen, B., 2017. SoilGrids250m: Global gridded soil information based on machine learning. *PLOS ONE*, 12 (2), e0169748.
- ITCOLD, 2009. La gestione dell'interrimento dei serbatoi artificiali italiani. Comitato Nazionale Italiano delle Grandi Dighe, No. 1.
- ITCOLD, 2016. La gestione dell'interrimento dei serbatoi artificiali italiani situazione attuale e prospettive. Comitato Nazionale Italiano delle Grandi Dighe, No. 2.
- Iverson, R.M., 2000. Landslide triggering by rain infiltration. *Water Resources Research*, 36 (7), 1897–1910.
- Jacob, D., Petersen, J., Eggert, B., Alias, A., Christensen, O.B., Bouwer, L.M., Braun, A., Colette, A., Déqué, M., Georgievski, G., Georgopoulou, E., Gobiet, A., Menut, L., Nikulin, G., Haensler, A., Hempelmann, N., Jones, C., Keuler, K., Kovats, S., Kröner, N., Kotlarski, S., Kriegsmann, A., Martin, E., van Meijgaard, E., Moseley, C., Pfeifer, S., Preuschmann, S., Radermacher, C., Radtke, K., Rechid, D., Rounsevell, M., Samuelsson, P., Somot, S., Soussana, J.-F., Teichmann, C., Valentini, R., Vautard, R., Weber, B., and Yiou, P., 2014. EURO-CORDEX: new high-resolution climate change projections for European impact research. *Regional Environmental Change*, 14 (2), 563–578.
- Karssenberg, D., Schmitz, O., Salamon, P., de Jong, K., and Bierkens, M.F.P., 2010. A software framework for construction of process-based stochastic spatio-temporal models and data assimilation. *Environmental Modelling & Software*, 25 (4), 489–502.
- Kreibich, H., Di Baldassarre, G., Vorogushyn, S., Aerts, J.C.J.H., Apel, H., Aronica, G.T., Arnbjerg-Nielsen, K., Bouwer, L.M., Bubeck, P., Caloiero, T., Chinh, D.T., Cortès, M., Gain, A.K., Giampá, V., Kuhlicke, C., Kundzewicz, Z.W., Llasat, M.C., Mård, J., Matczak, P., Mazzoleni, M., Molinari, D., Dung, N.V., Petrucci, O., Schröter, K., Slager, K., Thielen, A.H., Ward, P.J., and Merz, B., 2017. Adaptation to flood risk: Results of international paired flood event studies. *Earth's Future*, 5 (10), 953–965.
- Lamb, M.P. and Venditti, J.G., 2016. The grain size gap and abrupt gravel-sand transitions in rivers due to suspension fallout. *Geophysical Research Letters*, 43 (8), 3777–3785.
- Milanesi, L., Pilotti, M., Clerici, A., and Gavrilovic, Z., 2015. Application of an improved version of the Erosion Potential Method in Alpine areas. *Italian Journal of Engineering Geology and Environment*.
- Moran, G.W., 1984. Locally-Weighted-Regression Scatter-Plot Smoothing (LOWESS): a graphical exploratory data analysis technique. *NAVAL POSTGRADUATE SCHOOL MONTEREY CA*.
- Panagos, P., Borrelli, P., Poesen, J., Ballabio, C., Lugato, E., Meusburger, K., Montanarella, L., and Alewell, C., 2015. The new assessment of soil loss by water erosion in Europe. *Environmental Science & Policy*, 54, 438–447.
- Pearson, E., Smith, M.W., Klaar, M.J., and Brown, L.E., 2017. Can high resolution 3D topographic surveys provide reliable grain size estimates in gravel bed rivers? *Geomorphology*, 293, 143–155.
- Rappelli, F., 2008. Definizione delle soglie pluviometriche d'innescio frane superficiali e colate torrentizie: accorpamento per aree omogenee. Milano: IRER, Istituto Regionale di Ricerca della Lombardia.
- Roo, A., A.P.J. Wesseling, C.G., Jetten, V.G., and Ritsema, C., 1996. LISEM: A physically-based hydrological and soil erosion model incorporated in a GIS. In: K. Kovar & H.P. Nachtnebel (eds.), *Application of geographic information systems in hydrology and water resources management*. Wallingford (UK), IAHS, 1996. IAHS Publ. 235, pp. 395–403.
- Shobe, C., Tucker, G., and Barnhart, K., 2017. The SPACE 1.0 model: A Landlab component for 2-D calculation of sediment transport, bedrock erosion, and landscape evolution. *Geoscientific Model Development Discussions*, 1–38.
- Strauch, R., Istanbuloglu, E., Nudurupati, S.S., Bandaragoda, C., Gasparini, N.M., and Tucker, G.E., 2018. A hydroclimatological approach to predicting regional landslide probability using Landlab. *Earth Surf. Dynam.*, 6 (1), 49–75.
- Sutanudjaja, E.H., van Beek, R., Wanders, N., Wada, Y., Bosmans, J.H.C., Drost, N., van der Ent, R.J., de Graaf, I.E.M., Hoch, J.M., de Jong, K., Karssenberg, D., López López, P., Peßenteiner, S., Schmitz, O., Straatsma, M.W., Vannamettee, E., Wisser, D., and Bierkens, M.F.P., 2018. PCR-GLOBWB 2: a 5,arcmn global hydrological and water resources model. *Geoscientific Model Development*, 11 (6), 2429–2453.
- Tangi, M., Schmitt, R., Bizzi, S., and Castelletti, A., 2019. The CASCADE toolbox for analyzing river sediment connectivity and management. *Environmental Modelling & Software*, 119, 400–406.
- de Trincheria, J. and Otterpohl, R., 2018. Towards a universal optimization of the performance of sand storage dams in arid and semi-arid areas by systematically minimizing vulnerability to siltation: A case study in Makueni, Kenya. *International Journal of Sediment Research*, 33 (3), 221–233.
- Vetsch, D., Siviglia, A., Caponi, F., Ehrbar, D., Gerke, E., Kammerer, S., Koch, A., Peter, S., Vanzo, D., Vonwiller, L., Facchini, M., Gerber, M., Volz, C., Farshi, D., Mueller, R., Rousselot, P., Veprek, R., and Faeh, R., 2018. System Manuals of BASEMENT Version 2.8.

Electronic monitoring of natural hazards prone reservoir regions and catchment areas of Alpine dams

M. Carrel, S. Stähly, J. Gassner & S. Wahlen
GEOPRAEVENT AG, Zürich

ABSTRACT: In the Alps, many hydropower infrastructures could potentially be impacted by impulse waves or tsunamis triggered by natural gravitational hazards as landslides, large rock falls or glacier collapse occurring in the vicinity of reservoirs. Impulse waves in reservoirs overtopping dams have the potential to cause serious damage or even complete failure to these key infrastructures. Automatic electronic monitoring of the geomorphological processes involved can provide key information to take measures reducing the impact of natural hazards on these infrastructures. GEOPRAEVENT has been monitoring such hazards in the Alps for more than a decade applying various technologies and different approaches. In this paper, we present different cases of monitoring of slopes, rock cliffs and glaciers that could potentially generate impulse waves in reservoirs located in the Swiss Alps or endanger construction work on hydropower infrastructure. Among others, camera-based systems used to monitor the “Giétro” glacier in the vicinity of the Mauvoisin dam and monitoring of the “Schafselbsanft” area above the Limmeren reservoir with both crack meters installed locally and periodic interferometric radar measurements. These measurement systems provide useful data to monitor the evolution of key processes in the vicinity of these critical infrastructure.

RÉSUMÉ: Dans les Alpes, de nombreuses infrastructures hydroélectriques pourraient être affectées par des ondes d’impulsion ou des tsunamis déclenchés par des risques gravitationnels naturels tels que des glissements de terrain, des chutes de pierres importantes ou l’effondrement de glaciers à proximité des réservoirs. Les ondes d’impulsion dans les réservoirs qui débordent des barrages peuvent causer de graves dommages, voire une défaillance complète de ces infrastructures clés. La surveillance électronique automatique des processus géomorphologiques en jeu peut fournir des informations essentielles pour prendre des mesures visant à réduire l’impact des risques naturels sur ces infrastructures. GEO-PRAEVENT surveille ces risques dans les Alpes depuis plus d’une décennie en utilisant différentes technologies et approches. Dans cet article, nous présentons différents cas de surveillance de pentes, de falaises rocheuses et de glaciers qui pourraient potentiellement générer des vagues d’impulsion dans les réservoirs situés dans les Alpes suisses ou mettre en danger les travaux de construction d’infrastructures hydroélectriques. Entre autres, des systèmes basés sur des caméras ont été utilisés pour surveiller le glacier du “Giétro” à proximité du barrage de Mauvoisin et la surveillance de la zone “Schafselbsanft” au-dessus du réservoir de Limmeren à l’aide de fissuromètres installés localement et de mesures radar interférométriques périodiques. Ces systèmes de mesure fournissent des données utiles pour surveiller l’évolution des processus clés à proximité de ces infrastructures critiques.

1 INTRODUCTION

Mountain environments are naturally prone to natural hazards caused by geomorphological processes. The observed temperature rise over the last years led to permafrost melting (Harris et al., 2003) and the retreat or disappearance of glaciers (Huss and Fischer, 2016). These phenomena

and their combination are increasing the probability of occurrence of gravitational hazards such as rockfall (Fischer et al., 2006), landslides (Huggel et al., 2012), avalanches (Gilbert et al., 2015) or glacier lake outbursts floods (Harrison et al., 2018). Thereby, climate change exacerbates the already existing risk due to geomorphological processes, increasing the possibility of infrastructure destabilization or damage (Duvillard et al., 2015). In some cases, several processes combine in a hazard cascade that can have devastating consequences for infrastructure located in the vicinity and people living nearby (Mergili et al., 2020). A recent example of cascading events is the catastrophic mass flow caused by an extraordinary rock and ice avalanche and debris flow that left more than 200 people dead or missing, destroyed infrastructure and damaged two hydropower projects severely (Shugar et al., 2021).

The hydropower potential of the Alps has been extensively developed in the 20th century and the energy crisis that stroke Europe in 2022 fostered the development of new projects. Due to their location in a mountainous environment, key infrastructure such as dams, water intakes or conduits are exposed to gravitational natural hazards. Additionally, dam reservoir catchments are also of concern, as impulse waves generated by landslides or avalanches could also cause severe damage to the dam itself (Heller and Hager, 2010; Huang et al., 2016). To prevent or to develop mitigation strategies for such hazards, it is necessary to first identify, understand and monitor such problematic processes and to be able to alert in the case of critical situations.

In this study, we present three different case studies of hydropower infrastructure located in the Alps and endangered by either glacier retreat and possible subsequent collapse or important rockfall events. The problems faced in these different cases are very much dependent on the local topography and geology, which leads to the implementation of three customized technical solutions to optimally monitor the involved gravitational hazards.

2 MATERIAL AND METHODS

2.1 *Presentation of the study sites*

The three cases presented in this study are located in Switzerland, as illustrated on Figure 1. The first site is a glacier monitoring site with a camera system installed on a ridge close to “La Grande Ashle” above the Mauvoisin retention lake, close to the Verbier ski resort. This Giétro glacier caused a large flood in 1818 as its ice avalanches blocked the valley floor and formed a glacial lake, which failure caused a major flood, devastating the valley below (Ancy et al., 2019). The glacier remains potentially dangerous as it is retreating, and a potential collapse of its tongue reaching the retention lake could create an impulse wave endangering the dam structure.

The Schafselbsanft landslide is located above the Limmeren lake, which is the main reservoir of the massive Linth-Limmeren hydropower complex. This cliff is moving at a constant velocity of several millimeters per year, and contains several important cracks. Here again, any important failure of this cliff could potentially lead to an impulse wave endangering the dam structure.

The third study site is located in Ovella on the Swiss-Austrian border above a water intake on the Inn river that was recently built. The Northern side of the valley is prone to frequent rockfall events and potentially threatening the workers underneath.

2.2 *Giétro glacier above the Mauvoisin hydropower dam*

The system installed on the “Grande Ashle” mountain to monitor the Giétro glacier consists mainly of a high-resolution camera, a solar power supply, a data transmission unit and a waterproof casing. The camera is a digital single-lens reflex model with a resolution of 24 megapixels. The different electronic components were chosen carefully to minimize maintenance on site. The system is mounted on a rock pillar above the lake and in front of the glacier. The system is self-sufficient as its power supply is provided by a solar panel and a battery, allowing to overcome several days of bad weather.

Such a camera system can take photographs on an hourly basis. Cross-correlation algorithms have recently been applied to images of glaciers in order to quantify their displacement

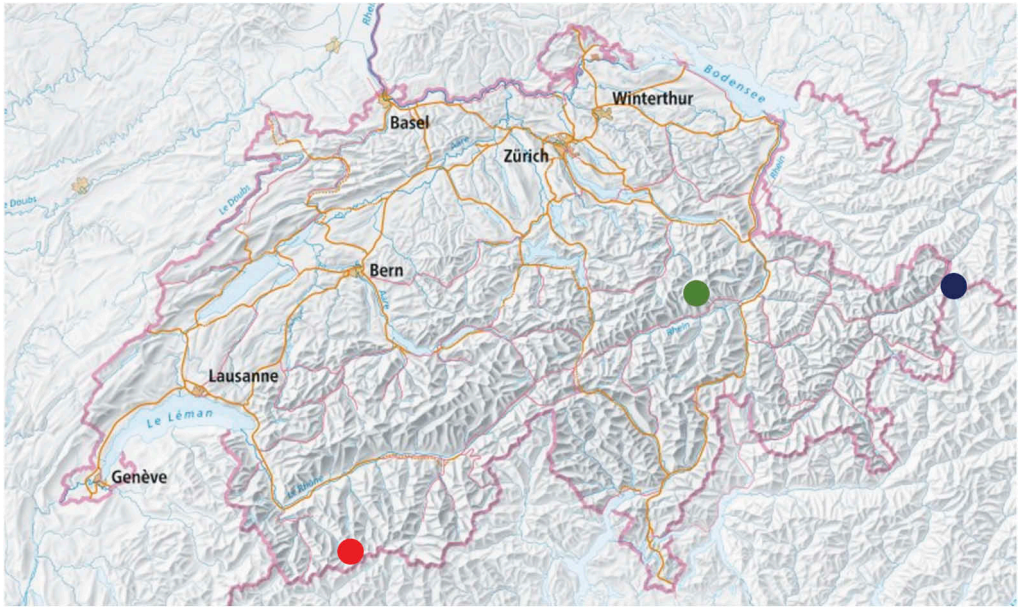


Figure 1. Map of Switzerland with the location of the Giétro glacier (red), Schafselbsanft cliff above the Limmeren lake (green) and Ovella rockfall site (blue) on the Swiss-Austrian border, background map: courtesy of swisstopo.



Figure 2. System installed on a rock pillar with the housing containing the camera, a solar panel and a control cabinet (left). View on the Mauvoisin reservoir and on the Gietro glacier (bottom right corner of the right panel).

(Giordan et al. 2016). Here, a cross-correlation algorithm allows to obtain the displacement field at the surface of the Giétro glacier. Images acquired on an hourly basis are used to measure displacement fields weekly. If necessary, the frequency analysis can be increased up to twice a day. Here, the local weather conditions substantially impact the quality of the photographs, so that during extended bad weather, the quality of the deformation analysis decreases substantially. The system has been operational in this alpine environment for more than 7 years without any maintenance on site.

2.3 Schafselbsanft landslide above the Limmeren reservoir

The Schafselbsanft rock cliff has been moving steadily at a speed of several millimeters per month for years. Different cracks are visible over tens of meters, see Figure 3. The monitoring

system installed there has two distinct components; first, crackmeters are mounted on cracks that were identified as potentially dangerous. These crackmeters have been used to measure displacements locally with time intervals of 10 minutes, so that any sudden local acceleration could be detected or measured. Altogether, nine different crackmeters were installed initially on cracks of length between 50 cm and 1.5 m. The cracks have been monitored since 2012, but due to avalanches events and snow pressure in this area, the material regularly must be checked, refurbished, or replaced. The crackmeters are powered with batteries that need occasional replacement. The data transmission is either performed via 3G or using the available local WAN network.



Figure 3. Aerial photograph of the Schafselbsanft cliff with the nine cracks that are monitored with crackmeters (left). Example of the installation on site with a crackmeter, the data logger and a transmission unit (right).



Figure 4. Two different locations where the interferometric radar was installed to monitor the Schafselbsanft rock cliffs.

With these crackmeters, it is possible to measure a sudden movement locally. In order to detect a more subtle acceleration of the entire cliff, another measurement technique was retained. Several campaigns were performed with a ground-based interferometric radar located on the other side of the Limmeren lake. The interferometric radar measures displacement in line of sight. To achieve optimal coverage of the entire cliff, measurements were taken from two different locations to monitor the entire region of interest. The distance between the locations of the radar and the Schafselbsanft rock cliff is of ca. 1 km or less. At this distance, it is possible to measure average submillimeter displacement with the interferometric radar with a spatial resolution of several square meters.

The locations where the interferometric radar was installed for the measurement campaigns are displayed on Figure 4. The terrain where the system was installed is quite challenging and required autonomous power supply that was provided by a system consisting of solar panels and batteries as well as a diesel generator.

2.4 *Rockfall in Ovella above a water intake*

The Ovella slope above is steep and frequent rockfall pose a serious threat to the safety of the workers building the water intake located underneath. More than 1200 m of rockfall barriers were installed on the slope to prevent important rockfall events that would eventually damage the water intake below or endanger the workers. To further increase the safety of the workforce, the barriers were equipped with more than 100 motion sensors (yellow device on Figure 5). These sensors are typically mounted on top of the masts or upper cable of the barriers. These sensors can either detect vibrations or a rockfall impact. Some so-called trigger lines are stretched between two adjacent sensors and the base of the mast. Large impacts in the rockfall barriers pull out the trigger lines. The combination of the vibration and trigger line pull-out signal allows for a differentiated interpretation of occurring events, e.g. small vibrations could imply an increase of activity after important precipitations or freeze and thaw events. Pulled out trigger lines would mean that important masses impacted the barrier and that an inspection visit should be performed rapidly to assess the state of the barrier. The motion sensors are also linked to audio-visual sirens installed close to the construction site. In case of an event, an alarm is triggered and the workers can escaped to protected areas.



Figure 5. Rockfall barrier installed above the construction site close to Ovella, with one of the motion sensors installed to detect vibration and rockfall impact.

3 RESULTS AND DISCUSSION

3.1 *Image-based monitoring of a glacier with deformation analysis*

The results of the deformation analysis are illustrated in Figure 5, with the displacement field indicated in color as pixels per day. If necessary, a conversion to m/day is also possible. In the present case, three different regions of interest were defined, namely the upper glacier zone, middle glacier zone and the glacier tongue. Additionally, stable zones were used as a reference for the atmospheric correction. The three regions of interest are delineated in white on the image in Figure 6, the stable zones in yellow. The average displacement in these different zones is displayed in the inset of Figure 6, where the black time series corresponds to the region of the glacier tongue, decelerating at the end of the ablation season, the brown and yellow data correspond to the middle and upper glacier zone, respectively. The blue data represents the average displacement in the stable areas and this time series confirms that these regions are not moving.

In Figure 6, two distinct regions of higher velocity (in blue) are visible in the region of the glacier tongue. A local acceleration was measured in these two zones towards the end of the ablation season. To monitor the situation more closely, the frequency of the deformation analysis was increased for several days. If desired, SMS and email warnings can be sent out when the deformation rate exceeds pre-defined thresholds. In the present case, the situation never posed a serious threat and was continuously monitored by experts.

Some zones of Figure 6 do not have a color coding because of the loss of correlation, meaning that the cross-correlation algorithm could not detect any movement because locally, the changes in the image were too important. This is the case in zones where vegetation may have grown, seracs collapsed or snow fell or melted.

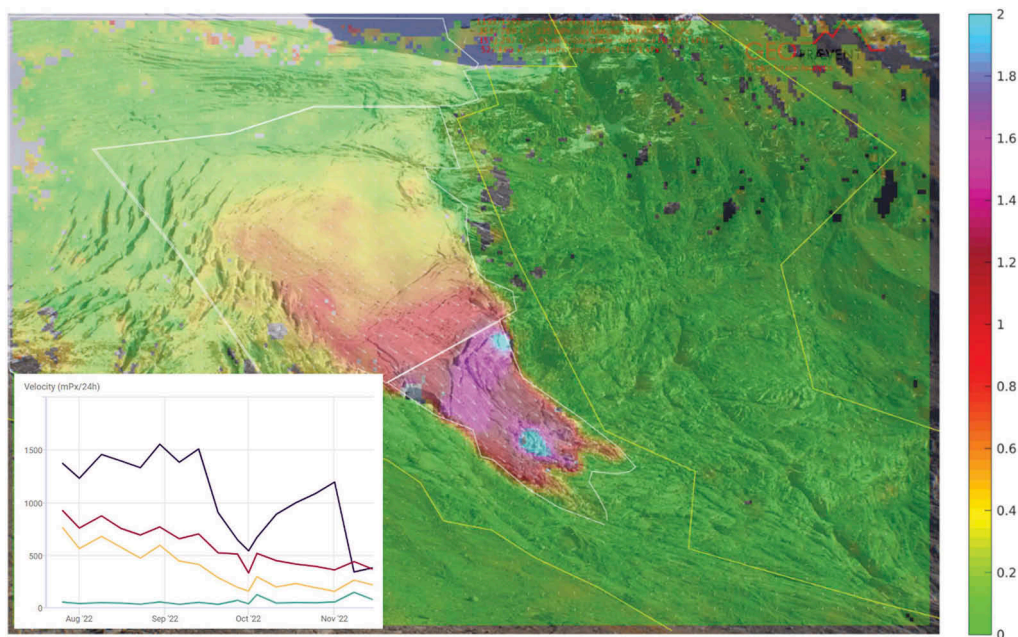


Figure 6. Displacement field in pix/frame of the Giétro glacier obtained from the deformation analysis on the 13th of September 2022. Inset: average displacement for an ablation season in the different regions of interest (black glacier tongue, brown middle zone, yellow upper glacier, blue stable zones).

3.2 Monitoring of the Schafselbsanft rock cliff above the Limmeren reservoir

The displacement measured in the Schafselbsanft region with different crackmeters is displayed in Figure 7. The unstable area shows a displacement of a few centimeters per year, which is reflected in the data measured by the crackmeters with yearly displacements ranging between 0 and 3 cm and depends on the orientation of the crackmeters with respect to the main displacement direction. Over the course of the 10 years of operation, the time series show several interruptions, which were mainly due damage caused by avalanches and snow pressure to some of the material installed (sensors, cables and loggers). Due to the remoteness of the site and its exposition to avalanches and rockfall, repair or maintenance operations could not always be performed directly, which caused some of the gaps observed in the time series.

A displacement field obtained by radar measurements averaged over a month is displayed in Figure 8, where the average displacement over this time span in the critical region is of ca. 1 mm. Zone A in pink is the zone where the crackmeters are installed. The green zones with black contours were assumed not to be moving and used as reference for the atmospheric correction.

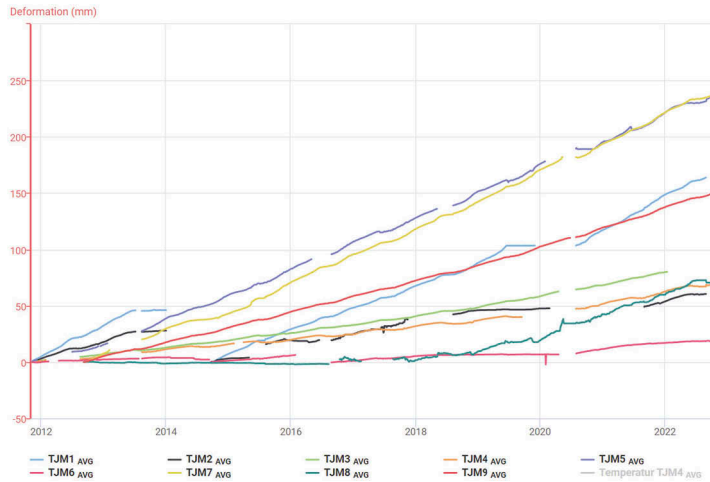


Figure 7. Ten years time series of displacement measured with crackmeters installed in the Schafselbsanft region.

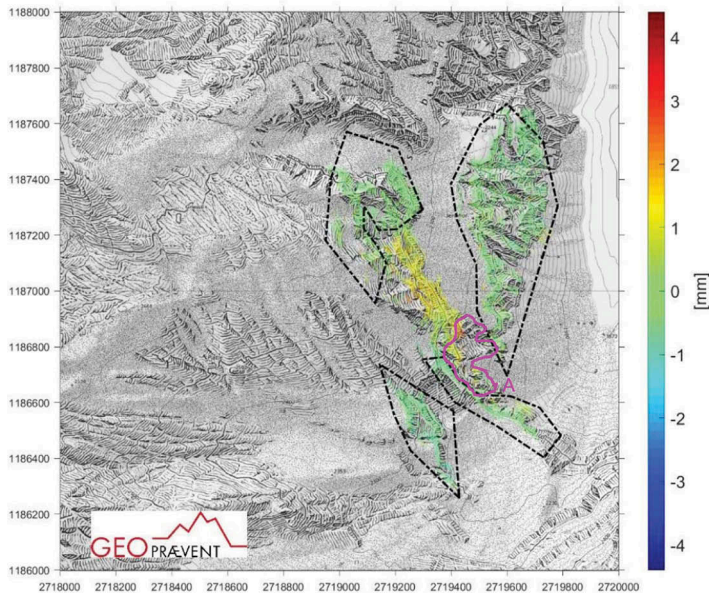


Figure 8. Displacement measured within 1 month of measurement. The black zones are stable areas used as a reference for the atmospheric correction, the zone A (pink) is the region where the crackmeters are installed.

3.3 Alarms system to detect rockfall events in Ovella above a water intake

The location of the more than hundred sensors installed on the rockfall barriers at Ovella are displayed in Figure 9. Unlike the systems presented above that are monitoring systems in the sense that they do not provide real-time or close to real-time information, the motion sensors installed in Ovella are used to provide trigger alarms in real-time (a few seconds). Therefore, it is critical to monitor their function continuously to detect any anomalies.

The sensors displayed in Figure 9 are all operating under normal conditions, as indicated by the green color-coding. In case of anomalies (data transmission interrupted, vibration detected, trigger line pulled out on one side or trigger line pulled out on both sides), the color-coding changes accordingly and alarms are triggered (notifications and alarm horns).

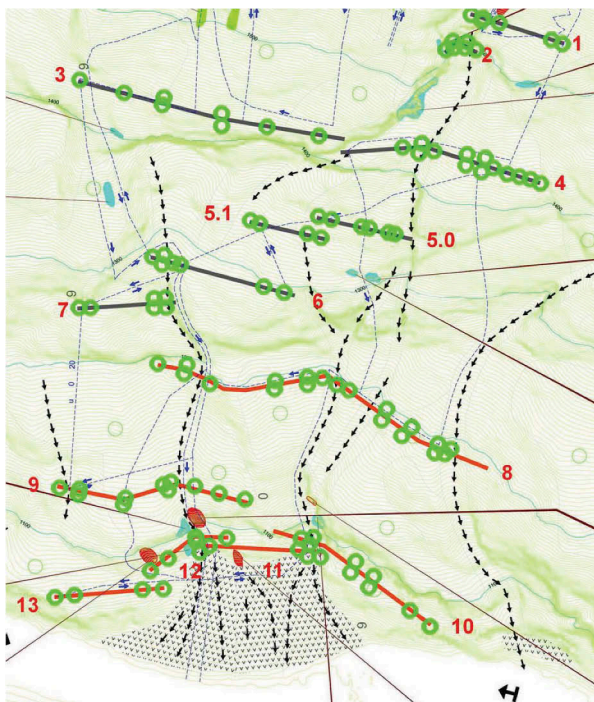


Figure 9. Location of different motion sensors close to the Ovella water intake (indicated by the green circles).

4 CONCLUSION

The different cases presented in this study show how different technologies can be used to monitor mass movements such as landslides, rockfalls, or ice avalanches that could potentially damage or endanger hydropower infrastructure. When necessary, monitoring systems can be upgraded to alarm systems to provide real-time alerting e.g., send alarm SMS and emails or activate sirens. The recent technological advances have the potential to substantially increase the reliability and accuracy of monitoring and alarm systems in a changing climate and therefore contribute to safer operation of mountain hydropower infrastructure.

REFERENCES

- Ancy, C., Bardou, E., Funk, M., Huss, M., Werder, M.A., Trehwela, T., 2019. Hydraulic Reconstruction of the 1818 Giétro Glacial Lake Outburst Flood. *Water Resour Res* 55, 8840–8863. <https://doi.org/10.1029/2019wr025274>
- Duvillard, P.-A., Ravel, L., Deline, P., 2015. Risk assessment of infrastructure destabilisation due to global warming in the high French Alps. *J Alp Res Revue De Géographie Alp*. <https://doi.org/10.4000/rga.2896>
- Fischer, L., Käab, A., Huggel, C., Noetzi, J., 2006. Geology, glacier retreat and permafrost degradation as controlling factors of slope instabilities in a high-mountain rock wall: the Monte Rosa east face. *Nat Hazard Earth Sys* 6, 761–772. <https://doi.org/10.5194/nhess-6-761-2006>

- Gilbert, A., Vincent, C., Gagliardini, O., Krug, J., Berthier, E., 2015. Assessment of thermal change in cold avalanching glaciers in relation to climate warming. *Geophys Res Lett* 42, 6382–6390. <https://doi.org/10.1002/2015gl064838>
- Harris, C., Mühl, D.V., Isaksen, K., Haerberli, W., Sollid, J.L., King, L., Holmlund, P., Dramis, F., Guglielmin, M., Palacios, D., 2003. Warming permafrost in European mountains. *Global Planet Change* 39, 215–225. <https://doi.org/10.1016/j.gloplacha.2003.04.001>
- Harrison, S., Kargel, J.S., Huggel, C., Reynolds, J., Shugar, D.H., Betts, R.A., Emmer, A., Glasser, N., Haritashya, U.K., Klimeš, J., Reinhardt, L., Schaub, Y., Wiltshire, A., Regmi, D., Vilimek, V., 2018. Climate change and the global pattern of moraine-dammed glacial lake outburst floods. *Cryosphere* 12, 1195–1209. <https://doi.org/10.5194/tc-12-1195-2018>
- Heller, V., Hager, W.H., 2010. Impulse Product Parameter in Landslide Generated Impulse Waves. *J Waterw Port Coast Ocean Eng* 136, 145–155. [https://doi.org/10.1061/\(asce\)ww.1943-5460.0000037](https://doi.org/10.1061/(asce)ww.1943-5460.0000037)
- Huang, B., Yin, Y., Du, C., 2016. Risk management study on impulse waves generated by Hongyanzi landslide in Three Gorges Reservoir of China on June 24, 2015. *Landslides* 13, 603–616. <https://doi.org/10.1007/s10346-016-0702-x>
- Huggel, C., Clague, J.J., Korup, O., 2012. C. HUGGEL, J. J. CLAGUE AND O. KORUP. *Earth Surf. Process. Landforms* 37, 77–91. <https://doi.org/10.1002/esp.2223>
- Huss, M., Fischer, M., 2016. Sensitivity of Very Small Glaciers in the Swiss Alps to Future Climate Change. *Frontiers Earth Sci* 4, 34. <https://doi.org/10.3389/feart.2016.00034>
- Mergili, M., Jaboyedoff, M., Pullarello, J., Pudasaini, S.P., 2020. Back calculation of the 2017 Piz Cengalo–Bondo landslide cascade with r.avaflow: what we can do and what we can learn. *Nat Hazard Earth Sys* 20, 505–520. <https://doi.org/10.5194/nhess-20-505-2020>
- Shugar, D.H., Jacquemart, M., Shean, D., Bhushan, S., Upadhyay, K., Sattar, A., Schwanghart, W., McBride, S., Vries, M.V.W. de, Mergili, M., Emmer, A., Deschamps-Berger, C., McDonnell, M., Bhabri, R., Allen, S., Berthier, E., Carrivick, J.L., Clague, J.J., Dokukin, M., Dunning, S.A., Frey, H., Gascoïn, S., Haritashya, U.K., Huggel, C., Kääb, A., Kargel, J.S., Kavanaugh, J.L., Lacroix, P., Petley, D., Rupper, S., Azam, M.F., Cook, S.J., Dimri, A.P., Eriksson, M., Farinotti, D., Fiddes, J., Gnyawali, K.R., Harrison, S., Jha, M., Koppes, M., Kumar, A., Leinss, S., Majeed, U., Mal, S., Muhuri, A., Noetzli, J., Paul, F., Rashid, I., Sain, K., Steiner, J., Ugalde, F., Watson, C.S., Westoby, M.J., 2021. A massive rock and ice avalanche caused the 2021 disaster at Chamoli, Indian Himalaya. *Science* 373, 300–306. <https://doi.org/10.1126/science.abh4455>

Role of water storage reservoirs management and flood mitigation in climate change conditions

T. Dašić

Faculty of Civil Engineering, University of Belgrade

ABSTRACT: The impacts of climate change are becoming increasingly pronounced in all aspects of human activity, but are especially evident in the field of water management. One of its most significant consequences is the increasingly pronounced temporal variability of river flows - frequent floods with increasing peak flows and long periods of low water flow. In such conditions, existing flood protection measures are often insufficient to secure the protected area. That is why flood protection systems must be constantly developed, considering their construction, as well as improvement of management measures. The paper presents the consequences of climate change on water resources on the territory of the Serbia. The main principles of water management in such conditions are defined, as well as the role of the estimation of flood hydrographs. The possibilities of applying mathematical models in order to improve the role of active flood protection measures of existing reservoirs are presented. The analyses are performed for water resources systems in the Trebišnjica and Vrbas river basins in the Republic of Srpska (Bosnia and Herzegovina). The main task was to analyse the reduction of peak flow in the urban areas downstream from the analysed reservoirs, taking into account the uncontrolled part of the watershed (between the urban area and the reservoir), from which the torrential tributaries originate. Performed analyses show that reservoirs (even of relatively small active storage) can significantly reduce the peak flow during flood events.

1 INTRODUCTION

Climate change is a process that is already occurring in all aspects of life. However, its greatest consequences are felt in the field of water resources. On one hand, there is an increase in high-intensity precipitation, resulting in shorter concentration times for flood waves and faster propagation of these waves. This is due to river training works that have raised river embankments and excluded or narrowed river flood zones, which were used to slow down and mitigate flood peaks. Consequently, the risk of flooding increases, and reservoirs play a more significant role in active flood protection. Their task is to mitigate the flood wave and to improve protection from high water levels downstream of the river, particularly in the urban areas and highly flood-sensitive industrial facilities.

On the other hand, the other hydrological extreme, low water periods, are significantly deteriorating in most rivers. Low water flows are decreasing, and their duration is longer. In general, flows are most drastically reduced during periods when water is most needed, such as vegetation periods, when the water demands of aquatic ecosystems and other water users are highest due to high temperatures.

The aforementioned consequences of climate change significantly change the conditions in the field of water resources. (a) There is a significant need for the construction of new reservoirs of all types of flow regulation, (b) Reservoirs are gaining additional objectives: creating conditions for reliable water supply for all users, active flood protection through the mitigation of flood waves, providing favorable conditions for the survival and development of aquatic ecosystems, etc. (c) The increasing number of objectives, especially in the field of flood protection, also affects the criteria for reservoir volume (larger reservoir volumes should be

pursued in accordance with spatial limitations), as well as the selection and disposition of release facilities.

2 WATER RESOURCES IN SERBIA UNDER CLIMATE CHANGE CONDITIONS

Even before the recent trends in climate change, Serbia had unfavorable hydrological regimes, characterized by pronounced spatial and temporal variability. Considering domestic water resources, the average annual water flow in Serbia is approximately 508 m³/s (Water Management Plan of Serbia 2001). However, during low-flow periods (which can last over 2 months) these quantities decrease below 50 m³/s, causing a serious crisis for social, ecological and economic systems. Many rivers in Serbia are torrential, with over 50% of the annual water quantities passing through short torrential floods followed by long low-water periods. The relationship between low monthly flow Q_{95%} (the 95 percentage exceedances flow) and the flood flow of 1% probability for most rivers is between 800 and 1200, but on small streams, it can reach over 1:2000 (up to 5000).

The area of Serbia is also characterized by pronounced spatial variability of water resources. The average specific runoff for the entire country is around 5.7 L/s·km². However, the northern part of Serbia, with the highest-quality soil resources suitable for agricultural production, faces the scarcest water resources, with a specific runoff of about 1-2 L/s·km² or even less. In the mountainous parts of Serbia, this value rises to over 30 L/s·km². There are large areas of the country where the average specific availability of water is less than 500 m³ per capita annually.

Water regimes in Serbia, already highly unfavorable, are further worsening due to climate change conditions. An analysis of climate change on water regimes was conducted in 2019 as part of the III National Communication on Climate Change. Two scenarios of GSB emissions according to the IPCC were considered: RCP4.5 (moderate scenario) and RCP8.5 (intensive scenario), for three future time intervals. According to these models, the average temperature will increase from 0.6°C in the near future to 2°C by the end of the century, according to the moderate scenario. According intensive scenario the increase ranges from 1°C to even 4.3°C (Đurđević et al. 2018). An increase in precipitation is expected from an average of 0.7% in the near future to 2.3% by the end of the century, according to RCP4.5, or from 1% to 4.5% according to RCP8.5. The situation is significantly more unfavorable when considering the expected decrease in precipitation during the summer vegetation period.

The results of the analysis for scenario RCP4.5 indicate a tendency towards a certain increase in average flows in most river basins, ranging from around 2 to 12% in the near future. However, from the middle to the end of the century, these flows are expected to decrease to approximately the values of the reference period, with deviations ranging from -3% to +3% (Đurđević et al. 2019). According to the more intensive scenario of GSB emissions (RCP8.5), a decrease in average annual flows is expected on most rivers, ranging from 1 to 5% in the near future, and from 3 to 17% by the end of the century.

The real danger of these changes becomes evident when analyzing the impact of climate change on average monthly and daily flows. The results indicate that flows during the low-flow and warm period of the year (typically from June to October for most rivers) will further decrease. Compared to the reference period, a decrease in average monthly flows can be expected from April to October. On the other hand, an increase in average monthly flow values is expected during December, January, February, and for some rivers, March. This means that the period with higher monthly flows is shifting towards the beginning of the year, or towards the winter months. Consequently, maximum daily flows during winter periods will increase by an average of around 10% (up to 20% in some rivers), while minimum daily flows during low-flow periods will be significantly reduced. According to RCP4.5, the average flow reduction ranges from 5% in the near future to 35% by the end of the century.

It is evident that extreme events are becoming more frequent in Serbia and it is similar in the entire region. Nine of the ten warmest observed years occurred after 2000. Disastrous floods are also becoming more frequent. In early December 2010, a flood event with a return period of 20-year, or even 50-year occurred in the area of Montenegro and Herzegovina. It was the result of heavy precipitation, in some parts of Herzegovina up to 360 mm in 24 h, and

in parts of Montenegro up to 260 mm in 2 days. In November 2019, heavy rainfall occurred again, with a maximum intensity of 312 mm in 24 h, and a total of 575 mm in 5 days (Vlahović 2020). The largest floods in the Sava River basin occurred in 2014, when parts of Serbia, Bosnia and Herzegovina and Croatia were affected. In some areas flood events of 100-year returned period have been recorded.

3 RESERVOIR MANAGEMENT DURING FLOOD EVENTS

It has already been emphasized that in the new hydrological conditions, the importance of reservoirs of all types of regulating storage is rapidly growing, especially those with the possibility of annual flow regulation. This paper deals with the problem of reservoir management in the conditions of the flood events, which is particularly significant when reservoir is located upstream of an urban area.

After the construction of the dam and reservoir, the downstream area is protected from floods, especially those with a shorter return period (2-year, 5-year, 10-year). Floods occur rarely and new urban facilities are very often situated closer to the river, sometimes even within the floodplain. Consequently, the urban area becomes more vulnerable to lower flood flows than before. In such conditions, reservoirs face the demanding task of mitigating flood waves more significantly than what was initially designed, and flood waves are more unfavorable, as a consequence of climate changes. To address this challenge, management decisions based on hydrology prognostic models and reservoir management models are necessary.

The article presents the results of the management model that provides optimal management of the releasing facilities on the dam (gates on spillways, valves on bottom outlets, operation of turbines in hydropower plant) in the case of flood event, according to the criterion of minimizing flow in the downstream urban area (Đorđević et al. 2012, Dašić et al. 2019). In addition to the flood wave in the main course of the river (which reaches the reservoir), there is also a flood wave that comes from the part of the catchment between the reservoir and the urban area, with no facilities to mitigate the flood wave (uncontrolled part of the catchment). The model was applied to two systems: the Trebišnjica Hydrosystem in East Herzegovina and the system on the Vrbas River in central Bosnia. The hydrological properties and reservoir storage capacities of presented examples are quite different. The Trebišnjica Hydrosystem, with annual regulating storage, is situated in one of most karstified regions of the world, with temporary rivers, underground flows, flooded karst poljes and extreme precipitations. The hydrosystem at Vrbas River, with weekly regulating storage, is characterised with well-developed surface river network and lower precipitation.

3.1 *Trebišnjica Hydrosystem case study*

The Trebišnjica Hydrosystem, located in Eastern Herzegovina (Bosnia and Herzegovina) is one of the most complex water resources systems in the region (Milanović 2002). Construction of the system began 60 years ago and is still ongoing. The backbone of the system is Trebišnjica River, the largest sinking river in Europe. Its catchment area is highly karstified with numerous sinkholes (ponors), springs, estaveles and underground connections with different capacity. It is the area with high precipitation and a high frequency of storm-induced events. The average annual precipitation in the region ranges between 1500 mm and 2000 mm, with extreme values reaching 3000 mm in the rainy years, and 700 mm in the droughty years. Most of the precipitation occurs in the cold part of the year, from October to March (75% of the total annual amount falling within that period), with especially heavy precipitation in the period between November and February. The summer period is often dry, with several months of little to no rainfall. The local population has been struggling with water-related challenges for centuries. During the cold (humid) period of the year (characterized by high precipitation when underground conduits are saturated and karst poljes are turned into lakes) they struggle with floods, while during the summer period (with low or without precipitation) they struggle with droughts.

With the construction of the complex Trebišnjica Hydrosystem, the recharge of the largest infiltration zones was reduced to specific, short-lasting, hydrological periods or completely

blocked. Water is stored in reservoirs and transported through the tunnels and channels from higher elevated parts of catchment areas ($\sim 1,000$ m a.s.l.) down to the sea. Along its route water is utilized for power production, irrigation, water supply and various of secondary benefits. The duration of flood events in karst poljes is limited and locally eliminated.

The Trebišnjica Hydrosystem consists of seven dams, six reservoirs, six tunnels (with a total length of 57 km), four channels with a total length of 74 km, and seven hydropower plants with a total installed capacity of 1069 MW.

Due to its complexity, the construction of the system has been divided into three phases. The I phase of the system (the most cost-effective part) includes the Grančarevo Dam, with HPP Trebinje I and the Gorica Dam with HPP Dubrovnik and HPP Trebinje II (Figure 1). This section serves as the „backbone“ of the entire hydrosystem and was completed in 1975. The management model discussed in this article refers to this part of the system.

The main element of the system is Bileća Reservoir, created by 123 m high arch Grančarevo Dam. It has a total water storage volume of $1280 \cdot 10^6$ m³, an active volume of $1100 \cdot 10^6$ m³ and a normal operating level of 400 m a.s.l. There are two lateral spillways with radial gates for flood discharges, with maximum capacity of 874 m³/s and two bottom outlets with maximum capacity of 266 m³/s. HPP Trebinje I, with three Francis turbines of installed capacity 3×60 m³/s, and installed power 171 MW, is located in the immediate proximity of the dam body.



Figure 1. Trebišnjica Hydrosystem (I phase).

The concrete gravity Gorica Dam (33.5 m high) is situated 13.5 km downstream from the Grančarevo Dam. It forms Trebinje Reservoir, with total storage volume of $15.6 \cdot 10^6$ m³ and normal operating level of 295 m a.s.l. There are two spillways in the center of the dam, with radial gates, providing a maximum capacity of 412 m³/s and two bottom outlets with maximum capacity of 800 m³/s. Two intakes for the HPP Dubrovnik are located at the left bank in the immediate proximity upstream of the dam body. HPP Dubrovnik is an underground hydro-power plant, with 16.5 km long head race (tunnel and penstock) and two Francis turbines with an installed capacity 2×45 m³/s and installed power of 2×108 MW. HPP Trebinje II with one Kaplan turbine (installed capacity 45 m³/s) is situated in the left bank immediately downstream of the dam. The Gorica Dam must maintain an environmental flow of 8 m³/s downstream.

The Trebinje Town is located 4 km downstream from the Gorica Dam. One of the important purposes of the system is flood protection of the Trebinje urban area. This purpose becomes increasingly important and complex in the climate changes conditions, when flood waves become more frequent and intense, as well as because of uncontrolled urbanization in the immediate vicinity of the river. Consequently, Trebinje is now endangered with flows exceeding 400 m³/s, whereas the boundary flood flow was approximately 900 m³/s before the development of this part of the Trebišnjica Hydrosystem.

Due to the high intensity of precipitation and the karst area characterized by high runoff coefficients and short concentration time, flood waves are very unfavorable. Analyzing the observed flood waves, the following characteristics can be defined: the time of concentration ranges from one to two days, the flow gradients can increase over $300\text{m}^3/\text{s}$ per day, the retardation time of waves is usually 6-8 days, it is possible for two or more flood waves to occur consecutively. The inflow from the watershed area between the Grančarevo and Gorica dams is torrential, with much shorter flood wave concentration time.

Although the Bileća reservoir has a large storage capacity, characteristics of flood waves and torrential inflows in Trebinje Reservoir make it difficult to manage the system and maintain the flows in Trebinje town below $400\text{ m}^3/\text{s}$. To prevent damages, reservoir rule curves have been defined, specifying maximum water levels for each month, which provide empty space in the reservoir for flood wave mitigation during the flood event. To enhance the system's operating performance and optimize the utilization of the active volume, a management model for flood conditions (including a module for hydrological prediction) is currently under development. Its objective will be to predict flood flows (based on predicted precipitation) and to propose an optimal system management, with a criterion of minimizing the flow through the Trebinje town.

This paper presents the effects of the prediction of flood event on flood wave mitigation, considering how early the flood event was announced. All current rules for managing the release structures (gates, hydropower plant, outlets etc.) are incorporated in the model. Analyses were conducted for a flood event occurring once in 100 years (FW100) and they included: several observed flood waves (with a maximum flow similar as the flows of the FW100 wave), a synthetic flood wave, and a wave resulting from three days of rainfall with a total precipitation of 282 mm and a maximum intensity of 95 mm in 3 hours in the central part of the rainfall episode. The results are presented for the 3-day rainfall wave, which is the most unfavorable among the analysed waves in terms of maximum flow and wave volume. The peak of the flood wave entering the Bileća Reservoir occurs approximately 40-44 hours after the most intense rainfall (with a maximum flow of $715\text{ m}^3/\text{s}$), while the peak of the flood wave from the catchment area between Grančarevo and Gorica dams, flowing into the Trebinje Reservoir (with a maximum flow of $300\text{ m}^3/\text{s}$) occurs after only 6-8 hours.

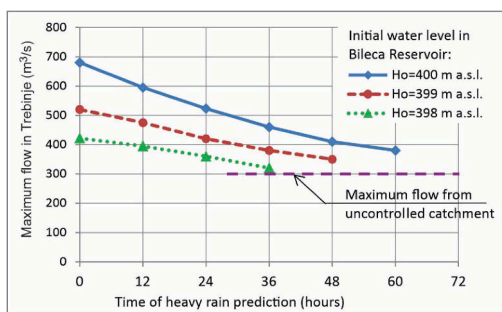


Figure 2. Maximum flow in Trebinje urban area for flood event of 100 year return period, for different initial water levels in Bileća Reservoir and for different times of heavy rain prediction.

The results of optimal management strategy for maximum flood wave mitigation through Trebinje town are presented at the Figure 2. Performed analyses indicate that if the Bileća Reservoir is full (water level 400 m a.s.l.), it is necessary to predict heavy rainfall at least 2 days in advance, to initiate timely reservoir emptying. The water level needs to be lowered to an elevation of 497.7 m to provide the volume of round $76 \cdot 10^6\text{ m}^3$, which is sufficient to completely accept flood wave. By employing the optimal management rules, it is possible to reduce the maximum flow through Trebinje town by over 50%, from $835\text{ m}^3/\text{s}$ to $400\text{ m}^3/\text{s}$, assuming that all facilities of the system (gates, turbines in hydropower plants) are fully operational. If rain is predicted only one day in advance, the water level in the reservoir can be lowered approximately 1.1 m, resulting in a maximum flood flow of around $520\text{ m}^3/\text{s}$ through

the urban area (assuming an initial reservoir level of 400 m a.s.l.). Even if optimal management begins during intense rainfall, it would still be possible to reduce the flood wave by nearly 150 m³/s compared to the maximum flow that would occur without the reservoirs (825 m³/s). Once completed with a prognostic hydrological module, this management model will enable the maximum utilization of the reservoir's active volume for hydropower production, while ensuring the safe transfer of flood waves without endangering Trebinje urban area.

3.2 *Vrba River case study*

A similar control model was applied to analyze the optimal management of Bočac Reservoir, situated on the Vrba River, with the aim of reducing flood waves in the city of Banja Luka. The Vrba River is a right tributary of the Sava River, located in the central part of Bosnia and Herzegovina (Figure 3). The watershed covers an area of 6,273 km², with 63.5% falling within the Republic of Srpska and 36.5% in the FBiH. In the downstream part of the basin, the river flows through Banja Luka, the capital of Republika Srpska with approximately 180,000 inhabitants. The Vrbanja River, a torrential tributary, joins the Vrba within the urban area. Banja Luka is protected from the flooding by passive protection measures - embankments along those two rivers. However, due to increasingly unfavorable flood events (such as the flood in 2014), which are a consequence of climate changes as well as changes in the watershed, additional protection measures are necessary in order to adequately protect the city.

There are four hydropower facilities in the Vrba River basin. In the upstream part of the catchment, there is a diversion HPP Jajce I, with the reservoir on the Pliva River, with an active storage capacity of $4.2 \cdot 10^6$ m³ (which enables daily flow regulation) and hydropower station on the Vrba River. Downstream from that HPP is the diversion HPP Jajce II with very small active storage volume of only $2.1 \cdot 10^6$ m³ (mostly backfilled) which operates as a run-of-river HPP. The only facility in the Vrba River basin that has a significant possibility of flow regulation is the Bočac Reservoir with HPP Bočac. The active storage of that reservoir is $42.9 \cdot 10^6$ m³ and it enables weekly flow regulation. HPP consists of two turbines, each with an installed capacity of 120 m³/s. The normal water level in the reservoir is 282 m a.s.l., maximal 283 m a.s.l., and a working level is 281 m a.s.l. The Bočac Dam has three releasing facilities:

- a spillway with radial gates located on the right side of the dam. The spillway crest elevation is at 272 m a.s.l., and it has a capacity of 1345 m³/s for water level of 283 m a.s.l.,
- a bottom outlet situated on the right side of the dam, with a maximum capacity of 127 m³/s for a water level in the reservoir at 283 m a.s.l.,
- a free lateral spillway on the left side of the dam, constructed subsequently to increase the hydraulic reliability of the dam during extremely large flood waves. The crest elevation is at 283 m a.s.l. and it has an overflow capacity of 567 m³/s for a reservoir water level of 286 m a.s.l.

HPP Bočac operates as a peak hydropower plant producing the variable energy. In order to protect the downstream area, particularly the town of Banja Luka, from sudden flow changes, a small reservoir with daily flow regulation was built downstream of the Bočac Dam. The gated structure is a low dam with two spillways, with a maximum capacity of 1450 m³/s, and small run-of-river HPP Bočac 2 with an installed capacity of 110 m³/s.

The average annual precipitation in the Vrba basin varies from 800 mm in the Sava confluence zone to approximately 1500 mm in the southern mountainous part of the basin. The average flow of the Vrba River is around $Q_{av}=132$ m³/s, and the average specific runoff is about 20.7 L/s·km². Flood flows of 1% occurrence for the Vrba River is more than 10 times higher compared to average flows. A special problem for the city of Banja Luka is the torrential river Vrbanja with flood waves of very steep ascending and recession branches and a relatively small base of the hydrograph. Despite the Vrbanja catchment area being four times smaller than that of the Bočac Dam (804 km² compared to 3448 km²), the maximum flood flows are higher for the Vrbanja River at the Vrba confluence profile. Currently, there are no dams or reservoirs on the Vrbanja River to mitigate such unfavorable flood waves. The most unfavorable hydrological event for the city of Banja Luka is the coincidence of flood

waves on Vrbas and Vrbanja rivers. In such circumstances, managing the Boćac Reservoir becomes crucial to reducing the maximum flows originating from the Vrbas River and delaying the peak flows until the flood wave from Vrbanja River has passed.

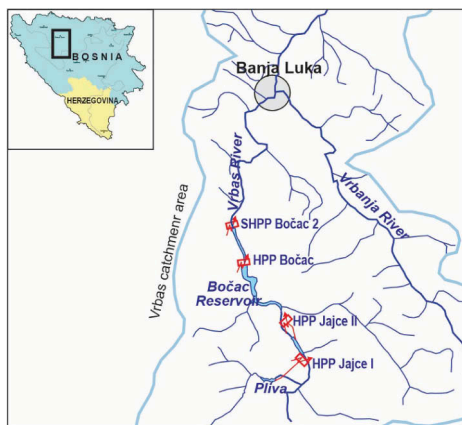


Figure 3. Part of the Vrbas River catchment.

Analyses were performed for flood waves of different return periods: 20, 50 and 100 years (FW20, FW50 and FW100), which were determined by applying a hydrological model based on the simulation of rain episodes (Topalović et al. 2018). The rain duration in the upstream part of the catchment was 12 hours, with intensities from 87 mm to 103 mm (for the 100 years return period). In the downstream part of the catchment (Banja Luka region), the rain duration was 24 hours, with an intensity of 169 mm. All current rules for managing the release structures (gates, hydropower plant, outlets etc.) were incorporated in the model. The analyses were performed under the assumption that the initial water level in the reservoir was at 281 m a.s.l (working level), the maximum water level was 282 m a.s.l., and the minimum level was 271 m a.s.l. (during the intensive emptying of the reservoir).

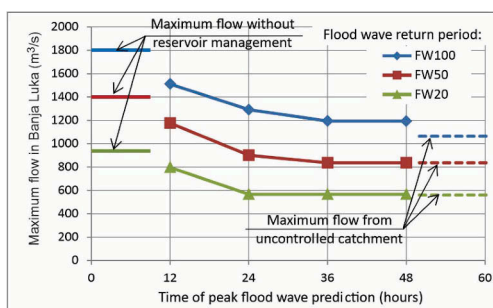


Figure 4. Maximum flows in Banja Luka for different flood waves return period and different times of peak flood wave prediction.

The results of performed analyses show that despite the relatively small reservoir volume it is possible to significantly reduce the maximum flows in the city of Banja Luka (Figure 4). By effectively managing the reservoir, it is possible to delay the peak of the flood wave from the Vrbas River, avoiding its coincidence with the wave from the Vrbanja River. This is particularly important for mitigating floods in Banja Luka due to the rapid occurrence and high peak flows of the Vrbanja flood waves. When the optimal reservoir management strategy begins 36 hours before the peak flow, the maximum flows through Banja Luka do not exceed the maximum

flows from the uncontrolled part of the catchment (Vrbanja River flood wave), for flood waves FW20 and FW50. Water is mostly discharged through the HPP Bočac. Gated spillways are open only a few hours (5 h for FW20 and 16 h for FW 50). For FW100 maximum flow is higher than the maximum flow from uncontrolled catchment (by 130 m³/s), and about 600 m³/s lower than the flow that would occur without the Bočac Reservoir. Even if the optimal reservoir management begins one day before the peak flow, significant mitigation of flood wave is possible. Maximum flow through Banja Luka in that case is slightly above maximum flow from the uncontrolled catchment for FW50, and flood wave FW100 can be significantly mitigated, with maximum flows 230 m³/s higher than the maximum flows coming from the Vrbanja River.

4 CONCLUSIONS

In the climate change conditions and the increasing variability of water regimes, the importance of reservoirs of all types of regulation increases. Their role is significant in providing the required quantities of water (by balancing water within the year) as well as in active mitigation of flood waves. In order to use the active volume of the reservoir in the best possible way, it is necessary to improve the management of the reservoirs.

The analysis of a management model applied on two hydrosystems (with different reservoirs sizes) with a goal to minimize flow in downstream urban areas, shows that these models can be used successfully, particularly when coupled with hydrologic models that simulate hydrograph of flood event. With improved and more reliable meteorological forecasts, these models can effectively contribute to active flood mitigation, even when dealing with reservoirs of relatively small volumes.

In the analysed case studies, predicting the flood wave two days in advance and implementing optimal management measures for the simulated wave result in mitigation to the extent that peak flows through downstream urban areas do not exceed the peak flow from the uncontrolled catchment (between the dam and the urban area). This mitigation is achieved by reducing and delaying the peak flow of the mitigated flood wave. The analyses also indicate that it is necessary to have release facilities on the dam with capacities that can provide efficient release operation. The trend of increasing the installed capacity at storage hydropower plants (with the ratio Q_{inst}/Q_{av} reaching 6) is also auspicious for the active flood defense, because a significant part of the discharge can be carried out by forced operation of the HPP, and only if it is not sufficient, by other releasing facilities.

REFERENCES

- Dašić, T., Đorđević, B., Sudar, N., Blagojević, V. 2019. Possibilities for active flood control management with the application of mathematical models – the case study of Bočac Reservoir on Vrbas River. *Vodoprivreda* 51(1-3): 69–84.
- Đorđević, B., Dašić, T., Sudar, N. 2012. Increase of the effectiveness of the reservoirs during the flood control – on the example of Trebišnjica Hydrosystem. *Vodoprivreda* 44(1-3): 43–58.
- Đurđević, V., Vuković, A., Vujadinović Mandić M. 2018. Report on the observed climate changes in Serbia and projections of the future climate based on different scenarios of future emissions, *Third National Communication on Climate Change*. Belgrade.
- Đurđević, V., Vuković, A., Vujadinović Mandić M. 2019. Report on the impact of observed climate change on water resources in Serbia and projections of future climate impacts based on different scenarios of future emissions, *Third National Communication on Climate Change*. Belgrade.
- Milanović, P. 2002. The environmental impacts of human activities and engineering constructions in karst regions. *Episodes, Journal of International Geoscience*. 25(1):13–21.
- Topalović, Ž., Blagojević, V., Sudar, N. 2018. Estimation of the flood hydrographs for the flood hazard and risk mapping – the case study of the Vrbas River basin in B&H. *Vodoprivreda* 50(1-3): 69–85.
- Vlahović, M. 2020. *Surface Reservoirs in the Nikšić Polje (Montenegro)*, Nikšić-Podgorica.
- Water Management Plan of Serbia*. 2001. Ministry of agriculture, forestry and water management.

XFLEX Hydro: Extending operation flexibility at EDF-Hydro Grand Maison PSP

Jean-Louis Drommi, Benoit Joly & Denis Aelbrecht
Electricité de France, Hydro Engineering Center, France

Christophe Nicolet & Christian Landry
Power Vision Engineering, Switzerland

Cécile Münch & Jean Decaix
Institute of Sustainable Energy, School of Engineering, HES-SO Valais-Wallis, Sion, Switzerland

ABSTRACT: Enhanced operation agility is now required from dispatchable generation means, hydro being top of the list. Increasing flexibility of legacy PSP has been implemented at Grand Maison scheme so as to provide regulating power in pump mode thanks to hydraulic short circuit technology. Extensive studies have been achieved to wave operational risk and provide operation boundaries. After 18 months, the demonstration has achieved 2500 hours of operation with full implementation onboard the EDF generating fleet.

1 INTRODUCTION

It is now a well known trump card of hydro power that its flexibility allows a large variety of ancillary services beyond bulk electric energy generation. Nevertheless, policy makers are requesting that hydro has to do more, and Hydro Industry shall answer to meet the challenge.

This is the whole purpose of XFLEX Hydro initiative, a consortium created to fulfill an EU call for extended flexibility services, beyond state of the art, in order to provide ever increasing grid support due to an ever larger of non dispatchable generating means blooming all over European power system.

Among the hydro assets whose flexibility is expected to play a key role in coming years, Pump Storage Plant have been fully assessed within XFLEX Hydro. At demonstration site, GRAND MAISON PSP (operated by EDF), an additional operation mode has been implemented to provide regulating power in pump mode which will be described in this article.

2 XFLEX HYDRO INITIATIVE

2.1 *Objective*

EU Horizon 2020, now Horizon Europe, research program aims to an extensive decarbonation of the energy sector all over the continent. One of the path followed by the EU is to seek solutions to build a low carbon and climate resilient future for the energy system mix.

In line with the EU vision, XFLEX Hydro objectives are to demonstrate how to increase the potential of the hydroelectric technologies in providing flexibility to the electric power system while achieving an improved average annual overall efficiency, providing high availability of the hydro plants and maximizing their performances.

XFLEX Hydro operational target is therefore to prove, through industrial scale demonstrator (TRL7), the system integration of hydroelectric technology solutions such as fixed and variable speed, pump power regulation, battery hybridisation, advanced monitoring and

digitalisation, and to draw the road-map for the deployment of this system integration to the all kinds of European hydroelectric power plants, run of river, storage and pumped storage of all sizes; being existing, uprated or new.

2.2 Consortium

The ambitious objectives of the XFLEX Hydro project are being addressed by a consortium of 19 partners, from 6 countries. Led by EPFL, the consortium includes academic, research institute, utilities and 3 major hydro industry companies.

The consortium has been working since mid 2019, on this 4 year project which represents more than 250 000 working hours and 20 million Euros overall budget.

2.3 Demonstrators

As mentioned in the XFLEX Hydro objectives, demonstration of extended flexibility shall be based on industrial scale examples.

The demonstration sites have been selected by the partner utilities in order to implement in each of them one of the additional flexibility feature. All demonstration sites are among the most powerful hydro scheme in Europe which proves the confidence, involvement, and expectancy that utility management puts in flexibility services for hydro.

Demonstration sites operated by EDP are Alqueva PSP, Alto Lindoso, Caniçada, and Frades II Variable Speed PSP. Demonstrator operated by ALPIQ is the Grand Dixence scheme and more specifically Z'MUTT pump turbine unit. Demonstrator operated by EDF include the RoR plant at Vogelgrun site, and Grand Maison PSP.

2.4 Flexibility services

The expression “Flexibility” applied to electric power system, and more specifically to generating means, describes their ability to adapt their operating set point in a controllable manner. This flexibility feature covers several time horizons, from millisecond regarding short circuit response, to several seconds when dealing with frequency support and up to hours or even years in case of energy storage. Hydro power can be found over the whole spectrum.

The first achievement of XFLEX Hydro has been to build up a comprehensive framework around flexibility and Electric Power Systems (EPS) support services with a strong link to Hydro Power Plants (HPP). The technical requirements associated to different services were revised in detail, as well as the positioning of those services within current and emerging market mechanisms. A full sorting matrix of hydro technologies vs flexibility services has been produced, see [1].

The ancillary services under evaluation include:

- Synchronous inertia; – Synthetic inertia; – Fast Frequency Response (FFR); – Frequency Containment Reserve (FCR); – Automatic Frequency Restoration Reserve (aFRR); – Manual Frequency Restoration Reserve (mFRR); – Replacement Reserve (RR); – Voltage/ reactive power.

2.5 Digitalisation

The goal of digitalization concept developed through XFLEX Hydro, (named “Smart Power Plant Supervisor” SPPS) is to integrate advanced hydroelectric technology solutions, including advanced monitoring, control and communication with all the hydropower plants functional levels to increase the availability, flexibility and lifespan of the units and the ancillary services provision to the power system.

The SPPS consists in two main parts: a database able to provide information about the behavior of the power plant in the different operating points, and an advanced control, driven by an optimization algorithm, which steers and optimizes the hydroelectric unit operation. Its function is to elaborate information coming from the database and from monitoring measurements and perform a real time computation of the optimum distribution of set points between

the different machines of a hydropower plant. By exploiting the additional knowledge given by the database, the SPSS can make choices oriented not only to respect the general set point given to the HPP, but also to maximise the efficiency or the lifetime of the different HPP components, eg to reduce the wear and tear on one given unit.

3 GRAND MAISON PSP

3.1 Description of PSP

The Demonstrator Grand Maison is part of the demonstration action of the XFLEX HYDRO; located in the French Alps, the scheme is part of the EDF fleet. With 1240 MW pumping capacity and 1800 MW generating capacity, Grand Maison is the largest PSP, Pumped Storage Power, plant in Europe, featuring four Pelton turbines (uprated from 150 to 170MW each) located at ground level and eight pump-turbine reversible units (150MW each) located 50 m below ground level, see Figure 1. It was commissioned in 1985/1986.

Major hydraulic figures about Grand Maison scheme are the following, for the eight pump-turbines (G1-G8):

- Maximum gross head 955.00 mWC;
- Minimum gross head 821.50 mWC;
- Turbine mode total discharge 140.80 m³/s;
- Pump mode total discharge 136.60 m³/s; and for the Four Pelton turbines (G9-G12):
- Maximum gross head 922.4 mWC;
- Minimum gross head 817.4 mWC;
- Turbine mode total discharge 76.0 m³/s.

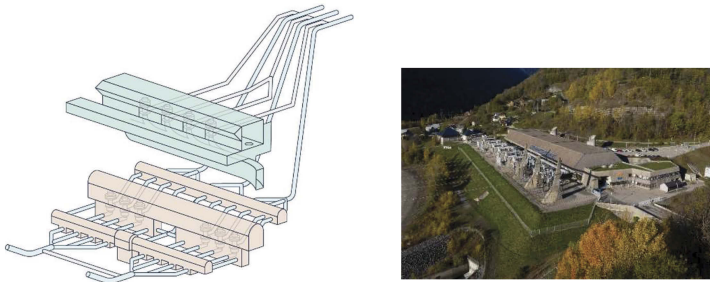


Figure 1. Schematic of the Grand Maison pumped storage power plant.

3.2 Ambition: Dispatchable pump mode

Grand Maison was designed and built in the early 80s as a complementary power mix to the French nuclear program, so as to use surplus energy during low demand periods (typically at night and over the weekends) and release it during peaking periods: arbitrage was the original economic pillar.

Grand Maison therefore, is fitted with 8 high head multi-stages reversible Francis pump-turbine units operating at fixed speed and which have no power adjustment ability, and 4 Pelton turbine units which are fully adjustable and provide grid support services.

Hence, the PSP operates with 2 basic modes: turbinng so as to generate power in a dispatchable manner, and pumping so as to store surplus energy but with fixed set points.

The aim and ambition of the Grand Maison demonstration is to prove that pumping mode may also become dispatchable and thus enhance provision of ancillary services to the grid in pump mode. There, the challenge and innovation include implementing hydraulic short circuit between pumps and Pelton units, in an extremely high head PSP where hydraulic transient and waterways behaviour may be project killers.

3.3 Constraints

Though, increased flexibility is a relevant target, it must remain a reasonable target on an asset management stand point. No need to say, that the implementation of the extra flexible feature must not at all deteriorate or put at risk in any manner the existing scheme, penstock, surge tank, or rotating machine. This is top one priority assigned to the project team.

The second constraint to be fulfilled deals with CAPEX required to implement dispatchable power in pump mode. Lowest CAPEX is obviously always the target in any project; in the case of Grand Maison PSP, the goal is zero CAPEX.

Third project assignment is to provide in pump mode an equivalent power reserve range as in turbine mode.

This is the deal that the project team had to tackle.

4 INCREASING FLEXIBILITY AT GRAND MAISON PSP USING HSC

4.1 HSC description, on the fly catch up

In order to provide balancing power when the PSP is overall in pump mode, choice was made to operate in so called “Hydraulic Short Circuit” (HSC) where pumps are operated at fixed set points and a dispatchable turbine (Pelton in the case of Grand Maison) operates simultaneously so that from the power grid view, adjustable power in pump mode is observed.

Grand Maison being fitted with 3 penstocks, each having a Pelton and a pump branch, several routes are possible to achieve the hydraulic short circuit. The short route involved pumps and Pelton turbine on the same penstock, there the water makes “a U turn” at the bifurcation level of that penstock. The long route involves pumps and Pelton located on different penstocks, there, the water flow diverge at the triple penstock junction point. Figure 2.

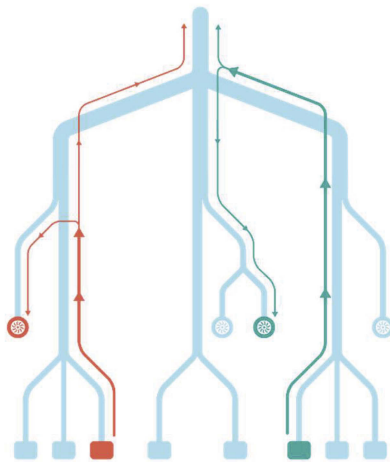


Figure 2. Grand Maison PSP – Waterway branching.

As it can be understood from the above description, the scheme as it exists, already embeds all necessary hardware to operate in hydraulic short circuit, so that no CAPEX is needed.

Analysing the plant SCADA sequence, an additional flexibility feature was brought to light. At Grand Maison, the pumps are launched with Pelton turbine using a back to back sequence. After launching Pelton is stopped. In view of operating in HSC mode, it makes sense to transfer directly the Pelton from launching to turbinning mode without stopping. Plant SCADA is to embed this improvement which saves start stop cycles.

4.2 HSC balancing power

Balancing power provided to grid by generating units contributes to frequency stability (50Hz). Beyond rotating mass inertia (which is an inherent non controllable feature of

synchronous generators or motors), two grid frequency control process are devoted to frequency containment. FCR (Frequency Containment Reserve, also known as primary reserve) is expected to deliver the contracted power within 30 s. A typical figure for FCR reserve is 10% of rated power to be delivered in case of -200mHz frequency deviation.

aFRR (Automatic Frequency Restoration Reserve, also known as secondary reserve) is to deliver the requested amount of power within 300 s.

At Grand Maison, both services are supplied by Pelton units. Compliance of the service to Transmission System Operator (TSO) requirement have been checked and documented during specific test. The same dynamic performance have been observed in HSC mode as they are in turbine mode. See Figure 3.

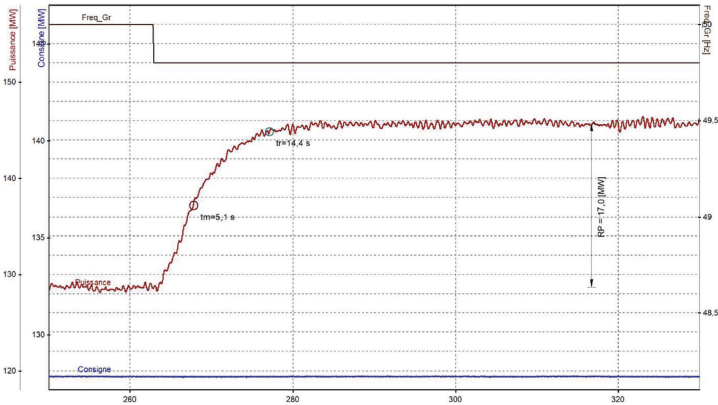


Figure 3. FCR Power response to -200mHz frequency step.

For both type of step response, the turbine power profile is well within acceptance criteria.

When in HSC mode, the balancing power of the Pelton units act as a demand side control. Based on Pelton unit balancing power span, Figure 4 shows the power set points and related reserve band that can be put on line; up to 500MW span can be made available in less than 300s when 4 Pelton are in use.

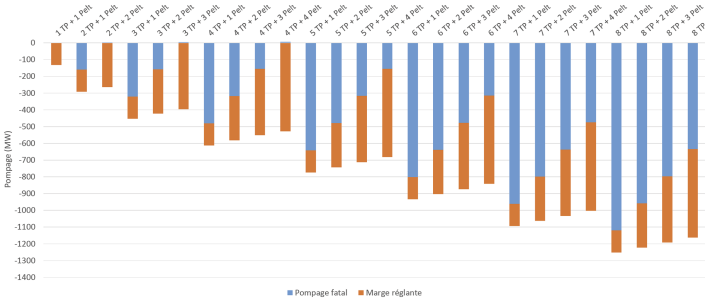


Figure 4. HSC operating points with power reserve span, orange bars.

4.3 Studies and modeling; simulation results

Despite a relatively simple implementation, the HSC mode induces operating conditions that were not necessarily studied during the commissioning of the hydraulic power plant. Therefore, in order to guarantee the safety of the installation, the introduction of such new operation mode requires to perform several investigations [2]. According to the hydraulic layout of the Grand Maison PSP, the following topics must be analyzed before allowing this new operation mode:

1. **Flow in bifurcation:** With a new HSC operating mode, the flow paths in the waterways of the power plant are different compared to the pump and turbine modes. CFD studies are

therefore carried out to assess the risk of hydraulic instabilities in bifurcations or trifurcations, induced by unfavorable flow patterns, such as recirculation, vortices, flow instabilities, pressure fluctuations, cavitation or vibrations in bifurcation structures, [3], [4], [5].

2. **Performance of the hydraulic machines:** The possible flow disturbances induced by the junctions could alter the flow pattern at the turbine and/or pump inlet, which could lead to vibrations, cavitation or a reduction in efficiency. For this demonstrator, the flow disturbances induced by the junctions do not affect the flow pattern at the injectors inlet because the junctions are located more than 120m upstream of the Pelton turbine (corresponding to more than 53 diameters distance).
3. **Cavitation of the pump:**For Grand Maison PSP, the flow at the Pelton turbine outlet goes through a separate tailrace channel directly to the lower reservoir and therefore the aeration of the turbined water cannot deteriorate the behavior of the pump, [6]. The advantage of having separate tailrace channels between the pump and the turbine is very beneficial for this type of operation.
4. **Interference between the units:** The pump trip or the turbine trip can prevent the normal operation of the other units in the same pressure shaft, [7]. For the Grand Maison PSP, the pump trip induces a head variation for the other units on the same pressure shaft and therefore an almost instantaneous drop of the power of the Pelton unit which may be accentuated by the possible Falaise Effect which may occur in Pelton turbines, [2].
5. **Hydraulic transient behavior:**An important point related to the safety of the hydraulic power plant is the verification of the hydraulic transient behavior of the units and the interactions with the hydraulic circuit occurring in case of normal, quick or emergency shutdown, [8]. With a 1D numerical model, different load cases can be simulated to identify the potential hydraulic transient issues, such as extreme water levels in the surge tanks, maximum static pressure along the pressure shaft and minimum static pressure along the waterways, [2].

After a validation of the 1D SIMSEN hydraulic model of the Grand Maison PSP, the most critical load cases were analysed in order to highlight the different operating limits for a new HSC mode. It is important to note that the critical load cases studied are specific to Grand Maison PSP and that the list may be quite different for another hydraulic power plant.

Among the list of load cases, the Normal Shutdown (NSD) of the 4 Pelton turbines operated at maximal power are simulated, followed by an ESD of the 8 pump-turbines at the worst moment for the minimum water level in the surge tank at minimum head. The transient behavior of the pump-turbine G1 in pump mode is illustrated in Figure 5. A negative static pressure of - 2.06mWC was detected in the headrace tunnel, close to the upstream surge tank, see Figure 6. To solve this problem, the PSP will not be operated in HSC mode when the water levels in the upstream reservoir is at minimum water level.

Finally, the transient analysis of the critical load cases did not revealed any significant operating limitations. Therefore, except for some water level limitations in the upstream reservoir, this new mode of operation can be used for Grand Maison PSP.

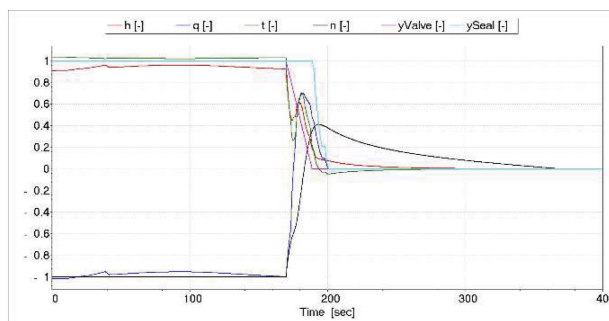


Figure 5. Time histories of the pump-turbine Unit G1 transient behavior after an ESD at 170s. The head (red line), the discharge (blue line), the torque (green line), the rotational speed (black line), the spherical valve (pink and light blue lines).

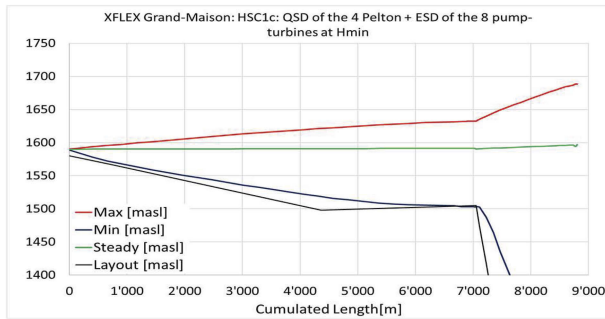


Figure 6. Pressure envelopes along the waterways. The maximum (red line), the minimum (blue line) and the steady piezometric pressure (green line). The pipe elevation (black line).

To determine the head losses and the flow topology in the junctions for the different HSC operating points considered, computational fluid dynamics (CFD) have been performed. Due to the lack of local measurements, hundreds of simulations have been carried out to provide a kind of uncertainty quantification regarding the numerical results. Figure 7 is an example showing the average and the standard deviation of the head loss coefficients (36 simulations) for the junction on penstock 2 and for 5 discharge ratios between the turbine(s) and the pump(s) ranging from pump mode to full HSC mode (all the discharge pumped is turbined). In overall, the standard deviation is low compared to the average value (less than 12%) with a maximum value for the discharge ratio of 0.75.

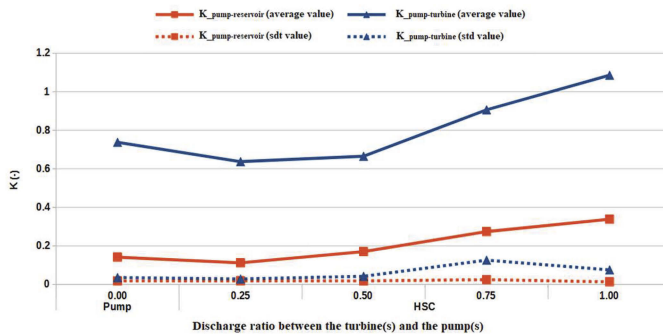


Figure 7. Average and standard deviation (std) of the head loss coefficients between the pump (s) and the upper reservoir and between the pump (s) and the turbine (s) for junction of penstock 2 and for 5 discharge ratios.

Regarding the flow topology, the HSC mode leads to the development of small instabilities in the junction (see Figure 8) however, the vortices do not extend far downstream in direction of the turbines. By consequence, no influence of the HSC mode is expected on the behaviour of the Pelton turbines.

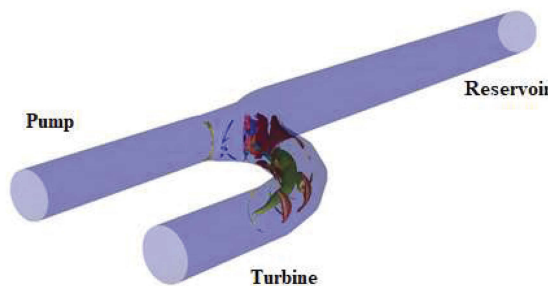


Figure 8. Visualization of the vortices in the junction of the penstock in HSC operating mode.

From the CFD investigation, it can be concluded that whatever the HSC operating mode (short or long route) considered, the head losses are less than 1% of the gross head and no large flow instabilities are transported far downstream. Therefore, the impact of the HSC mode on the flow is rather low.

4.4 Operating the PSP with HSC; operating statistics

From its industrial inception, the Grand Maison demonstrator has been operating daily. End of Feb 2023, the demo was totaling more than 2500 hours of operation with almost all kind of possible arrangement on the pump side (from 1 to 8 pumps operating in parallel with the Pelton turbine).

It must be noted at this stage, that HSC mode at Grand Maison PSP has become a regular third operating mode together with turbine mode and pump mode. HSC operation is now part of the daily life of the plant since more than 50% of pump time is spent with the Pelton turbine in HSC mode.

Together with the PSP operating statistics, EDF overall electric power generation shows evidence that fleet optimization calls for the Grand Maison PSP to offer balancing power prior to calling more expensive generating means typically coal or gaz. As a consequence, it has been possible to quantify the environmental benefit of the Grand Maison demo regarding CO² emission. Based on actual data of the demonstration and playing back the electric generation scenario, the demo led to ~40kilo tons CO² emission savings so far.

From the operating statistics performed through EDF monitoring systems, weekly and daily HSC operation schedule have been identified and show when the HSC mode provides the most relevant service for grid support.

Over a week (Figure 9) HSC mode is mostly called over week ends which is logical both with the fact that weekends are traditionally low power demand prone to pump cycles and that Grand Maison being a weekly PSP, large pumping cycles are taking place over weekends to refill upper reservoir. Otherwise, weekdays tend to be rather even as a matter of HSC best positioning.

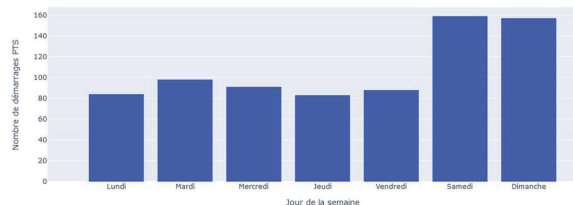


Figure 9. HSC mode weekly operating statistics – number of start of demo per weekday.

During the course of a day (Figure 10), it can be noted that HSC is mostly called during night-time and mid-afternoons. There also, these periods correspond to low power demand when pumping cycles can be positioned at most effective cost. The availability of HSC allows to offer balancing power thus avoiding the use of less efficient generating means to do so.

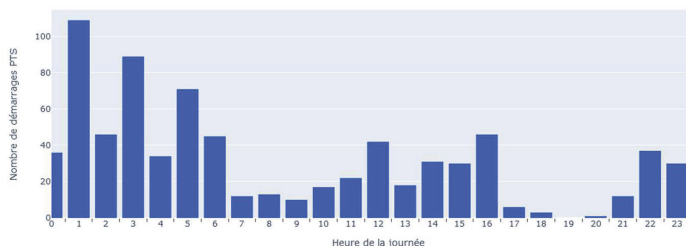


Figure 10. HSC statistics – number of HSC start vs HSC cycle duration.

On another hand, demo observation also helped assessing the average duration of HSC cycles. From Figure 10, it can be computed that HSC cycles run for 3 to 4 hours on average. Some are longer, up to 24 hours in the most extreme case experienced so far.

5 CONCLUSION AND PERSPECTIVE

The industrial demonstration of higher and more agile valuable flexibility service based on HSC (Hydraulic Short Circuit) technology at existing PSH station is now a reality thanks to the XFLEX-Hydro European project.

The demonstrator at Grand-Maison PSP offers a unique platform to test and qualify the HSC operating mode, optimize its performance and service to the grid, while controlling that no undesired potential risks have impact on the assets.

The technology has now reached a high maturity level (TRL 8) as expected, and extended deployment and its scalability potential is under close consideration.

It's now unquestionable that hydropower future lies in more agile operation features, whether load span, fast start/stop and ramping, continuous positive to negative loading for PSPs (Hydro battery like). As shown from TSO expectations, hydro plant specification from past century are no longer relevant and must make way to design worthy of the challenges ahead. The XFLEX-Hydro project has thus delivered more than the expected outcomes for the hydropower sector and gives a basis to extend flexibility service at existing or future PSP projects to help achieve the Zero Net target.

ACKNOWLEDGEMENT

The Hydropower Extending Power System Flexibility (XFLEX HYDRO) project has received funding from the European Union's Horizon 2020 research and innovation programme under grant agreement No 857832.

REFERENCES

- [1] XFLEX Hydro deliverable D2.1, "Flexibility, technologies and scenarios for hydro power", 2020.08.01, *xflexhydro.com*.
- [2] Landry, C., Nicolet, C., Badina, C., Pichon, H., Drommi, J.-L., *Contribution for the roadmap of hydraulic short circuit implementation: Case of Grand-Maison pumped storage power plant*, Proc. of the 31th IAHR Symposium on Hydraulic Machinery and Systems, Trondheim, Norway, 26 June – 1 July 2022, paper 19.
- [3] Ruprecht, A., Helmrich, T., Buntic, I., *Very large eddy simulation for the prediction of steady vortex motion*, 12th International conference on fluid flow technologies, Budapest, Hungary, September 3–6, 2003.
- [4] Huber, B., Korger, H. and Fuchs, K., *Hydraulic optimization of a T-junction hydraulic model tests and CFD-simulation*. Proc. XXXI IAHR Congress, Seoul, Korea, September 11–16, 2005.
- [5] Decaix, J., Drommi, J.-L., Avellan, F., Munch-Alligne, C., *CFD simulations of hydraulic short-circuits in junctions, application to the Grand Maison power plant*. Proc. of the 31th IAHR Symposium on Hydraulic Machinery and Systems, Trondheim, Norway, 26 June - 1 July, 2022, Paper 33.
- [6] Lais, A., Lucas, J., Wickenhäuser, M. and Kriewitz, C.R., *Lufitansport im Unterwasserkanal des Pumpspeicherwerks FMHL+*, Wasserbausymposium, Graz, Austria, September 12–15, 2012.
- [7] Dreyer, M., Nicolet, C., Alligné, S., Kolb, S., Dayer, J.-D., Vuignier, E., Michellod, Y., Sauthier, A., "Commissioning of Nant de Drance: delayed load rejection and hydraulic short-circuit operation transient tests", Proc. of 21th International Seminar on Hydropower Plants, 9–11 November 2022, Vienna, Austria.
- [8] Goekler, Gottfried, and PeterMeusburger. "KOPS II on the Grid–First Experiences and Lessons Learned." Proceedings Hydro2009 (2009).

Additional water and electricity storage in the Swiss Alps: From studies of potential towards implementation

Jonathan Fauriel

Head Civil Engineering and Environment, Alpiq Ltd, Switzerland

Jérôme Filliez

Senior Civil Engineer, Alpiq Ltd, Switzerland

David Felix

Senior Civil Engineer, formerly VAW of ETH Zürich; Aquased GmbH, Switzerland

Robert M. Boes

Professor and Head of the Laboratory of Hydraulics, Hydrology and Glaciology (VAW), ETH, Zurich

ABSTRACT: Storage hydropower from the Swiss Alps contributes considerably to the stability of the European electrical network and is key for the energy transition. Between 2010 and 2020, several research projects were carried out exploring the opportunities for the implementation of new reservoirs in regions of retreating glaciers as well as for the extension of existing reservoirs through dam heightening. The potential for additional electricity storage and production was estimated up to 3.9 TWh and 1.2 TWh/a, respectively.

Within the Energy Strategy 2050 and based on the above-mentioned research, a Round Table, gathering the main stakeholders identified 15 projects to increase the winter electricity production by 2 TWh. These projects have strong connections with existing hydropower schemes, and need to be further developed and refined to meet economic and environmental requirements.

After summarizing the potential studies, the present and future Swiss electricity landscape and the 15 projects of the Round Table, this paper presents a preliminary assessment of their technical risks and unit costs per kWh based on publicly available information. Then, two example projects developed by Alpiq, a main Swiss utility, and related operators are presented, namely the new multi-purpose reservoir at Gorner and the heightening of the Emossion dam.

1 INTRODUCTION

Hydropower (HP) is the backbone of the Swiss electricity system providing around 60% (36 TWh/a) of the total electricity generated on a yearly average (Boes et al., 2021). With the planned phase-out of nuclear power plants, HP and other Renewable Energy Sources (RES) will need to fill the substantial gap in domestic electricity generation, particularly in the winter season. Because of the intermittent nature of RES generation (mainly solar photovoltaics and wind) and their typically lower production in winter, the need for storage up to the seasonal time scale increases. Such large-scale storage is offered mainly by storage HP.

Existing HP infrastructure in the Swiss Alps is significant, with more than 220 large dams under federal supervision. A considerable number of artificial lakes (reservoirs) were implemented mainly during the 20th century. Their primary purpose is seasonal water storage for hydropower production.

In this contribution, an overview is given of recent studies on the production and storage potential by (i) the implementation of new multipurpose reservoirs in regions of retreating glaciers, and (ii) the extension of existing reservoirs by dam heightening. This potential is then

compared to target values stemming from recent energy policy, and ongoing societal and political discussions related to energy turnaround, security of energy supply, climate change and net zero goals. A consensus between the various stakeholders has led to a list of the most promising 15 storage HP projects at the national level. These are compared in a preliminary analysis of the technical risk and the unit cost per kWh, because these aspects were not considered in the selection of the 15 projects at the Round Table. An example of a new multipurpose reservoir and of a dam heightening are presented. Both projects aim to be in service by the end of 2030.

2 STUDIES OF SWISS HYDROPOWER POTENTIAL

HP production and storage can be increased by new HP schemes, upgrade and extension as well as renewal and refurbishment of existing ones. Herein, studies of (i) new HP schemes or stages using previously unexploited HP potential at new sites or higher intake locations and of (ii) upgrades and extensions of existing HPP are discussed. For the latter the focus is put on the dam heightening, because storage is expected to be more important in the future than production, and only large HP reservoirs are considered for economic reasons (economy of scale).

2.1 *New HP schemes in regions of retreating glaciers*

Ehrbar et al. (2018, 2019) presented an approach for the systematic analysis of the HP potential of the periglacial Swiss Alps, i.e. in regions which have recently or will in the near future become ice-free due to glacier retreat. Their consistent rating of 62 potential sites is based on an evaluation matrix with 16 economical, environmental and social criteria. Ehrbar et al. (2018, 2019) distinguished three different weighting models (e.g. focus on technical and energy economical aspects vs. focus on public acceptance). A low sensitivity on the weighting models was found for some of the best-rated sites. Various climate scenarios were taken into account in the estimation of future run-off. The eight best-rated sites (average of all three weighting models) and their energy key data are listed in Table 1. The potential of large HP schemes at the 20 best-rated periglacial sites is estimated as 1600 to 1800 GWh/a in a framework favorable for HP. The corresponding new reservoirs would have a total storage volume of 700 up to 760 Mio. m³ and a total stored energy equivalent of 1400 to 1600 GWh. The latter is defined as the energy that can be generated from one reservoir filling in the new and all existing Swiss medium- and high-head HPP (if applicable) downstream. With these 20 additional reservoirs, the electricity storage capacity of Swiss HP reservoirs of currently 8.88 TWh (SFOE, 2022) would increase by 18 to 20%.

Table 1. Eight best-rated sites for new storage HP in the Swiss periglacial environment (Boes et al. 2021).

Reservoir location	Annual generation [GWh/a]	Stored energy [GWh]	Storage volume [Mio. m ³]
Alalin Glacier	32	47	20
Aletsch Glacier	200	216	106
Gorner Glacier ¹	220	550	150
Oberaletsch Glacier	105	60	30
Schwarzberg Glacier	19	41	19
Trift Glacier ²	145	215	85
Turtmann Glacier	36	78	36
Unt. Grindelwald Glacier	112	150	84
Total	869	1357	530

1 after Lehmann (2020)

2 according to KWO (2020)

HP schemes may be developed for neighboring sites together, e.g. Allalin and Schwarzberg, and need to integrate into existing HP infrastructure. Only one of these best-rated sites, namely the Trift project, is currently in the licensing procedure. Most other sites, however, lie in or upstream of protected areas, likely causing controversial debates on the weighing of

interests, the legal feasibility and social acceptance. The numbers given above include sites with protected wetlands according to the Federal Inventory of Floodplains of National Importance, which are excluded from use according to the Energy Act (EnG) Art. 12. If these sites are not accounted for, the estimated periglacial generation potential decreases by about one third. The more realistic numbers then amount to 1000 to 1200 GWh/a for large HP schemes in roughly 12 out of formerly 20 best-rated glacier catchments in a framework favorable for HP. The corresponding new reservoirs would have a total storage volume of about 465 ± 25 Mio. m³ and a total stored energy equivalent of about 1000 ± 50 GWh.

2.2 Extension of storage reservoirs by dam heightening

A systematic study at ETH Zurich within the SCCER framework explored the potential of extending the capacity of existing Swiss reservoirs by dam heightening. In the study, 38 existing reservoirs in the Alps with a net storage volume of at least 20 Mio. m³ were investigated. For dam heightening options of 5%, 10% and 20% of the maximum dam height, the required adaptations on the reservoir area, at the dams including their appurtenant structures (spillways, outlets, intakes) and at the corresponding HPP were studied and rated based on eight criteria (Fuchs et al., 2019). For the options that were rated “well-suited” (scenario 1) and adding the “moderately-suited” (scenario 2), the additional storage capacities for water and electricity were estimated.

If 17 or 26 of the reservoirs were heightened, their electricity storage capacity would be increased by 2200 and 2900 GWh, respectively (Table 2). This corresponds to an increase of the existing storage capacity of 8820 GWh by 25 to 33 %. Using the additional storage volumes once every year, 2200 and 2900 GWh year could be additionally shifted from the summer to the winter half year. This would allow to increase the electricity generation of the Swiss storage HPPs in the winter half year from currently 48% of their annual generation to 59% or 62 %, respectively (Felix et al., 2020).

It should be noted that dam heightening results in no considerable additional generation (< 200 GWh/a) on an annual balance, as the increase in head of the corresponding HPP is negligible (≈ 2 %). The value of dam heightening lies in the production shift from the summer half year (with generation exceeding the demand) to the critical winter semester (with a significant import need).

Table 2. Summary of two Swiss dam heightening scenarios (adapted from Felix et al. 2020).

by	No. of reservoirs with dams heightened				Additional volume [Mio. m ³]	Additional energy storage [GWh/a]
	5 %	10 %	20 %	total		
Scenario 1	1	6	10	17	700	2200
Scenario 2	2	3	21	26	950	2900

3 ENERGY POLICY CONTEXT

3.1 Role of Swiss hydropower

HP is the most important domestic source of renewable energy in Switzerland. The Swiss net annual electricity production amounted to 63 TWh/a on average over the last ten years (SFOE, 2019). Thereof, 57% (36 TWh/a) stem from HP (net production after subtracting the consumption of pumps at water adductions), 36% (23 TWh/a) from nuclear and 7% (4 TWh/a) from conventional thermal power plants and “new” renewable energy sources (RES) (SFOE, 2019).

With 56%, the share of storage HPP on the production is unusually high in Switzerland compared to about one third on the global average. Thanks to its storage capabilities, Switzerland plays a central role as an on-demand electricity supplier in the European network.

Until 2004, Switzerland usually exported more electric energy over the calendar year than it imported (SFOE, 2019). From then on, the export has decreased, leading to occasional net imports of up to 6 TWh/a (Felix et al. 2020). In the winter half year, however, up to 10 TWh/ winter net have been imported since 2002, with an average value of 4.4 TWh/ winter (2010 to 2020), corresponding to 14% of the domestic winter net generation. In the winter 2016/17, when

the generation of the Swiss nuclear power plants was pronouncedly below average, the net import amounted to 10 TWh/winter (39% of the domestic winter net generation) (SFOE, 2019).

3.2 *Swiss energy strategy 2050 and energy perspectives 2050+*

After the nuclear disaster of Fukushima Daichii on 11 March 2011, the Federal Council and Swiss Parliament decided a stepwise phase-out of nuclear power plants. Adaptions of the Swiss energy supply system were formulated in the Swiss Energy Strategy 2050 (ES 2050), which targets in the Energy Act (EnG) a significant extension of the use of RES, particularly photovoltaics. The net HP production should increase to 37.4 TWh/a in 2035 (EnG); a target value of 38.6 TWh/a is foreseen for 2050 (Swiss Federal Council, 2013).

In 2019, the Swiss Federal Government additionally set the goal to reduce its net carbon emissions to net-zero by 2050 (Swiss Federal Council, 2019), which also affects the Swiss electricity supply system. In the so-called Energy Perspectives 2050+ (EP 2050+, SFOE 2020) it was analyzed how to develop an energy system compatible with the goal of net-zero greenhouse gas emissions by 2050 while ensuring a secure energy supply. In 2050, domestic electricity generation is anticipated to be almost exclusively by HP and renewable energies, including combined heat and cogeneration plants. In a base scenario, the new renewable energies should provide 39 TWh/a or 46% of the gross electricity generation, HP 45 TWh/a or 53%. The HP production and pump storage HP is thus supposed to increase significantly, which seems quite challenging to reach in view of the slow authorization procedures and the more severe residual flow requirements for new concessions requested by the Swiss Waters Protection Act.

Regarding HP generation in the winter half year and storage capacities, no target values were set in the ES 2050 nor the Energy Act. However, the Swiss Federal Commission on Electricity (ElCom) sees an increasing risk of winter supply shortages after decommissioning of the two largest nuclear power plants in Switzerland. ElCom has recommended a legally binding target to increase winter generation by at least 5 TWh/winter until 2035 by various technologies (ElCom, 2020). In November 2020, a target value of + 2 TWh/winter for storage HP until 2040 was stipulated by the Swiss Federal Department of the Environment, Transport, Energy and Communications (DETEC).

3.3 *Round table hydropower*

The identified options for both new multi-purpose reservoirs and extensions of existing reservoirs described in Section 2 touch various and partly conflicting interests such as the security of electricity and water supply, protection against natural hazards, landscape conservation as well as terrestrial and aquatic habitats. In an attempt to develop a common understanding between project developers, responsible authorities and other stakeholders of the challenges facing HP in the context of the Energy Strategy 2050, the net-zero climate target, security of supply and preservation of biodiversity, DETEC organized the so-called Round Table Hydropower which led to a declaration in 2021.

33 potential projects, of which the Federal Office of Energy (SFOE) collected short descriptions and key figures from project developers, were screened regarding biodiversity, landscape and energy. The projects with the presumably lowest specific impact on biodiversity and landscape per GWh of additional annual storage capacity received the highest grades. To meet the target of +2 TWh/winter of additional electricity production (Section 3.2), 15 projects with the highest grades were listed (SFOE, 2021). Figure 1 shows the expected additional winter electricity storage of these projects (blue bars), compared to earlier potential studies summarized in Sections 2.1 and 2.2 (rectangles). For the heightening projects, smaller degrees of heightening than assumed in the potential study were favored upon further analysis in several cases.

The list contains 11 reservoir extensions by moderate dam heightening (H) and four new reservoirs related to mainly existing or naturally forming future lakes (N). Note that three of the new reservoirs were already listed among the most promising options of new periglacial reservoirs in Table 1. The four new reservoirs are expected to contribute to about 1 TWh/winter, similar to the 11 dam heightening projects. The total expected additional electricity storage (2 TWh/winter) results mainly from an additional production shift from summer to winter and to a smaller extent from additional production.

The list is neither legally binding nor exhaustive. Depending on the history of the 15 projects so far, their level of detail and the extent of technical, ecological and economical investigations carried out to date varies considerably. Hence, it is likely that the list needs to be updated for various reasons. With the energy supply situation in Europe since the winter of 2021/2022, higher electricity prices in winter are more likely, which is favorable for the economic viability of such projects focusing on seasonal energy transfer. However, a staggering based on the economic viability of the projects on a comparable basis is recommended to first realize the most promising options.

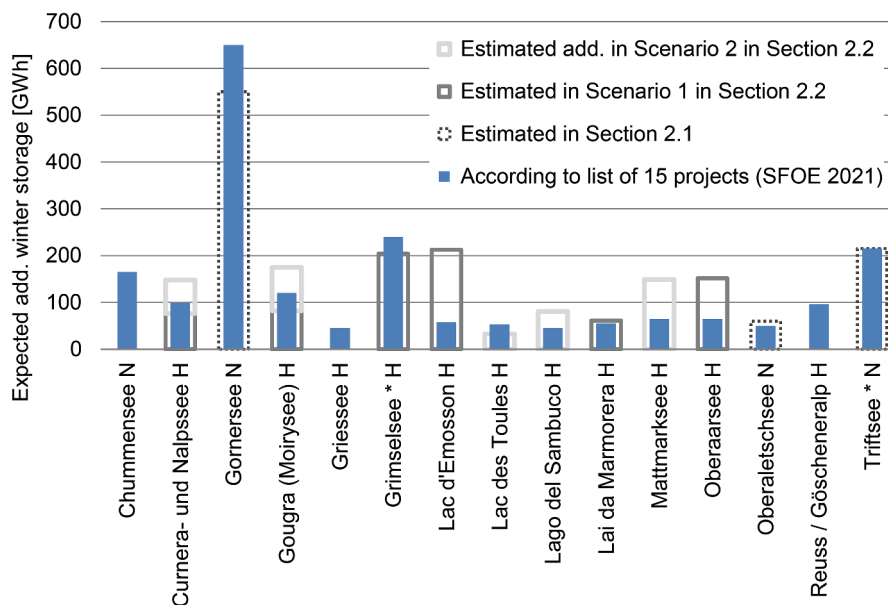


Figure 1. Expected additional electricity storage for winter production of the 15 projects of the Round Table Hydropower (SFOE 2021) in comparison to earlier potential studies in Switzerland (H = reservoir extensions by dam heightening, N = new reservoirs, * = currently in licensing procedure).

4 SIMPLIFIED COMPARATIVE ANALYSIS OF THE ROUND TABLE PROJECTS

As most of the projects were still in an early stage, the selection process of the Round Table did not include further technical and economic analyses. In order to estimate the chance of success and with the perspective of a systemic approach, Alpiq performed a simplified analysis of the 15 projects based on common hypotheses and available public data in 2022.

A technical risk or uncertainty level ranging from 0 (very low) to 5 (high) is assigned as a measure of potential difficulties such as geology, integration within existing infrastructure, lack of data and experiences in other projects. A high technical risk does not affect the safety aspects but the risk of cost overruns. Costs are estimated on the basis of construction material and excavation volumes, site accessibility, construction site facilities and installed capacity. A complexity factor is also added in function of the work peculiarities. The main goal was not to evaluate precisely the costs, but to compare the 15 projects.

The results show a great disparity between the projects (Table 3 and Figure 2). In general, the most economic projects are also those presenting the lowest technical risk level. The energy storage targets appear to be technically challenging to reach for five projects. In terms of unit costs per kWh stored, a factor of more than 5 can be observed. However, it is pointed out that a storage of more than 850 GWh is expected with unit cost < 0.05 €/kWh.

In the following, two projects in the canton of Valais, Switzerland, are presented as examples. The first is a multipurpose scheme developed by Alpiq and the municipality of Zermatt, while the second is a heightening of a major arch dam in a HP scheme in France and Switzerland.

Table 3. Comparative analysis of the 15 Round Table projects (H = reservoir extensions by dam heightening, N = new reservoirs; GWh according to SFOE 2021).

Name		Technical risk [1-5]	Electricity storage		Electricity generation		
			[GWh]	[cts €/kWh]	[GWh/a]	[cts €/kWh]	
1	Chummensee	N	4	165	> 10	18	> 20
2	Curnera-Nalps	H	2	99	< 5	-	-
3	Gornersee	N	1	650	< 5	200	< 10
4	Gougra Moiry	H	3	120	5 - 10	-	-
5	Griessee	H	3	46	5 - 10	12	> 20
6	Grimselsee	H	1	240	5 - 10	12	> 20
7	Lac d'Emosson	H	1	58	< 5	-	-
8	Lac Toules	H	4	53	>10	10	> 20
9	Lago del Sambuco	H	2	46	>10	6	> 20
10	Lai da Marmorera	H	3	55	5 - 10	-	-
11	Mattmarksee	H	2	65	5 - 10	-	-
12	Oberaarsee	H	1	65	< 5	-	-
13	Oberaletschsee	N	1	50	5 - 10	100	< 10
14	Reuss/Göscheneralp	H	3	96	5 - 10	44	> 20
15	Trift	N	1	215	5 - 10	145	10 - 20
Total				2023		547	

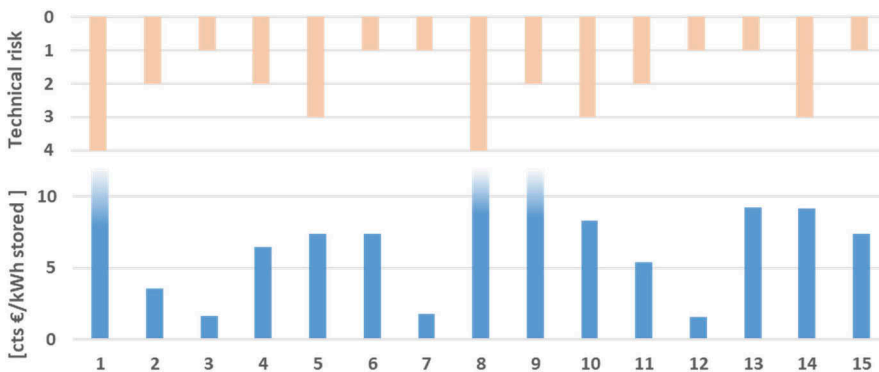


Figure 2. Preliminary analysis to compare the 15 Round Table projects.

5 PROJECT EXAMPLES ON THE WAY TO IMPLEMENTATION

5.1 Gorner reservoir: A typical multi-purpose project

The site of the Gorner reservoir project, also termed MZS Gornerli, is getting ice-free due to the strong melting of the Gorner glacier (Figure 3a). It includes the construction of a 90 m high arch dam in the Gorner gorge to create a multi-purpose reservoir of 150 Mio. m³ downstream of the glacier, with a 30 MW underground pumping station at the upstream toe of the dam (Figure 4, Felix et al. 2022). The main purposes of the project are:

- Natural hazard protection: Flood retention (peak flow reduced to 50% in Zermatt - Figure 3b), Glacial lake outburst flood damping, and mitigating impacts of landslides,
- Water resources management: Hydropower (Winter electricity storage 650 GWh and net electricity generation 200 GWh), supplying drinking and irrigation water to communities and agriculture, respectively.

The specificity of the project in terms of the hydropower purpose is the direct transfer of the accumulated water into Grande Dixence reservoir using an existing adduction tunnel passing beneath the gorge close to the dam site (Figure 4). This allows to shorten the water transfer length, optimize

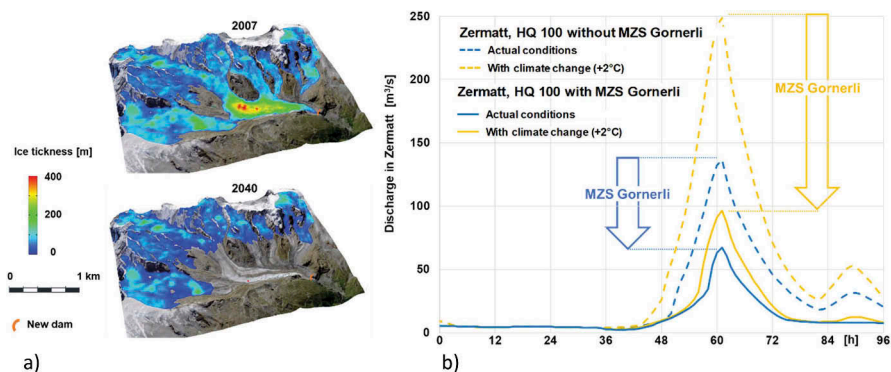


Figure 3. (a) Glacial melt modeling in the Gorner region, adapted from VAW (2011 and 2021), (b) 100-year flood (HQ100) estimations in Zermatt.

the existing facilities, mitigate the environmental impacts, and allow a favorable CO₂ footprint. At this stage of the project, the technical challenges lie in the selection of the exact location of the dam and the pumping station according to local geological conditions, the optimization of the access to the construction site in a harsh and very touristic Alpine area, and in the mitigation of the impacts on fauna, flora, and landscape, as well as the CO₂ footprint of the scheme. The construction works are expected to last 5 years, for a commissioning before the end of 2030.

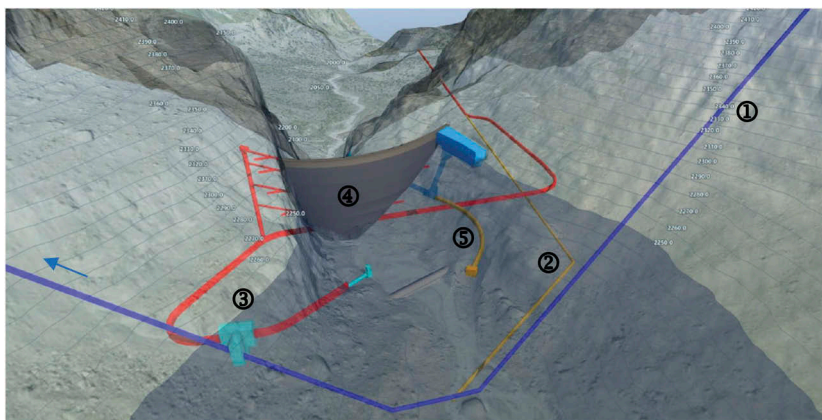


Figure 4. Designed structures for the multi-purpose reservoir Gorner, seen in flow direction (Lombardi, 2023). 1 Existing syphon of the main collector towards the Grande Dixence, 2 Existing access to the toe of the syphon, 3 Planned underground pumping station, intake from the reservoir and connection to the existing facilities, 4 Dam and access galleries, 5 Diversion tunnel.

5.2 Lac d'Emosson: An optimization of existing infrastructure

The purpose of the Emosson dam heightening project (SurESA) is to increase the storage capacity of the scheme. The use of existing infrastructure (dam and hydropower plant) is technically and economically advantageous, with limited impact on the environment. For example, the reservoir surface does not increase considerably (Figure 5). Feasibility studies have shown that the heightening by 6 % of the current maximum dam height is possible by a simple extension of both the existing double-curved dam and a small gravity section at one abutment. As a result, the crest width is reduced, and the volume of concrete needed remains low with respect to the increased storage capacity (Table 4). In addition, the utilization factors of the structure increase significantly. In particular, the amount of energy stored per cubic meter of dam concrete increases by 9 % from an already high value of 676 kWh/m³.

Table 4. Main characteristics of the existing and the heightened dam, adapted from AFRY, 2022.

		Existing dam	heightened dam	Difference	
Dam body					
Height	[m]	180	190	10	+6%
Crest length (arch dam)	[m]	424	430	6	+1%
Crest length (total)	[m]	524	790	266	+51%
Crest width	[m]	9	7	-2	-22%
Concrete	[m ³]	1 100 000	1 170 700	70 700	+6%
Reservoir					
Surface area	[km ²]	3.3	3.5	0.2	+6%
Stored energy/surface area	[kW/m ²]	228	249	22	+9%
Water storage	[hm ³]	225	259	34	+15%
m ³ of water/m ³ of concrete	[-]	205	221	16	+8%
Energy storage	[GWh]	744	860	116	+16%
Stored energy/m ³ of concrete	[kWh/m ³]	676	735	58	+9%

The Nant de Drance pumped storage plant inaugurated in 2022 located nearby offers improved accessibility and potential availability of construction materials. Another peculiarity of the project is its vicinity to the French-Swiss border (Figure 5). In the 1950s, an exchange of land between the two countries took place to allow the construction of the Emosson dam on Swiss territory. To avoid procedural difficulties, the heightening should remain on the Swiss side. As a bi-national project, the procedures are partly different from the other projects of the Round Table. At this stage of the studies, the construction works are expected to last four years, for a commissioning before the end of 2030.

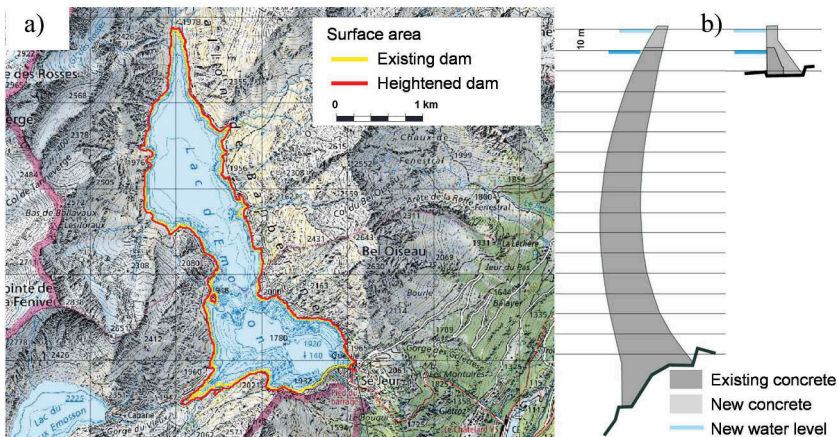


Figure 5. A) Reservoir area, adapted from Grenat (2022) b) typical dam sections, adapted from Stucky (2020).

6 CONCLUSION

The Fukushima incident in 2011 and the European energy crisis of 2022 have highlighted the need to speed up the transition to low-carbon energy. In Switzerland and in Europe, the hydroelectric potential has been widely exploited and only few new large-scale hydropower plants have been constructed for several decades. However, climate change and volatility of new renewable energies have changed the situation and hydropower is once again seen as a robust and reliable technology that can act as an enabler to foster the integration of new renewables. Recent studies of the Swiss storage and generation potential have given a good overview of new hydropower opportunities in the fast changing periglacial environment and

of extending existing facilities. Stakeholders (federal authorities, NGOs and utilities) have become aware of the chances and challenges, and found a consensus at the federal level in terms of ranking large hydropower projects that allow to increase energy storage by 2 TWh until 2040. Although there are still major disparities among the 15 projects selected, several promising projects are on track for commissioning before 2030.

REFERENCES

- AFRY 2022. Barrage d'Emosson, Surélévation du barrage, rapport de faisabilité (in French).
- Boes, R., Hohermuth, B., Giardini, D. (eds.), Avellan, F., Boes, R., Burlando, P., Evers, F., Farinotti, D., Felix, D., Hohermuth, B., Manso, P., Münch-Aligné, C., Schmid, M., Stähli, M., Weigt, H. 2021. Swiss Potential for Hydropower Generation and Storage, Synthesis Report, ETH Zurich, <https://doi.org/10.3929/ethz-b-000517823>.
- Ehrbar, D., Schmocker, L., Vetsch, D., and Boes, R. 2018. Hydropower Potential in the Periglacial Environment of Switzerland under Climate Change. *Sustainability* 10.8: 2794. DOI: 10.3390/su10082794.
- Ehrbar, D., Schmocker, L., Vetsch, D., Boes, R. 2019. Wasserkraftpotenzial in Gletscherrückzugsgebieten der Schweiz (Hydropower potential in regions of retreating glaciers in Switzerland). *Wasser Energie Luft*, 111(4): 205–212 (in German).
- ElCom 2020. Rahmenbedingungen für die Sicherstellung einer angemessenen Winterproduktion. D-B13A3401/32. Eidgenössische Elektrizitätskommission ElCom, Schweiz (in German).
- Felix, D., Müller-Hagmann, M., Boes, R. 2020. Ausbaupotential der bestehenden Speicherseen in der Schweiz (Potential of extending existing storage lakes in Switzerland). *Wasser Energie Luft*, 112(1): 1–10 (in German).
- Felix, D., Ehrbar, D., Fauriel, J., Schmocker, L., Vetsch, D.F., Farinotti, D., Boes, R.M. 2022. Potentials for increasing the water and electricity storage in the Swiss Alps. *Proc. 27th ICOLD Congress*, Marseille, France, Q.107-R.24: 367–387.
- Fuchs, H., Felix, D., Müller-Hagmann, M., Boes, R. 2019. Bewertung von Talsperren-Erhöpfungsoptionen in der Schweiz (Assessment of dam heightening options in Switzerland). *Wasserwirtschaft* 109(5): 146–149 (in German).
- Grenat 2022. Surélévation du barrage d'Emosson, Evaluation préliminaire des impacts sur l'environnement (in French).
- KWO (Kraftwerke Oberhasli AG) 2020. Neubau Speichersee und Kraftwerk Trift (Info sheet on project of HPP Trift with new reservoir). <https://www.grimselestrom.ch/wp-content/uploads/neubau-speichersee-kraftwerk-trift-kwo-web.pdf> (in German).
- Lehmann, D. 2020. Study on a dam for a multipurpose reservoir on the Gornera. Master thesis at VAW, ETH Zürich (unpublished, in German).
- Lombardi 2023. Ouvrage à buts multiples Gornerli, documents d'avant projet (in French).
- SFOE 2019. Schweizerische Elektrizitätsstatistik 2018. Bern: Swiss Federal Office of Energy. <https://www.bfe.admin.ch/bfe/de/home/versorgung/statistik-und-geodaten/energiestatistiken/elektrizitaetsstatistik.html> (in German).
- SFOE 2020. Energieperspektiven 2050+, Zusammenfassung der wichtigsten Ergebnisse (Summary Report). <https://www.bfe.admin.ch/bfe/de/home/politik/energieperspektiven-2050-plus.html> (in German)
- SFOE 2021. Medienmitteilung über den Runden Tisch Wasserkraft (Press release Round Table Hydropower) 13.12.2021: <https://www.admin.ch/gov/de/start/dokumentation/medienmitteilungen.msg-id-86432.html>
- SFOE 2022. Schweizerische Elektrizitätsstatistik 2021. Bern: Swiss Federal Office of Energy. <https://www.bfe.admin.ch/bfe/de/home/versorgung/statistik-und-geodaten/energiestatistiken/elektrizitaetsstatistik.html> (in German).
- Swiss Federal Council 2013. Botschaft zum ersten Massnahmenpaket der Energiestrategie 2050 (Revision des Energierechts). <https://www.admin.ch/opc/de/federal-gazette/2013/7561.pdf> (in German).
- Swiss Federal Council 2019. Federal Council aims for a climate-neutral Switzerland by 2050. <https://www.admin.ch/gov/en/start/documentation/media-releases.msg-id-76206.html>.
- VAW 2011. Gletscher- und Abflussentwicklung in den Einzugsgebieten Gornergletscher, Findelengletscher und Haut Glacier d'Arolla 1900-2100; Versuchsanstalt für Wasserbau, Hydrologie und Glaziologie, ETH Zurich (in German).
- VAW 2021. 21st century glacier and runoff evolution on yearly, daily, and hourly time scales in the catchment of Gornergletscher; Laboratory of Hydraulics, Hydrology and Glaciology, ETH Zurich.

Guidelines for modelling dam safety adaptation to climate change

J. Fluixa-Sanmartin

HYDRO Exploitation, Sion, Switzerland

A. Morales-Torres

iPresas Risk Analysis S.A., Valencia, Spain

I. Escuder-Bueno

Universitat Politècnica de València, Valencia, Spain

iPresas Risk Analysis S.A., Valencia, Spain

ABSTRACT: Risk analysis techniques are useful tools to support decision-making for dam safety by optimizing the economic resources and pointing at the most efficient ways of reducing risks. Climate change is likely to modify dam risks in the future and must be incorporated to long-term safety management strategies to increase economic efficiencies when defining the implementation sequence of risk reduction measures. This article presents a set of guidelines and recommendations to integrate impacts on dam safety, which complexity must depend on the data availability and the depth of the analysis. Three methodologies have been applied to a Spanish dam subjected to the effects of a changing climate, with a focus on hydrological loads. It has been found that simplified methods give valuable information but can oversimplify the reality, while more complex methods provide finer results but at the expense of a higher computational cost. Risk analysis methodologies have proved useful to tackle inherent uncertainties from climate or hydrometeorological information, and to design mitigation measures to counteract the effects of climate change.

1 INTRODUCTION

The implementation of long-term dam safety management programs ensures an adequate management of these critical infrastructures in a continuous and updated process. Risk analysis is a useful methodology that encompasses traditional and state-of-the-art approaches, integrating a variety of aspects in the risk calculation and assessment stages. The occurrence of extreme hydrological events, the dam's ageing process or the sedimentation of reservoirs are critical factors that can undermine the safety of dam-reservoirs systems.

Climate change impacts come on top of this and can cause amplifying risks of dam failures, progressively increasing costs of dam repair and maintenance, and loss of a dam's functionality and effectiveness (Duminda Perera et al. 2021). The increasing frequency and severity of such events can overwhelm the reservoir's and dam's design limits and undermine dam safety which was established for a different (and stationary) climatic situation. This makes the incorporation of climate change aspects into dam safety management increasingly important.

Although incipient, an increasing number of studies are being performed to analyze the effect of climate change on dam safety, be it at a regional level or on a macroscopic scale (Fluixa-Sanmartin et al. 2019; Ghimire and Schulenberg 2022; USBR 2014). However, the information remains scattered and challenging for its application for overall dam safety in general. Proper application of such approaches depends on the availability of data and adapted tools for the integration of dam risk and climate-related information (Larsson and Große 2023).

The authors present a concise set of guidelines and tools to address integrating climate change into dam risk calculation, which allows quantifying and structuring its effects and to design adaptation strategies that incorporate the non-stationarity of future risks, as well as the uncertainty associated with new climate scenarios. The application of such techniques represents as a key step for long-term safety management and will depend on the chosen scope and depth of the analysis. The example of an application to the Santa Teresa dam in Spain is described as well, focusing on the treatment of hydro-meteorological information.

2 BENEFITS OF INCORPORATING CLIMATE CHANGE ON DAM SAFETY MANAGEMENT

Dam safety management programs and decision-making strategies have traditionally assumed stationary climatic conditions based on past information. However, future patterns are likely to change due to climate change. In particular, changes in climate factors such as variations in extreme temperatures or frequency of heavy precipitation events (IPCC 2014) are likely to affect the different factors driving dam failure risks (Bowles et al. 2013; USACE 2016; USBR 2014). Dam owners and operators must adapt their mid- and long-term management and adaptation strategies to new climate scenarios.

In the context of the evaluation of adaptation strategies, revising risk assessments with future climate information can be advantageous for dam safety practitioners to:

- Update the current risk based on one or several future climate scenarios. This approach helps to evaluate the vulnerability of the dam to climate change, i.e. the additional risk imposed by climate change effects.
- Determine the contribution of each dam safety component to the overall risk, thus highlighting which is more susceptible to climate change or has more influence in the final risk level.
- Compare the future dam risk under different climate scenarios for adaptation and decision-making support on climate mitigation. While typical adaptation practices are developed for the short- to the mid-term, in a context of uncertain climate change a long-term planning is imperative.
- Justify whether specific long-term adaptation approaches should be conducted.
- Increase the efficiency and robustness of investments by defining flexible measures that can be implemented adaptively. Such is the case of the so called low-regrets measures, which provide benefits under both current climate and a wide range of future climate change scenarios.
- Prevent choosing risk reduction measures that would no longer be necessary in the future or missing some measures that could efficiently reduce future risk. This is of particular interest when adapting risk management strategies to future climate change impacts.

3 TACKLING CLIMATE CHANGE IMPACTS ON DAM SAFETY COMPONENTS

The information needed to assess climate change effects of each safety component is often vast and complex to integrate. In light of this situation, performing an analysis without a proper guidance can be unaffordable and induce to inefficiencies or conceptual errors. The authors propose in this work a set of guidelines and recommendation on how to quantitatively integrate climate change impacts on dam risk components.

3.1 *Risk analysis approach for structuring climate change impacts*

The projected effects of climate change are expected in different components of dam safety where interdependencies, uncertainties and cross-effects can be relevant. The assessment of such impacts must be addressed jointly and in a homogeneous way rather than by a simple accumulation of separate effects.

Risk analysis represents a useful methodology to manage dam safety in an accountable and comprehensive way (Bowles et al. 2013). In this context, risk models are the basic tool used for the quantitative assessment of risk, integrating and connecting most variables concerning dam safety. These models can be structured using influence diagrams, each node representing a variable related to each term of risk.

In Fluixa-Sanmartin et al. (2018) the authors presented a complete review on projected climate change impacts on dam safety to provide information for dam owners and dam safety practitioners in their decision-making process. The review follows the structure of dam risk models, which allows incorporating and connecting the different components of the risk: Loads of the system, System response and Consequences.

Such an approach has been proved effective for the structuring and assessment of the potential impacts of climate change on dam safety. The analysis can then be performed in a comprehensive way, evaluating the total risk and the climate change impacts as well as their evolution over time. And since all the risk components are jointly evaluated, we avoid neglecting certain factors that affect the global safety.

3.2 Adoption of the level of detail

When assessing the impact of climate change in risk models, it is convenient to define first the scope of the analysis. It is not always advisable to perform analyses with a high level of detail but to look for a balance between precision and effort. The authors propose three levels of detail: simplified, intermediate and advanced (coded as Lvl-1, Lvl-2 and Lvl-3 respectively). The selection of one of these should depend on the depth of the analysis, the data availability, the complexity of the model and the uncertainty degree of the concerned variables and predictions. A summary of the aspects to be considered in each level is presented in Table 1.

Depending on the importance of each node, more effort should be put into those that have a bigger impact on the resulting risk. It can thus be convenient to perform sensitivity analyses to find out which nodes are most influenced by climate change and how the risk model responds to their variation.

It is worth mentioning that risk impacts of climate change are conditioned by climatic but also by non-climatic drivers (IPCC 2014) such as population increase, economic development, or water management adaptation. In certain cases, these non-climatic drivers may have a significant influence in the dam risk calculation. However, the characterization of this type of relations is usually difficult and reserved for detailed studies.

Table 1. Aspects recommended for the application of each detail level.

Aspect	Level of detail		
	Lvl-1	Lvl-2	Lvl-3
Use of empirical results from external studies	x		
Consideration of climatic drivers	x	x	x
Application of ad hoc models	x*	x	x
Comparison between several climate scenarios	x*	x	x
Incorporation of uncertainty		x*	x
Consideration of non-climatic drivers		x*	x
Second-order effects			x*

* Subject to data and time availability

3.2.1 Simplified (Lvl-1)

Adopting a simplified detail level can be advantageous when:

- Dam engineers or decision-makers do not have the time or resources, or when the available information is limited or not pertinent enough to perform more detailed analysis.
- An initial stage of the assessment (screening level) is intended. This will help in defining if additional investigations are necessary, thus optimizing ulterior efforts.

- Assessing the overall vulnerability of a portfolio of dams, according to homogeneous criteria, which would help to identify those with more urgent need for adaptation measures.

At this level, the study of the impacts of climate change must rely on simple techniques or existing results directly applicable to the study cases. No extensive studies (or at the most few of them) should be necessary to accomplish the assessment and only the use of a few representative scenarios is envisaged. Moreover, uncertainty of climate effects should not be taken into account at this level. Main efforts must be put into changes of the hydrological loads, the water level probability distribution and eventually the consequences estimation.

3.2.2 *Intermediate (Lvl-2)*

This level is adopted when more precise results than in Lvl-1 are sought. This might be the case when:

- Effects of climate change need to be further studied after a Lvl-1 analysis shows a high vulnerability of a particular dam.
- Results of the analysis are meant to support decision-makers in the definition or the choice of adaptation measures.
- Time and available data are generally enough to reach a higher level of understanding of the problem. Ad hoc studies can be performed and applied to specific cases.

In this case, a complete set of climate scenarios should be analyzed. Techniques to extract valuable conclusions from wide and often disperse information are to be envisaged. The incorporation of uncertainty (and eventually of non-climatic drivers) is subjected to data availability and to the importance of the studied node. Ad-hoc models or studies are encouraged.

3.2.3 *Advanced (Lvl-3)*

This level is mandatory when we seek the maximum understanding of the climate processes that may affect dam safety. This is the case for instance when a detailed assessment of the performance of a particular portfolio of measures is required considering future climate uncertainties, as well as non-climate factors.

Eventually, second-order effects can be incorporated to the analysis. This happens when a component is directly affected by climate and/or non-climate factors but also by the changes in other components. For instance, an increase in temperatures might produce a decrease of water levels in reservoirs, but a prolonged situation or the implementation of adaptive policies might also entail a reduction of consumption and therefore of demand, leading to a balanced situation between available and required water volumes. This requires a deep understanding of how the different variables are expected to evolve and how they interact. The complexity of such approaches can rapidly increase and must be envisaged under a pragmatic perspective.

Moreover, participatory workshops or the use of expert judgment could improve the extent and depth of the analysis, since most of the effects and interactions taking place are highly complex and their assessment should involve multi-sectorial approaches.

3.3 *Selection of climate scenarios*

A key aspect to be considered when analyzing impacts of climate change is the selection of the climate scenario(s) and model(s) to be used. Different approaches can be undertaken.

The simplest and less time-consuming tactic is to choose only a few scenarios to perform the analysis. This is the case in many situations, when engineers do not have the time or resources to explore all scenarios or the outcomes of different models. A common practice is using the highest and lowest emission scenarios in order to have an idea of the spectrum of possible future climate hazards. However, this type of results may show an overestimation of climate risks and thus must be interpreted with special caution. Moreover, it is not always evident in advance which scenarios will produce higher/lower risks, since multiple interactions between the different risk components occur. An alternative can be to work with average scenarios from of a set of more or less adverse cases. Nonetheless, it is not advised to mix too different scenarios to avoid counterbalance positive/negative effects on risk.

To better capture the range of possible futures and integrate climate uncertainties in the analysis, different scenarios and climate models should be investigated (IPCC 2014). It is possible to combine multiple climate projections and, sometimes, different emissions scenarios and obtain probability distributions of future impacts by weighting each scenario considered. However, it can be sometimes difficult to practically construct robust quantitative probability distributions of climate change impacts. The same climate scenario chosen should be consistently applied to all the components of the risk model; otherwise, risk could be easily over or underestimated.

3.4 *Temporal horizon*

Since climate change impacts are expected to (greatly) evolve with time, another important aspect to take into account is the temporal horizon of the analysis (e.g. whether to use projections for 2030, 2050 or 2100). When the analysis aims at establishing the optimal sequence of risk reduction measures, this time horizon can be defined as the upper limit of the time interval during which the investments are justifiably financed. This allows foreseeing the events to be expected during this period, to define the risk reduction measures and to plan the implementation that maximize their effectiveness. Criteria for setting the decision time horizon cover a wide range of possibilities. These are the basis for the widespread application in diverse domains of economic and financial analyses such as cost benefit analysis (CBA), cost effectiveness analysis (CEA) or multi-criteria analysis (MCA). The decision time horizon can have a great influence on the prioritization of risk reduction measures.

Short-term analyses (time horizons of less than 20 years) are more suitable to be matched to conventional planning time scales. However, a longer-term policy is preferable when we seek strategies for adaptation, mitigation, and development that are robust over the long term and able to cope with uncertainties. The expected lifetime of the dam or the projected investments also contributes to the choice of a time horizon. For instance, newly constructed or in progress dams require considering longer scenarios than obsolete ones.

Analyses can be performed for a unique temporal horizon or for a succession of them, depending on whether only the final risk situation is significant or what is sought is how climate change will progressively affect dam safety.

4 CASE STUDY: SANTA TERESA DAM IN SPAIN

The case study of the Santa Teresa dam, a Spanish dam belonging to the Duero River Basin Authority, is used to assess how different levels of detail in the analyses carried out can affect the resulting risks of the dam and ultimately the decisions to be made.

The Santa Teresa dam is a concrete gravity dam with a height of 60 m and a length of 517 m. It is equipped with a spillway regulated by five gates, as well as with two bottom outlets. The dam is complemented with a 165 m long and 15 m high auxiliary gravity concrete saddle dam.

4.1 *Risk modelling*

As part of a quantitative risk analysis performed on several Spanish dams (Ardiles et al. 2011), the risk model of the Santa Teresa dam was set up with iPresas software for hydrological loading scenarios. This is a tool for quantitative risk calculation based on event trees to compute failure probability and risk. The software integrates the probability of occurrence of loads, the system response and any type of consequences using influence diagrams (Figure 1).

4.2 *Approaches for integrating hydrological loads under climate change*

Results from Fluixa-Sanmartin et al. (2019) showed that the effects of climate change on the dam failure risk are mainly explained by the changes in the flood loads and the changes in the reservoir water levels regime. Such components are directly related to the dam's hydrological contributions. Therefore, in this work we focus on the hydrological factors, which is the response of the catchment to meteorological drivers, which in turn are directly affected by climate change.

This section deals with the techniques aimed at incorporating the (vast) meteorological information issued from climate models into the dam risk model.

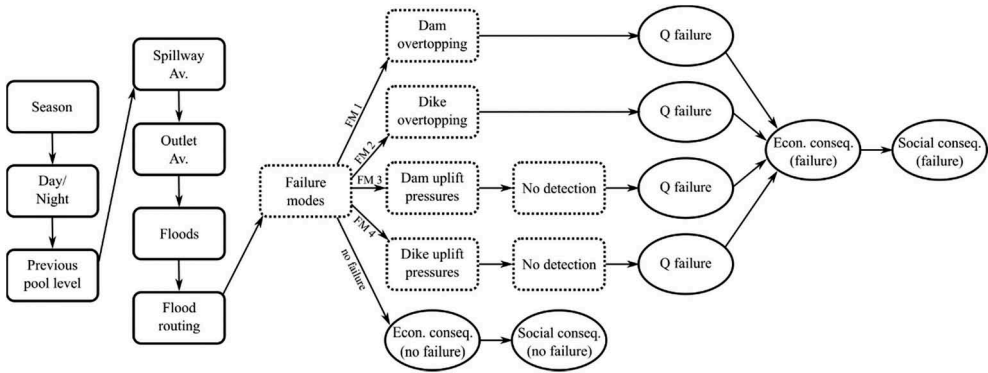


Figure 1. Diagram of the quantitative risk model for the Santa Teresa dam.

4.2.1 Simplified

As a first phase in the incorporation of climate change effects on hydrological aspects, a simplified analysis has been performed. In this case, only the effects on floods frequency and magnitude are investigated. For this purpose, the recent publication from the Spanish Center for Research and Experimentation of Public Works (CEDEX) has been used. The goal of the study (CEDEX 2021) was to assess the impact of climate change on annual maximum daily rainfall P_d , at different time intervals, based on the simulations of 15 EURO-CORDEX climate projections (CP). The study covers the following cases:

- Four study periods: a control period (1971-2000), and three impact periods (2011-2040, 2041-2070 and 2071-2100).
- Two greenhouse gas emission scenarios: RCP4.5 and RCP8.5, considered the most likely scenario in view of current trends according to the IPCC Sixth Assessment Report, and the worst-case scenario if no climate policies are adopted, respectively.
- Four return periods: 10-, 100-, 500- and 1,000-year.

Results are in the form of change rates of the quantiles of maximum observed precipitation $P_{d,T}$, for different return periods. For each combination of study period, RCP and return period, a unique change rate is calculated as the mean of the statistically significant ($\alpha=0.10$) changes of maximum daily precipitation from the 15 CPs.

The application of this information for our simplified analysis is schematized in Figure 2. To obtain the maximum daily precipitation for other the return periods, the corresponding rates of change are applied to the quantiles of maximum precipitation, to which a GEV distribution function is fitted. Finally the quantiles of precipitation for the necessary return periods are obtained.

It is worth mentioning that the methodology described here was only applied to the maximum precipitations that leads to the calculation of incoming floods. Since the results from CEDEX (2021) only contain information about maximum precipitations, the reservoir water levels were computed with the base case hydrological model (Fluixa-Sanmartin et al. 2019).

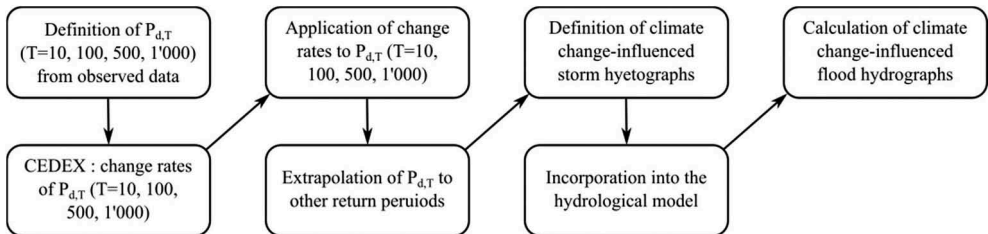


Figure 2. Methodology followed under the simplified approach for obtaining flood hydrographs based on the CEDEX study.

4.2.2 Intermediate

The authors have performed a comprehensive quantitative assessment of the climate change impacts on the risk of this dam under hydrological scenarios. The study Fluixa-Sanmartin et al. (2019) integrates the various projected effects acting on each component of the risk. We used the same 15 climate projections from the EURO-CORDEX project as in the simplified approach and two RCPs (RCP4.5 and RCP8.5).

A hydrological model was set up based on the physical characteristics of the basin and on the hydro-meteorological observations. On one hand, such model allowed performing the simulation of the system of water resources management to obtain the relation between previous pool level and probability at the reservoir, at the present situation and for future scenarios. The reservoir's exploitation rules considered were based on the current Duero's Hydrological Plan and adapted to fit population changes.

On the other hand, the hydrological model was used for the definition of the flood hydrographs. In order to calculate these flood events, a statistical analysis of the annual maxima of storm rainfall was performed, extracted from the daily precipitation data of the observation and climate projection series. Each annual maxima series was fitted to a Gumbel distribution with which an extrapolation to return period between 2 and 10^5 years was carried out.

Lastly, the risk model was used to calculate the evolution of risk and dam failure probability until the end of the 21st century for each CP-RCP combination. Results were extracted for 4 periods: 1970-2005 (Base Case); 2010-2039; 2040-2069; and 2070-2099. These results served as reference points (years 2005, 2039, 2069 and 2099, respectively) for the interpolation of risk.

The main steps of the methodology followed to integrate this information is presented in Figure 3. A complete description of such methodology and the results obtained can be found in Fluixa-Sanmartin et al. (2019).

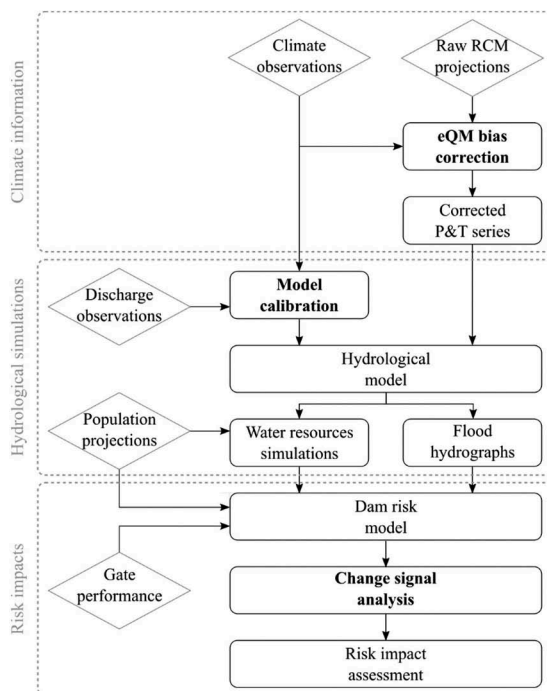


Figure 3. Workflow of the methodology followed to assess climate change impacts on dam failure risk.

4.2.3 Advanced

Risk calculations, and in particular those relative to floods, depend on observed and future extreme events whose probability of occurrence is extrapolated using extreme probability distributions, making them very sensitive to the fitted parameters. Furthermore, the use of short

annual maxima time series (<100 years) induces sampling errors in the estimation of these parameters, causing uncertainty to the estimated quantile-frequency relationship. In order to quantify the influence of extreme meteorological inputs on the resulting risk, a sensitivity analysis has been performed to the above-described intermediate assessment (Section 4.2.2).

Because of the sampling error, we can assume that the estimated maximum daily precipitation x_T for a T return period can be treated as a random variable (Su and Tung 2013). The maximum likelihood method is used to calculate the sampling error of the Gumbel-based quantile estimator. The variance for the year quantile estimator (x_T) can be expressed as:

$$s_e^2 = \frac{\beta^2}{n} \cdot (1.1087 + 0.5140 \cdot Y + 0.6079 \cdot Y^2) \quad (1)$$

where β = scale parameter of the Gumbel distribution; n = sample size; and $Y = -\ln(-\ln(1-1/T))$.

Assuming the sampling distribution of the quantile estimator to be normal with mean x_T and variance s_e^2 , 200 random quantiles are generated. Thenceforward, the corresponding hydrographs are obtained using the new quantile-frequency relationships to determine the maximum daily precipitations. Finally, the risk model is applied for each of the 200 aleatory cases.

Given the computational cost that this analysis represents, the sensitivity analysis has been applied only to the observation data. This gives an idea on how the rest of the cases would behave.

4.3 Results

Once the dam risk model is adapted following the effects of climate change, the social and economic risks are calculated for the Base Case (year 2005) and for all the CP-RCP combinations. For the Base Case, the failure probability is 2.91×10^{-6} year⁻¹, while the social and economic risks are 2.56×10^{-4} lives/year and 7.53×10^{-4} M€/year respectively.

Figures 4 and 5 present the evolution of social risks (economic risks follow a similar pattern and are not plotted for simplicity) for RCP4.5 and RCP8.5, respectively. For illustrative purposes, the y-axis is plotted on a logarithmic scale to better appreciate the order of magnitude of its values. Results of the intermediate analysis show that in most future scenarios from RCP4.5 an increase of the risk occurs in comparison to the present risk level. For RCP8.5, dispersion makes it hard to extract a generalized conclusion.

The bold dashed lines indicate the risk resulting from the simplified method. The general trend of risk is well captured by the results of the simplified analysis that also indicates a general deterioration of the dam's risk. However, while for the RCP4.5 the simplified risk corresponds approximately with the mean values of the intermediate risk results, for the RCP8.5 the simplified risk is within the upper range of the intermediate analysis. This is because for the simplified version, no ad-hoc hydrological models could be built to extract the Previous Pools Levels, and only the information from the base case model was used. In fact, for the RCP8.5 scenario the higher evapotranspiration related to the increase of temperatures are expected to reduce the water levels in the reservoir, which will ultimately lead to a lower risk for RCP8.5 compared to the RCP4.5 scenario. This can only be extracted when using a complete hydrological model for each of the CPs considered and can hardly be replaced with results of an averaged model.

Concerning the advanced approach, results of the analysis are displayed in Figure 6. Risks corresponding to the 200 sample points have been decomposed in its associated probability of failure and average social consequences. The Base Case risk is represented as a black point and its probability of failure and consequences are highlighted with two dashed black lines. Even though the analysis is only applied to the Base Case, similar results can be expected when applying it to the climate projections. Results show a significant dispersion of risk arising from the sensitivity to the statistical distribution fitting used to obtain maximum daily precipitations. This gives a larger uncertainty of results that comes on top of the one observed in the intermediate analysis. These uncertainties influence the reliability of the results and the adopted adaptation strategies, and must be handled with appropriate tools.

Furthermore, from the intermediate and advanced analyses a dispersion of the risk clearly appears. The ensemble of uncertainties propagates through input data and models, which inherit prior uncertainties and expand at each step of the process. This needs a proper uncertainty

treatment methodology to make the most of the results. Although procedures can be established to deal with each climate projection individually and obtain the optimal risk reduction approach, response strategies that explicitly recognize climate-related uncertainties must be incorporated into the decision-making process under a comprehensive approach. Under this perspective, the advantage of using the risk analysis approach is that the impact of all uncertainties on each component of the risk can be easily identified and analyzed, taking into account their potential interrelations. It is important to highlight that the incorporation of uncertainties in the process must not prevent decisions from being made and should rely on robust adaptation strategies.

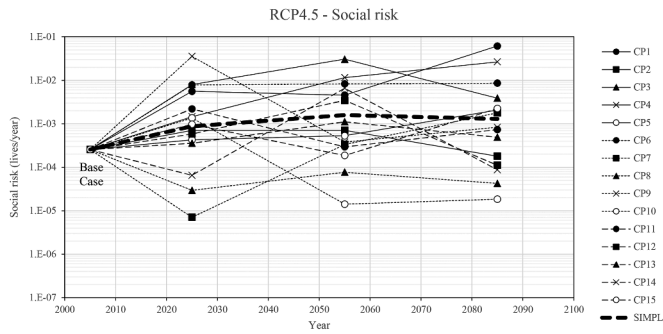


Figure 4. Evolution of the social risks of the dam considering the RCP4.5 scenario, classified by CP (for the intermediate approach) and with a bold dashed line (for the simplified method, called SIMPL).

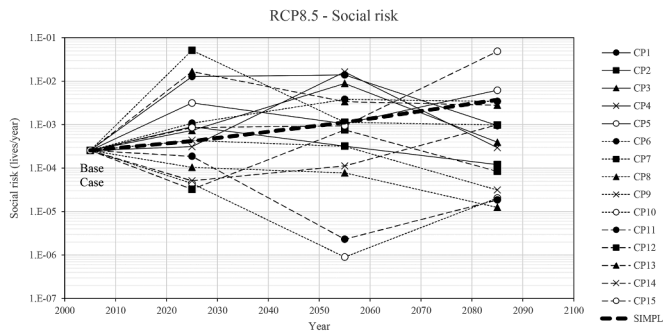


Figure 5. Evolution of the social risks of the dam considering the RCP8.5 scenario, classified by CP (for the intermediate approach) and with a bold dashed line (for the simplified method, called SIMPL).

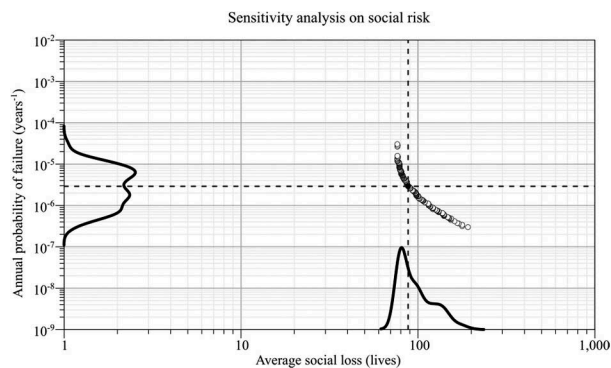


Figure 6. Effect of precipitation sampling uncertainty on social risk. The density of the resulting points is displayed on the x- and y-axes.

5 CONCLUSIONS

Under changing climatic scenarios, dam risk management approaches and decision-making strategies must be updated. In this work, a set of guidelines and recommendations are presented to tackle the modelling of climate change impacts on dam safety. Proposed approaches range from simple reuse of external studies in a unique (average) climate projection to sensitivity analysis applied to climate projections and intermediate variables. The chosen methodology should then depend on the data availability and the depth of the analysis.

Three increasingly complex methodologies, based on dam risk analysis methods, have been applied to a Spanish dam subjected to the effects of a changing climate. Simplified methods give valuable information on how the dam will react to future climate solicitations, but can oversimplify the reality. More complex methods provide finer results but at the expense of a higher computational cost.

It is worth mentioning that inherent uncertainties from climate or hydrometeorological information will have a direct impact on how to manage dam safety on the mid- and long-term but must not prevent decisions from being made. Risk analysis methodologies have proved useful to tackle such uncertainties, and to design mitigation measures to counteract the effects of climate change.

REFERENCES

- Ardiles, L., D. Sanz, P. Moreno, E. Jenaro, J. Fleitz, and I. Escuder-Bueno. 2011. Risk Assessment and Management for 26 Dams Operated By the Duero River Authority (Spain). *Proceedings of the 6th International Conference on Dam Engineering*, 15-17 February 2011, LNEC, Lisbon, Portugal. Singapore: CI-Premier Pte Ltd.
- Bowles, D., A. Brown, A. Hughes, M. Morris, P. Sayers, A. Topple, M. Wallis, and K. Gardiner. 2013. *Guide to risk assessment for reservoir safety management, Volume 1: Guide*. 329. Horison House, Deanery Road, Bristol, BS1 9AH: Environment Agency.
- CEDEX. 2021. *Impacto del cambio climático en las precipitaciones máximas en España*. Madrid, Spain: CEDEX - Centro de Estudios Hidrográficos.
- Duminda Perera, V. Smakhtin, S. Williams, T. North, and A. Curry. 2021. *Ageing Water Storage Infrastructure: An Emerging Global Risk*. UNU-INWEH Report Series, 11. United Nations University (UNU).
- Fluixa-Sanmartin, J., L. Altarejos-García, A. Morales-Torres, and I. Escuder-Bueno. 2018. Review article: Climate change impacts on dam safety. *Natural Hazards and Earth System Sciences*, 18 (9): 2471–2488.
- Fluixa-Sanmartin, J., A. Morales-Torres, I. Escuder-Bueno, and J. Paredes-Arquiola. 2019. Quantification of climate change impact on dam failure risk under hydrological scenarios: a case study from a Spanish dam. *Natural Hazards and Earth System Sciences*, 19 (10): 2117–2139.
- Ghimire, S. N., and J. W. Schulenberg. 2022. Impacts of Climate Change on the Environment, Increase in Reservoir Levels, and Safety Threats to Earthen Dams: Post Failure Case Study of Two Cascading Dams in Michigan. *Civil and Environmental Engineering*, 18 (2): 551–564.
- IPCC. 2014. *Climate Change 2014: Impacts, Adaptation, and Vulnerability. Part A: Global and Sectoral Aspects. Contribution of Working Group II to the Fifth Assessment Report of the Intergovernmental Panel on Climate Change*. Cambridge, United Kingdom and New York, NY, USA: Cambridge Univ. Press.
- Larsson, A., and C. Große. 2023. Data use and data needs in critical infrastructure risk analysis. *Journal of Risk Research*, 1–22.
- Su, H.-T., and Y.-K. Tung. 2013. Incorporating uncertainty of distribution parameters due to sampling errors in flood-damage-reduction project evaluation. *Water Resources Research*, 49 (3): 1680–1692.
- USACE. 2016. *Guidance for Incorporating Climate Change Impacts to Inland Hydrology in Civil Works Studies, Designs, and Projects*.
- USBR. 2014. *Climate Change Adaptation Strategy*. U.S. Department of the Interior. Bureau of Reclamation.

Upgrade of the Perlenbach Dam in Germany – A multi-purpose sustainability project

R. Haselsteiner, B. Ersoy & L. Werner
M&P Water Ltd., Germany

ABSTRACT: Perlenbach dam is located within the catchment of the Rur River close to the city of Monschau in West Germany at the border to Belgium. The main purpose of the reservoir is water supply, but it also serves the minimum flow requirements, recreation and hydropower.

During the devastating flood incident in July 2021 in western Germany the reservoir faced inflows exceeding a HQ_{10,000} event. Thanks to the conservative design of the existing spillway major harm did not occur. Contrary to the flood event, the 2018 and 2022 dry periods revealed that the capacity of the reservoir is not sufficient to cover such extreme droughts. The water supply association Perlenbach was forced to purchase water from other suppliers of the region.

The existing scheme is a reservoir volume of only 750.000 m³ which represents only 1.7 % of the annual mean inflow. The increase of the reservoir volumes shows positive effects not only onto the water supply security but also the energy production and minimum flow periods. Additionally, the reservoir could contribute to flood retention since the Perlenbach comprises about one third of the Rur catchment at its mouth. Particularly in summer the reservoir could contribute essentially to flood control downstream.

The existing dam is an earth-rockfill dam with an asphaltic surface sealing and a height of 18 m. The upgrade requires the heightening of the existing dam by approx. eight meters. All dam facilities need to be adjusted, the spillway has to be completely reconstructed and existing sediments need to be removed from the reservoir.

Upstream of the reservoir valuable fauna flora habitats are located which are affected by the future reservoir. This impact is a critical aspect and compensation is strongly required. An early participation of all stakeholders is anticipated in order to find a realizable solution.

1 INTRODUCTION

Climate change leads to extreme water regimes which include devastating floods and droughts as well. The unequal distribution of water resources leads to challenges in both flood protection measures and water supply assets among other knock-on impacts such as various supply chains, damage of critical infrastructure, endanger of life and property. Social welfare and safety may suffer from serious long-term destabilization with local and global range.

“Climate change is one of the great dangers we face, and it’s one we can prevent if we act now.” (Stephen Hawkin, 1942 – 2018) This statement of one of the masterminds in physics summarizes precisely the urgency of taking counter measures to diminish the effects of climate change. Up-to-date IPCC (2021) reports document that now is over and CO₂ emissions and subsequent temperature increase are inevitable.

Climate adaptation measures need to be realized in order to guarantee basic services and supply in terms of water, energy, communication, traffic, etc. Drinking water supply is one of the most critical services which are sensed as self-evident in most of the western countries such as Germany. Remarkable droughts during the past years have revealed the vulnerability of the water supply mains. In 2018 Germany suffered from a long drought period which lasted several months.

Also, for the Perlenbach Water Supply Association which is owner of the Perlenbach Dam the year 2018 was critical. During approximately 155 days almost no inflows entered the reservoir. The reservoir could not meet the requirements of the drinking water demand, so drinking water had to be purchased from a nearby water supply association. This experience and pessimistic prognosis triggered the preparation of studies which investigated feasible solutions and adherent measures and costs.

2 THE PERLENBACH DAM REGIME AND WATER SUPPLY REQUIREMENTS

The Perlenbach Dam is located on the Perlenbach river close to the city of Monschau in the western part of Germany very close to the Belgium border. The Perlenbach River flows into the Rur River two kilometer downstream. The Rur River discharges into the reservoir of the Rurtal Dam further downstream.

The Perlenbach Dam's main purpose is drinking water supply for 50,000 people and it is operated by the Water Supply Association Perlenbach. In emergency cases the association

Table 1. Main characteristics of the Perlenbach Dam and reservoir.

General data/hydrology	
Catchment area A_{EO}	60.93 km ²
Dam structure	
Type	Rockfill dam with asphalt surface sealing
Maximum height H_D	18.30 m (above foundation level)
Dam length L_D	117.00 m
Crest width W_C	4.75 m
Crest elevation	467.00 m asl
Freeboard height f	1.94 m
Reservoir data	
Total reservoir volume V_{tot}	925,000 m ³ (= utilized volume)
Degree of utilization α	1.7 %
Minimum reservoir level Z_{min}	452.35 m asl
Operation water level Z_S	464.25 m asl
Flood water level Z_{H1}	465.06 m asl
Flood water level Z_{H2}	465.20 m asl
Hydrological data	
Lowest low discharge NNQ	0.040 m ³ /s
Average low discharge MNQ	0.129 m ³ /s
Average discharge MQ	1.5 m ³ /s
Average flood discharge MHQ	18.39 m ³ /s
Flood discharge HQ_{10}	21.2 m ³ /s
Flood discharge HQ_{25}	29.0 m ³ /s
Flood discharge HQ_{50}	32.2 m ³ /s
Flood discharge HQ_{100}	36.1 m ³ /s
Design flood discharge $BHQ_1 = HQ_{1.000}$	40.5 m ³ /s
Design flood discharge $BHQ_2 = HQ_{10.000}$	55.75 m ³ /s
Maximum recorded flood discharge HHQ	56.00 m ³ /s (before flood in July 2021)
Operation facilities	
Spillway type	Overflow weir with one flap gate
Spillway length	28.6 m weir and 8.5 m gate
Raw water steel supply pipes diameter	2 x 300 mm
Steel bottom outlet diameter	1 x 800 mm
Concrete penstock pipe diameter	1 x 800 mm
Inflow pipe diameter (Francis turbine)	1 x 800 mm
Inflow pipe diameter (Ossberger turbine)	1 x 1.500/1.600 mm

withdraws drinking water from adjacent associations of a volume of 0.3 Mio. m³ per year. The storage volume of the current reservoir is 0.76 Mio. m³ whereas the annual average inflow is 45 Mio. m³ from a catchment area of 61 km². The utilization is less than 1.7 % which is the main reason that longer periods without rain or droughts leads to supply lacks.

The daily average supply demand is ranging between 8,190 and 8,800 m³/d and maxima of 10,500 and 12,900 m³/d, respectively. The peak factors result in values from 1.23 to 1.51. The raw water withdrawal from the reservoir is approx. 2.87 to 3.62 Mio. m³ per year. Losses are reaching maximum 11 %.

Accounting for climate change effects, a safety factor of 20 % for the drinking water demand and a safety factor of 1.6 for the daily peak demands shall be considered. These values are recommended by different professional and scientific associations (DVWG et al., 2021). Hence, the future scheme of the Perlenbach reservoir has to guarantee a daily supply of 13,700 m³/d or 3,75 Mio. m³/a drinking water which requires a raw water withdrawal of approximately 4.12 Mio. m³/a in consideration of 10 % process losses.

The dam itself is of embankment/rockfill type with an asphalt surface sealing. According to the national classification scheme of the DIN 19700 it is a class 1 dam; according to ICOLD criteria it is a large dam. The dam was commissioned in 1956. It is a multipurpose dam serving for drinking water supply, hydropower production, and low flow regulation. A hydropower station is placed nearby the downstream dam toe; it hosts a Francis turbine since 1956, and since 2004 an Ossberger turbine. The main characteristics are given in the table below.

In July 2021 a major flood incident struck Europe that especially impacted, Western Germany. The catchment of the Perlenbach Dam was affected, which resulted in a peak outflow of the reservoir of approximately 62 m³/s. This discharge represents a recurrence period larger than T = 10,000 a. Although, the flow was extreme the reservoir, dam and also the downstream region downstream to the Rurtal Dam were not severely harmed. The existing spillway shows a relatively long overflow crest and the flap gate was lowered so that the water level in the reservoir could be handled safely.

Due to the small reservoir volume and the relatively large inflow and the relatively high-water level there was no retention effect, such that the inflow equalled the outflow over the spillway.

3 FUTURE WATER DEMAND AND ADDITIONAL RESERVOIR VOLUME

The thread of climate change which is causing long drought periods were documented by the years 2018 and 2020 at the Perlenbach River. During both years the dam owner needed to purchase drinking water from other neighbouring association since the reservoir volume of the dam was not sufficient. A future prognosis scenario needed to be developed in order to define the required additional reservoir volume. For this purpose, the recorded inflow data of the year 2020 was considered and a longer drought period of 5.5 month was considered. A minimum reservoir volume of 400,000 m³ was considered to have the required safety margin and water quality guarantee.

The result is shown in Figure 1. The simple modelling approach results in a required initial reservoir volume of 2.3 Mio. m³ also considering an increased future demand. The prognosis was prepared for the year 2040.

The adjacent water treatment plant refurbishment or replacement was not addressed in the feasibility study.

4 STRUCTURAL ADAPTATION MEASURES

The need for a larger reservoir volume in order also to cover future drought scenarios results in several adaptation measures of the existing dam scheme which include following:

- Increase of the dam body by approximately 8 to 9 meters
- Strengthening of the downstream dam slope by additional fill

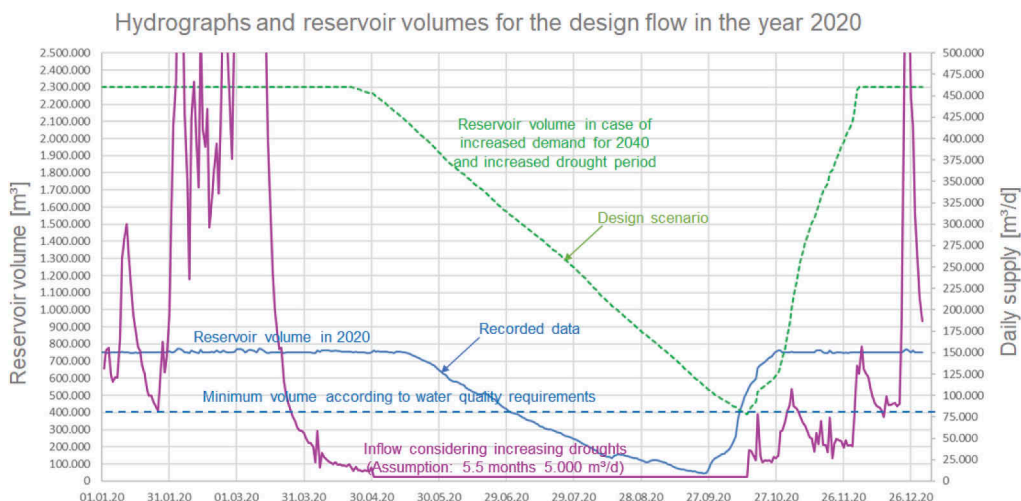


Figure 1. Determination of a required reservoir volume for a selected drought scenario.

- Adaptation and heightening of the left public road
- Adaptation and rehabilitation of the surface sealing
- Adaptation of the existing hiking tracks along the reservoir
- Adaptation/rehabilitation of the operation facilities such as bottom outlet and other operation outlets for water supply and hydropower
- Adaptation of the dam crest road and right bank bridge
- Renewal of the spillway
- Adaptation and refurbishment of the survey works and measurements

The new reservoir levels are as follows:

- Operation level Z_S : 473,00 m asl
- Flood water level Z_{H2} : 474,00 m asl
- Crest level: 474,75 m asl

The current reservoir shows also a sedimented volume of approximately 100,000 m³ which could be treated hand in hand with the general works. This also counts for future maintenance and renewal works for the bottom outlet inlet structure as well as for other components that need treatment.

Due to continuous sedimentation processes, the placement of an upstream sedimentation dam is discussed in order to keep sediments away from the main storage. With the increasing water level, the reservoir also increases and elongates upstream where single housing and another public road are affected.

In Figure 2 the adaption/heightening measures within the main dam area is illustrated.

5 ENVIRONMENTAL IMPACT

Since the water level needs to be increased by 8 to 9 meters the reservoir also extends several kilometres upstream. There, environmental protection areas and biotopes are affected. The affected area is considerable and according to European and national environmental laws compensation is required. During the feasibility study initial coordination meetings with the environmental agencies were held which revealed serious concerns as strictly protected biotopes and species could be affected.

Although, a study and evaluation of alternatives was performed within a forerunner study the extent of environmental impact is critical so that again general alternatives such as also



Figure 2. Structural adaption measures within the main dam area.

abandoning the Perlenbach reservoir and subsequent affiliation of the complete association to an neighbouring association. Before going ahead with the planning and realization of upgrading the Perlenbach Dam the fundamental feasibility of compensation had to be clarified and be evaluated in consideration of basic aims such as guaranteeing the water supply for the future, strengthening the autarchy of the local supplier and utilizing the local water resources.

6 FLOOD PROTECTION AND RETENTION BENEFITS

By increasing the reservoir volume, the retention volume is increased which may create flood detention potential especially when the reservoir level is low due to normal consumption and low inflows during the summer times.

The reservoir characteristic is given in Figure 3. The reservoir volume increase is 1.6 Mio. m³ from 0.75 to 2.35 Mio. m³. The operation water level is increased from $Z_{S,old} = 464,286$ m asl to $Z_{S,new} = 473,00$ m asl. The recorded flood hydrograph 2021 was considered for modelling flood hydrographs with different peak flows corresponding to selected

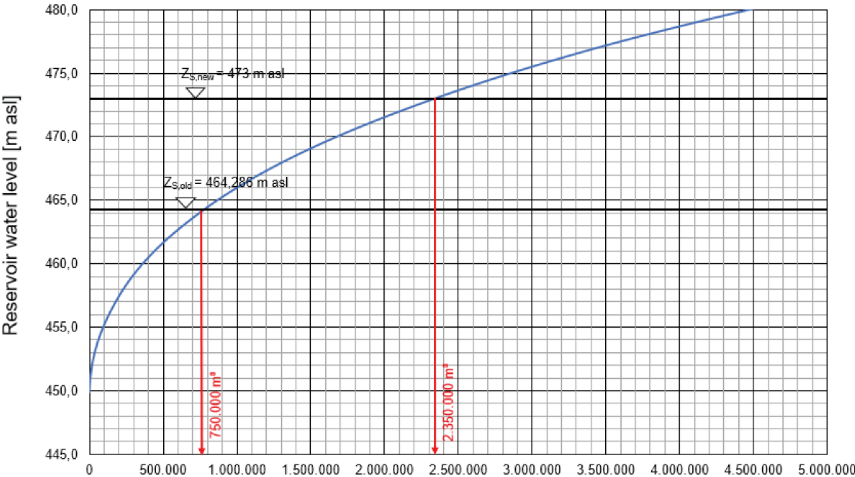


Figure 3. Reservoir characteristic and storage volume before and after heightening.

recurrence periods (see Figure 4). Since the 2021 event was a supercell storm event, the duration of the hydrograph is limited to 24 hours from mean flow to the peak flow. Recorded winter/spring flood events show longer durations.

The flood routing results for a selected flood event and operation scenario is shown in Figure 5. In this case, a lowering of the reservoir level was considered so that the outflow only reached approximately 2/3 of the peak inflow. The larger the flood volumes and its peaks the smaller the detention effect. This is reflected by the diagram in Figure 6.

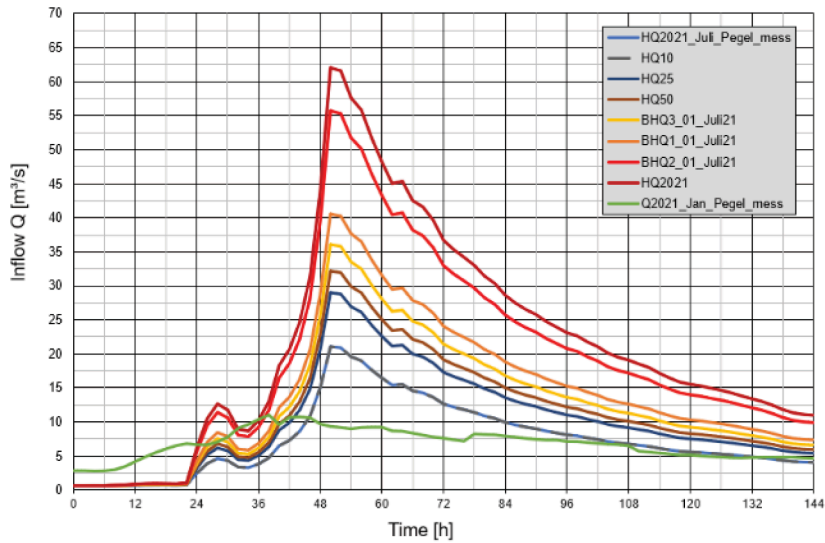


Figure 4. Considered flood hydrographs for flood routing.

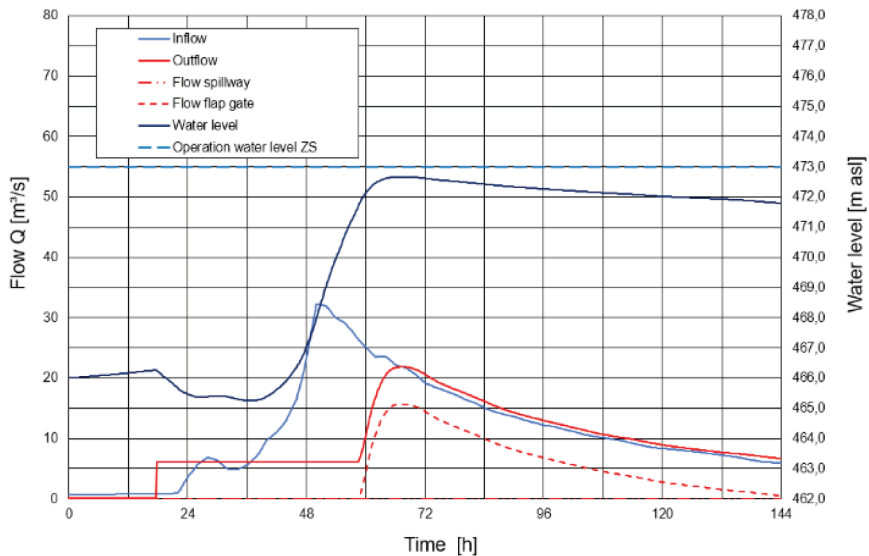


Figure 5. Flood routing results (selected flood scenario).

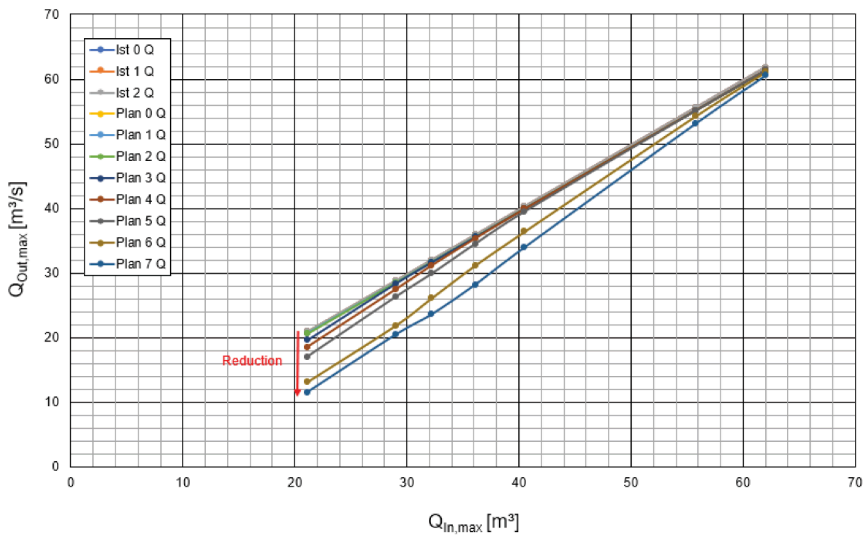


Figure 6. Detention effect by illustration of inflows and outflows of the reservoir.

For floods such as 2021 with a recurrence period $T > 10,000$ a no detention is achieved but for smaller floods with recurrence periods of $T = 10$ to 50 the inflow peaks could be decreased by 30 to 50 % if corresponding adaptations are done.

Thus, the increase of the Perlenbach reservoir does not only show a positive effect on the water supply security but also on flood safety for summer times, when also the Rurtal Dam provides only limited flood retention volume due to the reservoir operation scheme there.

ACKNOWLEDGMENTS

The authors would like to thank the colleagues of the Water Supply Association Perlenbach for the fruitful collaboration and the permission to publish the content of the feasibility study.

REFERENCES

- DIN 19700 2004. Dams. *Deutsches Institut für Normung (DIN)*, Berlin.
- DVGW et al. 2021. Bedarfe der Wasserversorgung in Zeiten des Klimawandels, Maßnahmenvorschläge des BDEW, DVGW und VKU, June 2021.
- IPCC 2021. Summary for Policymakers. In: *Climate Change 2021: The Physical Science Basis. Contribution of Working Group I to the Sixth Assessment Report of the Intergovernmental Panel on Climate Change Working Group I contribution to the Sixth Assessment Report of the Intergovernmental Panel on Climate Change (IPCC)*, Cambridge University Press.

PKW Spillways: An innovative, resilient and flexible solution from run-off river dams in plains to large dams in mountains suitable for climate change

F. Laugier

Dam Safety Expert, EDF-CIH, France

M. Ho Ta Khanh

Dam Safety Consultant, Vietnam

J. Vermeulen

Dam Hydraulics Expert, EDF-CIH, France

ABSTRACT: Two different examples of Piano Key Weirs spillways (PKW) projects are presented. It highlights the wide range of application and brought benefits: The existing La Raviege dam PKW (40 m high concrete gravity dam, France) initially originally equipped with 2 radial gates and improved with a PKW spillway on crest, and the new Van Phong run-off river dam (Vietnam) equipped with 60 PKW units and 10 large radial gates.

RÉSUMÉ: Le papier présente deux applications très différentes des évacuateurs de crue labyrinthe à touche de piano (PKW). Ces exemples illustrent la très large gamme d'application de ce système et les bénéfices apportées: Le barrage existant de La Raviege (barrage poids de 40 m de haut, France) équipé initialement de 2 vannes radiales et complété par un PKW en crête en rive gauche, et le projet neuf du barrage en rivière de Van Phong (Vietnam) équipé de 60 unités PKW et 10 grandes vannes radiales.

1 INTRODUCTION

Piano Key Weir (PKW) labyrinth spillway have been a quickly developing innovation during the past decade. In about 15 years since the first prototype was commissioned (Goulours dam, France in 2006), more than 30 PKW were built all over the world in the 5 continents.

PKW concept is based on the old traditional vertical labyrinth idea. However, their main drawback was solved. Due to a reduced footprint, PKW can be installed at the top of most concrete dams, gravity or even arch dams.

As free flow spillway, PKW operate without any mechanical equipment, human operator or energy source. They are intrinsically safe and significantly improve general dam safety.

PKW free flow spillway are quite flexible in case of hydrological increase due to climate change. PKW discharge capacity rises fast according to hydraulic head without the risk of discharge saturation than can affect gates above a given head.

PKW concept is suitable either for existing dam rehabilitation or for new dams. In the latter case, a combination “gates + PKW” has revealed many advantages by optimizing cost, reliability and other technical issues such as reservoir level control or sediment passage.

The paper will focus on two very different examples of PKW highlighting the wide range of application and brought benefit:

- The new Van Phong barrage (run-of river) dam (Vietnam) was commissioned in 2014. It is equipped with 60 PKW units and 10 large radial gates. PKW units can discharge $8700 \text{ m}^3/\text{s}$ and allow to reduce the number of gates from 28 (initial project) to 10.
- Raviege dam PKW (40 m high concrete gravity dam, France) was commissioned in 2015 as part of a dam safety rehabilitation project. It combines two existing radial gates and a new PKW unit installed on the narrow crest of the dam. It can discharge $300 \text{ m}^3/\text{s}$. Beyond the 30% discharge increase, it significantly improves dam safety level especially in case of gate dysfunction and common mode.

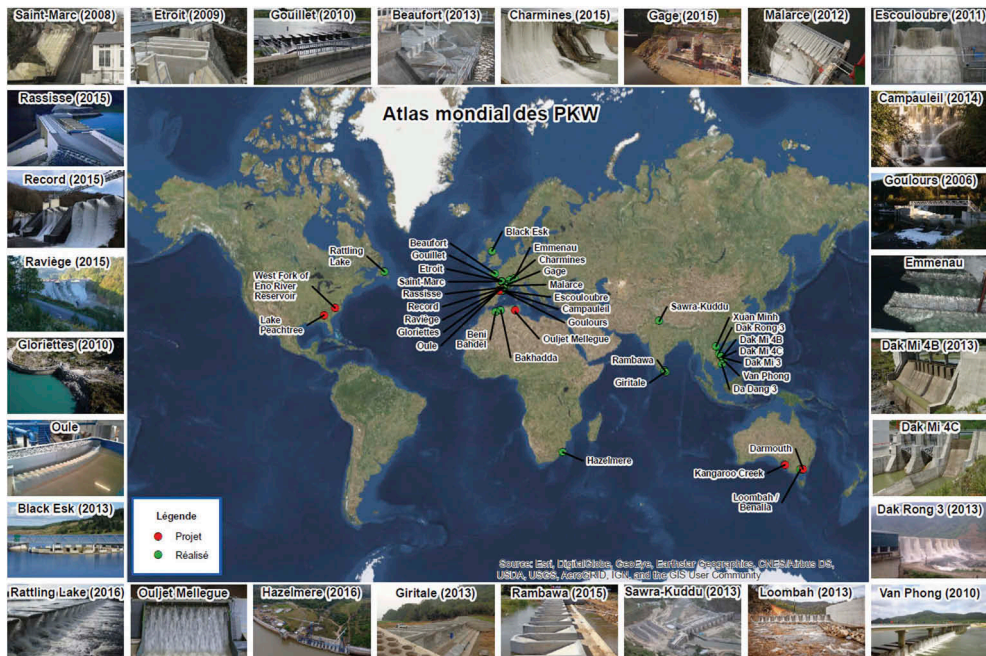


Figure 1. PKW worldwide in 2017 – See also https://www.uee.uliege.be/cms/c_5026433/en/world-regis-ter-of-piano-key-weirs-prototypes.

2 LA RAVIEGE DAM – IMPROVEMENT OF AN EXISTING LARGE DAM

2.1 General

La Raviege dam, operated by Electricité de France (EDF) is a gravity buttress dam 40 m high.

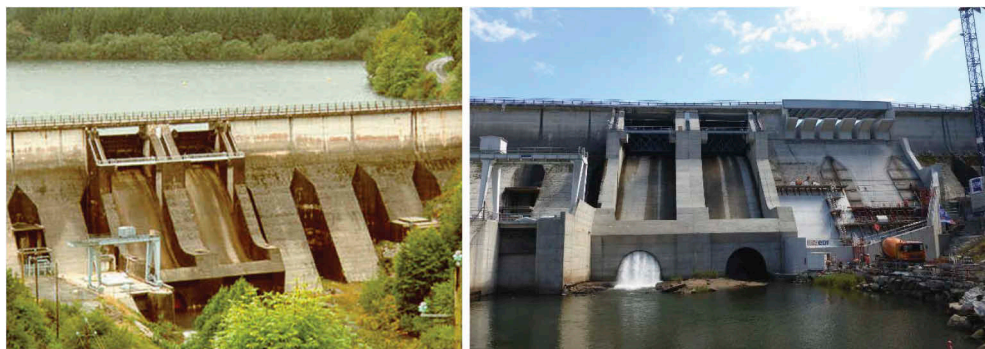


Figure 2. La Raviege dam before a), and b) during the construction of the PKW.

The release capacity of the two existing gated spillways, located in the centre of the dam, is 1 000 m³/s under the reservoir Maximum Water Level (MWL). Recent update of the hydrology calculations of the dam catchment area revealed new extreme floods. The design flood peak discharge has been raised from 1 000 m³/s to 1 720 m³/s and a project aiming at increasing the dam safety has been studied.

Most of the solutions to face safely the new extreme floods combine the use of the reservoir storage capacity and an additional spillway on top of the dam. Following technical and economical studies including safety considerations, the new spillway has been designed as a free overflow one. Finally the chosen solution consists of creating an additional structure on the left bank of the dam: this free surface spillway of the Piano Key Weir (PKW) type consists of 4 inlets, 5 outlets and 2 narrower closing inlets at each end. Considering that the existing gates will first operate, the new PKW will start to operate for major floods with return periods larger than 50 years.

The creation of the new PKW significantly improves the safety level of the dam:

- The PKW constitutes a new autonomous spillway whose failure rate is close to zero and the risks associated with the failure to open a gate will therefore be reduced thanks to this new PKW.
- With the consideration of a free space of 2 m above the PKW, the passage of floating debris during high flood will be improved

2.2 Main features

The PKW project combines the two existing radial gates and a new PKW spillway installed on the narrow crest of the dam. It can discharge 300 m³/s. Beyond the 30% discharge increase, it significantly improves dam safety level especially in case of gate dysfunction and common mode failure.



Figure 3. a) the hydraulic model, b) during the construction, c) end of works.

An hydraulic model Erpicum (2011), was made for the detailed design phase to study several configurations. This model allowed the three following elements to be determined:

- Optimisation of the PKW flow rate by adapting its geometry,
- Definition of the stilling basin design to guide the flow to the chosen zone downstream,
- Checking the impact of the PKW's flow on the flow of the two gated spillways.

The PKW has a height of 4.22m, a global width of 25.82 m and occupies the top of a little bit more than two blocks of the dam. Its crest is at the Full Supply Level (FSL). The weir



Figure 4. End of construction.

developed length is 176.6m. The energy dissipation structure has been designed as a converging smooth channel with varied slopes and downstream deflectors (Figure 4).

The final design of the flood control structures enables to maintain the FSL at its current elevation while releasing the updated design flood with a reservoir elevation 1.41 m above this normal level. In that case, peak discharge on the PKW is 300 m³/s and 1 100 m³/s through the gates fully opened.

Huge works were necessary to build this new structure on the top of the existing dam: 1000 m³ of dam concrete were demolished, the new spillway was built as well as a new road bridge over the crest of the dam, and a stilling basin to protect the structure's downstream toe and guide the flow.

Treating the contact between the old and new layers of concrete and the continuity of the dam block joints in the PKW are two important issues in ensuring the safety, stability and watertightness of this new structure and therefore its durability.

During this work, safety issues related to the management of reservoirs and in particular the routing of floods were essential, so the deconstruction works during seasonal floods were carried out with great care.

The total cost of the project was less than 5 M€ (including the new bridge, the dam retrofitting and the downstream structures) but the cost of the PKW was only 1.2 M€.

3 THE VAN PHONG RUN-OFF RIVER DAM – NEW SMALL DAM

3.1 *General*

The Van Phong barrage, Ho Ta Khanh (2013) & Dinh Sy Quat (2017), is about 70 km from Quy Nhon. The dam derives the water through a main canal for irrigation by gravity of 10 815 ha in the plain near the ocean. The reservoir FSL is determined by the highest possible entrance canal level and the MWL must avoid large inundated zones upstream with probable huge resettlement issues.

Among the 3 alternatives examined (Figure 5) in order to maximize the FSL and to make this scheme possible:

- Alternative 1: a barrage with 28 slide gates,
- Alternative 2: a barrage with 28 radial gates,

- Alternative 3: a combination of 60 PKW units on the Left Bank and Right Bank, and 10 radial gates (H= 3.5 m, L= 15 m) in the central part, this alternative was found as the most appropriated for the cost and the dam safety.

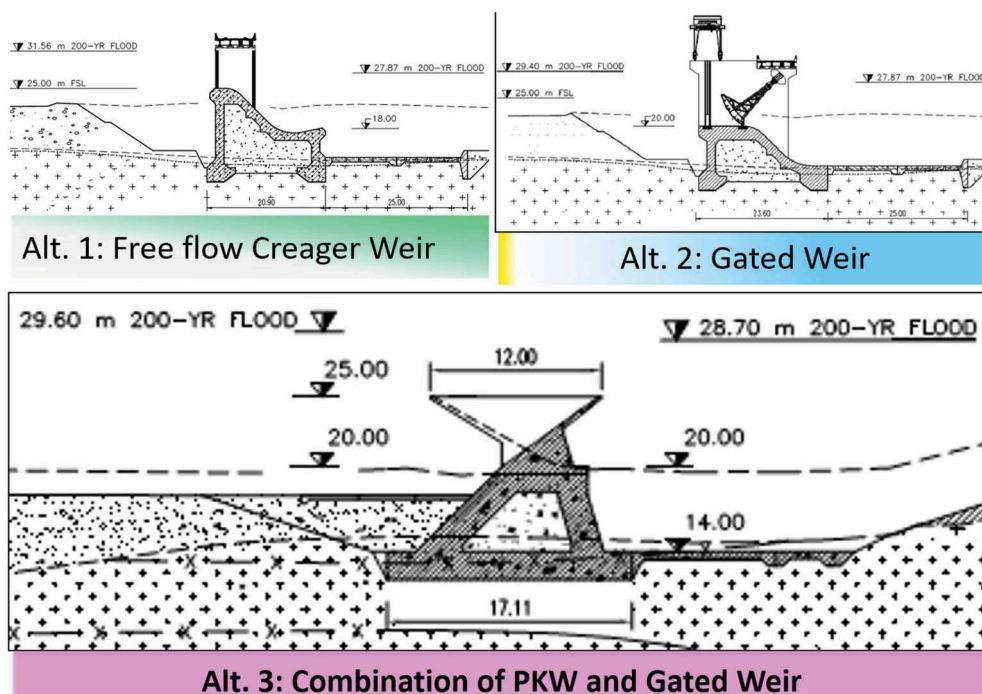


Figure 5. Comparison of 3 Van Phong alternatives at the feasibility stage.

To note that a minimum of gates is necessary to lower the FSL if necessary and to evacuate the sediments. In the case of the Van Phong barrage, this minimum is found inferior to 10, but this last number was retained with caution.

The table below shows a very significant investment cost saving for the Alternative 3, but this advantage is definitely greater if the operating and maintenance costs and the safety of functioning are taken into account in this comparison.

Table 1. Cost comparison of 3 Van Phong alternatives at the feasibility stage.

		Cost estimates in 10 ³ USD 2017		
Items		Alternative 1 with 28 slide gates	Alternative 2 with 28 radial gates	Alternative 3 with 10 radial gates + PKW
1	Civil works	24 000	24 000	20 000
2	Mechanic & Electric- Electronic Equipment	10 000	8 500	3 000
3	Project Management	350	350	250
4	Consultancy Service	750	750	600
5	Others	500	500	550
6	Contingencies	3 500	3 400	2 400
7	<i>Total</i>	<i>39 000</i>	<i>37 500</i>	<i>26 700</i>



Figure 8. a) and b) Hydraulic model tests for submerged flows.

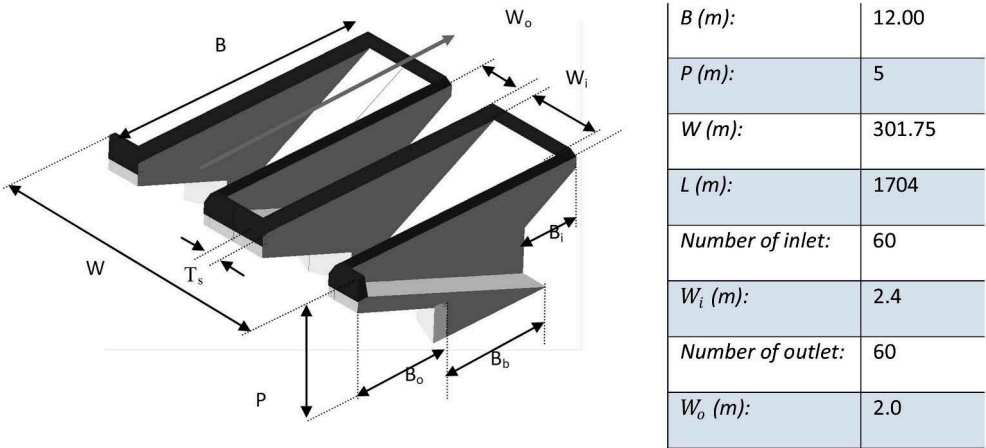


Figure 9. Main dimensions of Van Phong PKW units.



Figure 10. a) View of Van Phong dam barrage with the FSL, b) During construction.



Figure 11. View of Van Phong dam during a low overflow.

The water-surface profiles for the alternatives totally-gated or with PKW are very similar upstream to downstream. This shows the very good hydraulic behaviour of the PKW for submerged flows and the efficiency of the PKW for evacuating the floods with a limited raising of the upstream water level (Figure 13), Ho Ta Khanh & al. (2017).

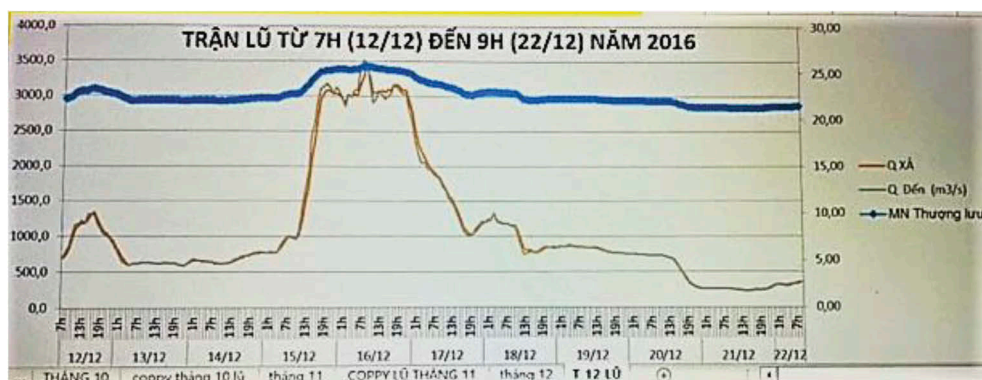


Figure 12. Maximum discharge and water level during 16th December 2016 flood.



Figure 13. Photos a) U/S and b) D/S) of the 16th of December 2016 flood on the PKW .

4 CONCLUSION

A PKW solution has been designed at existing La Raviege large dam to increase the dam safety towards extreme floods.

This example shows that with a PKW, a significant increase in the capacity of an existing spillway thanks to a new one placed on a short available length of the dam crest is possible. This solution has the advantage of being highly reliable and significantly improves the overall dam safety level especially in case of gate dysfunction. In addition, it requires a minimum of the operating and the maintenance of the structure. The feedback from other PKWs built at EDF facilities in France since 2006, Laugier & al. (2015, 2017), was used to build this new PKW. The methods, equipment and tools have improved and have been adapted to ensure the safety of the workers and faster execution.

The configuration is quite different for new Van Phong run-off river smaller dam (Vietnam). The new solution is a combination of gates (one third of dam length) and PKW (two thirds of dam length). Such a combination has many advantages for a long barrage in terms of costs for investment and operation and safety during high floods. When performing dam safety risk analysis, the combination of gates and efficient free flow spillway such as PKW, shows a significant increase of the overall dam safety level and a substantial improvement of dam failures modes and decreasing failure probabilities regarding flood situations.

The proposed hybrid solution of (PKW+Gates), compared with a traditional barrage, shows that the choice of a site, even with a broader stretch of the river, may be the best solution.

REFERENCES

- Dinh Sy Quat, Nguyen Luong Am, Nguyen Manh Hung. 2017. Study, Design and Construction of the Van Phong Piano Key Weir. International Workshop on Labyrinth and Piano Key weirs, Qui Nhon, Vietnam. *Labyrinth and Piano Key Weirs III – PKW 2017 – Erpicum et al. (Eds) © 2017 Taylor & Francis Group, London, ISBN 978-1-138-05010-5*.
- Erpicum, S., Laugier, F., Nagel V. 2011. “PKW design optimization at Raviege dam”. *International Workshop on Labyrinth and Piano Key weirs*, Liège, Belgium.
- Ho Ta Khanh, M., Truong Chi Hien, Pinchard, T., Pralong, J., 2013. “Utilization of Piano Key weirs for low barrages”. *International Workshop on Labyrinth and Piano Key weirs*, Paris, France.
- Ho Ta Khanh, M., Hai Nguyen Thanh & Thang Tang Duc, “Research on Piano KeyWeirs capacity for free and submerged flows”. International Workshop on Labyrinth and Piano Key weirs, Qui Nhon, Vietnam. *Labyrinth and Piano Key Weirs III – PKW 2017 – Erpicum et al. (Eds) © 2017 Taylor & Francis Group, London, ISBN 978-1-138-05010-5*.
- Laugier, F., Vermeulen, J. – “Lessons learnt on Design and Construction of Labyrinth Piano Key Weir (PKW) Spillway for a large set of dams: Specific cases and research actions” - 2015 – *ICOLD 25th Congress – Stavanger – Q97*.
- Laugier, F., Vermeulen, J. & Blancher, B. “Overview of design and construction of 11 Piano KeyWeirs spillways developed in France by EDF from 2003 to 2016 - *Labyrinth and Piano Key Weirs III – PKW 2017 – Erpicum et al. (Eds) © 2017 Taylor & Francis Group, London, ISBN 978-1-138-05010-5*”.

Enhancing dam safety through contractual strategies

M. Lino

Dam Expert, ISL Ingénierie, Ciboure, France

Stéphane Giraud

Contract Specialist & FIDIC, Adjudicator, Mauguio, France

Luciano Canale

Project Director, SCATEC, Naples, Italy

Bettina Geisseler

Lawyer, Founder of GEISSELER LAW, Freiburg i.Br., Germany

ABSTRACT: Dam safety is crucial to successfully ensure the long-term sustainability and the multiple benefits of a dam project and is the primary condition for its acceptance by civil society.

Dam failures worldwide continue to be too numerous, and the International Commission on Large Dams (ICOLD) has recently issued a “World declaration on Dam Safety” [1] and declared dam safety the highest priority of the organization.

The paper looks into dam safety aspects in different phases of the project life cycle and from different stakeholder perspectives, and analyses dam failure records to understand where gaps can be found for the construction of a new dam or the rehabilitation of an existing dam. The statistics on dam failure clearly indicates where corrective measures have to be taken and drives the authors in formulating a set of recommendations, based on their long experience and complementary expertise, to help dam owners, developers and lenders to better address dam safety in their projects. The authors finally analyse the link between dam safety issues and contractual strategy, in order to propose an enhanced contractual and organisational set-up in dam development.

1 INTRODUCTION

ICOLD recently issued a bulletin on statistical analysis of dam failures, i.e. Bulletin 188 [2]. When a problem occurs in a dam project, the first task is generally to determine whether its cause is related to a faulty design, poor quality in construction or insufficient operation and maintenance. The available data clearly shows that the first causes of dam failure are attributed to faulty and insufficient design; related in most cases to geotechnical issues, as presented in the following Figure:

Most of the failures on dams built in the 20th century and all failures of dams built after the year 2000 occurred during the 5 first years after construction, as the following examples of historical and recent accidents show: the Malpasset Dam (France; failure in 1959), the Teton Dam (USA; accident in 1976) and the more recent incidents or failures of Hydro Ituango (Columbia; 2018) and Xe-Pian Xe-Namnoy (Laos; 2018). These cases clearly show, that though the necessary conclusions have been drawn after analyzing the historical failures, there is still a lot to do.

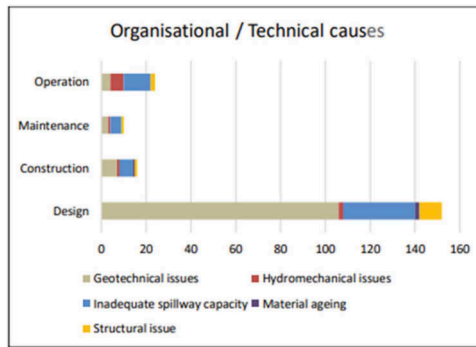


Figure 1. Organisational vs. Technical causes of dam failure. Source: ICOLD Bulletin 188 [2].

2 PAST AND PRESENT EXPERIENCES - DAM SAFETY REGULATIONS & POLICIES

2.1 *National dam safety regulations, the state of art requirement and internationally accepted best practice*

An extensive review of the dam safety regulatory framework in 51 countries, estimated to account for more than 95 percent of the ICOLD's register of world dams, has been carried out by the World Bank in 2018 [3]. The majority of the developed countries' members of ICOLD have established during the past decades comprehensive Dam Safety Regulations, which unfortunately is not the case in developing countries, even in those where large or mega projects are currently being designed and constructed.

In any dam project during the whole life cycle any party involved such as the future owner/operator, the designer or the contractor must comply at any time with the existing national regulations reflecting the binding regulatory framework. This also applies for the the state - of - the - art - requirement, reflecting the generally accepted good practice.

The National Dam Safety Regulations generally provide minimum design criteria to be adopted to ensure dam safety. Often those state laws request not only the compliance with the basic design criteria, including safety factors to achieve in various load conditions, return periods for design floods, seismic loadings to be considered, etc., but they stipulate additionally procedural rules to be observed such as the report of an independent expert engaged by the owner to verify the dam stability in predetermined regular intervals.

2.2 *Norms issued by national or international norming associations or other standards*

Whereas it is compulsory to comply with the national regulatory framework in place in the country where the dam will be/is located, this is not the case with regard to (sometimes more stringent) norms of private norming associations even though these standards might have a high reputation and acceptance in the dam industry. Examples are the DIN norms or ICOLD Bulletins, or norms of national COLDs such as the CFBR (French National Committee of ICOLD) Guidelines, British standards or USBR Guidelines, which all are not legally binding. As those norms are not part of the state laws, their application has to be agreed upon in the construction contract in order to be binding for the contractor.

It must also be noted that ICOLD Bulletins, which are essential sources of international state of the art in the dam industry, are in general not prescriptive documents and reflect the variety of practices all over the world. Their purpose is to establish, on different subjects, an international state of the art based, as much as possible, on worldwide knowledge and lessons learned from the dam industry. However, a particular challenge with dam design is that it is not possible to rely only on regulations, laws or codes. Norms and state of the art can guide the designer, but in the end the design shall involve a significant part of technical experience and engineering judgment.

2.3 *The Lender's interest, in particular the World Bank policy and the Dam Safety Panel of Experts*

Lending institutions (IFIs) have a vital interest that during the construction, erection, rehabilitation or operation of dams financed by them high and suitable safety standards are observed. Otherwise, they might be faced not only with a huge reputational, but as well with a tremendous financial damage. Thus: in countries, without a strong dam safety framework the observance of internationally accepted high safety standards is often imposed by the international lenders; the compliance to their dam safety requirements being a compulsory milestone in the financing agreement.

Additionally, the establishment of an independent Panel of Experts might be requested. The World Bank (WB) has led the way among development banks in raising dam safety standards by introducing in 1977 the policy Operational Manual Statement 3.80 "Safety of Dams", replaced in 2001 by the policy O.P. 4.37 [4], and superseded in October 2018 by the ESS4, Annex 1 [5], whose compliance is included as a condition in the implementation and financing agreements for all dams classified as "large". The policy is part of the wide range of safeguard instruments and calls for an "Independent Panel of International Experts in dam safety" with the responsibility of reviewing the investigation, design, and construction of the dam, including review of the four detailed dam safety plans to be prepared by the borrower as per the policy requirement, namely: (i) Construction Supervision and Quality Assurance plan, (ii) Instrumentation plan, (iii) Operation and Maintenance plan, and (iv) Emergency Preparedness Plan. The Panel reviews and advises the borrower on matters related to dam safety and other critical aspects of the dam project. The Dam Safety Panel of Experts (DSPoE) usually consists of three or more experts (e.g. dam specialist, a geological/geotechnical expert and a hydrologist), appointed by the borrower and acceptable to the WB, with expertise in the various technical fields relevant to the safety aspects of the particular dam.

After a few decades of application on more than 400 dam related projects funded WB, the DSPoE has proven to be a valuable technical resource for borrowers and their projects. To date no major failures or accidents have been recorded in WB funded projects for construction of new dams and rehabilitation of existing dams during their project life cycle.

3 THE ROLE AND TASKS OF AN INDEPENDENT EXPERT

3.1 *Reasons to engage an independent expert*

The dam failure cases investigated by the authors show how important the involvement of a body of independent experts within the project might be. These bodies, such as the DSPoE, can be nominated (as the case may be, upon request) by the project owner, a developer, the lender, a state authority in charge of supervising a dam or a private concessionaire.

Ensuring independency in the Panel's opinions, is a key aspect. Independency means that the expert is in the position to give his advice without being influenced by an interested party to the project, such as the owner and operator of the dam, the Engineer or the contractor. The monitoring and supervision of the behaviour of small or large dams starting from the planning and design through the construction phase will be (as provided for in most legislations) primarily the responsibility of the owner/operator of the dam. Even in countries where the regulatory framework doesn't call for the engagement of an independent expert, an owner/operator being responsible for the dam's safety should carefully evaluate whether he has the necessary inhouse expertise to assess the safe behaviour of the dam, or better should rely on the advice of an external expert.

3.2 *The tasks, rights and obligations of an independent expert*

The tasks and obligations of the dam safety expert will usually be defined by the contract through which the nominating party entrusts and mandates the expert to give his advice. The rights and obligations of the expert result directly from that contract and are described in its terms of reference, complemented by the law governing the contract.

A Panel or an expert acts like any other consultant or service provider, similarly to a technical advisor or an “Owner’s Engineer”. He/she must render his/her services within the defined scope of works and according to the terms of reference of the nomination contract with due care and diligence and will be fully liable if he neglects his duties. Considering that full liability means the obligation for compensating all damages resulting from his advice in case of an at least negligent breach of his obligations, the authors strongly advise the expert to contractually limit his liability amount (e.g. to x-times of the fees) and to try to exclude liability for normal negligence and (if possible under the applicable law) for gross negligence of the mandate. The liability for damages to life and physical property of third parties as well as for intentional breach of contract can never be excluded. It is the expert’s interest to subscribe a corresponding insurance covering his professional liability. This liability aspects are not always dealt with in dam safety panel contracts.

3.3 *Recommendation vs. legally binding opinion: How to impose the expert’s advice*

As observed in the case studies, one of the dam safety risks might result from the fact that the nominated expert often is engaged by the owner either upon request of lending institutions or upon his own interest. In this case he has no direct contractual relationship with the party (e.g. the contractor) who should follow the expert’s advice, and thus he cannot (unless additionally agreed upon in the construction contract) directly impose his recommendations on this party. Therefore, an owner being advised by an expert, has to either reserve the right to give instructions to contractors or will initiate “Variation orders” following the expert’s recommendation or directly impose by contractual means the DSPoE’s advice on the contractor.

The compliance with the expert’s advice might result in higher costs for the project execution or have consequences on the time for completion. It is therefore important that the construction contract properly allocates the (financial) risk if compliance with recommendations by a DSPoE leads to additional construction costs and an extension for the time for completion. The DSPoE recommendations should be recorded accordingly.

The authors are convinced that in well-defined cases it might be necessary to provide for strictly binding recommendations of the expert, which contractually means that the engaging owner himself is as well obliged to follow the expert’s advice.

3.4 *The independent expert in public vs. privately developed projects*

Dam safety should be addressed the same way irrespective of the source of fundings or the nature of the developer, whether a private entity and/or an investor as owner/operator or state owned company. But it can be observed that Dam safety standards and guidelines may also differ for public and private projects. In developed countries dam safety standards are usually well established, they correspond to national regulations or more stringent requirements, and any public or private owner must comply with them as far as they are legally binding or contractually agreed upon. In countries where a dam safety framework doesn’t exist, the Private sector usually adopts IFC Performance Standards (PS) or equivalent, whereas public sector infrastructures are implemented by using WB Environmental and Social Standards. Dam safety in IFC PS package is covered in PS1 “Assessment and Management of Environmental and Social Risks and Impacts” which calls for an independent review by one or more experts not associated with design and Owner’s engineering services. The WB has recently issued guidance notes [6] to help borrowers better understand the application of the dam safety policy, including how to address differences between private and public sector projects.

4 DAM SAFETY FROM DIFFERENT STAKEHOLDERS’ PERSPECTIVE

4.1 *From the Employer/Owner/Operator’s perspective*

As mentioned, the employer/owner (being a privately owned company or the state or a public-private partnership) of a dam and the operator of a dam (if it is separate from the owner) are ultimately responsible and liable for dam safety aspects during design, construction and operation.

Therefore, it is of utmost importance that a robust national dam safety framework is in place and applicable. But even in the absence of a detailed and compulsory national dam safety framework it will not only be at the employer's and operator's own discretion to strictly follow well established international standards; but the authors strongly advise the employer/owner/operator to do so and to ensure that the engaged contractor and/ or designer does the same. As mentioned, non-binding standards – in case of absence of a robust national regulatory framework or being more stringent - become only binding, if referred to as the contractor's obligation in the construction contract. A DSPoE will be certainly able to guide/advise the employer/owner in making the right technical choices. An early involvement of a DSPoE /a dam safety expert (if necessary together with a legal expert) from the beginning of the project development, to advise on the design and the contractual strategy or on the dam safety standards to include in the Employers' Requirements of the construction contract, is certainly desirable.

4.2 From the designer's perspective

When the dam designer is employed by the contractor in case of a Design-Build contract (e.g. the FIDIC Yellow or Silver book with lump sum (EPC) and the contractor being responsible for the design), the dam designer is sometimes in an awkward position; the project bankability and the objective of achieving the best competitive bid leads to a search for savings. On one hand the dam designer must respect the dam safety requirements, and on the other hand there is the risk that the contractor is requesting him to find ways of saving money. This is a common problem of all designers working as sub-contractors for the contractor. Legally speaking, the designer must diligently perform his work, otherwise he might be held liable in case of dam failures and/or damages towards the contractor and potentially other third parties. However, the subcontracting condition of the contractor's designer may put him into a difficult position, being confronted by requests from the contractor to save money, even though it is clear that the employer may not optimize his budget by sacrificing safety issues. He must resist those requests if they would lead to a design which does not respect adequate safety considerations. The situation might be different, when the designer is engaged by the employer in case of more traditional design-bid-build procurement strategy with a traditional construction contract e.g. the FIDIC Red book with Bill of Quantities. As consequence of the tendency to adopt a design-build scheme through EPC contracts dam designers, little by little, have lost their predominant role as designer for the employer. This might result in a deteriorating quality of the design when the contractor puts pressure onto the designer. Then obviously, this may badly impact dam safety aspects.

4.3 From the Contractor's perspective

Respecting dam safety aspects should be as important for the contractor as it is for the employer and for other stakeholders such as investors. Because of budget restrictions and the tender competition, there may be certain risks that contractors may be tempted to shift focus on short-term objectives such as budget limitation and completion time. If within his scope of works the contractor is responsible for the design, he bears the full responsibility even if he has subcontracted the works to a designer. In any case he should resist any temptation to sacrifice safety considerations for cost savings. As to the dam safety requirements, it may be an interesting way to involve the contractor at the outset of the project. In that case (Early Contractor Involvement), the consistency of the project and the adherence to dam safety requirements may be improved while the competition among the contractors may be maintained.

4.4 From the Financier/Banker/Insurer's perspective

Development banks, International Financial Institutions (IFI), public and private, have fully understood the importance of adopting adequate dam safety standards in the projects they finance. The potential hazard to the downstream communities with the risk of loss of life of people and their property, the high reputational risk and the financial consequence of a dam

failure and the awareness of risks due to faulty design, construction and erection or inadequate operation are enough reasons for them to prescribe enhanced dam safety requirements in their financing and loan agreements.

The insurance sector is one of the largest industries of the world. Insurance mechanisms can play a beneficial role and contribute to regulatory form of supervision of dam safety management when insurance premiums are linked to the level of dam safety being provided for dams.

5 DAM SAFETY ACROSS THE PROJECT LIFECYCLE

5.1 *Dam safety issues during preparation and procurement*

Dam safety requirements have to be captured in the whole process starting from site investigations, over the early stage of studies (preliminary design) and structuring of the financing. Some IFIs, such as WB, have established their dam safety policy including a set of the dam safety requirements considering type of interventions, potential risk of dams, complexity of projects, and so forth, which would require the early mobilization of the DSPoE and support the preparation of the dam safety plans and setting adequate design criteria for ensuring the safety of dams and downstream communities. Projects where the DSPoE has been mobilized only after validation of the studies have suffered delays in closing financing due to rediscussing of fundamental technical decisions not pre-scrutinized by the Panel.

Before entering into the tendering and procurement phase the suitable contractual strategy and the project set-up must be defined: Turnkey contract vs. multicontracting and a “Design-Bid-Build” (FIDIC - Fédération Internationale des Ingénieurs-Conseils - Red Book), or the “Bid-(Design-)Build” (Yellow or Silver book) delivery method? These two questions are fundamental having implications on dam safety requirements. In the case of a “Design-Bid-Build” scheme, all the dam safety requirements should be reflected by the designer hired by the employer before tendering for the construction contract or other dam safety associated works. The dam design criteria should be established prior to the tender and comply with the national regulatory framework, the dam safety requirements required by the employer and take into account the state-of-the-art requirement as well as well proven international guidelines such as the ICOLD bulletins.

In the case of a “Bid-(Design-)Build”, all the dam safety requirements should be strictly mentioned in the Employer’s Requirements (including norms and ICOLD Bulletins to be referred to) of the construction contract. In both cases, mobilization of the DSPoE in due time, at least before tendering, would allow the Panel to review the dam safety requirements including norms, standards and guidelines that will form part of the construction contract.

Another common issue that materializes during procurement is the lack of coordination and communication between the legal and technical teams the employer is using to prepare the tender. Often, the legal team is focusing mainly on the body of the contract with the General and Particular Conditions of Contract including the financial schedules, the insurances and other commercial provisions. The technical team is focusing on the technical specifications, the design requirements and other technical annexes such as the guaranteed performances or milestone plan. This gap must be filled by more collaborative works, as there is an interdependence between the different parts of the construction contract, which often cannot be understood in isolation e.g. the technical prerequisites and legal consequences of the performance guarantees.

There may be some gaps or even contradictions in different parts of the contract. A cross-check and final choice has to be made as to the priority of the contractual documents to ensure that the contract documentation is consistent and the dam safety requirements are without any legal ambiguity. A final legal review will be required to check the compliance with the law applicable to the construction contract (which is not necessarily the law of the country in which the project is constructed but can be chosen by the contractual parties).

5.2 *Responsibility for dam safety during construction and allocation of risks*

Depending on the delivery method the parties have chosen, the responsibility for the design and thus for safety considerations will a priori be with the employer or the contractor

respectively designers engaged by either of them, even though the ultimate responsibility for dam safety must be assumed by the owner and operator. The contractual parties can choose a Model Agreement such as the FIDIC Red, Yellow or Silver book or other Model Agreements such as the NEC or ICC Standard Forms of Contract. Of course, the parties are free to choose a specifically drafted contract or should, if necessary, modify a Model Agreement. They should evaluate whether the issue of any differing site conditions, such as adverse geological conditions, and which party bears the related financial risk and the consequence of a potential delay, is properly addressed in the Contract. Important is to allocate the risk of unforeseen events such as differing site -, in particular underground conditions to one party, who in case that the risk materializes then has to assume the financial consequences as well as the consequences on the time for completion. In the last years so – called Alliance agreements have been developed according to which both parties share the risk totally or above a certain threshold.

Regardless of the method of delivery respectively the contractual strategy the owner chooses Quality Assurance during the whole construction and erection phase is crucial. Usually, the Employer's requirements request from the contractor to set-up a Quality Assurance Program (QA) to be approved by the employer and then strictly respected by the contractor. Additionally, the employer (owner) can reserve himself ample inspection -, approval - (design drawings, engagement of subcontractors etc.) and instruction rights. Depending on the chosen contractual agreement the employer will be supported by an owner's engineer cross – checking the contractor's design and supervising the execution of the construction works. A DSPoE will help the owner to ensure compliance with safety regulations and standards.

5.3 *Dam safety issues during operation*

During testing and the initial operation and maintenance (O&M) period, the interface between the civil works (CW) contractor and the electromechanical (E&M) or hydromechanical (H&M) contractor shall be properly managed. At the time of taking-over and first filling of the reservoir to allow wet tests and early operations the consequence of a dam safety non-compliance may be difficult to determine if it affects both lots and the liability aspects are not cross-referenced and linked between the two contracts. This has to be clearly scrutinized at the time of the tender in order to avoid an ambiguous situation. As observed from the case studies and discussed above, the initial filling and the first 5 years of operations have demonstrated to be critical when it comes to dam safety. The Defects' Notification Period of contractors usually ends 12 to 24 months after completion of the works. Sometimes their liability is lifted even before the reservoir is completely filled. The handover of the dam with all safety requirements and procedures demands more time and requires a proper program of knowledge transfer to the dam operator. Often these aspects are left behind and in many cases the dam operator starts his mandate unprepared.

6 POTENTIAL CONTRACTUAL SOLUTIONS TO CLOSE DAM SAFETY GAPS

6.1 *The FIDIC contract environment*

Contractual solutions must be found within the existing contractual framework that is most adopted by the industry. Since 1957, FIDIC has edited several standard construction contracts, broadly used for the last 60 years in more than 150 countries.

Newly developed is the Emerald Book Ed. 2019 [7], under which the geological baseline can be reviewed during construction, accepting variation for new quantities due to the new site conditions to be paid on unit prices pre-agreed in the so-called "Schedule of Rates and Prices" and "Schedule of Baseline" and allowing the contractor, once the updated design is approved by the Engineer, to be compensated in case of differing site conditions. This useful contractual tool avoids lengthy discussions/claims/disputes from occurring in the course of the project.

6.2 *Definition of a robust geological and the hydrological baseline and extending the liability period*

The main construction risks identified as dam safety risks above are (i) geological risks (such as unforeseen ground conditions) and (ii) hydrological risks (such as flooding during and after construction) [2]. To allocate these two risks and to determine differing site conditions it is recommended to establish in the project preparation phase a clear baseline through a report containing assumptions on the main parameters and their interpretation for design; this is the so-called Geotechnical and/or Hydrological Baseline Report (GHBR), which will not only define site conditions, but as well the design flood and the threshold beyond which the responsibility to fix any damages caused by hydrological conditions at site move from the contractor to the employer.

In addition, the authors believe that the situation could be significantly improved by (i) increasing the period of responsibility of the Engineer and/or contractor for monitoring the dam behaviour after completion and (ii) extending the initial Defects' Notifications Period (DNP)/warranty period for the dam contractor by increasing it from the usual 2 years (while FIDIC recommends 1 year by default) to 5 years as the majority of the failures observed occurred in the five first years. The dam contractor's liability will be lifted (partially in some cases, as some legal liability may still apply) after all the dam components are finally approved and accepted.

6.3 *The evolving role of the Dam Safety Panel of Experts*

Fortunately for Dam Safety, the appointment of a DSPoE is now good practice in dam projects from the beginning of a project (preliminary studies). In the past years, it had been observed that the implementation of a DSPoE enhances the safety and quality of IFI funded projects. It involves safety in coordination with the employers, engineers, and ultimately contractors in a professional manner.

In dam safety matters, the cost and time implications of a DSPoE recommendations can be substantial. Therefore, there is a need to improve the contractual mechanism to address and implement in a more simple and direct way the independent opinions of the Dam Safety Panel. The role, scope and terms of reference for the Panel shall better fit into the contractual framework in which the other stakeholders operate. To fill this "contractual gap", the authors suggest different adaptations to the usual scheme by:

1. Adding a new role of the DSPoE, on top of its usual "review and advise role" during the project life. Essentially, the authors propose an evolving role of the DSPoE during the different phases of a project life cycle, where the DSPoE has capacity to issue binding instructions during construction on very technical and specific issues concerning Dam Safety (e.g. recommending not to reduce a freeboard against flooding, to treat a geological fault with special concrete filling, not to undersize the diversion scheme/system, not to excavate during heavy rain season, etc.), to be given to the Employer, and then to be transferred to the Engineer for their implementation.
2. Therefore, for this new DSPoE role, the following bodies should be appointed:
 - During the preparation phase, a DSPoE 1 for the independent design review at different milestones such as feasibility, basic design (incl. design criteria) for D&B, detailed design (for Red Book scenario) and tender.
 - During the construction phase, a DSPoE 2 (with same members from DSPoE 1 or new members) for technical design review, supervision of the works executed including commissioning and of the Provisional Acceptance Procedure including the impounding.
 - During the O&M operation phase a DSPoE 3 (with same members from DSPoE 2 or new members) for reviewing and auditing the dam behaviour and the dam safety procedures (with inspections at least every 6 months for the most critical first 5 years).
3. Adding the DSPoE new role, its rights and obligations in the construction contract and the provision that the DSPoE may issue binding instructions to the employer as to dam safety

requirements in circumstances to be detailed by the project. This is to keep the contractor continuously informed.

4. Ensuring that the binding recommendations of the DSPoE are well-recorded, so that in case of a dispute between one contractual party the dispute can be referred to either a Dispute Adjudication Board (DAB) or an Arbitration Tribunal respectively the competent state court.

7 CONCLUSION

All involved (contractual) parties should pay highest attention to safety considerations throughout the whole project life from the early research for suitable sites and the tendering/ procurement process throughout the construction/ erection phase and the first filling up to the operation of the dam. An adapted contractual strategy, the extension of the Defects' Liability Period and the establishment of a DSPoE advising the owner/stakeholders with decisive power in some limited cases related to dam safety will have a considerably positive impact on dam safety.

ACKNOWLEDGEMENT

The article is based on an article published in the issue 2/2023 of the international Journal on HYDROPOWER & DAMS. But it has been considerably modified for the ECS 2023 in Interlaken.

REFERENCES

1. ICOLD, World Declaration of Dam Safety, October 2019.
2. ICOLD, Bulletin 188 - Dam failure statistical analysis, 2021.
3. World Bank, "Laying the foundations", 2018.
4. World Bank, Operational Policy 4.37, 2010.
5. World Bank, ESS4-Annex1 on Dam Safety Panels, 2018.
6. World Bank, Good Practice Note on Dam Safety, April 2021.
7. FIDIC, Conditions of Contract for Underground Works (Emerald book), Edition 2019; see also www.fidic.org.

Risk management for the Lago Bianco reservoir in case of a rupture of the Cambrena glacier

J. Maier

Wettingen, Switzerland

R. Baumann

Rebau Engineering Ltd., Poschiavo, Switzerland

H. Stahl

AFRY Switzerland Ltd., Zurich, Switzerland

T. Menouillard

Swiss Federal Office of Energy, Berne, Switzerland

ABSTRACT: In 2014/15 it was detected that the retreating Cambrena glacier had introduced a new risk to the Lago Bianco reservoir in southeastern Switzerland. A melting glacier tongue could eventually lose its support, rupture off, move as an ice avalanche down to the reservoir and initiate an impulse flood wave with danger of a break of one of the reservoirs two dams. Therefore, the owner of the reservoir established a special emergency preparedness plan, based on two elements: (1) continuous surveillance of the Cambrena glacier by an automatic photographic camera to measure the ice flow speed; (2) lowering of the reservoir in case of a high ice flow speed to a level, which still guarantees the stability of the dam. In case the ice flow speed had increased faster than predicted before the safe reservoir level was reached, the emergency service of the Swiss civil protection would have alarmed the population to evacuate the danger zone. In November 2022 the Cambrena glacier tongue had melted down so far, that an ice rupture would not affect the Lago Bianco dams any more. Since then, the reservoir is back to normal operation.

Keywords: Lago Bianco, climate change, glacier rupture, avalanche, impulse flood wave, dam break, reservoir operation

1 INTRODUCTION

The average annual temperature in Switzerland has increased by 2°C since the start of systematic measurements in 1864. This increase is almost twice as high as for other land areas in the northern hemisphere. Today, the zero degree line in Switzerland is about 350 m higher than 60 years ago. Mainly because of the rising temperature the alpine glaciers melt.

In 2014/15, it was discovered that the retreating Cambrena glacier in southeastern Switzerland had introduced a new risk to the Lago Bianco reservoir: a melting glacier tongue was slowly retreating into a steep rock step and therefore losing its support at the front end and on both sides. According to the glacier specialists, there was a danger for a rupture of up to 1.5×10^6 m³ of ice. The ice rupture could generate a impulse flood wave in the reservoir and cause a sudden dam break. Therefore, the owner of the Lago Bianco reservoir Repower AG had to consider this new danger into his risk management.

2 LAGO BIANCO RESERVOIR

The Lago Bianco reservoir (Figure 1) is located just west of the Bernina pass in southeastern Switzerland, only a few kilometers from the boarder to Italy. The reservoir is part of the water divide between the Mediterranean Sea and the Black Sea. The highest peaks of the eastern Alps (with altitudes around 4000 m a.s.l.) flank the western side of the reservoir. The narrow gauge Bernina railway follows the eastern reservoir shore; the northeastern corner of the reservoir is close to the Bernina highway. Both traffic lines are open all-the-year, except winter days with high avalanche risk. The water stored in the reservoir is used in several power stations to produce electricity.

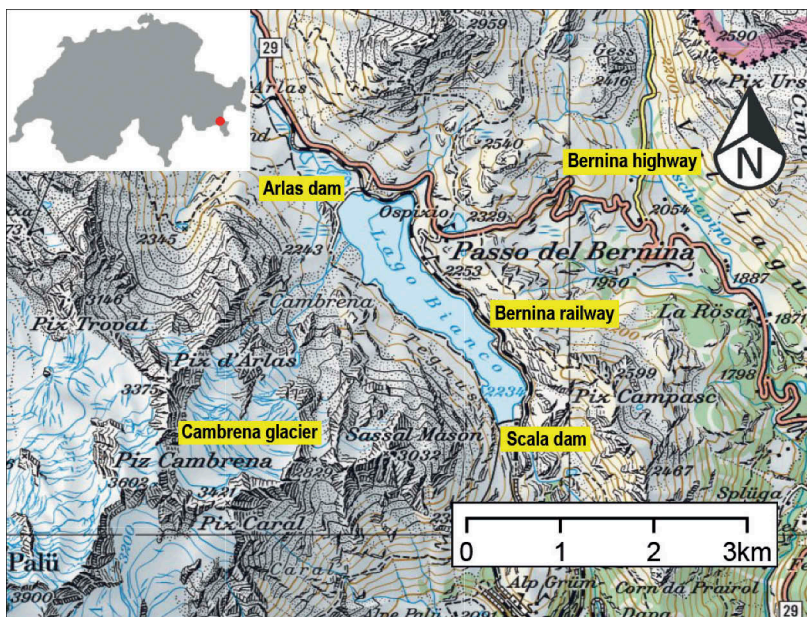


Figure 1. Location of the Lago Bianco reservoir in southeastern Switzerland.

The two dams of the Lago Bianco reservoir, the Arlas gravity dam in the north and the Scala arch-gravity dam in the south, were originally built in 1910–12 with cyclopean concrete. The impounding of the reservoir connected two natural lakes. In 1941/42 the height of the two dams was increased by adding at the crest 4 m of concrete and so enlarging the reservoir capacity. Later on this additional concrete started to show signs of alkali aggregate reaction; furthermore, an incomplete connection between the original and the additional concrete was discovered at the Scala dam. To solve these problems an extensive renovation of the two dams took place in 2000/01. The eastern two-thirds of the Arlas gravity dam were totally demolished and rebuilt with regular concrete above the old foundation. The demolition waste together with fresh rock material was used to cover the western third of the dam. The Scala arch-gravity dam got a shotcrete cover and PP-Dam sealing on the upstream face, a drainage and inspection gallery at the upstream foot, a new concrete crest and a systematic anchoring on the downstream face. Figure 2 shows pictures of the Arlas and Scala dams.

The characteristics of the Lago Bianco reservoir and its two dams are the following:

- Catchment area 10.85 km² (currently ≈15 % covered by glaciers)
- Reservoir area 1.43 km², volume 18.6 × 10⁶m³ and maximum level 2234.65 m a.s.l.
- Arlas dam length 290 m, height 15 m and crest level 2235.75 m a.s.l. (western part 2237.00 m a.s.l.)
- Scala dam length 190 m, height 26 m and crest level 2237.00 m a.s.l.

All outlets are located in the Scala dam. The bottom outlet has a maximum capacity of $6.0 \text{ m}^3/\text{s}$; the intermediate outlet with a base level of 2231.40 m a.s.l. allows a maximum discharge of $24.0 \text{ m}^3/\text{s}$. Flood waters are controlled with a 37 m long overflow section, whose crest is at the maximum reservoir level 2234.65 m a.s.l. The turbination capacity amounts to $4.4 \text{ m}^3/\text{s}$ and $0.75 \text{ m}^3/\text{s}$ can be pumped from the Lago Palü reservoir below. Today, the reservoir is used as a seasonal water storage with the maximum level in autumn and the minimum level in spring.



Figure 2. Scala arch-gravity dam with overflow section (left) and Arlas gravity dam (right).

3 RETREAT OF CAMBRENA GLACIER

During project work for the development of the current seasonal reservoir into a high-capacity pumped storage facility it was detected that the Cambrena glacier presented a risk of rupture of its southeastern tongue. In 2013 the reservoir owner asked glacier specialists from the ETH Zurich to study the situation and give their advice. Their findings (Funk & Bauder 2013) can be summarized as follows:

- Situation in 2013: The Cambrena glacier covers a surface of about 1.37 km^2 and has a volume of $50 \times 10^6 \text{ m}^3$. The current lower end of the southeastern glacier tongue is at an altitude of 2520 m a.s.l. Due to the strong glacier retreat a lake has appeared in front of it. The terrain behind the end of the glacier gets steeper and steeper over a distance of 550 m until a flattening starts at an altitude of 2820 m a.s.l. The inclination below the steep part is at 24° , in the steep part it is at 35° .
- Prognosis of glacier melting: Figure 3 shows the result of model calculations for the ice volume of the Cambrena glacier from 1900 until 2100. Between 1985 and 2008 the volume loss amounted to $40 \times 10^6 \text{ m}^3$ of ice. Furthermore, the diagram shows that the Cambrena glacier is expected to disappear totally between 2050 and 2080. Figure 4 presents the prognosis of the surface covered by the glacier between 2010 and 2050. Around 2025 the glacier is expected to retreat above the steep part.

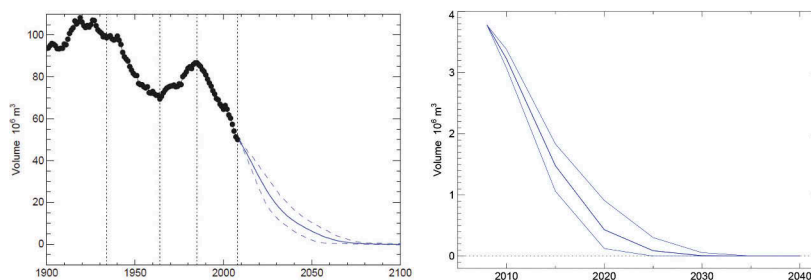


Figure 3. Development of the ice volume of the Cambrena glacier between 1900 and 2100 (left) and its southeastern tongue between 2008 and 2040 (right) (the potential future changes are given by an average value and a band width from 10 scenarios; the vertical dotted lines indicate dates with known extent of the glacier surface) (Funk & Bauder 2013).

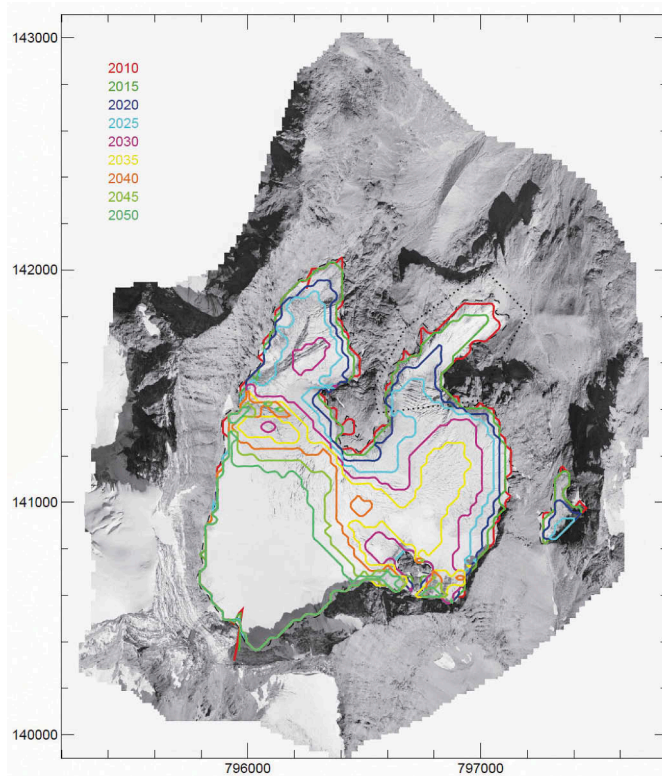


Figure 4. Prognosis of the surface of the Cambrena glacier until 2050 (the base photo shows the situation in 2008) (Funk & Bauder 2013).

- Threat of glacier tongue rupture: Currently the glacier tongue is stabilized by its lowest part with the inclination at 24° and the contact at its bottom and the two sides. As soon as the glacier tongue retreats into the steeper part with the inclination at 35° and gets thinner on both sides, the ice is only stabilized by the contact to the terrain at its bottom and a risk of sudden ice rupture emerges. According to studies at other glaciers, a rupture requires a water flow between the glacier and the terrain surface. Therefore, such events usually occur with alpine glaciers in the months of July to October.

4 RUPTURE OF CAMBRENA GLACIER TONGUE, ICE AVALANCHE AND IMPULSE FLOOD WAVE IN THE LAGO BIANCO RESERVOIR

The report of the glacier specialists (Funk & Bauder 2013) gives a forecast on the decrease of the ice volume in the steep part with time: in 2015 the potential rupture volume will equal $1.5 \times 10^6 \text{ m}^3$, this corresponds to the worst-case scenario to be taken into account in the risk management of the Lago Bianco reservoir. By 2020, the potential rupture volume will diminish below $0.5 \times 10^6 \text{ m}^3$ of ice.

The ruptured ice would move as an avalanche towards the Lago Bianco reservoir. The report (Pitsch 2014) presents the calculations carried out in 2014 by avalanche specialists with the computer program RAMMS (SLF/WSL). The calculation results showed that the ice rupture volume in the worst-case scenario of $1.5 \times 10^6 \text{ m}^3$ would give an avalanche with a volume of $1.8 \times 10^6 \text{ m}^3$, which could reach the reservoir with a speed of 10–20 m/s, a flow height of 5–10 m and a volume of approximately $0.25 \times 10^6 \text{ m}^3$ (Figure 5). On the other hand, an

avalanche produced by an ice rupture volume of $0.5 \times 10^6 \text{ m}^3$ could reach the reservoir with a neglectable volume of a few thousand m^3 .

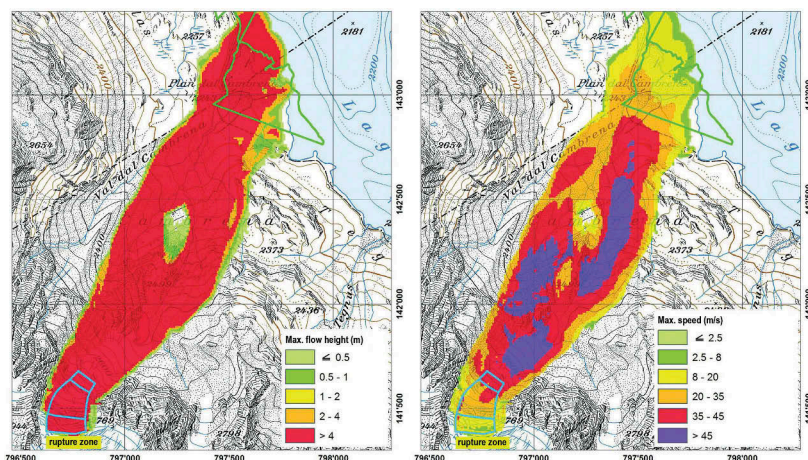


Figure 5. Maximum flow height (left) and speed (right) according to the RAMMS calculations for the ice avalanche produced by the worst-case glacier rupture of $1.5 \times 10^6 \text{ m}^3$ (Pitsch 2014).

Based on the results of the avalanche calculations the dam expert responsible for the Lago Bianco reservoir conducted in 2015 impulse flood wave calculations (Steiger 2015) with a spreadsheet program, which had been developed by the ETH Zurich (Heller et al. 2008) at the demand of the Swiss Federal Office of Energy. For the worst-case ice rupture and the maximum reservoir level of 2234.65 m a.s.l. the calculations for the Arlas dam gave a wave height of 1.5–4.5 m and an overtopping volume of 200–4000 m^3 (minimum freeboard of 1.1 m taken into account). The overtopping volume is rather small. It would only cause minor damages downstream of the Arlas dam. On the other hand, the flood wave reaches well above the danger level (= crest level of the eastern part of the dam at 2235.75 m a.s.l.) and therefore puts the stability of the dam at risk.

The impulse flood wave can only reach the substantially more distant Scala dam after several reflections. Thus, the wave height at the Scala dam would be much smaller and pass the dam by the overflow section. The significant freeboard of 2.35 m from the maximum reservoir level up to the crest level at 2237.00 m a.s.l. (= danger level) was expected to guarantee the integrity of the Scala dam.

5 ICE FLOW SPEED AS EARLY INDICATOR OF GLACIER RUPTURE

Experiences with several glacier ruptures have demonstrated, that the ice flow speed is a good early indicator for a situation becoming dangerous (Funk & Bauder 2013, Bauder 2018). Figure 6 presents the flow speed of the tongue of the Allalin glacier in the Saas valley in the southern Swiss Alps for the years 1965 to 1967. The two decreasing curves from 1965 were measured after the rupture of more than $2 \times 10^6 \text{ m}^3$ ice on August 30th 1965, which killed 88 people on the construction site of the Mattmark dam. The curves from 1966 and 1967 show speed increases by a factor of 10 or more from a few decimeters/day to several meters/day. Important is also the fact that the periods with increased speed lasted many days or weeks.

Based on the findings given above, the ETH Zurich glacier specialists recommended in the case of the Cambrena glacier the installation of an automatic photographic camera with energy supply from a photovoltaic panel and mobile phone data transmission to follow the ice flow speed on a daily basis. The camera (Figure 7) was installed in July 2015 at a cost of about 30,000 CHF \approx 30,000 EUR (Blum 2015). The annual costs amount to 12,500 CHF \approx 12,500 EUR and include the analysis of the daily pictures by the glacier specialists.

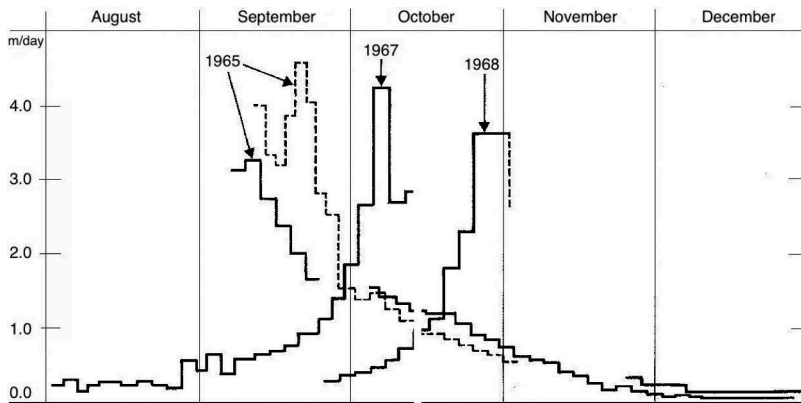


Figure 6. Flow speed of the Allalin glacier in the southern Swiss Alps for the years 1965 to 1967 (Funk & Bauder 2013).

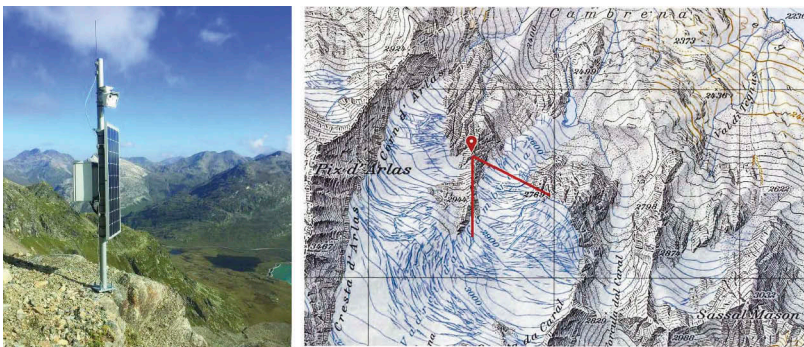


Figure 7. Automatic camera with photovoltaic energy supply and mobile phone data transmission for the surveillance of the Cambrena glacier (left) (Bauder 2018); camera position and view angle over south-eastern glacier tongue (right) (Blum 2015).

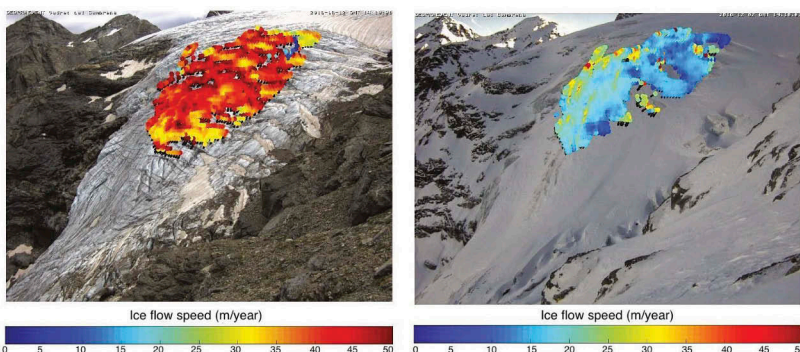


Figure 8. Ice flow of the southeastern tongue of the Cambrena glacier based on the analysis of camera pictures (left: high flow speed in August 2016; right: low flow speed in December 2016) (Bauder 2018).

Figure 8 Shows as an example the ice flow speed calculated from the camera pictures for two different periods of the year 2016. Ice flow speeds between 0.04 and 0.12 m/day, averaged over periods of several days, were evaluated for the steep part of the southeastern tongue of the Cambrena glacier.

6 EMERGENCY PREPAREDNESS PLAN

Emergency preparedness plans for reservoirs and their dams use five danger levels (SFOE 2015a, b), as it is common for different risks in Switzerland:

- Danger level 1 = normal situation → regular surveillance and maintenance
- Danger level 2 = moderate danger → preparation of emergency organization
- Danger level 3 = serious danger → emergency organization in action
- Danger level 4 = high danger → preparation of alarm of population
- Danger level 5 = very high danger → alarm and evacuation of population

The Supervision of Dams Section of the Swiss Federal Office of Energy assigned at a meeting with the reservoir owner, the ETH Zurich glacier specialists, the dam engineer, the dam expert and the geology expert danger level 2 for the Lago Bianco reservoir. Thereafter, the reservoir owner developed a special emergency preparedness plan for a rupture of the Cambrena glacier tongue (Repower 2017). This plan uses two basic elements:

- Continuous surveillance of the Cambrena glacier to measure the ice flow speed.
- Lowering of the Lago Bianco reservoir in case of a high ice flow speed to a level, which still guarantees the stability of the Arlas dam.

Based on the calculations presented in section 4 the safe reservoir level was determined by the dam expert for the worst-case glacier rupture of $1.5 \times 10^6 \text{ m}^3$ of ice to be 2232.15 m a.s.l., i. e. 2.50 m below the maximum reservoir level. The time needed for this lowering plays a key role in the emergency preparedness plan. With an inflow of $1.0 \text{ m}^3/\text{s}$ to the reservoir, the available outlets (see section 2) give the following times for reaching the safe level: turbination only = 10.9 days, bottom outlet only = 7.4 days and intermediate outlet only = 2.6 days. The use of the intermediate outlet at maximum capacity would cause substantial damage downstream of the Scala dam. To reduce this, it was decided to open the intermediate outlet stepwise as long as the danger does not reach level 4. Therefore, the lowering of the reservoir level including a preparation period of 24 hours is prolonged to 100 hours \approx 4 days. This agrees with the statement of the glacier specialists, that the increase period of the ice flow speed lasts many days or weeks before it comes to a glacier rupture. In case of danger levels 4 and 5, an immediate full opening of all outlets down to the safe level is intended.

Based on the previous statements the following conditions and procedures were established for the danger levels 2 to 5 (Figure 9):

- Danger level 2: The reservoir may be operated over its full range. The glacier specialists of the ETH Zurich check the ice flow speed, during the critical time of the year on a daily basis. The operation center of the reservoir owner is active on a 24 hours and 7 days basis.

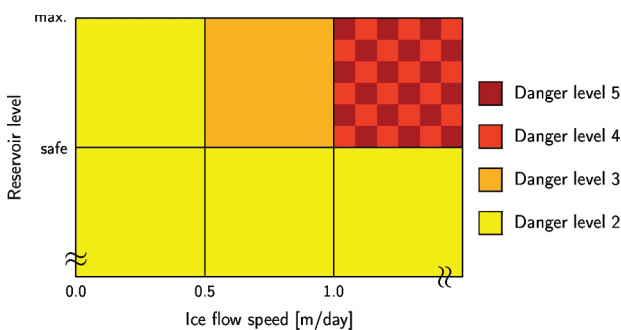


Figure 9. Danger levels 2 to 5 as a function of the ice flow speed of the Cambrena glacier and the water level in the Lago Bianco reservoir.

- Danger level 3: A reported glacier flow speed 0.5 m/day and a reservoir level $> 2232.15 \text{ m a.s.l.}$ (= safe level) triggers danger level 3. Between June 1st and November 30th, a camera

blackout of 5 days and a reservoir level > 2232.15 m a.s.l. would also lead to danger level 3. Immediately, the reservoir owner informs the emergency center of the police about the new danger level and sends personnel to the reservoir. After a 24 hours preparation period, the lowering of the reservoir with a stepwise opening of the intermediate outlet starts.

- Danger level 4: A reported glacier flow speed 1.0 m/day and a reservoir level > 2232.15 m a.s.l. (= safe level) triggers danger level 4. Immediately, the reservoir owner informs the emergency center of the police about the new danger level and the intermediate outlet is totally opened; if possible, the bottom outlet and the turbines are additionally used with maximum capacity. The water alarm center at the Lago Bianco reservoir is now permanently manned. The police closes down both railway and highway over the Bernina pass.
- Danger level 5: A glacier flow speed 1.0 m/day continuously reported over 5 days and a reservoir level > 2232.15 m a.s.l. (= safe level) triggers danger level 5. Immediately, the water alarm is activated and the Swiss civil protection sirens alarm the population to evacuate the possible flooding area of an Arlas dam break. The reservoir owner informs the emergency center of the police about the new danger level and the activation of the water alarm. The lowering of the reservoir continues with the totally opened intermediate outlet and, if possible, with the full capacity of the bottom outlet and the turbines.

7 DEVELOPMENT OF THE CAMBRENA GLACIER BETWEEN 2017 AND 2022

The measuring of the actual ice thickness allows a more precise estimate of the possible ice rupture volume. In May 2017, such a measurement was carried out with a helicopter-based Ground-Penetrating-Radar system on several profile lines (Grab & Bauder 2017). The measurements showed ice thicknesses between 40 and 60 m.

In mid-September 2019 the pictures from the automatic camera showed a horizontal crack crossing almost the whole width of the glacier tongue (Bauder & Farinotti 2020a). Was this the start of an ice rupture? In the following weeks and months, the situation was carefully supervised. But a year later in mid-September 2020 the crack had not developed any further (Bauder & Farinotti 2021). Figure 10 presents this crack from two different view-points and on different dates.



Figure 10. Horizontal crack (marked with yellow arrows) in the Cambrena glacier tongue: automatic camera picture on 15.09.2019 (left), situation from below on 27.09.2019 (middle) and automatic camera picture on 15.09.2020 (Bauder & Farinotti 2020a, 2021).

The diagram in Figure 11 shows the mean ice flow speed in the steep part of the Cambrena glacier tongue between January 2019 and December 2022 evaluated from the automatic camera pictures (Bauder & Farinotti 2023). All four years show a similar seasonal behavior: from October to April the ice flow is slow (20–30 m/year corresponding to 60–80 mm/day) and during the melting period from May to September an increased movement is present (60–80 m/year corresponding to 160–220 mm/day). The maximum is usually reached around the end of June and the beginning of July.

Figure 12 presents the loss of area of the Cambrena glacier tongue from 2015 to 2019 respectively to 2022 and its thickness in 2019 and 2022. The changes on the Cambrena glacier tongue are impressive: its surface shrank by a third from 2015 to 2019 and more than half the area had melted away in 2022; the mean thickness reduced by 20 % from 2015 to 2019 and by an additional 20 % until 2022 (Bauder & Farinotti 2020b, 2022).

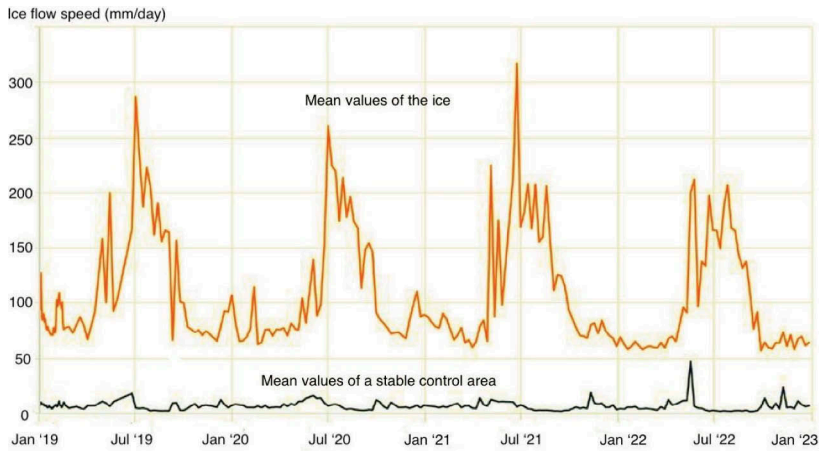


Figure 11. Ice flow speed of the Cambrena glacier tongue (Bauder & Farinotti 2023).

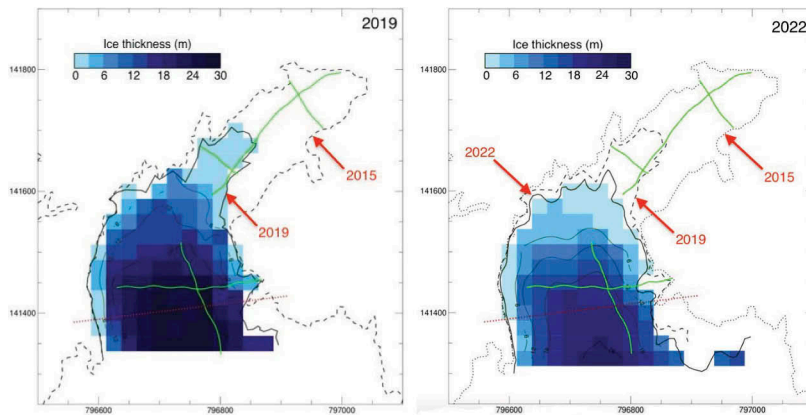


Figure 12. Loss of area and thickness of the Cambrena glacier tongue: situation in 2019 (left) and 2022 (right) (Bauder & Farinotti 2020b, 2022).

Three times—in 2015, 2019 and 2022—the maximal ice rupture volume was determined by the glacier specialists (Bauder & Farinotti 2022). The results are given in the following table:

Table 1. Estimated volume of the Cambrena glacier tongue in 2015, 2019 and 2022.

Year	Area of glacier tongue	Thickness of glacier tongue		Volume of glacier tongue = ice rupture volume
		max.	mean	
2015	85,000 m ²	32 m	14.6 m	$1.25 \pm 0.20 \times 10^6 \text{ m}^3$
2019	54,000 m ²	27 m	12.0 m	$0.64 \pm 0.08 \times 10^6 \text{ m}^3$
2022	41,000 m ²	22 m	8.9 m	$0.36 \pm 0.04 \times 10^6 \text{ m}^3$

As already stated in section 4, an avalanche produced by an ice rupture volume of $0.5 \times 10^6 \text{ m}^3$ would reach the Lago Bianco reservoir with a volume of only a few thousand m³ and produce a negligible impulse flood wave. The preceding table shows that the maximal ice rupture volume did fall below this value in 2022. As a consequence, the restricting safe reservoir level of 2232.15 m a.s.l. was lifted in November 2022 by the Swiss Federal Office of Energy. Since then, the Lago Bianco reservoir is back to a fully normal operation. It is planned to continue the camera monitoring of the southeastern tongue of the Cambrena glacier until 2024.

8 CONCLUSION

In 2014/15, the risk of an impulse flood wave in the Lago Bianco reservoir due to a rupture of the southeastern tongue of the Cambrena glacier was detected. Based on the ice volume reaching the reservoir a safe water level was assigned to prevent a dam break. Experiences with other glaciers have shown that an ice rupture is announced over several days or weeks with an increase of the ice flow speed by a factor of 10 or more. Therefore, the behavior of the Cambrena glacier tongue was continuously monitored with flow speed measurements. These measurements showed every year an increase of the flow speed during the melting period from May to September by a factor of 2 to 3. The repeated determination of the possible ice rupture volume allowed an update of the safe water level and of the emergency preparedness plan. Thus, the water level restriction for the Lago Bianco reservoir could be totally lifted in November 2022. The measurements carried out from 2015 until 2022 showed a very good agreement with the prognosis of the glacier specialists.

ACKNOWLEDGMENT

The authors want to express their thankfulness for the support given by C. Pelazzi (Repower AG).

REFERENCES

- Bauder, A. 2018, unpubl. Überwachung des Cambrena Gletschers. Presented at the conference *ATCOLD-STK Fachtagung 2017, Dornbirn*, July 28th 2017. VAW ETH Zurich.
- Bauder, A. & Farinotti, D. 2020a, unpubl. Vadret dal Cambrena 2019. Letter to Amt für Wald und Naturgefahren Graubünden. VAW ETH Zurich.
- Bauder, A. & Farinotti, D. 2020b, unpubl. Eisvolumen der Gletscherzunge des Vadret dal Cambrena. Letter to Repower AG. VAW ETH Zurich.
- Bauder, A. & Farinotti, D. 2021, unpubl. Vadret dal Cambrena 2020. Letter to Amt für Wald und Naturgefahren Graubünden. VAW ETH Zurich.
- Bauder, A. & Farinotti, D. 2022, unpubl. Eisvolumen der Gletscherzunge des Vadret dal Cambrena. Letter to Repower AG. VAW ETH Zurich.
- Bauder, A. & Farinotti, D. 2023, unpubl. Vadret dal Cambrena 2022. Letter to Amt für Wald und Naturgefahren Graubünden. VAW ETH Zurich.
- Blum, M. 2015, unpubl. Überwachung Vadret dal Cambrena — Vorprojekt Überwachung 2015–2019. Amt für Wald und Naturgefahren Graubünden.
- Grab, M. & Bauder, A. 2017, unpubl. Eisdickenmessungen auf dem Vadret dal Cambrena — Helikopter-gestützte Radarmessungen. IfG and VAW ETH Zurich.
- Funk, M. & Bauder, A. 2013, unpubl. Vadret dal Cambrena — Untersuchungen zur Gefahr von Eislawinen im Zusammenhang mit dem Projekt Lago Bianco. Report 70.03.2013, VAW ETH Zurich.
- Heller, V., Hager, W. H. & Minor, H.-E. 2008. Rutscherzeugte Impulswellen in Stauseen. VAW ETH Zurich.
- Pitsch, N. 2014, unpubl. Vadret dal Cambrena — Gefahrenanalyse betreffend Eislawinen. pitsch-ing.ch.
- Repower 2017, unpubl. Stauanlage Lago Bianco — Notfallreglement Cambrenagletscher. Poschiavo: Repower AG.
- SFOE 2015a. Directive on the Safety of Water Retaining Facilities—Part E: Emergency plan (version 2.0). Swiss Federal Office of Energy.
- SFOE 2015b. Beispiel Notfallreglement Stauanlage mit Wasseralarmsystem (version 2.0). Swiss Federal Office of Energy.
- SLF/WSL. Program RAMMS—Rapid Mass Movement Simulation (two-dimensional dynamics modeling of rapid mass movements in 3D alpine terrain). Program homepage <http://ramms.slf.ch/ramms/>.
- Steiger, K. M. 2015, unpubl. Stauanlage Bernina — Expertenbericht über die 9. Fünfjahreskontrolle 2014. AF-Consult Switzerland AG.

Inclinometer monitoring of a dam during hot weather

N. Manzini, S. Van Gorp & Y. Jobard
SITES SAS, France

ABSTRACT: The Bazergues Dam is a 156m long and nearly 20m high hydraulic dam located in the Allier department of France. This arch-type dam was built in 1953 and holds a water volume of 1,300 thousand m³ over an area of 14 hectares. Traditionally, the dam's movements have been monitored using direct pendulums. However, these instruments now reach their limit of measurement during very hot and dry conditions, preventing proper monitoring of the structure during these critical periods. To overcome this issue and monitor any movements of the dam, SITES has installed a remote monitoring system using an array of inclinometers. A total of 9 wireless sensors have been deployed on the downstream face of the dam by a team of rope access technicians. These sensors automatically collect data, transmit it to a wireless data logger, which then sends the data to SITES' servers for real-time monitoring with a dedicated interface. This paper focuses on the analysis of data acquired over the past 3 years, including a comparison and correlation of the inclinometers data with ambient conditions, especially during periods of intense heat. A comparison with traditional pendulum measurements is also conducted to validate the monitoring system's data.

RÉSUMÉ: Le barrage de Bazergues est un barrage hydraulique de 156m de long et de presque 20m de hauteur situé dans le département de l'Allier en France. Ce barrage de type voûte a été construit en 1953 et retient un volume d'eau de 1300 milliers de m³ sur une surface de 14 hectares. Les mouvements du barrage sont traditionnellement suivis à l'aide de pendules. Cependant ces derniers atteignent désormais leur limite de domaine de mesure lors des conditions très chaudes et sèches, empêchant le bon suivi de l'ouvrage dans ces périodes critiques. Pour palier cela et suivre d'éventuels mouvements du barrage, SITES a installé et mis en service un système de télésurveillance à l'aide d'une chaîne d'inclinomètres. Au total, une chaîne de 9 capteurs sans fils a été déployée sur le parement en aval par une équipe de cordistes. Les capteurs collectent automatiquement les données, les transmettent vers un collecteur sans-fil, qui transmet les données vers les serveurs de SITES pour un suivi en temps réel avec une interface dédiée. Cet article s'intéresse à l'exploitation des données acquises au cours des 3 dernières années: comparaison et corrélation des inclinomètres avec les conditions ambiantes, en particulier lors des périodes de forte chaleur. Une comparaison avec les mesures de pendule traditionnelle est également réalisée pour valider les mesures du système de monitoring.

1 INTRODUCTION

1.1 *Context*

The Bazergues Dam (Figure 1) is an arch-type hydraulic dam located in the municipality of La Celle on the Banne River and is operated by the SMEA (Mixed Syndicate of Allier Waters) – Commentry Local Commission. The water reservoir of the structure, the Bazergues pond, represents a volume of 1,300 thousand m³ of water for an area of 14 hectares, and is now a favored fishing site. The structure, with a height of 19.5m and a total length of 156m, is mainly used to supply industrial sites in Commentry.



Figure 1. Picture of the Bazergues dam - © Ville de Commentry.

1.2 Monitoring system

The monitoring of the Bazergues Dam is traditionally carried out by regular inspections, typically twice a month, which include:

- Measurement of the water level (since 1979).
- Measurement of the leakage volume (since 1979).
- Measurement of two direct pendulums installed on the structure (since 1986). For each pendulum, three readings are made, which allow the calculation of radial, tangential, and zenithal displacements detected by the pendulums.

The use of direct pendulums is a historical method of monitoring of potential movements and deformations of hydraulic dams (Pretorius et al. 2001, Sangaré 2003). However, these pendulums are now at risk of reaching the limit of their measurement range, particularly during the hottest and driest periods of the year, when deformations are the most important on the structure. This is due to the protective tubes that are installed around the pendulums: to protect the pendulums from external perturbations (notably wind), they are installed in solid and fixed tubes. Now, especially during hot weather, pendulums come close to touching the edges of these protective tubes.

In this context, the operator of the structure, the SMEA, has called on SITES to deploy inclinometer sensors to monitor the radial movements of the structure.

An inclinometer is a sensor capable of measuring its inclination with respect to the vertical: when fixed alone on a structure, it only allows the inclination to be monitored very locally. By installing the sensor on a rigid support (e.g., on a rod or metal plate), the sensor can monitor the inclination of the whole segment, which can then be used to calculate the relative displacement between the two ends of the segment.

To enable monitoring of the displacements along the entire height of the dam, SITES has deployed and put into service an array of 9 segments equipped with inclinometers installed vertically on the downstream face of the dam (Figure 2). These inclinometers are equipped with high-precision MEMS sensors ($\pm 0.01\text{mm}$), operate on batteries (5-year autonomy), and automatically transmit their data wirelessly to a close gateway that sends them to a remote server for data processing and analysis. It is then possible, based on a reference inclination for each sensor, to estimate the relative displacements of each segment, as well as

to estimate the cumulative relative displacements for several segments or for the entire array of inclinometers. Each sensor is also equipped with a temperature probe.



Figure 2. Wireless sensor array (left) and the associated wireless gateway (right).

The use of sensors to complement monitoring measurements has several advantages:

- Sampling rate: the system acquires data on each inclinometer every 2 hours, which allows for dense time series that can reveal daily movements of the dam.
- The use of 9 segments allows for a denser coverage of a similar vertical range as the existing pendulums: for instance, it is possible to precisely monitor radial deformations at several intermediate heights.
- The temperature probes of the sensors also allow for additional information to be collected.
- Inclinometers have no limit to the range of measurements that can realistically be reached by the structure.

In this study, inclinometers are used to monitor only radial displacements, but could be used to monitor tangential displacements as 3D inclinometers can be installed.

In this context, this paper aims to validate the data acquired by the inclinometer chain by comparing them to data from pendulums and standard models, and to propose additional analyses exploiting the advantages of using instrumentation.

2 DIRECT PENDULUM DATA ANALYSIS

2.1 *Pendulum data information*

The structure is equipped with two direct pendulums, labelled Pendulum #1 and Pendulum #2 in this paper. Pendulum #1 covers a vertical section similar to the inclinometer sensor array and will be used as a reference for monitoring data.

Measurements from the pendulums (Figure 3) were performed starting in 1986. From 1986 to 1998, two readings were made during regular inspections, allowing for the calculation of two displacement components: radial displacement and tangential displacement. Since 1998, a third reading is made, allowing for the calculation of the zenithal displacements.

For both pendulums, the largest displacements are observed in radial direction, with practically negligible tangential movements.

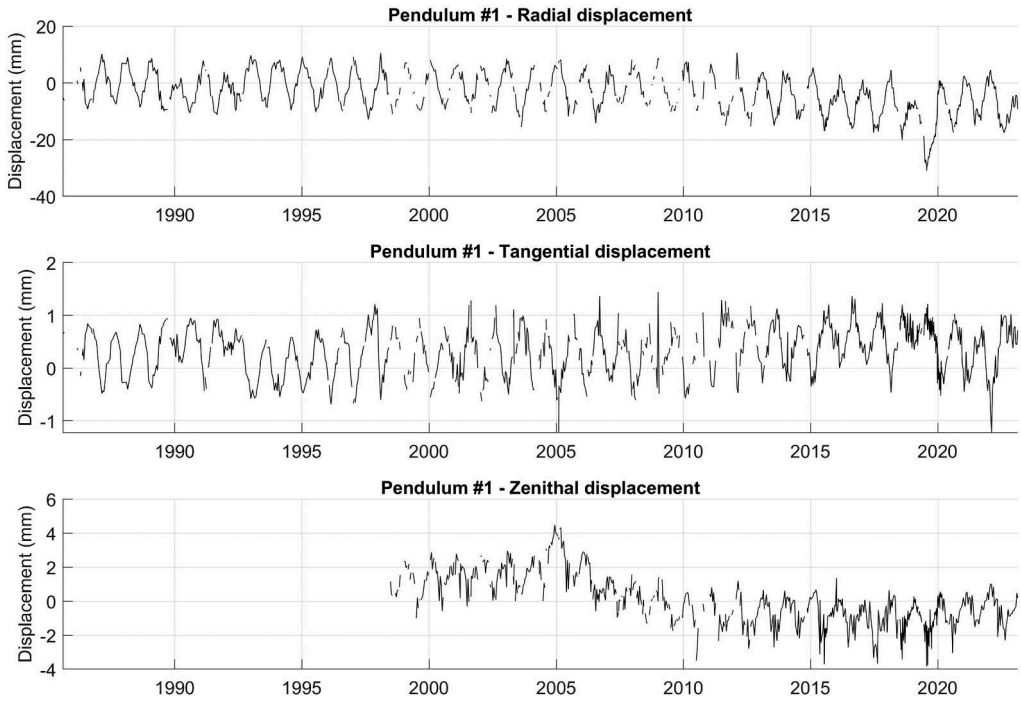


Figure 3. Displacements measured with Pendulum #1.

Over 1030 measurements of radial and tangential displacements, and over 750 measurements of zenith displacements have been made since 1986 and 1998, respectively. This represents approximately 28 measurements per year.

2.2 HST model principles

One of the historical data analysis tools for dams is the HST model (Andersson & Seppälä 2015, Gahlouz 2020, Hoonakker et al. 2012), which stands for Hydrostatic Seasonal and Temporal. The HST model is a polynomial model that assumes that all movements and deformations on a structure can be attributed to either:

- Reversible phenomena related to water load (Hydrostatic).
- Reversible phenomena related to seasonal environmental variations (Seasonal).
- Non-reversible time-related phenomena (Temporal).

The hydrostatic part of the model is expressed as a function f_H of the water level:

$$f_H = u_0 + u_1 Z + u_2 Z^2 + u_3 Z^3 + u_4 Z^4 \quad \text{with} \quad Z = \frac{h_0 - h}{h_0 - h_e} \quad (1)$$

Where h represents the current water level, h_0 represents the normal water level, and h_e represents the empty reservoir level.

The seasonal part of the model is expressed as a function f_S :

$$f_S = v_1 \cos(S) + v_2 \cos(2S) + v_3 \sin(S) + v_4 \sin(2S) \quad (2)$$

Where S represents an increasing angle value starting at zero at the beginning of the calendar year and completing one full rotation at the end of the calendar year (for example: 0-360° over a single year).

The temporal part of the model is expressed as a function f_T of the elapsed time t which includes a polynomial of degree n :

$$f_T = w_0 e^{-\frac{t}{\tau}} + w_1 t + w_2 t Z^2 + \dots + w_n t^n \quad (3)$$

Where τ represents the characteristic damping time. The degree n of this polynomial is generally between 1 and 4.

The HST approach therefore consists of expressing the model \hat{Y} of a data Y acquired a dam (deformation, displacement. . .) such as:

$$\hat{Y} = f_H(Z) + f_S(S) + f_T(t) + \varepsilon \quad (4)$$

The simplicity of the HST approach makes it a widely used tool, notably for identifying the impact of various phenomena affecting the structure, and for correcting data from reversible effects and thus facilitating further data analysis.

However, the HST approach has several limitations, notably because hydrostatic, seasonal, and temporal effects are assumed to be independent (Bonelli 2004, De Granrut 2019). This approach also does not consider the effects related to the thermal deformation of the dam except those that can be associated with the sinusoids in the seasonal term.

2.3 Comparison with HST model

To verify that the monitoring dataset does not contain any significant anomaly, it is proposed to model the acquired time series with a HST model. The objective of the approach presented here is not to use the model to interpret the behavior of the structure, but to verify that the measurements made with the pendulum correspond to a plausible theoretical behavior.

The model was generated using all available data. For quality control, the model was not trained on data from 2020 to 2023. A model with a degree 1 time polynomial was trained. The results obtained on the radial displacement from Pendulum #1 are presented in Figure 4.

The generated model offers a robust prediction of the time series: accurate modelling of the general trend and regular seasonal variations, as well as years with significantly different profiles from others (1992, 2019), confirming that these differences can be explained from the hydrostatic load of the structure.

However, it should be noted that the model is not able to predict shorter variations in the time series, which are assumed to be related to thermal variations of the structure and the associated deformations.

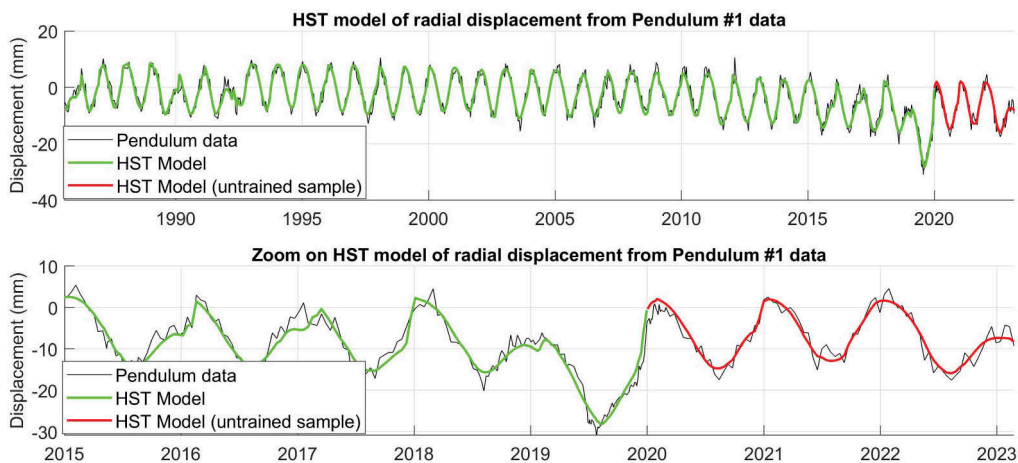


Figure 4. HST mode of Pendulum #1 radial displacement (positive displacements are towards downstream).

3 SENSOR DATA ANALYSIS

3.1 Data information

Data acquisition of the inclinometer array began during the month of August 2019. For each sensor, numbered from 1 to 9, the inclination and temperature (noted as $Inc\#_T$) are measured. From the inclination, the relative radial displacement observed along the sensor is calculated from its initial orientation, and noted as $Inc\#_D$. The cumulative displacements are then calculated at each sensor and noted as $Inc\#_DC$.

Data acquisition rate was initially set to 30 minutes but was slowed down to 2 hours to optimize system battery life.

3.2 Comparison with pendulum data

Cumulative displacement of the entire inclinometer array is calculated ($Inc9_DC$). Pendulum #1 follows the movements along the entire dam height, similarly to the inclinometer array. Instrumentation data are compared to the pendulum readings in Figure 5.

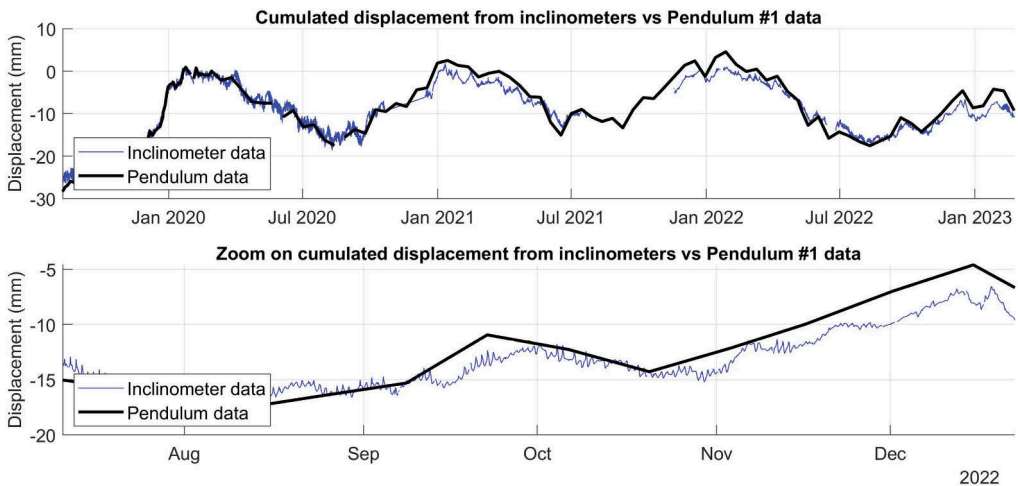


Figure 5. Comparison between inclinometer and pendulum data.

The two time series are strongly similar. The same annual and seasonal trends are observable. Some small differences are observed, which can be explained by:

- The fact that the pendulum and the inclinometer array are not located exactly at the same place (slight local variations, the inclinometer being located outside the structure).
- The fact that the pendulum measurement rate does not allow to account for short period thermal variations, whereas the inclinometers do so thanks to their higher sampling rate.

Regarding inclinometer data, part of the thermal effects can be identified in the daily variations. To better highlight this phenomenon, one proposes to filter the daily variations of the signal. This is done by estimating the slow component of the signal, calculated as the sliding daily average, and subtracting it from the complete signal. An illustration of this computation is presented in Figure 6 for a one-year sample.

Observation of the daily variations shows a seasonal difference over the span of a year: cumulative displacements show larger daily variations in summer than in winter. Variations of up to 1mm can be observed.

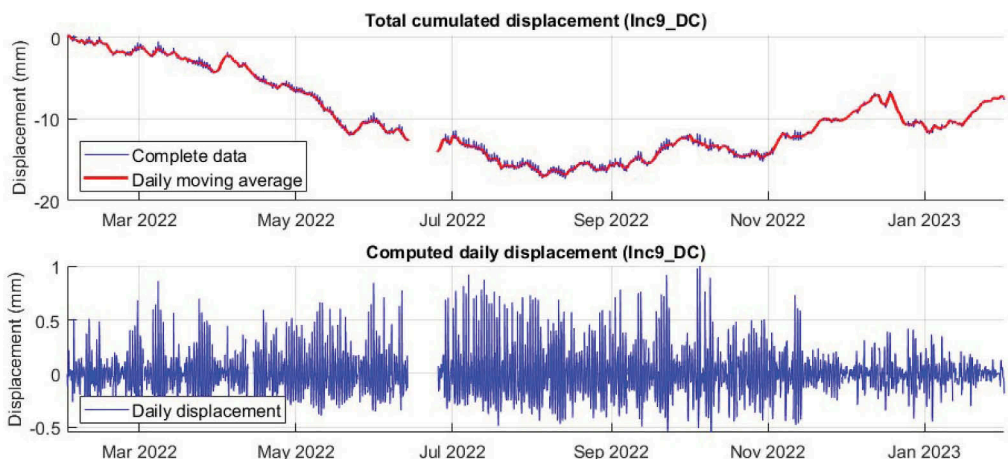


Figure 6. Estimation of daily cumulated displacement variations.

3.3 Correlation with temperature data

To study the relationship between these variations, it is proposed to evaluate the correlation between temperature, displacement and cumulative displacement data. The correlation is calculated here as the Pearson Correlation Coefficient (PCC). PCC is an indicator computed between two time series, ranging from -1 to 1 and whose value has the following meaning:

- A value tending towards 1 means that there is a positive linear relationship between the time series.
- A value tending towards -1 means that there is a negative linear relationship between the time series.
- A value tending towards 0 means that there is no linear relationship between the time series.

The PCC between all acquired time series are represented in a correlation map (Figure 7). A similar map was generated using only the daily variations of the time series (including temperatures).

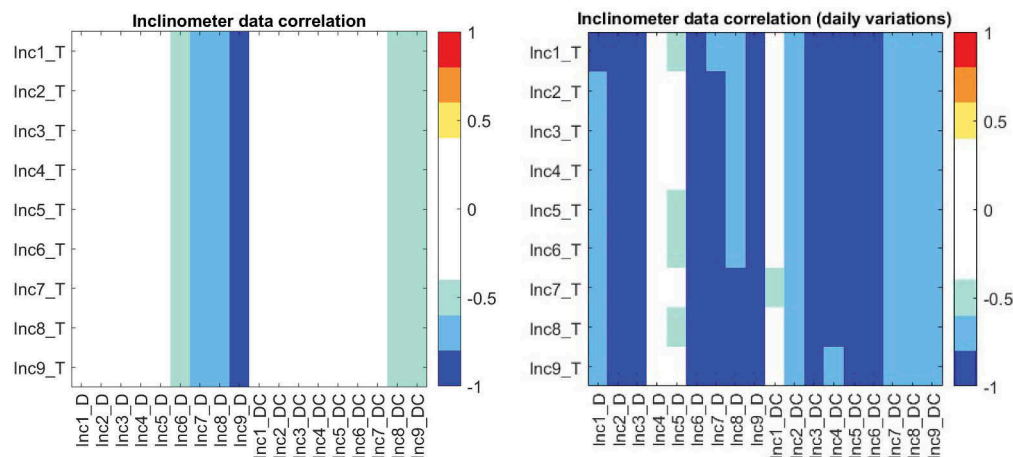


Figure 7. Correlation map of inclinometer array data. Full data (left) and daily variations (right).

Correlations are much stronger on the daily variation data. This result is expected since it has been previously shown that seasonal variations can be largely modeled by a HST model without temperature data.

It is noted that with several sensors, even when considering only the daily variations, the correlation remains moderate to low. This can be explained by the fact that there is a slight time delay between daily thermal variations and observed displacements.

This delay can be explained by the thermal inertia of the structure: the observed movements are related to temperature variations in the material of the dam. However, the temperature probes of the inclinometers are located on the surface, so the temperature variations they observe are ahead of the true temperature variations inside the material.

3.4 Proposal for HST+T model

The observations made so far have shown that:

- The data acquired by the inclinometer sensor chain is consistent with the associated pendulum measurements, and thus with the corresponding HST model.
- Inclinometer data provides more detailed tracking of radial movements, but a standard HST model does not allow them to be visualized.
- After filtering, temperature data can be correlated with the displacement data for a majority of inclinometers.

Based on these observations, one hypothesizes that thermal effects on the structure can be expressed as a linear function f_K of the temperature T of the structure and can be used to complete the HST model to form a HST+T model. Since it has been previously observed that the time series seem to be more strongly correlated when considering only daily variations, one proposes to incorporate daily variations T_Q as a variable in the temperature function.

The HST+T model is then expressed as:

$$\hat{Y} = f_H(Z) + f_S(S) + f_T(t) + f_K(T, T_Q) + \varepsilon \quad (5)$$

$$f_K(T, T_Q) = a_0T + b_0T_Q \quad (6)$$

However, inclinometers only record surface temperature data, and thus these measurements are not relevant of thermal inertia of the structure.

To address this, it is proposed to simulate the effects of thermal inertia by adding variables to f_K with multiple time delays $\Delta t_1, \Delta t_2, \dots, \Delta t_n$. The temperature function of the HST+T model is then expressed as:

$$f_K(T(t), T_Q(t)) = a_0T(t) + \sum_{i=1}^n a_iT(t - \Delta t_i) + b_0T_Q(t) + \sum_{i=1}^n b_iT_Q(t - \Delta t_i) \quad (7)$$

3.5 Sensor data models

To evaluate the proposed approach, three models are generated based on the total cumulative displacement from inclinometer data:

- A conventional HST model.
- A HST+T model without time delays Δt_i .
- A HST+T model using $\Delta t_i = 12h, 24h, \dots, 72h$.

The models were trained on all available data. The performance of the models is evaluated by comparing the root mean squared error (*RMSE*) and the maximum deviation from the model (Δmax), represented by the 99th percentile of the absolute difference between the data and the model. The results are presented in the following table:

Table 1. Comparison of multiple models of Inc9_DC.

Model	RMSE	Δ_{max}
HST	1.3mm	4.0mm
HST+T (no Δt)	1.0mm	3.1mm
HST+T (with Δt)	0.4mm	1.2mm

These results show the significant gains brought about by incorporating temperature data with time shifts. The *RMSE* and maximum error of the model are, in the case studied, divided by 3. A comparison between the HST model and the HST+T of *Inc9_DC* model with time shifts is illustrated in Figure 8.

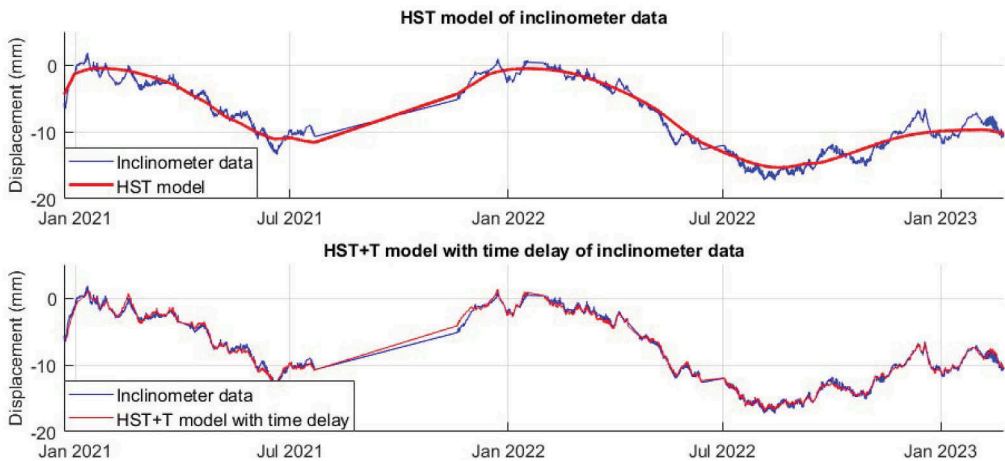


Figure 8. Comparison of HST and HST+T models.

The cumulative displacements of all inclinometers (*Inc2_DC* to *Inc9_DC*) were modeled using the same HST+T approach. The results are summarized in Table 2.

The results obtained show that by incorporating a simple temperature data from the sensors into a conventional HST model, it is possible to generate models with submillimeter precision capable of modeling the temperature-induced displacements along the dam. These results also demonstrate the usefulness of using an array of inclinometer, as it is possible to accurately track displacements at several levels of the structure.

It should be noted that the differences are smaller for the first sensors, which can be explained by the smaller amplitude of the cumulative displacements for those sensors (less relative displacements added).

Table 2. HST+T models of inclinometer data.

Sensor	RMSE	Δ_{max}
Inc2_DC	0.2mm	0.5mm
Inc3_DC	0.2mm	0.7mm
Inc4_DC	0.3mm	0.8mm
Inc5_DC	0.3mm	0.9mm
Inc6_DC	0.4mm	1.1mm
Inc7_DC	0.4mm	1.3mm
Inc8_DC	0.5mm	1.4mm
Inc9_DC	0.4mm	1.2mm

4 CONCLUSIONS

This paper presented the evaluation of an inclinometer array deployed on an arch-dam in order to complement traditional monitoring data. Sensor data was compared to historical monitoring measurements, validating the accuracy of the results obtained.

Time series acquired by the sensors allows for a much higher sampling rate and enables visualization of thermal effects not modeled by the traditional HST method. An approach combining an HST model with filtered temperature data was proposed and applied using surface temperatures acquired by the sensors. The results obtained illustrate the ability of this approach to model movements related to thermal variations despite the absence of information in the depth of the structure material. Such models could allow for a finer prediction the effects of daily temperature variations in continuous monitoring data.

The Bazergues dam is a medium-sized dam, and in the case of a structure with a thicker wall, the required modeling approach of thermal inertia could be more complex. Moreover, in the context of a thinner structure, the variation of water level could also have a more important effect on temperature variations. Thus, this study calls for applying the proposed approach to structures with different characteristics to validate it. These results also highlight the interest in using an array of sensors. While inclinometers have a specified range of operation (for high resolution purposes), this range is either greater than the movements expected on a dam or can be recalibrated if necessary. Thus, inclinometer arrays appear as viable tool for long-term dam monitoring, and offer complementary data acquisition to the measurements made with pendulums.

ACKNOWLEDGEMENTS

The data presented in this article is the property of the operator of the facility, the SMEA (Mixed Syndicate of Allier Waters) – Commentry Local Commission, which the authors would like to thank for the authorization and provision of the data presented in this article. The authors would also like to thank GEOS for providing monitoring measurements.

REFERENCES

- Andersson, O., & Seppälä, M. (2015). Verification of the response of a concrete arch dam subjected to seasonal temperature variations. Master thesis, *KTH, School of Architecture and the Built Environment*.
- Bonelli, S. (2004). Analyse retard des mesures d'auscultation de barrages. *Revue française de Géotechnique*, 108, 31–45.
- De Granrut, M. D. B. (2019). Analyse et interprétation de la pression d'eau en fondation des barrages-voûtes à partir des mesures d'auscultation, *Doctoral dissertation*, Université Grenoble Alpes.
- Gahlouz, M. (2020). Analyse et interprétation des données d'auscultation des barrages par le modèle HST, *Doctoral dissertation*, Université Mouloud Mammeri Tizi Ouzou.
- Hoonakker, M., Aigouy, S., Fabre, J., Geffraye, G., & Pons, E. (2012, November). Effets thermiques et maîtrise des sollicitations de voûtes en vallée large, surveillances particulières, *Colloque CFBR Auscultation des barrages et des digues-Pratiques et perspectives*, pp. 27–28, Chambéry.
- Pretorius, C. J., Schmidt, W. F., Van Staden, C. S., & Egger, K. (2001, March). The extensive geodetic system used for the monitoring of a 185 metre high arch dam in Southern Africa, *Proceedings of 10th FIG International Symposium on Deformation Measurements* (pp. 19–22).
- Sangaré, S. (2003). Déplacement des barrages en béton: comparaison entre mesures in situ et calculs par modèles statistiques et déterministes. Mémoire de maîtrise, *École Polytechnique de Montréal*.
- Yigit, C. O., Alcay, S., & Ceylan, A. (2016). Displacement response of a concrete arch dam to seasonal temperature fluctuations and reservoir level rise during the first filling period: evidence from geodetic data. *Geomatics, Natural Hazards and Risk*, 7(4),1489–1505.

Multipurpose dams – A European perspective

A. Palmieri

Independent Water Infrastructure Adviser, Italy

D. Maggetti & A. Balestra

Lombardi Engineering Ltd., Switzerland

ABSTRACT: The first draft of ICOLD bulletin 171 on Multipurpose Water Storage (MPWS) was circulated in May 2015 during the ICOLD Congress in Stavanger and finally published in 2017. The scope of the bulletin is to provide a view of the dynamics of MPWS in terms of essential elements and emerging trends. In December 2020 a national working group of the Italian Committee on Large Dams (ITCOLD) has been created and started its activities on this topic.

Before the end of the twentieth century, it was predicted (Keller et al. 2000) that one-third of the developing world would have faced severe water shortages by 2025. Since this prediction, it has been observed pressure growing on water resources, with key drivers being more people, growing economies, and increasing hydrological variability.

The true renewable water resource is precipitation, be it in the form of rain or snow. Sporadic, spatial and temporal distribution of precipitation rarely coincides with the demand. Whether the demand is for natural processes or human needs, the only way water supply can match demand is limiting demand itself to match supply, or through the creation of storage to supplement low flow periods.

A ‘Multipurpose’ role is recognized as a key factor in the development of projects involving dams and reservoirs. Sharing benefits between users and needs emphasizes the multiple benefits of dams and reservoirs and fosters acceptance by stakeholders and communities.

For many existing European dams, MPWS has often become a ‘de facto reality’, even for officially single-use dams, because additional requirements are often introduced to the initial single purpose during the life of the works. This introduces constraints that often conflict with each other and with the optimization of the original single purpose. Economic considerations, related to opportunity costs, are also relevant. Therefore, the different uses must be wisely managed, and fairly allocated among different beneficiaries.

A multifunctional approach can better assess the real value of dams and reservoirs, considering both economic and financial aspects.

RÉSUMÉ: La première version du bulletin 171 de la CIGB sur le stockage de l’eau à buts multiples (anglais Multipurpose Water Storage, MPWS) a été diffusée en mai 2015 lors du congrès de la CIGB à Stavanger et a finalement été publiée en 2017. L’objectif du bulletin est de fournir une vue d’ensemble de la dynamique des MPWS en termes d’éléments essentiels et de tendances émergentes. En décembre 2020, un groupe de travail national du Comité italien des grands barrages (ITCOLD) a été créé et a commencé ses activités sur ce sujet.

Avant la fin du vingtième siècle, on prévoyait (Keller et al. 2000) qu’un tiers du monde en développement serait confronté à de graves pénuries d’eau d’ici 2025. Depuis cette prédiction, nous avons observé une pression croissante sur les ressources en eau, dont les principaux facteurs sont l’augmentation de la population, la croissance des économies et le réchauffement climatique.

La véritable ressource en eau renouvelable est la précipitation, que ce soit sous forme de pluie ou de neige. La distribution spatiale et temporelle sporadique des précipitations coïncide rarement avec la demande. Que la demande soit liée à des processus naturels ou à des besoins humains, le seul moyen pour que l’approvisionnement en eau corresponde à la demande est de

limiter la demande elle-même pour qu'elle corresponde à l'offre, ou de créer des réservoirs pour compenser les périodes de faible débit.

Le rôle "polyvalent" est reconnu comme un facteur clé dans le développement de projets impliquant des barrages et des réservoirs. Le partage des bénéfices entre les utilisateurs et les besoins met l'accent sur les avantages multiples des barrages et des réservoirs et favorise leur acceptation par les parties prenantes et les communautés.

Pour de nombreux barrages européens existants, le MWPS est souvent devenu une réalité "de facto", même pour les barrages officiellement à usage unique, car des exigences supplémentaires sont souvent ajoutées à l'objectif unique initial au cours de la durée de vie des ouvrages. Cela introduit des contraintes qui entrent souvent en conflit les unes avec les autres et avec l'optimisation de l'objectif unique initial. Des considérations économiques, liées aux coûts d'opportunité, entrent également en ligne de compte. Par conséquent, les différentes exigences doivent être gérées judicieusement et équilibrées entre les différents bénéficiaires.

Une approche multifonctionnelle permet de mieux évaluer la valeur réelle des barrages et des réservoirs, en tenant compte des valeurs économiques et non économiques.

1 A RENEWED GLOBAL INTEREST IN MULTIPURPOSE RESERVOIRS

Dam sites, particularly storage sites, are scarce national resources, and so it makes sense to consider how to extract maximum benefit from them. In addition, since these civil works may last for 100 years or more, they represent strategic long-term investments in the future, and so should be viewed from this long-term perspective, which demands for flexibility in use over time.

As global warming contributes to increasing variability in rainfall, agricultural production, floods, etc., storage becomes more valuable, and dam projects need to be designed with this in mind. Countries that have developed significant storage capacity have become reluctant to develop more, while developing nations are struggling to build their stock. Therefore, in order to match the high demand, it is reasonable to expect the need to increase the use of the existing reservoirs. Indeed, in recent years there has been a gradual increase in interest in multipurpose water reservoirs (MPWS).

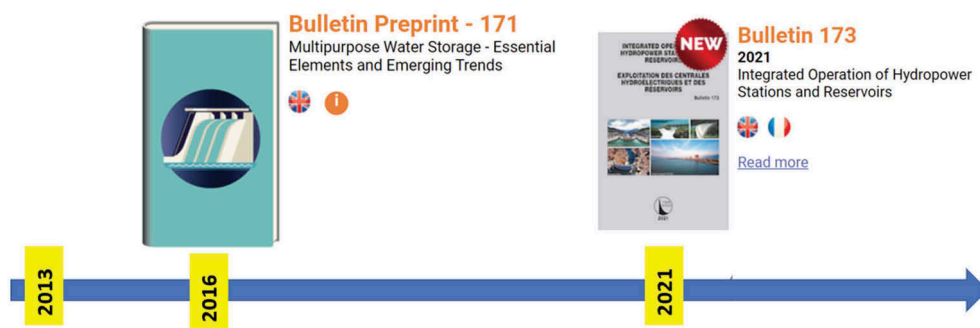


Figure 1. Timeline of ITCOLD Bulletin publications related to MPWS.

2 THE ITCOLD WORKING GROUP ON "EXISTING DAMS AND MULTIPURPOSE RESERVOIRS"

In 2021, ITCOLD (the Italian chapter of ICOLD) launched a working group on MPWS. Initial elaborations used ICOLD Bulletin 171 to analyze trends of mean annual flows and their variability of major Italian rivers (Balestra, A, 2021 unpublished). The analyses compared variations in two periods: 1970-2000 vs 2000-2020 and 1970-2010 vs 2010-2020 (Figure 2).

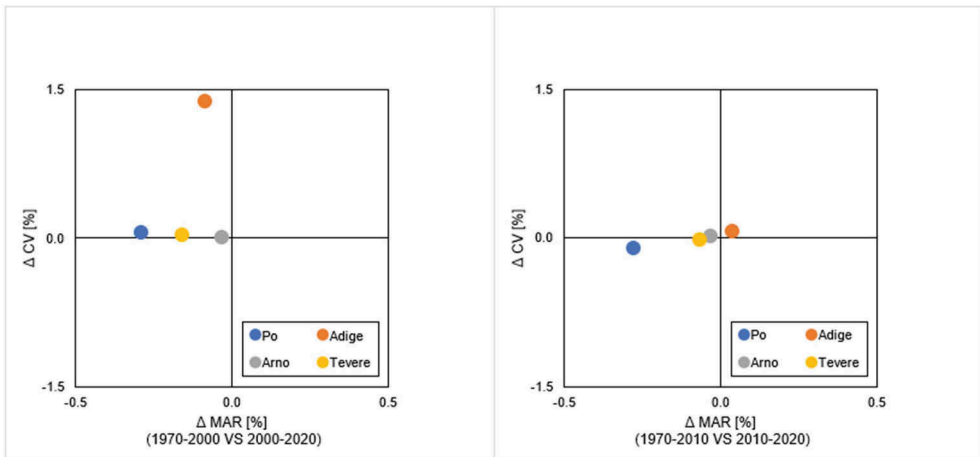


Figure 2. Trends of mean annual flows and their variability of major Italian rivers.

In both periods, a trend of declining flows (MAR) can be observed. A larger variability of the flows (CV) can be observed in the longer period, while the more recent period exhibits more stable flows.

These results indicate scenarios that are mostly unfavorable (Figure 3), or at least complex, for the realization of new storage in the analyzed water basins (ICOLD Bulletin 171 2016).

Soon, it should therefore be expected that adding new purposes to existing reservoirs will be a rising trend because of the increased economic value of water storage.

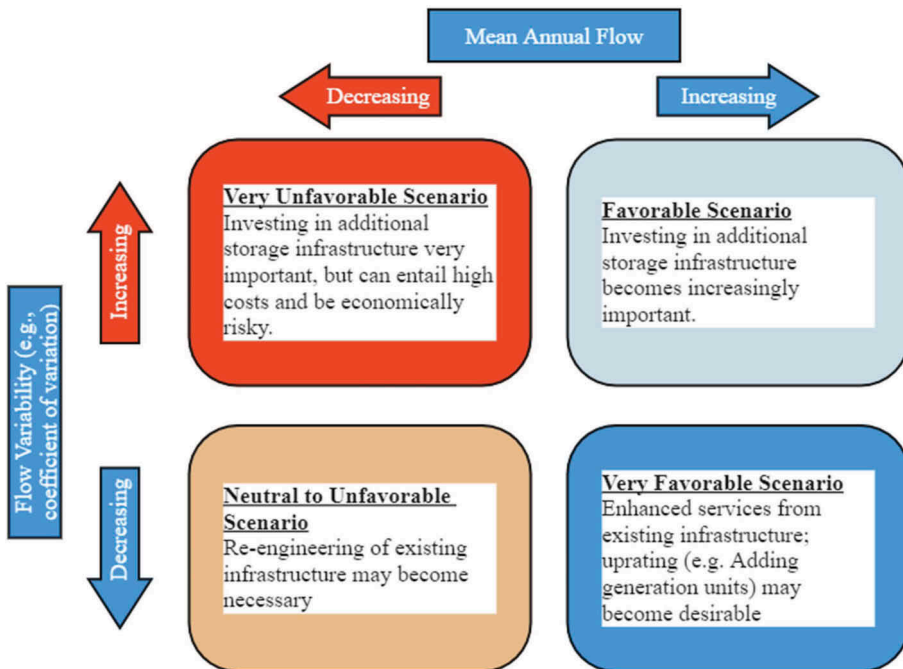


Figure 3. Interpretation key according to ICOLD Bulletin 171.

In this context, it is important to appreciate the difference between financial and economic analysis. In fact, the boundaries of analysis differ depending on whether the perspective is

economic or financial. The financial analysis concentrates on costs and benefits that accrue to the project entity and is of particular concern to the developer and investors.

Differently, the economic analysis seeks monetization of welfare gains and losses. That way economic analysis takes a wider view to determine the impact on society; it includes externalities and is of concern to the other stakeholders, particularly the government.

Consultations with operators of Italian water infrastructure, mainly hydro, revealed the following emerging topics¹:

Table 1. Emerging topics of Italian water infrastructure.

	Economic value	Financial viability
Priority rehabilitations	Moderate	Very high
Sedimentation management	High	Moderate to high
Supporting local economy	Very high	Negligible
Flood and drought mitigation	Very High	Negative
Water quality	High	Negligible

In accordance with the differentiation given above, the second and third columns of Table 1 assess, respectively, the economic value and the financial viability of the topics.

The perspective of the above analysis is that of a hydropower concessionaire, for whom the last three MPWS functions have negligible to negative financial viability, while being economically important for society. At the same time, the perspective would be different for a concessionaire that uses the reservoir to supply water for potable and industrial uses. Water quality and sedimentation management would have from high to very high financial viability for the water supply concessionaire.

Figure 4 shows, in qualitative terms, the difference between economic and financial perspectives for the most common water uses. It should be noted that the two perspectives coincide in the case of electricity generation, while they are always different for other uses.

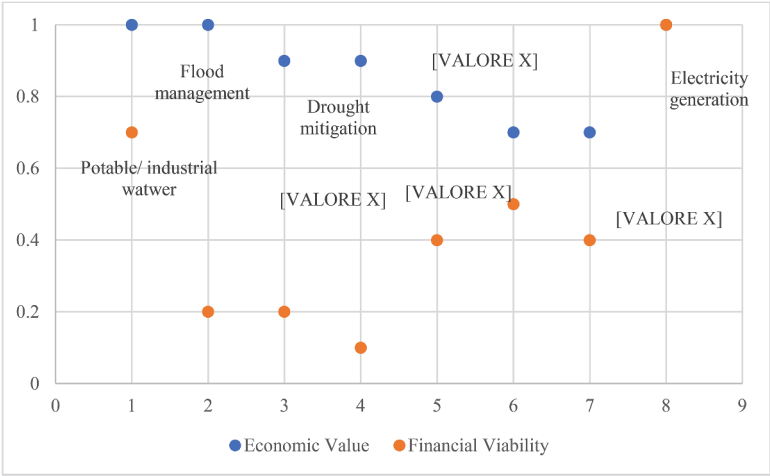


Figure 4. Qualitative difference between economic and financial perspectives for the most common water uses.

1. Another long-term ITCOLD’s initiative “Dams and Territories” also provided valuable information on the matter. In particular: Mazzà, G., and Frigerio, A. “Assessment of the relationship between dam owners and host territories: the Italian experience”. SANCOLD, Johannesburg, South Africa, May 2016.

In both economic and financial terms, the above considerations imply the existence of opportunity costs when uses other than those in the concession are made of the reservoir. As a matter of fact, the opportunity cost is the (monetary) value of water in its highest alternative use. A positive opportunity cost indicates losses with respect to the expected revenues, and a negative opportunity cost indicates added revenues.

3 THE OPPORTUNITY COST OF UNRECOGNIZED SERVICES

Naming the uses not foreseen in a concession agreement “other uses”, an empirical analysis of the opportunity costs was carried out with reference to hydropower concessions in Italy. The following methodology was used.

- i) Identify the main/ prevalent use (hydroelectric in all cases).
- ii) Use hydrological series of monthly inflows in the reservoir.
- iii) Define reference operating rules for the main use and the corresponding revenues.
- iv) Simulate reservoir operation for “other uses”, quantifying their impacts on water resources management.
- v) Quantify the opportunity costs associated with the “other uses”.

The following tables summarize the results obtained under different conditions for two hydropower schemes: the first, Taio-Santa Giustina, an alpine scheme designed for spot energy production (V_{in}/V_{active} ca. 10); the second, Corbara, a reservoir scheme with a greater reservoir turnover (V_{in}/V_{active} ca. 30).

Table 2. Opportunity costs associated with “other uses” of Taio Santa Giustina hydropower plant.

Case Study Taio Santa Giustina	Lost revenue compared to a reference scenario	
	Steady prices	Spot market
Continuous generation “average” year (2015)	12.6%	
Continuous generation “dry” year (2006)	29.7%	
“Static” flood control capacity “average” year (2015)	12.7%	0.9%
“Static” flood control capacity “dry” year (2006)	30.4%	0.9%

Table 3. Opportunity costs associated with “other uses” of Corbara hydropower plant.

Case Study Corbara	Lost revenue compared to a reference scenario	
	Steady prices	Spot market
Continuous generation “average” year (2013)	9.9%	
Continuous generation “dry” year (2007)	28.8%	
“Static” flood control capacity “average” year (2013)	5.8%	5.6%
“Static” flood control capacity “dry” year (2007)	6.3%	4.6%

In the case of flood mitigation, the order of magnitude of the “average loss” is between 1 and 6% of the expected revenue in the reference scenario. Such service entails “reasonable”, yet not necessarily acceptable, revenue losses.

On the other end, “continuous generation” has deleterious consequences particularly on reservoirs with smaller turnover ratios commonly used for spot market production (losses up to 30% of the expected revenue, in a dry year). Continuous generation corresponds to sustained releases of water to support “other uses” downstream. Since such an operation defeats the purpose of a regulating reservoir, the result is not surprising.

4 AN INTERNATIONAL CONSULTATION

The above results were discussed within the ITCOLD Working Group members, especially with the concessionaires. Different perspectives emerged, without clear indications that could

be used to move the process forward. Sensing a stalemate in the process, it was therefore decided to reach out a broader audience, outside Italy. The box in Figure 5 summarizes the circulated questionnaire.

<p>Context</p> <p>Water storage offers the possibility of meeting several demands, providing services as economies develop, as circumstances change, and as societal values evolve. Hydro with storage is a remarkable example of the above.</p> <p>Private entities, who operate hydro projects under a concession contract, may be requested, by regional/national authorities to provide services related to other purposes than hydro. Examples include emergency releases in severe drought periods, providing static flood routing capacity, maintaining a given water level for recreational purposes, etc.</p> <p>In most of the cases, such "other services" conflict with optimal hydropower generation and have, therefore, an opportunity cost for the hydro operator.</p> <p>Questions</p> <p>Q1: are such other services clearly spelled out in the concession contracts?</p> <p>Q2: are such other services compensated?</p> <p>Q3: is the compensation realized by reducing the concession fees?</p>
--

Figure 5. Circulated questionnaire.

Feedback was received from experts from Brazil, France, Japan, New Zealand, Norway, South Africa, and Switzerland². Contributions are individually acknowledged with thanks. The above countries are considered “mature” in terms of dams and hydro development and, as such, representative for reflecting their feedback in the Italian context.

The answers to the questionnaire are reported in the Annex at the end of the article, while the authors’ stocktaking of the feedback is presented in Table 4.

5 THE ROLE OF STRUCTURAL SOLUTIONS

Multipurpose use of existing water reservoirs represents a non-structural solution³ to provide services that meet evolving society’s demands. At the same time, it should be realized that, in the long run, structural solutions will inevitably be required. A couple of relatively unconventional solutions are discussed in the following.

The fact that glaciers are retreating in the Alps has been known since the late 1800s. In some areas, the phenomenon leaves empty depressions, which can be used as reservoirs with the construction of retention dams. To the authors’ knowledge this opportunity is being contemplated in the Swiss Alps, and could also be studied in other alpine countries.

2. Federal Energy Office, Cantons of Grisons, Ticino, and Valais.

3. While that can be broadly considered the case, in some situations, structural interventions may be required to consent multipurpose uses.

Table 4. Summary of the questionnaire’s main findings.

Subject	Preliminary feedback
Regulatory Framework aspects	Concessions contracts, from State entities to private operators, have similar structures internationally, albeit with different names, durations, and obligations.
Q1: are such “other services” clearly spelled out in the concession contracts?	Not in all countries/ jurisdictions. When that is the case, they mostly refer to flood management.
Q2: are such other services compensated?	No direct compensation is generally provided. Except for flood-preparation releases (Japan), and for project-specific agreements (Switzerland). Explicit compensation for “other services” can be an interesting way to make hydro with storage more <u>economically</u> viable again (Brazil).
Q3: do forms of compensation include reductions in the concession fees?	No experience was reported.

The Italian peninsula features remarkable differences between the North areas (Alps river basins) and the Central-South areas (Apennines river basins). A declining hydrological trend has been recorded in Italy in terms of water resource availability. In the last 30-year climatological period 1991-2020, with a value of more than 440 mm, water availability decreased by 20% compared to the historical reference value of 550 mm, about 166 km³ recorded between 1921-1950. Long-term estimates (1951-2021) also show a significant reduction, about 16% less than the historical average annual value according to ISPRA (2023). In the last decade, a trend of alternating droughts has been observed between the North and the Central-South regions. The distribution of water reservoirs (large dams), in the Italian peninsula, is shown in Figure 6⁴.

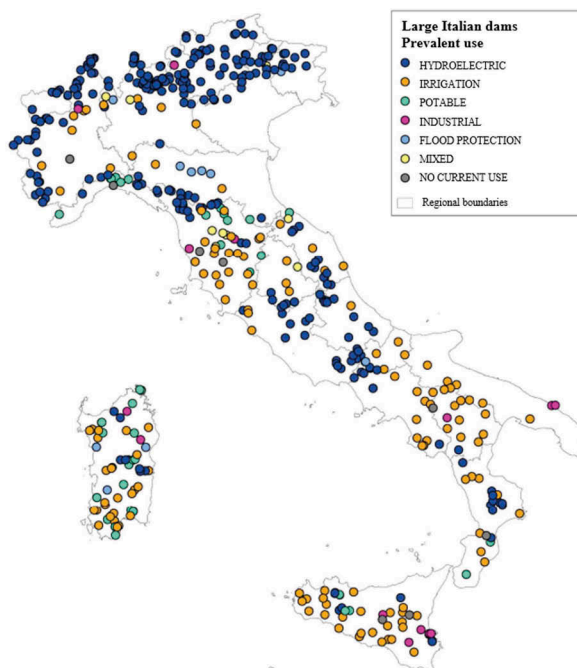


Figure 6. Distribution and purpose of reservoirs created by large dams in Italy (greater than 3 mio. m³), adapted from ISPRA (2020).

4. ISPRA (2020)

A structural solution for mitigating regional water scarcity was suggested by Fanelli, M. et al. (2018)⁵, which featured a long-range interconnection among existing reservoirs through a system of hydraulic galleries that would work by gravity. The system, which has been studied at the pre-feasibility level, would allow to re-distribute inflows, from high-intensity precipitations, within the entire system. That would both mitigate hydrogeological distress and facilitate water storage to face scarcity periods. Electricity generation would be increased and, in general, multipurpose uses of the water resource would be enhanced.

6 REFLECTIONS AND CONCLUSIONS

Private entities that operate hydro projects under a concession contract may be requested, by regional/ national authorities, to provide services related to other purposes than hydro. Since, in most cases, such “other services” conflict with optimal hydropower generation and, therefore, have an opportunity cost for the hydro operator, it is fair that the private entities are supported by appropriate management and compensation models for the services rendered. Clearly spelling out these other services in the concession contracts would contribute to facilitating the provision of such economically important functions of water reservoirs.

It is necessary to have better collaboration between all the stakeholders involved, so that all of them can take advantage of the multiple benefits of MPWS and foster acceptance by stakeholders and communities.

The provision of “other services” features different approaches outside Italy, from which some lessons can be derived. Explicit compensation for “other services” can be an attractive way to make hydro with storage more economically viable.

ACKNOWLEDGEMENTS

The authors acknowledge the inputs provided, by the professionals representing Italian Concessionary Utilities: Alperia Green Power, Compagnia Valdostana Acque, Edison, Enel Green Power, Ente Acque della Sardegna, Sorical. The contribution of Giuseppe Donghi (Senior Adviser, Edison) to the formulation and the analysis of case studies has been particularly appreciated.

Furthermore, the authors recognize that the feedback received represents the opinions of the individuals that kindly responded to the questionnaire, and not necessarily those of the Institutions in which they work. The experts that contributed their valuable responses are hereby acknowledged: Rogeiro Abreu Menescal (Brazil); Pierre Jacques Lorillou (France); Masayuki Kashiwayanagi (Japan); Craig Scott (New Zealand); Lervik Katrin (Norway); Quentin Shaw (South Africa); Rocco Panduri, Sandro Pitozzi, Beat Hunger, Joël Fournier (Switzerland).

REFERENCES

- Fanelli, M., Mazza, G., Frigerio, A., (2018) “The integrated management of water crises. The case for long-range hydraulic interconnections.”. *L’ Acqua magazine*, 6/2018.
- ICOLD (2016) “Multipurpose Water Storage- Essential elements and emerging trends” *Bulletin 171 International Commission on Large Dams*.
- ISPRA (2023) “Disponibilità idrica nazionale. BIGBANG ISPRA: nell’ultimo trentennio diminuita del 20%”.

5. Fanelli, M., Mazza, G., Frigerio, A., (2018) “The integrated management of water crises. The case for long-range hydraulic interconnections.”. *L’ Acqua magazine*, 6/2018.

- Mazzà, G., Frigerio, A. (2016) “Assessment of the relationship between dam owners and host territories: the Italian experience”. SANCOLD, Johannesburg, South Africa.
- Policicchio, R. (2020) “Le risorse idriche nel contesto geologico del territorio italiano. Disponibilità, grandi dighe, rischi geologici, opportunità”. ISPRA.

ANNEX

The following tables report the answers to the questionnaire.

Table 5. Regulatory framework aspects.

Country	Regulatory Framework aspects
Brazil	Hydropower plants, operated by non-public entities, are subject to concession contracts.
France	Hydro concessions in France started relatively recently (compared to other European countries). Most concessions are held by EDF.
Japan	Almost all major hydropower plants are owned and operated by nine utility companies (TEPCO, KEPCO, etc.) and another wholesale company of electricity of J-Power. These dams are used exclusively for hydropower according to contracts between dam owners and MLIT (Ministry of Land Infrastructure and Tourism).
New Zealand	The hydropower sector operates within a trading market. All hydropower assets have “resource consents” which are their licenses to manage discharges. Hence power generators do not operate in a simple concession structure seen in some countries.
Norway	The Norwegian system is license-based and does not involve the use of “concession contracts” as such. In Norway, multi-purpose use of reservoirs is not common, although it may occur that reservoir owners have entered into private contracts with e.g., water supply utilities or fish-farming companies concerning the right to use water from either reservoirs or from the waterways.
Switzerland	In all cantons, hydropower projects are subject to concession contracts.

Table 6. Answers to Q1.

Country	Q1: are such “other services” clearly spelled out in the concession contracts?
Brazil	In the case of hydro with regulating reservoirs, Brazil has increasingly witnessed conflicts between hydro and “other services”. Hydropower concession contracts do not explicitly address this issue. Almost all other large reservoirs are operated by federal, state, or municipal agencies. Being them public entities, aiming at economic results, rather than financial viability, conflict among uses loses its meaning.
France	Being hydro concessions relatively recent, the subject has not yet emerged.
Japan	The reservoirs of hydropower dams have been frequently operated for flood mitigation use. MLIT enacted guidelines on reservoir operation in 2020, with the aim of maximizing flood mitigation functions. Guidelines apply all over Japan to both hydropower and irrigation reservoirs.
New Zealand	On river systems, hydropower dam owners are required to actively manage flows according to flood rules, these rules are regulated by the “resource consents”.
Norway	Normally, the Norwegian licenses for hydropower plants and reservoirs do not spell other services, except a term relating to flood risk control. All licenses include a standard clause that states “When releasing the natural flood-discharge downstream, the reservoirs should as far as possible not be increased».
	When licenses are given for hydropower production, operation constraints might be given in terms of summer levels to be reached in the reservoirs, a minimum water flow to be released downstream, etc. These limitations are normally given to take due care to the interests of the public such as landscape, tourism, fish, biological values, etc. The other interests/ services are not clearly spelled out in the conditions themselves, only discussed in the government’s deliberations that form the basis of the license.
Switzerland	Depends on the Canton. “Other services” are contemplated in Grigioni and Vallese.

Table 7. Answers to Q2.

Country	Q2: are such other services compensated?
Brazil	No direct compensation is provided for “other services”. However, as most of the large hydros are part of the National Interconnected System (SIN), there is an implicit compensation, through the “guaranteed energy”, which is attributed to each hydro reservoir, based on the modeling of its connection to the SIN.
France	Being hydro concessions relatively recent, the subject has not yet emerged.
Japan	MLIT guidelines (2020) entitle dam owners to request compensation, in terms of opportunity costs, in case they need to lower reservoir levels in anticipation of floods. Flood forecasts are provided by Japan Meteorological Agency. Since 2020, no claims have arisen from any electricity company for such flood mitigation service.
New Zealand	There is no additional compensation to perform the flood management function, but operators will be fined (or in extreme cases license to operate removed) for not following the rules. Their only revenue comes from the hydropower market. Income varies according to the supply and demand situation in the market.
Norway	No. Limitations or changes in the operation of hydropower plants can only be prescribed at the time when the license is given, or when the license conditions are revised after 50 years. There is no compensation if the services are included. There is a limitation on how heavy the new terms and conditions might be when the license is revised.
Switzerland	Compensation is foreseen or possible according to project-specific agreements/ contracts. Details of the compensation are agreed between the entities responsible for the “other services” (flood protection in particular) and the respective hydropower operators.

Table 8. Answers to Q3.

Country	Q3: do forms of compensation include reductions in the concession fees?
Brazil	Nowadays, there is a systematic disincentive for the construction of new regulating reservoirs. Explicit compensation for “other services” can be an interesting way to make hydro with storage more economically viable again.
France	Being hydro concessions relatively recent, the topic has not emerged.
Japan	No.
New Zealand	No.
Norway	The concession fee is linked to the size of the plant, and it is based on a theoretical calculation of the foreseen production, not the actual production. Hence, when there are changes in the reservoir operation rules, there is no change in the concession fee. Other taxes such as income tax, resource rent tax, etc. are based on the surplus of the hydropower company from year to year. These taxes will indirectly be reduced when such services are imposed through the license, as most of the services lead to reduced production.
Switzerland	In general, that is not the case. The Grigioni’s cantonal law foresees water reserves for the municipalities, which have the right to withdraw an agreed volume of water for drinking purposes. Provided the withdrawal shall not compromise hydroelectricity production, in a significant manner, otherwise, compensation is due to the hydropower concessionaire.

How to evaluate arch dam's behaviour under increased thermal load such as heat waves and extreme cold

E. Robbe & L. Suchier

EDF-CIH, La Motte-Servolex, France

A. Simon & T. Guilloteau

EDF-DTG, Saint-Martin-le-Vinoux, France

ABSTRACT: Arch dam's behavior is generally strongly influenced by thermal load. In summer, concrete expansion generates displacement of the arch toward upstream, which can lead in some cases to the opening of cracks on the downstream face and instability of gravity abutment. In winter, the arch moves toward downstream, increasing the opening of the dam-foundation interface at the upstream toe for the arch concerned by such issue.

Generally, for the evaluation of the arch dam behaviour during winter or summer load, average seasonal temperatures are used. In 2018, the French guidelines for the safety assessment of existing arch dam behavior proposed to carry out additional analyses which considers increased thermal loads. Such analyses should be performed for dams that show a particular vulnerability to thermal conditions such as very thin arches or arch dams in wide valley which are affected by opening of the dam-foundation interface.

The characterization of increased thermal loads is rather difficult because it is strongly dependent of the inertia of the structure itself: a thin arch dam will react quickly to a short but intense cold weather whereas the behavior of a thicker structure will depend on the temperature of the previous months.

The objective of this communication is to present a uniform methodology based on the monitoring on the dam's crest and statistical analyses involving the HSTT (Hydrostatic Seasonal Temporal Thermal), (Penot,2009) method developed by EDF, to define increased thermal loads with a specified return period. In the same manner that statistical analyses of monitoring data allow to evaluate the radial displacement of the crest of an arch dam during seasonal effect, the methodology allows to define an increase of displacement of the arch under a ten-year return period in winter or summer. Numerical modellings can then be calibrated to represent such an increase of displacement and be used to evaluate the behavior of the dam for such situations.

1 INTRODUCTION

Arch dam's behavior is generally strongly influenced by thermal load. In summer, concrete expansion generates displacement of the arch toward upstream, which can lead in some cases to the opening of cracks on the downstream face and instability of gravity abutment. In winter, the arch moves toward downstream, increasing the opening of the dam-foundation interface at the upstream toe for the arch concerned by such issue. That's why safety assessment of arch dam generally required to consider summer or winter thermal load in addition to hydrostatic and gravity loads in the numerical analyses.

In 2018, the French guidelines for the safety assessment of arch dam behavior (CFBR 2018) proposed to carry out additional analyses which considers increased thermal loads. The main

purpose of this is to quantify this thermal sensitivity. Such analyses should be performed for dams that show a particular vulnerability to thermal conditions which could initiate a specific failure mode. The characterization of increased thermal loads is rather difficult because it is strongly dependent on the inertia of the structure itself. In addition, such load should be related to a probability.

The aim of this paper is to present an original method for existing dam, based on monitored displacement. For arch dams, the displacement at the crest is somehow representative of the whole behavior of the dam: the crest behavior is in a way “integrating” the behavior of the structure over its whole height.

The central assumption of the proposed methodology is that it only relies on the analyses of monitored radial displacement at the crest of arch dam, and when possible, at the crown cantilever, to evaluate and simulate the increased thermal load. This choice was motivated by the need to standardize and generalize the methodology.

In the frame of this first paper on this topic, only arch dams monitored by pendulums are considered. An example of the application of the proposed method for an arch dam is presented.

2 STATISTICAL PROCESSING OF MONITORING DATA AND METHODOLOGY

The establishment of the methodology requires the statistical analysis of two types of data:

- Reliable temperature series with at least more than 45 years of mean daily temperature measurements. Without temperature measurement, each dam is associated with one of the height reference stations throughout France according to its geographical location.
- Monitoring data of the arch dams, in particular the radial displacements at one point of the crest, and when possible, in the crown cantilever with at least 10 years of reliable data.

2.1 Monitoring data and the HSTT model

The Hydrostatic Seasonal Temporal Thermal model (HSTT) was developed by EDF (Penot 2009) to improve the well-known HST model following the 2003 heat wave event to take into account average seasonal thermal effect as well as real mean daily air temperature. The statistical model, calibrated using multiple linear regression on chosen monitored measurement, allows to highlight:

- irreversible effect related to time t :

$$g_1(t) = b_1 t$$

- reversible hydrostatic effect related to the reservoir level h , normal water level NWL and reservoir level when empty WL_{empty} :

$$g_2(Z) = b_2 Z + b_3 Z^2 + b_4 Z^3 + b_5 Z^4 \quad (2)$$

$$\text{with } Z = \frac{NWL - h}{NWL - WL_{empty}} \quad (3)$$

- thermal effect related to the temperature distribution in the structure, which can be divided into two terms:
 - A sinusoidal “seasonal” term representing at best the mean annual evolution of temperatures related to a seasonal variable S going from 0° the 1st of January and 360° the 31th of December,

$$g_{3a}(S) = a_6 \cos(S) + a_7 \sin(S) + a_8 \cos(2S) + a_9 \sin(2S) \quad (4)$$

- A component accounting for temperature deviation from the seasonal average.

$$g_{3b}(t) = K \Delta\theta_R(t) \quad (5)$$

With $\Delta\theta_R(t)$ the delayed temperature deviation from the mean seasonal temperature computed from the following formula involving the characteristic time T_0 of the thermal diffusion inside the dam.

$$\Delta\theta_R(t + dt) = \Delta\theta(t + dt) \left(1 - e^{-\frac{dt}{T_0}}\right) + \Delta\theta_R(t) e^{-\frac{dt}{T_0}} \quad (6)$$

This last component $g_{3b}(t)$, can be used to quantify the intensity and duration of an exceptional event. This component is a product of two factors computed at the end of the HSTT model calibration:

- K , computed from multiple linear regression. It quantifies the sensitivity of the phenomenon to temperature deviations from the mean. In the case of a displacement, K is expressed in $mm/^\circ C$.
- The second term $\Delta\theta_R$ results from a manipulation of the instantaneous temperature deviations from the mean seasonal temperature. Thanks to a numerical parameter, T_0 , derived from the HSTT model, this second term considers both the duration and the intensity of cold or warm periods considering the thermal inertia of the phenomenon.

The parameter T_0 is representative of the inertia of the structure for the phenomenon considered. While a low T_0 indicates short response times for thin structures, a higher T_0 will be more often encountered for thicker structures. This parameter is expressed in days, and the operation (6) computes what would be called the “delayed temperature deviations” corresponding to the parameter $\Delta\theta_R$ previously used, taking into account the heat propagation into a wall with a chosen thickness related to T_0 .

2.2 Gumbel's law for the evaluation of the probability of occurrence

The probability of occurrence of a critical event can be determined with the use of Gumbel's law, which is a special case of the generalized extremum law. This is a very satisfactory approximation of the law of maximum when analyzing a sample of independent random variables all of them following the same law. We use this law to determine the probability of occurrence of an event related to temperature.

From the maxima identified over a fixed period, we associate an empirical frequency F to these maxima which is given by the Hazen formula:

$$F[i] = \frac{i - 0.5}{n} \quad (7)$$

where i = rank of the maxima in the sorted list; n = number of years over which the statistic is calculated.

The Gumbel statistic G is then obtained by the formula:

$$G[i] = -\ln(-\ln(F[i])) \quad (8)$$

This allows us to associate a statistical probability with an event that is part of a list of events sorted in ascending order.

2.3 Outline of the methodology

To evaluate a radial displacement increment at the crest due to temperature deviations from the seasonal normal, it is necessary to know the parameters K and T_0 from the HSTT model

(see chapter 2.1) of the monitored phenomenon. Arch dams are instrumented by pendulums which provide sufficient data to perform a reliable HSTT analysis over a significant period, making it possible to obtain the K and T0 parameters.

The increased thermal load is thus expressed in the form of a displacement increment D_{10} , generally for a ten-year return period. This displacement must be found at the point studied at the crest, and then possibly, in the crown cantilever. Displacement increment should be computed in winter $D_{10winter}$ or/and in summer $D_{10summer}$.

Once this increase of displacement is quantified, calibration of the finite-element analyses is performed so as to find the loads that reach the displacement increment D10.

3 STATISTICAL TREATMENT OF MONITORING DATA AND APPLICATION OF THE METHODOLOGY

3.1 Steps of the methodology for the arch dams monitored by a pendulum at the crest

Figure 1 describes the method used to define the ten-year thermal loading of the arch dams tested by a pendulum at the crest. This methodology consists of the following two successive steps:

- The determination of a temperature increment θ_{10} from a Gumbel statistic performed on the delayed temperature deviation $\Delta\theta_R$ (steps 1a and 1b).
- The estimation of the increment of displacement increased D_{10} at the point studied at the crest (step 2) from a simple multiplication between the coefficient K of the associated phenomenon and the θ_{10} value found in the previous step.

Step 3 involves the numerical implementation of the ten-year thermic loadings.

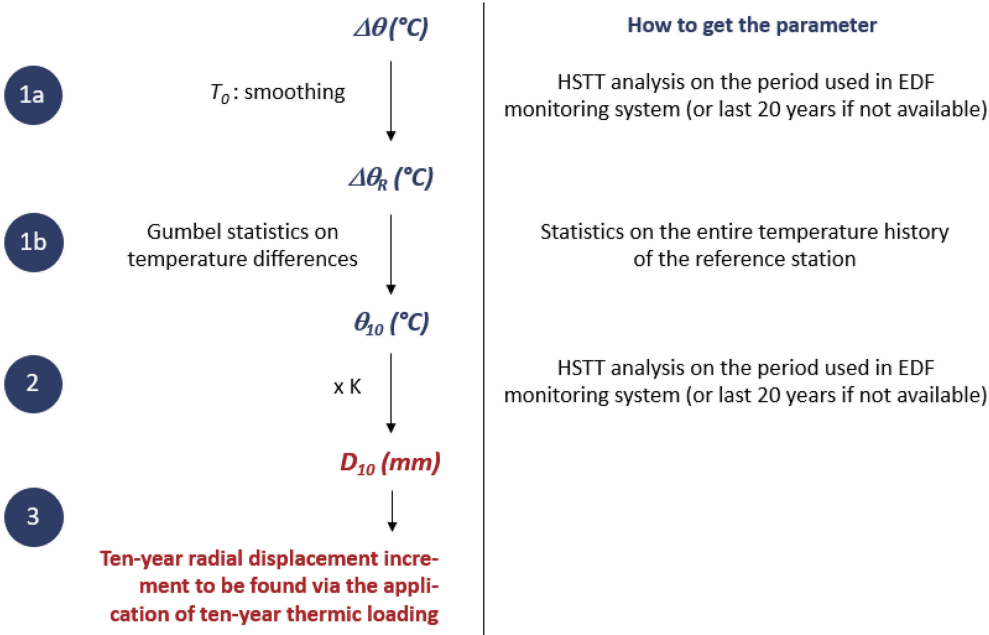


Figure 1. Methodology for obtaining the ten-year radial displacement increment for arch dams monitored by one or more pendulums at the crest.

3.2 Determination of the ten-year temperature deviation θ_{10}

Difference between instantaneous temperature and mean seasonal temperature provides instantaneous temperature deviation. The successive steps for the determination of the ten-year temperature deviation θ_{10} are summarized in Figure 2 and below.

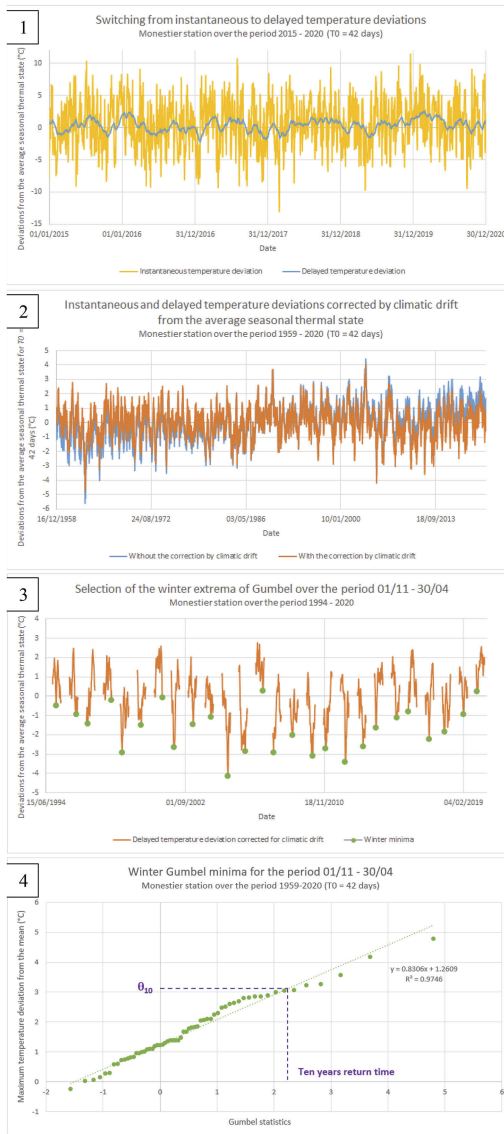


Figure 2. Successive steps for the determination of the ten-year temperature deviation $\theta_{10, winter}$.

- 1) Switch from instantaneous temperature deviation to delayed temperature deviations $\Delta\theta_R$ using equation (6),
- 2) Correction by climate drift due to climate change (about 2°C between 1980 and 2020 in France) so that climate change - distorting deviations from the mean - is not included in the study,
- 3) Determination of the annual extreme delayed temperature deviation. Depending on the event considered (heat of cold wave), the maximum annual delayed temperature deviation is picked: from 1st of November until 30th of April for winter event (as in Figure 2) or from the 1st of Mai until the 30th of October or summer event).
- 4) Use of the Gumbel statistic (§2.2) to determine the temperature associated with different occurrences (ten-year return-period of a cold event in this case).

3.3 Determination of the ten-year radial displacement increment in crest D_{10} for arch dams monitored by pendulums

From the parameter K calibrated by the HSTT modeling and the ten-year temperature deviation θ_{10} , the ten-year radial displacement increment at the point studied at the crest is obtained by the formula:

$$D_{10} = K \times \theta_{10} \quad (9)$$

This method has been applied to 28 EDF arch dams monitored by a pendulum in crown. A synthesis table allows to obtain for these arch dams the summer and winter ten-year radial displacement increments to be applied in crest.

Arch dam	Name of the pendulum	Position on the crest	Reference station	HSTT Data			Winter		Summer	
				Seasonal amplitude	T_0	K	θ_{10}	D_{10}	θ_{10}	D_{10}
							10-year event	10-year event	10-year event	10-year event
Arch dam 1	CD 600-584	Crest	Marcillac	8.29 mm	2.4 jours	-0.38 mm/°C	10.02 °C	3.81 mm	7.59 °C	2.88 mm
Arch dam 2	FG 668-625	Crest	Millau	8.34 mm	5.3 jours	-0.38 mm/°C	8.13 °C	3.09 mm	6.08 °C	2.31 mm
Arch dam 3	DE 566-307	Crown	Marcillac	13.78 mm	3.7 jours	-0.55 mm/°C	7.83 °C	4.31 mm	5.90 °C	3.25 mm
Arch dam 4	PA 1082-1031	Crown	Sentaraille	10.32 mm	6.0 jours	-0.49 mm/°C	7.24 °C	3.55 mm	4.84 °C	2.37 mm
Arch dam 5	PS 1555-1540	Crest	Sentaraille	5.57 mm	6.3 jours	-0.22 mm/°C	7.11 °C	1.56 mm	4.76 °C	1.05 mm
Arch dam 6	EF 411-368	Crown	Marcillac	16.21 mm	6.4 jours	-0.73 mm/°C	7.51 °C	5.48 mm	5.66 °C	4.13 mm
Arch dam 7	P 398-362	Crown	Lacaune	8.47 mm	6.9 jours	-0.38 mm/°C	7.71 °C	2.93 mm	5.25 °C	2.00 mm
Arch dam 8	DE 664-618	Crest	Marcillac	14.00 mm	9.8 jours	-0.76 mm/°C	6.32 °C	4.81 mm	4.82 °C	3.67 mm
Arch dam 9	PI 1552-1500	Crown	Monestier	4.04 mm	10.2 jours	-0.07 mm/°C	6.57 °C	0.49 mm	4.50 °C	0.33 mm
Arch dam 10	LI 582-481	Crest	Monestier	14.20 mm	10.4 jours	-0.56 mm/°C	6.52 °C	3.65 mm	4.97 °C	2.50 mm
Arch dam 11	EF 938-865	Crest	Millau	20.70 mm	12.3 jours	-0.81 mm/°C	5.78 °C	4.68 mm	4.41 °C	3.57 mm
Arch dam 12	GH 195-152	Crest	Marcillac	11.28 mm	12.4 jours	-0.57 mm/°C	5.66 °C	3.23 mm	4.95 °C	2.48 mm
Arch dam 13	FG 510-480	Crown	Marcillac	11.30 mm	13.1 jours	-0.64 mm/°C	5.51 °C	3.51 mm	4.24 °C	2.70 mm
Arch dam 14	KL1 2160-2081	Crown	Sentaraille	28.90 mm	13.2 jours	-1.05 mm/°C	5.13 °C	5.39 mm	3.56 °C	3.74 mm
Arch dam 15	PF 627-596	Crest	Lacaune	12.24 mm	13.6 jours	-0.55 mm/°C	5.69 °C	3.13 mm	4.02 °C	2.13 mm
Arch dam 16	EF 737-722	Crown	Castellane	7.72 mm	14.0 jours	-0.40 mm/°C	4.40 °C	1.76 mm	2.80 °C	1.12 mm
Arch dam 17	PD 1539-1406	Crown	Sentaraille	22.50 mm	14.0 jours	-1.05 mm/°C	4.98 °C	5.23 mm	3.46 °C	3.63 mm
Arch dam 18	Crown 766-678	Crown	Monestier	4.17 mm	14.2 jours	-0.11 mm/°C	5.68 °C	0.62 mm	3.88 °C	0.42 mm
Arch dam 19	KL 2212-2137	Crest	Sentaraille	27.00 mm	14.9 jours	-1.25 mm/°C	4.81 °C	6.01 mm	3.36 °C	4.20 mm
Arch dam 20	PS 1948-1924	Crest	Monestier	8.35 mm	15.8 jours	-0.34 mm/°C	5.40 °C	1.84 mm	3.69 °C	1.25 mm
Arch dam 21	FG 876-751	Crown	Castellane	10.85 mm	18.0 jours	-0.52 mm/°C	3.90 °C	2.03 mm	2.48 °C	1.29 mm
Arch dam 22	PIOT 5 301-290	Crown	Monestier	8.56 mm	18.1 jours	-0.54 mm/°C	5.05 °C	2.73 mm	3.45 °C	1.86 mm
Arch dam 23	CE 403-335	Crown	Castellane	10.67 mm	19.8 jours	-0.60 mm/°C	3.72 °C	2.23 mm	2.37 °C	1.42 mm
Arch dam 24	KL 1789-1565	Crown	Monestier	16.02 mm	20.1 jours	-0.52 mm/°C	4.78 °C	2.49 mm	3.27 °C	1.70 mm
Arch dam 25	GH 490-325	Crown	Monestier	17.15 mm	20.3 jours	-0.70 mm/°C	4.75 °C	3.33 mm	3.25 °C	2.28 mm
Arch dam 26	EF 515-438	Crest	Millau	8.56 mm	23.1 jours	-0.35 mm/°C	4.04 °C	1.41 mm	3.27 °C	1.14 mm
Arch dam 27	GF 1007-955	Crown	Millau	12.62 mm	42.2 jours	-0.81 mm/°C	2.74 °C	2.22 mm	2.42 °C	1.96 mm
Arch dam 28	OP 427-278	Crown	Monestier	20.24 mm	51.7 jours	-1.53 mm/°C	2.77 °C	4.24 mm	1.98 °C	3.03 mm

Figure 3. Application of the methodology to the 28 EDF arch dams monitored in crest.

For most arch dams, the radial displacement increment to be added to simulate a ten-year thermal load represents between 10 and 40% of the seasonal amplitude (obtained from annual temperature variations). This ratio is very dependent on the value of the T_0 : the thicker the dam, the larger the T_0 , and the less sensitive it is to temperature variations. On the other hand, the thinner the arch, the more likely it is to react quickly and significantly to a rapid or intense heat or cold wave.

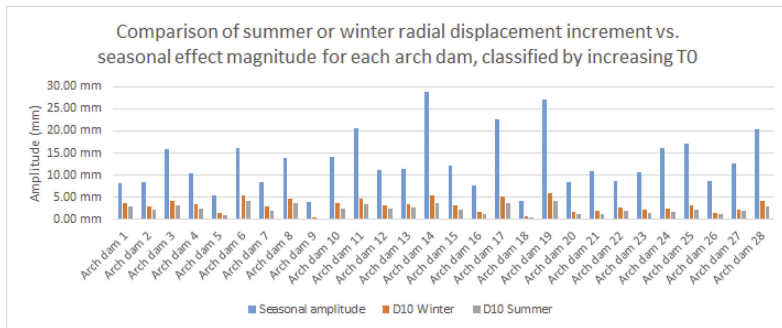


Figure 4. Comparison of summer or winter ten-year radial displacement increment vs. seasonal effect magnitude for each arch dam, ranked by increasing T_0 .

3.4 Numerical simulation of ten-year thermal load

With the aim of simulating increased thermal load with finite-element analyses, time-history analyses should be carried out to firstly simulate seasonal thermal load and secondly the increased thermal load.

Analyses involving seasonal thermal load are generally carried out using mean seasonal time-history air temperature at the crest and downstream face of the dam. Specific boundaries are also chosen at the upstream face of the dam considering the influence of the reservoir. Numerical model (properties, assumptions) is generally calibrated to fit seasonal displacement observed on different monitored points of the dam (including the crest).

Then the numerical implementation of the ten-year thermal modeling must be carried out with an increased scenario (Figure 5). The aim is to calibrate the temperature assumptions to reach the targeted ten-year radial displacement increment in crest D_{10} .

Warning: the numerical temperature increment used to find the peak radial displacement increment is different from the θ_{10} calculated using the Gumbel statistic and only related to the chosen phenomenon.

Following this calibration process, evaluation of the behavior of the dam can be carried out following CFBR guidelines criteria.

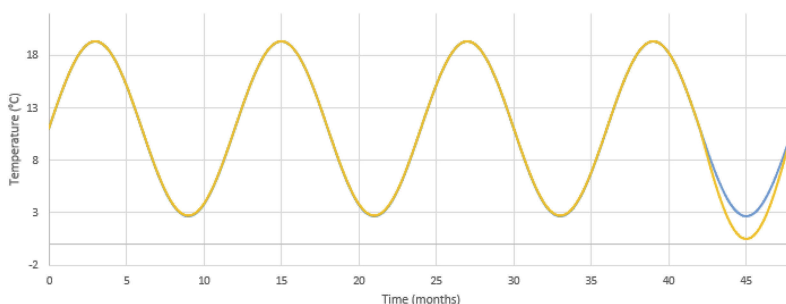


Figure 5. Simulation of an increased winter. (mean seasonal temperature in blue, with increased winter in yellow).

4 EXAMPLE OF THE APPLICATION OF A TEN-YEAR SUMMER THERMOAL LOAD ON AN ARCH DAM

In summer, expansion of the concrete with increasing temperature can lead to cracks on the downstream face, parallel to the abutment. Increase of the arch effect near the crest can also jeopardize the stability of a gravity abutment. In such case, the application of a ten-year summer thermal loading can be implemented to evaluate the consequences of an increased but probable thermal load.

An example on a French arch dam is proposed: downstream view of the dam and mesh used for the finite-element analyses, are given on the figures below.



Figure 6. Dam studied: view from downstream.

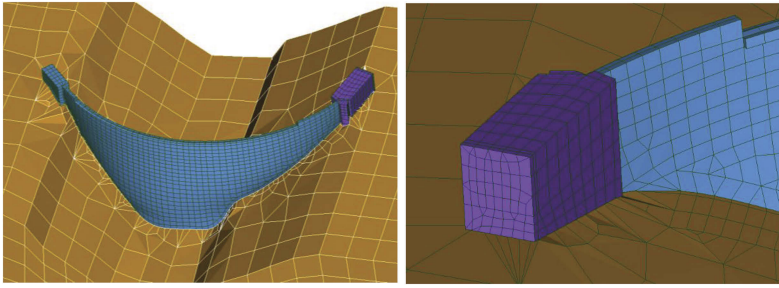


Figure 7. Geometry of the dam and zoom on the gravity abutment (in purple) studied at right bank.

Table 1. Evolution of the friction angle according to the thermal loading, on the gravity abutment studied at right bank.

Load case	NWL	NWL + Summer	NWL + ten-year Summer
ϕ^* (°)	24°	48°	54°
C** if $\phi = 45^\circ$ (kPa)	0 kPa	38 kPa	115 kPa
C** if $\phi = 50^\circ$ (kPa)	0 kPa	0 kPa	69 kPa

* ϕ (°) is the angle of internal friction require to assess the stability without any safety factor and without cohesion.

** C (kPa) is the cohesion required for a given friction angle.

Table 1 shows the stability evaluation of the gravity abutment studied at right bank under normal water level (NWL) with addition of summer or ten-year summer thermal conditions. It can be seen from this example that the friction angle required, initially 24° under NWL loading, reaches 48° when the summer thermal loading is applied and 54° under the ten-year summer thermal loading. For the stability evaluation of the gravity abutment, the increased thermal load has a strong influence on the results.

It is also interesting to measure the impact of a ten-year thermal scenario on the stresses observed on the upstream and downstream faces as presented in Figure 8 and summarized in Table 2. While there is a quite significant change in stress pattern between NWL load only and NWL + summer load, the stresses from summer to 10-year summer load remain in similar range: increase of compression and tensile stresses are respectively 0.1 and 0.5 MPa.

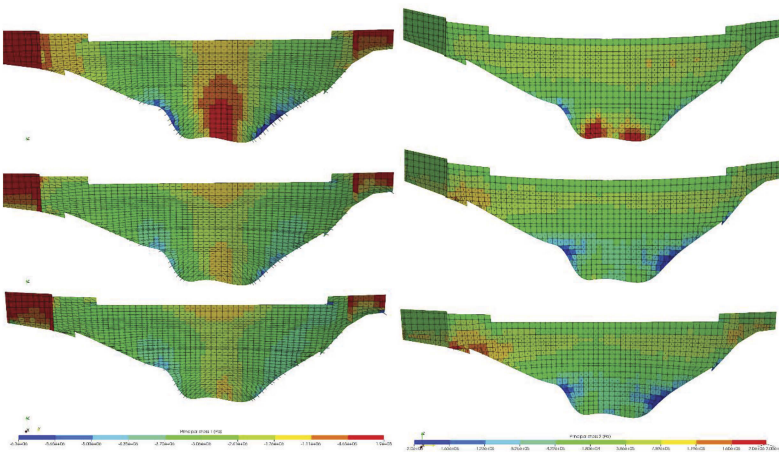


Figure 8. Comparison of the compression (left) and tensile (right) stresses on the downstream face of the dam at NWL (top), NWL + summer (middle) and NWL + summer10 (bottom).

Table 2. Evolution of stresses in faces near the left bank abutment (LA) and right bank abutment (RA) according to the thermal loading.

Load case	NWL	NWL + Summer	NWL + ten-year Summer
Max. crest displacement (mm)	22.1 mm	14.0 mm	11.7 mm
Downstream – Maximal compressive stress (LA)	-1.8 MPa (6.3 MPa)*	-5.1 MPa	-5.2 MPa
Downstream – Maximal tensile stress (RA)	0.3 MPa (2.3 MPa)*	1.3 MPa	1.8 MPa
Upstream – Maximal compressive stress (RA)	-2.4 MPa (5.4 MPa)*	-4.7 MPa	-5.6 MPa
Upstream – Maximal tensile stress (LA)	0.3 MPa (1.4 MPa)*	1.1 MPa	1.5 MPa

* For a better understanding, the maximum compressive and tensile stresses are indicated at NWL at the same location as for the other two loading cases with summer and ten-year summer (near the right bank (RA) or the left bank (LA) gravity abutment), in order to obtain comparable data. Absolute compressive and tensile maxima at the upstream and downstream faces are indicated in parentheses for information.

5 CONCLUSION

This paper presents an original methodology to characterize increased thermal load for arch dam based on monitored displacement and their analyses using HSTT method. The aim is to define a crest increased displacement of the dam related to a chosen period of return (typically a ten-year period) using Gumbel's law.

This methodology meets the requirements of the French guidelines for the safety evaluation of arch dam's behavior, which recommends studying certain arch dams under increased thermal load. The method presents the following negative and positive sides.

- Only relevant for existing operating dams since many years,
- Require having reliable and qualified air temperature and dam's crest displacement measurements.
- + Uniformity of the methodology allowing arch dams to be treated under equal conditions, simple to implement.
- + Easy to simulate several exceptional thermal loads with different time-return period.
- + Rely on monitored data representative of the real behavior of the dam.
- + Do not require to make hazardous assumptions relatives to thermal properties of the materials.

REFERENCES

- CFBR, 2018. Recommendations for the safety assessment of arch dam behaviour. In CFBR (ed.).
 I.PENOT & FABRE & DAUMAS, 2009. Analyse et modélisation du comportement des ouvrages de génie-civil par la prise en compte des températures de l'air: méthode HST Thermique, Q91 -R60, Commission internationale des grands barrages, Brasilia 2009.

Importance of hydropower reservoirs and dams in Europe to mitigate the energy crisis and to serve as a catalyst and enabler for the Green Deal

A.J. Schleiss

ICOLD-EPFL, Coordination Team ETIP HYDROPOWER, Switzerland

J.-J. Fry

EURCOLD, Coordination Team ETIP HYDROPOWER, France

M. Morris

Samui, Coordination Team ETIP HYDROPOWER, France

ABSTRACT: Hydropower has a long tradition in Europe and contributed significantly during the last century to industrial development and welfare in most of the countries in Europe. The ambitious plan for an energy transition in Europe now seeks to achieve a low-carbon climate-resilient future in a safe and cost-effective way, serving as an example worldwide. The key role of electricity will be strongly reinforced in this energy transition. In many European countries, the phase out of nuclear and coal generation has started with a transition to new renewable sources comprising mainly of solar and wind for electricity generation. However, solar and wind are variable energy sources and difficult to align with demand. The IEA (2021) concludes that hydropower provides “unmatched” flexibility and storage services required for ensuring energy security and delivering more solar and wind power onto the grid. In the future, these services will be in much greater demand to achieve the energy transition in Europe, and worldwide. Hydropower has all the characteristics to serve as an excellent catalyst and enabler for a successful energy transition. The HYDROPOWER EUROPE Forum brought together some 650 relevant stakeholders representing all sectors (including design, construction, production, sectoral associations, environmental and social issues), who participated actively for 40 months (2018-2022) through an extensive program of review and consultation addressing needs of the whole hydropower sector targeting an energy system with high flexibility and renewable energy share. The follow-up ETIP HYDROPOWER project (2022-2025) consolidates the strong network of the HYDROPOWER EUROPE Forum into a sustainable association and helps to unify the voices of hydropower in Europe. ETIP HYDROPOWER will facilitate, enhance and disseminate the Research and Innovation Agenda (RIA) and the Strategic Industry Roadmap (SIR) (drafted under the HYDROPOWER EUROPE project) taking into consideration the future needs of the sector and the R&I targets and the emerging policy priorities. This will help to ensure that hydropower can play the vital role of an enabler in the transition to a clean and safe energy system and the achievement of climate neutrality by mid-century. Furthermore, besides unifying the voices of hydropower, ETIP HYDROPOWER will further align and coordinate the industry RIA and SIR strategies to provide consensus-based strategic advice to the SET Plan (European Strategic Energy Technology Plan) covering analysis of market opportunities and research and development funding needs, biodiversity protection and ecological continuity. Another goal is, in one with Europe and the latest EU climate and energy related policies, deepening the understanding of innovation barriers and the exploitation of research results.

1 INTRODUCTION

Global warming is the biggest known threat for the 21st century. The European Union is the first continent to fight against global warming by announcing the European Green Deal, courageously showing the way for other countries and continents. The EU aims to be the first carbon-neutral continent by 2050. To fulfil this objective, PV and wind power will replace oil and coal for electricity generation. But PV and wind are very volatile energies. For integrating this huge amount of variable renewable electricity into the grid, Europe must also lead the development and integration of the high storage and flexibility capacity of hydropower into the new energy system, efficiently and cost-effectively. To provide an effective contribution to this unprecedented new European Green Deal in a sustainable, efficient, and cost-effective manner, the hydropower sector needs to develop strongly through technical and environmental innovations.

The current energy crisis reveals the importance of an independent electricity supply with high availability. Here the existing hydropower reservoirs already play an important role in helping to overcome the critical situation in winter 2022/23 as well as the following winters without the risk of blackout. New multi-purpose storage schemes and pumped-storage powerplants will be vital in future for a safe, independent and renewable electricity supply besides other services such as flood and drought protection to mitigate climate change effects. Nevertheless, to tackle environmental, societal, technological and market challenges, the hydropower sector needs to find novel approaches to future development in accordance with environmental and social demand.

The Research and Innovation Agenda (RIA) and the Strategic Industry Roadmap (SIR), released by the HYDROPOWER EUROPE Forum and now implemented under the ETIP HYDROPOWER project (both funded by the EU Horizon 2020 and Horizon Europe research and innovation programs), are key contributions to the growing debate on the net zero economy and the European Green Deal under the challenge of a safe and independent energy supply. They will be highly relevant for discussions on finding the best solutions to provide the new energy system with flexibility and high availability.

2 STATUS OF HYDROPOWER DEVELOPMENT IN EUROPE

Hydropower has a long history in Europe and in the first half of the last century contributed significantly to industrial development and welfare in most of the countries of Europe. Hydropower in Europe, and indeed worldwide, has many advantages such as:

- Renewable energy without direct emission of CO₂, excellent energy gain or pay back factor
- Excellent efficiency, production can be easily adapted to the demand (flexible peak energy)
- In-country independent energy creating jobs and financial resources in remote areas (taxes and concession fees)
- Strong contribution to flood and drought protection with potential for recreational and tourism activities
- Facilitation of navigation for the large rivers in Europe.

Today within Europe, including Turkey, almost 650 TWh are generated in an average hydrological year, which equates to about 65% of the economically feasible hydropower potential (Figure 1). For a few years, the yearly production of hydropower has stabilized near 650 TWh and the total installed capacity near 230 GW. It should be noted, however, that the yearly hydropower production is also influenced by the hydrological situation each year.

Figure 2 shows the situation for hydropower use and untapped potential in different countries within the Europe region. It can be noticed that in many countries there is still considerable potential for development. In Figure 2, the highlighted countries have developed less than 50% of the economical feasible potential, assuming that the market conditions would allow for it. For 14 countries the share of hydro in the overall electricity generation is between 25% and 50%, for three countries between 50% and 90% and for another two countries higher than 90%. This demonstrates that in more than half of the countries in Europe (as shown in Figure 2) hydropower

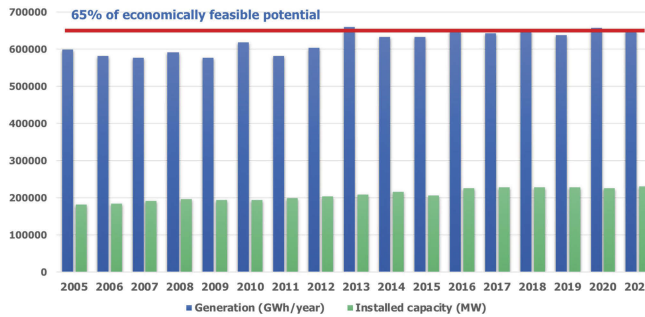


Figure 1. Evolution of yearly production and installed capacity of hydropower in Europe since 2005 (according to Hydropower & Dams World Atlas 2022).

represents an important share in the electricity generation, which is important for the success of a safe energy transition.

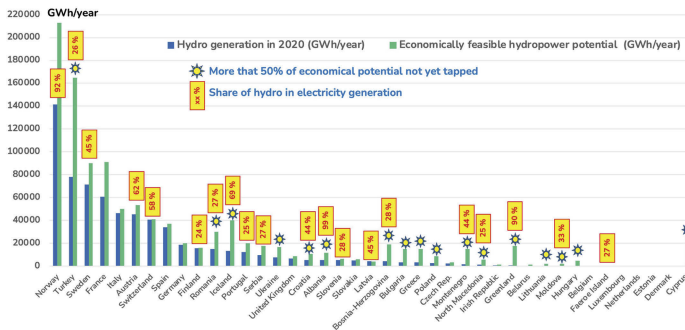


Figure 2. Generation and extension potential of hydropower in countries within the European region (according to Hydropower & Dams World Atlas 2021). The countries having developed less than 50% of their economical feasible potential (assuming market conditions have a demand for it) are highlighted. The share of hydro in the electricity generation is indicated for the countries with a share of more than 25%.

Nevertheless, relatively little investment has been undertaken over the last 15 years, as can be seen in Figure 3 which shows the installed capacity under construction. In 2012, a quite significant increase in the construction of new power plants reaching almost 10,000 MW can be seen. This may be attributed to the Fukushima catastrophe leading many countries to redefine their energy strategy towards renewable sources such as hydropower alongside the planned phasing out of nuclear energy. Since 2015, however, construction activity has been decreasing to some 3000 MW with an activity above 5000 MW in 2019.

The low investment level around 2021 can be attributed to the fact that electricity prices on the European spot market were very low due the following reasons:

- Production capacity in Europe was too high (especially via conventional thermal generators using coal)
- Cost of CO₂ certificates were very low
- The market was distorted due to the high subsidies provided for renewable energy sources such as solar and wind

Thus, under such market conditions hydropower generation was strongly penalized. However, the actual energy crisis reveals the important and vital role of hydropower – storage and pumped-storage - to help ensure a safe supply of electricity in the coming winters in Europe. Due to the energy crisis, the attractiveness of the extension and upgrading of existing hydropower plants, with the purpose of making them more flexible through the refurbishment of equipment and

increasing storage where possible, together with the construction of new pumped-storage power plants, has increased again strongly in countries with high storage potential. Furthermore, in many countries a significant amount of untapped hydropower potential still exists. However, in view of environmental and socio-economical constraints, the partial use of this remaining potential is extremely challenging and can be reached only through innovative and sustainable solutions for new hydropower plants.

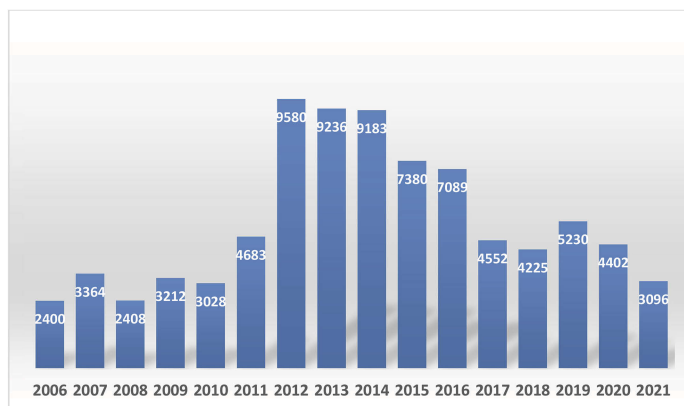


Figure 3. Installed capacity in MW under construction since 2006 (according to Hydropower & Dams World Atlas 2022 without Turkey).

3 OUTCOMES OF THE HYDROPOWER EUROPE FORUM: RESEARCH AND INNOVATION AGENDA – STRATEGIC INDUSTRY ROADMAP

The HYDROPOWER EUROPE Forum (<https://hydropower-europe.eu>) was supported by the EC under the Horizon 2020 programme LC-SC3-CC-4-2018 with the goals of developing a Forum through which an extensive programme of consultation could be undertaken to support the development of a Research and Innovation Agenda and a Strategic Industry Roadmap which would facilitate launching a series of innovations in the hydropower sector, targeting an energy system with high flexibility and renewable share.

The outcomes of the HYDROPOWER EUROPE Forum show the pathway to the vision for hydropower in Europe defined through wide consultation following four directions:

- Increasing hydropower production through the implementation of new environmentally friendly, multipurpose hydropower schemes and by using hidden potential in existing infrastructures
- Increasing the flexibility of generation from existing hydropower plants by adaptation and optimization of infrastructure and equipment combined with innovative solutions for the mitigation of environmental impacts
- Increasing storage by the heightening of existing dams and the construction of new reservoirs, which have to ensure not only flexible energy supply, but which also support food and water supply and thus contribute to the WEF NEXUS and achievement of the SDGs of the United Nations
- Strengthening the contribution of flexibility from pumped-storage power plants by developing and building innovative arrangements in combination with existing water infrastructure.

This vision was underlined by the Research and Innovation Agenda (RIA) and the Strategic Industry Roadmap (SIR), which also provide an inspiring example for hydropower development worldwide which is of high importance to the hydropower sector in Europe, which is already playing a major role in the worldwide market today. Eighteen research themes comprising some 80 topics were identified (RIA) as well as 11 strategic directions including some

40 detailed actions (SIR) ranging from regulation framework to social acceptance and innovative environmental strategies.

Besides the RIA and SIR (HPE, 2021b,c), the outcomes of the HYDROPOWER EUROPE Forum can be summarized as follows:

- A state-of-the-art report on Hydropower Technologies has been produced (HPE, 2021a).
- The HYDROPOWER EUROPE Forum has been launched, which includes a global network covering the whole sector of Hydropower, comprising some 650 participants in 2022.
- An extensive programme of consultation has been undertaken, comprising workshops, regional workshops and many online events to support the development and prioritisation of recommendations for the industry.
- A complex systems analysis of the European hydropower sector has been undertaken allowing priorities to be compared against findings from the wide consultation programme (HPE, 2020).
- A series of roundtables, discussions and dissemination events, including consultation with NGOs, has been implemented to better understand issues and priorities and to help raise awareness of how hydropower in Europe can support the clean energy transition (HPE, 2021d).
- The steps needed for a sustainable voice for hydropower in Europe, including a focus on facilitating R&I priorities, have been considered and an implementation plan proposed.

4 ETIP HYDROPOWER - UNIFYING THE VOICES OF HYDROPOWER

A European Technology and Innovation Platform (ETIP) is a community whose primary purpose is to define R&I priorities for its sector. The secondary purpose is to overcome barriers to the deployment of R&I outcomes: e.g., industrial strategy, market opportunities, exploitation of research results, international cooperation, education, environmental and social impacts. There is a need for a unified industry to be represented and recognized at a European level. The HYDROPOWER EUROPE Forum provided a first opportunity to gather some 650 stakeholders representing all the sectors of the value chain. Under the ETIP HYDROPOWER project (<https://etip-hydropower.eu>), the hydropower forum will continue to grow and offers an ideal opportunity to help unify the voices of hydropower in Europe (Fry et al., 2023).

ETIP HYDROPOWER will further detail the already developed industrial strategies as well as analysis of market opportunities and research and development funding needs, by a deepening of the understanding of innovation barriers and exploitation of research results, which are in line with the Recovery Plan for Europe and the latest EU climate and energy related policies.

The ETIP HYDROPOWER has the mission to:

- represent a consolidated and strong network of representatives from industry, academia, research centers, civil society and sectorial associations of the hydropower sector
- enhance and disseminate the Research and Innovation Agenda (RIA) and the Strategic Industry Roadmap (SIR) taking into consideration the future needs of the sector and R&I targets and emerging policy priorities
- align and coordinate the industry RIA and SIR strategies to provide consensus-based strategic advice to the European Commission and the SET Plan (European Strategic Energy Technology Plan) covering analysis of market opportunities and research and development funding needs, biodiversity protection and ecological continuity
- deepen the understanding of innovation barriers and the exploitation of research results in line with the latest EU climate and energy related policies

The ETIP HYDROPOWER aims to be a recognised interlocutor for the European Commission, Member States and Associated Countries about the hydropower sector specific R&I needs. ETIP Hydropower foresees working relationships with the relevant national/regional/EU-level platforms to ensure synergies between EU, national and regional activities.

In more detail, ETIP HYDROPOWER will answer the following questions:

- Which research and innovations projects are the most important in order that hydropower can fulfil the role of an enabler and catalyst in the energy transition?
- Which strategic actions have to be taken when, in order that hydropower can fulfil the role of an enabler and catalyst in the energy transition?
- How public awareness can be increased for hydropower in the transition to a clean energy system focusing towards a zero-emissions target?
- How hydropower projects can be carried out to create win-win situations with other renewables and other services contributing to the Water-Energy-Food Nexus and the achievement of the Sustainable Development Goals of the United Nations?
- What form of sustainable associate organisation representing the hydropower sector is required to ensure the vital role of hydropower in the energy transition?

ETIP HYDROPOWER will address these questions and challenges with working groups identified and launched based on consultation with the hydropower sector willing to participate with the sustainable associate organization beyond the ETIP lifetime. Potential working groups may cover a wide range of topics including, for example, the fields of economy, environment, equipment, structures, pumped storage hydropower (PSH), small hydro, digitalization, communication, market rules, legal frameworks etc. depending upon the specific need of the sector. Working groups will also include Civil Society Organisations for the identification of potential social impacts of hydropower.

This structure allows for robust outreach approaches and societal engagement actions to be implemented across the EU and associated countries. The outcome of the working groups will be position papers on specific themes prepared by joint workshops, thematic conferences, webinar series, regular exchanges and wide consultation. The activities of ETIP HYDROPOWER, involving an external scientific board and the above-mentioned working groups, is structured according 5 work packages as shown in Figure 4 below.

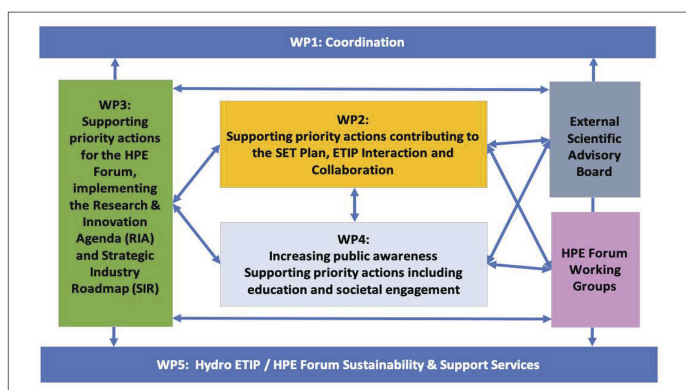


Figure 4. Structure and work packages of the ETIP HYDROPOWER project.

Figure 5 provides a generic representation of the mission and activities of ETIP HYDROPOWER at a strategic level within the hydropower sector. As illustrated by the anchor symbol the ETIP HYDROPOWER can unify and magnify the voice of hydropower to key stakeholders such as the European Commission and other EU institutions. It does not replace existing initiatives; rather it links them, allowing for presentation of key issues with one voice when appropriate. The job of the ETIP HYDROPOWER is to manage the linking and unified messaging process (arrows in brown in Figure 5). Existing initiatives continue with their own programmes and communications as before as shown in Figure 5 (blue dotted arrows).

The ETIP Hydropower project runs for three years from September 2022 to August 2025 and aims to be a facilitator for unifying the voices of the hydropower sector and to be a recognised interlocutor for the European Commission, Member States and Associated Countries regarding the hydropower sector specific deployment and R&I needs. The purpose

of the ETIP HYDROPOWER project is also to prepare for a transition into a sustainable, self-funded organization i.e. association which lasts after the duration of the project.

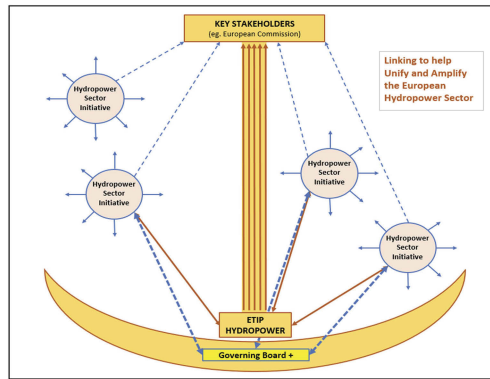


Figure 5. Generic representation of the mission and activities of ETIP HYDROPOWER at a strategic level within the hydropower sector.

With regards to *advocacy* in order to help unify and magnify the voice of hydropower, this association would have 3 main axes:

1) *Towards the decision makers:*

- Being the main contact point for all hydropower related activities as an EU association for the EU decision makers.
- Focused on lobbying, communication with stakeholders, increasing visibility of the hydropower sector, ensuring the inclusion of the voices of the hydropower sector, providing inputs for future energy policy, quantifying the added value brought by hydropower, highlighting the positive services hydropower provides to the environment.
- The technical expertise would be drawn from national hydropower entities.

2) *Towards the funding organisms:*

- Providing a clear research priorities list for the national and also the EU-level funding organisms by identifying and collecting the priorities from the association members.
- Increasing the funding amounts available for Hydropower research in national and European funding programmes. National research priorities or funding activities would be done through national hydropower entities.

3) *Between the stakeholders:*

The association would provide a network between all the relevant hydropower stakeholders in order to hear early in the process from new technologies, projects or activities related to the European and global hydropower sector.

In view of *collaborative R&I* this association may have three main types of research collaboration:

- Small projects programme: As part of the annual membership fee, each member pays a contribution into the small projects fund. This fund is used to directly contract 'small projects' addressing issues of priority to the forum members. Small projects are expected to cost in the €10-50K budget range.
- Co-funding projects programme: These projects would be significantly larger and more costly than those proposed under the small projects programme. Forum members will be invited to express interest and potential financial support for collaborative working on projects on this list. Where there is sufficient support and pledged finance, then:(i) a project specification will be developed in detail. (ii) a project budget will be developed in detail. (iii) a collaborative research agreement established. (iv) the project tendered for contract, proposals evaluated, tender selected and project implemented.
- Collaborative bidding programme: Where existing funded programmes of research (for example, EC Horizon Europe and other programmes) show opportunities for relevant

hydro industry research, these will be presented to the forum members with the opportunity to collaborate on a joint proposal submission. The costs associated with development of such submissions would be borne by individual members; the HPE Forum role here is to raise awareness with members and facilitate initial proposal team building.

5 CONCLUSIONS

ETIP HYDROPOWER will help to ensure that hydropower can play the vital role of a catalyst and enabler in the transition to a clean and safe energy system in Europe. Hydropower has proven to be a reliable supplier in the energy crisis. Its important contribution to secure storage with the lowest indirect CO₂ emissions amongst the renewable energies will become even more important in the energy transition towards the achievement of climate neutrality by mid-century. ETIP HYDROPOWER will help to unify the voices of hydropower in Europe and worldwide, to increase public awareness on its catalyst and enabler abilities as well as motivate innovative collaborative research towards environmentally compatible solutions. Besides electricity supply, hydropower can offer other services which are important to help mitigate climate change effects, like water supply, contribution to flood and drought protection with potential for recreational and tourism activities and facilitating navigation on the large rivers.

ACKNOWLEDGEMENT

ETIP HYDROPOWER ETIP has received funding from the European Union's Horizon Europe research and innovation programme under grant no 101075620. Project partners are: International Commission on Large Dams (ICOLD), European Association for Storage of Energy (EASE), European Renewable Energies Federation (EREF), Association of European Renewable Energy Research Centres (EUREC), International Hydropower Association (IHA), Samui France SARL (SAMUI), VGBE energy (vgbe) and ZABALA Brussels SPRL (ZABALA).

REFERENCES

- Fry, J.J.; Garcia, J.; Morris, M.; Schleiss, A.J. 2023. The need for a unified European hydropower voice. *Energetyka Wodna*, 45(1):14. ISSN 2299-0674
- HPE HYDROPOWER EUROPE Forum. 2020. *Hydropower in Europe in a complex world - A global system analysis approach*. Hydropower Europe Technical Report, June 2020. (https://hydropower-europe.eu/private/Modules/Tools/EUProject/documents/47/WP2-Rp-47_HPE_Complex_System_Approach_V2_1.docx)
- HPE HYDROPOWER EUROPE Forum. 2021a. *Current Status Hydropower Technology*. Deliverable D4.3. https://hydropower-europe.eu/publications/deliverables/WP4_DIRp_57_D4_3_StatusHydro-Tech_v5_2_Final-1629470232.docx. 20/08/2021.
- HPE HYDROPOWER EUROPE Forum. 2021b. Research and Innovation Agenda (RIA). Report WP4-DIRp-53. (<https://hydropower-europe.eu>).
- HPE HYDROPOWER EUROPE Forum. 2021c. Strategic Industry Roadmap (SIR). HPE report no. WP4-DIRp-54. (<https://hydropower-europe.eu>).
- HPE HYDROPOWER EUROPE Forum. 2021d. Environmental & Socio-Economic Challenges of Hydropower in Europe: the Experience of Non-Governmental Organisations. Conclusions from the Roundtable Event: 19th January 2021. Hydropower Europe document WP2-Rp-51.V3. www.Hydropower-Europe.eu. February 2021. (https://consultation.hydropower-europe.eu/assets/NGO/NGOExperiences_WP2-Rp-51_V3_1_AS.pdf)
- IEA (2021). Valuing Flexibility in Evolving Electricity Markets: Current Status and Future Outlook for Hydropower. IEA Hydro Annex IX, White Paper No 2, June 2021 (<https://www.ieahydro.org>).

From energy producer to water manager: A research-industry collaboration

X. Schröder

Alpiq SA, Lausanne, Switzerland

E. Reynard

University of Lausanne, IGD & CIRM, Lausanne, Switzerland

S. Nahrath

University of Lausanne, IDHEAP & CIRM, Lausanne, Switzerland

ABSTRACT: The hydropower industry is expected to play a central role in the double field of energy transition and water security, in a context of climate change, increasing pressure on water resources and geopolitical tensions. The role of alpine hydropower infrastructure in the deployment of a multifunctional water management policy needs to be considered. A research project involving Alpiq and the University of Lausanne is developing this reflection, by clarifying the origin of the concept of multiple use of water and hydraulic infrastructure, the perceptions of multifunctionality by the various water and energy stakeholders, and the issues of governance of resources “water” and “hydraulic infrastructures”, particularly in view of the dam relicensing. The work in progress demonstrates the common interest of this collaboration, which is fruitful for both science and industry.

RÉSUMÉ: L'industrie hydroélectrique est amenée à jouer un rôle central dans le double domaine de la transition énergétique et de la sécurité hydrique, dans un contexte de changement climatique, d'augmentation des pressions sur la ressource en eau et de tensions géopolitiques. Des réflexions doivent être menées sur le rôle des infrastructures hydroélectriques alpines dans le développement d'une politique de gestion multifonctionnelle de l'eau. Un projet de recherche associant Alpiq et l'Université de Lausanne développe cette réflexion, en précisant l'origine du concept de multiusage de l'eau et des infrastructures hydrauliques, les perceptions de la multifonctionnalité par les différents acteurs de l'eau et de l'énergie, et les enjeux de gouvernance des ressources « eau » et « infrastructures hydrauliques », notamment dans la perspective des retours de concessions. Les travaux en cours démontrent l'intérêt commun de cette collaboration, fructueuse autant pour la science que pour l'industrie.

1 INTRODUCTION

In the current context of strong pressure on water resources, linked to climate change, the energy transition and various political crises, the concept of “multiple use of water infrastructure” is put forward by various user sectors to deal with an increasingly complex distribution of the resource (Kellner and Brunner, 2021). For hydropower producers, this issue is becoming increasingly urgent and is being addressed at various levels. In order to better define the contours and challenges of this new paradigm and to develop proposals for future responses, Alpiq and the University of Lausanne (UNIL) have joined forces to conduct a research project on the multifunctionality of hydropower infrastructures in the Swiss Alps.

1.1 *Origin, actors and purpose of the project*

The first discussions between UNIL, more specifically its Interdisciplinary Centre for Mountain Research (CIRM), and Alpiq began in 2019. The aim was to define the contours of joint research and to identify the motivations and contributions of each party. In 2020, UNIL launched a call for applications for a post-doctoral work focusing on the origin of the concept of multipurpose use of alpine hydropower reservoirs in Switzerland, its actors and the past, present and future evolution of this new management model for hydraulic infrastructure. Alpiq wished to extend the research on a more institutional axis and to question the governance of the resource. In this context, Alpiq has been financing a doctoral thesis since October 2021 on the analysis of the governance of the multifunctionality of dams and its perspectives. These two lines of research are being carried out jointly in three research centres of Lausanne University – the CIRM, the Swiss Graduate School of Public Administration (IDHEAP) and the Institute of Geography and Sustainability (IGD) – and will continue until autumn 2025.

The subject of the research was discussed at length: was it a question of questioning multifunctionality solely (or primarily) from the point of view of the water resource, as the main issue of rivalry of uses and regulation, or was it a question of adopting a more holistic and integrative approach that also considered the infrastructural resources constituted by the hydropower schemes? From an integrated management perspective, it quickly became clear to us that hydroelectricity should be considered as a *system* of resources that is indissociably composed of water and infrastructure. Such an approach has the advantage of making it possible to study not only the regulation regimes of each of the two resources, but also, and above all, to study their interdependence at the functional scale of the hydropower basin, i.e. the use basin (Calianno et al., 2018) delineated by the hydraulic infrastructure. The postulate on which our research is based is therefore that the understanding of the management stakes of the multifunctionality of hydropower installations requires a combined analysis of the regulations – public law (public policies) as well as private law (concessions and other property rights) – concerning the two resources (water and infrastructure), in order to evaluate in particular the level of coherence between the various regulations.

2 CONTEXT

2.1 *Collaboration and motivations of each party*

2.1.1 *Motivation of the industrial partner*

In the context of current energy, political and climate crises and the renewal of hydropower concessions, the multiple use of water, and consequently the multifunctionality of hydropower dams, is a theme that an energy producer must integrate into business considerations. In the near future, Alpiq will probably no longer be a producer of hydroelectric energy alone, but will also be a water resource manager offering various services and products. This paradigm shift implies changes in terms of management and corporate philosophy; Alpiq needs to adapt its core business to the new direction of the hydropower market, in particular if multifunctionality is developing.

Collaboration with research allows developing a cross-disciplinary approach in which Alpiq can demonstrate its skills as a manager and not just as an electricity producer. This strategy will be necessary in discussions with the various stakeholders on hydropower relicensing. The integration of Alpiq, an industrial player, in this research project allows it to be part of a global societal project and to profile itself as a sustainable manager of water resources. Thanks to its expertise, Alpiq can provide its engineering point of view on its ability to manage large catchment areas and structures, and on the implementation of potential future developments, and also make available historical and current operating data to researchers.

2.1.2 *Motivation for the research*

During the period 2016-2021, UNIL Rectorate has placed the development of inter- and transdisciplinary research as one of its priorities. As mountain themes are very present within UNIL, the Interdisciplinary Centre for Mountain Research (CIRM) was created in this

context in autumn 2018. From the beginning, it has been placed in a resolutely transdisciplinary perspective (Reynard et al., 2020), with the objective of co-developing joint research with territorial actors. Collaborations have thus emerged, notably with local museums, regional nature parks, and associations active in the Valais and Vaud Alps, which have been defined as privileged territories for the development of CIRM research. The joint reflection undertaken with Alpiq is part of this dynamic.

For the UNIL research team, collaboration with an industrial player has several advantages. Firstly, it allows the conceptual models to be confronted to the concrete expectations of stakeholders. Secondly, the collaboration between research and industry augurs a potential application of the recommendations resulting from the research; such collaborations are rare in the field of human and social sciences. Finally, this research project is in line with CIRM’s commitment to develop transformative research, with the aim to transform Alpine territories towards greater sustainability.

2.2 Two lines of research

The first axis (Figure 1) is a socio-historical research. The objective is to find out when and how the term multifunctionality appeared in the scientific literature, in strategic documents on water and energy management, and in the public debate in Switzerland (task 1a), and how it is perceived and understood by water and energy stakeholders, both at the national and cantonal levels (1b) and at the level of the hydropower schemes themselves (1c).

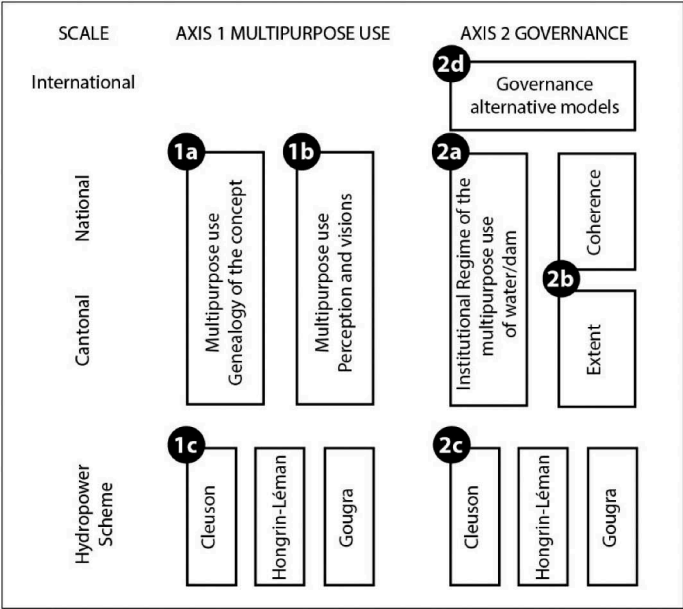


Figure 1. Research organisation.

The second axis focuses on the institutional side and the regulation of the various uses using the institutional resource regimes (IRR) analytical framework (task 2a). The aim is to describe the extent of regulated uses and the coherence of the governance of multifunctionality (2b). The problem is first addressed at the national and cantonal levels, before being studied in three case studies at the scale of specific schemes (2c). The second part of the project focuses on the study of institutional solutions developed abroad (2d) with the aim of establishing new governance scenarios that could be transposed to Switzerland.

3 METHODOLOGY

3.1 *Analysis of the multifunctionality of hydropower dams*

The first part of the work (Task 1a) focuses on the emergence of the concept of multifunctionality – of water and hydropower infrastructure – in Switzerland (Flaminio and Reynard, 2022, 2023). We studied the definitions associated with this concept, their evolution over time and the visions associated with them at the national and cantonal levels, using the example of the canton of Valais, the largest hydroelectric producer in Switzerland. The work is based on a corpus of documents (reports from various federal and cantonal offices, government messages and parliamentary interventions, scientific reports, etc.) as well as on 22 semi-structured interviews with various water and energy stakeholders in Switzerland and in Valais (politicians, members of the administration, scientists, representatives of professional or environmental associations).

In a second step (1b), we studied the documentary corpus and the interview transcripts from the perspective of the perception of the concept by the different groups of stakeholders. This allowed us to identify groups of representations that we aggregated around three main visions of the multifunctionality of water and alpine dams.

As multifunctionality is primarily seen as a possible adaptation to climate change at regional and local levels, case studies of existing schemes should investigate how multifunctionality is considered by water and energy stakeholders at local and regional levels (1c). For obvious reasons of ease of access to data, three case studies of Alpiq schemes were selected. Size, geographical and topographical location, mode of operation and multifunctional character were the main characteristics used to select the case studies. In Valais, the Cleuson dam in the Printse valley and the Gougra dam in the Anniviers and Turtmann valleys were selected. The Hongrin dam in the canton of Vaud completes the sample. These three schemes are very different both geographically and administratively and thus allow the broadest possible view of the existing or potential multifunctionality of dams.

For each case, after defining the perimeter of the study, which depends as much on the hydrological components (watershed) as on the infrastructures (basin of uses), we mobilise a corpus of documents (concessions and other administrative documents, scientific studies, study reports relating to projects, local press) and interviews with stakeholders concerned by the use of water and the infrastructure (15-20 interviews per case). The objective is to obtain an inventory and characterisation of the various uses, their temporal evolution, a quantification of water withdrawals and an analysis of rivalries and complementarity between uses. In the continuation of the study at national and cantonal level (Flaminio and Reynard, 2022), we also seek to establish what visions the actors involved in specific schemes have of water and aquatic environments, of hydropower and of multifunctionality.

3.2 *Analysis of the governance of the multifunctionality of hydropower dams*

The analysis of governance is carried out using the theoretical framework of institutional resource regimes (IRR) (e.g. Knoepfel et al., 2007; Varone et al., 2008; Gerber et al., 2009). The aim of this approach is to study the links between the multifunctionality of the uses of a resource, the institutional rules regulating and arbitrating these uses, the configuration of the actors concerned by the uses and regulations and, finally, the effects on the sustainability of resource management. It has already been used on numerous occasions to analyse the regulatory regimes of water resources (e.g. Varone et al., 2002) as well as those of various infrastructure resources (e.g. Nahrath et al., 2011).

More concretely, by combining a public policy analysis approach (Knoepfel et al., 2010) and an approach based on the institutional economics of resources (Ostrom, 1990), the framework for analysing IRR makes it possible (Knoepfel et al. 2007) to: (i) identify all the uses (goods and services) that are made of a given resource and to identify any phenomena of rivalry and scarcity resulting from this multifunctionality; (ii) systematically and exhaustively describe all the rules – both public law (public policies) and

private law (Civil Code, Code of Obligations, etc., defining property rights, in particular concessions) – that make up the IRR; rules that regulate the allocation of use rights over the various goods and services; (iii) to characterise the IRR using two dimensions: its extent – understood as the number of goods and services regulated by the regime – and its coherence – understood as the level of coherence or incoherence, both between different public policies (e.g. energy (hydropower), environment, tourism, flood control, agriculture (irrigation), etc.), and between public policies and property rights (e.g. incoherence between the turbinning rights conferred by concessions and the obligation to guarantee minimum flows imposed by water protection policy).

The study of the institutional regime of the multifunctionality of water and dams (Task 2a; Savoy et al., 2023) first required the elaboration of a list of all the uses that could theoretically be made of alpine hydroelectric schemes in Switzerland, classified into 9 main categories and 41 specific uses, as well as a definition of the resources “water” and “hydropower infrastructure” and their uses. Tables of the current uses of these two resources and of the negative externalities of hydraulic infrastructures were thus established. Four groups of rivalries between uses were established: rivalries over the allocation of water in the reservoir, rivalries over the use of the power schemes, rivalries over the use of the reservoir itself and finally, rivalries over the use of the infrastructures.

The analysis of the institutional regime of hydropower activity is based on legal texts (Constitution, laws and ordinances or decrees, Civil Code, Code of Obligations) and political texts (e.g. messages from the Federal Council or cantonal State Councils), both at national and cantonal level (Valais and Vaud). The characterisation of the regime is organised around seven major groups of uses defined according to their relevance in the governance of the multifunctionality of alpine dams and according to the institutional density, i.e. the “volume” of legislative texts concerning them. These uses are: hydropower production, ecosystems and landscape, flood management, agriculture and irrigation, drinking water supply, artificial snowmaking, other uses. For each use group, the history of regulation, the triangle of actors (Knoepfel et al., 2006) and the constituent elements of the political-administrative programme are analysed. For each group of uses, the formal property rights, the disposal rights and the use rights, as defined in particular in concessions and other private law documents, are then identified.

On this basis, we carry out a study of the extent and coherence of the regime (task 2b). For the extent, we establish how intensively the uses are regulated and we also identify which uses are not or only weakly regulated.

The same approach is then applied at the scheme level (Task 2c). The selected schemes are the same as for Task 1c. In contrast to the analysis at national and cantonal level, which is based primarily on a corpus of legislative, legal and political texts, the study at the scheme level also uses semi-structured interviews with actors managing and using the infrastructures. The aim is to define the contours of the local regulation arrangement (LRA; Schweizer, 2015; Viallon et al., 2019) and in particular to identify the mechanisms governing the multifunctional use of the resource and infrastructure that escape or complement the legal regulation by the national and cantonal regulation regime, and are subject to more or less formalised local arrangements (conventions, customary rules, informal oral agreements, etc.)

Finally, the aim is to identify and study, on the basis of scientific literature and possibly *in situ* case studies, forms of regulation of multifunctionality developed in other countries (task 2d). These cases will make it possible to reflect on alternative forms of regulation of multifunctionality that could be mobilised in Switzerland when relicensing power schemes.

4 FIRST RESULTS

4.1 *Genealogy and perception of the concept of multifunctionality of water and infrastructure*

The results of tasks 1a and 1b of the project (Flaminio and Reynard, 2022, 2023) show that the notion of multifunctionality of water and dams is still unclear for many actors. Nevertheless, it is beginning to stabilise. Its emergence in the literature on water and energy in

Switzerland is quite recent. The multifunctionality of dams was first mentioned in federal reports on climate change, and in scientific studies on the adaptation of the hydropower sector to climate change in the early 2010s. From the mid-2010s onwards, various documents give it more prominence. Since 2018, the concept of multifunctionality of water and dams has developed both in scientific publications and in reports from various federal and cantonal administrations. Overall, multifunctionality is discussed in connection with the debate on adaptation to climate change and could concern both existing infrastructure – which is the reason why, according to the sources consulted and the testimonies collected, it should be discussed before the relicensing of power schemes – and the construction of new infrastructures or the modification of existing ones.

The analysis of the interviews reveals three main visions of multifunctionality (Flaminio and Reynard, 2022, 2023): (i) the first is defined as a vision supporting the hydroelectric sector under pressure from environmental requirements, and considers it unnecessary and costly to implement; (ii) the second vision considers multifunctionality beneficial and interesting, particularly suitable as an instrument for adapting to climate change and decreasing water resources; (iii) the third vision, carried by actors particularly sensitive to the impacts of hydropower production on the environment, considers the notion of multiple use of water as purely rhetorical, with the objective to rehabilitating the image of hydropower, and not allowing for a paradigm shift towards more sustainable water management.

4.2 *First lessons from the Cleuson case*

The Cleuson dam is located in the Printse watershed, in the commune of Nendaz, on the left bank of the Rhone River. It was commissioned progressively from 1948 and has a capacity of 20 million m³. It is part of the Grande-Dixence hydropower complex. The water is not turbined directly, but pumped to the Grande-Dixence reservoir before being turbined in one of the Cleuson-Dixence power stations.

The first results of the analysis of uses and stakeholders (Flaminio, 2023) allow us to consider water as a multifunctional resource in this valley. Indeed, it is used and valued by many sectors of use. Various uses are present around the infrastructure and some even precede the construction of the dam, such as irrigation, practised since the Middle Ages thanks to a network of ten *bisses* (traditional irrigation channels) which divert the Printse waters, or fishing. Other uses have been added over time following the emergence of new needs, such as the production of drinking water, from the end of the 1960s, and artificial snowmaking, from the beginning of the 1990s. On the other hand, some uses have disappeared, such as the use of hydraulic power to drive mills and other hydraulic devices in the middle Printse valley (Beuson), which were replaced by electrical power following the construction of the Cleuson scheme (Reynard, 2000). The Cleuson reservoir also plays a role in flood hazard prevention by being integrated into the Minerve scheme (García Hernández et al., 2010), following an agreement signed in 2008 between the hydropower operator and the Canton of Valais. The water stored in the Cleuson reservoir is also used as a reserve in case of fire, via withdrawals from the drinking water network. The Cleuson lake also contributes to the valley's tourist image and thus has a certain tourist value, essentially during the summer period. Lastly, the withdrawals have a certain impact on the flows and aquatic environments.

Although the reservoir has multiple uses, it should be noted that uses other than hydropower production remain limited from a quantitative point of view, representing less than 5% of the volumes stored in the Cleuson reservoir. Hydroelectric use thus represents around 23.7 million m³, withdrawals for irrigation are only made in dry years and reach a maximum of 750,000 m³ (in 2022), while withdrawals for the production of drinking water and artificial snow are of the order of 90,000 and 130,000 m³ respectively. This means that approximately 1 million m³ per year (maximum) can be withdrawn from the Cleuson reservoir, i.e. 4.2% of the stored volume.

Today, this gives rise to fairly strong complementarity dynamics and little competition as regards the uses linked to the exploitation of water. On the other hand, there is a certain competition between the exploitation uses (withdrawals) and the protection of the resource.

During the interviews conducted with the various stakeholders in the region, the issue of climate change and the related challenges was raised. The majority of those interviewed are aware of the need in the more or less near future to better anticipate shortages and to implement integrated management of the resource, but for the time being, the sharing between the different uses is not anticipated, as water is still not under much pressure in this region.

5 CONCLUSION - STRENGTHS OF A RESEARCH/INDUSTRIAL PARTNERSHIP

Today, Switzerland is at the interface of two issues with different dynamics that need to be considered together: (i) the energy strategy which, in the dynamics of decarbonation of the economy and society, the gradual abandonment of nuclear production and the reduction of energy dependence on foreign countries, intends to reinforce the production of indigenous renewable energy, within which hydropower energy plays a central role; (ii) the water management strategy, which requires a paradigm shift towards greater integration, driven by climate and hydrological changes, of which the last twenty years have shown that Switzerland is not immune to extreme events and shortages, despite its relative water wealth. For this reason, the Federal Council (2022) has pointed out the need to strengthen water security. In this context, the implementation of integrated water management includes the use of the large alpine hydropower reservoirs as storage infrastructures to adjust water supply to demand. It also requires the development of shared water governance mechanisms, which are still underdeveloped at the moment.

The objectives of these two public policies – electricity supply and water supply – seem *a priori* to be competing, but hydropower producers could play a central role in this double transition because of their position at the interface between the two policies, because of the importance and geographical spread of the infrastructures and because of their expertise in hydraulic matters based on a century and a half of practice in the field. As for research, particularly in the human and social sciences, it provides the theoretical and methodological basis necessary to carry out a good diagnosis of the existing situation and to provide a solid foundation for relevant reflection on future scenarios. The importance given to the analysis of the perceptions of the issues by the stakeholders and the governance mechanisms at stake should thus make it possible to better understand tensions that could transform in conflicts when the concrete projects are implemented (Utz et al., 2017).

Through this research project, Alpiq and UNIL are seeking to link the fields of energy and water management, to go beyond existing operating models and develop broader socio-political models that cross these two fields. The industrial partner is often a driving force and proactive in these reflections on paradigm changes. In association with science, the industry can reflect on the possible transformations in water supply, both technical and in relation to hydrological evolution, uses and rivalries, etc. In parallel, they can carry out reflections on innovative modes of governance and comparative prospection work. Subsequently, the industrial partner hopes to be able to propose concrete solutions for the governance of the resource to politicians.

REFERENCES

- Calianno, M., Milano, M., Reynard, E. (2018). Monitoring water use regimes and density in a tourist mountain territory. *Water Resources Management*, 32, 2783–2799.
- Conseil fédéral (2022). *Rapport de base sur la sécurité de l’approvisionnement en eau et sur la gestion de l’eau*. Rapport du Conseil fédéral en réponse au postulat 18.3610 Rieder du 15 juin 2018. Berne: Conseil fédéral.
- Flaminio, S. (2023). *Analyse de la multifonctionnalité des aménagements hydroélectriques alpins: le cas de Cleuson (Valais)*. Working paper n°2 du projet « Multifonctionnalité des infrastructures hydroélectriques alpines ». Lausanne: Université de Lausanne, 77 p.
- Flaminio, S., Reynard, E. (2022). *Une généalogie de la multifonctionnalité des barrages-réservoirs en Suisse*. Working paper n°1 du projet « Multifonctionnalité des infrastructures hydroélectriques alpines ». Lausanne: Université de Lausanne, 30 p.

- Flaminio, S., Reynard, E. (2023). Multipurpose use of hydropower reservoirs: Imaginaries of Swiss reservoirs in the context of climate change and dam relicensing. *Water Alternatives*, under review.
- García Hernández, J., Horton, P., Tobin, C., Boillat, J.-L. (2009). MINERVE 2010: Prévission hydrométéorologique et gestion des crues sur le Rhône alpin. *Wasser Energie Luft*, 4, 297–302.
- Gerber, J.-D., Knoepfel, P., Nahrath, S., Varone F. (2009). Institutional Resource Regimes: Towards sustainability through the combination of property-rights theory and policy analysis. *Ecological Economics*, 68(3), 798–809.
- Kellner, E., Brunner, M. I. (2021). Reservoir governance in world's water towers needs to anticipate multi-purpose use. *Earth's Future*, 9, e2020EF001643.
- Knoepfel, P., Larrue, C., Varone, F. (2006). *Analyse et pilotage des politiques publiques* (2nd ed.). Zürich: Verlag Rüegger.
- Knoepfel, P., Nahrath, S., Varone, F. (2007). Institutional regimes for natural resources: An innovative theoretical framework for sustainability. In P. Knoepfel (Ed.), *Environmental Policy Analyses. Learning from the Past for the Future - 25 Years of Research* (pp. 455–506). Berlin: Springer.
- Knoepfel, P., Nahrath, S., Savary, J., Varone, F. (2010). *Analyse des politiques suisses de l'environnement*. Zürich/Chur: Ruegger Verlag.
- Nahrath, S., Pflieger, G., Varone, F. (2011). Institutional Network Regime: a new framework to better grasp the key role of infrastructure. *Network Industries Quarterly*, 13(1), 23–26.
- Ostrom, E. (1990). *Governing the Commons. The evolution of institutions for collective action*. Cambridge: Cambridge University Press.
- Reynard E. (2000). *Gestion patrimoniale et intégrée des ressources en eau dans les stations touristiques de montagne. Les cas de Crans-Montana-Aminona et Nendaz (Valais)*, Thèse de doctorat, Université de Lausanne, Lausanne: Institut de Géographie, Travaux et Recherches n° 17, 2 vol., 371 p.
- Reynard, E., Otero, I., Clivaz, M. (2020). The Interdisciplinary Centre for Mountain Research (CIRM): Fostering transdisciplinarity for transformation research in mountains. *Mountain Research and Development*, 40(2), P1–P3.
- Savoy, A., Nahrath, S., Reynard, E. (2023). *Analyse juridique du régime institutionnel de l'activité hydroélectrique*. Working paper n°3 du projet « Multifonctionnalité des infrastructures hydroélectriques alpines ». Lausanne: Université de Lausanne, in prep.
- Schweizer, R. (2015). *Stratégies d'activation du droit dans les politiques environnementales. Cas autour des bisces valaisans*. Zürich: Rüegger Verlag.
- Utz, S., Clivaz, M., Reynard, E. (2017). Processus participatifs et projets d'aménagement des cours d'eau. Analyse de l'implication des acteurs dans la planification du projet de 3ème correction du Rhône suisse entre 2000 et 2015. *Géocarrefour* [En ligne], <http://geocarrefour.revues.org/10140>
- Varone, F., Reynard, E., Kissling-Näf, I., Mauch, C. (2002). Institutional Resources Regimes. The case of water in Switzerland. *Integrated Assessment. An International Journal*, 3(1), 78–94.
- Varone, F., Nahrath, S., Gerber, J.-D. (2008). Régimes institutionnels de ressources et théorie de la régulation. *Revue de la régulation*, 2 [en ligne]. <http://regulation.revues.org/>
- Viallon, F.-X., Schweizer, R., Varone, F. (2019). When the regime goes local: Local regulatory arrangements and land use sustainability. *Environmental Science & Policy*, 96, 77–84.

The use of motor vessels on the reservoirs in Slovenia: A case study on the Sava River

N. Smolar-Žvanut, M. Centa, I. Kavčič & N. Kodre

Ministry of Natural Resources and Spatial Planning, Slovenian Water Agency, Celje, Slovenia

ABSTRACT: In accordance with the Slovenian Water Act, the Government of the Republic of Slovenia determines by the Decree individual inland waters or their sections where navigation with the use of motor vessels is permitted, taking into account enabling the general use of water, their protection against pollution and the preservation of the natural balance in the aquatic and riparian ecosystems. Currently, nine Decrees on the use of motor vessels in the river sections are in force in Slovenia. In order to determine the navigation regime in the reservoir of the Brežice Hydropower Plant on the Sava River, a study was made in which the environmental basis from the river basin management plan and bathymetry of the reservoir were taken into account. The indirect and direct impacts of possible pressures due to navigation, on the ecological and chemical status of the water were analyzed. The result of the study is a designated section of reservoir where the navigation with the use of motor vessels is permitted.

1 INTRODUCTION

The reservoirs in Slovenia were built for different purposes, such as hydropower generation, flood protection, industrial water use, irrigation, drought management as a priority use, but during the years many other uses of water like fisheries, aquaculture, navigation and recreation started to develop on them (Smolar-Žvanut et al. 2020).

Navigation on inland waters, which is divided into navigation with the use of motor vessels and navigation within general use of water, is regulated by the Water Act (Official Gazette of the Republic of Slovenia, No. 67/02, 2/04 – ZZdrI-A, 41/04 – ZVO-1, 57/08, 57/12, 100/13, 40/14, 56/15 and 65/20), Inland Waterways Navigation Act (Official Gazette of the Republic of Slovenia, No. 30/02, 29/17 – ZŠpo-1 and 41/17 – PZ-G) and bylaws. According to the first paragraph of Article 66 of the Water Act (Official Gazette of the Republic of Slovenia, No. 67/02, 2/04 – ZZdrI-A, 41/04 – ZVO-1, 57/08, 57/12, 100/13, 40/14, 56/15 and 65/20), navigation with the use of motor vessels on inland waters is prohibited. On the basis of the second paragraph of Article 66 of the Water Act (Official Gazette of the Republic of Slovenia, No. 67/02, 2/04 – ZZdrI-A, 41/04 – ZVO-1, 57/08, 57/12, 100/13, 40/14, 56/15 and 65/20), the Government of the Republic of Slovenia can, with the Decree on the use of motor vessels determine inland waters or their sections where the navigation with the use of motor vessels is permitted. There are currently 9 Decrees in force in Slovenia (Figure 1). All Decrees are located in the Danube River Basin.

Navigation on inland waters without motor vessels is a general use of water, for which you do not need a water right. However, it is necessary to get a water right for the use of water for a harbor or port.

The purpose of the paper is to show the restrictions of the navigation with the use of motor vessels on the reservoir of the Hydropower Plant Brežice (hereafter HP Brežice) in accordance with the second paragraph of Article 66 of Water Act (Official Gazette of the Republic of Slovenia, No. 67/02, 2/04 – ZZdrI-A, 41/04 – ZVO-1, 57/08, 57/12, 100/13, 40/14, 56/15 and 65/20),

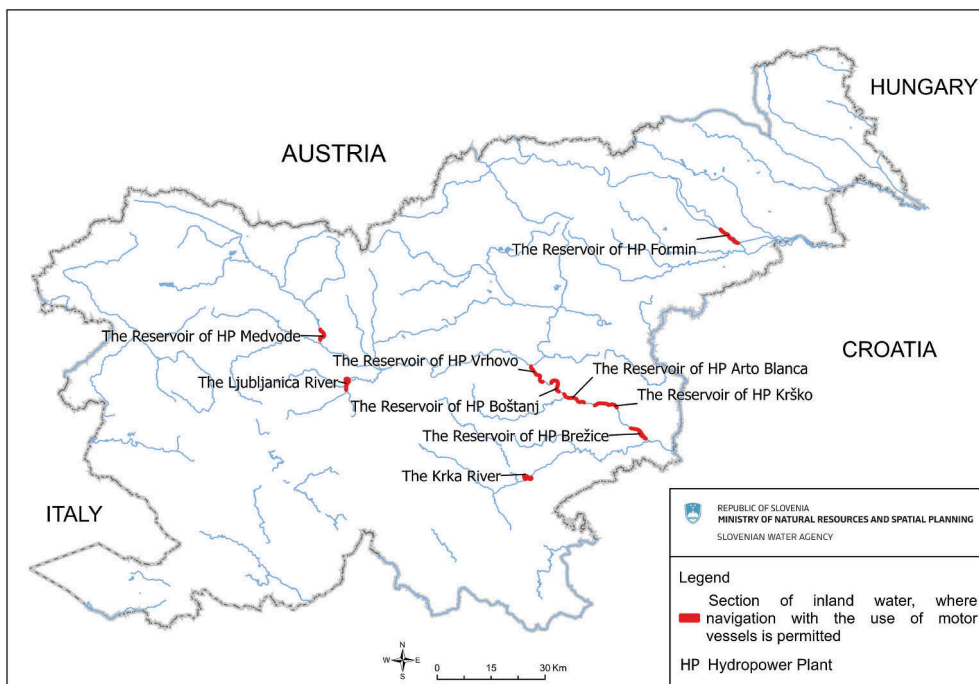


Figure 1. Sections of inland waters, on which the navigation with the use of motor vessels is permitted in Slovenia.

taking into account the possibility of general use of water, its protection against pollution and the preservation of the natural balance in the aquatic and riparian ecosystems. When preparing the expert basis for navigation with the use of motor vessels (Smolar-Žvanut et al. 2019), the impact of navigation on the water status was assessed by taking into account the Water Management Plan in the Danube River Basin for the period 2016-2021 (2016). The direct and indirect impacts on the water status were assessed and took into account the guidelines of the concessionaires and guidelines in the field of nature and fish protection. The expert basis were the starting points for the preparation of the Decree on the use of motor vessels on the reservoir of the Brežice Hydropower Plant on the Sava River (Official Gazette of the Republic of Slovenia, No. 105/20).

2 ENVIRONMENTAL BASIS FOR NAVIGATION WITH THE USE OF MOTOR VESSELS ON THE RESERVOIR OF THE HYDROPOWER PLANT BREŽICE

The Lower Sava River HP chain (HP Brežice is the last HP in the chain and it was constructed in 2018) is a run of the river cascade system, with some active storage capacity that provides a continuous and reliable supply of electricity, with flexibility of operation for daily fluctuations in demand through water flow that is regulated by the facilities. The Figure 2 shows the dam and HP Brežice.

The reservoir of HP Brežice is primarily used for hydropower generation, but also have a much broader role for people and environment (flood protection, groundwater level preservation, tributaries and habitats restoration, new habitats, recreation and water sports, etc.). During operation, the concessionaire of HP Brežice must take into account all existing water rights and not limit them.

The navigation section is located on the catchment area of the surface water body »Sava Krško – Vrbina« (Regulation on the definition and classification of surface water bodies (Official Gazette of the Republic of Slovenia, No. 63/05, 26/06, 32/11 and 8/18)), which has a good chemical status for the water and biota matrix together, without ubiquitous substances, and a good ecological status (both for the period 2014–2019), and in the area of the groundwater



Figure 2. HP Brežice dam.

body »Krška kotlina« (Regulation on the designation of groundwater bodies (Official Gazette of the Republic of Slovenia, No. 63/05 and 8/18)), which shows good quantitative and good chemical status (both for the 2014–2019 period).

For the surface water body »Sava Krško–Vrbina«, it is estimated that there are significant pressures on the water body due to the discharge and treatment of industrial waste water, agriculture, water abstraction and regulations of the riverbed and the river banks. For the water body, environmental goals are defined in accordance with the Water Management Plan in the Danube River Basin for the period 2016-2021 (2016), namely the prevention of deterioration of water status.

Data on the reservoir bathymetry are needed for a more precise determination of the navigable section of the reservoir. The bathymetric recording of the reservoir of HP Brežice was carried out from August 29 to August 31, 2017 and the data was received by the customer of the measurements, public company INFRA, d.o.o. It is also necessary to take into account the fact that the bottom of the reservoir changes, as the sediment in reservoir bed is moved especially during floods. In the reservoir, sedimentation itself could also be a problem for navigation.



Figure 3. Concrete pier, steps and benches for sitting.

The intended small ports and harbors in the area of the HP Brežice reservoir have not yet obtained water permits. During the field visit on April 2018, we recorded access ramps, concrete piers (Figure 3) that will also serve as platforms for access by firefighters and for rescue needs. Figure 4 shows artificial pebble islands for birds, which were made like environment mitigation and replacement measures during the construction of HP Brežice.



Figure 4. Artificial pebble islands.

When preparing conditions, bans and restrictions for the navigation of the use of motor vessels, we took into account the expert opinions and guidelines of the owner of HPs on the Lower Sava River (company HESS, d.o.o.), public company INFRA, d.o.o., Nuclear Power Krško (which is located upstream), the Institute of the Republic of Slovenia for Nature Protection - Novo mesto and the Fisheries Research Institute of Slovenia.

3 POTENTIAL PRESSURES AND IMPACTS CAUSED BY NAVIGATION WITH THE USE OF MOTOR VESSELS ON WATER STATUS

Possible pressures and impacts on the reservoir ecosystem due to activities related to use of motor vessels are:

- water pollution due to municipal waste water and waste due to the increased number of people near the water, which are related to the arrangement of tourist facilities along the reservoir (catering facilities, boat rentals, information points),
- spills of oil, fuel, engine exhaust (PAH - polycyclic aromatic hydrocarbon, benzene and other petroleum derivatives), waste,
- pollution from anti-fouling coatings on vessels (TBT - Tributyltin, copper),
- physical changes to the river banks (strengthening of the river banks, removal of riparian vegetation) and undulation,
- physical changes to the river bed (change in the structure of the river bed, lifting of sediment),
- direct contact of the vessel with organic or inorganic substrate and aquatic organisms,
- introduction of organisms attached to the vessel, if it was used elsewhere (e.g. non-native species of mussel, like zebra mussel, *Dreissena polymorpha*),
- transfer of non-native species of plants located in the river banks (e.g. Japanese knotweed *Fallopia japonica*),
- underwater noise.

The direct and indirect impacts of pressures that can be caused by the use of motor vessels were defined on individual quality elements of ecological status. On the basis of the analyses, it was concluded that navigation can directly have impacts on the hydromorphology (the structure and substrate of the river bed, the structure of the riparian zone), while on the chemical and physico-chemical elements of quality (oxygen conditions, nutrients, thermal conditions) can have impacts indirectly or directly. Indirect impact of navigation is possible on all biological quality elements (composition and abundance of phytobenthos and macrophytes, composition and abundance of benthic invertebrates, composition, abundance and age structure of fish).

4 RESTRICTIONS, CONDITIONS AND BANS FOR NAVIGATION WITH THE USE OF MOTOR VESSELS ON THE RESERVOIR OF HP BREŽICE

Based on the review of the indirect and direct impacts of navigation with the use of motor vessels on the quality elements of the water status and the aquatic ecosystem, taking into account the obtained expert opinions and guidelines, it was defined the navigation section inside the reservoir of HP Brežice.

Below are the restrictions, conditions and bans to reduce the negative impact of navigation with the use of motor vessels on the river ecosystem of the reservoir of HP Brežice.

4.1 Permitted use of motor vessels

The navigation area is divided into zone A and zone B (Figure 5). With the aim to reduce the negative impact on the water status and quality of the water, only vessels on electric motor can be used and vessels should be shorter than 24 m. In January, February, March, November and December, only one motor vessel can navigate at the same time in the navigation zone B, and only under condition if this navigation is intended for the implementation of educational processes or related to recreational sports (e.g. sailing, rowing).

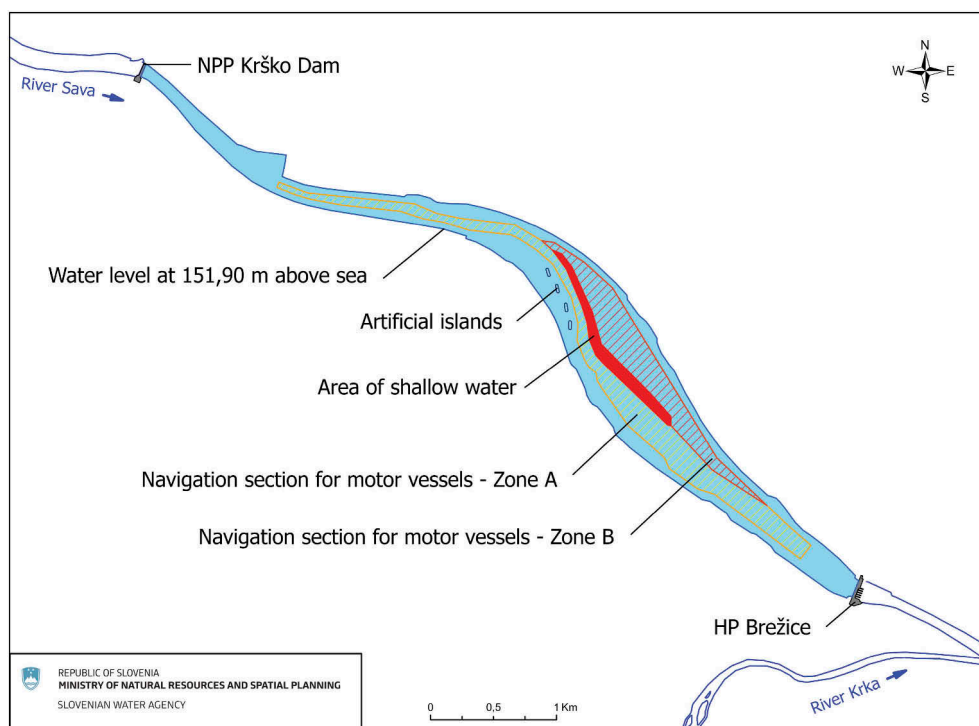


Figure 5. Navigation section with zone A and zone B.

4.2 *Conditions for navigation*

Navigation with the use of motor vessels must be carried out in such a way that:

- takes place outside the shoals and the shoals are marked with prescribed signalization,
- the maximum speed of motor vessels does not exceed 10 km/h or it can be higher in order to ensure the safety of passengers in case of emergency conditions in the navigation section (e.g. storm, increased water flow, rising water level),
- the recommended minimum distance between the maximum sinking of the vessel and the reservoir bottom is 2 m,
- waves are not caused along river banks with a wave height greater than 0.3 m,
- after mooring in the port, before leaving the vessel, all movable fuel tanks and all unattached objects should be removed from it,
- boarding and disembarking of passengers is carried out only in ports or harbors,
- during the ban of navigation, all vessels should be moored in ports or raised from the water outside the river bank,
- the maximum number of vessels that can be in the navigation section at the same time does not exceed the maximum number of berths in the ports,
- the leakage of pollutants (e.g. battery contents), oils and lubricants, protective coatings, organically loaded fecal waters and other harmful or toxic substances from vessels into the water is prevented, even in the event of sinking or damage to the vessel,
- the filling of batteries with electricity from land or their transfer to vessels is carried out only in the port area,
- the lifting or lowering of the vessel is carried out only at designated places,
- does not cause lift of sediment on the river bottom,
- all vessels, together with all equipment, should be cleaned before launching into the water in order to prevent the spread of invasive plants and animals,
- that in the case of fishing activities (fishing, competitions, etc.) the fishing activity is not disturbed,
- not affect the existing water rights and the production of electricity at the HP Brežice.

4.3 *Bans for navigation*

Navigation with the use of motor vessels is prohibited:

- in zone A from November 1 to March 31,
- at night time in zone A and zone B,
- when water overflows through the spillway of the HP Brežice,
- when the flows of the Sava River are higher than 500 m³/s,
- during the implementation of maintenance and other works (intervention) on river banks that affect the navigable section,
- if the water level is lower than the normal level of the reservoir,
- in the event of extraordinary events (floods or pollution).

4.4 *Monitoring*

Due to the sediment accumulation in the reservoir of HP Brežice, larger and new shallows can form. It makes sense to carry out measurements of sediments (bathymetric measurements of the reservoir bottom) annually or after major floods and, if necessary, change the navigation section or prepare a proposal for sediment removal/transportation program. If the results of ecological monitoring showed that navigation with the use of motor vessels has a negative impact on the achievement of the water status goals, additional measures must be taken to reduce the negative impact, or the navigation should be reduced or banned. In the case of deterioration of habitat types for plant and animal species or in the event of a significant impact of navigation during the nesting period of birds or fish spawning, the navigation is adjusted or restricted accordingly (e.g. space, time limit or limit on the number of vessels in the navigation section).

5 CONCLUSION

Navigation with the use of motor vessels can represent an important secondary use of reservoirs in Slovenia. Expert basis should take into account the guidelines and opinions of all key stakeholders and they form the basis for the preparation of the decrees on the use of motor vessels.

Decrees determine the navigation section where the use of motor vessels is permitted, the conditions, restrictions and bans for navigation. According to Slovenian Water Act (Official Gazette of the Republic of Slovenia, No. 67/02, 2/04 – ZZdrI-A, 41/04 – ZVO-1, 57/08, 57/12, 100/13, 40/14, 56/15 and 65/20), the conditions for navigation are crucial for the protection of water ecosystems against deterioration of ecological status, water pollution and the preservation of the natural balance, while the Inland Waterways Navigation Act (Official Gazette of the Republic of Slovenia, No. 30/02, 29/17 – ZŠpo-1 and 41/17 – PZ-G) and by-laws (including municipal ones) regulate the safety of navigation (Slovník Vraneš 2020).

REFERENCES

- Decree on the use of motor vessels on the reservoir of the Brežice hydroelectric power station on the Sava river (Official Gazette of the Republic of Slovenia, No. 105/20).
- Inland Waterways Navigation Act (Official Gazette of the Republic of Slovenia, No. 30/02, 29/17 – ZŠpo-1 and 41/17 – PZ-G).
- Regulation on the definition and classification of surface water bodies (Official Gazette of the Republic of Slovenia, No. 63/05, 26/06, 32/11 and 8/18).
- Regulation on the designation of groundwater bodies (Official Gazette of the Republic of Slovenia, No. 63/05 and 8/18).
- Slovník Vraneš, D. 2020. Problems of the state and municipalities competence in navigating inland waterways. Master Thesis. University of Ljubljana. The Faculty of Public Administration. Ljubljana: 110.
- Smolar-Žvanut, N., Centa, M., Kavčič, I., Damjanovič, B., Kolman, G., Hrovat, M., Krajčič, J. 2018. Expert basis for the preparation of the Decree on the use of motor vessels on the reservoir of the Brežice hydropower plant on the Sava River. Slovenian Water Agency, Ljubljana, July 2018: 73.
- Smolar-Žvanut, N., Meljo, J., Kodre, N., Prohinar, T. 2019. Multipurpose water uses of reservoirs in Slovenia. *The International Journal on Hydropower and Dams*, Volume 27 (2).
- Water Act (Official Gazette of the Republic of Slovenia, No. 67/02, 2/04 – ZZdrI-A, 41/04 – ZVO-1, 57/08, 57/12, 100/13, 40/14, 56/15 and 65/20).
- Water management plan in the Danube River Basin for the period 2016–2021. 2016. Ministry of the Environment and Spatial Planning of the Republic of Slovenia. Ljubljana, October 2016: 295.

Re-operationalization of dams to adapt to climate change in Romania

D. Stematiu

Romanian Academy of Technical Sciences

A. Abdulamit

Technical University of Civil Engineering Bucharest, Romania

ABSTRACT: Increased hydrologic variability has and will continue to have a profound impact on the water sector through the water availability versus water demand and water allocation. Dam construction is a long-standing strategy to reduce the spatial-temporal variability of natural regime of water. By regulating the water flow, dams alter the natural hydrograph to secure a reliable source of water for a wide variety of human and environmental needs.

The increase in the frequency and intensity of floods and droughts in Romania, combined with the reduced drought and flood storage buffering capacity of dams under a changing climate may have critical inferences for a region's water supply and economy. Building new dams in addition to dams' re-operation may be necessary to balance the climate change impacts on flooding and drought vulnerability.

The present paper deals with several examples of required changes in Romanian dam operation: the new constrains in operation of hydropower developments, the needed increase of flood protection volumes for the existing reservoirs, the new concept in characterizing a flood by its volume instead of the peak inflow and the reasonable procedures to cope with the large siltation of many existing reservoirs.

RÉSUMÉ: La variabilité hydrologique accrue a et continuera d'avoir un impact profond sur le secteur de l'eau à travers la disponibilité par rapport à la demande et allocation de l'eau. La construction de barrages est une stratégie de longue durée visant à réduire la variabilité spatio-temporelle du régime naturel des eaux.

Les augmentations de la fréquence et de l'intensité des inondations et des sécheresses en Roumanie, ainsi que la réduction de la capacité-tampon de stockage des barrages réservoirs en cas de sécheresse et d'inondation dans un climat changeant, peuvent avoir des implications critiques pour l'alimentation en eau et l'économie de la région. Construire des nouveaux barrages et reconsidérer l'exploitation des barrages existants peut être nécessaire pour équilibrer les impacts du changement climatique sur la vulnérabilité aux inondations et à la sécheresse.

L'article présente plusieurs exemples de changements requis dans l'exploitation des barrages roumains: les nouvelles contraintes d'exploitation des aménagements hydroélectriques, l'augmentation nécessaire des volumes de protection contre les crues pour les réservoirs existants, le nouveau concept de caractérisation de l'inondation par son volume au lieu du débit de pointe et les procédures raisonnables pour faire face à la sédimentation importante de certains réservoirs existants.

1 INTRODUCTION

A series of phenomena and processes from recent years - the global temperature rise, the increase in the frequency of heat waves, droughts, the change in the precipitations regime, the decrease of the snow layer, the change in soil moisture and surface runoff – are termed as

global climate changes (Alavian et al. 2009). For the reservoir operation they cause changes in the hydrological regime of the watercourses. Usually, dam safety management has been carried out assuming stationary climatic and non-climatic conditions. However, the projected alterations due to climate change are likely to affect different factors driving dam risk. This includes impacts and adaptations that relate to the operation and use of reservoirs. The main operating purpose of a dam (e.g. flood management, hydropower, water supply etc.) will influence dam re-operation strategies. Re-operation may require integration across sectors or involve multiple dams, enhancing benefits such as water supply or hydropower while simultaneously achieving ecosystem restoration.

Changes in the hydrological regime, characterized by more frequent and larger floods and, in opposition, by prolonged droughts, lead to important effects in the operation mode (rules) of dams and pose additional risks affecting their safety.

2 THE IMPACT OF CLIMATE CHANGE ON FLOOD ROUTING

The effect of the reservoir on the regulation of downstream flows is globally expressed by the volume of water retained and respectively discharged into and from the reservoir. For flood control, the actual effect is done not by the volume of the reservoir itself but by the ratio between the reservoir and the annual yield of the stream. An index of the degree of regulation can be defined as the ratio between the volume of water temporarily stored in a reservoir and the yield of the stream for the same period. Currently, the operating rules are based on the assumption that flood volume is constant, corresponding to the hydrological conditions at the design level. Figure 1 presents alteration of the Total Available Water resources (TAW) (Ehsani et al. 2017) due to climate change and considering regulation. These changes lead to re-evaluation of the needed attenuation volume provided by the existing operation rules.

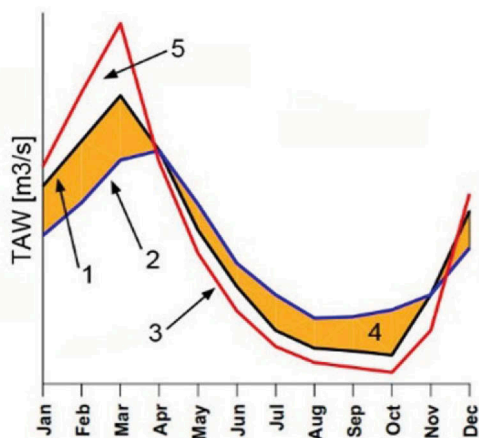


Figure 1. Changes in Effective degree of regulation (EDR). 1-Natural TAW, w/o dams; 2-regulated TAW, w dams; 3-Effect of climate change on TAW; 4-Water volume displaced by dams; 5-Additional storage/volume needed! (adapted from Ehsani et al. 2017).

The consequences of the changes of the inflow hydrograph corresponding to the maximum volume flood are rendered evident by the analysis of the hydrological safety of a very large flood control storage reservoir in Romania, i.e. Stanca-Costesti reservoir, with a total volume of 1.4 km³. Stanca-Costesti hydraulic development is located on the Prut River at the border between Romania and the Republic of Moldova (Figure 2).



Figure 2. Aerial view of Stanca-Costesti dam. 1-Right wing dam; 2-Spillways; 3-Intake; 4-Main dam; 5-Powerhouse; 6-Old quarry closure dam.

The retention front has a length of over 3 km and includes a series of dams of different types and characteristics, connected into a continuous larger structure or separated by sectors of natural ground with higher elevation. The maximum dam height is 47 m, the main dam length is 740 m. The hydraulic development was built in the 1973-1978 period and was commissioned in 1977.

The routing through the Stanca-Costesti reservoir of some significant floods occurred in the last years has shown some significant differences from the designed floods (Figure 3). The largest one was during 25 July - 02 August 2008 with maxim discharge 3380 m³/s (15% larger than the design flood) and a volume of 982 hm³ (Gabor & Hortopan 2008). Using the designed operation rules, the water elevation in the reservoir overpassed the upper limit of the flap gates on the main spillway (Drobot & Draghia 2012).

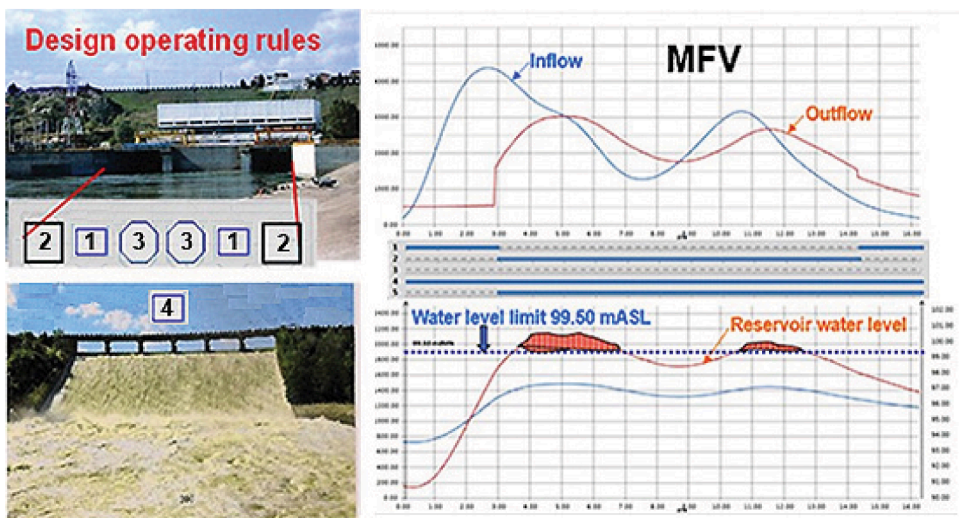


Figure 3. Stanca-Costesti dam flood routing according to the Design Operating Rules. Water level in the reservoir overpassed the flap gates. 1. . .3-opening rules for the bottom outlets; 4-flap gated spillways. (MFV-maximum flood volume).

In the case of Stanca-Costesti reservoir new operating rules are in development. One alternative would require increasing the attenuation volume. In this case, the reservoir level decrease will be in direct conflict with the hydropower output and with lake shore existing developments. In many other cases the need to provide flood mitigation volume for the protection of downstream communities by pre-emptying the reservoir is in direct conflict with the need to having available stored volumes of water to counteract for the effects of drought, supplying water for population and economic objectives and providing ecological flows. The reconciliation of the two options becomes much more difficult in the context of climate change, when both requirements are more acute - higher floods followed by prolonged droughts.

Changing the operating regime of the dams storage reservoirs (more recently called re-operation) can partially solve the impact induced by climate change, but certainly, if the current tendencies persist, new storage reservoirs will be needed.

3 THE IMPACT OF CLIMATE CHANGE ON THE OPERATION OF HYDROPOWER FACILITIES

Hydropower reservoirs alter the seasonal flow patterns and can be out of phase from the natural flow regime, reducing flow during higher-flow periods and increasing flow during lower-flow periods. The regular operation patterns can be significantly changed by climate change. In many rivers, climate change will affect water availability for hydropower and ecosystems. The impacts of climate change on hydropower developments are complex, often interactive issues. Many studies have already focused on climate change impacts on the hydrologic cycle. The gross hydropower potential is expected to increase with the increased river flows (Stanciu et al. 2010).

Even prior to the climate change issue, new conditions regarding the approach concerning the public security and environmental protection and changes in the way of operation and maintenance of the existing hydropower facilities were considered. They were imposed by the requirements to satisfy some additional stakeholders compared to those from the initial hydropower facility commissioning. The operation changes have to accommodate the new basin management policies: flood protection, supply water for population and irrigations, providing a minimum ecological flow, restoring some wetlands, tourism and leisure etc. These requirements increase with the climate change. In the vast majority of them, the re-operationalization led to a reduction in the energy produced. Thus, the increase in the guaranteed minimum flow downstream of the dam reduces the volume of water used by turbines, the maintenance of restricted lower elevations in the reservoir to provide the volume of flood mitigation reduces the power plant head, the restrictions on the seasonal variations of the water level in the reservoir imposed by tourism or fish farming affect energy regulation. In all these situations, optimizing the reconciliation between the different conflicting uses is essential.

In order to underline the effects of the re-operationalization, the case of Tarnita hydropower development is presented in the followings, were a supplementary water supply service led to a decrease in the amount of energy produced.

The Tarnita arch dam, with a total height of 97 m, and a crest length of 237 m was commissioned in 1974 and provides the storage and head for the power station located at the downstream toe of the dam. The power station is equipped with two Francis units of 22.5 MW each (Figure 4).

The reservoir has a volume of over 70 hm³ and is created on Somesul Cald River and its tributaries from a watershed of 491 km². The reservoir surface is 220 ha, with a maximum depth of over 70 m.

While built as a hydropower facility, the Tarnita reservoir currently has a triple role. In addition to the production of electricity, the reservoir is also used as source for water supply for the towns of Cluj-Napoca and Gilau. The dam also plays an important role in flood control. The change in the reservoir operation rules was imposed by the constrains induced by climate change on the existing water supply sources e.g. decrease of water wells yield due to a long drought period and a severe siltation of the Gilau reservoir that used to be an additional water supply source.

In order to accommodate the new reservoir use (as a water supply source), several hydraulic structures were built, including a water supply intake tower and a 5 km aqueduct (Figure 4, right).



Figure 4. Tarnita dam aerial downstream view. The new water supply intake tower (right).

Some concluding data regarding the effects of the new operation rules are: the water volume provided for population is some 32 hm³/year; the water power specific consumption is 3400 m³/MWh; the energy loss is 9.689 GWh/year.

On the other hand, it should be emphasized that the use of hydropower potential is a component of water management. Recently, there has been a tendency to design hydropower facilities with the sole objective of “profitability”, expressed as a specific investment and internal return rate. Such an approach inherently leads to reservoirs with minimum volumes required for hydropower, neglecting both the concept of assured power and the full utilization of the water resources in the site (Stematiu & Iacob 2015).

On the basis of the specific legislation and the national program for harnessing the hydropower potential, the hydropower development schemes with complex use must be updated, taking into account some requirements such as:

- the regulation of the natural hydrological yield of the watershed to provide, in the drought periods, the necessary water for population, industry, agriculture, environment;
- providing flood protection for localities, lifeline facilities and agricultural lands;
- development of the tourist and fishing potential in the cases of future developments.

4 DAM SAFETY UNDER INCREASED FLOODS

Exceeding the designed capacity of the dam spillways, followed by crest overflowing is, by far, the most common way of failure, with over 30% of cases worldwide. Obviously, the inflow is a random quantity, possibly to be transformed by upstream regulation processes. The capacity and location of the spillways depend on the type of the hydraulic structure and its availability. The attenuation volume provided by the reservoir depends inextricably on the initial water level in the reservoir at the time of flood incidence. All these are random variables that must be included in the operation rules of a certain reservoir.

The alteration in the hydrological regime imposed by climate change directly affects both factors that define the safety of the flood routing - the inflow and the water level in the reservoir. If for the first factor the effect is obvious, for the second one the effect is caused by the need to store as large volumes as possible in the reservoir, in order to ensure all water uses in the conditions of extended drought periods and therefore to keep a higher water level in the reservoir.

At the first glance, the engineering solution is to increase the capacity of the spillways adding supplementary hydraulic structures or extending the existing ones (e.g. turning a conventional spillway into a piano key weir). The solution is particularly erroneous. First, it involves high costs

and secondly, it leads to a decrease of flood attenuation capacity by spilling a higher discharge downstream and storing a lower volume of flood. A more rational approach consists in creating larger volumes to mitigate floods, either by pre-emptying the reservoir, or by adding lateral (additional) storage facilities.

For example, the case of the Mihailesti dam is presented. The reservoir, with a volume of 52.7 hm^3 is created behind a main concrete mobile dam with a maximum height of 25.50 m, a frontal earthfill dam on the right bank of 2 km and a longitudinal dam closing the left bank along 11.48 km, with a maximum height of 13 m.

The spillways of the dam consist of 3 discharge bays, 10 m wide, equipped with radial gates with flaps ($10 \times 5.75 \text{ m}^2$) and three bottom outlets equipped with radial valves ($10 \times 3 \text{ m}^2$). Additionally, the dam is provided with a safety spillway located near the end of the left bank lateral dam. Its aim is to increase the discharge capacity of the spillway system in the event of floods exceeding the design flood ($Q_{0.1\%} = 2,935 \text{ m}^3/\text{s}$).

According to the design operating rules, the design flood is partially retained into the reservoir, by lowering the water level from 85 maSL (normal operation level) to 82 maSL. For the routed flow the discharge is achieved by using the full capacity of the mobile dam spillways and by using, beside the gated bays, the safety spillway that can discharge an additional $385 \text{ m}^3/\text{s}$. Without the safety spillway the level in the reservoir could reach the dam crest elevation (89.50 maSL), situation that can raise concerns for the dam safety (Abdula-mit et al 2015).



Figure 5. Mihailesti dam general plan and downstream view.

The original designed operation rules are no longer valid. However, the activation of the safety spillway leads to the flooding of a large, inhabited area. At the design time the area was used as an agriculture land but, in the last 20 years, the use of land has been changed, by extending the inner-city limits to the vicinity of the left bank dam.

Under the new conditions, taking into consideration the possible increase of the river floods due to climate changes, flood routing through the reservoir must be reviewed (re-operationalization). The rational approach is to increase the attenuation volume by increasing the pre-lowering of the reservoir and relying on the main spillway. Based on an early hydro-meteorological prediction with a three-day anticipation period, it is possible to lower the reservoir to the level of 76.16 mSL keeping the downstream outflows in the limits of the riverbed capacity. The procedure has to be extended in case of an increase in flows and flood volumes due to climate change (Figure 6).

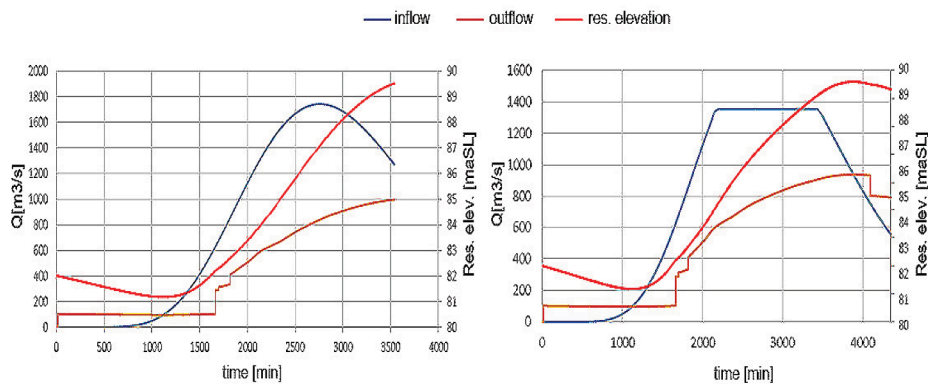


Figure 6. Volumes and levels during the transit of the design flood (according to the UTCB study, 2015).

5 INCREASED SILTATION AND ITS EFFECTS ON RESERVOIR OPERATION

Among the consequences of climate change are the increase in torrential flows on the basin slopes, the activation of torrents on streams that are usually with no water and flush-floods of increasing magnitude. These changes in the regime of surface runoff led to the amplification of erosion in the watershed and directly to the increase of the solid flow. Recent studies show an increase in solid transport by 1.7% for every 1% increase in precipitation volume.

For dam storage reservoirs, the phenomenon is extremely negative, leading to their increased congestion. The immediate effect is the decrease in operating volume, affecting both the use of raw water supply and the ability to mitigate floods for downstream protection. A situation often easily disregarded is the clogging at the tail of the reservoir, in the region of the reservoir inflow access. Over time, veritable alluvial dams are formed, densely vegetated, sometimes even forested, preventing water inflow into the reservoir. As a result, flood can bypass the reservoir with a direct effect on the dam safety, but especially with catastrophic effects for the localities adjacent or downstream of the dam. To illustrate the issue the case of Pucioasa dam is presented in the following.

The dam creating the Pucioasa reservoir is located in the upper basin of the Ialomita river, immediately upstream of the Pucioasa town. The dam has a height of 30.5 m. The gated dam has a 16 x 2.50 m² flap gate and 3 bottom outlets of 4 x 4 m², equipped with radial valves. The reservoir is bordered by lateral dams with a total length of 3,128 m (Figure 7).

At the design time (1971), the volume of the reservoir corresponding to the normal operation level was 10.6 hm³. In 1993 the volume was already reduced to some 5.08 hm³, that represents 47% siltation degree. In 2002, the volume dropped to only 3.49 hm³, with a degree of reservoir siltation of 67%. Currently the siltation degree is above 75% and the process is still ongoing.

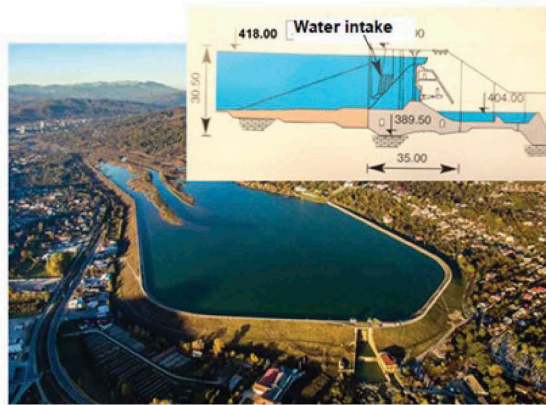


Figure 7. Pucioasa dam and reservoir.

Figure 8 shows a satellite view of the evolution of the reservoir siltation. It is visible that, in a time frame of some 35 years, the area at the access into the reservoir became more and more silted and covered with vegetation. The Ialomita River inflows into the reservoir through a narrow channel and during floods, even minor ones, the river by-passes the lateral dams of the storage reservoir and provokes inundations in the town of Pucioasa, located downstream.



Figure 8. The evolution of the silting of Pucioasa reservoir between 1985 and 2020.

6 CONCLUDING REMARKS

The increase in the frequency and in magnitude of floods and the increase of the severity and duration of drought periods, combined with the lack of regulation volumes in the reservoirs of existing dams can have critical consequences in social and economic security and sustainability. Therefore, the new tendency induced by climate changes leads to significant effects in the operation mode of the dams and poses additional risks concerning their safety.

In the context of climate changes, the operation of hydropower facilities must take into account the regulation of the natural hydrological yield of the watershed in order to supply water for population, industry, agriculture and environment. Their reservoirs have to provide also the safe flood routing protecting localities, lifeline facilities and agricultural land.

The change in the hydrological regime imposed by climate change may lead to larger floods that endanger the dam safety. The rational approach for maintaining safety requirements consists in creating larger volumes to mitigate floods by pre-emptying the reservoirs.

In the case of reservoirs with a very high degree of siltation, where the regulation volume is seriously affected, floods can by-pass the reservoirs with a direct effect on dam safety, but especially with catastrophic effects for the localities adjacent or downstream.

REFERENCES

- Abdulamit, A., Stematiu, D., Sirbu, N. 2015. Study to upgrading the operation rules for the storage reservoir Mihalesti. *Technical Report* (in Romanian). Bucharest, 2015.
- Alavian, V., Blankespoor, B., Danilenko, A., Dickson, E. Diez, S., Hirji, R., Jacobsen, M., Pizarro, C., Puz, G., Qaddumi, H. 2009. Water and climate change: understanding the risks and making climate-smart investment decisions. Washington, D.C. World Bank Group.
- Drobot, R., Draghia, A. 2012. Design floods obtained by statistical processing. *Proc. of 84th ICOLD Congress*, Kyoto.
- Ehsani, N., Vörösmart, C., Fekete, M., Stakhiv, E. 2017. Reservoir operations under climate change: Storage capacity options to mitigate risk. *Journal of Hydrology*. Vol. 555, Dec. 2017, Pages 435–446.
- Gabor, O., Hortopan, I. 2008. Mitigation of the July-August 2008 flood in the Stanca-Costesti reservoir (in Romanian). *Hidrotehnica*, Vol 53, No. 11-12, 2008.
- Stanciu, P., Oprisan, E., Tecuci, I. 2010. Some considerations on the hydropower potential of Romania. *Proc. Conference "Climate changes - Concrete solutions for Romania"*. (in Romanian). Bucharest, March 18.
- Stematiu, D., Iacob, I. 2015. Aspects regarding hydropower as a supporting source of energy for sustainable development (in Romanian). *Hidrotehnica*, Vol. 60, No. 3, 2015.

Design values for dams exceeded: Lessons learnt from the flood event 2021 in Germany

S. Wolf, E. Klopries & H. Schüttrumpf

Institute of Hydraulic Engineering and Water Resources Management, RWTH Aachen University, Germany

D. Carstensen

Institute of Hydraulic Engineering and Water Resources Management, TH Nürnberg, Germany

R. Grönsfeld

Waterboard Eifel-Rur (WVER), Düren, Germany

C. Fischer

WSW Energy and Water; Wupperverband, Wuppertal, Germany

ABSTRACT: Large parts of Germany, Belgium and the Netherlands were affected by a severe flood event in mid-July 2021. Dams and reservoirs in the Eifel Mountains reached their design limits and in some cases the design values for a return interval of 1 in 10,000 years were even exceeded. This shows us that planning, design, construction and maintenance of these dams are very safe and that a high level of resilience is guaranteed even in the case of very extreme events.

RÉSUMÉ: Une grande partie de l'Allemagne, de la Belgique et des Pays-Bas a été touchée par de graves inondations à la mi-juillet 2021. Les barrages et les réservoirs des montagnes de l'Eifel ont atteint leurs limites de conception et, dans certains cas, les valeurs de conception pour un intervalle de retour de 1 sur 10 000 ans ont même été dépassées. Cela montre que la planification, la conception, la construction et l'entretien de ces barrages sont très sûrs et qu'un niveau élevé de résilience est garanti même en cas d'événements très extrêmes.

1 INTRODUCTION

1.1 *General*

Large parts of Germany, Belgium and the Netherlands were affected by a severe flood event in mid-July 2021. The storm with precipitation rates of up to 200 mm in 24 hours hit the low mountain regions of North Rhine-Westphalia and Rhineland-Palatinate particularly hard. For comparison, the typical annual mean rainfall in the region is about 800 mm (City of Aachen). Due to the mountainous landscape with relatively short and steep valleys, the water levels of the rivers increased rapidly, creating enormous inundations. Peak water depths of up to 8 m above normal water levels were observed at the Ahr River and have caused considerable devastation to buildings, roads and other infrastructures in the affected valleys. The most severe damages were recorded in the Ahr valley in Rhineland-Palatinate and along the Erft and Vicht Rivers in North Rhine-Westphalia. More than 180 people lost their lives during the flood event in Germany. An economic damage in the order of 30 billion Euros occurred. This flood is therefore considered the worst natural disaster in Germany since the storm surge in 1962 and the Elbe flood in 2002.

Dams and reservoirs in the Eifel Mountains reached their design limits for a return interval of 1 in 10,000 years which – in some cases - were even exceeded. For example, the Urft dam, one of the oldest dams in the northern Eifel from 1905, has experienced an event with a probability of occurrence of more than 10,000 years. This extraordinary event did not leave any noticeable damage to the structure. Many other dams in the northern Eifel have also experienced their design event without failure or considerable damages. This shows us that planning, design, construction and maintenance of these dams are very safe and that a high level of resilience is guaranteed even in the case of very extreme events. Dams were even able to withstand an event higher than the design event.

A preliminary comparison between valleys with dams and valleys without dams also revealed the protective effect of dams even during extreme events. The severe damage on the Ahr, Vicht and Erft Rivers occurred in sections without large dams in the upper reaches. Although many large dams are multi-purpose facilities and are mainly designed for raw water supply at the respective locations, they contributed significantly to mitigating flood impacts due to retention effects. Nevertheless, the event was so severe that some damages even occurred in areas below large dams and in flatland regions.

One of the main challenges will be to transfer the lessons learned from this extreme event into a sustainable improvement of future flood protection and reservoir operation in the affected areas of 2021 as well as other areas.

1.2 *Flood area*

The 2021 flood event hit the mid-mountain regions of Northrhine-Westphalia and Rhineland-Palatine in Western Germany. Neighboring countries (The Netherlands, Belgium, Luxembourg) were also affected. Anyway, this paper focuses on the situation in Germany although the situation in NL, B and Lux was quite similar. The most affected river catchments in Germany were the Rur catchment in the Northern part of the Eifel mountains, the Erft catchment in the North-Eastern part of the Eifel mountains, the Ahr catchment in the Southern Eifel mountains and the Wupper-catchment east of the river Rhine. The Rur is a 165 km long river with a total catchment area of 2,360.8 km². The headwaters are at an altitude of 660 m above sea level, while the mouth to the river Meuse is at 30 m above sea level close to Roermond in NL (Nilson, 2006). The Erft catchment originates at an altitude of 527 m above sea level, the river length is about 106.6 km, the catchment area of 1,837 km², and the mouth to river Rhine close to Neuss. The Ahr River flows from Northrhine-Westphalia to Rhineland-Palatine, starting close to Blankenheim and flowing to Rhine River at Sinzig after 85.1 km. The catchment area is 897 km². Finally, the Wupper River has a length of 116.5 km, with a catchment area of 813 km², and is a right-side tributary to the Rhine River at Leverkusen. All four rivers have numerous tributaries, the major ones are presented in Figure 1.

The landscape of these river catchments is characterized by steep and narrow valleys, which are typical for the low mountain regions in Germany. Due to the volcanic origin of the Eifel mountains, the soil structure is composed by a thin topsoil and rocky subsoils resulting in restricted water retention capacities.

1.3 *The Flood event of July 2021*

The flood event of July 2021 can be described as a flash flood, especially in the low mountain ranges. Flash floods are characterized by the fact that they occur without a long warning period, cause water levels to rise in a relatively short time, and have high flow velocities. Depending on the soil properties in the catchment, flash floods can transport a lot of coarse material, deadwood, and, in the case of the event in July 2021, also cars, caravans, and other objects, which increase the force of the water when it hits buildings, bridges or other infrastructure. In low mountain valleys in particular, this often leads to damages to buildings and their foundations.

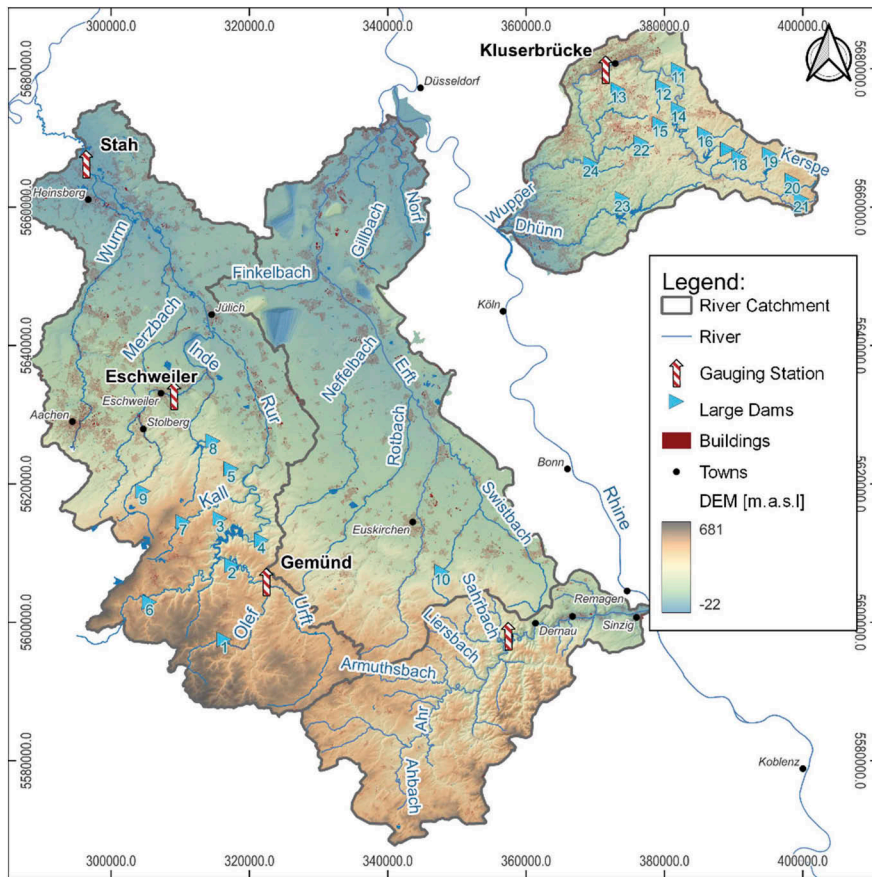


Figure 1. Flood area of July 2021 and locations of dams (source IWW).

When the river has left the low mountain range with its mostly narrow sections, the gradient decreases and the flooded areas increase, resulting in a decrease in water depths and flow velocities. Therefore, damages in these areas are mainly caused by water penetrating into buildings. Damage caused by the impact of flowing water on the building envelope is less frequent. However, since large areas outside the narrow valleys in the low mountain ranges can be flooded and the population density in the foothills is higher, the number of affected buildings and people usually increases considerably in the lowlands.

The flood event of 2021 exceeded all water levels and discharges measured up to that time in the affected regions. Table 1 gives an overview of some selected stations in the Ahr, Inde, Rur, Urft, and Wupper catchments. However, historical water levels are not considered here. For example, the Altenahr gauge was commissioned on 01.01.1991, Eschweiler on 01.01.1966, Stah on 01.06.1905, and Gemünd on 01.11.1949 (sources: LfU, LANUV). Historical flood events such as those in 1804 and 1910 in the Ahr River are not included in these flood statistics (Roggenkamp and Herget, 2015). Particularly along the Ahr River, there are a large number of flood marks that allow a reconstruction of historical Ahr River floods (Roggenkamp and Herget, 2022). Taking these events into account would have led to different recorded peak discharges (HHQ) in preparing the flood hazard and flood risk maps, at least for the Ahr River.

The observed water levels and discharges in the floodplains inevitably lead to a change in the discharge statistics. For water management, this results in the urgent question of how to deal with the new water levels and discharges. In this context, both the question of how the HQ_{100} and EHQ (EHQ = extreme discharge often related to a return period of 1,000 years) values change and the extent to which existing flood protection concepts must be adapted to

Table 1. Hydrological characteristics of the flood event 2021 compared to previous extreme values.

River	Gauge	HHQ* [m ³ /s]	HQ ₂₀₂₁ ** [m ³ /s]	Previous HHW	Water level 14.07.2021	Source
Ahr	Altenahr	236	1000 – 1300	3.71 m (02.06.2016)	≈ 7.00 m	1.)
Inde	Eschweiler	89.48	270	2.48 m (28.09.2007)	> 3.5 m	2.)
Rur	Stah	129.35	n.a.	2.77 m (27.05.1983)	> 3.0 m	2.)
Urft	Gemünd	142.92	n.a.	3.04 m (10.12.1966)	> 5.5 m	2.)
Wupper	Kluser- brücke	211.28	n.a.			3.)

* HHQ: highest peak discharge since start of gauge operation

** HQ₂₀₂₁: peak discharge during the flood event in mid-July 2021

1.) Kreienkamp et al. (2021); LFU Rheinland-Pfalz;

2.) Ministerium für Umwelt, Landwirtschaft, Natur- und Verbraucherschutz NRW (2021), LANUV NRW (2021);

3.) Schüttrumpf et al. (2022)

the new water levels must be discussed. This is not a trivial question to which there are simple answers, as the measured water levels from July 2021 stand out from the previous extreme value statistics and can be statistically characterized as outliers.

1.4 Dams in the flood area

In total, 24 large dams are operated in the flood prone areas of the 2021 event. 10 large dams are situated in the Eifel mountains left to the Rhine River, while some additional 14 dams are situated in the Bergisch Land right to the Rhine River. Table 2 gives an overview of the main characteristics of the 10 dams located on the left side of the Rhine River, while Table 3 gives an overview of the 14 dams located on the right side of the Rhine River.

Table 2. Summary of large dams located on the left side of the Rhine River, WVER = Water Board Eifel-Rur, WP = Perlenbach Water Supply Organisation, WAG = Water Extraction and Treatment Company Nordeifel, WES = Water Supply Organisation Euskirchen-Swisttal.

Dam	Year of Construction	Height of dam [m.a.g.]	Capacity [Mio. m ³]	Operator
1 Olef Dam	1959	59.0	19.3	WVER
2 Urft Dam	1905	58.5	45.5	WVER
3 Rur Dam	1938/1959	77.2	202.6	WVER
4 Heimbach Dam	1935	13.5	1.21	WVER
5 Obermaubach Dam	1934	6.7	1.65	WVER
6 Perlenbach Dam	1956	21.0	0.76	WP
7 Kall Dam	1935	40.0	2.10	WAG
8 Wehebach Dam	1981	49.0	25.1	WVER
9 Dreilaegerbach Dam	1911	38.0	3.67	WAG
10 Steinbach Dam	1936	23.4	1.05	WES

The largest dam in the region is the Rur Dam with a capacity of 202.6 Mio. m³ followed by the Grosse Dhuenn Dam (81.0 Mio. m³) and the Urft Dam (45.5 Mio. m³). In general, the age of the dams in Northrhine-Westphalia is quite old. The first dams in the region were constructed in 1899 (Lingese Dam), 1905 (Urft Dam), and 1909 (Neye Dam). Although the Urft Dam is small compared to international dams nowadays, it was the largest dam and the largest hydropower station in Europe during the start of operation in 1905.

The dams have different purposes. Some dams are operated for flood protection, hydro-power generation, drinking and process water production, low water elevation, irrigation, fish

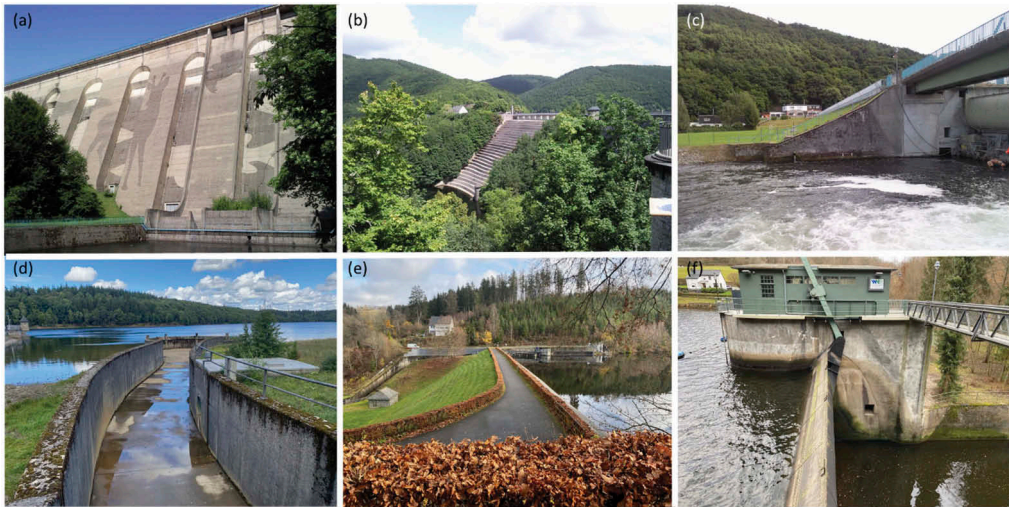


Figure 2. Large Dams in the Eifel Mountains (a) Olef Dam, (b) Urft Dam, (c) Obermaubach Dam, (d) Dreilaegerbach Dam, (e) Perlenbach Dam, (f) Heimbach Dam (all photos: Schüttrumpf).

Table 3. Summary of large dams located on the right side of the Rhine River (source: www.wupperverband.de).

Dam	Year of Construction	Height of dam [m.a.g.]	Capacity [Mio. m ³]	Operator
11 Beyenburg Dam	1953	8.6	0.47	Wupperverband
12 Herbinghauser Dam	1901	34.0	2.90	Wupperverband
13 Ronsdorfer Dam	1899	23.5	0.12	Wupperverband
14 Wupper Dam followed by the Dalhausen Dam	1987 1921	40.0 11.0	25.60 0.07	Wupperverband
15 Panzer Dam	1893	16.1	0.19	Wupperverband
16 Bever Dam	1939	35.0	23.70	Wupperverband
17 Neye Dam	1909	31.0	6.00	Wupperverband
18 Schevelinger Dam	1941	22.0	0.31	Wupperverband
19 Kerspe Dam	1912	34.6	15.50	Wupperverband
20 Lingese Dam	1899	25.8	2.60	Wupperverband
21 Brucher Dam	1913	27.8	3.37	Wupperverband
22 Eschbach Dam	1891	20.0	1.12	Wupperverband
23 Grosse Dhuenn Dam	1985	63.0	81.00	Wupperverband
24 Sengbach Dam	1903	43.0	2.80	Stadtwerke Solingen



Figure 3. Large Dams in the Bergisch Land Mountains (a) Grosse Dhuenn Dam, (b) Bever Dam, (c) Kerspe Dam (all photos: Schüttrumpf).

farms, recreation, and leisure. Exact rules for dam operation exist to either provide water for different purposes or for flood protection. It should be noted that flood protection was not part of the operating rules for some dams (e.g. Wupper Dam) in summer since the occurrence of flood events in summer months was not regarded as very likely.

2 OBSERVATIONS

2.1 *Flood damages*

Flood damages are not in the scope of this paper. Anyway, a short description of flood damages will be given to inform the reader about the severity and the consequences of this flood event. In total 186 people died during this event in Germany, thereof 134 in the Ahr valley. Due to the nature of the flood event as a flash flood, the most severe damages were found in the narrow valleys of the rivers Ahr, Vicht, and Erft.

Buildings were not only inundated but partly or totally destroyed by high flow velocities, debris impacts, scouring, wash-out of oil, chemicals, or waste water (Korswagen et al., 2021). Bridges were destroyed by overflow, the impact of debris, scouring of fundaments, uplift of the bridge and other causes (Burghardt et al., 2022). Roads and railways were destroyed among other processes by erosion and wash-out (Szymczak et al, 2022). Observed damages were not restricted to physical destruction. The loss of bridges, roads, and railways resulted in an interruption of all transport systems. Cascade effects accelerated the impact of the flood event to the population. As an example, due to the interruption of the transport systems, it was impossible to send help to affected people at the beginning of the disaster, rescue teams had problems reaching the people, medical help was not possible, and food and drinking water were missing.

Water supply systems and waste water treatment plants were destroyed by the flood. The quality of the water decreased since contaminants were leached into the water. The contamination by heavy metals was high and reached maximum values in some of the flood regions (Lehmkuhl et al., 2022).

Finally, sediments were transported by the river resulting in significant morphological changes, erosion, and sedimentation in large volumes. In some cases, the rivers have tried to find their historical courses again without disregarding existing anthropogenic activities (Lehmkuhl et al., 2022). All these aspects are investigated by national and international research teams, some results have been already published (Burghardt et al., 2022; Korswagen et al, 2021; Lehmkuhl et al., 2022; Mohr et al., 2022; Szymczak et al., 2022).

2.2 *Overflow of spillways*

Overflow of spillways is rare in Germany since large dams are designed for design events with a return interval of 1 in 10,000 years. Therefore, from the view of a dam designer the 2021 flood event was a possibility to verify the design conditions in the field. A number of dams experienced not even their design event but beyond.

As mentioned above, the Urft Dam which was constructed between 1900 and 1905 is the oldest dam in the Eifel mountains. It is certain that design guidelines from more than 120 years ago are different from modern design guidelines. Anyway, this old Urft gravity dam could withstand its design event in 2021. The maximum inflow to the Urft Reservoir was in the order of 610 m³/s which is more than the BHQ2 (1 in 10,000-year event). The maximum discharge over the spillway was in the order of 370 m³/s while the design discharge for the spillway is 220 m³/s. (WVER, 2021)

Water from the Urft Dam flows directly into the Rur Reservoir, which is divided into an upper reservoir and the Rur dam Schwammenauel. The Rur Reservoir is the second largest reservoir in Germany after the Bleiloch dam in Thuringia (related to the storage capacity). Therefore, this reservoir provided enough storage capacity to retain the water coming from the Urft Dam. This resulted in the fact that the overflow of the spillway of the Rur Dam could be



Figure 4. Selected examples of flood damages caused by the 2021 flood event: (a), (b), (c), (d), (i) Ahr valley; (e), (f), (g), (h) Vicht valley (photos: Schüttrumpf, 2021).



Figure 5. Overflow of spillways: (a) Urft Dam, (b) Perlenbach Dam, (c) Rur Dam (photos: (a) and (c) Vonden, (b) Schüttrumpf).

reduced to a maximum of 10.3 m³/s in addition to 60 m³/s released by the bottom outlet. This is far below the design flood of 450 m³/s for the spillway of the Rur Dam. (WVER, 2021)

In addition to the Rur Dam, three other dams (Dreilaegerbach Dam, Perlenbach Dam, Steinbach Dam) experienced their design events. The situation of the Steinbach Dam is discussed in chapter 2.3. The Dreilaegerbach Dam and the Perlenbach Dam (HQ2021 = 62 m³/s) showed significant overflow of the spillway far above the respective design events.

In the Bergisch Land region, three dams experienced their design events. The Schevelinger Dam is designed for a BHQ2 of 10.77 m³/s, the flood discharge in 2021 was 10.8 m³/s. The Neye Dam is designed for 16 m³/s, and a flood discharge of 17 m³/s was measured in 2021. Finally, the Wupper dam is designed for 165,1 m³/s and the maximum flood discharge over the spillway was 190 m³/s (Schüttrumpf et al., 2022).

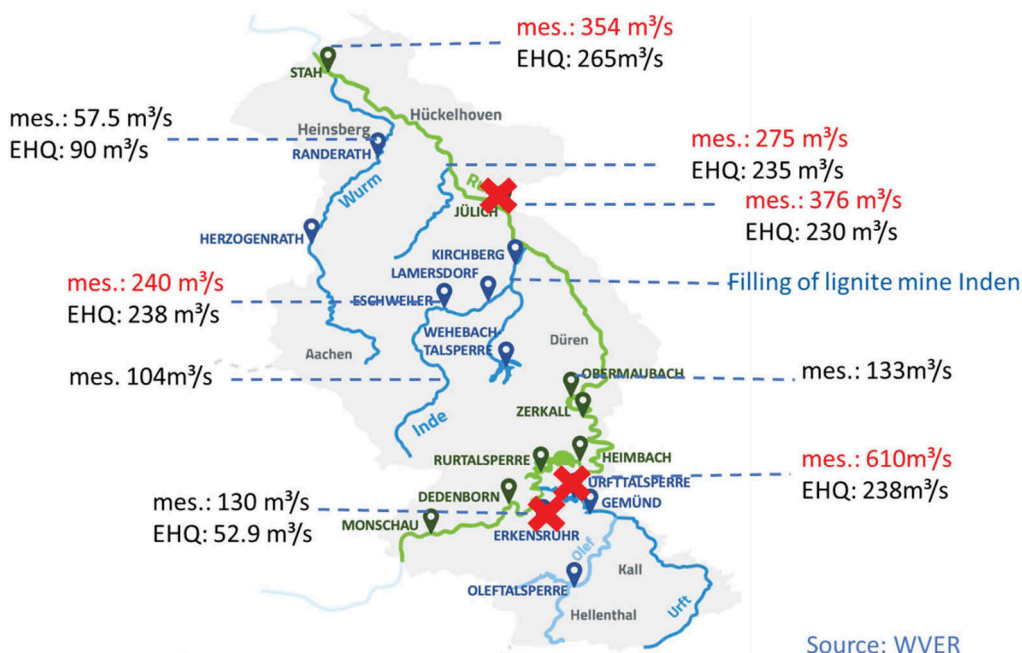


Figure 6. Peak discharges in the Rur catchment during the 2021 flood event (source: WVER) (Not all values finally confirmed by LANUV!).

2.3 Flood protection downstream of dams

Reservoirs provide a good level of flood protection for downstream regions. This can be shown by the example of the dams situated in the upper reaches of the Rur catchment. As mentioned in the previous chapter, a peak discharge of 610 m³/s flowed into the Urft Reservoir. The total inflow to the reservoirs was even in the order of 760 m³/s (WVER, 2021). Anyway, the flood wave is dampened to about 90 m³/s released at the downstream end of the reservoir cascade. Thus, the flood wave was decreased by a factor of over 8 by the cascade of reservoirs of the Northern Eifel.

Anyway, we have to distinguish between that part of the catchment which can be controlled by reservoirs, and that part of the catchment which is still uncontrolled. For the uncontrolled part, we can again distinguish two areas. Significant flood damages occurred upstream of the Urft Dam in the small cities of Gemünd and Schleiden. This area is not controlled by the Urft Dam and the flood wave with a peak discharge of 610 m³/s was able to create considerable devastation. On the other hand, tributaries downstream of the area controlled by large reservoirs were able to generate a new flood wave which resulted in flood damages in the downstream parts of the cascade of reservoirs in the Eifel mountains.

2.4 Steinbach dam case

The Steinbach Dam is situated in the upper reaches of the Erft River in the Eifel mountains south of the city of Euskirchen. The Steinbach dam which was constructed between 1934 and 1936 is a dam with a crest height of about 17.7 m above the river bed. The total storage volume is in the order of 1.05 Mio. m³. The Steinbach dam was close to rupture during the 2021 flood event due to an overflow of the dam crest. The new spillway which was designed for 20.3 m³/s before 2021 was overflowed by a discharge of 37.6 m³/s and unable to discharge the enormous amount of water. During the 2021 flood, a peak discharge of 31 m³/s flowed over the dam crest resulting in large erosion gullies on the landward dam side and clogging of the bottom outlet on the landward side. Therefore, the situation of the dam became very

critical, and no normal operation was possible. The fact that the upstream asphaltic membrane of the dam had been renewed in the years before the flood event had a positive effect.



Figure 7. Steinbach Dam: (a) Dam crest, asphaltic membrane and embasure, (b) empty reservoir, (c) erosion gullies on landward dam side (all photos: Schüttrumpf).

As an emergency measure, the bottom outlet was opened, and pipes were installed to decrease the water level in the reservoir. At the same time, the population downstream of the dam was evacuated to be prepared in case of a dam breach with a resulting flood wave. Fortunately, the disaster management teams were able to decrease the water level in the reservoir slowly and stop the overflow of the dam crest. The situation came back under control and the emergency case could be ended. The dam was not in good technical condition after the event due to the damages on the landward side. Therefore, a large V-shaped embasure was dug into the dam to avoid any refill of the reservoir.

3 CONCLUSIONS

The 2021 flood event in the Eifel mountains was the most disastrous flood event in mid-mountain areas in Germany during the last century. Flood protection in Germany is in general designed to withstand flood events with a return interval between 100 and 1,000 years. Anyway, the 2021 flood event was far above a return interval of 1,000 years. Therefore, the 2021 flood event has unsparingly shown both, the weak points in flood protection and the high resilience of hydraulic engineering infrastructures such as dams during extreme events.

Especially in areas with a number of very large dams the flood wave could be dampened significantly by the system of reservoirs resulting in a comparatively small flood wave at the outflow section of the reservoir cascade system. Anyway, downstream tributaries were able to generate a new flood wave which was low compared to a fictive flood wave without the dams but still destructive. The downstream regions in the German Rur catchment as well as the Meuse River in the Netherlands were protected significantly.

In addition, it was possible to verify in practice if dams are able to withstand their design conditions. It can be concluded that even old dams which have been perfectly maintained over the last decades were able to withstand not only their design conditions but even higher events. This means that the dams are loadable according to their technical design and do not fail if the design conditions are exceeded.

In general, river catchments with dams were in a comparatively better situation than river catchments without dams or with dams with low storage capacity. From an engineering perspective, the dams fulfilled their tasks perfectly. Anyway, the population which is often unaware of the physical processes and interrelations has blamed the operators for flooding and inundation in downstream areas. Dam operators had to explain the situation and their contributions to buffer the flood wave and protect the population.

REFERENCES

- Burghardt, L.; Klopries, E.; Wolf, S. & Schüttrumpf, H. 2022. Analyse der Schäden an den Brückenbauwerken in Folge des Hochwasser 2021 an der Ahr. Wasser und Abfall. 11/2022 <https://www.springerprofessional.de/analyse-der-schaeden-an-brueckenbauwerken-in-folge-des-hochwasse/23686968>
- Korswagen, P.; Harish, S.; Oetjen, J. & Wüthrich, D. 2021. Post-flood field survey of the Ahr Valley (Germany) Building damages and hydraulic aspects. Technical report
- Kreienkamp, F.; Philip, S.; Tradowsky, J.; Kew, S.; Lorenz, P.; Arrighi, J.; Belleflamme, A.; Bettmann, T.; Caluwaerts, S.; Chan, S.; Ciavarella, A.; De Cruz, L.; de Vries, H.; Demuth, N.; Ferrone, A.; Fischer, E.; Fowler, H.; Goergen, K.; Heinrich, D.; Henrichs, Y.; Lenderink, G.; Kaspar, F.; Nilson, E.; Otto, F.; Ragone, F.; Seneviartne, S.; Singh, R.; Skalevag, A.; Termonia, P.; Thalheimer, L.; van Aalst, M.; Van den Bergh, J.; Van de Vyver, H.; Vannitsem, S.; van Oldenborgh, G.; Van Schaeybroeck, B.; Vautard, R.; Vonk, D. & Wanders, N. 2021 Rapid attribution of heavy rainfall events leading to the severe flooding in Western Europe during July 2021. World Weather Attribution.
- Lehmkuhl, F.; Schüttrumpf, H.; Schwarzbauer, J.; Brüll, C.; Dietze, M.; Letmathe, P.; Völker, C.; Hollert, H. 2022. Assessment of the 2021 summer flood in Central Europe. Environmental Science Europe. <https://doi.org/10.1186/s12302-022-00685-1>
- LfU Rheinland-Pfalz. 2021. <https://www.hochwasser-rlp.de/karte/einzelpegel/flussgebiet/rhein/teilgebiet/mittlerhein/pegel/ALTENAHR>. Zugriff: 07. 01.2022
- LANUV NRW. 2021. Anfrage Hochwasser-Pegeldaten. Eschweiler, 21.12.2021.E-Mail an Stefanie Wolf. ausgewählte Pegeldaten
- Ministerium für Umwelt, 2021. Landwirtschaft, Natur- und Verbraucherschutz NRW. ELWAS-WEB. Karte. Hg. v. Landesamt für Natur, Umwelt und Verbraucherschutz NRW. Landesbetrieb Information und Technik Nordrhein-Westfalen (IT.NRW). Online verfügbar unter www.elwasweb.nrw.de, zuletzt geprüft am 07.01.2022
- Mohr, S.; Ehret, U.; Kunz, M.; Ludwig, P.; Caldas-Alvarez, A.; Daniell, E.; Ehmele, F.; Feldmann, H.; Franca, M.; Gattke, C.; Hundhausen, M.; Knippertz, K.; Mühr, B.; Pinto, J.G.; Quinting, J.; Schäfer, A.M.; Scheibel, M.; Seidel, F. & Wisotzky, C. 2022. A multi-disciplinary analysis of the exceptional flood event of July 2021 in Central Europe. Part 1: Event description and analysis. Natural Hazards and Earth System Sciences. <https://doi.org/10.5194/nhess-2022-137>
- Nilson, E. 2006. Flusslandschaften im Wandel - Untersuchungen zur Mäanderentwicklung an zwei Maas- Tributären anhand von historischem Bild- und Kartenmaterial. In: Reineke T, Lehmkuhl F, Blümel H (eds) Grenzüberschreitendes integratives Gewässermanagement, 1. Aufl. Academia-Verl, Sankt Augustin
- Roggenkamp, T. & Herget, J. 2015. Historische Hochwasser der Ahr - Rekonstruktion von Scheitelabflüssen ausgewählter Ahr-Hochwasser. Heimatjahrbuch Kreis Ahrweiler.
- Roggenkamp, T. & Herget, J. 2022: Floods of the Ahr in July 2021 - discharge estimation and classification. Hydrology and Water Management. HW 66. H. 1
- Schüttrumpf, H. & Kirschbauer, L. 2022. Was haben wir aus dem Hochwasser 2021 gelernt? Wasser und Abfall. 9/22 <https://www.springerprofessional.de/en/was-haben-wir-aus-dem-hochwasser-2021-gelernt/23480092>
- Schüttrumpf, H., Wingen, M. & Reinert, J. 2022. Dokumentation und Untersuchungen zur Talsperrenbewirtschaftung der Wuppertalsperren während des Hochwassers 2021 - Vorläufige Abschlussergebnisse 04. 05.22 [https://www.wupperverband.de/internet/mediendb.nsf/gfx/C60F486A6AB948E8C125883800490C37/\\$file/20220504_Praesentation_Gutachten_RWTH_Aachen.pdf](https://www.wupperverband.de/internet/mediendb.nsf/gfx/C60F486A6AB948E8C125883800490C37/$file/20220504_Praesentation_Gutachten_RWTH_Aachen.pdf)
- Szymczak, S., Backendorf, F., Bott, F., Fricke, K., Junghänel, T. & Walawender, E. 2022. Impacts of Heavy and Persistent Precipitation on Railroad Infrastructure in July 2021: A Case Study from the Ahr Valley, Rhineland-Palatine, Germany. Atmosphere 2022, 13, 1118. <https://doi.org/10.3390/atmos13071118>
- J. Reichert, J. & Demny, G. 2021. WVER 2021 Hochwasserereignis Juli 2021- Einordnung und Ablauf an der Rur. Bürgerinformation 02.11.2021



Taylor & Francis

Taylor & Francis Group

<http://taylorandfrancis.com>

Theme C: Impact mitigation of dams and reservoirs



Taylor & Francis

Taylor & Francis Group

<http://taylorandfrancis.com>

New Poutès dam (France): Innovative retrofitting to reconcile environment and hydropower

T. Barbier

Civil Engineer, EDF Hydro Engineering Centre, Le Puy En Velay, France

S. Lecuna

Territory Delegate, EDF Hydro, Le Puy En Velay, France

P. Meunier

Project Manager, EDF Hydro Engineering Centre, Brive La Gaillarde, France

ABSTRACT: Poutès dam was at the heart of debates initiated in the 80's for wild river and salmon restoration. Since the expiry of the previous licensing in 2007, Authorities have been looking for a tradeoff solution which might be acceptable to all: EDF Hydro, NGO's and municipalities officials. The objective is to limit the environmental impact as much as possible while maintaining the hydroelectric generation performance.

The renewal of the Monistrol d'Allier hydropower scheme licensing, including Poutès dam, was granted to EDF Hydro in 2015 for a period of 50 years. The new licensing specifications include a significant lowering of the reservoir operating level and the optimizations made to the reconfigured structures ensuring environmental functions.

The reconfiguration of the dam, the work of which took place from 2019 to 2021, consisted of the following tasks:

- Demolishing part of the Creager spillway weirs and piles of the current concrete dam, as well as dismantle the sluices and mechanical components equipping the structure;
- Adapting and lowering the partially demolished dam to get a limited operating level, equipped with a new gated central sluice passage, to ensure free continuity of the structure for sediments and fish during certain periods of the year;
- Reshaping the existing fish pass facilities (for upstream and downstream migration), to adapt them to the new reservoir operating level and improve their performance.

This unusual dam reconfiguration could make it possible to significantly improve fish and sediment transit, and to maintain a performant site's hydroelectric production.

RÉSUMÉ: Le barrage de Poutès est au cœur de discussions engagées dans les années 80 pour le retour à une rivière sauvage sur la thématique du saumon. Depuis l'échéance de la précédente concession en 2007, l'Etat recherche une solution de compromis acceptable par tous: EDF Hydro, les ONG et les élus. L'objectif est de limiter l'impact environnemental tout en maintenant la production hydroélectrique de la chute.

Le nouveau cahier des charges de l'aménagement prévoit un abaissement significatif de la cote de retenue et intègre les optimisations apportées aux ouvrages reconfigurés.

La reconfiguration du barrage, dont les travaux se sont déroulés de 2019 à 2021, a consisté à:

- Démolir une partie des seuils Creager et des piles du barrage actuel, ainsi qu'à démanteler la vantellerie et les organes mécaniques équipant l'ouvrage;
- Aménager le barrage partiellement démolit pour retenir une hauteur d'eau limitée (8 m) et l'agréments d'une passe centrale vannée, pour permettre d'assurer la mise en transparence de l'ouvrage (sédimentaire et piscicole) certaines périodes de l'année;
- Reprofiler les ouvrages piscicoles existants (montaison et dévalaison), pour les adapter à la nouvelle cote de retenue et en améliorer le fonctionnement;

Cette reconfiguration atypique permet d'améliorer significativement le transit piscicole et sédimentaire, tout en maintenant la production hydroélectrique du site.

1 NATIONAL CONTEXT

In France, the environmental code classifies watercourses into two distinct lists:

- List 1: Rivers with very good ecological status, requiring full protection of migratory fish and whose aquatic environments should not be degraded;
- List 2: watercourses or sections of watercourses requiring actions to restore ecological continuity (sediment transport and fish circulation).

The Allier River is classified in list 2 under the L214-17 of the French environmental code. The Poutès dam must therefore ensure the circulation of migratory fish and the sufficient transport of sediments.

EDF Hydro has a research and development unit equipped with a physical modelling laboratory, developing its own numerical tools and several integrated engineering units: one for measurement (DTG) and one for hydraulic engineering (CIH). The latter has used its environmental skills (design of fish breeding and sediment transit structures), but also civil engineering (partial demolition and reconstruction of the dam), electromechanical engineering (installation of new gates and flap gates) and control engineering (regulation of the reservoir and production set points) to meet the challenge of the “Nouveau Poutès” project.

2 PRESENTATION OF THE MONISTROL D’ALLIER SCHEME AND THE POUTÈS DAM

The Monistrol d’Allier scheme is located in the Haute Loire department (43), in France, about 40 km southwest of Le Puy en Velay. It consists of two water intakes and waterways (Figure 1):

- The Allier waterway on the Allier (catchment area 1014 km²; mean annual discharge 16.7 m³/s for the period 1948-2010; installed capacity 18 MW), to which the Poutès dam is related;
- The Ance waterway on the Ance du Sud, left bank tributary of the Allier (catchment area 225 km², mean annual discharge 2.87 m³/s at Pouzas for the period 1969-2009; installed power 15 MW).

Before reconfiguration, the Poutès reservoir, 3.5 km long, occupied an area of 39.15 ha at the normal reservoir level 650.20 m NGF (m a.s.l.). The total capacity of the reservoir was about 1.7 hm³ at normal water level.

The Poutès dam, impounded in 1941, was a gated gravity dam. Its crest height reached 652.00 m NGF. Its height was 17.7 meters above the natural ground. Its crest length measured 85 meters, half of which was occupied by 3 spillways equipped with radial gates, each 14 meters wide, whose sill was set at 644.00 m NGF.

3 LOCAL CONTEXT

3.1 *The Allier, a salmon river*

At the end of the 80s, the significant decline in salmon populations led to the mobilization of environmental associations; Poutès was then identified as one of the black spots on the Allier axis for salmon migration, despite the construction of fish pass structures in 1986, with a fish elevator for upstream fish migration and a specific downstream migration pass. In 1994, the French state decided to set up the first “Plan Loire Grandeur Nature”. This plan provides for the construction of the largest salmon farm in Europe at Chanteuges to support the salmon populations of the Loire basin and thus avoid the extinction of the species. It also provides for the dismantling of two dams: Maison-Rouge on the Vienne and St Etienne du Vigan on the Allier (20 km upstream of the Poutès dam), which has been dismantled in 1998.

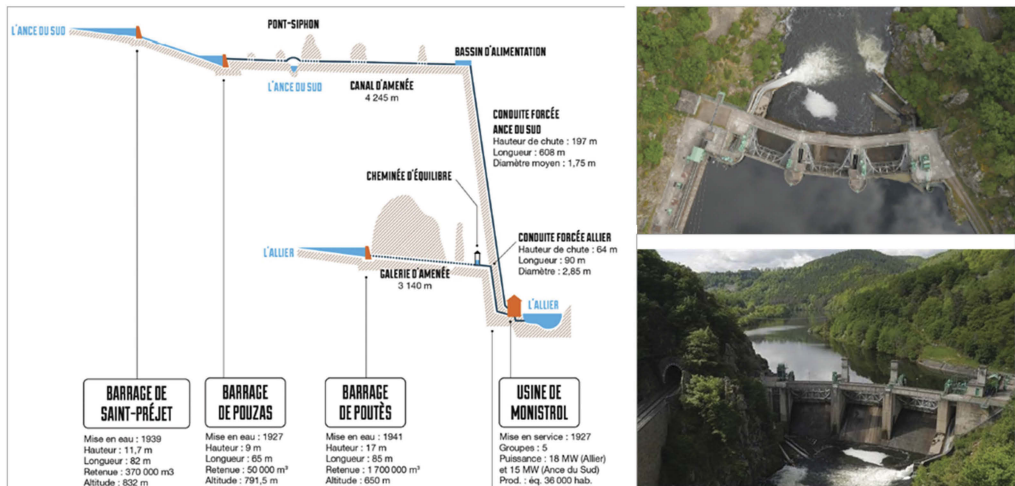


Figure 1. On the left, schematic synoptic of Monistrol d'Allier facility. On the right, aerial view of the Poutès dam (before retrofitting).

3.2 *Renewal of the Monistrol d'Allier concession and objections*

With a view of the hydroelectric concession licensing expiration in 2007, in 2002, EDF submitted a first file for initial examination and a public inquiry. This was an opportunity for all the stakeholders to express their views: elected representatives grouped together in an association for the protection of the dam joined EDF in calling for the renewal of the licensing with improvements; and environmental associations (in particular SOS Loire-Vivante, WWF, the fishing federation) who maintained their desire to see the complete dismantling of the Poutès dam.

At the same time, in 2006 the French state commissioned a study from experts who recommended the removal of the structure. Nevertheless, the same year, the public inquiry resulted in a favorable opinion to keep the dam but with reservations. The situation was blocked and everyone was sticking to their positions. This situation of deadlock finally led to the first real exchanges between associations, elected officials and EDF, at the end of which the idea of a possible consensus emerged.

3.3 *Original crossing device and problems*

In 1986, the dam was equipped with a fish elevator on the right bank. This elevator is connected to the downstream side of the dam by a fish pass and a fish pass with delays. This setting of 3 devices makes the upstream migration complex and causes important delays for the salmon.

A downstream spillway on the left bank allows young salmon to reach the downstream. If the spillway proves to be efficient, the difficulty for the fish to find it because of the long reservoir (3500 m) causes delays that can reach several weeks and important losses (estimated at 50% according to the hydrology).

4 CO-CONSTRUCTION OF THE “NEW POUTÈS

4.1 *Evolution of the project to reconcile environment and electricity production*

The project, since the first exchanges between administrations, elected officials, NGOs and EDF in 2009, has undergone many changes. Indeed, no less than 4 versions of the project have been developed. The implemented project is the result of this long process which is based on exchanges between stakeholders and experiments carried out in the field. All these evolutions, which are the marker of this project, allow to reach the most efficient project from environmental as well as from energy point of views.

4.2 Description of the final project

The work carried out to adapt the layout to its new configuration is as follows, from the left bank to the right bank:

- Changing the trash racks of the water intakes;
- Reshaping the downstream migration structure;
- Levelling of the dam crest at 642 m NGF and creation of a new central spillway;
- Adapting the upstream migration structure;
- Modifying the automated outlet of the powerplant;
- Re-establishing pedestrian and vehicle access through the construction of a bridge.

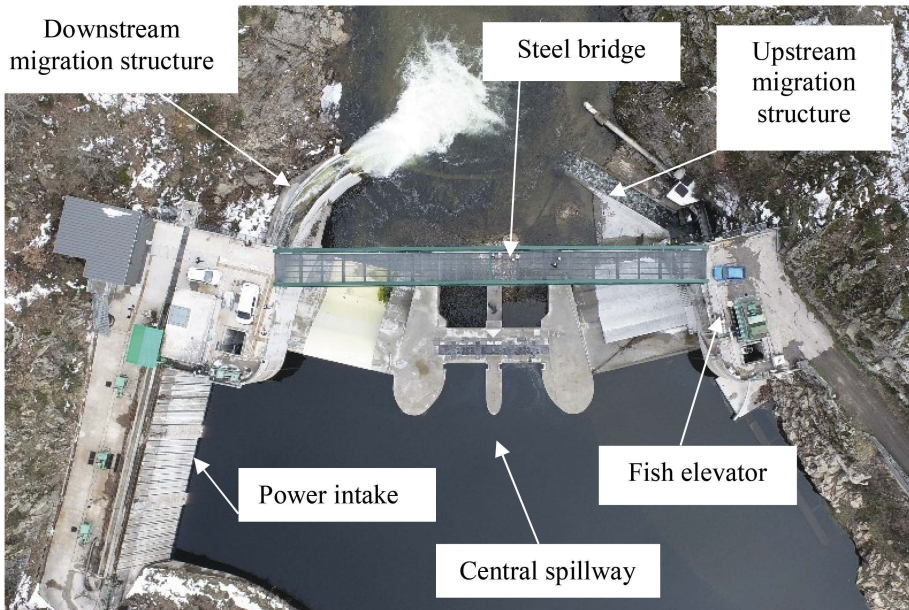


Figure 2. Aerial view of the reconfigured dam and identification of the main structures.

4.2.1 Water intake

The water intake is about 20 m wide. At 642.00 m NGF, the height of the trash rack in water is about 5 m (bottom at 637 m NGF; quasi-vertical grids). The surface is thus of approximately 100 m² and the average normal velocity of the order of 0.3 m/s for the maximum turbine flow (28 m³/s). This average value being sufficiently low, the grids of the water intake were changed by modifying their air gaps from 30 mm to 12 mm which corresponds to the 1/10th of length of the smallest smolt.

4.2.2 Downstream migration structure

The downstream migration structure is located on the left bank, in the extension of the water intake grid plane. It is made up of an upstream flap gate whose shape allows a progressive water velocity, of a 3% slope chute at the end of which, at the downstream end, a device of “spoon” dispersion of the jet downstream makes it possible to ensure good conditions of reception of the fish and to avoid a parasitic attraction with the rise. It is fed by a flow of 3 to 4 m³/s, corresponding to 10.7% to 14.3% of the maximum turbine flow, and less of 10% of the average flow rate of the river. The minimum water level on the flap gate is 0.80 m and the minimum water height in the reception pit is 1.50 m.



Figure 3. Overview of the new grid plane.



Figure 4. Reconfiguration of the downstream structure. Left, upstream view of the spillway (flap gate). Right, view of the downstream extremity of the spillway chute and the "spoon".

4.3 The dam

In its new configuration, the Poutès dam is levelled at 642.00 m NGF, leading to a decrease in height of 10 m. The radial gates have been removed.

The dam is composed of two free overflow spillways, about 18 m long on the left and right banks. In the central part, a sediment transit pass has been created and equipped with two lifting sluice gates of 5 m wide x 3.50 m wide, whose sill is set at 634.00 m NGF. These gates allow, by their opening, the setting in complete continuity of the installation.

The length of the reservoir has been reduced from 3500 m in the old configuration to a few hundred meters in the current one, thus facilitating the transit of smolts but making electricity production more complex.



Figure 5. Retrofitting of the Poutès dam. On the left, before works. On the right, after works.

4.3.1 Operation of the dam

In order to ensure fish migration continuity, the dam is transparent during:

- 5 weeks in spring (mid-May to mid-June);
- 8 weeks in fall (October - November).

An analysis of salmon runs from 1986 to 2017 at the Poutès elevator showed that these two periods cover an average of 80% of the salmon runs.

In addition to these provisions and in order to ensure sediment transport continuity, the operator will make the facility transparent during morphogenic floods, hence for discharges larger than 100 m³/s.

4.3.2 Design of the central pass

In order to check the hydraulic conditions in the central channels during the continuity episodes, a one-dimensional hydraulic model using Mascaret software has been used.

For flows less than or equal to 70 m³/s, the Froude number is always less than 1. There will therefore be no hydraulic jump because the flows are always fluvial. This is favorable to the fish run.

This model made it possible to verify that the flow velocities were compatible with the upstream migration of the various fish species (salmon, trout, eel, etc.).

A particularity of the design of the central fishway is that its invert has been built below the downstream level, so that it is always covered by one meter of water, thus allowing the passage of fish at low flow.

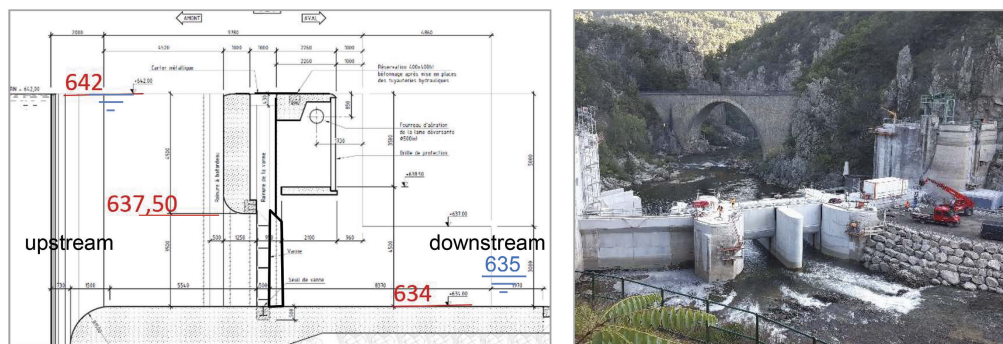


Figure 6. Central pass: on the left, cross section; on the right, view of the central pass with gates open at the end of the retrofitting work.

4.4 The upstream migration structure

In order to allow the upstream migration to occur outside of continuity periods, the initial upstream migration structure was completely reconfigured to provide a multi-species crossing despite the limited proportion of salmon migrating outside of these periods.

The selected solution consists, from downstream to upstream, in:

- Replacing the existing speed bump pass with a macro-rug pass that is 2.55 m wide, 13 m long with a 7% slope. The structure is fed by a flow of 1 m³/s and makes it possible to make up for a difference in level of 0.9 m;
- Creating a stilling basin located upstream of the macro-rug pass: the water line elevation is 635.80 m NGF. The basin is fed by the flow coming from the elevator and by the instream flow;
- Modifying the fish elevator (fish discharge rating), while removing the old pool pass and creating a horizontal invert inlet channel. The adaptation of the screens, the cage and the flow delivery system of the elevator were also carried out.

The upstream structure is functional for inflows from 4 m³/s to 100 m³/s. Beyond that, the dam is made transparent (sediment continuity objective). These transparencies are in addition to the transparencies targeted for salmon.

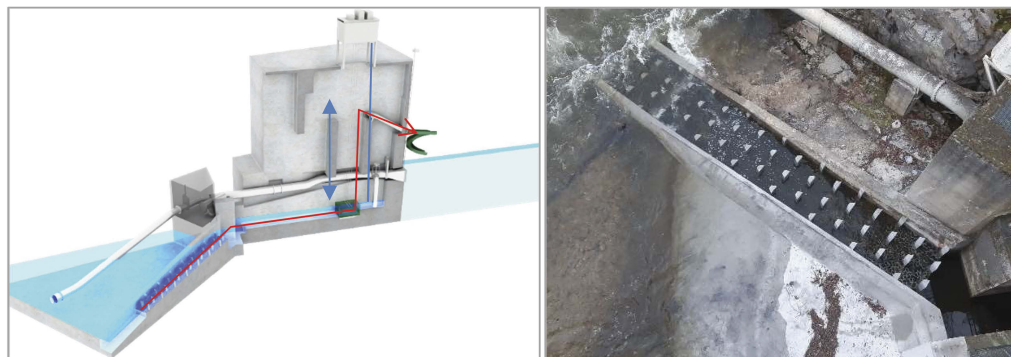


Figure 7. Reconfigured fish passage structure. On the left, 3D view of the run inside the right bank abutment (in red the migration of fish). On the right, the completed macro-rug pass.

A specific device for the crossing of eels was installed, the bar of the elevator shaft not being fine enough to capture eels.

The most suitable type of structure, given the small size of the site, is the brush ramp. It is developed in the form of alternating flights separated by stilling basins between 635.5 and 646.5 m NGF and ends with a trap basin that discharges the eels into a PVC pipe, which in turn discharges into the return chute of the elevator.

4.5 Adaptation of the power plant operation

The main modification concerning the operation of the power plant is the elimination of hydropeaking, in connection with the very significant reduction in the length of the reservoir (and therefore its volume). The Monistrol d'Allier power plant now operates on continuous flow.

This new operating mode, as well as the reduction of the head and the consideration of the periods of continuity of the dam, leads to a loss of 15% of the power production of the Monistrol d'Allier HPP development, from now on estimated at 53 GWh/year.

The development was redesigned to address the following issues:

- Respect for environmental constraints: maintain the level regardless of the inflow so that the upstream and downstream discharges deliver the right flow;
- Respect of the number of generation unit starts.

This automatic control is ensured by a “Programmable Logic Controller”.

5 WORK SCHEDULE

The retrofitting work, planned between 2019 and 2022, was carried out according to an optimized phasing, alternating emptying, work and return to operation, to limit the plant's operating losses and limit the impact of the work on the environment. The phasing also took into account the hydrology of the Allier, avoiding the planning of sensitive work during periods of high-water levels.

Two phases of work as well as an operation phasing were selected for the realization of the project:

- Work 2019 - Phase 1 (June - October 2019) - Empty reservoir: development of the construction site base; creation of an access track and a platform at the foot of the dam; removal of the 3 radial gates; first modification of the upstream structures.

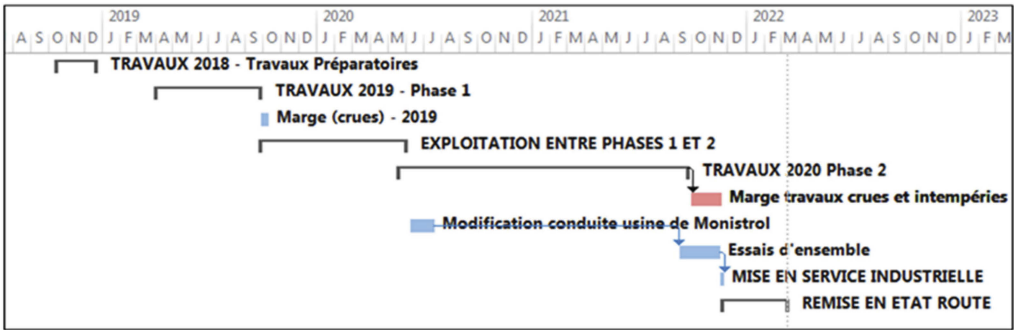


Figure 8. Phasing of the retrofitting work.

- Back to operation (October 2019 to June 2020): during this period, the structure is operated on a run-of-river basis; the dam spills as soon as the level of the reservoir exceeds 644.00 m NGF
- Works 2020/2021 - Phase 2 (June 2020 - End of 2021) - Empty reservoir: installation of temporary structures (cofferdams); partial demolition and reconfiguration of the dam; modification of fish migration structures (upstream and downstream); construction of a new operating room; construction of a bridge to cross the new dam.

6 SOME FEATURES

The main quantities of the construction are listed below:

- 4,500 m³ of concrete and rock demolition (100% reused as on-site fill);
- About 1500 m³ of C35/45 concrete; about 1,700 m² of formwork; 115 tons of steel reinforcement;
- Two cofferdams, 3.5 m to 9 m high (flood protection), total length of 80 m;
- 2 wagon gates of 10 tons each (central pass); 1 lowering gate of 3 tons (downstream).

The amount of the operation is 15.6 M€, distributed as follows: Civil Engineering works: 7.9 M€; Electromechanical works: 2.8 M€; control-command system works: 900 k€; Operation modification: 500 k€; Specific expenses for the implementation of the project: 260 k€; Project management (project manager and project supervisor), from the detail design to the end of the works: 3.3 M€.



Figure 9. Aerial views of the dam reconfiguration during the construction phase.

7 CONCLUSION

The new Poutès project, beyond the technical innovations, is above all a territory project, designed, elaborated and implemented with all the stakeholders: elected officials, NGOs,

administrations. It thus allows to answer the public expectations of renewable energy production as well as preservation of the environment.

The modern and shared governance process and the co-construction throughout the project make it an exemplary project.

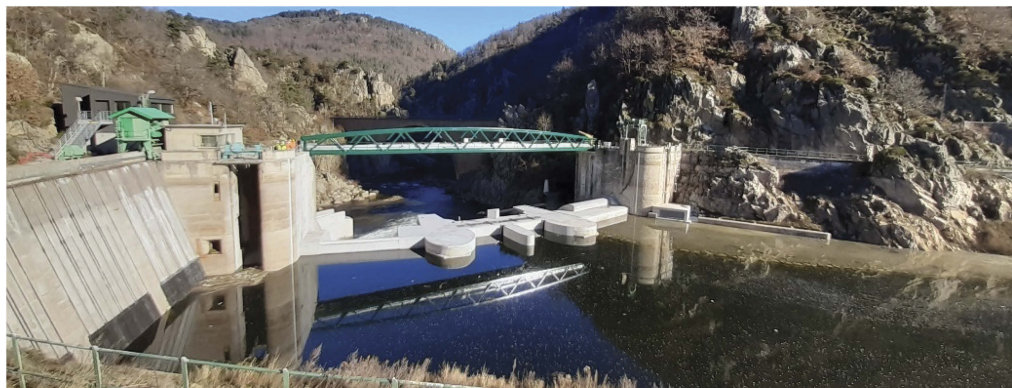


Figure 10. General view of the reconfigured dam from upstream when it was first impounded.

Monitoring of the upstream migration structure (acoustic camera) and of the downstream migration structure (acoustic study) are in progress, with a year of monitoring of the fish migration using the elevator. The preliminary results are very encouraging (passage of more individuals of various species than before, demonstrating the improvement of the pass). The first videos on the run show that transparency is effective.

ACKNOWLEDGEMENTS

This project would not have been possible without the participation and strong support of SOS Loire-Vivante, European Rivers Network, SAGE Haut-Allier, Les Gorges de l'Allier, European Union and FEDER. Financial assistance was also provided by Loire Bretagne Water Agency and the support of the European Union

REFERENCES

- Dumont, L., 2020. Detailed Preliminary Project of the New Poutès - Sizing of the fish migration structures. ref. EDF n°H-30575713-2019-000389
- Tétard, S., De Oliveira, E., Lecuna, S., Le Brun, M., Morel, S., Henault, F., Rancon, J., 2019. Adaptive operational management of a hydropower complex to protect downstream migrating Atlantic salmon. Case study: The Poutès dam on the Allier River (Haute-Loire, France). *AMBER report – D4.2 - AMBER Project - H2020 - Grant Agreement #689682*

Effects of water releases and sediment supply on a residual flow reach

C. Blanck, R. Schroff & G. De Cesare

Plateforme de Constructions Hydrauliques (PL-LCH), École Polytechnique Fédérale de Lausanne (EPFL), Lausanne, Switzerland

ABSTRACT: An artificial floods program has been implemented on the Sarine residual flow reach, downstream of the Rossens dam. Two artificial floods were released in 2016 (coupled with sediment augmentation) and in 2020. A natural flood occurred in 2021. The indicator set on habitat diversity (FOEN) was applied on a Sediment Augmentation and a Control Reach after each flood. Additional data sets comprise the macrohabitats, trout redds and population evolution. The effects of the 2020 artificial flood and the 2021 natural flood on the hydromorphology, the trout reproduction sites and population were compared. To generalize the previous results, hydrological descriptors were analyzed for statistical correlation with the hydromorphological and ecological responses of the river. Results show that the natural flood was larger and had a significantly higher morphological impact, reflected in the increase of the trout redds surface area. The decline in hydromorphological diversity underlines the lack of sediment supply. The correlation analysis confirms the importance of gravel bars as an indicator for trout redds. The role of morphogenic floods for redds availability and hence for trout population is also emphasized. The Sarine residual flow reach's need for regular morphogenic floods, coupled with adequate sediment augmentation measures, is highlighted.

RÉSUMÉ: Un programme de crues artificielles a été implémenté sur le tronçon à débit résiduel de la Sarine, en aval du barrage de Rossens. Deux crues artificielles ont été relâchées en 2016 (couplée à un apport de sédiments) et en 2020. Une crue naturelle a eu lieu en 2021. Le jeu d'indicateurs portant sur la diversité des habitats (OFEV) a été appliqué sur deux tronçons à dépôts de sédiments et de contrôle après chacune des crues. Des jeux de données supplémentaires utilisés sont l'évolution des macrohabitats, les sites de frai et la population des truites. Les effets des crues artificielle (2020) et naturelle (2021) sur l'hydromorphologie, les sites de frai et la population des truites ont été comparés. Pour généraliser ces résultats, des descripteurs hydrologiques ont été analysés pour des corrélations statistiques avec les réponses hydromorphologiques et écologiques de la rivière. Les résultats montrent que la crue naturelle a été plus puissante et a eu un impact morphologique plus important. Cela a été reflété dans l'augmentation de la surface des sites de frai. Le déclin de la diversité hydromorphologique met en évidence le manque d'apport en sédiments. L'analyse de corrélation confirme l'importance des bancs de gravier comme indicateur pour les sites de frai. Le rôle des crues morphogènes pour la disponibilité des sites de frai et donc pour la population de truites est également souligné. Les résultats soulignent le besoin du tronçon à débit résiduel de la Sarine pour des crues morphogènes régulières, combinées à des mesures adéquates d'apports de sédiments.

1 INTRODUCTION

The morphology and ecology in river systems are strongly determined by two key factors: the flow and sediment regimes. They generate and influence a wide diversity of constantly evolving aquatic and terrestrial habitats, thereby promoting a developed biodiversity (Döring et al., 2018, Allan et al., 2021). Storage dams alter the natural flow and sediment regimes, which

causes significant risks to biodiversity and ecosystem functions (Allan et al., 2021). An artificial floods program is a possible rehabilitation measure to mitigate the detrimental effects of dams. To maximize their efficiency, the frequency and magnitude of artificial floods should be carefully planned (Stanford et al., 1996, Peter, 2010). Sediment augmentation should be considered as a complementary measure in a holistic restoration approach (Wohl et al., 2015).

Morphological and ecological deficits have been documented in the Sarine residual flow reach (known as the Petite Sarine), located downstream of the Rossens dam in the canton of Fribourg. These deficits result from decades of monotonous discharge regime and interrupted sediment continuum induced by the storage infrastructure (Mivelaz, 2004). Recently, an experimental flood program was implemented as a rehabilitation measure. The first artificial flood was released in September 2016 and was combined with a sediment augmentation measure. Immediate effects showed a significantly increased morphological diversity (Döring et al., 2018, Stähly et al., 2019). However, in the long-term, the positive effects on the ecomorphological conditions do not persist (Schroff et al., 2021a, Schroff et al., 2021b). In October 2020, another artificial flood was released, without additional sediment supply. Temporary positive effects were observed but the lack of sediment supply caused bed incision and reduced the overall hydromorphological diversity (Schroff et al., 2022). Most recently, a natural flood occurred in summer 2021.

The indicator set on habitat diversity from the Swiss Restoration Outcome Evaluation (ROE) was applied on a Sediment Augmentation Reach (SAR) and an upstream Control Reach (CR) after each of these floods. Additional data sets are available, including macrohabitats evolution, trout spawning sites and trout population data.

Previous studies have examined the effects of influencing factors (mainly hydrological and sediment conditions) on morphological or ecological responses (Tonolla et al., 2021, Stähly et al., 2019). At present, no study has been found that investigated all the above-mentioned variables in a joint analysis for the Sarine residual flow reach. Furthermore, the effects of the natural flood of 2021 on the morphological and ecological conditions have not yet been assessed. The objectives of this study are to assess the results of the monitoring campaigns and compare the effects of both the artificial flood (2020) and the natural flood (2021) on the river bed morphology, bed substrate, diversity of habitats, trout reproduction sites and population. This study also includes a correlation analysis between various descriptors of the flood characteristics and the hydromorphological and ecological responses of the river. This analysis will contribute to generalizing the previous results in both space (the entire residual flow reach) and time (the period 1997 to 2022). It was expected that the natural flood of 2021 had more beneficial effects than the artificial flood of 2020, since it was larger. Hypotheses for the correlation analysis are listed below:

1. Strong positive correlation between the spawning grounds surface area and the gravel surface area (Gravel habitat constitutes suitable substrate for trout spawning grounds (Pulg et al., 2013)).
2. No strong correlation between the trout population and the duration or mean discharge of floods or overflows, of the same and preceding years (Ortlepp and Mürle (2003) found that the trout population remained constant after floods on the Spöl).
3. Strong positive correlation between the gravel habitat surface area and the flood and flood frequency historic variables (Floods promote gravel bar formation (Barry et al., 2008, Mürle et al., 2003)).
4. Positive correlation between the spawning grounds surface area and the floods and overflows variables of the same and preceding years (Floods remove clogging and spawning grounds surface area increase significantly after floods (Mürle et al., 2003, Ortlepp and Mürle, 2003)).
5. Positive correlation between the adult trout population and the ancient mean discharge of floods and overflows (Former spawning ground creation is favored by floods and overflows).
6. Positive correlation between the trout population and the gravel surface area of the same and preceding years (based on the relationship between gravel surface area and spawning grounds, and spawning grounds and trout population).

2 DATA & METHODS

The study period extends from 1997 to 2022 and the field site comprised of the entire residual flow reach, from the Rossens dam to the powerhouse of Hauterive (Figure 1).

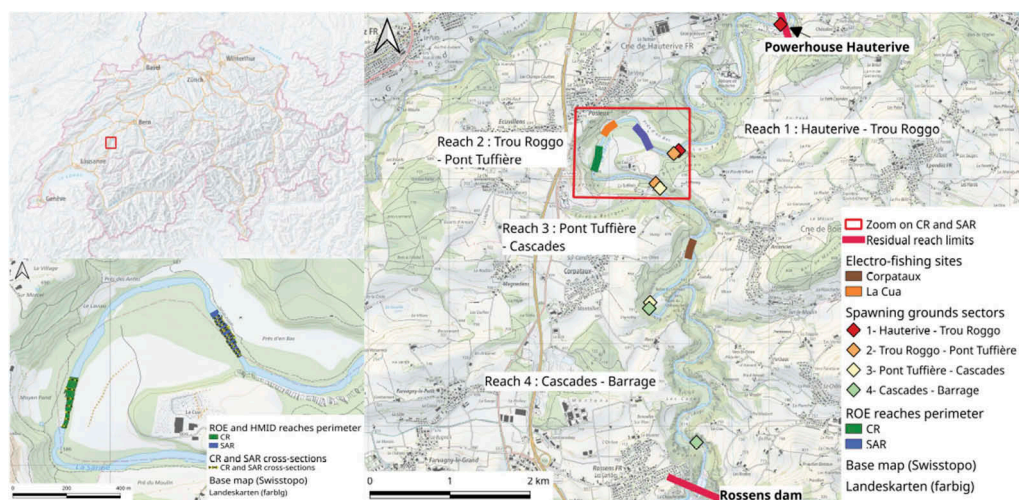


Figure 1. Situation map; Location of the study site in Switzerland (up left); ROE reaches (CR and SAR) and cross-sections location (down left); Electro-fishing sites, Spawning grounds sector limits, ROE reaches location in the residual reach (right); Background: © Swisstopo.

Several data sets were used in this study:

- Discharge data was provided by Groupe E for the period from November 1996 to October 2022. This data includes the released water through the spillway as a volume or a discharge. For the period from 2010 to 2022, the data includes the residual discharge. Overflows and floods occurrences were extracted. The criteria for the definition of a flood was based on volume: $V_{12h} > 1.75$ million m^3 (Schroff et al., 2022). The following characteristics were extracted: beginning and ending date and time, duration, peak and mean discharge and total released volume. As shown in Table 1, the flood of 2021 was larger than the flood of 2020 in terms of peak discharge, duration and volume. Its peak discharge is greater than 300 m^3/s , so larger than the one of a two-year return event (257 m^3/s). The peak discharge of the artificial flood was 224 m^3/s , so larger than the one of a one-year return event (82 m^3/s) (OFEV, 2021).
- Macrohabitats evolution: Habitats digitalization was performed on aerial images from Swiss-topo and ZHAW drone imagery, on the sectors 1 and 2 of the trout spawning grounds monitoring campaign (Figure 1). Two habitat types were distinguished: bare sediments (gravel) and wetted surface. Already digitized layers provided by the Ecohydrology group from ZHAW were used for the years 2007 and 2013.

Table 1. 2016 and 2020 artificial floods and 2021 natural flood characteristics; discharge data provided by Groupe E.

	2016 (artificial flood)	2020 (artificial flood)	2021 (natural flood)
Beginning date and time	14/09/2016 03:00	22/10/2020 01:30	11/07/2021 22:00
Ending date and time	15/09/2016 06:15	22/10/2020 22:00	20/07/2021 17:15
Duration	27.25 h (> 1 day)	21h (< 1 day)	211.5h (~ 9 days)
Maximum discharge	255 m^3/s	224 m^3/s	> 300 m^3/s
Total released volume	~11.7e+06 m^3/s	~6.6e+06 m^3/s	~72.3e+06 m^3/s

- Field measurements for the ROE indicator set 1 on habitat diversity were performed on 14 profiles on the SAR and 7 profiles on the CR before and after the 2020 and 2021 flood events. Indicators 1.3 (Water depth) and 1.4 (Flow velocity) and the HMID (Hydro-Morphological Index of Diversity) were computed from flow velocity and water depth measurements. Detailed descriptions of the indicators can be found in Hunzinger et al. (2019) and Gostner et al. (2013). The attributes of indicator 1.6 (Substrate) on substrate composition and mobilisability were also assessed.
- Trout spawning grounds data was provided by the NGO La Frayère. Data was available for 4 sectors on the residual flow reach starting in 1997. The study focuses on the sectors 1 and 2, that have been monitored almost every year.
- Trout catch data was also provided by La Frayère. Data is available starting in the year 2000, but not for every year. Electro-fishing is executed on 2 sites, usually in October. Trout population and biomass estimation were computed using the depletion after k-pass method developed by Carle and Strub (1978). Juvenile trouts were differentiated from adult trouts, based on a length criteria: juveniles were defined as fishes of a length inferior to 130 mm.

In order to analyze correlations between hydrological variables and morphological and ecological responses, a data frame containing the explanatory factors and the target variables was built. Each line corresponds to a year from 1997 to 2022 and gathers all the corresponding data related to the explanatory factors or target variables of the columns if available. A list of the created variables with a short description is presented in Table 2. The variables can be divided into 4 main categories: discharge-related variables, morphological variables, spawning grounds variables and electro-fishing variables. Historic variables were derived from the original variables using the value of preceding years and included in an extended version of the data frame.

Table 2. Data frame variables code, name, unit and description.

Code	Variable name	Unit	Description
D-1	Years_peak_Q_sup_Q2	-	Number of consecutive years for which the yearly peak discharge is greater than a two-year return event ($Q_2 = 257 \text{ m}^3/\text{s}$) within the last five years
D-2	Years_since_flood_Q2	-	Number of years since the last flood superior to a Q_2
D-3	Years_peak_Q_sup_Q1	-	Similarly as for D-1, greater than a one-year return event ($Q_1 = 82 \text{ m}^3/\text{s}$)
D-4	Years_since_flood_Q1	-	Similarly as for D-2, since the last flood superior to a Q_1
D-5	Days_overflows	-	Number of days of overflow episodes in the year
D-6	Mean_Q_overflows	m^3/s	Mean discharge of overflow episodes in the year
D-7	mean_Q_overflows_5	m^3/s	Mean discharge of overflow episodes of the last five years
D-8	ancient_overflows_Q	m^3/s	Mean discharge of overflow episodes of the years-4 and -5
D-9	Days_floods	-	Number of days of flood events in the year
D-10	Mean_Q_floods	m^3/s	Mean discharge of flood events in the year
D-11	mean_Q_floods_5	m^3/s	Mean discharge of flood events of the last five years
D-12	recent_floods_Q	m^3/s	Mean discharge of flood events of the years-1 to -3
D-13	ancient_floods_Q	m^3/s	Mean discharge of flood events of the years-4 and -5
D-14	Days_Flood	m^3/s	Number of days of the largest flood event of the year
D-15	Mean_Q_Flood	m^3/s	Mean discharge of the largest flood event of the year
M-1	Gravel_surf	m^2	Total absolute gravel surface area in the sectors 1 and 2
M-2	Gravel_surf_5	m^2	Similarly as M-1, mean area in the past five years
E-1	N0	-	Estimated trout population
E-2	N0_ha	ha^{-1}	Estimated trout population density per hectare
E-3	Biomass_ha	g/ha	Estimated trout biomass density per hectare
E-4	Biomass_ad_ha	g/ha	Similarly as E-3 for adult trouts
E-5	N_ad_ha	ha^{-1}	Similarly as E-2 for adult trouts
E-6	N_juv_ha	ha^{-1}	Similarly as E-2 for juvenile trouts
S-1	Sector_1	m^2	Spawning grounds surface area reported for the sector 1
S-2	Sectors_1_2	m^2	Spawning grounds surface area reported for the sectors 1 and 2
S-3	Sector_3	m^2	Spawning grounds surface area reported for the sector 3
S-4	Sector_4	m^2	Spawning grounds surface area reported for the sector 4

A correlation matrix was created in order to identify significant strong correlations between variables of different categories. The chosen method for computing a correlation metric was the Pearson correlation coefficient. The significance threshold for the p-value was set at 0.05, and a correlation could be considered large if its absolute value was greater than 0.5 (Field et al., 2012). In addition to the verification of the stated hypotheses, the largest correlation coefficients were more closely examined.

3 RESULTS

3.1 Comparison of the effects of the artificial flood (2020) and the natural flood (2021)

As it can be observed in Figure 2, the HMID value steadily decreased for both reaches from 2020 to 2022. The decline is more pronounced for the CR (- 5.2; SAR: - 1.2). The indicator 1.3 follows the same trend for both reaches: it decreases following the artificial flood of 2020 and slightly increases again after the natural flood of 2021, without reaching the indicator value of 2020. The values for indicator 1.4 sharply decline for the CR (- 0.4), whereas it remains almost constant (with a slight decrease) for the SAR (~ 0.7) between 2020 and 2022.

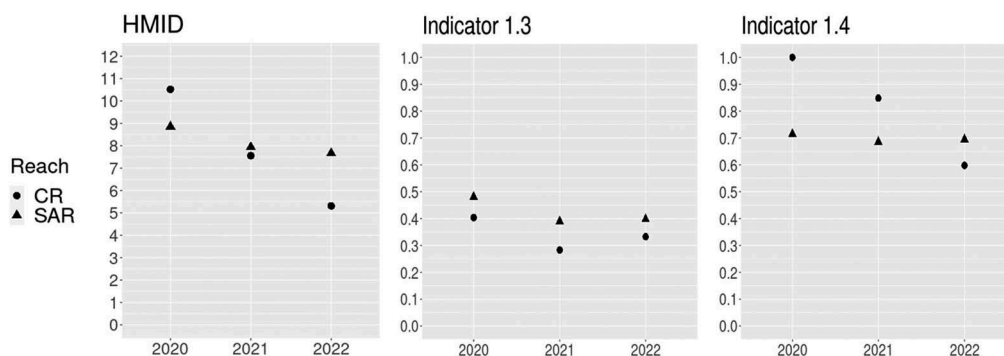


Figure 2. HMID and ROE indicators results for the years 2020 to 2022, differentiated across reaches CR: circle, SAR: triangle (a) HMID (b) Indicator 1.3 (c) Indicator 1.4.

The digitized gravel habitat surface area generally increased between 2020 and 2022 (+ 6443 m²), and the increase is larger between 2021 and 2022 (+ 5805 m²). The indicator 1.6 score remains identically low between 2020, 2021 and 2022, at 0.25. The proportion of bed load increased for both reaches between 2020 and 2022 (CR: + 10.1%; SAR: + 4.4%), while the proportion of suspended particles diminished (CR: - 5%; SAR: - 10.5%). Concerning the substrate composition, the dominant substrate type in both reaches is large stones (> 50%). The proportion of rock continuously increased for both reaches between 2020 and 2022 (CR: + 5.9%; SAR: + 20.9%) whereas the one of gravel (CR: - 1.9%; SAR: - 0.5%) and fine sediments (CR: - 17.9%; SAR: - 6.3%) decreased in both reaches.

As demonstrated in Figure 3a, the spawning grounds surface area in 2020 does not deviate from the declining trend ongoing since 2014 despite the peak discharge caused by the artificial flood. On the other hand, the trend is inverted in 2021, as the peak discharge resulting from the natural flood is associated with the largest cumulative spawning grounds surface area recorded for the two sectors.

The estimated trout population, differentiated among adult and juvenile trouts, is represented in Figure 3b. It is observed that the population evolution is similar to the one for the spawning grounds surface area. The trout population is larger after the artificial and the natural floods than before, but it remains low compared to the population in 2007 and 2012. The proportion of juveniles is nevertheless high in 2021 (~ 82%) and 2022 (~ 77%).

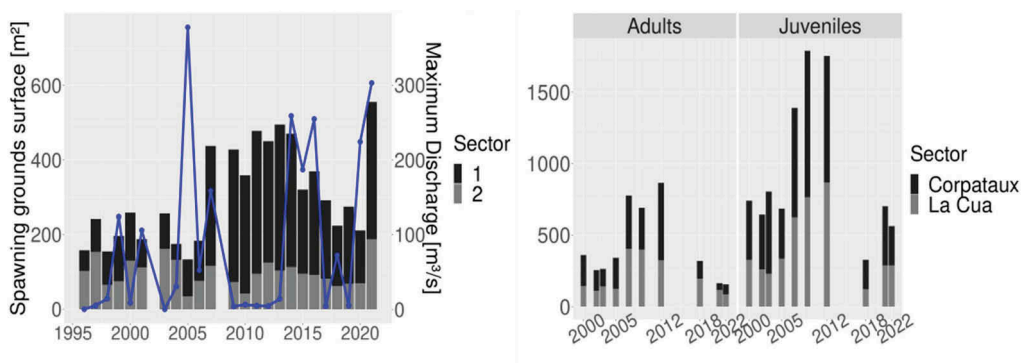


Figure 3. (a) Spawning grounds surface area evolution on the sectors 1 and 2 [m²], plotted as stacked bar diagram, and yearly maximum discharge [m³/s] between 1996 and 2021, plotted as a blue line (b) Estimated trout population N₀ using the k-pass removal method developed by Carle and Strub (1978), for Corpataux and La Cua sectors, for the years 2000 to 2022 (years for which data was available); data provided by La Frayère.

3.2 Effects of discharge variations on morphological and ecological variables

The most important relationships, including historical variables, have been selected from the correlation analysis results and are presented in Table 3. The total trout population (E-1) has a strong positive correlation with the mean gravel surface area of the past five years (M-2), while the adult trout population (E-5) has a strong positive correlation with the time elapsed since the last two-year return flood event (D-2). The spawning grounds surface area in different sectors (S-1, S-3, S-4) has a strong positive correlation with the trout biomass density of the year before (E-3) and with explanatory factors related to past overflows and floods mean discharge (D-13, D-7). The mean gravel surface area of the past five years (M-2) is negatively correlated with the frequency of one-year return flood events (D-3) and the mean discharge of overflow episodes (D-7) in the past five years.

Table 3. Most important correlations between the investigated variables (retrieved from the correlation analysis on the basis of decreasing absolute value of the Pearson correlation coefficient); lines of the table are ordered by variable code of Variable 1; n is the number of samples used for calculating the correlation.

Variable 1	Variable 2	Correlation coefficient r
E-1: N ₀	M-2: Gravel_surf_5	0.81 (n=10)
E-5: N_ad_ha	D-2: Years_since_flood_Q2	0.90 (n=10)
S-1: Sector_1	E-3: Year.1_Biomass_ha	0.99 (n=7)
S-3: Sector_3	D-13: ancient_floods_Q	0.86 (n=8)
S-4: Sector_4	D-7: mean_Q_overflows_5	0.76 (n=13)
M-2: Gravel_surf_5	D-3: Years_peak_Q_sup_Q1	-0.82 (n=23)
M-2: Gravel_surf_5	D-7: mean_Q_overflows_5	-0.67 (n=23)

The results of a representative selection of correlations related to the hypotheses are presented in Table 4 and described hereafter:

1. The spawning grounds surface area in different sectors (S-1, S-2) is positively correlated with the mean gravel habitat surface area in the past five years (M-2).
2. No statistically significant correlation has been observed between the trout population and floods and overflows variables of the same year. Only one strong negative correlation is observed with the duration of overflows (D-5) of four years before.

Table 4. Correlation analysis results (examples) for the formulated hypotheses, n is the number of samples used for calculating the correlation.

N°	Mathematical formulation (selection of correlations)	Verification
1	$r(\text{Sector}_1, \text{Gravel_surf}_5) = 0.52$ (n=20)	Verified
2	$r(\text{N0_ha}, \text{Year.4_d_overflows}) = -0.71$ (n=9)	Verified
3	$r(\text{mean_Q_floods}_5, \text{Gravel_surf}_5) = -0.58$ (n=21)	Rejected
4	$r(\text{Years_peak_Q_sup_Q1}, \text{Gravel_surf}_5) = -0.82$ (n=23)	Partly verified
	$r(\text{ancient_floods_Q}, \text{Sector}_3) = 0.86$ (n=8)	
	$r(\text{mean_Q_floods}_5, \text{Sector}_3) = 0.69$ (n=9)	
	$r(\text{Years_peak_Q_sup_Q2}, \text{Sector}_4) = 0.76$ (n=13)	
5	$r(\text{Years_since_flood_Q2}, \text{Sector}_3) = 0.66$ (n=13)	Partly verified
	$r(\text{Biomass_ad_ha}, \text{Year.5_d_Flood}) = 0.67$ (n=9)	
	$r(\text{Biomass_ad_ha}, \text{Year.5_mean_Q_Flood}) = 0.69$ (n=9)	Verified
6	$r(\text{N0_ha}, \text{Gravel_surf}_5) = 0.79$ (n=10)	
	$r(\text{N_ad_ha}, \text{Gravel_surf}_5) = 0.79$ (n=10)	
	$r(\text{N_juv_ha}, \text{Gravel_surf}_5) = 0.76$ (n=10)	

- The gravel habitat surface area has both positive and negative correlations depending on the flood and flood frequency variables. It is negatively correlated with the floods mean discharge (D-11, D-12) and the one-year return flood event frequency (D-3), but it is positively correlated with the time elapsed since the last one- and two-year return flood event (D-2, D-4).
- The spawning grounds surface area in different sectors has a strong positive correlation with the mean discharge of flood and overflow events (D-7, D-8, D-11, D-13) and with the frequency of one- and two-year return flood events (D-1, D-3). It is also positively correlated with the time elapsed since the last one- or two-year return event (D-2, D-4), although the correlations are slightly weaker.
- No statistically significant correlation is observed with the adult trout population. The adult biomass density (E-4) is positively correlated with the mean discharge (D-15) and the duration (D-14) of ancient maximum flood event but negatively with the duration of ancient overflows (D-5).
- The total trout population (E-1, E-2) as well as the adult (E-5) and juvenile (E-6) trout population has a strong positive correlation with the mean gravel habitat surface area of the past five years (M-2), as shown in Figure 4 for the example of trout density per hectare.

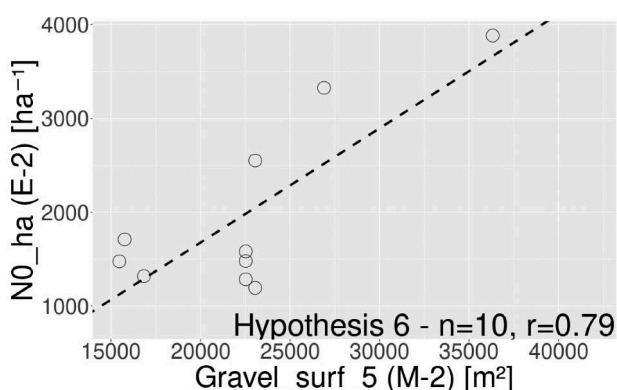


Figure 4. Scatterplot showing the correlation result for the variables E-2 (Estimated trout population density per hectare) and M-2 (Mean area of gravel surface in sectors 1 and 2 over the past five years).

4 DISCUSSION

The 2020 artificial flood had a smaller peak discharge than the artificial flood released in 2016. The sediment deposits on the SAR, that were pre-eroded in 2016, were hence barely mobilized with the flood of 2020. The lack of sediment supply could have contributed to the overall decrease in hydromorphological diversity, reflected in the indicators 1.3 and 1.4 and the HMID. On the other hand, the larger natural flood of 2021 mobilized additional sediments out of the alluvial plain and from the sediment deposits. The indicator values and the proportion of bed load thus rise after the flood of 2021. The sediment deposits on the SAR helped to mitigate the loss of hydromorphological diversity but were not sufficient to compensate for the deficit. On the CR however, since there is no sediment supply, the general decrease in the indicators' scores is more pronounced than for the SAR. The natural flood of 2021 can be considered as morphogenic, as its peak discharge is higher than the one of a two-year return event (Barry et al., 2008). The rise in the proportion of gravel habitat in 2022 can then be related to the morphological changes induced by the flood. Both floods presumably washed away the fine sediments, which results in reduced clogging. This is particularly beneficial for trout spawning (Pulg et al., 2013). The large increase in rock surface in both reaches shows the continued sediment depletion of the reach and indicates progressive channel incision. The trout spawning ground surface area after the artificial flood of 2020 follows the declining trend ongoing since 2014. The artificial flood had then no tangible effects on the spawning grounds surface area. This is confirmed by the findings of Schroff et al. (2022), that underline concerns about long-term detrimental effects of floods under sediment-starved conditions. On the other hand, the flood of 2021 seems to have triggered a favorable dynamic for aquatic species, as the elevated peak discharge coincides with a large increase in the spawning ground surface area in 2022. This rise is not particularly reflected in the trout population, although it is higher than before both flood events and the proportion of juveniles in 2021 and 2022 is high. The fish population might react with a time delay, since juveniles take several years to grow into sexually mature adult trouts that can spawn and contribute to the growth of the total population (Alp et al., 2003).

The gravel habitat surface area was expected to depend solely on hydrological explanatory factors, as hydrological variations, especially morphogenic flood events, promote morphological changes and gravel bar formation (Barry et al., 2008). Strong correlations are indeed observed between the gravel surface area and the flood and flood frequency variables, the correlation signs are however opposite to what could have been expected. The positive correlations between the gravel habitat surface area and the trout population and the spawning grounds surface area is in accordance with the suitability of gravel as adequate substrate for spawning, which is favorable to the trout population (Pulg et al., 2013). The strong positive correlation between the adult trout population and the time elapsed since the last two-year return flood event might be a purely statistical coincidence. Similarly, the occasional correlation with the duration of overflow episodes is not enough to conclude on systematic relationships between the trout population and floods and overflows mean discharge or duration. This implies that the trout population is not negatively impacted by hydrological variations, as Ortlepp and Mürle (2003) observed on the Spöl. Spawning grounds availability is favored by hydrological variations. This is confirmed by the strong positive correlations between the spawning grounds surface area in different sectors and discharge and overflows variables. It underlines the role of these variables in removing clogging and promoting spawning habitat (Mürle et al., 2003, Ortlepp and Mürle, 2003). The positive correlation with a priori contradictory flood frequency variables (D-2, D-4 and D-3) was however not expected. The spawning grounds surface area correlation with the trout biomass density of the year before is supported with similar correlations with the total trout population and adult trout biomass and population of the year before. These correlations were expected, as spawning grounds are built by sexually mature adult trouts (Alp et al., 2003).

4.1 *Limitations of the study*

Several approximations were made in this study. A particularly limiting constraint was the restricted number of samples for the correlation analysis, which was derived from data gaps

that were not consistent between the different data sets. A more complete data set could have helped in determining clearer systematic correlations and in avoiding contradictory trends. The influence of other factors, such as water temperature, chemistry, turbidity and macroinvertebrates abundance and diversity, that were not accounted for in this study, might also play an important role. Future studies could examine the interactions with these factors so as to complete the investigation. Another limitation originates from the lack of geographical overlapping in the available data for spawning grounds surface area and electro-fishing. Future studies could correct this bias in investigating the relationships between local morphological conditions and trout population at the electro-fishing sites. An additional limitation stems from the procedure applied for habitats digitalization. The source-dependent quality of aerial images may have induced errors in the absolute recorded surfaces. Although the method was performed according to the category classification described by Tonolla et al. (2021), bias can be introduced due to the manual digitalization.

5 CONCLUSION

An essential part of this study was to assess the effects of the artificial flood in 2020 and the natural flood in 2021 on the morphological and the ecological conditions. Results have shown that the morphogenic natural flood induced larger morphological changes, which seem to have promoted the spawning grounds surface area formation. This trend is not yet reflected in the trout population estimation. It can be estimated that the natural flood of 2021 had overall beneficial ecological effects. The artificial flood of 2020 did not have a significant positive influence on the trout population nor on the spawning ground surface area. Both flood events contributed to the washout of fine sediments and the reduction of stream bed clogging. However, the decline in hydromorphological diversity reflects the lack of adequate sediment supply and implies that such floods do not provide sustainability over the long term. The sediment deposits in the SAR seem to have played a mitigative role in the loss of morphological diversity. It is recommended that future experimental floods should be combined with properly designed sediment augmentation measures.

The correlation analysis between hydrological, morphological, and ecological variables revealed interesting relationships. The dependence of bare sediment bars on hydrological variations and the suitability of gravel as substrate for trout spawning were confirmed. The contradictory trends observed in some of the hypotheses confirm the difficulty of detecting statistical patterns between hydrological, morphological and ecological data, even over a period longer than 20 years on a reach scale. Some of these trends could be due to bias sources described in the study. A more complete data set and the addition of other explanatory factors could help to generalize these results in future studies. The examined relationships underline the role of hydrological variations, especially morphogenic floods, on the trout population. Restoration measures for the Sarine residual flow reach should ensure regular medium-sized floods (Q2 to Q5), along with sediment augmentation measures. These measures could be completed with less frequent larger floods (Q10, Q30). Trouts could also benefit from a more dynamic residual discharge regime, mimicking the natural flow variations, coupled with an increase in the residual discharge.

ACKNOWLEDGEMENTS

We would like to thank La Frayère, the Eco-hydrology Group of ZHAW as well as Groupe E for providing the underlying data of this study. We also thank Montana Marshall for the proofreading.

REFERENCES

- Alp, A., Kara, C., and Büyükçapar, H. M. (2003). Reproductive biology of brown trout, *Salmo trutta macrostigma* Dumeril 1858, in a tributary of the Ceyhan River which flows into the eastern Mediterranean Sea. *Journal of Applied Ichthyology*, 19(6):346–351.

- Barry, J. J., Buffington, J. M., Goodwin, P., Asce, M., King, J. G., and Emmett, W. W. (2008). Performance of Bed-Load Transport Equations Relative to Geomorphic Significance: Predicting Effective Discharge and Its Transport Rate. *Journal of Hydraulic Engineering*, 134(5):601–615.
- Döring, M., Tonolla, D., Robinson, C., Schleiss, A., Stähly, S., Gufler, C., Geilhausen, M., and Di Cugno, N. (2018). Künstliches Hochwasser an der Saane - Eine Massnahme zum nachhaltigen Auenmanagement. *Wasser Energie Luft*.
- Field, A., Miles, J., and Field, Z. (2012). *Discovering Statistics using R*. Ashford Colour Press, sage publications edition.
- Gostner, W., Alp, M., Schleiss, A. J., and Robinson, C. T. (2013). The hydro-morphological index of diversity: A tool for describing habitat heterogeneity in river engineering projects. *Hydrobiologia*, 712(1):43–60.
- Hunzinger, L., Armin, P., and Schweizer, S. (2019). Jeu d'indicateurs 1 – Diversité des habitats. Office fédéral de l'environnement OFEV.
- J. David Allan, María M. Castillo, and Krista A. Capps (2021). *Stream Ecology: Structure and Function of Running Waters*.
- Mivelaz, L. (2004). Augmentation du débit de dotation de la Petite Sarine en aval du barrage de Rossens. *Entreprises Electriques Fribourgeoises, Direction Production Energie*.
- Mürle, U., Ortlepp, J., and Zahner, M. (2003). Effects of experimental flooding on riverine morphology, structure and riparian vegetation: The River Spöl, Swiss National Park. *Aquatic Sciences* 2003 65:3, 65(3):191–198.
- OFEV (2021). *Probabilité des crues (crues annuelles), Sarine - Fribourg*. Technical report, Office fédéral de l'environnement (OFEV).
- Ortlepp, J. and Mürle, U. (2003). Effects of experimental flooding on brown trout (*Salmo trutta fario* L.): The River Spöl, Swiss National Park. *Aquatic Sciences*, 65:232–238.
- Peter, A. (2010). A Plea for the Restoration of Alpine Rivers: Basic Principles Derived from the “Rhône-Thur” Case Study. *Hdb Env Chem*, 6:247–260.
- Pulg, U., Barlaup, B. T., Sternecker, K., Trepl, L., and Unfer, G. (2013). Restoration of spawning habitats of brown trout (*Salmo Trutta*) in a regulated chalk stream. *River Research and Applications*, 29(2):172–182.
- Schroff, R., Mörtl, C., and De Cesare, G. (2021a). Ultrasonic Doppler flow velocity measurements as a co-indicator for the eco-morphological assessment in a residual flow reach. *Proceedings of the 13th Symposium on Ultrasonic Doppler Methods for Fluid Mechanics and Fluid Engineering*, pages 107–111.
- Schroff, R., Mörtl, C., and De Cesare, G. (2021b). Wirkungskontrolle einer Sedimentzugabe: Habitatvielfalt und Kolmation ||| Eco-morphological evaluation of a sediment augmentation measure. *Wasser-Wirtschaft*, 111(9-10):68–76.
- Schroff, R., Mörtl, C., Vonlanthen, P., and De Cesare, G. (2022). Impacts et enjeux de charriage d'une crue artificielle – Exemple de la Petite Sarine 2020 | Wirkung und Geschiebeproblematik eines künstlichen Hochwassers – Beispiel der Kleinen Saane 2020. *Wasser Energie Luft*, 114(2):75–84.
- Stähly, S., Franca, M. J., Robinson, C. T., and Schleiss, A. J. (2019). Sediment replenishment combined with an artificial flood improves river habitats downstream of a dam. *Scientific Reports*, 9(1):1–8.
- Stanford, J. A., Ward, J. V., Liss, W. J., Frissell, C. A., Williams, R. N., Lichatowich, J. A., and Wiley, J. (1996). A general protocol for restoration of regulated rivers. *Regulated Rivers: Research and Management*, 12(4-5):391–413.
- Tonolla, D., Geilhausen, M., and Doering, M. (2021). Seven decades of hydrogeomorphological changes in a near-natural (Sense River) and a hydropower-regulated (Sarine River) pre-Alpine river floodplain in Western Switzerland. *Earth Surface Processes and Landforms*, 46(1):252–266.
- Wohl, E., Bledsoe, B. P., Jacobson, R. B., Poff, N. L., Rathburn, S. L., Walters, D. M., and Wilcox, A. C. (2015). The Natural Sediment Regime in Rivers: Broadening the Foundation for Ecosystem Management. *BioScience*, 65(4):358–371.

Bedrock scour prediction downstream of high head dams due to developed rectangular jets plunging into shallow pools

A. Bosman

Department of Civil Engineering, Stellenbosch University, Stellenbosch, South Africa

G.R. Basson

Emeritus Professor, Department of Civil Engineering, Stellenbosch University, Stellenbosch, South Africa

ABSTRACT: Rock scour formation near the foundation of a dam due to a plunging jet could compromise the safety of the structure. It is therefore essential to predict the geometry of the equilibrium scour hole during the hydraulic design of the dam. Rock scour is normally predicted by analytical-empirical formulae and methods. Despite extensive research since the 1950s, presently there is no universally agreed method to accurately predict the equilibrium scour hole dimensions caused by plunging jets at dams. The main purpose of the research is to contribute to the body of knowledge in predicting the equilibrium geometry of a scour hole in bedrock downstream of a high dam caused by a fully developed rectangular jet plunging into a shallow plunge pool. Both physical and numerical modelling were used to investigate the hydrodynamic and geo-mechanical aspects of rock scour. The physical model investigated the equilibrium scour hole geometries of an open-ended jointed, movable rock bed for different discharges, dam heights, plunge pool depths, rock block sizes, and joint orientations. Novel contributions to science made by the research were the measurement of the dynamic pressures at the joint openings at the water-rock interface of a movable pool bed, while the jet was issued from a rectangular horizontal canal and not a nozzle. From the experimental results, non-dimensional formulae for the scour hole geometry were developed using multi-linear regression analysis. The experimental scour results from this study were compared to various analytical methods found in literature. The equilibrium scour hole depth established in this study best agrees with that predicted by the Critical Pressure method, followed by the Erodibility Index Method. A three-dimensional, multi-phase numerical model, in combination with the developed scour depth regression formula, was used to simulate the equilibrium scour hole geometry in an iterative manner. The proposed three-dimensional numerical model is capable of accurately simulating the scour hole depth, and to a lesser extent the scour length and width.

1 INTRODUCTION

A free-falling jet from a high head dam requires significant energy dissipation to limit scouring of the foundations downstream of a dam. A scour hole will form in the plunge pool bed downstream of the dam if the energy dissipation of the jet is underestimated. The foundation of the dam could be endangered if the scour hole geometry becomes extensively large. The assessment of the equilibrium scour hole geometry (ultimate depth, width, and length) is important in the hydraulic design of high head dams to ensure that the foundations of the dam are not endangered by the scour hole during its lifetime (Van Aswegen et al., 2001).

Scouring of the bottom of the plunge pool downstream of the dam has been reported at several dam sites worldwide. Well documented cases, such as the Kariba Dam on the Zambezi River (border between Zimbabwe and Zambia, Africa) and Wivenhoe Dam, situated on the Brisbane River (Australia) are prime examples where plunge pool scouring had drastic consequences. Currently, the depth of the scour hole of the Kariba Dam is 80 m, which is

approximately two thirds of the dam height of 128 m (Bollaert et al., 2012). The scour hole depth at the Wivenhoe Dam was one-third of the dam height of 33.87 m (full supply level to lip of spillway bucket) after the January 2011 flood (Stratford et al., 2013).

Bedrock scour downstream of a dam is a complex physical process and the complete understanding of the air-water-rock phase interaction in the scouring process is required. Rock scour is normally predicted by analytical-empirical formulae and methods. Although sophisticated computer models are available, most existing three-dimensional (3D) numerical models use two-phase simulation, using either water-and-rock or water-and-air.

The assessment of rock scour in the current study was limited to fully developed jets plunging into shallow plunge pools for different discharges, fall heights, rock block sizes and joint structure orientations that may be commonly found in dam prototypes. The research makes specific contributions, that are novel to science, towards the hydraulic design of high head spillways. These include that the dynamic pressures at the water-rock interface was accounted for by using a movable bed that could change continuously with a 3D interconnected joint structure, and that air entrainment was taken into account via a low-frequency turbulent jet, issued from a horizontal canal and not a nozzle.

The main purpose of this investigation was to contribute to the body of knowledge on the prediction of the equilibrium scour hole geometry downstream of high head dams. Rock scour at the plunge pool bottom due to a free-falling jet was investigated using both physical and numerical modelling.

2 ROCK SCOUR ANALYSES

Rock scour downstream of a dam due to a plunging jet is governed by air-water-rock phase interaction (Bollaert & Lesleighter, 2014). The free-falling jet can be apportioned into three different energy dissipation mechanisms: firstly, the disintegration and aeration of the jet as it travels through the air, secondly, the diffusion and aeration of the jet in the plunge pool, and finally, the impact with the plunge pool bottom as shown in Figure 1.

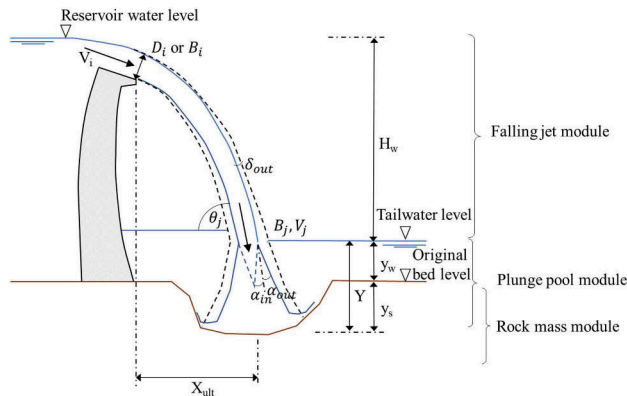


Figure 1. Free-falling jet modules involved in the rock scouring process (Bosman & Basson, 2020).

The hydrodynamics of a free-falling jet in the air and plunge pool involved in the rock scour process have been studied by various researchers. The behaviour of the jet through the air is influenced by the fall height (H_w), issuance velocity (V_i), discharge (Q), air entrainment, initial turbulence (T_u), and issuance cross-section (B_i) (Van Aswegen et al., 2001). The jet trajectory and energy at impingement with the plunge pool water surface are dependent on the impingement jet thickness (B_j) and mean velocity (V_j). If the plunging jet travels a sufficient distance through the air, the core loses its coherence and breaks up completely, becoming a developed jet (Bollaert, 2002). The jet breakup length (L_b) is dependent on the discharge, initial turbulence intensity and air entrainment (Manso et al., 2008). According to Duarte (2014) and Kuroiwa (1999), the scouring capacity of the free-falling jet is affected by the air entrainment rate over the fall height.

The jet experiences additional diffusion as it travels through the plunge pool until it impinges on the pool bed (Van Aswegen et al., 2001). The jet impact angle (θ_j), impinging mean velocity (V_j), and turbulence intensity when entering the plunge pool water surface (Manso et al., 2008), as well as the plunge pool depth (Y) and geometry (Manso et al., 2009) determine the amount of energy that would be dissipated and how much of the jet core remains intact at impact with the bedrock.

Scouring of the plunge pool bed would occur when the erosive capacity of water exceeds the ability of the rock to resist it. Scouring of rock in turbulent flow is not a shear process, but results from turbulent pressure fluctuations (Annandale, 2006). Factors that influence the vulnerability of rock include lithology, the rock strength, and the spacing, orientation and condition of the rock joints (Bollaert et al., 2004).

3 PHYSICAL MODELLING

3.1 *Physical model setup*

The physical model (Figure 2) emulating rock scour downstream of a dam was constructed in the Hydraulics Laboratory of Stellenbosch University, South Africa, as illustrated in Figure 3. The transient data collected from the physical model were used to calibrate the numerical model. The three-dimensional physical model (based on Froude scale laws) consisted of a rectangular horizontal issuance canal, replicating an uncontrolled spillway. The issuance canal could be adjusted to three levels relative to the movable rock bed, namely 3 m, 4 m, and 5 m. The plunge pool depths (TWD) that were tested were 0.5 m and 1.0 m. Free-falling jets were investigated for unit discharges of 0.010 m³/s/m to 0.224 m³/s/m. The broken-up, movable rock bed comprised of tightly hand-packed concrete paver blocks (cobblestones) emulating a uniform 3D open-ended horizontal and vertical interconnecting rock joint network. The two rock sizes tested were rectangular concrete blocks with x,y,z dimensions of 0.1 m \times 0.1 m \times 0.05 m and 0.1 m \times 0.1 m \times 0.075 m. Since gravity cannot be scaled, a similar prototype rock density of typically 2 650 kg/m³ must be used in the model. The concrete block densities used were 2 355.4 kg/m³ and 2 388.1 kg/m³ respectively. The three joint structure orientations relative to the inflow jet investigated are 0°, -45°, and 45° with the horizontal axis.

An undistorted model scale of 1:20 was recommended for the experimental results from this study. With the available laboratory height, a 1:20 model scale is able to replicate realistic prototype spillway heights (i.e. 60 m up to 100 m). Moreover, due to the air-water-rock nature of the model and the scaling effects of surface tension (Weber number), a relatively large model scale was used to ensure that air entrainment and the generation of fluctuating pressures at the plunge pool bottom and inside the joint network were suitably represented (Duarte, 2014).

The joint entrance of the movable rock mass was fitted with internal conduits to allow for the remote measurement of dynamic pressures at several locations on the plunge pool bottom (water-rock interface) using pressure transmitters fitted at the ends of the pipes. Additional data that was collected included discharge, water levels inside the issuance canal and plunge pool, flow velocity (using a Nortek Vectrino Acoustic Doppler Velocimeter), air concentration of the plunging jet (using a Thermal Needle Probe), while a 3D laser scanner surveyed the scour hole profile.

For each experiment, the rock scouring by the plunging jet was monitored until scouring of the rock mass stopped and equilibrium conditions were reached, called Case A. The bed profile was then surveyed. Thereafter, the same test was repeated with the deposited rocks downstream of the scour hole being continuously removed until equilibrium conditions were reached again, called Case B. The contour maps for the scour holes of the model for Case A and Case B are shown in Figure 4 (a) and (b) respectively for the maximum flow rate, highest fall height, and deepest plunge pool. The scour hole depth, length, width and volume all increase when the deposited rocks downstream of the hole are removed.

Further details regarding the model and its design, construction, setup, data capturing methodology, measurements accuracy, and scaling effects are described in Basson and Basson (2020) and Bosman (2021).



Figure 2. Physical model for lowest fall height (Bosman, 2021).

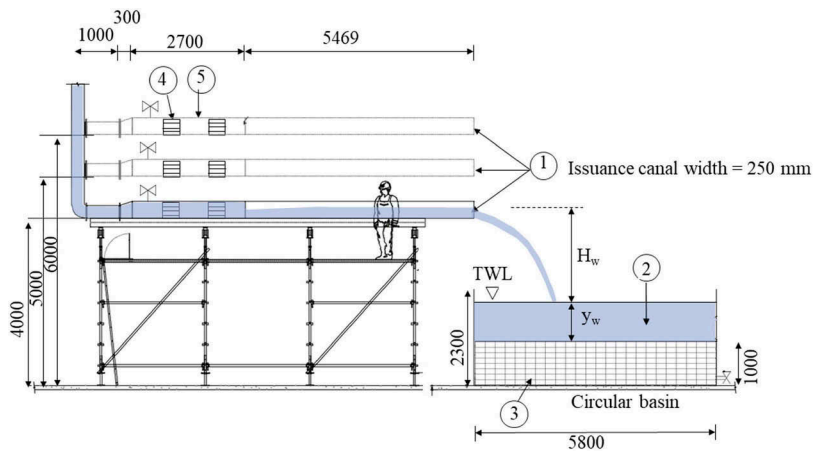


Figure 3. Model setup: (1) issuance canal; (2) plunge pool; (3) movable rock blocks; (4) flow straighteners; and (5) pressure box (adapted from Bosman & Basson, 2020).

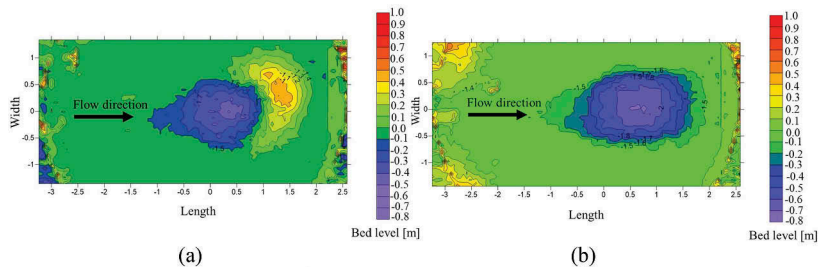


Figure 4. Final bed level for $Q = 80 \text{ m}^3/\text{s}/\text{m}$, $H_w = 100 \text{ m}$, $TWD = 20 \text{ m}$ for (a) Case A (scour and deposition) and (b) Case B (scour with deposited rocks removed).

3.2 Regression analysis

An Ordinary Least Squares regression analysis was performed on the collected physical model data, with due consideration given to the parsimony principle, to develop non-dimensional equations that predict the scour hole geometry caused by fully developed jets plunging into

shallow plunge pools. Based on literature and experimental tests, multiple variables were incorporated in the regression analysis, such as discharge, fall height, plunge pool depth, impinging jet velocity and Froude number (Kuroiwa, 1999), stream power (Annandale, 2006), rock diameter, submerged weight of rock block, and uplift pressures and forces (Bollaert, 2002). The regression analysis did not explicitly incorporate the bed shear stress, since rock scour is not a shear process but is caused by turbulent and fluctuating pressures at the pool bottom (Annandale, 2006). Therefore, the movability number that incorporates the settling velocity of the rock block (V_{ss}), and the particle Reynolds number based on the shear velocity (V^*) were used to analyse rock scour. The parameters were made dimensionless by applying the Buckingham- π theorem. The non-dimensional formulae* for vertical rock joints obtained from the regression analysis for Case A (deposited rocks intact) and Case B (deposited rocks continuously removed) are defined as follows:

$$\begin{aligned} \ln\left(\frac{D_{ScaseA}}{H_w}\right) &= -468.532\ln\left(\frac{d_{s0}}{H_w}\right) - 322.102\ln\left(\frac{V_j}{\sqrt{gB_i}}\right) + 4.502\ln\left(\frac{H_w}{L_b}\right) \\ &- 483.385\ln\left(\frac{V_{SS}}{V_i}\right) - 0.804\ln\left(\frac{F_{lift}}{G_b}\right) - 0.817\ln\left(\frac{v_w}{H_w}\right) - 473.991\ln\left(\frac{V_i B_i}{\nu}\right) \\ &+ 158.264\ln\left(\frac{q^2}{gH_w^3}\right) - 0.419\ln\left(\frac{P_{SP}}{P_{uplift} \cdot V_{SS}}\right) + 0.006\ln\left(\frac{P}{P_{crit}}\right) \\ &- 473.536\ln\left(\frac{V^*}{V_{SS}}\right) + 474.587\ln\left(\frac{V^* d_{s0}}{\nu}\right) \end{aligned} \quad (1)$$

$$\begin{aligned} \frac{D_{ScaseB}}{H_w} &= -0.196\ln\left(\frac{d_{s0}}{H_w}\right) - 0.578\ln\left(\frac{V_j}{\sqrt{gB_i}}\right) - 0.942\ln\left(\frac{V_{SS}}{V_i}\right) - 0.216\ln\left(\frac{F_{lift}}{G_b}\right) \\ &- 0.129\ln\left(\frac{P_{SP}}{P_{uplift} \cdot V_j}\right) - 0.079\ln\left(\frac{v_w}{H_w}\right) - 0.279\ln\left(\frac{V_i B_i}{\nu}\right) + 0.129\ln\left(\frac{q^2}{gH_w^3}\right) \\ &+ 0.006\ln\left(\frac{P}{P_{crit}}\right) - 0.145\ln\left(\frac{V^*}{V_{SS}}\right) + 0.315\ln\left(\frac{V^* d_{s0}}{\nu}\right) \end{aligned} \quad (2)$$

*Prototype ranges: Discharge: 35 – 80 m³/s/m, Drop height: 60 – 100 m, Tailwater depth: 10 – 20 m

The joint structure angle factors for orientations 45° in and against the direction of the flow (Table 1) should be applied to the scour hole profile determined for the horizontal and vertical joint formulae obtained from Equations 1 and 2. Similar to the well-known rock scour case of Ricobayo Dam in Spain (Annandale, 2006), the stabilising factors (Table 1) indicate that the rock is more conducive to scour failure when the dipping angle of the rock measured from the horizontal is dipped 45° in the direction of the flow.

Table 1. Joint structure angle factors (adapted from Bosman & Basson, 2020).

Scour hole geometry	Dipping angle 45° of rock relative to the horizontal against the flow direction	Dipping angle 45° of rock relative to the horizontal in the flow direction
Case A	0.93	1.29
Case B	0.89	1.06

3.3 Comparison with scour prediction methods in literature

At present there is no universally agreed upon method to accurately predict the equilibrium scour hole depth due to plunging jets at dams, despite extensive research since the 1950s. The scour depth results from this study for a full-scale prototype were compared to various analytical methods and empirical formulae found in literature as seen in Figure 5 for the 45 m³/s/m flow, a 100 m fall height (H_w), a 20 m deep plunge pool (TWD), and horizontal and vertical aligned joints. The rock scour depth prediction methods from literature yield a wide range of scour depths for the same input conditions as seen in Figure 5.

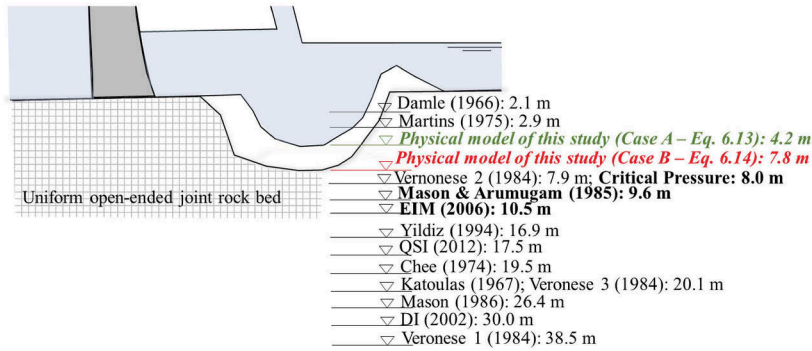


Figure 5. Prototype equilibrium scour depth from physical model and literature scour prediction methods for $Q = 45 \text{ m}^3/\text{s/m}$, $H_w = 100 \text{ m}$, $TWD = 20 \text{ m}$ (Bosman & Basson, 2020).

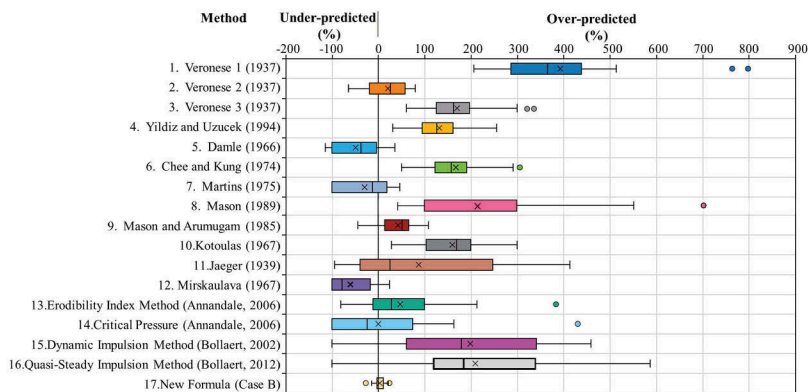


Figure 6. Scour depth distribution a percentage difference for the different scour prediction methods from the experimental work for Case B (Bosman, 2021).

The scour depth percentage difference results shown in Figure 6 indicate that the scour prediction methods have limited agreement with each other and generally overestimate the observed scour depths with a mean difference of 108% for Case B and 240% for Case A. The analytical method agreeing the best with the experimental results is the Critical Pressure method (Annandale, 2006), as the median percentage difference (-25.2%) is near zero and the method has the lowest mean percentage difference of 1% to the experimental scour depth results. However, the safest scour prediction method (accurate and conservative) would be the Erodibility Index method (Annandale, 2006), followed by Mason and Arumugam's empirical equation (1985), since the first quartile (25th percentile) nears the zero percentage difference (-12% and 15%, respectively) with a narrow statistical spread. The developed regression formula (Equation 2) to predict the scour depth for Case B agrees well with the experimental results with a compact statistical range of differences with a median difference percentage close to zero (0.8%) with the first quartile just below zero (-3%).

4 NUMERICAL MODELLING

4.1 Numerical model setup

The 3D hydrodynamic numerical model simulating the free-falling jet plunging into a plunge pool was built using the Fluent module of ANSYS 19.2. The time-averaged hydrodynamics of the plunging jet were modelled with a transient, two-phase and volume of fluid (VOF) numerical model. A variety of turbulence models were tested, though the Shear Stress Transport

(SST) $k - \omega$ Reynolds-averaged Navier Stokes (RANS) turbulence module proved to emulate the dynamic pressures on the bedrock and the flow velocity in the plunge pool when calibrated against the physical model. Various other researchers have also concluded that the SST $k - \omega$ turbulence module is the most suitable to emulate a plunging jet (Fiorotto et al., 2016, Lauria & Alfonsi, 2020, Castillo et al., 2014, and Castillo & Carrillo, 2011). A mesh refinement exercise was also conducted on the model.

The data collected from the physical model was used to calibrate the numerical model. The indicative calibration results show that a bedrock roughness constant of $C_s = 0.8$ gives a more accurate representation of a plunge pool bottom surface, corresponding to a non-uniform bed as recommended by ANSYS (2018). After calibration, the surface roughness (k_s) parameters were determined to be 0.2 m for the 0.1 m \times 0.1 m \times 0.05 m rock blocks, and 0.4 m for the 0.1 m \times 0.1 m \times 0.075 m rock blocks (Bosman, 2021). A more complete data set and explanation of the calibration results are available in Bosman (2021).

4.2 Numerical solution procedure for determining the scour hole geometry

The complex 3D dynamics of a falling jet initially impinging onto an originally flat plunge pool bed were simulated in the CFD numerical model. The equilibrium scour hole geometry was determined by applying the scour depth regression formula (Equation 1 for Case A and Equation 2 for Case B) iteratively to obtain the static scour limit (maximum scour hole dimensions) using the hydrodynamic results obtained from the CFD model as input values.

The numerical results were collected in a grid fashion. The 1% exceedance dynamic pressures at the plunge pool bottom surface (Castillo et al., 2018) and the horizontal flow velocity (x -direction) in the plunge pool were recorded at each grid point. The mobility and particle Reynolds numbers were determined by using the mean horizontal flow velocity between the pool bottom and the maximum flow velocity at the specific grid point, together with the flow depth to the maximum velocity.

Finally, the block movement was determined manually by solving the scour depth regression equation (Equation 1 for Case A and Equation 2 for Case B) for each grid point. According to the regression formula setup, a positive value indicates scour, and a negative value is taken as zero scour. The numerical simulation is then repeated with the newly calculated scoured pool bottom elevations, with the additional scour added to the previous scour depth at each specific grid point. Iterations cease when a reasonable percentage difference is found (i.e. 0% for the maximum scour depth and < 3% for all the grid points).

4.3 Numerical model results

The experimental and simulated bed deformation results as longitudinal and lateral cross-sections are compared to each other in Figure 7, while Figure 8 records the contour maps for Case B (deposited rocks continuously removed) and the numerical model for the maximum discharge, medium fall height, and deepest plunge pool depth. Although the scour profile cross-sections from the experimental and numerical tests in Figure 7 are not identical, the simulated scour contours reasonably agree with the experimental test measurements in terms of maximum scour depth and the scour width. The numerical model was successful in capturing the variation in the scour hole size for various discharges, fall heights, tailwater levels, rock sizes and joint structure orientations. The simulated scour hole contours are not entirely symmetrical as seen in Figure 8, suggesting that the numerical model is able to incorporate the randomness of scouring in nature.

The simulated scour depth results compared well with the maximum experimental scour depth observed, indicating that the numerical model can predict the maximum scour depth due to a free-falling jet for different discharges, fall heights, tailwater levels, rock sizes and joint structure orientations. The simulated equilibrium scour depth was generally over-predicted with a mean percentage error of 11%. The simulated results indicated that the proposed numerical model predicts the scour width and length with less accuracy. The maximum simulated scour width and length for Case B compared to the experimental measurements were under-predicted with a mean percentage error of -13% and -33%, respectively.

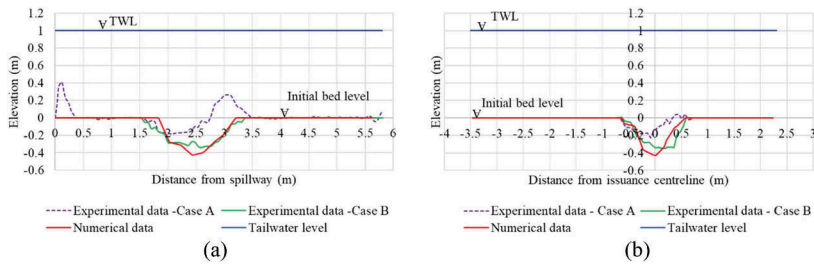


Figure 7. Experimental and simulated (a) longitudinal and (b) lateral bed profile results for Q_{max} , H_{med} , TWD_{max} for Case B.

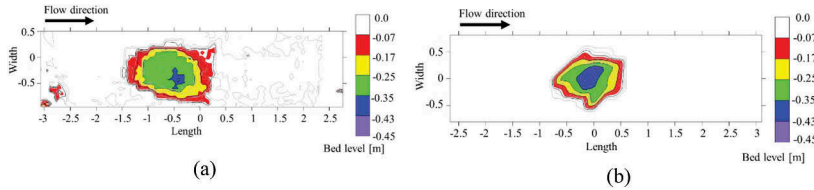


Figure 8. (a) Experimental and (b) simulated contour plot results for Q_{max} , H_{med} , TWD_{max} for Case B.

In general, the numerical model predicted a deeper, shorter, and narrower scour hole compared to the experimental measurements. A possible explanation for the disparity in the scour hole dimensions could be that the air entrainment of the jet in the air and plunge pool of the numerical model is less than in the physical model, resulting in a more compact jet being simulated. However, despite the perceived limitations, the numerical model performs well in predicting the maximum scour depth due to a rectangular jet plunging into a shallow plunge pool.

5 CONCLUSION

The erosive power of a high-velocity plunging jet, issued from a dam spillway, could create a scour hole downstream of the dam. The foundation of the dam could be endangered if the scour hole geometry becomes extensively large. The assessment of the equilibrium scour hole geometry is of crucial concern in the hydraulic design of a high head dam to ensure that the foundation is not endangered by the scour hole during the lifetime of the dam. The main objective of this research was to contribute to the body of knowledge on predicting the equilibrium geometry of a scour hole in bedrock downstream of a high dam caused by a fully developed rectangular jet plunging into a shallow plunge pool.

Both physical and numerical modelling were used to investigate rock scour for different discharges, fall heights, plunge pool depths, rock block sizes and rock joint structure orientations. The influence on the pressure characteristics at the water-rock interface by the highly irregular shape of the pool bottom was accounted for by using a movable bed with open-ended, interconnected rock joints. The research studied the scour hole geometry formed by a low-frequency turbulent jet issued from a horizontal canal, and not from a nozzle. Results from the physical model were used to develop non-dimensional multi-linear regression formulae to predict the scour hole geometry. The scour depth results from the physical model were compared to various analytical methods found in literature. The scour prediction methods were found to have limited agreement with each other, yielding a wide range of varying scour depths for the same input conditions. No single scour prediction method is conclusively superior, however, from this research the Critical Pressure method (Annandale, 2006), followed by the EIM (Annandale, 2006) method and Mason and Arumugam's (1985) empirical formula are recommended.

Furthermore, the proposed 3D numerical model, in conjunction with the scour depth regression formula developed in this study (Equation 1 for Case A and Equation 2 for Case B), is capable of accurately simulating the depth of the scour hole, and to a lesser extent the scour hole length, width and volume.

6 NOTATION

B_i	Issuance thickness of rectangular jet
$B_g = \frac{q}{\sqrt{2gH_w}}$	Core thickness at impingement for rectangular jet (Castillo et al., 2014)
$B_j = \frac{q}{\sqrt{2gH_w}} + 4 \times (1.14T_u)\sqrt{B_i}(\sqrt{2H_w} - 2\sqrt{B_i})$	Impingement jet thickness for rectangular channel (Castillo et al., 2014)
$C_I = 0.0035\left(\frac{y}{B_g}\right)^2 - 0.119\left(\frac{y}{B_g}\right) + 1.22$	Dynamic impulsion coefficient (Bollaert et al., 2015)
D_S	Scour depth
$F_{uplift} = C_I\gamma_w(x_b \cdot y_b)\frac{V_j^2}{2g}$	Lift force underneath block (Bollaert, 2002)
$G_b = V_b(\rho_r - \rho_w)g$	Submerged weight of rock block (Bollaert, 2002)
H_w	Fall height
$L_b = 6q^{0.32}$	Jet breakup length (Horeni, 1956)
P	1% exceedance dynamic pressure head
$P_{crit} = P_{uplift} \cdot 1/\gamma$	Critical pressure head
$P_{SP} = \gamma Q_w H_w / (B_{jrock} \cdot W_{jrock})$	Stream power per unit area at rock bed (Annandale, 2006)
$P_{uplift} = C_I\gamma V_j^2/2g$	Uplift pressure (Annandale, 2006)
$Q_{down} = A_{wall\ jet} \times 18\log\left(\frac{12 \times R}{d_{50}}\right)\sqrt{R \cdot S_f}$	Discharge of wall jet downstream of impingement region based on Bollaert (2012)
$R = \frac{A_{wall\ jet}}{W_{jrock}}$	Hydraulic radius of wall jet
S_f	Energy slope of wall jet (for Chèzy equation)
T_u	Initial turbulence intensity
V_b	Rock volume
V_i	Issuance velocity
$V_j = \sqrt{V_i^2 + 2gH_w}$	Impingement velocity (Annandale, 2006)
V_{SS}	Rock block settling velocity
$V^* = \sqrt{g \cdot y_{down} \cdot S_f}$	Shear velocity
W_i	Flow width at issuance
W_{jrock}	Thickness of impinging jet onto bedrock, with jet's outer spreading angle taken as 15° (Ervine & Falvey, 1987)
x_b, y_b, z_b, d_{50}	Rock block size
y_{down}	Wall jet thickness downstream of impingement
y_w	Initial plunge pool depth
θ_i, θ_j	Issuance and impingement jet angle
ρ_r, ρ_w	Rock density, water density

ACKNOWLEDGEMENTS

The authors would like to express their sincere gratitude to PERI Formwork Scaffolding, Continental Cobbles, Kaytech Engineered Fabrics, and Horts Geo-Solutions, as well as Mr NF Katzke and Mr DE Bosman for their valued support.

REFERENCES

- Annandale, G. W. (2006). *Scour Technology: Mechanics and Engineering Practice*. New York: McGraw-Hill Companies.
- ANSYS. (2018). *ANSYS® academic research fluent, release 18.1, help system, fluent theory guide*. Pennsylvania: ANSYS.
- Bollaert, E. (2002). *Transient water pressures in joints and formation of rock scour due to high-velocity jet impact*. Lausanne, Switzerland: PhD Thesis, Ecole Polytechnique Fédérale de Lausanne (EPFL).

- Bollaert, E. (2012). Wall jet rock scour in plunge pools: a quasi-3D prediction model. *International Journal on Hydropower & Dams*, 1–9.
- Bollaert, E., & Lesleighter, E. (2014). Spillway Rock Scour Experience and Analysis - the Australian Scene over the past Four Decades. *11th National Conference on Hydraulics in Civil Engineering & 5th International Symposium on Hydraulic Structures: Hydraulic Structures and Society-Engineering Challenges and Extremes*, (p. 189). Brisbane, Australia.
- Bollaert, E., Manso, P., & Schleiss, A. (2004). Dynamic pressure fluctuations at real-life plunge pool bottoms. *International Conference on Hydraulics of Dams and River Structures* (pp. 117–124). Tehran, Iran: A.A. Balkema Publishers.
- Bollaert, E., Munodawafa, M., & Mazvidza, D. (2012). Kariba Dam Plunge Pool Scour: quasi-3D Numerical Predictions. *6th International Conference on Scour and Erosion*, (pp. 627–634). Paris.
- Bollaert, E., Stratford, C., & Lesleighter, E. (2015). Numerical modelling of rock scour: Case study of Wivenhoe Dam (Australia). *7th International Conference on Scour and Erosion* (pp. 397–404). Perth, Australia: CRC Press. DOI: 978-1-138-02732-9.
- Bosman, A. (2021). *High dam scour hole geometry prediction for fully developed jets plunging into shallow pools on bedrock*, PhD Thesis. Stellenbosch: Stellenbosch University.
- Bosman, A., & Basson, G. (2020). Physical model study of bedrock scour downstream of dams due to spillway plunging jets. *Journal of South African Institute of Civil Engineering*, 62(3), 36–52.
- Castillo, L., & Carrillo, J. (2011). Numerical simulation and validation of hydrodynamics actions in energy dissipation devices. *34th IAHR World Congress* (pp. 4416–4423). Madrid, Spain: International Association for Hydro-Environment Engineering and Research.
- Castillo, L., Carillo, J., & Sordo-Ward, A. (2014). Simulation of overflow nappe impingement jets. *Journal of Hydroinformatics*, 16(4), 922–940.
- Castillo, L., Carrillo, J., & Marco, F. (2018). Advances in the characterization of pressures and velocities in the overtopping of arch and gravity dams. *3rd International Conference on Protection against Overtopping (6-8 June)*, (pp. 1–9). United Kingdom.
- Duarte, R. (2014). *Influence of air entrainment on rock scour development and block stability in plunge pools*. Lausanne, Switzerland: PhD Thesis, EPFL.
- Ervine, D., & Falvey, H. (1987). Behaviour of Turbulent Water Jets in the Atmosphere and in Plunge Pools. *Proceedings of the Institution of Civil Engineers, Part 2*, (p. 83).
- Fiorotto, V., Barjastehmaleki, S., & Caroni, E. (2016). Stability analysis of plunge pool linings. *Journal of Hydraulic Engineering*, 142(11), 04016044-1 to 04016044-11.
- Horeni, P. (1956). Disintegration of a free jet of water in air. *Byzkumny ustav vodohospodarsky prace a studie, Sesit 93*.
- Kuroiwa, J. M. (1999). *Scour caused by rectangular impinging jets in cohesionless beds*, PhD Dissertation. Colorado: Colorado State University.
- Lauria, A., & Alfonsi, G. (2020). Numerical investigation of ski jump hydraulics. *Journal of Hydraulic Engineering*, 146(4), 04020012-1 to 04020012-8.
- Manso, P., Bollaert, E., & Schleiss, A. (2008). Evaluation of high-velocity plunging jet-issuing characteristics as a basis for plunge pool analysis. *Journal of Hydraulic Research*, 46(2), 147–157. DOI: 10.1080/00221686.2008.9521852.
- Manso, P., Bollaert, E., & Schleiss, A. (2009). Influence of plunge pool geometry on high-velocity jet impact pressures and pressure propagation inside fissured rock media. *Journal of Hydraulic Engineering*, 135(10), 783–792.
- Mason, P., & Arumugam, K. (1985). Free jet scour below dams and flip buckets. *Journal of Hydraulic Engineering*, 111(2), 220–235.
- Stratford, C., Bollaert, E., & Lesleighter, E. (2013). Plunge pool rock scour analysis techniques: Wivenhoe dam spillway, Australia. *Hydro 2013 Conference*. Innsbruck, Austria.
- Van Aswegen, W., Dunkley, E., & Blake, K. (2001). *Plunge pool scour reproduction in physical hydraulic models*. Stellenbosch, South Africa: Water Research Commission

Fish passes on the Rhine River – Major structures at EDF Hydro plants to restore fish continuity

Guillian Brousse

Project Manager, EDF Hydro Engineering Centre, Mulhouse, France

Régis Thevenet

Assets Manager, EDF Hydro East Unit, France

Antoine Vermeille

Operating Manager, EDF Hydro East Unit, France

ABSTRACT: At the 16th Rhine river Ministerial Conference on February 13, 2020 in Amsterdam, a new “Rhine 2040” program was adopted. One of the objectives of this program is to complete the restoration of fish continuity between the North Sea and the Schaffhausen falls, a restoration initiated during the Rhine 2020 program with the commissioning of fish passes on Strasbourg and Gerstheim EDF Hydro run-of-river plants.

To do this, two fish passes have been included in the “France Relance Plan” in September 2020 and are in progress: one on Rhinau Hydropower scheme and another one on Marckolsheim Hydropower scheme. These run-of-river hydropower systems each consist of a dam and a diversion canal equipped with shiplocks and a hydro plant. In order to guarantee fish attractiveness, passes are installed downstream of the plant in the tailrace canal and designed to be non-selective with respect to fish species.

The two ‘twin’ fish passes for Rhinau and Marckolsheim sites, designed by EDF engineering teams, in consultation with local NGO’s, the French administration and river foreign stakeholders (Germany, Switzerland), consist of the following structures:

- 8 entrances distributed on the left bank and on the right bank of the tailrace canal, allowing adaptation to river flowrate or level conditions to make the pass as best attractive as possible;
- An attraction flow of 15 m³/s delivered by pumps or turbines depending on the banks;
- A bank-to-bank fish conveying bridge-canal 120 m long allowing fishes to be collected on the right bank;
- A series of basins allowing to pass the plant’s head (12 m) and upstream levee up to the headrace canal.

It should be reminded that EDF had initially proposed to study and implement an innovative solution on Rhinau scheme, based on a fish capture-transport and floating barge system, in order to guarantee the deadline for the restoration of fish farming continuity on the Upper Rhine in 2020. This proposal was ultimately not selected by the Authorities.

Fish pass works at Rhinau Hydropower site started in 2022, with a target completion date of 2025. The provisional timetable for Marckolsheim site is 2022-2026.

These major environmental measures and structures will improve fish migration conditions while adapting to the operating conditions of the Hydropower schemes.

1 PRESENTATION OF THE SYSTEMS OF THE RHINE RIVER

1.1 *The Rhine River*

10 large hydroelectric power plants and 3 ones line Rhine River between Basel and Lauterburg, on almost 185 kilometres of common border between France, Switzerland and Germany.

Built between 1932 and 1977, the system operated by EDF produce an average of more than 7 billion kWh per year, about 20% of EDF's hydropower in France and more than half of the electricity consumption of Alsace (1.8 million inhabitants)

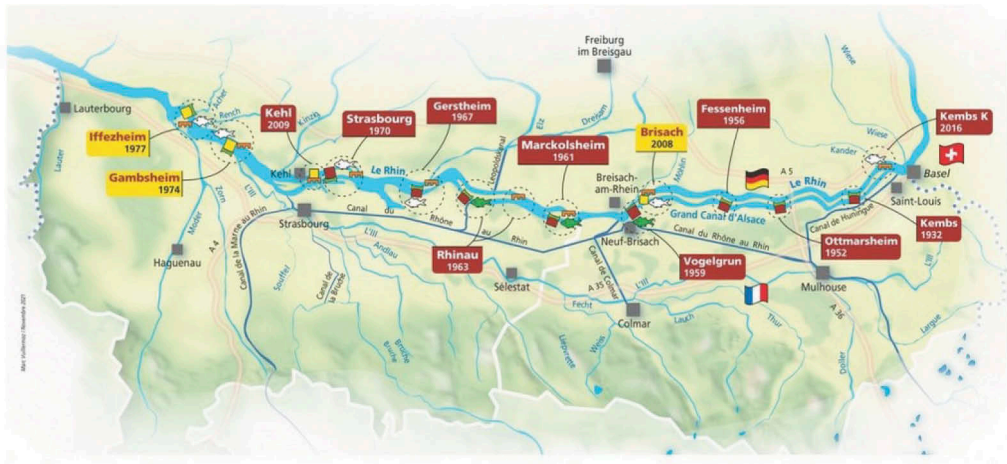


Figure 1. The Rhine River system.

1.2 The different types of systems

Hydroelectric schemes have been built from upstream to downstream. They comprise three main works: a dam, a shiplock consisting of two chambers, and a hydroelectric plant. The headwork of the Rhine River, the Kembs dam, allowed the construction of the Grand Canal d'Alsace (Alsace channel), equipped with 4 hydroelectric power plants and 4 shiplocks. Subsequently, the fittings were carried out in festoons, i.e. with headworks (dam) and a hydroelectric power station accompanied by a lock a few kilometres downstream. From the Gamsheim scheme onwards, the structures have been designed on a same line.

All of these facilities are called “run-of-river”, i.e. they turbine water coming from upstream without storage in a reservoir.

The hydraulic control and monitoring centre (CCSH) in Kembs, supervises the Rhine River's hydroelectric facilities, 24 hours a day, 365 days a year to optimise production according to energy demand. It monitors water levels in the port of Basel's, Ottmarsheim and Strasbourg, the draught of water and air under the bridges, for the needs of navigation. It also contributes to flood management, in coordination with the French and German authorities.

1.3 The system of Rhinau

The Rhinau system, which went into operation in 1963, is the sixth section of the Rhine River development since Basel, and the second hydroelectric power plant built as a bypass on the dyked Rhine River. It consist of a dam, a shiplock consisting of a large and a small chamber, and a hydroelectric powerplant. The latter is equipped with 4 Kaplan turbines. It has a head of 13.2m for an installed capacity of 160MW. Its flow rate capacity is 1400m³/s. In case of stopping of the groups, the flow is released downstream by 4 discharge valves located in the middle of the powerplant.

The dam has 7 passes of 20m width. Each pass is closed by a 9m high radial gate equipped with a flap valve which allows the passage of low flows and floating debries by spilling.

The Rhine River is completely closed off by a dike built across the bed in the extension of the dam.

1.4 The system of Marckolsheim

The layout of Marckolsheim is almost identical to the Rhinau scheme. It was commissioned in 1961 and is the fifth reach in the development of the Rhine River from Basel, and the first hydroelectric



Figure 2. Aerial photo of the Rhinau powerplant and lock (left photo) and Marckolsheim (right photo).

power plant built as a bypass on the dyked Rhine River. The bridge located downstream of the hydroelectric power plant and the shiplock allows road traffic between Germany and France.

2 LOCAL CONTEXT

2.1 *The Rhine River until the 19th century*

Until the 18th century, the Rhine River was the largest and most important salmon-farming river in Europe. In 1815, at the Congress of Vienna, the Rhine River became a navigable waterway to the sea. But the Rhine River's bed constantly meandered in a labyrinth of meanders that changed during floods, over a width of 3km. Also in 1840 to 1876, works to correct the bed of the Rhine River are carried out to concentrate the river into a bed about 250m wide, thanks to two correction dikes called the Tulla dike. This development solves the problem of flooding, but these rectifications are accompanied by a shortening of the Rhine River bed, generating higher current velocities and causing very significant erosion (6 to 7m) which discover rocky bars such as the one at Istein, near Kembs, which became practically impassable in 1930.



Figure 3. Salmon fisherman in the Rhine River, year 1920.

During the construction of the Kembs system, commissioned in 1932, in close proximity of its dam starting the grand canal of Alsace, a fish pass has been built, allowing the crossing of this structure by the Old Rhine (short-circuited section).

Furthermore, since the 19th century, the water of the Rhine River is increasingly polluted by domestic and industrial water, with a peak in the middle of the 20th century.

Thus, in the 1950s, salmon almost completely disappeared from the river.

2.1 *The SANDOZ accident*

Following a fire in a Sandoz AG warehouse on 1 November 1986, extinguishing water with up to thirty tonnes of pesticides flows into the Rhine River, causing the death of fish and other organisms over several hundred kilometres of river.

Following this accident, Ministers in charge of the Rhine River adopted the ambitious “Rhine River Action Program” and entrust the ICPR¹ with its coordination and monitoring of the results. The program plans to reduce by half discharge of 40 hazardous chemicals within ten years. Its objective: to make the Rhine River so clean that salmon can return to live in it.

2.2 ICPR and recovery plan program

In January 2001, the Ministers in charge of the Rhine River adopted the “Rhine 2020” program. In this way, they have defined measurable objectives for ecology, flood protection, water quality and groundwater protection.

The Salmon 2020 program has been incorporated into the Rhine 2020 program, which itself succeeded the “Rhine Action Program” implemented from 1987 to 2000. It has assisted in the construction of four fish passes on the large dams on the Upper Rhine River in Iffezheim (2000), Gamsheim (2006), Strasbourg (2016) and Gerstheim (2019), allowing the river fish passage downstream to Rhinau. The fish passes in Strasbourg and Gerstheim give migratory fish access to the 59 ha of potential (salmon) spawning grounds in the Elz-Dreisam Forest hydrosystem.

The “Rhine 2040” program was adopted in February 2020. This program aims to make the Rhine River a sustainably managed basin, resilient to the impacts of climate change and whose watercourses are valuable living places for nature and people.

In line with the objectives of the previous “Rhine 2020” program, the “Rhine 2040” program defines new ambitious, concrete and measurable objectives for 2040, including the restoration of the ecological continuity of the Rhine River for migratory fish from the mouth to the Rhine Falls, and in particular by the construction of the Rhinau and Marckolsheim fish passes.

The restoration of ecological continuity for fish at the Rhinau and Marckolsheim dams on the Rhine was included in the “France Relance” Plan² dated of the 3 September 2020.

3 THE MOBILE FISH PASS

3.1 Project description

The Rhine 2020 program declines the objectives ecological continuity defined by the ICPR and is reflected in the need to ensure fish migration on French hydroelectric schemes. Considering the deadlines and the costs of constructing migration works on each of the schemes, EDF has proposed a capture-transport solution and floating barge system on the Rhinau powerplant. This solution consisted of recovering the fish downstream of Rhinau and directing them to a capture/sorting station in order to bring them, according to their species, to the most suitable sites for the continuation of their life cycle.

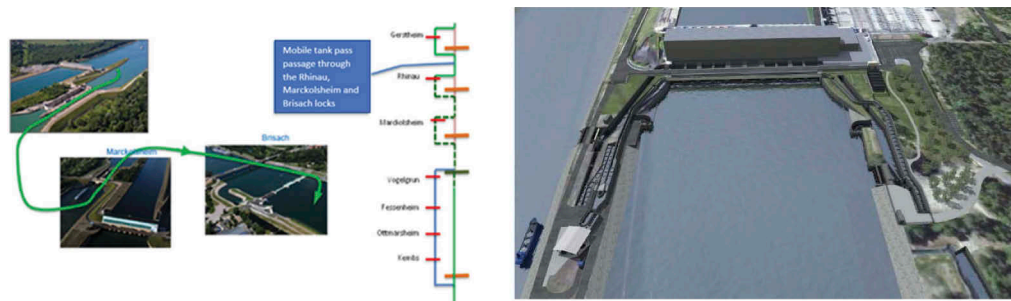


Figure 4. Design of the fish pass: Crossed facilities (left) and architectural view of the project (right).

The transport of fish upstream of the river was designed by waterway. This allowed for a gradual acclimatization of the fish by a permanent renewal of the water, which is not possible with road transport. The distance between the Rhinau power plant and the Old Rhine is about 32km long and has 3 shiplocks. The total travel time there and back is estimated to be between 7 and 11 hours,

4 FISHWAYS OF RHINAU AND MARCKOLSHEIM

4.1 Organization of the project

Following the inclusion of the Rhinau and Marckolsheim fish passes in the France Relance Plan in September 2020, the EDF engineering team immediately took over the design of the fish passes based on the historical mobile fish pass project. This reactivity was necessary to meet the deadlines for the commissioning of fish passes, planned in 2025 for Rhinau and 2026 for Marckolsheim.

In addition, a monitoring committee was set up with the participation of the DREAL Great Eastern, of the French Office for Biodiversity (OFB), the Rhine Meuse Water Agency and the Association Salmon Rhin, to share design progress along the way.

4.2 Project description

4.2.1 Input data and functionality

The upstream structure is designed for the range 500m³/s - 2000m³/s, i.e. between low water and a flow of the order of 2 times the modulus of the river. The target species are Atlantic salmon, sea trout, shad, lamprey, eel, bream, river barb, hotu, and asp.

The structure provides five functions:

- A collection function: the fish in the power plant's return channel will be attracted by the jets from the fish entrances on the bank and above the groups, and this, on the right and left bank;
- A transfer function: given the large size of the structure, seven transfer channels are necessary to collect the fish at the entrance to the hatcheries, bring them to the same counting point (on the right bank) and, by optimising the topographical insertion of the structure, bypass the plant and return to the upstream intake channel;
- A function of elevation: the crossing of the hydroelectric installation (~13 m) will be split (6 m then 7 m) and ensured by four tank passes (one on the left bank, one on the right bank, a transfer pass on the right bank and one upstream);
- A monitoring function: a video counting room will allow the counting of fish and checking the checking of the biological functionality of the structure;
- A capture function: a capture station will be inserted into the structure, upstream of the counting room, to be able, on request, to capture fish for marking purposes (in particular salmon for which the homing phenomenon justifies capture as close as possible to the breeding zones).

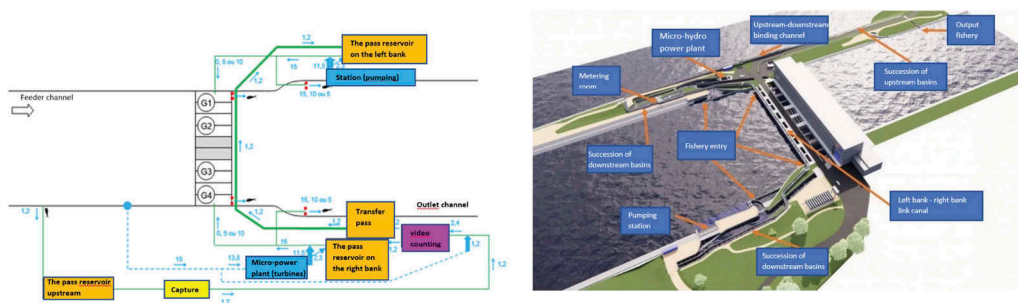


Figure 6. Block diagram of the Rhinau fish pass (left) and architectural view (right).

4.2.2 The case of inlets

As the dominant flows on the system are located in the vicinity of the hydroelectric power-plant, the inlets have been positioned in the tailrace of the plant. Since the attractiveness of the inlets jets does not extend to the other bank, it is necessary to equip both banks

with fish inlets. For a better attractiveness, shore entrances and “group” entrances are planned to ensure maximum attractiveness of the pass, depending on the swimming ability of the fish.

The calibration of the entries was carried out on the basis of in-situ observations, but also thanks to numerical simulations using the Saturn code produced by EDF Research and Development³ and a physical model produced at the EPFL⁴ accompanied by a Flow3D model.

The Saturn model was used to model the propagation of a jet perpendicular to the channel in order to evaluate its range and therefore its potential attractiveness to fish. For a turbinig configuration corresponding to the factory saturation, the simulation shows that the jet is diverted by the recirculations. Its range remains very limited.

Different configurations of bank inlets have been considered. Simulation using the Saturn code showed that inclined configurations were particularly unfavorable as they generate a large recirculation on the bank immediately downstream of the entrance.

The physical model produced at the EPFL enabled the design of the bank entrances to be refined to their final design, parallel to the banks.

4.2.3 Attractive features

Given the width of the tailrace where the inlets are located, the turbulent flows and the presence of the plant’s dischargers in the center of the structure, the attraction flow was chosen at 30m³/s, i.e. 15m³/s per bank, or 2.7% of the Rhine River module

The left bank intake system consists of a lift station with six pumps equipped with downstream control valves to ensure a constant flow rate. The pumped water is then discharged into 2 injection basins comprising rows of dissipators ending in a grid pattern.

The right bank intake system is composed of a micro power with a 1.3 MW Kaplan turbine. This turbine is fed by an upstream hydraulic circuit taking water from the intake canal through an intake equipped with a grid plan and Screen cleaning machine. The turbined intake water discharges into a dissipation basin comprising rows of dissipators and ending in a grid pattern.

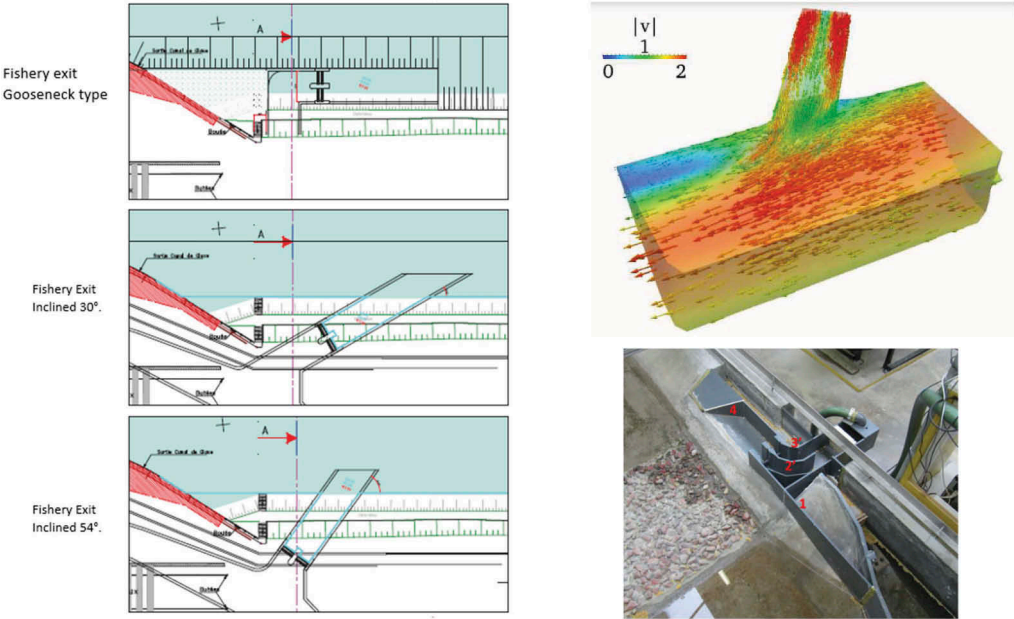


Figure 7. Possible shoreline entrance configurations (left), Saturn code simulation of the flow (right) and photo of the EPFL⁴ physical model (bottom right).

4.3 Operation

Each inlet has 2 gates. Thus, 8 regulating fish gates are installed on this fish pass. These gates will regulate a constant head at the fish entrances on both banks. This height is 25cm +/-5cm if the inflow to the facility is less than 1400m³/s and 30cm +/-5cm if the inflow to the facility is greater than 1400m³/s. In addition, depending on the flow rate of the bank groups, and in order to ensure the best possible visibility of the inlet jet, the inlet gates are regulated to concentrate the attraction flow rather towards the group inlets in case of low flow rate in the main plant (below 200m³/s for the bank group) and to the bank inlets in case of high flow rate in the main plant (above 300m³/s for the bank group). Similarly, if the level in the downstream channel exceeds 160.50mNN, the entire attraction flow is concentrated on the 2 gates of the downstream inlets.

5 THE WORKS

5.1 Schedule

Works on the Rhinau fish pass started in the autumn of 2022; works on the Marckolsheim fish pass began in the spring of 2023.

The stages of realization are as follows: realization of the foundations, execution of civil engineering, installation of the hydromechanical elements and hardware, electrical connection and installation of the automats and finally the commissioning of the works.

5.2 Some figures

For each fish pass, it is planned:

- 30,000m³ of excavated material
- 300t of sheet piling
- 10,000m³ of concrete
- 600t of reinforcement
- 200m of GRP pipe
- 27 valves, 8 of which are fishgates
- 1 turbine of 1.3MW
- 6 pumps of 2.5m³/s
- 1 bridge-channel of 120m length

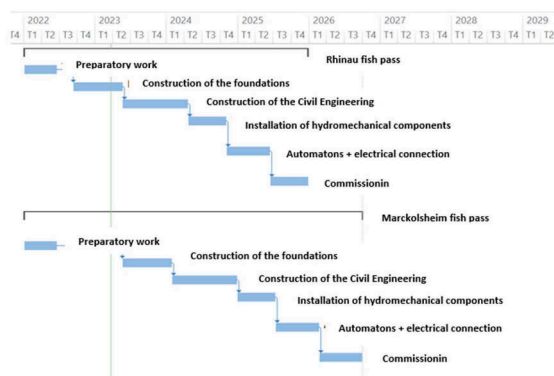


Figure 8. Macro-planning of the Rhinau and Marckolsheim fish passes.

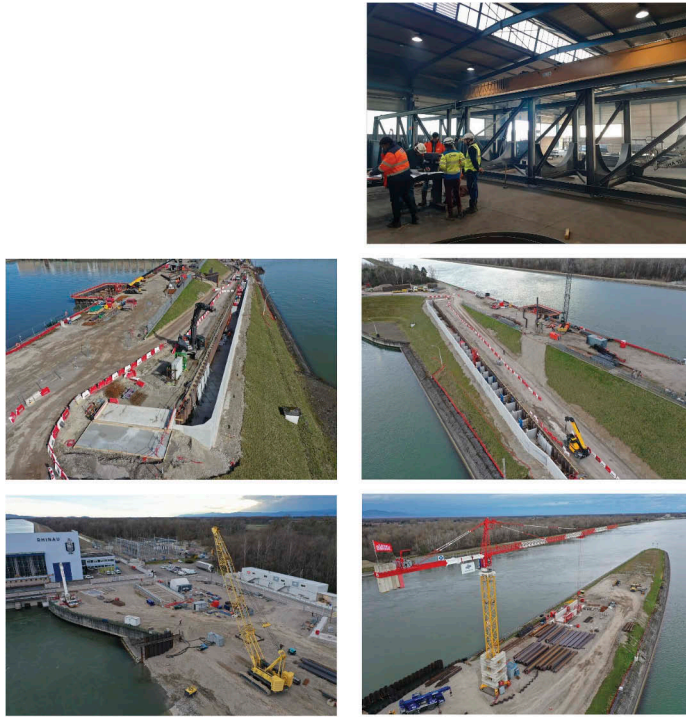


Figure 9. Photos of the construction of the Rhinau fish pass (March 2023). From left to right and from top to bottom: Supporting structure of the canal bridge, upstream pond flight and wastewater intake, upstream pool flight, downstream entrance left bank downstream entrance right bank.

6 CONCLUSION

Fish continuity on the Rhine River has been a strong commitment since the construction of the first hydroelectric systems. The fish passes at Rhinau and Marckolsheim will open up continuity as far as the Old Rhine, and therefore as far as Basel, Switzerland. These large-scale projects demonstrate EDF's expertise in the design, construction and operation of these structures. This is a technical and ambitious project carried out by EDF, initiated by the ICPR and financed by the French recovery plan France Relance.

REFERENCES

- 1 Program: <https://www.iksr.org/fr/>
- 2 Plan de Relance France Relance: <https://www.economie.gouv.fr/plan-de-relance>
- 3 Leroy, A., Bourqui, P., Dumond, L. & De Cesare, G. 2018. Physical and 3D Numerical Simulations of the Flow in the Trailrace of a Hydroelectric Power Plant to Design Fishway Entries. *Advances in Hydroinformatics*: 855–866. Springer, Singapore
- 4 Bourqui, P., Bron, C., De Cesare, G., 2018. Flow measurement for the design optimization of fish pass entries in a run of river hydropower plan. *11th International Symposium on Ultrasonic Doppler Methods for fluid Mechanics et fluid Engineering*, Berlin, Germany

Efficiency evaluation and simulation of sediment bypass tunnel operation: Case study solis reservoir

S. Dahal

Doctoral Researcher, Laboratory of Hydraulics, Hydrology and Glaciology (VAW), ETH Zurich, Switzerland

M.R. Maddahi

Visiting Researcher, Laboratory of Hydraulics, Hydrology and Glaciology (VAW), ETH Zurich, Switzerland
Doctoral Researcher, Department of Water Engineering, Shahid Bahonar University of Kerman, Iran

I. Albayrak

Executive Scientific Collaborator & Lecturer, Laboratory of Hydraulics, Hydrology and Glaciology (VAW), ETH Zurich, Switzerland

F.M. Evers

Senior Research Assistant & Lecturer, Laboratory of Hydraulics, Hydrology and Glaciology (VAW), ETH Zurich, Switzerland

D.F. Vetsch

Group Head & Lecturer, Laboratory of Hydraulics, Hydrology and Glaciology (VAW), ETH Zurich, Switzerland

L. Stern

Operations Manager, Kraftwerke Mittelbünden, ewz, Switzerland

R.M. Boes

Director & Professor, Laboratory of Hydraulics, Hydrology and Glaciology (VAW), ETH Zurich, Switzerland

ABSTRACT: Hydropower is the major source of electricity in Switzerland contributing about 57% (36 TWh/yr) of the total annual generation. Therefore, water storage in hydropower reservoirs is crucial to balance the electricity demand over variable river flow. With the increase in storage demand and climate-related stress it becomes important to sustain the existing reservoir storage capacities. Sedimentation impairs the sustainable operation of reservoirs by reducing the storage volume and may also cause dam safety related issues by the interference of sediment deposits with dam outlets.

Sediment Bypass Tunnels (SBTs) are an effective countermeasure to reduce or even stop sedimentation and contribute to a sustainable use of reservoir storage capacity. This study investigates the performance of an SBT constructed at Solis reservoir in the Swiss Alps, operated by ewz. The SBT was commissioned in 2012 to mitigate continuous propagation of sediment aggradation towards the dam since its construction in 1986. As the inlet of the SBT is located within the reservoir and therefore typically submerged, optimized reservoir operation is required during the intended period of sediment bypassing.

Annual field measurements were conducted to measure the reservoir bathymetry, sediment concentrations, transport rate and sediment particle sizes on the bed to derive the reservoir's sediment balance. The measurements between October 2018 and August 2019 are analyzed to

investigate bypass efficiencies of the SBT. The results indicate that the efficiency of the SBT was 80%, and thus considerably higher than the previous efficiency rate of 17%, due to adaptation of the reservoir operation to a lower water level during SBT operation. This implies that with proper synchronization of SBT and reservoir operation, this type of SBT can be highly efficient.

Furthermore, a 1D numerical model is applied to investigate the processes of sedimentation and sediment management for the Solis reservoir. The data from the field measurements is used to set-up, calibrate and validate the model aiming at investigating the performance of the SBT. The model can reproduce the sedimentation as well as SBT operation in terms of longitudinal bed profile evolution and deposition volume. Moreover, the model also allows for simulating additional scenarios, including e.g. no SBT operation, to compare the effects of different operation modes.

1 INTRODUCTION

Reservoirs worldwide are affected by sedimentation which causes a progressive loss of storage capacity as well as other functional problems (Wisser et al. 2013, Kondolf et al. 2014, Schleiss et al. 2016). The sedimentation rate varies globally depending on the reservoir and catchment characteristics. The global average rate of sedimentation is estimated to be in the range of 0.5 to 1 % (Basson 2009). The impact of reservoir sedimentation becomes more severe as water demand and climate-related stresses increase, while the limited feasible storage sites are already exploited to a large extent (Annandale et al. 2016).

Depending on reservoir size and catchment characteristics, Swiss reservoirs have an infill period in the range between 30 and more than 1000 years (Ehrbar et al. 2018). However, this infill period is rather a theoretical value for the operation of reservoirs. A loss of reservoir functionality may occur much earlier if sediment deposits interfere with the operation of dam outlets (Graf et al. 2010). Although the sedimentation rate in Switzerland is less than the global average, it is an important issue to be dealt with as the dependency on hydropower storage is quite high (Boes et al. 2021a). Therefore, it becomes essential to investigate the sedimentation processes to formulate proper sediment management strategies. However, the lack of monitored sediment management data is a limiting factor for conducting more detailed investigations.

Reservoir sedimentation involves dynamic processes of flow hydraulics, sediment transport and reservoir operation. It is crucial to understand these processes for planning any kind of sediment management strategy. A detailed investigation of the underlying processes is necessary to understand the sedimentation dynamics. This requires field monitoring of sedimentation as well as sediment management actions. Additionally, such processes can also be investigated by using numerical models which represent the governing physical processes in the form of mathematical equations. The main advantage of numerical models is that they allow for simulating complex dynamic processes such as sediment sorting along a reservoir, which are rather difficult to study analytically (Ehrbar et al. 2018, Dahal et al. 2021). However, the main challenge is to have sufficient field data to validate their performance.

Depending on the nature of sedimentation, different types of countermeasures are available (Morris 2020). At catchment scale, measures to reduce erosion and sediment transport can be implemented. At reservoir scale, sedimentation can be minimized by either removal of already deposited sediment or by preventing sediment settlement. Among these alternatives, sediment routing helps to restore the river sediment continuity to a certain extent. This may be achieved by sluicing of sediment laden flow through dam outlets or bypassing through Sediment Bypass Tunnels (SBTs). Japan and Switzerland have effectively implemented SBTs to prevent sedimentation and restore sediment continuity (Kondolf et al. 2014).

The SBT efficiency (ratio of sediment volume bypassed through SBT to incoming sediment volume into the reservoir) depends on many parameters, mainly the inflowing sediment transport rate as well as reservoir and SBT operations (Albayrak et al. 2019). The investigation of SBTs in operation allows for properly understanding the underlying processes and provides the basis for optimizing the operation to enhance bypassing efficiency. However, it is costly and, in many

cases, impractical to investigate the effects of the above-mentioned parameters on SBT efficiencies purely by means of field measurements. Therefore, numerical simulations are helpful tools in such studies, provided sufficient data for model setup and validation are available.

The main goal of this study is to demonstrate an approach for 1D numerical modelling of reservoir sedimentation and SBT operation for the case of the Solis reservoir in Switzerland, based on extensive field measurements. Solis reservoir and SBT operation have been well-monitored (Albayrak et al. 2023) providing useful data required for modelling. The validated numerical model allows for simulating further scenarios which provide the basis for optimizing SBT operation to enhance bypassing efficiency.

2 STUDY SITE

Solis is a reservoir operated by ewz (Municipal Electric Utility of Zurich, Elektrizitätswerk der Stadt Zürich) in the Swiss Alps and is highly affected by sedimentation. The reservoir is located on the Albula river in the Canton of Grisons, Switzerland. The 61 m high arch dam constructed in 1986 created a reservoir with an initial storage capacity of 4 Mm³. As shown in the layout map of Figure 1, it is a narrow reservoir extending about 3 km upstream from the dam. The inflow is supplied by a watershed of approximately 900 km² which includes two more reservoirs on the Julia river tributary. In 2012, an SBT was put into operation as a countermeasure against sedimentation.

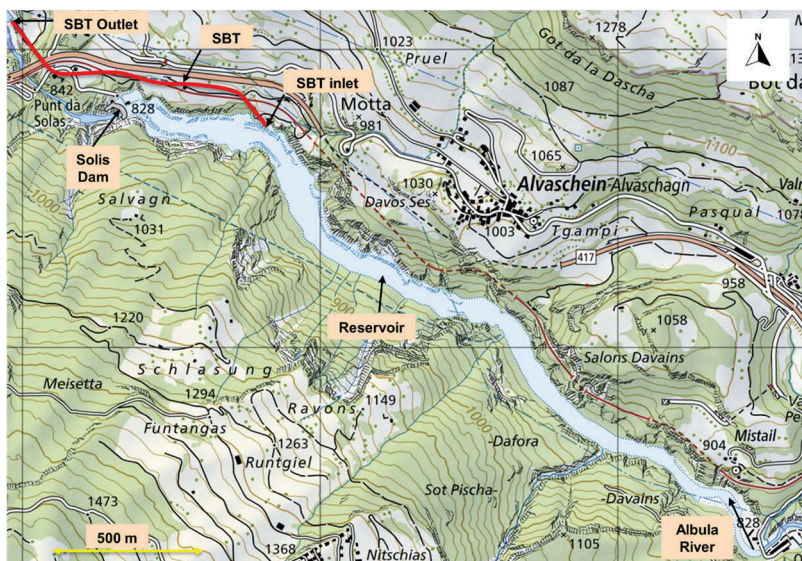


Figure 1. Layout map of Solis reservoir (background map source: Federal Office of Topography).

The Albula river is the main source of supplying sediment to the reservoir. Until 2009, the high rate of sedimentation had caused a reduction of about 50% of the reservoir's storage volume since its construction in 1986 (Auel & Boes 2011). The evolution of the reservoir bed profile over time is shown in Figure 2. As of 2011, the sedimentation delta had advanced close to the dam which not only caused a loss of storage volume but also threatened the safe operation of the dam outlets.

To mitigate the sedimentation problem, an SBT was commissioned in 2012 to divert high sediment loads during flood events (Oertli & Auel 2015). It belongs to the category of "type-B" SBTs which have the inlet at the middle reach of the reservoir (Albayrak et al. 2019, Hager et al. 2020). As the inlet is submerged during normal reservoir operation, the reservoir level should be lowered during the intended period of SBT operation to ensure effective sediment bypassing.

3 METHODS

This study involves the analysis of sedimentation and SBT operation at the Solis reservoir during the period from October 2018 to August 2019. Three main procedures are applied to achieve the objectives of this research: fieldwork, data analysis, and numerical modelling.

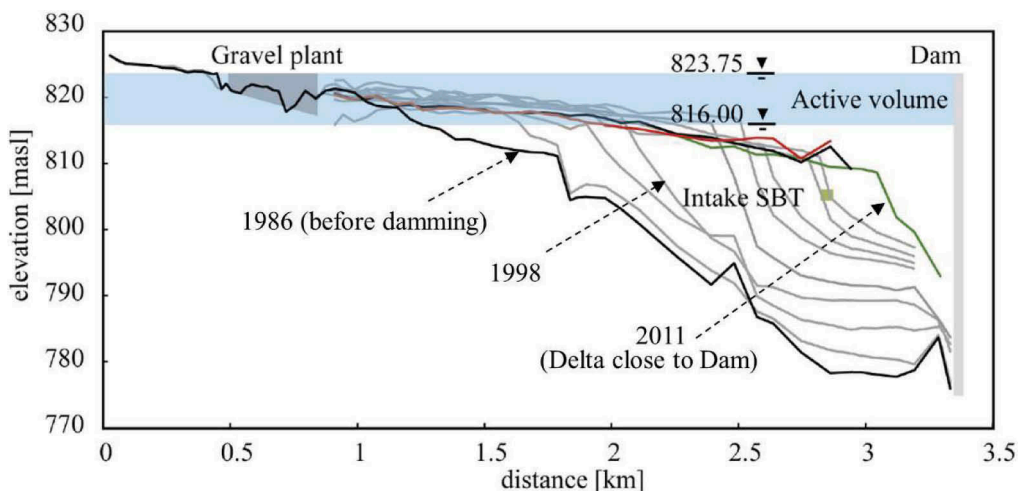


Figure 2. Temporal and spatial evolution of Solis reservoir bed profile, and location of the SBT intake structure; flow from left to right (modified from Müller-Hagmann 2017).

3.1 Fieldwork

Fieldwork campaigns were conducted in October 2018 and August 2019 to measure the reservoir bathymetry and bed sediment parameters (Albayrak et al. 2023). A River Pro 1200 kHz Acoustic Doppler Profiler (ADCP) mounted on a remote-controlled boat (Q-boat) (manufacturer: Teledyne Marine) was used to measure the bathymetry of the reservoir bed. A bed sediment grabber was used to collect bed samples at different locations along the reservoir.

Apart from annual field measurements, continuous monitoring systems were also installed in the SBT for recording the sediment transport (Albayrak et al. 2022). Bedload was monitored indirectly using a Swiss Plate Geophone System (SPGS) (Müller-Hagmann 2017, Müller-Hagmann et al. 2017), and Suspended Sediment Concentration (SSC) was measured using turbidimeters.

3.2 Data analysis

The ADCP raw data are analyzed using WinRiver II and ArcGIS to prepare bathymetry maps for each year. Bathymetry difference maps are prepared to observe the areas of erosion and deposition within the reservoir. The sedimentation volume between two fieldwork campaigns is computed from the bathymetry difference map. Longitudinal bed profiles are plotted to see the evolution of the bed profile due to sedimentation and SBT operation. The analysis of hydraulic conditions within the reservoir is done by using inflow data and reservoir water level time series provided by the operator.

The overall sediment transport in the reservoir is classified into Bedload (*BL*) and Suspended Load (*SL*). There are various locations of inflow sources and outflow sinks as illustrated in Figure 3.

The Albula river is the main source of sediment inflow which carries both *BL* and *SL*. The Julia river does not supply substantial amounts of sediment directly due to trapping in upstream reservoirs. The outflow of the upstream Tiefencastel HPP supplies fine sediment (*SL*) into the Solis reservoir.

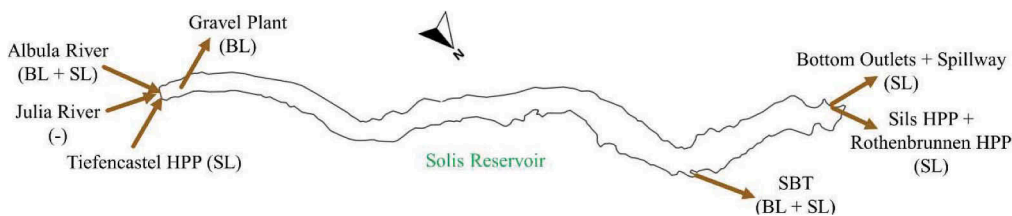


Figure 3. Locations of sediment inflow and outflow in the Solis reservoir; flow from left to right.

The main location of sediment outflow is the SBT which releases both *BL* and *SL* during its operation. A part of fine suspended sediment (*SL*) releases downstream through the dam's low-level outlets, spillway, and the two powerplant intakes of Sils HPP and Rothenbrunnen HPP. A gravel extraction plant is located at the upstream end of the reservoir which takes out some portion of deposited *BL*.

BL supplied by the Albula river is computed with an empirical sediment transport equation to derive similar average values as suggested by literature (Müller-Hagmann 2017). The *BL* extracted from the gravel plant is already accounted for while computing net *BL* inflow from the Albula. A rating curve is available for *SSC* in the Albula river (Albayrak et al. 2023) which is used to derive *SL* inflow into Solis reservoir. There is no data available for *SL* released by the Tiefencastel HPP, so it is assumed to have similar concentrations as that of another monitored powerplant in the same region (Sils HPP) (Müller-Hagmann 2017). The outflowing *BL* through the SBT is based on the monitored SPGS data (Albayrak et al. 2022). Outflowing *SL* through the SBT is also derived from a relation between inflowing *SSC* (from Albula river) and the reservoir water level based on monitored data of SBT operations in 2013 and 2014 (Albayrak et al. 2023). Fine sediment released through dam outlets is computed based on a linear dilution profile of *SSC* along the vertical axis at the dam location (Müller-Hagmann 2017).

The overall sediment balance in the reservoir is analyzed based on the inflow and outflow from various locations. Then the SBT bypass efficiency is evaluated as the ratio of bypassed sediment volume to the inflowing sediment volume.

3.3 Numerical modelling

The dynamic processes of reservoir sedimentation and SBT operation of the Solis reservoir are investigated with 1D numerical modelling. The BASEMENT software is applied for modelling which allows for the numerical simulation of unsteady flow, multiple grain sediment sizes, bedload transport (*BL*), and suspended load transport (*SL*) (Vetsch et al. 2022). The modelling period is from October 2018 to August 2019 which includes SBT operations.

The goal of this numerical simulation is to identify a set of parameters that can reproduce the processes of sedimentation and SBT operation under the given boundary conditions of water and sediment inflow, and reservoir operating water levels. The calibration targets are to match the simulated longitudinal bed profile with the measured profile as well as to match the simulated sedimentation volume with the measured value.

Bathymetry data of October 2018 is processed to derive a geometry input file to model the reservoir. The geometry of Solis reservoir is discretized into 89 cross-sections. The upstream boundary conditions are defined with water, *BL*, and *SL* inflow time series. The downstream boundary is located at the dam which is defined in the model as reservoir water level time series. In addition, one more outflow boundary condition is imposed at the location of the SBT to extract water, *BL*, and *SL*.

The sediment particles are discretized into four fractions to well represent the sediment sorting process. From the available particle size distribution (PSD) of the Albula riverbed materials, the fractions of 6.4 mm and 39.4 mm are taken as coarse materials. For fine sediment particles, a PSD is available from a water sample collected during the flood of June 2019. From this PSD, two fractions of 0.012 mm and 0.055 mm are adopted to represent the suspended particles. These particle sizes are selected by conducting trial simulations to achieve closest match with

measurements. Overall, all these four sediment fractions take part in dynamic sediment transport processes in the model. The inflow SL is derived from the rating curve of the Albula river. The BL inflow is computed using the empirical sediment transport equation of Meyer-Peter & Müller (MPM). The time series of sediment outflow through the SBT is computed from the analysis of monitored data as explained in Section 3.2. The initial bed composition is defined based on the PSD of bed material sampled at different locations along the reservoir.

Finally, the numerical model is applied to numerically simulate the processes of sedimentation and SBT operation. Furthermore, a scenario of no SBT operation is simulated for the same period. The purpose is to visualize how the sedimentation delta would have evolved if the SBT had not been operated. This also gives a comparison of sedimentation volumes with and without SBT operation, which is useful to evaluate the effectiveness of the SBT as a mitigation measure against sedimentation.

4 RESULTS

4.1 Data analysis

Figure 4 shows the 15-minute interval time series of the hydraulic conditions in the reservoir during the period from October 2018 to August 2019. A 5-year flood occurred in June 2019 during which the water level in reservoir was lowered to around 813 masl to operate the SBT. Apart from that, the SBT was in operation a few times in October 2018 and July 2019.

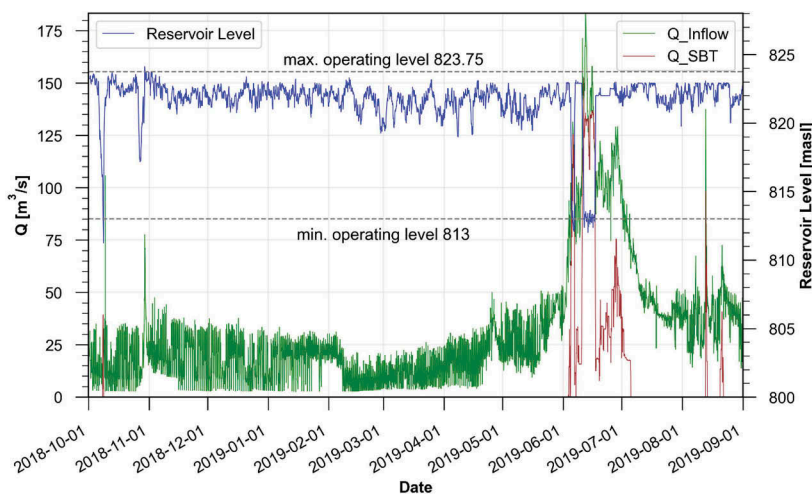


Figure 4. Time series of hydraulic conditions in the reservoir.

Figure 5 shows the erosion/deposition locations along the reservoir at different time intervals, as well as the bathymetry difference from October 2018 to August 2019. The reservoir is divided into three zones: Zone 1 at the upstream end, Zone 2 in the middle reach upstream of the SBT inlet structure, and Zone 3 downstream of the SBT inlet. The deposited sediment volume is computed as $63,414 \text{ m}^3$, while $40,002 \text{ m}^3$ of sediment are eroded. This results in a net deposition of $23,412 \text{ m}^3$. The deposition mainly occurred in Zones 1 and 3, while Zone 2 experienced a large amount of erosion. Deposition in Zone 1 is likely due to settling of coarse particles carried by floods during high reservoir water levels. Erosion in Zone 2 is due to combined effects of sediment diversion through the SBT and high bed shear stress during reservoir lowering. While most of the BL particles were diverted through the SBT, some coarser SL particles might still have travelled downstream of the SBT causing deposition in Zone 3.

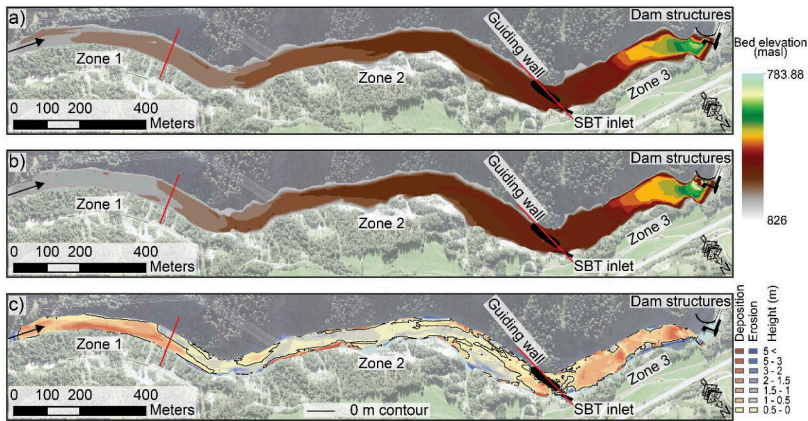


Figure 5. A) Measured bathymetry in October 2018, b) measured bathymetry in August 2019, and c) bathymetry difference map; flow from left to right (source of background map: Federal Office of Topography).

The analytically computed sediment balance volumes based on the methodology given in 3.2 are shown in Table 1. The total sediment inflow is 205,157 m³ and the total outflow is 178,674 m³, of which 163,732 m³ is bypassed through the SBT. The net deposition volume is 26,483 m³ which corresponds closely to the volume given by the bathymetry difference (23,412 m³). This indicates that the approach and assumptions for the computation are reasonable. The ratio of bypassed sediment volume to inflowing sediment volume gives an SBT bypass efficiency of 79.8% which indicates a good performance of the SBT. The high efficiency of SBT operation is mainly achieved by lowering of the reservoir water level to around 813 masl (Figure 4).

Table 1. Sediment balance in the Solis reservoir from October 2018 to August 2019 (analytical approach).

Sediment type	Volumes (m ³)				
	Albula*	Tiefencastel HPP	SBT	Dam outlets	Total
BL inflow	49,273	-	-	-	49,273
SL inflow	151,484	4,400	-	-	155,884
Total inflow	200,757	4,400	-	-	205,157
BL outflow	-	-	34,563	-	34,563
SL outflow	-	-	129,169	14,942	144,111
Total outflow	-	-	163,732	14,942	178,674

*Gravel extraction by gravel plant at the Albula river is already deducted.

4.2 Numerical modelling

The simulated longitudinal bed profile (thalweg) evolution due to sedimentation and SBT operation is shown in Figure 6. The deposition profile downstream of the SBT inlet is closely reproduced by the model (green lines). The deposition volume given by the model is 24,788 m³ and lies between the volume given by bathymetry difference (23,412 m³) and the analytically computed volume (26,483 m³). The inflowing volume of sediment is 205,157 m³ (Table 1), i.e., the net deposition volume is substantially smaller than the inflowing sediment volume. This highlights the good performance of the model in replicating the sediment bypassing process. The sediment balance volumes computed as boundary conditions and results of numerical modelling are shown in Table 2.

The effectiveness of SBT operation is demonstrated by comparing the reservoir bed evolution with the scenario of no SBT operation (red line in Figure 6). In absence of an SBT, the incoming sediment would have migrated downstream of the inlet of the SBT to form a deltaic deposit. The location of this delta is very close to the dam that might threaten the safe operation of the dam outlets. In terms of volumes, the deposition volume without SBT operation would have been 74,652 m³ which is approximately three times the volume with SBT operation (24,788 m³). Thus, this also highlights how effective the implementation of the SBT has been to mitigate the sedimentation in the Solis reservoir.

Table 2. Sediment balance in the Solis reservoir from October 2018 to August 2019 (numerical modelling).

Sediment type	Volumes (m ³)			Total
	Upstream boundary*	SBT	Downstream boundary	
<i>BL</i> inflow (6.4 mm)	43,643	-	-	43,643
<i>BL</i> inflow (39.4 mm)	5,630	-	-	5,630
Total <i>BL</i> inflow	49,273	-	-	49,273
<i>SL</i> inflow (0.012 mm)	116,913	-	-	116,913
<i>SL</i> inflow (0.055 mm)	38,971	-	-	38,971
Total <i>SL</i> inflow	155,884	-	-	155,884
Total inflow	205,157	-	-	205,157
<i>BL</i> outflow (6.4 mm)	-	24,194	-	24,194
<i>BL</i> outflow (39.4 mm)	-	10,369	-	10,369
Total <i>BL</i> outflow	-	34,563	-	34,563
<i>SL</i> outflow (0.012 mm)	-	96,877	**	96,877
<i>SL</i> outflow (0.055 mm)	-	32,292	**	32,292
Total <i>SL</i> outflow	-	129,169	17,425	146,594
Total outflow	-	163,732	17,425	181,157

*Inflow from Albulra river and Tiefencastel HPP including deduction from gravel extraction.

**Only total *SL* volume available.

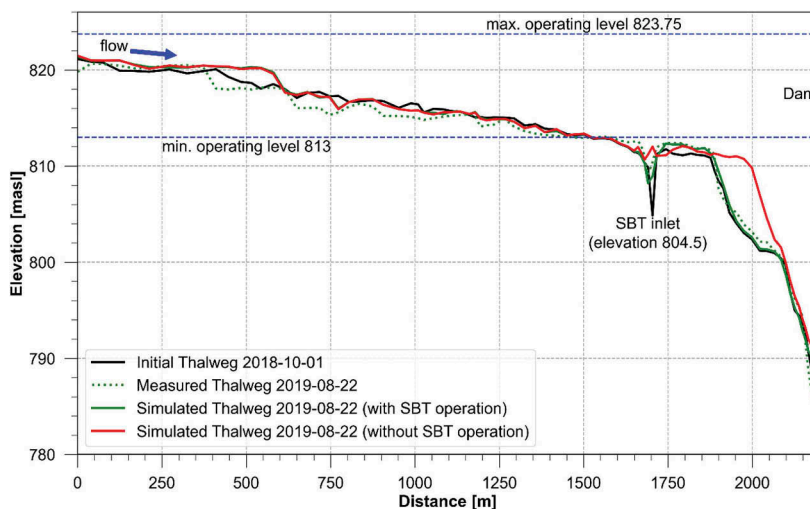


Figure 6. Numerical simulation of longitudinal bed profile (thalweg) evolution due to sedimentation and SBT operation scenarios.

5 DISCUSSION AND CONCLUSION

Bathymetry data and sediment data obtained from the field measurement campaigns are useful to analyze the sedimentation processes and locations as well as sediment-bypassing in the Solis reservoir. We captured the effect of a 5-year flood on the reservoir sedimentation and evaluated the SBT performance during that period. The sediment balance in the reservoir is computed by considering various locations of sediment inflow and outflow by using monitored data and applying justified assumptions for unmonitored values. The ratio of inflow BL (including gravel extraction) to inflow SL is 1:1.94 herein, which is in the range of 1:1 to 1:2 for typical Swiss torrents (Rickenmann 2001, Turowski et al. 2010). This analytical approach is validated by comparing the results with the sedimentation volumes given by bathymetry differences. The deviation is only around 13% which is a reasonably good match for sediment studies.

The bypassing efficiency of the SBT is computed to be 80% which is quite high in contrast with a previous study of Albayrak et al. (2019) for Solis SBT operations before 2018. Referring to the hydraulic conditions, we see that the reservoir was operated at a low level of around 813 masl during SBT operation in the flood of June 2019. This suggests that for a “type-B” SBT with the inlet located within the reservoir, the bypass efficiency can be increased by maintaining low reservoir water levels during the bypass operation. This efficiency is close to the reported efficiencies of “type-A” SBTs in Switzerland (Albayrak et al. 2019, Boes et al. 2021b), which have their inlet at the reservoir head and are less dependent on reservoir water levels during operations. Lowering the reservoir water level during type-B SBT operation facilitates the transport of coarser particles and even mobilizes already deposited sediments towards the SBT inlet. Thus, it is essential to have a synchronous operation of the reservoir and the SBT to achieve optimal performance.

The data available for the Solis reservoir are key to setup the numerical model. The simulation helps to investigate the related physical processes in a more dynamic approach. The developed numerical model can closely reproduce the longitudinal bed profile evolution as well as the associated sediment volumes. The numerical model is most sensitive to the discretization of PSD, which is essential to replicate the sediment sorting phenomena that is usually found in unsteady non-uniform flows within a reservoir. Furthermore, the model provides additional options for simulating different scenarios, such as the scenario of no SBT operation. Without SBT operation the sedimentation delta would have advanced further downstream from the SBT inlet towards the dam. This shows that numerical modelling is a powerful tool for evaluating the performance of sediment management techniques by comparing the magnitude of sedimentation with and without sediment management operation. Overall, numerical modelling provides further opportunities of developing sediment management strategies and testing different scenarios, including climate changes scenarios, to achieve a sustainable use of reservoirs.

REFERENCES

- Albayrak, I., Arnold, R., Yüzügüllü-Demiral, D., Müller-Hagmann, M., & Boes, R. 2022. *Field monitoring of sediment transport, hydraulics and hydroabrasion at Swiss Sediment Bypass Tunnels*. Final report of the research project funded by Swiss Federal Office of Energy (SFOE). <https://www.aramis.admin.ch/Dokument.aspx?DocumentID=69420>.
- Albayrak, I., Maddahi, M., & Boes, R. 2023. *RESEMO, Reservoir sedimentation, management and operation at the case study reservoir Solis*. Final report of the research project funded by Swiss Federal Office of Energy (SFOE). <https://www.aramis.admin.ch/Grunddaten/?ProjectID=41723>.
- Albayrak, I., Müller-Hagmann, M., & Boes, R.M. 2019. Efficiency evaluation of Swiss Sediment Bypass Tunnels. In Proc. 3rd Intl. Workshop on Sediment Bypass Tunnels, Taipei, Taiwan, 239–245.
- Annandale, G.W., Morris, G.L., & Karki, P. 2016. *Extending the life of reservoirs: sustainable sediment management for dams and run-of-river hydropower*. The World Bank.
- Auel, C., & Boes, R.M. 2011. Sediment bypass tunnel design – review and outlook. *Proc. ICOLD Symposium “Dams and reservoirs under changing challenges”* (A.J. Schleiss & R.M. Boes, eds.), 79th Annual Meeting, Lucerne. Taylor & Francis, London: 403–412.

- Basson, G.R. 2009. Management of siltation in existing and new reservoirs. General Report Q. 89. In *Proceedings of the 23rd Congress of the International Commission on Large Dams CIGB-ICOLD*, May 25–29, 2009, Brasilia, Vol. II.
- Boes, R., Hohermuth, B., Giardini, D., Avellan, F., Burlando, P., Evers, F., Farinotti, D., Felix, D., Manso, P., Münch-Aligné, C., Schmid, M., Stähli, M., & Weigt, H. 2021a. *Swiss Potential for Hydro-power Generation and Storage*, Synthesis Report, ETH Zurich. <https://doi.org/10.3929/ethz-b-000517823>.
- Boes, R.M., Baumer, A., Pfeifer, S., Albayrak, I., & Felix, D. 2021b. Techniques to reduce sedimentation in bed load and suspended load dominated reservoirs. In *Proc. 27th Congress of the international commission on large dams (ICOLD)*, June 2021, Marseille, France.
- Dahal, S., Crosato, A., Omer, A.Y., & Lee, A.A. 2021. Validation of Model-Based Optimization of Reservoir Sediment Releases by Dam Removal. *Journal of Water Resources Planning and Management*, 147(7), 04021033 [https://doi.org/10.1061/\(ASCE\)WR.1943-5452.0001388](https://doi.org/10.1061/(ASCE)WR.1943-5452.0001388).
- Ehrbar, D., Schmocker, L., Doering, M., Cortesi, M., Bourban, G., Boes, R.M., & Vetsch, D.F. 2018. Continuous seasonal and large-scale periglacial reservoir sedimentation. *Sustainability*, 10(9), 3265. <https://doi.org/10.3390/su10093265>.
- Graf, W.L., Wohl, E., Sinha, T., & Sabo, J. L. 2010. Sedimentation and sustainability of western American reservoirs. *Water Resources Research*, 46(12). <https://doi.org/10.1029/2009WR008836>.
- Hager, W.H., Schleiss, A.J., Boes, R.M., & Pfister, M. 2020. *Hydraulic Engineering of Dams*. Taylor & Francis, London. <https://doi.org/10.1201/9780203771433>.
- Kondolf, G.M., Gao, Y., Annandale, G.W., Morris, G.L., Jiang, E., Zhang, J., Cao, Y., Carling, P., Fu, K., Guo, Q., Hotchkiss, R., Peteuil, C., Sumi, T., Wang, H., Wang, Z., Wei, Z., Wu, B., Wu, C., & Yang, C.T. 2014. Sustainable sediment management in reservoirs and regulated rivers: Experiences from five continents. *Earth's Future*, 2(5), 256–280. <https://doi.org/10.1002/2013EF000184>.
- Morris, G.L. 2020. Classification of management alternatives to combat reservoir sedimentation. *Water*, 12(3), 861. <https://doi.org/10.3390/w12030861>.
- Müller-Hagmann, M. 2017. Hydroabrasion in high speed flow at sediment bypass tunnels. *VAW-Mitteilung 239* (R. Boes, ed.) and Doctoral dissertation no. 24291, ETH Zurich.
- Müller-Hagmann, M., Albayrak, I., & Boes, R. M. 2017. Field calibration of bedload monitoring system in a sediment bypass tunnel: Swiss plate geophone. *Proceedings of the 37th IAHR World Congress*, Kuala Lumpur, Malaysia, 995–1004.
- Oertli C., & Auel, C. 2015. Solis sediment bypass tunnel: First operation experiences. In *Proc. First International Workshop on Sediment Bypass Tunnels*, VAW-Mitteilung 232 (R. Boes, ed.), Laboratory of Hydraulics, Hydrology and Glaciology (VAW), ETH Zürich, Switzerland, pp. 223–233.
- Rickenmann, D. 2001. Comparison of bed load transport in torrents and gravel bed streams. *Water Resources Research* 37(12): 3295–3305. <https://doi.org/10.1029/2001WR000319>.
- Schleiss, A.J., Franca, M.J., Juez, C., & De Cesare, G. 2016. Reservoir sedimentation. *Journal of Hydraulic Research*, 54(6), 595–614. <https://doi.org/10.1080/00221686.2016.1225320>.
- Turowski, J.M., Rickenmann, D., & Dadson, S.J. 2010. The partitioning of the total sediment load of a river into suspended load and bedload: A review of empirical data. *Sedimentology* 57, 1126–1146. <https://doi.org/10.1111/j.1365-3091.2009.01140.x>.
- Vetsch, D., Siviglia, A., Bürgler, M., Caponi, F., Ehrbar, D., Facchini, M., Faeh, R., Farshi, D., Gerber, M., Gerke, E., Kammerer, S., Koch, A., Mueller, R., Peter, S., Rousselot, P., Vanzo, D., Veprek, R., Volz, C., Vonwiller, L., & Weberndorfer, M. 2022. *System Manuals of BASEMENT*, Version 2.8.2, Laboratory of Hydraulics, Hydrology and Glaciology (VAW), ETH Zürich, Switzerland. Available from <http://www.basement.ethz.ch>. [Accessed on 03.03.2023].
- Wisser, D., Frolking, S., Hagen, S., & Bierkens, M. F. 2013. Beyond peak reservoir storage? A global estimate of declining water storage capacity in large reservoirs. *Water Resources Research*, 49 (9), 5732–5739. <https://doi.org/10.1002/wrcr.20452>.

Reduction of riverbed clogging related to sediment flushing

R. Dubuis & G. De Cesare

Platform of Hydraulic Constructions LCH, ENAC, École Polytechnique Fédérale de Lausanne, Lausanne, Switzerland

ABSTRACT: The ecological effects of dams on sediment and river flow have been subject to an increasing attention, leading to the implementation of mitigation measures such as environmental flow release and sediment replenishment. However, fine sediment dynamics have been subject to less attention. To prevent fine sediment accumulation and maintain reservoir capacity, dam operators conduct sediment flushing operations that can release a significant amount of sediment into the downstream river, potentially damaging the ecosystem and clogging the riverbed. These flushing operations raise questions about their frequency, magnitude, and duration in order to minimize losses to the dam operator while ensuring that the downstream river maintains or improves its ecological services. From a clogging perspective, research is needed to investigate the various options available and their effects on fine sediment dynamics. In this study, the influence of a sediment flushing event on the clogging of riverbeds is analyzed using flume experiments, with a focus on the mobilization of the substrate and the conditions during the falling limb of the hydrograph. Four different scenarios have been tested using silt size sediment in suspension flowing over a bed composed of sand and gravel ranging between 0.1 and 8 mm. Scenarios are characterized by different durations of mobilization phase and falling limb, with different decrease of the suspended sediment concentration during this last phase. The experimental setup allows for the measurement of the permeability of the bed, associated with the presence of an infiltration flow, as well as the vertical distribution of silt in the bed. It appears that the mobilization of the substrate limits the effect of fine sediment on the permeability of the riverbed, although deposition is still taking place. At the end of each flushing event, the permeability was lower in the absence of mobilization. However, mobilization promotes the deposition of fine sediment below the active layer, where fine sediment forms a dense layer. The duration and concentration are key variables to limit the clogging of the substrate below the bed mobilization threshold. When the concentration and flow conditions decrease faster, a smaller reduction of the permeability is observed. Finally, a scenario characterized by low flow conditions followed by the mobilization of the substrate to declog the bed showed a limited impact of the fine sediment deposition while reducing the water volume of the flushing event. This research, although limited to some specific cases, shows that the design of sediment flushing events has an influence on the clogging of the riverbed. The deposition of silt under mobilized bed conditions reveals different results in comparison with a static bed. More research is however needed to take into account the large variety of situations that can arise in riverbeds.

1 INTRODUCTION

The deposition and accumulation of fine sediment (particles < 2 mm) in the riverbed is a natural component of river system, which results in the clogging of the substrate and limits the exchanges between the surface flow and the hyporheic layer (Dubuis and De Cesare, 2023). In excessive quantity, fine sediment has a negative impact on the benthic fauna, for instance by reducing oxygen exchange with the hyporheic zone needed for fish eggs and benthos.

Reservoirs along rivers alter the transport of sediment by interrupting bedload and suspended load fluxes. To limit the impact of sediment deposition on the storage capacity of reservoirs and on dam safety, regular sediment flushing operations are performed which release large quantities of suspended particles like silt and clay (Kondolf et al., 2014) and can lead to a significant impact on the ecosystem (Ramezani et al., 2014). Clean water flushing operations are also performed to give more dynamics to the river, combined with sediment replenishment measures that improve the habitat conditions for fish and benthos (Batalla and Vericat, 2009; Loire et al., 2019; Schroff et al., 2021). The impact of sediment flushing events on the aquatic fauna has been subject to multiple studies, including recent research like Espa et al., (2019), Folegot et al., (2021) or Panthi et al., (2022). In these studies, the deposition of fine sediment and clogging of the riverbed is only marginally treated even though the effect of clogging as a general aspect is always mentioned. Part of fine sediment deposits in pools and low flow areas in the form of surface clogging, which can be easily eroded in subsequent events (Legout et al., 2018). Some fine sediment can also deposit in the substrate with long term negative effects on hyporheic exchanges. Mobilizing the substrate releases fine sediment trapped in the riverbed. It is therefore relevant to understand the clogging and declogging processes under variable flow conditions. Only very few studies cover fine sediment exchanges between the surface flow (bedload, suspended load) and the riverbed under variable flow conditions. In the laboratory, only the experiments conducted by Schälchli, (1993) document the influence of declogging on the permeability of the riverbed. Changes in the morphology of the riverbed are important in the removal of fine sediment (Diplas, 1994; Frostick et al., 1984), since they allow for the mobilization of entire layers of the substrate filled with fine sediment. The evolution of the permeability during flood events with important suspended load has not been documented so far, nor the influence of concentration and flow conditions on the clogging of the riverbed during sediment flushing.

Given the large variety of river morphology and sediment characteristics, investigating different situations that can be met along rivers would allow for a better understanding of the clogging process in such variable flow conditions. The experiments carried out in this study will focus on the deposition of silt in the case of partial mobilization of the substrate, with a ratio of fine sediment to substrate particle diameter allowing for inner clogging near the surface of the riverbed. To show the impact of different flushing events on fine sediment deposition, we tested the hypothesis that the falling limb of sediment flushing operation is critical regarding the possible clogging of the riverbed, as well as the impact of bed mobilization on the permeability of the riverbed. Four main scenarios have been tested. They correspond to different discharge scenarios that could be implemented for sediment flushing operations, or to different situations that can arise along a river during a flood.

2 THEORETICAL BACKGROUND

Fine sediment in suspension deposits depending on the local flow conditions, the characteristics of the substrate and the river morphology. The accumulation of fine sediment, promoted by hyporheic flow and seepage flow, can result in the reduction of the permeability of a layer of the bed, either on the surface or within the substrate.

Declogging, i.e. the removal and resuspension of fine sediment from the riverbed, needs high flow shear stresses to either allow for surface clogging to be eroded or allow for the mobilization of the substrate to resuspend fine sediment trapped in the pores of the riverbed. Schälchli (1993) identified two shear stress thresholds for declogging, a first one when the riverbed starts to be mobilized and a second one when reaching the complete mobilization of the substrate. It can be hypothesized that the clogging process has a stronger impact on the permeability when the flow conditions do not allow for the mobilization of the riverbed, but no studies document this behavior. In such a case, the falling limb of flood and sediment flushing hydrographs would be critical for the clogging of the riverbed resulting from the sediment flushing event.

In the field, the efficiency of clean water flushing to reduce the clogging of riverbed downstream of reservoirs shows variable results (Loire et al., 2019; Mürle et al., 2003). Also, pre-existing conditions are critical in the success of flushing flow (Antoine et al., 2020).

3 METHOD AND EXPERIMENTAL SETUP

3.1 Experimental setup

Four experiments were carried out in a recirculating flume at the Platform of Hydraulic Constructions at EPFL (Figure 1). The channel was 6.25 m long and 15 cm wide, with a 33 cm thick substrate bed and a false bottom to set an infiltration flow across the substrate. The substrate had a longitudinal target slope of 0.9 %. The infiltration flow, set with the outside weir, allows for the determination of the permeability of the substrate and its evolution with time. It is also responsible for an important part of the deposition of fine sediment and clogging of the substrate. The flume is equipped with a pump that can deliver a discharge up to 6 L/s. The concentration of fine sediment is measured at both ends of the flume using two turbidimeters, calibrated for silt used in the experiments. The surface flow, infiltration flow and water level in two locations along the flume were measured continuously. 10 piezometers placed in the same two locations in the substrate allow for the visual measurement of head loss in the substrate at regular intervals. Fine sediment in suspension, with a grain-size distribution ranging mainly between 1 and 63 μm (Figure 1), was fed directly into the main tank at predetermined time. Coarser sediment corresponding to the grain size of the substrate (Figure 1), transported as bedload in sliding or saltation mode, was fed with a vibrating box placed upstream of the flume when the riverbed was mobilized (Figure 1). Transported coarse sediment was collected in a bucket at the end of the flume. The fine sediment grain-size was chosen to obtain inner clogging in the subsurface of the substrate, with $d_{85,f} = 36 \mu\text{m} > d_{15,s}/15.4 = 32 \mu\text{m}$ (Gibson et al., 2010).

The slope has been designed to obtain the start of the substrate mobilization at about 3.5 L/s, corresponding to a theoretical dimensionless shear stress of 0.045 ($d_m = 3.4 \text{ mm}$). The feed rate was adapted in function of the discharge, and adjusted to maintain the initial level of the substrate. At full discharge (around 6 L/s), all grain sizes were mobilized, but no general movement of the surface layer was observed.

3.2 Scenarios

Four scenarios have been tested (Table 1), with different mobilization phases and falling limbs, and a similar initial percolation gradient i . All scenarios took place over 8.5 hours and reproduced a controlled flood. They were characterized by a fast increase of the discharge from the base flow up to a given maximum discharge, which is kept between 1 and 2 hours, followed by a longer falling limb with different decrease rates until it reached the initial discharge. The concentration was increased up to the peak concentration of 2 g/L during the rising limb, and kept approximately constant over 2 hours. After that point, no more fine sediment was added and concentration slowly decreased due to deposition or change of the water in the system.

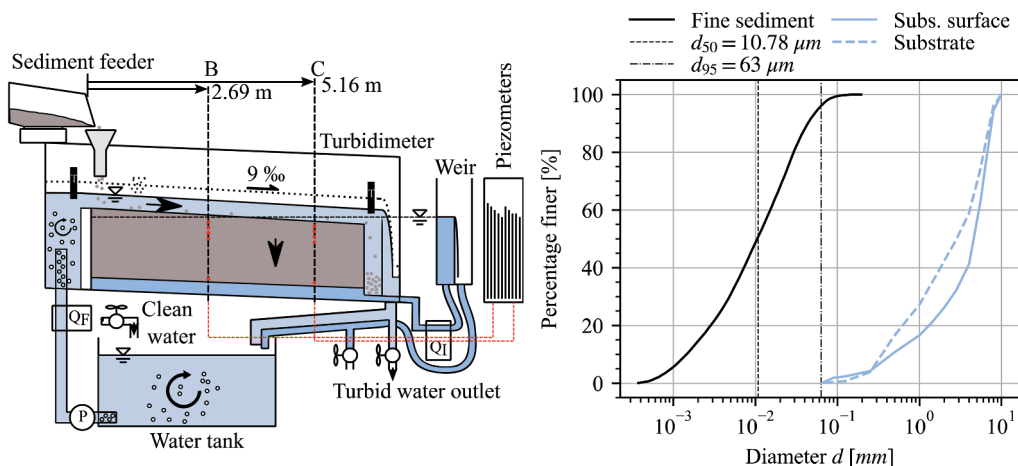


Figure 1. Experimental setup (left), substrate and fine sediment characteristics (right).

Table 1. Summary of the 4 different scenarios tested with the experimental setup.

Scen.	High flow phase	Falling limb	Initial i [%]
a	Mobilized 1h	Long	7.4
b	Mobilized 2h	Short	8.9
c	Static with 2h peak	Long	6.5
d	Short mob. after 2h	Short	7.6

The base scenario (a) consisted in a mobilized substrate over 1 hour followed by a slow decrease of the shear stress and discharge. The second scenario (b) exhibited a longer time at the highest shear stress (2 hours), followed by a faster decrease. The concentration was also artificially decreased during the falling limb (see Section 3.3 and Figure 2). The third scenario (c) consisted in a non-mobilizing flood with a peak discharge lasting 2 hours and a slow decrease of the discharge over a similar duration as scenario (a), without possible declogging. Scenario (d) had the same first phase as scenario (c). However, a declogging event followed the first phase, with the mobilization of the substrate, obtained by increasing the discharge at a similar level as (a). Discharge and concentration decreased similarly to scenario (b). In this scenario, a smaller water volume flowed over the riverbed than in scenario (b).

3.3 Protocol

Each experiment followed a similar protocol. After setting the weir level to obtain a pre-determined initial infiltration discharge, the flow was gradually increased according to each scenario. Fine sediment was added in the main tank to reach the maximum concentration when the top discharge was reached. The percolation gradient was set constant between the surface flow and the weir level, instead of the bottom of the substrate layer, which led to an increase of the percolation gradient with the decrease of bed permeability. The global permeability of the substrate was calculated using the surface-averaged percolation gradient, considering the piezometer measurements and a theoretical surface flow level from a fitted backwater curve model.

Concentration change in experiments (a) and (c) was driven by the deposition rate. In experiments (b) and (d), the concentration was “artificially” reduced by adding clear water to the system (about 8 L/min) while evacuating the same amount of the system at the outlet of the flume. This concentration reduction was started at the end of the peak discharge phase.

At the end of each experiment, substrate samples were collected to analyze the vertical distribution of fine sediment in the substrate. They were only collected in position B (Figure 1), near the center of the flume. Six layers with a thickness ranging between about 10 and 25 mm were collected. Fine sediment was separated from the substrate and both fractions weighted.

4 RESULTS

The concentration, dimensionless shear stress, infiltration discharge and percolation gradient over time are presented in Figure 2, corresponding to the scenarios presented in Table 1. The permeability reduction (Figure 3) resulting from the clogging process starts in all scenarios with a slow initial reduction of the permeability, and an acceleration of the process until permeability reaches a minimum value. Relative to the initial permeability, all experiments except (c) show a very low reduction of the permeability at the end of the mobilization phase. Mobilization was observed for dimensionless shear stress $\theta > 0.046$, which corresponds approximately to the critical shear stress as defined in Shield’s diagram. The permeability appears to decrease in all scenarios as soon as fine sediment is available in the surface flow, regardless of the mobilization of the substrate. This can be explained by the presence of an infiltration flow that filters suspended sediment through the substrate. The reduction is however much slower in the presence of substrate mobilization. This can be explained by the deposition in a more diffused way in comparison to the scenario without mobilization. High shear stresses and the mobilization of the substrate impede the creation of a dense layer of fine sediment near the surface of the substrate, typical in the absence of substrate mobilization.

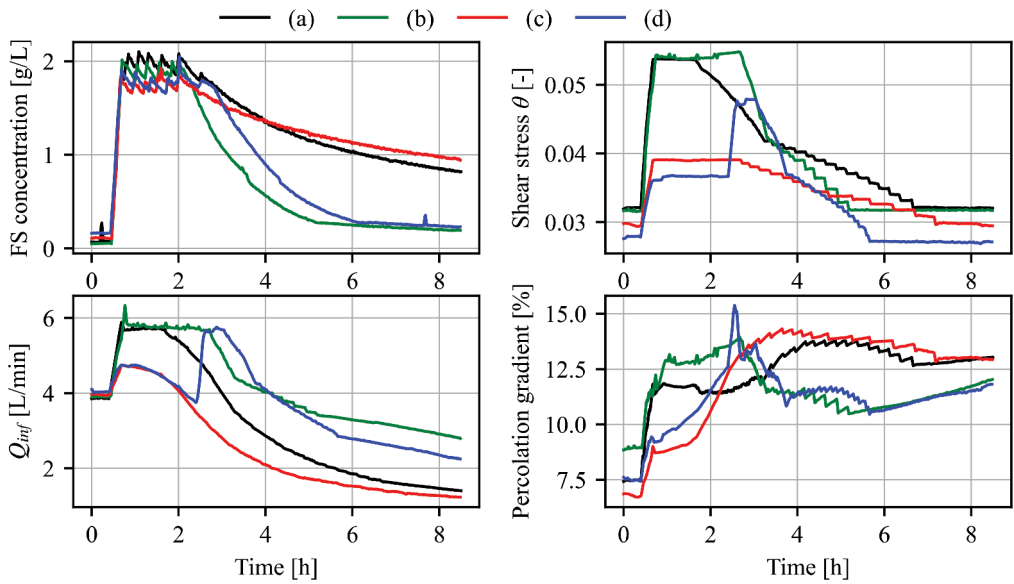


Figure 2. Measured suspended sediment concentration, dimensionless shear stress ($d_m=3.4$ mm), infiltration discharge and percolation gradient as a function of time for all four scenarios.

When looking at the evolution of the permeability with time, all scenarios show very different results (Figure 3, left). Experiment (a) resulted in a faster clogging than the other experiments with mobilization and a strong clogging of the substrate at the end of the experiment. Expressed as a function of deposited fine sediment m_k , the evolution of the permeability (Figure 3, right) shows that experiment (a) evolved in a similar way as experiment (b) and (d) for an equal deposited quantity. Scenario (b) shows a moderate reduction of the permeability at the end of the experiment (45 %), which can be attributed to the lower quantity of fine sediment accumulated due to the “artificial” decrease of the concentration but also to the mobilized substrate.

Scenarios (c) and (d) show similar initial reduction of the permeability, linked to similar flow conditions and fine sediment concentrations. The two curves diverge as soon as the substrate is mobilized in experiment (d), which release fine sediment into the surface flow. Scenarios (c) and (d) show similar initial reduction of the permeability, linked to similar flow conditions and fine sediment concentrations. The two curves diverge as soon as the substrate is mobilized in experiment (d), which release fine sediment into the surface flow. Based on the change of concentration, it is estimated that about 18 to 26 % of deposited fine sediment, concentrated near the surface, was eroded during the declogging event, which resulted in an increase of the permeability from 55 % to 82 % of its initial value. After declogging, permeability reaches values equal or

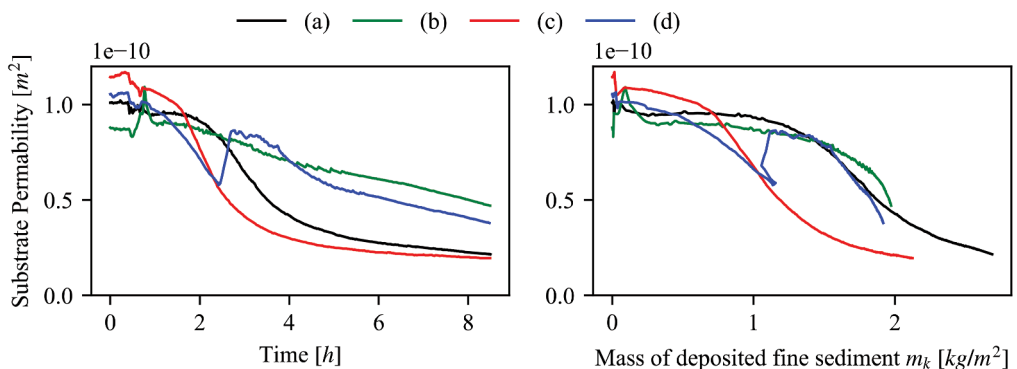


Figure 3. Evolution of the permeability with time and deposited mass of fine sediment for all 4 scenarios.

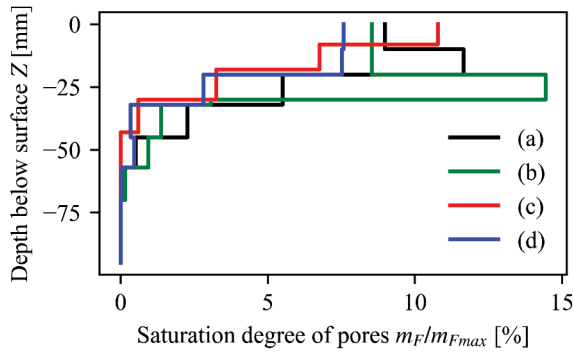


Figure 4. Vertical distribution profiles of the fine sediment in the substrate, expressed as the proportion of the mass of fine sediment m_F to the maximum mass m_{Fmax} that can enter the pore volume.

larger than the one for scenarios (a) and (b). However, a stronger reduction of the permeability is observed in the falling limb of experiment (d). The decrease of the permeability despite low fine sediment deposition at the end of experiment (b) and (d) may be explained by the rearrangement of fine sediment in the substrate into denser layers of fine sediment, due to the high percolation gradient present in the clogged layer and a reduced availability of fine sediment. This means that during the falling limb, when mobilization was stopped, the amount of fine sediment available in the surface flow was not sufficient to create a dense clogged layer near the surface of the substrate in a similar way to the other experiments.

To consolidate the previous analysis, it is interesting to look at the vertical distribution profiles of fine sediment in the substrate at the end of the experiments (Figure 4). Vertical distribution profiles (a) and (b) show a reduced amount of fine sediment near the surface, on the top layer, in contrast with experiment (c) where the maximum is clearly reached at the top layer. The higher fraction of fine sediment below the first layer is first due to the fact that fine sediment can hardly deposit in a mobilized layer. Kinetic sieving (Dudill et al., 2017) can also take place in the mobilized layer, with finer particle (silt and sand) settling below coarser particles at the end of the mobilization phase. The result of scenario (c) corresponds to vertical distribution profiles observed in experiments without mobilization (Dubuis and De Cesare, 2022). Experiment (d) exhibits a distribution situated in between experiments with and without mobilization, possibly due to the refill of the top layer during the falling limb. Under mobilized substrate, clogging seems to take place deeper in the substrate where grains are not mobilized. It is also possible that the observed increase of the substrate level due to an imbalance between the transport capacity and the feed rate reinforce that effect.

5 DISCUSSIONS

The different scenarios analyzed in this set of experiments can be seen as different controls of sediment flushing events. Two criteria have been observed to increase the clogging of the substrate. First, the absence of substrate mobilization results in the formation of a clogged layer close to the surface that reduces substantially the permeability and exchange between the surface flow and the hyporheic layer. Secondly, the quantity of fine sediment available for deposition after the end of the riverbed mobilization, i.e. the concentration of suspended sediment or their duration over which suspended sediment takes place, has an influence on the reduction of permeability. The longer and the higher the concentration of fine sediment stays, the stronger the reduction of permeability is. In the presence of an infiltration flow, deposition of fine sediment takes place regardless of the presence of substrate mobilization, but mobilization increases the clogging depth. In practical terms, the results of these experiments show that, in the presence of infiltration flow, mobilization of the substrate followed by a long falling limb with high fine sediment concentration can induce a clogging of the riverbed that combines both a deep

intrusion of fine sediment and a low permeability of the substrate. To this regard, a flood event in the absence of mobilization can be more favorable, since clogging close to the surface is more easily removed by a subsequent mobilization event (Evans and Wilcox, 2013).

If the concentration can be managed over time, reducing the concentration when flow conditions are unable to mobilize the riverbed can be beneficial to avoid a significant reduction of the permeability. The combination of clogging without mobilization of the substrate followed by a mobilization that allows at least a partial declogging of the substrate may offer the best solution. In this case, clogging only takes place near the surface of the substrate, it is directly followed by declogging, and a smaller quantity of water is used. However, the mobilization tested in experiment (d) was not sufficient to result in the resuspension of an important part of deposited fine sediment and therefore resulted in a limited declogging. In such a scenario, it is important to avoid large quantities of fine sediment during the falling limb to prevent a new clogging phase with an important reduction of the permeability that would cancel the benefits of the declogging event. These observations apply only to places where inner clogging takes place, in combination with downwelling. The large variety of morphologies with different mobilization thresholds and flow conditions present in rivers should not be neglected. Also, riverbed mobilization below dams should be combined with sediment replenishment measures or sediment bypass to avoid the erosion and coarsening of the riverbed (Kondolf et al., 2014). In the presence of surface clogging, increasing the shear velocity with time with an artificial shape similar to experiment (d) (hydrograph opposite to natural flood curves) could also present benefits, and could be tested in future experiments. The slow increase of the flow would allow, in a first phase, for the resuspension of fine sediment on top of the substrate, before the declogging of the substrate by mobilization at the end of the flushing event once the surface layer is washed off.

No reduction of the deposition rate was observed during the substrate mobilization phase. However, this should be further analyzed since the important infiltration flow may have reduced some effects which hinders deposition, and that could be observed in the presence of substrate mobilization. The flux of water in the substrate due to turbulence and advective pumping (Fries and Taghon, 2010; Mooneyham and Strom, 2018) may play a more important role in the deposition and resuspension of fine sediment in the absence of infiltration flow.

Finally, small changes in the substrate surface level have been observed in most experiments due to the accumulation or erosion of substrate material. This can have a substantial effect on the clogging of the riverbed. In the case of an aggradation of the riverbed (as typically observed in this set of experiments), fine sediment deposited on the previous surface layer cannot be resuspended. On the other hand, an erosion of the substrate leads to the resuspension of all fine sediment that clogs eroded layers of the substrate.

6 CONCLUSION

This study explores how the clogging process can take place over various sediment flushing event scenarios. The experiments conducted in this research revealed that clogging can also take place in the presence of substrate mobilization, especially when combined with an infiltration flow. In that case, the deposition of fine sediment differs from clogging under non-mobilizing conditions, with a deeper penetration and a more limited impact on the overall permeability of the substrate. The falling limb is critical with regard to the quantity of fine sediment that can deposit in the previously mobilized layer. Mobilization events over a clogged riverbed allows for the resuspension of part of the fine sediment accumulated near the bed surface. The clogging of riverbed areas with flow conditions that do not allow for surface clogging can therefore be limited depending on flow and concentration conditions over time. However, fine sediment can also affect spawning areas that might be less prone to surface clogging, but where inner clogging can still have consequences. More research is needed to explore the diversity of situations that can take place in the field, with different degrees of mobilization, grain-size effects, and how the clogging process evolves over multiple events of mobilization.

REFERENCES

- Antoine, G., Camenen, B., Jodeau, M., Némery, J., Esteves, M., 2020. Downstream erosion and deposition dynamics of fine suspended sediments due to dam flushing. *J. Hydrol.* 585. <https://doi.org/10.1016/j.jhydrol.2020.124763>
- Batalla, R.J., Vericat, D., 2009. Hydrological and sediment transport dynamics of flushing flows: implications for management in large Mediterranean Rivers. *River Res. Appl.* 25, 297–314. <https://doi.org/10.1002/rra.1160>
- Diplas, P., 1994. Modelling of fine and coarse sediment interaction over alternate bars. *J. Hydrol.* 159, 335–351. [https://doi.org/10.1016/0022-1694\(94\)90265-8](https://doi.org/10.1016/0022-1694(94)90265-8)
- Dubuis, R., De Cesare, G., 2023. The clogging of riverbeds: A review of the physical processes. *Earth-Sci. Rev.* 239, 104374. <https://doi.org/10.1016/j.earscirev.2023.104374>
- Dubuis, R., De Cesare, G., 2022. Influence of Vertical Fluxes on the Clogging of Riverbed by Fine Sediment, in: *39th IAHR World Congress, IAHR*. Granada, pp. 659–666. <https://doi.org/doi:10.3850/IAHR-39WC2521711920221145>
- Dudill, A., Frey, P., Church, M., 2017. Infiltration of fine sediment into a coarse mobile bed: a phenomenological study. *Earth Surf. Process. Landf.* 42, 1171–1185. <https://doi.org/10.1002/esp.4080>
- Espa, P., Batalla, R.J., Brignoli, M.L., Crosa, G., Gentili, G., Quadroni, S., 2019. Tackling reservoir siltation by controlled sediment flushing: Impact on downstream fauna and related management issues. *PLoS ONE* 14, e0218822. <https://doi.org/10.1371/journal.pone.0218822>
- Evans, E., Wilcox, A.C., 2013. Fine Sediment Infiltration Dynamics in a Gravel-Bed River Following a Sediment Pulse. *River Res. Appl.* 30, 372–384. <https://doi.org/10.1002/rra.2647>
- Folegot, S., Bruno, M.C., Larsen, S., Kaffas, K., Pisaturo, G.R., Andreoli, A., Comiti, F., Maurizio, R., 2021. The effects of a sediment flushing on Alpine macroinvertebrate communities. *Hydrobiologia* 848, 3921–3941. <https://doi.org/10.1007/s10750-021-04608-8>
- Fries, J.S., Taghon, G.L., 2010. Particle Fluxes into Permeable Sediments: Comparison of Mechanisms Mediating Deposition. *J. Hydraul. Eng.* 136, 214–221. [https://doi.org/10.1061/\(ASCE\)HY.1943-7900.0000169](https://doi.org/10.1061/(ASCE)HY.1943-7900.0000169)
- Frostick, L.E., Lucas, P.M., Reid, I., 1984. The infiltration of fine matrices into coarse-grained alluvial sediments and its implications for stratigraphical interpretation. *J. Geol. Soc.* 141, 955–965. <https://doi.org/10.1144/gsjgs.141.6.0955>
- Gibson, S., Abraham, D., Heath, R., Schoellhamer, D., 2010. Bridging Process Threshold for Sediment Infiltrating into a Coarse Substrate. *J. Geotech. Geoenvironmental Eng.* 136, 402–406. [https://doi.org/10.1061/\(ASCE\)GT.1943-5606.0000219](https://doi.org/10.1061/(ASCE)GT.1943-5606.0000219)
- Kondolf, G.M., Gao, Y., Annandale, G.W., Morris, G.L., Jiang, E., Zhang, J., Cao, Y., Carling, P., Fu, K., Guo, Q., Hotchkiss, R., Peteuil, C., Sumi, T., Wang, H.-W., Wang, Z., Wei, Z., Wu, B., Wu, C., Yang, C.T., 2014. Sustainable sediment management in reservoirs and regulated rivers: Experiences from five continents. *Earths Future* 2, 256–280. <https://doi.org/10.1002/2013EF000184>
- Legout, C., Droppo, I. G., Coutaz, J., Bel, C., Jodeau, M., 2018. Assessment of erosion and settling properties of fine sediments stored in cobble bed rivers: the Arc and Isère alpine rivers before and after reservoir flushing. *Earth Surf. Process. Landf.* 43, 1295–1309. <https://doi.org/10.1002/esp.4314>
- Loire, R., Piégay, H., Malavoi, J.-R., Beche, L., Dumoutier, Q., Mosseri, J., Kerjean, C., 2019. Unclogging improvement based on interdate and interreach comparison of water release monitoring (Durance, France). *River Res. Appl.* 35, 1107–1118. <https://doi.org/10.1002/rra.3489>
- Mooneyham, C., Strom, K., 2018. Deposition of Suspended Clay to Open and Sand-Filled Framework Gravel Beds in a Laboratory Flume. *Water Resour. Res.* 54, 323–344. <https://doi.org/10.1002/2017WR020748>
- Mürle, U., Ortlepp, J., Zahner, M., 2003. Effects of experimental flooding on riverine morphology, structure and riparian vegetation: The River Spöl, Swiss National Park. *Aquat. Sci.* 65, 191–198. <https://doi.org/10.1007/s00027-003-0665-6>
- Panthi, M., Lee, A.A., Dahal, S., Omer, A., Franca, M.J., Crosato, A., 2022. Effects of sediment flushing operations versus natural floods on Chinook salmon survival. *Sci. Rep.* 12, 15354. <https://doi.org/10.1038/s41598-022-19294-2>
- Ramezani, J., Rennebeck, L., Closs, G.P., Matthaei, C.D., 2014. Effects of fine sediment addition and removal on stream invertebrates and fish: a reach-scale experiment. *Freshw. Biol.* 59, 2584–2604.
- Schälchli, U., 1993. Die Kolmation von Fliessgewässersohlen: Prozesse und Berechnungsgrundlagen (Doctoral Thesis). ETH Zurich. <https://doi.org/10.3929/ethz-a-001322977>
- Schroff, R., Mörtl, C., De Cesare, G., 2021. Wirkungskontrolle einer Sedimentzugabe: Habitatvielfalt und Kolmation. *WasserWirtschaft* 68–76.

Norwegian sediment handling technologies - recent developments and experiences from projects

Tom Jacobsen

SediCon AS, Trondheim, Norway

ABSTRACT: The author has 30 years' experience in designing sediment removal equipment for intakes, desanders, tunnels and reservoirs. Hydrosuction dredging has proven to be an effective way of maintaining reservoir storage, and gravity powered hydrosuction dredges has been supplied tom among others to Tinguiririca and Trichahue reservoirs in Chile in 2022. The capacity of the remotely and automatic operated 400 mm hydrosuction dredge was measured to 183 m³sediments per hour. In 2001 the author designed an ejector dredge with a 160 kW water jetting system and mechanical cutter to disintegrate cohesive clay. The dredge was used to reopen lower parts of the intake at 116 years old Necaxa reservoir in Mexico. Since 2020 the author have developed a boulder excluder which is capable of removing boulders of more than one in size meter from intakes. The boulder excluder is completely without movable parts and still operates autonomously during floods, using only the excess water. A 1,2-meter diameter boulder excluder has been successfully tested at Ulvik power plant in Hardanger in Norway and has since 2020 kept the intake completely clean and free from sediments without any human intervention at all.

1 INTRODUCTION

Norway has less sediment transport than most countries but has still seen the development of a range of sediment handling technologies, among other technologies for sediment removal from desanders, tunnels intakes and reservoirs. Since 1999 sediment removal equipment has been sent from Norway to hydropower plants ranging from 400 kW to 1500 MW in 22 countries in all parts of the world. Through practical implementation of these new technologies, it has been gained a unique portfolio of experience – not only on removal of sediments but also on assessment of sediment transport, knowledge about properties of sediment deposits and dimensioning and layout of open and underground de-sanding structures. Adding to this, Norwegian companies have supplied design for several innovative dredging technologies used in the offshore wind, oil and gas industry including pumping of rock up 500 mm with ejectors, disintegration and cutting of clay with water jetting up to 1000 bar and remote operation down to 2000 m water depth. The interaction between the offshore and the hydropower sectors av truly added to a remarkable development. In the following sections three projects are presented where the Norwegian sediment handling technologies have been used to increase hydropower production.

2 BACKGROUND

Daily peaking reservoirs have an increasingly relevant function for balancing new renewable energy sources, mainly solar and wind. A major obstacle is however sedimentation that reduces water storage capacity quickly and affects the operation. Large reservoirs may not fill up so quickly, but sedimentation can cause problems due to blocking of intakes and bottom outlets before loss of reservoir storage volume becomes a problem. Even in countries where sedimentation is a lesser problem the sediment transport in steep brooks and creeks may affect the operation of secondary (brook) intakes and reduce the amount of water transferred to storage in reservoirs.

3 HYDROSUCTION OF SEDIMENTS IN THE TINGUIRIRICA RESERVOIRS

Hydrosuction uses gravity to power a flow of a water-sediment mixture through a pipe leading out of, and to a lower level than the reservoir surface, and to create suction at the inlet of the suction head. The technology enables sediment removal in a controlled and continuous way without requiring external energy input.

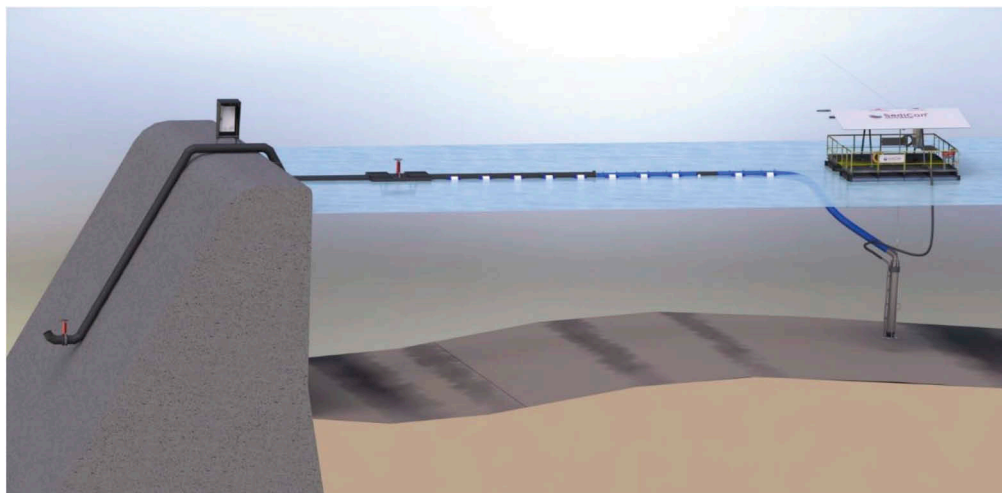


Figure 1. Principle sketch of the SediCon Hydrosuction Dredge. The suction head is operated from a raft and connected to an at least partly flexible outlet pipe. The outlet pipe passes over the dam and the siphon therefore must be primed (air removed) before the system operates.

1.200.000 m³ Tinguiririca and 150,000m³ Tricahue reservoirs belong to the 325 MW Tinguiririca complex commissioned in 2011. In spite of desanders at the intakes much of the sediments below 0,20 mm passes into the reservoirs and causes heavy sedimentation. After achieving an environmental permit, the owner Tinguiririca Energía therefore commissioned a SediCon Hydrosuction Dredge in 2021. The dredge was supplied and installed in late 2022 and uses gravity only to pump sediments out of the reservoirs, over the dam crest and into the downstream river (Figure 2 and 3).

The dredge is connected to perpendicular ropes across the reservoir and is remotely operated by winches on the raft pulling the raft in x and y directions. The suction head is operated up and down and valve closing and opening is also remotely operated. Due to the automatic balancing of sediment concentration the system also includes an automatic operation mode where the raft and suction head are moved in a pre-programmed pattern, without risking blocking of the outlet pipe. Measuring of flow and concentration in the dredged sediment water mixture is done with floating Capacity Measuring System (CMS) which allows measurement of velocity and concentration based on actual weight of the dredged slurry. Features of the equipment are indicated in Table 1.

Table 1. Salient features of the SediCon Hydrosuction Dredge for Tinguiririca Energía.

Inlet diameter = largest rocks	250 mm
Suction hose diameter	400 mm
Discharge pipe	450 mm HDPE
Sediment disintegration system	20 kW
Water consumption	1382 m ³ /h
Nominal sediment discharge	80 m ³ /h
Measured sediment discharge	183 m ³ /h

The experience from commissioning is that sediments are mainly silt and fine sand somewhat cohesive, but it was still possible to achieve a continuous, high output and a sediment concentration much higher than design criteria was measured. Among the challenges, strong winds and waves must be mentioned as it subjects pipes and hoses to significant forces if anchoring is inadequate. The other challenge is measuring concentration as the flow is 3-phase consisting of water, sediments and gases released from sediments or due to low pressure in the pipes.



Figure 2. Overview of the dredge in Tinguiririca reservoir. Notice the wind and waves in the reservoir are two of the challenges during operation.



Figure 3. Discharge downstream of the dam crest. The discharge of sediments is controlled and corresponds to the capacity of the river.

4 RE-OPENING OF LOW-LEVEL INTAKES AT NECAXA RESERVOIR

The Necaxa reservoir has been in operation since 1905 and feeds the 199 MW Necaxa Hydroelectric System in Juan Galindo, Puebla in Mexico. The reservoir has been in operation for 118 years and accumulation of 16-meter-thick sediment deposits in front of the intake tower caused the lower gates to be blocked. Due to the thickness and the age of the sediment deposits highly cohesive sediments were expected a sediment study was conducted prior to design and supply of the equipment to investigate the sediments. Based on samples obtained with a drop-core sampler and its analysis, sediments are as described in Table 2.

Table 2. Sediment properties Necaxa based on 11 samples.

Average particle size, d_{50}	0,0023 – 0,025
Average clay content	25%
Plasticity Index, IP	24% - 45%, Av. = 33%
Dimensioning IP (Av. + 2 St Dev)	50%

Undrained shear strength is the most important factor when designing disintegration systems by water jetting. The undrained shear strength is deducted from the Bjerum (1972 “aged”) relationship shown in Figure 4, below is $C_u = 0,5 \times 16 \text{ m} \times 10 \text{ kN/m}^3 = 80 \text{ kPa}$. As these were old sediments and only upper layer was investigated, a safety factor of 2 was introduced, which gave as a maximum undrained shear strength $C_u = 160 \text{ kPa}$.

Based on the assessed sediment properties it was supplied an ejector dredge to remove 50.000 m^3 sediments in front of the intake, down to a water depth of more than 40 meters. The dredge was equipped with a non-blocking suction head with a powerful 264 kW water jetting system and a rotating hydraulic cutter to cut wood and other debris that may potentially block the inlet of the suction head. The sediment water mixture was pumped with an unrestricted flow ejector pump. The suction head is operated from a winch on the main raft whereas the pumps for jetting and the ejector as well as the ejector itself were installed on

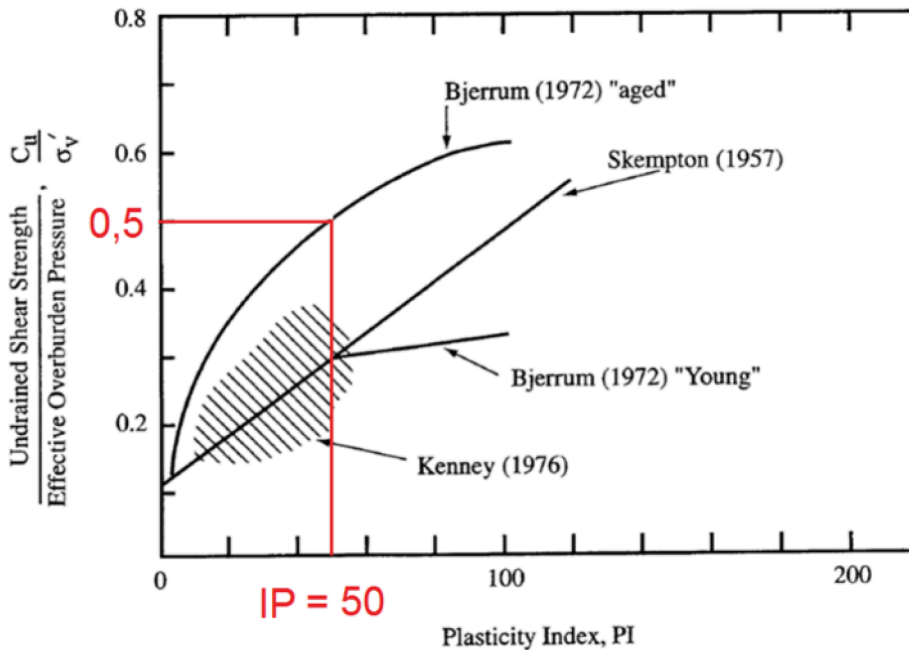


Figure 4. Relationship between the proportion of the undrained shear strength and the effective overburden pressure with the plasticity index for normally consolidated clays. The red line shows conservative estimate for Necaxa clays. (Munfakh, Arman, Samtani, & Castelli, 1997).

a separate pump raft. The general layout of ejector dredge is shown in Figure 5 and the actual equipment is shown in Figures 6 and 7. Features of the equipment are indicated in Table 3.

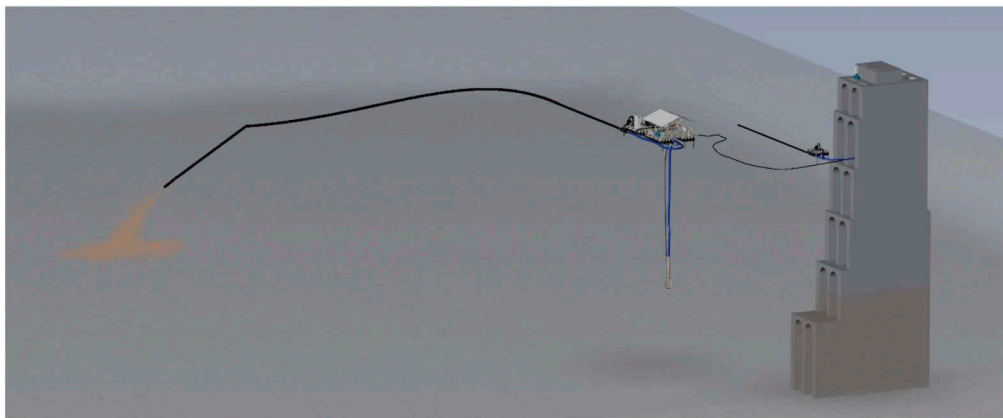


Figure 5. Principle sketch of the SediCon Ejector Dredge. The suction head is operated from a raft and sucked through a suction hose to the ejector pump from where sediments pass through the outlet pipe to the point of discharge.

The experience from operation is that sediments are fine and cohesive and contains debris, but the disintegration systems and the powerful ejector pump made it possible to achieve a continuous, high sediment output with a sediment concentration much higher than design criteria, and sediments were dredged close to the bottom of the 16 m thick deposits. It was also observed that the sediment plume plunged quickly and that the release of sediments did

Table 3. Salient features of the SediCon Ejector Dredge for Necaxa.

Inlet diameter = largest rocks	200 mm
Suction hose diameter	250 mm (internal diameter)
Floating discharge pipe	400 mm diameter HDPE, 200 m long
Sediment disintegration system	264 kW (Nominal power)
Maximum undrained shear strength, S_u	160 kPa (Nominal power)
Nominal sediment discharge	25 m ³ /h
Measured sediment discharge	80 m ³ /h

not cause any visual impact except in a local area (The dredge was designed to discharge sediments on the bottom in a location where they are harmless).



Figure 6. The floating ejector dredge operating in Necaxa Reservoir in 2022.



Figure 7. Discharge of sediments from the ejector dredge during SAT.

5 MAINTAINING A SECONDARY INTAKE AT ULVIK HYDROPOWER PLANT

Hardly any Norwegian reservoirs are affected by storage loss due to sediment deposition, as most reservoirs are constructed by raising the level of natural lakes by dams and lowering of the drawdown level by lake tapping's. However Norwegian and other reservoirs are sometimes affected indirectly by sediments that either blocks secondary intakes or passes into the transfer tunnels and reduces their cross section, in both cases, reducing the capacity of intercepting and transferring small rivers and brooks into reservoirs. In Norway this is a substantial problem as the number of brook intakes are in the order of thousand and may contribute to 20% of the water stored in reservoirs (authors own and very rough assessment).

In 2019, The author introduced its newly developed Boulder Excluder to the Norwegian research program HydroCen and the western-Norway power producer Eviny, with purpose of testing a prototype at one of Eviny's brook intakes. A suitable site was found at Ulvik powerplant in western Norway, where one brook intake alone contributes nearly 30 GWh of the power plants annual production of 102 GWh. The river is steep, and due to floods up to 30-40 m³/s it carries substantial amounts of sediments including gravel, stones and boulders up to almost a meter in size. Since commissioning in 1974, it has therefore been necessary to remove sediments from the intake regularly to maintain its capacity. However, the intake is three km from any road and substantial amounts of water have been lost in periods before cleaning and during cleaning itself when water must be bypassed. Another issue is that the transfer tunnel has a very mild slope and withdrawn sediments have tended to settle on the bottom and reduce its capacity. Finally, there has been a substantial CO₂ footprint as an excavator must be flown in by helicopter for each mechanical removal action (Figure 8).

A 1200 mm diameter Boulder Excluder (Figure 9) was designed and supplied in 2020. The boulder excluder has a special inlet, is designed with air vent that secures start during overflow and stopping when water recedes in such a way that only excess flood water is used for removal of sediments. The boulder excluder is made from extremely durable and strong

HDPE and Designed to tolerate large floods stones and ice floes passing the intake. The equipment is shown in Figures 9, 10 and 11, and its features are indicated in Table 4.

The boulder excluder has been operational since October 2020. There are no electricity or network at site, but the boulder excluder has been monitored by a conventional game camera. The first autonomous operation was recorded in 2021. Later that year an operator observed the boulder excluder working during a flood and pictures and video were recorded. In 2022 Eviny

Table 4. Salient features of the SediCon Boulder Excluder for Ulvik power plant.

Inlet diameter	1040 mm
External diameter	1200 mm (external diameter)
Head difference	2,5 m
Autonomous start and stop during floods	yes
Induced start and stop by operators	yes
Velocity	5 m/s
Estimated flow	5 m ³ /s
Diameter of largest rocks	1000 mm
Weight each component (due to helicopter)	< 1000 kg
Material	HDPE
Method of joining pipes	Electrofusion
Installation time	2 days



Figure 8. Conventional maintenance with excavator that has to be brought in by helicopter.



Figure 9. Boulder excluder after installation.

performed a provoked test where the water level was raised artificially. It was then possible to observe the autonomous priming and stopping of the boulder excluder (Figure 10). Prior to the test was also proven that the boulder excluder could be started by operators as intended.

The boulder excluder stood a major test later in 2022: On 11th November the largest flood since recording started in 1983 hit the area. It was 25% larger than the estimated 50-year flood and may therefore well have been above the 100-year flood. Some weeks later the intake was inspected, and as shown in Figure 11, it appeared that absolutely no sediments were blocking the trash rack at the intake. Even more amazing was the fact the sediment level was continuously flat quite far from the suction inlet of the boulder excluder. One can only conclude that the boulder excluder has passed even the most optimistic expectations, and that this is a promising technology not only for brook and secondary intakes but for intakes in sediment carrying rivers in general.



Figure 10. Boulder excluder during operation in September 2022.



Figure 11. Boulder excluder after the > 50-year flood 11th November 2022.

6 CONCLUSIONS

There is little doubt that sediment transport cause substantial problems to many hydropower plants, such as blocking of water intakes in rivers and submerged intakes in reservoirs as well as by sediment deposition in reservoirs. Sediments reduce withdrawal of water and the ability to store water for balanced power production. Through practical implementation of sediment removal methods, it has verified that sediments can be removed with innovative methods and that problems caused by sediments can be mitigated.

REFERENCES

Munfakh, G., Arman, A., Samtani, N., & Castelli, R. (1997). Geotechnical and Foundation Engineering. Module 1 Surface Investigations. Federal Highway Administration, Arlington, Virginia:

Study on the sedimentation process in Boštanj reservoir, Slovenia

M. Klun, A. Kryžanowski, A. Vidmar & S. Rusjan

Chair of Hydrology and Hydraulic Engineering, University of Ljubljana, Faculty of Civil and Geodetic Engineering, Ljubljana

A. Hribar

HESS, d.o.o., Hidroelektrarne na spodnji Savi, Brežice

ABSTRACT: The paper presents a study case of Boštanj reservoir on the Sava River in Slovenia. The reservoir for a run-of-the-river dam has been in operation since 2006. The total capacity of the reservoir is 8,000,000 m³, with 1,170,000 m³ of live storage, the maximum operational denivelation in the reservoir is 1 m. The combined rated discharge of the powerhouse is 500 m³/s, while the mean annual discharge of the Sava River is 229 m³/s. The Sava River is a sub-Alpine River with a predominantly torrential character, the discharge conditions in the river can vary substantially, e.g. 3100 m³/s during a 100-year flood. Approximately 3.3 km upstream of the Boštanj dam, in the convex on the right riverbank, a large amount of sediment has been already deposited. During a regular reservoir denivelation, in a length of approximately 400 m, the sediment deposition area is now peaking above the reservoir level. Based on available documentation the material in this part of the reservoir has been already removed in the past, while the aim of this study was to find a permanent solution which would contribute to improved sediment management.

Using the HEC-RAS hydrodynamical model, a full 2D hydraulic model of the reservoir has been constructed. In this study the entire Boštanj reservoir area was considered since local conditions at the convex are affected by global behavior of the sediment in the reservoir. As input data for the hydraulic model a 1×1 m digital terrain model was created using combined lidar and bathymetry measurements. Furthermore, the model was calibrated based on hydro-metric measurements in a reference profile. The model consisted of 50,950 calculation cells and the results of the model were used to redesign the area of the reservoir to provide for the sediment continuity and consider the multipurpose use of the reservoir.

Results of the hydraulic model confirm that flow velocities within the area of the reservoir with an increased sediment deposition are low under all flow conditions, meaning the area is generally prone to sediment deposition. Even if the sediment is now completely removed, the natural processes in the river will again start to create a sediment dune in the same location. Therefore, the final solution is designed as a nature-based solution, a plateau of approximately 5900 m² and 400 m of length, re-designed as a riparian habitat for various aquatic and riparian plants and animals. Instead of fighting the natural processes a redesign of this section of the reservoir is a more appropriate solution; the final solution has been confirmed with a hydraulic model. By raising the plateau level at the mean reservoir level and by providing proper vegetation cover we can create good conditions for the riparian habitat and provide sufficient protection against the erosive power of water.

1 INTRODUCTION

Sediment deposition is a major problem worldwide, both in terms of the available reservoir storage volume and the possibility of removing and depositing potentially contaminated

sediment from reservoir areas (Brack et al., 2017). Based on Vörösmarty et al. (2003), globally, there are over 100 billion metric tons of sediments deposited in the reservoirs constructed in the last 50 years. In the smaller reservoirs the deposited sediments alter the flow properties and may cause an accelerated sedimentation, which can shorten the predicted life span of reservoirs and/or causes large maintenance interventions in the reservoir area. The design of modern, integrated management of reservoirs is crucial in mitigating negative effects of sediment accumulation and in assuring the natural dynamics and continuity of sediment transport, as well as in terms of extending the reservoir's life span.

The aim of the study presented in this paper is to provide a permanent technical solution for a local sedimentation issue in the reservoir of a run-of-the-river dam, located on the Lower Sava River in Slovenia. The Sava River is the major drainage basin of Southeastern Europe and the biggest tributary to the Danube River. The 97,713 km² large catchment is extended over Slovenia, Croatia, Bosnia and Herzegovina, and Serbia. In Slovenia, the Sava River has a characteristic of an alpine river, which is evident from the high temporal dynamics of the flows during contrasting hydrological conditions (Mikoš et al., 2015). The torrential character has also a significant impact on the sediment transport, as intensive sediment displacement processes occur in relatively short periods of high discharge conditions. The inflow of sediments from headwater parts is relatively large, mainly due to hydro-meteorological and hydrogeological conditions, e.g. high annual and high-intensity rainfall and erodibility of the subsoil (Colarič, 1985). The natural dynamics of sediment transport was disturbed by construction of the run-of-the-river hydropower plants (HPP) with a limited storage capacity along the river course, which resulted in changes in interception and deposition of sediment within the reservoir volumes. The cascading system on the Lower Sava River consists of 5 dams, built between 1993 and 2017: Vrhovo HPP (1993), Boštanj HPP (2006), Arto-Blanca HPP (2009), Krško HPP (2012), and Brežice HPP (2017) (HESS, 2017; SLOCOLD, 2022). The cascading system and location of the area of the Lower Sava is presented in Figure 1 below.

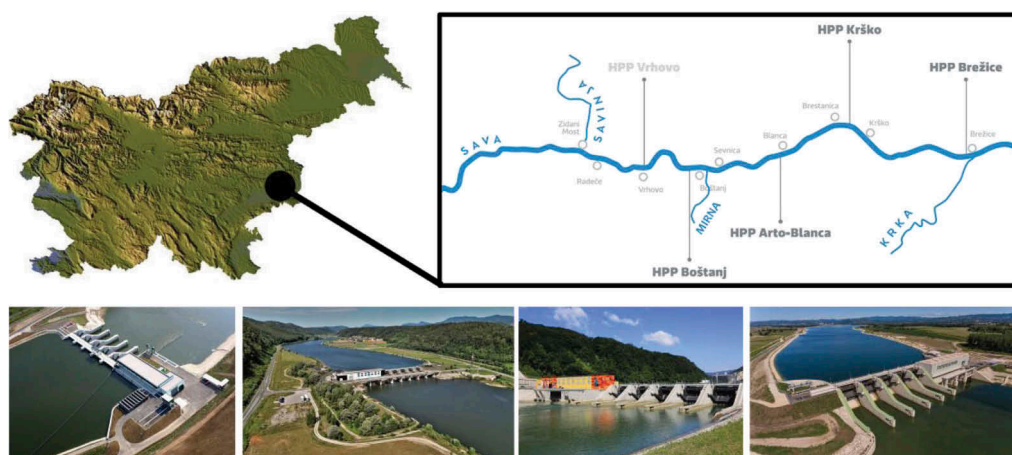


Figure 1. Reservoirs in the Lower Sava River area.

This investigation focuses on the Boštanj reservoir, which is the 2nd reservoir in the cascading system and where in the reservoir area, larger amounts of fine-grained sediment have deposited and formed a sediment deposition dune, which is now partly already reaching above the water level in the reservoir during regular daily denivelation, due to the operation of the Boštanj HPP.

2 THE DESIGN AND IMPLEMENTATION OF THE INVESTIGATION

2.1 Description of the site

Boštanj HPP is the second HPP in the cascading system of run-of-river dams on Lower Sava River section. The dam was constructed in 2006 when also the reservoir was first impounded, and the trial-run operation started. In the powerhouse there are 3 double-regulated horizontal bulb-type Kaplan turbines installed, which operate at $500 \text{ m}^3/\text{s}$ of combined rated discharge and at 7.5 m of rated head. The spillway of the dam consists of 5 overspilling sections, equipped with radial gates with a flap. The 100-year flood for this section of Sava River is estimated at $3100 \text{ m}^3/\text{s}$, while the designed spillway capacity is $4600 \text{ m}^3/\text{s}$ (IHR, 2003). The Boštanj reservoir has a total capacity of $8,000,000 \text{ m}^3$ and a live storage of $1,170,000 \text{ m}^3$. The reservoir is approximately 10 km long and has a maximum of 1 m operational denivelation (ICOLD, 2023). The Vrhovo dam is located on the upstream boundary of the Boštanj reservoir. In Figure 2 below we present the run-of-river Boštanj reservoir and the locations of Boštanj and Vrhovo HPPs, the area where the issue with the deposited sediment is occurring and the location where we performed hydrometric measurements on the Sava River.

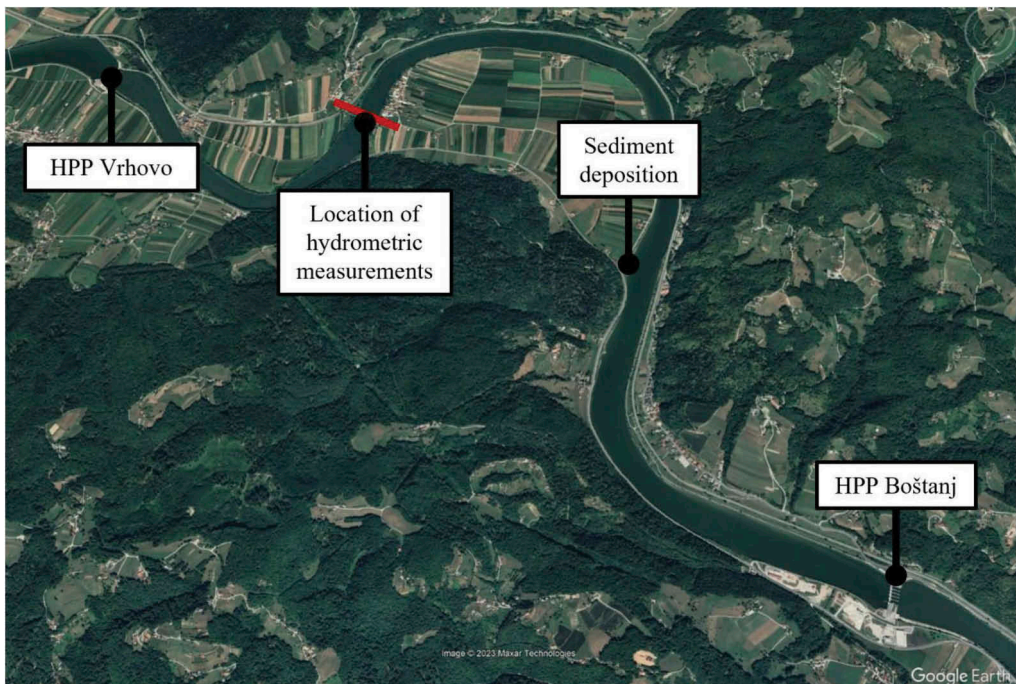


Figure 2. Boštanj reservoir (Google Earth capture).

The critical area of the reservoir, which is the subject of our investigation, is located approximately 3.3 km upstream from the Boštanj dam. The section is located on the right bank and is approximately 400 m long. Along the right bank an alluvium has formed; currently the extent of sedimentation is progressed to the level where the deposits already form a large deposition area, reaching above the normal elevation of the reservoir. Figure 3 presents a panoramic view of the situation as it was captured during a field investigation.



Figure 3. Panoramic view of the deposition area in the Boštanj reservoir.

2.2 Measurements and data preparation

Digital terrain model (DTM) was constructed using: the official LIDAR data obtained in 2015, when the entire area of Slovenia was captured in a resolution of 1×1 m (MOP, 2015), bathymetric survey of the reservoir area conducted by HESS d. o. o. in 2021, and the additional fine resolution LIDAR scanning of the deposition area site in 2022, since it was found that the LIDAR data from the official LIDAR database of the Republic of Slovenia do not precisely describe the topography of the reservoir bank in the denivelation range and the deposit formation under the investigation. By combining all 3 data point clouds we created a single DTM with a cell size of 1×1 m for the entire area of the Boštanj reservoir. For the narrower area along the right bank in Kompolje, where the sediment deposit is located, the DTM of the existing state is shown in Figure 4.

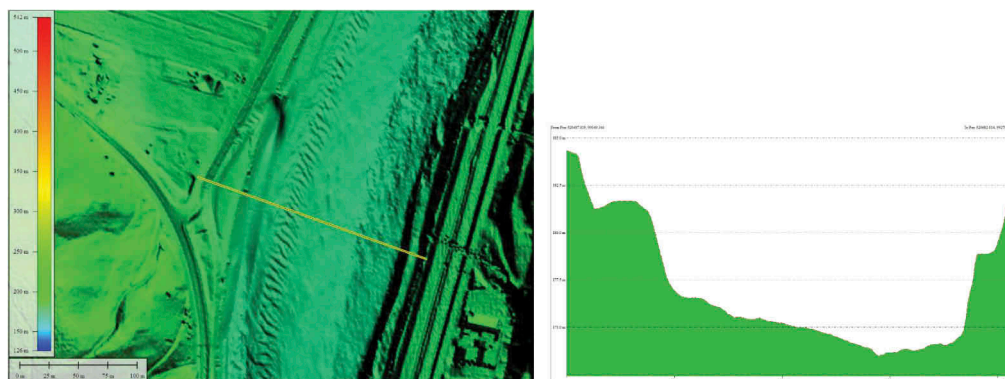


Figure 4. DTM of the Boštanj reservoir (left) and one of the cross-sections in the area of deposit formation (right).

In a profile in the upper part of the reservoir, downstream from the Šmarčna settlement, we also performed hydrometric measurements using ADCP Sontek River Surveyor M9. The discharge of the Sava at the time of the field measurements was relatively low, only $178 \text{ m}^3/\text{s}$, and the mean flow velocity was 0.41 m/s . The spatial distribution of flow velocities in the cross-section is presented in Figure 5.

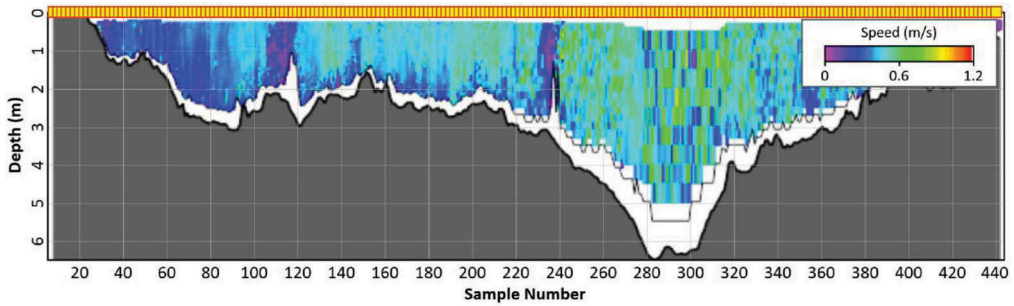


Figure 5. Distribution of measured flow velocities in the profile downstream from the Šmarčna settlement.

2.3 Modelling

A full 2D hydrodynamic model of the Boštanj reservoir was built using HEC RAS 6.2 (HEC, 2022). To be able to comprehensively analyze locally hydrodynamic phenomena at the section of the reservoir under consideration and to properly consider the boundary conditions we modeled a major part of the reservoir area. The downstream boundary condition was applied at approx. 370 m upstream from the Boštanj dam, and the upstream boundary of the model is at 380 m downstream from the Vrhovo dam. The total length of the modeled section of the reservoir is 7.5 km. Computational cell size in the hydraulic model is 5×5 m and the entire mesh consists of 49,169 cells. The upstream boundary condition was considered as inflow hydrographs with 8h peak flows for various peak flow values up to $3500 \text{ m}^3/\text{s}$. The extended time of the hydrograph peak assured virtually stable hydraulic conditions along the entire reservoir section during the high flow conditions. Since we are observing local hydraulic phenomena at a smaller section of the reservoir, it is important to establish a stable runoff situation along the entire section under consideration. For the downstream boundary condition, a denivelation curve for the Boštanj reservoir was considered. The denivelation curve is presented in Figure 6. The model was calibrated by considering the hydrometric measurements and by fine fitting the Manning coefficient of the Sava River. By setting the Manning coefficient at 0.026, the modelled flow velocity distribution and reservoir level in the control profile downstream of Šmarčna matched the measured velocity field very well.

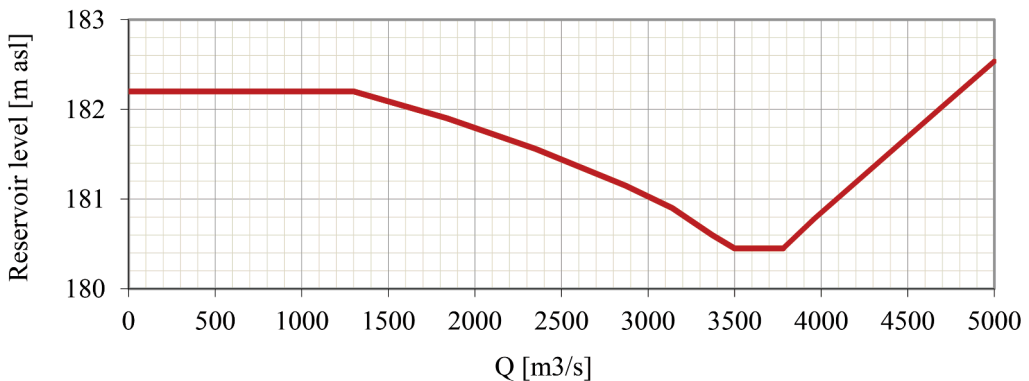


Figure 6. Denivelation curve - downstream boundary condition in the Boštanj reservoir.

3 RESULTS AND DISCUSSION

The hydraulic model of the Boštanj reservoir was used to perform a series of simulations to evaluate the local hydraulic phenomenon at the location where the sediment deposition area

has formed and where flows ranging up to $3500 \text{ m}^3/\text{s}$ were considered. The situation in Figure 7 represents local hydraulic conditions considering the $2000 \text{ m}^3/\text{s}$ discharge of the Sava River. The formation of the fine-grained sediment deposit is at the left bank side; in Figure 7 the location is marked with a black dotted line. As can be seen from the figure the location of the main flow is moved towards the left side of the cross-section, while the flow velocities closer to the right bank drop drastically, especially in the area where the fine-grained sediment deposit is formed. The flow depth across the computational cross-section is presented in Figure 9; with a dashed box we marked the area of the formation of the fine-grained deposition area. In this area along the Sava River right bank, the depth of the water flow varies between 0.5 and 1 m at flows of up to approx. $1300 \text{ m}^3/\text{s}$. With a further increase of the discharge and due to the reservoir operation condition at the downstream boundary condition of the Boštanj reservoir, the water depth starts to decrease, e.g. at a discharge of $3500 \text{ m}^3/\text{s}$, the water depth at the location of the formation of the sediment deposit is below 0.5 m. When observing flow velocities in Figure 8, we can clearly notice significantly lower flow velocities at the area of the sediment deposition (marked with dashed black line), which are approx. 0.1 m/s at flow of $500 \text{ m}^3/\text{s}$. With increasing inflow, the velocities gradually rise to about 0.5 m/s . At $Q = 3000 \text{ m}^3/\text{s}$ in the entire deposition area the flow velocity is under 0.35 m/s . Moreover, at $Q = 3500 \text{ m}^3/\text{s}$ due to further denivelation of the water level in the reservoir, the velocities drop even further; however, then, with a continuous increase of inflow, the velocities again start to increase with the increasing flow. We need to emphasize that the depth of flow and flow velocities rapidly increase in the direction toward the central part of the river cross-section, e.g. at the discharge of $2000 \text{ m}^3/\text{s}$ and above, flow velocities towards the main river flow section rise above 2 m/s . Moreover, during the high flow condition, when the hydraulic gates at the Boštanj dam are completely opened, the natural flow condition is established along the entire section of the reservoir.

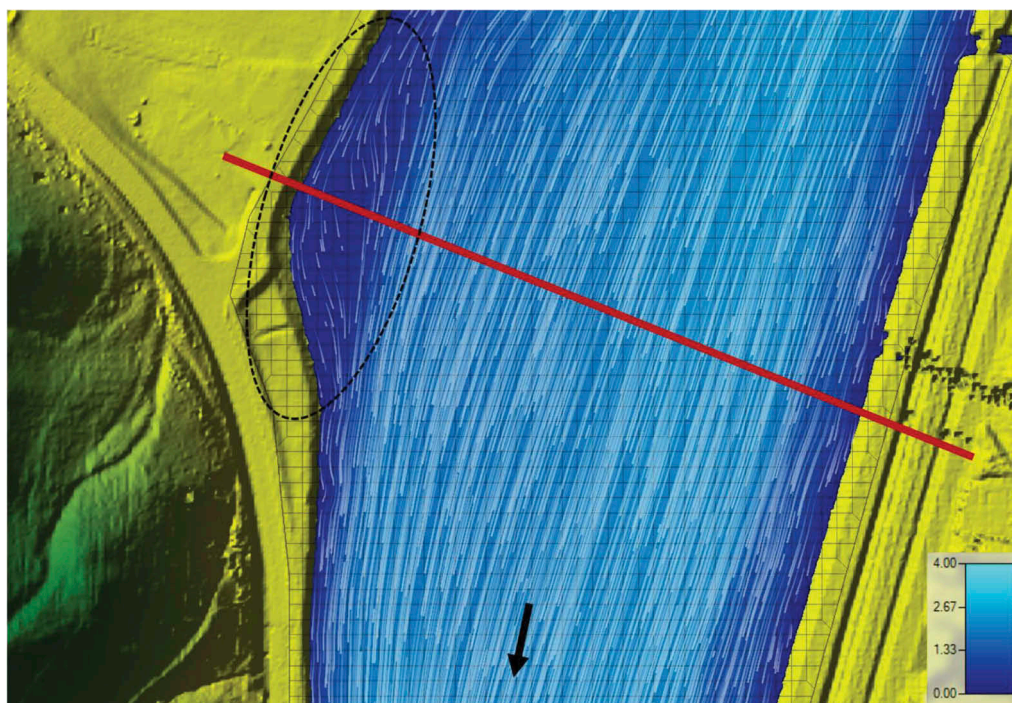


Figure 7. Local hydraulic conditions at the area of the formation of the fine-grained sediment deposit. The red line marks the location of the cross-section with more detailed results in the following figures. The black arrow marks the direction downstream and the dotted black line the location of the dune formation.

Results of the hydraulic model confirm that flow velocities decrease under all flow conditions within the area of the reservoir where intensified sediment deposition is occurring, meaning the area is generally prone to sediment deposition. As an optimal solution we propose a redesign of this section of the reservoir in a way that the shape of the bank slopes corresponds to the local hydraulic conditions.

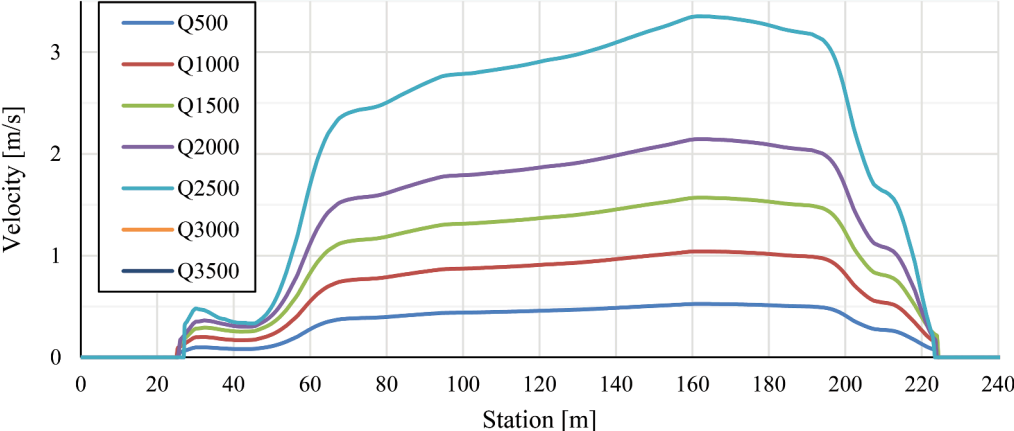


Figure 8. Flow velocities along the computational cross-section for various inflow hydrographs.

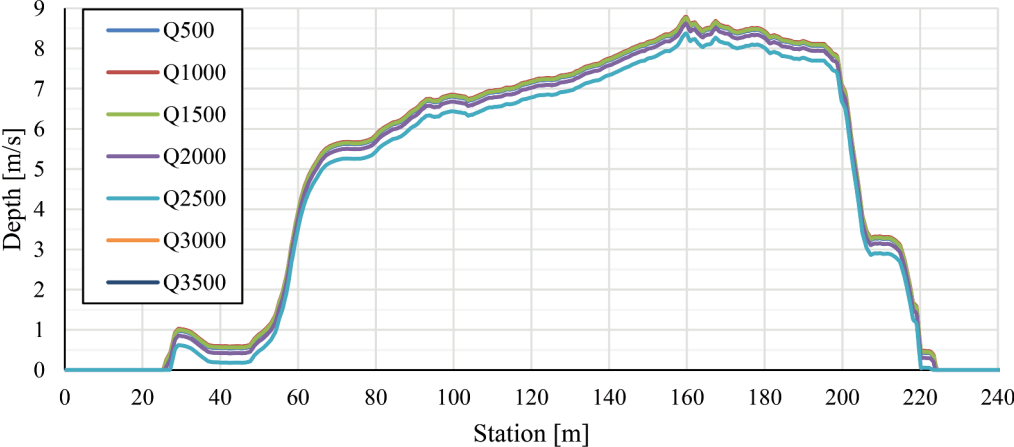


Figure 9. Flow depth along the computational cross-section for various inflow hydrographs.

4 PROPOSED REMEDIATION WORKS

By conducting field surveys, hydraulic modelling, and revision of the past measures we proposed implementation of a nature-based solution in the form of ecological remediation works where a part of the right bank is re-designed as a new riparian habitat. Due to specific local hydraulic conditions, the area is prone to sedimentation; even during high flows in the Sava River local hydrodynamic conditions do not enable re-mobilisation of the sediment, but the location remains prone to further deposition of the fine-grained sediment. Therefore, even if the sediment had been removed, the natural processes in the river would again start to create a fine-grained sediment deposition area in the same location. Instead of fighting the natural

processes, an area of approximately 5900 m² and 400 m of length (see Figure 10(b)) should be re-designed as a riparian habitat supporting the ecological functions of the riverbanks. One variant of such solution is presented in Figure 10(a).

To verify and refine the proposed measures, new DTMs were constructed, considering various arrangements of the new riparian habitat. Figures 11 and 12 present the flow depth and velocities in the computational cross-section for one of the proposed solutions where the area of 5900 m² is designed as a riparian habitat for various aquatic and riparian plants and animals. The proposed solution includes construction of a plateau at the mean daily reservoir level, which means that the reservoir level in the area would vary on a daily basis and enable the growth of riparian plants and additional habitat for animals. Protection against the erosive action of water flow would be assured by vegetation growth and consequent stabilisation of the banks. Results of the hydraulic simulation shown in Figures 11 and 12 demonstrate that the flow velocities in the area of the plateau would remain below 0.3 m/s for all flow regimes and the depth of water would be below 0.5 m.

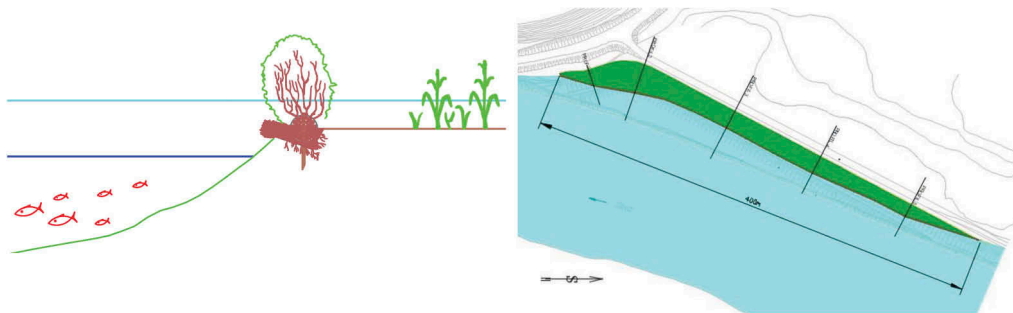


Figure 10. Proposed solution.

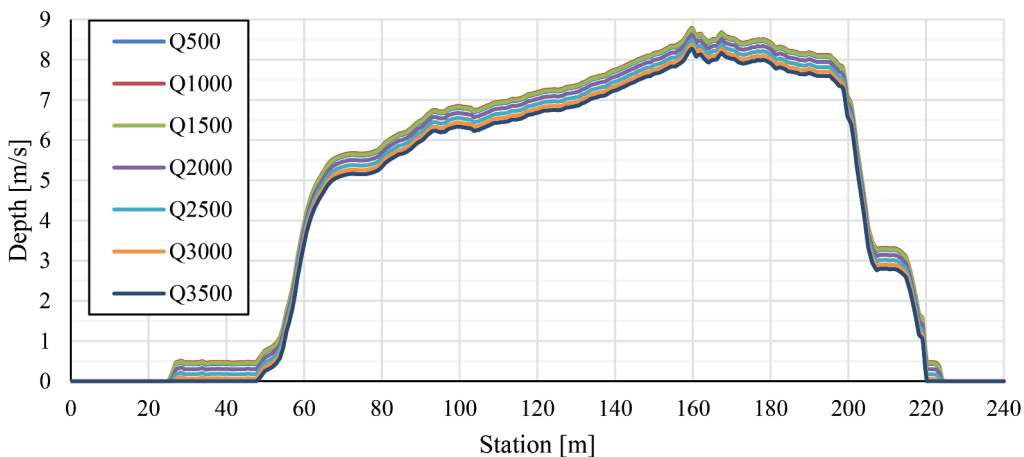


Figure 11. Flow depth along the computational cross-section for various inflow hydrographs.

5 CONCLUSIONS

Sediment deposition is a common issue for many dam operators in terms of the available reservoir storage volume and maintenance costs. In this paper we presented a study case from the Boštanj reservoir on the Sava River in Slovenia, where we designed a nature-based solution to permanently tackle the sedimentation issue in a smaller area of the Boštanj reservoir.

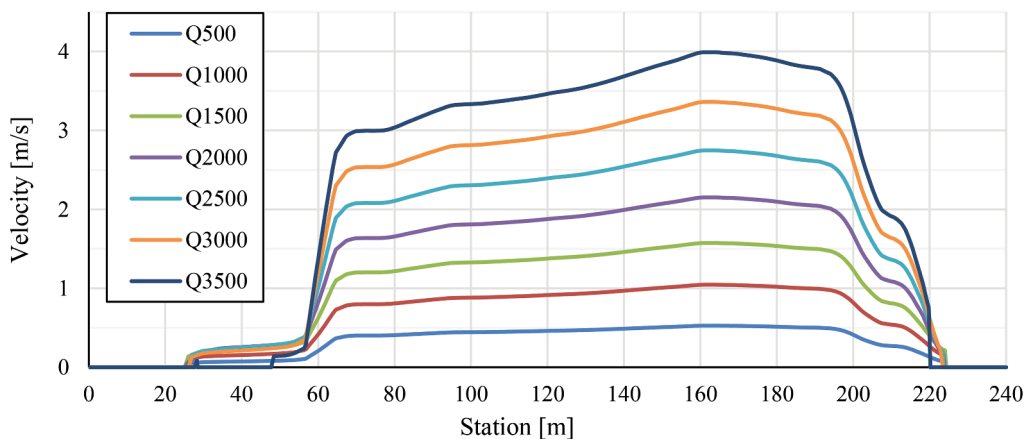


Figure 12. Flow velocities along the computational cross-section for various inflow hydrographs.

In the scope of the project, we created a full 2D model of the reservoir and performed multiple simulations under various flows for the existing terrain condition and for the suggested design solution. The proposed final solution is designed as a nature-based solution, a vegetated area where a new riparian ecosystem could be established.

ACKNOWLEDGEMENT

The study was financed by HESS, d.o.o., Hidroelektrarne na spodnji Savi, Brežice. The work was also partially supported by the Slovene Research Agency (ARRS) through grant P2-0180.

REFERENCES

- Brack, W., Dulio, V., Ågerstrand, M., Allan, I., Altenburger, R., Brinkmann, M., Bunke, D., Burgess, R.M., Cousins, I., Escher, B.I., Hernández, F.J., Hewitt, L.M., Hilscherová, K., Hollender, J., Hollert, H., Kase, R., Klauer, B., Lindim, C., Herráez, D.L., Miège, C., Munthe, J., O'Toole, S., Posthuma, L., Rüdél, H., Schäfer, R.B., Sengl, M., Smedes, F., van de Meent, D., van den Brink, P.J., van Gils, J., van Wezel, A.P., Vethaak, A.D., Vermeirssen, E., von der Ohe, P.C., Vrana, B. 2017. Towards The Review of The European Union Water Framework Directive: Recommendations for More Efficient Assessment and Management of Chemical Contamination in European Surface Water Resources. *Sci. Total Environ.* 576, 720–737.
- Colarič, O. 1985. Assessment of Riverbed and Water Level Elevation of the Vrhovo HPP Reservoir, VGI Ljubljana, Technical Report 831, pp. 29
- HEC, 2022. HEC-RAS User's Manual, Version 6.2, U.S. Army Corps of Engineers, Hydrologic Engineering Center, Davis, CA.
- HESS, 2017. [Online]. Available: https://www.he-ss.si/pdf/brosura_hess_2017_eng.pdf. [Accessed: 01 March 2022].
- ICOLD, 2023. The World Register of Dams, Official database.
- IHR, 2003. Hidravlična modelna raziskava HE Boštanj na prostorskem modelu (in Slovenian), Institute for hydraulic research, Ljubljana, Slovenia.
- Vörösmarty, C.J., Meybeck, M., Fekete, B., Sharmad, K., Greena, P., Syvitskie, J.P.M. 2003. Anthropogenic Sediment Retention: Major Global Impact from Registered River Impoundments. *Glob. Planet. Change*, 39,169–190.
- Mikoš, M., Muck, P., Savič, V. 2015. The Sava River Channel Changes in Slovenia, *Acta Hydrotechnica* 28/49, 28/49, 101–118.
- MOP, 2015. Laser Scanning of Slovenia, Official database.
- SLOCOLD, 2022. List of Large Dams in Slovenia, SLOCOLD – Slovenian National Committee on Large Dams [Online]. Available: http://www.slocold.si/e_pregrade_seznam.htm. [Accessed: 01 March 2022].

Submerged wood detection in a dam reservoir with a narrow multi-beam echo sounder

T. Koshihira

Kyoto University, Kyoto, Japan

S. Takata

Public Works Research Institute, Tsukuba, Japan

K. Murakami

Sea Plus Co., Ltd., Yokohama, Japan

T. Sumi

Kyoto University, Kyoto, Japan

ABSTRACT: In 2017, the Susobana Dam in Nagano prefecture became uncontrollable because sediments and submerged driftwood clogged the bottom outlet during flood control. This incident was induced by a combination of large amounts of sedimentation residue which reached the bottom of the gate and driftwood clogged the gate travelling through the flushing water. Such incidents will occur more frequently as now more and more reservoirs are suffering from sedimentation and climate changes, which are a result of these severe flood events nowadays. However, there are few studies on the process of how driftwood is generated, submerged and transported by a flood, thus the driftwood movement during the incident is still a matter of speculation. In this study, as a first step for understanding the dynamics of driftwood movement in reservoirs, we applied the Narrow Multi-Beam Echo Sounder (MBES) system to detect the current distribution of driftwood in the Susobana reservoir.

1 INTRODUCTION

In recent years, it has been reported that driftwood discharged into river channels during floods accumulates on piers and weirs, causing river levels to rise and leading to increased flood damage. In response to these reports, studies on driftwood disasters have been conducted, including driftwood production and the relationship between the accumulation of driftwood on bridge piers and the rise in water levels. On the other hand, driftwood that flows into a dam reservoir is captured by booms installed in the reservoir, and the effect of this on reducing damage downstream has been attracting attention. For example, in Japan, about 10,000 m³ of driftwood was trapped at the Terauchi Dam in Fukuoka Prefecture in 2017. The driftwood trapping effect of dams is expected to continue with the increasing inflow of driftwood (MLIT, 2018).

On the other hand, there have been cases where driftwood has affected the safe operation of dam reservoirs. At Susobana Dam in Nagano Prefecture, Japan, an incident occurred in 2017. Gate operation was disabled during flood control due to sediment reaching the gate during flood control operations and the pulling of sediment in the vicinity. This case is a combined phenomenon of reservoir sedimentation progression and the large driftwood inflow during heavy rainfall events (Figure 1). However, how and when driftwood floating on the reservoir surface reached the sediment surface has yet to be studied. Also, the gate blockage mechanism is still a matter of conjecture.

The case of the gate closure at the Susobana Dam is an example of the manifestation of the risk caused by the combined factors of sedimentation and sedimentation, which has not been paid attention to until now, and there is a possibility that similar cases will occur in the future as sedimentation progresses. Therefore, it is necessary to elucidate the dynamics of sedimentation in dam reservoirs.

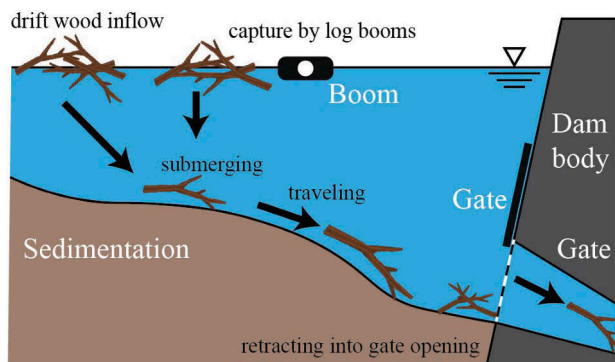


Figure 1. Anticipated gate blockage mechanism.

As a part of such efforts, the authors have conducted a sedimentation survey using a multibeam echosounder (MBES) at the Susobana Dam. This paper describes the principle of MBES, the actual sinking tree survey method used at the Susobana Dam, and the characteristics and detectability of sinking trees obtained by analyzing microscopic protrusions, which have yet to be paid attention to in the past. Future issues and the direction of the analysis method are also presented.

2 PREVIOUS RESEARCH ON SUNKEN WOOD

There have been many studies on driftwood in the field of river and erosion control (for example, Seo et al., 2008). Many essential findings have been accumulated from the viewpoint of disaster prevention, such as the mechanism of driftwood generation, flood magnitude and the amount of driftwood generated, and blockage of bridge piers (Schalko et al., 2019). At the same time, not only the negative aspects of driftwood but also the positive aspects have been studied. Driftwood and fallen trees play an important role in the dynamics of river channels and ecosystems and be indispensable to rivers (Bertoldi et al., 2003).

On the other hand, although there have been cases of driftwood in dam reservoirs recognized at the level of individual managers, there needs to be knowledge of the process and amount of driftwood generated and their dynamics within the reservoirs. However, there are reports of dam management problems caused by sedimentation in dams overseas, including the Susobana Dam. The Bureau of Reclamation of the United States Bureau of Reclamation introduced a case in which sediments and sedimentation buried the outlet of Paonia Reservoir during a reservoir lowering operation and proposed solutions for similar cases (USBR, 2016). However, the authors did not mention the process of generation or migration of siltation, which is a knowledge that is still awaited in Japan and abroad. There have been no cases where sediment progression immediately upstream of a dam has been considered a risk factor for dam function. It is considered increasingly necessary to understand the risk and consider countermeasures based on sediment progression, including the combined effects of sedimentation and wood sinking.

The first question that needs to be addressed is, "How does sunk wood occur and move in a dam reservoir?" There are two possible mechanisms: (1) indirect sink, in which driftwood entering a reservoir during a flood is trapped for a long period in a screened area and becomes plunged with water, increasing its specific gravity and causing it to settle; and (2) direct

transport of driftwood to the reservoir bottom by flood or density currents. By studying the mechanisms of sinking and clarifying the dynamics of sedimentation in a dam lake, it is expected that the sinking of driftwood can be suppressed and cases such as the one at the Susobana Dam can be prevented.

3 MULTIBEAM ECOSOUNDER (MBES) MEASUREMENT

3.1 Introduction

In Japan, sedimentation rate surveys are conducted once a year or every two years to determine the reservoir capacity and maintain and manage reservoir facilities. Since the multibeam echosounder (MBES) development in 1988, the use of MBES has gradually increased. Currently, SBES or MBES are used for sediment volume surveys, depending on the degree of sediment progress and cost.

Compared to SBES, MBES has a much higher resolution and has been used for bathymetry surveying in oceans and lakes worldwide. Accordingly, many studies have been conducted to improve noise reduction and measurement data resolution to analyze bottom materials (Calder 2003, Hellequin et al., 2003, Brown et al., 2019, Roberts et al., 2005). However, there are a few examples of its use for object detection, including sunken wood in dam reservoirs.

3.2 The principle of MBES

The SBES (single-beam echosounder) uses the reference points on the left and right banks of the reservoirs as measuring lines for the bathymetry survey. The SBES navigates back and forth across the valley (between the reference points) and measures the cross-sectional shape of the reservoir bed directly below the measuring line. In contrast, the MBES emits sound waves in a fan shape (swath width) and measures the cross-sectional shape (line shape) directly below the measuring line in a band shape. The information from multiple band measurements is combined to cover the reservoir. In contrast to SBES, which traverses the area between the left and right bank reference points, the MBES measures the reservoir longitudinally to maintain a fixed measurement depth for each navigation.

MBES needs to be evaluated in terms of distance and azimuth resolutions. Bathymetry is the resolution of the distance, and various corrections are made to eliminate any influence on the distance resolution. Azimuth resolution is an instrument specification for beamwidth, where each beam has an angle. The unit of information is the beamwidth within the beamwidth at the point of arrival. The resolution is not improved by making the beam spacing finer than the beam width at a depth of interest. If detailed information is to be obtained, the model should be selected so that the footprint (the area where the beam illuminates the reservoir bottom) can be made up of several points of the object (e.g., a sunken tree with a diameter of 60 cm).

An image of survey point acquisition by MBES surveying is shown in Figure 2. A simple calculation yields the following equation for the distance between survey points on the reservoir bed.

$$\Delta X = \frac{V}{L} \quad (1)$$

$$\Delta Y = 2 \frac{D}{N} \tan \frac{\theta}{2} \quad (2)$$

Where, ΔX : measuring interval in the X direction [m], ΔY : measuring interval in the Y direction [m], V : navigation speed [m/s], L : frequency of launch [shots/s], D : water depth [m], θ : swath width [degrees]. N : number of received beams [points/shot]. Equation (2) shows the average spacing of measuring points in the Y direction, with the spacing widening at both ends of the swath width (angle of the beam launch range) and decreasing in the centre. Therefore, the smallest topographic resolution is found just below the ship's bottom, calculated by the following equation.

$$\Delta y = \varphi d \quad (3)$$

Here, Δy : maximum resolution in the y-direction [m], d : water depth at the bottom of the ship [m], φ : beam width [rad]. The beam width is generally the swath angle divided by the number of beams. The beam width setting is, therefore, critical for detailed topographic mapping.

3.3 Postprocessing

The bathymetry survey is subject to various corrections because they contain errors. Measurement errors are classified as systematic and random errors. Systematic errors are values that deviate systematically from the actual value due to environmental factors, even if measurements are carried out using the same method. If the causes of systematic errors and the amount of correction based on them are known, they can be eliminated. Random errors remain even after systematic errors have been removed from the measured values. The most accurate value is obtained from the mean or standard deviation of several measurements at the same location.

Differences in equipment installation and survey position also significantly affect the bathymetry survey's accuracy. There are several methods for avoiding accuracy loss, such as GPS calibration using a reference point, overlapping survey lines at a certain rate (lap rate), intersecting survey lines, and calculating correction values using patch tests.

In sediment volume surveys, topographic information and noise are separated based on the corrected bathymetry data. This process is called filtering. The main objects to be removed by filtering are noise, vegetation on the reservoir bottom, and fish shoal. Generally, the noise emitted when measuring suspended objects in the water, including gas bubbles from the reservoir bottom and upright structures such as dam sites, is random regarding position and time of detection.

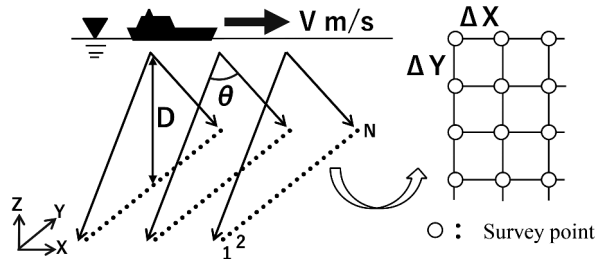


Figure 2. Image of survey point acquisition by MBES surveying (Koshiha, et al., 2022).

Table 1. MBES specification used for Susobana reservoir bathymetry survey.

item	Specification
Survey method	Cross-fan beam
frequency	200 ~ 400 kHz
Beam width	0.5°×1.0° (400 kHz Left/Right x Direction of travel)
Survey points/swath	Max. 1024 points/swath (Normal 256 points/ swath)
Survey mode	Isobar survey, equidistant survey
Swath width	10 ~ 160°
Applicable depth	Approx.. 400 m
Range resolution	1.25 cm
Pulse width	15 μ_s ~ 1 ms
Max. launch frequency	60 times/sec
Weight	16.2 kg

4 BATHYMETRY SURVEY AT THE SUSOBANA DAM

4.1 MBES specifications

The MBES used for the reservoir sedimentation survey at Susobana Dam was the Sonic 2024 (R2Sonic, LLC), a cross-fan beam MBES, the flagship model of the company's MBES range for shallow sea applications. Two hundred fifty-six points can be acquired in a single launch, and the data can be sent to the ship in a strip of data. A vessel navigates on the measuring line while launching several to several dozen times per second, and strips of point cloud data can be acquired. The point cloud data of the measurement area is acquired by connecting them with the neighboring survey lines.

The performance of Sonic 2024 is shown in Table 1. The measurement frequency can be varied between 200 and 400 kHz to prevent interference when used simultaneously with other acoustic equipment. The maximum depth measurement depth is approximately 400 m. The maximum launch frequency depends on the depth range, and the ping rate decreases inversely as the range increases. For example, when measuring a depth of 40 m with a swath width of 120° , the range is considered to be about 100 m, in which case the oscillation frequency is about 7 Hz (seven launches per second). However, when measuring a depth of 40 m with a swath width of 60° , the range is only about 50 m, in which case the launch frequency is about 15 Hz. The beam width is $0.5^\circ \times 1.0^\circ$ at 400 kHz and $1.0^\circ \times 2.0^\circ$ at 200 kHz. 400 kHz was mainly used in this study because of the need to determine the shape of the sink wood.

4.2 Survey overview

The survey was carried out on 23 and 24 September 2020. A small survey vessel was equipped with an MBES, a motion sensor, GNSS for position and heading, and a recording PC. A base station was installed on land for radio communication with the survey vessel and remote control. The base station consisted of a radio antenna, a PC for controlling the survey vessel, and a PC for remote control of the recording PC in the survey vessel. The base station was installed near the dam in this experiment, and manned navigation was conducted. The MBES was installed on a boat and navigated around the Susobana reservoir, as shown in Figure 3. The navigation trajectory's overlap ratio (lap rate) was approximately 50%.

The measurements were carried out with a beam width of 0.5° , a beam count of 256 points, a swath width of 120° and a launch frequency of approximately ten shots/sec (at a swath width of 120° and a water depth of 30 m). Using the formula described in Section 3, the launch point interval is determined by the water depth at the survey location and the boat's navigation speed. When considering the risk of blockage of the permanent flood discharge at the middle elevation of the dam, the target can be considered to be to identify sink trees with a water depth of approximately 50 m (= difference between the elevation of the dead water

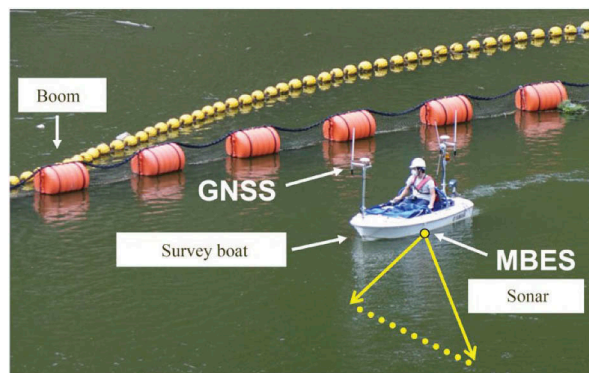


Figure 3. MBES bathymetry survey in the Susobana reservoir (Koshiba, et al., 2022).

zone and the normal full water level) and a trunk diameter of about 30 cm. In contrast, a beam width of 0.5° is considered to ensure the required resolution (a beam width of 0.5° (1800") at a water depth of 50 m a footprint of about 0.5 m (50 cm) at 206,265": 1,800" ≈ 100:1). Note that in actual surveying, the Y direction can be observed at a higher density because the navigation track can be overlapped according to the water depth.

4.3 *Distribution of sink wood*

Observing the random data after removing noise, objects that appeared to be sink wood were visually extracted. In general, sedimentation by scouring sand is formed from upstream to downstream of the reservoir, and sediment deposition with suspended load is deposited across the entire bottom of the reservoir. The sedimentation surface shows little undulation because the suspended load in the turbid water is deposited on the bottom of the reservoir as it settles. Therefore, we extracted sink wood based on the difference in the undulation shape of the surface in the reservoir bottom. Specifically, the two criteria were that there was no difference in depth of more than several tens of centimeters between adjacent bathymetric points and that the protrusion of the reservoir bottom was recorded at the same point on multiple bathymetric lines (Figure 4).

The Figure 5 shows the results of these two points superimposed on the gray scaled plan of the reservoir bottom. At the same time, the central axis of the reservoir is indicated by a line segment passing through the approximate center of the transverse direction. Only the downstream area where much sink wood was observed is shown in this figure. The red line indicates the sink wood, and its direction indicates that of the sink wood. The approximate length (m) of each sink wood is shown next to each sink wood.

A total of 52 sink wood were identified by MBES bathymetry. The distribution of the sink wood is characterized by the fact that most of them are located downstream of the sedimentation iDelta (about 500 m from the bank), near the right and left banks of the reservoir and around the boom, and that relatively large sink wood is located near the boom. Except for the sink wood near the left and right banks, most of the sink wood was deposited in a direction parallel to the streamline, suggesting that it was influenced by running water. In addition, this survey found no sink wood near the gate. However, this may be because the sink wood was removed during sedimentation excavation to reduce the risk of gate blockage.

Among the sink wood identified in this survey, we extracted the following characteristics and explained them below.

- (1) Those presumed to be sink wood (Figure 6a)
They have knots and root nodules clearly sink wood (Figure 6b). The elevation increases from the upper end to the lower end, and the upper end impales on the lake bottom. These are expected to be cylindrical trunks of trees that have lost their branches and leaves and are highly probable to be sink wood.
- (2) A partially buried sink wood (Figure 6b)
The elongated shape and the root-like bumps suggest it is sink wood, but the central part is buried. The tree is presumed to be a sink wood because of its elongated shape and root-like knob, but the central part of the tree is buried.
- (3) Presumed to be sink wood, but its shape is distorted (Figure 6c).
The object is presumed to be sink wood because it has a trunk-like part, but it has a complicated shape and maybe the root part of a large tree with many branches remaining. However, it may be a root of a large tree with a complicated shape and many branches.
- (4) Difficult to determine if it is sink wood or not (Figure 6d)
Some objects are certainly at the bottom of the reservoir, but they are not clearly shaped enough to be identified as sink wood. A part of a large piece of sink wood may be visible even if it is not a large object, and future floods may wash the surrounding sediment to reveal it, so further observation is important.

5 CONCLUSION

In order to confirm the feasibility of sink wood exploration using MBES bathymetry survey, which is widely used for sedimentation surveys in Japanese dam reservoirs, a bathymetry survey was conducted on Susobana dam, and the results were analyzed. The findings are as follows.

- MBES has sufficient accuracy in detecting large sink wood at a depth of Susobana Dam Lake (about 30 m). Note that the horizontal resolution depends on the beam width.
- To detect sink wood, it is important to effectively map the unevenness of about 1 m on the sediment surface without removing protrusions, using random data after noise processing.
- There is a possibility that many objects exist on the reservoir bottom, but it is difficult to determine whether they are sink wood or not.
- Sink wood buried in sediment cannot be detected. Sink wood may be buried or exposed due to sediment movement caused by the progress of sediment deposition and changes in water level, so it is not safe to judge safe just because sink wood is not visible.

This survey provided valuable data for understanding the distribution of sink wood in the Susobana Dam reservoir bed. In the future, we plan to conduct additional measurements when large movements of sink wood are expected, such as after a flood, to clarify how they will move further and how much and how sink wood will be newly generated. In addition, it is necessary to develop survey methods and future forecasting methods that contribute to “sink wood triage,” namely, how to sort out those that cannot be left untreated from the viewpoint.

REFERENCES

- Bertoldi, W., Gurnell, A. M., and Welber, M. 2003. Wood recruitment and retention: The fate of eroded trees on a braided river explored using a combination of field and remotely-sensed data sources, *Geomorphology*, 180: 146–155.
- Brown, C. J., Beaudoin, J., Brissette, M., and Gazzola, V. 2019. Multispectral multibeam echo sounder backscatter as a tool for improved seafloor characterization, *Geosciences*, 9(3), 126.
- Calder, B. R., and Mayer, L. A. 2003. Automatic processing of high-rate, high-density multibeam echosounder data, *Geochemistry, Geophysics, Geosystems*, 4(6).
- Hellequin, L., Boucher, J. M., and Lurton, X. 2003. Processing of high-frequency multibeam echo sounder data for seafloor characterization, *IEEE Journal of Oceanic Engineering*, 28(1), 78–89.
- Koshiha, T., Kiyono, Y., Murakami, K., Takata, S., and Sumi, T. 2022. Possibility of Driftwood Detection in a Dam Reservoir with a Narrow Multi-Beam Sonar System, *Journal of Japan Society of Dam Engineers*, 32(1): 4–15.
- Ministry of Land, Infrastructure, Transport and Tourism, Japan, 2018. A Guide for Dam Reservoir Driftwood Control (in Japanese).
- Roberts, J. M., Brown, C. J., Long, D., & Bates, C. R. 2005. Acoustic mapping using a multibeam echosounder reveals cold-water coral reefs and surrounding habitats. *Coral Reefs*, 24(4): 654–669.
- Seo, J. I., Nakamura, F., Nakano, D., Ichiyanagi, H., and Chun, K. W. 2008. Factors controlling the fluvial export of large woody debris, and its contribution to organic carbon budgets at watershed scales, *Water Resources Research*, 44(4).
- Schalko, I., Lageder, C., Schmocker, L., Weitbrecht, V., and Boes, R. M. 2019. Laboratory flume experiments on the formation of spanwise large wood accumulations: I. Effect on backwater rise, *Water Resources Research*, 55(6): 4854–4870.
- U.S. Department of the Interior Bureau of Reclamation, 2016. Reservoir Debris Management.

HYPOS – Sediment management from space

M. Leite Ribeiro & M. Launay
GRUNER STUCKY, Switzerland

K. Schenk & F. von Trentini
EOMAP, Germany

M. Bresciani & E. Matta
Consiglio Nazionale delle Ricerche, Italia

A. Bartosova & D. Gustafsson
SMHI, Sweden

ABSTRACT: The HYPOS tool provides comprehensive, reliable, and scalable access to key hydrological, sediment and water quality parameters to be used in supporting different stages of hydropower installation life cycles. To support the ecological and economical assessment during design and operation phases, HYPOS transforms satellite-based water quality and sediment information together with a worldwide hydrological model, which can be adapted to local conditions at the user's request, and on-site measurements into data useful for decision-making. The water quality and physical parameters supporting the analysis of sediment dynamics in hydropower installations and planning phases are operationally derived from multispectral satellite data from different sensors such as Sentinel-2, Landsat 8/9 or very high-resolution data from Planet SuperDoves. Land use and land cover changes as well as a combination of hydrological and meteorological re-analyses and forecasts complement the analysis. It is showcased in a use case in the Banja and Moglice HPPs, in Albania.

1 INTRODUCTION

Sediment monitoring is highly important for the design of new reservoirs, ensuring the prediction of the incoming fluxes which can be useful to dimension the reservoir infrastructure and to estimate the necessary maintenance in the future. However, sediment monitoring can be expensive, require know-how, commitment, and can be extremely lengthy. Often, it is not implemented before the project is well advanced. By that time, it is usually late to the actual sediment transport dynamics in the location of the future reservoir into account in the design. This can lead to disastrous consequences like failed investments and security concerns (e.g., bottom and middle outlet for routing floods can become blocked).

Sediment monitoring networks can collect sediment transport data continuously for the operational monitoring of flushing events, but are limited, at best, to a few points along the river reach of interest. In more complex morphologies, this may not be enough. Satellites can close this gap with generally seamless monitoring of all relevant river reaches.

An innovative Decision Support Tool is developed within the Hypos project to provide essential assets for asset managers, planners, and decision-makers facing sediment management issues in their existing or future reservoirs.

The integrated approach aims to bring together high-quality satellite-based measurements, state-of-the-art hydrological modelling, and available in-situ data to develop better reservoir

management strategies. The tool enables the retrieval and processing of both historical and near real-time data, contributing to improved sediment management and reduced environmental impacts. In this paper, the developed tool is showcased for the Banja Reservoir, in Albania, where it provided valuable information to understand sediment dynamics.

2 STUDY SITE

The Devoll cascade in Albania consists of two existing hydropower plants (HPP) constructed in the Devoll River and owned by Statkraft (Norway), the Banja and Moglicë HPPs. The Banja HPP is located in Cërrik Municipality in Elbasan County, 65 km southeast of Albania's capital Tirana, and has been officially commissioned in September 2016. Moglicë HPP, located further upstream has been commissioned in 2019. In total, the two plants have an annual production of around 700 GWh, which represents a 17 % increase in Albania's total energy production.

At the end of 2015, a sediment transport measurement research station has been installed to monitor the suspended sediment concentration (SSC) every 30 minutes. The station has been logging continuously from January 2016 until May 2018 in periods where the river had a water depth of more than 1 m at Kokel bridge (Aleixo, et al., 2018).

3 METHODOLOGY

HYPOS, the online tool developed in the frame of a European Union funded project (2019-2022) includes several functionalities to access, visualize, analyze, and calculate data relevant to hydrological and sediment studies in the hydropower sector. Various data sources originating from satellite images, hydrological models and in-situ measurements can be introduced into the tool. It includes for example the ingestion of SMHI's (Swedish Meteorological and Hydrological Institute) worldwide HYPE model data to include river discharge data, precipitation, specific runoff, and other variables (Bartosova, et. al, 2021).

Satellite-based products are another data source, which can be operationally processed with the Modular Inversion and Processing System MIP (Heege et al. 2014, Matta et al., 2023) of EOMAP. It accesses various satellite data archives from satellite providers such as ESA, USGS, or Planet Labs to generate quantitative and independently derived data such as turbidity, organic absorbers, chlorophyll, water surface temperature (Bresciani et al. 2019), and water level.

The spatial resolution of satellite-based measurements is related to the respective satellite sensor, e.g. 10 m for data from Sentinel-2, or 30 m for data from the Landsat sensor family. Most water-related satellite-based data products are provided in specific raster formats, which contain the entire spatially expanded measurements for each satellite record with a given time stamp. Typically, several records per week can be utilized under good weather conditions, whereas clouds create spatiotemporal data gaps.

For the pilot areas, the backend further ingests SMHI's HYPE model data into the system every day, which are immediately visualized in the portal. Users can upload in-situ measurements where available, such as measurements of total suspended matter or discharge. The basic requirement for such data is proper metadata that relates the measurements with time stamps, geographical coordinates, and a user-defined name.

The tool can display all these data sources in one map and creates time series plots for selected variables of point data and spatially aggregated raster data (satellite data). This enables the user to quickly oversee the catchment and identify trends or certain periods with interesting behavior (extremes).

Figure 1 presents a view of the Hypos portal, accessed through the following address: <https://hypos.eoport.de>.



Figure 1. View of the Hypos portal (<https://hypos.eoportal.de>).

Data ingested into the HYPOS portal is used to calculate sediment-related parameters, such as sediment fluxes upstream and downstream of a dam, or monthly and yearly sedimentation trapping rates in the reservoir. For the calculation of sediment flux, suspended sediment concentration (SSC) in g/m^3 is multiplied by the discharge at a given location, e.g. the inlet and outlet of the reservoir. In absence of in-situ measurements, the tool can use discharge data generated by hydrological models such as SMHI's HYPE model into the portal, included in the portal. SSC can be calculated through calibration of the turbidity measurements from the satellite at the given locations. In the absence of in-situ data, an initial assessment of the given environmental conditions can be used (e.g. a fixed factor between turbidity and SSC or any given formula from the literature). In case nearby in-situ measurements of SSC, representative of the inflow area, are available for concurrent satellite and in-situ measurements, the calibration accuracy can be improved in a few clicks using the nonlinear regression tool. The calculation of sediment fluxes at any meaningful river section (e.g., inflow and outflow) is then a simple workflow that assigns the SSC calibration formula, the turbidity data set from the satellite with the respective virtual station, the discharge data set from the hydrological model for a representative, nearby point. The output data are displayed in a graphical pop-up window and can then be stored as new data set to the system.

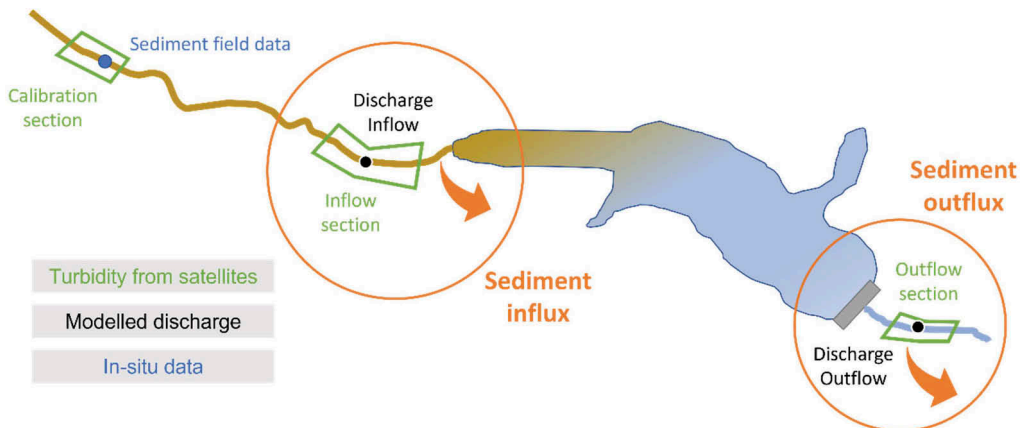


Figure 2. Calculation of sediment fluxes based on different input.

4 VALIDATION

The satellite-derived turbidity measurements were validated with a specific in-situ campaign performed between 22 and 25 September 2021 (Figure 3). Hyperspectral above-water remote sensing reflectance and subsurface irradiance reflectance were measured using WISP-3, Spectral Evolution sr-3500 and ROX spectroradiometers.

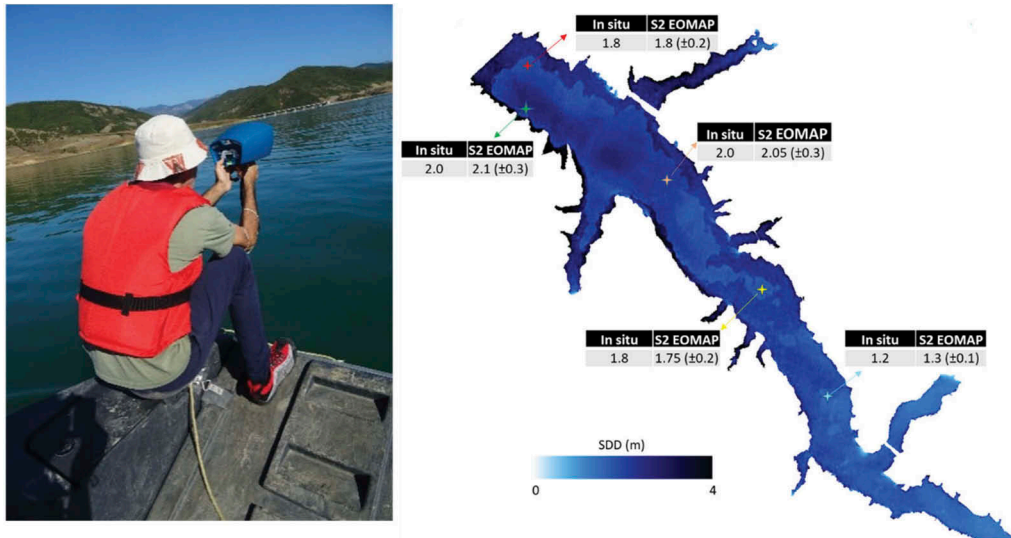


Figure 3. Photos of the in-situ activities conducted at Banja (left) and location of the measured points in the reservoir (right).

Radiometric data collected with in situ hyperspectral sensors were quality controlled and processed, and the mean and standard deviation of the data were calculated resulting in one hyperspectral remote sensing reflectance measurement per measured station. These hyperspectral measurements were resampled at Landsat8-OLI bands and Sentinel 2-MSI bands to enable direct comparison with satellite observations using the Signal Response Function (SRF) of the respective sensors. The SRF of a sensor defines the probability that a photon of a given wavelength is detected by the sensor.

The water quality parameters derived by using the MIP code applied to satellite images have been validated based on the comparison with respect to the in-situ data. The focus on the water quality parameters validation was mostly on Total Suspended Matter (TSM) and Transparency (Secchi disk depth), which are crucial parameters for the evaluation of the status of HYPOS hydropower case studies.

In Figure 4, the TSM maps obtained applying MIP code to Sentinel-2 MSI and Landsat-8 OLI for all HYPOS case studies were compared to in situ derived TSM values, including two sites from other study sites in Switzerland (Verbois and Gebidem dams). The results clearly denote the good match-up between satellite products and in situ data, both for waters characterized by low concentrations and for those with higher concentrations. The application of statistical metrics to evaluate the accuracy of the products shows results that indicate a very good product validation (Figure 4) with R^2 close to 1 and with comparable average in situ data with respect to average satellite products.

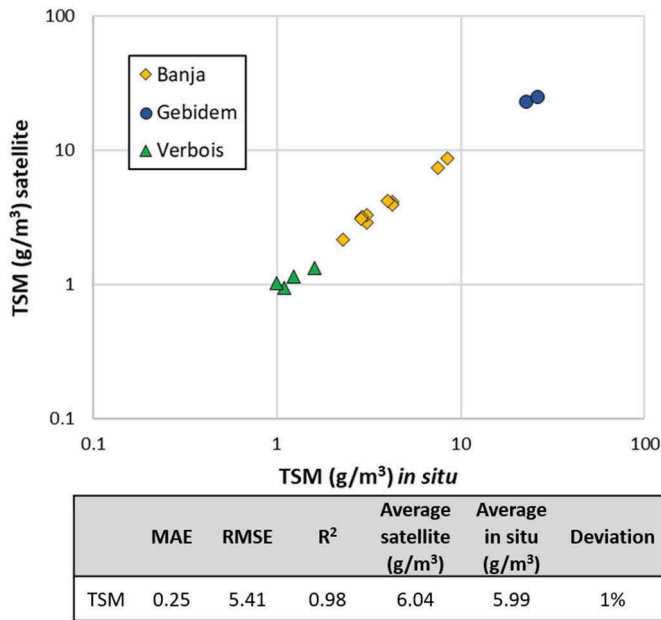


Figure 4. Scatter plots of satellite-derived products and in situ concentrations of TSM for the different HYPOS case studies; in yellow for Banja reservoir, in green for Verbois Chancy-Pougny site (Switzerland), in blue for Gebidem dam (Switzerland).

5 RESULTS

By processing archived satellite imagery from 2016 onwards, as well as conducting operational monitoring of new acquisitions, the commissioning of the two power plants could be tracked from space (Figure 5). The beginning of operations of the Moglice dam in summer 2019 is visible in the turbidity measurements from space at the outflow (blue time series). Due to the high re-suspension along the riverbed, this signal gets mostly lost for river sections further downstream at Kokel (orange) and near the inflow of the Banja reservoir at Gramsh (green). This relatively simple analysis can be performed in the HYPOS tool within seconds, once all data is processed and already reveals valuable information on the sediment dynamics along the Devoll River in a spatial dimension.

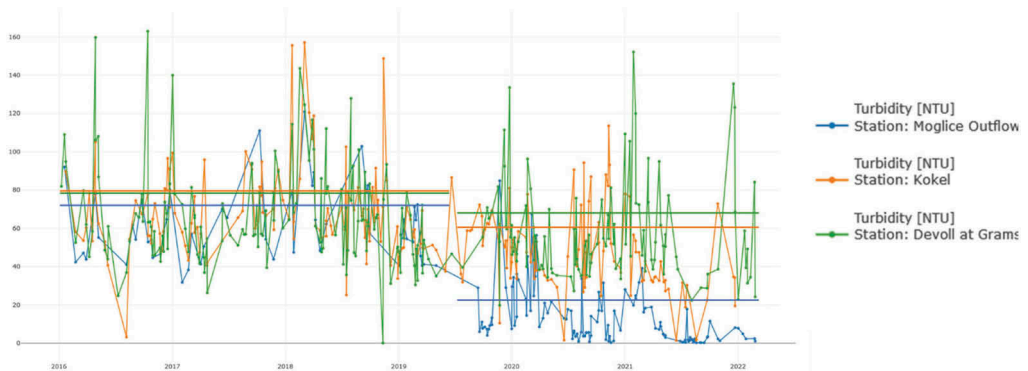


Figure 5. Turbidity time series from satellite measurements for the years 2016 to 2022. The horizontal lines depict the mean values for the two periods before and after the operation beginning of the Moglice dam.

Additionally, the spatial dynamics of sediments in the reservoirs and in the Devoll river can be observed with the HYPOS tool. Figure 6 shows the HYPOS portal with a timeseries overlay. These timeseries were extracted for the polygon at the shown location. The turbidity in the high-flow season from 2018 to 2021 peaks around 10 – 20 NTU at the outflow and up to 200 NTU at the inflow from Devoll river. The satellites reveal how much the turbidity values differ in their spatial distribution.

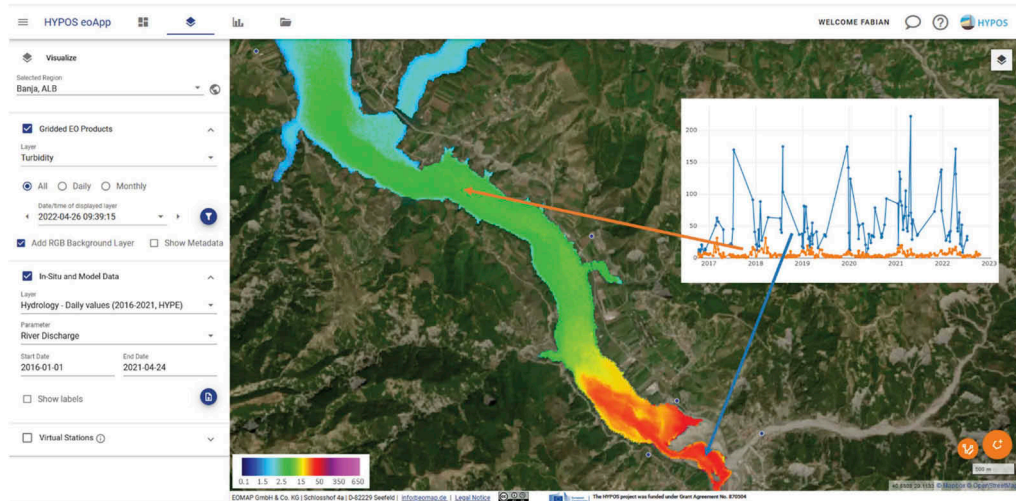


Figure 6. Virtual Stations at the entrance (blue time series) and at the middle (orange time series) of the Banja Reservoir showing the turbidity in Nephelometric Turbidity Unit (NTU).

By using the modelled discharge at the inflow section of the Devoll River to the Banja reservoir near Gramsh and the outflow directly downstream the Banja dam, as well as the associated concentrations from satellite-based turbidity measurements, the system can calculate the sediment fluxes at these two river points (Figure 7). The outflow is much less than the inflow and the trapping efficiency of the reservoir is around 40 %.

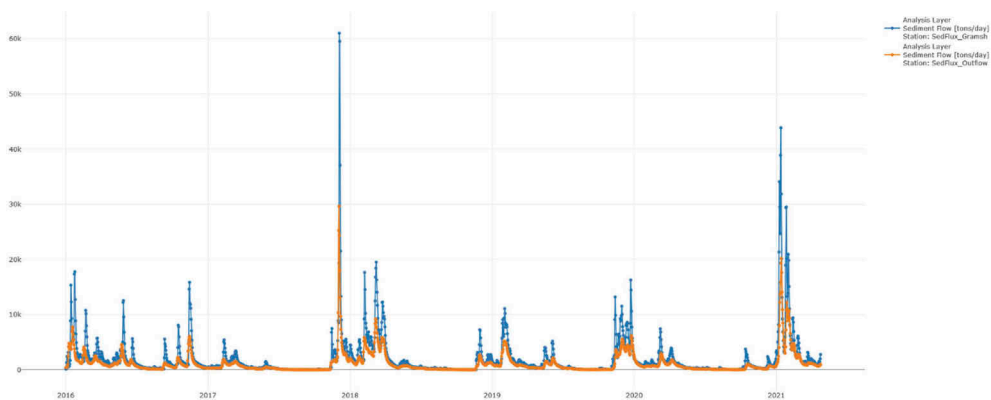


Figure 7. Sediment fluxes (tons/day) at the inflow (blue) and outflow (orange) of the Banja reservoir, as calculated with the modelled discharge and SSC from satellite measurements.

6 CONCLUSIONS

The great advantage of the HYPOS solution is the relative independency of in-situ measurements and the special dimension of the analysis of sediments. The turbidity measurements by satellites reach back until 2015 for Sentinel-2 (10 m resolution) and even back to the 1980's for Landsat (30 m resolution), which enables the system to estimate long-term sediment dynamics. This includes trends, but also seasonality identification, or the assessment of high-impact events (floods). The river discharge can be modeled with the globally available HYPE model, which can also be adjusted and refined for local conditions if demanded by the customer. By combining sediment dynamics from satellites and river discharge from a model, the user can calculate sediment fluxes and estimate the trapping efficiency of a reservoir. On the other side, it is easily possible, and often of value, to integrate time series of in-situ measurements into the tool's calculations. Even short periods of measurements (e.g., one year of sediment concentrations from an old station 10 years ago) can help to robustly extend this short time series into a much longer data set. This enables the user to set up a better sediment management plan or even newly built infrastructure, such as dams and bypasses.

This work has presented the results of the application of the Hypos tool to the Banja and Moglice HPPs, in Albania. Results of the analysis of the data derived by satellite, validated by a field campaign show the influence of the commissioning of the Moglice HPP in the reduction of the sediment transport of the Devoll River, as well as the trapping efficiency of the Banja reservoir.

ACKNOWLEDGEMENTS

This work was supported by the EU Horizon 2020 program with the project HYPOS, under the Grant Agreement No. 870504.

For further information, visit the website: <https://hypos-project.eu/> or access the portal directly at: <https://hypos.eoportal.de>.

REFERENCES

- Aleixo, R., Gerrero, M., R  ther, N. And Stokseth, S. (2018): Development of a method for suspended sediment transport monitoring by means of ADCP measurements, E3S Web of Conferences 40:05016, January 2018.
- Bartosova, Alena, Arheimer, Berit, de Lavenne, Alban, Capell, Ren  , & Str  mqvist, Johan. (2021). Large-Scale Hydrological and Sediment Modeling in Nested Domains under Current and Changing Climate. [https://doi.org/10.1061/\(ASCE\)HE.1943-5584.0002078](https://doi.org/10.1061/(ASCE)HE.1943-5584.0002078)
- Bresciani M, Giardino C., Stroppiana D., Dessena M.A., Buscarinu P., Cabras L, Schenk K., Heege T., Bernert H., Bazdanis G. & Tzimas A. (2019): Monitoring water quality in two dammed reservoirs from multispectral satellite data, European Journal of Remote Sensing, 10 pages, DOI: 10.1080/22797254.2019.1686956
- Heege, T., Kiselev, V., Wettle, M., Hung N.N. (2014): Operational multi-sensor monitoring of turbidity for the entire Mekong Delta. Int. J. Remote Sensing, Special Issues Remote Sensing of the Mekong, Vol. 35 (8), pp. 2910–2926
- Matta, E., Bresciani, M., Tellina, G., Schenk, K., Bauer, P., Von Trentini, F. and Ruther, N (2023). Data Integration for Investigating Drivers of Water Quality Variability in the Banja Reservoir Watershed. Water 15, no. 3: 607. <https://doi.org/10.3390/w15030607>

Comprehensive assessment of sediment replenishment and downstream hydro-geomorpho-ecology, case study in the Naka River, Japan and the Buëch River, France

Jiaqi Lin, Sameh A. Kantoush & Tetsuya Sumi

Water Resources Research Centre, Disaster Prevention Research Institute, Kyoto University, Japan

ABSTRACT: Sediment replenishment is one common restoration technique to tackle the sediment deficit problem caused by dam construction. The additional sediment supply from replenishment site is beneficial for recovering downstream morphology and aquatic ecosystem. In this paper, we would like to develop a novel methodological approach for assessment of the riverine system during implementation of sediment replenishment in the Naka River, Japan and the Buëch River, France. Key factors for replenishment (placed volume and transported volume, magnitude and duration of flushing flow), and downstream impacts (habitat structures, flow velocity, water depth, riverbed level and substrates, fish species) are considered. Several indices for replenishment and riverine assessment, such as Transported ratio (TR), GUS (Geomorphic Units Survey), BCI (Bed Change Indicator), and Fish Diversity Index (H Value) are determined to statistically evaluate the replenishment works. The results show that the efficiency of SR erosion of France project is higher than Japanese project due to the different optimization strategies. Moreover, both projects can enhance the downstream morpho-ecology by increasing the numbers of GU and promoting the diversity of fish species. It is recommended to conduct continuous SR with adaptable sediment supply to maintain such positive impacts on downstream reach.

1 INTRODUCTION

SR, as a common mitigation approach for river restoration, has already been implemented around the world, for instance, the Naka River (Lin et al., 2021), the Tenryu River (Okano et al., 2004), and the Uda River (Kantoush and Sumi, 2011) in Japan, the Trinity river (Gaeuman, 2014) in America, and the Buëch River (Brousse et al., 2019), the Sarine River (Stahly et al., 2019), and the Old Rhine River (Paquier et al., 2018) in Europe. Typical projects for those river basins, the running of SR leads to some positive impacts on downstream reach, for instance, the reproduction of shallow geomorphic units (riffle, rapid, and run) (Lin et al., 2021), recovery of the riverbank incision and instability (Paquier et al., 2018). However, adverse impacts should also be considered, such as the increasing turbidity at downstream reach due to the utilization of the in-channel stockpile method for replenishment (Ock et al., 2013). The differences in implantation characteristics, such as implementation methods of replenishing, flushing flow, the placed volume of sediment, as well as the grain size of the scouring sediment are the main reasons that generate successful or unsuccessful outcomes.

The current research gaps are the lack of a comprehensive approach to assess the downstream responses of SR to judge whether the projects are successfully conducted or not. There is rare research that mentioned the relationships between the characteristics of SR (volume, grain size, arrangement, and injection method), flow conditions, and the downstream morpho-ecological responses. Previous research mainly emphasized the geomorphological and ecological parts of SR solely. For instance, the alteration of river cross sections, riverbed substrates, and habitat structures are the three common aspects that have always been investigated for downstream geomorphology (Kantoush et al., 2010). While for ecology, the key points are the characteristics

of habitat quality, such as water temperature, turbidity, and POM (Particulate organic matter). Hence, we still need to create a simple and integrated method to fill the blank among river geomorphology, aquatic habitat, and characteristics of SR.

In this paper, we develop a comprehensive methodology for the assessment of the replenishment, including the efficiency of the replenishment and the downstream hydrogeomorpho-ecological responses. Several assessed indicators are considered to statistically analyze the impacts, including Transported ratio (TR), GUS (Geomorphologic Units Survey), BCI (Bed Change Indicator), and Fish Diversity Index (H Value). In the end, some discussions related to the assessment results and recommendations for sediment replenishment were highlighted.

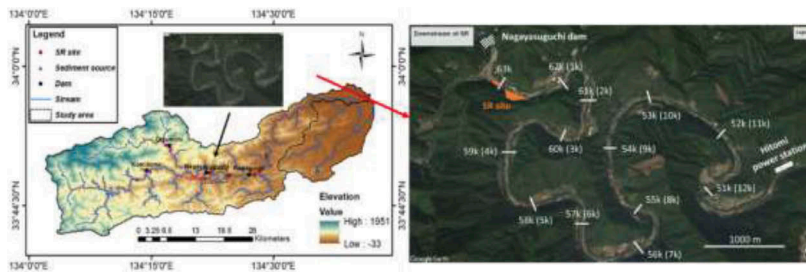


Figure 1. The study area in the Naka River. Left figure: the location map of the Naka River Basin. Right figure: the SR site at Kohama and the 12 km study reach.

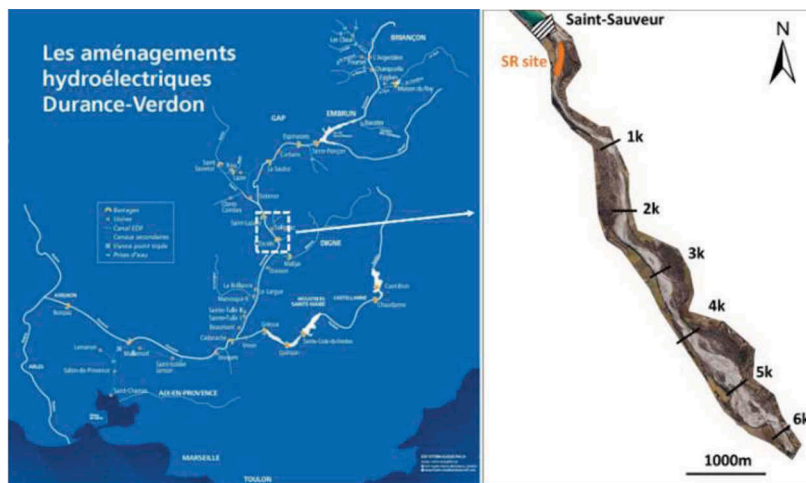


Figure 2. The study area in the Buëch River. Left figure: the location map of the Buëch River. Right figure: the SR site at Saint-Sauveur dam and the 6 km study reach.

2 STUDY AREAS

The SR project conducted in the Naka River was selected as one of the study areas. It is located in the Tokushima prefecture, Japan (see the left figure in Figure 1). The SR has been started to be implemented at 6 locations downstream of Nagayasuguchi dam since 1991. Nevertheless, only the SR works at the Kohama site are maintained now with an annual placed sediment of around 200,000 m³. Hence, the target area is the 12 km reaches downstream of the SR site at Kohama with an interval of 1 km (see the right figure in Figure 1). The maximum releasing discharge from the upstream dam is varied from 400 m³/s to 5000 m³/s annually since it is related to the precipitation.

Another SR project is the Buëch River, which is located in the Southern French Prealps. The SR was implemented downstream of the Saint-Sauveur dam in 2016 and 2018 with a placed volume of around 43,500 m³. The target area is the 6 km reach downstream of the site (see Figure 2). The mean daily discharge from the upstream dam is around 14 m³/s and the maximum daily discharge is varied from 100 m³/s to 300 m³/s (Brousse et al., 2019).

3 METHODOLOGY

A unified methodological approach for the assessment of the riverine system during SR was developed. First of all, the efficiency of the SR for transporting the scouring sediment under different flushing flows was discussed based on two newly discovered parameters called the transported ratio (TR) and the total flushing water volume (TFWV) (see A in Figure 3). Meanwhile, several indicators for riverine assessment from the literature have been utilized to present the downstream responses of SR, for instance, the Geomorphic Units Survey (GUS) (Belletti et al., 2015), the Bed change indicator (BCI) and Fish Diversity Index (H value) (Lakra et al., 2010) (see B in Figure 3).

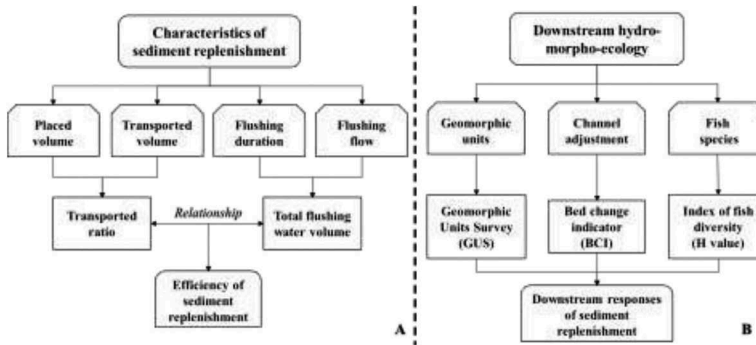


Figure 3. The flow chart of the comprehensive assessment approach. A: the assessment of SR efficiency. B: the assessment of downstream hydro-morpho-ecology.

3.1 Erosion efficiency of sediment replenishment

To evaluate the efficiency of sediment replenishment, we considered the relationship between total flushing water volume (TFWV) and transported ratio (TR), which can be calculated by:

$$TFWV = \sum_{i=1}^n \bar{Q}_{i,i-1} * \Delta t_{i,i-1} \quad (1)$$

$$TR = \frac{\text{Transported volume (m}^3\text{)}}{\text{Placed volume (m}^3\text{)}} * 100\% \quad (2)$$

Where, $\bar{Q}_{i,i-1}$ is the average magnitude of the flushing flow between two time steps in m³/s, and $\Delta t_{i,i-1}$ is the interval of the time step in seconds.

3.2 Geomorphic units survey

To simply analyze the data of the geomorphic units, the Geomorphic Units Survey (GUS) was considered, which is a common classification and assessment system utilized in European countries (Belletti et al., 2015). The system first classifies the macro-units at the reach (riffle, pool, puddle, etc.), and then several subtypes of each macro unit (forced pool, scoured pool, etc.) are recognized if a detailed geomorphic survey is required. For our study, we only considered the first level of classification (macro units) since the data is limited. Two sub-

indicators, the GUS Richness index (GUSI-R) and GUS Density index (GUSI-D) were applied in our study, which can be calculated by:

$$GUSI - R = \sum \frac{NT_{GU}}{N} \quad (3)$$

$$GUSI - D = \sum \frac{N_{GU}}{L} \quad (4)$$

Where, NT_{GU} and N_{GU} are the total number of types and quantities of macro units within the investigated reach respectively. While N is the total number of all possible types of units (including macro-units and sub-types) within the reach. Because we only considered the macro units in our study, the N is equal to N_{GU} here. L is the length of the study reach, which is equal to 1 km.

3.3 Channel adjustment

The additional sediment supply from the SR site usually leads to bed aggradation at the downstream reach. To assess such alterations of the riverbed, we calculated the average bed level changes based on the BCI value (Esmaili et al., 2017):

$$BCI = \left(\sum_{i=1}^n (z_{i_{y2}} - z_{i_{y1}}) \right) / n \quad (5)$$

Where $z_{i_{y2}}$ is the bed level at node i in the next year, and $z_{i_{y1}}$ is the bed level at node i in the previous year. And n is the total number of nodes.

3.4 Index of fish diversity

The variation of fish species and numbers is a straightforward way to investigate the quality of the spawning grounds in the river reach. We would like to utilize the Shannon-Wiener index of diversity (H value) to analyze the diversity of species (Lakra et al., 2010), which can be calculated as:

$$H = \sum_{i=1}^n \left(\frac{n_{si}}{n_{st}} \log_2 \left(\frac{n_{si}}{n_{st}} \right) \right) \quad (6)$$

Where, n_{si} is the total number of individuals of one specie and n_{st} is the total number of individuals of all species.

4 RESULTS

4.1 The assessment of SR efficiency

Regarding the Naka River, the analysis of SR efficiency was conducted at two replenishment sites upstream and downstream of the Kohama bridge from 2009 to 2020. The representative flow was calculated when the releasing discharge from the Nagayasuguchi dam was larger than 200 m³/s (submergence of replenishing stockpile happened). According to Figure 4 A, before 2015, both two SR sites (double sites) existed and the maximum TR is 10% higher than the single site case (after 2015). It is a suitable countermeasure to divide the replenishing sediment and placed them at multiple downstream locations to promote the SR efficiency since the placed volume is higher.

Considering the Büech River, SR was only conducted in 2016 and 2018, and the data for analysis of the relationship between TR and TFWV was very limited, and we only calculated the placed sediment, transported sediment, and corresponding TR. During the first replenishing in 2016, the majority of the sediment that was placed at the middle channel and the right bank was efficiently eroded, while limited sediment was scoured downstream at the left bank. To mitigate such issues, sediment from the left bank was moved and a new berm was created in the middle of the channel. The movement of sediment from low flushing area to high flushing area is an

efficient way to increase the TR value from 50% in 2016 to 83% in 2019 and thus can be proved as a successful strategy for replenishment implementation (Figure 4 B).

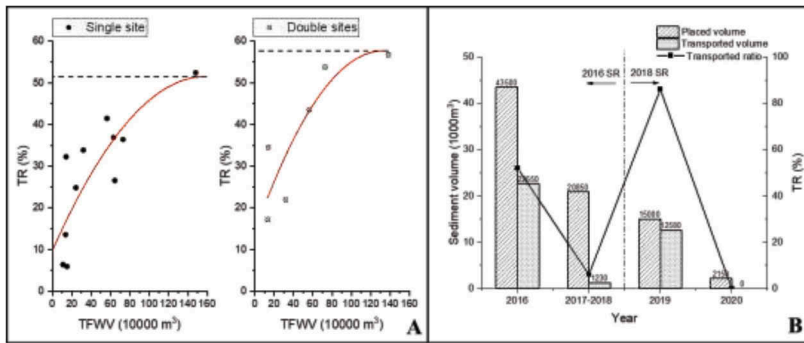


Figure 4. The assessment results of SR efficiency. A: the results in the Naka River that consider the single and double SR sites. B: the results in the Büech River that considering the two SR implemented in 2016 and 2018.

4.2 The assessment of downstream hydro-geomorpho-ecology

For the downstream responses of SR implementation, the assessment was conducted based on several developed indicators and approaches (GUS, BCI, H value,). Regarding the geomorphic unit survey (GUS), large and integral toros (glide) were transferred to pools, small runs, and rapids after the significant flood in 2015 (transported volume around 300,000 m³), and the geomorphic units tended to be evenly distributed in the Naka River (Figure 6). Moreover, after the SR was implemented in 2016, the run was transferred to rapid and pool in the Büech River. The additional sediment supply from SR tended to break the integrated units into semi-units and therefore enhance the diversity of the habitat structures (Morgan, 2018).

As a consequence of geomorphic unit alterations, the GUSI-D indicators were increasing after the SR in both cases, while the opposite tendency can be observed for GUSI-R (Figure 6 and Figure 7). Due to the significant sediment supply and flushing flow, the quantities of GU downstream were raised, while the types of GU were not promoted. Thus, the density index (GUSI-D) increased while the richness index decreased (GUSI-R).

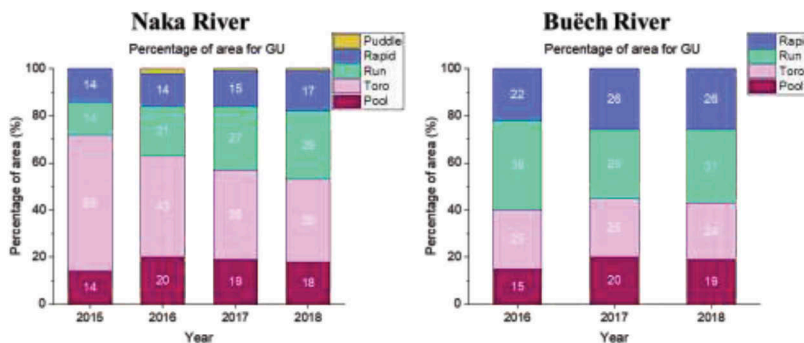


Figure 5. The percentage of area of geomorphic units (GU) in the Naka River and the Büech River.

Regarding the channel adjustment, the BCI value has a close correlation to the sediment supply from the SR site in both cases (Figure 8). It means that the transported sediment from the SR site was mainly deposited downstream. Such deposited sediment can not only enrich the bed substrate (tackle armouring issues) but also promote the formation of GU (riffles), and thus, restoring the downstream geomorpho-ecology.

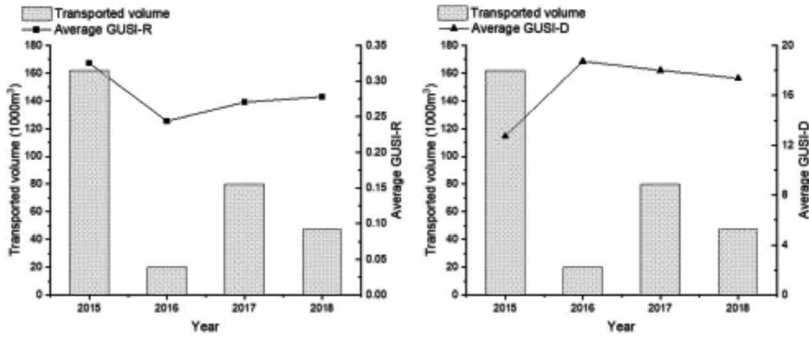


Figure 6. The variation of GUSI-R and GUSI-D indicators with the changes of transported sediment from SR site in the Naka River.

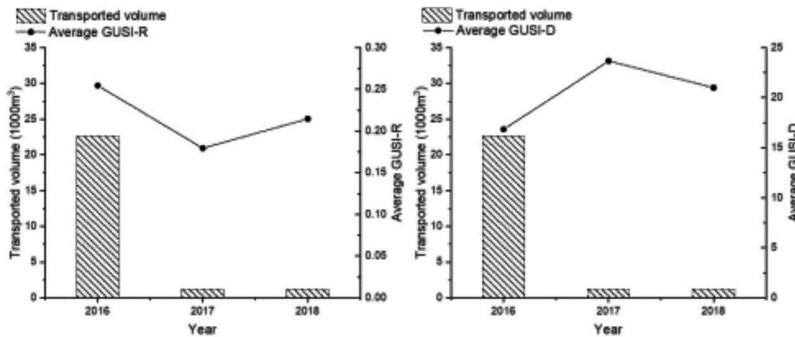


Figure 7. The variation of GUSI-R and GUSI-D indicators with the changes of transported sediment from the SR site in the Bučeh River.

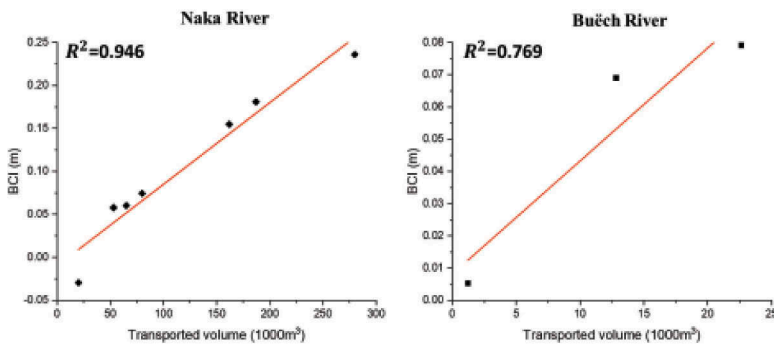


Figure 8. The relationship between BCI and transported volume from SR site in the Naka River and the Bučeh River.

For the ecological consideration, the time series of H values were calculated at three main spawning grounds, which were located 0.5 km, 2 km, and 11 km downstream of the replenishment site from 2009 to 2017 in the Naka River (Figure 9). We can roughly analyze that the H value started to increase from the implementation of SR in 2010 at all spawning grounds. Such promotion of habitat quality stopped and adverse impacts can be observed after 2015 in the near two spawning grounds (0.5 km and 2 km). It can be noticed that the transported sediment started decreasing after 2015 (from 390,000 m³ to 160,000 m³), which may be the main reason to cause the turning points of the H value. A delay of such reduction occurred at

11 km (from 2016) which may be because sediment needs time to be transported to the site far away from the replenishment location. Furthermore, the same increasing tendency can be founded after the SR implementation in 2016, while reduced after the SR stopped in 2017 and 2018 in the Buëch River (Figure 9). In summary, fish diversity has a close correlation to the sediment supply from the SR site since the geomorphological alterations are linked to the habitat quality and diversity. Therefore, it is recommended to conduct continuous SR to maintain the adapted sediment supply annually for the consideration of river restoration.

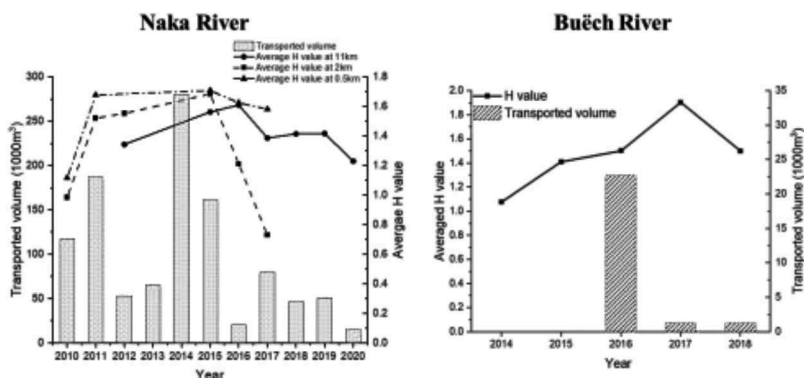


Figure 9. The relationship between the average H value and the transported volume from the SR site in the Naka River and the Buëch River.

5 CONCLUSIONS

In conclusion, a compressive assessment of SR works was conducted in the Naka River, Japan, and the Buëch River, France. The replenishment characteristics and downstream hydro-geomorpho-ecology were evaluated based on several simple indicators, including TR, TFWV, GUSI-R, GUSI-D, BCI, and H value. The results of the assessment can be utilized to optimize the SR strategies at two rivers in the future.

Regarding the Naka River, the efficiency of replenishment is not higher due to the location of the stockpile and the considerable volume of placed sediment. Furthermore, new riffles and pools were formatted due to the sediment supply from SR. The alterations of geomorphic units were beneficial for the fish species and the corresponding H values were promoted. However, a decrease in such benefits can be observed after the significant flood occurred in 2015 since the volume of transported sediment from SR was reduced. Therefore, it is necessary to promote the SR efficiency under low flushing flow (lower than 1000 m³/s) to maintain an adaptable sediment supply to the downstream annually. Future countermeasures with multiple replenishment sites and lower placed volume should be considered.

Considering the Buëch River, efficient replenishment works were successfully conducted due to the appropriate strategy of stockpile placement. For downstream responses, the SR also enhanced the formation of new geomorphic units (pools and rapid) and the corresponding H value was increased as well. However, the responses were reduced after the SR since the remaining sediment at the replenishment site was small and there was no sufficient sediment supply downstream. Thus, it is recommended to conduct continuous SR in the Buëch River instead of the one-time project to restore the sustainability of the downstream habitat.

ACKNOWLEDGEMENT

This work was supported by JSPS KAKENHI Grant Number JP21H01434 and Japan Science and Technology Agency (JST SPRING). The Authors appreciate the support from Naka River Office in Japan and the EDF in France.

REFERENCES

- Belletti, B., Rinaldi, M., Comiti, F., Nardi, L., Mao, L. & Bussetini, M. (2015) The Geomorphic Units survey and classification System (GUS). Proceedings IS Rivers, 2nd International Conference.
- Brousse, G., Arnaud-Fassetta, G., Liébault, F., Bertrand, M., Melun, G., Loire, R., Malavoi, J. R., Fantino, G. & Borgniet, L. (2019) Channel response to sediment replenishment in a large gravel-bed river: The case of the Saint-Sauveur dam in the Buëch River (Southern Alps, France). *River Research and Applications*, 36, 880–893.
- Esmaeili, T., Sumi, T., Kantoush, S. A., Kubota, Y., Haun, S. & Rütger, N. (2017) Three-Dimensional Numerical Study of Free-Flow Sediment Flushing to Increase the Flushing Efficiency: A Case-Study Reservoir in Japan. *Water*, 9, 900.
- Gaeuman, D. (2014) Analyses to support gravel augmentation recommendations for the Trinity River, California. Weaverville, California, TRRP, Trinity River Restoration Program.
- Kantoush, S. & Sumi, T. (2011) Sediment replenishing measures for revitalization of Japanese rivers below dams. Proceedings of the 34th World Congress of the International Association for Hydro-Environment Research and Engineering: 33rd Hydrology and Water Resources Symposium and 10th Conference on Hydraulics in Water Engineering. Engineers Australia.
- Kantoush, S., Sumi, T. & Kubota, A. (2010) Geomorphic response of rivers below dams by sediment replenishment technique. *River Flow 2010*, 1155–1164.
- Lakra, W. S., Sarkar, U. K., Kumar, R. S., Pandey, A., Dubey, V. K. & Gusain, O. P. (2010) Fish diversity, habitat ecology and their conservation and management issues of a tropical River in Ganga basin, India. *The Environmentalist*, 30, 306–319.
- Lin, J., Kantoush, S. A., Sumi, T. & Takemon, Y. (2021) Comprehensive Assessment of Sediment Replenishment in Naka River: Hydrological, Morphological, and Ecological Perspectives. *Journal of Japan Society of Civil Engineers, Ser. B1 (Hydraulic Engineering)*, 77, I_379-I_384.
- Morgan, J. (2018) The effects of sediment supply, width variations, and unsteady flow on riffle-pool dynamics.
- Ock, G., Sumi, T. & Takemon, Y. (2013) Sediment replenishment to downstream reaches below dams: implementation perspectives. *Hydrological Research Letters*, 7, 54–59.
- Okano, M., Kikui, M., Ishida, H. & Sumi, T. (2004) Reservoir sedimentation management by coarse sediment replenishment below dams. Proceedings of the Ninth International Symposium on River Sedimentation.
- Paquier, A., Chardon, V., Schmitt, L., Piégay, H., Arnaud, F., Serouilou, J., Houssier, J., Clutier, A. & Rivière, N. (2018) Geomorphic effects of gravel augmentation on the Old Rhine River downstream from the Kembs dam (France, Germany). *E3S Web of Conferences*, 40.
- Stahly, S., Franca, M. J., Robinson, C. T. & Schleiss, A. J. (2019) Sediment replenishment combined with an artificial flood improves river habitats downstream of a dam. *Sci Rep*, 9, 5176.

Experimental modeling of fine sediment routing: SEDMIX device with thrusters

Montana Marshall, Azin Amini & Giovanni De Cesare
Platform of Hydraulic Constructions (PL-LCH), EPFL, Switzerland

ABSTRACT: Reservoir sedimentation is a key challenge for storage sustainability because it causes volume loss, affecting hydropower production capacity, dam safety, and flood management. A preliminary EPFL study proposed and studied an innovative device (called SEDMIX), which uses water jets to keep fine sediments near the dam in suspension and ultimately allows the sediments to be released downstream. The SEDMIX device is composed of two rigid steel parts: one floating and one on the basin bottom holding a multi-jet manifold frame. The jets induce a rotational flow which creates an upward motion and keeps fine sediments in suspension near the dam and water intakes. The sediment can then be continuously released downstream through the power waterways at acceptable concentrations, without additional water loss or required energy. The efficiency of the SEDMIX device has been confirmed through recent experimental simulations and numerical analyses at EPFL. This study involves updated experimental simulations to include thrusters in the device design, instead of jets, because they lead to a less complex arrangement that requires less energy to operate. The experimental setup is similar to the previous experiments (utilizing a glass tank), and tests different thruster parameters to understand the resulting changes in tank turbidity (using turbidity meters).

1 INTRODUCTION

1.1 *Scientific background*

In high-altitude alpine reservoirs, turbidity currents are the main inflow process for sediments (De Cesare, 1998). Turbidity currents mainly occur during floods, when a sediment-laden river enters the reservoir downstream of the root delta. These currents transport fine sediments downstream to the deepest part of the reservoir, close to the dam. This causes two main issues: increased sedimentation at the dam (decreasing the available storage volume for hydropower and flood control), as well as negatively impacting operation of the bottom outlets and/or water intakes.

Reservoir sedimentation is a key challenge for storage sustainability because it causes volume loss, affecting hydropower production capacity, dam safety, and flood management. According to a recent UN University study (Perera et al, 2023), it is forecasted that dams around the world will lose nearly a quarter of their storage capacity due to sedimentation by 2050. In Switzerland, their forecast is even more dramatic (albeit slightly unrealistic), predicting that the country-wide storage capacity will see one-third reduction from sedimentation by 2050. This storage loss rate is of particular concern for mid-altitude reservoirs which must regularly conduct costly sediment management operations which affect their sustainability. The SEDMIX device is designed to help solve this exact issue: decreasing ongoing sedimentation issues in existing dams.

1.2 *Existing technologies and solutions*

To combat reservoir sedimentation and the negative impacts of turbidity currents, there are several sediment management strategies that are being investigated and applied worldwide.

These include venting, flushing, and mechanical dredging, among others. While these strategies have benefits, they also have practical challenges that hamper using them as successful techniques (Chamoun, 2016).

For example, venting allows for the release of sediments downstream during a flood event but requires a substantial amount of water release in the process (decreasing hydropower availability and production). Mechanical dredging allows for removal of large quantities of deposited sediment but is costly and requires ongoing maintenance and disposal of the dredged material. Flushing is more cost effective but may require powerplant outage for a limited period and may have larger potential for adverse downstream impacts.

1.3 *SEDMIX device concept*

This study focuses on an innovative concept for such a system that does not have as many negative aspects when it comes to dam reservoir operation. The SEDMIX device is a more flexible and versatile solution that has the potential to be employed in reservoirs with a diverse range of design details and location-specific criteria than each of the solutions mentioned above.

A PhD thesis that was completed at EPFL PL-LCH (Jenzer-Althaus, 2014) proposed and lab-tested an innovative system (called SEDMIX), which used water jets to keep fine sediments near the dam in suspension and allows them to be routed downstream. This study involves updated experimental simulations to include thrusters in the device design, instead of jets, because they lead to a less complex arrangement that requires less energy to operate.

The thrusters induce a rotational flow which creates an upward motion. This circular thruster arrangement is beneficial for sediment release as it keeps fine sediments in suspension near the dam and water intakes. The sediment can then be continuously routed downstream through the power waterways at suitable concentrations, without additional water or energy loss. This study involves updated experimental simulations to include thrusters in the device design, instead of jets, because they lead to a less complex arrangement that requires less energy to operate.

The SEDMIX device consists of a composed of two rigid parts: one floating at water level and one on the basin bottom holding a multi-thruster manifold frame. The thrusters will require electrical power supply. Once constructed, the thruster manifold frame will be suspended from a floating platform (anchored onshore) and lowered underwater into position. As such, the system can be mobile and can be moved around the reservoir to find the position that provides optimal sediment evacuation. The facility is modular and combines the use of different materials, taking into consideration structural resistance, weight, workability, aging properties, and cost.



Figure 1. Conceptual graphic showing SEDMIX design (source: PL-LCH).

2 EXPERIMENTAL SETUP

This study involves a physical experiment to study thruster performance and ability to keep fine sediments in suspension. The goal of the study is to better understand the influence of the SEDMIX device on reservoir hydrodynamics, and the resulting turbidity. A plan view of the experimental setup is shown in Figure 2, and described in the below sub-sections.

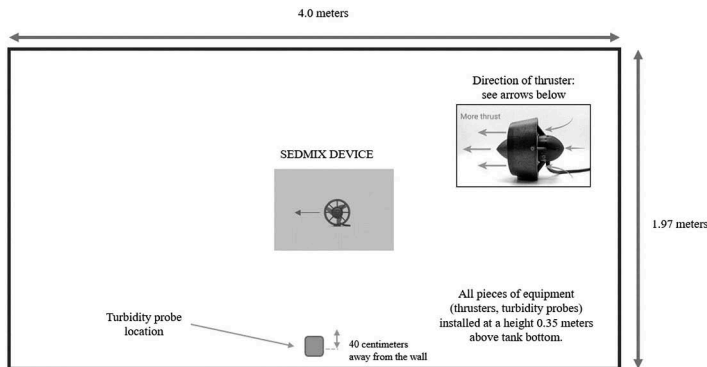


Figure 2. Plan view schematic of tank experiment (including measurement devices).

2.1 Laboratory tank

The physical experiments were carried out in a prismatic tank with vertical walls. The tank has a total inner basin length of 4.0 meters (m), an inner width of 1.97 m and a total basin height of 1.50 m (for a total volume of 11.8 m³). The horizontal bottom of the tank is a steel plate. Three quarters of the right lateral wall and the majority of the front wall are made of glass, providing transparency for visual observations, whereas the other walls are made out of steel plates.

The tank is a closed system, and for simplicity does not have any incoming or outgoing flow. The water height was kept constant at a depth of 1.0 m. The temperature of the water was kept at room temperature (between 15 - 20°C), and as such, the viscosity does not vary significantly.



Figure 3. Photograph of experimental tank, including thrusters.

2.2 Thrusters

The thrusters used for this experiment are Blue Robotics T200 thrusters¹, which consist of a fully flooded brushless motor with encapsulated motor windings and stator as well as coated magnets and rotor. The thruster body and propeller are made from polycarbonate

1. <https://bluerobotics.com/store/thrusters/t100-t200-thrusters/t200-thruster-r2-rp/>

plastic and the only exposed metal components are made from marine grade 316 stainless steel. Based on information from the manufacturer, the thrusters have a (approximate and theoretical) maximum velocity output of 4.5 m/s, and a maximum discharge of 0.0125 m³/s. For this phase of the experiment, one thruster was used. This thruster was installed in the center of the tank, at an off-bottom clearance of 0.35 m, using a designed and constructed structure that held it in place.

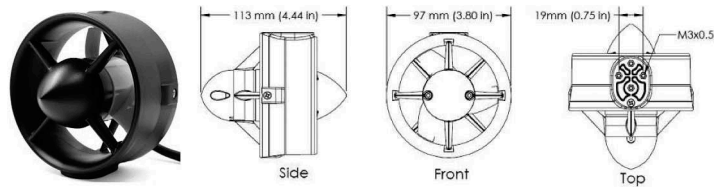


Figure 4. Blue robotics thruster T 200 schematic (images provided by Blue Robotics).

The thruster can generate thrust both in the forward and reverse directions, although the reverse direction has a lower force and efficiency. The thruster throttle can be controlled using a programmed electronic speed controller (ESC), which then uses a Pulse Width Modulation (PWM) signal to control the throttle of the thruster. Figure 5 shows the potential range in the PWM signal (from 1100 μ s to 1900 μ s), which allows for both forward and reverse throttle.

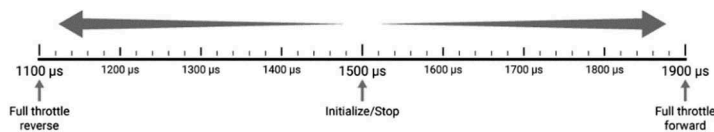


Figure 5. Pwm signal range for thruster throttle control (Source: Blue Robotics).

2.3 Turbidity meters

Turbidity meters (Zülig COSMOS-25 turbidity measurement system) were used to measure the turbidity as a function of time. The acquisition system is composed of two turbidimeters *Cosmos-25* linked to a Zülig AG *b-line multi* amplifier (Figure 6). To connect the probes to a computer, an acquisition card *NI-USB-6259 M series* (NI Instruments) is used between the transmitter and the computer. The thruster was installed with an off-bottom clearance of 0.35 m, and in a location shown in Figure 2.

The transmitter has an analogic output in voltage (V). The voltage values output from the transmitter are read via the acquisition card and then transferred to the computer via LabVIEW software. The LabVIEW script was written and utilized to record voltage values from the turbidity sensor with a precision of 0.1 mV. The results are recorded every 100 milliseconds. These results are then averaged using a moving window of 100 recorded values. The output current of the transmitter is 0-20 mA (milliamps), an electrical resistance of 510 Ω is used in the acquisition setup which creates a range of values from 0.0 - 10.2 V. Through experimentation, this voltage was then related to the turbidity unit (FNU).

At this phase of the study, water without sediment was used for testing turbidity changes. As such, the change in turbidity is a result of the various suspension contents of the water in the tank.



Figure 6. Züllig Transmitter (left) and COSMOS-25 Turbidity Probes (right).

3 METHODOLOGY

The focus of this phase of the experiment was to test the influence that one thruster had on the turbidity of the tank. The thruster was initiated and then set to a series of different throttle values, and then eventually turned off. As such the turbidity was monitored prior to thruster initiation, during thruster usage, and then monitored after the thruster was turned off. This method was tested under two conditions: 1) the thruster was set to forward throttle, and 2) the thruster was set to reverse throttle. This allowed for the comparison of the tank turbidity under a scenario with a more efficient thruster force and one with a less efficient thruster force. The throttle values, and all other tank conditions, were kept constant between the two test conditions.

4 RESULTS

Figure 7 provides the turbidity time series information for both the forward and reverse throttle conditions, as well as the thrust regime used for both scenarios.

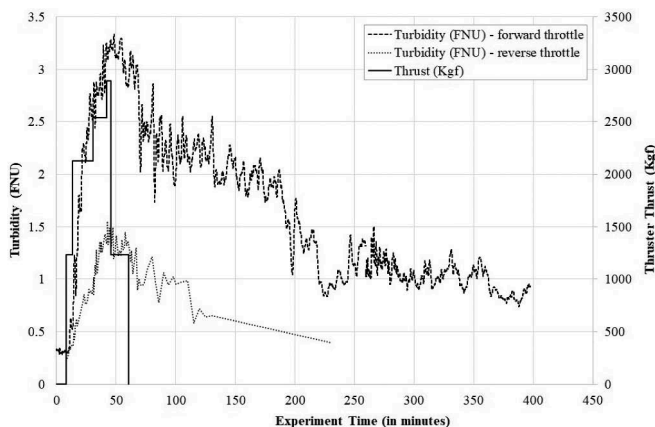


Figure 7. Turbidity (FNU) in the SEDMIX Experimental Tank, under two throttle conditions.

Both conditions show that the initiation of the thruster leads to a relatively rapid increase in turbidity in the tank, meaning that the thruster is beneficial for keeping in suspension, or resuspending, fine material. Once the thruster is turned off, the turbidity declines but at a slower speed. This behavior is to be expected given the fine material that is causing the

turbidity. The forward throttle condition results in a higher degree of turbidity. The maximum turbidity observed in the forward throttle condition is approximately double the maximum turbidity observed in the reverse throttle condition. Lastly, because the turbidity value reached a higher maximum in the forward throttle condition, the time needed to reach the initial turbidity value prior to thruster initiation (due to turbulence decay) is longer than for the reverse throttle condition.

5 ONGOING RESEARCH

Now that single thruster behavior has been observed and analyzed, ongoing studies are focused on testing different thruster configurations and parameters, including the multi-thruster systems, the location (including distance and off-bottom clearance) and angle of thrusters, and the magnitude of induced flow from the thrusters. In addition to turbidity meters, employing Ultrasonic Velocity Profilers (UVP) to better understand the resulting flow patterns and velocity fields that result is also being done. These ongoing studies will lead to the determination of optimal configurations of the thrusters for effective sediment suspension.

Ultimately, these simulation results will aid in the next step of the project, which is prototype installation of a SEDMIX device in a reservoir for further testing and observation in real, full-scale conditions. Information gleaned from these studies will allow for continued optimization of the device and industrial development for use in reservoirs that have fine sedimentation issues.

ACKNOWLEDGEMENTS

The authors would like to thank everyone who helped to make this experiment happen. Cédric Bron designed the thruster structure and helped with the selection, setup, and programming of the different measurement tools. Kilian Gertsch also helped with the design of the experimental tank and constructed the specific experiment elements. André Stakowian was incredibly helpful in helping to parametrize and set up the turbidity meters and the measurement methodology.

REFERENCES

- Amini A., Manso P., Lindsey N., Venuelo S., Schleiss A.J. 2017. *Computational hydraulic modeling of the sediment stirring and evacuation through the power waterways at the Trift reservoir*. In the Proceedings of the Hydro Conference 2017. Spain.
- Amini A., Onate-Paladines A., De Cesare G., Schleiss A.J., Mongiardino B., Binder F.M. 2019. *Short- and long-term storage volume recovery in a reservoir using a combined mixing-dredging device*. In the Proceedings of the Hydro Conference 2019. Portugal.
- Boes, R., Auel, C., Haggmann, M., Albayrak, I. 2014. *Sediment bypass tunnels to mitigate reservoir sedimentation and restore sediment continuity*. In Reservoir Sedimentation, CRC Press: Switzerland.
- Chamoun S., De Cesare G., Schleiss A. J. 2016. *The importance of venting turbidity currents on the sustainable use of reservoirs*. In the Proceedings of Hydro Conference 2016, Montreux, Switzerland.
- De Cesare, G. Boillat, J. 1998. *Alluvionnement des retenues par courants de turbidité*. Thèse EPFL, 1820.
- Fernandes J., Boes R., Titzschkau M., Hammer A., Haun S. and Schletterer M. 2016. *Suspended sediment concentrations and turbine wear during the drawdown of two Alpine reservoirs*. In the Proceedings of the 2016 Hydro Conference, Montreux, Switzerland.
- Guillén-Ludeña S., Manso P.A., Schleiss A.J. 2018. *Multidecadal Sediment Balance Modelling of a Cascade of Alpine Reservoirs and Perspectives Based on Climate Warming*. In Water.
- Jenzer-Althaus J., De Cesare G., & Schleiss A. J. 2014. *Sediment evacuation from reservoirs through intakes by jet-induced flow*. In Journal of Hydraulic Engineering, 141 (2).
- Perera, D., Williams S., and Smakhtin V. 2023. *Present and Future Losses of Storage in Large Reservoirs Due to Sedimentation: A Country-Wise Global Assessment*. In Sustainability 15, no. 1: 219.
- Schleiss A. J., Franca M. J. Juez C., De Cesare G. 2016. *Reservoir Sedimentation*. In Journal of Hydraulic Research. Volume 54 (6), pp. 595–614.

Dynamic environmental flows using hydrodynamic-based solutions for sustainable hydropower

S. Martel, P. Saharei, G. De Cesare & P. Perona

Platform of Hydraulic Constructions PL-LCH, ENAC, IIC, EPFL, Switzerland

ABSTRACT: Water diversions from rivers and torrents for anthropic uses of the resource alter the natural flow regime. As a measure, environmental flows have been prescribed and often are enforced by law to follow policies (e.g., minimal flow, proportional redistribution, etc.) that may vary from geographical location, environmental constraints and country-dependent environmental protection laws. There is not yet general consensus about the optimal release policy to be adopted, although scientific research generally agrees that flow variability for environmental flows should be a hydrological attribute fundamental for maintaining riverine biodiversity. Along with the previous assumption, non-proportional flow release strategies both for small hydropower and for traditional hydropower were proposed to generate optimal solution (*sensu* Pareto) for energy production and riverine ecology. Although non-proportional flow redistribution can easily be achieved by regulating flow devices (e.g., hydraulic gates), there is an interest to avoid the use of blocking structure for both safety control and energy consumption reasons. In this work, we study the redistribution capacity and flow hydrodynamics of asymmetric plate geometries that we propose as a technical and zero-operational-costs solution for generating the desired non-proportional repartition rule. Such plates can be easily mounted to partially cover the metallic rack installed at water intakes and used to intercept the stream while guaranteeing technical and environmental constraints (e.g., minimal and maximal turbined flow, minimal flow release and fish passage scales, transport capacity during high flow, etc.). We perform our study analytically and compare some performances also numerically. In summary, we demonstrate via the proposed analytical framework that different plate geometries correspond to different non-proportional fraction of water left to the environment for varying incoming flow. This work sets the premises for further studies where our approach could be adopted also for design purposes.

1 INTRODUCTION

Hydropower is considered a renewable energy source which, compared to other generation techniques (e.g., fossil-fuel based), produces fewer greenhouse gases while ensuring enough flexibility to meet production demand and the fluctuations of market electricity prices. Nevertheless, the environmental footprint of hydropower is not negligible and numerous studies have shown its detrimental impact on aquatic life and ecosystems (Perona et al. 2021, Razurel et al. 2018). These have been shown to result from the perturbation of the natural flow regime (Arthington et al. 2006) and the lost of hydrograph quantiles variability with obvious consequences for related ecosystem functions, which tends to homogenize at regional scales and beyond (Poff et al. 2007).

In a time when hydropower development for many countries (included Switzerland) is affected by the low feasible potential still available and the imminent renewal of concessions for water exploitation for existing power plants, then claiming an increase of environmental flows may appear questionable. This is particularly true considering that environmental flow releases (EFR) based on the minimal flow policy have been shown to be of low utility for preserving the riverine ecosystem (Poff et al. 2007). Some authors (Pfamatter & Semadeni 2018)

have for example demonstrated that the renewal of concessions strictly applying new foreseen efr rules in Switzerland might contrast with the 2050 strategy of energy production. This opens the question on whether actual efr should instead not be valorized, for example by redistributing the released water in a dynamic way so as to regain part of the natural variability of the flow regime.

Perona et al. (2013) and Gorla & Perona (2013) have proposed dynamic flow releases to redistribute the fraction of flow exceeding the Q_{347} (prescribed by the Swiss law as the basis for negotiation, e.g. see Assemblée fédérale de la confédération Suisse 1991) as a way to restore part of the original natural variability. This would have the effect of increasing the value of the actual minimal flow policies without the need of augmenting them in magnitude. Other authors have tested such considerations on a family of infinite flow redistribution rules and showed the existence of more ecologically efficient policies allowing to guarantee the same energy production (Razurel et al. 2015, Razurel et al. 2018, Niayifar & Perona 2017). Figure 1 shows for example the Pareto frontier arising from thousands of non-proportional redistribution rules, some of which clearly define a set of efficient (*sensu* Pareto) solutions (red borderline). Hence, several explored power plants typically show to perform below the frontier, thus leaving space for improvement both ecologically and in productivity. Such improvement require to generate one of the redistribution policy lying on the Pareto front (e.g., NP1-NP3), and do so at zero operational costs (e.g., without steering hydraulic gates). This challenge can be achieved by adopting hydrodynamic-based solutions like the one we show in this work or other proposed by Gorla & Perona (2013) and by Bernhard & Perona (2017).

We propose to investigate the performances of several intake rack geometries with asymmetric profiles as a way to generate non-proportional flow redistribution rule at zero operational costs. Our approach is based on developing a 1D analytical modelling framework and then compare some of the leading quantities with the results of a CFD model for the same geometry.

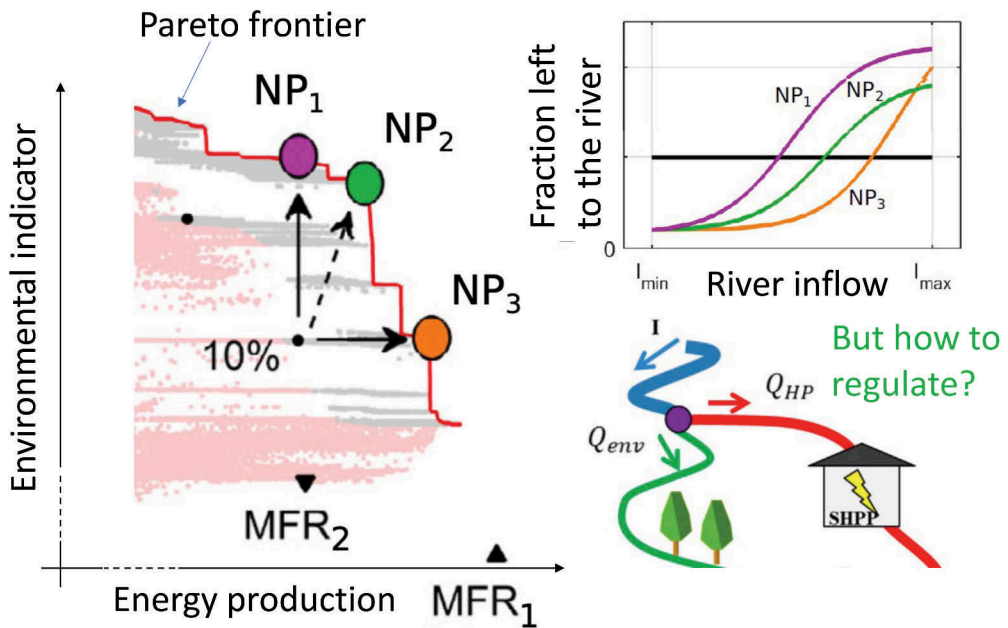


Figure 1. Example of Pareto frontier resulting from the implementation of non-proportional allocation policies (gray and rosa dots) in comparison with a 10% the minimal flow policies with 1 (MFR1) and two (MFR2) thresholds. Three exemplary efficient (*sensu* Pareto) solutions are shown corresponding to the three non-proportional allocation functions NP1, NP2, NP3 shown in the uppermost right panel. The challenge is to implement such non-proportional allocations at zero-energy operational costs.

2 ANALYTICAL MODEL

We consider the case of a stream of breadth b and falling freely into a trench through a metallic rack of assigned texture (Figure 2). The fraction of water f_T captured by the trench of longitudinal aperture length $l(y)$ and varying with the transversal coordinate y , is diverted to a generic water use (e.g., hydropower). The difference $f_{env} = 1 - f_T$ keeps flowing downstream and represents the residual environmental flow. This scheme is thus general and suitable to represent water intakes serving, for example, a reservoir or a small hydropower plant, or any other water use withdrawing water from the main channel through a simple diversion node. Therefore, the incoming natural flow discharge $I(t)$, the total flow going to the water use, Q_T and the residual environmental flow Q_{env} are related via the continuity relationships $I(t) = Q_T + Q_{env}$. We derive now the analytical steps that describe the amount of flow per unit width q_T captured by a trench of longitudinal length $l(y)$ under the assumption that the stream form a free falling jet, normally referred to as “end overfall” in the hydraulic literature (Hager 2010). The height difference between the beginning and the end of the trench divided by the maximum aperture length, L defines the slope angle of the rack covering the trench.

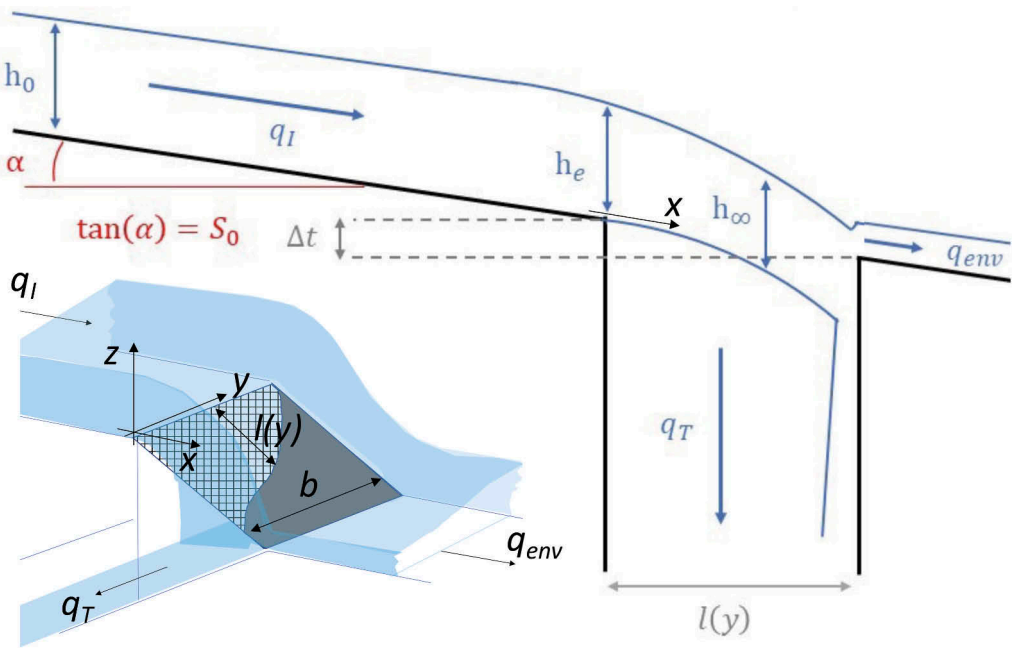


Figure 2. General scheme for the problem being considered in both a 3D and cross section representations. h_0 is the stream depth in normal flow conditions, h_e the depth at the beginning of the overfall representing the water intake, h_∞ the width of the jet far from end overfall. S_0 represents the slope of the river, and Δt the height difference between the beginning and end of water intake. q_I is the incoming specific discharge, q_{env} the fraction of flow that remains to the environment and q_T the fraction that falls into the intake.

Given a maximum flow per specific width, $q_I = Ilb$, there is a critical length $l_{c1}(y)$ of the trench that allows to capture the whole jet. For $l < l_{c1}$ only part of the jet falls into the water intake whereas the difference remains to the river beyond the intake. In order to proceed, we first derive the expression linking q_I and l_{c1} . Notice, that when the rack has a slope higher than the riverbed slope, then there is a second critical length, $l_{c2}(y)$ for which all the jet “jumps” the trench and will not be intercepted by the intake.

Consider the scheme of Figure 2, under the assumptions of a wide riverbed channel with slope, S_0 , homogeneous Manning’s roughness, n , the stream for $x < 0$ flows under normal flow conditions and has a water depth h_0 given by the Manning’s equation (e.g., see Julien (2018)).

$$h_0 = \left(\frac{nq}{\sqrt{S_0}} \right)^{\frac{3}{5}} \quad (1)$$

Also, we consider only incoming subcritical flow conditions for which the stream will become supercritical during the free fall within the rack. In the following model, we will make use of dimensionless values, so that all lengths are normalized to the depth of the incoming flow h_0 .

2.1 Jet longitudinal profile

Under the assumption above specified, Hager (2010) provides the equation of the bottom jet profile. By indicating $X = \frac{x}{h_0}$ and $Z = \frac{z}{h_0}$, the dimensionless shape of the jet is

$$X = \left(\frac{F_0}{T_e} \right)^2 \left[(Z_0'^2 - 2\epsilon Z)' - Z_0' \right], \quad (2)$$

where $Z_0'^2 = 2(1 - T_e F_0^{-2})(1 - T_e)^2$ and $T_e = h_e/h_0$ the normalized end depth. Note that the jet has a parabolic profile, as one could expect from a free fall problem. Thus, by inverting Eq.(2), and considering the negative solution (the jet falls toward negative z), one obtains the inverted relationship $Z = f^{-1}(X)$. The value for T_e is specified by Hager (2010) as a function of the upstream Froude number $T_e = \frac{F_0^2}{0.4 + F_0^2}$. Hager (2010) also provides the value of the jet thickness,

which has been determined both experimentally and theoretically, $T_\infty = \frac{2F_0^2}{1 + 2F_0^2}$. As one is interested in determining the profile at distances $x = O(l)$, the values of T_e and T_∞ are very close one each others, then the upper profile of the jet can be approximated by $Z_u = f^{-1}(X) + T_\infty$. According to Hager (2010), for incoming subcritical flows, the jet becomes critical when falling and so the relevant Froude number to be considered in the relationships for T_e and T_∞ is 1. The dimensional equation of the jet is then given by

$$z(x) = h_0 f_{F_0=1}^{-1}(x/h_0), \quad (3)$$

where the link to the incoming flowrate enters through h_0 and $T_e = 0.715$ and $T_\infty = \frac{2}{5}$.

2.2 Critical lengths 1 & 2

The two critical lengths are such that:

- l_{c1} : Critical length 1. This is the shortest length such that all the jet falls into the water intake, that is for $l > l_{c1}$, then $q_T = q_I$.
- l_{c2} : Critical length 2. This is the largest length such that all the jet jumps above the water intake, that is for $l < l_{c2}$, then $q_T = 0$.

The values of l_{c1} and l_{c2} is a function of the incoming flow and of the height difference Δt between the beginning and the end of the rack.

Again referring to Figure 2 and making use of the bottom and upper equations of the dimensionless jet profile $X = L : Z = f^{-1}(L)$ and $Z = f^{-1}(L) + T_\infty$. Therefore, $L = L_{c,1}$ if $Z(L) + T_\infty = -\Delta T$, where $\Delta T = \frac{\Delta t}{h_0}$. This gives $Z(L_{c,1}) = -(T_{infty} + \Delta T)$, and so

$$L_{c,1} = f(-(T_\infty + \Delta T)) \quad (4)$$

For the calculation of $L_{c,2}$, we use the same reasoning, but with the lower profile hitting the end of the rack. This translates in physical terms to impose that $Z(L_{c,2}) = -\Delta T$. Accordingly,

$$L_{c,2} = f(-\Delta T) \quad (5)$$

for which a solution exists only if $\Delta T > Z'_0 L$, i.e. the rack slope loses in elevation downstream more than the jet does.

2.3 Turbine and environmental discharge fractions

We now calculate the fraction of the flow directed to the turbines and the one released to the environment. The fraction going to the turbine as

$$f_T(y) = \frac{q_T(y)}{q_I} \quad (6)$$

where $q_T(y)$ is the flowrate intercepted by the intake at the coordinate y and going to the turbines, and q_I the incoming specific flow. The fraction of the flow that goes to the turbine is the fraction of the jet below $-\Delta T$, therefore:

$$f_T(y) = \frac{-\Delta T - Z(L)}{Z(L) + T_\infty - Z(L)} = -\frac{\Delta T + Z(L)}{T_\infty} \quad (7)$$

Some comment is in order here: the condition $L_{c1} \leq L(y) \leq L_{c2}$ implies that $0 \leq f_T(y) \leq 1$. Moreover, our model does not take into account a possible pressure increase at the point of contact between the wall and the jet, that could push part of the water upward and reduce f_T locally. The environmental fraction, $f_{env}(y)$ is defined as $f_{env}(y) = 1 - f_T(y)$.

The total discharge going to the turbine can thus be computed by simply integrating over the y coordinate,

$$Q_T = \int_0^b f_T(y) q_I dy \quad (8)$$

which implies that $Q_{env} = I - Q_T$

To the purpose of making the model more realistic, the losses introduced by the presence of a metallic rack texture should be taken into account. This can be done by adopting a reduction coefficient, which will however not be discussed further here.

3 RESULTS

We show now the results for some exemplary rack profiles, which are instructive to understand the principle leading to non-proportionality in the redistribution. In particular, we begin by considering the effect of a metallic rack having opening length $l(y)$ that varies linearly with the coordinate y and minimum aperture in the range $0 \leq l_{c1} \leq 4$. This corresponds to the case shown in Figure 3(a), bottom panel. The upper panel shows the corresponding total fraction left to the environment. For varying the incoming flow rate in the range $0 \leq I \leq 10 \text{ m}^3 \text{ s}^{-1}$. When the minimum aperture is non zero, then also the total fraction left to the environment is and becomes nonzero starting from the critical specific flowrate that first intercepts the rack. This type of rack shape thus produces a linearly varying non-proportional redistribution. Figure 3(b), lower panel shows the effect of a tri-linear profile as a perturbation of the linear one shown in panel (a). The steeper is the middle reach, the higher the shift of the redistribution to the environment for low flow conditions as a result of the interception due to the minimal length $l_{c1}(y)$. Notice that close to the extreme case of a vertical mid reach, the situation would correspond to only half a rack with constant aperture equal to $2m$, for which the fraction left to the environment in the range of the incoming flow considered approaches the proportional value of 0.5.

The tri-linear profile, introduces some interesting non-proportional behaviour compared to the simple linear profile. Figure 3(c) is the case of a tri-linear profile with fixed slope of the mid reach and varying location. This configuration generalizes further the results shown in Panel (b) (purple case) for which the range of (almost) proportional redistribution can be steered by

shifting the mid profile. Accordingly, the redistribution factor f_{env} shifts towards higher values. Such a profile could be adopted to represent a redistribution made of a non-proportional part up to a certain incoming flow and then non-proportional for higher discharges. It is now instructive to refer to the example of efficient non-proportional redistribution obtained by Fermi-like type of functions (Figure 1). To the purpose, we show how a redistribution similar to the NP1-NP3 curves could be obtained when designing the rack profile as, for example, done in panel (d), bottom figure. In the upper figure, a Fermi-like function was fit to the resulting redistribution shown almost a perfect matching but for very high incoming flowrate. A better match would require a further modification of the profiled rack.

In order to appreciate the effect of the simplifications made, we compared the results of the jet profile (water depth h_e) with that obtained from a 3D numerical flow solver like Flow 3D for the case of the linearly profiled rack. Results are shown in Figure 4 together with the trajectories seed view that illustrate well the partial capturing effect imposed by the linearly varying intake profile. As far as the water depth h_e of the incoming jet is concerned, the bottom panel shows the comparison between Hager (2010)'s solution implemented in our model and the CFD one. Our model provided h_e under the assumption of a Froude number always equal to unity. This produces an overestimation of the water depth towards low flows and an underestimation of it as the Froude number becomes larger than one.

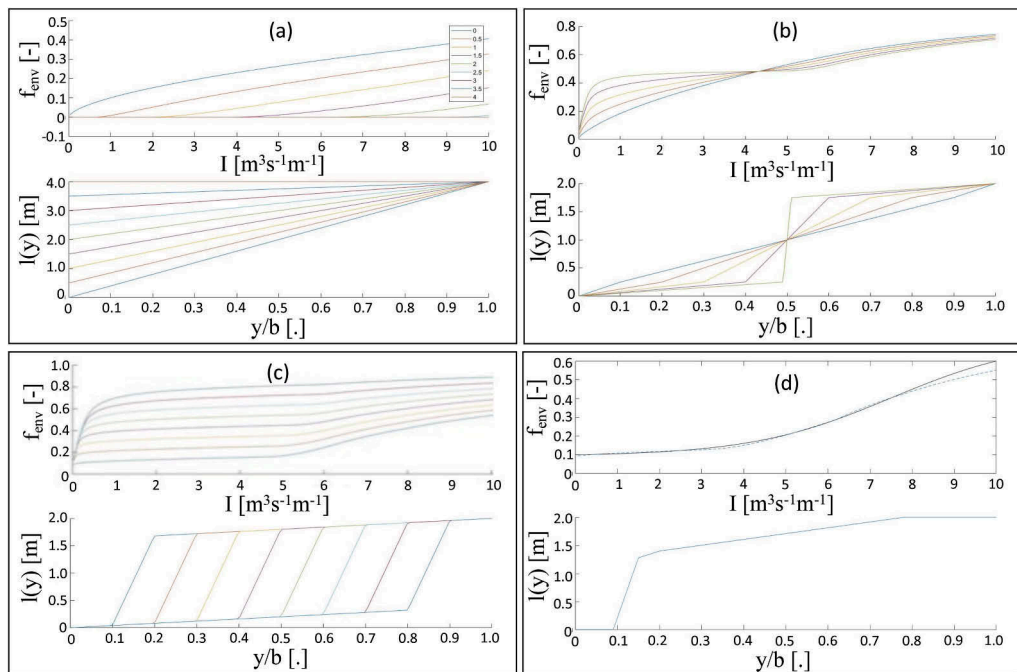


Figure 3. Varying rack shape and related total fraction left to the environment for varying total incoming flow rate, I : (a) linear profile with different minimal aperture; (b) tri-linear profile with changing mid profile slope; (c) tri-linear profile with shifted steeper mid profile. Panel (d) shows an exemplary profile and the corresponding fit on the resulting non-proportional redistribution with a Fermi-like function.

4 DISCUSSION

For subcritical flow conditions the dimensionless jet profile is the same for every discharge value because of the assumption $F_0 = 1$. Therefore, the main parameter impacting the trajectory of the jet is the normal height of the incoming flows, which is used to normalize the different length of the problem, and depends on the discharge value. Due to its simplicity, the model neglects several

elements that could affect the final results. First, we consider a 1D flow, which implies that all velocity components along the transversal and the vertical coordinates are ignored. Such velocities can have different origins, for example: the difference in height along the y axis of the end of river bed ($x=0$): as the discharge flowing through the intake changes along y , so does the flowdepth thus generating weak transversal currents; in a real 3D overfall, the jet tends to widen during the fall due to pressure and gravity effects (Hager 2010); the approximation of large width allowing $R_h \approx h$, may not be justified at all flow conditions. A second source of error is the impact of the rack protecting the water intake: first of all, the rack causes a reduction of discharge flowing through the intake, due to head losses caused by the rack. The consequence is an increase in the fraction of water left to the environment. A corrective factor for discharge should then be applied following, for example the Frank's type of approximation. This, however, would provide an estimation of the losses for the maximal design discharge, only. Jet fragmentation when hitting the rack might produce local chocking and this effect depends on rack texture. Despite the limitation above said, the analytical model seems to perform very similarly to the CFD solution and certainly deserves additional investigations.

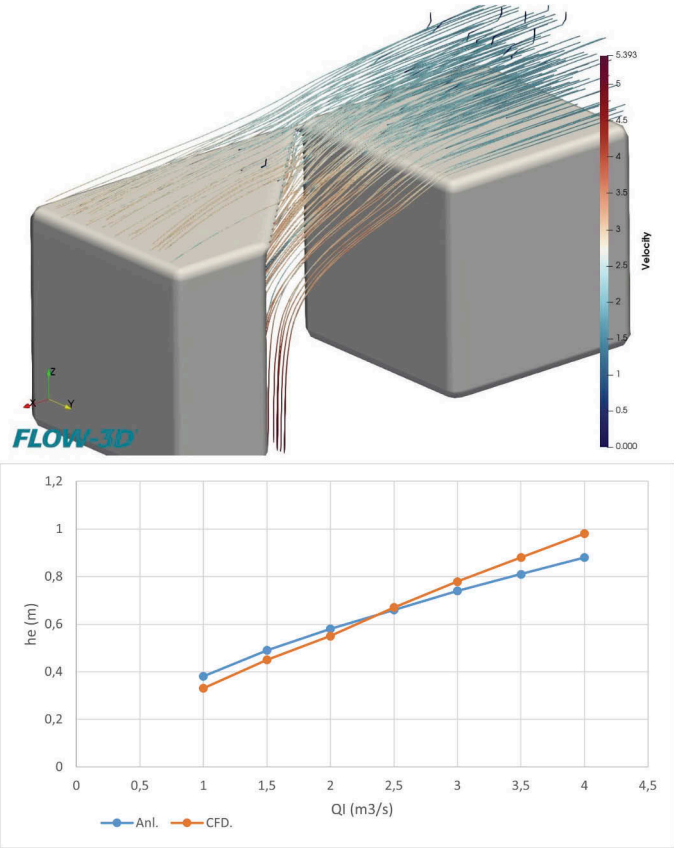


Figure 4. CFD representation of the functioning of a linearly varying intake profile (upper panel) and the comparison between the modeled initial jet water depth h_e and the CFD resulting one (lower panel).

5 CONCLUSIONS

Designing an intake able to reproduce non-proportional redistribution policies that maximises both production and ecological benefits (see Figure 1) at zero operational costs is appealing. We showed that this can be done by adopting hydrodynamic-based solutions to re-design the

geometry of the rack at water intakes. This solution would be flexible and perfectly adaptable for water uses either with or without storage reservoir. The purpose of pursuing an analytical approach like the one done in this work was to show that such solutions exist and should be considered in a time where energy savings are strategic for both the people and the environment. Naturally, the proposed model needs some further improvement, but we showed the possibility of using it also for design purposes. Mathematically, this would require to study the inverse problem, that is finding the rack profile $l(y)$ that reproduces the desired non-proportional (i.e., *sensu* Pareto) redistribution policy. This step has not been done here, and it requires to invert the problem, that is finding the profile of the rack, $l(y)$, once the non-proportional rule $f_{env}(I)$ is assigned for varying incoming flow $I(t)$. For example, f_{env} would correspond to one of the Fermi-like family functions shown in Figure 1 (see also, Razurel et al. 2015, Razurel et al 2018), which should be equalized to an integral function that contains $l(y)$. Then, the problem would take the form of a Fredholm integral equation of the first type with fixed extremes of integration. Some challenges thus arise here also from the mathematical point of view, which enhance also the pure speculative scientific aspects of the work. The refinement of the model and the latter step are therefore left to future works.

REFERENCES

- ASSEMBLÉE FÉDÉRALE DE LA CONFÉDÉRATION SUISSE 1991. *Loi fédérale sur la protection des eaux*, Bern
- Arthington, A. H., Bunn, S. E., Poff, N. L. & Naiman, R. J. 2006. The challenge of Providing Environmental Flow Rules to Sustain River Ecosystems. *Ecological Applications* 16: 1311–1318.
- Bernhard, F.A. & Perona, P. 2017. Dynamical behavior and stability analysis of hydromechanical gates. *J. Irrig. Drain. Eng.* 143 (9): 0401703
- Gorla, L. & Perona, P. 2013. On quantifying ecologically sustainable flow releases in a diverted river reach. *Journal of Hydrology* 489: 98–107
- Hager, W. H. 2010. *Wastewater Hydraulics*, Chapter 11: End overfall. Springer.
- Julien, P. J. 2018. *River Mechanics*. London: Cambridge university press.
- Niayifar, A. & Perona, P. 2017. Dynamic water allocation policies improve the global efficiency of storage systems. *Adv. Water Resour.* 104: 55–64.
- Perona, P., Dürrenmatt, D.J., Characklis, G.W. 2013. Obtaining natural-like flow releases in diverted river reaches from simple riparian benefit economic models. *J. Environ. Manag.* 118: 161–169.
- Perona, P., Niayifar, A., Schwemmler, R., Razurel, P., Flury, R., Winz, E., Barry, D. A. 2021. Frontier of (Pareto) optimal and sustainable water resources management for hydropower and ecology. *Frontiers in Environmental Sciences* 9: 703433
- Pfamatter, R. & Semadeni Wicki, N. 2018. Energieeinbussen aus Restwasserbestimmungen – Stand und Ausblick. *Wasser Energie Luft* 110(4)
- Poff, N.L., Allan, J.D., Bain, M.B., Karr, J.R., Prestegard, K.L., Richter, B.D., Sparks, R.E., Stromberg, J.C. 1997. The natural flow regime. *BioScience* 47 (11): 769–784
- Poff, N.L., Olden, J.D., Merritt, D.M., Pepin, D.M. 2007. Homogenization of regional river dynamics by dams and global biodiversity implications. *Proc. Natl. Acad. Sci.* 104 (14): 5732–5737
- Razurel, P., Gorla, L., Tron, S., Niayifar, A., Crouzy, B., Perona, P. 2018. improving the ecohydrological and economic efficiency of Small plants with water diversion. *Advances in Water Resources* 113: 249–259

Improving fish protection and downstream movement at the Maigrauge Dam (Switzerland) using an electric barrier

Anita Moldenhauer-Roth

Laboratory of Hydraulics, Hydrology and Glaciology, ETH Zurich, Switzerland

Delphine Lambert & Michael Müller

IUB Engineering Ltd., Berne, Switzerland

Ismail Albayrak

Laboratory of Hydraulics, Hydrology and Glaciology, ETH Zurich, Switzerland

Georges Lauener

Groupe E Ltd., Granges-Paccot, Switzerland

ABSTRACT: The main intake of the Maigrauge Dam is protected by a vertically inclined trash rack with 30 mm bar spacing. The bypass entrance for downstream fish passage is located next to the main turbine intake. A PIT tag study showed that many fish approach the bypass but only few enter it. In this project, structural measures were analyzed to improve fish protection at the turbine intake and bypass acceptance. To reduce rack passages, two options to electrify the rack were compared: 1) Placing electrodes on the front of the bars of the rack and 2) using the rack as a cathode and placing a row of electrodes 10 cm downstream. Based on numerical simulations of the electric field and comparison to laboratory and literature data, both setups are expected to significantly reduce rack passages. Furthermore, improvements for bypass attraction and acceptance were developed.

1 INTRODUCTION

1.1 *Fish protection at the Maigrauge Dam*

On the Saane River (Switzerland), a hydropower cascade consisting of three large dams and hydropower plants (HPP) is run by the company Groupe E. Just upstream of the City of Fribourg, Lake Pérolles, classified as a protected nature reserve, is impounded by the Maigrauge Dam. The heavily forested catchment area presents a technical challenge for the management of floating debris. The Pérolles Lake presents a diverse fish community consisting mainly of cyprinids and brown trout (*Salmo trutta*). European Eel (*Anguilla anguilla*) are not present in the lake. From the main turbine intake structure, water is guided through a pressurized waterway towards the Oelberg HPP. The intake is protected by a vertical inclined trash rack with a bar spacing of 30 mm and an inclination of 65°. Turbine operation is dependent on the operation of the upstream Hauterive HPP. The discharge varies several times a day between 0 l/s and a maximum of 99 m³/s. Therefore, the approach flow velocity at the trash rack is highly variable. In 2005, a fish elevator for upstream movement and a downstream fishway (bypass) consisting of a channel followed by multiple spillway basins were built to establish up- and downstream fish passage, respectively (Figure 1). The bypass entrance is located adjacent to the main water intake and provides an attraction flow of 350 l/s. Close to the main dam, 370 l/s of water is extracted for the fish elevator and an environmental flow is provided via the residual flow turbine in the historical powerhouse to the Saane River downstream of the dam site (total residual flow of 4 m³/s).

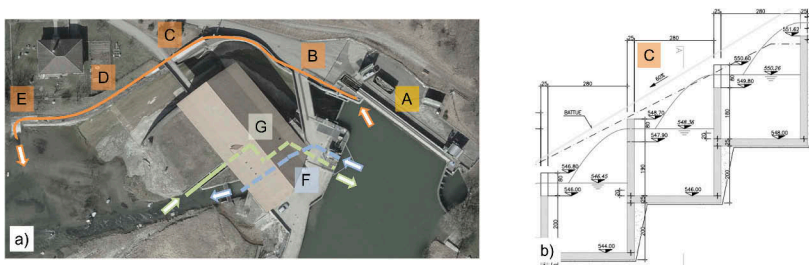


Figure 1. (a) Orthophoto of the Maigrage dam. A: main intake with vertical bar rack, B: bypass entrance and upstream channel, C: spillway basins, D: downstream channel, E: restitution basins, F: intake for residual flow turbine, G: fish elevator in the historic power house (b) Longitudinal profile of the spillway basins in the downstream fishway.

A PIT tag study carried out between 2016 and 2019 tagged and monitored just over 1000 fish to evaluate the functioning of the measures implemented in 2005. It concluded that many fish approached the bypass but only few entered it. During periods of standing water, fish entered the main intake seeking shelter in the area behind the rack. Upon turbine start-up, they could not withstand the high flow velocities and were entrained towards the turbines. (Zurwerra et al., 2019).

The existing bypass facility does not fulfill the most recent Swiss Guidelines for downstream fish passes (FOEN, 2022). Flow velocities at the entrance are too low compared to the velocities towards the main intake. The water levels in the upper channel are too low and energy dissipation in the spillway basins needs to be improved. In a preliminary project in 2021, various potential improvement measures were evaluated (IUB, 2021). To improve fish protection, electrification of the existing rack, an electrified cable barrier (“Fish Protector” by HyFish®), a plunging wall as well as a fine rack with horizontal bars were compared. For the improvement of the bypass, an increased attraction flow, an enhanced entrance geometry and a continuous flow acceleration from the intake zone through the entrance and towards the bypass channel were determined as key factors to improve bypass acceptance.

1.2 Electric barriers

Electric barriers are generally used to prevent upstream moving fish from entering tailrace channels (Burger et al., 2015). Such installations are in place in Switzerland i.e. at the tailrace tunnel Veytaux HPP (de Cesare et al., 2016) and Vessy HPP (GREN, 2009). To the authors knowledge, no electrified barrier for downstream fish passage is currently in operation in Switzerland. The fish reaction to an electrified structure mainly depends on the strength and orientation of the electric field, the fish species and the swimming behavior of the approaching fish (Beaumont, 2016). Figure 2 shows the electric field between two point electrodes. For the same electric field strength, the fish may experience a strong repulsion impulse when is oriented perpendicular to the equipotential lines (dotted black lines) or avoid the electric field by aligning parallel to the equipotential lines (Beaumont, 2016). Upon encountering an electric field, a fish approaching with positive rheotaxis (head oriented upstream) can flee directly in upstream direction while a fish approaching with negative rheotaxis (head oriented downstream) first needs to turn around in order to escape away from the rack.

Generally pulsed direct current is used at electric barriers because alternating current was found to cause more injuries and has been prohibited for electrofishing (Snyder, 2003). Direct current is always flowing in the same direction which leads to corrosion of the anodes and, depending on the setup, corrosion of the existing rack. Recently pulsed direct current with a regular switch of polarization has been proposed to reduce corrosion without being as harmful as alternating current (Haug et al. (2022b); Weibel and Ness (2014); Smith Root, personal communication). First results show no increased risk of injuries and strongly reduced corrosion (Haug et al., 2022b) but systematic live fish tests are yet to be conducted.

Recent research electrifying the bars of horizontal and vertical bar racks as well as retrofitting them with electrodes placed on the upstream and downstream side of the rack have

shown that high protection rates up to $\geq 90\%$ are possible depending on the fish species, the bar spacing and the electrification setup. However, immobilization and injuries can be incurred by slight changes of electrode geometry and applied voltage, which must be carefully considered when designing such fish protection structures (Beck, 2020; Haug et al., 2022b; Meister et al., 2021; Moldenhauer-Roth et al., 2022).

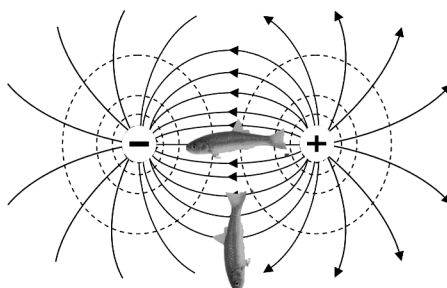


Figure 2. Electric field generated by two point electrodes. The dotted lines represent equipotential lines while the continuous lines represent the flow of the current. The fish swimming to the left experiences a strong electric impulse while the fish swimming towards the bottom is aligned with the equipotential lines and is therefore much less exposed.

2 METHODOLOGY

2.1 Possibilities to electrify the bar rack at Maigrauge HPP

Large amounts of floating debris arrive at the Maigrauge Dam and the main intake is equipped with a rack cleaning machine. Additional electrodes therefore need to be constructed such that they do not interfere with the rack cleaning machine. Based on this constraint, two types of electrification are considered:

1. Electrodes placed on the upstream side of the bars of the existing rack (Figure 3).
2. Bar rack electrified as cathode, vertical poles used as anode placed 10 - 15 cm downstream (Figure 4).

Placing electrodes on the upstream side of the bars of existing racks (Setup 1) was tested by Haug et al. (2022a,b) in a laboratory and small field setup. A Patent for fixing an electrode to the front of bars of a rack has been granted to Aufleger et al. (2021). The connection between the electrodes and the bars may experience high lateral forces due to large floating debris being pressed against the electrode by the rack cleaning machine. To increase the lateral stability and to create a similar electric field as Haug et al. (2022a), placing the electrode in a depression in the front of the bars is a possibility (Figure 3a). Using the bar rack as cathode and vertical poles placed downstream as anode (Setup 2) allows creating an electric barrier without modification of the existing rack.

The electric fields of both setups were numerically modelled using Comsol Multiphysics 5.5. The numerical results were compared to literature data and live fish tests conducted at the laboratory of hydraulics, hydrology and glaciology at ETHZ (VAW, unpublished) with a pulse duration of 2 ms and a frequency of 10 Hz.

2.2 Numerical simulation of the electric field

The numerical simulations were run for a rack conductivity of $35.5 \cdot 10^{10} \mu\text{S}/\text{cm}$ and the average water conductivity of $437 \mu\text{S}/\text{cm}$ measured at the NADUF station Gümmenen in 2015. The water conductivity varies between $347 \mu\text{S}/\text{cm}$ and $521 \mu\text{S}/\text{cm}$ throughout the year. These variations did not significantly influence the extent of the electric field. The simulations were run on a 2D horizontal section through the rack, assuming a large body of water around the rack and no other metallic structures influencing the electric field.

3 RESULTS AND DISCUSSION

3.1 Electric field

3.1.1 Setup 1: Electrodes placed on the upstream side of the bars of the existing rack

The electric field for an applied potential of 150 V with an electrode placed on every second bar is shown in Figure 3b. The electrodes are grouped as three anodes and three cathodes. This creates a larger extent of the electric field in front of the bar rack than by electrifying each electrode alternating as anode and cathode. The electric field $E \geq 0.2$ V/cm extends 13 cm upstream of the rack. The equipotential lines are mostly oriented parallel to the rack, which is favorable for fish protection as fish are likely to feel the voltage potential over their full body length. However, at each change from the group of anodes to the cathodes, the equipotential lines are oriented parallel to the bars (Figure 3b). In these areas, a fish only feels a potential difference across its tail fin or across the width of its body, which reduces the deterrence effect of the electric field.

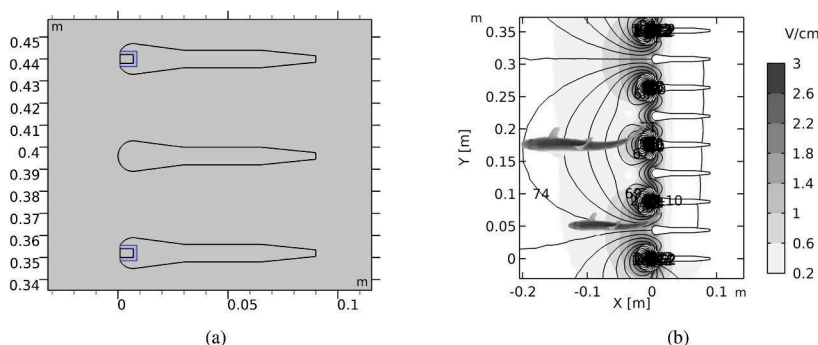


Figure 3. Setup 1: Electrodes placed in a depression on the upstream side of the bars. a) Geometry of the bars with a layer of insulation between the electrode and the bar of the rack. b) Electric field generated using three electrodes as anodes and subsequent three electrodes as cathodes. The applied potential is 150 V. The black lines represent equipotential lines and the colors electric field strength E [V/cm].

3.1.2 Setup 2: Bar rack electrified as cathode, anode downstream

The rack is used as a cathode and a row of vertical poles placed downstream of the rack acts as anodes. The poles have a diameter of 15 mm, a distance of 17.6 cm between the poles and a distance of 10 cm between the poles and the rack. The applied potential is 33 V. The geometry and resulting electric field are shown in Figure 4. This configuration was chosen to ensure a maximum electric field strength of ≤ 2.4 V/cm and a minimum field strength ≥ 2 V/cm a fish will pass if it swims through the rack. The spacing of 17.6 cm between the vertical poles, much larger than the bar spacing, minimizes the risk for fish or wood getting blocked between the rack and the poles. A small distance between the poles and the rack ensures that fish passing the rack are swept through the electric field quickly.

The orientation of the electric field for setup 2 is more favorable than for setup 1, as the equipotential lines are always oriented parallel to the rack, which means that it is impossible for a fish to orientate itself parallel to the equipotential lines and evade the effect of the electric field while passing the rack. However, due to the small bar spacing, the electric field gets stronger than 0.2 V/cm only 6 cm behind the bar tip. This indicates that a fish only experiences a significant electric impulse when a part of its body is already between two bars of the rack.

3.2 Protection efficiency, risk of injuries and risk of corrosion

Live-fish tests were conducted for similar electric setups as numerically evaluated here but with a larger bar spacing (50 mm and 90 mm) at the etho-hydraulic flume of VAW (unpublished). The fish protection efficiencies obtained from these experiments with a pulse duration

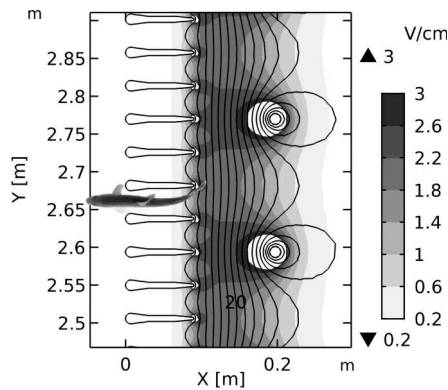


Figure 4. Setup 2: Electric field generated by electrifying the rack as a cathode and downstream placed vertical poles as anodes. The applied potential is 33 V. The black lines represent equipotential lines and the colors electric field strength E [V/cm].

of 2 ms and a frequency of 10 Hz and the literature data with pulse durations of 0.3 ms (Haug et al., 2022a,b) were used as a reference to estimate fish protection efficiencies for both setups evaluated for the Maigrage Dam.

3.2.1 Non electrified 30 mm bar rack

At the Maigrage Dam a vertically inclined bar rack with a bar spacing of 30 mm is installed. A bar spacing of 30 mm is not sufficient for physical fish protection FOEN (2022). However it does influence the fish swimming behavior in front of the rack and can have protection efficiencies for salmon smolts around 60 – 70% with favorable approach flow conditions (Courret et al., 2014). Similar protection efficiencies were observed for various species by Haug et al. (2022a,b). Therefore, for comparison of the electrified setups, a base protection rate of 60% was assumed without electricity and a high probability of a change of rheotaxis upstream of the rack was assumed due to the hydrodynamic and visual impact of the rack.

3.2.2 Setup 1: Electrodes placed on the upstream side of the bars of the existing rack

Haug et al. (2022a), observed an increase in fish protection efficiency from 62% to 96% for for a species mix consisting mainly of cyprinids when placing electrodes on the front of a bar rack with 30 mm bar spacing. In live-fish tests conducted at VAW, electrodes were mounted on a bar rack bar with a bar spacing of 90 mm. This created a very similar electric field but with a larger extent of $E \geq 0.2$ V/cm up to 40 cm upstream of the rack compared to 15 cm at Maigrage (Figure 3b). Therefore, approaching fish had more time to react but due to the larger bar spacing, the fish protection efficiency without electricity was 0%. The tested electrified bar rack increased the fish protection efficiency up to 48% for trout and up to 73% for chub. Combined with the 30 mm bar rack at the HPP Maigrage, a significant improvement of the fish protection up to $\geq 80\%$ is expected for the species mix present in Lake P erolles.

Haug et al. (2022a) observed some immobilization of fish, which recovered immediately after being swept through the rack. During the tests at VAW, no immobilization of chub and trout was observed. Since the existing rack is oriented at an angle to the approach flow, it is expected that potentially immobilized fish pass the rack or are transported away from the electric field by the water velocity. Theoretically, a person swimming towards the rack could touch both anode and cathode simultaneously. To date, there have been no studies of the effect of such an electric field on humans. Consequently, this access to the electrified rack needs to be prevented to ensure that no person can swim into the vicinity of the rack.

The trash rack at Maigrage HPP consists of galvanized iron. Due to the placement of electrodes with variable potential on the front of the bars, the rack acts as an anode towards the cathodes resulting in an increased corrosion risk compared to a non-electrified rack. This risk can be reduced by applying a coating of insulating paint to the rack which also reduces power consumption of the setup. Another promising approach is the application of a modified pulse

pattern which regularly changes polarization of anode and cathode. However, the risk of injuries and the effect of such a modified alternating direct current on fish protection have been studied only in exploratory manner in Haug et al. (2022b). Therefore, this type of electrification demands a close monitoring both for potential blockage due to immobilization in front of the rack, potential fish injuries and corrosion.

3.2.3 *Setup 2: Bar rack electrified as cathode, anode downstream*

Electrifying the rack as a cathode and a metal mesh downstream as anode was tested with a horizontal bar rack with 50 mm bar spacing with Spirlin by Meister et al. (2021) at VAW. Despite the large bar spacing protection efficiencies up to 96% were observed. In a recent study, a vertical bar rack with 90 mm bar spacing was tested in the same flume with Chub, trout and eel (VAW, unpublished). At a low approach flow velocity of 0.15 m/s, chub approached the rack with varying rheotaxis and 78% of the tested chub were prevented from rack passage. This increased to 90% at an approach flow velocity of 0.6 m/s when almost all chub approached the rack with positive rheotaxis. The tests with trout were abandoned after 6 trout passed the rack at 0.15 m/s without showing any reaction to the electric field. The difference in reaction among species and approach flow velocity was attributed to their swimming behavior when approaching the rack. Trout often changed to negative rheotaxis 15 to 20 cm upstream of the rack and then passed the rack head first. Due to such behavior, a setup where the electric field extends behind the rack cannot provide protection for trout, unless an additional incentive induces a change of rheotaxis. The relatively small 30 mm bar spacing of the rack at the HPP Maigrauge is expected to induce a change to positive rheotaxis upstream of the rack for all species present in the lake. This results in an expected protection efficiency up to $\geq 70\%$ for trout and $\geq 80\%$ for chub.

No injuries or immobilization were observed if the downstream anode is constructed of vertical poles with a large spacing among them. It is unlikely that this setup poses a risk to humans or other animals present in the vicinity since the electric field is created behind the rack. Therefore it is not possible to touch anode and cathode simultaneously.

Electrifying the rack as a cathode protects it from corrosion. The vertical poles are consumables and need to be replaced after some 10 - 15 years unless the newly proposed pulse patterns with regularly changing polarity are used.

3.3 *Constructional challenges of an electrified bar rack*

Large floating debris arrive regularly at the main intake of Maigrauge HPP. Electrodes mounted on the upstream side of the bars (Setup 1) of the rack are exposed to high impact forces and lateral forces during the rack cleaning process. Electrodes mounted directly on the rack need to be separated from the latter with a layer of insulating material. Fixation cannot be done by traditional screws as these would create a conducting connection between electrode and bar rack which would lead to a short circuit. Placing electrodes in a depression on the front of the bars would be very difficult to retrofit so manufacturing a new rack would most likely be more economical. Since the anodes are exposed to corrosion if direct current is used, the electrodes should ideally be easily replaceable in case of necessary maintenance. Possible fixation modes using glue and different electrode geometries to provide enough resistance are currently being discussed with the company HyFish[®].

If a setup is proven to be sufficiently robust against the forces present at the Maigrauge Dam, its mode of fixation and geometry will have a big impact on the cost of manufacturing of the electrodes. Furthermore, depending on the exact geometry and width of insulation, the maximum current that is flowing varies between 2700 and 5300 A. The maximum current only flows during less than 2% of the time but determines the number of pulsators needed. It can be significantly reduced to around 1700 - 1900 A if insulating paint is applied on the bars.

Mounting circular electrodes downstream of the bar rack (setup 2) also presents a constructional challenge. Due to the dynamic hydraulic forces and the very thin bar geometry, the anodes may suffer from resonance phenomena if anchored to the concrete walls. The distance between electrodes and rack should be smaller than 20 cm to keep the extent of the electric field small. This constraint is challenging as the forces need to be transmitted to the

concrete walls directly behind the rack. A system of two horizontal steel ropes between which the vertical electrodes are fixed is considered to be the most suitable construction. Since it is flexible, it is much more resistant to resonance phenomena. This setup is expected to use a maximum electric current of 1800 A.

Which setup will be pursued for realization at Maigrauge is yet to be determined. Advantages of the Setup 2 are: less modification is required on the existing trash rack, the rack is not exposed to corrosion if direct current is used, and fish and human injuries are unlikely. However, fish protection is expected to be slightly more favorable for setup 1. Manufacturing a new rack structure with electrodes placed in bar depressions would be very costly. If an alternative sufficiently robust electrode fixation can be developed, setup 1 could become economically interesting.

3.4 Planned improvements of the bypass design

To improve the attraction flow towards the bypass, the residual flow turbine intake is displaced near the bypass inlet (Figure 4a). This increases the attraction discharge to 4 m³/s which amounts to more than 4% of the concurrent turbine discharge at the main intake. The inlet section is enlarged for the new attraction flow with a maximum flow velocity of 2 m/s (Figure 4a). A vertical bar rack with a spacing of 10 to 20 cm is positioned at the bypass inlet to prevent large floating debris from entering. The upstream part of the bypass channel is designed to have a constant approach flow velocity of 0.5 m/s without abrupt flow changes or dead zones. A 3D numerical modeling allowed to verify velocity profiles at different characteristic sections, for different exploitation levels of Lake Pérolles. The new lateral intake for the fish lift and the residual flow turbine is protected by a screen with a 20 mm vertical bar spacing. Discharge towards the bypass channel is controlled by a gate valve equipped with two regulation orifices downstream of the new intake. In a completely opened position, this gate valve allows flushing the bypass system, in periods with increased (light) floating debris such as leaves and small branches. To fulfill the ecological criterion of minimum water depths for fish passages, the discharge in the downstream fish passage facility is increased to 600 l/s. However, to reduce water losses and thus minimize costs related to reduced power generation, a temporal reduction of the bypass discharge is currently discussed with the authorities. The spillway basins are adapted to increase energy dissipation levels and water depths (Figure 5b). Half-arched walls in the basin corners improve flow paths and thus enhance fish guidance. In each basin, a 30° bottom ramp toward the spillway section ensures the safe passage for both surface and bottom swimming fish.

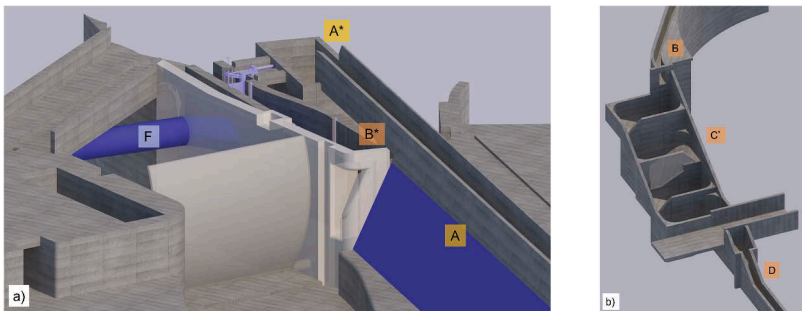


Figure 5. 3D Construction model of the enhanced bypass design. (a) View from upstream towards the bypass entrance, with A: existing main intake with 30 mm vertical bar rack and A*: the new position of trash collection, B*: enhanced bypass entrance, F*: new intake for residual flow turbine and fish elevator with 20 mm bar rack. (b) Enhanced spillway basins with B: upstream channel, C*: optimized basin geometry, D: downstream channel.

4 CONCLUSIONS AND OUTLOOK

At the Maigrauge HPP fish protection at the turbine intake and attraction flow to the bypass channel need to be improved. To this end, two different setups to electrify the existing 30 mm

vertically inclined trash rack are possible: 1) Placing electrodes on the upstream side of the bars of the existing rack and 2) using the existing rack as cathode and placing anodes a short distance downstream. Numerical simulations of the electric field allow to evaluate how to adapt the voltage and electrode geometry to replicate the electric fields tested in laboratory conditions.

Based on comparable laboratory experiments and literature data, both electrification setups in combination with the behavioral effect of the existing rack are expected to provide good protection for cyprinids, especially at high flow velocities where fish approach the rack with positive rheotaxis. For trout, setup 1 is expected to provide slightly better protection. For setup 1, the electrodes are exposed to high lateral forces from wood pressed against them by the rack cleaning machine. How to fix the electrodes in a sufficiently robust manner is yet to be determined. Subsequently, a final decision between the setups will be taken based on a cost-benefit-analysis.

The developed improvements of the downstream bypass system allow to fulfill current recommendations in terms of flow velocity and flow depths in the bypass channel as well as energy dissipation in the basin cascade. The displacement of the residual flow turbine intake near the bypass inlet improves approach flow conditions towards the bypass entrance. After realization of the enhancement project, a detailed monitoring of the fish behavior and hydraulics will be conducted to verify the effect of the implemented improvements.

REFERENCES

- Aufleger, M., Brinkmeier, B., Haug, J., and Tutzer, R. (2021). Hybrid fish protection on intake screens. European Patent Office, EP4110994A1.
- Beaumont, W. (2016). *Electricity in fish research and management*. Wiley.
- Beck, C. (2020). Fish protection and fish guidance at water intakes using innovative curved-bar rack bypass systems.
- Burger, C. V., Parkin, J. W., O'Farrell, M., and Murphy, A. (2015). Improving technology designed for deterrence offers hydroelectric facility managers options to both control and protect fish as they move through and around hydro projects. *Hydro Review*, 34:15–20.
- Courret, D., Larinier, M., and Travade, F. (2014). La migration piscicole dans les cours d'eau utilisés par l'homme-Problèmes et solutions techniques.
- de Cesare, G., Furlan, P., Cilvaz, C., Micoulet, G., and Decaillet, Y. (2016). Elektrische Fischsperre des Pumpspeicherwerkes Hongrin- Léman FMHL+.
- FOEN (2022). Wiederherstellung der Fischwanderung. Gute Praxisbeispiele für Wasserkraftanlagen in der Schweiz. *Umwelt-Wissen Nr. 2205*, page 109.
- GREN (2009). Centrale Hydroélectrique de Vessy - Suivi du système de repulsion de poissons (suivi de mise en service). GREN Biologie Appliquée, unpublished.
- Haug, J., Auer, S., Frees, C., Brinkmeier, B., Tutzer, R., Hayes, D. S., and Aufleger, M. (2022a). Retrofitting of existing bar racks with electrodes for fish protection—an experimental study assessing the effectiveness for a pilot site. *Water*, 14:850.
- Haug, J., Frees, C., Brinkmeier, B., and Aufleger, M. (2022b). Ethohydraulic experiments investigating retention rates of an electrified bar rack. *Water*, 14:4036.
- IUB (2021). Barrage de la maigrauge - assainissement de la dévalaison - Étude détaillée de variantes. Technical report, IUB Engineering AG, Bern. unpublished.
- Meister, J., Moldenhauer-Roth, A., Beck, C., Selz, O. M., Peter, A., Albayrak, I., and Boes, R. M. (2021). Protection and guidance of downstream moving fish with electrified horizontal bar rack bypass systems. *Water*, 13:2786.
- Moldenhauer-Roth, A., Selz, O. M., Unterberger, F., Albayrak, I., and Boes, R. M. (2022). Development of low-voltage electrified fish guidance racks for safe downstream fish migration. *Proceedings of the 39th IAHR World Congress (Granada, 2022)*.
- Snyder, D. E. (2003). Invited overview: conclusions from a review of electrofishing and its harmful effects on fish. *Reviews in Fish Biology and Fisheries*, 13:445–453.
- Weibel, U. and Ness, A. (2014). Verfahren zum Schutz von Fischen. European Patent Office, EP2770824A1; US2014238307A1; WO2013060320A1.
- Zurwerra, A., Richard, A., M, E., and Brunner, D. (2019). Assainissement de l'ouvrage de dévalaison piscicole de la maigrauge - biomonitoring et propositions des variantes d'assainissement. Technical report. Unpublished.

Assessment of the hydromorphological effectiveness of sediment augmentation measures downstream of dams

C. Mörtl & G. De Cesare

Ecole Polytechnique Fédérale de Lausanne, Switzerland

ABSTRACT: This article presents assessment methods for the hydromorphological effectiveness of sediment augmentation measures downstream of dams. First, we describe different ways of quantifying hydromorphological effectiveness based on typical objectives of sediment augmentation. Then we show how field observations and physical and numerical modelling can be combined to investigate the influence of design criteria and site conditions on hydromorphological evolution following sediment augmentation. We provide examples of the influence of geomorphic units on bedload transport patterns and the influence of augmentation repetition frequency on hydromorphological variability. The results show that geomorphic units can influence deposition patterns and that consecutive sediment augmentation increases morphological and hydromorphological variability. Finally, we discuss the results and summarize some practical implications.

RÉSUMÉ: Notre article présente des méthodes d'évaluation de l'efficacité hydromorphologique des mesures d'augmentation des sédiments en aval des barrages. D'abord, nous décrivons différentes manières de déterminer l'efficacité hydromorphologique en fonction des objectifs typiques de l'augmentation des sédiments. Ensuite, nous montrons comment les observations sur le terrain et la modélisation physique et numérique peuvent être combinées pour étudier l'influence des critères de conception et des conditions du site sur l'évolution hydromorphologique suite à l'augmentation des sédiments. Nous donnons des exemples de l'influence des unités géomorphologiques sur les tendances du transport de charriage et de l'influence de la fréquence de répétition de l'augmentation sur la variabilité hydromorphologique. Les résultats montrent que les unités géomorphologiques peuvent influencer les schémas de déposition et que l'augmentation consécutive des sédiments accroît la variabilité morphologique et hydromorphologique. Enfin, nous discutons les résultats et résumons quelques implications pratiques.

1 INTRODUCTION

Sediment augmentation refers to the direct or indirect addition of sediment into a watercourse. Downstream of large dams, sediment augmentation measures are often implemented to compensate for a bedload deficit and re-establish sediment continuity across the reservoir. Sediment can be supplied from different sources. It can be excavated from the alluvial floodplain, the reservoir, or the reservoir's delta or transported from an external source. Global case studies have shown potential benefits and limitations for the eco-geomorphological evolution following one-time (e.g. Arnaud et al., 2017) or consecutive sediment augmentation measures (Ock et al., 2013). However, the transferability of results and, thus, the exchange of experience remains challenging, as site conditions, objectives, design and evaluation criteria can vary strongly between different measures (Mörtl & De Cesare, 2021). Table 1 shows different assessment methods used in scientific case studies of sediment augmentation measures.

Table 1. Objectives and assessment methods of sediment augmentation measures.

Site*	Year	Target process/Objectives	Assessment methods**	References
[1]. RFR Murou Dam (JA)	2006 - 2010	Sediment continuity, spawning habitat	Imagery, GSD	(Kantoush, Sumi, Kubota, et al., 2010; Kantoush & Sumi, 2011)
[2]. RFR Nunome Dam (JA)	2004, 2005, 2007 - 2009	Sediment continuity, riverbed incision, sediment transport, clogging, eutrophication	Imagery, GSD, water temperature, POM	(Kantoush, Sumi, & Kubota, 2010; Ock et al., 2013)
[3]. RFR Rossons Dam (CH)	2016	Bed morphology	CS-Profiles, HMID, RFID	(Stähly et al., 2019)
[4]. RFR Saint-Sauveur Dam (FR)	2016	Channel dynamics, riverbed incision	LIDAR, RFID	(Brousse et al., 2020)
[5]. By-pass reach Kembs Dam (DE)	2010	Sediment transport, bed morphology, recreational value	Airborne imagery, bathymetry, RFID, macroinvertebrates, macrophytes, riparian plants	(Arnaud et al., 2017; Staentzel et al., 2018)
[6]. RFR Lewiston Dam (USA)	2010, 2011, 2015	Bed morphology, spawning habitat	Airborne imagery, LIDAR, bathymetry, bedload sampler, seismometers	(Gaeuman, 2014; Gaeuman et al., 2017)

* Sites: RFR residual-flow reach. Country codes: CH Switzerland, DE Germany, FR France, JA Japan, USA United States of America.

** Assessment methods: CS-Profiles Cross-sectional bed-level profile measurements, HMID hydromorphological index of diversity (Gostner et al., 2013), RFID bedload particle tracking using radio frequency identification passive integrated transponder tags, LIDAR Light Detection and Ranging, GSD grain size distribution analysis, POM particulate organic matter.

Erosion rates and processes can be assessed from time-lapse images and topographic surveys [1,2]. Impact distance and pulse propagation behaviour of the augmented sediment can be assessed from bedload particle tracking using Radio Frequency Identification (RFID) Passive Integrated Transponder (PIT) tags [3-5] or seismic measurements [6].

One principal objective of sediment augmentation measures is diversifying bed morphology to enhance in-stream habitat conditions for fish, macroinvertebrates, or macrophytes. Common assessment methods for bed morphology complexity are analogue bed-level profile measurements [3] or bathymetric surveys [5,6]. The complexity can be quantified by the *Hydro-Morphological Index of Diversity* (HMID; Gostner et al., 2013) or the *normalized Bed Relief Index* (BRI*; Liébault et al., 2013). Satellite- and airborne imagery [5,6] and Light Detection and Ranging (LIDAR) surveys [4,6] are often used for the assessment of channel dynamics. Historic channel forms and flow patterns can be reconstructed from old maps or aerial photographs. Implications for the hyporheic flow exchange were assessed using water temperature measurements [2]. Beyond hydromorphological assessment, some studies also investigate the link between physical habitat changes from sediment augmentation measures and ecological evolution. Biological indicators can be the particulate organic matter particulate organic matter (POM) retention capacity of geomorphic units [2], the assessment of macroinvertebrate taxa richness and invasive species [5], or fish counts (e.g. Sellheim et al., 2016).

The following sections describe a multi-methodical approach to assess the hydromorphological effectiveness of the 2016 sediment augmentation measure at the Sarine River.

2 METHODOLOGY

2.1 Multi-methodical approach

A schematic overview of the main methodological approaches is shown in Figure 1.

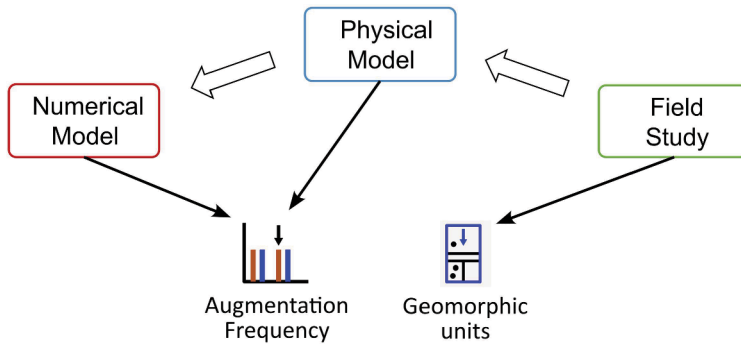


Figure 1. Schematic overview of the main methodological approaches for the hydromorphological assessment. The large arrows indicate the reference study used for the conceptual design for each approach. The small arrows indicate which approach was used to address different study objectives. Modified from Mörzl (2023).

The field study site is a 300 m-long section of the Sarine River residual-flow reach, including the 2016 sediment augmentation measure's artificial deposits at its upstream end. The physical model's main dimension criteria are a scaled representation of the study site. These main criteria are the channel geometry, bed elevations, roughness, characteristic discharge, and the sediment augmentation measure's grain size distribution (GSD) and blocking ratio. The numerical model is a digital representation of the experimental flume with a constant mesh at different experimental states.

In this multi-methodical approach, the field study provides field observations for reference, the physical model allows to reproduce and investigate hydromorphological processes for different design criteria and site conditions, and the numerical model can be used to calculate hydraulic parameters for a given channel state and simulated flow at a high resolution.

2.2 Field Study

In 2016, 1,000 m³ of sediment from the adjacent floodplain was placed in four in-channel deposits along both sides of the Sarine River residual-flow reach, nine kilometres downstream of the Rossens Dam. At the study site, the average channel slope is 0.3%, and the average channel width is 25 m. The residual flow discharge is 3.5 m³/s in summer and 2.5 m³/s in winter. The mean diameter (d_m) of the augmented sediment is 57 mm. The artificial deposits were partly mobilized in two artificial floods with a peak discharge of around 200 m³/s (2016, 2020) and in one natural flood event outside the study period (2021).

A number of 489 tracer stones equipped with radio frequency identification (RFID) passive integrated transponder (PIT) tags were distributed evenly amongst the artificial deposits and localised after a flood event using a mobile antenna (Stähly et al., 2019). Geomorphic units were mapped in several field campaigns according to the *Swiss Federal Office for the Environment* (FOEN) guideline for *Evaluating the Outcome of Restoration Projects* (EOR; Weber et al., 2021). Several reference studies include more details on the sediment augmentation measure, the site conditions, and the morphological and ecological effects (Döring et al., 2018; Schroff et al., 2022; Stähly et al., 2020). A picture of the remnants of an artificial deposit at the Sarine River after the first mobilizing flood event is shown in Figure 2.



Figure 2. Picture of the remnants of an artificial deposit at the Sarine River residual-flow reach 9km downstream of the Rossens Dam. The picture was taken on the 24th of October 2016, eleven days after an artificial flood © EPFL Platform of Hydraulic Constructions (PL-LCH). Picture: Severin Stähly.

2.3 Physical Model

The experimental flume is a 34 m-long straight wooden channel with a trapezoidal cross-section. The width is between 0.55 m and 0.78 m, and the slope is between 0.16% and 0.64%. The bed is fixed in place everywhere except in a downstream widening section, where a horizontal bed layer is created with mobile sediment (Figure 3).

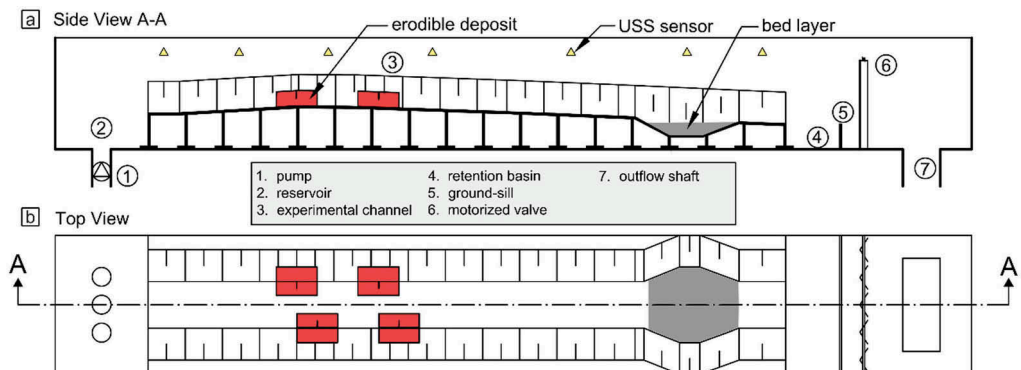


Figure 3. Schematic sketch with the control elements of the experimental flume. a: side view (A-A), b: top view. The grey area represents an initial bed layer. Modified from Mörtl (2023).

The fixed bed is coloured red to distinguish it from the mobile sediment. The channel banks are covered with a geotextile to increase their roughness. Sediment augmentation is performed in the form of four artificial sediment deposits in the upstream part of the channel. Their dimensions are shown in Figure 4.

The mobile sediment's median grain size diameter ($d_{50, \text{mobile}}$) is 5.9 mm, and the GSD range is 4-8 mm. The fixed bed sediment's d_{50} ($d_{50, \text{fix}}$) is 7.3 mm, and the GSD range is 4-16 mm.

Floods with a symmetrical hydrograph, a peak discharge of 50 l/s and a total duration of seven hours were released in the experimental flume for mobilizing the artificial deposits. Assuming Froude similitude and a scaling factor (λ) of 10, the peak discharge corresponds to 15.8 m³/s and the flood duration to 22 hours in field conditions. With this scaling, the experimental flume is representative of a 5.5 to 7.8 m-wide and 340 m-long river section and the total volume of a single sediment augmentation corresponds to 210 m³ at field scale. For the $d_{50, \text{mobile}}$, the standard cross-section width and the mean channel slope of 2.8‰, the model's peak discharge results in a *Shields Number* (θ) of 0.054.

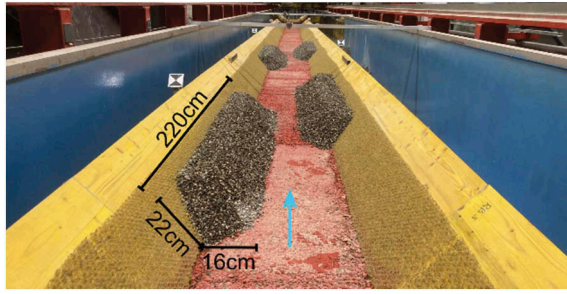


Figure 4. Pictures of the experimental flume with artificial sediment deposits in the downstream direction. The arrow indicates the direction of flow. © EPFL Platform of Hydraulic Constructions (PL-LCH). Picture: Christian Mörtl. Modified from Mörtl (2023).

After every flood, the artificial deposits were rebuilt with additional sediment to their initial dimensions. Up to four consecutive floods coupled with sediment augmentation were performed. The geomorphological evolution of the channel bed was recorded with a 3D laser scanner (scanner) of the type *LEICA SCANSTATION P20*. The scans were performed in dry conditions at different stages of the experiment. To obtain dry conditions, the discharge in the flume was stopped, and the remaining water left to flow out. After a scan or the rebuilding of the artificial deposits, the discharge was slowly resumed within a few minutes, not to flush out any sediment during the restart.

2.4 Numerical model

The numerical model is built in *BASEMENT* version 2.8.2. (VAW, 2022). The model we present is designed for steady-state simulations with a constant mesh representing a fixed bed. No morphodynamical simulations were performed, but different input meshes were created from the scans of the physical model during different stages of the experiment. With those geometries, hydrodynamic, steady-state flow simulations were carried out.

The maximum triangle size of the quality mesh is equivalent to a maximum grid length of 2 cm (small) and 4 cm (large). The higher grid resolution was used for the bed area and the bank area in the artificial deposits' vicinity. The bank's hydraulic *Strickler Roughness* (K_{st}) is $25 \text{ m}^{1/3} \text{ s}^{-1}$, and the bed's K_{st} is $40 \text{ m}^{1/3} \text{ s}^{-1}$. The numerical model's hydraulic roughness was calibrated with water level and flow velocity measurements at the physical model in the initial empty channel state during four different constant discharges (Mörtl, 2023).

The upstream boundary condition is a constant inflow with a gradient equal to the mean channel slope. The downstream boundary condition is a free surface elevation with a zero-gradient assumption. The simulations are run with a constant inflow of 2.2 l/s, corresponding to low-flow conditions in the field ($\pm 0.7 \text{ m}^3/\text{s}$). Simulations are run until a steady state is reached. The standard simulation time was 320 s.

3 RESULTS

The first part of this section provides a result of the field study's geomorphic unit mapping and RFID-particle tracking. Figure 5 shows the geomorphic units and the tracer distribution in the study section after the second morphological flood event following the 2016 sediment augmentation measure.

After two floods, the recovery rate of tracers is 41%. Only 19% of detected tracers were moved at least 2m during the flood. The longest distance of a tracer from the artificial deposits is 334 m. The dominant geomorphic unit type is *glide* (42%), followed by *run* (26%) and *shallows* (14%). Tracer density is highest in type *bar*, *shallows* and *riffle* ($[1,263; 418; 311] \text{ ha}^{-1}$) and lowest in type *glide*, *pool* and *run* ($[81; 95; 161] \text{ ha}^{-1}$). Most parts of the largest *pool* unit ($[230, 265] \text{ m}$) could not be searched for tracers because the mobile antenna could not be used in water depths greater than 1.5 m.

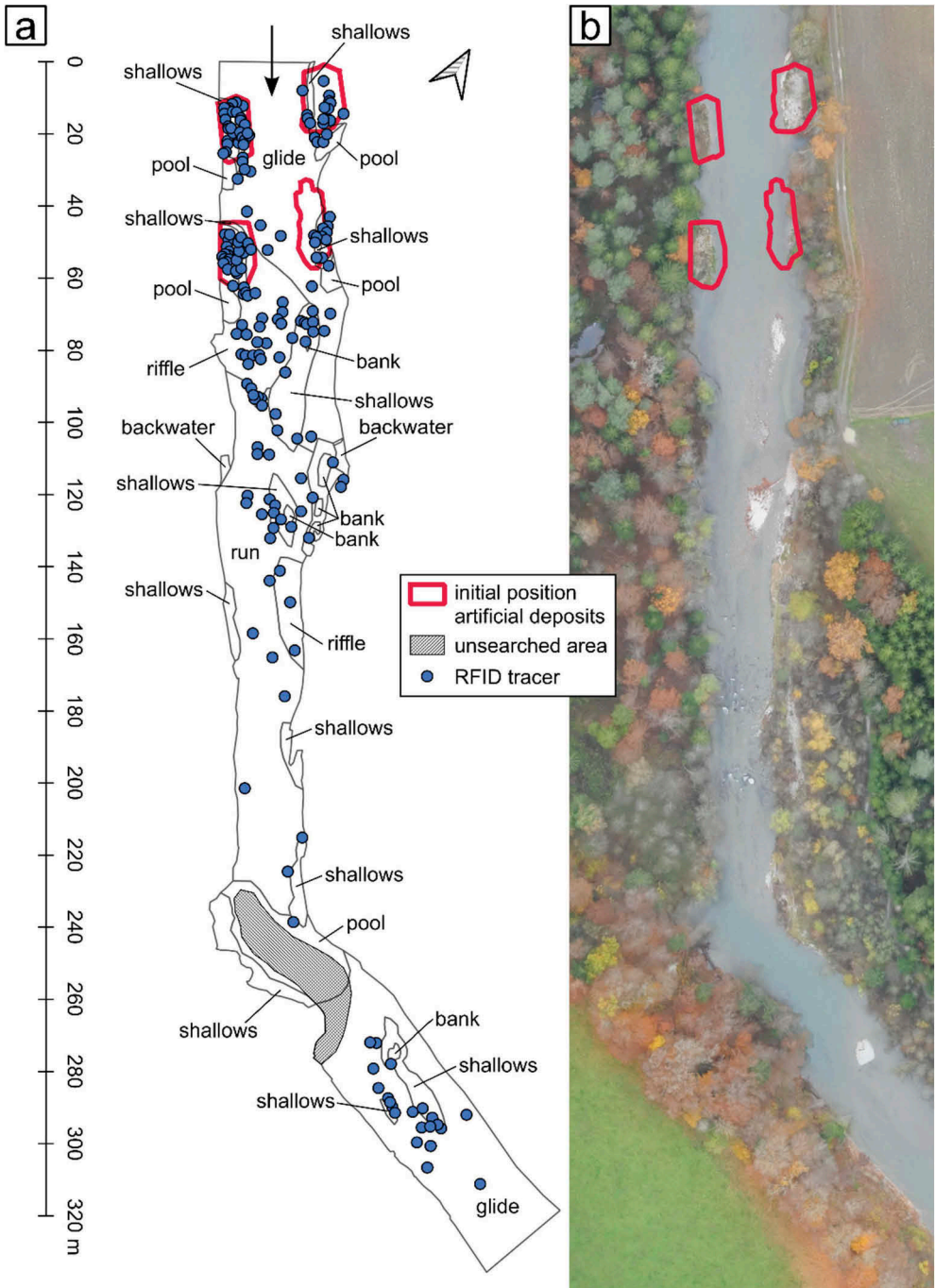


Figure 5. Plan view with RFID tracer positions (a) and ortho photo (b) of the downstream section of the artificial deposits after two morphological flood events, in November 2020. The labels mark the geomorphic units (CGUs). The unsearched area represents an area with water depths greater than 1.5m. The black arrow marks the flow direction from top to bottom. Ortho photo: Research unit Ecohydrology, Zurich University of Applied Sciences (ZHAW).

If tracers were detected in the unit type *glide* or *riffle* after the first flood, they mainly remained in the same geomorphic unit type during the second flood ([80; 89]%). If those tracers were first detected in the unit type *run* or *shallows*, around half relocated to a different geomorphic unit type during the second flood ([53; 40]%).

The following part of this section describes results of the hydromorphological channel evolution in response to consecutive sediment augmentation from the physical and numerical model study. Figure 6 shows the morphological change in the physical model between the empty channel before the placement of the artificial deposits (initial state) and the channel after four successive floods coupled with sediment augmentation. A detailed representation and discussion of morphological changes during the floods is available in Mörtl (2023).

After four floods coupled with sediment augmentation (Figure 6.b), the bed morphology is strongly diversified compared to the initial channel state (Figure 6.a). The total volume of added mobile sediment is 2.2 times the initial volume of artificial deposits. No sediment was transported outside the experimental flume. Large parts of the upstream deposit remained uneroded. The percentage area covered with augmented sediment (POC) is 73%. About 38% of the augmented sediment's volume is deposited in the channel's widening section.

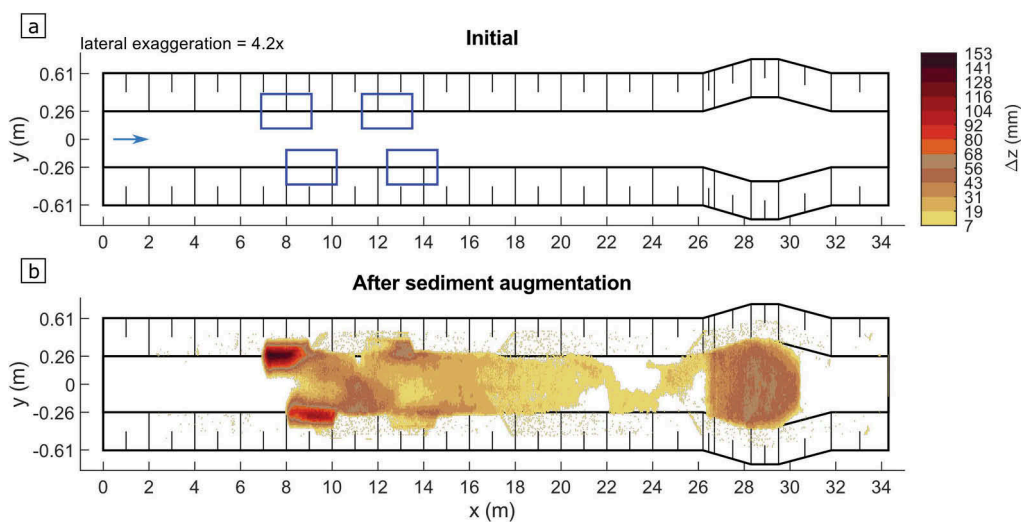


Figure 6. Graphic display of the vertical changes (Δz) between the experimental flume's initial state (a) and its state after the sediment augmentation (b). Variable x is the longitudinal channel coordinate, and y is the lateral channel coordinate. The blue squares mark the four artificial deposits' initial placement positions. The blue arrow marks the direction of flow during the experiments.

Figure 7 shows the flow fields resulting from steady-state, low-flow simulations with the channel morphology of the physical model before (Figure 6.a) and after consecutive sediment augmentation (Figure 6.b).

The simulated flow field after consecutive sediment augmentation (Figure 7.b) is more heterogeneous than at the initial state (Figure 7.a). At the height of the artificial deposits' initial positions ([7, 15]m), the main flow is deflected by the remnants of the artificial deposits. Further downstream ([15, 26]m), irregular deposition diversifies the flow field and water depth distribution, with the maximum values increased by 62% and 72%. In the section of the channel widening ([26, 31]m), a newly-formed island diverts the flow towards both banks. Compared to the initial state, the HMID increases from 7.2 by 67% to 12.0, indicating a morphologically pristine site with fully developed spatial dynamics after the sediment augmentation (Gostner et al., 2013).

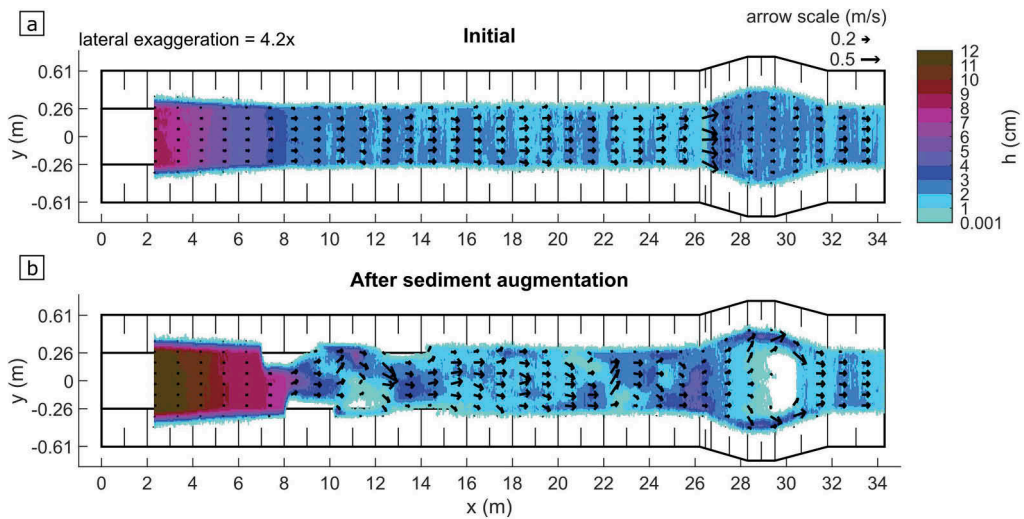


Figure 7. Graphic display of the simulated water depth (h) and flow field for the experimental flume's initial state (a) and its state after the sediment augmentation (b). Variable x is the longitudinal channel coordinate, and y is the lateral channel coordinate. The black arrows represent the two-dimensional (2D) flow field.

4 DISCUSSION

The field observations suggest that geomorphic units can influence the augmented sediment's deposition pattern. The mapped tracer distribution indicates that the proximity to the artificial deposit does not alone determine the spatial distribution of tracers alone but that the geomorphic unit types in the downstream section also have an influence. Few studies investigate the interaction of bedload transport and various geomorphic units. In an unregulated, high-gradient, pool-riffle stream, Thompson et al. (1996) showed that the distributions of coloured pebbles placed in small patches at few locations were not uniformly distributed after several low-magnitude, bed-forming floods but depended on their grain size and the geomorphic unit pattern in the downstream section. The results we present also suggest that the geomorphic unit type influences particle persistence during a flood. High particle persistence in the type *riffle* can result from relatively low shear stress during a flood due to reduced water depth along the elevated portion of the riverbed, consequently favouring bedload deposition and the covering of particles by other sediments. On the other hand, in the unit type *run*, a steep slope increases shear stress and transport rates. The interaction of bedload transport and geomorphic units is important for estimating pulse evolution and impact length and intensity of sediment augmentation measures.

The physical and numerical modelling results show that consecutive sediment augmentation increases morphological and hydromorphological variability. In conditions with sufficient bedload available, floods with a peak discharge of at least 1.5 times the entrainment threshold of the d_{50} are known to positively affect the restructuring of a mobile bed (Rachelly et al., 2021). The results we present suggest that in a sediment-starved reach, several repetitions of sediment augmentations are first required to re-establish a mobile bed layer that covers at least two-thirds of the target section before the bed can be effectively restructured while maintaining high hydromorphological variability.

Hydromorphological assessment in the form of topographic surveys, physical habitat mapping, or particle tracing can help to develop tailor-made design strategies and to make long-term predictions of the impact of sediment augmentation measures. However, especially in morphologically complex reaches, the impact of single measures is hard to isolate. The multi-methodical approach we used helped to address different physical processes and reduce

uncertainty. Similar success was achieved by coupling physical and numerical modelling (e.g. Vonwiller et al., 2018) or field observations and physical modelling (e.g. Stähly et al., 2020).

5 CONCLUSION

Consecutive sediment augmentation can help to increase the morphological- and hydraulic complexity of a sediment-starved reach. The pre-existing bed morphology thereby influences pulse propagation and deposition patterns. The mapping of geomorphic units helps obtain a process-based understanding of morphological evolution. Constant hydromorphological and ecological assessment beyond the project period can provide valuable information for proactive and adaptive decision-making and increase the long-term cost-benefit ratio of sediment augmentation measures.

ACKNOWLEDGEMENTS

This research was conducted within the framework of the River Engineering and Ecology project, funded by the Swiss Federal Office for the Environment (FOEN).

REFERENCES

- Arnaud, F., Piégay, H., Béal, D., Collery, P., Vaudor, L., & Rollet, A.-J. (2017). Monitoring gravel augmentation in a large regulated river and implications for process-based restoration. *Earth Surface Processes and Landforms*, 42(13), 2147–2166. <https://doi.org/10.1002/esp.4161>
- Brousse, G., Arnaud-Fassetta, G., Liébault, F., Bertrand, M., Melun, G., Loire, R., Malavoi, J., Fantino, G., & Borgniet, L. (2020). Channel response to sediment replenishment in a large gravel-bed river: The case of the Saint-Sauveur dam in the Buëch River (Southern Alps, France). *River Research and Applications*, 36(6), 880–893. <https://doi.org/10.1002/rra.3527>
- Döring, M., Tonolla, D., Robinson, C. T., Schleiss, A. J., Stähly, S., Gufler, C., Geilhausen, M., & Di Cugno, N. (2018). Künstliches Hochwasser an der Saane – Eine Massnahme zum nachhaltigen Auenmanagement [Artificial flood at the Sarine - A measure for sustainable floodplain management]. *Wasser Energie Luft*, 2, 119–127.
- Gaeuman, D. (2014). High-flow gravel injection for constructing designed in-channel features. *River Research and Applications*, 30(6), 685–706. <https://doi.org/10.1002/rra.2662>
- Gaeuman, D., Stewart, R., Schmandt, B., & Pryor, C. (2017). Geomorphic response to gravel augmentation and high-flow dam release in the Trinity River, California. *Earth Surface Processes and Landforms*, 42(15), 2523–2540. <https://doi.org/10.1002/esp.4191>
- Gostner, W., Alp, M., Schleiss, A. J., & Robinson, C. T. (2013). The hydro-morphological index of diversity: a tool for describing habitat heterogeneity in river engineering projects. *Hydrobiologia*, 712(1), 43–60. <https://doi.org/10.1007/s10750-012-1288-5>
- Kantoush, S. A., & Sumi, T. (2011). Sediment replenishing measures for revitalization of Japanese rivers below dams. In E. M. Valentine, C. J. Apelt, J. Ball, H. Chanson, R. Cox, R. Ettema, G. Kuczera, M. Lambert, B. W. Melville, & J. E. Sargison (Eds.), *Proceedings of the 34th World Congress of the International Association for Hydro- Environment Research and Engineering: 33rd Hydrology and Water Resources Symposium and 10th Conference on Hydraulics in Water Engineering* (Issue July, pp. 2838–2846). Engineers Australia.
- Kantoush, S. A., Sumi, T., & Kubota, A. (2010). Geomorphic response of rivers below dams by sediment replenishment technique. In A. Dittrich, K. Koll, J. Aberle, & P. Geisenhainer (Eds.), *Proceedings of the River Flow 2010 Conference* (pp. 1155–1163).
- Kantoush, S. A., Sumi, T., Kubota, A., & Suzuki, T. (2010). Impacts of Sediment Replenishment Below Dams on Flow and Bed Morphology of River. *First International Conference on Coastal Zone Management of River Deltas and Low Land Coastlines*, 285(March), 285–303.
- Liébault, F., Lallias-Tacon, S., Cassel, M., & Talaska, N. (2013). Long profile responses of alpine braided rivers in SE France. *River Research and Applications*, 29(10), 1253–1266. <https://doi.org/10.1002/rra.2615>
- Mörtl, C. (2023). *Hydromorphological assessment of sediment augmentation measures in gravel-bed rivers* [Thesis]. EPFL.

- Mörtl, C., & De Cesare, G. (2021). Sediment Augmentation for River Rehabilitation and Management— A Review. *Land*, 10(12), 1309. <https://doi.org/10.3390/land10121309>
- Ock, G., Kondolf, G. M., Takemon, Y., & Sumi, T. (2013). Missing link of coarse sediment augmentation to ecological functions in regulated rivers below dams: Comparative approach in Nunome River, Japan and Trinity River, California, US. In S. Fukuoka, H. Nakagawa, T. Sumi, & H. Zhang (Eds.), *Advances in River Sediment Research* (pp. 1531–1538). CRC Press. <https://doi.org/10.1201/b15374>
- Rachelly, C., Friedl, F., Boes, R. M., & Weitbrecht, V. (2021). Morphological Response of Channelized, Sinuous Gravel-Bed Rivers to Sediment Replenishment. *Water Resources Research*, 57(6). <https://doi.org/10.1029/2020WR029178>
- Schroff, R., Mörtl, C., Vonlanthen, P., & De Cesare, G. (2022). Impacts et enjeux de charriage d'une crue artificielle – Exemple de la Petite Sarine 2020 [Effects and bedload related challenges of an artificial flood - Example of the Petite Sarine 2020]. *Wasser Energie Luft - Eau Energie Air*, 114(2–2022), 75–84. <https://www.swv.ch/wel/fachzeitschrift-wel/wasser-energie-luft-2-2022>
- Sellheim, K. L., Watry, C. B., Rook, B., Zeug, S. C., Hannon, J., Zimmerman, J., Dove, K., & Merz, J. E. (2016). Juvenile Salmonid Utilization of Floodplain Rearing Habitat After Gravel Augmentation in a Regulated River. *River Research and Applications*, 32(4), 610–621. <https://doi.org/10.1002/rra.2876>
- Staentzel, C., Arnaud, F., Combroux, I., Schmitt, L., Trémolières, M., Grac, C., Piégay, H., Barillier, A., Chardon, V., & Beisel, J.-N. (2018). How do instream flow increase and gravel augmentation impact biological communities in large rivers: A case study on the Upper Rhine River. *River Research and Applications*, 34(2), 153–164. <https://doi.org/10.1002/rra.3237>
- Stähly, S., Franca, M. J., Robinson, C. T., & Schleiss, A. J. (2019). Sediment replenishment combined with an artificial flood improves river habitats downstream of a dam. *Scientific Reports*, 9(5176), 1–7. <https://doi.org/10.1038/s41598-019-41575-6>
- Stähly, S., Franca, M. J., Robinson, C. T., & Schleiss, A. J. (2020). Erosion, transport and deposition of a sediment replenishment under flood conditions. *Earth Surface Processes and Landforms*, 45(13), 3354–3367. <https://doi.org/10.1002/esp.4970>
- Thompson, D. M., Wohl, E. E., & Jarrett, R. D. (1996). A revised velocity-reversal and sediment-sorting model for a high-gradient, pool-riffle stream. *Physical Geography*, 17(2), 142–156. <https://doi.org/10.1080/02723646.1996.10642578>
- VAW. (2022). *BASEMENT – Basic Simulation Environment for Computation of Environmental Flow and Natural Hazard Simulation* (2.8.2). Versuchsanstalt für Wasserbau, Hydrologie und Glaziologie (VAW), ETH Zurich.
- Vonwiller, L., Vetsch, D., & Boes, R. (2018). Modeling Streambank and Artificial Gravel Deposit Erosion for Sediment Replenishment. *Water*, 10(4), 508. <https://doi.org/10.3390/w10040508>
- Weber, C., Sprecher, L., Åberg, U., Thomas, G., Baumgartner, S., & Haertel-Borer, S. (2021). Summary and content. In *Evaluating the outcome of restoration projects – collaborative learning for the future* (V1.02). Federal Office for the Environment FOEN.

Revitalization of the Salanfe river (Valais, Switzerland): A multi-faced project

M. Perroud & C. Gabbud

Alpiq, Lausanne, Switzerland

P. Bianco

iDEALP, Sion, Switzerland

J. Rombaldoni

Bureau d'ingénieur Joël Bochatay Sàrl, St-Maurice, Switzerland

V. Degen

Patrick Epiney Ingénieurs Sàrl, Sierre, Switzerland

ABSTRACT: Due to the construction of the Salanfe SA hydroelectric dam in 1952, the river is disconnected from the upper watershed. On reaching the plain, the river suddenly flows into an artificial bed, between rock banks, an underground sector and a weir at its mouth in the Rhone.

A series of measures resulting from various projects, carried out by different actors, will be implemented over the next 20 years in the Salanfe plain area. The planning and implementation of these measures must be coordinated since the perimeters of these measures and their temporality overlap.

The reflections on the upstream sector of the Salanfe plain area have led to the elaboration of a revitalization project for the watercourse with ambitious fish stakes. The project aims to promote the reproduction and growth of brown trout, and to create a sculpin reserve. The project provides for a widening and lengthening of the watercourse, as well as a diversification of the banks and streambed. Outside the watercourse, a project to safeguard biodiversity, with the creation of ponds favorable to the existing population of yellow-bellied ringers, has been established. A relaxation area, an educational pathway, a waterfall observation mound and paths dedicated to soft mobility are integrated into the overall project.

RÉSUMÉ: De par la construction du barrage de l'aménagement hydroélectrique de Salanfe SA en 1952, la rivière est déconnectée du bassin versant supérieur. En atteignant la plaine, le cours d'eau s'écoule soudainement dans un lit artificiel, entre des berges en enrochements, un secteur souterrain et un seuil à son embouchure dans le Rhône.

Un ensemble de mesures découlant de divers projets, portés par des acteurs différents, verront le jour d'ici à 20 ans dans le périmètre de la Salanfe en plaine. La planification et la mise en œuvre de ces mesures doivent se faire de façon coordonnée, tant les périmètres de celles-ci et leur temporalité se chevauchent.

Les réflexions sur le secteur amont de la Salanfe en plaine ont conduit à l'élaboration d'un projet de revitalisation du cours d'eau aux enjeux piscicoles ambitieux. Il s'agit notamment de favoriser la reproduction et le grossissement de la truite fario et d'aménager une réserve de cha-bots. Le projet prévoit un élargissement et un allongement du cours d'eau, de même qu'une diversification des berges et du lit. Hors espace cours d'eau, un projet de sauvegarde de la biodiversité, avec la création de mares favorables à la population existante de sonneurs à ventre jaune a été établi. Un espace détente, un sentier didactique, une butte d'observation de la cascade et des chemins dédiés à la mobilité douce sont intégrés au projet global.

1 INTRODUCTION

The Salanfe is a small river located in the Canton of Valais, Switzerland, which originates at the foot of the Dents du Midi and flows into the Rhone. Due to the construction of the dam and the operation of the Salanfe SA hydroelectric power plant in 1952, the river is now disconnected from the upper watershed, and its flows are greatly reduced compared to a “natural” situation. Shortly after reaching the plain, the water turbinated at the Miéville hydroelectric power station is returned to the river, causing hydropeaking effects (sudden and artificial variations in water level). The concession granted to Salanfe SA for 80 years expires in 2032. A working group has been set up to prepare a project for the renewal of the concession.

In order to meet the environmental requirements in accordance with the Federal Law on Water Protection (LEaux, 1991) and the Ordinance on Environmental Impact Assessment (OEIE), a series of environmental measures will be implemented over the next 2 to 20 years on a large part of the Salanfe river in the plain, a highly anthropized sector. The potential for development of this sector is strong, both from an ecological and morphological point of view, as well as from a tourist and landscape point of view.

This article proposes an overview of the different joint measures, the expected added value and the interrelationships between the different actors, project holders, schedules and objectives. It then presents the large-scale coordination of all these measures and the preparation of a public inquiry file for a first package of measures on the upstream sector of the Salanfe in the plain.

2 STUDY SITE

The Salanfe catchment area covers an area of 25.7 km², between the altitude of 447.5 m.s.m. and 3'257 m.s.m. On the upstream sector, the Salanfe dam collects the waters of this catchment area, as well as those derived from the adjacent Saufla catchment area.

In the intermediate watershed, downstream from the dam, the river crosses a variety of natural and forested environments, with alternating gorges, pools, and waterfalls.

Upon reaching the plain, at the foot of the Pissevache waterfall, the Salanfe flows along a natural stretch of about 50 m. A first weir of 2 m high marks the upstream limit of the dammed watercourse (Figure 1a). A second (Figure 1b) and a third weir (Figure 1c) segment the embanked watercourse into a trapezoidal, straight and monotonous channel until downstream of the Miéville power plant.

The river then flows towards the Bois de Miéville (Figure 1d), with flows increased by the turbinated water and that of the lateral channels of the plain. Its morphology remains rectilinear along its entire length but becomes more natural as it approaches the mouth of the Rhone (despite a passage under the highway of about 200 metres and the railroad line).

3 INVENTORIES OF ENVIRONMENTAL AND SAFETY MEASURES

In the Salanfe sector on the plain, various measures are or will be implemented to provide additional environmental value. These measures have overlapping perimeters, objectives that in some cases overlap, but different deadlines, implementation costs and project holders. Figure 2 shows the location of the set of environmental measures. The project holders and the year of implementation of the measures are indicated in the titles of the sub-chapters.

3.1 *Watercourse remediation – Salanfe SA – 2023/2024*

Art. 80 of the LEaux aims to remediate water withdrawals on a temporary basis until the concessions are restored, by setting up an endowment flow, implementing artificial floods or



Figure 1. Photographs of the Salanfe River in the plain a) at the foot of the Cascade la Pissevache, with weir 1 in the foreground, b) on the channelled section at weir 2, c) then at weir 3, and d) in the Bois de Miéville.

carrying out compensation measures, within the limits of what is economically feasible. After negotiations, a compensation measure was decided in 2021, with a triple objective:

- Structure the bed to allow for trout reproduction and growth,
- diversify the shoreline to accommodate valuable riparian environments, and
- provide new biotopes for other species that depend on aquatic and wetland environments.

3.2 *Hydropeaking remediation – Salanfe SA – 2025/2026*

The aim of the hydropeaking remediation (Art. 83 of the LEaux) is to reduce the impact on aquatic fauna and flora caused by the sudden and artificial variation of the watercourse during hydropeaking. The Confederation subsidizes the studies and the measures carried out (Art. 34 of the Low on Energy) provided that the realization begins before 2030. Salanfe SA, which is subject to this remediation obligation, is in the process of evaluating the hydrological and ecological deficits of the watercourse, in order to establish the objectives to be reached and the variants of measures allowing to meet them.

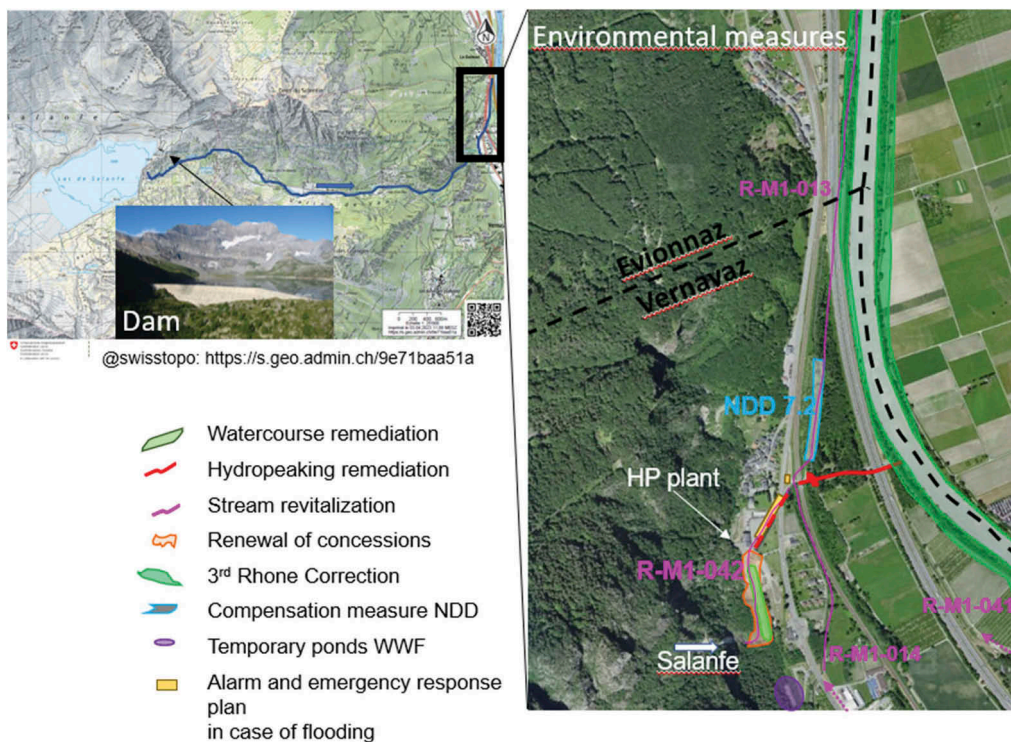


Figure 2. Watershed of the Salanfe River with location of the dam and the environmental measures.

3.3 Stream revitalization – Municipalities – 2024 (< 80 years)

The cantonal strategic planning for the revitalization of watercourses (Art. 62b of the LEaux) defines the objectives and priorities of the measures to be implemented by the municipalities. Priority 1 measures are generally those with a flood protection objective. Their realization is generally fixed at 20 years. The measures in priority 2 extend over 80 years depending on the opportunities. The Confederation and the Cantons grant subsidies for these projects ranging from 65 to 90% depending on the achievement of the objectives (i.e. objectives set through a Program Agreement renewed every 5 years).

Three revitalization measures from the cantonal catalog of measures are located in the Salanfe plain area:

- R-M1-013: improvement of fish habitat, its land-water connection, extensive management of its riparian vegetation, its connection to the Rhone and its habitat diversity.
- R-M1-014: preservation of riparian vegetation and placement of small structures.
- R-M1-042: habitat diversification to support natural trout reproduction, restoration of extensive riparian environments, removal of barriers to fish passage, habitat diversification.

3.4 Renewal of concessions – Future Salanfe SA concessions holder – 2032

The Saufla and Salanfe rivers have been used for the production of hydroelectric power for nearly 70 years. All the facilities belong to the company Salanfe SA, founded in October 1947. The concessions expire on 31 December 2032. As part of the procedure for the renewal of its concessions for a further period of 80 years from 1 January 2033, in accordance with Art. 58a of the Federal Law on the use of hydropower, the Salanfe SA facility is subject to an environmental impact assessment (EIA) for the granting of a water rights concession. Within the

framework of this procedure, the implementation of a measure in favour of nature and the landscape was proposed in the Salanfe sector on the plain, upstream of the discharge of the turbine water. Its objective is to increase the ecological and public benefits of the measures already planned in this area.

3.5 *3^{ème} correction of the Rhône – Canton Valais and Vaud – coming decades*

The third correction of the Rhone aims at various modifications of the river for safety purposes over several decades. The removal of the weir at the mouth of the Salanfe in the Rhône will be carried out within the framework of this project.

3.6 *Other measures*

Other specific environmental measures have already been implemented. These will have to be preserved during the realization of future projects.

The Nant de Drance pumped storage power plant went into operation in 2022. To compensate for the environmental impact of its construction and the high-voltage line, it has implemented fifteen environmental measures, most of which aim to encourage the recolonization of the environment by certain animal and plant species that are rare or threatened with extinction in Switzerland. Two measures are located in the plain sector of the Salanfe, and more specifically on parts of the sections inventoried in the cantonal strategic planning for the revitalization of watercourses (see Section 3.3). These are the measures:

- NDD 7.1bc: Development of biotopes favourable to amphibians
- NDD 7.2: Creation of wetlands separated from the watercourse by excavations, with variation in depths to obtain a proportion of approximately 60% of flooded environments and control of invasive species.

The WWF has created small water bodies for the yellow-bellied toad, a protected species of amphibian, on the right bank of the Salanfe, a few dozen meters from the Cascade de la Pissevache.

4 COORDINATION

The actions described above have implications for those sharing a common boundary or, in the case of a change in hydrologic regime, for those further downstream. Examples include:

- The viability of measure NDD 7.2 (Section 3.6) can only be ensured if possible enlargements of the watercourse do not affect the section of the Salanfe concerned after the hydropeaking remediation (Section 3.2). The same constraints apply to the implementation of the Salanfe revitalization concept R-M1-013 (Section 3.3).
- The watercourse remediation measure (Section 3.1) is included in the scope of the measure proposed within the renewal of concessions project (Section 3.4). Coordination between these two measures is necessary to avoid any constraints.
- The ecological measures upstream of the hydropower plant tailrace (Sections 3.1; 3.3; 3.4) have a common interface with the hydropeaking remediation measure (3.2). Management of this interface is essential.

A global and integrated approach is therefore fundamental, in terms of territorial scope, technical and environmental constraints, interfaces and dependencies between these measures (hydrology, ecological networks, and so on). Aware of these stakes, Salanfe SA (present and future concessions holders) and the Municipalities have joined forces as project holders to carry out the large-scale coordination of all these measures.

The coordination mandate is given to an assistant project manager with multidisciplinary skills, able to conceptualize, consider, process, plan, coordinate and monitor the measures as a whole and their transdisciplinarity (technical and environmental aspects).

The assistant project manager ensures the smooth running of the project in terms of organizational, administrative, legal and budgetary aspects. He is the link between the project holders and the specialized branches offices and ensures coordination with the authorities and third parties involved. In particular, he leads the decision-making meetings.

The technical skills are provided by a group of specialized offices, appointed by all the project holders. The assistant project manager can thus rely on experts in the fields of hydrology, hydraulics, hydroelectric developments, civil engineering, geotechnics, hydrogeology, aquatic biology, riparian environments, heritage.

5 COORDINATION DURING THE IMPLEMENTATION PHASE

The first phase of this coordination began in 2021. The group of specialized offices has been mandated to draw up project outline for the upstream sector of the Salanfe in the plain, i.e. the area between the Cascade de la Pissevache and the hydropower plant tailrace. This section concerns 1) the watercourses remediation (Section 3.1), 2) the stream revitalization - R-M1-042 (Section 3.3) and 3) the renewal of concessions (Section 3.4).

From the various outlines, the project holders selected the most favorable, based on environmental, safety, tourism, and financial criteria. The detailed project was then started. In parallel, coordination meetings with the cantonal authorities are regularly organized to ensure that the project complies with the legislation in force.

By agreement between the project holders, the global project (Figure 3) was then divided into 4 sectors, one for each of the 3 projects discussed above plus one for other potential projects. Technical reports and impact statements were prepared for each measure simultaneously to ensure that the interface between the systems was coherent and that the objectives, especially for fish, were achieved in a comprehensive manner. The construction permit applications will be filed separately, and the implementation of the measures staggered over time.

6 THE PROJECT

The overall project under consideration is shown in Figure 3.

In the watercourse area, the revitalization project (iDEALP SA 2023, Patrick Epiney Ingénieurs Sàrl 2023) plans, on the one hand, to widen the streambed while softening and diversifying the slopes on both banks and, on the other hand, to smooth the longitudinal profile to increase the slope and promote the dynamics.

The section to be developed, with a total length of 250 m, will be subdivided into 2 subsections:

- A “trout sector”, downstream (see North sector on Figure 3), with a dynamic natural bed, allowing the formation of alternating gravel banks, diversified habitats and conditions favorable to the natural reproduction of river trout. In this sector, a few large boulders will be placed on both sides of the minor river bed in order to initiate diversification of the flows. The development of this section of stream is attributed to the watercourse remediation measure.
- A “sculpin sector” upstream (see South sector on Figure 3), with a more or less fixed sinuous bed, developed with a predominance of pebbles, allowing to reproduce the current habitat conditions very favorable to the maintenance of sculpin. In this sector, the heights of the banks of the major river bed will be adjusted so as to be flooded approximately 30 days per year, thus relieving the constraints on the minor bed during ordinary flooding episodes. The development of this section of stream is attributed to the stream revitalization measure.



Figure 3. Overall view of the revitalization project on the upstream sector of the Salanfe in the plain.

Weir n°1 (existing), located downstream of the section, will be redesigned to make it passable for trout and sculpin.

Weir n°2 (existing), with a height of 1.4 m, will disappear by recharging the bed up to threshold n°1. The slope of the bed will thus be slightly increased, with the aim of recreating a dynamic allowing the formation downstream of alternating banks. This target morphology should favour the alternation of pools and riffles necessary for the habitat and reproduction of trout (structuring of the minor river bed).

A new weir will be built between the current weir n°1 and n°2, in the middle of the section, in order to separate the “trout sector” from the “sculpin sector”. It will be built in such a way as to make the upstream sector inaccessible for trout and to preserve the sculpin population currently present in this sector.

The presence of gravel in the river bed is an essential element to promote trout reproduction. An access to the river will be built downstream of the new weir to dump, if necessary, gravelly materials that would have been washed away by a flood event.

Finally, weir n°3 (existing), upstream of the section, will be redesigned with riprap blocks to give it a natural appearance.

The project plans to reclaim the materials on site. The smallest blocks of the current riprap and the excavation materials will be used to fill and develop the new river bed. The larger blocks will be used to build the 3 weirs and to concentrate the current locally (preferential channel) in the “trout sector”.

The excess material will be used to build the stream dike, an observation dike (an attractive viewpoint on the Pissevache waterfall, also serving as protection against boulders), and a noise barrier.

To prevent the colonization of the banks by invasive neophyte plants, a riparian cordon will be planted on the banks with native species. Walls will be built on the banks with the excess blocks to provide habitats for amphibians, reptiles, small mammals and insects.

Outside the watercourse, the renewal of concessions project (Bureau d'ingénieur Joël Bochatay Sàrl 2023) foresees the creation of a string of ponds on the left bank of the Salanfe, between the foot of the Pissevache and the hydroelectric power station. The objective of this measure is to safeguard biodiversity in general, with a particular focus on amphibians and aquatic fauna in lentic environments. The target species is the yellow-bellied toad *Bombina variegata*, a small and rare toad whose population has been observed 150 m from the project. The string of ponds planned will serve as relay biotopes between the existing population to the south and the recently created ponds in the Miéville woods to the northeast, about 300 m away (Section 3.6).

Tourism and landscape objectives are also integrated into this measure, notably by enhancing the Cascade (observation mound) and the site's industrial heritage (educational trail) and optimizing the access roads to this sector.

A recreational area is reserved on the right bank for potential future projects. This area will be dedicated to playgrounds, picnic areas and pastures. Soft mobility is also taken into account, with the improvement of the Vernayaz - Miéville villages, and easier access for people with reduced mobility.

7 CONCLUSION

In order to meet the legal environmental requirements, a series of measures will be carried out in the Salanfe plain area over the next 10 years. At the initiative of the hydroelectric company Salanfe SA, the project holders have agreed on a global management of these measures. A first revitalization project was elaborated on the channeled section located between the foot of the Pissevache waterfall and the tailrace of Salanfe SA hydroelectric power plant in Miéville.

The ambitious detailed project brings a significant ecological added value to a highly anthropized section of the river. Without joint measures, preserving the sculpin population and promoting trout reproduction on the same stretch of water would have been a difficult task. The widening and lengthening of the stream, as well as the creation of pools fed by the Salanfe River, gives the stream more space. In accordance with the expectations of the LEaux, the perimeter of the project will be registered as a reserved space for water, preserving it from any further construction.

The collaboration undertaken with the municipalities is welcomed by all the actors, including the cantonal authorities. The know-how and the multidisciplinary knowledge of the employees of the hydroelectric companies are assets for the deployment of municipal projects. By working together, objectives that go beyond those targeted by the revitalization have been integrated, with concrete solutions brought in particular to safety issues (rock falls and protection against floods). As for the population, it will benefit from these spaces of well-being and relaxation where landscape, soft mobility and heritage preservation aspects are maximized. Everyone wins, the cost of the project being minimized.

In view of the popularity of the project in the upstream sector, the second phase of the project, on the section between the power station and the mouth of the Rhone, has begun. The analysis of variants will be finalized during 2023 and shared with the authorities and the concerned municipalities.

REFERENCES

- Bureau d'ingénieur Joël Bochatay Sàrl. 2023. Restoration and replacement measure of Miéville. Technical report and environmental impact notice, St-Maurice, Switzerland.
- iDEALP SA. 2023. Salanfe SA - Commune de Vernayaz, Revitalization of the Salanfe at Miéville. Mise à l'enquête publique - Rapport technique, Sion, Switzerland.
- Patrick Epiney Ingénieurs Sàrl. 2023. Revitalization of the Salanfe river in the plain: Miéville (Commune of Vernayaz). Environmental impact statement (NIE), Sierre, Switzerland.

Storage tunnels to mitigate hydropeaking

W. Richter & G. Zenz

Institute of Hydraulic Engineering and Water Resources Management, Graz University of Technology, Graz, Austria

ABSTRACT: The optimization of hydraulic systems in diversion tunnel power plants can provide significant economic and ecological benefits. By designing these systems as storage tunnels with differential surge tanks, power plants can be improved to handle surge and sunk compensation to mitigate hydropeaking by optimizing the associated construction costs, allowing for increased flexibility and improved storage management.

1 INTRODUCTION

New diversion power plants with tunnel water conveyance systems are currently designed and constructed as new as well as replacements for old power plants in terms of re-commissioning.

The transportation of water in tunnels offers the opportunity to go underground and thus utilize both economic and ecologic advantages, such as preserving protection zones and reducing fluctuations in water levels. For example, the Romanche-Gavet hydropower project (97 MW, 560 GWh/year), consisting of 6 old power plants and 5 reservoirs were replaced with a diversion power plant in one river section. Table 1 refers to Alpine hydropower projects utilizing underground storage infrastructure.

Table 1. Overview of underground storage of hydropower plants (Richter, 2022).

Power plant	Type of underground storage	Volume	Installed capacity	Standard production capacity	Design discharge
		m ³	MW	GWh	m ³ /s
Innertkirchen (CH)	Storage tunnel and hydropeaking compensation basin combined in tailwater	60,000 20,000	390	720	64
Fieschertal (CH)	Storage tunnel headwater	64,000	64	144	15
Forbach PSH (G)	Storage cavern in tailwater for expansion	200,000	50		16.9 TU 15.7 PU
Nassfeld PSH (A)	Storage cavern in tailwater for expansion	175,000	31.5	50	11.6 TU 9.2 PU
Obervellach II (A)	Storage tunnel in headwater and hydropeaking compensation basin in tailwater	60,000 60,000	38	125	9.0
Salvesenbach (A)	Storage tunnel	10,000		17	1.0
Stanzertal (A)	Storage tunnel headwater	51,000	13.5	52.2	12
St. Anton (IT)	Storage tunnel in as hydropeaking compensation basin in tailwater	95,000	90	300	18
Starkenbach (A)	Storage tunnel	4,700	17.8	17.8	0.85

The following example projects already show the effectiveness of storage tunnels in power water ways.

Obervellach II power plant project - currently under-construction - will replace an old cascade of power plants in the Möll valley in Carinthia. The project has a storage tunnel in parallel with the main tunnel and in balance with a retention basin with the same volume to allow an energy shift by storage operation by keeping the inflow and outflow to the river system at the same quantity.

The Stanzertal hydropower plant is operated with a 4.6 km long storage tunnel in the main pressure tunnel, which allows for energy to be shifted to peak periods. The approved pumped-storage hydropower plant (PSH) Forbach in the Black Forest in Germany will feature a 200,000 m³ tailwater storage expansion by a mostly unlined storage cavern attached to the existing river retention basin to enable efficient pumped storage operation in combination with the existing upper reservoir with 14 hm³.

The St. Anton hydropower plant near Bolzano was renovated with a 95,000 m³ storage tunnel in the tailrace for compensation of water level fluctuations. As part of the expansion of the Innertkirchen I hydropower plant, the tailrace was equipped with a storage tunnel and a balancing basin to reduce water level fluctuations in the Hasliaare river.

Pressure tunnels for hydro power generation with medium head and high discharge rates often have greater lengths and necessarily large cross-sectional areas, which also contain a large volume of water. Traditionally, the hydraulic use of pressure tunnels is mostly intended for the transport of water from the reservoir to the surge tank and then to the turbines via the pressure shaft. In hydropower plants with large storage reservoirs, the volume proportion of the tunnel is in general small and serves purely for transport. The pressure tunnel is part of a hydraulic pressure system, changes in flow might occur very quickly due to the rapid propagation of pressure waves, with accompanying compensatory oscillations in the surge tank.

The additional use of the water conveyance system as a storage volume for short-term storage such as daily storage or flood peak compensation can significantly increase the usable water volume. This can make the operation of a hydroelectric power plant more flexible, especially in alpine catchment areas. For small or medium-sized diversion power plants, the operation can be based on the electricity demand and be adapted by the intermediate storage in the tunnel. In combination with the requirements of compensating for flood and low flow in the river as well as the residual water flow, the storage of water volume can offer advantages for the operation.

Additionally, by using bypasses with energy dissipators around turbines, the power regulation of the machines and the water flow rate can be decoupled. This can be used for environmental flow compensation in case of load rejections. Specifically designed regulated energy dissipators are currently investigated to ensure stable control circuits in combination with environmental benefits.

2 TUNNEL STORAGE CONCEPT

In addition to the amount of water and the head, the ability to store water efficiently determines the effective generation of renewable energy by hydroelectric power plants. In some cases, the storage reservoir can be effectively supplemented by hydraulic storage utilization implemented in the water transport tunnel. Tunnel systems are particularly used in storage power plants, diversion power plants, or pumped-storage power plants. For small or medium-sized diversion power plants, an adapted operation can be carried out based on the electricity demand through the intermediate storage in the tunnel. New power plants or revitalization projects are also subject to higher requirements for flood and low flow compensation. These can be partially or entirely relocated to the tunnel for their damping effect, enabling flexible participation in grid control services with higher ecological acceptability. In pumped-storage power plants, the capacity of the storage reservoirs usually prevails, and they can provide peak power without flood or low flow impact, especially with sufficiently large reservoirs downstream, making them an ideal storage and load balancing technology for the energy transition. The combination of tunnel storage in the head race tunnel and compensating reservoir

downstream also enables turbines to operate beyond the amount of water available, in order to operate the storage volumes during peak power times or during low water seasons without negative impacts on river flows. Any suspended sediment accumulations in storage tunnels can also be addressed through daily emptying in a bypass.

2.1 *Diversion power plant with bypass energy dissipator*

The combination of a tunnel storage with a bypass that includes an energy dissipator allows for flexible operation to maintain the hydropeaking compensation through the water volume in the diversion tunnel. An adequate bypass system enables the decoupling of the power-controlled turbine operation and water flow. This allows for steep power gradients of the units and flat flow gradients to meet the requirements of hydropeaking compensation in the river system. Figure 1 shows a schematic section through a diversion power plant with a tunnel storage in the head race, a tunnel storage surge tank, and an energy converter in the power cavern. The tunnel is shown in the empty state. A control element after the intake enables independent control of the storage volume. An aeration shaft enables that the ventilation of the storage tunnel takes place and not through the intake structure ensuring safe operation. By using the energy dissipator downstream, a possible compensation basin can be optimized in size since in this case, storage water can pass from the head race even when the turbines are throttled. In particular, by holding the hydropeaking compensation in the tunnel, the level in the compensation basin can be lower, thus ensuring higher energy generation, which is relevant for medium-head systems with high flow rates. The energy dissipator in the turbine bypass allows the hydropeaking compensation volume to be maintained in the head race tunnel. The dissipator depicted corresponds to the pressure regulator of the turbines in the Tonstad power plant (960 MW) in Norway, which are successfully used for pressure surge reduction. Dissipators or pressure regulators were built in many power plants associated with Francis turbines, especially in the first half of the 20th century. Pressure regulators in Austria are, for example, in operation in Rodundwerk I (1943) pumped-storage power plant and Limberg I pumped storage power plant (1955). Possible further designs of a control element in the bypass are modified cone jet valves and axial piston valves.

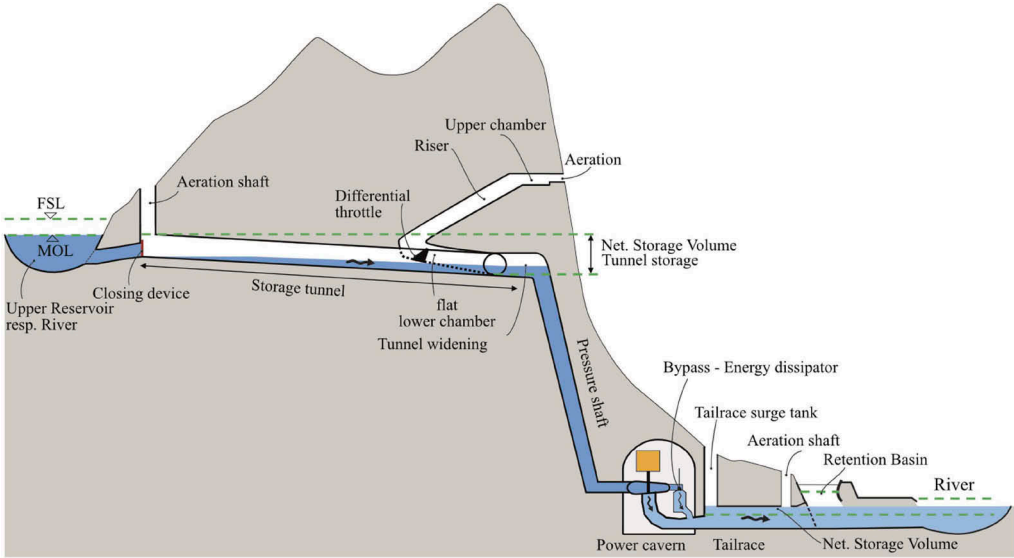


Figure 1. Schematic longitudinal section of a diversion power plant with tunnel storage and differential storage surge tank, bypass with energy converter, optimized compensation basin, and optimized surge tank concept. (Richter et. al, 2022 modified).

3 HYDRAULIC REQUIREMENTS

3.1 *General requirements*

Due to its operation as a storage tunnel, the hydraulic flow behavior of the tunnel changes from pure pressure flow to a free surface flow and vice versa. Thus, the requirements for the design and dimensioning of the tunnel and the surge tank are crucial. The head race tunnel must therefore be designed to ensure safe flow between pressurized flow and free surface flow. These boundary conditions, as well as the necessary venting before the intake structure, influence the design of the surge tank and the necessary inclination of the pressure tunnel. Venting in the tunnel prevents air blowouts when the power plant is unloading and the surge tank is upsurging. An ideal, possibly low inclination of the storage tunnel can be determined specifically for each system. A gentle inclination enables high heads even with partial filling, therefore the inclination can be in the range of 0.1% to 0.2% (Design and operation of the Stanzertal hydro power plant headrace tunnel as reservoir, 2015). However, even lower inclinations in the range of the energy line gradient can also be effective.

3.2 *Requirements for the surge tank*

A surge tank for hydraulic separation between pressure surge and mass oscillation of the penstock is necessary in hydropower plants featuring tunnel systems of a certain length to ensure the controllability of the turbines (Thoma, 1910). To prevent the surge tank from showing a resonance event due to independent control processes, it must have a sufficiently large horizontal cross-section that interacts with volume changes caused by switching operations with head changes affecting the power output. Particularly for large flow rates and lower heads, the stability criterion for the surge tank shaft may require large horizontal cross-section areas. This criterion is usually calculated according to Thoma or Svee (Thoma, 1910 and Jaeger C., 1949) or (Svee, 1972 and Leknes, 2016). A flat surge tank tunnel with surge tank chambers arranged at an angle in the head height range of the power plant has very large cross-sections, which thus meet the stability criterion for adequate controllability and also store water. Since the frictional losses in the pressure shaft, which have an adverse effect on stability, are not considered in Thoma's criterion, a safety factor must be multiplied by it. Values of 1.5 [-] to 1.8 [-] are proposed (Jaeger, 1958). More precise calculations of the required cross-section can be carried out using calculation formulas from Svee, 1972 or Leknes, 2016, or with 1D numerical stability calculations. Short pressure shafts and operating ranges in which the efficiency gradient of the turbines increases (before the optimal efficiency value) have a favorable effect on stability. A decreasing efficiency gradient of the turbines (after the peak load value) has an unfavorable effect on the required stability cross-section. Thus, for diversion power plants with low or medium head heights, the safety factor of 1.5 [-] for the stability cross-section typically used can be reduced, or best being calculated in terms of 1D numerical simulations.

The surge tank also reduces the pressure surge load on the pressure tunnel and allows for quick start-up and shutdown of the hydraulic machines, with the inertia of the water masses in the tunnel enabled by the water volume in the surge tank. The water in the pressure tunnel is accelerated by the water level and thus pressure difference between the surge tank and the reservoir. It must ensure both start-up without the water column separation and shutdown without the surge tank overflowing. For the start-up operation, a different condition arises for tunnel storage surge tanks compared to the usual high-pressure systems. For storage tunnel operation the tunnel may have a free surface flow. However, the water column must not separate creating macro cavitation, prevented by the lower chamber design on low head level in connection to the tunnel. It is important that the pressure tunnel cross-section is widened before the transition to the pressure shaft in order to compensate for the varying flow velocities without causing the flow to break.

The specific representation of a possible tunnel storage surge chamber from a 3D CFD simulation in the emptying state (Figure 2) shows a low-lying lower chamber with a free water level that is able to drop into the tunnel without flow separation during the downsurge. Due to the low tunnel inclination and the surge tank, any intermediate switching operations are also enabled.

In the event of shutdown or emergency shutdown, the differential surge tank arrangement allows the kinetic energy in the gallery and surge tank to be damped by the upsurge via the overflow weir and the differential throttle. The overflow height thus defines the pressure maximum for the mass oscillation at the surge tank base. A differential chamber is provided directly after the lower chamber separated by the differential throttle. The two chambers are provided as inclined tunnels, the latter being designed on the required volume from the mass oscillation and the stability criterion. From a construction point of view, both chambers can thus be excavated up from the same access. The deep differential chamber significantly reduces the dynamics of water flowing back from the surge tank to the basin in case of shutdown. The throttle is necessary to efficiently dampen the mass oscillation and separate water from the lower chamber as much as possible in case of a shutdown. The throttle must be sized to an optimum diameter, leaving enough air in the upper chamber to retain volume in the event of shutdown. Several constructive design variations of a surge tank surge chamber are conceivable.

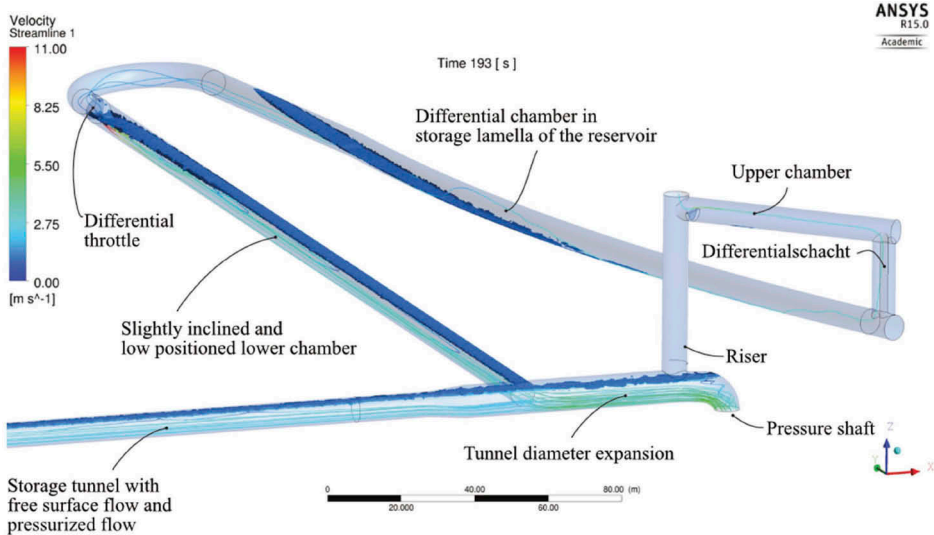


Figure 2. 3D view, surge shaft surge chamber, emptying process, expansion of the surge shaft before the transition to the pressure shaft, effect of the differential throttle (Richter et. al, 2022 modified).

Since a vertical surge shaft is unthrottled, and connected directly at the transition to the pressure shaft, the design enables ideal pressure pulse reflection. The shaft has very low inertia values and thus can physically respond quickly to pressure surges. This design can also be omitted if it is demonstrated that the pressure surge can be sufficiently mitigated by the inclined gallery and ventilation of the lower chamber is assured. Figure 3 shows a horizontal differential throttle with a lower loss coefficient in outflow direction compared to filling direction defining a differential throttle.

3.3 1D numerical simulation

The hydraulics of pressure tunnel systems are being investigated efficiently in a goal-oriented approach by means of 1D numerical simulations. The transient processes such as mass oscillation and pressure surge events are calculated for the headrace waterways and in particular the surge tank, that are designed for most unfavorable transient operations. In order to model the free surface flow in the pressure tunnel appropriately, adequate 1D numerical simulations are demanded. Based on a Master’s thesis at the Institute of Hydraulic Engineering and Water Resources Management at the Graz University of Technology, the hydraulics of a tunnel reservoir of a medium-sized hydropower plant were studied. The 1D numerical simulation software Wanda V4.2 was evaluated for these problems (Wechtitsch, 2014).

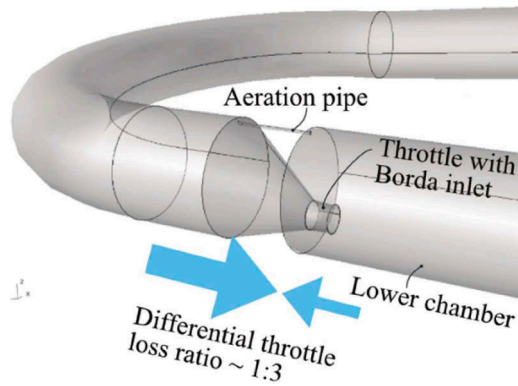


Figure 3. 3D view, horizontal differential throttle with aeration pipe (Richter et. al, 2022 modified).

In the hydraulic engineering laboratory of the Graz University of Technology, hybrid model tests (numerical and physical) were used to calibrate the 1D numerical simulations using large surge chamber models (Richter, et al., 2013). Flow transitions from pressurized flows to free surface flow occur in surge tanks, especially in the lower chambers. The experience of the hydraulic behavior of the lower chambers will be applied to both the hydraulics of the pressure tunnel and the design of storage tunnel surge tanks.

3.4 Case study for storage tunnel featuring a storage surge tank

1D simulations are carried out on the basis of a case study. Load cases for start-up and shut-down as well as stability simulations are performed. Penstocks usually have large flow cross sections and high Reynolds numbers. For back-calculations of existing flow losses in headrace tunnels, Strickler coefficients are usually determined in Austria. For transient 1D numerical calculations these roughness values are converted into equivalent sand roughness. The Strickler coefficient of smooth concrete pressure tunnels was converted from measurements of the pressure tunnel of the Lünarseewerk PSH from D_i 3.05 m, $K_{ST} = 85 \text{ m}^{1/3}/\text{s}$ to $K_S = 0.276 \text{ mm}$ (Buecheger, 1961). Due to the neglect of the Reynolds number in the Strickler approach, the Strickler coefficient decreases for the same roughness for larger pressure tunnel cross-sections.

The power plant dimensions for the case study are defined as follows:

- Gross head: 64 m
- Expansion water flow: 130 m^3/s
- Storage gallery length: 13 700 m, $D = 7.2 \text{ m}$, $K_{ST} = 80 \text{ m}^{1/3}/\text{s}$
- Gross gallery volume: 557 800 m^3
- Expansion capacity: 66 MW
- Pressure shaft: $L = 80 \text{ m}$, $D = 6 \text{ m}$, $K_{ST} = 110 \text{ m}^{1/3}/\text{s}$

Due to the low head and the relatively high discharge in the pressure tunnel, the required stability cross-section for the surge chamber is 888 m^2 with a safety factor of 1.5 [-].

Figure 4 shows the evaluation for the usable volume of the case study as a function of slope. A distinction is made between emptying at design water discharge (Q_d) and staggered emptying discharge $Q_d - Q_{d/2} - Q_{d/4}$. In the case of emptying with Q_d , the water column separates at a point, whereby emptying degrees of 50% - 65% are achieved. With staggered emptying between 90% - almost 100% can be achieved depending on the inclination. The friction slope for pressure discharge is 0.74 ‰, which can be a minimum design slope specification.

Thus, depending on the plant, it is possible to reserve both a part of the storage tunnel for flexible power plant operation and a partly for hydropeaking compensation.

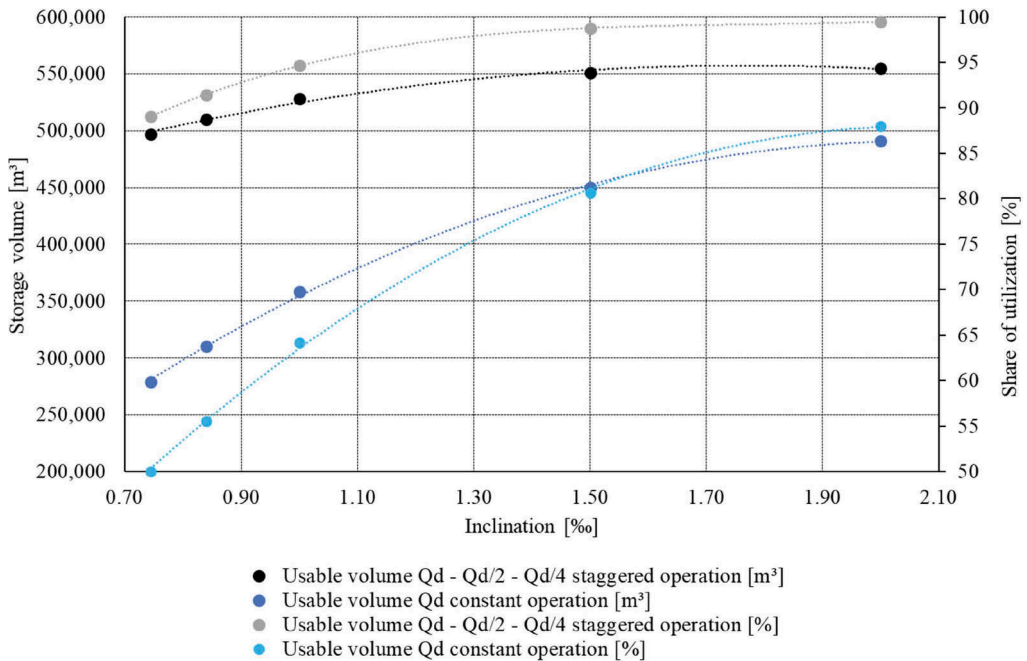


Figure 4. Drainage of storage galleries, useful volume and useful fraction, case study, (Richter et. al, 2022 modified).

3.5 Design criteria for storage tunnel surge tanks

For the hydraulic dimensioning of storage tunnel surge tanks, the following parts are to be designed by means of transient simulations:

- Lower chamber for the most unfavorable opening load case, or a resonance load case in storage tunnel operation, to avoid separation of the water column.
- Upper chamber, or inclined shaft to the most unfavorable shutdown load case, in connection with the throttle dimensioning to avoid overflow.
- The horizontal water surface area in the surge chamber is designed for the stability criterion in a 1D numerical stability analysis.

Due to the low inclination, storage tunnels have low internal pressures, especially in diversion power plants. When a storage tunnel surge tank with differential effect is arranged, higher pressures are generated only briefly. Therefore, for specific pressure tunnel situations and with good geological conditions, an unlined pressure tunnel can offer hydraulic stability and enough volume as well as design and economic advantages. The throttle generates a differential effect. Since the lower chamber overlaps in height with the pressure tunnel, startup events can be permitted until a free level discharge is reached in the pressure tunnel if the design is appropriate. In particular, a low positioned lower chamber also allows increased flexibility in operation with free surface flow discharge with respect to cyclic power plant operations. 3D numerical flow simulations and/or physical model tests are recommended to investigate a concrete design hydraulically with respect to transient effects of filling and emptying, as well as the behavior of the air. In addition, 1D numerical stability simulations allow an economic design of the surge tank cross-sections.

4 DISCUSSION

Power plant constructions in times of climate crisis, resource efficiency and energy generation in particular are reconsidered in comparison with the energy input for construction and operation. Since low inclined pressure tunnels, which are designed as storage tunnels, are also exposed to

a low maximum internal pressure, the tunnel lining can be optimized due to geotechnical requirements. Thus, in load-bearing rock, unlined pressure tunnels can also be designed in a targeted manner, taking the criterion of internal pressure versus mountain water table into account. For the hydraulic design of diversion power plants with a defined inflow level, it may also be advisable to design the headrace tunnel for free surface flow operation as normal operation mode.

5 SUMMARY

Diversion power plants with headrace tunnels can offer both economic and ecological advantages in terms of hydropeaking compensation by increasing flexibility and enabling reservoir management if the hydraulic design is optimized as storage tunnels with differential surge tanks.

A storage tunnel surge tank consisting primarily of a shallow lower chamber with a necessary volume also allows for flexible hydraulic use of the tunnel volume. 1D numerical calculations show that a well-designed surge tanks can perform this function. This allows the free surface flow discharge in the tunnel to be independent of the cyclic load operations. In addition, the use of energy dissipators can decouple the power control of the machines and the hydraulic flow downstream. This allows upstream tunnel volume to be used for hydropeaking compensation as well. Simulations show that with staggered discharge and an optimized tunnel inclination up to nearly 100% of the tunnel storage volume can be utilized. However, current research on dissipators in control operation is necessary in order to safely manage the durability on the one hand and the flexible control capability of the overall system on the other hand. In addition, dissipators can achieve a reduction of the pressure surge load if designed appropriately. Specific investigations by means of 3D-numerical hydraulic simulations as well as physical model tests allow the most economical and structural safe and appropriate design of storage tunnel systems and surge tanks.

REFERENCES

- Buchegger, W. 1961. *Fallhöhenverluste in der Wasserführung des Lünenseewerkes*. Jahrgang 51, Heft 5/6, Seiten 136-142: Österreichische Wasserwirtschaft.
- Deltares. 2013. *Wanda 4.2, User Manual*. Delft.
- Die Oberstufe des Tauernkraftwerkes Glockner-Kaprun. 1955. Zell am See: Tauernkraftwerke A.G.
- Jaeger, C. 1949. *Technische Hydraulik*. Basel: Birkhäuser.
- Jaeger, C. 1958. Contribution to the Stability Theory of Systems of Surge Tanks.
- Leknes, E. 2016. *Comparison of the Svee and Thoma Stability Criteria for Mass Oscillations in Surge Tanks*. Masterthesis, NTNU Trondheim.
- Müller, M., Kaderli, R., Keller, Y., Gehri, M., & Kost, M. 2016. Ausgleichs und Regulierbecken Innertkirchen Planung, Realisierung und Inbetriebnahme des ersten Beckens zur Reduktion von Schwall und Sunk in der Schweiz. *Konferenzbeitrag, 18. Wasserbau - Symposium, Technische Universität München, Obernach*.
- Richter, W. 2020. *Surge Tank Design for Flexible Hydropower*. Dissertation: Graz University of Technology.
- Richter, W., Schneider, J., Zenz, G., & Innerhofer, G. 2013. *Hybrid Modelling and Development of a long Upper Chamber in a Surge Tank*. Proceedings of Hydro Congress, Innsbruck.
- Richter, W., Schneider, J., Zenz, G., & Kolb, S. 2012. Hybrid Modelling of a Large Surge Tank. *Proceedings of 17th International Seminar on Hydropower Plants, Vienna*.
- Richter, W., Zenz, G. Stollenspeicher für Ausleitungskraftwerke. *Österr Wasser- und Abfallw* 74, 383–388 2022. <https://doi.org/10.1007/s00506-022-00879-0>
- Svee, R. 1972. *Fordelingsbasseng ved vannkraftverk; Formler til bestemmelse av svingegrenser og kritiske tverrsnitt, Surge tanks for hydropower plants – Equations for deciding the surge limits and critical areas Bericht - Norwegisch*. Trondheim.
- Thoma, D. 1910. *Theorie des Wasserschlosses bei selbsttätig geregelten Turbinenanlagen*. Dissertation, Kgl. Technische Hochschule zu München: R. Oldenbourg.
- Wechtitsch, R. 2014. *Modellierung von Stollenspeicher*. Masterarbeit, Institut für Wasserbau und Wasserwirtschaft, TU Graz.
- Widmann, W., Lebesmühlbacher, T., Eder, A., & Knorpp, K. 2015. Design and operation of the Stanzerthal hydro power plant headrace tunnel as reservoir. *Hydro Congress*. Bordeaux

Can hydropeaking by small hydropower plants affect fish microhabitat use?

J.M. Santos

Forest Research Centre, School of Agriculture, University of Lisbon

R. Leite & M.J. Costa

CERIS, Instituto Superior Técnico, University of Lisbon

F.N. Godinho

Hidroerg, Lisbon, Portugal

M.M. Portela, A.N. Pinheiro & I. Boavida

CERIS, Instituto Superior Técnico, University of Lisbon

ABSTRACT: Despite the numerous benefits of hydropower, this renewable energy source can have serious negative consequences on freshwater fish, as a result of short-term artificial flow fluctuations downstream, often known as hydropeaking. Alterations in species habitat use are expected to occur, as a result of variations in the physical environment. However, such assessments conducted at the microhabitat scale, and stratified by season and ontogeny, have rarely been assessed, yet they are fundamental to improve our mechanistic understanding of hydropeaking influences on fish. The goal of this study was to assess fish microhabitat use and availability of leuciscids at upstream undisturbed (2) and hydropeaking-affected (2) river sites located downstream from two small hydropower instalments (SHP), Douro basin, NE Portugal. Fish surveys (juveniles and adults) were performed in spring and summer by electro-fishing followed by the establishment of river transects to acquire use and availability data, respectively. A multivariate approach was then employed to analyse both datasets. Cover and depth were found to be the most important variables driving microhabitat use of species at both the reference and hydropeaking sites. Fish exhibited similar patterns of non-random microhabitat use between the reference and the hydropeaking sites, mainly occupying deeper and more sheltered ones than those available. Overall, seasonal and size-related patterns in species microhabitat use were similar between the reference and hydropeaking sites, with the species showing seasonal patterns in microhabitats use from spring to summer, but, in most of the cases, revealing no size-related difference between both types of sites. This work showed that artificial peak-operations by SHP had negligible effects on fish microhabitat use downstream from SHP when compared to the reference sites, and that the high resilience of the hydropeaking sites appears to be related to the amount of cover habitat and the availability of undisturbed substrates, which provide conditions that still support similar driving patterns of fish habitat use at sites fragmented by SHP.

1 INTRODUCTION

Hydropower currently stands as one of the leading renewable energy sources worldwide, known to reduce the dependence on greenhouse gas emissions and attenuate the effects of climate change (Owusu & Asumadu-Sarkodie, 2016). Approximately half (48%) of the global

river volume is altered by flow regulation and/or river fragmentation as a consequence of the construction of hydropower schemes (Grill et al., 2019). However, increasing emphasis has been placed in the widespread development of small hydropower plants (SHP) as a result of governmental incentives and the private sector to enable electrification in remote regions and to encourage the transition to new forms of market-based renewable energy (Couto & Olden, 2018). Typically, hydropower plants operate according to short-term, sub-daily changes of the electricity market, undergoing sudden variations of flow discharge, and significantly changing downstream water levels. This operation known as hydropeaking cause negative impacts on river ecosystems downstream SHP. Most common ones are fish drift and stranding, blockage to fish migratory movements, alterations in food-web sources and in water temperature, as well as modification of sediment transport, for which studies have been carried out over the past decade (Young et al., 2011).

However, hydropeaking also causes changes in species habitat use, namely on fish, which under such conditions face significant changes in key hydraulic variables that structure habitat, i.e. in depth and velocity (Capra et al., 2017). However, such assessments considering these core variables have been rarely investigated at the microhabitat use scale, which roughly corresponds to an “hydraulic unit,” described by a combination of distinct hydraulic and physical factors, usually at a scale of 1 m² or less (Hohensinner et al., 2018). In addition, most studies do not consider, the effect of other variables that also change during hydropeaking, such as river substrate and cover, which are also considered as major factors driving fish microhabitat use elsewhere (Nestler et al., 2019). Therefore, microhabitat assessments should encompass the joint effect of all these variables (depth, velocity, substrate and cover) in hydropeaking rivers, while integrating sampling stratified by season and ontogeny (i.e., size-related) on species microhabitat use and availability.

The goal aims to address the effects of hydropeaking by SHP on species microhabitat use, stratified by season and ontogeny to understand how fish microhabitat use at river segments downstream from such plants, are affected when compared to those located reference ones (i.e. lacking ant river regulation structures). This information will prove useful to better understand how hydropeaking impact fish life stages to drive future conservation actions but also to inform possible mitigation measures to counteract the effects of such induced peak-flows.

2 MATERIAL AND METHODS

2.1 Study area

The work was conducted in rivers Couto and Avelames, tributaries of the Tâmega River, NE Portugal. Couto and Avelames rivers are partially regulated by SHP (i.e. plants with installed capacity < 10 MW), namely Covas do Barroso and Bragado, respectively. The cases studies are of run-of-river type although capable of storing part of the daily inflows smaller than the minimum design discharges, namely during low flow periods. These operations cause abrupt variations in the river discharges downstream the powerhouses' tailraces which configure a hydropeaking exploitation mode on river segments downstream. The mean annual flow and the design discharge at Covas do Barroso SHP are 3.33 and 5.70 m³/s, respectively. The equivalent values for Bragado SHP are 1.28 and 2.20 m³/s. The discharge assigned to ecological and irrigation purposes is 0.170 m³/s, at Covas SHP, and 0.114 m³/s, at Bragado SHP. Four 150m long river sites - 2 located in the affected river segments downstream from Covas do Barroso and Bragado SHP and the other 2 located upstream from both SHP in the lotic segment and taken as reference sites were selected. The latter lacked induced peak flows or other human pressures. The fish fauna is dominated by the native leuciscids Northern straight mouth nase (*P. duriense*; henceforth, nase) and the Northern Iberian chub (*S. carolitertii*; henceforth, chub). The brown trout (*S. trutta*) also occurs in the study area, namely in Couto River.

2.2 Fish sampling

Fish sampling was performed in late-spring and early-summer, coinciding with the spawning and growing period, respectively, for nase and chub (Ferreira et al., 2007). It is also a critical period for the trout, when this species actively searches for thermal refugia to avoid warmer temperatures (Ayllón et al., 2010). Each of the four sites was sampled by a modified point electrofishing procedure (Garner, 1997) to avoid pushing the anode forward in the water and cause fish to displace from their original positions. The team (3 persons, 1 maneuvering the anode) moved upstream in a zag-zag to ensure full coverage of all habitats. Each time a fish or a school of fishes was captured or spotted, a numbered location marker was anchored to the streambed for the subsequent microhabitat use measurements. Captured fish were transferred to small buckets to avoid repeated counting and were immediately measured for total length (TL), to further account for ontogenetic (i.e., size-related) differences in microhabitat use. The following size-classes were considered according to the literature (Santos et al., 2011; Nicola & Almodóvar, 2002): ≤ 11 and > 11 cm TL for nase, ≤ 7 and > 7 cm TL for chub and < 12 and ≥ 12 cm TL for trout.

2.3 Microhabitat use and availability sampling

After fish sampling, several microhabitat use parameters were measured, including i) water depth (cm), measured with a graduated dip net pole, ii) mean water velocity (cm/s), measured at 60% of the distance from the surface to the substrate if depth was less than 80 cm; otherwise, it was the mean of measurements recorded at 20% and 80% of depth; iii) dominant substrate composition, measured according to a modified Wentworth scale (Bovee, 1986) and assessed visually in 0.8 x 0.8 m quadrats directly below the location of the captured/spotted fish and iv) percent cover, estimated at each fish/shoal location in 10% increments, by the same operator to minimize potential errors. It was considered as any natural structure occurring in the riverbed that could provide protection to fish. After microhabitat use measurements at each site, availability of the same variables was randomly assessed at 15-25 equidistant transects perpendicular to the flow to allow comparisons with microhabitat use and to search for non-random microhabitat use patterns.

2.4 Data treatment

Principal component analysis (PCA) with varimax rotation including availability and use data for the reference and hydropeaking sites was performed to explore for non-random microhabitat use by fish and to examine possible seasonal and size-related microhabitat use patterns (Santos et al., 2018). To approach normality, all variables were previously $\log(x+1)$ transformed, except percent cover, which was arcsin square root transformed. Only components with eigenvalues >1 and variable with loadings $\geq |0.70|$ were retained for interpretation (e.g., Santos et al., 2018). Mann-Whitney (MW) U-tests were then conducted on the PCA scores to search for seasonal and size-related differences on species microhabitat use. The analyses were conducted on the software STATISTICA (StatSoft, Inc., Tulsa, OK, USA).

3 RESULTS

3.1 Non-random microhabitat use

PCA on the microhabitat availability and use by nase at the reference and hydropeaking sites yielded two principal components (PCs) with eigenvalues >1 , which explained 65.7% and 68.7% of the variance in the data, respectively (Table 1). Depth and cover were found to be positively loaded on PC1 at both type of sites, with individuals selecting specific microhabitats (i.e. showing non-random microhabitat use), being over-represented in deeper and sheltered positions (MW U-tests on PCA scores, $P < 0.001$). Substrate correlated high with PC2 at both types of sites, but only the hydropeaking sites showed non-random microhabitat use with nase being over-represented in finer substrates (MW U-test on PCA scores, $P < 0.01$).

Table 1. Loadings of environmental variables on the first two components extracted by PCA on the seasonal and size-related microhabitat use by nase (*P. durienne*) in reference and hydropeaking sites. An asterisk (*) denotes non-random microhabitat use for a specific variable.

Sites	Environmental variable	PC axes	
		1	2
Reference	Depth	0.83*	
	Substrate		0.78
	Cover	0.85*	
	% of explained variance	65.7	
Hydropeaking	Depth	0.79*	
	Substrate		0.80*
	Cover	0.89*	
	% of explained variance	68.7	

PCA on the microhabitat availability and use by chub at the reference and hydropeaking sites produced two PC with eigenvalues >1, which both explained 65.0% of the variance in the data (Table 2). Depth and cover were found again to be positively loaded on PC1 at both type of sites, with this species showing non-random microhabitat use, being over-represented in deeper and sheltered positions (MW U-tests on PCA scores, $P < 0.001$). Substrate was the single variable correlating high with PC2 at both types of sites, but only the reference sites showed evidence of non-random microhabitat use, with individuals being over-represented in finer substrates (MW U-test on PCA scores, $P < 0.01$).

Table 2. Loadings of environmental variables on the first two components extracted by PCA on the seasonal and size-related microhabitat use by chub (*S. carolitertii*) in reference and hydropeaking sites. An asterisk (*) denotes non-random microhabitat use for a specific variable.

Sites	Environmental variable	PC axes	
		1	2
Reference	Depth	0.84*	
	Substrate		0.77*
	Cover	0.85*	
	% of explained variance	65.0	
Hydropeaking	Depth	0.87*	
	Substrate		0.82
	Cover	0.83*	
	% of explained variance	65.0	

PCA on the microhabitat availability and use by trout at the reference and hydropeaking sites produced two PC with eigenvalues >1, which both explained 73.4% and 64.9% of the variance in the data, respectively (Table 3). Depth and cover were found to be positively loaded on PC1 at both type of sites, with this species showing non-random microhabitat use at the hydropeaking sites, in which it was found to be over-represented in deeper and sheltered areas (MW U-tests on PCA scores, $P < 0.001$). Velocity was the single variable correlating high with PC2 at the reference sites, whereas substrate was more important at the hydropeaking ones, both showing no indication of non-random microhabitat use (MW U-tests on PCA scores, $P > 0.05$).

Table 3. Loadings of environmental variables on the first two components extracted by PCA on the seasonal and size-related microhabitat use by trout (*S. trutta*) in reference and hydropeaking sites. An asterisk (*) denotes non-random microhabitat use for a specific variable.

Sites	Environmental variable	PC axes	
		1	2
Reference	Depth	0.87	
	Velocity		0.81
	Cover	0.88	
	% of explained variance	73.4	
Hydropeaking	Depth	0.82*	
	Substrate		-0.80
	Cover	0.84*	
	% of explained variance	64.9	

3.2 Effects of season and size on microhabitat use

MW tests on PCA scores of PC1 showed a significant effect of season on microhabitat use by nase at both the reference and hydropeaking sites (Table 4), where individuals were found to shift to deeper and more covered habitats from spring to summer. Evidence of size-related microhabitat use was also found on this component but only for the reference sites (adults used deeper and more covered areas than juveniles). Regarding PC2, a significant effect of season was also reported in both types of sites, with fish shifting to finer substrata from spring to summer. The effect of size-class was not significant for both types of sites.

Table 4. Results of the Mann-Whitney (MW) U-tests on PCA scores addressing the effect of season and size class on fish microhabitat use in reference and hydropeaking sites, in relation to the extracted principal components (PCs).

Species	PC	Variation	Reference		Hydropeaking	
			Z	P	Z	P
Nase	1	Season	-2.93	< 0.01	-8.09	< 0.001
		Size-class	-3.83	< 0.001	-0.72	0.471
	2	Season	4.67	< 0.001	4.82	< 0.001
		Size-class	1.82	0.070	0.71	0.478
Chub	1	Season	-2.27	< 0.05	0.06	0.950
		Size-class	-1.22	0.222	0.59	0.552
	2	Season	4.07	< 0.001	4.35	< 0.001
		Size-class	0.29	0.774	-0.58	0.559
Trout	1	Season	-3.76	< 0.001	-1.17	0.241
		Size-class	-4.86	< 0.001	-2.75	< 0.01
	2	Season	4.58	< 0.001	2.99	< 0.01
		Size-class	1.08	0.063	0.89	0.373

For chub, the effect of season was significant at the reference sites only, as MW tests on PC1 scores showed that fish shifted to deeper and more covered areas from spring to summer. Size-class had no influence on microhabitat use by fish on this component for both types of sites. As found for the nase, season was reported to have a significant effect on microhabitat use at both the reference and hydropeaking sites, with fish shifting to finer substrata from spring to summer.

A significant seasonal (individuals shifting to deeper and more covered areas in summer) and size-related effect (adults using deeper and more covered habitats than juveniles) on microhabitat use was found for trout at the reference sites (MW U-test on PC1 scores, $PP < 0.05$). For the hydropeaking sites, a significant effect on this component was solely reported for size-class, with adults using deeper and more covered habitats than juveniles. Concerning PC2, significant effects were only found for season for both types of sites: at the reference sites individuals shifted to slower-flowing areas from spring to summer, whereas at the hydropeaking sites, fish shifted to coarser substrata from spring to summer.

4 DISCUSSION

One of the most relevant results from this work was that the variables that structured microhabitat use for fish species at the reference and hydropeaking sites were cover and depth, as shown by the high loadings on the first axis PCA, which explained most of the variation. This agrees in part with initial expectations in which that depth and water velocity should be the most important variables for habitat use, particularly at the reference sites, because they are not subjected to abrupt flow variations, and hence fish should not be dependent on the use of cover against potentially harsh environmental conditions as those experienced under induced peak-flow conditions (Boavida et al., 2017).

The role of cover for fish microhabitat use has been highlighted in several works (e.g., Allouche, 2002 and references therein), providing: i) protection against predators, ii) visual isolation reducing competition risk and iii) hydraulic shelter against detrimental environmental conditions, such as those imposed during peak-flow operations. Cover is therefore a critical factor in most fish life-cycle stages, including spawning or growth and diel life activities, such as foraging, resting, or avoiding predators. In the present study, additional forms of cover could have also been provided by the well-structured and continuous riparian vegetation galleries. Besides offering cover, vegetation also has important functions in terms of ecological structure and river functioning, namely by providing structural protection for instream habitats, regulation of the river flow, as well as substratum fixation for algae and periphyton (Vesipa et al., 2016).

All leuciscids species exhibited similar patterns of non-random microhabitat use between the reference and hydropeaking sites. At both types of sites, nase and chub, occupied non-randomly deeper and sheltered microhabitats than those available, as shown by PC1 high loadings. Both species showed non-random microhabitat use on PC2, which was substratum-related, being overrepresented in habitats with finer substrata. Taken together, these patterns seem to suggest an association of both species with pool habitats. Similar results have been reported by other authors in Iberian rivers (e.g., Ferreira et al., 2007), suggesting that both species mainly adopt a pool-dwelling behaviour to both counteract the effects of water shortage at warmer seasons and also the effects of floods and peaking events at the wet ones (Boavida et al., 2020).

Contrarily to leuciscids, there was no evidence of non-random microhabitat use by trout at the reference streams, confirming their plasticity in habitat selection that has been already described (Ayllón et al., 2009). This species can flexibly change selection behaviour as a function of habitat features, which is in turn, determined by the interaction of the structural features of the channel and the hydrological regime (Maddock, 1999). In rivers characterized by a Mediterranean regime of high intra and interannual flow variability as in the study area, river hydrology can be a relevant driving force for trout dynamics, as this species may display higher habitat plasticity in such variable environments (Ayllón et al., 2010). However, under induced peak-flow conditions, trout were found to display non-random microhabitat use, occupying deeper and sheltered positions than those available. As habitat use by trout is highly based on the profitability of territory in terms of potential net energy intake rate (Railsback & Harvey, 2002) and thus, on the trade-off between energy gain and risk, it is believed that the selection of deeper and sheltered positions provided increased protection against peak-induced flow variations making them able to cope against excessive current velocity and drifting (Saltveit et al., 2020).

Overall, seasonal and size-related patterns in species microhabitat use were similar between the reference and the hydropeaking sites, with the majority of species displaying seasonal patterns in microhabitats use from spring to summer (though such shifts were more expressive at the reference sites), but, in most of the cases, revealing no size-related difference between both types of sites. The most common species showed a shift to deeper and more covered areas from spring to summer, along with the selection of areas with finer substrata. This would be naturally expected, particularly in rivers that seasonally experience water shortage due to its Mediterranean regime, and where fish need to find deep and sheltered positions in summer to increase their survival chances during the harsh environmental season (e.g., Varkadas et al., 2020), typically in pools where substratum coarseness is in general dominated by finer particles, i.e., sand and gravel (Bonada et al., 2020). A possible reason for finding the same patterns in the peak-operation affected sites is that flow-variation may not be sufficient to exceed the environmental range needed to alter the role of key variables structuring species microhabitat use.

Unlike seasonal patterns, significant size-related differences in microhabitat use of species were barely noted, both at the reference and hydropeaking sites. A few exceptions were noted for the nase at the reference sites and for trout at both types of sites, in which adults used deeper and more covered habitats than juveniles. This is in accordance with the frequently documented larger fish – deeper habitat association, either for leuciscids (Santos et al., 2018) or salmonids (Ayllón et al., 2010). Such patterns often result from predation by gape-limited piscivores that increase the predation risk to smaller fish in deeper habitats (Morán-López et al., 2012). The absence of differences – in this case, in size-related habitat use patterns – between the reference and hydropeaking sites, seems to point out the effect of habitat heterogeneity, and the availability of high undisturbed coarse substratum and cover in overcoming the effects of induced peak-flow variations.

5 CONCLUSIONS

This work showed that the effects on fish microhabitat use downstream from SHP of peak-induced flow variations were negligible when compared to reference sites upstream. Cover and depth were found to be the most important variables structuring habitat use, both at the reference and hydropeaking sites, being therefore critical as they also elicited non-random responses for all species as shown by PCA results. Potential mitigation measures should consider maintaining and controlling the strips of riparian vegetation and the mosaics of submerged aquatic macrophytes downstream from SHP that are critical for fish, in particular during unfavorable flow conditions as those imposed by induced peak-flow conditions. The provision of large coarse substrata (e.g., boulders), to the river channel may provide hydraulic shelter against excessive current velocities (Allouche, 2002; Santos et al., 2006), hindering fish from being washed away by sudden discharges.

ACKNOWLEDGEMENTS

This study received funding from Foundation for Science and Technology (FCT) through the EcoPeak4Fish project – an integrated approach to support self-sustaining fish populations downstream hydropower plants (PTDC/EAM-AMB/4531/2020). The authors are grateful for the FCT's support through funding UIDB/04625/2020 from the research unit CERIS.

REFERENCES

- Allouche, S. 2002. Nature and functions of cover for riverine fish. *Bulletin Français de la Pêche et de la Pisciculture* 365-366: 297–324.
- Ayllón, D., Almodóvar, A., Nicola, G.G. & Elvira, B. 2009. Interactive effects of cover and hydraulics on brown trout habitat selection patterns. *River Research and Applications* 25(8): 1051–1065.

- Ayllón, D., Almodóvar, A., Nicola, G.G. & Elvira, B. 2010. Ontogenetic and spatial variations in brown trout habitat selection. *Ecology of Freshwater Fish* 19: 420–432.
- Boavida, I., Ambrósio, F., Costa, M.J., Quaresma, A., Portela, M.M., Pinheiro, A., Godinho, F.N. 2020. Habitat use by *Pseudochondrostoma duriense* and *Squalius carolitertii* downstream of a small-scale hydropower plant. *Water* 12(9): 2522.
- Boavida, I., Harby, A., Clarke, K.D. & Heggenes, J. 2017. Move or stay: habitat use and movements by Atlantic salmon parr (*Salmo salar*) during induced rapid flow variations. *Hydrobiologia* 785(1): 261–275.
- Bonada, N., Cañedo-Argüelles, M., Gallart, F., von Schiller, D., Fortuño, P., Latron, J., Lloren, P., Múrria, C., Soria, M., Vinyoles, D., Cid, N. 2020. Conservation and management of isolated pools in temporary rivers. *Water* 12(10): 2870.
- Bovee, K.D. 1986. Development and evaluation of habitat suitability criteria for use in the instream flow incremental methodology, Fort Collins, CO, U.S. Fish and Wildlife Service Biological Report 86(7).
- Capra, H., Plichard, L., Bergé, J., Pella, H., Ovidio, M., McNeil, E. & Lamouroux, N. (2017). Fish habitat selection in a large hydropeaking river: strong individual and temporal variations revealed by telemetry. *Science of the Total Environment* 578: 109–120.
- Couto, T.B. & Olden, J.D. 2018. Global proliferation of small hydropower plants – science and policy. *Frontiers in Ecology and the Environment* 16: 91–100.
- Ferreira, M.T., Sousa, L., Santos, J.M., Reino, L., Oliveira, J., Almeida, P.R. & Cortes, R.V. 2007. Regional and local environmental correlates of native Iberian fish fauna. *Ecology of Freshwater Fish*, 16: 504–514.
- Garner, P. 1997. Sample sizes for length and density estimation of 0+ fish when using point sampling by electrofishing. *Journal of Fish Biology* 50: 95–106.
- Grill, G., Lehner, B., Thieme, M., Geenen, B., Tickner, D., Antonelli, F., Babu, S., Borrelli, P., Cheng, L., Crochetiere, H., Ehalt Macedo, H., Filgueiras, R., Goichot, M., Higgins, J., Hogan, Z., Lip, B., McClain, M. E., Meng, J., Mulligan, M., Nilsson, C., Olden, J.D., Opperman, J.J., Petry, P., Reidy Liermann, C., Sáenz, L., Salinas-Rodriguez, S., Schelle, P., Schmitt, R.J.P., Snider, J., Tan, F., Tockner, K., Valdujo, P.H., van Soesbergen, A. & Zarfl, C. (2019). Mapping the world's free-flowing rivers. *Nature* 569: 215–221.
- Hohensinner, S., Hauer, C. & Muhar, S. 2018. River morphology, channelization, and habitat restoration. In: S. Schmutz, S. & J. Sendzimir (eds.), *Riverine Ecosystem Management*: 41–65. Aquatic Ecology Series. Amsterdam, The Netherlands: Springer.
- Maddock, I. 1999. The importance of physical habitat assessment for evaluating river health. *Freshwater Biology* 41(2): 373–391.
- Morán-López, R., Pérez-Bote, J.L., Da Silva, E. & Perales Casildo, A.B. (2012). Hierarchical large-scale to local-scale influence of abiotic factors in summer-fragmented Mediterranean rivers: structuring effects on fish distributions, assemblage composition and species richness. *Hydrobiologia* 696(1): 137–158
- Nestler, J.M., Milhous, R.T., Payne, T.R. & Smith, D.L. 2019. History and review of the habitat suitability criteria curve in applied aquatic ecology. *River Research and Applications* 35: 1155–1180.
- Nicola, G.G. & Almodóvar, A. 2002. Reproductive traits of stream-dwelling brown trout *Salmo trutta* in contrasting neighbouring rivers of central Spain. *Freshwater Biology* 47: 1353–1365.
- Owusu, P.A. & Asumadu-Sarkodie, S. 2016. A review of renewable energy sources, sustainability issues and climate change mitigation. *Cogent Engineering* 3: 1167990.
- Railsback, S.F. & Harvey, B.C. 2002. Analysis of habitat-selection rules using an individual-based model. *Ecology* 83(7): 1817–1830.
- Saltveit, S.J., Brabrand, Å., Juárez, A., Stickler, M. & Dønnum, B.O. 2020. The impact of hydropeaking on juvenile brown trout (*Salmo trutta*) in a norwegian regulated river. *Sustainability* 12(20): 8670.
- Santos, J.M., Reino, L., Porto, M., Oliveira, J., Pinheiro, P., Almeida, P.R., Cortes, R. & Ferreira, M.T. 2011. Complex size-dependent habitat associations in potamodromous fish species. *Aquatic Sciences* 73(2): 233–245.
- Santos, J.M., Rivaes, R., Boavida, I. & Branco, P. 2018. Structural microhabitat use by endemic cyprinids in a Mediterranean-type river: implications for restoration practices. *Aquatic Conservation: Marine and Freshwater Ecosystems* 28(1): 26–36.
- Vardakas, L., Kalogianni, E., Smeti, E., Economou, A.N., Skoulikidis, N.Th., Koutsoubas, D., Dimitriadis, C. & Datry, T. 2020. Spatial factors control the structure of fish metacommunity in a Mediterranean intermittent river. *Ecohydrology & Hydrobiology*, 20(3), 346–356.
- Vesipa, R., Camporeale, C. & Ridolfi, L. 2016. Recovery times of riparian vegetation. *Water Resources Research* 52(4): 2934–2950.
- Young, P.S., Cech, J.J. & Thompson, L.C. 2011. Hydropower-related pulsed-flow impacts on stream fishes: a brief review, conceptual model, knowledge gaps, and research needs. *Reviews in Fish Biology and Fisheries* 21: 713–731.

The Cimìa dam in Sicily. A relevant case of rehabilitation

L. Serra

Waterways, Roma, Italy

G. Gatto & E. Costantini

Studio Speri, Rome, Italy

ABSTRACT: Cimìa is an zoned embankment dam with clay core, built in the period 1975-1980 in Sicily. The dam has a maximum height of 39 m and determines a reservoir volume of 10 Mm³. Over the years the structure has undergone a progressive silting due to the influx of solids during floods and actually the bottom discharge is compromised and requires important re-efficiency interventions. The dam shows an excessive lowering of the crest level and cracks due to the consolidation of the embankment. The seismic assessment, carried out accounting for the new Italian guidelines, has shown a potential vulnerability of both the dam and the complimentary works. The planned verification and remediation interventions are complex and expensive, however the work is strategic, as it provides water resources for agriculture. The analysis of these issues and the remedies must therefore involve not only technical verification and planning, but also technical and economic support and training plans that guarantee the sustainability of strategic works. The approach methodology is relevant, given that there are hundreds of dams of the same type, where efforts have been made important for the management of water resources in arid areas, with the aggravated impact of climate change.

1 INTRODUCTION

The construction of the Italian modern large dams began at the end of the 19th century. Some plant even earlier. The average age of the dams currently operating and registered as large dams, over 500, is 65 years. Some are more than a century old.

The management system for these strategic resources must be developed and made the most of them. Currently many plants are responsibility of Concessionaries having difficulty operating, due to lack of personnel and economic resources, tied to other local problems. Entities managing plants producing energy benefits from direct returns and are facilitated to provide adequate maintenance and operation. For others, especially in the case of plants mainly for irrigation purposes, the current structure has difficulties.

2 THE CIMIA DAM CASE

The reservoir is strategic for irrigation, but there are no resources for essential interventions of maintenance, in consequence of which the provisions of the control entities impose drastic lowering of the level of the reservoir, with the consequence that a large part of the reservoir capacity is lost.

The plant was in charge of a Consortium for 32 years, and then passed on to the Sicily Region.

The Reservoir is heavily silted, but the economic resources to desilt are not available. The re-efficiency of the bottom outlet alone, which is presented here, will cost around 9 million euros, to move 32,500 cubic meters (the interventions on the electromechanical systems have a very little impact) giving a unit cost of around 280 euro per cubic meter.

The work was designed to facilitate subsequent mud removal operations, which affect at least 700,000 cubic meters currently within the useful capacity volume, plus approximately 100,000 cubic meters per year entering the reservoir.

In 10 years, to make a number, at least 1.7 Mm³ will have to be removed, so, depending on the distance of the landfill in which to place the sediment, or its placement as a soil improver, if it were ever accepted by farmers (which if it happens is a free of charge and with severe resistance to accept it), could perhaps cost from 100 to 200 million.

It would be advisable to raise the dam and retain the sediment in the reservoir. Also to maximize the flushing, which however is difficult given that the inflows are lower than the irrigation demand and that there are strong difficulties in obtaining authorizations to release flows into the river with high solid densities, for environmental reasons.

Furthermore, the Cimia dam requires important restructuring interventions to guarantee the stability of the dam and complementary works; therefore, a super-elevation would be an effective solution.

3 THE ASSIGNMENT OF THE JOB

The task was awarded by the Sicily Region to RTI studio Speri/Waterways and includes:

1. the hydraulic and hydrological revaluation of the dam and complementary works;
2. seismic revaluation of the dam and complementary works;
3. the reservoir management plan;
4. the re-efficiency of the bottom discharge

The assignment includes investigations for:

1. geometrization of the actual state of the works;
2. bathymetric surveys for measuring deposits in the reservoir;
3. characterization of the constituent materials of the dam and ancillary works;
4. characterization of the sediment deposited in the reservoir.

4 IDENTIFICATION AND STATUS OF THE WORK

The Cimia dam is located in Sicily, in the province of Caltanissetta. It was built in the period 1975-1980 and can be classified as an earth embankment dam, with an internal impervious core. The dam is 39 meters high and forms a reservoir of 10 million cubic metres (Figure 1).

The reservoir dominates the Gela plain and provides an essential irrigation supply service. Additional flow is diverted from nearby Disueri dam, which for various reasons has exhausted its water storage capacity. The outlet organs consist of a labyrinth spillway and a tunnel bottom outlet.

The dam can be divided into five zones (Figure 2):

- zone 1: impervious core;
- zone 2: abutment;
- zone 3: transitional material;
- zone 4: upstream abutment;
- zone 5: upstream facing.

Since the first reservoir filling, a progressive subsidence has been recorded at the crest, such as to trigger the development and propagation of an extensive crack pattern in the pavement and roadbed.

In 40 years there has been a consistent sedimentation of fine materials, which have conditioned the intake of the bottom outlet, which is at risk of clogging, while the bottom outlet gallery and the relative discharge channel are full of sediments and require of extraordinary maintenance.

The electromechanical parts of the bottom discharge have reached the end of their useful life and need to be overhauled and largely replaced.

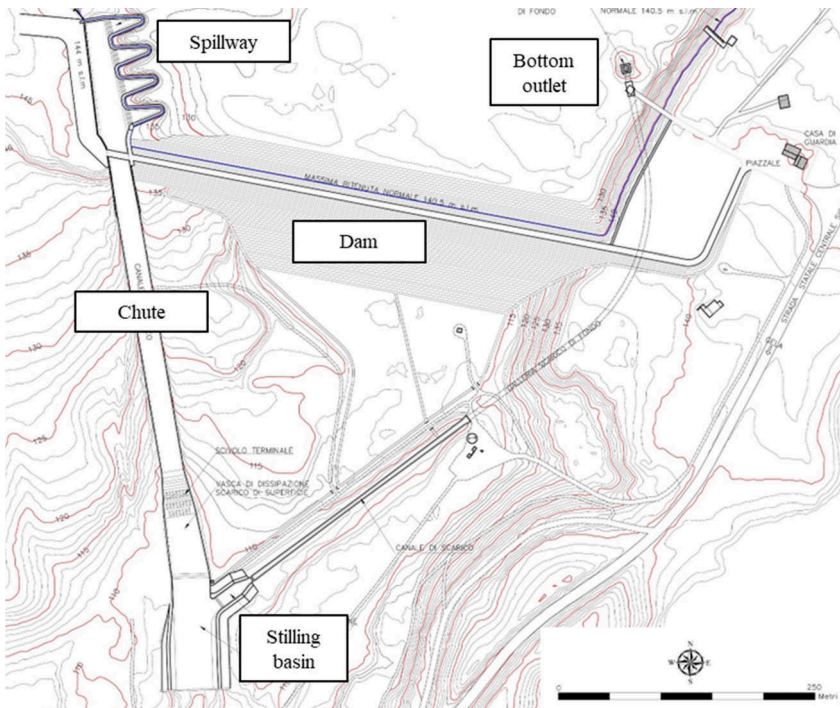


Figure 1. Dam body plan.

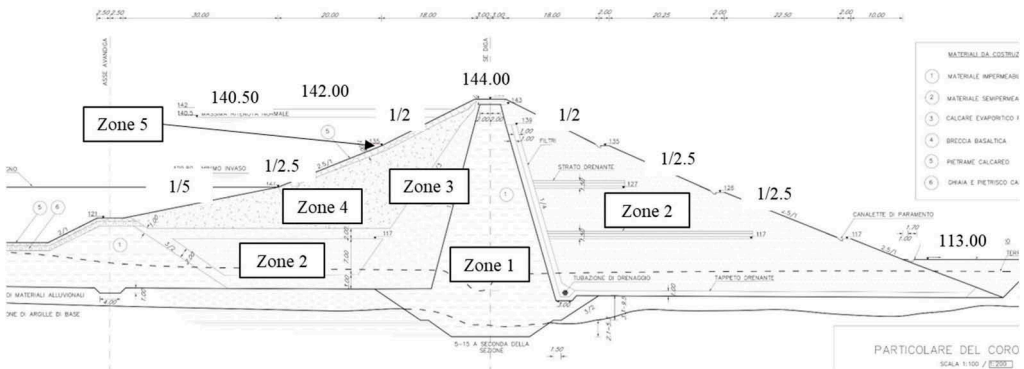


Figure 2. Cross section.

5 SEISMIC REASSESSMENT OF THE DAM AND ANCILLARY WORKS

As part of the seismic reevaluation of the dam and ancillary works, an extensive campaign of geognostic and diagnostic investigations was carried out aimed at increasing the degree of knowledge on the mechanical characteristics of materials and at identifying their dynamic characterization.

Specifically, the characterization of the coarse-grained materials of the backfills was based on site tests (SPT and DPSH), while that of the fine-grained materials of the core and foundation was based on laboratory tests performed on undisturbed samples taken in boreholes.

The dynamic field characterization of the dam body materials was carried out with down-hole geophysical tests. The dynamic analyzes were performed on a two-dimensional finite element model (FEM), in the hypothesis of flat deformations, adopting a linear visco-elastic type

constitutive relationship, in which the stiffness and damping characteristics are updated iteratively as a function of the level of deformation reached during the considered seismic event.

The foundation elements were modeled with a linear elastic behavior and as massless (massless model), therefore they were constrained to have zero horizontal and vertical displacements at the domain boundaries.

The contribution of the foundation in terms of local seismic response was studied in a decoupled way, through dedicated analyses. In the model, the foundation constitutes only an elastic type of support for the dam, in order to take into account the effects of dam-foundation kinematic interaction and neglect, as a precautionary measure, the effect of the geometric damping of the waves that propagate in the foundation domain.

After the dynamic analyses, the permanent displacements accumulated along the potential sliding surfaces were evaluated using the method of Newmark (1965). This approach made it possible to determine the conditions of compliance of the work based on the regulatory requirements.

The static analyzes have highlighted the downstream abutment as a critical element of the work, in fact, the safety factor relating to the downstream critical surface is very small and close to unity. The reduced degree of safety of the valley abutment is congruent with the high yielding observed in the surface layer of the facing during the operation of the work.

The dynamic analyzes have shown that:

- the seismic response of the dam to the SLD (damage limit state) is positive as the average of the dynamic permanent slip is in the order of a centimeter, therefore congruous with the performance required by the legislation for this limit state;
- expected level of damage to the SLC (limit state of collapse) is serious according to the criterion of Swaisgood (2003), the average lowering of the crest, equal to about 2% of the height of the dam, is greater than the limit of the 1% indicated in the Italian regulation.

Therefore, the collapse of the structure due to the direct effect of inertial actions cannot be excluded. The high permanent displacements calculated at the SLC are essentially linked to the small safety margin of the valley abutment in static conditions.

Therefore, in order to achieve the safety level required by current regulations, it was proposed to reduce the average slope of the sidewall by reinforcing the facing. The intervention is aimed at increasing the degree of stability of the abutment in static and seismic conditions and allow for the recovery of the dam freeboard.

The ancillary works, spillway, bottom outlet tower, access walkway to the control room and guard house are not seismically tested.

6 THE HYDROLOGICAL-HYDRAULIC REVALUATION

The filling of the dam began in 1979. The non-fulfillment of the requests formulated by the supervisory authority resulted in the present reduction to an altitude of 135 m a.s.l., well below the maximum admissible level (140.50). The maximum flow rates that can be released through the outlet devices and which can be derived from the irrigation intake structure, with the level in the reservoir at the maximum height equal to: 142.00 m a.s.l., are as follows:

- from spillway 1,100.00 m³/s
- from the bottom outlet 55.00 m³/s
- from the irrigation intake structure 2.30 m³/s

The spillway structure consists of a labyrinth-type on the right abutment, positioned at an altitude of 140.50 m a.s.l., approximately 348 m long, equipped with an aeration system for the overflowing vein, headed by vertical aerophores protruding from the threshold (Figure 3).

Downstream of the labyrinth sill there is a collector channel, of variable width from 20 to 30 m, which enters, via a shaped connection, into a steeply sloping drain channel, 20 m wide and approximately 318 m long, at the foot of which is located a section of plano-altimetric connection, followed by the stilling basin.

This is of the depressed type, with breakwater blocks, 75 m long and variable in width from 29.40 m to 36 m, with a bottom elevation of 96.00 m a.s.l.

The bottom outlet consists of an intake on the left bank, at an altitude of 119 m a.s.l., horizontal, 5.40 x 5.40 m, with a grid of concrete beams, a curvilinear duct, which connects it to the base of the circular tower where the interception devices are located (Figure 4).

Downstream of the sluice chamber, the discharge structure consists of a tunnel with a circular section, with a diameter of 3.80 m, which crosses the left bank and, after 383 m, flows into a channel with a trapezoidal section, width at the base of 3 m and slope of the banks 1/4; the channel has a length of 270 m and ends in a dissipation basin which connects to the section of channeled riverbed downstream of the spillway.

The discharge interception gates, two in series, have dimensions of 1.5 x 2 m, which can be operated on site and remotely, from the control cabin, located on top of the access tower, by means of a hydraulic device, powered by electricity, from the electric network and from a generator set, from an internal combustion engine and manual actuator; the command can also take place from the guard house.

It has been verified that the original design approach is adequate and compliant with the requirements of the technical standards. An exception is the freeboard, which is insufficient due to the detected subsidence. The inconvenience can be remedied with a curb, but given that the dam needs to be rehabilitated, it is reasonable to envisage the re-efficiency of the franc at the same time as the rehabilitation of the dam.



Figure 3. Labyrinth-type spillway.

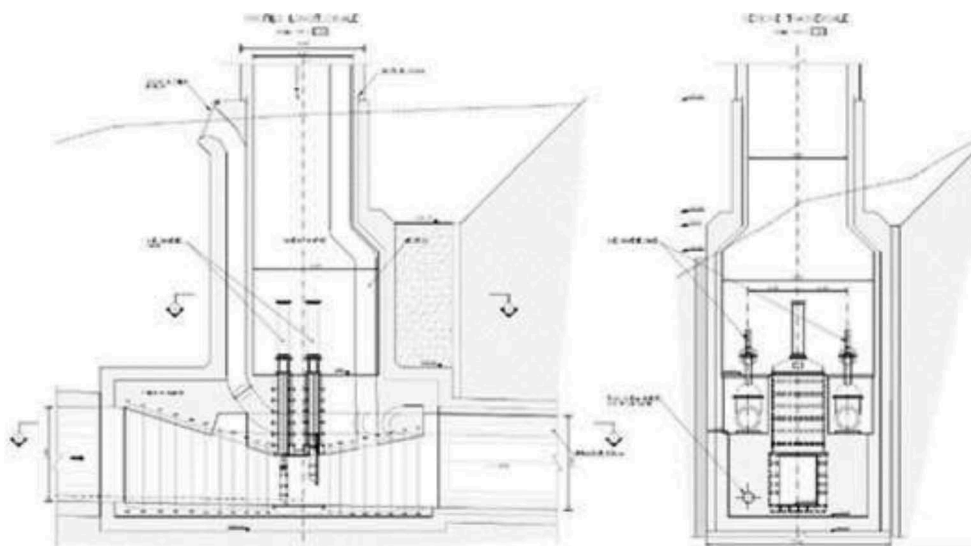


Figure 4. Bottom outlet.

7 THE BOTTOM OUTLET RE-EFFICIENCY PROJECT

The critical issues consist of:

- silting of the inlet, still functioning at low flows, but subject to collapse of the impending and certainly unstable sedimented mass.
- the age of the electromechanical equipment, which in part needs to be replaced.
- clogging of the discharge tunnel and the return channel, which are now inaccessible.

Conditioning factor is not to empty the reservoir to ensure the supply of irrigation. It was therefore decided to operate in the presence of water.

The inlet area of the bottom outlet will be delimited by a substantially impermeable Larsen-type sheet pile. The purpose of the sheet pile is to prevent the sludge from flowing back into the entrance area following dredging and to ensure, in cases of emptying of the reservoir for maintenance or mud removal, a minimum useful volume to ensure irrigation supplies and to safeguard aquatic life (Figure 5).

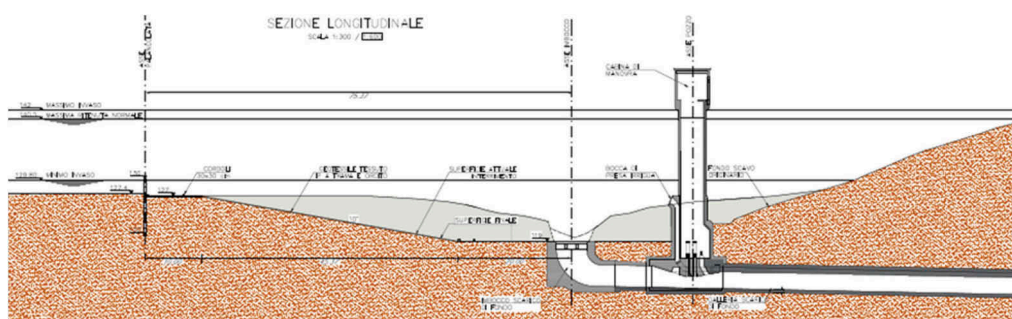


Figure 5. Longitudinal section of the bottom outlet.

The sediment delimited by the sheet piles is dredged with a suction pump, without agitators, mounted on a pontoon. The pumped sediment is conveyed via mud pipes above the dam to an available space downstream, where the sediment is contained in large non-woven drainage bags, with a process that allows the transfer of 32,500 m³ of sediment in addition to the liquid vector, which brings the total volume to 220,000 m³.

The bags drain the water fraction quite quickly, which is tested and pumped back into the reservoir. Once the dredging has been completed, the mouth of the bottom outlet is completely free, satisfying the first operational plan of the reservoir management project.

The elimination of the other sediments of the reservoir (according to the reservoir management plan) is foreseen in a second phase.

Simultaneously with this operation, the bottom outlet tunnel is cleaned, taking the sediment to the landfill. This allows you to access the sluice gates from downstream to check their status. It is foreseen to open a manhole in the ventilation pipe in order to access the tunnel, without having to go through the entire bottom outlet tunnel, which is quite long.

Once the preparatory operations have been completed, the interventions on the sluice gates are carried out. These interventions must be carefully prepared, having the pieces ready to be assembled and pre-assembled, in order to limit the time of exposure to hydrological risk.

In fact, the reservoir at these levels does not have lamination capacity, and the irrigation derivation pipes cannot be used since the entrances are located in the area separated from the reservoir. The project foresees the re-efficiency of the two sluice gates in one/two weeks, working in shifts and without interruption for the critical period. In this period, weather monitoring and flood warnings are expected, with communication systems and procedures for the rapid evacuation of workplaces at hydrological risk.

In the project, the alternative of a prefabricated turret to be built above the current entrance was evaluated, with the commitment of launching equipment and controls with divers.

The sheet pile solution was preferred because a tower:

- It weighs on the current structure, which is founded on well-consolidated Pliocene clays, but in correspondence with a paleo-riverbed which is causing consolidation problems for the dam.
- It is vulnerable to earthquake, so it requires good foundations and sizing.
- The waters are murky and assistance from divers for the delicate operation of launching and positioning the prefabricated elements is possible but certainly difficult.

The pontoon and the dredger are expected to remain available to the site for maintenance operations to complete the re-efficiency project, and to also be used for the current removal of sediments upstream of the sheet pile in the reservoir.

8 RESERVOIR MANAGEMENT PLAN

8.1 *Basin and reservoir characteristics*

The hydrographic basin of the Gela river is located in the southern slope of Sicily and occupies an area of 559.16 km². The Gela river basin has an elongated shape in the N – S direction which widens towards the east in its central portion (Figure 6). The reservoirs of the Cimìa dam and the Disueri dam which block the course of the Porcheria river fall within the Gela river basin.

As far as protected areas are concerned, the basin in question partially includes the following nature reserves:

- in the provincial territory of Caltanissetta: the natural reserve of the Sughereta di Niscemi, subject to the protection regime of article 7 of the Regional Law n° 98/81 and subsequent amendments, which constitutes the most important wreck of mixed cork oak wood existing in central Sicily;
- in the province of Enna: the natural reserve of Rossomanno – Grottascura Bellica.

For the chemical-physical characterization of the sediments, three sediment samples were taken from the bottom of the reservoir. The physical characteristics of the sediments are silt with high water content clay. The result of the laboratory analyzes have highlighted that the sedimentation material can be considered free of polluting elements.

The sampling and evaluation of the water in the reservoir was carried out. Furthermore, the measurements of some parameters detected with a multi-parameter probe and a probe for measuring the turbidity of the water were carried out on site.

The analyzes carried out show that the presence of toxic substances or both organic and inorganic pollutants was not found in the waters of the reservoir and very low concentration values were determined for the metals present, always lower than the instrumental quantification limit.

For the purposes of classifying the ecological status of the water body of Lake Cimìa, the physico-chemical elements monitored in support of the organic are total phosphorus, transparency and hypolimnic oxygen; they are integrated in a descriptor called LTLeco (trophic level of lakes for ecological status).

8.2 *Management plan contents*

The management plan consists of two parts:

- the first part of the project includes all the cognitive activities that have been carried out for the definition of the basic characterization of the plant and of the physical system connected to it;

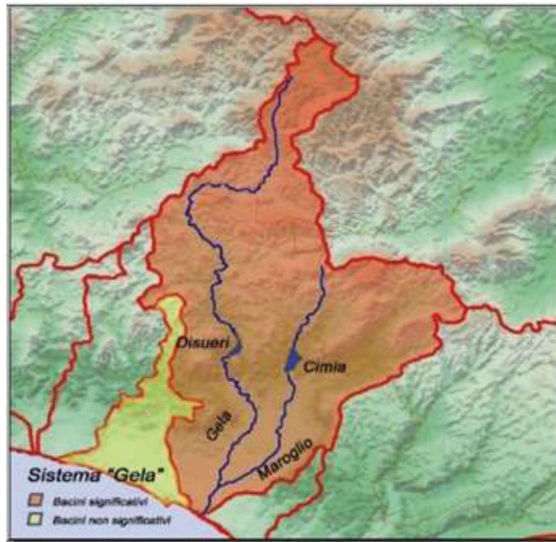


Figure 6. Gela river basin.

- the second part includes the reservoir management program with the identification of the optimal method of managing the reservoir from a technical and economic point of view with the aim of preserving the useful capacity of the reservoir in the medium to long term.

Among the ordinary periodic interventions, the following actions are envisaged:

- opening of the sluice gates of the bottom outlet during flood events for purges/expulsions to limit the deposit of sediments;
- hydraulic dredging with suction pumps on a pontoon or dinghy or periodic mechanical removal for the portions not discharged with flushes. With reference to extraordinary interventions, the following activities are envisaged;
- the safety and re-efficiency plan for the bottom outlet which provides for the removal of approximately 32,500 cubic meters of sediment by hydraulic dredging;
- the plan for the recovery of the useful capacity of the tank which provides for the removal of approximately 660,000.00 m³ of sediment deposited in the useful volume of the tank between the minimum use level of 129.80 and the maximum use level of 140.50.
- the plan for the containment of erosion in the basin.

9 CONCLUSIONS

The studies and investigations carried out on the Cimlia reservoir have highlighted a fact that involves many works that are in similar conditions, in Italy and around the world.

Many dams require extraordinary maintenance, due to natural aging, new safety rules and regulatory requirements, the need to preserve and increase water storage to compensate for climate change.

The dam managers should be supported financially and technically, to guarantee the preservation and safety of these infrastructures, which are vital for the environment and for public well-being and safety.

In the initiatives of the sector associations, it will be important to develop, alongside the project and monitoring techniques, also the tools providing the dissemination of information and the support of the most effective and sustainable practices. for the management of dams and reservoirs.

Assessing the carbon footprint of pumped storage hydropower – a case study

R.M. Taylor

Director, RMT Renewables Consulting Ltd, UK

V. Chanudet

Environmental Engineer, EDF Hydro Engineering Center, France

J-L. Drommi

Electricity Expert, EDF Hydro Engineering Center, France

D. Aelbrecht

Head of Technology – Deputy Technical Director, EDF Hydro Engineering Center, France

ABSTRACT: The role of pumped storage is changing because of the energy transition. Several research initiatives are ongoing to investigate the enhancements in the operational flexibility to support the greater integration of low-carbon variable renewable energies. This paper summarizes a study to estimate the carbon footprint of pumped storage activities. The case of EDF's Grand Maison pumped storage plant was selected. The study presents a methodology for estimating life-cycle emissions which will enable further comparative assessments. These may include the evaluation of the carbon benefit of pumped storage services to the electricity grid, comparison with other pumped storage projects, and with other storage technologies.

RÉSUMÉ: La transition énergétique amène un nouveau regard vis-à-vis du rôle des stations de transfert d'énergie par pompage (STEP). De nombreuses études sont en cours pour améliorer leur flexibilité d'exploitation afin de permettre une meilleure intégration des énergies renouvelables faiblement carbonées. Cet article décrit une étude visant à estimer l'empreinte carbone des STEP avec comme cas d'usage l'aménagement de Grand Maison exploité par EDF. Cette étude présente une méthodologie d'estimation des émissions sur le cycle de vie de l'aménagement, base pour des analyses comparatives ultérieures. Ces dernières peuvent inclure l'évaluation du gain en carbone apporté par les services d'une STEP sur le système électrique, la comparaison avec d'autres projets de STEP ou avec d'autres technologies de stockage d'énergie.

1 INTRODUCTION

Grand Maison is the largest pumped storage plant (PSP) in Europe, with 1,800 MW installed capacity. The PSP is involved in a pan-European research project to investigate digital and operational innovation in relation to increased flexibility services to the electricity grid. The name of this study is Hydropower Extending Power System Flexibility (XFLEX HYDRO), funded by the European Union's Horizon 2020 research programme (No. 857832). To augment this work, the PSP owner, Electricité de France (EDF), commissioned a parallel study to look at the carbon impact of providing its services to the grid, and this paper reports on this study's findings.

Grand Maison PSP is equipped with four Pelton units in an above-ground powerhouse, and eight reversible (pump-turbine) units in an underground powerhouse. This high-head PSP (+900 m) is located in the French Alps. The upper reservoir has an active storage capacity of 150 million m³, sufficient for long-duration energy storage, while the lower reservoir has a capacity of 15 million m³.

Commissioned in 1987, Grand Maison is an important source of peaking power and grid stabilization services for the French electricity system. In an average year, the PSP exchanges 3094 GWh with France's Transmission System Operator (RTE); that is, 1704 GWh is taken from the grid during pumping operations and 1392 GWh is returned by generation.

In 2022, a study was carried out to assess the carbon footprint associated with the PSP's construction and operation. This considered the net consumption the PSP takes from the grid, plus the greenhouse-gas (GHG) emissions embedded in its construction materials and equipment, and the biogenic GHG emissions related to the creation of related water bodies.

An objective was to normalize the carbon footprint caused by electricity consumption, construction, and biogenic sources. This would make it possible to establish a total annual emissions rate, in tons of carbon dioxide equivalent (tCO_{2eq}/y). This could then be used to assign a carbon footprint for each unit of energy exchanged annually by the PSP in its provision of services, per gigawatt-hour (tCO_{2eq}/GWh).

2 ASSUMPTIONS AND METHODOLOGY

This study was carried out to assess the carbon footprint of the Grand Maison PSP relating to its full range of operating activities. The scope of the study includes three components mentioned above. The first assessment analysed the net consumption of grid-supplied electricity. The second part was a retrospective assessment of the possible emissions relating to the construction of the project. The third was the estimation of biogenic GHG emissions likely to occur during the life of the two associated reservoirs. This part was led by Université du Québec à Montréal (UQAM), and a full report is available separately (Mercier-Blais & Prairie, 2022).

In accordance with the United Nations Framework Convention on Climate Change, the global warming potential for each GHG species (carbon dioxide and methane) was assigned at the 100-year time horizon (UNFCCC, 2022). After conversion of emissions into rates of carbon dioxide equivalent (CO_{2eq}), the total amounts were allocated at an annual rate. The useful life of the PSP asset was also assumed to be 100 years, with periodic modernization of original equipment having a small impact on the carbon footprint of materials and construction.

3 EMISSIONS ASSOCIATED WITH ELECTRICITY CONSUMPTION

On an annual basis, the Grand Maison PSP exchanges 3094 GWh. Within this total, it consumes 1704 GWh for pumping operations and generates 1392 GWh from turbine mode operations. Note that, through the hydraulic short-circuit mode of operation, which is being tested through the XFLEX HYDRO project, Grand Maison will be both generating and consuming at the same time. There is also a part of generation which is derived from natural inflow into the Grand Maison reservoir, which represents 215 GWh/y, and is included in the total generation mentioned above.

Taking the above into consideration, the net consumption of Grand Maison is:

$$1704 - 1392 = 312 \text{ GWh/y}$$

To allocate GHG emissions to the consumption of 312 GWh, it is necessary to know the overall emissions within the system. Figure 1 shows an example of the generation in the French system and indicates the composition by generation type (ENTSOe 2022). Based on average emissions at times of bulk pumping at Grand Maison (and other PSPs in France), it was estimated that the grid-mix emissions were 26.8 tCO_{2eq}/GWh. Emission rates are disclosed on the grid operator's website (RTE 2022). It should be noted that this rate is relatively

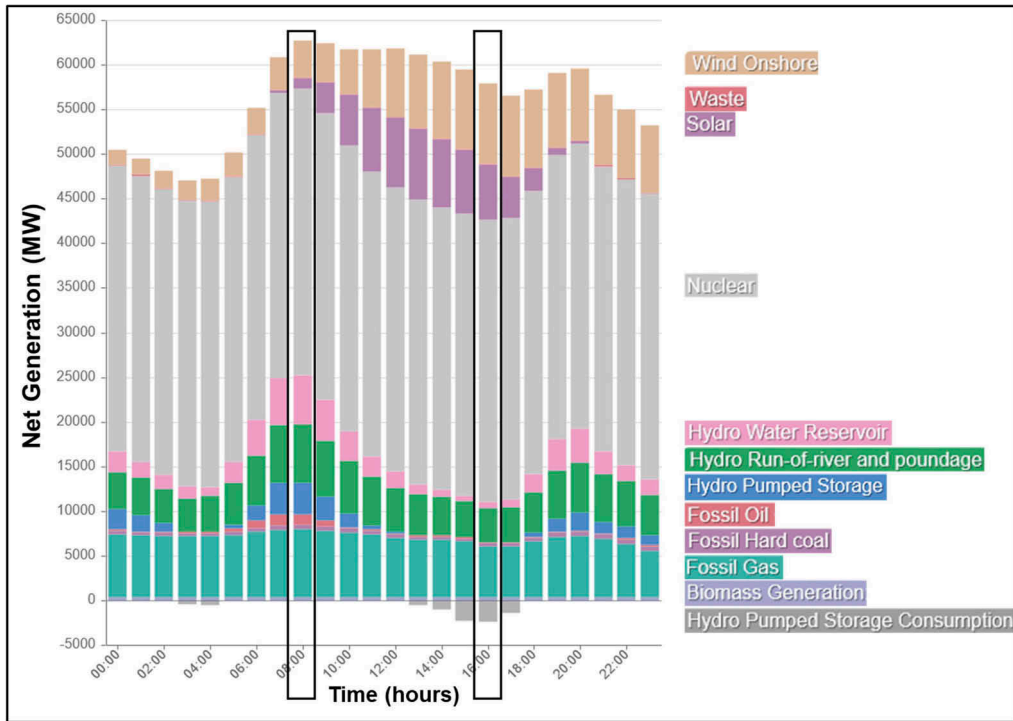


Figure 1. Example of the generation mix in the French power system, showing generation per production type at typical times of bulk PSP generation (08:00, left) and times of pumping (16:00, right).

low because pumping tends to occur when the main baseload is nuclear generation, with peak feed-in from variable renewable energies (VRE).

Knowing the French system emissions rate applicable to PSP activities, it then is possible to allocate a carbon footprint to the net consumption at Grand Maison in tons of CO_{2e} per year:

$$312 \text{ GWh/y} \times 26.8 \text{ tCO}_{2\text{eq}}/\text{GWh} = 8362 \text{ tCO}_{2\text{eq}}/\text{y}$$

4 EMISSIONS ASSOCIATED WITH CONSTRUCTION

This section utilizes a methodology developed to estimate the carbon footprint of the main materials and equipment embedded in the construction of large-scale infrastructure. The first part of the section describes the layout of Grand Maison PSP and estimates the volumes of key materials and their transportation distances. The second part of the section presents the methodology to allocate a carbon footprint to the construction and the inclusion of this in the overall life-cycle analysis. The third part presents the results.

4.1 Estimation of key material volumes

The Grand Maison dam is an embankment structure on the L'Eau d'Olle River, which is a tributary of the Romanche River. The primary purpose of the dam is to serve as the upper reservoir for the PSP. The Verney rockfill dam, located downstream in the valley, creates the lower reservoir. The dams were constructed between 1978 and 1985, with the PSP being commissioned in 1987.

Grand Maison is a rockfill dam with a central clay core (see Figure 2). It has a height of 140 m from the riverbed and 160 m from the lowest foundations. It is 550 m long and has a fill volume of 12,000,000 m³.

The smaller Verney dam has a maximum height of 42 m and a crest length of 430 m. It is composed of compacted alluvial gravels and has an upstream bituminous-concrete facing. The overall volume of the Verney dam is 1,550,000 m³.

The majority of the fill material for both dams was sourced from borrow pits within the project area. It is assumed that the total volume of embankment material for the overall scheme is 13.5 hm³. Most of the materials were placed by a fleet of 50 t dumper trucks, supplemented by a conveyor system in the case of Grand Maison. A 5 MW diesel generator was also utilized during the construction period.

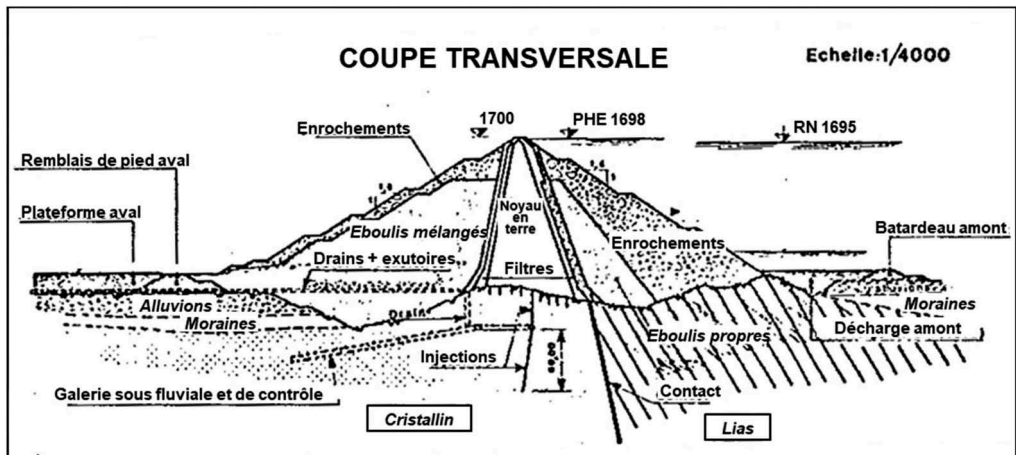


Figure 2. Cross-section of Grand Maison dam (Redon 1982).

The two powerhouses are located adjacent to the Verney reservoir. The surface powerhouse is 35 m wide, 15 m high and 110 m long. The underground powerhouse comprises upstream and downstream valve chambers, and the main power cavern is 15 m wide, 15 m high and 122 m long (see Figure 3). Both powerhouses are connected to the Grand Maison reservoir through a -7100 m long head-race tunnel with a maximum diameter of 7.1 m. The headrace is partly steel lined. The headrace then splits into three 1450 m long penstocks, which then split further into secondary penstocks feeding the units of the surface powerhouse and those of the underground

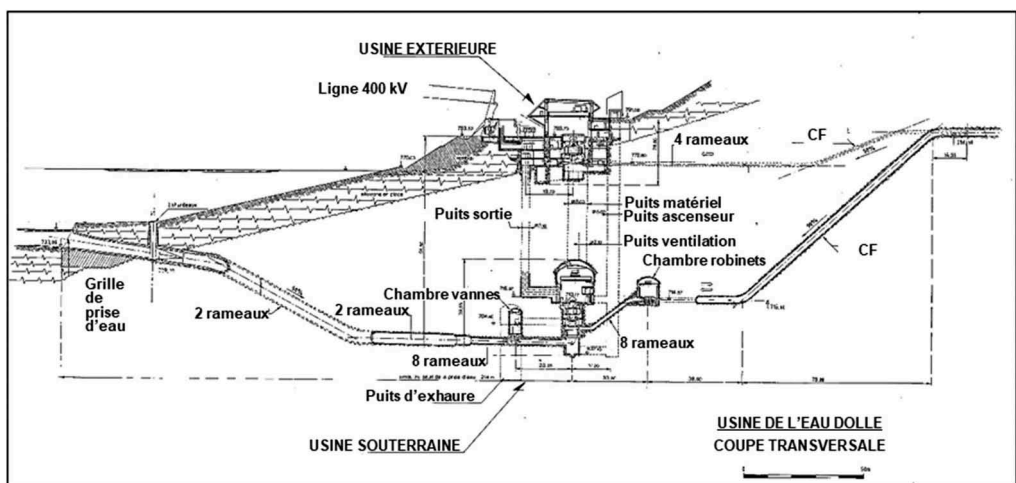


Figure 3. Cross-section showing the Grand Maison powerhouses (source: Aménagement de Grand Maison, Plan views and profiles, December 1986).

cavern immediately beneath it (Figure 4). The headrace tunnel also includes a steel-lined vertical surge chamber, which is 190 m high and 4.6 m in diameter.

The volume of concrete utilized in the overall construction includes the lining of tunnels and power waterways, powerhouses, other caverns, dam spillways and facing elements, and the intakes at both Verney and Grand Maison reservoirs. It is assumed cement was supplied from within the region (<50 km) and that mixing was carried out on site. The total volume of concrete used is estimated to be 87,000 m³.

The amount of steel used in the construction and equipment is estimated to be 26,000 t. This amount is dominated by steel used for the power waterways (see Figure 4), estimated to be 17,000 t. Turbines and generator/motors total 4600 t, and transformers, switchgear and transmission equipment are about 1900 t. Gates and valves represent 2500 t. The steel components were sourced from within France and Switzerland, with an estimated average transportation distance of about 1000 km.

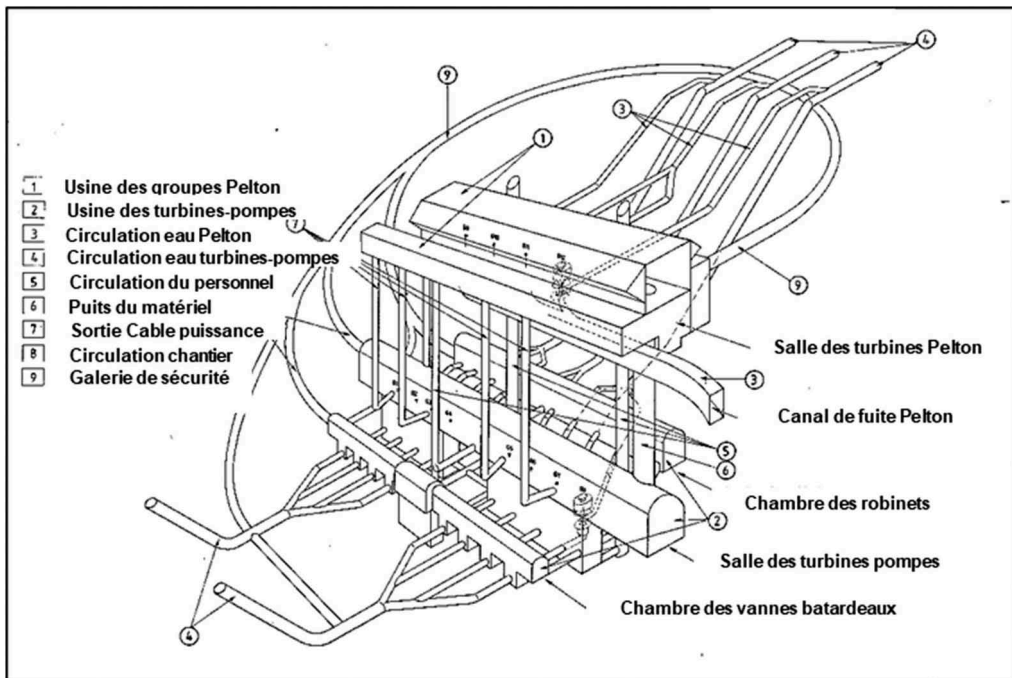


Figure 4. Schematic showing the Grand Maison complex of conduits (source: Aménagement de Grand Maison, Plan views and profiles, December 1986).

4.2 Methodology to estimate construction emissions

The manufacture, transportation and installation of equipment and infrastructure will lead to emissions of GHG. These emissions are a one-off source of GHG that can be attributed to the services that the infrastructure provides during its operational life. The method utilized here provides an indicative estimate of the construction phase emissions which includes the manufacture of raw materials (the embodied carbon), transportation of materials to, from and around the site, and the energy use from equipment used for installation of the infrastructure. The assessment only attempts to provide an 'order of magnitude' level of accuracy. In some cases, detailed information will be readily known; however, in cases of longstanding infrastructure, such information is not as easily available. For this study, original specification documents and published literature provided a partial source of the data needed.

The calculation of GHG emissions is based on a simple equation that relates the amount of a material, plant, or unit of transport to a GHG emission factor, along the following logic:

$$\text{GHG Emissions} = \text{amount of consumption/activity} \times \text{emission rate per unit of activity}$$

Material consumption is specified in terms of volume or mass depending on the material in question. Construction site operation is specified in terms of energy use from the construction equipment, whether that is direct combustion or electricity use. Finally, construction transport is specified in terms of ton-kilometres; this is a unit that combines the amount of material being transported over a given distance.

The methodology described above is incorporated in the G-res Tool, see Prairie et al. (2017), which is an online resource to estimate emissions relating to hydropower and other water-related infrastructure.

In the G-res Tool, the total CO₂ emissions are calculated based on the inputs of basic information and more detailed data, when available. A set of key materials and assets have been included in the tool that allow carbon emissions to be calculated. This requires the user to specify the amount of these materials and assets for the project being assessed. The model calculates carbon emissions for each material that have been used in the project, using known or estimated quantities that are input by the user. They are set up to produce the most accurate results possible with the data available.

4.3 Results of the construction analysis

The estimation for key materials gives indicative quantities of emissions as follows (see also Table 1):

- Embankment material: 13.6 million m³, transported over 5 km = 325,893 tCO_{2eq}
- Concrete material: 87,000 m³, transported 50 km = 31,196 tCO_{2eq}
- Steel incorporated: 26,000 t, transported 100 km = 70,947 tCO_{2eq}
- Total construction emissions embedded in the materials = 428,036 tCO_{2eq}
- Annualised emissions, assuming a 100-year life of the infrastructure = 4280 tCO_{2eq}/y

The above was further reviewed on the basis of other studies in the literature. It was noted that mass concrete will have varying amounts of carbon embedded, based on the energy input for the manufacture of the cement, preparation of aggregate, proportion of the concrete mix and transportation method for placement. Cement emission footprints have been stated in the literature between 600 and 900 kgCO_{2eq}/t and resulting mass concrete at 70 to 80 kgCO_{2eq}/t. The density of mass concrete has been assumed to amount to 2.5 t/m³ in this review. It is understood that the concrete was exclusively mixed on-site, but an allocation of 50 km was included to account for transport of cement from various points of production.

Transportation for embankment material for both dams was entered as only 5 km, as it is understood that these materials were sourced from borrow pits within the project areas.

For steel, again there is a considerable discussion in the literature as to the carbon embedded in each unit. This is based on the various approaches to life-cycle analyses, source and processing, forming and transportation. As steel manufacture remains inextricably linked to fossil fuel-based energy in the production process, rates tend to be allocated at 1.85 tCO_{2eq} per ton of steel. A transportation value of 1000 km was allocated to the steel materials; this attempts to cater for the wide range of sources of origin of the steel for equipment and construction.

Table 1. Carbon footprint of the construction of Grand Maison and Le Verney reservoirs and associated power stations, taking into account material quantities and estimation of transportation distances.

Material	Amount	Distance (km)	Carbon embedded (kgCO _{2eq})	Carbon embedded (tCO _{2eq})	Allocation (tCO _{2eq} /y)
Fill material (m ³)	13,500,000	5	325,893,375	325,893	3259
Concrete (m ³)	87,000	50	31,195,808	31,196	312
Steel (t)	26,000	1000	108,089,800	108,090	1081
Totals			428,036,163	428,036	4652

5 EMISSIONS ASSOCIATED WITH THE RESERVOIRS

As mentioned above, this part of the study was carried out separately by Université du Québec in Montréal (UQAM). Presented here is a summary of the study and the results.

Two studies were carried out on the biogenic emissions related to the two reservoirs (see Figure 5 for the general characteristics of the reservoirs and their catchments). The first study utilized the industry standard method of the G-res Tool, which assesses the net GHG emissions associated with the creation of reservoir on a life-cycle basis (see Prairie et al. 2017).

In addition, a second approach was taken because the two reservoirs are interconnected by the regular exchanges of water through the pumped storage operations. To take this into account, a second study was conducted, utilizing a new process-based biogeochemical model which is known as PB-res (see Prairie et al. 2023).

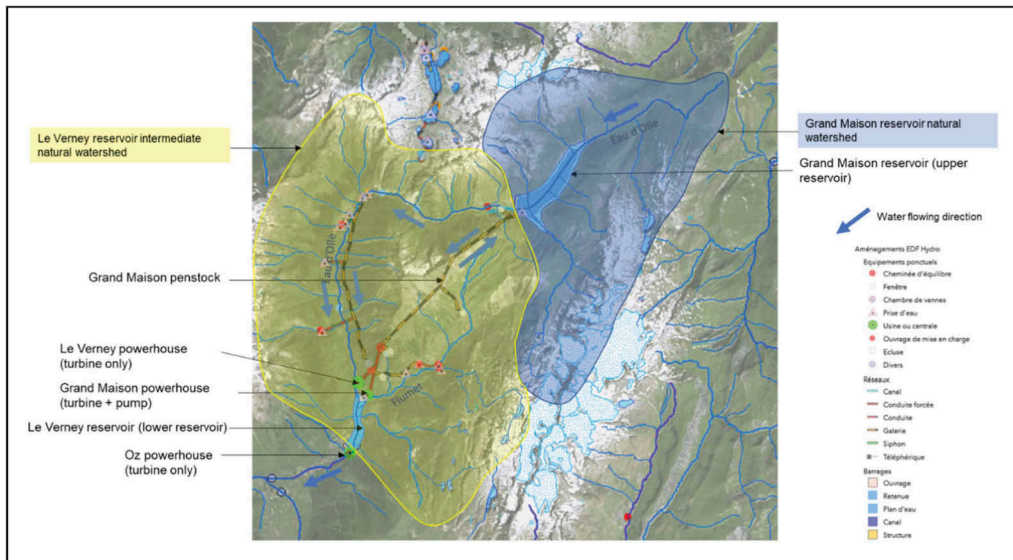


Figure 5. Grand Maison scheme showing the two reservoirs and catchments (source: <https://geoportail.gouv.fr/>).

5.1 Analysis of the G-res Tool results

Table 2 presents the results of both reservoirs for each of the possible emission pathways. All four emissions pathways are low compared to worldwide reservoirs. CO₂ diffusive emissions are the largest source of emissions to the atmosphere for Grand Maison, representing 50% of the total post-impoundment emissions. The remaining half of emissions are almost equally represented by CH₄ diffusive and CH₄ bubbling emissions pathways, with CH₄ degassing emissions being almost zero. For Le Verney reservoir, CH₄ bubbling emissions are predicted to be the highest contributor to net GHG emissions, while CO₂ and CH₄ diffusive emissions are both lower and similar in size.

As temperature plays an important role in GHG production and emissions, low emissions can be linked to the monthly average water temperatures, which are always below 15°C for the two reservoirs. Temperature is directly involved in both diffusive models (CO₂ and CH₄) and indirectly influences CH₄ bubbling and degassing emissions. The higher CH₄ bubbling emissions in Le Verney reservoir can be linked to the higher extent of littoral area in this reservoir.

At full supply level, the area of Grand Maison is 2.19 km² and Le Verney is 0.75 km². In terms of metric tons, the emission rates are 137 tCO_{2eq}/km²/y and 250 tCO_{2eq}/km²/y, respectively. Hence, the emissions for the two reservoirs represents:

Table 2. Grand Maison and Le Verney reservoir G-res Tool version 3.1 results. Results are in gCO_{2eq}/m²/y and integrated over a 100 year lifetime. Post-impoundment emissions are the sum of the four first rows. The numbers in parenthesis for net GHG footprint represents the 95% confidence intervals.

	GHG emissions (gCO _{2eq} /m ² /y)	Grand Maison	GHG emissions (gCO _{2eq} /m ² /y)	Le Verney
Diffusive CO ₂ emissions	29		39	
Diffusive CH ₄ emissions	14		33	
Bubbling CH ₄ emissions	12		103	
Degassing CH ₄ emissions	1		15	
Post-impoundment emissions	57		190	
Pre-impoundment emissions	-80		-60	
Unrelated Anthropogenic sources	0		0	
Lifetime net GHG footprint (100yrs)	137 (130-144)		250 (228-276)	

- Grand Maison = 2.19 km² x 137 tCO_{2eq}/km²/y = 300 tCO_{2eq}/y
- Le Verney = 0.75 km² x 250 tCO_{2eq}/km²/y = 188 tCO_{2eq}/y

Consequently, the total contribution from reservoir biogenic sources to the overall carbon footprint is 488 tCO_{2eq}/y.

5.2 Process-based biogeochemical (PB-res) approach

To further validate whether the G-res Tool is estimating an accurate result for a pumped storage hydropower project, a PB-res modeling approach was also applied (Prairie et al. 2023). The annual stratification pattern obtained confirms that the Grand Maison reservoir is stratified for about half of the year at a depth of around 2 m, compared to a thermocline depth of 3.8 m estimated in the G-res Tool. For such a deep reservoir and water intake, the small difference between the two methods has no impact on the final GHG results. For the Le Verney reservoir, different trends were observed between the G-res and the PB-res approaches, as the G-res does not consider the effect of the upstream reservoir, but both methods predict low CH₄ emissions.

Comparing both annual thermal profiles, it could be seen that the turbine/pump exchanges of water have almost no effect on the thermal condition in the water column and therefore little effect on the emissions.

It would be important to re-apply this dual approach on other assessments of pumped storage projects because the local conditions, especially the relative depths of the inlet/outlets could have a significant impact. In the case of Grand Maison, both approaches predict similar results for the overall GHG emissions. Although slightly different results are predicted for the lower reservoir (due to the difference in the stratification pattern), the two approaches indicated low values in the same order of magnitude.

6 OVERALL SUMMARY OF RESULTS

Three carbon footprints associated with the Grand Maison PSP have been assessed:

- Net consumption from the French electricity system
- Carbon embedded in the construction materials and equipment
- Biogenic carbon emissions associated with both reservoirs

After conversion of emissions into rates of carbon dioxide equivalent (CO_{2eq}), the total amounts were allocated to an annual rate, based on the assumption that the useful life of the asset is 100 years. The global warming potential for each GHG species (carbon dioxide and methane) was also assigned at the 100-year rate.

Having normalized the rates from consumption, construction and biogenic sources, it is possible to establish a total annual emissions rate. This is shown below:

- Electricity consumption emissions = 8377 tCO_{2eq}/y
- Carbon footprint of construction and equipment = 4652 tCO_{2eq}/y
- Biogenic reservoir emissions = 488 tCO_{2eq}/y
- Total carbon footprint for the Grand Maison PSP = 13,517 tCO_{2eq}/y

With this information, it is possible to assign a carbon footprint for each unit of energy exchanged annually by the PSP in its provision of services. As mentioned previously, on an annual basis, Grand Maison PSP exchanges 3094 GWh. Within this total, it consumes 1704 GWh for pumping operations and generates 1392 GWh from turbine mode operations. Note that, through the hydraulic short-circuit mode of operation, Grand Maison is capable of generating and consuming electricity through different units at the same time for the provision of grid stability services.

By apportioning the carbon footprint to each unit of electricity exchanged with the grid, the following result is obtained:

$$13,517 \text{ tCO}_{2\text{eq}}/\text{y} \div 3094 \text{ GWh}/\text{y} = 4.37 \text{ tCO}_{2\text{eq}}/\text{GWh} \text{ (} 4.37 \text{ gCO}_{2\text{eq}}/\text{kWh)}$$

If we allocate the total carbon footprint only to the electricity supplied back to the power system by Grand Maison, then the result is:

$$13,517 \text{ tCO}_{2\text{eq}}/\text{y} \div 1392 \text{ GWh}/\text{y} = 9.71 \text{ tCO}_{2\text{eq}}/\text{GWh} \text{ (} 9.71 \text{ gCO}_{2\text{eq}}/\text{kWh)}$$

Allocating to the generation output only the construction and biogenic emissions (excluding the consumption emissions relating to the grid), the result is:

$$5140 \text{ tCO}_{2\text{eq}}/\text{y} \div 1392 \text{ GWh}/\text{y} = 3.43 \text{ tCO}_{2\text{eq}}/\text{GWh} \text{ (} 3.69 \text{ gCO}_{2\text{eq}}/\text{kWh)}$$

7 CONCLUSION

Of the three main components of the carbon footprint, the largest impact was the net consumption of electricity from the grid by pumping (and not returned through generation). This represented 64% of the carbon footprint. The embedded emissions in the construction (steel, concrete and embankment material) represented 33%, and the biogenic emissions related to the reservoirs contributed 4%. Clearly these proportions will vary from one site to another, especially when there are higher proportions of fossil fuel in the power system mix.

Given that emissions are effectively ‘spent’ prior to the provision of PSP services, the higher the use of the asset, the more dilute the carbon footprint will be. That is, the emissions have already been created within the electricity system prior to any consumption by the hydro-power station, as well as embedded in the building of the powerplant and water bodies. Increasing the role of the PSP in delivering power and energy to the grid will further lower the rate of emissions per unit of service.

Future work might look at conducting similar studies on other PSPs. This will bring further confidence in the methodology utilized and allow for comparative analyses with other storage technologies.

REFERENCES

- UNFCCC 2022. Global Warming Potentials (IPCC Second Assessment Report); <https://unfccc.int/process/transparency-and-reporting/greenhouse-gas-data/greenhouse-gas-data-unfccc/global-warming-potentials>
- RTE 2022. éCO2mix - Les émissions de CO2 par kWh produit en France <https://www.rte-france.com/eco2mix/les-emissions-de-co2-par-kwh-produit-en-france>
- ENTSOe 2022. Transparency Platform; <https://transparency.entsoe.eu/>

- Redon J.C. 1982. Construction des barrages de Grand'Maison et du Verney. *Travaux*, Issue 566, pp 79–86
- Prairie Y.T., Alm J, Harby A, Mercier-Blais S, Nahas R. 2017. The GHG Reservoir Tool (G-res) Technical documentation v3.2 (2022-12-19). *UNESCO/IHA research project on the GHG status of freshwater reservoirs*. UNESCO Chair in Global Environmental Change and the International Hydropower Association.
- Prairie YT, Mercier-Blais S, Vachon D, Bilodeau F, and Tremblay A. 2023. Methane emissions from reservoirs: a comparison of estimates from G-res and PB-res, a new process-based model: Submitted
- Mercier-Blais S and Prairie YT. 2022. GHG assessment of Grand Maison/Le Verney pump storage reservoirs using the G-res Tool (v3.1) and the PB-res model. Report available from the authors of this paper.

Exploring the efficacy of reservoir fine sediment management measures through numerical simulations

S. Vorlet, M. Marshall, A. Amini & G. De Cesare

Hydraulic Constructions Platform, Ecole Polytechnique Fédérale de Lausanne (EPFL), Lausanne, Switzerland

ABSTRACT: Reservoir sedimentation is one of the main challenges in the sustainable operation of large reservoirs because it causes volume loss, affecting hydropower production capacity, dam safety, and flood management. To ensure the sustainability of deep reservoirs by maintaining sediment flow continuity, it is essential to understand the mechanisms of the sedimentation process. The prediction of sediment deposition can enable adequate sediment management, including the design and implementation of prevention and mitigation measures. Different countermeasures are now being used to tackle sedimentation problems. However, many of these measures have a considerable ecologic and/or economic impact. It is therefore paramount to develop new efficient measures to ensure fine sediment transport through large reservoirs. This paper presents three innovative measures for fine sediment management in reservoirs and summarizes how state-of-the-art numerical modeling might help to assess the efficiency of these measures.

1 INTRODUCTION

Reservoir sedimentation is one of the main challenges in the sustainable operation of large reservoirs because it causes volume loss, affecting hydropower production capacity, dam safety, and flood management. The construction of a dam alters the sediment inflow and outflow balance that is observed for natural conditions and the sediment flow continuity is interrupted, resulting in sedimentation (Schleiss et al., 2016). On a global scale, storage capacity loss due to sedimentation is estimated to be between 1 and 2% annually. According to a recent UN University study (Perera et al., 2023), it is forecasted that dams around the world will lose nearly a quarter of their storage capacity due to sedimentation by 2050. The evolution of storage capacity and of volume loss due to sedimentation is a substantial problem for sustainability, as the annual increase in storage volume due to construction of new reservoirs is close to 1% (Müller, 2012). It has been estimated that Alpine reservoirs have a mean annual sedimentation rate of approximately 0.2% (Beyer & Schleiss, 2000). This low sedimentation rate is mainly due to geological characteristics of the catchment areas. However, safe and sustainable operation of Alpine reservoirs, which are predominantly used for hydropower production, is threatened by the deposition of sediment after decades of operations. The accumulation of fine sediment in large reservoirs has negative impacts on hydropower production and can lead to serious issues, such as reduction of live storage, blockage of power intakes, turbine abrasion and dam safety in case of bottom outlet blockage (Guillén-Ludeña et al., 2018; Müller et al., 2014). In addition, downstream river reaches are negatively impacted by the decrease in sediment supply.



Figure 1. Sedimentation of Sufers reservoir, Grisons, Switzerland (Amini et al., 2020).

Sedimentation is a serious issue for most Alpine reservoirs, as many of them were built in the second part of the last century and have been experiencing ongoing sedimentation for decades. In large seasonal storage reservoirs in partially glaciated catchments, sediment inflows are mostly fine-graded, supplied by glacier melt flows and moraine sediment transport during rainfall events in the summer and autumn months in the catchment area. Coarse-graded sediment is mainly deposited in the delta area, while fine-graded sediment is transported and deposited near the dam by turbidity currents (De Cesare et al., 2001). These reservoirs are often part of hydro-power plants composed of multiple reservoirs with a range of reservoir size and morphology, including pumped-storage facilities, facing new challenges with sedimentation.

In order to ensure the sustainability of large reservoirs by maintaining sediment flow continuity, it is essential to understand the mechanisms of sedimentation. The prediction of sediment deposition can enable adequate sediment management, including the design and implementation of prevention and mitigation measures. Several technical methods are now being used worldwide to combat sedimentation in large reservoirs. However, most of these methods have a considerable ecologic and/or economic impact. It is therefore paramount to develop new measures to ensure fine sediment transport through large reservoirs. This paper presents innovative methods developed at the Hydraulic Constructions Platform (PL-LCH) of Ecole Polytechnique Fédérale de Lausanne (EPFL) for fine sediment management in reservoirs and presents how state-of-the-art numerical modeling can be used to help to assess the efficiency of these measures.

2 INNOVATIVE METHODS FOR FINE SEDIMENT MANAGEMENT IN LARGE RESERVOIRS

Numerous technical solutions have been developed in recent decades for sediment management in reservoirs. These measures are commonly distinguished between solutions in the catchment area (soil conservation, slope and banks protection, bypass structures, etc.), in the reservoir (flushing operations, controlling turbidity currents, etc.), at the dam (intake/bottom outlet heightening, etc.) or downstream (Jenzer Althaus et al., 2010). However, these measures usually have a significant economic or ecological impact. In this context, innovative methods to combat the trapping of fine sediment by large reservoirs still need to be developed. The PL-LCH has been developing innovative solutions for enabling fine sediment transport through large reservoirs.

2.1 *Fine sediment routing*

Sediment routing is one innovative method that aims to keep fine sediment in suspension in large reservoirs for subsequent routing through power waterways, without additional water

consumption or adverse impact on hydropower operations. Turbulence levels in the reservoir and close to the waterways should be maintained above a minimum threshold level to ensure fine sediment transport for given particle sizes and physical properties. This can be achieved via operational stirring, where the level of turbulence is related to the hydropower operations and power intake structures, or via forced stirring, where the level of turbulence is controlled by an external device. Both methods help to keep fine sediment in suspension, and/or the mobilization of deposited sediment in specific conditions.

2.1.1 *Operational stirring*

Operational stirring makes use of hydrodynamics induced by inflows and outflows in large reservoirs (De Cesare et al., 2019). The interplay between inflows and outflows help to maintain a proper turbulence level in vicinity of these structures. In pumped-storage facilities, the water intake works in both flow directions. The hydrodynamics induced by the inflow and outflow sequences (and the turbulence maintained or increased by the cyclic flow exchanges) inhibit sediment settling (Guillén-Ludeña et al., 2018). Previous studies have shown that reservoir stratification and sediment transport dynamics are altered by pumped-storage operations, and that the settling of fine sediment can be considerably reduced near the outlet structures by inflow and outflow sequences (Guillén Ludeña et al., 2017; Müller et al., 2017). Therefore, the assessment of reservoir hydrodynamics and turbulence levels, and the resulting sediment motion, is of paramount importance in selecting the most suitable location, orientation, and layout of the power intake and outlet structures. These elements can then be integrated into the design of new or expanding hydropower schemes.

2.2 *Forced stirring*

Depending on the reservoir morphology and operations management, the interplay between inflows and outflows might not be sufficient to maintain fine sediment in suspension and ensure fine sediment transport through the reservoir. In this case, additional tools are needed to locally generate an upward sediment motion at critical locations within the reservoir. One such tool is the innovative SEDMIX device, which uses thrusters to keep fine sediments near the dam in suspension and allows these sediments to be routed downstream. The SEDMIX device is composed of two parts: one floating and one close to the basin bottom holding a multi-thruster manifold frame. The thrusters induce a rotational flow which creates an upward motion and keeps fine sediments in suspension near the dam and water intakes. The sediment can then be continuously routed downstream through the power waterways at suitable concentrations, without additional water or energy loss. Once deployed, the thruster manifold frame is suspended from a floating platform and lowered underwater into position. As such, the system can be mobile and can be moved around the reservoir to find the position that provides optimal sediment evacuation.

2.3 *Turbidity currents venting*

In high-altitude reservoirs, turbidity currents are the main inflow process for sediment (De Cesare et al., 2001). During floods, the density of river water usually increases due to an increase in the concentration of the suspended sediment that the river carries. Once the river enters the reservoir downstream of the root delta, the denser river water plunges underneath the free surface of the ambient clear water of the reservoir. After plunging, a turbidity current is triggered and travels along the reservoir's bottom and, in case of high enough concentrations, can reach the dam. This causes two main issues: increased sedimentation at the dam (decreasing the available storage volume for hydropower and flood control), as well as negatively impacting operation of the bottom outlets and/or water intakes.

Turbidity current venting involves the evacuation sediment-laden flows through the bottom outlets during flood events. This allows for the direct transport of turbidity currents and prevents the settling and sediment and subsequent blockage of the outlet structures (De Cesare et al., 2019).

3 NUMERICAL INVESTIGATIONS OF INNOVATIVE FINE SEDIMENT MANAGEMENT METHODS

Understanding reservoir hydrodynamics, together with efficient timing of reservoir operations, is crucial for successful fine sediment management. State-of-the-art computational fluid dynamics can help to predict the fine sediment motion in large reservoirs and provide insight for use in the design and operational planning of structures. At PL-LCH, numerical investigations have been performed for operational stirring, forced stirring, and venting of turbidity currents, using ANSYS CFX software. This software is based on the finite-volume method (FVM) to discretize governing equations in the computational domain.

3.1 Operational stirring: Flow patterns and sediment deposition prediction in large reservoirs

The aim of this study was to enhance knowledge on the hydrodynamics and sedimentation processes in large reservoirs for various inflows and outflows arrangements, and for multiphase simulations (Vorlet, 2018). The numerical model considered a simple geometry with different inlet and outlet arrangements located at mid-height. The water density was assumed to be $\rho_f = 999 \text{ kg/m}^3$ and the dynamic viscosity was assumed to be $\mu_f = 1.3059 \cdot 10^{-3} \text{ kg/ms}$. Fine sediments were modeled using spheric particles with diameter $d_s = 4 \text{ }\mu\text{m}$, with density of $\rho_s = 2650 \text{ kg/m}^3$, and with a porosity of 35% when settled. An inhomogeneous Eulerian-Eulerian multiphase model was used to simulate the behavior of suspended fine sediment in the reservoir, where fine sediment is considered as an extra Eulerian phase, considering different flow fields for water and sediment. The Particle model was used, in which the dispersed phase particles are assumed to be spherical. An inlet flow velocity of 1 m/s and a static pressurized outlet were considered. The no slip condition was used for the walls and the free slip condition for the free surface. The initial flow velocity is zero in the computational domain. For multiphase simulation, a concentration of 88 mg/l is considered for fine sediment uniformly distributed in the computational domain and at the inlet.

Results showed that the presence of suspended fine sediment changes the hydrodynamics and the turbulence levels in deep reservoirs. For identical inlet and outlet relative locations and hydraulic conditions, flow patterns were different with the presence of sediment. This is accordance with (Kantoush et al., 2008)'s findings in laboratory tests. In addition, jet energy dissipation is larger in the case with sediment. The presence of sediment in the reservoir also modified the turbulence levels due to the damping effect of turbulence. The interaction between particles and fluid resulted in a loss of energy because of the drag effect.

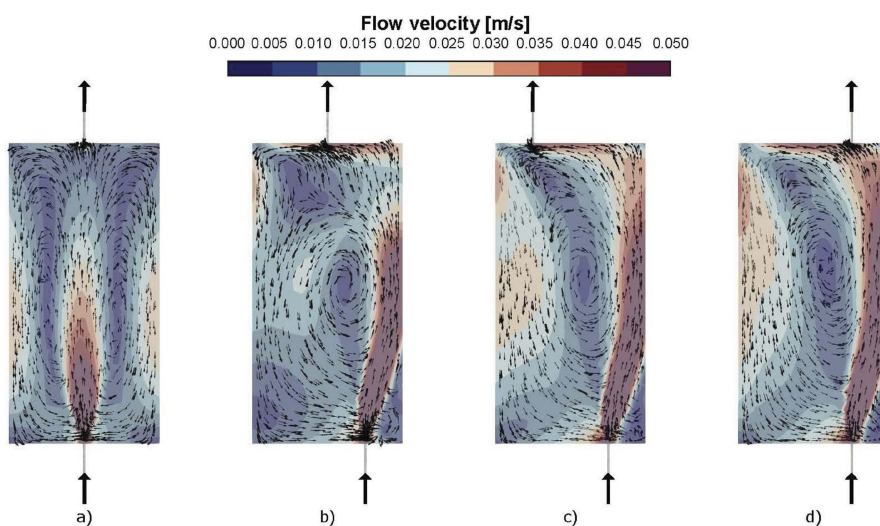


Figure 2. Horizontal flow patterns at steady state for multiphase simulations at steady state for various inlet and outlet arrangements at mid-height: centered-centered (a), right-centered (b), right-left (c), right-right (d).

Results from this study also highlighted that the motion of suspended fine sediment is linked to the observed hydrodynamics and flow patterns. Indeed, preferential regions of deposition coincide with regions with low flow velocities are observed, and vice versa. It should be noted that the deposition of fine sediment depends on the magnitude of flow velocities near the bottom of the reservoir, and not at the height of the inlet and outlet..

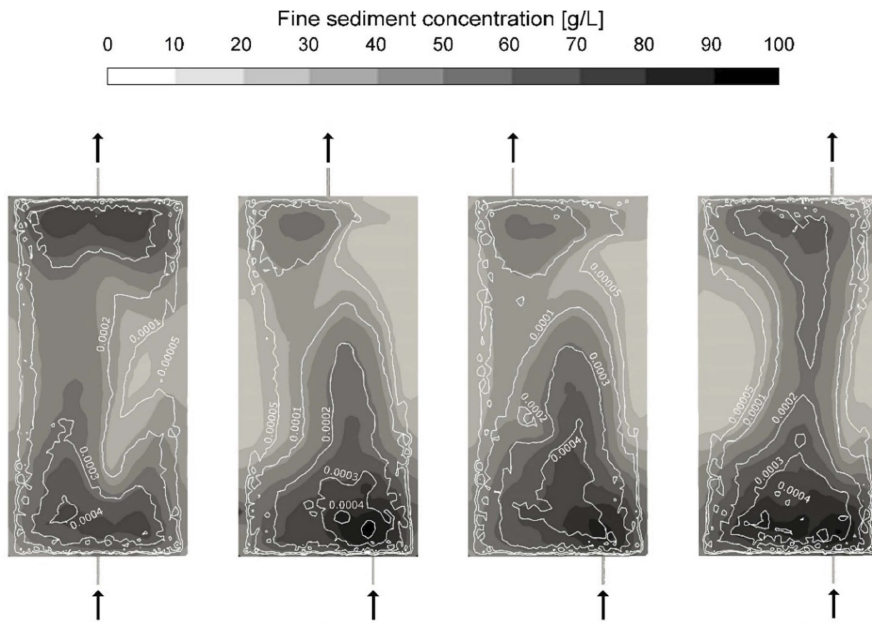


Figure 3. Fine sediment concentration [g/L] (contours) and turbulence kinetic energy dissipation rate [m²/s³] (isolines) at steady state for multiphase simulations at the bottom of the reservoir for various inlet and outlet arrangements: centered-centered (a), right-centered (b), right-left (c), right-right (d).

Results also showed that the deposition pattern near the bottom of the reservoir depends on the turbulence kinetic energy dissipation rate, with the highest deposition located in regions with the highest energy dissipation rate. In regions where flow velocities are low, the upward effect of turbulence on particles transport was small. On the other hand, in regions where flow velocities are higher, the upward effect of turbulence and suspension transport capacity was larger and coincides with regions exhibiting minimal sediment deposition. Zones with the largest deposition volume were mostly observed at locations below the inlet and the outlet, where flow velocities are smaller, and the energy dissipation rate is high

3.2 Forced stirring: SEDMIX device

The feasibility and efficiency of the SEDMIX device has been validated through experimental and numerical simulations at EPFL PL-LCH for several different scenarios and case studies. These studies include the use of jets in different geometric configurations in a rectangular tank (J. M. I. Jenzer Althaus et al., 2015), the use of jets at the Trift Reservoir (Amini et al., 2020), and an approximation use of thrusters (instead of jets) at the Trift Reservoir (Onate-Paladines et al., 2019).

In the 2011 study, the influence of jets on the hydrodynamics of a rectangular tank were analyzed for various combinations of the off-bottom clearance and water intake height. These results were eventually compared to experimental tests that were conducted with the same geometric parameters to test physical model feasibility. In general, this study found consistency in the results when comparing the experimental and numerical models. In the 2018 study, the Trift Reservoir was used as a case study to numerically model the SEDMIX device in

a reservoir, instead of a tank. The numerical simulations are performed for different positions and off-bottom clearance of the SEDMIX device. The analysis of the numerical simulation results shows that the presence of SEDMIX creates a vortex flow pattern and upward sediment movement. This study also showed that the evacuated volume of fine sediments increases for simulations using the SEDMIX device comparing those without the device and determined optimal locations and dimensions of the device. In the 2019 study, the performance of using thrusters instead of jets was examined using an approximation of thruster behavior. Thrusters are a more ideal mechanism for use in the SEDMIX device because they lead to a less complex arrangement, that requires less energy and operational costs to operate. This study was able to confirm that thrusters could achieve the same sedimentation evacuation efficiency at Trift Reservoir as was found when using a jet configuration. The analysis also identified the optimal thruster geometric and operational parameters to maximize beneficial flow patterns.

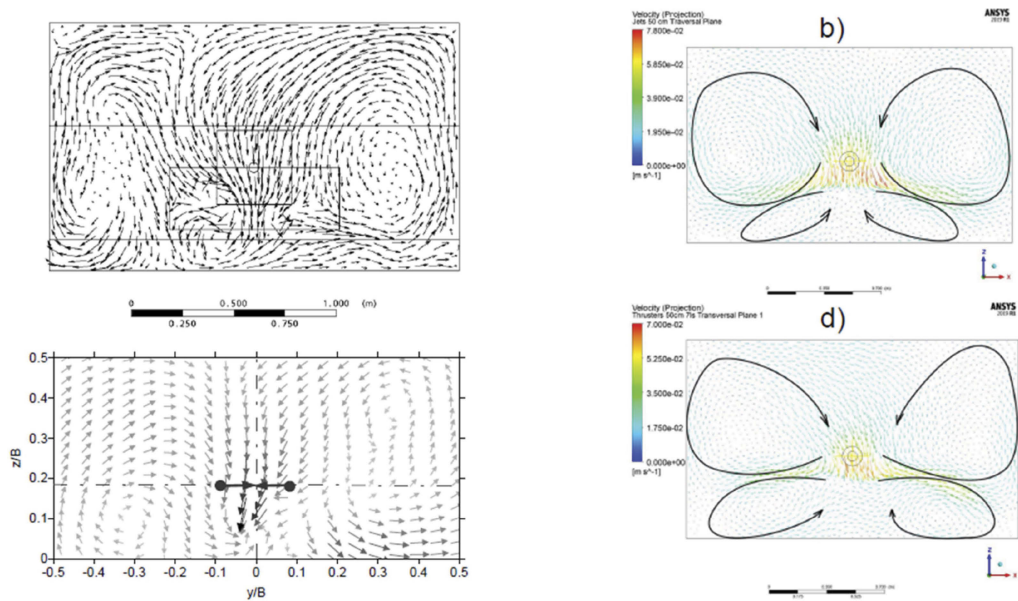


Figure 4. Results comparing experimental and numerical results for identical model set-ups. Top: numerically obtained transversal flow pattern, Bottom: experimentally obtained transversal flow pattern (left) (Jenzer Althaus et al. 2015); Bottom: results comparing numerically modeled results for jets (top) and thrusters (Onate-Paladines et al. 2019).

Most recently, PL-LCH has been conducting both experimental and numerical models in an experimental tank configuration in order to study, in detail, thruster flow behavior and different thruster configurations (including the number and size of thrusters, location and angle of thrusters, and the magnitude of induced flow). Flow patterns and velocity fields are observed to determine optimal configurations for effective sediment release. Ultrasonic Velocity Profiling (UVP) and turbidity meters are used for the experimental model, and ANSYS CFX is used for the numerical model. The numerical model acts as a “digital twin” of the experimental setup to validate the results and performance indicators, specifically regarding thruster flow behavior and suspended sediment concentrations. The goals for this ongoing work are to investigate the influence that different thruster configurations have on reservoir hydrodynamics, and to define the optimal position, design, and timing of the device for possible deployment at the reservoir scale.

The next step in this project is to deploy the SEDMIX device at the field scale, in a reservoir. Although experimental studies have shown the effectiveness of this system, its performance has not been tested in site-specific reservoir conditions, or at full-scale. The next phases of the project are currently being planned, which involve the installation, testing,

operation, and optimization of a real-size demonstrator that includes the SEDMIX device, the command and monitoring facilities, and the detailed protocols for implementation, operation and relocation. Potential downstream ecomorphological and ecohydrological effects of the device operation will be assessed and evaluated. Finally, this will allow for future industrial development for use in other reservoirs that have fine sedimentation issues.

3.3 Venting: Case study of the Rudbar Lorestan dam

The goal of this study was to numerically evaluate the efficiency of turbidity current venting for evacuating fine sediments in the Rudbar Lorestan dam reservoir in Iran (Amini et al., 2017). The numerical model was first validated using experimental tests in a laboratory flume (Chamoun, 2017). The experimental model consists of a long and narrow laboratory flume in which continuously fed turbidity currents were triggered and monitored. A wall was placed at the downstream end of the flow channel with a fixed rectangular bottom outlet. Venting was implemented by opening the bottom outlet and evacuating the turbidity currents that approached the wall. A variety of parameters were tested, including the outlet discharge, and the venting timing. Additionally, several measurements were taken throughout the tests, including velocity profiles, sediment concentrations of the inflowing and outflowing turbidity currents, and the mass of the deposited sediment.

The physically tested configurations were then simulated numerically. Once the numerical model was calibrated and adjusted, it was used to simulate venting of the turbidity current in the case of Rudbar Lorestan reservoir. The scheme impounds the river with a 153 m high Earth Core Rockfill Dam (ECRD) at the Rudbar River to create a reservoir that is approximately 20 km long with an estimated useful storage capacity of 248 hm³. The catchment area is 2'255 km², producing an average flow of approximately 30 m³/s. The dam is equipped with two bottom outlets. The reservoir model was built over a total length of 11 km.

Knowing the arrival time of the turbidity current is crucial as it directly determines the optimal timing for the opening of the bottom outlets. By opening the outlets at the current's arrival time, the current can exit the reservoir directly, enabling continuous sediment evacuation during the venting process while still allowing the reservoir to be filled. In the following discussion, the term "arrival time" refers to moment when the turbidity current reaches the reference section, located 300 m upstream of the dam. Generally, the arrival time can be identified by the sudden change in the sediment volume fraction and sediment flow rates at the reference section. Analysis of the velocity and sediment concentration profiles serves as an additional tool to confirm the obtained results.

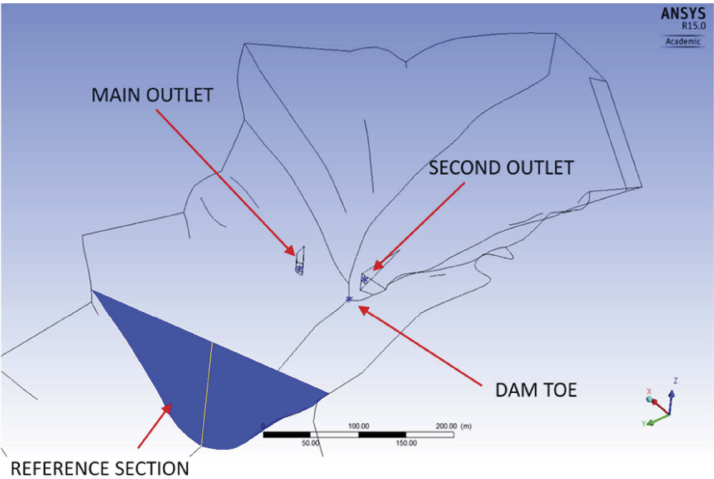


Figure 5. Location of the reference section, approximately 300 m upstream the dam body toe, used to identify the arrival time of turbidity currents to the dam vicinity.

Venting is an operation which aims to reduce the amount of sediment deposition in the reservoir (Chamoun et al., 2016) and thus avoid sedimentation related problems in the vicinity of the dam (e.g., bottom outlet clogging). For this reason, the venting efficiency is evaluated both globally (with respect to the entire reservoir) and locally (with respect to the area close to the dam). As such, two definitions of venting efficiency are applied:

- Global venting efficiency
- Local venting efficiency

The global efficiency is computed as the ratio between the amount of sediment passing through the outlets during the venting process, and the amount of sediment entering the reservoir over the entire duration of the flood event simulation:

$$\epsilon_{global} = \frac{\sum_{time} Q_{sediment\ out}}{\sum_{time} Q_{sediment\ in\ (inlet)}} \quad (1)$$

The local efficiency is computed as the ratio between the amount of sediment passing through the outlets during the venting process, and the amount of sediment passing through the reference section during the duration of the entire simulation:

$$\epsilon_{local} = \frac{\sum_{time} Q_{sediment\ out}}{\sum_{time} Q_{sediment\ in\ (reference\ section)}} \quad (2)$$

This latter definition allows for the computation of the amount of vented sediment that travelled through the reference section and thus reached the area close to the dam. The venting efficiency for each return period flood event is evaluated for four different bottom outlet opening scenarios: 25%, 50%, 100% opening of the main and the second bottom outlet (at the same time), as well as when the second bottom outlet alone is 100% open.

In Figure 6, the venting efficiency results are compared for different outlet opening scenarios. For the case with 25% opening of bottom outlets, it was found that the local efficiency was half of the case with 100% opening. Additionally, it was found that the local efficiency value is 10% less for the case with 50% opening compared to the case with 100% opening. The results for the case with 100% opening of the second bottom outlet alone are similar and slightly improved (in terms of the venting efficiency) compared to the results obtained for the case with 50% opening of both outlets. For the global venting efficiency, the 100% opening scenario leads to an efficiency that is almost five times greater than the 25% opening, and twice that for the case with 50% opening.

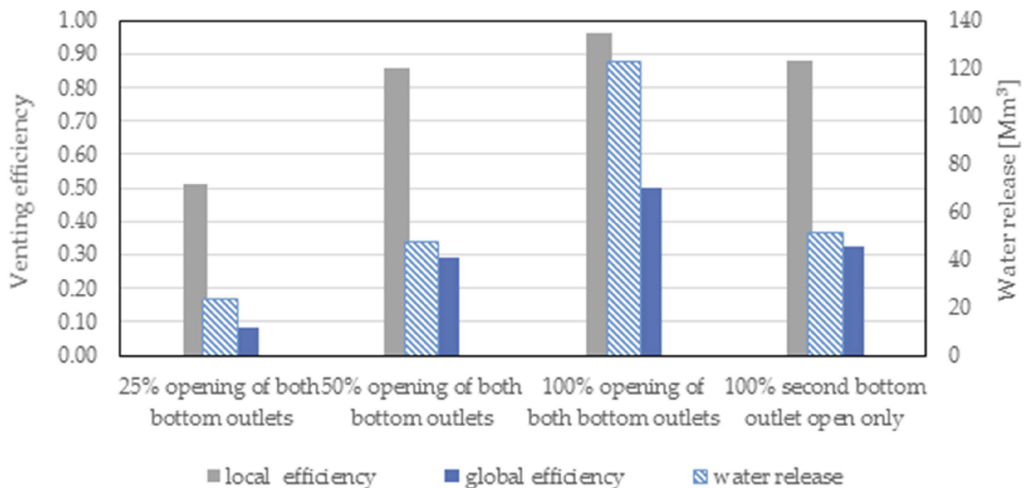


Figure 6. Global and local venting efficiency and water release comparison for different bottom outlet openings (for a 2-year flood and normal water level).

4 CONCLUSIONS

This paper presents innovative methods for fine sediment management in large reservoirs and how state-of-the-art numerical modeling can help in the design and implementation of these methods. Three-dimensional numerical modeling has been shown as a highly-capable and cost-effective approach for conducting such investigations. It provides a solid basis for assessing the efficacy of the aforementioned methods. The following conclusions can be derived for each specific case:

Operational stirring: Suspended fine sediment motion in the reservoir is linked to hydro-dynamics and flow patterns, with preferential deposition in regions of low flow velocities. The deposition pattern correlates with turbulence kinetic energy dissipation rate, with higher deposition in areas of higher energy dissipation.

Forced stirring: The use of the “SEDMIX” facility presents similar advantages to the previous solution, with the added benefit of allowing adjustments according to specific condition in each reservoir. Computational investigations conducted at a prototype scale indicate significant sediment release rates for a specific case studied in the Swiss Alps. These results are promising and will be further strengthened through additional research and prototype demonstrations in the upcoming years.

Venting: The obtained results are promising, demonstrating effective sediment evacuation through bottom outlets during venting operations across various scenarios. The study offers general recommendations to enhance the efficiency of such operations.

REFERENCES

- Amini, A., Chraïbi, A., & Manso, P. (2020). Numerical Simulations of an Innovative Water Stirring Device for Fine Sediment Release: The Case Study of the Future Trift Reservoir. In P. Gourbesville & G. Caignaert (Eds.), *Advances in Hydroinformatics* (pp. 967–978). Springer. https://doi.org/10.1007/978-981-15-5436-0_73
- Amini, A., Venuleo, S., Chamoun, S., De Cesare, G., Schleiss, A., & Takhtemina, F. (Eds.). (2017). Investigation of venting turbidity currents in the Rudbar-Lorestan reservoir in Iran. In *Abstract Book of the 85th ICOLD Annual Meeting*.
- Beyer, N., & Schleiss, A. (Eds.). (2000). Bodenerosion in alpinen Einzugsgebieten in der Schweiz. *Wasserwirtschaft*, 90(3), 88–92.
- Chamoun, S., De Cesare, G., & Schleiss, A. J. (2016). Managing reservoir sedimentation by venting turbidity currents: A review. *International Journal of Sediment Research*, 31(3), 195–204. <https://doi.org/10.1016/j.ijsrc.2016.06.001>
- De Cesare, G., Manso, P. A., Chamoun, S., Amini, A., & Schleiss, A. J. (2019). Innovative methods to release fine sediments from reservoirs developed at EPFL, Switzerland. *HydroLink*, 2.
- De Cesare, G., Schleiss, A., & Hermann, F. (2001). Impact of Turbidity Currents on Reservoir Sedimentation. *Journal of Hydraulic Engineering*, 127(1), 6–16. [https://doi.org/10.1061/\(ASCE\)0733-9429\(2001\)127:1\(6\)](https://doi.org/10.1061/(ASCE)0733-9429(2001)127:1(6))
- Guillén Ludeña, S., Manso, P. A., & Schleiss, A. J. (2017). Fine sediment routing in a cascade of alpine reservoirs: Influence of the inlet angle on settling of fine sediments. *Proc. Hydro 2017*. Hydro 2017, Seville, Spain.
- Guillén-Ludeña, S., Manso, P. A., & Schleiss, A. J. (2018). Multidecadal Sediment Balance Modelling of a Cascade of Alpine Reservoirs and Perspectives Based on Climate Warming. *Water*, 10(12), 1759. <https://doi.org/10.3390/w10121759>
- Jenzer Althaus, J., De Cesare, G., & Schleiss, A. J. (2010). Verlandung der Stauseen gefährdet die nachhaltige Nutzung der Wasserkraft. *Wasser, Energie, Luft - eau, énergie, air*, 102(1), 31–40. <https://doi.org/10.5169/seals-941640>
- Jenzer Althaus, J. M. I., Cesare, G. D., & Schleiss, A. J. (2015). Sediment Evacuation from Reservoirs through Intakes by Jet-Induced Flow. *Journal of Hydraulic Engineering*, 141(2), 04014078. [https://doi.org/10.1061/\(ASCE\)HY.1943-7900.0000970](https://doi.org/10.1061/(ASCE)HY.1943-7900.0000970)
- Kantoush, S. A., De Cesare, G., Boillat, J. L., & Schleiss, A. J. (2008). Flow field investigation in a rectangular shallow reservoir using UVP, LSPIV and numerical modelling. *Flow Measurement and Instrumentation*, 19(3), 139–144. <https://doi.org/10.1016/j.flowmeasinst.2007.09.005>
- Müller, M. (2012). *Influence of in- and outflow sequences on flow patterns and suspended sediment behavior in reservoirs* [Ecole Polytechnique Fédérale de Lausanne (EPFL)]. <https://doi.org/10.5075/epfl-thesis-5471>

- Müller, M., De Cesare, G., & Schleiss, A. J. (2014). Continuous Long-Term Observation of Suspended Sediment Transport between Two Pumped-Storage Reservoirs. *Journal of Hydraulic Engineering*, 140(5), 05014003. [https://doi.org/10.1061/\(ASCE\)HY.1943-7900.0000866](https://doi.org/10.1061/(ASCE)HY.1943-7900.0000866)
- Müller, M., De Cesare, G., & Schleiss, A. J. (2017). Experiments on the effect of inflow and outflow sequences on suspended sediment exchange rates. *International Journal of Sediment Research*, 32(2), 155–170. <https://doi.org/10.1016/j.ijsrc.2017.02.001>
- Onate-Paladines, A., Amini, A., & De Cesare, G. (2019). Computational Modelling of Fine Sediment Release Using SEDMIX Device with Thrusters. *Proceedings of the SCCER-SoE Annual Conference*. SCCER-SoE Annual Conference 2019, Luzern, Switzerland.
- Perera, D., Williams, S., & Smakhtin, V. (2023). Present and Future Losses of Storage in Large Reservoirs Due to Sedimentation: A Country-Wise Global Assessment. *Sustainability*, 15 (1), Article 1. <https://doi.org/10.3390/su15010219>
- Schleiss, A. J., Franca, M. J., Juez, C., & De Cesare, G. (2016). Reservoir sedimentation. *Journal of Hydraulic Research*, 54(6), 595–614. <https://doi.org/10.1080/00221686.2016.1225320>
- Vorlet, S. (2018). *Preventing fine sediment settling with jet-like inflows and intake-like outflows in reservoirs* (STUDENT). Infoscience. <http://infoscience.epfl.ch/record/253549>



Taylor & Francis

Taylor & Francis Group

<http://taylorandfrancis.com>

Theme D: How to deal with ageing dams Dam safety



Taylor & Francis

Taylor & Francis Group

<http://taylorandfrancis.com>

Ageing dams in Switzerland: Feedbacks of several case studies

Nicolas J. Adam

Civil Engineer, Alpiq Ltd, Switzerland

Jérôme Filliez

Senior Civil Engineer, Alpiq Ltd, Switzerland

Jonathan Fauriel

Head Civil Engineering and Environment, Alpiq Ltd, Switzerland

ABSTRACT: Swiss dams, mainly built for electricity generation, are monitored by an organization composed by the dam owner, the dam operator, qualified professionals, and the Swiss Federal Office of Energy.

The paper presents different case studies of how ageing dams is addressed, including dams affected by alkali-silica reaction (ASR) or subjected to a change in thermal loading. The panel of case studies allows to identify the different stages of ageing and highlight the investigation process. It includes the deviation of the structural behavior, the crack appearance, and the detailed on-site investigation. These feedbacks challenge the existing processes, the studies used to help the decision and highlight strengths and weaknesses and when it is necessary to act. Furthermore, different solutions are highlighted from the rebuild or reinforcement to a reinforced monitoring.

The synthesis suggests a rehabilitation decision process to ensure an adequate response for both safety and economical aspects. The rehabilitation monitoring is finally discussed to control the effectiveness of the owner's response.

1 INTRODUCTION

1.1 *Large Dams and health monitoring in Switzerland*

There are around 200 large dams in Switzerland with an average age of 70 years (Schleiss & Pougatsch, 2011). Most of these dams are for hydroelectric power generation and were mainly built during the period 1950-1970. The Swiss large dams are subject to the Water Retaining Facilities Act (WRFA) and its implementing ordinance, the Water Retaining Facilities Ordinance (WRFO). These legal documents require, among other things, the owner of these structures to set up a monitoring system to detect any deterioration in their safety.

Four monitoring levels are defined in the WRFO. Figure 1 shows the four levels and their main tasks according to the WRFA and WRFO. This paper focuses on the synergies between these levels and their main contributions, especially:

- The annual report (AR) written by the qualified professional based on the measurements performed by the operational staff.
- The five-yearly safety assessment (FSA) performed by the geology and civil experts based on the ARs.



Figure 1. The four levels and their main tasks (non-exhaustive) according to WRFA and WRFO.

1.2 Asset management

From a legal point of view (WRFA and WRFO), the operator, who is responsible for the dam surveillance, is the one who has obtained the operating permit. Thus, a distinction shall be made between the operating staff and the owner operator. The owner operator (thereafter “operator”) must set-up the surveillance organization as briefly described in Figure 1 and Section 1.1. The asset management technical support of the operator can take over the tasks of qualified professionals (L2) and cumulates both vision of an asset management and a monitoring point of view.

This paper aims to show how these two visions allow an operator to optimize the life span of its facilities under surveillance and to anticipate the work to be carried out.

2 DESCRIPTION OF CASE STUDIES

2.1 Hongrin

2.1.1 Dam description and issues

Hongrin dams (Figure 2) are two double curved arch dams linked by a central buttress, which were completed in 1969. Hongrin Lake is operated by FMHL SA (Forces Motrices Hongrin Léman) and whose water is used for the Veytaux I & II pumped storage power station (480 MW).

Hongrin dams has faced to two different issues during last years:

- 1) There have been weaknesses in the right bank grout curtain since the commissioning.
- 2) A downstream displacement drift and horizontal cracks have been highlighted in the central buttress (Figure 3).

Both issues were solved with rehabilitation works in 2018 (Wohnlich, 2022). This paper however focuses on the radial buttress displacement.

2.1.2 Drift observations, analyses, and reactions

The radial and tangential deformations of the buttress are measured by an inverted pendulum at two different levels (Figure 2). They have been recorded in a database since 1985. The radial displacements are drawn in Figure 3 from 1985 to 2023.

First, a deviation of the radial upper displacement was reported in 1996 by the qualified professional (L2) in the annual report, while there were visible seepages on the downstream

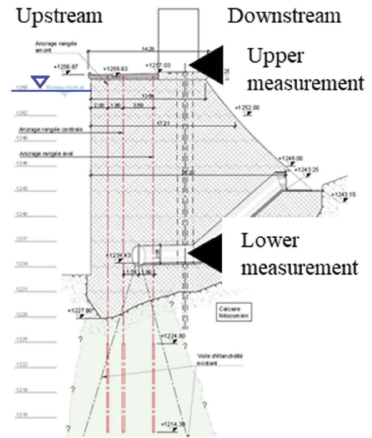


Figure 2. Hongrin dams and the central buttress (right) and vertical section of the central buttress (left).

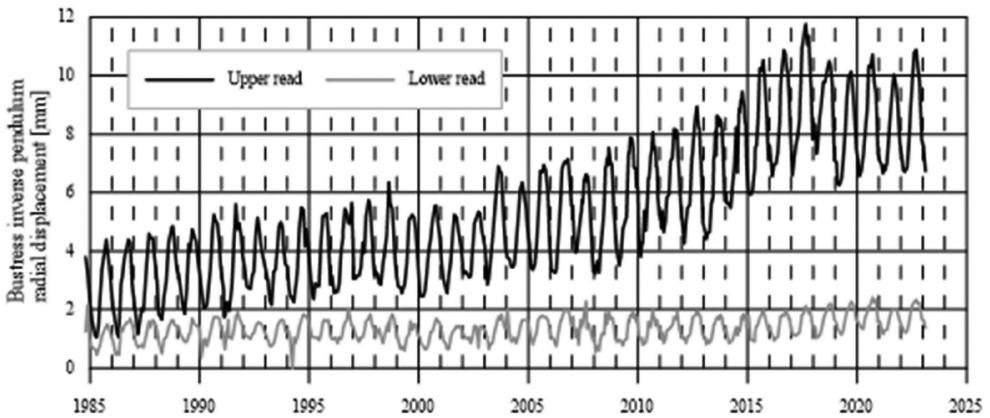


Figure 3. Radial displacement of the buttress (two readings).

buttress face. Both qualified Professional and civil engineer expert agreed to measure the horizontal cracks opening. Table 1 shows the accelerating drift of the upper displacement, even though there is no trend for the lower measurement.

Secondly, the 2007 FSA triggered several additional analyses: detailed inspection, vertical drillings (and concrete analysis) and the creation of a 3D numerical model. The detailed inspection of the buttress confirmed the existence of 3 through-wall horizontal cracks. The vertical drillings gave information on the internal crack networks: one old network every 20-30 cm and another new with smaller cracks. The numerical analysis revealed that the global stability of the two arch dams were not affected. A new monitoring was set-up to follow the drift acceleration after 2003.

Thirdly, the 2012 FSA launched different assessments. The buttress stability was not insured in case of extreme earthquake (return period of 10'000 years). In addition, Summer 2015 accelerated the implementation of maintenance work. Indeed, the warm conditions caused a significant downstream shift.

Figure 4 summarizes the different observations (erratic behavior and visual), the enhancement of the monitoring, the investigations and analysis, which were performed.

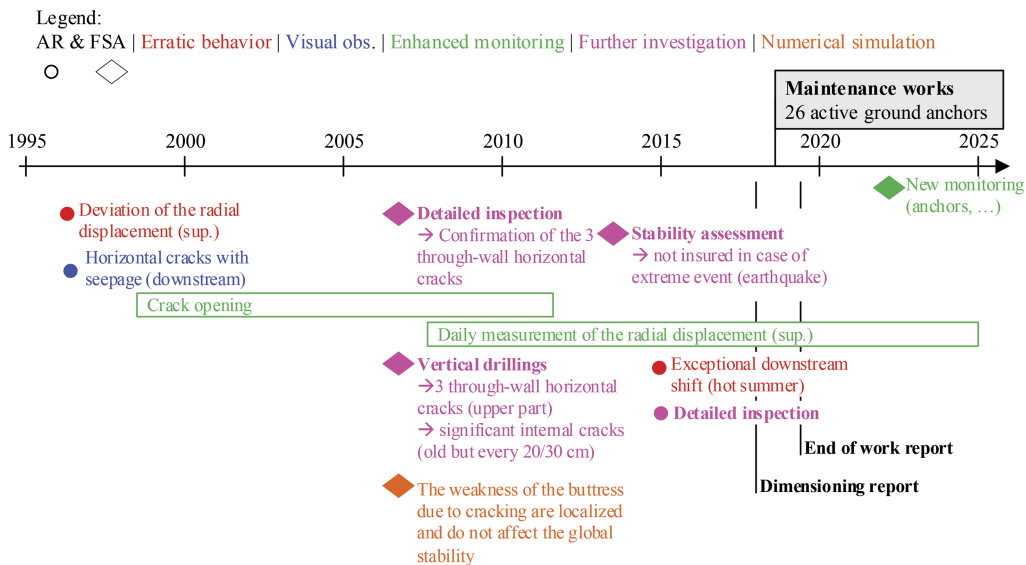


Figure 4. Timeline of all interventions, analyses and reports performed on the Hongrin buttress.

Table 1. Buttress - Displacement drift (mm/yr.) (+ downstream; - upstream) (from FSA 2022).

	1984-1996	1991-2001	1996-2006	2001-2011	2006-2016
Upper read	0.11	0.04	0.10	0.21	0.35
Lower read	0.02	-0.02	0.00	0.00	0.00

2.1.3 Feedback of the maintenance works

Maintenance works were performed from March (slab sawing) to December (anchor tensioning) 2018 with the installation of 26 active ground anchors and new monitoring instruments were installed.

Figure 3 shows, that the downstream deviation has been stopped. The displacement amplitude, caused by the concrete thermic, remains constant.

2.2 Salanfe

2.2.1 Description

Salanfe dam (Figure 5) is a concrete gravity dam commissioned in 1952. Salanfe Lake is operated by Salanfe SA and turbined in Miéville power station (70 MW).

2.2.2 Observations, analysis, and reactions

The dam is equipped with several monitoring systems, including pendulums and extensometers, and has been fitted with a geodetic and levelling network since 1993 to follow the evolution of its deformations. A drift started soon after the dam was built and then accelerated in the 1970s. Since the dam commissioning, the total irreversible downstream-upstream displacement is approximately 35 mm.

Two concrete analysis campaigns (mechanical, physicochemical, and residual expansion) in 2001 and 2008 revealed the development of an alkali-reaction, the presence of numerous cracks within the cement paste and interfaces between the binder and the aggregates. Following this, new monitoring devices were installed, i.e., 3 new pendulums (2 more in 2013) and 1 distivar in 2005 and 18 new levelling points around the left elbow in 2007. In addition, detailed inspections were conducted every 5 years. All this allowed to better understand the behavior of the dam due to concrete expansion and to calibrate the numerical model in 2007.

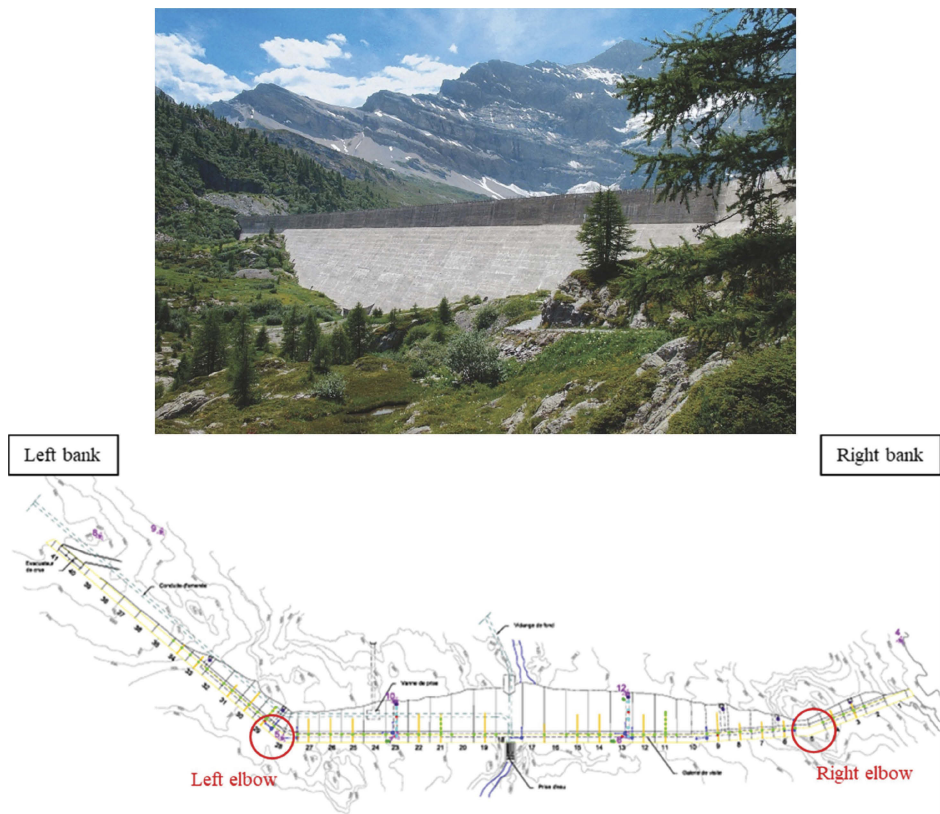


Figure 5. Salanfe dam (up) and top view (down).

This monitoring reinforcement also highlight the irreversible movements of the dam: downstream-upstream movements and a vertical displacement of the crest, which have continued over time. The upstream drift of the crest is amplified by the horizontal angles, giving an “arched” of the structure. This situation is typical of arch dams where swelling of the concrete leads to an increase in the length of the arch, which is only possible outwards, namely upstream.

To mitigate the effects, part of the concrete was removed by cutting saw cuts through the dam in the upstream-downstream direction. The cutting work was done between 2012 and 2014, resulting in 22 cuts with a total sawing area. Other works were also conducted, including refurbishment of the crest, reconstruction of the bottom drainage building, replacement of geotectic pillar No.1, and various drillings. Figure 7 shows the location of the saw cuts in yellow.

Figure 6 summarizes the different observations (erratic behavior and visual), the enhancement of the monitoring, the investigations and analysis, which were performed. In complement to this paper, Droz et al. (2012) summarizes the issues, e.g., alkali-silica reaction (ASR), that the dam has faced for a long time. The new monitoring, developed after the slot cuttings, is exposed in Droz et al. (2015).

2.2.3 Feedback of the rehabilitation project

The swelling of concrete is a recognized issue that causes various symptoms. It is interesting to observe how rehabilitation project has influenced these symptoms (Table 2). After a reduction due to slot-cuttings, the irreversible trend towards upstream increased again in the period 2016-2020. The slot-cuttings allowed some blocs to move laterally, which showed a temporary reduction in irreversible movements.

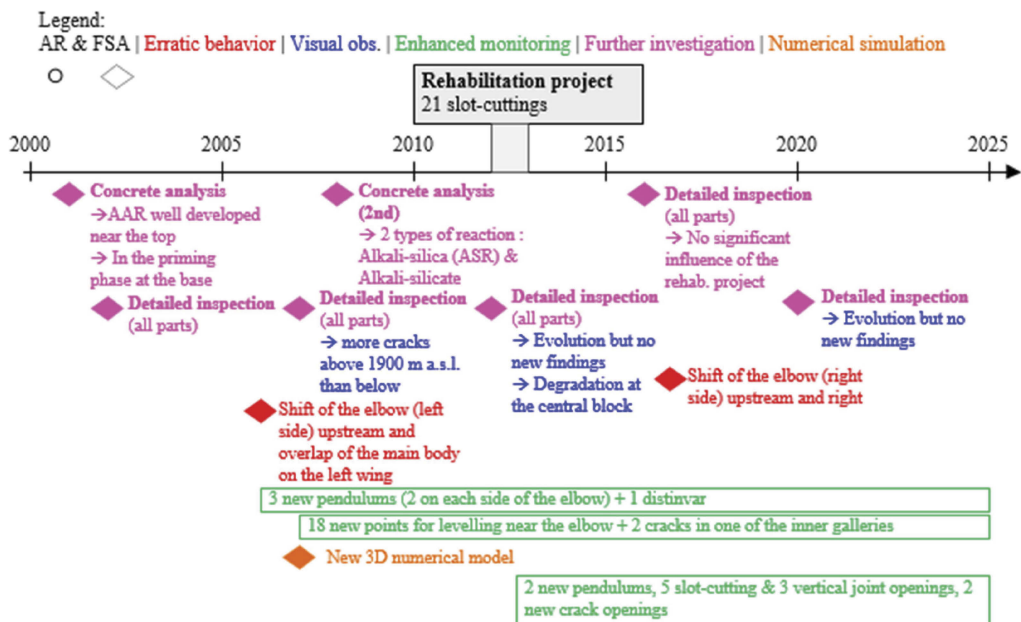


Figure 6. Timeline of all interventions, analyses and reports performed on Salanfe dam.

Table 2. Average irreversible displacements (mm/yr.) (+ downstream; - upstream) for the different parts of the dam (from FSA 2021).

	1996-2000	2001-2006	2006-2013	2013-2015	2016-2020
Left elbow				-1.08	-1.51
Central part	-0.82	-1.21	-1.24	-0.97	-1.36
Right elbow			-3.48	-1.44	-2.71

2.3 Cleuson

2.3.1 Description

The Cleuson (1947-1951) buttress dam is a hollow gravity dam which is 87 m tall. It retains 20 million m³ of water the waters of which are pumped to the Lac des Dix. The Cleuson dam is a part of Grande Dixence complex.

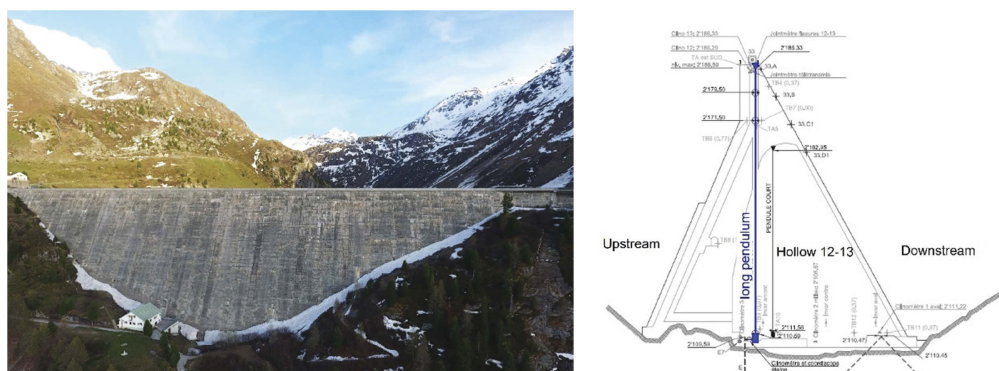


Figure 7. Cleuson dam and vertical section of a central hollow (n°12/13) with the long pendulum in blue.

2.3.2 Drift observations

The existing monitoring allows to follow the behavior of the dam body from the first impounding. In the central part of the dam, the displacement can be controlled by two direct pendulums, one measuring the movement from the crest to the foundation, the other one measuring the lower part (Figure 7). The drift of the upper part towards the downstream direction (Figure 8) has been continuously measured since 1955, with an average downstream displacement of 0.65 mm/year.

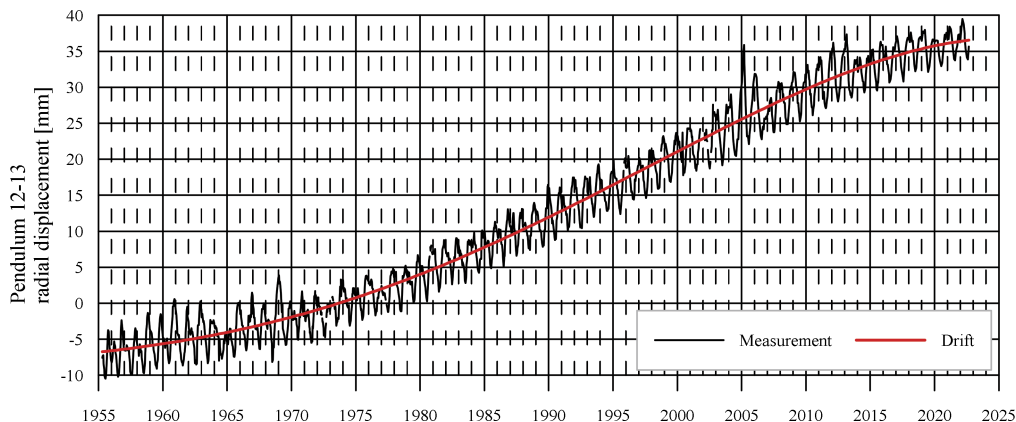


Figure 8. Measurement and drift for the long pendulum in hollow 12-13.

2.3.3 Observations, hypothesis, analysis, and reactions

During the first FSA in 1967, downstream displacement of the dam was observed on both pendulums, which was associated with plastic movement of the rock foundation. In 1971, a short pendulum and rockmeters were installed in excavation 12/13 to confirm this hypothesis. A polygonal and a leveling survey of the dam crest have been conducted since then. During the next FSV in 1976, the rock foundation was confirmed to be elastic based on measurements from the rockmeters and the short pendulum, and the plasticity hypothesis was discarded. New measurements were installed to understand the downstream displacement, and in 1980, inclinometers were installed at the foundation and dam crest to measure the rotation of the dam body.

In 1986, the expert noticed that plastic deformation downstream was mainly localized in the top 23 meters of a dam. The expert hypothesized abnormal concrete creep as the cause. Laboratory tests were conducted on samples taken from the downstream face in 1992 and 1997, but no significant expansive degradation was found. In 2002, a crack was observed for the first time at the drainage well of excavation 12-13, but the expert still favored the hypothesis of ongoing creep. In 2005, a survey revealed one or more transverse cracks spanning the dam from one bank to the other, about 10 meters high, in the upper part of the dam.

A pseudo-static stability calculation was carried out in 2008, considering the cracking with conservative assumptions. This study demonstrated the stability of the upper part of the dam under dynamic loading up to the water level of 2185.5 meters above sea level. The Swiss Federal Office of Energy (the supervisory authority in Figure 9) requested a restriction of the reservoir filling in 2008 to the level of 2184.50 meters above sea level, which is 2 meters below the normal operating level. At the same time, investigations were launched with the aim of identifying and explaining the observed damages, but it was not possible to conclude. Internal or external sulphate reaction, alkali reaction, delayed ettringite formation are suggested or, in some cases, excluded.

Further surveys and investigations were carried out in 2013 to characterize the transverse cracking of the upper part of the structure and to characterize the mechanical and chemical concrete characteristics. These new investigations make it possible to question the conservative hypotheses admitted for the verification of the safety of the upper part of the dam in

2008. Based on these observations, a new numerical modelling by finite element makes it possible to determine the cause of the cracking observed and to show that the safety of the structure was guaranteed without operating restrictions. In 2016 and 2022, the galleries, wells, excavations, and the faces were again inspected to check the good performance of the structure. In 2022, a numerical modeling is underway to check the long-term performance of the structure.

2.3.4 Timeline

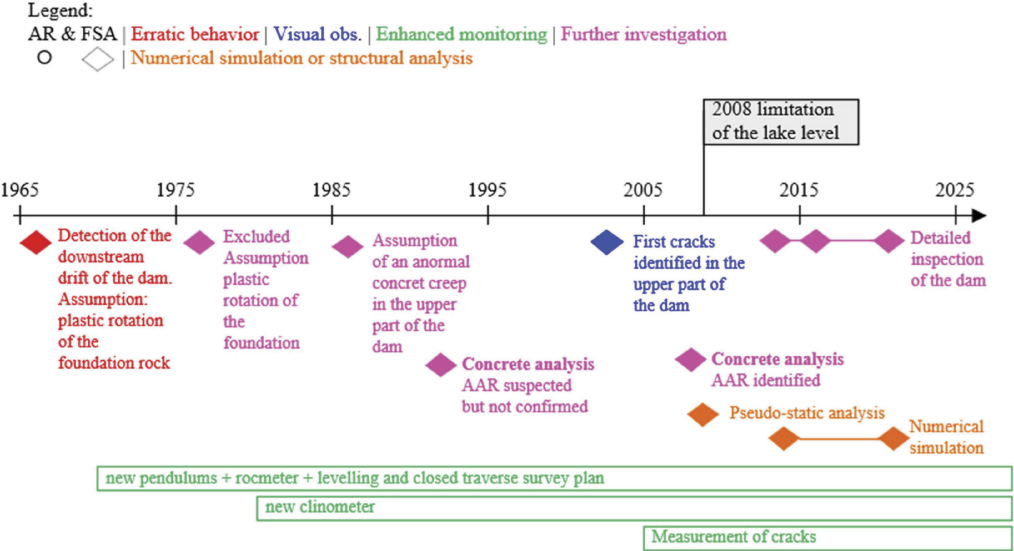


Figure 9. Timeline of all interventions, analyses and reports performed on Cleuson dam.

2.3.5 Feedback of the ageing of the Cleuson Dam

The irreversible displacement of the barrage was detected less than 20 years after its construction and was continuously monitored through instrumentation. No rehabilitation measures were necessary. Restrictions on exploitation were imposed in 2008 following the appearance of cracks and structural analysis. Since then, investigations have focused on modeling the structure’s degradation and estimating its structural safety.

3 DISCUSSION AND CONTRIBUTION OF DECISION-SUPPORT ALGORITHMS

The ageing effects of three concrete dams were presented in Section 2. These problems come from different causes, such as concrete expansion, increased thermal loads and a combination of causes (geological displacement and concrete expansion).

These different examples show how the monitoring levels described in Section 1.1, and more specifically the qualified professional (L2) and the experts (L3), interact with each other. Through ARs and FSAs, the owner-operator can anticipate and commission additional investigations to understand and characterize the drift of a dam to extend its life. It is, however, interesting to see that the first trigger is conducted by the experts, who has the necessary perspective.

The three cases show how the thinking of the responsible engineers (experts and qualified professionals) evolves as the investigations progress:

- As in the Hongrin case (Section 2.1), the implementation of an enhanced monitoring may be abandoned in favor of another one when the first one is not relevant.
- For Salanfe, the detailed inspections at short intervals (every five years) allow to follow the degradations.

- For Cleuson, various observations and hypotheses have been made since the dam was commissioned. Combined with a reinforced auscultation and structural analysis, the complementary investigations allow to follow the effect of the drift on the structure.

Finally, it is interesting to note the degree of resolution of the damage or drift noted. Indeed, in the case of the Hongrin, it can be said that the static structural behavior was recovered by stopping the drift of the central abutment. The other two examples allowed the structures to continue to operate, but under different conditions than initially. The rehabilitation works or the level constraint did not allow to solve the drift observed.

4 CONCLUSION

In conclusion, asset management and structure health monitoring with the help of experts are crucial for maintaining dams. They enable proactive issue detection, informed decision-making, cost savings, and improved efficiency. Integration of these tools and the decision of the qualified professionals extend asset life and maximizes return on investment for sustainable operations.

Dam owners can use asset management strategies and structure health monitoring technologies to identify and address potential issues before they escalate into more significant problems, leading to cost savings and improved operational efficiencies. By making informed decisions at the right time about asset maintenance, owners can extend the useful life of assets and ensure long-term sustainability of operations.

In this paper, three examples demonstrate the effectiveness of the Swiss dam monitoring system. The four levels of monitoring, described in Figure 1, work together to ensure the longevity of dams. Different solutions have been discussed such as rehabilitation of the initial dam statics, release of the stress state in the dam or a numerical modeling to check the long-term performance of the structure.

REFERENCES

- Droz, P., Seignol, J. F., Leroy, R., & Boldea, L. 2012. Strategy for the Rehabilitation of the Salanfe Dam. In 14th International Conference on Alkali-Aggregate Reaction (pp. 10–p).
- Droz, P., Vallotton, O., Menouillard, T., & Leroy, R. 2015. Monitoring of an AAR affected dam. Q99-R33, ICOLD, Stavanger.
- Koliji, A., Bussard, T., Wohnlich, A., & Leroy, R. (2011). Abutment stability assessment at the Hongrin arch dam. *The international Journal on Hydropower & Dams*, 18(ARTICLE), 56–61.
- Schleiss, A.J. & Pougatsch, H. 2011. *Les Barrages: du projet à la mise en service* (TGC volume 17). Lausanne: PPUR Presses polytechniques
- Wohnlich, A., Leroy, R., 2022. Hongrin Arch Dams, Rehabilitation Works of the Central Artificial Gravity Abutment EUROCOLD, Interlaken

Geological hazard evaluation for the dams constructed at Drin valley

S. Allkja, A. Malaj & K. Petriti

A.L.T.E.A. & Geostudio 2000, Tirana, Albania

ABSTRACT: The Drin River valley is very important for Albania, on the energy sector, and electricity production. The most important dams constructed in this valley are Fierza, Komani, Qyrsaqi, Rragami, Zadeja dam and the newest one (currently under study process), Skavica dam. This article will present some of our findings regarding the geological hazards identified on these dams, give recommendations to reduce the risk and keep them under surveillance.

RÉSUMÉ: Le Drin est un élément clé de l'économie Albanaise, notamment pour sa production électrique. Relativement, les plus barrages importants ont été construits sur cette vallée. Nous pouvons mentionner, Fierza, Komani, Qyrsaqi, Rragami, le barrage de Zadeja et aussi le plus récent (actuellement à l'étude), le barrage de Skavica. Nous allons traiter des phénomènes géologiques et des risques identifiés dans les zones où ces barrages sont construits et nous donnerons des recommandations pour réduire le risque et maintenir sous surveillance et exploitation plus longtemps.

1 INTRODUCTION

The Drin is a river located in Southern and South-eastern Europe. Its catchment area extends across Albania, Kosovo, Serbia, Greece, Montenegro, and North Macedonia. The Gulf of Drin is formed by the river itself and its stream branches. The Drin, 335 kilometres long, is the longest river in Albania of which 285 kilometres pass across Albania and the remaining part through Kosovo and North Macedonia. It has two headwaters, namely the Black Drin and White Drin. It originates in the mountainous northern mountain range, flows westwards through the Albanian Alps and Dukagjin Highlands, and drains into the Adriatic Sea.

The Drin is a key component of the Albanian economy, especially for its electrical potential production. Other than hydro power production, the cascade provides a variety of public services including tourism, water sport/transport, aquaculture, fishing, flood protection, and lately has been considered solar energy production as well.

It has a basin area of 11,756 km², and an estimated discharge of 352 m³/s.

Three hydropower facilities produce most of Albania's electricity power (over 1200MW capacity), named Fierza HPP, Komani HPP, Vau i Dejes HPP, with total 6 dams already constructed over this cascade.

The artificial Lake Fierza created by the dam at Fierzë is the largest artificial lake in Albania with a surface of 73 km². The second largest artificial lake built on this river is Vau i Dejës Lake and has an area of 25 km². Despite Fierza, Komani, Qyrsaqi, Rragami, and Zadeja existing dams over the river cascade, we want to mention the newest, large, currently under study process, the Skavica dam.

1.1 *General overview of dam location, types, technical data representation*

The design of the cascade started over half a century before. From the very beginning of the exploitation of hydropower potential, in early 1961, it was necessary to design very high dams. Some of their most prominent characteristics are summarized in the pictures and tables below: [KESH sh.a., Albanian National Committee of Large Dams, ALTEA & Geostudio 2000]

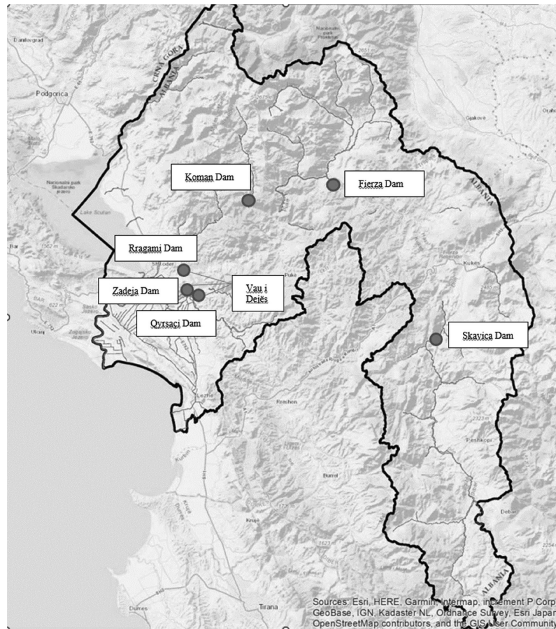


Figure 1. Layout of water basin of Drin – Buna with six large dams’ location, part of Shkodra Prefecture [ALTEA & Geostudio 2000].

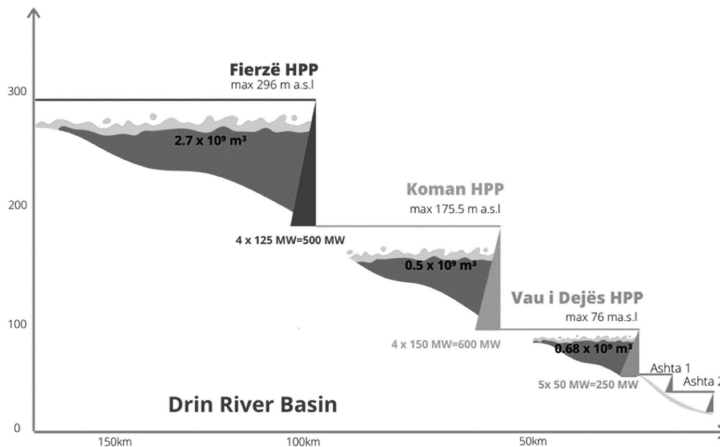


Figure 2. Hydropower facilities data, over Drin cascade. [Albanian National Committee of Large Dams].

The data mentioned in the above tables [Tables 1–3] is gathered and summarized from the information available on the official website of KESH corporate, updated in coordination with the technical data received from Albanian National Committee of Large Dams. Dam owner and user is KESH sh.a.

The characteristics in tables are prepared from the authors of this paper.

Over the years of its operation, our company has had the chance to participate in many geological surveys for the region and give geological and geotechnical expertise for the maintenance of existing dams. In 2012, our company participated in the slope stability project, conducted for Fierza Dam with another international company. Later, in 2021, evaluated the erosion potential and stability of Komani dam area.

Table 1. Technical data for Fierza, Zadeja and Rragami dams. [KESH sh.a.].

	Fierza	Zadeja	Rragami
Dam type/s	Rockfill dams with clay core		
Dam Height	166.5 m	60.0 m	54.0 m
Dam Crest length	380.0 m	387.0 m	514.0 m
Dam body volume	8 000 000 m ³	3 100 000 m ³	1 800 000 m ³
Spillway Capacity	2670 m ³ /s	2100 m ³ /s	2100 m ³ /s
Intake Capacity	4 x 123.5 m ³ /s	-	-
Surface of catchment area	11 829 km ²	14 173 km ²	14 173 km ²
People in the risks in the case of dam failure	195 550	196 200	196 200
Completion Data	1978	1971	1971

Table 2. Komani Dam technical data. [KESH sh.a.].

Dam type	Rockfill dam with reinforced concrete face
Dam Height	115.5 m
Dam Crest length	275.0 m
Dam body volume	5 708 700 m ³
Spillway Capacity	3600 m ³ /s
Intake Capacity	4 x 184.0 m ³ /s
Surface of catchment area	12 850 km ²
People in the risks in the case of dam failure	196 400
Completion Data	1986

Table 3. Qyrsaqi Dam technical data. [KESH sh.a.].

Dam type	Rockfill dam with clay core+concrete dam
Dam Height	54.0 m
Dam Crest length	514.0 m
Dam body volume	1 800 000 m ³
Spillway Capacity	3900 m ³ /s
Intake Capacity	5 x 113.0 m ³ /s
Surface of catchment area	14 173 km ²
People in the risks in the case of dam failure	196 200
Completion Data	1971

During the last two years, we have been involved in the feasibility study for the construction of the Skavica HPP. Our task was to conduct detail geological and geotechnical investigations for the hydro power plant facilities construction area.

2 GEOLOGICAL HAZARDS EVALUATION

This section will deal with the geological phenomena faced during construction and operating phase of the hydro power plants build over the Drin cascade and their facilities.

Our laboratory has performed careful and detailed desk studies, geological mapping, drilling, sampling, other field tests, and of course laboratory testing to characterize soils and rocks encountered on each required specific site.

Based on the available geological and geotechnical investigations from different authors, and our field tests and laboratory testing results in the region from our company, we have distinguished four main geological hazards risking the stability and efficiency of the dams over Drin River cascade:

1. Rock sliding and Landslides, present on the slopes of each dam.
2. Erosion phenomena: coming from surface waters and from Drini river itself.

3. Water Leakage from the reservoirs, presents a fundamental problem that could threaten dam stability.
4. Alluvial deposits, which fill the reservoirs of the dams (sedimentation).

All the above phenomena are encountered in the hydropower plant, at times one of them, sometimes all four, or as combinations of the above-mentioned geo-hazards. To get a clear picture of our investigations let's explain them below:

Rock sliding & Landslides: identified from feasibility studies, during construction or exploitation phase of each dam construction.

We would like to highlight that for the biggest suspected and verified landslides, devices have been installed to monitor the movements and the efficiency of the already taken protective measures of the operating dams. The area's most at risk from landslides and collapse of rock blocks fall are near the Koman Dam and the Fierza Dam.

Vau i Dejës HPP is of the dam and lake type, with four main dams' part of its unit: Qyrsaqi, Zadeja, Rragami and Gjocaj Dam. All these dams are supported on limestone formations. They are stable, regarding the overall safety of the dams, but also the stability of the slopes of the area of the dams and the reservoir.

Both Komani and Fierza were constructed over 50 years ago, in the narrowest part of Drini valley. In the areas where these dams are located there are present a variety of rock formations. These rock formations have been evaluated in our laboratory. The studies comprised the geomorphological aspects, geological aspects petrographic investigations, chemical analysis, physical properties, and most important their mechanical resistance features. The results showed that these rocks are fractured and under atmospheric agents are prone to weathering processes.

A large tectonic fault passes through Drini river valley, which is accompanied by other smaller faults, which are the main causes of rock fractures. These factors have caused the creation of active landslides of diluvial and eluvial masses, but also the rock masses.

While studying these formations over the years, we noticed that each area displays a different typology of these phenomena, that's why they are treated separately. For example:

- Komani Dam is the second and most powerful hydropower plant of the Drin River Cascade. Considering the installed power, position, and the volume of the reservoir, this HPP plays an important role for the exploitation of the entire cascade. Koman dam was built in the narrowest part of the Drini valley where the Vau i Dejes lake ends. The slopes of the valley are built of slate limestone rocks of Upper Cretaceous age (Cr2). The rocks are very fractured, on the slope there are also some large rock blocks which are ready to move towards the end of the valley. On the right side of Drini river there are present rock masses that have been moved and are seen in other parts which are in a critical state and ready to fall. The left side of the river is the side where many facilities of the hydropower plant reside.

We have performed horizontal and vertical drillings, sampling, field testing, and laboratory testing. [Figures 3–11].

Table 4. Komani Dam typical site geotechnical parameters. [A.L.T.E.A. & Geostudio 2000].

GSI	52
γ (kN/m ³)	26.50
c (MPa)	0.48
ϕ (°)	48.40
Es (MPa)	38465.7
E (MPa)	4258.76
UCS(MPa)	65.80
G (MPa)	578.4
ν	0.253
mi	12
D	0.50

Data interpretation and results showed that there is a debris flow and some detached rocks on the slopes near Komani dam. At the area indicating debris flows, rock falling protection with wire nets were built, with a capacity of rock falling protection up to 10-20 tons. Rock masses will either be destroyed by using small mines or anchors will be used to stabilize the slopes.

In our investigation reports we have recommended continuous monitoring of the slope protection measures and their efficiency.

The table above summarizes some typical values, resulting from tested rock samples taken from the Komani dam area, and characterisation of present rock mass formations.



Figure 3. Plan of geological works identifying landslide area [A.L.T.E.A. & Geostudio 2000].

The picture above gives a general view from Komani Lake, Komani Dam and the additional geological works performed by our company to identify the landslide areas, or other risk factors threatening the dam site. After the investigation was completed, several engineering measures were taken to stabilise the erosion phenomena, to protect the site from falling rocks, and to stabilise and keep the landslides under monitoring. The preventing measures comprised the construction of a pile wall, the use of wire nets, and inclinometer installation or other monitoring devices. [A. L.T.E.A. & Geostudio 2000 archives]



Figure 4. View from horizontal borings at Komani Hydropower. [A.L.T.E.A. & Geostudio 2000].

Figures 3–11, represent a generic view of geological and geotechnical works taken on site and laboratory for each specific dam evaluation study.

- Fierza dam: Fierza is the upper HPP of the Drin River Cascade, its construction began in 1970, but the first unit become operational in 1978, only to become full operational in 1980. The dam is filled with stones and has a clay core. [KESH sh.a.].

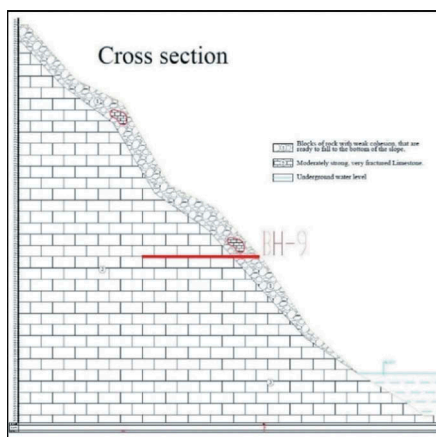


Figure 5. Typical cross-section representation from borings near Hydropower Koman. [A.L.T.E.A. & Geostudio 2000].



Figure 6. Typical core box sample representation from borings near Hydropower Koman. [A.L.T.E.A. & Geostudio 2000].

It was built in the narrow part of the Drin River valley, just after the Koman lake ends. The valley where the dam is built has steep, inclined slopes. The slopes are built from granite rocks, which are fractured rocks. The Fierza dam body rests on granite rock formations.

On the left side of the valley, two large landslides were encountered, Porava and Gropaj landslide, named respectively after the near villages.

At the HPP Fierza dam, all pressure piezometers were out of function, and seepage measurement instruments were installed but no available data since 1987.

Monitoring equipment for water level measurement were installed, but data transfer was manually processed and therefore prone to uncertainties. Monitoring of two main landslides (Porava landslide with a volume of 22 million m³ and Gropaj landslide with a volume of 4 million m³) was a real challenge.

Due the reasons mentioned above and the importance of this power plant, a detailed geological and geotechnical investigation was carried out by our company, in late 2012. A summary of the tested rock samples characteristics and the rock mass characterization is presented in the Table 5.

Gropaj landslide located on the left side of the valley, it has the shape of a large armchair. This landscape was formed either by an old landslide or it is an erosional terrace of the Drin River. In-depth studies proved that this is an old slide which is in an equilibrium state nowadays. In this area, sedimentary and volcanic rock are present, melanges of Upper Jurassic age (J3). the layers of mudstones that are between the volcanic rocks are the main cause for the activation of the big slide. In this area, the electric substation of the Fierza hydropower plant was built. This slide has reached its equilibrium and has not been seen to be moving since the construction period of the Fierze hydropower plant. Later studies comprising borings, mapping, and laboratory analysis revealed that this terrace was created by a rockslide.

The stabilization of this slide has been influenced by the dam, the hydropower plant building, and the reduction of the erosion phenomena due to the construction of the Fierza hydro-power plant. A sudden reactivation of the landslide will be fatal to the facilities of the hydropower plant, but most important for the habitants of the villages nearby these facilities.

We emphasize the importance of digital devices and tools installation to serve the monitoring purposes of sliding events, rock fall, seismic events, water level measurements, etc. . .

In our study, we have recommended installing inclinometers on the terrace of this slide and in the head of the area where the sliding body and non-sliding part met.

Porava slide is on the left side of Fierza lake, close to the crown of the dam.

This slide has very large dimensions due to the presence of the effusive sedimentary deposits (B T2-J1). These formations consist of mudstone, sandstone, and basalts. For this slide there have been performed many tests, since its first stage and during design and construction phases. But in 2012 our company conducted a detailed study comprising mappings, drillings, sampling, laboratory analysis and inclinometer installation and readings.

This analysis showed safe ground with a high possibility for a re-activation.

There are found that there is up to 100 m rock predisposed to slide. The high level of water in Fierza lake has played a huge role on the stability of this area with weak stability.

Table 5. Fierza Dam area typical site geotechnical parameters. [A.L.T.E.A. & Geostudio 2000].

GSI	45
γ (kN/m ³)	25.80
c (MPa)	0.42
φ (°)	36.50
Es (MPa)	28942.6
E (MPa)	34567.8
UCS(MPa)	28.60
G (MPa)	345.7
v	0.357
mi	12
D	0.50



Figure 7. Gropaj landslide view at Fierza dam. [A.L.T.E.A. & Geostudio 2000].

Erosion phenomena from surface waters and the waters of the Drin River itself

Erosion phenomenon often takes place after the rock has been disintegrated through weathering process. This phenomenon has been detected, identified at Komani dam area, but measures have been taken to prevent it and this dam is under monitoring. This phenomenon has been observed in the outside part of the dams in times of discharges when the reservoir is in full capacity.

In the Komani dam, the affected area is on the left side of the river flow. There are present gravel, sand, and clay deposits, which are easily eroded by water currents. There must be noted that if we don't take measures to protect the dam from this phenomenon, the erosion would advance, and it would be dangerous for the dam itself and the hydropower plant area in general.

Table 6. Porava landslide typical geotechnical parameters. [A.L.T.E.A. & Geostudio 2000].

GSI	54
γ (kN/m ³)	27.90
c (MPa)	0.58
ϕ (o)	38.70
Es (MPa)	45789.3
E (MPa)	43278.7
UCS(MPa)	45.70
G (MPa)	542.8
ν	0.357
mi	12
D	0.50



Figure 8. Landslide view at Porava area, Fierza dam. [A.L.T.E.A. & Geostudio 2000].

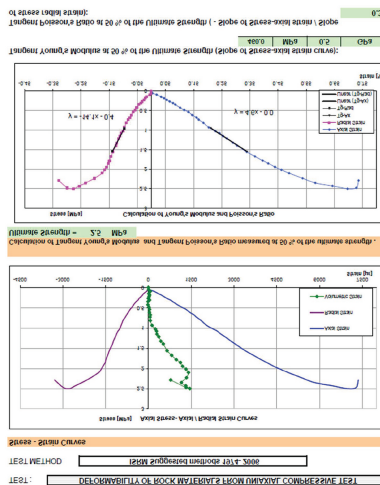


Figure 9. Deformability from Uniaxial Compressive test on encountered rock deposits. [A.L.T.E.A. & Geostudio 2000].

To protect the riverbed, a geological study was carried out in 2021. Based on the data of the geological study, geotechnical calculations were made, and the most effective engineering measures were taken.

It was decided to construct a row of piles [Figure 11] to help with the stability, and this was proven sufficient and successful until nowadays.

As a conclusion, for the dams of the Fierza hydropower plant, the Komani hydropower plant and the Vau i Dejes hydropower plant, we can say that the erosion phenomenon is



Figure 10. During field works at Porava landslide. [A.L.T.E.A. & Geostudio 2000].

present, but with low activity and is not endangering so far, the important facilities of the constructed hydropower plants.

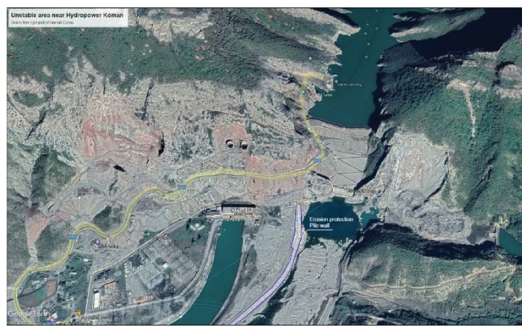


Figure 11. The pile wall built near Komani dam as a measure dealing with the erosion phenomena. [A.L.T.E.A. & Geostudio 2000].

Water leakage from the reservoir of each dam under the foundation of the dam or from the slopes

Leakage can present a fundamental problem, especially if it also carries sediments, an indication that erosion could threaten dam stability, but more pronounced in Vau i Dejes dam and Komani dam. Devices have been installed to evaluate and monitor the amount of water leaving each lake. Several studies carried out in past years, especially in the Komani dam, have noticed that in this area leaks that go up to 900 l/sec of water. [KESH sh.a.]. Based on our investigations, we think that these waters come from the banks of the Drini river and from Komani dam. During the construction of the dam, the anti-filtration curtain was damaged and does not serve its purpose. A part of the dam is placed on the alluvial deposits of the Drin River. There is a possibility, that the water comes from these alluvial deposits and from the upper part of the rock formations. Several piezometers and a catchment have been installed in this dam to monitor the amount of water that filters from Komani dam.

Since our investigation was limited, we recommend a detailed geological study to find the exact place where the groundwater flows in the Komani dam to take the necessary engineering measures to reduce the amount of water flowing from the Komani dam.

Filling reservoirs with alluvial deposits

An important issue for the reservoirs of the hydropower plants over the Drin cascade is the risk of their filling with solid materials.

The Drin River has steep slopes, many mountains' streams flow into these reservoirs, which in cases of rainfall, deposit a lot of solid material into the reservoir. The deposits of solid materials reduce the amount of water in the reservoirs.

So far, no measurements of the bathymetry of these reservoirs have been made. Now, in our knowledge there is undergoing a project from the Albanian Elektroenergjitike Koorporata (KESH) to make bathymetric measurements to estimate the amount of solid materials that have been deposited in these reservoirs since their construction period. This assessment will show us, depending on the data of accumulated materials, what measures we should take to clean them or to predict the future life service of these reservoirs.

Skavica is the last dam on the “dam chain” in Drini valley, which will serve to produce energy but also for regulating the economic use of water for energy production.

From the results of the study of the area of the construction of the Skavice dam on the Drin River, we are faced with two main issues: dam safety and storage of water in the reservoirs.

From the results of the study of the area of the construction of the Skavice dam on Drini river, we are faced with two main problematics:

- Dam stability
- Storage of water in the reservoir

Since the rocks in the area of the dam are more fissured and the tectonic activity is very developed, the optimal type of dam to be considered is a rockfill dam with clay or asphalt core.

In order to preserve the water in the reservoir, it is necessary to take engineering measures like building an improved area under the dam and in its side parts, in order to create an impermeable area from water.

Alluvial deposits filling the lakes: many measurements have been carried out to measure the landscape on the bottom of the lakes and it turns out that there lay a large amount of the deposits.

We propose a detailed economical estimation about the quantities, to evaluate the right time to intervene or abandon the dams where the lake is filled.

3 CONCLUSIONS

After a careful study and evaluation process of the current condition of the large dams built over the Drin River cascade, their monitoring and maintenance, as well as their safety assessments and geohazard aspects the authors have concluded the following main geological hazards:

1. Rockslides and landslides, present on the slopes near all above-mentioned dams.
2. Erosion phenomena, from surface waters and the waters of the river itself.
3. Leakage of water from the reservoir of each dam under the foundation of the dam or from the side slopes.
4. Filling of reservoirs with alluvial deposits.

For a full efficiency operation of the large/small dams built over the Drin cascade in Albania, we propose that the dam operator should consider and keep an eye of the evidenced hazards, especially the geological phenomena, which are developed near the facilities of hydro power plants.

Considering the above-mentioned risks, the dam operator must develop a modern operational program, insuring dam's safety, continuous monitoring systems, risk control and assessment and asset evaluation, since all the large dams built over the cascade have a major role on the Albanian economy.

ACKNOWLEDGEMENT

The authors thank the specialists of the company A.L.T.E.A & GEOSTUDIO 2000, who helped with data for the preparation of this paper.

REFERENCES

- Albanian National Committee of Large Dams, Tirana, Albania.
A.L.T.E.A. & GEOSTUDIO 2000. 2012-2022. *Geological & geotechnical study for Hydropower Plants at Drin River*. Albania
KESH sh.a. <https://www.kesh.al/en/>

Galens arch dam strengthening works

F. Andrian, N. Ulrich & P. Agresti

ARTELIA, Grenoble, France

Y. Fournié

SHEM, Toulouse, France

ABSTRACT: The Galens dam is a 20m high thin arch dam built in a wide valley. Because of this unfavorable configuration, a transverse crack has developed at the base of the central cantilevers near the contact with the ground level. Moreover, the higher-than-usual monitored displacements caught the attention of the dam operator, the Société Hydro-Électrique du Midi (SHEM). These displacements were further amplified by the thermal sensitivity of the arch, especially during winter in one of the coldest regions of France. The stability analyses conducted by ARTELIA from 2014 revealed a non-conformity during rare winter loadings. Although the short and mid-term safety was not compromised, the strengthening works of the dam was considered by the SHEM. In the first part, the paper will describe the studies that led to the choice of the strengthening principle. The “cyclic calculation” method will be discussed, an approach which makes it possible to model one aspect related to the ageing of the dam. The reasons that led to the choice of the strengthening solution will also be discussed. In the second part, the technical specificities involved in the works will be described. The mass concrete mix optimization, the bonding between the new mass concrete to the existing arch, the simplified groutable contraction joints and the upgrade of the monitoring system will be detailed.

RÉSUMÉ: Le barrage des Galens est une voûte mince en vallée large d’une vingtaine de mètres de hauteur. A cause de cette configuration défavorable, une fissure traversante s’est développée en pied des consoles centrales, près du contact avec le terrain naturel. De plus, les déplacements auscultés inhabituellement élevés ont attiré l’attention de l’exploitant, la Société Hydro-Électrique du Midi. Ces déplacements sont par ailleurs amplifiés par l’effet thermique, notamment pendant l’hiver dans l’une des régions les plus froide de France. L’étude de stabilité menée par ARTELIA dès 2014 a montré une non-conformité pour le chargement hivernal rare. Bien que la sécurité à court et moyen terme ne fût pas compromise, des travaux de renforcement ont alors été envisagés par la SHEM. Dans la première partie, les études qui ont menées au choix du principe de confortement seront décrites. La méthode de « calculs cycliques », permettant de simuler le vieillissement de la voûte, sera abordée. Le choix de la solution de confortement sera également expliqué au travers des avantages et inconvénients de chaque option.

Dans la seconde partie, les spécificités techniques liées aux travaux seront abordées. En particulier, le choix de la formulation du béton, la jonction avec la voûte existante, les joints de dilation injectables, et l’amélioration du dispositif d’auscultation seront les points discutés.

1 INTRODUCTION

The Galens dam is an arch dam built between 1966 and 1967 in the French department of Aveyron. This dam is operated by SHEM, the French 3rd hydropower supplier.

It is a thin arch, about 20m high (H) whereas the thickness varies from 1.5m at the crest to 3m at ground level.

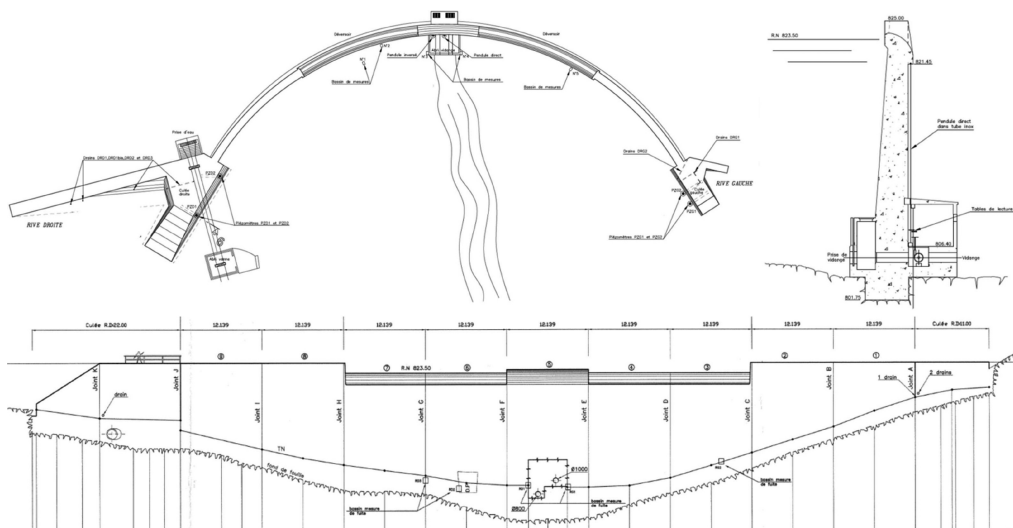


Figure 1. Galens dam: plane view (top left), cross section of the central cantilever (top right) and downstream developed elevation (bottom).

Moreover, because the dam is constructed in a wide valley, the straight distance exceeds 90m (L) between its two thrust blocks ($4 < L/H < 5$). Likewise, the slenderness coefficient is equal to 38 as per Lombardi (Lombardi, 1988). Hence, the dam is particularly sensitive to thermal variations and based on international feedback, an extended decompression/crack opening is expected to occur at the upstream base of the central cantilevers.

2 NON-CONFORM BEHAVIOR AND DECISION OF RETROFITTING

The monitoring data of the dam exhibit seasonal reversible radial displacements of about 1cm at the crest and 2mm at the toe, mainly governed by seasonal effect. As a comparison, one may expect the similar value at the crest and almost one quarter at the toe of a 40-50m high arch dam built in a more suitable valley shape. Moreover, in the case of Galens dam, a few occurrences of unusual tangential displacements at both the crest and the toe are recorded by the monitoring system during winter without being able to relate such events with data collection errors.

In addition, the downstream base of the dam shows a leaking crack which is suspected to cross the entire base thickness at least at the center of the valley. This crack occurring on the dam body side, near the connection with the ground level and along the lift joints is unfavorable due to rather certain low shear strength of the crack. Visual inspections of this crack show a previous sliding of a few millimeters and highlight an obvious freeze-thaw issue.

ARTELIA, acting as SHEM's assistant, performed a series of stability analyses to assess the short, medium, and long-term risks, to help in decisions to be taken, and to design possible strengthening works.

Rather innovative numerical analyses simulating the usually noticed early-year downstream irreversible displacement of arch dams (Fabre, Bourdarot, 2003) were performed. Actually, this approach referred to as "cyclic calculations" (Andrian, Roy, Agresti & Fournié, 2018; Roy, Andrian, Mathieu, Yziquel, 2018; CFB, 2018) proved to be the only way leading to an acceptable calibration of the numerical model to the monitoring data.

The calculations depict a totally cracked dam base with a lifting of the central cantilevers, related to the arch stresses which do not appropriately reach the thrust blocks. This may explain the quite high dam base reversible seasonal displacements. Moreover, for a 100-yr return period winter, the dam base would exhibit a computed sliding of about 3cm along the crack. In addition, the sliding would concern 5 cantilevers out of 9, which exceeds the

maximum range of allowable value as per the current French guidelines (CFBR, 2018). However, the calculations do not highlight any failure mechanism.

Hence, SHEM decided to engage in retrofit works aiming at securing the dam behavior in case of the occurrence of 100-yr return period winter and at guaranteeing the structure’s durability against freeze-thaw.

From 2016 to 2023, ARTELIA’s assistance to SHEM for the strengthening works includes the confirmation of the thrust blocks stability (Andrian, Agresti, Gbiorczyk, 2018), the feasibility, the basic, the detailed and tender design, as well as the assistance to works supervision.

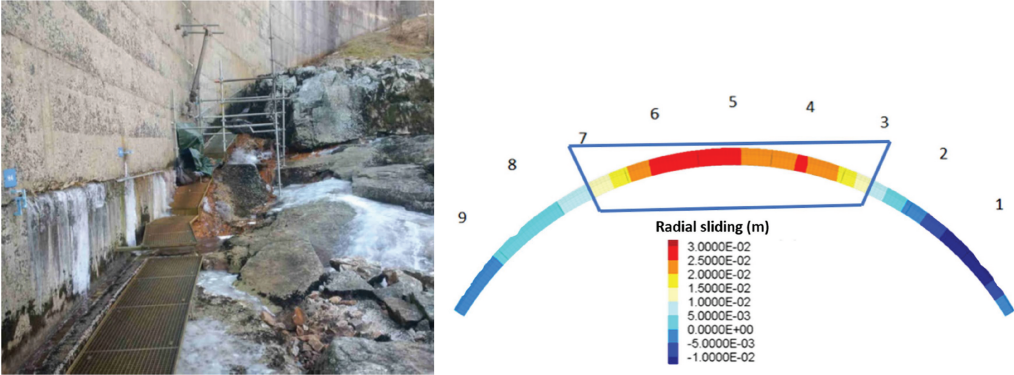


Figure 2. Galens dam base crack: winter picture of cantilever #4 (left) and calculated radial sliding under a 100-yr winter.

3 EXPLORED RETROFIT ALTERNATIVES

3.1 Downstream thermal insulation wall

This rather elegant solution often applied in the Nordic countries consists in installing an insulating wall which is expected to alleviate the thermal sensitivity of the structure.

However, this solution was rapidly disregarded for practical reasons: the possible impact of water sprays from the overflow spillway on the implementation and durability of the membrane, the hidden downstream face which will not allow appropriate surveillance and maintenance, and the insulation membrane lifetime which may require regular replacements.

3.2 Downstream prop-up plinth

The main principles of this alternative, adapted from the case of Kölnbrein dam (Oberhuber, 1991), consist in propping up the dam downstream toe by means of a plinth anchored to the rock using post-tensioned threadbars.

The calculations show that the 100-yr winter sliding is prevented but high tensile stresses are generated in the concrete just above the plinth. This creates a risk of transferring the crack higher up through other lift joints, unless rather complex provision is adopted. Furthermore, the need in follow-up of the threadbar tension with time is also a negative aspect from an operational point of view.

3.3 Post-tensioned vertical tendons

This solution, inspired by the Pont-Du-Roi dam (Bourgeois, Perche, 2016), applies several post-tensioned vertical tendons from the dam crest. The tendons are anchored deep in the bedrock.



Figure 3. Downstream prop-up plinth: perspective illustration view (left) and typical cross section (right).

According to the calculations, this alternative considerably improves the shear strength at the crack and appears to be the most effective in reducing the sliding displacement. However, the installation of the tendons in the overflowing cantilevers proves to be rather complex. Moreover, the significant loading of the foundation bedrock and the effect of the creep due to the heavily tensioned tendons raise several questions, including the issue of interpretability of monitoring data. Finally, the need of follow-up and maintenance of the tendons along with the construction cost pleaded in favor of abandoning this alternative.

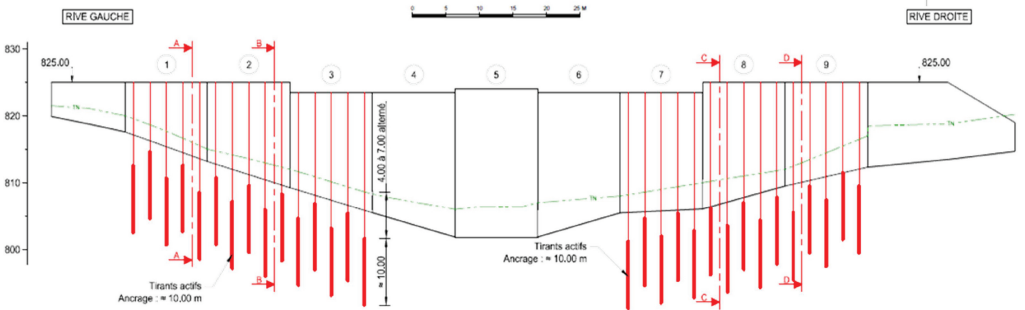


Figure 4. Post-tensioned vertical tendons – developed upstream elevation.

3.4 Thickening of side cantilevers

Inspired by the case of Les Toules dam (Mouvet, 2011), this alternative consists in gradually thickening the cantilevers from the valley center to the banks. The objective is to provide the dam with a shape which better suits the valley geometry. With this new layout, the remaining thin arch (between dashed lines in Figure 6) has acceptable dimensions and benefits from stronger side cantilevers.

Finally, this solution was chosen because its main purpose is not to fix the symptoms of the dam pathology but rather its root causes. Hence, the thermal vulnerability as well as the dam flexibility at the side cantilevers are expected to significantly reduce.

The stepped 1400m³ mass concrete thickening has a downstream slope of 0.5H/1V and a maximum base thickness of about 6m. At the end cantilevers, the taller thickening secures the gravity-type behavior highlighted by the calculations, which also show a resulting maximum 3mm base sliding for the central cantilevers under a 100-yr load case. This magnitude, and the localized nature of the sliding is in line with the current French guidelines.

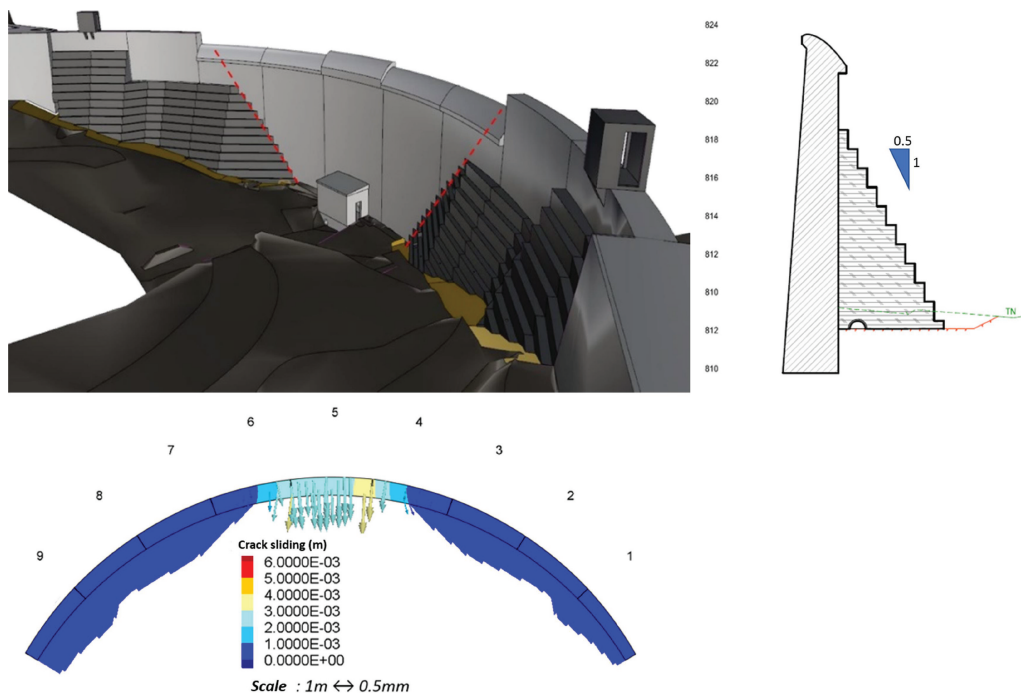


Figure 5. Strengthening by side thickening: perspective illustration view (top left), typical cross section (top right), 100-yr winter calculated sliding (bottom).

4 WORKS DETAILS

Started in spring 2021 by the bedrock excavations, the main works are now completed with the mass concrete being placed between summer and autumn of the same year. By doing so, a reservoir drawdown was not required in a mechanical point of view. Actually, the mass concrete was placed when the dam exhibits its usual summer upstream displacement. Therefore, in winter where its beneficial effect is most wanted, the mass concrete is mobilized by the opposite displacement of the dam. Still the water level was slightly lowered in order to prevent overspilling under 10-yr seasonal flood during the works as a means of protection.

4.1 Concrete mix

The selected concrete mix includes 250kg/m^3 of cement with only 28.5% of clinker and 71% of GGBS (Ground Granulated Blast-furnace Slag). The high Blaine fineness of both the cement (4600g/cm^2) and the limestone filler (5500g/cm^2), combined with the rounded sand, the plasticizer and air-entraining admixtures led to a rather fluid concrete (S4 slump class).

This results in a concrete with a compressive strength of 30MPa at 28 days, 36MPa at 90 days and very probably exceeding 40MPa at 365 days. The maximum mass concrete measured core temperature is 53°C during construction despite the construction in summer and autumn. The 56-day autogenous shrinkage is only 30microstrain, and the entrained air content is between 4.6 and 5.5%. Hence, all the measured parameters exceeded the required criteria.

4.2 Construction sequence and block joint details

The downstream mass concrete was constructed in a symmetrical way. One of two adjacent blocks is always constructed in advance so as to install or to check the installation of the

Table 1. Concrete mix.

Component	Nature	Mix
Cement	CEMIII/B 42,5 N - LH/SR CE PM NF	250kg
Filler	Limestone filler	75kg
Sand	0/4R	910kg
Gravel	6/14C	510kg
	12/20C	320kg
Admixtures	Sika Plastiment 24R	0.25%
	Sika Techno 90	0.70%
	Sika AER 200	0.05%
Water	Réseau	165litres

simplified block joint grouting provisions on the hardened face of the block constructed in advance.

The downstream mass concrete block joints, with a spacing of 12m, are installed at mid-distance between the existing arch dam block joints, allowing specific shear keys to be avoided.

Each mass concrete block joint is equipped with a grouting compartment protected with a closed loop PVC waterstop joint encasing the grouting pipes: one main peripheral (close to the waterstop joint) and one secondary in a diagonal layout. The flexible pipes are equipped with non-return longitudinal valves and were pressure-grouted with epoxy grout in April 2022 after the concrete hydration heat had dissipated. The grout take was rather low and relates approximately 1mm joint opening confirming the low autogenous shrinkage concrete.

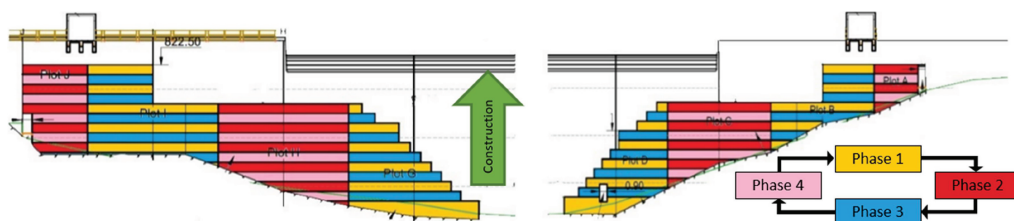


Figure 6. Construction sequence.



Figure 7. Details of the mass concrete block joints equipped with grouting compartments.

4.3 Bonding to the existing dam

The connection to the existing dam is made by means of regularly distributed T25 rebars concentrated at the higher part of the mass concrete, where the opening between both structures would have been forecast without these anchors as demonstrated by the thermo-mechanical analysis.

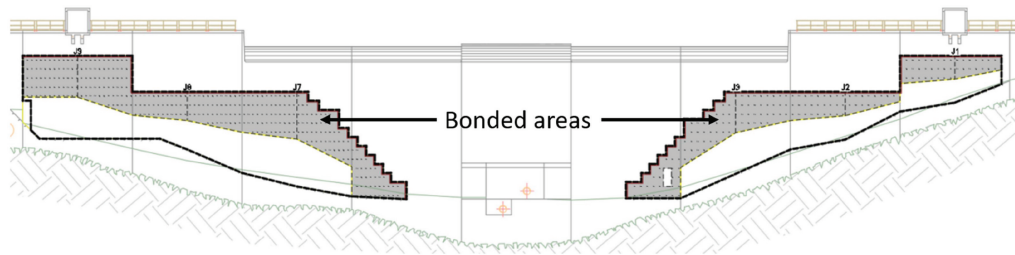


Figure 8. Layout of the rebars connecting the stepped mass concrete to the arch.

This optimized layout allows to reduce interferences with the mass concrete placement. On the other hand, the whole contact surface with the existing dam was chipped by water blasting in order to generate clear asperities ($2\text{cm}@10\times 10\text{cm}^2$), as a safety provision with regards to contact shear stresses, and to possibly achieve some bonding. A chemical grouting is used to anchor the reinforcement in the existing arch.

The upper edge where the mass concrete connects to the existing dam is protected against water seepage under spilling events or during heavy rain by means of hydrophilic joints and a surface Hypalon band.



Figure 9. Bonding details: rebars during construction (left) and Hypalon band finish (right).

4.4 Upgrade of monitoring system

Many monitoring devices of the dam could not be reached under overspilling conditions before the works. This was a significant impediment to the dam close follow-up as the rainy season coincides with winter for this dam, which was then very sensitive to cold weather.

Hence SHEM decided to take advantage of the planned works to undertake an ambitious upgrade of the monitoring system with more than 25 new instruments equipped with data remote transmission system. The new instruments include seepage measurement weirs at the end of the extensive drainage system at the connection between the existing dam, the downstream mass concrete and the bedrock (surface-perforated pipe and drain holes). New crackmeters, inverted plumb lines as well as 3-way head piezometers were installed, making the Galens dam one of the most equipped SHEM's dams in terms of monitoring system.

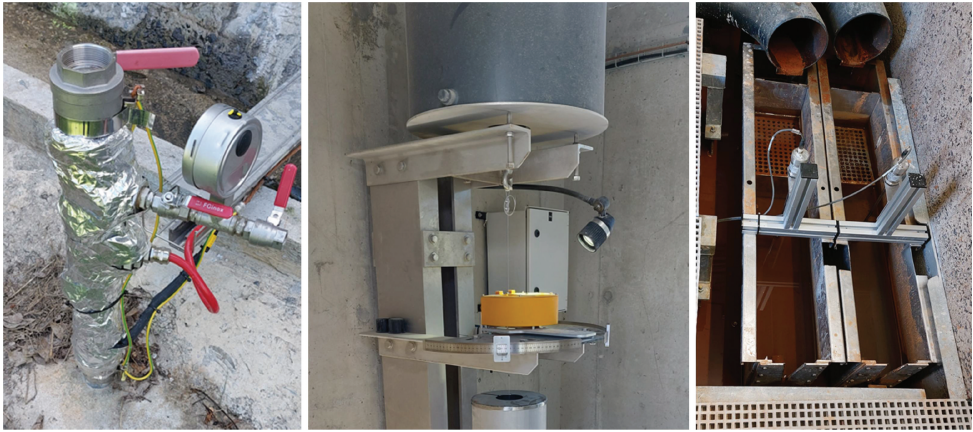


Figure 10. New monitoring devices (from left to right): 3-way head piezometer, inverted plumbline, v-notch weirs with data remote transmission system.

5 CONCLUSIONS

One of the consequences of the works is the apparent drying of the remaining visible leaking crack at the base of cantilever #4 although it was not subjected to any specific direct repairment. Hence, freeze-thaw risk at this precise location can now be excluded.

Moreover, a noticeable decrease in total leakage rate has also occurred without any visible increase in the measured bedrock pore pressure.

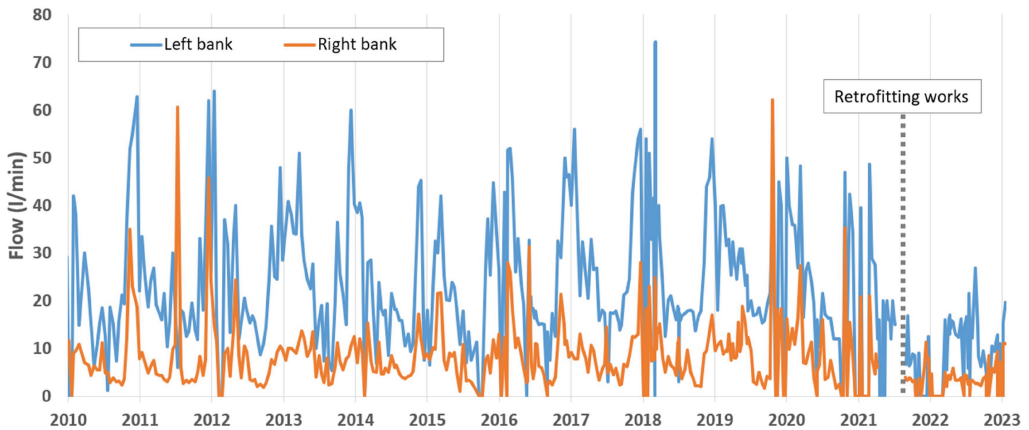


Figure 11. Leakage flow before/after the works.

Time is still needed to assess the mechanical effect of the works by means of the monitoring system, as 2023 is the first winter for which the hydration heat of the new concrete was totally dissipated. In any case, the cyclic calculations predict a 20% reduction in central cantilever crest seasonal displacement as well as a slight and short drift of the dam base toward downstream due to the new load distribution in the arch system. To be thoroughly analyzed in the coming years but there is confidence in the efficiency of the strengthening solution given its passive nature.

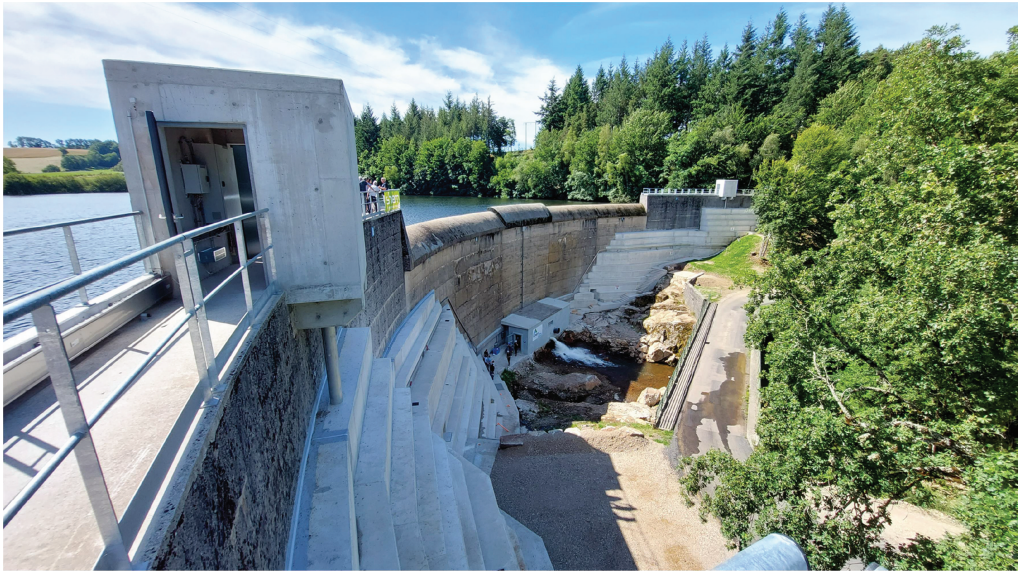


Figure 12. Strengthened Galens dam.

REFERENCES

- Andrian, F., Roy, M., Agresti, P. & Fournié, Y. 2018. On the use of cyclic calculations as a support for the surveillance and monitoring of arch dams, *Méthodes et techniques innovantes dans la maintenance et la réhabilitation des barrages et des digues*, Colloque CFBR Chambéry, 2018, p. 163–173
- Andrian, F., Agresti, P., Gbiorczyk, V., 2018. Reconnaissances approfondies pour déterminer la résistance des culées à la poussée des barrages voûtes, *Méthodes et techniques innovantes dans la maintenance et la réhabilitation des barrages et des digues*, Colloque CFBR Chambéry, 2018, p. 371–380
- Bourgeois, C., Perche, A., 2016, Travaux de confortement du barrage du Pont-du-Roi, *Symposium du CFBR, Chambéry*.
- CFBR. 2018. Recommendations for the safety assessment of arch dam behaviour.
- Fabre, JP., Bourdarot, E., 2003. Analyse du comportement mécanique à long terme des barrages-voûtes, *21th ICOLD congress, Q82-R43 Montréal*.
- Lombardi, G., 1988, Querkraftbedingte Schäden in Bogensperren. *Wasser, energie, luft – eau énergie, air*, 80. Jahrgang, Heft 5/6, 1988, pp. 119–125
- Mouvet, L., 2011, Confortement du barrage des Toules – Pourquoi et comment, *Symposium du CFBR, Paris*.
- Oberhuber, P., 1991, Remedial works for the Kölnbrein dam: Design and Analysis, *XVII ICOLD-CIGB, C.7, Wien*.
- Roy, M., Andrian, F., Mathieu, G., Yziquel, A. 2018. Thermo-Mechanical Calculations of the Janneh Dam, *14th ICOLD International Benchmark Workshop on Numerical Analysis of Dams, Stockholm*, p. 662–671.

Design concept for sustainable cut-off walls made of highly deformable filling materials

K. Beckhaus

BAUER Spezialtiefbau GmbH, Germany

J. Kayser

Federal Waterways Engineering and Research Institute, Germany

F. Kleist

SKI GmbH + Co.KG, Germany

J. Quarg-Vonscheidt

Koblenz University of Applied Sciences, Germany

D. Alós Shepherd

Karlsruhe Institute of Technology, Germany

ABSTRACT: Currently, a joint working group of the German Association for Water, Wastewater and Waste (DWA), the Hafentechnische Gesellschaft e.V. (HTG) and the Deutsche Gesellschaft für Geotechnik e.V. (DGGT) is working on recommendations for a new design concept for sustainable cut-off walls made of “highly deformable cut-off wall materials”. The focus lays essentially on a higher utilisation of the visco-elastic and also plastic deformation capacity of low-strength cement-bound filling materials. This allows for a lower required cement content and thus offers a sustainable advantage, as the equivalent carbon footprint will be significantly lower. Compared to the classical design method, a lower compressive strength shall be allowed. This should be high enough to ensure erosion safety, but with the lowest possible deformation modulus, while at the same time allowing deformation without exceeding the permissible compressive and tensile stresses. The article presents how this high deformation capacity can be applied in the design and thus ensure that more economical and resource-saving cut-off walls can be planned.

RÉSUMÉ: Actuellement, un groupe de travail conjoint d’associations allemandes concernées (DWA, HTG et DGGT) travaille à l’élaboration de recommandations pour un nouveau concept de design de parois moulées durables faites de “matériaux de parois moulées hautement déformables”. L’accent est mis essentiellement sur une meilleure utilisation de la capacité de déformation viscoélastique et plastique des matériaux cimentaires à faible résistance. Cela permet de réduire la teneur en ciment nécessaire et offre donc un avantage environnemental, puisque l’empreinte CO₂ équivalente sera considérablement réduite. Par rapport à la méthode de conception classique, une résistance à la compression plus faible peut être autorisée. Cette résistance à la compression doit être suffisamment élevée pour garantir la sécurité contre l’érosion, mais avec le module de déformation le plus bas possible, tout en permettant une déformation sans dépasser les contraintes de compression et de traction admissibles. L’article présente la manière dont cette capacité de déformation élevée peut être appliquée lors de la conception, ce qui permet de planifier des murs de soutènement plus économiques et plus économes en ressources.

1 MOTIVATION AND SCOPE

In preparation for the impacts of climate change, operators of dams in particular are obliged to take precautionary measures on existing facilities or to plan new facilities according to the current state of the art.

In hydraulic engineering, very high demands are consequently also placed on the vertical dam, dike and subsoil sealing elements (hereinafter: “cut-off walls”); especially regarding their impermeability over the entire service life of the hydraulic engineering installation under the currently given and in future expected impacts.

During the design process of a maintenance, retrofitting or new construction project, the technical properties of the cut-off wall materials (hereinafter also referred to as “filling materials”) must be determined. If hydraulically bound filling materials are used as vertical sealing elements, such as those described as self-hardening suspensions in guideline DWA-M 512-1E “Sealing systems in hydraulic engineering, part 1: earthwork structures”, specific technical dependencies of the deformation properties and the hydraulic parameters on the material composition are also associated with this. According to current experience, the visco-elastic and even markedly plastic deformation capacity of low-strength filling materials is not sufficiently taken into account in the assessment. Instead, in addition to the requirement for maximum water permeability, often only a minimum strength to ensure sufficient erosion resistance is required. The “contractual” requirement of a minimum strength, however, leads in consequence - after the addition of a preliminary dimension in the execution - to a strength that is too high for the actual purpose and thus also to a less ductile material behaviour. However, for the above-mentioned basically required maximum permeability - under the usual conditions of use - the filling material must also be highly ductile.

The challenge was identified in establishing objective criteria for highly ductile diaphragm wall materials, which are already defined in the planning phase and tendering.

The solution strategy can be worked out, at least in part, on the basis of a practical example from Bavaria. At the Sylvenstein reservoir (responsible water management office Weilheim), retrofitting measures were necessary for which, among other things, a deep cut-off wall was constructed. In the course of the tendering process and the definition of the quality criteria, no minimum value but a “target value” for the unconfined compressive strength of the filling material was defined, in addition to other parameters. At the same time, direct test criteria were defined for the essential properties of permeability and deformability.

The relevance of the material parameters on the function of the planned cut-off wall must be specified. Accordingly, a high deformability of a filling material must be taken into account in the design of cut-off walls. In addition, the influence of such highly deformable filling materials on structural sustainability in the sense of climate protection should be demonstrated within the framework of responsibility for society as a whole. Specifically, by reducing the cement content (with lower strength requirements on average), savings in greenhouse gas emissions of almost the same order of magnitude can be expected.

The solution is seen in the formulation of specific design rules and recommendations for planning and execution, which are essentially based on building material technology and its importance for the robustness or resilience of cut-off walls and thus for the effective durability of hydraulic structures. For this purpose, the German Association for Water, Wastewater and Waste (DWA), together with the Hafentechnische Gesellschaft e.V. (HTG) and the Deutsche Gesellschaft für Geotechnik e.V. (DGGT), has set up a joint working group on “Highly deformable cut-off wall materials” (No.: WW 6.6), which, within the same framework, addresses the possible sustainability to be improved in water management through a more resource-efficient use of hydraulic binders. The new recommendations will refer to cement-bound filling materials of different compositions and are to be understood as a supplement to the existing guideline DWA-M 512-1E. The status of the work is presented here in essential points and the authors as members of the working group look forward to a technical discussion, criticism and suggestions on this matter.

2 DESIGN CONSIDERTATIONS

2.1 *Requirements for sealing elements*

Vertical sealing elements in earthworks must fulfill various requirements:

Permeability: The sealing element must meet the sealing requirements of the structure. Here, the permittivity of the sealing element is the relevant parameter. For example, a 1.0 m thick diaphragm wall can have a higher permeability than a 0.1 m thin wall (like a vibrated beam slurry wall) with the same permittivity.

Erosion stability: The erosion stability determines the durability. Here, the solids content of the cut-off wall material and the final strength achieved play an important role in the assessment. In the case of high-solids cut-off walls (density $\rho > 1.2 \text{ t/m}^3$), a strength of $q_u > 0.3 \text{ MN/m}^2$ is often sufficient to achieve a permanently erosion-resistant sealing element with high hydraulic gradients of up to $I = 100$ (see DWA-M 512-1E).

Strength: Often a strength requirement is placed on the cut-off wall material, which is erroneously based on the fact that the sealing element is assigned a load-bearing function in the earthwork or subsoil, which is not actually assumed or does not have to be assumed by the sealing element. Looking at an earth dam or a dike, it can be seen that - except in the case of statically effective seals - a damage-free “co-deformation” of the sealing element with the deformations of the earth structure is desired and can bring great constructive advantages.

Stiffness: If the deformations in the earthwork to be sealed are considerable, “stresses are attracted” by stiff components. In the area of critical deformation points, the permissible strengths of the sealing element are then very quickly exceeded. Such critical deformation points can be located, for example, at rock embedment. When designing sealing elements, the aim is therefore to create low stiffnesses of the sealing element.

Stiffness and strength of a filling material for cut-off walls are usually almost proportionally correlated, so that a conflict of objectives can arise in the design of the sealing element if too high strength requirements also drive the stiffness of the component upwards. What is desired is a flexible sealing element that can absorb the occurring deformations without damage and without losing the required permanent sealing effect.

The highly deformable sealing element does not take on any load-bearing effect as planned, deforms with its surroundings and must not lose the required sealing effect in the process.

2.2 *“Classical” design method*

Deformations in sealing elements in hydraulic engineering can occur as planned from settlements of the surrounding foundation soil or dam body as well as from operational stresses (changes in the water level, traffic and live loads). This results in stresses that are the basis for the design of highly deformable sealing elements.

In many cases, the aforementioned stresses can be absorbed as planned by the elastic deformation capacity of the filling material. For static verifications, the “module of the uniaxial compression test” (E_u) described in DIN 18136 is generally used, corresponding to the inflection point tangent in the (compressive) stress-strain diagram, Figure 1.

Due to the largely proportional dependence of stresses and compressions in the elastic range ($E = \Delta\sigma / \Delta\varepsilon$), the resulting compressive stress increases equally with the imposed deformation, which remains clearly below the compressive strength with correspondingly limited compression.

A bending stress can usually only be verified by an “overpressure” of otherwise resulting bending tensile stresses. In the case of differentiated verifications with main tensile stresses, tensile stresses of up to 5% of the characteristic cylinder compressive strength $f_{m,k}$ on which the design is based can be permitted for simplification purposes (see Figure 1 from DIN 4093:2015, Section 4.4.4 (3)) without having to assume cracking. For higher tensile stresses, it must be assumed that the wall can crack. In this case, it is recommended to verify the hydraulic and mechanical functionality on the non-cracked residual cross-section.

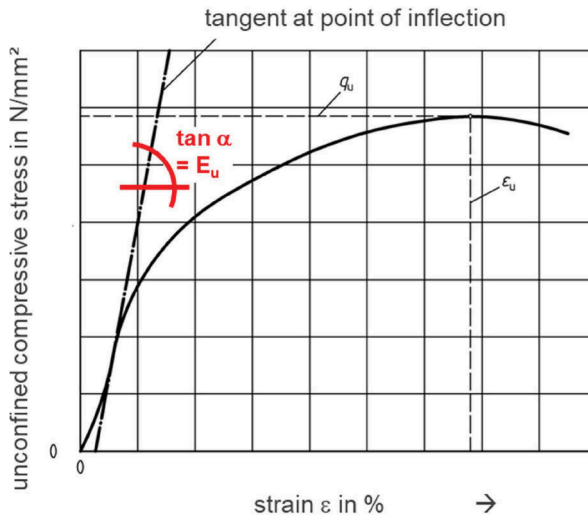


Figure 1. Stress-strain diagram for an unconfined compressive strength test (qualitative) with the deformation modulus E_u defined for an ideal-elastic material behaviour.

2.3 Design concept for highly deformable cut-off walls

2.3.1 Differentiation from the classical design method

The main effects on cut-off walls are deformations from the sealing element system and the surrounding ground, dam material or structure. The basis of the design is a calculation of the stresses and deformations in the structure, if necessary with corresponding load-bearing resistance conditions according to the German standard DIN 19700 for dam plants. The results of these calculations are the input values for the design of the cut-off wall and show the integrity of the entire construction. Due to the often complex boundary conditions at dams and dykes, calculations according to the Finite Element Method (FEM) are suitable.

From the deformations, loads are induced as stresses or stress changes in the cut-off wall, which correlate directly with the stiffness of the cut-off wall when viewed elastically. In order to keep the stress changes from deformations as low as possible, the cut-off wall should generally have as low a stiffness as possible and thus not significantly influence the deformations of the overall system.

Compared to the classical design method taking into account only elastic deformations (see Figure 1), the ductility beyond the aforementioned elastic range is used according to plan to take the properties of highly deformable sealing elements into account.

A reduced deformation modulus E_u^* is introduced as an essential design parameter for this purpose. The deformation-controlled (uniaxial) unconfined compressive strength (UCS) test based on DIN 18136 is suitable for determining E_u^* . The deformation rate during the test should be selected depending on the water permeability of the material and, in deviation from DIN 18136, should generally not exceed a value of 0.1% of the initial sample height per minute. The deformation modulus results from the tangent of the secant between the zero point of the inflection point tangent formed in the elastic range (for determining E_u) and the highest point of the stress-strain curve (at q_u , see Figure 2).

2.3.2 Material characterisation of highly deformable filling materials for cut-off walls

Compared to more brittle building materials, highly deformable cut-off wall materials are characterised by their pronounced plastic deformation capacity. In order for the material stiffness of these highly deformable building materials to be recorded realistically in the calculation, the material stiffness must not be limited to the consideration of a linear-elastic range, in deviation from the conventional calculation and design methods. The plastic stress-strain behaviour is to be included in the design concept of highly deformable filling materials. By

reducing the deformation modulus from E_u to E_u^* , as a result of accepted plastification of the sealing element, stresses in the material are reduced during imposed deformation.

The load-deformation behaviour is described in the following via the ‘model of the internal structure’ (see Figure 2) for a body subjected to compressive stress. The model makes it possible to describe the principal stress ratio in a cement-bound material by defining the two parameters ‘angle of the internal structure’ and ‘internal tensile strength’. The ‘internal tensile strength’ describes the cohesive resistance of the structure, the ‘angle of the internal structure’ indicates the extent to which a force is transmitted in the material. In an ideally structured material, force transmission takes place exclusively in the direction of loading ($\omega = 0$). If there is a deviation from this ideal force transmission, the angle of the inner structure is not equal to zero and tensile stresses arise. The interaction of internal structure and cohesive resistance and the resulting critical principal stress ratios are described in [Tynior et al., 2020] using the example of asphalt seals.

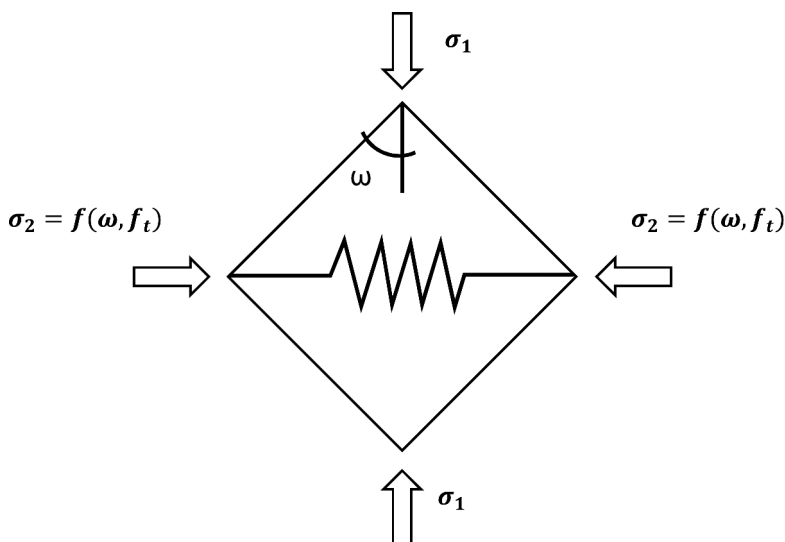


Figure 2. Element of the ‘internal structure’ model.

The variables and parameters shown in Figure 2 are:

σ_1 resp. $\sigma_{2/3}$	Main stresses	[Pa]
ω	Angle of the inner structure	[°]
f_t	Internal tensile strength of the material	[Pa]

For the model shown in Figure 3, it is assumed that a tensile stress is mobilised by load-induced deformation (top) and reaches its maximum value, i.e. the tensile strength, at the end of the elastic deformation range (middle). The elastic range is characterised by the fact that the ‘angle of the inner structure’ remains constant during deformation. As the deformation goes beyond this point, the angle changes while the tensile stress remains constant, which leads to an overall increase in the load-bearing capacity of the inner structure (bottom).

Plastic material behaviour can therefore be attributed to a correspondingly large potential for structural change and described by the material parameters ω_0 and ω_u . Brittle materials generally have no significant potential for change; the internal structure is determined, e.g. in concrete, by a stiff cement matrix. After complete mobilisation of the ‘internal tensile strength’, no further load application is possible ($\omega_u = \omega_0$), the test specimen thus fails spontaneously and without further notice. In this case, the internal energy, which is stored as potential energy in the elastic mobilisation of the tensile strength, is abruptly released as kinetic energy. If, on the other hand, the examined material has a corresponding potential for

change (such as a highly deformable filling material), the load transmission in the material is increasingly oriented in the direction of the load and increases the load-bearing capacity of the inner structure of the material. With additional load application beyond ω_u , the tensile strength is exceeded and unstable crack growth occurs.

For the utilisation of a plastic transition area in highly deformable filling materials, it must be ensured that the sealing effect is maintained. For this, according to the above-mentioned 'model of the internal structure', the 'internal tensile strength' must not be exceeded, which in turn is not exceeded until the compressive strength q_u is reached.

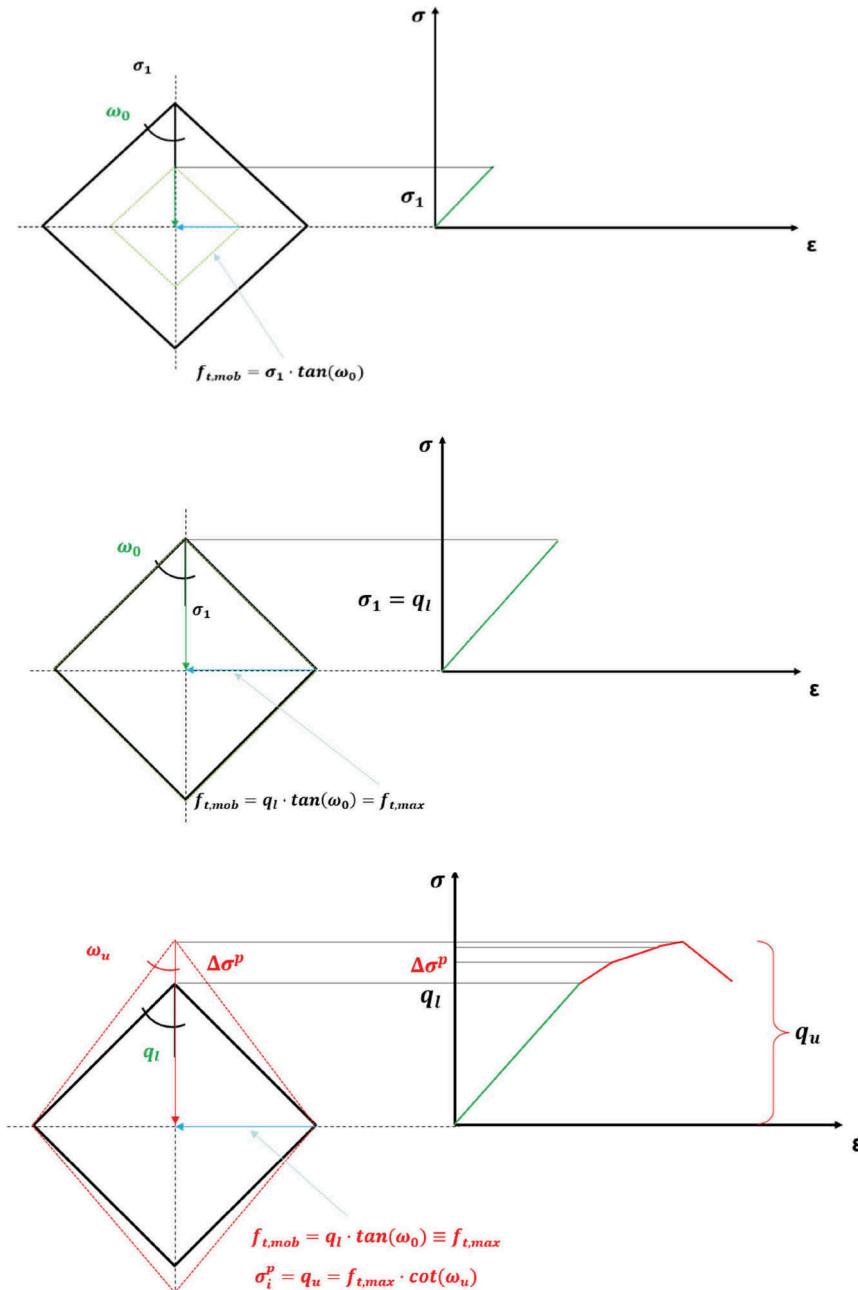


Figure 3. Load-compression behaviour in the 'model of the internal structure'.

2.3.3 Specifications for the compressive strength and stiffness of the filling material

The aim of the proposed design concept is to specify the material requirements for a cut-off wall. The design of the overall structure results in deformations that specify the deformation of the cut-off wall (see 2.1), and the maximum strain state in the wall is decisive for the functional performance of the cut-off wall. This characteristic deformation pattern can be calculated, for example, using the finite element method (FEM).

The characteristic value of the strain to be used for the design $\varepsilon_{k,COWM}$ is the maximum strain (tensile and compression, if applicable) from all investigated load cases. Another input value is the target compressive strength of the filling material q_{target} . The basis for the specification is the required minimum compressive strength q_{req} of the cut-off wall, which usually results from geohydraulic requirements (e.g. erosion) independent of the mechanical stress. The allowance of tolerance for the determination of the target compressive strength depends on the expected scattering of the building material. For an initial estimation, it should be possible to select 50% of q_{req} , but at least 0.2 MPa:

$$q_{target} = \max\left[1.5 q_{req}; q_{req} + 0.2\right] \quad (1)$$

For further design, a deformation modulus $E_{u,upper*}$ is calculated from the quotient of q_{target} and $\varepsilon_{k,COWM}$, which thus marks the upper limit of the compatible stiffness of the filling material.

$$E_{u*,upper} = q_{target}/\varepsilon_{k,COW} \quad (2)$$

The cut-off wall is to be planned accordingly with the following characteristic values:

$$q_k \geq q_{req} \quad (3)$$

$$E_{u*,k} \leq E_{u*,upper} \quad (4)$$

2.3.4 Stress verification

For the above-mentioned design of the overall structure, an “appropriate” deformability of the cut-off wall itself is to be assumed, defined by the characteristic deformation modulus $E_{u*,k}$. This results in characteristic stresses $\sigma_{k,COW}$, which must be verified.

The characteristic stress $\sigma_{k,COW}$ is to be increased with a partial safety factor γ_G to the design value $\sigma_{d,DWM}$

$$\sigma_{d,COW} = \gamma_G \times \sigma_{k,COW} \quad (5)$$

with γ_G = partial safety factor on stresses = 1.35 (for persistent design situation “BS-P”), see table A 2.1, DIN 1054.

If additional (smaller) tensile strains occur in the selected construction, it is suggested to verify the compatibility following DIN 4093. Derived from the compressive strength $q_{ud,m}$, the following tensile strength should be used as the resistance of the material (m) in this case:

$$f_{t,d,m} \leq 0.05 \times q_{ud,m} \quad (6)$$

with $q_{ud,m} = q_{req}$

In a subsequent design step, the decisive cross-section must be verified as follows:

$$\sigma_{d,COW} \leq q_{ud,m} \quad (7)$$

for compressive stresses

$$\sigma_{d,COW} \leq f_{t,d,m} \quad (8)$$

for tensile stresses

In the opinion of the working group, a local exceedance of the tensile strength or compressive strength in the cut-off wall should be allowed if the stress verification and the geohydraulic safety are fulfilled for 80% of the cut-off cross-section.

3 HIGHLY DEFORMABLE FILLING MATERIALS FOR CUT-OFF WALLS

3.1 *General*

The following filling materials for cut-off walls can achieve a high deformability, i.e. substantial usable plastic deformation fractions beyond the elastic range, if they are composed appropriately. They can be used in intersected bored pile walls, diaphragm walls and also in walls made of overlapping soil mixing elements. These construction methods are regulated in the relevant European Norms for execution (EN 1536 for Bored Piles, EN 1538 for Diaphragm Walls and EN 14679 for Deep Mixing).

- (1) Filling material made of self-hardening suspension,
- (2) Filling material made of Plastic Concrete
- (3) Filling material made from deep mixing, also “soilmix material” produced by the wet or dry soil-mixing process.

The type of filling material for cut-off walls to be used for a specific project depends largely on the applicable construction method. Very deep cut-off walls, for example, require a two-phase method, so that only a filling material made of Plastic Concrete can be considered from the above selection.

For all the above-mentioned building materials, target strengths in the following range and with a maximum permeability are suggested for the area of application as highly deformable filling materials, which are to be checked or adapted project-specifically depending on available building materials and other boundary conditions:

- $q_u = 0,5$ to 2.5 MPa
- $k \leq 10^{-8}$ m/s

3.2 *Filling material from self-hardening suspension*

Filling materials made of self-hardening suspension, serve as a supporting liquid during excavation and, together with fine particles from the natural soil, form the final hardened filling material. This limits the processing window as well as the depth of the cut-off wall.

An self-hardening suspension material is a suspension that contains cement, water and additions (e.g. bentonite or other clay mineral) as a stabiliser. Also, (chemical) admixtures may be included. Aggregates are usually not added. Often, ready-mixed dry powders are used, which are mixed by the manufacturer in the factory and only need to be mixed with water at the construction site.

3.3 *Filling material made of Plastic Concrete*

Filling materials made of Plastic Concrete are usually produced in a concrete mixing plant and installed in a previously excavated trench using the two-phase or tremie method.

Plastic Concrete consists of cement, water and bentonite (similar to self-hardening suspension material) and a high proportion of aggregate (sand and fine gravel). Admixtures and additives can also be added. Due to its composition, Plastic Concrete is most similar to normal concrete according to the relevant European Norm EN 206 (Concrete - Specification, performance, production and conformity), but has a significantly higher w/c ratio and lower cement content.

The concrete formulation is adapted to the requirements for strength, deformability and impermeability and checked during the initial test. Due to the controlled installation in the two-phase process (tremie method), the mechanical properties of the hardened filling material are essentially determined by the concrete mix design.

Further information on the fresh and hardened concrete properties and mix design of Plastic Concrete can be found in [Alós Shepherd et.al. 2020].

3.4 *Filling material from deep soil grouting*

Filling material from deep soil grouting is produced by mechanical disintegration by rotating mixing tools and mixing with cement suspension or cement without removing the support of the adjacent soil. Due to its composition, this filling material can also be referred to in simplified terms as soilmix material.

Bentonite or other clay minerals, other additives and (chemical) admixtures can be added to control the properties in the fresh and hardened state. The type and quantity of the remaining soil, as well as its natural water content, have a significant influence on the mechanical properties of the hardened filling material.

Soilmix material as a filling material for cut-off walls can be classified between self-hardening suspension and Plastic Concrete in terms of its technical properties. If the mixed-in natural soil is e.g. gravel sand, properties close to Plastic Concrete can be achieved. The finer the granularity of the mixed soil, the closer the achievable properties are to those of self-hardening suspensions.

4 SUSTAINABILITY

The sustainability of buildings and the building products used is increasingly in focus, at least since the global community adopted the 2030 Agenda in 2015. The 17 Sustainable Development Goals (SDGs) are political objectives of the United Nations that are intended to ensure sustainable development on an economic, social and ecological level worldwide [Sustainability policy of the Federal Republic of Germany; <https://www.bundesregierung.de/breg-en/issues/sustainability>]. By definition, sustainability is not limited to climate protection or the protection of natural resources.

However, with regard to this DWA guideline and the construction of cut-off walls made of highly deformable filling materials, the focus should be on reducing the environmental impact as much as is technically possible by selecting the raw materials and the mix composition in order to guarantee the function of the cut-off wall. The concept for the design of highly deformable cut-off walls proposed in section 2.3 leads in particular to a reduction of the cement content compared to the “classical design” and thus in total to a reduction of the emission of climate-damaging gases for the fulfilment of the set construction task.

By using the soil as a building material in the “soilmix material”, in addition to reducing the cement content, the potential for reducing transport is also exploited, including for the removal of excavated material and the delivery of cement. A particular challenge is posed by the greater scatter to be expected in the properties of soilmix material compared to factory-produced cut-off wall construction materials such as Plastic Concrete. In order not to get into the conflict of objectives of a low required strength for a high deformability, the quality assurance must be approximated project-specifically.

The relevant equivalent carbon footprint created for the planning, construction and maintenance of a cut-off wall can be calculated. In order to make the reduction of the environmental impact through the use and utilisation of a highly ductile filling material visible in figures, comparative calculations can be limited to the construction phase. And if no other significant changes in the composition of the filling material or in the construction process are to be expected, it is sufficient to know by what proportion the cement is reduced in order to assess the effect.

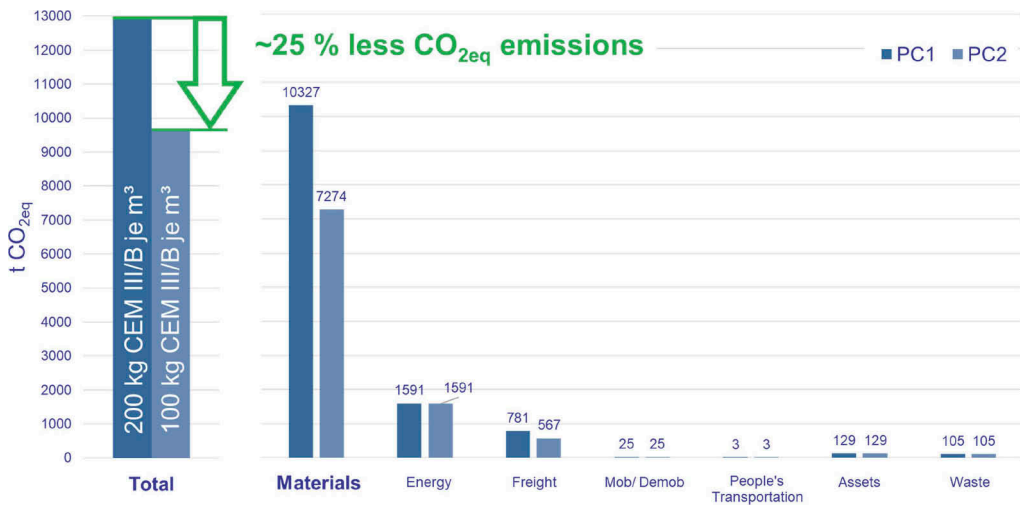


Figure 4. Result of a comparative calculation of the equivalent CO_{2eq} emissions for a deep cut-off wall (calculation with the EFFC Carbon Calculator by Bauer).

Figure 4 shows an example of the result of a comparative calculation for the production of a two-phase cut-off wall 1 km long, 100 cm thick and 100 m deep. Only the mix composition of the cut-off wall concretes (Plastic Concrete PC 1 and PC 2) was varied to achieve a different strength. If the cement content can be reduced from 200 to 100 kg/m³, i.e. by 50 %, a total reduction in the emission of CO_{2eq} of around 25 % is achieved. The target strength is also reduced, assumingly from approx. 3 MPa to approx. 1 MPa.

REFERENCES

- Guideline DWA-M 512-1E - Sealing Systems in Hydraulic Engineering, Part 1: Earthwork Structures - February 2012; check 2016 approved by experts.
- DIN 18136:2003-11 (en): Soil, investigation, and testing - Unconfined compression test.
- DIN 4093:2015-11 (en): Design of strengthened soil – Set up by means of jet grouting, deep mixing or grouting.
- DIN 1054: 2021-04:Subsoil - Verification of the safety of earthworks and foundations - Supplementary rules to DIN EN 1997-1: Geotechnical design - Part 1: General rules; German version EN 1997-1:2004 + AC:2009 + A1: 2013.
- David Alós Shepherd, Engin Kotan, Frank Dehn, Plastic concrete for cut-off walls: A re-view, Construction and Building Materials, Volume 255, 2020, 119248, ISSN 0950-0618, <https://doi.org/10.1016/j.conbuildmat.2020.119248>.
- Tynior, R., Meier, T. and von Wolffersdorff, P.-A. (2020), Neuartiger Nachweis für die Gebrauchstauglichkeit von Asphaltinnendichtungen in Staudämmen. *geotechnik*, 43: 224–236, <https://doi.org/10.1002/gete.202000012>.

Digitalization for a targeted and efficient dam management

F. Besseghini, C. Gianora, M. Katterbach & R. Stucchi

Lombardi Engineering Ltd., Giubiasco, Ticino, Switzerland

ABSTRACT: Dams are not only extraordinary engineering structures; they play a crucial role in the management of our most important vital resource, namely water. Currently, the expression “energy crisis” is familiar even to non-professionals. This is an important issue that plant operators are confronted with. A shutdown of the plant or lowering of the reservoir for extraordinary maintenance or to mitigate water scarcity, leads to major economic losses, both for dam owners, and homeowners, who are facing rising electricity costs. Is there a better way to adequately manage dams and appurtenant structures? The key lies in digitalization. Digitalization becomes more and more important to operate and maintain the facilities efficiently and adequately. The implementation of digital models allows the plant owner to undertake appropriate and faster business decisions and, therefore, to proactively manage the risks associated with aging dams’ infrastructure without affecting their operation. Digital models allow to overcome a common problem in dam monitoring: the dispersion of a large part of data volumes in multiple archives. In this way, all monitoring data can be kept in a single platform and effectively and efficiently visualized. These models also make real-time monitoring possible, thanks to the implementation of remote sensors for monitoring. New technologies, along with deterministic predictive models, enrich the digital twin and create a more complete picture over time without impeding the plant operation. It enables proper life cycle management of the structure, resulting in an exponential rise in the model’s efficacy over time.

1 INTRODUCTION

Dams offer an array of economic, social and environmental benefits and are useful for most problems pertaining to water conservation and its crisis management.

Following ICOLD’s World Register, dams existing worldwide can be classified according to their main purpose or typology as illustrated in the following graphs (Figure 1 & 2).

The constructive complexity of this important and fascinating infrastructure and its interaction with the surrounding ecosystem, implies an important owner’s commitment in their management. As a result, there is a specific need to describe and control their behavior. For this purpose, an enormous amount of data is constantly collected, sorted, and analyzed to provide meaningful future predictions. Digitization is undoubtedly a step in the right direction towards managing data properly and rationally, which, when combined with judicious interpretation by specialized engineers, enables substantial enhancements in O&M and it allows to control and manage the structure in respect of the ecosystem.

2 DIGITALIZATION

The economy and society are undergoing a transformation, taking advantage of digitization. For companies, implementing the digital into their business models is an added value since the adoption of new technologies simplifies processes and increases productivity. Customers are

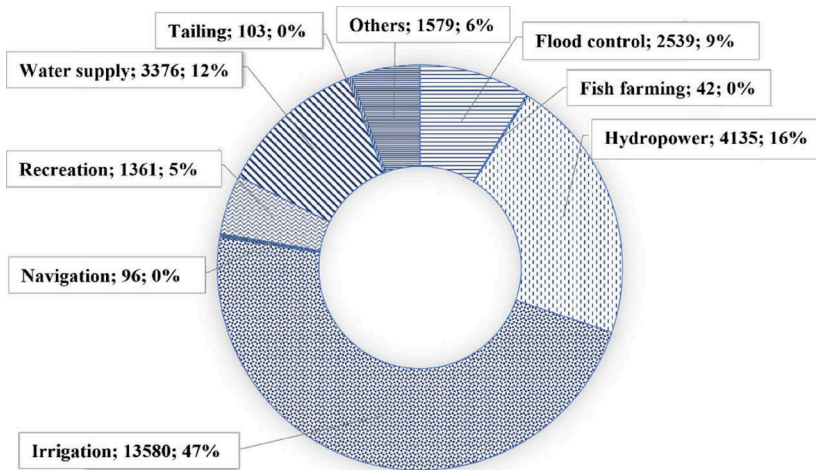


Figure 1. Single purpose dams distribution.

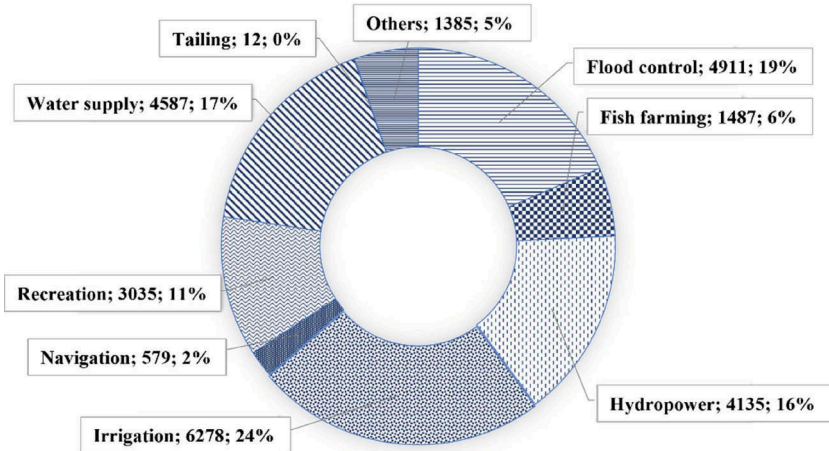


Figure 2. Multipurpose dams distribution.

more demanding and want companies to provide services and products in a short time. Customer-centric enterprises are transforming by adopting digital processes and taking advantage of new technologies, for instance IoT.

Hereby, it is essential that companies keep the focus on transformation rather than the technology itself, designing and implementing a digital strategy that promotes the adoption of lean methodologies and streamlines internal processes (Westerman, 2017). Undoubtedly, technology can help companies to innovate if implemented properly, but the innovation itself is only achievable with clear strategy and vision (Westerman, 2012).

Even the construction sector, characterized by very traditional procedures that have proven themselves over a long period of time, is not exempt from a digital transformation. Consequently, also the complex hydropower system and dams are affected by this transformation phase. One of the main benefits of dam digitization is an optimized decision-making process, in routine maintenance, life cycle management and even when an extraordinary event occurs, such as, a heavy rainfall. By gathering and accurately analyzing data from trustworthy sources, dam operators can identify trends and models, enabling them to make better, more

informed decisions related, for instance, to the level of water to be released on time, how to optimize power generation, and how to promptly respond to changing weather conditions. Hence, thanks to an on-spot intervention, the result is a better and lower-risk outcome.

Digitization and artificial intelligence allow to build smart algorithms to analyze the region's weather conditions by comparing temporal data. For instance, in the case of exceptional events, such as heavy rainfall, AI is able to advise the dam operator what decision-making process to be taken to manage the bottom outlet before any deformations/infiltrations exceed a specific critical threshold value.

An additional benefit of digitizing dams is the improved operational efficiency. By collecting and analyzing data, dam operators can identify areas of inefficiency and potential areas for improvement, optimize the maintenance practices as well as the power generation or reduce evaporative water losses. This leads to an improved operational effectiveness to relevant cost savings and to enhanced public safety.

The data retrieved from smart, real-time-transmitting technologies installed on the dam, such as crack gauges and pendulums, but also in the nearby location, like inclinometers in the ground or GNSS sensors capable of detecting millimetric displacements, adamantly help dam operators to identify potential risks and take appropriate corrective actions to address possible emergency situations. These scenarios may include unexpected water spill or breach of a part of the dam that can produce irreparable and serious damages to the villages located downstream of it. The result is, therefore, a substantial prevention of potential floods and of safety hazards or developing plans to respond to emergency situations.

The implementation of digital models also eliminates a common issue in dam monitoring: the scattering of data across multiple archives. In digital modeling, all monitoring data can be stored and visualized in one platform and better interpreted. Digital models enable real-time monitoring of all sensors placed inside the dam or on the reservoir shores. In other words, IoT enables efficient data exchange, data management and storage. New technologies, combined with predictive models enrich the digital twin since they provide a more detailed and clearer picture over time. This enables a significant optimization of the facility's operations and maintenance and ensures a proper lifecycle management of the facility.

3 DIGITALIZATION FOR DAM MONITORING

Predictive maintenance and behavior monitoring of dams are two major areas where digitization is especially advantageous, as previously highlighted.

Although an appropriate design ensures a sufficient level of safety, it does not eliminate it and, thus, monitoring a dam becomes critical in order to manage the residual risk. The primary role of dam monitoring is to immediately detect any anomalies in the dam's behavior to ensure that in the event that they pose a risk to dam safety, suitable corrective action can be performed. However, an adequate monitoring plan can also avoid the opposite risk of overestimating a deviation from the expected behavior of the dam and undertaking unnecessary measures.

New cutting-edge methods for managing, analyzing, and interpreting monitoring data better support and facilitate the coordination between all the stakeholders engaged in the various stages of a dam's monitoring process. In this regard, an emblematic example is MIC (*Modello Interpretativo Combinato*, Combined Interpretative Model, Stucchi et al. 2022). MIC is a software-as-a-service (SaaS) platform designed specifically for dam monitoring, combining the ease of use of a spreadsheet with the security and management capabilities of a large database.

Dam monitoring relies on data collected in a variety of ways around the world, including visual observations, manual instrument readings, automatic readings from the latest Internet-connected sensors. However, since the monitoring process is not based only on a mere collection of data, the information gathered needs to be processed and interpreted after a preliminary set of plausibility checks. MIC helps the user with a specific procedure developed to accurately identify erroneous data and to compare the information retrieved with historical data (i.e. uplift pressure) or with a typical seasonal pattern (i.e. temperatures).

Furthermore, the most common method to evaluate whether the dam's behavior meets expectations, is to compare it with a set of references to assess whether or not its behavior meets expectations. These references or models can be either statistical or deterministic in nature.

Statistical models are mathematical relationships calibrated on the past behavior of the dam and they only highlight if it behaves similarly to the past. In the case of an exceptional event that has never occurred, the dam's reliability becomes questionable.

On the other hand, deterministic models compare the monitored behavior of the dam to an expected behavior based on a structural model that can reproduce the dam's response to loading. They can also provide a reliable estimate for unusual events (e.g., extremely low water level due to sediment removal or unusual temperature for a particular season) since they represent a specific loading condition for the structural model. For instance, displacements at arch dams are primarily caused by two factors—hydrostatic water pressure and concrete temperatures—values that can be inferred from monitoring data.

Currently, the comparison between the measured and expected behavior is performed only for selected measures, which could be, for instance, the displacement of a dam. Therefore, in case of unexpected behavior, more detailed analyses should be performed by using specific numerical models. However, in the future, digital twins should be used to provide a more in-depth understanding of a dam's behavior, which would bring several advantages.

First of all, by linking the dam's digital twin to an automated numerical model (Figure 3), it could be possible to quantify the dam's response to changes in external conditions, improving the effectiveness of assessing the dam's safety status.



Figure 3. An automated numerical model for the assessment of the dam safety in real time.

Secondly, the numerical model could also take into account the nonlinearities in the dam's response that are usually neglected by deterministic models. This would provide a more accurate estimate of the expected dam's reaction, especially if it is considered that the response of arch dams to a change in reservoir level can be affected by the temperature of the dam body and that low temperatures may cause the vertical contraction joints to open and, thus, a less rigid dam's response.

In addition, by connecting the digital twin to a numerical model, difficulties associated with getting local stress measurements in concrete dams might be overcome. The numerical model allows for the estimation of stresses at any point in the dam under actual operating circumstances, highlighting potential places for compressive overload or the most likely sites for tensile cracking.

Regarding earth dams, the numerical model linked to the digital twin could calculate the seepage flow velocities and pore pressure distribution in real time in accordance with the operating conditions. As a result, pore pressures and the measurements recorded can be compared, and seepage velocities can be used to assess the likelihood of internal erosion and piping. The examples clearly highlight how dam digitalization is crucial since it allows for an optimized decision-making process for life cycle management and managing extraordinary events. Furthermore, it enables to gather and to process data in an easier manner, significantly improving the operational efficiency of a dam.

However, it should be noted that the exclusive use of automated numerical models may have negative risks that should be carefully evaluated. Despite being a helpful and important tool for assessing the safety condition of a dam, it might have inherent limitations related to the assumptions made in their creation that may affect the reliability of the input parameters. Therefore, it is suggested to leave the final evaluation to an experienced engineer who can properly weigh the model results with other observations and especially with his own experience.

4 GEOMATICS AND ITS ROLE FOR DIGITALIZATION IN THE HPP SECTOR

Geomatics is a multidisciplinary area playing a key role in the digital age. It is a combination of geographic information science, surveying, remote sensing, photogrammetry, cartography, geographic information systems (GIS) and global navigation satellite systems (GNSS). This discipline has become important in a digital world since it provides the technology and methods to collect, model, analyze, visualize, store, and manage physical objects in a digital context.

Geomatics is essential in the management of dams and other water infrastructure projects because it allows to assist the planning, construction, and operation of dams, as well as to monitor dams' performance.

In the planning phase, two useful tools for saving resources and time are: GIS and Satellite data. GIS allows to manage in a single platform various data related to the territory, geology, and meteorology and provides targeted information to evaluate the optimum construction site or to run simulations of reservoir breaching. Satellite data remotely provides a detailed historical and updated view of the geological movement, forest advancement, or water resources. The historical analysis combined with advanced algorithms offers valuable answers in the millimeter range over a short time.

During the construction phase, geomatics can be used to survey, track, and monitor site measurements. The typical instrumentation is the total station, which is used for its millimeter accuracy, while additional tools such as UAV drones allow to keep track of material storage areas. Advanced tools enable comparison of different photogrammetric flights and can establish the residual volume of raw materials on site. GIS can simulate transports to and from the construction site, enabling a resource optimization.

Real-time monitoring equipment can be installed on both the dam and the reservoir slopes during the reservoir filling and when the dam is in operation. Sensors like piezometers, strain gauges, and inclinometers are placed on a dam's key installation points to accurately take specific measurements throughout the year. In fact, to make a full evaluation of potential structural problems of a dam, the data must be compared with the sporadic measurements provided by the geodetic surveys. However, the knowledge gap occurs for those areas where no sensors are installed, i.e. slopes or embankments that are long several kilometers.

Dam operators are also looking for remote monitoring tools as drones, which are especially useful in routine maintenance and inspections and for UAVs to conduct large-scale assessments. Although drones reduce health and safety risks for the staff involved in visual inspection of hard-to-reach areas, their accuracy ranges between 20 and 50 millimeters, which is considerably below the granularity that can be obtained with the new technologies available. These advanced monitoring systems can detect ground movements and seepage and send real-time alerts where there is a potential risk.

As previously mentioned, also hydropower projects now benefit greatly from the use of geomatics, which ensures the most efficient and cost-effective design, construction, and

operations. For instance, bathymetric surveys with multibeam echosounders (MBESs) enable the detection of anomalies at the bottom outflow or discover sediment deposits in shallow water and for depths above 100 meters. Moreover, by comparing scans taken over time to determine the actual volume inside the reservoir, the administrator can choose whether to perform a cleanup. Taking into consideration the numerous advantages brought by geomatics, it is clear how it is becoming an even more essential component of the digital world as new technologies and methods continue to evolve.

5 IMPACT ON DECISION MAKING AND O&M

The right implementation of digitalization and dam monitoring through the finest geomatics equipment will have a substantial impact on the ability to make informed decisions.

The process of digital transformation entails making several critical decisions based on available data and information to refine current procedures, validate new approaches, and assess technologies. Therefore, to unlock the full potential of digital transformation, it is always important to have an open-minded approach and to have the curiosity to seek more pertinent data. Undoubtedly, digitalization has significantly enhanced and facilitated dams' operation and maintenance (O&M), enabling to address any issue remotely, providing a significant optimization of the procedures and generating relevant cost savings. Innovative solutions have improved data collecting, analysis, and asset monitoring. They can now foresee and quickly diagnose errors, resolve issues, and optimize an asset's operation.

Five main functions define the digitalization of maintenance services: monitoring, diagnosis, prediction, troubleshooting and optimization with real time data (Figure 4) (Chen et al., 2018).

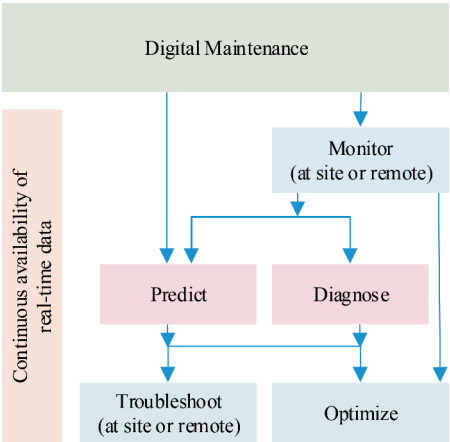


Figure 4. Basic building blocks of modern digital maintenance (Chen et al., 2018).

The evolution of maintenance from reactive to proactive has changed the equipment or asset technologies (Jantunen et al., 2010) by introducing advanced technologies such as machine learning, artificial intelligence, analytics, big data and cloud computing which empower the traditional O&M services, transform them into smart, effective and efficient operations and minimize waste and energy consumptions, save time, and eventually help in promoting a positive environmental impact (Karki et al., 2021).

By predicting, addressing, and remotely preventing errors, the digital approach to O&M significantly lowers accidents. This fosters a culture of safety, encourages responsible behavior, and ensures a secure and healthy workplace.

Table 1 enlists various benefits of the O&M digitalization and is categorized according to different sustainability impacts.

Table 1. Benefits of digitalization on a dam's O&M services.

Topic	Benefits of digitalization
Economic	Use of advanced tools and real-time data helps in detecting and preventing failures in advance; this saves time and money. Digitalization applied to dam monitoring and O&M facilitates remote maintenance functions which imply less service engineers on site, lower maintenance and travel costs and more time-savings.
Environmental	Up-to-date equipment process and data helps in monitoring, accurately diagnosing and troubleshooting, predicting, and optimizing. The reduction in downtimes and well-maintained equipment means high availability and performance capability. By using a correct type of tools and technologies that offer real-time predictions and diagnosis, it is possible to minimize waste and reduce energy consumptions as well as the carbon footprint. (Karki et al., 2021).
Governance	Digitalization makes the maintenance service reliable, safe, effective and keeps the dam and associated facilities operating to its maximum potential. This helps organization in decision making and strategic planning (Chen et al., 2021, Jain et al. 2014).
Social	Digital maintenance contributes to reducing accidents and to empowering safe behavior and assuring a safer and healthier work environment (Karki et al., 2021).
Technological	The use of vast historical and live data enhances the maintenance functionalities such as monitoring, diagnosing, troubleshooting, predicting and optimization. This is a positive technological outcome since it promotes secure and reliable transmission of data as well as effective and on spot maintenance services.

Considering the above-mentioned advantages, it is clear how the implementation of digital transformation is the right path towards a sustainable, efficient, and effective maintenance, regardless of the challenges or difficulties that must be overcome.

6 CONCLUSIONS

The economy and society are undergoing a transformation, taking advantage of the digital trend. In this framework, the article describes the role of digitalization as a key factor to properly manage dams and appurtenant structures and highlight how companies should also keep the focus on the cultural shift associated to such transformation. Moreover, a proper digital strategy must be identified to have a digital organization with lean methodologies and processes.

A detailed geometrical description of dams and appurtenant structures can be achieved with geomatics, which is multidisciplinary area that combines geographic information science, surveying, remote sensing, photogrammetry, cartography, geographic information systems (GIS) and global navigation satellite systems (GNSS). This discipline has become significantly important in a digital world, as it provides the technology and methods to collect, model, analyze, visualize, store, and manage physical objects in a digital context. Geomatics has become a valuable tool also for hydropower projects, helping to ensure the most efficient and cost-effective design, construction, and operation feasible. The added value of geomatics is increasing proportionally to new technology and methodologies.

The implementation of digital models and real-time monitoring allows to undertake more adequate and faster business decisions to proactively manage the risks associated with aging dam infrastructure without affecting their operation and to keep track of all the data in multiple archives without dispersing key information.

An additional benefit is that dam monitoring immediately detects any anomaly in a dam's behavior, however an adequate monitoring plan is suggested to avoid the opposite risk of over-estimating a deviation from the expected behavior of the dam, with the consequence of taking unnecessary measures. However, there are also new and innovative methods for managing, analyzing, and interpreting monitoring data to support all stakeholders involved in the various phases of a dam's monitoring process, such as MIC (Modello Interpretativo Combinato, Combined Interpretative Model, Stucchi et al. 2022). MIC helps the user through a specifically developed procedure to identify erroneous data, which are excluded from the subsequent analysis

and interpretation phases. The most common method for evaluating the regularity of a dam's behavior is to compare it to a set of references to assess if its behavior meets expectations. These references or models can be either statistical or deterministic in nature (Stucchi et al. 2022). An emphasis is placed on the deterministic models, which compare the observed behavior to an expected behavior of the dam in response to loading. Nevertheless, all these improvements may also carry some hazards related to the use of automated numerical models, including the possibility that the assessment of a dam's safety depends entirely on such models. Consequently, the final evaluation should be left to an experienced qualified engineer.

Finally, to make a full and accurate assessment and undertake the most appropriate decisions, the most performant geomatics technologies should be integrated in dam monitoring systems. This is important since organized, controlled and detailed information of a specific dam leads to highly skilled workforce within the microeconomic and macroeconomic environment. Thanks to new digital solutions, data collection and analysis has significantly improved; as well as all the functions to monitor assets, predict and diagnose any defaults, troubleshoot failures, and optimize the asset or its operating performances.

The shift in maintenance from reactive to proactive has compelled equipment or asset manufacturers to adopt cutting-edge technologies like machine learning, artificial intelligence, analytics, big data, and cloud computing. These technologies empower conventional O&M services and transform them into smart, effective, and efficient services by improving service delivery efficiency. New technologies and deterministic predictive models provide a more accurate picture of dams without interfering with plant operations, which allows to manage the structure's life cycle more effectively.

Digitization is undoubtedly a step toward an optimal administration and application of data. Specifically, it considerably helps to optimize the O&M operations, offers a better control over the structure, and enables the implementation of suitable measures to prevent detrimental impacts on the entire ecosystem.

REFERENCES

- Stucchi, R., Crapp, R., Fern, I. 2022. Development of a software as a service platform for dam monitoring. *HYDRO 2022*, Strasbourg, France.
- Karki, B. R., Porras, J. 2021. Digitalization for sustainable maintenance services: A systematic literature review, *Digital Business* 1 (2021).
- Coombs, M., Braithwaite C. 2021. Satellite technology enhances dam safety monitoring. *The international journal on hydropower & dams*, 2021, vol 28, issue 5. Wellington.
- The World Bank 2020. *Operation & Maintenance strategies for hydropower - Handbook for Practitioners and Decision Makers*.
- Johansson, N., Roth, E., Reim, W. 2019. Smart and sustainable emaintenance: capabilities for digitalization of maintenance. *Sustainability* (Switzerland), 11(13).
- Chen, J., Zhang, R., Wu, D. 2018. Equipment maintenance business model innovation for sustainable competitive advantage in the digitalization context: connotation, types, and measuring. *Sustainability* (Switzerland), 10(11).
- Goyal, D., et al. 2017. Optimization of condition-based maintenance using soft computing. *Neural Computing and Applications*, 28(s1), 829–844.
- Westerman, G. 2017. Your company doesn't need a digital strategy. *MIT Sloan Management Review*, spring 2018 vol 59, issue 3. Boston: Massachusetts Institute of Technology.
- Fontana, A., et al. 2016. An advisory tool for sustainability-driven maintenance. A real case in mould and die industry. *Proceedings of 2015 international conference on industrial engineering and systems management, IEEE IESM 2015* (pp. 1268–1276). Institute of Electrical and Electronics Engineers Inc.
- Susto, G. A., et al. 2015. Machine learning for predictive maintenance: A multiple classifier approach. *Industrial Informatics, IEEE Transactions on*, 11, 812–820.
- Jain, A., et al. 2014. Total productive maintenance (TPM) implementation practice: A literature review and directions. *International Journal of Lean Six Sigma*.
- Westerman, G., Bonnet, D., McAfee, A. 2012. *The advantages of digital maturity*. MIT Sloan Management Review, November 20, 2012. Boston: Massachusetts Institute of Technology.
- Jantunen, E., et al. 2010. Economical and technological prospects for e-Maintenance. *International Journal of Systems Assurance Engineering and Management*, 1(3), 201–209.

Digital cloud-based platform to predict rock scour at high-head dams

E.F.R. Bollaert

AquaVision Engineering Llc, Ecublens, Switzerland

ABSTRACT: This paper presents novel methods for prediction of scour of unprotected rock in plunge pools downstream of high-head dams. These methods allow a quasi-3D prediction of the evolution of the plunge pool. The methods have been bundled into a cloud-based numerical platform, based on user-defined parametric settings of the spillway geometry, the turbulent flow and the rock mass. A case study simulates the scour hole that was observed downstream of Chucàs Dam in Costa Rica, following the 2017 tropical storm flood with a return period of 100 years.

RÉSUMÉ: Le présent article détaillé de nouvelles méthodes pour estimer l'affouillement de massifs rocheux en aval des grands barrages. Ces méthodes définissent la fosse en 3D et ont été regroupées sur une plateforme digitale, basé sur un paramétrage spécifique utilisateur de la géométrie, de l'écoulement turbulent et du massif rocheux. Un cas d'étude simule la fosse constatée en aval du barrage de Chucàs au Costa Rica, suite au passage de la tempête tropicale en 2017 avec un temps de retour de 100 ans.

1 INTRODUCTION

Rock scour downstream of high-head dams and in unlined channels and stilling basins is more and more frequent. Climate change and related regulatory requirements generate more frequent functioning of dam spillways. Hence, unlined rock masses experience more action of hydrodynamic pressures. Sound prediction of rock scour potential becomes increasingly pertinent, especially for cases where the scour may potentially regress towards the dam.

This paper presents a novel digital software platform that has been developed with the aim to bundle and offer to its users the current state-of-the-art in the field of numerical predictions of scour of rock downstream of dams and in unlined channels and stilling basins. Users will be able to apply and compare a wide range of proven as well as new methods within one single numerical environment, based on user-defined tailored parametric settings of the dam, the turbulent flow and the rock mass.

Moreover, a novel digital database platform has been developed complementary to the software platform, allowing to freely consult any type of worldwide rock scour case studies that have been performed and published, either real-life or laboratory generated. As such, this platform aims at offering a practical and continuously updated database with the potential of informing specialists and engineers on the most relevant results, parameters and calibrations that have been used for each of the available scour computational methods.

The platform focuses on enhancing parametric pertinence and experience. It aims widespread distribution and exchange, so that shared benefits may be expected.

It is believed that this is the first attempt in this field to combine on one single digital platform both powerful and cutting-edge computational potential and directly related up-to-date database availability of published practical experiences and results.

2 THE ROCSC@R CLOUD

2.1 General

The rocscor® cloud contains two digital platforms: X_pl@re is a licensed computational platform, while X_ch@nge is a free database platform (Bollaert, 2021). Both platforms solely offer web-based remote access and storage. Cloud users benefit from personalized data encryption. Data results can be stored on user-specific allocated space in the cloud, or on the user's local IT infrastructure.

X_pl@re comprises the rocscor® software, i.e. a suite of the latest computational methods for numerical prediction of rock scour downstream of dam spillways and in unlined channels and stilling basins. The range of methods covers both oblique and vertical impingement of turbulent jets, and is compatible with any other turbulent flow at the water-rock interface, such as free surface flows and hydraulic jumps. X_ch@nge offers a free-access database platform for any type of publicly available rock scour cases at hydraulic structures. For each case, specific geometric, flow and rock mass parameters are provided, in parallel to the observed or computed scour for the related flow event.

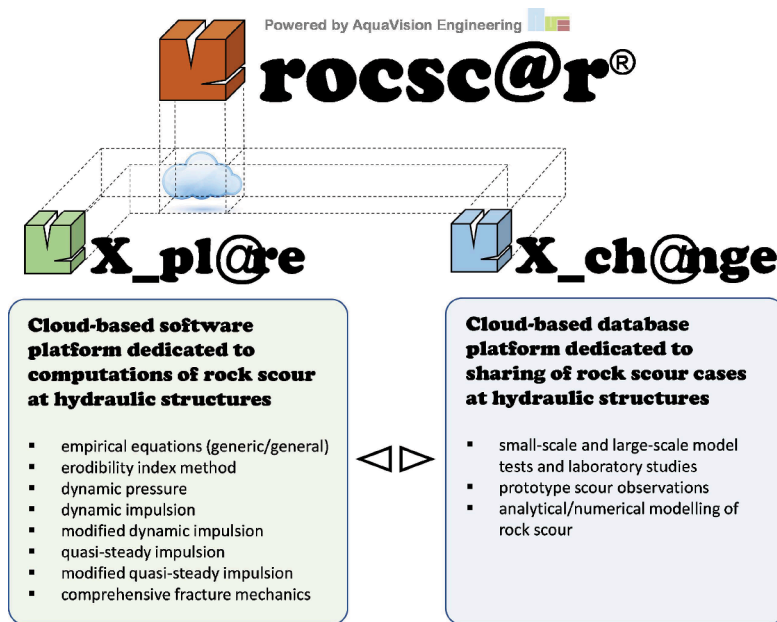


Figure 1. The rocscor® cloud and its main digital platforms implementing scour software (X_pl@re) and worldwide database of scour cases (X_ch@nge) (Bollaert, 2021).

2.2 Physics implemented

From the topological point of view, the software is subdivided in three main parts: GEOMETRY, FLOW and ROCK MASS. First, the user has to implement the geometry of the dam spillway and the downstream plunge pool or stilling basin. This is done by using a set of 2D vertical profiles in the X-Z plane, as shown in Figure 2, which shows examples of 2D vertical profiles that have been determined in a 3D geometrical situation of an arch dam and its downstream plunge pool. The profiles can be oriented freely, for example following the river axis (profile 1), or following the dam and spillway concentric curvature and geometry (profile 2). The dam and the spillway are introduced in a simplified manner, i.e. by determining the coordinates of the invert at jet issuance. The downstream rock bottom is introduced by user-defined X-Z coordinates. The scour computations are performed along each of these profiles separately.

By assembling these 2D results, a quasi-3D result may be obtained. A fully 3D version of the software is scheduled for 2023.

Next, the software allows to implement the 2D turbulent flow in two ways. First of all by making use of 2D flow matrices that use analytical expressions to determine the main hydraulic parameters with depth of scour for turbulent jets (i.e. mean and fluctuating dynamic pressures, impulsion coefficients, average flow velocities along the interface, stream power). Second, a generic interface is available, allowing the user to determine the hydrodynamic parameters at the water-rock interface, with a customizable vertical decay with increasing scour depth. Furthermore, this generic interface can be directly coupled to the Flow-3D® CFD software by means of the RemoteSc@r™ application, in which the former continuously updates the hydraulic parameters based on scour progression computed by rocsc@r.

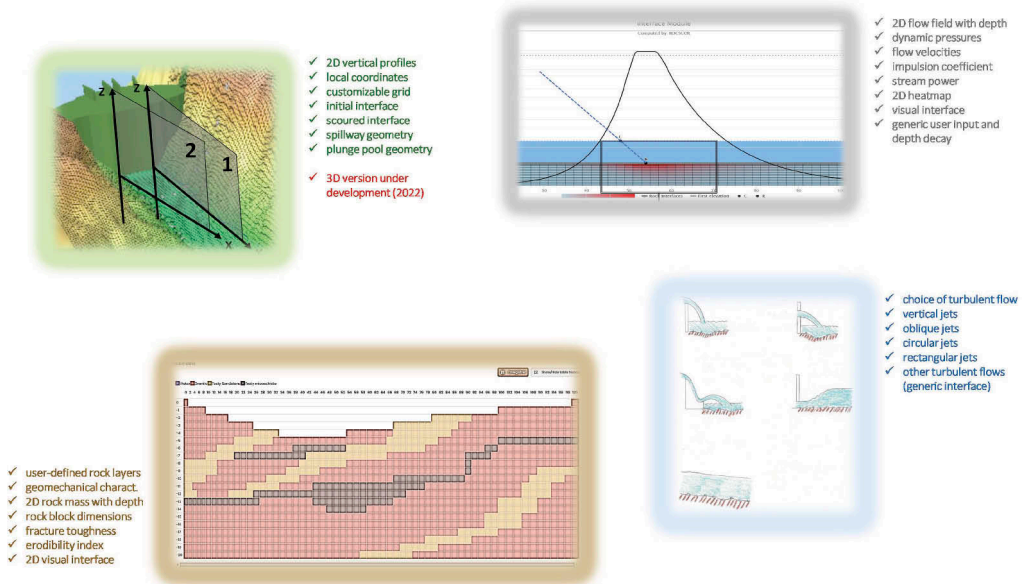


Figure 2. 2D vertical profiles and visual interfaces used in the rocsc@r digital environment.

As shown in Figure 5, the visual interface of rocsc@r allows to present and check the hydraulic parameters by use of 2D heatmaps and curves. Another topologic choice is the type of turbulent flow, from vertical and oblique jets to differently shaped jets and finally any type of turbulent flow, by using the generic interface.

Furthermore, a 2D rock mass interface has been set up allowing the user to determine the different rock mass layers and lithologies at the site in question, and to set up a rock mass model with depth in each 2D vertical profile (Figure 2). For each lithology, the necessary geo-mechanical characteristics can be defined, such as the UCS strength, the density, the initial degree of fracturing, the typical block shape, and so on.

Aeration issues are accounted for by using analytical equations for the hydrodynamic parameters that take into account flow aeration of jets and plunge pools. Second, by using the Flow-3D® coupling, automatic numerical coupling between air and water is obtained during the modelling for all types of turbulent flows.

The implemented flow physics account for the basic issues like flow trajectory and air drag, impact angle of jets, gravitational contraction and turbulent diffusion, formation of wall jets along the rock interface, velocity and pressure decay functions, both radially outwards and with increasing scour depth.

In terms of rock break-up mechanisms, fracture mechanics is accounted for, by both brittle and fatigue failure of rock joints, based on transient 2-phase pressures propagating through

these joints. Second, a force balance is implemented throughout the numerical grid, accounting for the main forces of influence, such as gravity, buoyancy, dynamic water pressures, shear forces in joints and drag and lift forces for inclined joints. This is directly coupled with rigid body dynamics, accounting for added mass, and block acceleration and deceleration phases during movement, allowing to define the net uplift height of the block while moving. Finally, fluid-solid interaction is implemented indirectly by accounting for block protrusion using quasi-steady and fluctuating drag and lift forces on protruding blocks, depending on their local geometrical situation that can be chosen by the user.

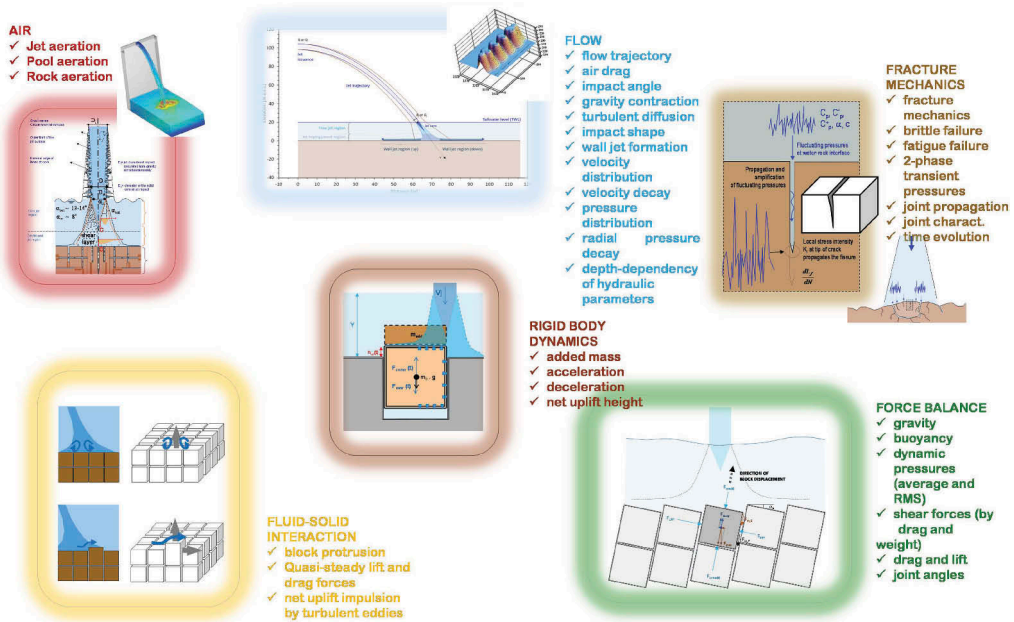


Figure 3. Main physics implemented in the rocsc@r digital environment.

2.3 Plunging turbulent flows

The hydraulic parameters of 2D plunging turbulent flows (Figure 4) are determined analytically along the initial water-rock interface and vertically down into the rock mass, and are stored as 2D matrices used by the software during the computations. The analytical equations make the assumption of a quasi-horizontal and quasi-flat interface between the rock and the water.

The equations allow storing the values of the main hydraulic parameters in 2D matrices. These matrices respect the network of computational nodes of the 2D vertical profiles, along which the scour computations are being performed (Figure 4). As such, in every computational node, the hydraulic parameters that are needed for the scour computations are being predefined before start. The corresponding values account for the progressively increasing flow depth during scour formation. The following hydraulic parameters are predefined with depth and stored in 2D matrices, based on analytical solutions of the flow environment:

The pressure coefficients have to be multiplied by $\rho V^2/2g$ to obtain the pressure values in $[N/m^2]$, and the impulsion coefficient by $\rho AV^2L/c$ to obtain impulsions in $[Ns]$, with V the jet velocity at impact in the pool, c the wave celerity, L the joint length and A the horizontal rock block area. Figure 5 illustrates an example of the average dynamic pressure coefficient C_p at the interface, due to a rectangular jet impacting the pool under an angle of 70° with the horizontal. The spatial distribution of the pressure at the rock is represented by the black curve

(right-hand side axis), while the evolution with depth is represented by a graded heatmap (legend on the right). Similar curves are defined in the model for all hydraulic parameters listed at Table 1. This 2D matrix system covers both circular and rectangular-shaped jets, as well as vertically or obliquely impinging jets for angles between 20 and 90°. Moreover, both compact and broken-up jets are accounted for, as well as the air concentration and degree of break-up of the jets at impact, and the initial turbulence intensity at issuance from the dam.

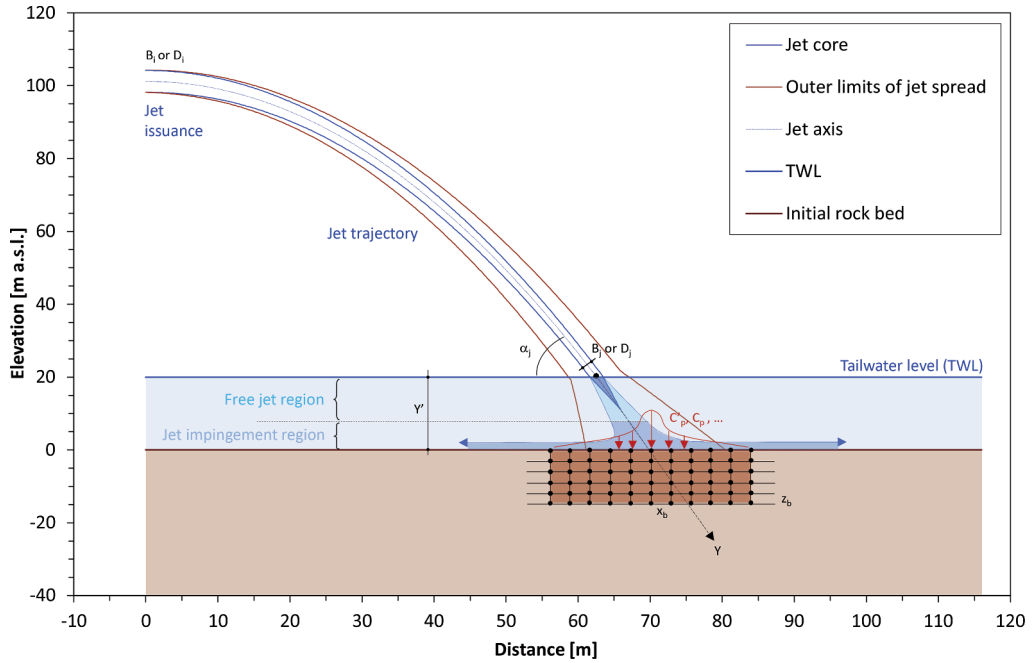


Figure 4. Sketch of obliquely plunging turbulent flow diffusing through plunge pool and impacting the water-rock interface (source: rocsc@r® Technical Manual, AquaVision Engineering 2022).

Table 1. List of hydraulic parameters pre-defined in 2D flow matrices.

Parameter	Description
C_p	Mean dynamic pressure coefficient
C'_p	Fluctuating (RMS) dynamic pressure coefficient
C_{max}	Maximum dynamic pressure coefficient
CI	Dynamic impulsion coefficient
VEL	Average flow velocity quasi-parallel to interface
SP	Average stream power at interface

2.4 Computational methods

The rocsc@r® software contains both novel and existing computational methods, expressing the different break-up mechanisms of fractured rock masses. Moreover, these methods have been implemented such that users may freely customize the related parameters and equations. The following methods are currently available:

- *Empirical equations*: A wide range of empirical formulae are available. These distinguish between a generic formula that can be user-defined, and more general and simplified formulas (Castillo and Carrillo, 2017). More information can be found in Bollaert (2021).

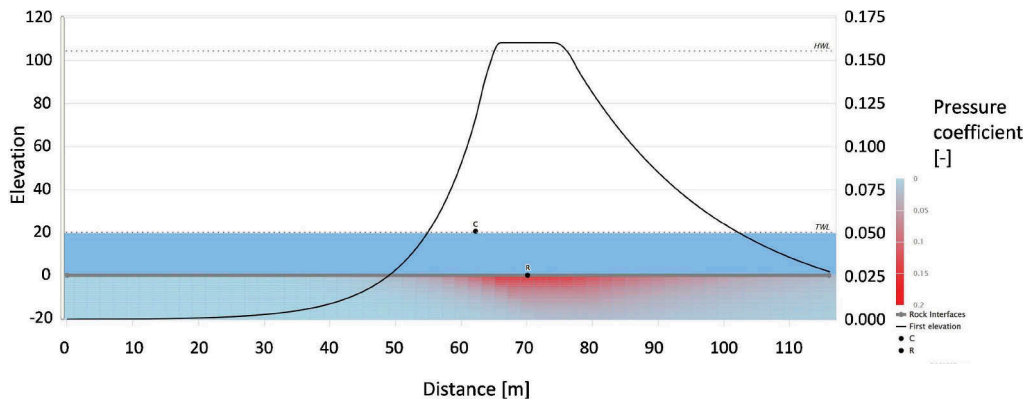


Figure 5. Example of 2D determination of average dynamic pressure at water-rock interface generated by an obliquely impacting jet (source: rocsc@r® Technical Manual, AquaVision Engineering 2022).

- *Erodibility Index method (EIM)*: The Erodibility Index Method is based on Kirsten’s ripability index and has been adapted by several researchers to scour in unlined plunge pool and stilling basins, based on a large dataset of case studies. This method relates the energy dissipation rate or stream power to the resistance of the rock as expressed by the erodibility index (EI), i.e. a geomechanical index incorporating the mass strength and different characteristics related to the size of the block, the joint roughness and alteration, and the structure of the discontinuities. information can be found in Bollaert (2021).
- *Dynamic Impulsion methods (DI/MDI)*: The DI method developed by Bollaert and Schleiss (2005) considers the maximum dynamic impulsion underneath a rock block, obtained by time integration of the pressure forces under and over the block, of the immersed weight and of shear forces on the block. The net uplift impulsion considers a time duration of forces and uses a net uplift coefficient Cup [-] determined based on large-scale laboratory experiments. Second, the MDI method developed by Bollaert (2021) uses similar physics of block uplift but computes the net uplift force as a function of the RMS values of the pressure fluctuations at the block upper surface and a multiplication coefficient based on large-scale 3D block uplift experiments. Both methods express block failure by comparing the vertical block displacement to the block height.
- *Dynamic Pressure method (DP)*: Bollaert (2021) developed a 2D implementation of the block uplift method developed by Maleki & Fiorotto (2019). This method determines the net uplift force on a block based on analytical determination of jet characteristics, as well as by accounting for the RMS coefficient of pressure fluctuations at the block upper face multiplied by a surface reduction coefficient. This approach defines the necessary thickness for a block to be stable, accounting for its submerged weight.
- *Quasi-Steady Impulsion methods (QSI/MQSI)*: The QSI method developed by Bollaert (2012) computes the scour potential by detachment or peeling off of protruding rock blocks, due to wall jet flows deviated by such blocks at the water-rock interface and generating quasi-steady lift forces on the blocks. The MQSI developed by Bollaert (2021) extends the previous method for both circular and rectangular jets and obliquely impinging jets, and allows to compute both quasi-steady and fluctuating detachment forces. The related lift forces are defined by an uplift coefficient Cup. The stability of the block is expressed by a force-balance equation.
- *Comprehensive Fracture Mechanics method (CFM)*: This method developed by Bollaert and Schleiss (2005) computes progressive fracturing of existing joints in rock masses as a function of time, based on linear elastic fracture mechanics theory and the cyclic character of dynamic pressures generated by turbulent flows. The method expresses scour evolution as a function of time.

3 CASE STUDY AT CHUCAS DAM

3.1 Site and project

The Chucás hydroelectric project, owned by Enel Costa Rica, was developed as a BOT project (Figure 6, Capuozzo & Jiménez, 2017). It is located about 40 km west of San José, the country's capital. The project, in operation since November 2016, dams the Tárcoles river with a - 63 m high dam. A surface penstock, about 400 m long and 6.5 m in diameter, leads to a powerhouse where two Francis units generate a total output of 50 MW.

For flood control, the dam is equipped with four radial gates, 15 m by 12.4 m, capable of discharging 5400 m³/s under design conditions (Capuozzo & Jimenez, 2017). This large discharge is conveyed through a ski-jump spillway chute discharging into the rock bed downstream of the dam. Scour formation in this unprotected rock mass was expected and a pre-excavation was planned but never executed. The corresponding plunge pool formation, in this particular case, may endanger the exposed penstock, because of the risk of lateral expansion of the scour hole, which might affect this structure. In addition, there is the risk that backwards erosion of the plunge pool may affect the dam foundations.



Figure 6. Jet trajectory and scour damage following 2017 flood (source: O. Jiménez).

3.2 Geology

Based on Capuozzo & Jiménez (2017), the in-situ rock mass consists of volcanic rocks such as andesitic lava, ignimbrite pyroclastic flows and occasionally thin layers of tuff and ash deposits. Good outcrops are observed on both banks of the river, however, the bedrock cannot be observed as a result of the constant flow of the river. The rock mass consists of aphanitic (fine grain) and aphanitic porphyritic (coarse grain) andesitic lava flow. The aphanitic mass is hard and highly fissured, and has good weathering resistance. The aphanitic porphyritic contains abundant calcite giving a brecciated textured appearance (called the 'coarse grain'), it is soft to moderately hard, moderately fissured andesite, susceptible to weathering. The rock mass has

been affected by a hydrothermal process, which has made it very susceptible to accelerated weathering when exposed to the environmental conditions of the area (rain and sun).

Borehole investigations indicate a variable RQD, however, at the left abutment the rock is more fissured. The RQD percentage at the left abutment ranges from 0 to 76 per cent with an overall average of 40 per cent, which classifies the rock mass as poor quality.

The joint spacing produces flat-shaped rock blocks of only 0.04 to 0.5 m sidelength. These results would indicate that a plunge pool formation is very likely to occur relatively rapidly. As the smaller range of values correspond to gravel and cobbles generated by ball-milling, only a block sidelength of 0.5 m has been used, together with a height-to-sidelength ratio of 1:2.

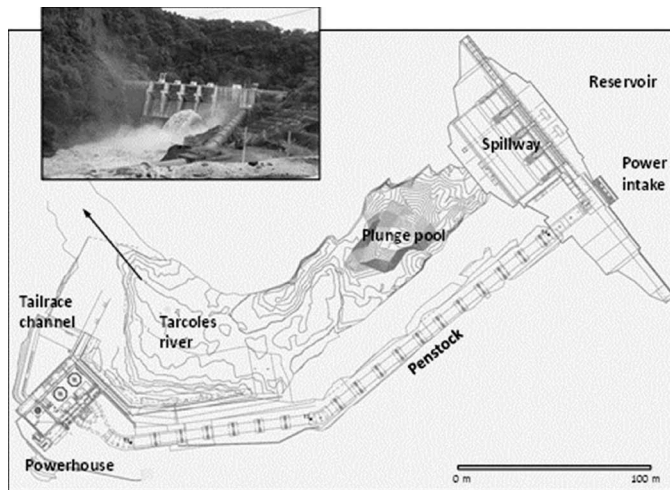


Figure 7. General layout of Chucàs HEP (source: O. Jiménez).

3.3 Tropical storm “Nate”

Based on Capuozzo & Jiménez (2017), the tropical storm Nate hit Costa Rica between 4 and 6 October 2017. The storm remained almost stationary for two days, close to the Caribbean coast of Costa Rica, displacing humidity from the Pacific Ocean toward the dam’s watershed. Rain fell for 48 hours, reaching precipitation levels of between 200 to 400 mm over the whole basin of the Chucás powerplant. As a result, peak flows of more than 3000 m³/s were discharged through the radial gates, starting in the early hours of 5 October and lasting for about 24 hours. According to the records, this flood has a return period of more than 100 years.

Although the powerplant suffered relatively little damage, and was back in operation after two days, it was clear that important scour downstream of the dam had taken place because of the natural formation of the plunge pool. Bathymetric measurements showed that a plunge pool had been formed, with a maximum depth of 25 m, larger than the 20 m initially assumed based on hydraulic model tests. Fortunately, the observed damage and scour did not pose threats to the existing structures. It was estimated that about 15’000 m³ of material was removed and deposited downstream.

3.4 Numerical reproduction of scour formation

The scour formed during tropical storm Nate has been numerically reproduced. The maximum observed discharge of 3’000 m³/s has been used for the computations. These are based on dynamic block uplift and quasi-steady peeling off (DP, MDI and MQSI methods), on the erodibility index method (EIM), as well as on progressive fracturing of rock joints (CFM method).

Figure 8 illustrates the scour computed by these different methods. For the DP and EIM methods, the computed scour is somewhat underestimated, i.e. 4-8 m less for a total depth of 23 m. For the MDI and MQSI methods, the computed scour is in slightly better agreement with the bathymetric survey, i.e. only 2 m less for MDI and 0-1 m less for MQSI. The agreement not only concerns the deepest observed scour, but also the shape of the scour hole, especially towards upstream.

Figure 9 presents similar results by using the CFM method. This method allows to obtain scour as a function of time period of discharge. By considering the 24h time period of the flood event, for a constant discharge of 3'000 m³/s, it may be observed how the scour progresses with time and how the computed scour after 24h is in good agreement with the observed scour for this particular event, predicting slightly deeper scour of about 25 m.

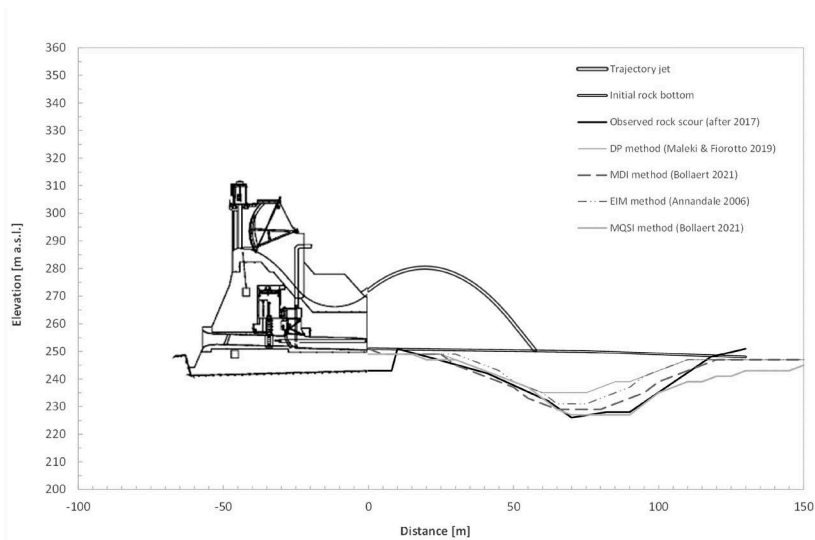


Figure 8. Numerical reproduction of scour during 2017 flood (MDI, MQSI, EIM and DP methods).

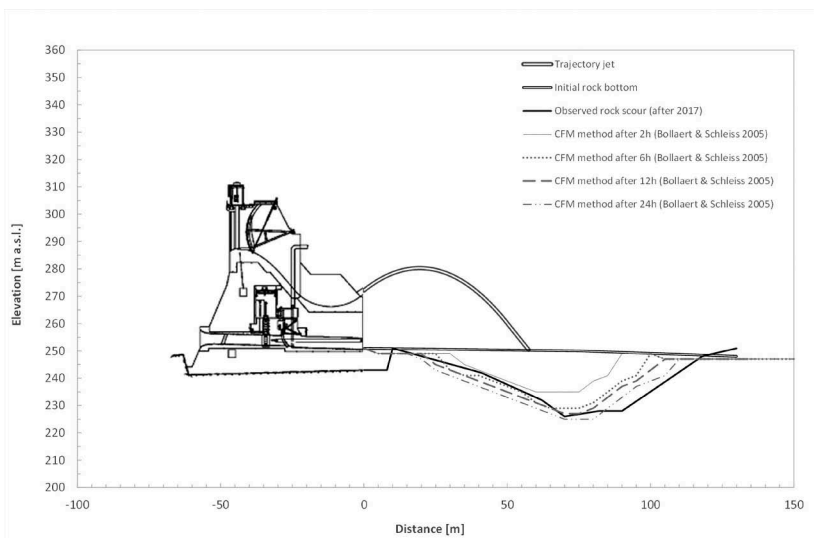


Figure 9. Numerical reproduction of scour during 2017 flood (CFM method).

4 CONCLUSIONS AND OUTLOOK

This paper presents a new cloud-based tool for sound and detailed assessment of rock scour incidents that may occur downstream of high-head dams following spillway functioning during flood events.

This next-gen software platform procures physics-based scour estimates using a series of 2D vertical profiles, allowing so a quasi-3D reconstitution of the scour hole. It is based on a 2D assessment of the geo-mechanical characteristics of the rock mass layers with depth, and proposes several novel computational methods, as well as some well-known and widely used existing methods for rock scour assessment.

These methods were applied and compared through a case study involving real-life ski-jump jets generating plunge pool scour observed in the unprotected rock mass downstream of Chucàs Dam in Costa Rica during the 2017 tropical storm flood event with a return period of about 100 years.

First-hand comparative results of the novel methods, together with the 20 years of practical experience and real-life calibrations gained by the author with the EIM, CFM, DI and QSI methods, provide a sound and promising basis for future applications of the different methods to real-life cases and projects.

In this sense, the presented rocsc@r® cloud offers future users the digital framework they need, combining cutting-edge computational power and versatility with off-the-shelf numerical methods.

ACKNOWLEDGEMENTS

Sincere thanks go to M. O. Jiménez from DLZ Carbon Ingenieria for his kind transmission of the photos and the hydraulic and geologic information needed to correctly perform the scour computations.

REFERENCES

- Annandale, G.W. (2006). Scour Technology: Mechanics and Engineering Practice, *McGraw-Hill*.
- Beltaos, S. (1976). "Oblique impingement of circular turbulent jets." *Journal of Hydraulic Research*. IAHR, Vol. 14, No 1.
- Bollaert, E.F.R. (2021). The rocsc@r™ cloud: An innovative digital platform to compute and record rock scour. *Intl. Journal on Hydropower and Dams*. Issue 5.
- Bollaert, E.F.R. and Schleiss, A.J. (2005). "A physically-based model for evaluation of rock scour due to high-velocity jet impact". *Journal of Hydraulic Engineering*. March 2005.
- Capuozzo, L. and Jimenez, O. (2017). Model and prototype studies for the Chucàs hydro scheme, Costa Rica. *Intl. Journal of Hydropower and Dams*. Issue 6.
- Castillo, L.G. and Carrillo, J.M. (2017). Comparison of methods to estimate the scour downstream of a ski jump. *International Journal of Multiphase Flow*. 92, 171–180.
- Maleki, S. & Fiorotto, V. (2019). Blocks Stability in Plunge Pools under Turbulent Rectangular Jets. *Journal of Hydr. Engng*. 145(4).

Sharing elements of EDF feedback on the operation and maintenance of pendulums

P. Bourgey, T. Guilloteau & J. Sausse

Dam safety expert, EDF, France

ABSTRACT: Although pendulums are widely used in monitoring for their reliability, precision and robustness, the fact remains that they can present material and functional problems which require regular control and maintenance actions, or even replacement in some cases. Through concrete and illustrated cases, this article presents in a qualitative way the different problems encountered.

RÉSUMÉ: Si les pendules sont des appareils très utilisés en auscultation pour leur fiabilité, leur précision et leur robustesse, il n'en demeure pas moins qu'ils peuvent présenter des problèmes matériels et fonctionnels, qui nécessitent des actions régulières de contrôle et de maintenance, voire de remplacement dans certains cas. Au travers de cas concrets et illustrés, cet article présente de manière qualitative les différentes problématiques rencontrées.

1 INTRODUCTION

EDF Hydro has been operating many dams for more than 75 years and they are often equipped with direct and inverted pendulums (about 500 out of a fleet of more than 300 dams monitoring) to measure horizontal and vertical displacements. This article analyzes various problems encountered on them and the solutions implemented to keep them operational. It does not present the maintenance actions that are part of the operator's routine maintenance (control of the absence of blocking of wires, water level in the tanks, ...).

Problems will be discussed:

- anchoring: breaking, disassembly-reassembling of removable anchorage,
- degradation/entrapment of wires in casings,
- corrosion: the different components of the pendulum,
- electrolysis according to the materials chosen for the tables and their supports.
- free domain that are no longer sufficient under the effect of exceptional thermal loading or under the effect of the swelling of the concrete of the dam,
- highly environmentally sensitive vertical measurements,

2 INVERTED PENDULUM ANCHORS

2.1 *First generation*

Until the late 1990s, inaccessible inverted pendulum anchors at the bottom of deep boreholes were made with sealing baskets (see diagram below):

This system was less used in the late 1990s following various problems encountered on these anchors:

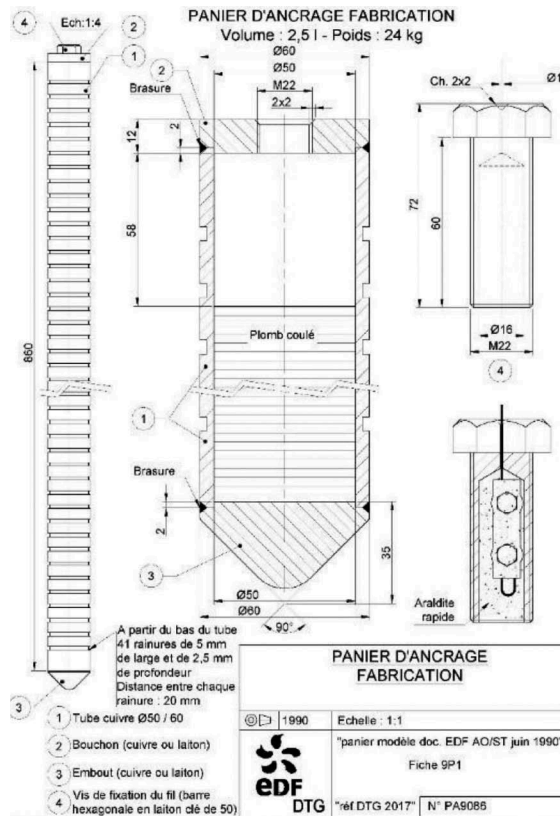


Figure 1. Anchor basket elements.

- Waiting a minimum of 21 days for the sealing before proceeding with the commissioning of the pendulum,
- Some basket seals were defective (grout not having been set, grout washed out by water circulations at the bottom of the borehole). Even the tensile tests at the reception that could be carried out, up to 1.5 times the operating tension, could never avoid this problem,
- Recovery of the anchor is impossible,
- Sensitivity to the under-pressures between the sealing and the borehole which caused many loosening on our pendulums,
- The final position of the basket is sometimes different from that initially planned because of fluctuations due to the setting of the grout,
- Suspicion of creep of the wire sealing resin (hypothesis formulated in some cases of anomalies of zenith measurements see § 7.1).

That's why, at the end of the 90s, we developed a removable anchoring system that will be watertight.

2.2 Second generation

This anchoring process uses the principle of conical jamming (Morse cone type) which guarantees axial repositioning.

At the bottom of the casing is fixed a cap on which can be screwed a socket machined in female cone and comprising, in the upper part, a hanging key allowing its eventual disassembly. Mounted before the casing is lowered, this socket will receive the movable male anchor cone which is extended by a wire hanging head (see schema below).

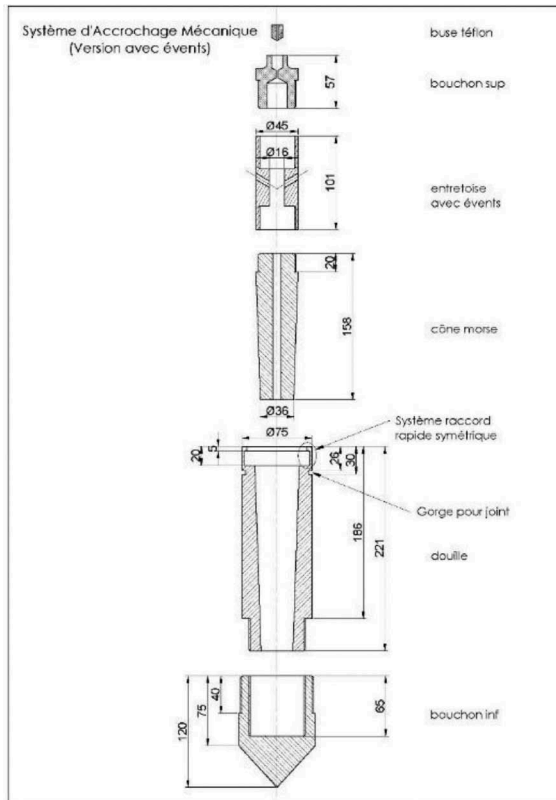


Figure 2. Removable anchorage details.



Figure 3. Cable clamp with corroded screws.

Nevertheless, we had the case in 2022 where a wire detached from the removable anchor on a 30-meter inverted pendulum. It was possible to disassemble the anchorage to find that the decommissioning of the pendulum was due to corrosion of the screws of the cable clamp which was not made of stainless steel.

3 CORROSION

The pendulums are installed in humid environments and suffer the effect of corrosion that is found on all the components of the device as evidenced by these few examples:

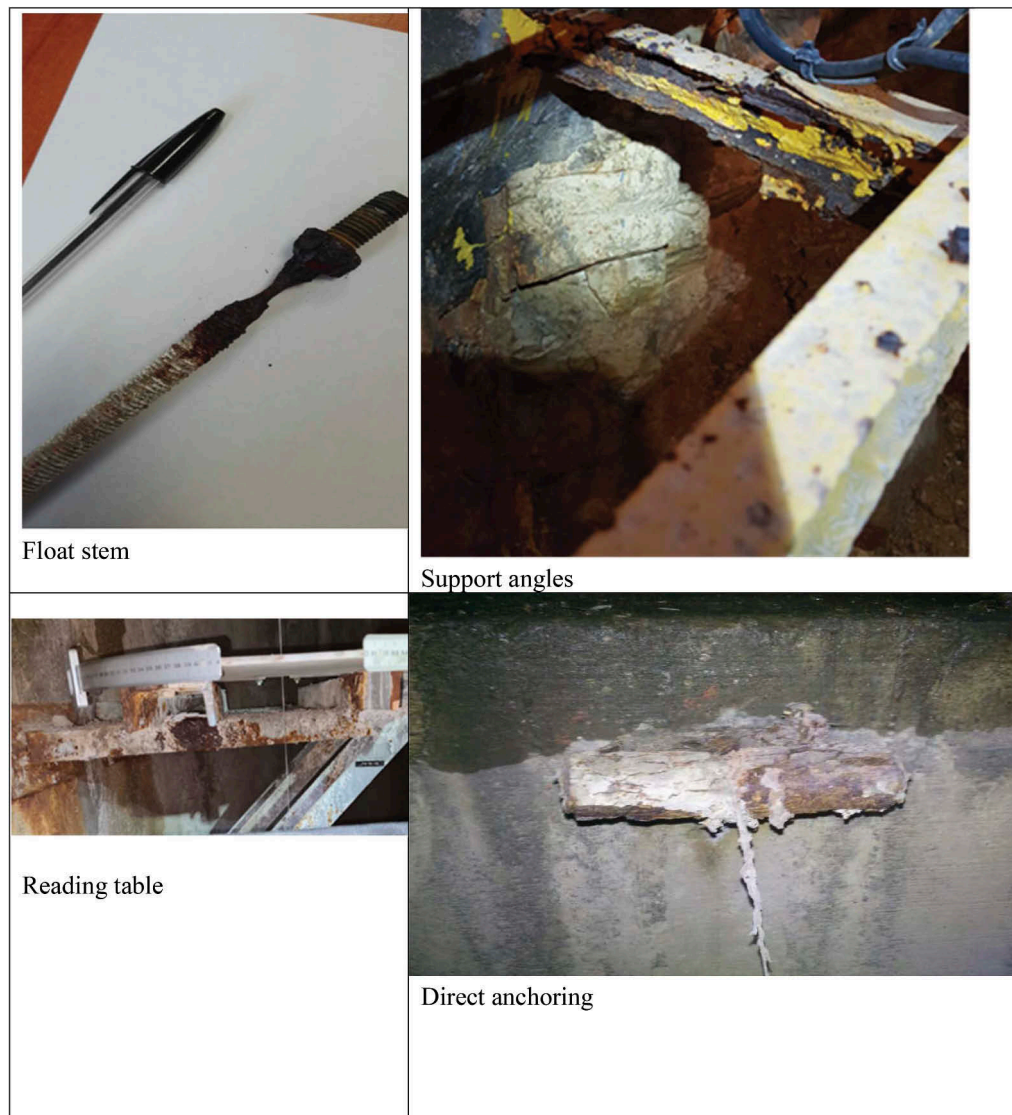


Figure 4. Examples of corrosion on different components of pendulums.

This corrosion is very active, especially when the pendulum anchors are located under the dam crest subject to climatic hazards but also rainwater and winter salting of pavements when the crest of the dam is a road open to traffic. This corrosion is also severe in tropical environments and forces us to change components of the device very regularly.

Today, we regularly change pendulum components corroded with stainless steel parts.

4 CALCITE

Calcite, which can be strongly present on our dams, can, by settling on the various components of the pendulums, prevent their correct operation. It is mainly found on the anchors and in the upper part of the casings of the inverted pendulums as shown in the examples below:



Figure 5. Examples of calcite on pendulum components.

To avoid blocking the wire by calcite, the easy-to-implement palliative solution that has been found is to move the pendulum wire after each manual measurement. This makes it possible to “break” the calcite film that can form on the surface of the water of an inverted pendulum tube that would not be waterproof (Figure 5). This also breaks a spider web that can also block a wire in a casing. In case of formation of a larger layer of calcite in a pendulum casing inverted in water (at the connection between tubes as frequently observed), the use of a specific tool “scraper”, a kind of sliding mass along the wire, makes it possible to blow up the calcite deposit and release the free domain of the wire.

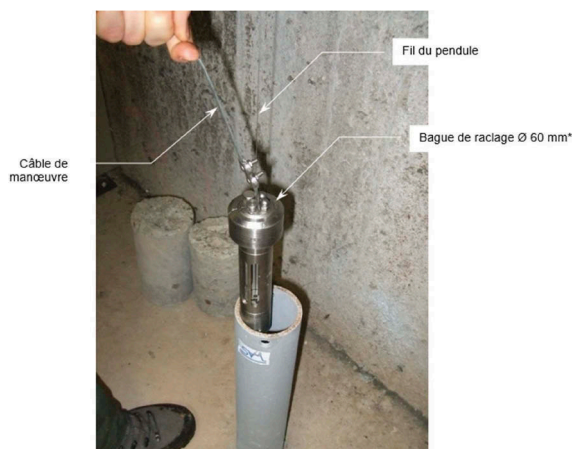


Figure 6. Using a “scraper”.

5 ELECTROLYSIS

In the past, pendulum tables and the angles supporting them may have been made of different materials resulting in an electrolysis reaction.



Figure 7. Pendulum table achieved electrolysis.

This was also the case encountered at the anchor rods of inverted pendulums when the bolts were not made of stainless steel.



Figure 8. Corroded float stem.

The only solution found to this problem was to replace all the pendulum tables affected by this phenomenon by devices of the same metal as the angles, without forgetting all the screws. Today, all the components of the pendulums are made of stainless steel.

6 FREE DOMAIN

Pendulums are monitoring devices designed to measure, with precision, relative horizontal or vertical displacements, whose maximum amplitude remains low (about 50 mm), which determines the requirement of a free domain fixed at 60 mm around the wire of the pendulum, at all points.

The field of evolution of the wire is delimited by a well, a borehole, or a sleeve attached to a facing, so that in no case is the wire unprotected, in the open air. It is frequently checked upon receipt of the pendulum.

But it happens that under the effect of reversible or irreversible displacement that the pendulum wire encounters one of these components distorting the measurement.

These cases are mainly found during heat waves or extreme cold, but also on dams affected of concrete swelling which leads in the long term to significant displacements that can exceed the free domain of the pendulum.



Figure 9. Controlling the free domain of a pendulum.



Figure 10. Pendulum wire touching the table during a heat wave.

To anticipate these problems, an application has been developed which makes possible, with past measurements, to predict when the pendulum could encounter an obstacle hindering measurement. The example below shows the prediction of the position of the wire in 2026 relative to the physical elements of the table. The wire will be at the limit of its free domain and it will be necessary to move the table at that time.

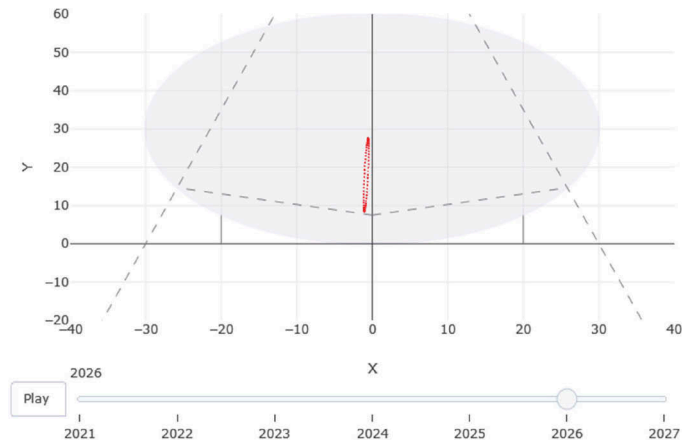


Figure 11. Rendering the application to anticipate a crash.

It has also happened that under pressure in the ground PVC tubing break and come to move or block the wire. It is then necessary to remove the debris from the first tubing to be able to replace it with a steel tubing.

7 VERTICALS MEASURES

Vertical measurements on pendulums have many advantages: simplicity of installation and measurement, low cost, possibility of installation on existing devices and the possibility of measuring deformations on more than ten meters.



Figure 12. Pendulum equipped with a vertical measuring device.

Nevertheless, this technology can have some disadvantages.

7.1 Anchor of first generation

Inverted pendulums whose anchorage is a sealing basket (see §2) may have presented a problem of creep of the resin trapping the cable tie before it reaches the top. The effect of this creep is visible only 1 to 2 years after tensioning of the wire and results in an irreversible artificial displacement oriented downwards (from 1 to 2 mm) which is not representative of the structure. Currently, the problem is eliminated using removable anchors.

It has also happened that this type of anchorage is unsealed.

7.2 Pendulum wire creep

The creep of the wire is clearly visible between 1 and 3 years after tensioning. The creep of a stainless-steel wire placed under a tension of 20 kg results in a total elongation of the order of 50 $\mu\text{m}/\text{m}$ after 3 years. This creep with log damping is very significantly reduced beyond these 3 years. These evolutions generate irreversible artificial movements oriented downwards, unrelated to the actual behavior of the dam as illustrated below.

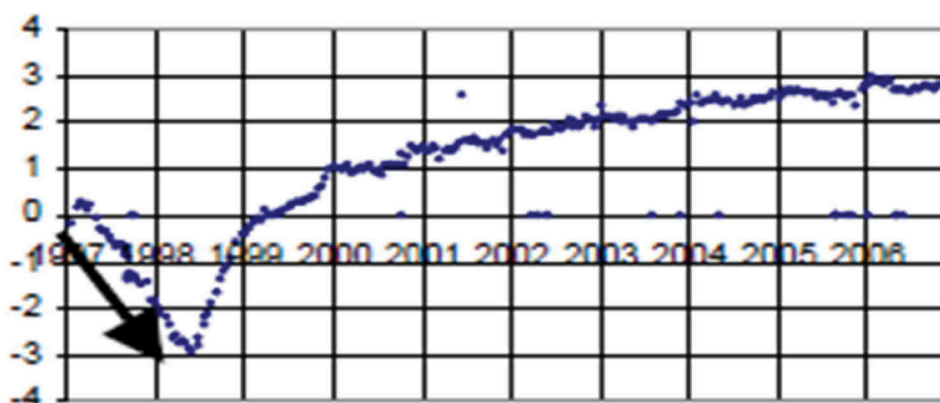


Figure 13. Example of pendulum wire creep measured over the first years of commissioning.

This inconvenience has been considered and dealt with using pre-fluited wires. It is also recommended to install a zenith measurement 3 years after the pendulum wire is commissioning.

7.3 Thermal expansion of the wire

The coefficients of thermal expansion of wire and concrete are different. The cumulative result of the thermal effect of the wire and the structure generally follows the thermal fluctuations of the wire. The seasonal reversible effect is therefore not representative of that of the dam. A correction of the expansion of the wire is nevertheless possible by measuring the temperature.

8 CONCLUSION

If pendulums are widely used in monitoring for their reliability, precision and robustness, the fact remains that there are frequently encountered hardware and functional problems. These are not to be neglected because they can lead to a deterioration in monitoring, or even errors in diagnosing the behavior of the structures examined.

Regular checks of all components, as well as up-to-date and anticipatory verification of functionality in the coming years, are highly recommended. In view of the difficulties encountered, maintenance actions are necessary; They can be complex and sometimes expensive, for example in the case of replacing an inverted pendulum in foundation. Improvements in the design of these devices are also possible and desirable. All exchanges in this direction within the profession should be encouraged.

Lifetime analysis of the Sta. Maria arch dam behaviour

M. Bühlmann, S. Malla & R. Senti

Axpo Power AG, Baden, Switzerland

ABSTRACT: The Sta. Maria arch dam was built between 1965 and 1967. After 40 years of operation, the Gotthard Base Tunnel (GBT) was constructed in the area of the dam. The tunnelling caused rock mass displacements, leading to irreversible deformations of the dam. To study the current behaviour of the dam as well as the effects of the tunnelling, a statistical analysis of the dam deformations was performed. For each of the 28 measurement stations, a statistical model was set up and calibrated. To analyse the entire lifetime of the dam considering the concrete temperature data, which are available only since 1980, a novel approach was applied: the temperature effects were simulated by a seasonal function until 1980 and later the measured temperatures were considered. After calibration, the contributions of water load, temperature and time-dependent effects could be separated. These results were used to determine the adjusted behaviour indicators (ABI), which can be employed as a powerful tool to evaluate dam behaviour over the whole lifetime. The case study presented in this paper shows that tunnelling is responsible for around 25 % of the irreversible dam deformations since the first impoundment.

RÉSUMÉ: Le barrage-voûte de Sta. Maria a été construit entre 1965 et 1967. Après 40 ans d'exploitation, le tunnel de base du Saint-Gothard (GBT) a été construit dans la zone du barrage. Le creusement du tunnel a provoqué des déplacements de la masse rocheuse, entraînant des déformations irréversibles du barrage. Afin d'étudier le comportement actuel du barrage ainsi que les effets du creusement du tunnel, une analyse statistique des déformations du barrage a été réalisée. Pour chacune des 28 stations de mesure, un modèle statistique a été mis en place et calibré. Pour analyser la durée de vie du barrage en tenant compte des données de température du béton, qui ne sont disponibles que depuis 1980, une nouvelle approche a été appliquée: les effets de la température ont été simulés par une fonction saisonnière jusqu'en 1980 et, par la suite, les températures mesurées ont été prises en compte. Après le calibrage, les contributions de la charge d'eau, de la température et des effets dépendant du temps ont pu être séparées. Ces résultats ont été utilisés pour déterminer les indicateurs de comportement ajustés (ABI), qui peuvent être utilisés comme un outil puissant pour évaluer le comportement du barrage pendant toute sa durée de vie. L'étude de cas présentée dans cet article montre que le creusement de tunnels est responsable d'environ 25 % des déformations irréversibles du barrage depuis la première mise en eau.

Traduit avec www.DeepL.com/Translator (version gratuite).

1 INTRODUCTION

Concrete dams are subjected to long-term processes, such as concrete swelling or valley deformation. If these processes lead to excessive dam deformations, structural damage and, in the worst case, even failure may occur. Hence, a proper monitoring is essential to detect irreversible deformations in dams. As concrete dams get older, greater attention needs to be paid to this aspect.

As underground works in the vicinity of a dam can cause valley deformations, a close monitoring of dam deformations is very important. When an exploratory gallery was built in 1978 near the Zeuzier arch dam, the rock mass displacements caused serious damage to the dam, due to which the reservoir had to be lowered to the minimum operating level (Swiss Committee on Dams, 1982). Hence, also in the case of the Sta. Maria arch dam, significant irreversible rock mass displacements were expected to occur at the dam site due to the nearby tunnelling project. It was therefore decided to carry out an enhanced monitoring of the dam during and after the tunnelling.

This paper presents the results of a statistical analysis performed using a novel methodology to evaluate the current state of the irreversible displacements of the Sta. Maria arch dam. These results help to determine the contribution of the tunnelling to these irreversible displacements.

2 STA. MARIA ARCH DAM

The Sta. Maria arch dam is a part of the hydroelectric power plant owned by Kraftwerke Vorderrhein AG with a catchment area of 315.8 km². The double curvature arch dam was built between 1965 and 1967. It has a height of 117 m and a crest length of 560 m. The reservoir with a storage volume of 67 million m³ is operated seasonally.

After 40 years of operation, the Gotthard Base Tunnel (GBT) was constructed in the area of the dam. The tunnel axis is located at a depth of 1300 m and a horizontal distance of 2200 m from the dam (Figure 1a). Due to the drainage of the rock mass caused by the tunnelling, irreversible rock mass displacements were expected to occur at the Sta. Maria dam site. To prevent any undesirable effects, the monitoring of the dam was enhanced during the construction period of the GBT project. The measured displacements were compared to critical values that were determined as the maximum tolerable limits based on a structural analysis of the dam. The displacements of the Sta. Maria dam due to the tunnelling remained well below these critical values. Nevertheless, due to the still ongoing mountain drainage, the valley deformation is still taking place, although the rate of deformations has slowed down considerably after 10 years since the completion of the tunnel. In particular, the rate of the irreversible dam displacement in the stream direction has dropped to a very low level. However, a slight increase of tilting of the dam in the cross-stream direction is still being observed. In order to

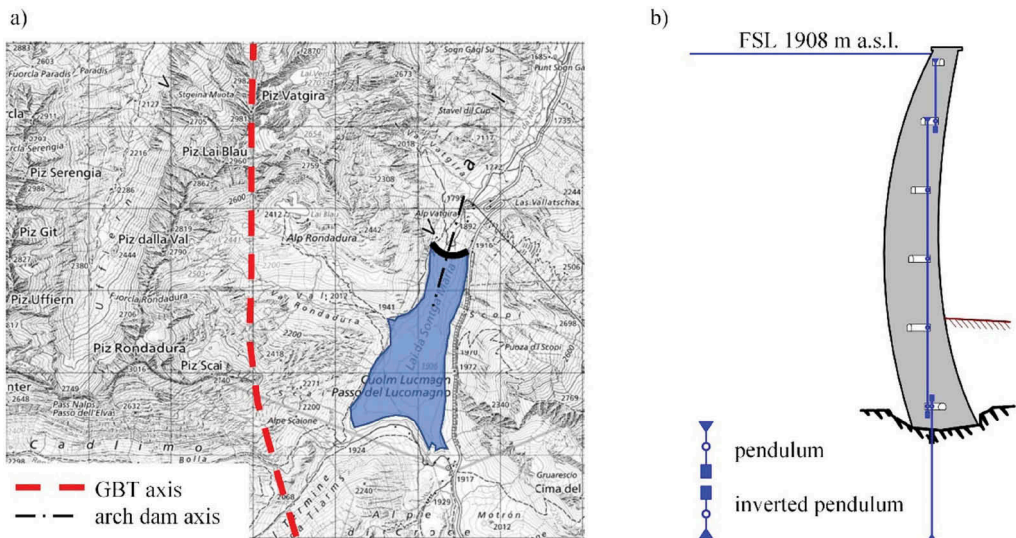


Figure 1. a) situation of the Sta. Maria arch dam; b) cross section of the central section with pendulum measurements.

assess the current behaviour of the dam and its foundation as well as to determine the additional irreversible displacements due to the GBT project, an extensive statistical analysis of the measured displacements during the whole lifetime of the dam was performed.

The dam displacements are monitored by five pendulums with a total of 28 measuring stations. The displacements are measured in each inspection gallery in the radial (upstream-downstream) and tangential (left-right) directions (Figure 1b).

3 METHODOLOGY

3.1 Investigated displacements

Dam displacements from pendulum measurements and the water level data are available from monthly readings since the first impoundment. In addition, monthly data of concrete temperature measurements are available since 1980. For the present investigation, all the available displacement data from the monthly pendulum measurements were considered. The dam displacements were transformed from the local $x'-y'$ (radial-tangential) coordinate system to the global $x-y$ coordinate system. For each of the 28 measurement locations, a statistical model in the x and y directions was set up.

3.2 Statistical models

Statistical models are widely used to analyse deformations of concrete arch dams (Mata, et al., 2013). In most cases, multiple linear regression (MLR) models are employed, since they are straightforward to set up and easy to interpret. The MLR models are based on model equations that define the relation between the influencing variables (regressors) and the behaviour indicator (dependent variable). The MLR models of displacements of concrete dams as behaviour indicators usually employ water level, temperature and time as influencing variables (Swiss Committee on Dams, 2003).

Some of the earliest publications on MLR models for the statistical analysis of deformations of concrete dams were those by Willm & Beaujoint (1967) and Widmann (1967). These so-called HST models (hydrostatic, seasonal, time) are still the most common statistical models (Tatin et al., 2015). In an HST model, the behaviour indicator is related to the loads on the dam due to the fact that the water level h , the seasonal effects S and some irreversible time-dependent effects t are used as influencing variables. The hydrostatic loading is represented by a fourth-order polynomial function of the water level h (Equation 1). The temperature effects are described by a second-order sinusoidal function of the seasonal variable $S=j2\pi/365.25$, where j is the number of the day in the year since the 1st of January. In the model of Willm & Beaujoint (1967), the irreversible effects are represented by a logarithmic function and an exponential function of time t (Equation 1). However, other suitable approaches to represent the time effects, such as those described in Swiss Committee on Dams (2003), can be used.

$$P(H, S, T) = \beta_0 + \beta_1 h + \beta_2 h^2 + \beta_3 h^3 + \beta_4 h^4 + \beta_5 \sin(S) + \beta_6 \cos(S) + \beta_7 \sin(2S) + \beta_8 \cos(2S) + \beta_9 \exp(t) + \beta_{10} \ln(t) \quad (1)$$

Equation (1) leads generally to a relatively good agreement between measurements and predictions (Bühlmann, 2018). Nevertheless, in situations with extreme temperature periods, such as the heat wave in Europe in 2003 or during exceptional operating conditions, there can be significant deviations between the predictions of the HST model and the measurements. In such cases, temperature-based models may lead to better results. If concrete temperature readings inside the dam are available, HTT models (hydrostatic, temperature, time) can be set up, for which there are several approaches. The most common one uses either temperature measurements directly, or the mean temperature T_m and the temperature difference T_d calculated

by thermal analysis based on temperature measurements. In Bühlmann (2018), these two approaches are compared. The present study employed the following HTT model (Léger & Leclerc, 2007):

$$P(H, T, T) = \beta_0 + \beta_1 h + \beta_2 h^2 + \beta_3 h^3 + \beta_4 h^4 + \sum_{i=1}^{i=n_t} \beta_{m,i} (T_m - T_{ref}) + \sum_{i=1}^{i=n_t} \beta_{d,i} T_d + \beta_5 t + \beta_6 \exp(-t) \quad (2)$$

For the analysis of the Sta. Maria arch dam, a combination of the two models described by Equations (1) and (2) was used, as concrete temperatures from measurements were available only from 1980 onwards. Hence, only an HST model could have been set up over the whole lifetime of the dam. On the other hand, in the case of a more precise HTT model using concrete temperatures, the dam behaviour in the first years of operation with large irreversible deformations could not be analysed. Therefore, a novel approach was introduced. From 1967 until 1980, a seasonal function is used to represent the temperature effects. From 1980 onwards, the data from the concrete temperature measurements were considered. In order to achieve a smooth transition between the two approaches, a step function was introduced on 01.01.1980. The temperature measurements were pre-processed to calculate the mean temperature T_m and the temperature deviation T_d . This involved the solution of an inverse heat conduction problem considering the distances of the temperature sensors from the boundaries (Weber et al., 2010). The effects of the water level were represented by a polynomial function up to the fourth order, with the order being determined by hypothesis testing (Montgomery et al., 2012). The better the representation of time effects in the statistical model, the better the modelling of the effects of water level and temperature (Bühlmann, 2018). In view of the various non-linear effects due to the irreversible rock deformations and creep, the time was modelled with a spline function $s(t)$. A spline function makes only sense for an inference-based analysis, in which past measurements are analysed, but not for prediction purposes. To sum up, the statistical model used in the present study can be expressed as follows:

$$P(H, S, T, T) = \beta_0 + \beta_1 h + \beta_2 h^2 + \beta_3 h^3 + \beta_4 h^4 + \beta_5 \sin(S) + \beta_6 \cos(S) + \beta_7 \sin(2S) + \beta_8 \cos(2S) + \beta_9 shift_{1980} + \sum_{i=1}^{i=n_t} \beta_{m,i} (T_m - T_{ref}) + \sum_{i=1}^{i=n_t} \beta_{d,i} T_d + \beta_{10} s(t) \quad (3)$$

3.3 Model calibration

The calculations were performed in the statistical software R (R Core Team, 2021). The linear regression analysis was performed using the stats library in R. For the spline approach, a generalized additive (GAM) model was used (James et al., 2013). In R, this is implemented in the mgcv library (Wood, 2006).

The variable selection was performed mainly based on two criteria. Firstly, to detect multicollinearity, which could lead to unstable models, the variance inflation factor (VIF) was evaluated. If the value of VIF was greater than 10, the correlated variables were removed from the models. Secondly, only significant variables with a p -value below 0.05 were considered in the models. The variable selection was done automatically by means of a best subset algorithm (Montgomery et al., 2012) based on the above two criteria.

The data from 1972 to 2021 were used for the model calibration. The data prior to 1972 was not considered for the calibration, since the concrete properties were still changing with time in the first few years of the dam operation. This approach allows the statistical inference of the contributions of water level, temperature and time to the dam deformations taking into account all the available data (Bühlmann, 2018). The aim of an inference-based model is to look at the entire data to draw conclusions on the dam behaviour. It should not be confused with a prediction-based model for ongoing monitoring.

The models were calibrated using routine statistical procedures. The goodness of fit was judged based on the coefficient of determination R^2_{adj} and the residual standard error (RSE). In addition, standard statistical plots to evaluate regression models, such as partial residuals were used.

3.4 Behaviour analysis

After calibration, the deformations due to water level δ_h , temperature δ_T and time δ_t were calculated based on the calibrated regression models. Thus, the adjusted behaviour indicator ABI was calculated as follows (Bühlmann, 2018):

$$ABI = M - P_{rev} = M - \delta_h - \delta_T \quad (4)$$

In this approach, the calculated reversible deformation P_{rev} is subtracted from the measured deformation M . In the case of a concrete dam, P_{rev} consists of the contributions of water level and temperature, as represented by δ_h and δ_T , respectively. Thus, the ABI represents the total irreversible deformations. In contrast to the observation-prediction comparison (Swiss Committee on Dams, 2003), in which the behaviour must be evaluated based on the residuals and the time function used in the model, the long-term dam behaviour is easier to identify based on the ABI.

The value of ABI was set to 0 at the start of the first impoundment on the 5th of April 1968. For a better understanding of the dam behaviour, a moving average was calculated by the LOESS (locally estimated scatterplot smoothing) approach (Dettling, 2015). Afterwards, the ABI values analysed separately for the x and y directions were plotted against each other. In these plots, the decades are depicted in different colours, so that the temporal course can be readily followed. Based on the temporal path of the deformations in the x- and y-directions for each measurement location of the pendulums, the dam behaviour can be evaluated. Furthermore, the results of the smoothed ABI were used to investigate the deformations caused by the construction of the GBT.

4 RESULTS

4.1 Statistical models

The statistical models showed a very good agreement between the measurements and the predictions. Generally, the goodness of fit was excellent at the crest level. In the central block, R^2_{adj} is equal to 0.99 in the x direction and 0.98 in the y direction. The agreement was quite good at the base of the blocks as well. For instance, at the base of the central block 18 (position see Figure 3), R^2_{adj} is equal to 0.98 in the x direction and 0.94 in the y direction.

The proposed temperature approach worked very well. The residuals are smaller since the start of the concrete temperature measurements in 1980. Nevertheless, the seasonal approach yielded satisfactory results even in the period 1968-1980, due to which the deformation paths could be assessed since the first impoundment.

In Figure 2, the results of the statistical analysis of the radial displacement at the crest level of the central block 18 are presented. There is an excellent agreement between the measured and computed displacements (Figure 2a). However, during the first impoundment, there are relatively large deviations, which could be related to the changes of the material properties of concrete and rock during this period. In Figure 2b), the displacements due to water level, temperature and time effects are shown. The effect of the water level is greater and out-of-phase with respect to the temperature effect. The change of approach in the modelling of the temperature effect is evident in the plot of residuals, which are larger prior to 1980 (Figure 2c), when a seasonal approach was used due to the lack of concrete temperature data. Nevertheless, the seasonal approach is a fairly good approximation to simulate the temperature effect. In Figure 2d), the ABI is depicted, representing the irreversible displacement overlaid with the modelling errors. The LOESS smoothing of the ABI yields a function representing the long-term trend of the irreversible displacement.

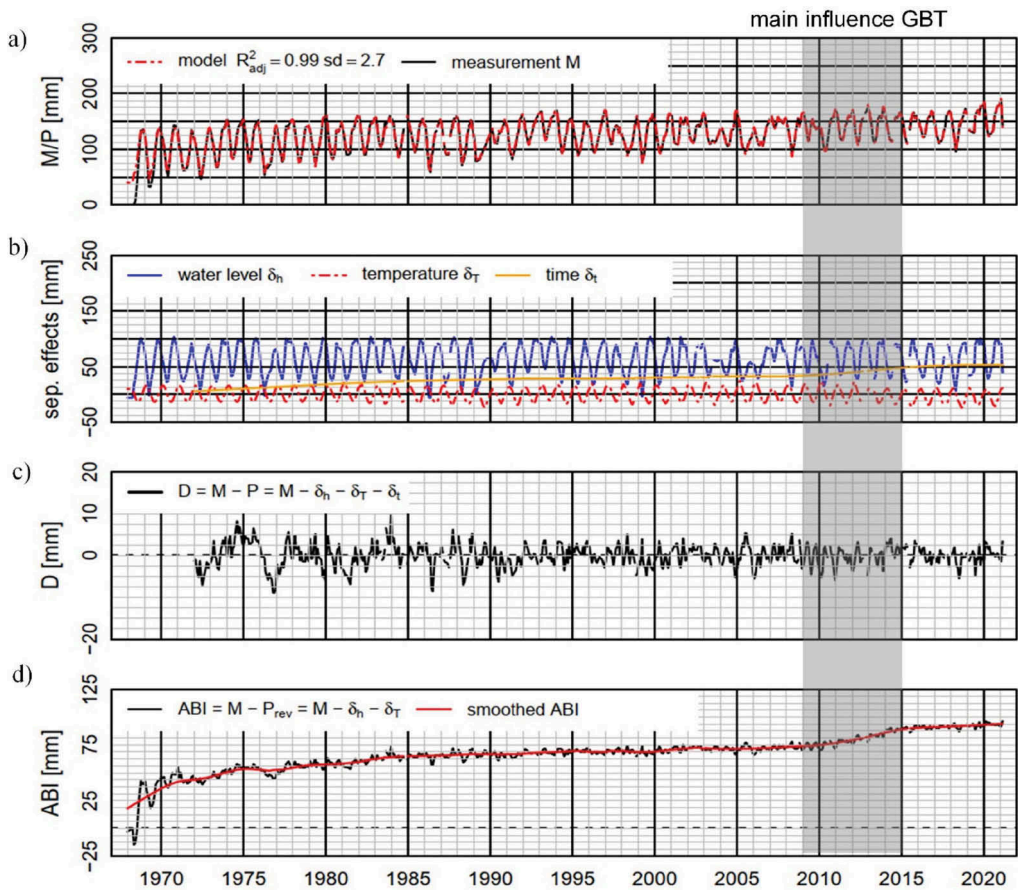


Figure 2. Results of statistical analysis of the radial displacement at the crest level of the central block 18: a) comparison between measured and computed displacements; b) displacements due to water level, temperature and time effects; c) residuals for the calibration period; d) adjusted behaviour indicator (ABI).

4.2 Behaviour analysis

The behaviour of the structure can be interpreted based on the ABI. At the crest level of the central section in block 18, an initial irreversible deformation occurred during the first three years of operation (Figure 2d). Since the beginning of the dam operation in 1968, a significant creep deformation in the stream direction was observed up to around 1990. From 1990 until the construction of the GBT, the ABI stayed at an almost constant level. From 2010 to 2015, the effect of the tunnelling can be recognised very well.

Furthermore, as described in Section 3.4, Figure 3 shows the deformation paths of the ABI in the global x (stream) and y (cross-stream) directions at the crest level of each of the five blocks equipped with pendulums. The value of ABI was set to 0 at the start of the first impoundment. In all the blocks with pendulum measurements, irreversible (creep) displacements took place in the stream direction during the first 20-30 years of operation. Afterwards, the irreversible displacements slowed down considerably. In the 1990's, there was only a very minor increase of the irreversible displacements. After 2009 onwards, when the tunnelling works for the GBT project started, the rate of irreversible displacements increased significantly. Besides an irreversible displacement in the stream direction, irreversible displacements towards the left were observed in the pendulums 10, 14, 18 and 22. By 2015, most of the irreversible displacements had stabilized (Figure 2). In the central block 18, the irreversible displacement increased in the period 2009-2016 by around 20 mm in the stream direction and by

around 4 mm towards the left as a result of the GBT project. In blocks 14 and 22, the tunnelling resulted in an irreversible displacement in the stream direction of around 15 mm each, which was somewhat smaller than the value in the central block.

In the cross-stream direction, the increase of the irreversible displacements in the period 2009-2016 indicates a tilting of the valley in cross-stream direction due to the tunnelling, as can be seen in Figure 4a. All the pendulum measurements show a tilt of around 0.018 mm/m. As expected, this is almost equal to a valley tilt of 0.020 mm/m determined by the geodetic measurements. The lateral tilt of the valley corresponds to a rigid body rotation towards the tunnel (see Figure 4b), which would not cause any significant deformations (stresses) in the dam structure.

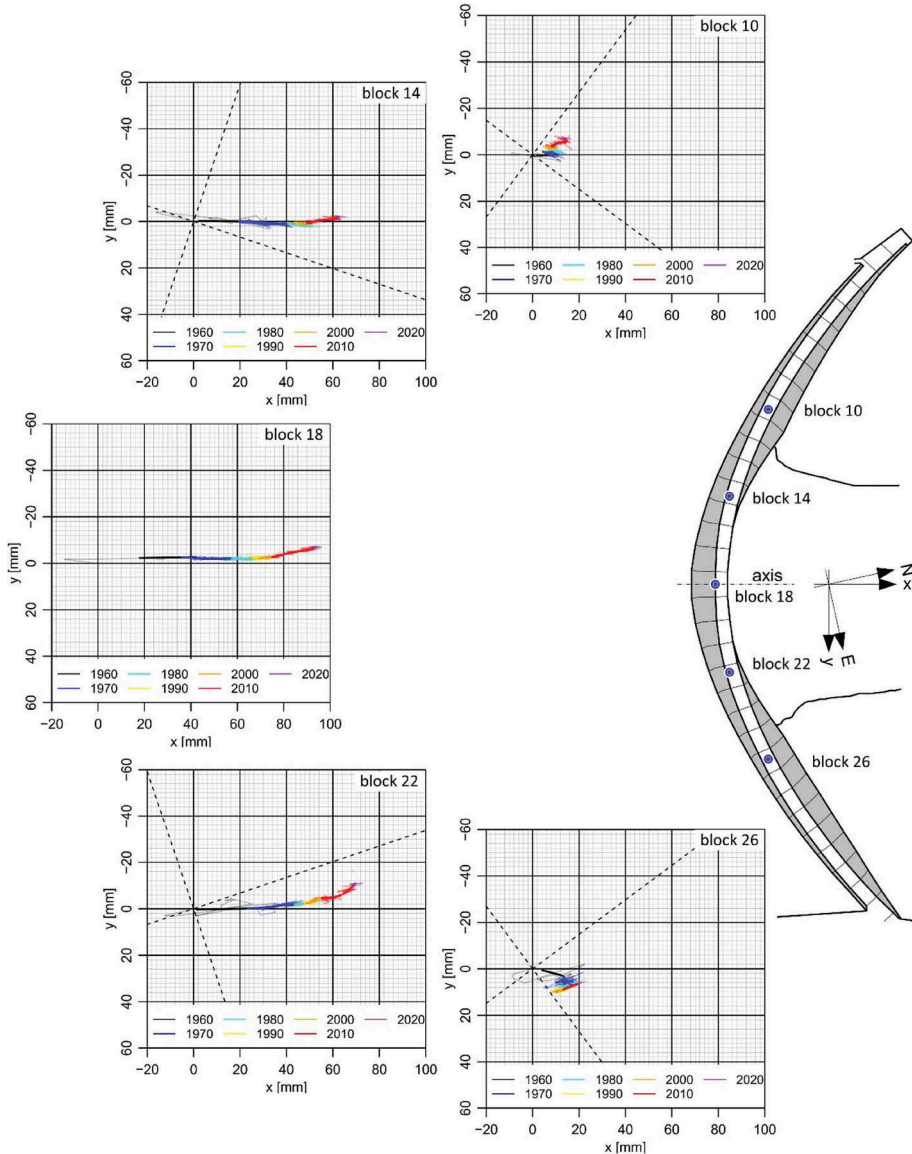


Figure 3. Deformation paths of ABI in the global x (stream) and y (cross-stream) directions at the crest level of each of the five blocks equipped with pendulums.

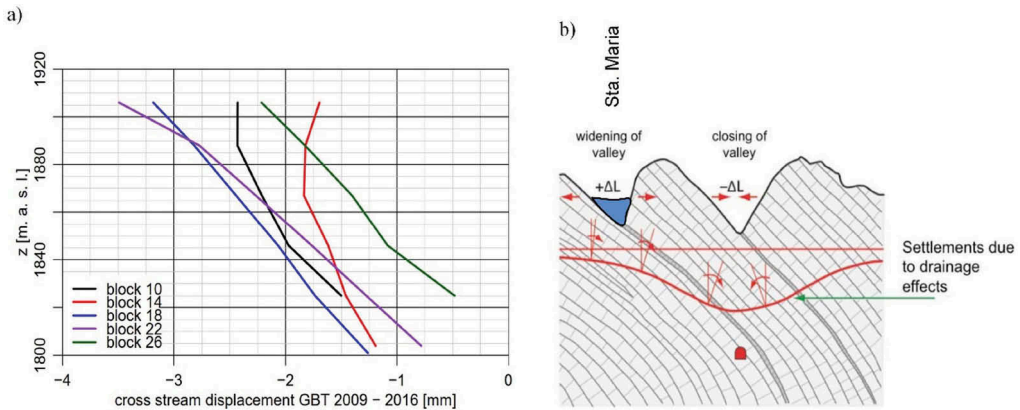


Figure 4. a) Irreversible displacements in the cross-stream direction in the period 2009-2016; b) valley widening at Sta. Maria arch dam site (Ehrbar et al., 2012).

5 SUMMARY AND CONCLUSIONS

The behaviour of the Sta. Maria arch dam was investigated by means of an extensive statistical analysis. The displacements obtained from the monthly pendulum readings since the first impoundment were analysed at all the measurement locations with the help of the adjusted behaviour indicator (ABI). Based on the results of this analysis, the dam behaviour can be summarised as follows:

- The construction of the GBT resulted in a significant increase of the irreversible dam displacements in the stream direction. This process has, however, stabilized now and the irreversible displacement is again occurring at a very slow rate, as observed also prior to the start of construction of the GBT.
- The present analysis shows that the construction of the GBT has resulted in a lateral tilting of the valley, resulting in irreversible dam displacements in the cross-stream direction. However, this does not cause any significant deformations in the dam. This tilting process is still ongoing, but it is progressing at a much slower rate.
- The GBT project has caused approximately 25 % of the total irreversible dam displacement in the stream direction since the initial impoundment.

The proposed methodology can be applied to analyse the irreversible deformations over the whole lifetime of the arch dam. Thus, the deformation caused by the construction of the GBT could be determined and put in relation to the total irreversible deformations since the first impoundment. The novel approach used to model the temperature deformations based on a seasonal function until 1980 and postprocessed temperature measurements since 1980 worked well. This approach can be applied to dams that have been retrofitted with concrete temperature measurements.

The results of the analysis presented in this paper show that the interpretation of the ABI can be a valuable tool to analyse the long-term behaviour and to investigate the structural safety of a concrete dam.

REFERENCES

- Bühlmann, M. (2018). Statistical Methods for Dam Behaviour Analysis. VAW-Mitteilungen 242, Versuchsanstalt für Wasserbau, Hydrologie und Glaziologie (VAW), (R. M. Boes, ed.), ETH Zürich, Schweiz.
- Detting, M. (2015). Applied Statistical Regression, ETH Zurich.
- Ehrbar, H.; Bremen, R. & Otto, B. (2012). Gotthard Base Tunnel - Mastering surface deformations in the area of two concrete arch dams - innovative solutions. World Tunneling Congress Bangkok.

- Mata, J., de Castro, A. A. & da Costa, J. S., 2013. Constructing statistical models for arch dam deformation. *Structural Control and Health Monitoring*, 21(3), pp. 423–437.
- James, G.; Witten, D.; Hastie, T.; Tibshirani, R. (2013). *An Introduction to statistical learning - with applications in R*. Springer, New York, USA. <http://www.springer.com/de/book/9781461471370>.
- Léger, P.; Leclerc, M. (2007). Hydrostatic, Temperature, Time-Displacement Model for Concrete Dams. *Journal of Engineering Mechanics (ASCE)*, 133(3): 267–277. [http://dx.doi.org/10.1061/\(ASCE\)0733-9399\(2007\)133:3\(267\)](http://dx.doi.org/10.1061/(ASCE)0733-9399(2007)133:3(267)).
- Montgomery, D. C., Peck, E. A. & Vining, G. G., 2012. *Introduction to Linear Regression Analysis*. 5. ed. Hoboken: John Wiley and Sons.
- Tatin, M.; Briffaut, M.; Dufour, F.; Simon, A.; Fabre, J. P. (2015). Thermal displacements of concrete dams: Accounting for water temperature in statistical models. *Engineering Structures*, 91: 26–39. <http://dx.doi.org/10.1016/j.engstruct.2015.01.047>.
- R Core Team (2022). *R: A language and environment for statistical computing*. R Foundation for Statistical Computing, Vienna, Austria. ISBN 3-900051-07-0, URL <http://www.R-project.org/>.
- Swiss Committee on Dams (1982). Abnormal Behaviour of Zeuzier Arch Dam. *Wasser Energie Luft*, 74 (3), pp. 64–112.
- Swiss Committee on Dams (2003). Methods of analysis for the prediction and the verification of dam behaviour. *Wasser Energie Luft*, 95(3/4), pp. 73–110.
- Weber, B.; Perner, F.; Obernhuber, P. (2010). Displacements of Concrete Dams Determined from Recorded Temperatures. *Proc. of the 8th ICOLD European Club Symposium: dam safety - sustainability in a changing environment*. Austrian National Committee on Large Dams (ATCOLD), Graz, Austria: 623–628.
- Widmann, R. (1967). Evaluation of deformation measurements performed at concrete dams. *Proc. 9th ICOLD Congress. International Commission on Large Dams (ICOLD)*, Istanbul, Turkey. Q.34, R.38: 671–676.
- Willm, G.; Beaujoint, N. (1967). Les méthodes de surveillance des barrages au service de la production hydraulique d'Electricité de France — Problèmes anciens et solutions nouvelles ('Surveillance methods of dams of EDF — Old problems and new solutions'): *Proc. 9th ICOLD Congress. International Commission on Large Dams (ICOLD)*, Istanbul, Turkey. Q.34, R.30: 529–550.
- Wood, S. N. (2006). *Generalized Additive Models: An Introduction with R*. ISBN 9781584884743. Chapman and Hall/CRC, Boca Raton, USA.

Effect of invert roughness on smooth spillway chute flow

M. Bürgler, D.F. Vetsch, R.M. Boes & B. Hohermuth

Laboratory of Hydraulics, Hydrology and Glaciology (VAW), ETH Zurich, Zurich, Switzerland

D. Valero

Institute for Water and River Basin Development (IWG), Karlsruhe Institute of Technology (KIT), Karlsruhe, Germany

Water Resources and Ecosystems department, IHE Delft, Delft, The Netherlands

ABSTRACT: Spillway chutes are appurtenant dam outlet structures with the purpose to safely convey large discharges during extreme flood events. During such events, hydraulics plays a major role in the safety of the structure. Along a spillway chute, water is accelerated by gravity and may reach flow velocities in the order of 10 to 50 m/s, implying a considerable cavitation risk. On the spillway invert, turbulence is generated by shear stresses and surface roughness, which results in self-aeration of the flow once the turbulent boundary layer interacts with the free surface. For reliable design guidelines of spillways, knowledge of air concentrations along the spillway chute is essential, as entrained air concentrations can mitigate the risk of cavitation at the expense of risking overtopping of the chute walls due to flow bulking, or further accelerating the flow due to drag reduction. While it is well known that the invert roughness is the controlling parameter for boundary layer development and the self-aeration process (for a given slope and discharge), the quantitative understanding of roughness effects on air-water flow properties is still limited by the availability of data sets that target this variable. In this research, the effects of invert roughness on smooth spillway chute flow are investigated in a large-scale physical model. The investigated flow properties include the clear water and air-water mixture flow depths, depth-averaged flow velocities, air concentrations, and friction factors. Based on the experimental data, we demonstrate that the streamwise development of depth-averaged air concentration is significantly affected by invert roughness, which in turn also affects the bottom air concentration downstream of the inception point. Further, we found that friction factors are significantly affected by the relative boundary layer thickness in the developing non-aerated flow region, but also by bottom air concentrations in the aerated flow region. Good agreement between experimentally determined friction factors and established theoretical relations was found. Overall, our findings contribute to a qualitative description of invert roughness effects on air-water flow properties for a robust design of spillways, thus contributing to safer dam infrastructure.

1 INTRODUCTION

Spillways are the dominant outlet structures of dams. They are engineered to safely pass the most extreme floods to prevent uncontrolled overtopping. Spillway chutes are often classified based on the surface characteristic, including smooth, micro-rough, and macro-rough inverts (Severi & Felder 2017); where the latter is normally encountered in the form of stepped spillways. Depending on the roughness characteristics, residual flow energy at the downstream end of the structure may significantly differ, which may imply the need for different types of energy dissipators.

Flow along smooth and micro-rough spillways can be distinguished into several characteristic regions (Wood 1991). In the most upstream, non-aerated region, the flow is generally described by the acceleration of water by gravity and the resulting drawdown of the water-surface (Castro 2009), starting from a critical depth closely upstream of the spillway crest. A turbulent boundary layer develops above the chute invert, thereby generating large amounts of turbulence (Pope 2000). The layer between the free surface and turbulent boundary layer consists of irrotational flow. As the upper edge of the turbulent boundary layer approaches the free surface, the water surface roughens until it breaks up, and air-entrainment occurs as the destabilizing turbulent forces overcome the stabilizing forces of gravity, surface tension, and viscosity (Wood 1991, Brocchini & Peregrine 2001, Valero & Bung 2018).

In the aerated region, downstream of the inception point, air is entrained at the free-surface and gradually distributed over the water column by turbulent diffusion, thereby resulting in *S*-shaped air concentration profiles over the mixture flow depth (Straub & Anderson 1958, Wood 1991, Chanson 1996). For sufficiently long spillways, with steep slopes ($> 30^\circ$), invert-normal air concentration profiles approach a quasi linear distribution over the entire depth, yielding considerable air concentrations close to the invert (Straub & Anderson 1958). For the design of spillways, knowledge of air concentrations along the spillway chute and across the depth is essential, as sufficiently large air concentrations close to the invert reduce the risk of cavitation (Peterka 1953, Falvey 1990), but also increase the risk of overtopping the chute walls due to flow bulking (Boes & Hager 2003, Wilhelms et al. 2005). Further, the presence of air in the vicinity of the invert reduces the effective shear stress and, thereby, the local friction factors compared to clear water flow (Straub & Anderson 1958, Wood 1991, Chanson 1994, Kramer et al. 2021).

Straub & Anderson (1958) published an extensive data set on air concentrations for various chute slopes between 7.5° and 75° . Until today, this data set, together with data from Killen (1968) and Cain (1978), remain the foundation for most engineering approaches to describe self-aerated flows on smooth and micro-rough spillways (e.g. Wood 1983, 1991, Wilhelms & Gulliver 2005, Wilhelms et al. 2005). For instance, the data sets are the basis for the calculation core of SpillwayPro (Wahl & Falvey 2022), a software for state-of-the-art modelling of self-aerated flows on spillways.

Besides the chute slope, the roughness of the spillway invert is the controlling parameter for boundary layer development, production of turbulence, and the self-aeration processes. While effects of invert roughness on boundary layer growth and flow development in the non-aerated flow region are well understood (e.g. Castro 2009), current engineering approaches to describe bulk air-water flow properties do not explicitly account for roughness effects, which may be equivalent to different levels of turbulence in prototype (for instance, with larger velocity, for a given roughness). The chute invert in the experiments of Straub & Anderson (1958) and Killen (1968) was a sand-coated surface with a mean grain size and spacing of 0.71 mm and 1 mm, respectively, while Cain (1978) assumed an equivalent sand grain roughness of 1.5 mm for the spillway of the Aviemore dam. Therefore, empirical relations based on the mentioned data sets, such as Wilhelms & Gulliver (2005), Wilhelms et al. (2005), and Hager (1991) implicitly assume a certain invert roughness and, under comparable velocities, a similar effect of turbulence.

Anderson (1965) compared depth-averaged air concentrations from Straub & Anderson (1958) and additional experiments with a smooth channel bed and found that channel roughness affected depth-averaged air concentrations and air concentration distribution over the flow depth. An improved quantitative understanding of roughness effects is currently limited by the availability of data sets over a range of invert roughness and slopes. Further, the data set of Straub & Anderson (1958) only has limited data on the developing aerated flow region, between inception point and uniformly aerated flow. With regard to cavitation risk, this is typically the most critical region of spillways due to large velocities and insufficient air concentrations in the vicinity of the invert.

To address the above-mentioned knowledge gaps, a large-scale physical spillway model was set up. Based on experimental results for two distinct invert roughnesses, we highlight *qualitative* effects of invert roughness on relevant air-water flow properties in the developing aerated

flow region of spillways. More specifically, we investigate effects of invert roughness on depth-averaged air-concentrations, flow bulking, bottom air concentrations and friction factors. While further investigations are necessary for a detailed *quantitative* description of roughness effects on self-aerated boundary layer flows on spillways, this work identifies potential limitations of existing approaches and thereby contributes to safer dam infrastructure.

2 EXPERIMENTAL SETUP, INSTRUMENTATION & METHODS

The experiments were conducted in a large-scale physical spillway model located in the Laboratory of Hydraulics, Hydrology and Glaciology at ETH Zurich, Switzerland (Figure 1a). The model features an inlet tank with a width of 1.2 m and a smooth convergence to an uncontrolled broad crested weir characterized by an upstream and downstream quadrant according to USACE guidelines and a design head H_D of 0.35 m. The crest width and length are 0.5 m and 0.65 m, respectively. The spillway chute exhibits a total length of 9 m, including the downstream weir quadrant, a width of 0.5 m and an inclination angle of 50° .

The smooth chute side walls are made of PVC and glass, respectively. The invert of the downstream weir quadrant and the chute consists of concrete plates with a washed concrete surface. Two sets of roughness plates are used, for which the washed concrete surface is characterized by particle diameters d in the range from 1.0 mm to 1.5 mm and from 10.0 mm to 12.5 mm, respectively (Figure 1b,c). Detailed invert surface scans were made for 25 patches along the centerline of the chute, using a Baumer OM70-P0250.HH0180.VI laser distance sensor with a point accuracy of 0.16 mm. Patch areas were $3 \times 3 \text{ cm}^2$ for the small roughness and $9 \times 9 \text{ cm}^2$ for the large roughness, respectively, amounting to 275,400 measurement points for each roughness configuration.

We found that determining the hydraulic roughness in terms of equivalent sand roughness k_s based on measured drawdown curves is difficult at steep slopes. Therefore, k_s was determined with the approach of Flack & Schultz (2010) given in Eq. (1) by making use of statistical parameters of the surface scans:

$$k_s = 4.423k_{rms}(1 - S_k)^{1.37} \quad (1)$$

The root mean square surface variations k_{rms} of the two roughness configurations are 0.17 mm and 1.15 mm and skewness of the surface elevation distribution S_k are -0.01 and 0.30, respectively. The obtained k_s values of 0.74 mm and 7.34 mm are in reasonable agreement with the grain diameters of the washed concrete surfaces.

The experimental program consists of six flow rates between $0.1 \leq q \leq 0.6 \text{ m}^2/\text{s}$, covering each roughness configuration. Water was supplied to the inlet tank in a closed recirculating system via a constant head tank for a specific chute discharge q of $0.1 \text{ m}^2/\text{s}$ or directly via a frequency-controlled pump for specific flow rates q between 0.2 and $0.6 \text{ m}^2/\text{s}$. The flow rate was measured with magnetic-inductive flow meters (MID) with an accuracy of $\pm 0.5 \%$. Water depths in the non-aerated region were measured with a Baumer UNAM ultrasonic distance sensor (0.5 mm accuracy) in steady flow conditions for 120 s. Flow velocities in the non-aerated region were measured for 120 s with a three-component Laser Doppler Anemometer (LDA) with beam pairs oriented in both streamwise and invert-normal direction.

The measured flow depth h and velocity time series were filtered iteratively using the Robust Outlier Cutoff (ROC) (Valero et al. 2020) until no more outliers were rejected. The boundary layer thickness δ was determined as the invert-normal distance from the top of the grains constituting the invert roughness to the point where the time-averaged velocity was equal to 99 % of the free stream velocity \bar{u}_{fs} . The latter was determined from LDA measurements. Measurements in the aerated region were conducted with a dual-tip conductive phase-detection probe with a side-by-side design manufactured in-house. The inner electrodes consist of a platinum wire with 0.125 mm diameter and the outer electrodes of hypodermic needles with an outer diameter of 0.5 mm, respectively.

Local air concentrations c were determined with a single-threshold criteria based on 50% of the intermodal voltage range (Cartellier & Achard 1991) and local flow velocities using the adaptive-windows cross-correlation (AWCC) technique (Kramer et al. 2019, 2020) with ten particles per window. Obtained velocity time series were filtered iteratively using the ROC until no more outliers were rejected. The bottom air concentrations c_b were evaluated at an invert-normal distance $z = 6.1$ mm, corresponding to the lowest measured elevation of Straub & Anderson (1958). Further, mixture flow depths h_{98} were determined as the invert-normal distance where $c = 0.98$ is reached. The equivalent clear water depth h_w was calculated as:

$$h_w = \int_{z=0}^{h_{98}} (1 - c(z)) dz \quad (2)$$

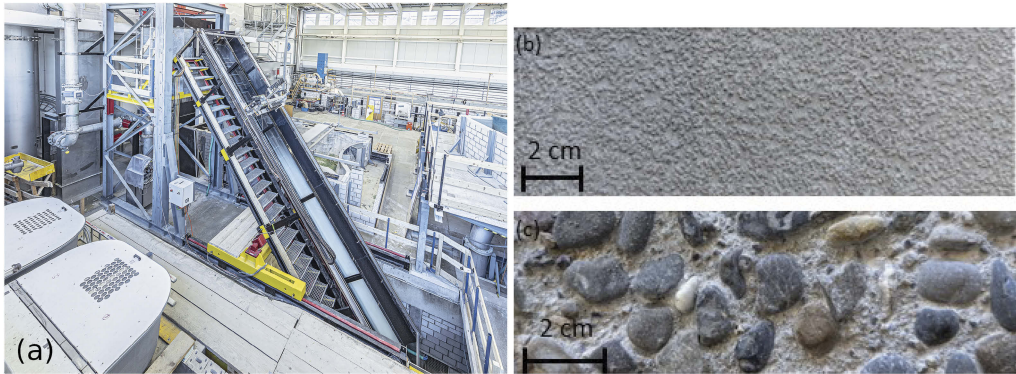


Figure 1. Large-scale spillway model consisting of water supply pipes, inlet tank and a chute of 9 m length and 0.5 m width (a); and a top view of the washed concrete surfaces characterized by particle diameters d (equivalent sand roughness k_s) in the range from (b) 1.0 mm to 1.5 mm (0.74 mm) and (c) 10.0 mm to 12.5 mm (7.34 mm), respectively.

The air concentration averaged over the mixture depth h_{98} is defined as:

$$C_{98} = \int_{z=0}^{h_{98}} (c(z)) dz \quad (3)$$

The inception point locations x_{Li} were determined as the points of intersection between measured boundary layer thicknesses and clear water flow depths. Shear velocities u_* were calculated with two methods. In the developing non-aerated flow region defined where $\delta/h < 1$, u_* was calculated with the von Kármán integral equation for momentum conservation within the boundary layer (Bauer 1954):

$$u_* = \sqrt{\frac{\bar{u}_{fs}^2}{2} \left[2 \frac{d\delta_m}{dx} + (\Lambda + 2) \frac{\delta_m}{\bar{u}_{fs}^2} \frac{d\bar{u}_{fs}^2}{dx} \right]} \quad (4)$$

where δ_m is the momentum thickness, and $\Lambda = \delta_d/\delta_m$ is a shape parameter of the velocity profile. Further, δ_d is the displacement thickness. The displacement and momentum thickness were calculated from measured time-averaged velocity profiles $\bar{u}(z)$ and the measured free stream velocity \bar{u}_{fs} (Bauer 1954):

$$\delta_d = \int_{z=0}^{\delta} \left(1 - \frac{\bar{u}(z)}{\bar{u}_{fs}} \right) dz \quad (5)$$

$$\delta_m = \int_{z=0}^{\delta} \left[\frac{\bar{u}(z)}{\bar{u}_{fs}} - \left(\frac{\bar{u}(z)}{\bar{u}_{fs}} \right)^2 \right] dz \quad (6)$$

Downstream of the inception points, shear velocities were calculated from the energy line gradient I_E as $u_* = \sqrt{ghI_E}$ (Auel et al. 2014). Darcy-Weissbach friction factors f were calculated with Eq. 7 from u_* and depth-averaged velocities $\langle u \rangle$:

$$f = 8 \left(\frac{u_*}{\langle u \rangle} \right)^2 \quad (7)$$

3 EXPERIMENTAL RESULTS AND DISCUSSION

3.1 Air concentration and flow bulking

Accurate predictions of depth-averaged air concentrations along the spillway are of utmost importance for a robust design of spillway, since most other flow properties and processes such as flow bulking, bottom air concentrations and friction reduction are derived thereof. Flow bulking is typically quantified in terms of the mixture flow depth h_{98} (Wilhelms et al. 2005, Wahl & Falvey 2022), since C_{98} , the air concentration integrated up to h_{98} , proved as the uppermost robust estimate for total conveyed air. The bulk flow depth can be calculated by Eq. 8:

$$h_{98} = h_w / (1 - C_{98}) \quad (8)$$

When computing clear water depths h_w , roughness effects are accounted for via the friction factor or in drawdown curve computations. In contrast, currently available relations for the streamwise development of C_{98} (e.g. Wilhelms & Gulliver 2005) are based on the data of Straub & Anderson (1958), Killen (1968), and Cain (1978) for invert roughnesses between 0.71 mm and 1.5 mm, but do not explicitly account for roughness effects.

Figure 2 shows the streamwise development of C_{98} in the developing aerated flow region as a function of the distance from the inception point ($x - x_{Li}$) normalized by the critical flow depth h_c for the two investigated invert roughnesses. A larger invert roughness results in a swifter increase of C_{98} . This suggests that depth-averaged air concentrations might be under or overestimated, if invert roughness is not considered appropriately, which in turn also affects flow bulking predictions. Based on the streamwise development of C_{98} in Figure 2, it is not clear whether effects of invert roughness on C_{98} persist as uniform aerated conditions are approached asymptotically. Nevertheless, the observations highlight the necessity for incorporating effects of invert roughness in empirical relations for air concentrations along spillways, in particular, since most spillways are too short to reach uniform aerated conditions under their respective design discharge.

3.2 Bottom air concentrations

Accurate predictions of air concentrations c_b close to the spillway invert are of particular importance for identifying regions at risk of cavitation (Falvey 1990), but also to evaluate friction reduction (Kramer et al. 2021). Based on the data of Straub & Anderson (1958), Hager (1991) suggested a simple relation for c_b in the uniform aerated flow region as a function of the chute slope only. For the prediction in the developing aerated flow region, Wilhelms et al. (2005) proposed an empirical relation for c_b as a function of the entrained air concentration. Since, the depth-averaged air concentration in the developing aerated flow region increases more rapidly with larger invert roughness (Figure 2), a similar effect is expected for c_b . This is confirmed by the measured bottom air concentrations depicted in Figure 3. While up to $(x - x_{Li}) / h_c \approx 5$, both configurations exhibit similar bottom air concentrations close to zero, the larger invert roughness results in an increase in c_b at a smaller relative distance from the inception point and a more

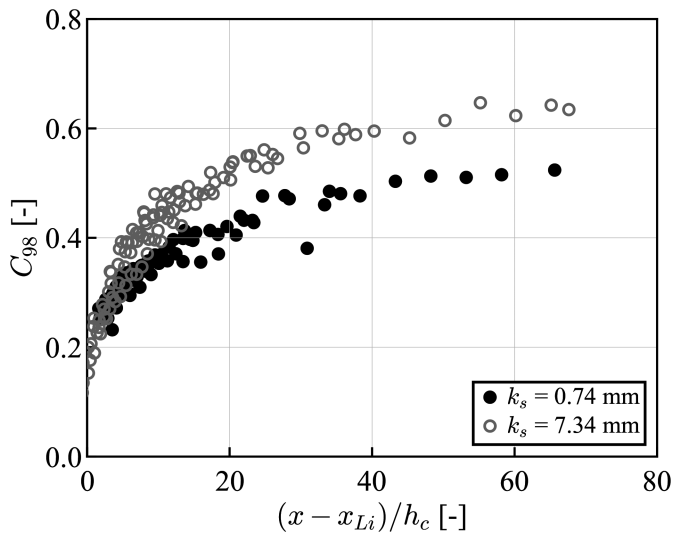


Figure 2. Streamwise development of the air concentration C_{98} downstream of the inception point for the two tested invert roughnesses.

rapid growth of the bottom air concentration. The greater growth rate with increased invert roughness may be explained by higher turbulence levels and, therefore, larger mixing rates. Overall, our findings indicate that predictions of bottom air concentrations and, thereby, assessment of cavitation risk and drag reduction might be improved, if effects of invert roughness are considered accordingly.

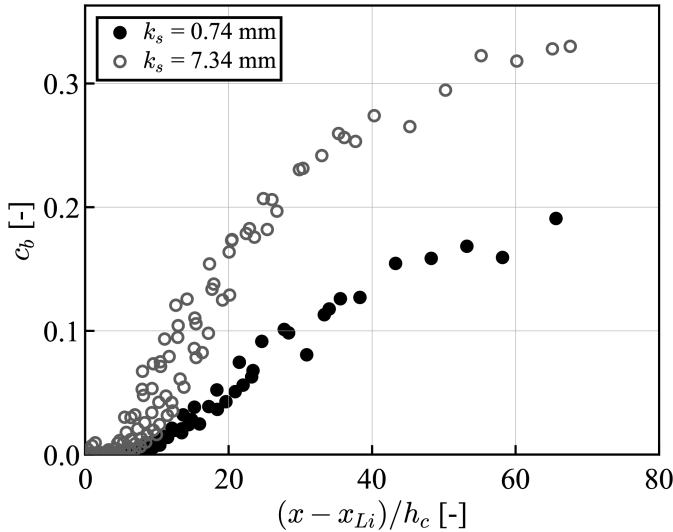


Figure 3. Development of the bottom air concentration c_b in streamwise direction downstream of the observed inception point for the two tested invert roughnesses.

3.3 Friction factors

Reliable estimations of friction factors are crucial for the design of spillways and energy dissipation works, such as stilling basins or flip buckets. Friction factors calculated with the Colebrook-White equation for fully developed turbulent rough pipe flows (Montes 1998) typically provide adequate accuracy for fully developed open channel flows without air entrainment.

For steep spillway chutes, however, this relation may not be sufficient as flow is either not fully developed or drag reduction effects in the presence of entrained air come into play. In the developing non-aerated region, friction factors are more adequately described by the approach of Castro (2009) accounting for the relative boundary layer thickness δ/h :

$$f^{-1/2} = 8^{-1/2} \left[\frac{1}{\kappa} \ln \left(\frac{\delta}{k_s} \right) + 8.5 + \frac{2\Pi}{\kappa} - \frac{1}{\kappa} \frac{\delta}{h} \left(\frac{11}{12} + \Pi \right) \right] \quad (9)$$

where h is the (clear) water depth (h_w), $\kappa = 0.41$ is the von Kármán constant, and $\Pi = 0.2$ is the wake parameter. For fully developed flows ($\delta/h = 1$), and neglecting the wake component, Eq. 9 is equivalent to the Colebrook-White equation for fully developed turbulent flows (Montes 1998).

Darcy-Weissbach friction factors f in the developing non-aerated region are presented in Figure 4a. Experimental results are only illustrated for the regions upstream of $\delta/h \leq 0.8$, as the calculation of shear velocities close to the inception point ($\delta/h \approx 1$) involves considerable uncertainties. Overall, experimental results indicate larger friction factors for smaller δ/h , given a constant relative roughness k_s/h_w . For comparison, the approach of Castro (2009) (Eq. 9) for different δ/h is plotted in Figure 4a. The friction factors for both roughness configurations are in reasonable agreement with values predicted by Eq. 9, with few exceptions. Overall trends confirm that the larger roughness results in increased frictions factors, as it is expected from theory.

In the aerated flow region, friction factors reduce with increasing air concentration (Wood 1983, Chanson 1994, Kramer et al. 2021). Figure 4b compares Darcy-Weissbach friction factors in the aerated region from all experimental configurations to a recently proposed semi-theoretical approach of Kramer et al. (2021) evaluated for different c_b . As the calculation of shear velocities close to the inception point involves considerable uncertainties, experimental results are only illustrated for $c_b \geq 1\%$.

Overall, the experimental data are well represented by the theoretical approach of Kramer et al. (2021), Eq. (10) with $K=0.8$, apart from a few values with small bottom air concentrations:

$$f = (1 - c_b)^{1+K} 0.115 \left(\frac{k_s}{h_w} \right)^{1/3} \left(1 + 0.5 \frac{k_s}{h_w} \right) \quad (10)$$

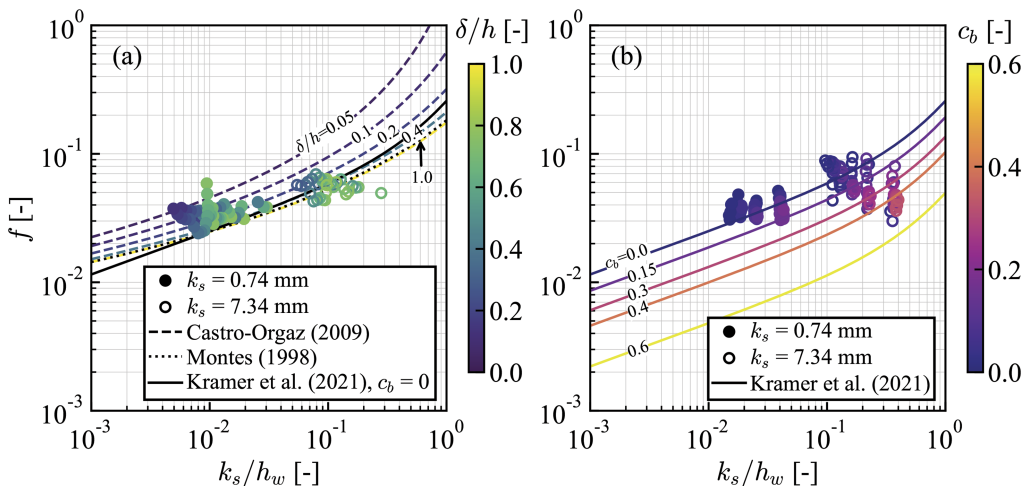


Figure 4. Darcy-Weissbach friction factors f for the two investigated roughness heights in (a) the developing non-aerated flow region, compared to the approach of Castro (2009) for developing boundary layer flow for different δ/h , the Colebrook-White equation for fully developed turbulent flows (Montes 1998) and the approach of Kramer et al. (2021) for $c_b=0$; and (b) the developing aerated flow region compared to the approach of Kramer et al. (2021) for different bottom air concentrations c_b .

Altogether, the experimental results clearly indicate that friction factors are reduced in the presence of air close to the invert. Our previous observations suggest that invert roughness considerably affects streamwise development of bottom air concentrations. Therefore, the quantification of roughness effects on entrained air concentrations can further improve predictions of drag reduction in spillway design.

4 CONCLUSION

In this research, physical experiments were conducted in a large-scale physical spillway model for six flow conditions ranging from $0.1 \text{ m}^2/\text{s}$ to $0.6 \text{ m}^2/\text{s}$ and two distinct invert roughness heights with k_s of 0.74 mm and 7.34 mm, respectively. The investigated flow properties include the clear water and air-water mixture flow depths, depth-averaged flow velocities, friction factors, and air concentrations. We found that the invert roughness has a considerable impact on the depth-averaged air concentrations in the developing aerated flow region downstream of the inception point. Our results show that larger invert roughness leads to greater depth-averaged and bottom air concentrations at the same normalized distance from the inception point.

Our findings are of practical relevance, as currently available methods for describing depth-averaged and bottom air concentrations along spillway chutes do not explicitly account for the effects of invert roughness. For given flow conditions, these methods may produce inaccurate air concentrations when the invert roughness deviates significantly from that of the data used to derive the relations (0.7 mm to 1.5 mm). This may have further implications for spillway design, in particular for assessment of flow bulking, cavitation risk, and drag reduction and emphasizes the need for a more quantitative understanding of the effects of invert roughness on self-aerated boundary layer flows on spillways. Furthermore, our experiments showed that friction factors in the *non-aerated* flow region are larger than those predicted by the Colebrook-White equation for fully developed flow and are better represented by the approach of Castro (2009). Whereas in the *aerated* flow region, the friction factors obtained from our experiments are more accurately represented by the theoretical approach proposed by Kramer et al. (2021), which accounts for drag reduction effects. Overall, our study highlights the importance of a quantitative understanding of invert roughness effects, for the development of more accurate models for designing and optimizing spillway structures.

ACKNOWLEDGEMENT

M. Bürgler and B. Hohermuth were supported by the Swiss National Science Foundation (SNSF) [grant number 197208]. The work of C. Friz in the framework of her Master's thesis is gratefully acknowledged.

REFERENCES

- Anderson, A. G. 1965. Influence of channel roughness on the aeration of high-velocity, open-channel flow. *Eleventh Congress IAHR*. Leningrad. 1(1.37).
- Auel, C., Albayrak, I., & Boes, R. M. 2014. Turbulence characteristics in supercritical open channel flows: Effects of Froude number and aspect ratio. *Journal of Hydraulic Engineering*, 140(4), 04014004.
- Bauer, W. J. 1954. Turbulent boundary layer on steep slopes. *Transactions of the American Society of Civil Engineers*, 119(1), 1212–1233.
- Boes, R. M., & Hager, W. H. 2003. Hydraulic design of stepped spillways. *Journal of Hydraulic Engineering*, 129(9), 671–679.
- Brocchini, M., & Peregrine, D. H. (2001). The dynamics of strong turbulence at free surfaces. Part 1. Description. *Journal of Fluid Mechanics*, 449, 225–254.
- Cain, R. 1978. *Measurements within Self-Aerated Flow on a Large Spillway*. PhD Thesis, University of Canterbury, Christchurch, New Zealand.
- Cartellier, A., & Achard, J. L. 1991. Local phase detection probes in fluid/fluid two-phase flows. *Review of Scientific Instruments*, 62(2), 279–303.

- Castro-Orgaz, O. 2009. Hydraulics of developing chute flow. *Journal of Hydraulic Research*, 47(2), 185–194.
- Chanson, H. 1994. Drag reduction in open channel flow by aeration and suspended load. *Journal of Hydraulic Research*, 32(1), 87–101.
- Chanson, H. 1996. *Air bubble entrainment in free-surface turbulent shear flows*. Academic Press.
- Falvey, H. T. 1990. *Cavitation in chutes and spillways*. Engineering Monograph No. 42, Bureau of Reclamation.
- Flack, K. A., & Schultz, M. P. 2010. Review of hydraulic roughness scales in the fully rough regime. *Journal of Fluids Engineering*, 132(4).
- Hager, W. H. 1991. Uniform aerated chute flow. *Journal of Hydraulic Engineering*, 117(4), 528–533.
- Hohermuth, B., Kramer, M., Felder, S., & Valero, D. 2021. Velocity bias in intrusive gas-liquid flow measurements. *Nature communications*, 12(1), 4123.
- Killen, J. M. 1968. *The surface characteristics of self aerated flow in steep channels*. PhD thesis, University of Minnesota. USA.
- Kramer, M., Valero, D., Chanson, H., & Bung, D. B. 2019. Towards reliable turbulence estimations with phase-detection probes: an adaptive window cross-correlation technique. *Experiments in Fluids*, 60(1), 2.
- Kramer, M., Hohermuth, B., Valero, D., & Felder, S. 2020. Best practices for velocity estimations in highly aerated flows with dual-tip phase-detection probes. *International Journal of Multiphase Flow*, 126, 103228.
- Kramer, M., Felder, S., Hohermuth, B., & Valero, D. 2021. Drag reduction in aerated chute flow: Role of bottom air concentration. *Journal of Hydraulic Engineering*, 147(11), 04021041.
- Montes, J.S. 1998. *Hydraulics of Open Channel Flow*. ASCE Press, Reston VA.
- Peterka, A. J. 1953. The effect of entrained air on cavitation pitting. In Proceedings: *Minnesota International Hydraulic Convention* (pp. 507–518). ASCE.
- Pope, S. B. 2000. *Turbulent flows*. Cambridge University Press.
- Severi, A., & Felder, S. 2017. Boundary layer development on a flat-sloped spillway with micro-roughness. In Proceedings: *13th Hydraulics in Water Engineering Conf* (Vol. 35).
- Straub, L. G., & Anderson, A. G. 1958. Experiments on self-aerated flow in open channels. *Journal of the Hydraulics Division*, 84(7), 1–35.
- Valero, D., & Bung, D. B. 2018. Reformulating self-aeration in hydraulic structures: Turbulent growth of free surface perturbations leading to air entrainment. *International Journal of Multiphase Flow*, 100, 127–142.
- Valero, D., Chanson, H., & Bung, D. B. 2020. Robust estimators for free surface turbulence characterization: A stepped spillway application. *Flow Measurement and Instrumentation*, 76, 101809.
- Wahl, T. L., & Falvey, H. T. 2022. SpillwayPro: Integrated Water Surface Profile, Cavitation, and Aerated Flow Analysis for Smooth and Stepped Chutes. *Water*, 14(8), 1256.
- Wilhelms, S. C., & Gulliver, J. S. 2005. Bubbles and waves description of self-aerated spillway flow. *Journal of Hydraulic Research*, 43(5), 522–531.
- Wilhelms, S. C., Gulliver, J. S., Ling, J. T., & Ling, R. S. 2005. Gas transfer, cavitation, and bulking in self-aerated spillway flow. *Journal of Hydraulic Research*, 43(5), 532–539.
- Wood, I. R. 1983. Uniform region of self-aerated flow. *Journal of Hydraulic Engineering*, 109(3), 447–461.
- Wood, I. R. (Ed.). 2018. *Air Entrainment in Free-surface Flow: IAHR Hydraulic Structures Design Manuals 4*. Routledge.

Nonlinear deterministic model for a double-curvature arch dam

E. Catalano & R. Stucchi

Lombardi Engineering Ltd., Switzerland

ABSTRACT: Deterministic models allow predicting dam response during the structure life-cycle. They are usually based on structural models and assume linear elastic behavior for the structure. However, model precision and reliability could be affected whenever nonlinear effects influence the structure response. We present the case of Emosson dam where nonlinear behaviour of vertical construction joints was found to influence the dam response. Including such aspect in the model enhanced its precision but limited its applicability.

RÉSUMÉ: Les modèles déterministes permettent de prédire la réponse du barrage pendant la durée de vie de la structure. Ils sont généralement basés sur des modèles structuraux et supposent un comportement élastique linéaire pour la structure. Une telle hypothèse pourrait affecter la précision et la fiabilité du modèle lorsque des effets non linéaires influencent la réponse de la structure. Nous présentons le cas du barrage d'Emosson où le comportement non linéaire des joints de construction verticaux s'est avéré influencer la réponse du barrage. L'inclusion de cet aspect dans le modèle a amélioré sa précision tout en limitant son applicabilité.

1 INTRODUCTION

1.1 *Predictive models*

Predictive models are widely used in the field of dam surveillance, providing a crucial tool in monitoring protocols to prevent accidents.

Predictive models can be distinguished in two typologies: statistical models that are based on mathematical/statistical relationships calibrated considering the past behavior of the dam and deterministic models that are based on the response of a structural model to loading conditions. In this latter case, the dam response is usually computed under the assumption of elastic behavior, and its response to all possible combinations of loads, even rare and/or unexpected, can be computed using the superposition effect.

Both approaches have some limitations. Statistical models nothing say on the behavior of the structure, its structural peculiarities. In addition, all exceptional events that go beyond the range of behavior used for the model calibration may produce an alert even if safety is not at risk. This could be somehow reasonable but may produce inconvenient situations. Regarding deterministic models, their precision might be questionable if the behavior of the dam is strongly influenced by some nonlinear effects of one or more than one of its structural components.

In this paper we present the case of Emosson dam, for which a deterministic model based on structural considerations was prepared. The behavior of the dam for low reservoir levels was found to be highly influenced by the nonlinear behavior of vertical construction joints.

1.2 *Dam description and instrumentation*

The Emosson dam, built in the years 1967-1974 in the Swiss Alps, is an arch-type dam with a maximum height on the foundation of 180 m and a length of the crown of 424 m. It is made up of 26 blocks, numbered from the left bank, ranging in width from 9 to 18 m. The thickness of the dam varies between 48.5 m at the base (level 1750.00 m asl) and 9.0 m at the crown (level

1931.50 m asl). Due to the topography on the right flank, the vault extends towards a 130 m long gravity wall.

In 2008 works began for the new Nant de Drance project, a 900 MW pumped storage scheme exploiting the reservoir of the Emosson dam, which was commissioned in 2022. Due in part to the significant change in the operating regime caused by the new project, it was decided to develop a new reliable interpretative model based on structural analysis.

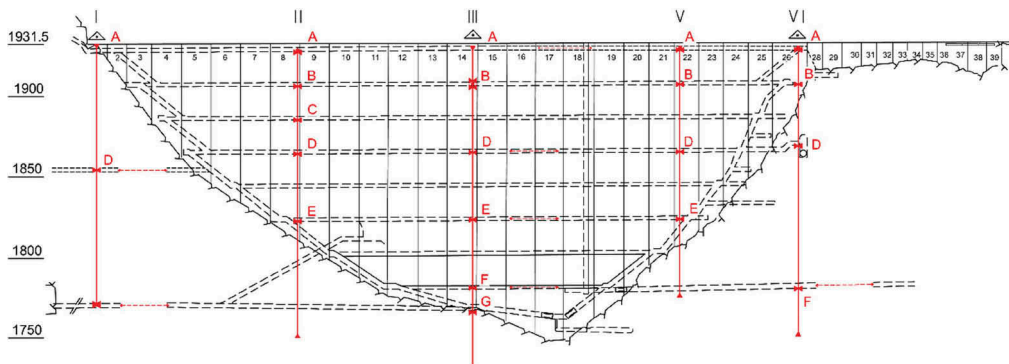


Figure 1. Pendulums installed in the dam body to monitor the structure displacements.

The dam is equipped with a monitoring system including 5 pendulums, direct and inverted, installed during the dam construction to monitor the displacements of the dam (Figure 1). The original temperature monitoring system, consisting in 92 thermometers, showed issues due to ageing. 19 new thermometers were installed in 2015 to replace them. (Figure 2) (Stahl 2021).

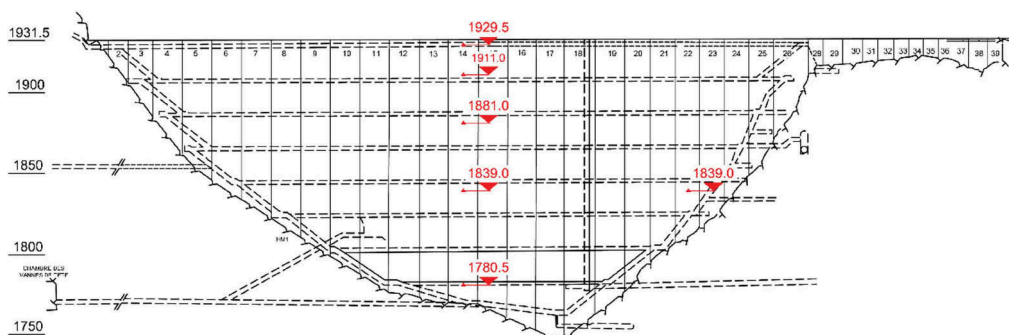


Figure 2. Elevations of the thermometers installed in the dam body to measure concrete temperature.

2 A DETERMINISTIC MODEL FOR EMOSSON DAM

2.1 Elastic model

To set up the deterministic model, a numerical model was prepared with the aim of reproducing the behavior of the dam-foundation system under varying external loading. The finite-difference code $FLAC^{3D}$ (Itasca 2019) was adopted. The numerical model reproduced with high precision the geometry of the dam (Colenco 1972). The implemented geometry of the foundation rock is simplified but included some peculiarity that topography shows on the right and left flanks, as shown in Figure 3.

As usually done when a deterministic model is set up, the dam response was evaluated assuming a linear elastic behavior for both the concrete of the dam and the rock.

The dam response to hydrostatic load was computed by varying the water level in the numerical model. A polynomial relationship between the water level and the dam

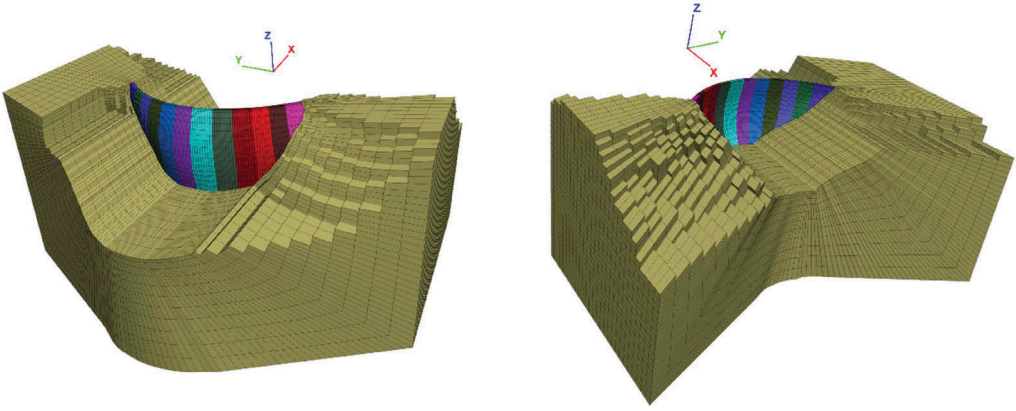


Figure 3. 3D view of the numerical model (left: view from upstream, right: view from downstream).

displacement at a certain point i of the model (i.e. the point of measurement of a pendulum) is then established. With this function, named $\delta_{R,i}$, the expected dam displacement for a given water level can be computed.

Variations in concrete temperature also play a role in the response of a dam. In order to account for this effect, the numerical model was used to compute the displacement due to unit thermal loads. The definition of thermal loads is represented in Figure 4. Considering the elevations of the thermometers, each thermal load is equal to 1 at one elevation and is zero at the other elevations.

By combining the effects of each unit thermal load, multiplied by the actual concrete temperature as measured by the thermometers, a function relating the temperatures with the dam displacement at a certain point i of the model (i.e. the point of measurement of a pendulum) can be established. With this function, named $\delta_{T,i}$, the expected dam displacement for a given concrete temperature distribution can be computed.

The final deformation is obtained applying the superposition effect. The deformation computed by the numerical model at one measurement point i is based on the following expression:

$$\delta_{C,i} = K_i + K_{R,i} \cdot \delta_{R,i} + K_{T,i} \cdot \delta_{T,i} \quad (1)$$

where:

- $\delta_{C,i}$ is the final computed deformation at the i -th measurement point.
- $\delta_{R,i}$ is the deformation induced by the hydrostatic load at the i -th measurement point.
- $\delta_{T,i}$ is the deformation induced by the thermal loads at the i -th measurement point.
- K_i is a calibration constant.
- $K_{R,i}$ is a calibration parameter that allows to modify the global stiffness of the model.
- $K_{T,i}$ is a calibration parameter that allows to modify the concrete thermal expansion coefficient.

The numerical model parameters (concrete and rock stiffnesses and thermal expansion coefficient being the most relevant) were calibrated to fit pendulums' measurements in the period from December 2015 to May 2019. The model precision was evaluated through the computation of the standard deviation of the residuals $\Delta\delta$ (difference between the measured displacement and the one predicted by the model), in the radial and the tangential direction.

$$\Delta\delta_i = \delta_{M,i} - \delta_{C,i} \quad (2)$$

After the calibration process, the following concrete and rock properties were obtained:

- Elastic modulus of concrete, $E_c = 30$ GPa
- Elastic modulus of rock (left bank), $E_{r,l} = 10$ GPa
- Elastic modulus of rock (right bank), $E_{r,r} = 6$ GPa
- Thermal expansion coefficient of concrete, $\alpha = 10^{-5} \text{ } ^\circ\text{C}^{-1}$

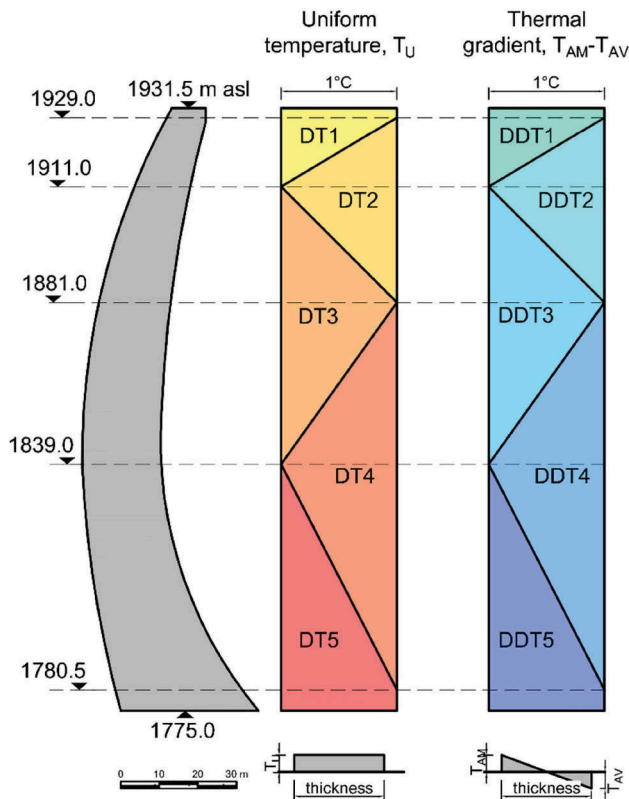


Figure 4. Unit thermal loads.

2.2 Peculiar behavior of the dam for low reservoir level

Setting up the numerical model for Emosson dam, a peculiar behavior was observed while trying to reproduce the behavior of the dam-foundation system. The behavior is expressed by the “elastic model” line in Figure 5, where measured/computed radial displacements at crest elevation (pendulum III in Figure 1) are shown: the computed dam response was found to properly match field measurements for high levels of the water in the reservoir, whereas the dam stiffness is clearly overestimated for low levels of the water in the reservoir.

All calibration efforts were inherently inefficient. It was not possible to match the real behavior of the dam for low reservoir with the model by changing the stiffness of the materials and/or the thermal expansion coefficient. The dam behavior was in fact associated to a dependency of the stiffness of the dam-foundation system on the water level in the reservoir, which cannot be properly reproduced by the equation (1), which operates in the linear regime.

The observed difference was associated to the fact that vertical joints could be opened when the reservoir level is low (usual condition in winter) (Amberg 2021). When joints are open, the arch effect is absent, and the dam behavior is basically associated to the mechanics of independent blocks, more deformable than the monolithic dam. When the level in the reservoir arises and joints close, the arch effect is gradually recovered and the global stiffness of the dam increases.

Joints opening for low reservoir levels was confirmed by measurements, the dam being equipped with joints opening measurements. Joints opening information was available at three different elevations, 1926, 1863 and 1800 m asl.

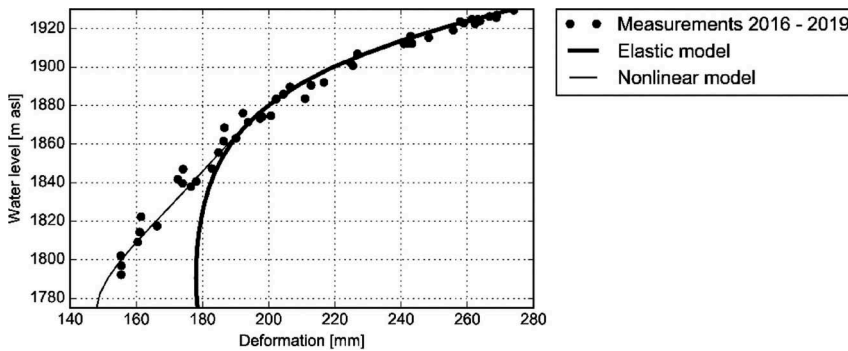


Figure 5. Radial displacements measured/computed at crest elevation, pendulum III - Effects of the introduction of joints nonlinear behavior in model precision.

2.3 Nonlinear model

To account for the nonlinear behavior of vertical joints, the numerical model needed some modifications. The dam was divided into blocks by means of nonlinear interfaces simulating the behavior of vertical contraction joints. The number of blocks that were introduced in the model was lower than the actual number but considered sufficient to capture the influence on the dam's response.

Having to simulate the nonlinear behavior of the dam, dam response depends on loading path. The load history must therefore be correctly considered. Self-weight was simulated considering the dam blocks as independent. The simulation of the injection of the contraction joints has been performed after the completion of the dam construction. In these conditions (empty reservoir), vertical joints are all in contact, but tangential stresses are none.

To reproduce joints opening for the empty/low reservoir configurations, as confirmed by the measurements, a fictitious (cooling) thermal loading is introduced into the model. The fictitious thermal loading allowed introducing the opening of vertical joints for the empty reservoir condition, ensuring the gradual activation of arch effect as the water level increases, and the consequent increase in dam stiffness.

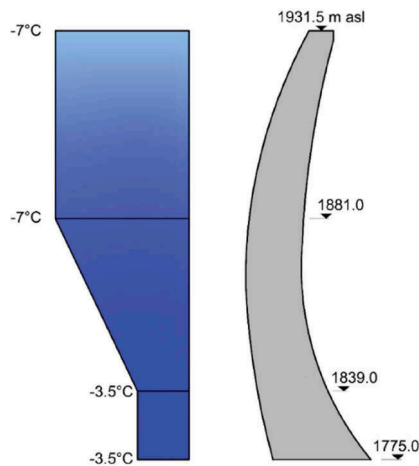


Figure 6. Temperature profile defined for the reference configuration to ensure joints opening prior to the reservoir filling.

To define the fictitious thermal loading, the information was processed according to the following procedure:

- The sum of joints opening measurements in wintertime for low reservoir was computed at the three available elevations (1926, 1863 and 1800 m asl).
- The computed values were assumed as equivalent to a shortening of the arch.
- Given the arc length at those elevations, it was possible to compute the average shortening deformation of the arches. The obtained values, ranging between 70 $\mu\text{m}/\text{m}$ and 35 $\mu\text{m}/\text{m}$, are listed in Table 1.
- Average deformation was assumed as constant and equal to 70 $\mu\text{m}/\text{m}$ from the crest at elevation 1931.50 m asl to elevation 1863 m asl, to vary linearly between 70 $\mu\text{m}/\text{m}$ and 35 $\mu\text{m}/\text{m}$ between elevations 1926 and 1863 m asl, and constant and equal to 35 $\mu\text{m}/\text{m}$ below elevation 1863 m asl.
- Temperatures equivalent to those deformations are finally computed assuming a thermal dilation coefficient of $10^{-5} \text{ }^\circ\text{C}^{-1}$. The distribution of the equivalent temperatures is shown in Figure 6.

Table 1. Opening of joints for empty reservoir configuration.

Elevation [m asl]	Joint opening [mm]	Arc length [m]	Avg. deformation [$\mu\text{m}/\text{m}$]	Equivalent temperature [$^\circ\text{C}$]
1926	29	420	70	-7
1863	25	350	70	-7
1800	7	200	35	-3.5

By introducing the fictitious thermal loading in the numerical model, the displacements predicted by the model as function of the water level are expressed by the “nonlinear model” line in Figure 5. For low reservoir levels, vertical joints are opened, arch effect is absent, and the deformability of the dam is higher. As the reservoir level increases, vertical joints close progressively, the dam monolithic structure is recovered, and deformability decreases.

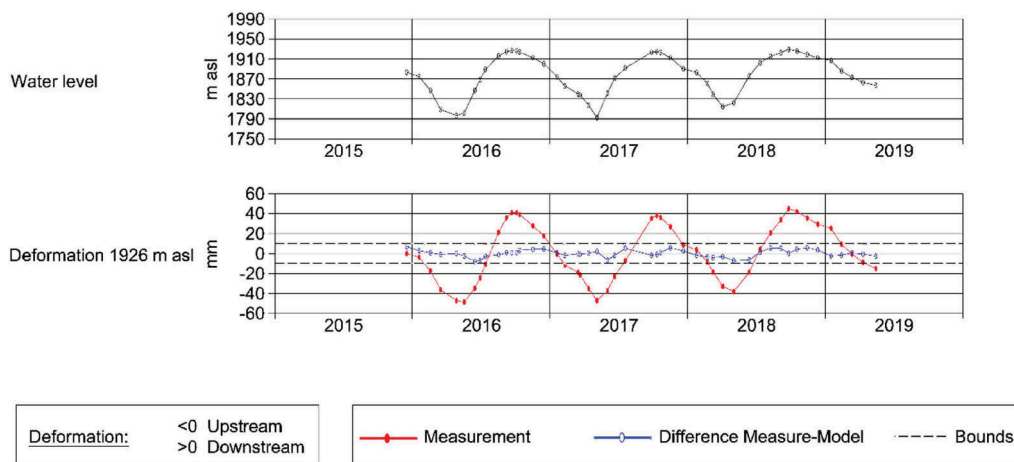


Figure 7. Radial displacements at crest elevation, pendulum III - comparison between model results and measurements and definition of alert bounds.

Figure 7 shows the results obtained by the model in the calibration period: measured radial displacements at crest elevation, pendulum III, are represented by the red line, whereas the difference between the computed and the measured displacement is represented by the blue line. Alert bounds are defined through definition of maximum and minimum bounds of variation of this difference.

It is worth noting that the introduction of this nonlinear element in the model restricts its applicability to usual operating conditions, characterized by low water level in the reservoir during winter and high water level during summer. In fact, joints open in winter, when the water level in the reservoir is low and the concrete is cold. In case a reservoir drawdown would occur in summertime, the dam response would probably correspond to the one of the elastic model (“elastic model” line in Figure 5), with closed joints.

3 CONCLUSIONS

The paper has presented the case of Eموsson dam, for which a deterministic model based on structural considerations was prepared. The behavior of the dam at low levels of the reservoir was found to be highly influenced by the nonlinear behavior of vertical construction joints.

The introduction of joint nonlinear behavior allowed capturing such complex behavior of the dam and reproducing the dam behavior.

The result that was obtained should not be intended as a weakness of the deterministic model but rather the expression of a complex behavior of the dam that doesn’t allow the use of one of the basic principles of structural deterministic models, that is the superposition effect.

REFERENCES

- Colenco, 1972. *Eموsson Arch Dam, geometrical definition*.
- Amberg, F. 2021. Advanced deterministic models to assess dam displacements. Application example at three large dams. *27th ICOLD World Congress*. Marseille, France.
- Stahl, H. & Amberg, F. 2021. Ugrading of monitoring system of Eموsson dam for the construction and operation of a pump-storage plant. *27th ICOLD World Congress*. Marseille, France.
- Itasca Consulting Group, Inc. 2019 *FLAC3D — Fast Lagrangian Analysis of Continua in Three-Dimensions, Ver. 7.0*. Minneapolis: Itasca.

Breach analysis of the Lozorno II. Dam

E. Cheresova, T. Mészáros & M. Mrva

VODOHOSPODÁRSKA VÝSTAVBA, SOE, Bratislava, Slovakia

ABSTRACT: The main objective of the reported manuscript is to analyze the breach of an earthfill embankment, specifically the Lozorno II. dam, serving for further purposes to possible reclassification of the hazard category of the dam. The Lozorno II. dam is located in the Slovak republic, lying in the Záhorská Lowland, where the need for reclassification results from intensive urban development downstream of the dam. For our work purposes we developed an HEC-RAS model from a digital terrain model (DTM) creating geospatial data in RAS Mapper to represent the river system and floodplain area specifically for performing a dam breach analysis with HEC-RAS Version 6.3.1. Results of the analysis, and the brief discussion on it are included in the presented paper.

1 INTRODUCTION

Inspired by the interest to revise the current dam safety program and management of the Lozorno II. dam, due to intensive urban development downstream of the dam in the past 3 decades, we performed a dam breach induced break wave analysis with HEC-RAS.

The presented dam breach and the break wave analysis has a purpose to further serve as a main entry to the dam hazard potential reclassification.

1.1 *Hazard potential classification*

Engineers in the dam safety industry generally use “risk” concepts as a guiding philosophy for design, construction, operation, and maintenance of dams. Risk is generally described as having two components: likelihood of failure, and consequences of failure. Both components contribute to the total risk profile of a dam, however, the two components are independent of each other. The present-day condition of a dam factors into the likelihood component, whereas the failure potential of a dam factors into the consequence component. Arguably, the most common categorization is the anticipated downstream consequences of a dam failure, also known as hazard potential classification or hazard rating. Dam safety engineers most commonly use the hazard potential classification system as a prioritization tool to focus attention on those dams with the most severe potential consequences of failure. It is important to understand that the hazard potential classification of a dam is not a reflection of the present-day condition of a dam (Schoolmeesters).

Hazard creep, also known as risk creep, is a term describing the gradual increase in anticipated consequences of a dam failure due to infrastructure development. Even though the physical condition of a dam may not have changed, hazard creep can result in an immediate adverse impact on the overall risk profile of a dam because the consequence component has increased (Schoolmeesters).

In the Slovak republic hydraulic structures are classified in categories from I. to IV., where the I. category represents the most severe potential consequences of failure. The overall risk profile, or factor and the classification itself is based on 4 main factors:

$$F = FOB + F\check{S} + FN\check{S} + FZ \quad (1)$$

where F = overall risk factor; FOB = population threat factor; F \check{S} = factor of financial losses from direct damages; FN \check{S} = factor of financial losses from indirect damages and FZ = loss of benefits from the operation of the hydraulic structure.

The hazard potential category of the dam then sets the legislative foundation for dam safety measurements and supervisions density and governs the obligation to build an autonomous warning and notification system.

1.2 *The Lozorno II. dam*

The Lozorno II. dam is a 16 m high earthfill embankment located in the west of Slovakia, in the Bratislava Region, Malacky district - Lozorno municipality. The dam is built on Suchý stream, situated below the confluence of Suchý and Záhorský streams, forming a multipurpose water reservoir with a max. storage capacity of 2 050 946 m³.

The structure was put into permanent operation in 1986, however the hazard category of the dam was first evaluated in 1979 based on the “Expert report for determining the category for Lozorno Dam”, according to which it fell into the III. hazard potential category. In 1994 the maintenance and administration of the dam went from the former State Reclamation Administration to the Slovak Water Industry State Owned Enterprise, and after developing a new expert report the Ministry of Agriculture of the Slovak Republic on February 1, 1995 reclassified the structure into II. category.

Since 1995 (last hazard potential reclassification of the structure), intensive construction and urban development have been taking place downstream of the dam, that impacts the overall risk profile of the dam. See Figures 1 and 2.



Figure 1. Aerial shot (orthophoto) of the Lozorno II. dam from 2012.
(Source: www.mapy.cz)

2 DAM BREACH AND BREAK WAVE ANALYSIS

For the purposes of the indicated dam breach and break wave analysis we developed a numerical 2D model in HEC-RAS from a digital terrain model (DTM) creating geospatial data in RAS Mapper to represent the river system and floodplain area.



Figure 2. Aerial shot (orthophoto) of the Lozorno II. dam from 2020. (Source: GKÚ Bratislava).

2.1 Theoretical basis

The presented analysis includes a dam breach estimation and a following 2D unsteady flow hydrodynamic model of the induced break wave.

Realistic estimation of the dam breach is crucial in order to make an accurate estimate of the outflow hydrographs and downstream inundation. Currently, to estimate breach location, size and development time, HEC-RAS offers three breaching methodologies. In our analysis we used the “User Entered Data” method, where the software requires either to manually enter the dam breach parameters (in this case estimation of the parameters should be done outside of the software) or by using one of the built-in regression equations.

Several researchers have developed regression equations for the dimensions of the breach, as well as the failure time. From the regression equations, which are built-in the software HEC-RAS we used the one developed by Dr. Froehlich in 2008 by utilizing 74 earthen, zoned earthen, earthen with a core wall, and rockfill dam data sets.

Froehlich’s regression equations:

$$B_{ave} = 0.27 K_0 V_w^{0.32} h_b^{0.04} \quad (2)$$

$$t_f = 63.2 \sqrt{V_w / (g h_b^2)} \quad (3)$$

where B_{ave} = average breach width (meters); K_0 = constant (1.0 for piping); V_w = reservoir volume at time of failure (cubic meters); h_b = height of the final breach (meters); g = gravitational acceleration; t_f = breach formation time (seconds) (Brunner, 2014).

After breaching the modelled dam, the resulting flood wave is routed downstream using the unsteady flow equations.

In practical applications, the continuity equation is often used along with leading equations, such as the Navier-Stokes equation, to simulate fluid flow and predict the behavior of a fluid system. The Navier-Stokes equation is a mathematical expression of the conservation of the mass and the momentum for the fluid. It describes the relationship among the pressure, the velocity of the fluid, and the internal forces due to viscosity and gravity. It is expressed as follows:

$$\rho \left(\frac{\partial v}{\partial t} + v + \nabla v \right) = -\nabla p + \nabla \cdot \tau + \rho g \quad (4)$$

where:

ρ = the fluid density;

v = the fluid velocity vector;

t = time;

∇ = the gradient operator;

p = the pressure;

τ = the viscous stress tensor;

g = the acceleration due to gravity.

The Navier-Stokes equations describe the motion of fluids in three dimensions. In the context of channel and flood modeling, further simplifications are imposed. One simplified set of equations is the Shallow-Water (SW) equation (Brunner, 2020).

The Shallow-Water equations considered in this analysis consider only the depth-averaged flows and hence cannot reproduce certain phenomena that occur in nature and in which some velocity variation with depth has to be allowed for (Zienkiewicz).

2.2 2D Numerical model

The 2D numerical model is based on the Digital Terrain Model (DTM) presented on Figure 3, which represents the Lozorno II. dam and its surroundings with accuracy higher than 1 meter. The used DTM was further modified in QGIS by building overlay, so that the model considers not only the elevation of the terrain, but also the height of the buildings located beneath the dam. This modification can provide a more accurate representation of the terrain, as buildings can significantly affect the flow of water.

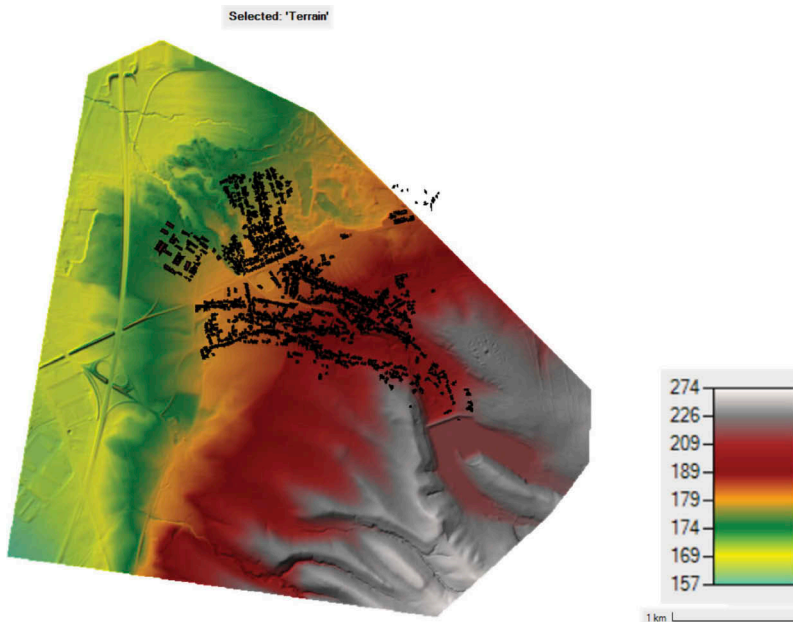


Figure 3. DTM of the Lozorno II. dam and its close area.
(Source: GKÚ Bratislava).

Further, orthophotos were utilized to identify natural and man-made features like vegetation, buildings, and structures that can affect flow dynamics. HEC-RAS does have a built-in tool called “ArcGIS World Imagery” that allows to load an orthophoto directly into the project. Simply entering the coordinate system (S-JTSK 5514) is enough to use this tool correctly.

After loading the relevant DTM and orthophotos, we used the Storage Area/2D Flow Area (SA/2D) breach model configuration option of the utilized software (HEC-RAS), with the

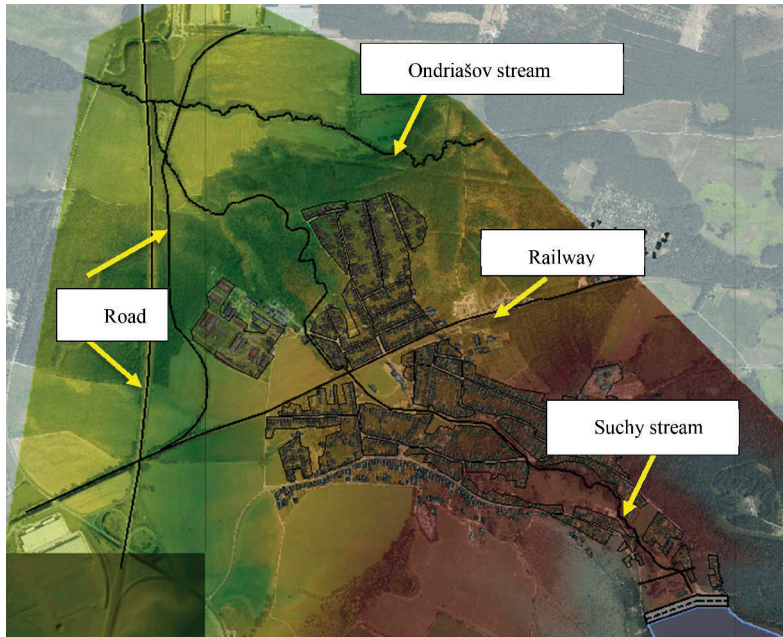


Figure 4. Natural and man-made features identified in the considered area.

Pool Routing method applied for directing the incoming flood hydrograph through the 2D Flow Area. The dam body, which connects the reservoir (Storage Area) and the down-stream area (2D Flow area), was represented by a SA/2D area connection as presented in Figure 5.

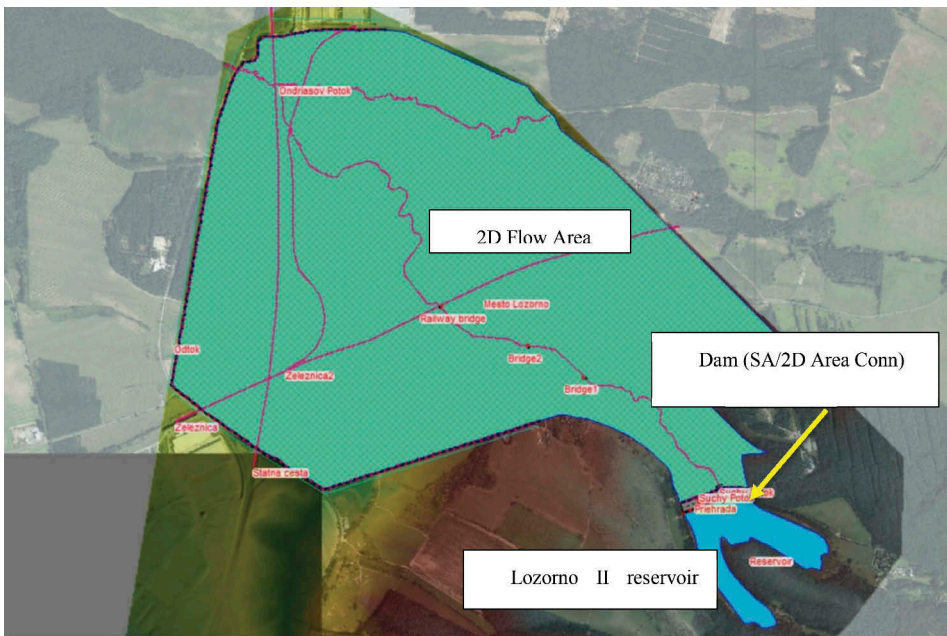


Figure 5. Model geometry and the breach model configuration option.

For the defined 2D Flow Area the default Manning's n value was set to 0,06, which corresponds to areas with light brush and trees in summer. For the purposes of the performed numerical analysis we further specified corresponding Manning's n values for the considered subsequent downstream areas, based on rages given in (Brunner, 2020), as shown on Figure 6.

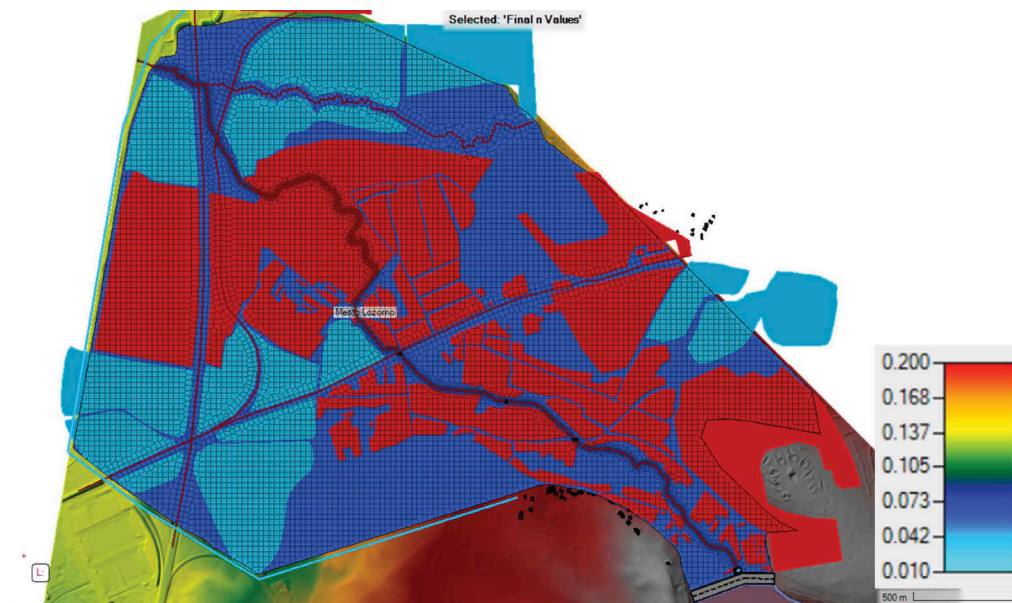


Figure 6. Areas defined with different manning's n values.

Three bridges located in the 2D Flow Area are important for this model. In order to enter the bridge parameters (including their width, length, and thickness), a visual inspection was conducted on site.

Further, the subsequent task involved the creation of break-lines, that were established in areas like as embankments, roads, and directly along the channel itself.

2.3 Time stepping and boundary conditions

In the reported calculation, at the 2D Flow Area perimeters, we used the normal depth (Manning's equation) boundary condition as the actual water level corresponding to a specific flow rate at the downstream end of this model is unknown. Whereas, the initial condition used for this calculation was the water surface elevation within the storage area equal to the max water sur-charge level: 219,00 m a. s. l.

To simulate the desired dam breach induced break wave we conducted a 2D unsteady flow hydrodynamic analysis. The duration of the simulated 2D unsteady flow hydrodynamic analysis was set to 8 hrs., with 2 sec. computational interval, 5-minute mapping output interval and a 15-minute detailed output interval. In order to fill the downstream river base (to model a realistic hydrological event) we set the initiation of the dam breach to 2 hrs. 20 min, with an estimated breach formation time equal to 35min (i.e. full dam breach at 2hrs 55min), and at the downstream dam toe we defined river inflow in the form of an additional boundary condition (inflow hydrograph).

3 LAYOUT OF TEXT

The maximum breach flow ($919.33 \text{ m}^3 \cdot \text{s}^{-1}$) was calculated 35 minutes after initiating the dam breach. Inundation mapping, depths and velocities of the computed flood wave at this time are presented on Figures 7 and 8 respectively.

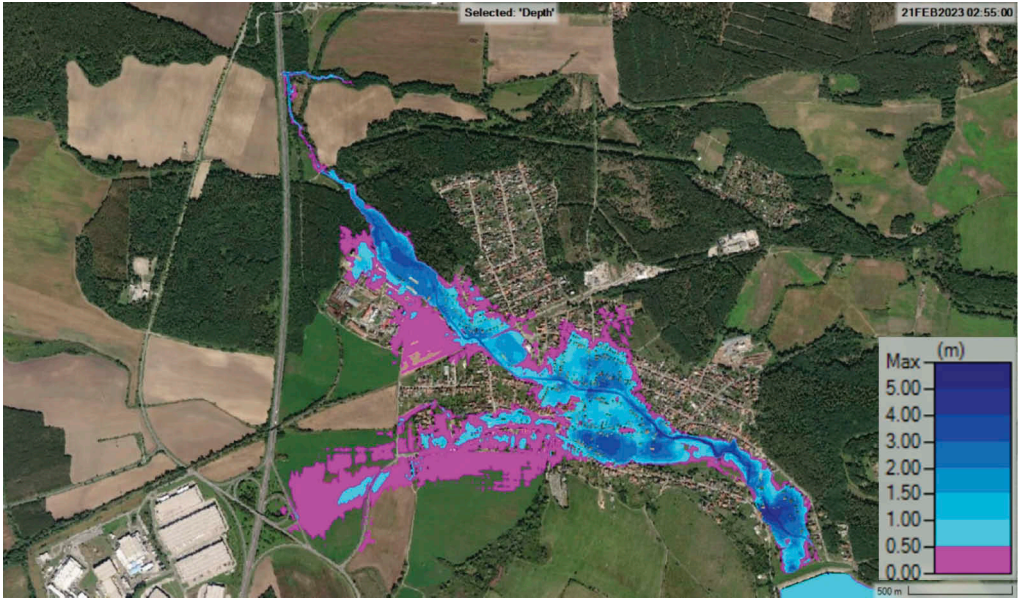


Figure 7. Inundation depths calculated at 2hrs 55min modeled time (35 min. after initiating dam breach).

As shown on Figures 7 and 8, 35 minutes after the dam breach initiation a relatively wide area of the Lozorno municipality was already impacted. Whereas, the buildings situated closest to the dam would be hit by the break wave in less than 15 minutes, which has a significant influence on effective warning and notification of the impacted population.

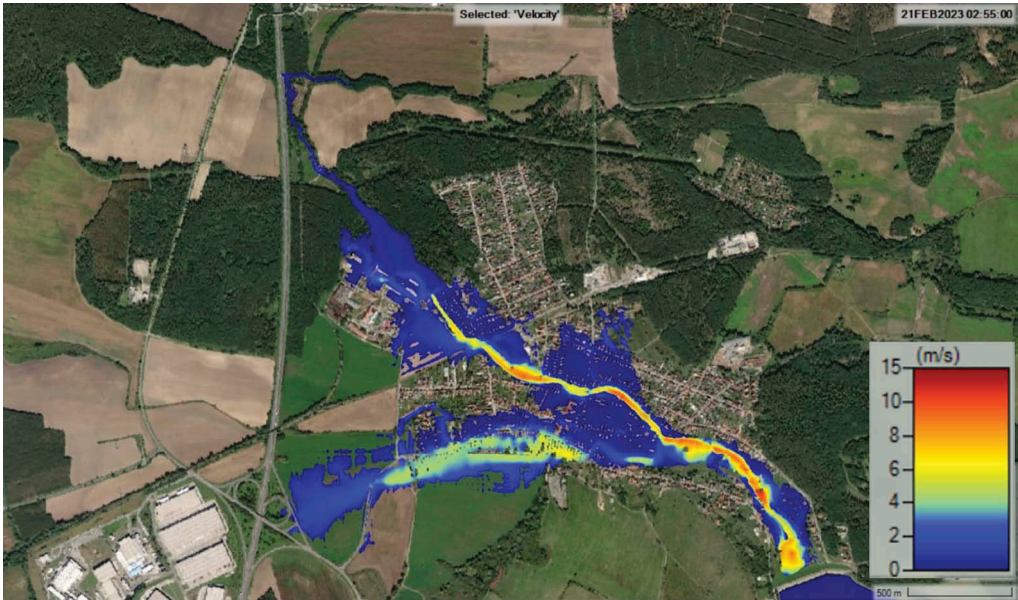


Figure 8. Break wave velocities calculated at 2hrs 55min modelled time (35 min. after initiating dam breach).

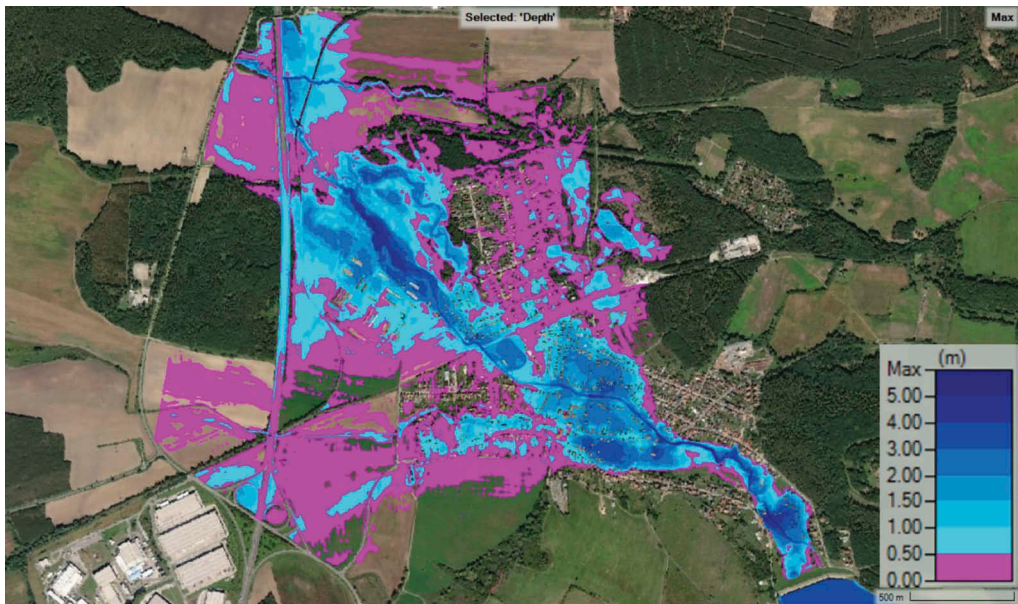


Figure 9. Maximum inundation depths calculated throughout the numerical solution.

The maximum achieved inundation reach and breach flow depths and velocities throughout the entire considered time frame are presented on Figures 9 and 10 respectively.

As shown on Figures 9 and 10 considerably large areas of the Lozorno municipality will be flooded with a depth higher than 3 m. This indicates relatively high population threat factor and factor of financial losses, which should be further calculated for the hazard potential reclassification.

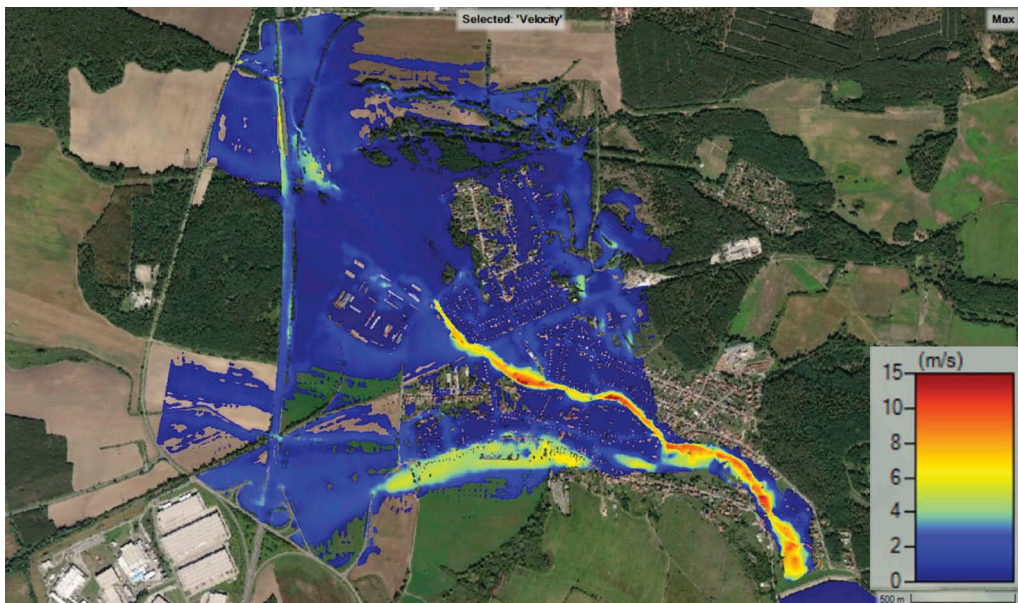


Figure 10. Maximum breach flow velocities calculated throughout the numerical solution.

Figure 11 displays a hydrograph plot from an Inline Structure, that was used to model the Lozorno II. dam. The plot shows the total flow rate of water in in $\text{m}^3 \cdot \text{s}^{-1}$, represented by a black solid line on the left vertical axis. The water stage elevation data is also shown on the plot, with the Head Water level represented by a black dotted line (Stage HW) and the Tail Water level represented by a black dashed line (Stage TW). The water stage elevations are in m a. s. l. and are displayed on the right vertical axis.

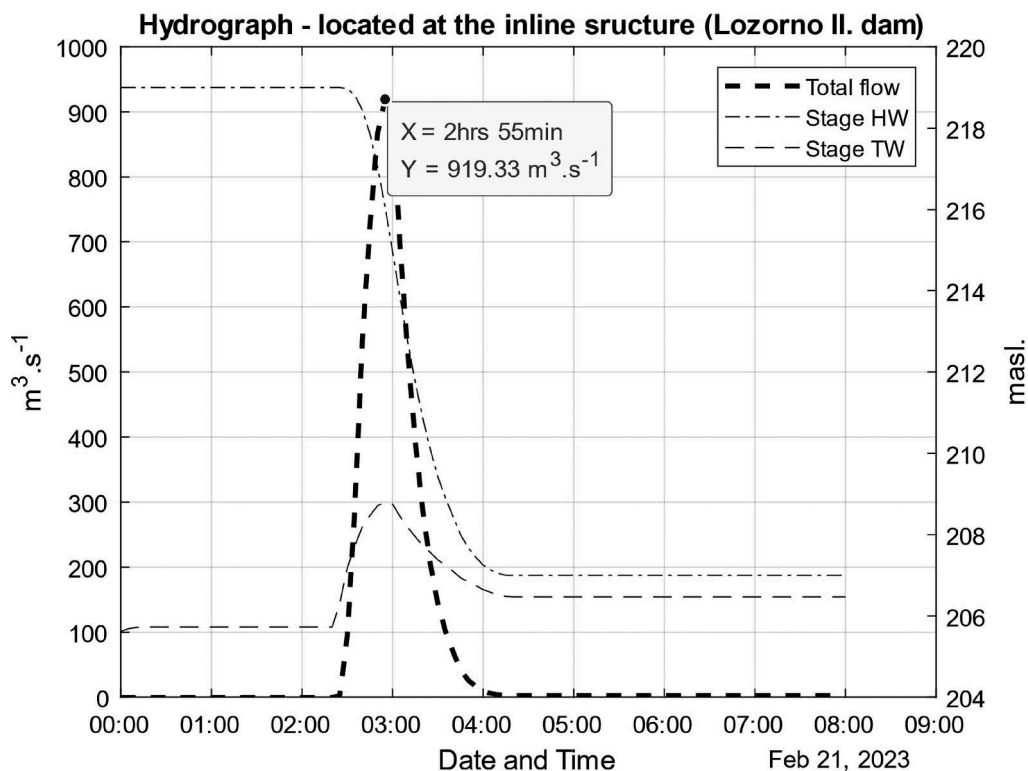


Figure 11. Hydrograph plot from the Lozorno II. dam inline structure.

4 CONCLUSIONS AND FURTHER DEVELOPMENTS

In this numerical solution, we performed a breach analysis of the Lozorno II. dam. The main revelations and conclusions of the presented work are as follows:

1. Although it is crucial to carefully determine all four partial risk factors that contribute to the overall risk profile of the investigated dam (as required by the Slovak legislation this needs to be done in a separate study based on the presented results), the analysis suggests that in the event of a Lozorno II dam breach, the Lozorno municipality would be affected by the breach wave in less than 15 minutes. Additionally, approximately 360 buildings would lie within an inundation area deeper than 1.5 meters, and around 800 buildings would be affected by an inundation between 0.5 to 1.5 meters.
2. Assuming that the inundation deeper than 1.5 meters would affect 100% of the population and that the inundation between 0.5 and 1.5 meters would affect 50%, and taking into account an estimated average of 4 people per building, the approximated population threat factor (FOB) is equal to 3040. This is calculated as follows: 360 buildings at a depth greater than 1.5m ($360 \times 4 = 1440$ people) and 800 buildings at a depth between 0.5m and 1.5m ($800 \times 2 = 1600$ people), resulting in a total population at risk of 3040 people.

3. Based on the estimated population threat factor (FOB) of 3040, it can be concluded that the overall risk profile of the Lozorno II. dam is greater than the criteria ($F > 1000$) for reclassifying dams into the I. category, which represents the highest hazard potential category in the Slovak Republic. Therefore, it is important to prioritize further safety measures and consider appropriate risk reduction strategies for the dam.

The presented paper highlights the importance of the dam breach analysis in determining the hazard potential of a dam. To enhance the accuracy of the analysis, the following factors should be considered for future improvements:

1. While the breaching methodology used in this analysis provides a realistic estimation of the dam breach parameters for the dam type being investigated, it is recommended to use several methods to predict a range of breach sizes and failure times for each hydrologic event.
2. An iterative process should be used for determining the extent of the modelled downstream flood area. Our recommendation is to consider areas with a flood wave depth higher than 0,5 m.

ACKNOWLEDGEMENTS

We gratefully acknowledge Ing. Martin Orfánus, PhD. for his valuable suggestions and discussions.

REFERENCES

- Brunner, G., 2014. *Using HEC-RAS for Dam Break Studies*. Davis: U.S. Army Corps of Engineers'.
- Brunner, G.W., 2020. *HEC-RAS, River Analysis System Hydraulic Reference Manual*. Davis: U.S. Army Corps of Engineers'.
- Schoolmeesters, R. Lesson Learned: The hazard classification of a dam can change over time (hazard creep). In <https://damfailures.org/lessons-learned/the-hazard-classification-of-a-dam-can-change-over-time-hazard-creep/>. Association of State Dam Safety Officials.
- Zienkiewicz, O.C., Taylor, R.L., Nithiarasu, P., 2014. *The Finite Element Method for Fluid Dynamics, Seventh Edition*. Waltham: Elsevier.

Dam safety and surveillance: Return of experience from the perspective of the Swiss Federal authorities

M. Côté, R.M. Gunn & T. Menouillard

Swiss Federal Office of Energy, Dam Safety and Surveillance Section, Bern, Switzerland

ABSTRACT: This paper provides a return of experience from the perspective of the Dam Section of the Swiss Federal Office of Energy, SFOE, on a range of challenging safety and surveillance issues that the Swiss dam industry is facing today. These include the implementation of new regulations, pumped storage schemes, flood verifications, dam ageing, climate change, the prioritization of safety measures, reservoir slope stability, sedimentation, hydraulic discharge structures, bi-national safety and surveillance requirements, the impact of solar photovoltaic panels on dam safety, surveillance and other subjects. In accordance with Art. 29 of the WRFO (Water Retaining Facilities Ordinance, Status on the 1st January 2023) the main objectives of the paper are to ensure the exchange of information at an international level, secure expertise, promote research and to outline some of the tasks undertaken by the Swiss authorities, putting the emphasis on challenging problems. The conclusions allow dam owners and operators to perhaps reassess their dam surveillance and safety concepts and take appropriate measures in a timely manner.

1 SWISS DAM SAFETY CONCEPT

1.1 Overview

The rupture of a dam can cause considerable loss of life and damage to property in the downstream reach and they are considered as structures with a high hazard potential. For this reason, Switzerland has adopted a Federal Act on Water Retaining Facilities (WRFA, SR 721.101) to guarantee the safety of people and property and to describe the responsibilities of the parties.

The Swiss legislation relevant to WRFA is defined in references (SFOE 2010, 2022). The supporting directives and accompanying help manuals are listed in references (SFOE 2014; 2015a, b, c, 2017, 2018, 2021). The safety of Swiss WRFA is founded on *three key pillars* which constitute the Swiss dam safety concept: (I) structural safety; (II) surveillance and maintenance and (III) emergency concept. Pillar I is based on *state-of-the-art* design and construction techniques, pillar II *object-orientated* surveillance and maintenance methods and pillar III, *emergency awareness and preparation*. The inter-connected relation between pillars I and II is the *minimization of risk* and between pillars II and III, the *mastering of residual risks*. The criteria to define whether a WRFA is subjected to Swiss legislation are (1) *retention height and reservoir capacity* and; (2) *particular risk potential*. The latter subordination criterion is based on a presumed scenario (breach) and the impact of that scenario (risk to human life or major material damage), the SFOE web site provides more details.

2 SAFETY OF WATER RETAINING FACILITIES, PILLAR I: STRUCTURAL SAFETY

2.1 Overview

The structural safety of dams is mainly based on directives (SFOE 2017, 2018, 2021) and further details related to the framework, recent changes and future perspectives of Swiss dam

legislation can be found in the SFOE reference (Schwager et al. 2023). These directives have been purposely written by representatives of the dam engineering community under the auspices of the SFOE. They endeavour to consider the latest state-of-the-art technologies and concepts that are continually developing with time.

2.2 *Return of experience and future challenges*

The previously mentioned directives are more orientated towards existing dams with the ultimate legal goal to guard against an *uncontrolled release of water*ⁱ rather than the design and construction of new dams whereby a multitude of other objectives must be handled. However, some dam heightening projects in the context of pumped storage schemes or upgrading have been successfully realised with a combined use of SFOE directives and other Swiss, associated European Standards (SIA). Experience from these projects has clearly demonstrated the importance of well-coordinated work schedules that involve the SFOE at the *early stages* of the project with particular reference to *first-reservoir filling* and *operational* dam safety requirements.

2.2.1 *The impact of new flood verification studies on Swiss regulations*

Swiss directive C2 on flood safety (SFOE 2018) was first published in 2017 and includes the latest *design flood* methodologies related to estimating natural inflow based on statistical inflow (M1) and precipitation (M2) measurement series. *Flood safety level* methodologies as a function of the Design flood and probable maximum precipitation (PMP) procedures are also given. Two other methods referred to as “SG”, synthetic hydrograph and “NAM”, precipitation discharge model, are also provided in directive C2. For the latter, recent extreme flood estimation studies named EXAR, *Extremhochwasser an der Aare* (Andres 2021) and *Extremhochwasser Schweiz* have been published or are under preparation respectively (Schwager et al. 2023).

EXAR studies *reduce flood verification uncertainties* and the results have already been implemented in approximately 75% of the 19 dams referred to in the EXAR report (Andres 2021).

2.2.2 *Discharge structures*

In general, functionality tests as per appendix 2 of the directive C2 (SFOE 2018) have been successfully performed and the SFOE experience has shown that the *organisation* of these tests in relation to particular discharge events, such as high natural inflows, is a critical element of the test procedures. In some cases, the outlet capacity has also been reassessed and corrective measures have been taken to allow for *normal*, *extraordinary* and/or *extreme* inflow events. Moreover, regular testing of local and remote-control gate systems needs to be followed to avoid the possibility of blocked gates or the overloading of hydraulic systems when manoeuvring gates.

3 SAFETY OF WATER RETAINING FACILITIES, PILLAR II: SURVEILLANCE AND MAINTENANCE

3.1 *Overview*

The main objective of surveillance is to obtain quantitative and qualitative information, respectively, on the behaviour, condition and functionality of the dam to determine possible measures in case of detected anomalies. Herein, “*dam*” refers not only to the dam body itself, but also to the outlet works, the reservoir, the abutments and the foundation.

An important secondary aspect of the surveillance is also to have a database of observations and measurements that can be used in future studies, especially in case of the unexpected behaviour or changes in the condition of the structure. Surveillance is based on the following elements:

i. Text shown in *italics* is aimed at highlighting a key point or subject.

- visual checks of the condition;
- measurements and their interpretation to characterise the behaviour;
- the correct control and operation of gated outlet structures in accordance with regulations.

3.2 *Return of experience and future challenge*

3.2.1 *Prioritizing safety measures into “must” and “nice to have” categories*

According to Swiss legislation, the operator must carry out measurements and visual inspections in accordance with the surveillance regulation. This is referred to as *first level* surveillance.

The operator must also ensure that a qualified and experienced professional engineer evaluates the results of measurements on an ongoing basis, carries out a visual inspection of the water retaining facility once a year and records the findings in an annual measurement and inspection report. The annual inspection in accordance with Art. 18 of (SFOE 2022) is the *second level* of surveillance. The objective of the annual report is to verify the behaviour of the dam based on technical evaluations and observations to ensure conformity with dam safety requirements (SFOE 2010) to (SFOE 2022).

For dams with a water height of at least 40 meters or if the water height is at least 10 meters and the storage capacity is greater or equal to 1 million m³, the operator must ensure that experienced experts in the fields of civil engineering and geology carry out a comprehensive safety assessment every five years. This is referred to as the *third level* of surveillance.

The annual report of the qualified professional and the expert five-year expertise report must provide a global synthesis of the results and observations. The objective is to relate all the observations, measurements and tests, with conclusions regarding the condition and behaviour of the facility, its surroundings (banks) and auxiliary installations. Any deviations from standard behaviour or normal condition must be clearly emphasised and a follow-up of the recommendations already listed above must be provided.

The annual report is submitted to the operator, when he is not the author, and transmitted to the supervisory authority. This is known as the *fourth level* of surveillance. The same process is followed for the five-year expert report. Every year, the supervisory authority and its specialists receive a considerable number of annual and five-year reports with many recommendations. Over the years, the supervisory authority has come to the conclusion that it is sometimes difficult to distinguish between essential (must) and desirable (nice to have) recommendations in the context of SMART (*Specific, Measurable, Attainable, Relevant and Time-based*) solutions. There is often a wide margin of interpretation about the implementation or not of recommendations and this has led to many discussions between the operators and the authorities. To improve this situation, the authority asked qualified professionals and experts to present their recommendations at the end of the reports into two categories: “*must*” and “*nice to have*”. The *must* recommendations are considered to be compulsory and have to be implemented in a timely manner. This is fixed between the professional engineer/experts and the operator and thereafter, agreed by the authorities. *Nice to have* recommendations are voluntary and may sometimes just be reminder points to be re-evaluated during the next safety evaluation period.

When submitting an annual or a five-year report, the authority systematically asks the operator to submit an accompanying *position statement* on the recommendations of the professional engineer and/or experts ensuring that all parties understand the recommendations including when and how they will be implemented. The SFOE experience has shown that the parties do in general agree on the content of recommendations, but not always on the time-based implementations due to financial or other non-technical reasons. This emphasises the importance of classifying recommendations into *must* and *nice to have* categories.

3.2.2 *Dam safety and surveillance for pumped storage schemes*

Given the current situation of the energy market in Europe, pumped storage projects have increased significantly in recent years. This type of facility makes it possible to meet the

growing demand for renewable energy and to benefit from their flexibility and energy storage capacity. They are designed to respond to peak energy needs, particularly in urban areas where electricity demand varies considerably. In addition, technological advances have made pumped storage projects more cost-effective by reducing operational and maintenance costs and improving efficiency.

Pumped storage dam facilities often involve significant economic stakes and social and environmental responsibility on the part of the operators, which are of considerable importance when making management decisions for this type of development. The supervisory authority has seen in recent years that having two different operators involved in the same development can lead to many issues that need to be resolved in advance. Careful planning of the different interactions must be done properly in the interest of short- and long-term safety. Indeed, coordination between the two operators can be difficult, particularly with regard to the management of water levels in the reservoir, equipment monitoring, maintenance management and emergency plans. Management conflicts between *multiple operators* can lead to delays in monitoring, maintenance, and repair operations, which can have long-term negative consequences for safety. A good example of this is the execution of geodetic measurement campaigns whereby the water level in the reservoir must remain stable over a certain period of time.

It is therefore essential that the multiple operators work closely together to ensure the safety of the facility in terms of monitoring, operation of outlet structures, flood management and residual risk management. This can be achieved through clear contractual agreements and open and frequent communication between the parties involved, as well as the implementation of strict safety processes and/or regulations for the management of pump and turbine operations. The supervisory authorities are particularly vigilant in approving documents and ensuring that the monitoring regulations, operation of outlet structures and emergency procedures of the different dams that are part of a pumped storage facility are compatible. *Common regulations* can be of considerable, if not essential, benefit to this type of facility. This is particularly true for emergency planning where the common priority of the operators must be to prevent or mitigate the consequences of an accident or unplanned incident. Establishing a common emergency management strategy allows operators to quickly and effectively coordinate emergency response, minimise loss of life and property damage, and protect the environment. These rules should define warning procedures, responsibilities and obligations of stakeholders, the means of communication and coordination, and contact information for the various parties involved in the emergency strategy.

3.2.3 *Monitoring the (creep) sliding of dam reservoir slopes*

Digital tools are being increasingly used to monitor landslides, especially in the vicinity of dams. Using motion sensors, remote sensing systems, and numerical models, monitoring experts can closely track areas at risk and anticipate landslides near dams. Satellite imagery can also track cracks and landslides from a distance. These digital tools are invaluable for the management of potential risks from dams and thus for the protection of people living downstream.

In recent years, the SFOE has identified two systems that are particularly useful for the five-yearly assessments of Swiss dams. They allow geologists to illustrate the evolution of the terrain in the vicinity of the dam, respectively of its reservoir, and facilitate the understanding and discussions of the different people involved in the surveillance and the resulting decisions. These are the Guardaval (Rouiller et al. 2004, 2005) and INSAR (Fielding & Rosen 2011, Hanssen & Meurs 2001, Li et al. 2018) systems, two remote sensing technologies used to monitor landslides (Mandel et al. 2005). These technologies differ in their approach and measurement methods.

Guardaval (Rouiller et al. 2004, 2005) uses high-resolution optical satellite images to detect surface changes and identify landslides. It uses image processing algorithms to track surface features and detect subtle changes. On the other hand, INSAR (Fielding & Rosen 2011, Hanssen & Meurs 2001, Li et al. 2018) uses radar images to measure changes in ground deformation by detecting changes in the distance between the satellite and the ground. It measures

landslides by measuring the phase changes of radar waves reflected from the earth's surface. The main difference between Guardaval and INSAR is therefore the measurement method used. Guardaval focuses on surface changes, while INSAR measures changes in ground deformation. Therefore, Guardaval is more suitable for detecting subtle landslides, while INSAR is more suitable for detecting larger and faster landslides.

3.2.4 Knowledge transfer and the importance of monographs

Many dams in Switzerland have been built over 50 or more years ago and the Design and Performance Criteria are in some cases not available or incompatible with current Standards and Directives. Moreover, those responsible for dam safety, whether they be Dam Wardens (N1), Professional Engineers (N2) or Expert Engineers/Geologists (N3) are becoming more increasingly difficult to replace following their retirement, see their age distribution in Figure 1-1. To ensure; (a) the passage of knowledge between the outgoing and incoming dam safety staff; (b) to maintain a clear record of the design criteria used at the time of construction and for structural rehabilitation projects performed over the lifespan of the storage facility; (c) track surveillance and monitoring concepts and evaluations and (d) monitor the adaptation of emergency regulations, the preparation of a monograph of the dam and water storage facility becomes an essential part of dam safety. This proposed requirement is valid for all three Swiss dam classes and therefore, not just for class I dams for which a five-year expertise is legally required. The contents of such a monograph have been elaborated by (SwissCOD 2001) and the SFOE has referenced this document in their Directives (SFOE 2015b). Experience at the SFOE has shown that more effort is still needed by operators and owners to elaborate and update monographies at regular intervals, for example every 10 years and in particular, special attention is needed to ensure that *geotechnical* and not just geological data are reported along with the core information related to flood and seismic verifications. This information may be even more relevant for decisions in regard to any future dam heightening projects.

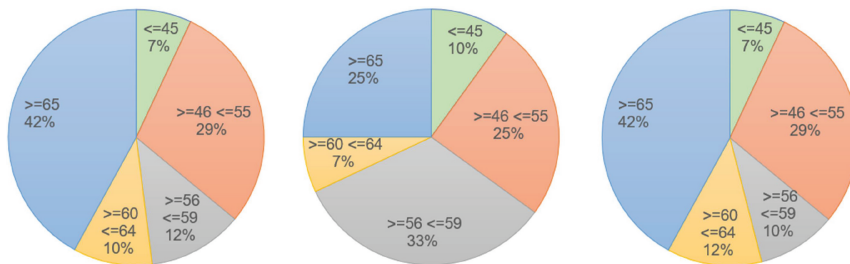


Figure 1-1. Distribution of the age of Swiss Expert Federal Geologists (Left) and Engineers (Middle) and both Geologists and Engineers (Right).

3.2.5 Future ways to manage the effects of concrete swelling based on past experience.

The SFOE has provided both financial and technical support over many years to investigate the swelling behaviour of dam mass concrete due to the chemical reaction between the silicate found in aggregates and the alkali in cements under certain environmental and load regime conditions. Research studies performed at EMPA (Leemann & Griffa 2013), EPFL (Ben Hal 2006), (Dunant 2009), (Giorla 2013), (Cuba Ramos 2017), (Gallyamov 2021) have focused on a detailed program of laboratory and numerical experiments leading to a better understanding of the diagnostic phases of alkali-aggregate (AAR) and alkali-silicate reactions (ASR).

The work performed by the AAR working group of (SwissCOD 2015) also provides a comprehensive study of AAR for Swiss Dams and the more recent (SwissCOD 2021) gives a return of experience on the behaviour of post-rehabilitated dams affected by concrete swelling.

References (Gunn et al. 2017, Gunn 2021) propose a strategy on how to identify AAR and its extent based on specific laboratory tests and field monitoring data and a simplified method for the long-term prognosis of AAR affected dams as shown in (Gunn et al. 2017). Reference (Gunn 2021) also provides instructions on where core samples can be taken from the dam noting that the extent of AAR may be different in different locations of the dam. To be able to carry out both diagnostic and prognostic evaluations of dams that are suspected of concrete swelling including any potential rehabilitation works, the authors recommend performing laboratory tests on core samples especially at the *early phases* of swelling and then at five-year intervals to build-up a database of information that reduces the risk of uncertainties.

Despite the achievements that we have made in the understanding and handling of AAR, we are still faced with many challenges when making a prognosis about AAR affected dams and in particular, what and when to perform, remedial measures and what long-term gains are made in terms of dam safety. The use of practical numerical methods that are able to capture the *true* physical processes of AAR at micro-meso and macro scales could help in this respect.

To achieve this goal, one would need; (a) simple model calibration tests like the ones recently proposed by (RILEM 2021); (b) prototype AAR affected dams with long duration monitoring data and; (c) rehabilitated dams for which slot-cuts are still open or partially open. Such prototype dams do exist in Switzerland (SwissCOD 2021) and the SFOE is working together with industry and academia to extract out the most relevant data that would allow both the calibration and validation of numerical models based on the *physics of the problem statement* rather than a holistic approach.

3.2.6 *The effect of climate change on dam surveillance evaluations and operational conditions*

According to the (MeteoSwiss website), *globally, the past decade was already 1.2°C warmer than the pre-industrial mean, and in Switzerland the increase was even higher at 2.5°C*. Climate change is affecting the behaviour of Swiss dams and the surrounding environments and the SFOE advocates care and attention to this important subject when performing safety evaluations of water-retaining facilities. Monitoring data recorded at many dam site locations in Switzerland indicate the increases stated by MeteoSwiss and it is important that this trend is clearly distinguished and not misinterpreted as irreversible displacements that are normally associated with plasticity, concrete swelling, damage and/or cracking. To assist with these evaluations, the SFOE along with the ETH Zürich have developed and made available to the public the software tool (DamBASE 2015) including the source code. Moreover, training courses (SFOE 2019) that focus of the fundamentals of statistical models, heat transfer analysis, behaviour analysis and hybrid models whereby the results from deterministic models can be imported and how hybrid models can be created within DamBASE, have been organised in particular for professional engineers (N2) and experts (N3) that are responsible for dam monitoring and assessments.

Global warming is also having an impact on glaciers and care is needed to assess the effects on dams due to for example, the sudden release of trapped glacial waters into the dam reservoir or the formation of mudslides and the increase in sediment transportation.

Although reservoir operation is in general clearly separated from dam safety, care must nevertheless be taken when *flushing* the increased sediment deposits associated with glacial retreats and also the *frequent use of bottom outlets* to avoid downstream erosion and/or the dissolution of foundation grouting (curtain, contact and consolidation).

3.2.7 *Sedimentation in the context of dam safety*

The increase in sedimentation in the reservoirs of Alpine regions is a phenomenon directly related to climate change. Indeed, climate change has significant consequences on the hydrological regimes of alpine regions, which are characterized by high precipitation and often high snow accumulation in winter. The increase in temperature in the Alpine regions leads to faster snowmelt and an increase in the amount of water flowing into rivers and reservoirs in summer. This increase in water also leads to an increase in the amount of sediment carried by rivers, which eventually settles in dam reservoirs.

Reservoir sedimentation can have a significant impact on the bottom outlet capacity of dam systems. Sediment carried by rivers can be deposited in drainage channels, bottom outlets or penstocks of dams. This can reduce the discharge capacity of the entire system, which can lead to flooding in the event of heavy rainfall. The supervisory authority must be particularly alert to this phenomenon since the approved flood and emergency management strategies were developed on the assumption of full operation of gated outlet structures. In the case of the water storage facilities are heavily affected by sedimentation problems; a revision of discharge capacities may be necessary. This may also lead to the revision of flood and emergency management strategies.

(SwissCOD 2004) addressed this issue and it continues to be a subject of importance due to the effects of climate change and the adapting flow characteristics of tributaries and the main reservoirs. SFOE experience has shown that a number of key dam safety subjects must be handled such as; (a) bathymetric surveys of the reservoir basin to ensure that outlet structures are free of deposited sediments and other debris; such surveys are typically performed on a five-year to ten-year basis (SwissCOD 2004); (b) ensuring that the effects of reservoir sedimentation management do not impair the stability of the dam by erosion of the supporting foundation such as might be the case for some run-of-the-river facilities (Wüthrich et al. 2018) and (c) adaptation of the inlet structures such as variable height intakes (SwissCOD 2016).

4 SAFETY OF WATER RETAINING FACILITIES, PILLAR III: EMERGENCY CONCEPT

4.1 Overview

SFOE directive E (SFOE 2015c) describes the requirements of an emergency concept that operators must comply with and that must also be approved by the Federal and/or Cantonal supervisory authorities. The contents of this document must contain *dam break flood maps*, *risk analyses*, and emergency responses related to *strategy*, *organisation* and the *dossier*.

4.2 Return of experience and future challenges

Following the publication of directive E (SFOE 2015c) in 2015, and after more than 5 years of intensive efforts, Swiss operators have diligently fulfilled their legal obligations. The work performed has also highlighted strengths and weaknesses in previous emergency plans and the need to update the contents of the regulations based on new risks and uncertainties, for example, flood and seismic verifications. The future development of regulations will also be based on *planned emergency exercises* that are to be performed within the coming years. Experience of just a few exercises has shown the importance of the cooperation of the different emergency organisations and the optimisation and definition of their respective duties and tasks.

4.2.1 Dam safety concepts applied to frontier dams

Swiss frontier dam safety refers to all measures taken to ensure the safety of people and infrastructures downstream of the dam, as well as to prevent risks associated with potential failures of the dam. Coordination problems between two countries can affect the safety of frontier dams.

Indeed, the safety of a frontier dam often involves cooperation and coordination between the regulatory authorities of each country involved, as well as the opportunities provided by the legislation of each country to accept such a collaboration. History has shown that it is in the common interest of both countries to work together to improve the surveillance conditions of the dam, to prevent potential risks by developing emergency plans in case of dam failure. When revising the law on water storage facilities (SFOE 2010) in 2010 and its ordinance in 2022 (SFOE 2022), the SFOE ensured that possible *derogations* from Swiss dam safety requirements set out in the legislation were legally established. This means that for frontier

facilities, the supervisory authority may define *special common agreements* or arrangements with neighbouring states/countries for storage facilities in adjacent waters and ensure that an equivalent level of safety can be maintained.

To overcome the challenges of managing frontier dam safety, a collaborative, problem-solving approach is needed. Both countries must be committed to working together to develop common security strategies, share information and communicate effectively. Comparative tables of each country's requirements and comparison of organisations can be particularly useful in helping to identify the optimal requirements, thereby ensuring an equivalent level of security. It is particularly important to involve the neighbouring country's regulatory authority in emergency management plans to ensure effective communication in the event of an accident or incident. The various agencies for public safety of both countries should be involved in the operator's emergency exercises.

5 WATER-STORAGE FACILITIES WITH SOLAR PHOTOVOLTAIC SYSTEMS, SPVS

(Kougias et al. 2016, Maddalena et al. 2022) have shown that a potential exists for solar photovoltaic systems, also called SPVS, placed on dams and storage reservoirs. In Switzerland, four photovoltaic installations are already in service: one floating SPVS on the reservoir Les Toules, one SPVS on the downstream face of Muttsee dam, and two SPVS on the upstream face of the concrete dams of Albigna and Valle di Lei. For such projects, the SFOE has to provide a *position statement* to the concerned Cantons on the safety of the dam and corresponding particular conditions. The goal is always to ensure that dam safety remains guaranteed with the addition of SPVS during construction and after.

It should be firstly recognised that photovoltaic installations on dams complicate visual inspections and in particular, the new possibilities with drones. Second, there are cases with severe destruction of a floating photovoltaic installation, e.g., at Yamakura Dam in September 2019 in Japan (Rogers & Bartle 2021), where a typhoon had lifted anchors resulting in the islands of panels splitting, and a fire. In that case, the anchor arrangement was considered as a cause of failure, and the wind speed was determined not to be the cause, see (Rogers & Bartle 2021). The reconstruction consisted of rearranging the panels in new shapes, since rectangular shapes mitigate stress deviations and concentrations compared to initial installation. Reinforcement measures on the anchors were also added.

5.1 Possible risks imposed by photovoltaic installations

The following is a list of possible risks to consider with photovoltaic installations placed on dams and storage reservoirs:

- Obstruction of the outlet by photovoltaic panels or their related holding structures,
- Spillway jamming during flooding including the influence of floating wood,
- Modified dam behaviour (thermal, static, dynamic) due to the photovoltaic installation covering previously exposed surfaces,
- Modification of the flows and diminution of the discharge capacity in case of flooding,
- Restricted personnel access to the dam facility due to fire or electrical dangers.

The photovoltaic installation placed on the dam or on its reservoir has to be considered within the Swiss safety concept of the storage facility and in particular, its impact on all three pillars.

5.2 First pillar: Structural safety with solar photovoltaic installations

The first pillar dealing with the structural safety must be fulfilled for both usual and exceptional load cases. The safety of the dam during and after the earthquake and the flood, must be guaranteed. The following cases related to construction design are:

- Static case: The influence of the photovoltaic installation must be analysed and the modification on the dam and reservoir evaluated. Moreover, the verification of the mounting structures and fasteners must be proven for the corresponding load cases. Particular additional load case like wind and waves may have to be considered as significant.
- Flood: A minimum distance between photovoltaic panels under flooding water and the spillway can be considered, or the real force due to the water flow on the panels has to be evaluated to prove the resistance of the pull-out system for the corresponding flood cases.
- Earthquake: The verification of the SPVS pull-out systems must be proven.

5.3 *Second pillar: Surveillance and maintenance with solar photovoltaic installations*

The second pillar dealing with the surveillance and maintenance of the dam must be guaranteed and not hindered by the photovoltaic installation allowing the following to be performed:

- Visual inspections as before the installation of joints and also unrestricted checks after exceptional events, such as earthquake or floods;
- Measurements including geodetic surveys,
- Treatment of the measures: the modification of the static behaviour of the dam should be considered in the treatment of the measurement. The photovoltaic installation has to be considered in the use of statistical models to monitor and control the behaviour of the dam,
- Controls and monitoring measures of the photovoltaic installations for safety purpose.

For the existing installations in Switzerland, Figure 2-1 shows different views during inspections.



Figure 2-1. View of the water face and joints with photovoltaic installation.

5.4 *Third pillar: Emergency concept with solar photovoltaic installations*

The third pillar dealing with the emergency concept has to be fulfilled as well. An additional risk is that the photovoltaic panel can burn, which could damage the fasteners and mounting structures (as well as cables for floating photovoltaic installation), they can fall and lead to obstruction of the outlet or spillway. The following measures, not exhaustive list, have to be taken into account:

- Regarding electrical problem, the photovoltaic panels should be connected to ground,
- A lightning protection must be installed,
- The emergency switch of the inverter must be accessible for the operator and fire department.

6 CONCLUSION

The main objective of this article is to provide the reader with a *return of experience* with respect to tasks performed by the Dam Surveillance Section of the Swiss Federal Authorities, SFOE. Often the dam owner or operator receives a *position statement* or *feedback* from SFOE concerning his particular water storage facility and he and the dam community at large are not always aware of the particular issues and problems that other operators have and the results of SFOE evaluations. This article is intended to close this knowledge gap. The main conclusions are summarised as follows:

- First reservoir filling should be handled well-coordinated in advance with the SFOE.
- New flood verification methods referred to as *EXAR* and *Extremhochwasser Schweiz* reduce uncertainties.
- The capacity of existing discharge structures may need to be reassessed.
- The prioritisation of dam safety recommendations into two SMART categories; “must” and nice-to-have” and a status of Pending Points database tool is described.
- Pumped-storage schemes with multiple operators require a common regulation and remote monitoring of the facilities to ensure the implementation of emergency concepts.
- The Guardaval and INSAR remote sensing technologies can greatly facilitate the monitoring of creeping landslides.
- Many Federal experts have reached or are reaching retirement age in the next 5 years and operators need to be aware of potential staff problems and ensure the transfer of knowledge with the due preparation of dam safety and surveillance monographs.
- The swelling of ageing concrete dams requires a closer collaboration between operators, consultants, academia and the authorities to ensure reliable long-term safe solutions. Emphasis is given to the diagnostic and especially the prognostic phase of concrete swelling.
- Climate change must be addressed in dam surveillance making use of tools like DamBASE to avoid confusing temperature trends with other detrimental phenomena.
- Recently SFOE approved emergency regulations must be followed by dry-run exercises to be performed in the coming 5 years that may result in further improvements.
- Common bi-lateral safety agreements between the authorities are needed for frontier dams to ensure dam safety concept.
- The installation of solar photovoltaic installations, SPVS must also satisfy all the three pillars of dam safety requirements.

ACKNOWLEDGMENTS

The authors would like to sincerely thank the water-storage facility owners and operators, the dam wardens, professional engineers and experts for their work and dedication to dam safety and surveillance in Switzerland. The SFOE dam section staff are also thanked for sharing both their experience and knowledge and a special thanks goes to Balz Friedli for reviewing the manuscript. Finally, the authors acknowledge the continued support of the Swiss Federal Office of Energy.

REFERENCES

- Andres, N., Steeb, N., Badoux, A. & Hegg, C. 2021. Extremhochwasser an der Aare: Hauptbericht Projekt EXAR: Methodik und Resultate. WSL Berichte, 104.
- Ben Haha, M. 2006. Mechanical Effects of Alkali Silica Reaction in concrete studied by SEM-image analysis. PhD Thesis N° 3516. École Polytechnique Fédérale de Lausanne.
- Cuba Ramos, A. I. 2017. Multi-Scale Modeling of the Alkali-Silica Reaction in Concrete. PhD Thesis. École Polytechnique Fédérale de Lausanne.
- DamBASE. 2015. Dam Behaviour Analysis Software Environment. User Manual. ETHZ-VAW.
- Dunant C. 2009. Experimental and Modelling Study of the Alkali-Silica-Reaction in Concrete, PhD Thesis N° 4510, École Polytechnique Fédérale de Lausanne.
- Fielding E. J. & Rosen P. A. 2011. Interferometric Synthetic Aperture Radar (InSAR): Principles and Signal Processing, IEEE Press.
- Gallyamov, E. 2021. Mechanics of Alkali-Silica Reaction in Concrete Across Scales, PhD Thesis, École Polytechnique Fédérale de Lausanne.
- Giorla, A. B. 2013. Modelling of Alkali-Silica Reaction under Multi-Axial Load, PhD Thesis N° 5982, École Polytechnique Fédérale de Lausanne.
- Gunn, R. M. 2021. New Concept for Concrete Swelling Evaluations Based on Surveillance and Monitoring Data, 27th ICOLD Congress, Q106c, Marseille.

- Gunn, R. M., Scrivener, K. & A. Leemann A. 2017. The identification, extent and prognosis of alkali-aggregate reaction related to existing dams in Switzerland, CFBR Chambéry.
- Hanssen, R. F. & Meurs, E. H. 2001. InSAR Principles: Directives for SAR Interferometry Processing and Interpretation. Delft University Press.
- Kougiass, I., Bódis K., Jäger-Waldau A., Monforti-Ferrario F. & Szabó S. 2016. Exploiting existing dams for solar PV system installations Prog. Photovolt: Res. Appl., 24:229–239.
- Leemann, A. & Griffa, M. 2013. Diagnosis of alkali-aggregate reaction in dams, SFOE Publication N° 290934, Project N° 500863, Empa, Laboratory for Concrete/Construction Chemistry.
- Li, B. et al. 2018. A Review of Interferometric Synthetic Aperture Radar (InSAR) Principles and Its Applications for Geophysical Studies. Earth-Science Reviews, vol. 181, pp. 1–28.
- Maddalena, G., Hohermuth B., Evers F., Boes R. & Kahl A. 2022. Photovoltaik und Wasserkraftspeicher in der Schweiz – Synergien und Potenzial. Wasser Energie Luft – 114, Heft 3.
- Mandel, A. et al. 2005. Detection and monitoring of landslide movements using high-resolution satellite imagery, Natural Hazards and Earth System Sciences.
- MeteoSwiss. website. <https://www.meteoswiss.admin.ch>.
- RILEM. 2021. Diagnosis & Prognosis of AAR Affected Structures.
- Rogers, M. & Bartle, A. 2021. Floating solar PV on dam reservoirs: The opportunities and the challenges, Hydropower & Dams Issue Four.
- Rouillier, J.-D., Ornstein P. & Délèze J.-Y. 2004. GUARDAVAL: un système de télésurveillance adapté aux régions de montagne. GéoQuébec 2004, 57ième Congrès Canadien de Géotechnique, G33.996
- Rouillier, J.-D., Ornstein P. & Délèze J.-Y. 2005. GUARDAVAL: la télésurveillance appliquée à la gestion des risques naturels en milieu alpin, Géoline 2005 - Lyon, France
- Schwager, M. V., Askarinejad A., Friedli B., Oberender P. W., Pachoud A. J. & Pfister L., 2023. Swiss dam safety regulation: Framework, recent changes and future perspectives. 12th ICOLD European Club Symposium, Interlaken, Switzerland.
- SFOE. 2010. Federal Act on Water Retaining Facilities, The Swiss Federal Office of Energy, 721.101.
- SFOE. 2014. Directive on the Safety of Water Retaining Facilities Part B: Particular risk potential as subordination criterion. Swiss Federal Office of Energy. Version 2.0.
- SFOE. 2015a. Directive on the Safety of Water Retaining Facilities Part A: Introduction. Swiss Federal Office of Energy. Version 2.0.
- SFOE, 2015b. Directive on the Safety of Water Retaining Facilities, Part D: Commissioning and operation, Commissioning - Maintenance - Surveillance. Swiss Federal Office of Energy. Version 2.0.
- SFOE. 2015c. Directive on the Safety of Water Retaining Facilities, Part E: Emergency plan. The Swiss Federal Office of Energy. Version 2.0.
- SFOE. 2017. Directive on the Safety of Water Retaining Facilities, Part C1: Design and construction. Swiss Federal Office of Energy. Version 2.1.
- SFOE. 2018. Directive on the Safety of Water Retaining Facilities, Part C2: Flood safety and lowering the reservoir water level. Swiss Federal Office of Energy. Version 2.02.
- SFOE. 2019. ETH-VAW, Training Course, Dam behaviour Analysis with DamBASE, Zürich.
- SFOE. 2021. Directive on the Safety of Water Retaining Facilities, Part C3: Earthquake safety. Swiss Federal Office of Energy. Version 2.1.
- SFOE. 2022. Water Retaining Facilities Ordinance, The Swiss Federal Office of Energy, 721.101.1.
- SIA. Swiss Society of Engineers and Architects - <https://www.sia.ch/en/the-sia/the-sia/>.
- SwissCOD. 2015. (Swiss Committee on Dams). Alkali-Aggregate Reaction (AAR) in Swiss Dams, Workshop, Switzerland.
- SwissCOD. 2001. (Swiss Committee on Dams). Monographie de barrage, Recommandations pour la rédaction, (contenu et structure), French and German.
- SwissCOD. 2004. Fachtagung/Journées d'études, Deposits and sediments: investigations, flushing, environment. Martigny.
- Heller, P. et al. 2016. Solutions constructives au problème d'ensablement du lac du Vernex sur la Sarine, Wasser Energie Luft, Eau énergie air, Acqua energia aria.
- SwissCOD. 2021. Fachtagung/Journées d'études. Sanierungsarbeiten An Talsperren: Erfahrungen Und Erkenntnisse Assainissement Des Barrages: Retour D' Expérience, Crans-Montana.
- Wüthrich, D., Chamoun S., Bollaert E., De Cesare G & Schleiss A. J. 2018. Hybrid Modelling Approach to Study Scour Potential at Chancy-Pougny Dam Stilling Basin, Springer Nature Singapore Pte Ltd.

Failures and incidents in Greek dams

G.T. Dounias

Edafos SA, Athens, Greece

S.L. Lazaridou

Hydroexigiantiki Consulting Engineers, Athens, Greece

Z.R. Papachatzaki

Public Power Corporation SA, Athens, Greece

ABSTRACT: The paper presents and discusses incidents and failures that have occurred in Greek Dams. The incidents and failures are grouped according to the mechanism that caused the incident. The first and most common mechanism involves internal erosion, mostly in homogeneous embankment dams. There are nine cases reported. In some, the deficiency was treated, and the dams are properly operating. In others, the reservoir is lowered waiting for remedial measures. In a few cases, erosion was not controlled and led to dam breach. The second mechanism involves overtopping of dams. There are seven reported cases. In many cases, the dam was badly damaged and had to be repaired. In some cases, very little or no damage occurred, mainly due to the rockfill of the downstream shoulder. A review of design floods and probable works to enhance spillway capacities are needed. The last group concerns excessive leakage. Four cases are reported, one concerning extreme leakage in the reservoir. The other cases involve excessive leakage through the foundation/abutments which are difficult to treat successfully. Investigations are ongoing to find a solution in each case. Most of the incidents would have been avoided if well-established principles, such as presented by ICOLD Bulletins, had been followed. The need for dam design and construction made by specialists and not by inexperienced personnel is apparent.

1 INTRODUCTION

1.1 *Dams in Greece*

Dam construction in Greece intensified in the 1960's and peaked in the 1990's and 2000's. The Greek Committee on Large Dams keeps a record of existing large dams in Greece, following the ICOLD definitions. The dam construction evolution is presented in Figure 1.

Nearly 69% of all dams are lower than 40 m high, 16% are between 40 and 60 m, 6% between 60 and 80 m, 4% between 80 and 100 m, 2% between 100 and 120 m, 2% between 120 and 140 m, one dam is 150 m high and two dams are over 160 m.

In the vast majority, dams were properly designed and constructed, following geological and geotechnical investigations. Big dam owners, like the Public Power Corporation, the Ministry of Infrastructure and the Ministry of Agriculture followed international good practice in the construction of their dams.

On the other hand, dams built by municipalities did not always follow the state of the art. Frequently, they were designed and built by inexperienced agencies and supervised by equally inexperienced personnel. Dams in this category frequently exhibited problems during their first filling, or shortly afterwards.

Currently, there are 151 completed large dams in Greece according to ICOLD definition, and approximately 20 in various completion stages. There are also many small dams that fall under the jurisdiction of the Dam Administration Authority.

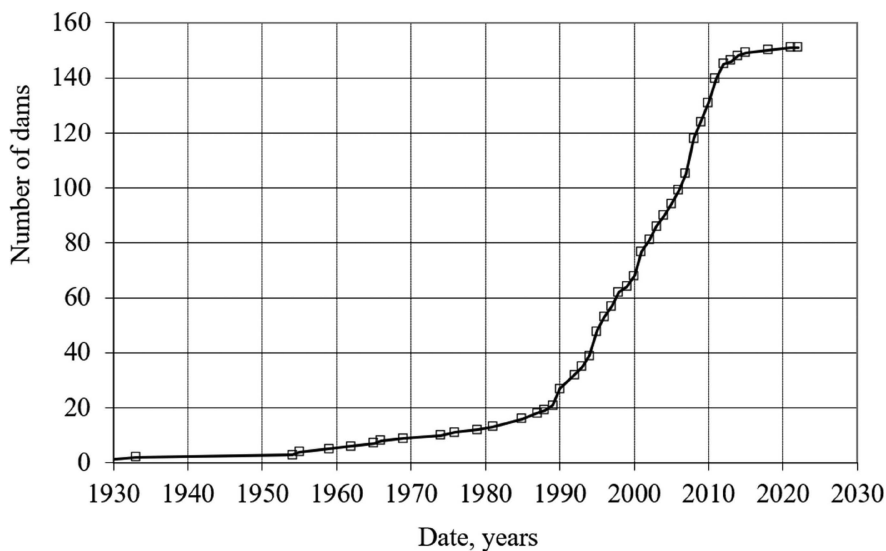


Figure 1. Dam construction evolution in Greece.

1.2 Incidents data base

The ICOLD Bulletin 99 on “Dam Failures - Statistical analysis” (ICOLD, 1995) is an update of the “Lessons from Dam Incidents” (ICOLD 1974), restricted only to failure cases. Many more similar presentations have been made without altering the basic findings of Bulletin 99.

The most common incidents and failures are related to external erosion, internal erosion, and structural dam failure.

A Working Group on dam incidents has been recently formed by the Greek Committee on Large Dams (GCOLD). The current article presents some initial findings on incidents and failures in Greek Dams.

In Greece, many incidents and some failures have occurred. Fortunately, all failed dams were relatively small, and the consequences of failure mild. No fatalities or injuries have been reported.

An Incident and Failures Data Base will be built, following closely the relevant proposal for an ICOLD Dam Incident Data Base (Poupart, 2016). The following information will be included in the Data Base:

- [a] Dam characteristics following the World Register of Dams (WRD) requirements
- [b] Incident characteristics including Year, Dam stage (i.e., construction, first filling, operation etc.)
- [c] Incident mode – failure mechanism
- [d] Severity of the incident
- [e] Description of the failure, including consequences
- [f] Incident causes (main, secondary)
- [g] Applied remedial measures (type and description).

2 DAM INCIDENTS AND FAILURES IN GREECE

A summary of recorded incidents is presented in Tables 1 and 2. Table 1 presents the Dam characteristics and Table 2 the Incident characteristics.

Table 1. Summary of dam characteristics.

Name, Completion Year	Height (m)	Type	Purpose	Watertight element		Reservoir (x10 ⁶ m ³)
				Position	Type	
Perdika, 1962	22	TE	S	i	e	10
Kremasta, 1965	165	TE	H	i	e	4750
Pelekanos, 1990	12?	TE	I	h	e	?
Monolithi Kilkis, 1992	8	TE	I	h	e	0.07
Exochis, 1998	17	TE	I	i	e	0.7
Aghias Chania, 1929	5	TE	H	f	c	?
Gages Kalivion, 1990	25	TE	I	?	e	?
Kouti Livadiou, 2000	20	TE	I	h	e	0.1
Ampelakia Dam, 1995?	10	TE	I	h	e	0.2
Kamare Sifnos, 2003	21	PG	C	-	-	?
Mylopotas Ios, 1996	23	TE	S. I	f	p	0.24
Dilofo, ?	?	TE	?	?	?	?
Triadio Thermis, 1997	36	TE	S. I	h	e	0.25
Raches Ikarias, 1995	29	TE	S. I	i	e	0.92
Gennas Crete, ?	11	PG	?	f	c	?
Panayiotiko, 2003	41	CFRD	I. S	f	c	1.8
Valsamiotis, 2014	67	HF	I.Sf	f	c	6
Paleomonastiro Kalivion, 1990	17	TE	I	h	e	0.08
Sparmos Elassona, 1990	16	TE	I	h	e	0.05
Kokinopilos, 1997?	12	TE	I	h	e	0.035

The acronyms used are according to ICOLD WDR:

Dam Type: CB buttress dam, BM barrage, ER rockfill dam, MV multiple arch, PG gravity dam (masonry or concrete), TE earthfill dam, VA arch dam, XX unlisted. Additional acronyms used are CFRD Concrete faced rockfill dam and HF Hardfill dam.

Position of watertight element: f upstream face, i internal/central, h homogenous

Watertight element: a bitumen, e earthfill, c concrete, p membrane or other synthetic, m metallic, x other.

Purpose: C flood protection, I irrigation, S water supply, H power generation, R recreation, X other (e.g., industrial usage, aquifer recharge etc.)

The following acronyms are also used to classify the incidents, as proposed by Poupart (2016):

Incident time: T1 During construction, T2 During first filling, T3 During first five years, T4 After five years, and T5 Not available.

3 PRESENTATION OF INCIDENTS

3.1 General

The incidents are grouped into four categories and a short description of the incident is presented for all cases. Some cases are well known while for others there is little information.

Some incidents involve both internal erosion and overtopping. These were grouped somehow arbitrarily, according to the severity or the graveness of the incident.

Table 2. Summary of Incident characteristics.

Name, year of completion	Year of incident	Dam stage	Incident type	Comments
Perdika, 1962	1962	T2	A5, F3	Reservoir leakage
Kremasta, 1965	1966	T2	A2, A5	Abutment leakage
Pelekanos, 1990	1991	T3	A5	Internal erosion
Monolithi Kilkis, 1992	1993	T1	F1	Internal erosion
Exochis, 1998 1999,	1999, 2018	T2, T4	A1	Internal erosion, overtopping
Aghias Chania, 1929	2000	T4	A1	Overtopping
Gages Kalivion, 1990	2000?	T4	A1	Internal erosion
Kouti Livadiou, 2000	2001	T3	A1	Internal erosion
Ampelakia Dam, 1995?	2002	T3	A1	Internal erosion
Kamares Sifnos, 2003	2003	T1	F1	Internal erosion, overtopping
Mylopotas Ios, 1996	2003	T4	A1	Overtopping
Dilofo,	?		F1	Internal erosion, overtopping ?
Triadio Thermis, 1997	2007	T4	A1	Internal erosion, overtopping
Raches Ikarias, 1995	2010	T4	A1	Overtopping
Gennas Crete, ?	2014	T2	F1	Abutment erosion, structural
Panayiotiko, 2003	2014*	T4	A5	Excessive seepage
Valsamiotis, 2014	2014*	T2	A5	Excessive seepage
Paleomonastiro Kalivion, 1990	2015	T4	A1	Internal erosion
Sparmos Elassona, 1990	2016	T4	F2	Internal erosion
Kokinopilos, 1997?	2017	T4	A1, R1	Overtopping, internal erosion

* Progressive increase of seepage over the years

Table 3. Type of incident (modified from ICOLD 1974 and Poupart 2016).

Type of Incident	Description
A1	An incident to a dam in operation, prevented from becoming a failure by remedial measures including control of reservoir water level.
A2	An incident observed during initial filling of the reservoir, and which was prevented from becoming a failure by remedial measures including control of reservoir water level.
A3	An incident to a dam during construction, i.e. by settlement of foundations, slope instabilities, etc., which occurred before impoundment and where remedial measures were carried out and the reservoir was then safely filled.
A4	An incident to another structure than the dam (appurtenant works, gates, reservoir sliding, etc.) but which has been prevented from leading to a dam incident by immediate remedial measures including possible drawdown of the water.
A5	An incident related to excessive water loss from the reservoir, not treated and posing restrictions on the dam operation.
F1	A major failure involving dam breach.
F2	A failure which at the time may have been severe but was successfully repaired and the dam brought again into operation.
F3	A failure that while causing inability of operation, does not pose a structural or public safety threat.
R1	Following an incident A1 or A2 the dam was removed.

3.2 *Excessive reservoir or foundation/abutment leakage*

Under this category are the dams that exhibit excessive leakage either in the reservoir or in the dam foundation abutments. A leakage is classified as an incident if it meets one of the following conditions:

- The volume of the leakage is excessive for the dam size. The definition of excessive leakage is somewhat subjective and is based on experience and recorded seepage in similar structures.
- The volume of the leakage is so large that it affects the operation of the reservoir. Again, the definition is subjective.
- The volume of the leakage is increasing with time and/or sediment is transported with the leakage.

There are four such cases known so far in Greece. Incidents in off-stream lined ponds are not included.

Perdika Dam (Moutafis, 2008; Liakouris, 1995)

Perdika dam is a 22 m high earthfill dam with a central core, built 2 km from the Perdika village of Ptolemais Municipality. It was completed in 1962 and when it was filled to approximately 2/3 of its height a considerable leakage occurred into underlying karstic limestones and the reservoir was emptied. The dam is resting on a 100 m thick watertight clay marl formation but some faulting within the reservoir brings the limestones near the surface, leaving only a small cover of clay marls. Erosion and piping occurred downwards through the marls and into the karstic limestone.

Some unsuccessful attempts were made in 1964 to fill the sinkholes, to no avail. Presently the reservoir holds little water and is used for recreation.

It is a case of design failure probably due to limited site investigation.

Kremasta Dam (Liakouris, 1995)

Kremasta is an earthfill dam, 165 m high, with a central core and shoulders made of river gravel. The dam is built on Flysch formations of the Gavrovo Zone that consists of layers of siltstone and conglomerates.

The dam was completed in 1965 and the reservoir was impounded. Considerable leakages occurred on both abutments. In an attempt to control the leakages and improve the stability of the abutments, drainage and grouting tunnels were constructed in both abutments and a substantial additional grouting program was carried out up to 1967. The leakages were reduced but not to acceptable levels. An additional grouting program was carried out from 1970 to 1973. The leakages were further reduced but still not to acceptable levels and it was decided to operate the reservoir at a slightly lower level than originally designed.

Various proposals have been made ever since for construction works that could limit the leakage and allow operation of the reservoir at full supply level, but none was considered viable.

Panayiotiko Dam (Dounias, Mamasis & Georgalas, 2016)

Panayiotiko is a 41 m high Concrete Faced Rockfill Dam (CFRD), with a reservoir capacity of 1.800.000 m³. It is built on schists with intercalations of clay schists, locally highly disturbed.

Following its first filling in 2003, considerable leakage occurred at the toe of the dam. The leakage, for full reservoir level, increased from 17 lt/sec in 2003 to 61 lt/sec in 2013 and to 74 lt/sec in 2014. It was reported to the team of GCOLD that visited the site in 30-09-2015 that the leaking water is always clear.

The causes for the leakage are still not known. No action to limit the leakage has been taken. The leaking water is collected and used.

Valsamiotis Dam (Personal communication OAK AE)

Valsamiotis is a 68 m high Hard Fill Dam (HF). It was completed in 2004 and during its first filling considerable leakage developed on the right abutment, emerging into the dam inspection and drainage galleries.

Additional grouting was performed from within the inspection galleries with only limited success. The dam now operates at a highly reduced reservoir level, while investigation and design for the final treatment of the problem are under way.

3.3 Overtopping

Overtopping has been observed in many dams. In most cases it was due to very low design floods and inefficient spillways. Accidentally blocked or modified spillways by the operators without any permission or design revision, are frequently the cause of overtopping.

Overtopping can also occur following excessive crest settlement and loss of free board.

Overtopping observed at the advanced stage of internal erosion is not classified as overtopping herein.

There are seven cases of overtopping so far reported. Some cases are not well documented, and the cause of overtopping is not known.

Exohis Pieria Dam (Dounias et al, 2020)

Exohi dam was first built in 1998, 1500 m west of the village of Exohi, Municipality of Katerini. It was initially a 16.7 m high homogeneous dam with no filters and drains but probably with a centrally placed plastic membrane acting as the watertight element (information not verified by limited site investigations). In 1999 the dam was overtopped, following severe floods. The dam suffered considerable surface erosion but was not breached. The consultant appointed to investigate and design remedial measures also reported indications of internal erosion.

A new spillway was constructed, and the dam was raised by 2.0 m to accommodate a much larger flood. A downstream berm with inverse filter was designed to defend against internal erosion. The works were partly constructed in 2004 but problematic behavior continued.

A Dam Administration Authority (DAA) team was called to inspect the dam in 2020, following a report by Municipality engineers. The team noted that there were signs of continuing internal erosion most probably along the route of the water conveyance pipe that crosses the embankment obliquely. The pipe appears to be blocked and water is drawn by pumping over the crest. The DAA team proposed, among other measures, the establishment of an Emergency Preparedness Plan and the construction of additional works to minimize the dam failure risk.

Aghias Chania Dam (Moutafis, 2008)

Aghia Dam is located 9 km west of Chania, Crete. It is a 5 m high and 480 m long earthfill dam with an upstream concrete slab. Two cases of overtopping are mentioned, one in 1968 and another in 2000. In both cases, surface erosion and sliding of part of the downstream slope was reported. The erosion was repaired and the dam is in operation.

It is a case of low design flood and insufficient spillway capacity.

Kamares Sifnos Dam (Moutafis, 2008)

Kamares dam is located 2 km SE from the Kamares village on Sifnos island. It is a 21 m high gravity masonry dam for flood protection. Dam construction began in 2002 and in early February 2003 it had reached an approximate height of 16 m. Heavy flooding occurred, and the dam was overtopped on the 18th of February. The foundation of the dam on the right abutment was eroded for the full dam height, creating a gap approximately 2 m wide. Part of the dam acted as a cantilever and cracked.

The overtopping was mainly due to inadequate diversion provisions during construction. The erosion was due to poor foundation contact.

The dam was later repaired and redesigned and now it is operating properly.

Mylopotas Ios Dam (Moutafis, 2008)

Mylopotas dam on the island of Ios is located 1.5 km East of Mylopotas Village. It is a - 23 m high embankment with an upstream High Density Polyethylene (HDPE) geomembrane. There is a 5 m wide frontal spillway whose sill was raised arbitrarily, without design approval in order to increase the reservoir capacity.

Following heavy rainfalls in January 2003, the dam was overtopped for a few hours across its crest with an estimated overflow height of 0.4 m. The flood exceeded considerably the design flood and overtopping would have occurred even with the original spillway crest. What saved the dam was a 3 m wide rockfill protection zone on the downstream face. Small erosion easily repaired occurred along access roads and secondary embankments.

The incident was caused by a considerable underestimation of the design flood.

Dilofo Thessaly Dam (Siskos & Thanopoulos, 2013)

Dilofo dam was a homogeneous embankment, 10 to 15 m high, most probably without filters and drains. Estimated time of construction is in the late 1990's. The dam was overtopped and destroyed following heavy floods in the mid-2000's.

In similar dams in the region, lacking filter and drainage zones, intense internal erosion was observed before the dam was overtopped and breached. A similar process is probable for the failure of Dilofo Dam.

Raches Ikarias Dam (Author's personal communication)

Raches Dam is a 29 m high, 260 m long, rockfill dam with a central clay core built in 1995, 3.5 km S-SW of Raches Christos village on the island of Ikaria. In 2010, following large floods, the dam was overtopped for a few hours. The maximum estimated overflow depth was 10 to 20 cm. The overtopping occurred mainly near the two abutments. The overtopping did not cause noticeable erosion of the downstream slope, mainly due to the rockfill zone that protects the downstream face of the dam. The design flood requires reconsideration following new hydrological data.

Kokkinopilos Thessaly Dam (Thanopoulos et al, 2017)

Kokkinopilos dam is located approximately 1 km SW of Kokkinopilos village, Municipality of Elassona, District of Thessaly. It is a 12 m high, and 120 m long homogeneous embankment most probably without any internal filter or drainage zones, like many other dams in this municipality. An unlined spillway channel is excavated on the left abutment.

The reservoir is empty in a series of Google Earth views from 2003 onwards. Some signs of seepage through the embankment are detected in the time series of Google Earth photos.

On the 9th of March 2017 there was heavy rainfall, the reservoir filled, and the spillway operated. The water level was rising fast and the dam was overtopped on the 10th of March 2017. The local authorities acted quickly by opening the water supply/bottom outlet valve and by enlarging and deepening the spillway inlet. The overtopping stopped midday on the 10th of March.

Since the water of the reservoir had only limited usage in the area, it was discussed to abandon the dam by opening a wide channel to accommodate the flow of the stream. So far, a deep cut on the left abutment has been made and the risk of overtopping and flood wave propagation has been minimized.

3.4 *Internal erosion*

The mechanism of internal erosion is commonly observed when the well-known principles of filtration and safe drainage are not applied. The mechanism is treated in ICOLD Bulletin 164 (ICOLD, 2017). There are many cases reported in Greece. Nine such cases are presented here. Unfortunately, most of them are not properly documented.

Pelekanos dam (Author's visit)

Pelekanos dam is located 850 m E-SE of the village of Pelekanos, Voio Municipality in Western Macedonia. It is a homogeneous embankment dam, approximately 12 m high, built in 1990. Water from an adjacent stream was diverted to the reservoir formed.

Immediately after first impoundment in 1991, considerable leakage was detected, gradually increasing and carrying sediment. The reservoir was emptied, and the diversion from the adjacent stream was stopped.

The dam was abandoned.

Monolithi dam (Nikos Naskos, personal communication)

Monolithi dam was an 8 m high homogeneous embankment, located near Monolithi Village of Kilkis Municipality. Excessive leakage and advancing internal erosion were observed soon after first filling. As there were no adequate means to control the reservoir level, the internal erosion progressed.

Internal erosion eventually caused the breaching of the dam in 1993.

Gennas (Crete) dam (Nikos Moutafis, personal communication)

Gennas Dam on the Island of Crete is an approximately 11 m high concrete dam. In 2014, a large hole developed low in the body of the dam, close to the right abutment. Most probably, inadequate foundation of the dam facilitated erosion of the foundation that caused local loss of support to the concrete dam. When the resulting pipe was enlarged, it probably caused failure along ill-constructed concrete joints. This is speculation since there are no descriptions of the evolution of the failure.

Gages Kalyvion, Dam (Dounias, Moutafis & Mamasis, 2016)

Gages Dam is located 2.7 km N-NE of the village of Kalyvia, Ellassona Municipality in Thessaly District. It is an embankment dam, approximately 25 m high, built around 2000.

The dam exhibited excessive leakage and signs of internal erosion soon after its first filling. A membrane was placed on the upstream face and the dam is operating ever since.

No further details are known at this stage.

Kouti Livadiou dam (Siskos & Thanopoulos, 2013)

Kouti Dam is located near the Livadi town, Municipality of Ellassona in Thessaly District. It is an embankment dam, probably homogeneous, approximately 20 m high and 60 m long, built around 2000.

Soon after its first filling, considerable leakage was observed near the toe. The leakage was gradually increasing carrying sediment. The reservoir was emptied and a 4 m deep trench, filled with compacted clay, was constructed along the upstream toe of the dam. A two-zone filter (fine filter plus drainage zone) was placed on the downstream face, protected by additional shoulder material. A 4 m deep trench, filled with filter material was placed at the toe of the additional downstream shoulder.

The works were completed in 2003 and the dam is operating properly ever since.

Ampelakia dam (Siskos & Thanopoulos, 2013)

Ampelakia Dam is located 4.5 km S-SE of the town of Ampelakia, Larissa Municipality in Thessaly District. Originally it was an embankment dam, approximately 10 m high and 200 m long, built around 2000. It was most probably homogeneous and had an unlined spillway of small capacity. Over the initial years of operation leakages developed indicating slowly advancing internal erosion. The dam was also frequently overtopped, causing surface erosion of the downstream face.

To face the problems, the dam was increased to 12.5 m and a new concrete spillway was built. Additionally, a filter protected by a zone of embankment material was placed on the downstream face. At the downstream dam toe, a trench was excavated, filter material was placed on its upstream face continuing the filter on the dam face, and the rest was filled with embankment material.

The dam is operating properly ever since.

Triadio Thermis Dam (Kazilis, 2008)

Triadio Dam, Thermi, Prefecture of Thessaloniki, is a 36.5 m high homogeneous embankment dam that was built in 1997. Soon after its first filling, seepage was observed on the downstream face that evolved slowly over the years. In July 2007, with the reservoir almost full, a large erosion pipe (of approximately 1 m diameter at its exit) was formed close to the right abutment, 25 m below the crest level. The reservoir was emptied above this level, and the dam suffered cracks and slumps on the upstream face, but it did not collapse. It was later repaired and is now a touristic attraction. No further incidents have been reported.

Paleomonastiro Kalivion dam (Dounias, Moutafis & Mamasis, 2016)

Paleomonastiro Dam is located 1.4 km NE of the village of Kalyvia, Municipality of Ellassona in Thessaly District. It is an embankment dam, probably homogeneous, approximately 17 m high and 120 m long, built around 1990. An unlined spillway was excavated on the left abutment.

Considerable leakage was observed at the downstream face of the dam and the reservoir was lowered to prevent piping and probable dam breaching. Sinkholes have developed just downstream of the crest, another sign of internal erosion.

The spillway was deepened, and the reservoir is controlled to remain very low.

The GCOLD team that inspected the site in 2016 has proposed means of rehabilitation that will allow the full operation of the reservoir. No works have been reported so far.

Sparmos Ellassona dam (Dounias, Moutafis & Mamasis, 2016; Dounias et al, 2017; Dounias & Bardanis, 2019)

Sparmos Dam is located 3 km NE of the village of Sparmos, Municipality of Ellassona in Thessaly District. It was a homogeneous embankment dam, approximately 16 m high and 210 m long, built around 1990. An unlined spillway was excavated on the right abutment. It formed an off-stream reservoir, fed by an adjacent tributary to Ellassonitis River.

The dam developed seepage on the downstream slope soon after its first filling. Signs of internal erosion appeared early on but were never treated. It is surprising that internal erosion was evolving gradually for almost 25 years before it developed into an uncontrolled piping that led to dam breach in March 2016.

3.5 *Other incidents*

Other kinds of incidents that have been reported are not included in this presentation. The most notable involves failure of cofferdams, such as in Marathon dam, Kremasta dam and Faneromeni Naxos dam (Moutafis, 2008).

Slope instabilities encountered during dam construction are also not presented herein.

4 DISCUSSION

The incidents reported in this paper represent approximately 10% of the Greek dams, and can be grouped in three main types of incidents. The types, percentage and numbers of the incidents are shown in Figure 2.

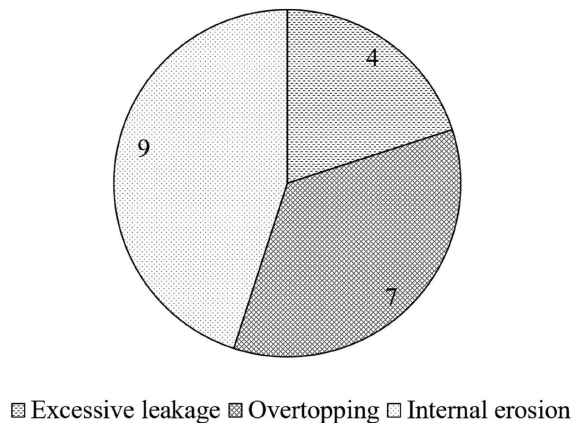


Figure 2. Percentages of incidents in Greek dams.

The majority of the incidents involves internal erosion. Nearly all reported cases of internal erosion are due to missing or inadequate filter and drainage zones, and/or insufficient

preparation of dam foundation. All these incidents would have been avoided if the well-established design practice had been followed.

The second largest group of incidents is overtopping. It is caused by very low design floods and thus insufficient spillway capacity. Occasionally this is due to inadequate stream flow measurement and reliance on very approximate assumptions regarding rainfall and runoff coefficients. It is apparent that there is a need to revise the design floods in most existing dams.

In many of the incidents, overtopping caused little damage to the dam, mainly because the downstream shoulders were made of good rockfill that is resistant to large shear stresses of the overflow.

The last group concerns excessive leakage. In the studied cases, excessive leakage was due to not detected unfavorable geological conditions and/or due to inadequately constructed grout curtains. It is known from reported cases that details in the construction of diversion culverts and in the sealing of joints between culverts and core (or plinth) are very important for preventing excessive leakage and internal erosion. It would be even better to adapt dam designs with no crossings of embankment dams by any culverts or outlets to avoid preferential flow paths at the interface between soil and solid structure which may also readily develop into internal erosion.

From all the reported cases the need for dam design made by specialists and not by inexperienced personnel becomes apparent.

REFERENCES

- Dounias G., Mamas N. and Georgalas G. 2016. Panayiotiko dam at Municipality of South Pelion, Thessaly District – Final report of GCOLD Panel of Experts. *Greek Committee on Large Dams Report*, April 2016 (in Greek)
- Dounias G. Moutafis N. and Mamas N. 2016. Report on the visit of GCOLD team at Sparmos dam and two other dams at Kalivia, Municipality of Elassona, District of Thessaly. *Greek Committee on Large Dams Report*, 10 May 2016 (in Greek)
- Dounias, G.T., Moutafis, N. and Mamas, N. 2017. The failure of Sparmos embankment dam of Elasona Municipality due to internal erosion – Description of the case. *3rd Greek Dams and Reservoirs Conference*, Athens 2017 (in Greek)
- Dounias, G.T. 2018. Key elements of National Dam Safety Regulation – The example of Greek Dam Safety Regulation. *5th International Symposium on Dam Safety, 27-31 October 2018*, Istanbul, Turkey
- Dounias, G.T. and Bardanis, M. 2019. The failure of homogeneous dams by internal erosion – The case of Sparmos Dam, Greece. *Sustainable and Safe Dams Around the World – Tournier, Bennett & Bibeau (Eds)*, © 2019 Canadian Dam Association, *ICOLD 2019*, Ottawa, ISBN 978-0-367-33422-2, p.8333
- Dounias G., Lazaridou S., Papachatzaki Z.R. and Tsiknakou P. 2020. Exohi Dam at Katerini Municipality - Inspection report. *Greek Committee on Large Dams Report*, 10-01-2020 (in Greek)
- ICOLD 1995. Dam failure and statistical analysis. *ICOLD Bulletin 99*, Paris
- ICOLD 2017. Internal erosion of existing dams, Levees and Dikes, and their Foundations. *ICOLD Bulletin 164*, Paris
- Kazilis, N. 2008. The failure conditions of Triadi dam of Thermi Municipality, Thessaloniki Prefecture, Greece, June 2007. *1st Greek Dam Conference*, Larissa 2008 (in Greek)
- Liakouris D. E. 1995. Geology and the Dams of Public Power Corporation. *Education Section of Public Power Corporation* (in Greek).
- Moutafis, N. I. 2008. Failures and incidents of Greek Dams. *1st Greek Dam Conference*, Larissa 2008 (in Greek)
- Poupart M. 2016. ICOLD Dam Incident Data Base - Objectives, Data definition, Data Base Management (Draft V1). *ICOLD/CODS/Project for a Dam Incident Data Base, 06/04/2016*
- Thanopoulos, I., Konstantinidis, Th., and Kollatou, A-M. G. 2017. Incidents in Small dams, the case of “Kokkinopilos” dam overtopping. *3rd Greek Dam Conference*, Athens 2017 (in Greek).
- Siskos, I.M. and Thanopoulos, I. 2013. Failure rehabilitation in small dams, the case of small Livadi and Ampelakia dams in Larissa district. *2nd Greek Dam Conference*, Athens 2013 (in Greek).

A dam-foundation seismic interaction analysis method: Development and first case studies

G. Faggiani & P. Masarati

Ricerca sul Sistema Energetico – RSE S.p.A., Italy

ABSTRACT: To accurately and realistically define the response of concrete dams to earthquakes it is often necessary to carry out complex FEM (Finite Element Method) analyses able to consider the three-dimensionality of the problem, the semi-unbounded size of the foundation, the non-linear behaviour of the system and the dynamic interactions of the dam with the foundation and the reservoir. An advanced approach to deal with dam-foundation seismic interaction was recently implemented and tested with the objective of appropriately simulating the propagation of seismic waves in a realistic massed foundation, considering its semi-unbounded extent. The approach, indicated by the acronym SAM-4D (Seismic Advanced Model for Dams), was developed by RSE to overcome the main deficiencies (above all the excessive conservativeness of the results) of traditional and simplified methods. Artificial non-reflecting (or absorbing) boundaries are used to delimit the semi-unbounded foundation and effective earthquake forces, computed with reference to the elastic wave vertical propagation theory, provide the seismic motion: the method can be adopted within the framework of FEM codes able to address all the above-mentioned complexities and allows to reduce the recognized excessive conservativity of the results obtained with simplified traditional approaches (e.g. the massless approach). Pre-processing software tools were developed to automate the calculation and the assignment of the effective earthquake forces to be applied to the artificial boundaries of the foundation. The method, including the pre-processing tools, was validated using theoretical and numerical solutions available in technical literature. Three case studies of dam-reservoir-foundation systems (one 2D case and two 3D cases) were carried out, allowing to verify the reliability of the method for real applications and to highlight the strong conservativity of the traditional analysis approaches with respect to the proposed method.

1 INTRODUCTION

Hydroelectric power plants provide the largest renewable contribution to generation, in Italy and worldwide; moreover, thanks to their flexible generation and storage capacity, they play a strategic role in the transition process towards a low-carbon, sustainable and resilient energy system. In contexts such as Italy, where most of the existing dams have more than 50 years and there is no possibility to build new large-scale plants, it is particularly important to encourage studies and methods to improve their efficiency, flexibility and safety. Regarding safety, a topic of considerable importance in the last years, is the assessment of the response of dams to earthquakes. International recent regulations, recommendations and guidelines require the reassessment also of existing dams, imposing seismic actions and performances much higher than in the past (at the age of their designing and building). The traditional and simplified analysis methods, often based on unrealistic assumption (e.g. neglecting the mass of the foundation), tend to significantly overestimate the seismic response of dams, sometimes leading to the conclusion that an existing dam is unsafe according to the current regulations (Chopra 2014, Hansen & Nuss 2013, Zang & Jin 2008). To overcome the main deficiencies

highlighted by the traditional and simplified methods for the seismic analysis of dam-reservoir-foundation systems (above all the excessive conservativeness of the results), it is therefore necessary to adopt advanced analysis methods, able to represent more reliably and realistically the structural response of dams to earthquakes. In this context a structure-soil dynamic interaction model, able to reproduce the propagation of seismic waves considering the dissipation effects through the boundaries of the artificially truncated massed foundation, was recently implemented and validated by RSE (Faggiani et al. 2019, 2020, 2021) and indicated by the acronym SAM-4D (Seismic Advanced Model for Dams).

Section 2 summarizes the main features of SAM-4D, mentioning some theoretical aspects of the method (§ 2.1), the adopted modelling solutions and the pre-processing tools (§ 2.2). In Section 3 three case studies of dam-reservoir-foundation systems are described: the 2D case of Pine Flat Dam (§ 3.1), the 3D case of Monticello Dam (§ 3.2) and the 3D case of a large Italian arch dam located in a high seismicity zone (§ 3.3). The main overcomes are focused on Section 4.

2 THE DAM-FOUNDATION SEISMIC INTERACTION ANALYSIS MODEL SAM-4D

The dam-foundation seismic interaction model SAM-4D allows to ideally reproduce the behaviour of the actual semi-unbounded foundation representing the wave propagation in a computation domain delimited by appropriate artificial boundaries and realistically provided with mass: the main properties of the model are deduced from Chen et al. 2012, Liu et al. 2006, Liu & Chen 2013, Zhang et al. 2009; Løkke & Chopra 2017, 2018, 2019 were considered as important references too. The model was implemented both in the commercial FEM code Abaqus (Dassault Systèmes 2021) and in the in-house FEM code CANT-SD (Masarati & Meghella 2000, Faggiani & Masarati 2011): Abaqus reliably simulates the non-linear behaviour of the concrete; on the other hand CANT-SD, specifically designed for the analysis of dam-reservoir systems, allows a quick and easy processing of the results, doesn't need commercial licenses for its use and accurately models the structural discontinuities in concrete dams.

The validation of the model includes the reproduction of the theoretical solution of the vertically propagating elastic wave problem for a flat foundation box (half-space) subject to impulsive or seismic excitation (Salamon 2018) and the reproduction of the analytical or numerical solutions available in literature for a semi-cylindrical canyon cut in a foundation half-space subject to sinusoidal excitation (Løkke & Chopra 2018, 2019, Trifunac 1972, Wong 1982).

2.1 *Theoretical notes*

The semi-unbounded extension of the foundation is achieved using artificial non-reflecting (or absorbing) boundaries at the truncations of the computational domain: one horizontal (the bottom boundary) and four vertical (the side boundaries) planes. The artificial boundaries consist in a layer of normal and tangential dampers and springs; if only dampers are used, the classic non-reflecting boundaries are obtained (Lysmer & Kuhlemeyer 1969). The incoming seismic waves are specified by means of effective earthquake forces, applied on both the bottom and the side boundaries of the foundation and computed, starting from the free-field ground motion, using the theoretical solution of the vertically propagating elastic wave problem in a half-space; the non-reflectivity of the boundaries allows the exit from the foundation of the outgoing waves, scattered by the dam-reservoir system that propagate towards infinity. In case the half-space is homogeneous and undamped the incident motion at the bottom boundary is equal to one-half the free surface motion: this simplification may be appropriate if the rock is assumed homogeneous and with no or little (up to 2%) material damping (Løkke 2017, Løkke & Chopra 2018).

2.2 *Modelling solutions and pre-processing tools*

To simulate the non-reflecting boundaries in the frame of a FEM model, two alternative solutions have been experienced: the infinite elements and the orthotropic elements. The infinite elements provide non-reflecting boundaries to the finite element model through the effect of

just a damping matrix (Dassault Systèmes 2021) and can be a practical solution if the FEM code is equipped with this type of element. Instead, if infinite elements are not available or the stiffness behaviour of the non-reflecting boundaries is considered important, the orthotropic elements can be introduced: these elements must be characterized by massless material with orthotropic linear behaviour where stiffness and damping characteristics are defined independently. The orthotropic elements can be easily obtained provided that the FEM code is able to simulate both the orthotropic material behaviour and the Rayleigh damping behaviour.

The calculation and assignment of the effective earthquake forces is not at all straightforward (particularly in the case of the side boundaries) and requires the use of specific pre-processing tools. Since in FEM codes the forces are usually expressed as sum of products of space and time functions, two pre-processors have been developed: one is aimed at writing the set of files with the space information (face of element and direction of the applied force), the other one at writing the set of the corresponding files with the time information (time history). Three types of seismic waves must be applied (P, S_x and S_y) and the side boundaries of the computational domain must be vertically divided into uniform layers.

3 CASE STUDIES

Three case studies of dam-reservoir-foundation systems are here presented: the 2D case study of Pine Flat Dam and the 3D case studies of Monticello Dam and of a large Italian arch dam located in a high seismicity area.

The seismic dam-foundation interaction is approached using the seismic wave propagation model SAM-4D, described at Section 2. The effective earthquake forces are computed considering the incident motion at the bottom foundation boundary equal to $\frac{1}{2}$ the surface motion (homogeneous foundation with no or small damping). The computed forces are applied both at the bottom and at the side boundaries of the foundation. The analyses are also carried out using the massless approach: in this case, the earthquake is uniformly applied to the boundaries of the massless foundation. The dynamic interaction between the dam and the reservoir is achieved through the classic structural-acoustic coupling on the upstream face of the dam (Zienkiewicz 1977), that allows to consider both the compressibility of the water and the damping effects at the boundary of the fluid domain. The upstream truncation of the reservoir is provided with non-reflecting acoustic condition; in the last two cases damping effects at the boundary of the fluid domain are assumed, using a reflection coefficient equal to 0.8 (Ghanaat 2000).

3.1 *Pine Flat Dam*

The seismic analysis of Pine Flat Dam was proposed in the frame of the ICOLD 15th *International Benchmark Workshop on Numerical Analysis of Dams* (Salamon et al. 2020) and before in the USSD workshop *Evaluation of Numerical Models and Input Parameters in the Analysis of Concrete Dams* (Salamon 2018). Pine Flat Dam (Fresno, California, USA) is a large concrete gravity dam consisting of thirty-six 15.25 m wide monoliths and one 12.2 m wide monolith.

The case study considers the tallest non-overflow dam monolith no.16, 15.24 m wide and 122 m high. The structural problem is schematized as a 2D (plane strain) problem applying appropriate symmetry conditions at side boundaries of the 3D FEM model, reported in Figure 1. The different parts of the mesh (dam, foundation and reservoir) are discretized quite uniformly, with element size ranging from 3 m to 6 m. The fluid domain is obtained by extruding the upstream face of the dam mesh up to the upstream boundary of the foundation. At the base and at the side boundaries of the foundation, damper and spring elements are placed to model the semi-unbounded extent of the foundation. The model of the foundation is characterized by elements of uniform height equal to about 6 m, that allows to describe with good accuracy frequencies up to about 15 Hz. Foundation rock and dam concrete are assumed to behave linear-elastically. The principal physical-mechanical properties of the materials are summarized in Table 1. The viscous damping, assumed equal to 2% for both the dam and the foundation, is defined using the classic Rayleigh modelling. The case study was approached with both the commercial FEM code Abaqus and the in-house FEM code CANT-SD.

The static loads are the self-weight of the dam and the hydrostatic pressure (applied both on the upstream face of the dam and on the surface of the foundation). The seismic action is the Taft horizontal (upstream component) acceleration time-history record of the M 7.3 Kern County, California, earthquake (peak ground acceleration of 1.77 m/s^2), considered as a free field ground motion at the surface of the foundation.

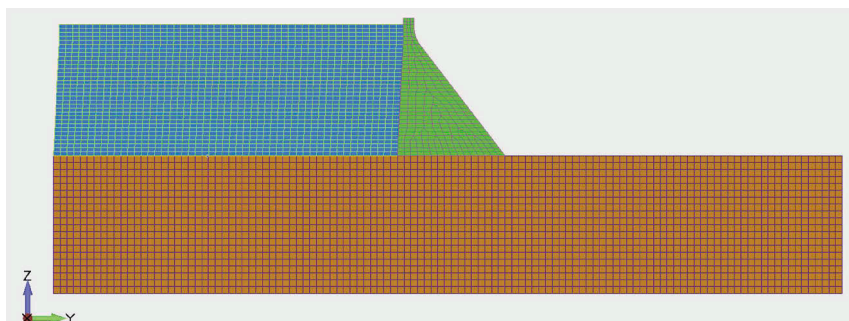


Figure 1. FEM model of the dam monolith, the foundation and the reservoir.

Table 1. Materials properties.

Parameter	Concrete	Rock	Water
Density [kg/m^3]	2483	2483	1000
Elastic modulus [MPa]	22410	22410	
Poisson's ratio [-]	0.2	0.2	
Compressional wave velocity [m/s]		3167	
Shear wave velocity [m/s]		1939	
Sound velocity [m/s]			1439

The following figures report the comparison of the results of the analyses performed with both the FEM codes (Abaqus and CANT-SD) and both the dam-foundation interaction methods (SAM-4D and massless approach) in terms of maximum principal stress envelope (Figure 2, Abaqus, and Figure 3, CANT-SD) and in terms of acceleration response spectra at dam toe and dam crest (Figure 4). The analyses carried out with the two codes provide actually the same results, in terms as of stress as of acceleration, proving that the model and the pre-processing tools were correctly developed in Abaqus as well as in CANT-SD. The seismic response obtained from massless approach is about 2 times greater than the response obtained from SAM-4D: tensile stress on downstream and upstream faces decreases from about 1.5 MPa to about 0.5 MPa and the maximum, at dam toe, draws down from about 8 MPa to about 6 MPa; peak acceleration (spectral acceleration at zero period) drops from about 15 m/s^2 to about 7 m/s^2 at dam crest.

3.2 Monticello Dam

The assessment of the seismic response of Monticello Dam was proposed in the *Blind Prediction Analysis Workshop* organized in the frame of the 2016 USSD Conference. Monticello Dam (Napa County, California, USA) is a large concrete arch dam, built between 1953 and 1957. The dam, 93 m high, 30 m thick at the base and 3.7 m at the crest (crest level at 139 m a.s.l.), is equipped with instrumentation at both the foundation and the dam crest, that recorded the acceleration time histories of a moderate earthquake occurred on May 22, 2015, not far from the dam site.

The case study was addressed with the FEM code Abaqus, using the 3D model reported in Figure 5 that includes the dam (4 elements in the thickness and 24 elements vertically in the main section), the foundation rock and the fluid domain (water level at 124.4 m a.s.l. on May 22, 2015) obtained by extruding the upstream face of the dam up to the upstream boundary of the foundation. The overall dimensions of the foundation model are

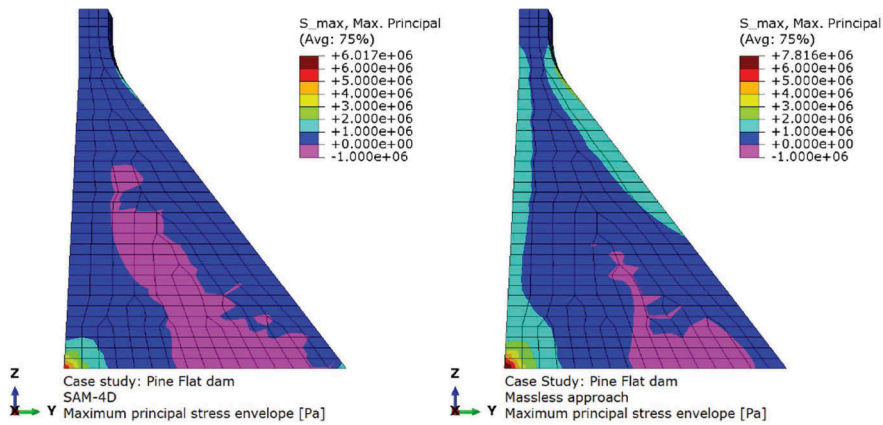


Figure 2. Maximum principal stress envelope (contour plot): comparison between SAM-4D and Massless approach (Abaqus code).

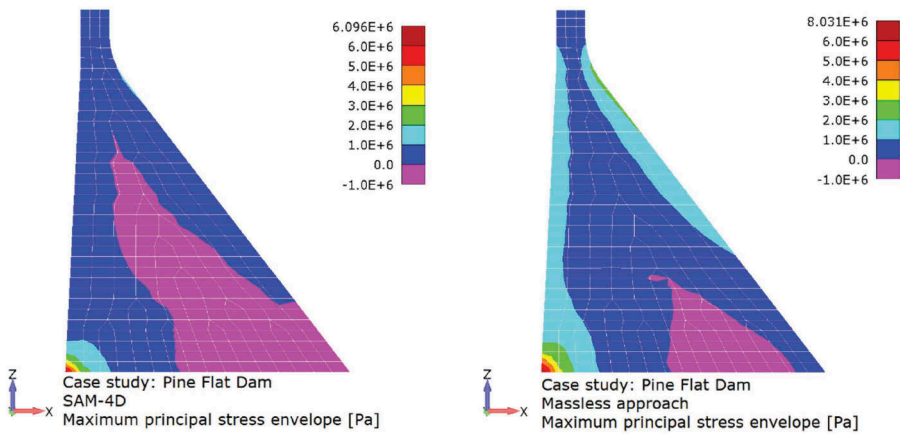


Figure 3. Maximum principal stress envelope (contour plot): comparison between SAM-4D and Massless approach (CANT-SD code).

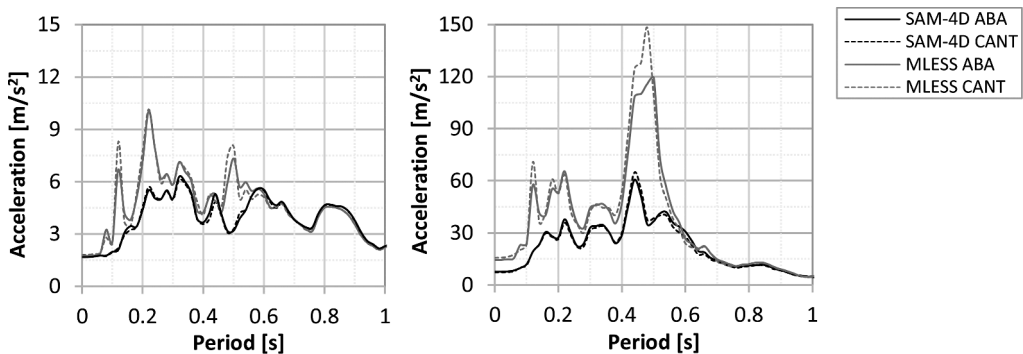


Figure 4. Acceleration response spectra (2% damping) at dam toe (left) and dam crest (right): comparison between the analyses performed with Abaqus (ABA) e CANT-SD (CANT) codes using the SAM-4D model (SAM-4D) and the massless approach (MLESS).

700 m×700 m×400 m, corresponding to approximately 7H×7H×4H, where H is the height of the dam. At the base and at the side boundaries of the foundation, infinite elements are included to model the semi-unbounded extent of the foundation. The model of the foundation is characterized by elements of uniform height equal to 10 m that allows to describe with good accuracy frequencies up to about 10 Hz. Foundation rock and dam concrete are assumed to behave linear-elastically. The principal physical-mechanical properties of the materials are summarized in Table 2. The viscous damping, assumed zero for the foundation and 2.5% for the dam, is defined using the classic Rayleigh modelling.

The static loads are self-weight, hydrostatic pressure and thermal gradient from a preliminary seasonal thermal transient analysis. Either the record at MONA, near the left abutment, or the record at MONF, near the dam toe, is considered as free field ground motion; these two monitoring points are shown in Figure 6 together with the two monitoring points MONC at the dam crest centre and MONQ at the dam crest left quarter). The peak acceleration is very moderate, about 0.1 m/s² in the upstream direction.

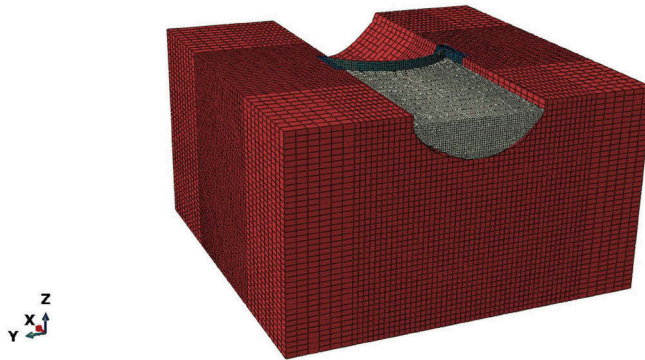


Figure 5. FEM model of dam-reservoir-foundation system.

Table 2. Materials properties.

Parameter	Concrete	Rock	Water
Density [kg/m ³]	2500	2500	1000
Elastic modulus [MPa]	32000	27200	
Poisson's ratio [-]	0.2	0.2	
Compressional wave velocity [m/s]		3477	
Shear wave velocity [m/s]		2129	
Sound velocity [m/s]			1440

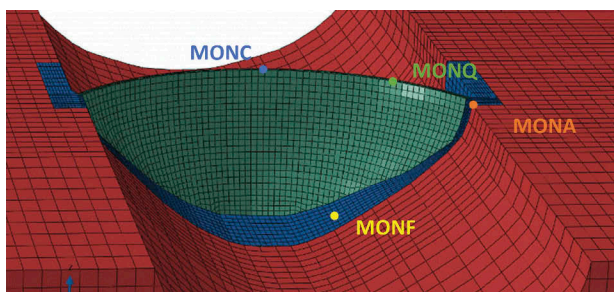


Figure 6. Monitoring points: MONA near the left abutment, MONF near the dam toe, MONC at dam crest centre and MONQ and the dam crest left quarter.

The results of the seismic analyses performed with the SAM-4D model, and the massless approach are reported in terms of upstream acceleration response spectra and compared with the corresponding experimental measures at monitoring points MONA and MONF in the foundation, MONC and MONQ on the dam crest. The following figures report the results of the analyses considering as seismic input either the record in MONA (left) or the record in MONF (right).

Figure 7 (left) and Figure 8 (right) show the comparison between the results of the analyses and the corresponding seismic input in MONA and MONF: the seismic input is well reproduced by the analyses with the massless approach (as expected considering that seismic waves propagate unchanged at infinite velocity throughout the foundation); the analyses with the SAM-4D model are a bit overestimated when the seismic motion recorded in MONA is used, only slightly underestimated when the seismic motion recorded in MONF is used. The results of the analyses well fit the records in the point in the foundation different from the one used to define the seismic input (Figure 7 right and Figure 8 left).

At MONC (Figure 9) the analyses with the massless approach greatly overestimate the actual response of the structure, instead better reproduced by the analyses with the SAM-4D model (however the simulated accelerations result higher than the measured ones): at this monitoring point, the analyses with the massless approach provide results almost double than those obtained with the SAM-4D model.

At MONQ (Figure 10) all the performed analyses provide results quite greater than records: the analyses considering the record in MONA, about 2 times, the ones considering the record in MONF, about 1.5 times, almost irrespective of the adopted dam-foundation interaction method.

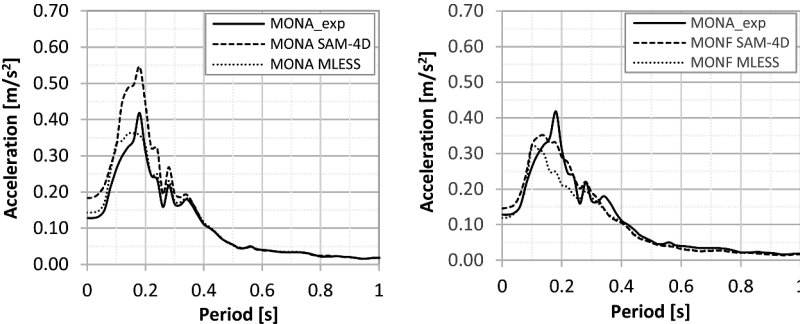


Figure 7. Response spectra (2.5% damping) of upstream acceleration at MONA. Comparison between the recorded data (MONA_exp) and the results of the analyses performed with the SAM-4D model (SAM-4D) and the massless approach (MLESS), with seismic input in MONA (left) and in MONF (right).

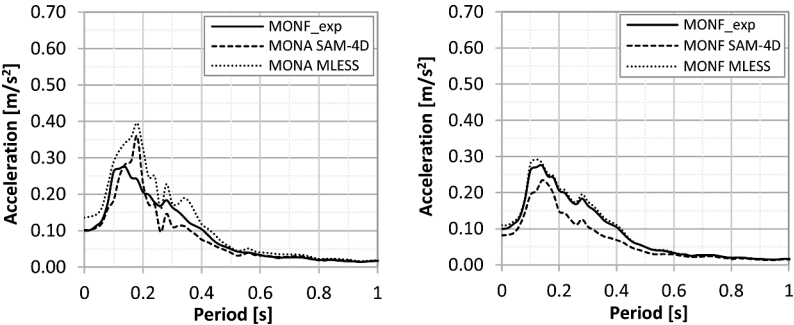


Figure 8. Response spectra (2.5% damping) of upstream acceleration at MONF. Comparison between the recorded data (MONF_exp) and the results of the analyses performed with the SAM-4D model (SAM-4D) and the massless approach (MLESS), with seismic input in MONA (left) and in MONF (right).

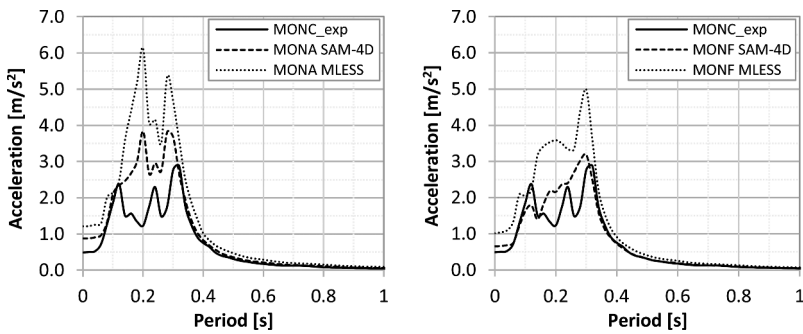


Figure 9. Response spectra (2.5% damping) of upstream acceleration at MONC. Comparison between the recorded data (MONC_exp) and the results of the analyses performed with the SAM-4D model (SAM-4D) and the massless approach (MLESS), with seismic input in MONA (left) and in MONF (right).

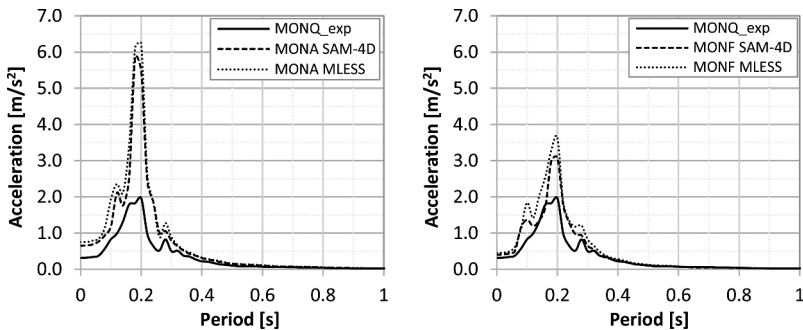


Figure 10. Response spectra (2.5% damping) of upstream acceleration at MONQ. Comparison between the recorded data (MONQ_exp) and the results of the analyses performed with the SAM-4D model (SAM-4D) and the massless approach (MLESS), with seismic input in MONA (left) and in MONF (right).

3.3 Large Italian arch dam

The last case study deals with a large concrete arch dam (about 70 m high, about 160 m crest length), located in an area of high seismic hazard in Northern Italy.

The case study was carried out with the FEM code Abaqus, using a 3D model that includes the dam and the “pulvino” (4 elements in the thickness and 25 elements vertically in the main section), the foundation rock and the fluid domain (at maximum regulation level) obtained by extruding the upstream face of the dam up to the upstream boundary of the foundation. Infinite elements are located at the bottom and at the side boundaries of the computation domain (700 m×700 m×400 m) to model the semi-unbounded extent of the foundation. The model of the foundation is characterized by elements of uniform height equal to 10 m that allows to describe with good accuracy frequencies up to more than 10 Hz. Foundation rock and dam concrete are assumed to behave linear-elastically. The principal physical-mechanical properties of the materials are summarized in Table 3. The viscous damping, assumed zero for the foundation and 5% for the dam, is defined using the classic Rayleigh modelling.

The static loads are self-weight, hydrostatic pressure and thermal gradient from a preliminary seasonal thermal transient analysis. The seismic input consists in a high-intensity earthquake (with a return time of about 2000 years, as prescribed by the Italian regulation) with peak acceleration of about 4 m/s² in the upstream direction.

The results of the seismic analyses performed with the SAM-4D model and the massless approach are reported in terms of maximum principal stress (Figure 11 and Figure 12

Table 3. Materials properties.

Parameter	Concrete	Rock	Water
Density [kg/m ³]	2400	2400	1000
Elastic modulus [MPa]	43500	48500	
Poisson's ratio [-]	0.12	0.34	
Compressional wave velocity [m/s]		5577	
Shear wave velocity [m/s]		2746	
Sound velocity [m/s]			1440

respectively) and of upstream acceleration response spectra (Figure 13). The massless approach provides a more severe seismic response than that of the SAM-4D model: neglecting the maximum at dam-foundation interface that depends on the monolithic model, tensile stress on downstream and upstream faces in the case of massless foundation are about 1.5-2 higher than in the case of SAM-4D model; peak acceleration (spectral acceleration at zero period) decreases from about 30 m/s² to about 20 m/s² at dam crest and from about 4.5 m/s² to about 3.9 m/s² at dam toe.

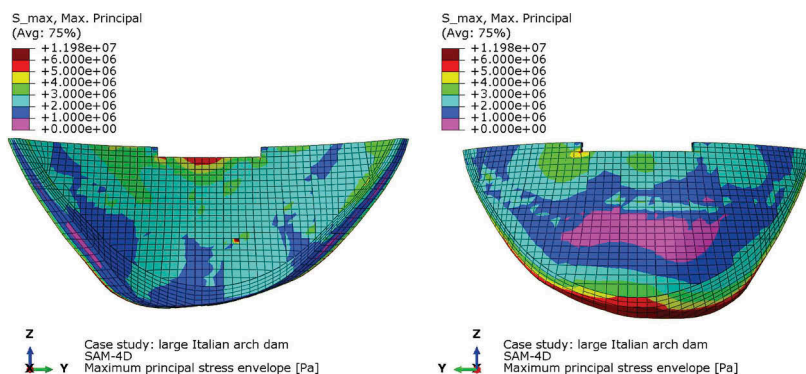


Figure 11. Maximum principal stress envelope (contour plot): analysis with SAM-4D. Downstream view (left) and upstream view (right).

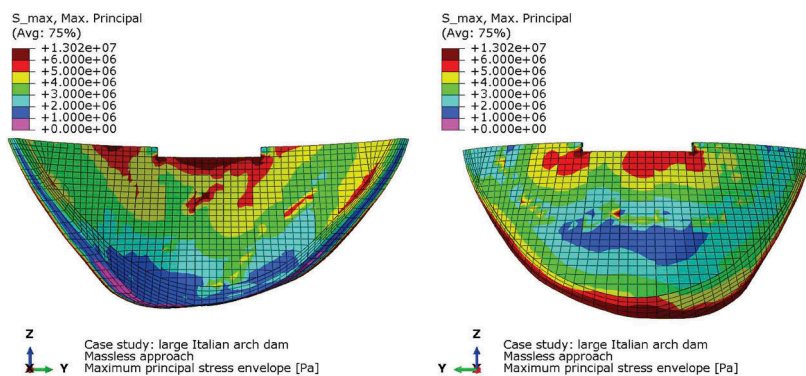


Figure 12. Maximum principal stress envelope (contour plot): analysis with massless approach. Downstream view (left) and upstream view (right).

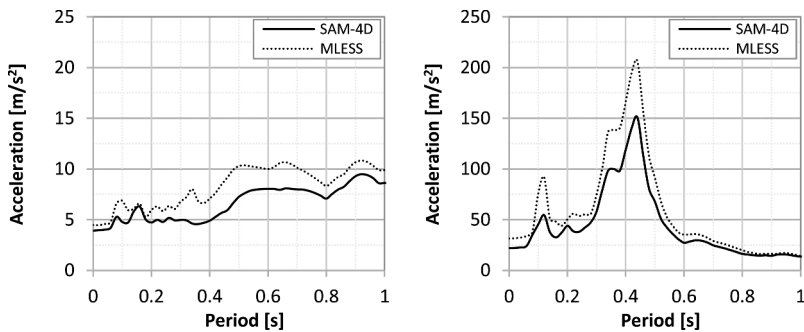


Figure 13. Response spectra (5% damping) of upstream acceleration at dam upstream toe (left) and dam crest (right). Comparison between SAM-4D and massless approach (MLESS).

4 CONCLUSIONS

The SAM-4D (Seismic Advanced Model for Dams) model was recently implemented by RSE in the frame of the commercial FEM code Abaqus and of the in-house FEM code CANT-SD, with the main purpose to reduce the excessive conservativeness of traditional and simplified methods for the seismic safety assessment of dams. It is an advanced structure-soil dynamic interaction model, able to simulate the propagation of seismic waves in a realistic massed foundation, considering its semi-unbounded extent. Suitable modelling solutions and pre-processing tools are studied, developed and tested to efficiently support the adoption of the model, especially in the context of the numerical analysis of 3D cases. The model was validated using theoretical and numerical solutions available in technical literature.

Three case studies of dam-reservoir-foundation systems were carried out with the main objective to compare the results obtained with the SAM-4D model and the traditional and consolidate massless approach: the 2D case of the Pine Flat gravity dam, the 3D cases of the Monticello arch dam and of an Italian large arch dam located in a high seismicity zone. The strong conservativity of the massless approach was highlighted by the results of all the three case studies. Moreover, the comparison with the experimental data recorded during a small earthquake in one of the case studies allows to demonstrate the reliability of the model, able to well reproduce the overall seismic behaviour of the dam, with minor overestimation than the massless approach.

Further investigation to compare numerical results with measured data, also in case of more severe earthquake, would be very important to improve the confidence and the reliability in the use of this advanced numerical method.

ACKNOWLEDGMENTS

This work has been financed by the Research Fund for the Italian Electrical System under the Three-Year Research Plan 2022-2024 (DM MITE n. 337, 15.09.2022), in compliance with the Decree of April 16th, 2018.

REFERENCES

- Chen, D.H., Du, C.B., Yuan, J.W. & Hong, Y.W. 2012. An investigation into the Influence of Damping on the Earthquake Response Analysis of a High Arch Dam. *Journal of Earthquake Engineering*, 16(3): 329–349.
- Chopra, A.K. 2014. Earthquake Analysis Of Concrete Dams: Factors To Be Considered. In *Proc. of the 10th National Conference in Earthquake Engineering*. Anchorage, Alaska
- Dassault Systèmes S.A. 2021. *SIMULIA Abaqus Unified FEA*.
- Faggiani, G. & Masarati, P. 2011. *Il programma di calcolo strutturale CANT-SD (versione 16.4) e suoi pre/post-processori: manuali d'uso*. Ricerca di Sistema, RSE, n. 12001259, Milano.

- Faggiani, G., Masarati, P., Polidoro, F. & Bruno G. 2019. *Modellazione dell'interazione diga - fondazione nell'analisi sismica delle dighe. Applicazione a casi bi-dimensionali*. Ricerca di Sistema, RSE, n. 19012845, Milano.
- Faggiani, G., Masarati, P., Polidoro, F. & Bruno G. 2020. *Analisi sismica dei sistemi tridimensionali diga-bacino-fondazione con modelli di interazione avanzata*. Ricerca di Sistema, RSE, n. 20010749, Milano.
- Faggiani, G., Masarati, P., Polidoro, F. & Bruno G. 2021. *Analisi sismica dei sistemi tridimensionali diga-bacino-fondazione, con modelli di interazione avanzata: applicazioni e confronti numerico-sperimentali*. Ricerca di Sistema, RSE, n. 21010320, Milano.
- Ghanaat, Y., Hall, R.L. & Redpath, B.B. 2000. Measurement of dynamic response of arch dams including interaction effects. In *Proc of 12th WCEE*.
- Hansen, K.D. & Nuss, L.K. 2013. Seismic Upgrades for Concrete Dams Then and Now. *The Journal of dam Safety* 11(4): 21–35.
- Hilber H.M., Hughes T.J.R. & Taylor R.L. 1977. Improved numerical dissipation for time integration algorithms in structural dynamics. *Earthquake Engineering and Structural Dynamics*, 5: 283–292.
- Liu, J., Du, Y., Du, X., Wang, Z. & Wu, J. 2006. 3D viscous-spring artificial boundary in time domain. *Earthquake Engineering and Engineering Vibration*, 5(1): 93–102.
- Liu, Y.S. & Chen, D.H. 2013. Earthquake Response Analysis of a Gravity Dam Considering the Radiation Damping of Infinite Foundation. In *APCOM & ISCM*. Singapore.
- Løkke, A. 2017. A researcher's perspective on modelling unbounded domains for earthquake analysis of dams. In *2nd Dams & Seisms EWG Workshop Lessons learn from earthquakes occurring in Italy. Qualification of dynamic analyses of dams and their equipments and of probabilistic assessment of seismic hazard in Europe, Rome 6th February 2017*.
- Løkke, A. & Chopra, A.K. 2017. Direct finite element method for nonlinear analysis of semi-unbounded dam–water–foundation rock systems. *Earthquake Engineering and Structural Dynamics*, 46(8): 1267–1285.
- Løkke, A. & Chopra, A.K. 2018. Direct finite element method for nonlinear earthquake analysis of 3-dimensional semi-unbounded dam–water–foundation rock systems. *Earthquake Engineering and Structural Dynamics*, 47(5): 1309–1328.
- Løkke, A. & Chopra, A.K. 2019. Direct finite element method for nonlinear earthquake analysis of concrete dams: Simplification, modeling, and practical application. *Earthquake Engineering and Structural Dynamics*, 48(7): 818–842.
- Lysmer, J. & Kuhlemeyer, R.L. 1969. Finite dynamic model for infinite media. *Journal of the Engineering Mechanics Division*, 95(4): 859–878.
- Masarati, P. & Meghella, M. 2000. *The FEM computer code CANT-SD for non-linear static and dynamic analysis of dams*. Enel.Hydro PIS n. 6045, Milano.
- Salamon, J.W., Wood, C. Hariri-Ardebili, M.A., Malm, R., & Faggiani, G. 2020. Seismic analysis of Pine Flat concrete dam. Theme A – Formulation and Synthesis of Results. In *Proc. of 15th ICOLD International Benchmark Workshop, Milano, 9–11 September 2019*. Cham: Springer.
- Salamon, J.W. 2018. *Evaluation of numerical models and input parameters in the analysis of concrete dams – A summary report of the USSD Workshop, Miami 3 May 2018*. USBR DSO-19-13.
- Trifunac, M.D. 1972. Scattering of plane SH waves by a semi-cylindrical canyon. *Earthquake Engineering and Structural Dynamics*, 1(3): 267–281.
- Wong, H.L. 1982. Effect of surface topography on the diffraction of P, SV, and Rayleigh waves. *Bulletin of the Seismological Society of America*, 72(4):1167–1183.
- Zhang, C. & Jin, F. 2008. Seismic Safety Evaluation Of High Concrete Dams Part I: State Of The Art Design And Re-search. In *Proc. of the 14th World Conference on Earthquake Engineering, Beijing, 12–17 October 2008*.
- Zhang, C., Pan, J. & Wang, J. 2009. Influence of seismic input mechanisms and radiation damping on arch dam response. *Soil Dynamics and Earthquake Engineering*, 29(9): 1282–1293.
- Zienkiewicz, O.C. 1977. *The Finite Element Method*. 3rd Edition, McGraw-Hill.

Concrete swelling: Studies and pragmatic results. Case study of Cleuson dam

Jonathan Fauriel

Head Civil Engineering and Environment, Alpiq Ltd, Switzerland

Andrea Abati

Projet manager, Gruner Stucky SA, Switzerland

Milaine Côté

Supervision of Dams Specialist, Swiss Federal Office of Energy SFOE, Switzerland

Reynald Berthod

N3 Expert, Gruner Stucky SA, Switzerland

ABSTRACT: Concrete swelling affects most of the existing concrete dams in Switzerland. The peculiar case study of the Cleuson dam, a 87 m hollow gravity dam, is proposed.

Irreversible movements of the dam body have been measured almost since the first impoundment and significant cracking in the upper part of the structure has been monitored since 2005. Based on the observation of the cracking and preliminary calculations, an operating restriction of 2 m was decided in 2008. In 2012, further investigations led to characterization of the cracking and determination of the concrete pathology. On this basis, a finite element model was made in 2013, implementing the movements, the cracks and the concrete swelling. The results showed that the structural safety was guaranteed.

In view of the dam body swelling pursuit, new studies were carried out in 2021 and 2022 to estimate the time frame in which the safety of the structure would no longer be guaranteed. Analyses of the probable failure mechanism associated with a damage model showed that a risk of failure should not appear before 30 years.

1 INTRODUCTION

The lifespan of a storage facility can be several centuries, but at the time of construction, the structure is often designed for a time horizon of 80 to 100 years. If the first impoundment is clearly the most sensitive moment from the structural safety point of view, taking into account the evolution of the structure over time leads to complex considerations. For the engineer, the question is how to guarantee the dam safety whilst avoiding the simplicity of over-conservative solutions that would have a strong impact on the existing facilities and on the environment. Finding the right balance between a coherent and reasonable solution is a real challenge for all stakeholders. A common will of the operating staff, the structural engineers, the owner/operator and the supervisory authorities is needed to find such solutions. Thus, the objective is to achieve a result that is beneficial to society at large, both from an economic and environmental point of view.

The vast majority of dams in Switzerland were built between 1920 and 1990 (Figure 1) with an average of more than 1 dam constructed per year. With a value of 4.2 dams per year, the peak of construction took place between 1945 and 1975. In 2023, we celebrate an average age of 70 years for Swiss dams. 154 concrete retaining facilities are under federal supervision. An analysis of the Swiss Committee on Dams (SCD) concluded that concrete expansion affects between 35% and 45% of Swiss concrete dams (SCD, 2017).

The example of the Cleuson dam is given here. After a brief description of the dam, the various observations and preliminary analyses are presented. The results of the discussions on the structural assessment for the next few years (20 to 30 years) are then proposed. The last paragraph gives information on the monitoring of the structure and on the feedback from the main stakeholders.

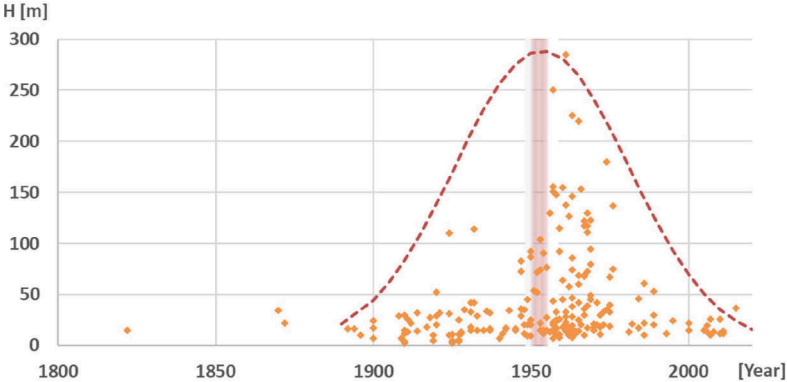


Figure 1. Dam construction in Switzerland: height and year of achievement, adapted from SCD.

2 DAM DESCRIPTION

The Cleuson reservoir stores water from the Haute Printze and Tortin catchment areas and pumps it into the Grande Dixence reservoir in all seasons. The uses of the water and the existing infrastructure are numerous (drinking water, irrigation, tourism...) but the main goal remains the production of electricity, with a net energy output of about 100 GWh per year.

The dam is a 87 m high concrete structure. Located at an altitude of 2,187 meters (crown level), the structure is set in a favorable topographic site, allowing it to hold a 19.5 hm³ reservoir. It was designed as a hollow weight dam (Noetzli type) with 18 pillars and a spacing of 12 m. The volume of concrete put in place was 88,000 m³ up to the levels 2,130 and 2,134 m.s.m. Due to military constraints, every second hollow space had to be filled in to resist a possible attack. Therefore, above 2,166 m s.m. level (last 21 m), the dam is massive. The volume of concrete used finally amounted to 405,000 m³.

Geologically, the conditions can also be considered to be favorable with a good quality chlorite gneiss and micaschist. Construction of the dam began in 1947 and was completed in 1950.

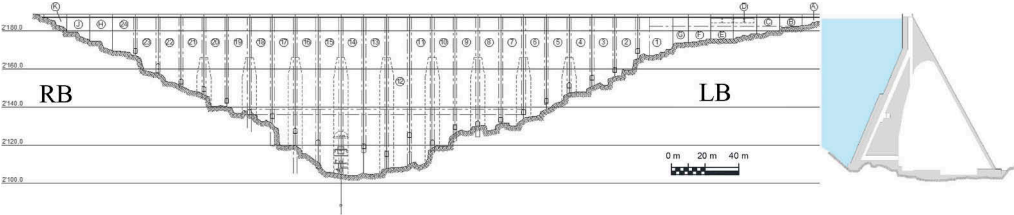


Figure 2. Cleuson dam. Elevation from downstream and cross section (hollow 12-13).

3 PRELIMINARY ASSESSMENTS

Irreversible movements have been measured since almost the first impoundment and significant cracking in the upper part of the structure has been monitored since 2005 (3.1). The results obtained from the first analyses (3.2) do not indicate a known mechanism and/or internal reaction

to explain the behaviour of the structure. The study of the available information has led to a new basis for analysis. With this in mind, an action plan was presented to the Federal Office of Energy in December 2012, and then validated by the Office in March 2013. The investigations (3.3) are focused gaining a better understanding of the mechanical and chemical characteristics of mass concrete, as well as of the apparent cracking observed from vertical shafts. This new knowledge is a solid basis for the development of structural safety verification models (3.4).

3.1 Main observations and measurements

Since its construction, the Cleuson dam has been subject to a special follow-up. As soon as it was impounded, a deterioration of the concrete was observed on the upstream and downstream faces of the dam. From 1994 to 1998, repair works were carried out on the upstream face, the crest and the spillway. In 2002, vertical cracks were found in the drainage shafts of the hollows. Finally, the measurements indicate irreversible downstream displacements of about 1 mm/year (Figure 3) as well as a rise of the same order of magnitude at the crest.

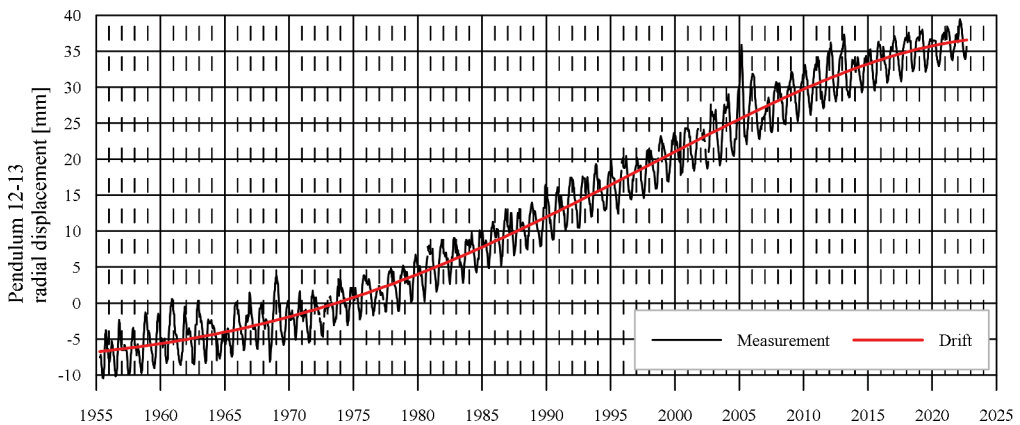


Figure 3. Irreversibility of Cleuson dam movement, hollow 12-13.

3.2 2007 and 2008 first analysis

In 2007 and 2008, the safety of the upper part of the structure was analysed using the pseudo-static method. In agreement with the supervisory authorities, an operating restriction of 2 m was decided, i.e. a maximum operating level of 2184.5 m.s.m. At the same time, investigations were launched with the aim of identifying and explaining the observed damage. Three samples were taken from the upstream face of the mass concrete. The samples were then analysed by three independent laboratories for chemical and thermal analyses, X-ray diffractometry, scanning electron microscopy, petrographic examinations with polarising optical microscopy and transmitted light microscopy. Each laboratory provided significantly different results, explaining the degradation of the concrete by various pathologies and with sometimes opposite conclusions. Internal or external sulphate reaction, alkali reaction, delayed ettringite formation were suggested or, in some cases, excluded.

3.3 Additional investigations

3.3.1 Mechanical and chemical concrete characteristics

For a calculation based on a damage and performance loss model, a test campaign was launched to determine the spatial distribution of the elasticity modulus in the concrete. Several large-diameter core samples were taken from the mass concrete in November 2012 and the elasticity modulus values were determined for each sample. With an average value of more

than 40 GPa, the measured value was considered rather high for mass concrete, although the variation between different samples could be significant (standard deviation of 3.8 GPa).

From December 2012 to February 2013, X-ray diffraction powder analyses and scanning electron microscope observations ruled out the role of sulphate in the swelling of the structure. Although the presence of a high concentration of sulphate in the grout coming from an injection work (1951-1953) was confirmed, a migration of sulphate between the grout and the concrete is excluded due to a clear separation of the two sulphate contents. In addition, the small amount of pyrite, confirmed by spectrometry, allows to ban this material as the source of a continuous supply of sulphate.

In the previous test campaigns, the alkali-silica reaction was not systematically detected. However, the swelling characteristics of the dam are consistent with such a reaction. This can be explained by the fact that in order to be detected in the laboratory, the reaction must have reached a minimum advancement threshold. Below a certain deformation, the swelling of the concrete can be measured without significant damage to the structure. This is all the more true when a large volume of concrete is involved. For the Cleuson dam, the swelling phenomenon has been regular since the 1970s and reaches a total irreversible deformation of about 0.025%, which is of the order of magnitude as the detection limit (Figure 4a). Based on this observation, a long-term test based on the SIA MB 2042 standard was initiated. Three specimens were placed in a water-saturated atmosphere at 60°C for six months. The deformation of the specimens is measured regularly to monitor the development of swelling. At the end of the test, the average swelling observed was of the order of magnitude of the detection limit (0.028% after 160 days). In addition, a scanning electron microscope analysis carried out at the end of the test on the three specimens revealed the presence of silica gel (Figure 4b) and degradation linked to GAN. It can therefore be concluded that the cores taken from the mass concrete are reactive, but of low intensity.

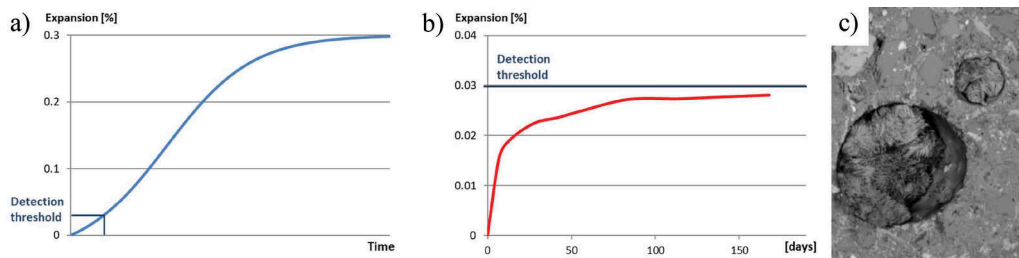


Figure 4. a) Expansion model and detection threshold, adapted from Larive b) Average observed swelling of the long-term test for Cleuson dam concrete, adapted from LMC-EPFL c) Visualization of silica gel (LMC-EPFL).

3.3.2 Characterisation of the observed cracking

The observations of the usual inspections focus on the visible parts of the structure (the concrete surface) and it is difficult to describe the expansion of the cracks into the concrete mass. A crack opening of several millimetres may suggest that the depth of the crack is significant, leading to very conservative design assumptions.

In addition to the observations of the visible parts on the surface, two specific investigations were carried out in 2012 and 2013. A borehole was drilled in the direction of the main vertical crack of block 13, open by 2 mm, from the vertical drainage shaft, 8 m below the crest. The drilling shows that the depth of the crack from the side of the shaft towards the shore is only 45 cm (Figure 5a).

In the summer of 2013, coloured water was injected in horizontal boreholes drilled from the downstream wall in an upstream direction (Figure 5b). The aim of these water tests is to reach possible through cracks in the left bank - right bank direction between two drainage shafts. The results show that a vertical through-cracking connecting the drainage shafts is not present, even in the upper part. Thanks to the investigations described above, systematic through-cracking in the direction left bank - right bank could be excluded (Figure 5c).

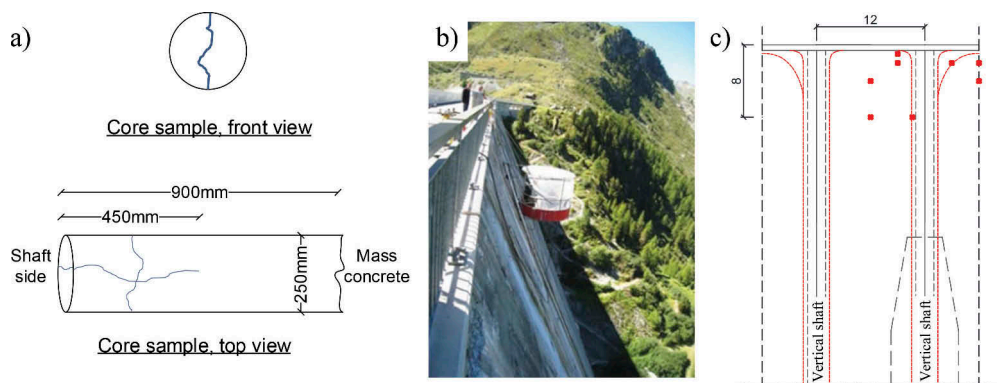


Figure 5. a) core sample and depth of cracking b) water testing and installation b) borehole (red points) and maximum cracking limit (red line).

3.4 Structural safety

The structural analysis has required unconventional calculations. A numerical model of the central blocks of the dam was performed. Based on the observed behaviour of the dam, the mechanical properties were obtained by calibration of the calculated temperature and displacements with the measurements available from the monitoring system. The reversible part of the dam behaviour was obtained separately by purging the observed deformation from the observed drifts. The irreversible part of the deformation was subsequently reproduced by means of a “thermo-mechanical analogy”. The stress-strain state obtained by the “thermo-mechanical analogy” was subsequently introduced in a simplified elasto-plastic analysis of the top part of the dam to reproduce the cracking in the concrete.

The so-obtained numerical model was therefore used to define the initial state of a dynamic time-history analysis to check the dam safety to the Safety Evaluation Earthquake. The safety assessment involved checking of both dynamic tensile and compressive stresses within the concrete mass, the eventual evolution of the cracking pattern during the earthquake, the dynamic stability of blocks in the top part of the dam.

As it was recognized that the cracking pattern in the top part of the dam was evolving with time together with the irreversible deformation, the focus was moved in defining a correlation between the dam safety and the evolution of the crack, i.e. in obtaining a definition of an Ultimate Limit State as a function of the penetration of the crack (“critical depth”) in the top part of the dam. Such “critical depth” was defined as the depth of a continuous crack between two shafts for which, as a consequence of the dynamic vibration induced by the earthquake, a concrete slab upstream the crack could fall into the reservoir leaving exposed the drainage shafts to the water and thus inducing an uncontrolled release of water.

In a further stage, a numerical prediction was obtained for when such a “critical depth” of the crack would have been achieved. Finally, a study was performed to define how to monitor the obtention of this Ultimate Limit State condition.

4 LONG TERM APPROACH

4.1 Numerical model

A full three-dimensional model of the dam was developed with the aim of improving the prediction of the cracking in the top part of dam. Numerical analyses were performed in order to reproduce the present cracking pattern observed within the drainage shafts. The cracking was reproduced by modelling the irreversible component of the dam deformation with the “thermo-mechanical analogy”. Several assumptions were made to take into account both damaging and creep in an aged concrete while avoiding producing an unrealistic stress state in the dam body, which is the typical drawback of the “thermo-mechanical analogy approach”.

The model allowed reproducing with a good agreement the three-component irreversible deformation, i.e. the bank-to-bank and the upstream-to-downstream drift in the deformation of the top part, as well as the heave in the dam crest.

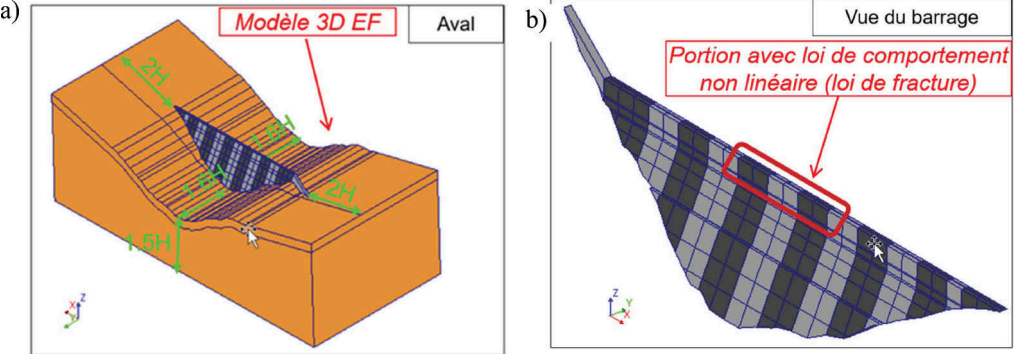


Figure 6. A) Geometry of the three-dimensional model of the dam and its foundation b) Three-dimensional model of the dam, with all the blocks: highlighted in red, the part of the model where the access shafts have been modelled in detail together with a non-linear smeared crack model for the concrete.

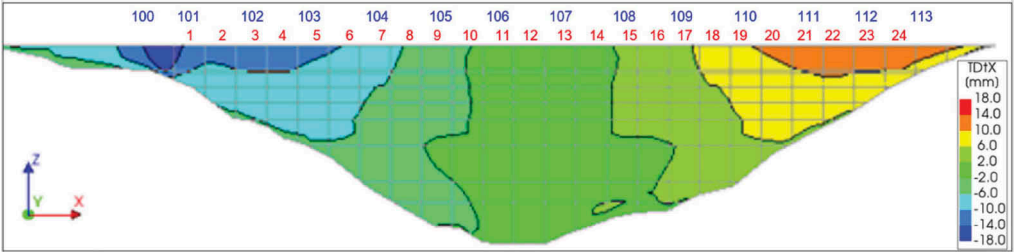


Figure 7. Bank-to-bank cumulated displacements (estimated at 2022), upstream view.

As a consequence of the bank-to-bank compressive state generated by the induced deformation, the cracking has been reproduced in the central blocks, where the actual geometry of the drainage shafts was modelled by means of a local mesh refinement and considering a “smeared crack” model. The penetration in depth and between two shafts was reproduced by progressively adjusting by a “trial and error” procedure the assumptions on the material properties. In particular, it was found that a good agreement with the observed crack pattern was obtained assuming a decay in the tensile strength of the concrete in the most superficial part of the dam, which is consistent with an increased damaging in the concrete.

4.2 Crack evolution

Since the cracking in the top part of the dam is a continuously evolving process, the scope of the model was to provide a tool to estimate the time horizon for the crack to reach that “critical depth” constituting an Ultimate Limit State for the seismic safety assessment.

Being the cracking in the top part intimately linked with the irreversible component of the deformation, in particular in the bank-to-bank direction, an assumption on the evolution of such irreversible deformation was made by a linear projection within the time. Such approach was considered conservative as it does not consider the “saturation” of the Alkali Aggregate Reaction with the development of a compressive state, i.e. the expansion tends to slow down in the direction where a compressive state tends to be higher.

Despite the simplifying conservative assumptions, it was concluded that the depth of a cracking passing through two shafts could achieve a “critical depth” (about 8 m below the crest) in the next few decades with a cautious estimate of 30 years.

4.3 *Dam monitoring and cracking follow-up*

The numerical model must be considered a support tool than it cannot replace a good monitoring practice which, on the other hand, can be adjusted to provide in time supporting information than can be compared with the results of the numerical analyses.

Considering the dam monitored behaviour and the results of the numerical analyses, it was found that the follow up of the dam could be complemented in order to include some “parameters” of the dam behaviour which can be used to predict the crack deepening with time. Three possible approaches were evaluated:

4.3.1 *Global indirect parameters*

The global indirect parameter which is more intimately linked to the crack evolution is the irreversible component of the bank-to-bank deformation of the dam, which is presently monitored both by pendulum and by geodetic surveys. Indeed, both the vertical heave and the upstream to downstream drift are not considered meaningful as the link between these deformation components and the development of the compressive stress in the bank-to-bank direction is indirect and it tends to become less evident with time, as the dam will tend to deform more in the directions where the compressive stress is lower.

On the other hand, even if the link is more evident, even the bank-to-bank deformation component must be considered only as a qualitative parameter, in view of the constitutive assumptions which are required to correlate the induced compressive stress with the reproduced cracking pattern. As a consequence, the bank-to-bank component of the irreversible deformation is kept only as a tool to judge eventual changes in trends.

4.3.2 *Local indirect parameters*

Local indirect parameters include those measures which can be taken in the drainage shafts and that could be correlated with the crack penetration between two shafts. For example, the crack opening is constantly monitored. However, a correlation between the crack opening and the penetration within the concrete is difficult to be achieved. The numerical modelling is able to qualitatively reproduce the cracking. However, branching of cracks and occurrence of different secondary cracks in reality cannot be reproduced with a “smeared crack”.

As a consequence, the direct observation of the surface cracks is kept as a information useful for the qualitative assessment of the crack evolution but it is not considered as an estimate to understand the crack penetration.

4.3.3 *Local direct parameters*

Finally, the crack can be directly monitored. Two possible approaches are considered. The depth of the penetration of the crack can be followed by drilling from the shafts. This approach has the advantage of being of ease implementation, but its main drawback is that the crack can be “lost” by the drilling due to deviations in its development or branching.

An alternative approach which has been implemented in other dams in Switzerland consists in monitoring the cracks by the use of sliding micrometer along boreholes. The extensometers can either detect an existing or newly formed crack at any location by comparing the tensile strain between two successive gauging stations. The number, position and depth of the extensometers can be adjusted to the required level of accuracy of information that is required.

5 LESSONS LEARNED AND CONCLUSION

The Cleuson dam is considered as a large dam according to Article 3, paragraph 2, letter a of the Federal Act on Water Retaining Facilities (WRFA, RS 721.101) and is therefore subjected to direct federal supervision by the Federal Office of Energy’s Dam Supervision Section (SFOE-TS). In accordance with the Swiss 3-pillar safety concept, the SFOE-TS ensures that the operator fulfils its legal obligations in terms of construction requirements, surveillance and emergency preparedness. The Cleuson dam has been monitored since it was commissioned in 1951.

The annual reports of the Cleuson dam provide a summary of the condition and behaviour based on the inspections and measurements carried out. Experts in civil engineering and geology intervene every 5 years in order to carry out a long-term analysis of the condition and behaviour and issue recommendations. Monitoring of the Cleuson dam quickly identified the appearance of an irreversible deformation downstream, as well as a rise in the crest. Over the years, vertical cracks have appeared in the tangential direction inside the vertical shafts, suggesting a common cracking plane in all shafts and therefore a dissociation of the upper part of the dam. A study to verify the stability of the upper part was requested by the SFOE-TS, with the hypothesis that the upstream and downstream parts of the crest behave like two independent blocks.

In 2008, the SFOE ordered a restriction on the operation of Cleuson reservoir to 2,184.50 msm (-2 m) for reasons of insufficient safety of the structure (upper crack in the shafts and displacement of the dam downstream and to the left) as a precautionary measure. During the five-yearly assessment of the Cleuson dam in 2012, the SFOE-TS asked the operator to provide a plan of the activities to restore the structure's ultimate safety.

Several documents were submitted to the supervisory authority, including: an action plan, an adapted service and operating regulation, a light microscopy and detailed analysis of the concrete microstructure, including degradation (TFB report, 2008), an examination of the dam's concrete (LCPC report, 2008), an examination of the concrete using a scanning electron microscope (SEM) (EPFL report, 2009), a laboratory analysis of the concrete (EPFL report, 2011), and an as-built remediation plan. Although the safety of the dam could be demonstrated, the conclusions of the concrete analysis reports and the various investigations carried out can be summarised as follows:

1. The elasticity modulus values of the concrete are in accordance with the expected values. A systematic degradation of the concrete characteristics is ruled out.
2. The observed swelling cannot be justified by an internal sulphate reaction.
3. The concrete is weakly reactive to the Alkali Aggregate Reaction.
4. The presence of a systematic vertical through crack connecting the drainage shafts could not be clearly identified in the upper part of the dam but the growth of the crack is expected.

The studies for the structural assessment were carried out in two phases. First, a calculation based on the observed state of the structure allowed to verify that the safety of the dam was guaranteed. In the second step, the question was to know in which time horizon the safety could be affected. The main failure mode was defined, then a finite element model specifically based on this failure mode was developed. The results indicate that the safety of the dam is not engaged before several decades without any reinforcement. Specific monitoring will have to be implemented to ensure that the dam behaviour is in line with expectations.

Coordination and transparency between all stakeholders are essential for the monitoring of the structure. Everyone's role is clearly defined, and each participant can focus on his specifications. The common goodwill allows to obtain safe and technically relevant solutions that allow all parties to benefit.

REFERENCES

- Alpiq, 2013, Vérification de la sécurité structural, Investigations complémentaires, rapport de synthèse, Document n°ECH8625, Lausanne (in French)
- K. Li, O. Coussy et C. Larive, 2004, modélisation chimico-mécanique du comportement des bétons affectés par la réaction alcali-silice. Expertise numérique des ouvrages d'art dégradés, coll. ERLPC, série OA43, LCPC.
- LMC, 2012, Carottes du Barrage de Cleuson, Rapport de synthèse, Procès verbal 361/13/LMC (in French)
- Swiss Committee on Dams, 2017, Concrete Swelling of dams in Switzerland, Report of the Swiss Committee on Dams on the state of concrete swelling in Swiss Dams swissdams.ch/fr/les-barrages/liste-des-barrages-suissees

The safety assessment of buttress, hollow gravity and multiple arch/slab dams. The contribution of numerical modeling

A. Frigerio & M. Colombo

Ricerca sul Sistema Energetico -RSE S.p.A., Italy

G. Mazzà

ITCOLD, Italy

F. Rogledi & A. Terret

Consorzio di Bonifica di Piacenza, Italy

ABSTRACT: An overview of the typical problems concerning buttress, hollow gravity and multiple arch/slab dams is presented, emphasizing the support that advanced numerical modeling can provide for the evaluation of their safety and for the definition of the most effective interventions to guarantee long-term safety conditions.

Even if the construction of this type of dams is nowadays practically abandoned, the problem of assessing their safety remains an important and challenging issue considering the obsolescence of most existing structures of this type and the peculiarities connected with their structural behavior, in particular referring to the effects of aging and seismic loadings.

In the Italian context there are numerous cases of this type of works built between the two World Wars and immediately after the II World War. A total of 37 dams are in operation (40% buttress, 30% hollow gravity, 30% multiple arch/slab dams). The problems connected with these structures are well-known: cracks (e.g., caused by phenomena of thermal origin, differences of the buttresses height, expansive chemical reactions, etc.), degradation associated with environmental conditions (e.g., due to corrosion of reinforcement bars when present), and aging. Other criticalities are related to compliance with current legislation which requires the verification of more stringent conditions not foreseen in the design phase (for instance higher seismic loads).

Some of the above-mentioned problems have been investigated in the frame of Benchmark Workshops proposed by the ICOLD Technical Committee A “*Computational Aspects of Analysis and Design of Dams*”, and are analyzed by an Italian Working Group, established by ITCOLD, the Italian National Committee on Large Dams.

Above all, in this paper the application of the eXtended Finite Element Method to evaluate the propagation of cracks in concrete dams and the seismic reassessment of an Italian multiple arch dam are discussed.

1 INTRODUCTION

In the early twentieth century, the hydropower sector was the backbone of the industrial development in many European countries. The need to exploit the water resources for the energy production accelerated the construction of increasingly large dams. Italy, for instance, went from a dozen of dams at the end of the nineteenth century to almost 400 large dams in the first half of the twentieth century.

To underpin this rapid development and cope with rising labor costs, efforts were soon made to reduce the construction time and costs while ensuring an adequate degree of safety. This process was fostered by new technological developments - mainly related to more performant materials and construction techniques and equipment - progress in geological and

geotechnical investigations, knowledge acquired through the monitoring systems installed on previously constructed works. All these innovative aspects, together with increasingly advanced assessment methods, resulted in the search for geometric shapes that could reduce the use of materials and, therefore, the costs of realization.

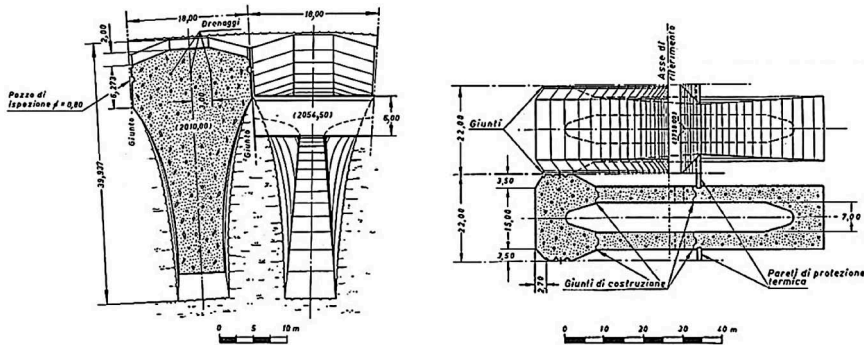


Figure 1. Typical section of a buttress dam (left), and a hollow gravity dam (right).

The first slab/arch dams were built in the first twenty-five years of the 1900. However, in 1923 the collapse of the Gleno dam, the only example in the world of mixed gravity and multiple arches dam, and the following judicial processes (Barbisan 2007), prompted engineers to design more massive structures, including buttress and hollow gravity dams (Figure 1). Nevertheless, the construction of this type of dams required rather complex construction techniques and skilled workers; thus, the increase in labor costs soon made this typology no longer convenient so it was abandoned in favor of massive gravity structures, simpler to build. Recently, the evolution of machinery has allowed the construction of the Rolled Compacted Concrete (RCC) dams, which are cheaper than concrete dams because of the relatively easy construction techniques and their lower cement content.

In this paper an overview of the typical problems concerning this type of dams is presented, emphasizing how ever more advanced numerical methods are needed to assess their safety and, eventually, to support the proper design of rehabilitation works.

2 THE MAIN PROBLEMS AFFECTING THIS TYPE OF DAMS

This type of dams has shown over time specific problems; in particular, they have a rather distinctive crack pattern whose genesis is often related to thermal phenomena occurred since the early stages of construction (Figure 2). The propagation of cracks can subsequently be affected by thermal environmental conditions or by geometric factors such as the different height between adjacent buttresses.



Figure 2. The Lago Eugio dam operated by IREN Energia in Piedmont (Italy), and the crack pattern in a buttress.

Other problems are the aging of materials due to environmental conditions or chemical phenomena, such as the alkali-aggregate reaction, and the corrosion of steel rebars in slabs and multiple arches. In some cases, the deterioration of concrete is closely related to its poor quality, or its high porosity determined by the limits of the vibration technology available at the time of construction.

Finally, other problems arising during the operation are caused by leakage through the upstream face, loss of resistance to sliding due to the development of excessive uplift pressures, limited resilience to seismic actions mainly along the transversal direction. Some structures have also shown inadequate flow capacity of outlets due to the limited availability of hydrological data at the design stage.

2.1 The Italian situation

In Italy there are 37 dams belonging to this construction type: 1 slab dam, 8 multiple arch dams, 13 buttress dams and 15 hollow gravity dams (Figure 3, left). Many of these structures, built in the last century, have recently required rehabilitation works to comply with the safety levels of the new regulations (Figure 3, right).

Hollow gravity dams represent the type that has undergone more interventions (10 out of 15) followed by multiple arch dams (4 out of 8). The Combamala dam (Piedmont), the only slab structure in Italy, built in 1913, was recently decommissioned by ENEL Green Power due to the extensive degradation of concrete. Some passages of adequate diameter have been opened through the bottom of the dam to allow the outflow of water even in case of flooding (ITCOLD 2022). The hydraulic and structural safety of the residual works of the dam has been duly verified, accordingly to the current Italian legislation (MIT 2014).

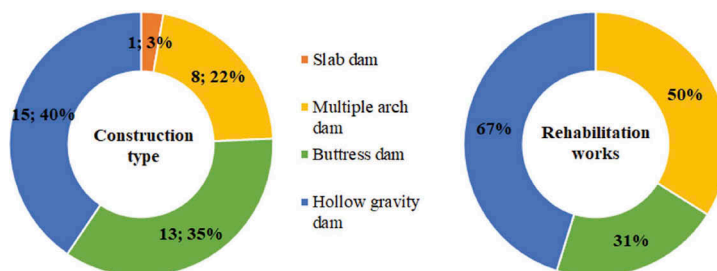


Figure 3. Number of Italian dams belonging to the construction type discussed in this paper (left) and percentage of dams subject to rehabilitation works in relation to their typology (right).

To address the issues related to this type of dams and share the knowhow among the engineering community, ITCOLD has set up the Working Group “*Behavior, problems, rehabilitation of hollow gravity, buttress and multiple archslab dams*”. Control and monitoring systems, criteria for safety assessment and rehabilitation works carried out to solve criticalities are discussed during meetings, generally held at the dam site. All this information is being documented in a Bulletin whose drafting is still in progress.

In the Bulletin several case histories are presented to outline how some remedial works have been effective in solving problems or have allowed to meet the new regulatory requirements.

One of the documented cases for instance is that of Ancipa dam, a hollow gravity structure, more than 110 m high, operated by ENEL Green Power in Sicily. A steel insulating shield, built on the downstream face from 2003 through 2005, has strongly reduced the seasonal thermal gradients allowing to significantly slow down the propagation of cracks in the buttresses over time (Figure 4, left). Moreover, in the central part, five gravity buttresses, 30 m high, have been built between the existing ones to reduce their height and improve the resistance to seismic loads in the transversal direction. After achieving new stable thermal conditions in the dam body, from 2009 to 2011 all relevant cracks were filled with epoxy resins.

Another interesting case refers to San Giacomo di Fraele dam (Valgoi 2009), a structure more than 90 m high with 25 buttresses, operated by A2A in Lombardy. The weighting of the



Figure 4. The steel insulating shield built to cover the buttresses of Ancipa dam (left), operated by ENEL Green Power in Sicily (Italy), and the weighting of San Giacomo di Fraele dam (right), operated by A2A in Lombardy (Italy).

downstream lower part, realized through concrete castings, has allowed to prevent sliding, and comply with current safety requirements (Figure 4, right). The remaking of the existing drainage perforations in the dam foundation and the grouting of a waterproof curtain at the base of the dam have contributed to decrease uplift. In 2010, after 6 years of experimental reservoirs, the initial storage capacity was completely recovered.

3 THE USE OF NUMERICAL MODELING TO ASSESS THE STRUCTURAL SAFETY

Since the early 1990s, numerical modelling has made a valuable contribution to the safety assessment of this type of structures in different operational and extreme loading conditions, also in presence of relevant crack patterns. Increasingly advanced numerical analyses have allowed to better understand the impact of thermal phenomena or degradation, as well as their evolution, on the structural behavior of these dams.

When traditional safety assessment methods provide results that do not meet the current legislation, advanced numerical modeling can help remove the conservative assumptions on which these methods are based to describe with greater accuracy the real behavior of dams. This avoids unnecessary operating restrictions that directly impact on the clean energy production of these power plants, and their storage capacity. These drawbacks represent a step back on the way to achieve the European Union energy and climate targets. In fact, hydroelectric power plants are playing a key role in the transition towards a decarbonized energy system, thanks to their capacity for delivering balancing services to the power network, thus fostering the exploitation of other renewable energy sources. Furthermore, considering that ever more long periods of drought are affecting European countries, the storage capacity of these plants must be preserved to provide mitigation services that will prevent costly catastrophes for agriculture and society in general.

Finally, to cope with problems that do not allow to meet regulatory requirements in any way, numerical modeling can support designers and engineers in defining the most effective interventions to guarantee the safety of these dams.

3.1 *The numerical studies proposed by the ICOLD Technical Committee A*

In the past years, the ICOLD Technical Committee A (TC-A) on “*Computational Aspects of Analysis and Design of Dams*” has studied some aspects inherent to this type of dams in the frame of Benchmark Workshops generally organized every two years.

In this regard, it is recalled the Benchmark Workshop (BW) held in 1994 in Gennevilliers (France) where the Theme A2 concerned a crack stability problem, specifically the evaluation of the uniform decrease in temperature capable of giving rise to the propagation of a pre-existing crack in an idealized 2D buttress dam (Figure 5, left). Five different initial crack lengths were considered, and two types of foundation: rigid and deformable (ICOLD TCA 1994).

In the next BW, held in 1996 in Madrid (Spain), the Theme A2 proposed a fracture mechanics problem on the same idealized dam but, in this case, a finite element 3D model was considered

to evaluate the stress intensity factor along the tip of the pre-existing crack under thermal gradient effects. For sake of simplicity, the crack tip was assumed to cross the entire thickness of the buttress with a straight path, normal to the external surfaces (ICOLD TCA 1996).

After several years, in the BW held in 2005 in Wuhan (China) the effects of the alkali-aggregate reaction on the stability against sliding of the main block of an Italian hollow gravity dam (Poglia dam) were studied under operational and ultimate conditions (Figure 5, right). The total vertical drift displacement at the top of the main block was provided to calibrate the numerical method adopted to describe the expansion phenomena (ICOLD TCA 2005).

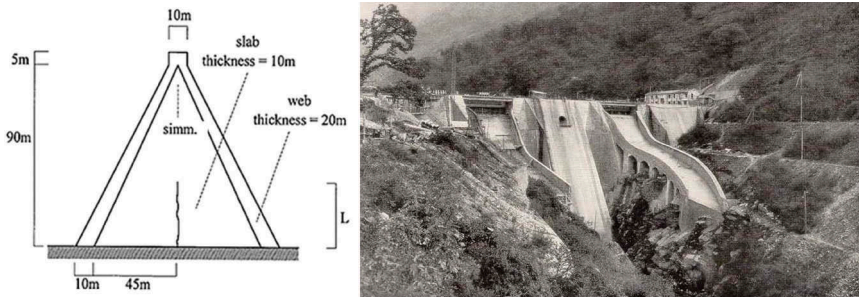


Figure 5. The idealized buttress dam studied with a 2D, and 3D model respectively in the BW held in France in 1994 and in Spain in 1996 (left) and the downstream view of the Poglia dam, the Italian hollow gravity structure, operated by EDISON in Lombardy (Italy), analyzed in the BW held in China in 2005 (right).

A critical evaluation of the abovementioned BWs will be available in the Bulletin “*Capitalization of the results of Benchmark Workshops on Numerical Modelling*” devoted to concrete dams that the TC-A is completing and will be issued in 2024.

In short, in the first two BWs the results provided by participants were generally in good agreement although different finite element models, numerical methods and computer codes were used to solve the proposed problems. In the third BW, the limited number of participants did not allow to carry out a constructive comparison of results. Some useful lessons learned were however drawn such as the need to properly model the dam-foundation interface and the recommendation to use suitable methods to describe complex physical phenomena and the realistic concrete behavior only if adequate and quality data are available.

3.2 *An innovative approach to simulate the crack propagation: The eXtended Finite Element Method*

In literature, two different concepts are generally used to simulate crack initiation and propagation in quasi-brittle materials, such as concrete.

On one side the smeared crack approach, introduced by Rashid (1968), is based on the continuum theory, thus assuming cracks can form over a band. The material behavior is described by constitutive laws, formulated in the stress-strain space, that combine the elasto-plasticity theory with the continuum damage mechanics. Crack initiation is controlled by a failure envelope that changes the initial isotropic material formulation to an orthotropic one that allows to describe the crack propagation. The softening part of the stress-strain curve depends on the crack opening displacement while the material damage is represented through the reduction of the elastic stiffness. In the smeared crack approach, the topology of the original finite element mesh is preserved, and there are no restrictions to the orientation of the crack planes. The main drawback is related to the softening curve which may imply mesh sensitivity problems (no convergence to a physical solution if mesh is refined).

On the other side, the discrete approach, first introduced to concrete structures by Ingraffea & Saouma (1981), is based on the principles of fracture mechanics in which cracks are

modelled by geometrical discontinuities. The cracks can be modelled by interface elements whose behavior is described by constitutive laws that relate the crack opening and sliding displacements to the normal and shear stresses. The interface strength is governed by a failure envelope. Various criteria for crack propagation have been formulated: the models based on linear elastic fracture mechanics assume infinite stresses at the crack tip while those based on nonlinear fracture mechanics consider a fracture process zone with cohesive stresses ahead of the crack tip. The main drawbacks related to the discrete approach are the continuous changes in nodal connectivity, and the need to constrain the path of cracks along the element edges.

To overcome the limits of these approaches, the eXtended Finite Element Method (XFEM) was developed by Moës et al. (1999) for modelling crack growth without remeshing an performing failure analysis. A standard displacement-based approximation is enriched by local functions in conjunction with additional degrees of freedom to model cracks. This technique allows simulating the crack path independently of the mesh. A short description of the XFEM theory will be available in the Bulletin “*Nonlinear modelling of concrete dams*” that the TC-A will issue in 2023.

Recently, the XFEM has been applied by Frigerio (2020) to simulate the crack propagation in a concrete buttress dam using the finite element code ABAQUS. A crack initiation surface was inserted a priori into the geometric model along the foundation interface (Figure 6, left). Generally, this type of fractures takes place during construction but, in this test case, the thermal phenomena occurring during the casting sequence was not modelled because the aim of this preliminary numerical study was to evaluate how XFEM was effective in simulating the crack propagation considering a seasonal temperature variation over several years. The numerical results have confirmed the capability of XFEM in modelling the crack propagation towards the upper part of the buttress (Figure 6, right): the rate of propagation is greater in the first year and it slows down in the following ones. The STATUSXFEM parameter, whose contour is shown in Figure 6 (left), is equal to 1.0 if the element is completely cracked and 0.0 if the element contains no crack.

In the second half 2023, the study will be extended, referring to a real test case. First the model parameters will be calibrated based on the measurement data related to crack initiation and propagation; then, the calibrated model will be used to predict the future trend of cracks.

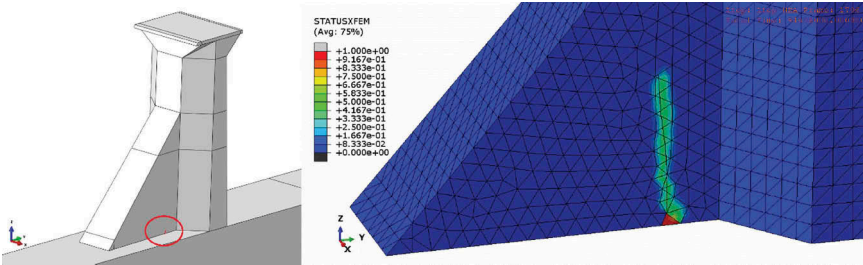


Figure 6. Geometric model of a concrete buttress with the crack initiation surface outlined into the red circle (left) and propagation of the crack (right).

3.3 The case history of Molato dam, an Italian multiple arch structure

Molato dam is a reinforced concrete multiple arch and buttress structure with gravity shoulders (Figure 7), 55 m high and a crest length of 335 m, located in Emilia-Romagna (Italy). The dam, built in 1921-1928, bars the gorge of Tidone River and has a total storage capacity of 8.1 Mm³. The Consorzio di Bonifica di Piacenza operates this structure to provide water for irrigation while ENEL Green Power operates the 2 MW hydroelectric power plant located in the span next to the concrete spillway on the left bank of the dam.

The 17 reinforced concrete arches, whose generatrices are inclined 45° to the horizontal plane, rest upon 16 intermediate buttresses and the lateral gravity shoulders (ANIDEL 1953). The arches have a circular section with a constant extrados radius of 5 m and a variable thickness from 1.20 m at the base to 0.45 m at the top but in the 80s all arches were thickened

(0.15 m over 340 m asl and 0.15 m + 0.01 m every meter of depth under 340 m asl). The reinforced buttresses have a distance of 10 m and a variable thickness from 2.40 m at the base to 0.90 m at the top. At the base, both the arches and the buttresses are anchored on concrete slabs that completely cover the spans, forming the foundation of the dam.

Seven series of reinforced concrete T-shaped beams were arranged at different elevations to connect the buttresses in the transversal direction (Figure 7, left). In the central part of the dam, the discharge of the concrete spillway, consists of three sluices 8.80 m wide.



Figure 7. Downstream and upstream view of Molato dam, operated by Consorzio di Bonifica di Piacenza in Emilia-Romagna (Italy) for irrigation.

3.3.1 *The limits of the design calculations*

The arches were designed and verified applying the cylinder formula, assuming an elastic response of the ring sections and fixed constrains at the abutments. The contribution of the reinforcement was neglected to be conservative. The buttresses were verified against overturning and sliding adopting the traditional methods for gravity dams.

The design calculation did not consider either the uplift pressures or the seismic loads, the latter introduced into the Italian standards only after 1959.

3.3.2 *The problems faced over time and the resulting rehabilitation works*

During the construction, design engineers decided to entirely cover the spans between adjacent buttresses with large concrete slabs to protect the foundation rock from atmospheric agents. This solution led to the need to drill the slabs several times, in different points, to reduce the uplift pressures but nevertheless the safety assessment against sliding of the four highest buttresses did not fulfill the Italian standards when considering the uplift pressures. In addition to this, changes in the Italian regulations showed that the flow discharge of the outlets was no longer adequate, and the structure had a poor resistance to seismic loads in the transversal direction.

For all these reasons, the Italian Authority limited the operation of the dam several times; thus, many in situ investigations and numerical studies were carried out to properly design the rehabilitation works in order to meet the new regulatory requirements.



Figure 8. Weighting of the dam foundation (left), strengthening of T-shaped beams with tie rods (center) rehabilitation of the surface spillway.

The most important structural and hydraulic works, divided in five steps, have been carried out from 1991 to 2022 and they interested several parts of the dam as shown in Figure 8 (e.g., buttresses consolidation, waterproofing of the upstream face of gravity shoulders and arches,

weighting of the dam foundation between spans, strengthening of some T-shaped beams with tie rods, restoration of drains, construction of an auxiliary free spillway on the right bank, rehabilitation of the existing spillway and outlets, etc.).

3.3.3 The seismic reassessment

The finite element model used in the seismic reassessment of Molato dam consists of solid elements for buttresses, slabs, concrete weightings among spans, gravity shoulders and rock foundation; beam elements for the T-shaped beams; shell elements for the multiple arches; acoustic elements for the reservoir (Figure 9).

A Mohr-Coulomb frictional model has been assigned to the interface between the dam and the rock foundation. A shell to solid coupling interaction has been adopted to join shell elements to solid ones: the displacement and rotation of each shell node is coupled to the average displacement and rotation of the solid surface in the vicinity of the shell node. The acoustic elements of the reservoir are connected only with the upstream dam elements (not with the ground ones).

Nonlinear concrete behavior has been simulated using an elasto-plastic damage constitutive model (Lee et al. 1998), while for the rock foundation a linear elastic behavior has been assumed.

In order to obtain the structure response of the dam-foundation-reservoir system, the traditional massless approach (Clough, 1980), based on the simplified hypothesis of rock foundation without mass, has been adopted. This method is still widely used in the field of dam engineering, but it does not take into account the energy dissipated in the rock foundation during the seismic motion. For this reason, the massless approach is considered based on a conservative hypothesis.

Time history analyses have been performed to evaluate the seismic structural response of the dam under gravity loads, hydrostatic pressures, uplift, winter thermal condition (which is the worst one), and seismic forces. For the latter, three natural accelerogram terns have been chosen for the serviceability and the ultimate limit states, and for three different water level conditions (i.e., maximum level of regulation, intermediate level, and empty reservoir). In Figure 10 (left) the upstream-downstream (X), shoulder-to-shoulder (Y) and vertical direction (Z) of the accelerogram tern called MRM is shown. The results of the seismic analyses have been evaluated in terms of maximum principal stresses envelop (Figure 10, right) and tensile damage.

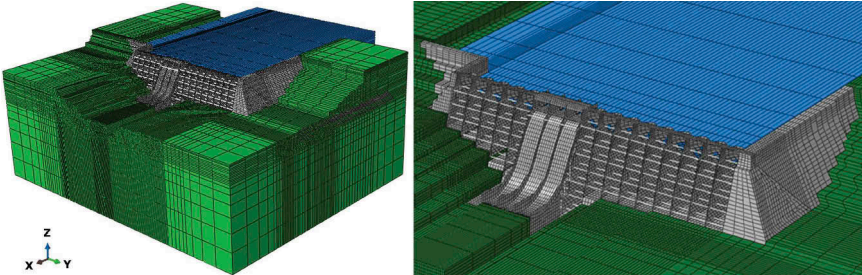


Figure 9. Finite element 3D model of Molato dam: dam-foundation-reservoir system.

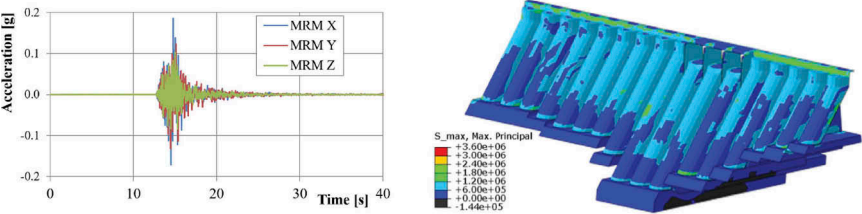


Figure 10. The accelerogram tern MRM (left) and the corresponding maximum principal stresses envelop on the upstream face, obtained considering the maximum level of regulation (right).

According to USACE (2007), in arch structures the maximum principal stresses can be up to twice the tensile strength of concrete, equal to 1.8 MPa in this case, but in a limited area of the upstream and downstream face (20% of the total surface) and for a cumulative duration not exceeding 0.3 s. As shown in Figure 10 (right), the maximum principal stresses do not overcome the tensile strength in all multiple arches. The tensile damage is not reported because it is not significant in the whole model.

For the reinforced concrete T-shaped beams and arches, starting from the geometrical and mechanical parameters of the section, a bending moment versus axial force diagram has been computed to define the strength domain. A reinforced cross-section is verified if the acting forces are inside this domain at any time steps of the analysis. In Figure 11, the comparison between the strength domain and the acting forces for the most stressed T-shaped beam (left) and arch (right) are shown. Four different force couples are reported: static loading condition in purple; maximum tension and compression over the seismic analysis respectively in light blue (only for the T-shaped beam) and pink; final condition in yellow.

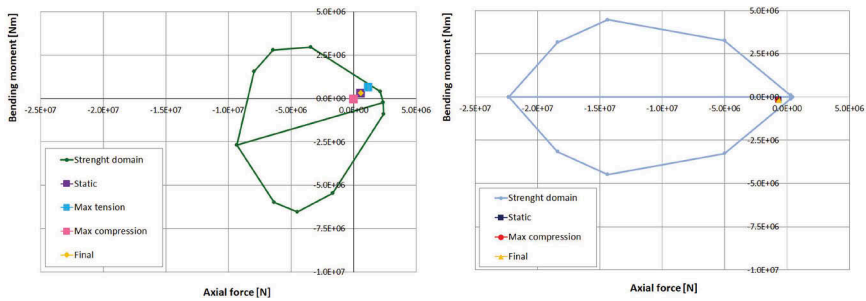


Figure 11. Bending moment versus axial force diagram for the most stressed T-shaped beam (left) and arch (right).

In order to understand the improvements of the new geometrical model with respect to the old ones, in which all the geometrical elements were modeled by means of solid elements, a comparison of the results in terms of stresses at the end of the static analysis is reported. The gravity load has been applied in one step (i.e., the casting construction sequence has not been simulated).

With the old model (Figure 12, left) the dam showed high stresses near the left shoulder: the lateral arch hangs on the shoulder, since a monolithic behavior has been considered and only a solid element was introduced along the arch thickness. Therefore, due to rock foundation deformability and the vertical section asymmetry of the gravity shoulder, the last one tends to rotate, compressing the close arch and generating horizontal (arch) stresses. These stresses could produce significant cracks, which did not really occur. With the new model, the use of shell elements to model the arches and of the shell to solid coupling interaction allows to describe realistically the stress-strain conditions of the structures (Figure 10 right) after the application of the gravity load (even in a single step). The stresses in Figure 12 are in N/m^2 .

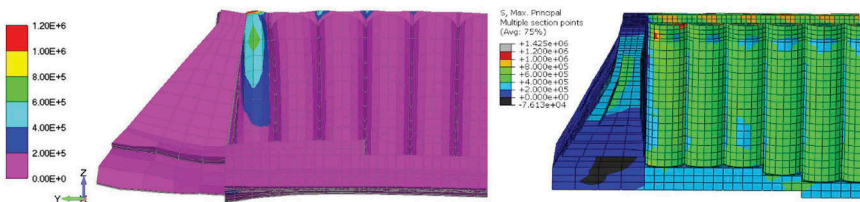


Figure 12. Stresses after gravity load application in the old model (left) and in the new one (right).

4 CONCLUSION

The paper provides an overview of the typical problems concerning the buttress, hollow gravity and multiple arch/slab dams, and emphasize the support that advanced numerical modeling can provide for the evaluation of their safety and for the definition of the most effective interventions to guarantee long-term safety conditions.

To address the issues related to this type of dams and share the knowhow among the engineering community, ITCOLD has set up the Working Group “*Behavior, problems, rehabilitation of hollow gravity, buttress and multiple arch/slab dams*”. Some numerical studies have also been carried out in the Benchmark Workshops that the ICOLD Technical Committee A (TCA) on “*Computational Aspects of Analysis and Design of Dams*” has organized since 1991.

The application of the eXtended Finite Element Method to evaluate the propagation of cracks in concrete dams is discussed; this innovative approach is effective in simulating the crack propagation considering a seasonal temperature variation over several years.

Finally, the seismic reassessment of Molato multiple arch dam, operated by Consorzio di Bonifica di Piacenza, is presented. This case study demonstrates how advanced finite element models allow to avoid unrealistic numerical behavior and the effectiveness of the rehabilitation works in meeting new regulation requirements.

ACKNOWLEDGEMENT

The work done by Frigerio and Colombo, except that related to the seismic assessment of Molato dam commissioned by Consorzio di Bonifica di Piacenza, has been financed by the Research Fund for the Italian Electrical System under the Three-Year Research Plan 2022-2024 (DM MITE n. 337, 15.09.2022), in compliance with the Decree of April 16th, 2018.

REFERENCES

- Barbisan, U. 2007. *Il crollo della diga di Pian del Gleno: errore tecnico?* Tecnologos editor.
- ITCOLD. 2022. *Osservatorio Dismissioni e Declassamenti Dighe*. Italian Bulletin.
- Ministero delle Infrastrutture e dei Trasporti (MIT). 2014. *Decreto Ministeriale 26 giugno 2014. Norme tecniche per la progettazione e la costruzione degli sbarramenti di ritenuta (dighe e traverse)*. Gazzetta Ufficiale n. 156.
- Valgoi, P. 2009. *Extraordinary maintenance of San Giacomo di Fraele dam*. 23rd Congress of ICOLD. Brasilia.
- ICOLD TCA. 1994. *Theme A2. Evaluation of critical uniform temperature decrease for a cracked buttress dam*. 3rd Benchmark Workshop on Numerical analysis of dams, Gennevilliers, France.
- ICOLD TCA. 1996. *Theme A2: Evaluation of stress intensity factor KI along the tip of the crack in a buttress dam under thermal gradient effects (3D analysis)*. 4th Benchmark Workshop on Numerical analysis of dams, Madrid, Spain.
- ICOLD TCA. 2005. *Theme A: Evaluation of alkali-aggregate reaction effects on the behaviour of an Italian hollow gravity dam*. 8th Benchmark Workshop on Numerical analysis of dams, Wuhan, P.R. China.
- ANIDEL. 1953. *Dams for hydroelectric power in Italy*. Vol.7.
- Frigerio A. 2020. *Attività scientifiche e di diffusione svolte nel 2020 a livello nazionale e internazionale per il settore idroelettrico*. Ricerca di Sistema. RSE, n. 20010750. Milan, Italy.
- Rashid, Y.R. 1968. *Ultimate Strength Analysis of Prestressed Concrete Pressure Vessels*. Nuclear Engineering and Design 7(4): 334–344.
- Ingraffea, A.R. & Saouma, V. *Numerical modeling of discrete crack propagation in reinforced and plain concrete*. Engineering Application of Fracture Mechanics 4: 171–225.
- Moës N., Dolbow J. & Belytschko, T. 1999. *A finite element method for crack growth without remeshing*. International Journal for Numerical Methods in Engineering 46(1): 131–150
- Lee J. & Fenves G. L. 1998. *A plastic-damage concrete model for earthquake analysis of dams*. Earthquake Engineering and Structural Dynamics 27(9): 937–956.
- Clough R.W. 1980. *Non-linear mechanisms in the seismic response of arch dams*. Proceedings of the international research conference earthquake Engineering, Skopje, Yugoslavia.
- US Army Corps of Engineers (USACE). 2007. *Engineering and Design - Earthquake Design and Evaluation of Concrete Hydraulic Structures*. EM 1110-2-6053.

Rehabilitation and upgrade of old small dams

Brigitta Gander

Dam Safety Authority, Canton of Zürich, Switzerland

ABSTRACT: There are more than 350 small dams in the Canton of Zurich, Switzerland. Some date back to the medieval ages and many were built between 1750 AD and 1900 AD. Today, these small dams are often protected for environmental or historical reasons. As the Federal Act on Water Retaining Facilities came in force in 2010, the supervision of small dams was handed over from the Federal Government to the cantons. The review of the dams by the Dam Safety Authority of the Canton of Zurich showed that hardly any of these small dams meet the requirements of the Federal Act. In this paper the reasons for dam rehabilitation and some examples of cost-effective measures to improve the safety of small dams are discussed. From several upgrading projects, the renewal of the spillway of the Sülbachweiher near Bauma and the retrofitting of the Sternensee above Richterswil are selected as case studies.

1 INTRODUCTION

Anyone who wants to dam or retain water in the Canton of Zurich needs a concession to do so, regardless the intent use such as running a mill, electricity generation or a just a pond.

Art. 3 of the Federal Act on Water Retaining Facilities (WRFA) states: “Large water retaining facilities are installations: a. with a storage height of at least 25 meters; b. with a storage height of more than 15 meters and a storage capacity of more than 50,000 cubic meters; c. with a storage height of more than 10 meters and a storage capacity of more than 100,000 cubic meters; d. with a storage capacity of more than 500,000 cubic meters.”

In the Canton of Zurich, only one dam meets one of these criteria. Thus, all the others are “small” dams. Many are very small, with a volume of less than 5000 cubic meters and a dam height of less than 2 meters.

Some of the dams date back to the medieval ages. Most were built between 1750 AD and 1900 AD during industrialization to use the power of the water, be it as a grain mill, sawmill, twisting mill, weaving mill, ice pond, for power transmission and a little later for electricity generation. In the middle of the 20th century, the power generation of these small plants became less important. Today, only about fifty hydroelectric plants still produce electricity. Most of them dam up rivers with weirs not embankment dams. However, most embankment dams still exist and are often protected for environmental or historical reasons. Unfortunately, many of these small dams have been “forgotten” and their regular maintenance has been neglected.

The original concessions from the 19th century already contain requirements for the safety of the dams (see example in Section 3.3). With progress in the state of the art in dam safety and concentration of infrastructure and residential areas downstream of the dams, the legal requirements were continuously tightened.

In the Canton of Zurich many dams were upgraded according to the requirements in the mid-1980s to the 1990s. In particular, spillways were improved or new ones were constructed. A second wave of renovations takes place since the end of the 2010s. The new wave was triggered by the enactment of the WRFA and is matched with establishment of the Dam Safety Authority of the Canton of Zurich. This second wave concerns mostly the dams that are or might be subject to the WRFA.

2 REASONS FOR RETROFIT A DAM

The reasons for upgrading dams are manifold. Often dams need to be upgraded due to a change in the legal basis such as laws, ordinances, directives and concessions. For example, since the implementation of the WRFA, the cantons in Switzerland must review the “special hazard potential” of small dams according to art. 2 para. 2 WRFA. If the review determines that a dam ought to be subject to the WRFA, the operator of the dam usually has two options:

- a) Adaptation to the requirements of subsection under the WRFA or
- b) Adjustment of the dam in order to avert subsection under the WRFA.

Neglected or inadequate maintenance by the owner can lead to a leaking dam. If a seepage trough a dam is not detected or remediated, this can lead to a dam breach and the failing of the dam. Upon renewal of the concession, the authority poses the dam safety requirements according to the state of the art.

An example of how requirements for dams have become stricter over time is the required height of the freeboard. In the 1920, when the “Federal Law for the Utilization of Hydraulic Powers” enacted, a freeboard of 0.5 meter above the “normal” water level was required. The regulations today require a freeboard of at least one meter for dams subject to the WRFA in the event of an exceptional situation, a 1000-year flood event. Thus, the allowable minimum freeboard has been more than doubled in the last hundred years. Similar enforcements exist for almost all specifications concerning the safety of dams.

3 MEASURES TO IMPROVE THE SAFETY OF SMALL DAMS

Some dams in the Canton of Zurich are owned by the public. But more often private owners are responsible and pass the dam on from one generation to the next. Especially in the case of private owners, financial resources are very limited, why deconstruct a dam often is the only option to avert future obligations.

In contrast, public owners try to keep their dams and undertake various measures to improve the safety of small dams. Often, only the combination of several retrofit methods leads to an optimal solution.

The most important measures are:

- Building a new spillway or improving the existing one
- Strengthening the dam
- Flattening the embankment slopes
- Lowering the water level and reducing the reservoir volume
- Renewal of the bottom outlet
- Deconstruction

On some neglected embankment dams, trees grew turning them into forests. In Switzerland the forest is protected by the Federal Act on Forest (ForA) and deforestation is prohibited. With the exception: “Trees and bushes on dams and in the immediate foreground of dams are not defined as forest” (art. 2 para. 3 ForA). Thus, a forest on a dam can and must be removed to prevent damaging the dam from windthrow or seepage along roots. This measure is not very popular with the public and must therefore be communicated intently. On the other hand, it is a cheap measure and improves the situation quickly. The embankment can finally be visually checked.

3.1 *Methods to improve flood safety*

The primary objective of flood safety measures is to prevent overtopping of the dam crest or to design the dam in such a way, that overtopping does not lead to erosion. If a dam that is not adequately secured gets overtopped, there is a risk that the dam surface and the base of the dam will be eroded, finally leading to a breach in the dam. A higher freeboard and the implementation of an upstream rake are quick and easy ways to prevent overtopping.

Dams built before 1950 often have no spillway or it is too small. Around the year 1990 some spillways have been built or enlarged. A successful example is the Sülibachweiher in Bauma. The spillway was built on top of the existing dam in 1991 by lowering the top of the dam by about one meter over a width of six meters. On the downstream embankment the spillway runs to a stilling basin and is lined up with grass pavers. The grass pavers are fixed into the embankment with hoe nails. In winter 2018/2019 the dam crest of the Sülibachweiher was lowered by three meters (see Schmocker 2021) as to prevent the dam to be subjected to the WRFA. In the process, the spillway was also lowered three meters and reconstructed as the same as in 1991 (see Figure 1). This action reduced the height of the dam and the volume of the reservoir to such an extent that the flood wave of the Sülibachweiher no longer poses a “special hazard potential” and therefore does not have to be subject to the WRFA.



Figure 1. Spillway of Sülibachweiher (Gander 2019).

3.2 *Methods to improve dam stability*

The requirements for dam stability became also stricter over time. Dams 150 years old or even older no longer meet the current guidelines in Switzerland that are required of dams being subjected to the WRFA. To prevent dams from deconstruction or total rebuilding, there are a few measures to renovate dams cost-effectively and adequately according to the state of the art. The most effective approach is to combine different measures.

Often, the only option to improve dam stability is to strengthen the dam itself. An example for this is to flatten the embankment slopes. Dams with slopes steeper than 1:2 hardly meet the specifications. Often the upstream and the downstream slopes are too steep.

As today most dams are no longer used as reservoirs, the accumulation of sediments has been allowed. The sediment deposit in the ponds is often contaminated with heavy metals or PAHs and organic material. When dredged, the disposal of the sediments is very expensive.

Therefore, the authority of the Canton of Zurich allows this material to be reused within the dam, for example to strengthen the upstream embankment. Although the sediments must be improved and stabilized, this reuse of material reduces transports and prevents costly landfilling.

Old dams often have quite narrow dam crests. By lowering the water level in the reservoir by at least one meter, not only the crest can be widened, but the specifications regarding free-board also can be met. This also releases material that can be used to level or flatten the downstream embankment.

For dams that are not subject to the WRFA, further actions can be implemented, as the requirements for such dams are less strict. For example, berms can be adjusted to the foot of the upstream or downstream embankment. Those dams can be reinforced with a sheet-pile wall or simple hydraulic engineering techniques, such as palisades or fascines.

3.3 Example of Sternensee

Sternensee is located above Richterswil on Lake Zurich. This site is a typical example of an old small dam in the Canton of Zurich. Its history in short is as follows:

In 1873, a concession was granted to dam up the water of the river Mühlebach for the operation of a silk twisting mill (from the Government Council Decision No. 2915 of 13 December 1873). Already at that time, specifications for the construction of the dam and thus for the dam safety were enforced: “The dams must be of a strength that corresponds to the pressure of the water and must be constructed with all the care and precision required for such a system; a free spillway must be installed at a suitable point to prevent the weir from overtopping”.



Figure 2. Labyrinth weir at Sternensee (Gander 2019).

In 1929 with the renewing of the existing concession further conditions were set concerning the freeboard: “It is stipulated that the dam crest shall be at least 0.5 meter above the crown of the spillway” (from the Government Council Decision No. 2534 of 28 November 1929).

In 1972 the production of silk twisting was abandoned and one year later the community of Richterswil took over the Sternensee. On 29 August 1985, the dam was subjected to the forerunner act of the WRFA. Thus, the dam had to meet stricter requirements and those led to investigations into flood safety and dam stability. In 1988, the bottom outlet was renewed, and in the winter of 1990/1991, an extensive upgrade followed: The dam was sealed with a sheet-pile wall to lower the seepage line in the embankment and the discharge capacity of the spillway was increased by constructing a labyrinth weir (see Figure 2). Piezometers were installed to monitor the seepage line in the dam and a geodesics survey was initiated.

With the transfer of the supervision of small dams from the federal government to the cantons, Sternensee was handed over to the Dam Safety Authority of the Canton of Zurich. Investigations in recent years have shown that the steep downstream embankment (up to 1:1.7) does not meet today’s requirements for dam stability. The measurements of the seepage water line in the existing piezometers also prove to be incomprehensible, as they show strong fluctuations in the water level (in some cases over one meter), although the water level in the reservoir fluctuates by a maximum of two centimeter. As an immediate action in winter 2022/2023, the trees that had grown on the downstream embankment slope since the renovation in 1990 were removed. As Sternensee is a popular destination for excursions, it was important to communicate the action to gain the people understanding it. Further measures are planned.

4 CONCLUSIONS

Today, the rehabilitation or upgrade of old small dams is possible but often costly, especially as most small dams produce no income. In the Canton of Zurich, old small dams being newly subjected to the WRFA never fulfill the requirements and therefore always need a renovation.

REFERENCES

Schmocker, L. et al. 2021. Renovation of small dams in the Canton of Zürich. In *Mitteilungen 262, Wasserbau in Zeiten von Energiewende, Gewässerschutz und Klimawandel, Tagungsband 1 Wasserbau-Symposium 2021:57–64*. Prof. Dr. Robert Boes: VAW, ETH Zurich.

Experimental investigation of the overtopping failure of a zoned embankment dam

M.C. Halso, F.M. Evers, D.F. Vetsch & R.M. Boes

Laboratory of Hydraulics, Hydrology & Glaciology (VAW), ETH Zurich, Zurich, Switzerland

ABSTRACT: The failure of dams poses an immense risk to settlements and infrastructure throughout the world. As extreme flood events become more likely in many parts of the world, dams become increasingly vulnerable to overtopping. Earthen embankment dams are made of erodible materials, and are therefore susceptible to erosion by an overtopping flow. Erosion of a dam to the point of uncontrolled outflow constitutes a dam breach. The erosive processes that lead to breaching depend on the type of dam. Zoned earthen dams with a mineral core erode differently than homogeneous earthen dams, due to the core material's resistance to entrainment by the overtopping flow. The process of breaching a zoned dam by overtopping has been scarcely observed at laboratory, field, or prototype scales. In this study, we perform a laboratory experiment to investigate the breaching due to overtopping of a zoned earthen embankment dam. A prototype-scale zoned dam was designed based on multiple large zoned earthen dams in Switzerland, with particular focus on the Jonenbach Dam in Affoltern am Albis. The prototype dam, which includes shell, filter, and core zones, was reduced to laboratory scale for experimentation. The laboratory-scale dam was breached by overtopping, and the failure processes of each zone were observed. The breaching process began with formation of a breach channel on the downstream slope of the dam. The breach channel incised downstream of the core, and expanded laterally due to mass slope failures of shell material. The filter material remained temporarily stable after departure of the supporting shell material, due to effects of apparent cohesion, but gradually failed with mass detachments. Erosion of the shell and filter zones left the core unsupported on the downstream side. The forces of water and soil pressure from upstream gradually became too large for the core to resist, causing the core to bulge, crack, and eventually break. Once the core broke, water and shell material from upstream flowed uncontrolled through the breach. Similar morphodynamic and hydrodynamic processes that occurred in this experiment would also be expected to occur during the overtopping failure of a prototype-scale zoned dam. The resistance of the core to the soil and water pressures can be a valuable output for calibration of statics calculations of core stability. Such calculations could be implemented in parametric or numerical dam breach models, for use by engineers to estimate the timing and resulting discharge of zoned earthen dam breaches.

1 INTRODUCTION

The breaching of a dam can have catastrophic consequences for communities downstream. The destructive power of dam break flows has been observed on multiple occasions, such as the 1976 Teton Dam failure in Idaho in 1976, the Tous Dam failure in Spain in 1982, and the cascading failure of two dams on Michigan's Tittabawassee River in 2020. According to the World Register of Dams (ICOLD 2003b), the majority of large dams worldwide are earthen embankment dams – a large share of which are zoned – and the most common cause of failure for earthen embankment dams is breaching due to overtopping (Costa 1985). With the

increasing likelihood of extreme flood events due to climate change (Milly et al. 2002), the risk of overtopping will increase for many dams (Lee and You 2013; Ahmadisharaf and Kalyanapu 2015).

The rate and manner in which an overtopping dam breach occurs impacts the magnitude of the resulting flood discharge. It is important that the erosive processes that lead to a dam failure are sufficiently well-understood, so that reliable flood forecasts and evacuation plans can be made. The overtopping of homogeneous embankment dams – those consisting of the same material throughout their entire volume – has been investigated extensively with laboratory and field experiments, as summarized by ASCE (2011), Amaral et al. (2020), and others. However, the overtopping of non-homogeneous embankment dams – those containing a shell zone for structural stability and a sealing element for impermeability – has been studied much less often.

A variety of designs can be employed for non-homogeneous embankment dams, based on the location and type of sealing element, inclusion of filter zones, and type of shell material. The sealing element may be located inside the center of the dam or along the upstream face. It can be a mineral clay-containing core, or a diaphragm made of concrete, steel, geomembrane, or cement-bentonite slurry. If the dam features a mineral core, one or multiple filter zones may be needed between the core and shell zones, to reduce the likelihood of internal erosion of the core material. The shell zone may consist of earthfill or rockfill (U.S. Bureau of Reclamation 2012), with earthfill being far more common in large dams (ICOLD 2003a).

Laboratory experiments to investigate the overtopping failure of non-homogeneous dams have been rare. Dams with diaphragms were investigated by Simmler and Samet (1982), Bornschein (2014), and Rüdiger (2017) for earthen dams, and by Franca and Almeida (2002) for rockfill dams. Laboratory experiments with fuse-plug spillways were performed by Pugh (1985), Fletcher and Gilbert (1992), and Schmockler et al. (2013). Field experiments of rockfill dams with moraine core were carried out during the IMPACT project (Vaskinn et al. 2004; Morris et al. 2007). Sadeghi et al. (2020) performed laboratory breach experiments of earthen dams with central mineral clay-containing cores. Several of the studies of dams with centrally-located impervious elements observed erosion of outer zones, while the central impervious element remained stable. Erosion of the outer layers left the impervious element increasingly unsupported, which eventually failed due water pressure, material pressure, and its own weight (Simmler and Samet 1982; Pugh 1985; Fletcher and Gilbert 1992; Schmockler et al. 2013; Sadeghi et al. 2020).

This study investigates the overtopping-induced failure of a zoned earthen embankment dam that contains a central vertical mineral core, a filter zone, and an earthen shell zone. The experiment depicts a prototype-scale dam that was designed to represent a typical zoned earthen dam. Inspiration for the design of the prototype dam came from three large zoned earthen dams in Switzerland: Jonenbach Dam in Affoltern am Albis, Aabachweiher Dam in Horgen, and Hühnermatt Dam near Einsiedeln. A particular focus is given to Jonenbach Dam.

1.1 *Earthen embankment dams in Switzerland*

Embankment dams play a major role in Switzerland's history, landscape, energy production, and plans for adaptation to climate change. The Swiss Federal Office of Energy currently supervises over 220 major dams and auxiliary structures, of which 69 are embankment dams (2022). Those embankment dams range from less than 10 to over 150 meters (m) tall, with the vast majority (94%) being less than 40 m. Those 69 embankment dams have an average height of 19.7 m. Three large zoned earthen dams in Switzerland were used to develop the design for the prototype-scale dam on which the experiment would be based. Those three dams are described in the following sections.

1.1.1 *Jonenbach Dam*

Jonenbach Dam is a zoned earthen embankment dam on the Jonenbach River, upstream of the town of Affoltern am Albis (Figure 1). It was built between 2006 and 2008, to provide flood protection to Affoltern am Albis. Jonenbach Dam was designed to manage the 100-year flood before the spillway becomes activated. The 21-km² catchment of the dam produces

a 100-year peak flood of $34 \text{ m}^3/\text{s}$, which the retention reservoir reduces to $15 \text{ m}^3/\text{s}$. Only during flood events on the Jonenbach River is water stored in the reservoir (Hochstrasser et al. 2008). Figure 2 shows Jonenbach Dam under normal hydrologic conditions, in which the reservoir is empty.

Jonenbach Dam is 19.35 meters tall (Swiss Committee on Dams), with a crest elevation at 516.35 m.a.s.l. The dam has a freeboard of 3 m above the 100-year flood level, 2 m above the 1000-year flood level, and 1.65 m above the safety flood level (1.5 times the 1000-year flood). A spillway with an overflow crest at 513.35 m.a.s.l is in the middle of the upstream face. Along the northeast side of the reservoir, a road sits at an elevation 1 m below the dam crest. This was done purposefully, to provide additional spillway length over the paved road for extreme floods, and thus reduce the possibility of overtopping the dam crest (Hochstrasser et al. 2008).

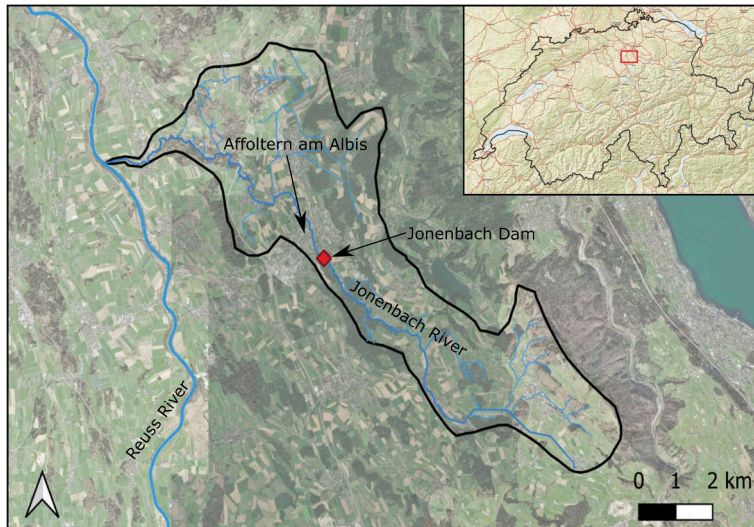


Figure 1. Location of Jonenbach Dam (background map: Swiss Federal Office of Topography).

The crest of Jonenbach Dam is between 5 and 7 m wide (Hochstrasser et al. 2008), with a length of 163 m (Swiss Committee on Dams 2021; Swiss Federal Office of Energy 2022). The dam extends approximately 141 m from upstream toe to downstream toe. The face slopes are at least 3:1 (horizontal:vertical, H:V). These slopes are milder than was deemed necessary, and were selected for integration with the local landscape, rather than for geotechnical stability.

Jonenbach Dam contains a central vertical core that is approximately 40 m wide at its base and 5 m wide at its crest, which is 1 m below the dam crest. The core is made of a compacted moraine material containing clay, silt, sand, and gravel, with approximately 14% clay and 61% fines. Along the downstream side of the core, there is a 2-m thick filter zone of sand and gravel. The shell zone contains regions of the same moraine material as the core, but with less strict installation requirements in some sections, as well as regions of a locally-excavated clayey silt with gravelly sand (Hochstrasser et al. 2008).

1.1.2 Aabachweiher Dam

Aabachweiher Dam is a zoned embankment dam on the Aabach River in Horgen, Switzerland. It was constructed in the 1880s, and contains two zones: an earthen shell and a central vertical core. The earthen shell has a wide grain size distribution, containing silt, sand, gravel, cobbles, and boulders. The central core contains clay and silt. Aabachweiher Dam is approximately 14.5 m tall, with a crest elevation of 535.35 m.a.s.l. The dam is approximately 54 m long from upstream toe to downstream toe, with face slopes of 1.6:1 (H:V) on the upstream side and 2:1 on the downstream side. The crest is 7 m wide. The central core is approximately 13 m tall, with a thickness of 1 m at

the top and 13.5 m at the base (Ingenieurburo Kälin 1986). The zoning of Aabachweiher Dam is typical for a zoned embankment dam that contains no filter or transition zones.

1.1.3 Hühnermatt Dam

Hühnermatt Dam is a zoned earthen dam on the Sihlsee, a lake in Switzerland's canton Schwyz. Hühnermatt Dam, constructed in 1937 (Swiss Federal Office of Energy 2022), is a saddle dam on the northwest side of the lake, near the town of Einsiedeln. The dam is 15 m tall, with face slopes between 1.5:1 and 2.75:1. The dam is approximately 71 m long from upstream toe to downstream toe, and the dam crest is 5-6 m wide. Hühnermatt Dam is a zoned dam with a central core, a filter on the downstream side of the core, and a shell zone. The central core is 15 m wide at the base and 2.5 m wide at its crest. The core is made of a moraine material containing gravel, sand, silt, and clay, with approximately 17% clay, and 40% fines. The filter is approximately 1.2 m wide, and is made of fine sand. The shell contains regions of poorly-graded gravel and silty gravel (Lombardi AG 2008). The zoning of Hühnermatt Dam is typical for a 3-layer zoned embankment dam.



Figure 2. Jonenbach Dam upstream slope with spillway intake structure (top left), dam upstream slope with low-level outlet intake (top right), dam crest (bottom left), and dam downstream slope with combined outlet structure for spillway and low-level outlet (bottom right).

2 EXPERIMENTAL METHODS

The laboratory experiment was based on a prototype-scale dam, that was designed to represent typical large zoned earthen embankment dams in Switzerland, as exemplified above. The prototype dam was scaled down to model scale. Experimentation took place in a recirculating hydraulic flume in the Laboratory of Hydraulics, Hydrology and Glaciology (VAW), ETH Zurich. The model dam was breached by overtopping. Morphodynamic and hydrodynamic processes were observed, recorded, and measured throughout the experiment.

2.1 Prototype zoned dam

The prototype dam is based on the three large zoned dams described in Section 1. The dimensions, zoning, and material types of the prototype dam are described in the following sections.

2.1.1 Dimensioning

A height of $h_{prototype} = 20$ m was selected for the prototype zoned dam. This height is similar to that of Jonenbach Dam, as well as the average height of embankment dams listed by the Swiss

Committee on Dams. The upstream and downstream face slopes are 2:1. The crest width is 6 m, and the total streamwise length of the dam is 86 m from upstream toe to downstream toe.

2.1.2 Zoning

The prototype dam contains three zones: a core zone, a filter zone, and a shell zone. The core zone is a central vertical core, located beneath the dam crest. The core is 18 m tall, 20 m wide at the base of the dam, and 8 m wide at its crest. The filter zone is located on the downstream side of the core. Like the core, it is 18 m tall. It is 3 m thick at the base, and 1.5 m thick at its crest. The shell zone surrounds the core and filter layers. It is 20 m tall, 86 m wide at the base, and 6 m wide at the crest. The dimensions and zoning of the prototype dam are shown in Figure 3a.

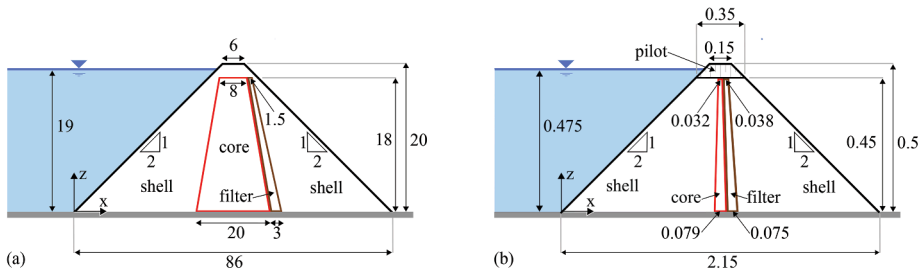


Figure 3. Schematic streamwise profiles of (left) prototype-scale dam and (right) model-scale dam (figures not to scale, all units in meters).

2.1.3 Material

The core zone is made of a mineral material that includes cohesive fines. It was designed to be similar to the core of the Jonenbach Dam. The material consists of 5% clay, 37% silt, 50% sand, and 8% gravel. The filter zone consists of 15% sand and 85% gravel. The shell zone is made of an earthfill material, containing 59% gravel and 41% coarse material (cobbles and boulders).

2.2 Model zoned dam

The model dam is a scaled-down version of the prototype dam, containing the same three zones as the prototype (shell, filter, and core). It has a height $h_{model} = 0.5$ m. With the prototype dam height of $h_{prototype} = 20$ m, this gives a scale factor $\lambda = h_{prototype}/h_{model} = 40$. The model dam represents a slice at the center of the prototype dam. With the flume width of 1 m and $\lambda = 40$, the model represents a dam length of 40 m in the transverse direction, i.e. between its abutments.

2.2.1 Scaling and dimensions of the shell and filter zones

The hydraulic processes of dam breaching are controlled by gravitational and inertial forces. Accurate representation of these processes at model scale requires Froude similarity between the model dam and prototype dam (Amaral et al. 2020). According to Froude similarity, lengths can be scaled according to λ . The dimensions of the shell and filter zones of the model dam are scaled in this way, and are therefore 40 times smaller than the corresponding dimensions at prototype scale. This gives a streamwise model dam length of 2.15 m, a crest width of 0.15 m, and face slopes remain 2:1. The filter height is 0.45 m, and its thickness ranges from 0.075 m at the base to 0.038 m at its crest. The dimensions and zoning of the model dam are shown in Figure 3b.

2.2.2 Material of the shell and filter zones

The grain size distributions of the model dam's shell and filter materials are initially scaled from the prototype materials using the scale factor of $\lambda = 40$. However, the processes that drive material erosion are related to the Reynolds number, which is not scaled correctly under Froude similarity (Pugh 1985; Amaral et al. 2020). A correction for this was developed by Pugh (1985, 2008), in which material size is adjusted so that its settling velocity is scaled according to Froude similarity. This increases the size of model material that had scaled to diameters of less than 2 mm. This method led to increasing 100% of the filter material, and

70% of the shell material. The model filter material consists of 100% sand, and the shell material consists of 61% sand and 39% gravel.

2.2.3 *Scaling, dimensions, and material of the core zone*

Previous experimental studies showed that the cohesive core zone should experience a different type of failure than the mainly non-cohesive shell and filter zones. A negligible amount of core material will be entrained by the overtopping flow. For this reason, the grain size of the core does not need to be scaled, and the model core therefore contains the same material as the prototype core (5% clay, 37% silt, 50% sand, and 8% gravel). Past research showed that the core should fail due to cantilever rotation, with large chunks detaching from the core (Schmocker et al. 2013; Sadeghi et al. 2020). A scaling method for this failure process is presented by Schmocker et al. (2013), and was utilized by Sadeghi et al. (2020). A similar method was also described by Pugh (1985). This method scales the thickness of the core zone by $\lambda^{1.5}$. With $\lambda = 40$, this gives a model core thickness of 0.079 m at the base and 0.032 m at the crest. The core height still scales with λ , giving a model core height of 0.45 m. Figure 3b shows the dimensions of the model core zone.

2.3 *Experimental setup*

The model dam was constructed in a 1-m wide, 1-m deep, and 11.9-m long recirculating hydraulic flume. The model dam was built on a 0.53 m deep raised test section in the upstream portion of the flume. A seepage collection system is built into the raised floor of the test section, and a sediment collection basket is directly downstream of the test section. A 0.05-m deep and 0.2-m wide triangular pilot channel was cut through the dam crest, in the center of the dam. The flume has a transparent wall along one side, allowing for observation of the dam profile during construction and experimentation.

2.4 *Measurements*

Ultrasonic Distance Sensors (UDSs) were used to measure water surfaces in the impoundment and the seepage collection tank. An inductive discharge measurement device was used to measure the rate of inflow to the impoundment. Based on those measurements, a continuity calculation was employed to calculate the rate of discharge Q_b exiting the impoundment through the breach. Similar approaches were used in dam breach experiments by Coleman et al. (2002), Cestero et al. (2015), Frank and Hager (2015), Frank (2016), Bento et al. (2017), and Halso et al. (2022).

The rate of material erosion V_e was also measured. Eroded material was collected in the sediment basket, which was weighed continuously by three force transducers. The water surface at the basket was measured by a UDS. This measurement system is described in Halso et al. (2022).

The evolving shape of the dam was measured throughout the experiment using a photogrammetric measurement system. The photogrammetric system generates two-dimensional depictions of the dam surface, allowing for reconstruction of dam cross sections and profiles at any moment during the experiment. This system is described by Frank and Hager (2015) and Frank (2016).

2.5 *Experimentation*

The experiment was begun by filling the impoundment at a constant rate of 1 mm/s (Figure 4a). As the water level approached the invert of the pilot channel (0.45 m above the base of the dam), the filling was slowed to 0.33 mm/s. Once the water level reached midway between the pilot channel invert and the crest elevation, it was held approximately constant for the duration of the experiment. The constant head is intended to represent a very large reservoir. The experiment lasted for another 118 seconds, until approximately 22 seconds after initial failure of the core zone. At that point, the breach had reached the side walls of the flume, and the experiment ended.

3 RESULTS AND DISCUSSION

3.1 *Initial breach channel*

Overtopping of the model dam started with a small flow through the pilot channel. This initial overtopping flow began making a breach channel through the upper portion of the downstream

dam slope. The shell material that was eroded to form this channel was slowly transported at the front of the overtopping flow. The overtopping flow front gradually progressed down the dam slope, reaching the downstream toe of the dam approximately 43 seconds after first exiting the pilot channel. At this time, the breach discharge Q_b , defined as the flow through the breach as measured at the downstream toe of the dam, became greater than 0. This moment is defined as time $t = 0$ for the experiment. Figure 4b shows the experiment at $t = 0$.

3.2 *Shell erosion*

Once the initial breach channel had formed through the entire downstream slope, the overtopping flow began incising the breach channel. The incision began in the initial pilot channel, quickly exposing the crest of the core (Figure 4c). The incised channel was nearly rectangular in shape, with steep sidewalls that the shell material could not sustain. The shell material along the channel sidewalls began detaching in a series of mass slope failures. The detached material slid towards the breach channel, and was gradually carried away by the overtopping flow. After each detachment, the remaining shell material (beneath the since-detached material) stabilized momentarily at an angle of approximately 30-35 degrees. After the detached material was carried away, the overtopping flow continued incising and widening the breach channel, leading again to steep sidewalls and thus more mass slope failures. This process gradually changed the breach channel to a trapezoidal shape, first near the downstream end of the initial pilot channel, and then in the lower part of the downstream slope by the time of core collapse. The timing of the first, final, and other large mass detachments of shell material are indicated in Figure 5. Figures 4d and 4e show the dam before and after large mass detachments of shell material on both sides of the breach channel.

3.3 *Filter erosion*

When incision of the breach channel exposed the filter zone, the exposed filter material was eroded by the overtopping flow. But outside the breach channel, the filter zone remained protected by the shell. After several detachments of shell material, sections of the filter zone became unprotected, and had nearly vertical slopes. However, the filter material did not immediately fail. The material had become slightly wet during the experiment, and appeared to be stabilized due to apparent cohesion. This may have occurred because the water level in the impoundment was higher than the crest of the core, so water could have seeped over the core into the filter zone. Also, water that flowed over the core fell into the breach channel approximately 0.2 m below. Splashes from the falling water may have contributed to wetting of nearby filter material. The stabilizing effect of apparent cohesion has been observed in multiple homogeneous dam breach experiments with sand, as summarized by Amaral et al. (2020) and Rifai et al. (2021). Sections of filter material eventually detached in large apparent-cohesive chunks, falling into the breach channel, where they separated and were carried away by the overtopping flow. The apparent cohesion caused the lateral expansion of the filter zone breach to be slower than that of the shell zone. The timing of filter material detachments are indicated in Figure 5. Figures 4f and 4g show the experiment before and after mass detachments of filter material on both sides of the breach channel.

3.4 *Core failure*

Due to incision of the breach channel, the downstream face of the core became exposed. Despite exposure to the overtopping flow, the core material did not become entrained by the flow. Instead, the core remained stable and intact while shell and filter material eroded around it. Where shell material had eroded from above the core crest, water flowed freely over the core, which acted like a weir. Mass detachments of filter material exposed the core laterally, to the edges of the remaining filter zone. Where the core was exposed, it had no support against water and soil pressures from upstream. As the core became increasingly unsupported, it appeared to remain unaffected until $t = 87$ s. At that time, the core began to bulge, with the center moving downstream at approximately 1 mm/s. At $t = 103$ s, when the exposed portion of the core was approximately 0.37 m wide and 0.2 m deep, a vertical crack appeared on the downstream face of the core, in the center of the bulge (Figure 4h). Two seconds later, at $t = 105$ s, the core broke along the crack, and was pushed open through cantilever rotation. A large piece of core from each side of the crack detached near

the lateral extent of the shell erosion (Figure 4i). The core had thus breached, and water and shell material from upstream rushed through the suddenly large breach (Figure 4j). The breach discharge Q_b and erosion rate V_e both rapidly increased. After 22 seconds, at $t = 127$ s, the core failure began to be impacted by the sidewalls of the flume, and the experiment ended. Before the impact of the sidewalls, the breach top width was 0.83 m, and the breach discharge was approximately 108 l/s. In prototype scale, this corresponds to a breach top width of 33 m, and a breach discharge of nearly 1100 m³/s. The timing of the core failure events, as well as the breach discharge and erosion rate hydrographs, can be seen in Figure 5.

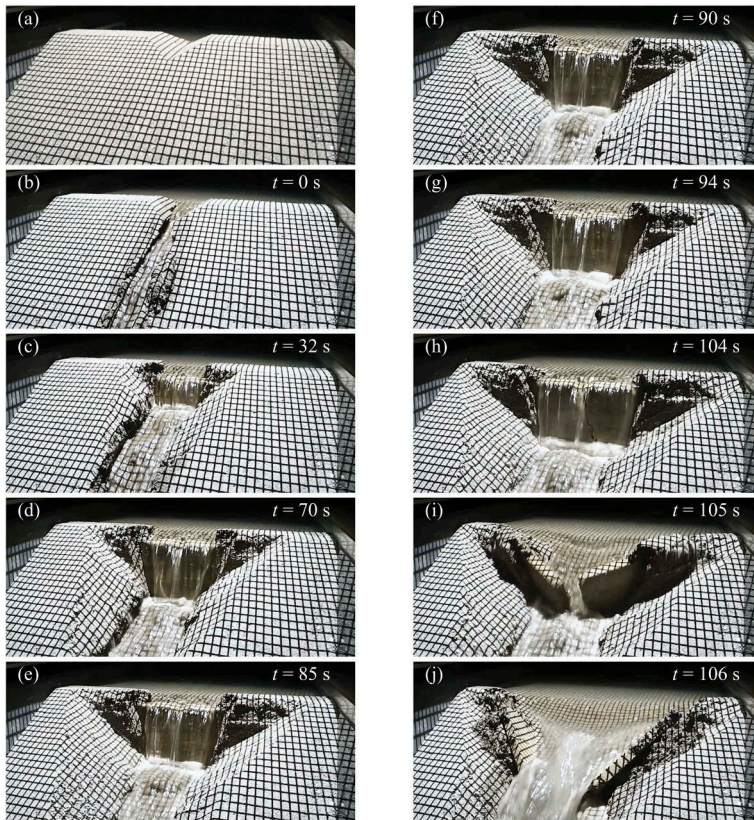


Figure 4. Breach experiment of a zoned embankment dam. Initial dam (a), $t = 0$ (when breach discharge at toe was first $Q_b > 0$, b), breach channel incision (c), before and after shell slope failures (d,e), before and after filter detachments (f,g), core crack appears (h), core failure (i), rapid increase in breach discharge (j).

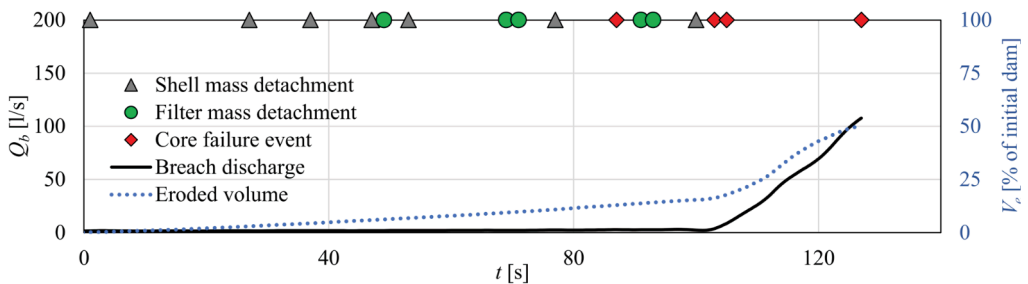


Figure 5. Breach discharge Q_b and material erosion rate V_e for zoned dam breach experiment, with timing of failure events of the shell, filter, and core zones.

4 CONCLUSIONS AND OUTLOOK

The overtopping-induced failure of a zoned dam was investigated by a laboratory experiment. A prototype-scale zoned dam, representing typical large zoned earthen dams in Switzerland, was designed and scaled down to laboratory scale for this experiment. The experiment demonstrated the failure processes that would be expected to occur during breaching of the prototype dam.

Breaching began with formation of a breach channel in the downstream shell. The breach channel deepened and expanded laterally across the shell zone, exposing the filter and core. The filter material, stabilized temporarily by apparent cohesion, failed in large chunks. Erosion of the shell and filter zones left the core exposed and unsupported on the downstream side. When the core could no longer resist the pressures of water and soil from upstream, it cracked in the middle, then broke along the crack, and two large pieces detached. This left a large breach in the embankment.

The observed failure processes of the shell material were expected. The erosion processes that occurred during initial breach channel formation, breach channel deepening, and lateral expansion were also observed in homogeneous dam breach experiments by Frank and Hager (2015), Frank (2016) and Halso et al. (2022), in which similar materials and experimental setups were used.

The failure process of the filter zone was not as expected. The filter zone was a thin, steep section of material that was expected to immediately undergo a slope failure in the absence of support from the shell zone. This would have quickly exposed the core, thus the filter would have had negligible effect on the timing of core exposure related to shell breach expansion. If the filter material had remained completely dry, this likely would have been the case. However, the filter material was wetted during the experiment, and it was temporarily stabilized due to effects of apparent cohesion. It is not clear if the continued presence of filter material, after departure of the shell material, contributed a stabilizing effect to the core zone.

Failure of the core zone was the process of most uncertainty prior to the experiment, due to the low number of experiments in which core failures have been observed. The core failed as a result of cantilever rotation, by first bulging, then cracking in the middle, followed by large pieces completely detaching from the rest of the core. The area of core exposure prior to its failure was larger than expected. The area of core exposure at the time of failure is a valuable result, as it can be used to evaluate methods for predicting core failure through statics calculations. Such methods could be implemented in parametric or numerical models, for use by engineers to estimate the timing and magnitude of breach outflow due to overtopping of specific prototype zoned dams.

ACKNOWLEDGEMENTS

This study was made possible by funding from the Swiss National Science Foundation (project #192223). A special thank you to Franklin Fuchsli for his help in building the model dam.

REFERENCES

- Ahmadisharaf, E. and A. J. Kalyanapu (2015). Investigation of the impact of streamflow temporal variation on dam overtopping risk: Case study of a high-hazard dam. *In World Environmental and Water Resources Congress 2015*, pp. 1050–1057.
- Amaral, S., L. Caldeira, T. Viseu, and R. M. L. Ferreira (2020). Designing experiments to study dam breach hydraulic phenomena. *Journal of Hydraulic Engineering* 146(4).
- ASCE/EWRI Task Committee on Dam/Levee Breaching (2011). Earthen embankment breaching. *Journal of Hydraulic Engineering* 137(12), 1549–1564.
- Bento Ana, M., S. Amaral, T. Viseu, R. Cardoso, and R. M. L. Ferreira (2017). Direct estimate of the breach hydrograph of an overtopped earth dam. *Journal of Hydraulic Engineering* 143(6), 06017004. doi: 10.1061/(ASCE)HY.1943-7900.0001294.
- Bornschein, A. (2014). Breschenentwicklung bei Dämmen mit Dichtungen ('Breach development for dams with seals'). In *Wasserbauliche Mitteilungen, Institut für Wasserbau und Technische Hydromechanik, TU Dresden*, Volume 50, pp. 303–312 (in German).

- Cestero, J. A. F., J. Imran, and M. H. Chaudhry (2015). Experimental investigation of the effects of soil properties on levee breach by overtopping. *Journal of Hydraulic Engineering* 141(4).
- Coleman, S. E., D. P. Andrews, and M. G. Webby (2002). Overtopping breaching of noncohesive homogeneous embankments. *Journal of Hydraulic Engineering* 128(9), 829–838.
- Costa, J. E. (1985). Floods from dam failures. Report 85–860. Reston, USA: USGS.
- Fletcher, B. P. and P. A. Gilbert (1992). Center Hill fuseplug spillway, Caney Fork River, Tennessee: hydraulic model investigation. Report HL 92–15., USACE WES.
- Franca, M. and A. Almeida (2002). Experimental tests on rockfill dam breaching process. In *IAHR-Int. Symp. on Hydraulic and Hydrological Aspects of Reliability and Safety Assessment of Hydraulic Structures*, St. Petersburg, Russia, pp. 29–31.
- Frank, P.-J. (2016). Hydraulics of spatial dike breaches. Doctoral thesis, ETH Zurich. *VAW Mitteilung* 236.
- Frank, P.-J. and W. H. Hager (2015). Spatial dike breach: Sediment surface topography using photogrammetry. In *Proc., 36th IAHR World Congress*, The Hague, the Netherlands. IAHR.
- Halso, M. C., F. M. Evers, D. F. Vetsch, and R. M. Boes (2022). Composite modeling of the effect of material composition on spatial dam breaching due to overtopping. In *Proc., 39th IAHR World Congress*, Granada, Spain, pp. 4600–4608.
- Hochstrasser, H., M. Aemmer, and A. Sorgenfrei (2008). Hochwasserrückhaltebecken am Jonenbach, Affoltern am Albis ('Flood retention basin on the Jonenbach River, Affoltern am Albis'). *Wasser Energie Luft* 100(4), 281–288 (in German).
- ICOLD (2003a). Bulletin on risk assessment in dam safety management. Paris, France.
- ICOLD (2003b). World register of dams. Paris, France.
- Ingenieurburo Kälin (1986). Sicherheitsüberprüfung Stauanlage Aabach ('Safety inspection Aabachweiherr Dam'). Report, Gemeindewerke Horgen, Switzerland.
- Lee, B.-S. and G. J.-Y. You (2013). An assessment of long-term overtopping risk and optimal termination time of dam under climate change. *Journal of Environmental Management* 121.
- Lombardi AG (2008). Staudamm Hühnermatt- Erhöhung der Hochwassersicherheit. Report 7022.1-R-10, Eitzelwerk AG.
- Milly, P. C. D., R. T. Wetherald, K. Dunne, and T. L. Delworth (2002). Increasing risk of great floods in a changing climate. *Nature* 415, 514–517.
- Morris, M. W., M. A. A. M. Hassan, and K. A. Vaskinn (2007). Breach formation: Field test and laboratory experiments. *Journal of Hydraulic Research* 45(sup1), 9–17.
- Pugh, C. A. (1985). Hydraulic model studies of fuse plug embankments. Report REC-ERC-85-7, US Bureau of Reclamation, Denver, USA.
- Pugh Clifford, A. (2008). Sediment transport scaling for physical models. In *Sedimentation Engineering: Processes, Measurements, Modeling, and Practice*. Reston, USA: ASCE.
- Rifai, I., K. El Kadi Abderrezzak, W. H. Hager, S. Erpicum, P. Archambeau, D. Violeau, M. Pirotton, and B. Dewals (2021). Apparent cohesion effects on overtopping-induced fluvial dike breaching. *Journal of Hydraulic Research* 59(1), 75–87.
- Rüdiger, B. (2017). Einfluss der Kornverteilung des Schüttmaterials und einer Oberflächendichtung auf die Breschenentwicklung und die Abflusskurve beim Versagen eines Schüttdammes durch Überströmen ('Effect of shell grain-size distribution and the facing element on breach-processing and discharge curve by embankment dam failure due to overtopping'). Doctoral thesis, Technical University of Vienna (in German).
- Sadeghi, S., H. Hakimzadeh, and A. B. Amini (2020). Experimental investigation into outflow hydrographs of nonhomogeneous earth dam breaching due to overtopping. *Journal of Hydraulic Engineering* 146(1).
- Schmocker, L., E. Höck, P. A. Mayor, and V. Weitbrecht (2013). Hydraulic model study of the fuse plug spillway at Hagneck Canal, Switzerland. *Journal of Hydraulic Engineering* 139(8).
- Simmler, H. and L. Samet (1982). Dam failure from overtopping studied on a hydraulic model. In *Proc., 14th Int. Congress on Large Dams*, Rio de Janeiro, Brazil. ICOLD.
- Swiss Committee on Dams (2021). List of dams in Switzerland. Accessed April 19, 2021.
- Swiss Federal Office of Energy (2022). Dams under federal supervision (dataset).
- U.S. Bureau of Reclamation (2012). Design Standards No. 13: Embankment dams. US Bureau of Reclamation, Denver, USA.
- Vaskinn, K. A., A. Løvoll, K. Höeg, M. Morris, G. Hanson, and M. Hassan (2004). Physical modeling of breach formation: Large scale field tests. In *Proc., Dam Safety Conference*, Phoenix, USA, pp. 1–16. Association of State Dam Safety Officials.

Reconstruction of hydrographs of the maximum annual flood event at dam site

Working Group of the Italian National Committee on Large Dams, ITCOLD (*)

(*)*The Working Group was made up of members from the national dam authority, dam owners and universities: F. Santoro & F. Pianigiani (Italian Dam Authority, Rome, Italy), A. Bonafè, L. Ruggeri & D. Feliziani (Enel Green Power Italy, Venice and Terni, Italy), M. Maestri (Alperia, Bolzano, Italy), F. Piras (ENAS, Cagliari, Italy), F. Sainati (Edison, Milan, Italy). P. Claps (Turin Polytechnic, Turin, Italy), A. Brath (Bologna University, Bologna, Italy)*

ABSTRACT: In 2000, the Italian Dam Authority issued a procedure to regulate the measures that should be carried out during each significant flood event, with the aim of obtaining a hydrological database of annual maximum flows.

After 15 years of applying this procedure, the Italian Dam Authority revised it in 2018 and required dam owners to reconstruct the most significant hydrological event of the year and the most significant events of the previous five-year period. They also provided further technical indications to improve and optimize the procedure. However, the experience gained in the last three years has shown that the reconstruction of hydrological events was affected by errors due to tolerance in reservoir level measurements, uncertainties in the measurement of flow rates, and discharge curves that were not always adequately calibrated.

With the aim, shared by the operators and the authority, to increase the database of the maximum annual flows with values that are “reliable hydrological data”, ITCOLD constituted the Working Group on the reconstruction of the maximum annual hydrographs. In March 2023 the group published the final report, providing more detailed technical indications for the reconstruction of hydrographs of the maximum annual flood event and defining shared criteria for the identification of cases of exemption from this obligation.

1 INTRODUCTION

In 2000, the Italian Dam Authority, hereafter referred to as DGD, regulated the measures to be carried out in the event of a flood, requiring special attention to be paid to the reconstruction of inlet hydrographs. After over 15 years of procedure application, in a period characterized by frequent and important flooding events, the DGD revised the procedure itself, in light of the experience gained and noting its partial and inefficient application. Therefore, with Circular Prot. No. 3356 of 13.02.2018, the DGD, moved by the need to improve the hydrological and hydraulic knowledge of Italian dams, ordered operators to reconstruct the most significant annual hydrological event, as well as one or more significant events of the previous five years. From the implementation of the Circular, a database of reliable hydrological data should be obtained within a few years.

After one year of application of the Circular, the DGD promoted a technical roundtable on 20 September 2019, with the major dam operators in order to improve the procedure and the quality of the hydrological data transmitted. The technical roundtable made it possible to gather all valid indications for improving and optimizing the procedure and the data transmitted by operators.

To date, the experience gained over the last three years, however, shows that for several dam sections, the reconstruction of the flow rates can be affected by errors due to the

tolerance of the level measurement or uncertainties in the measurement of connected flow rates, or to the use of discharge curves that are not always correctly calibrated, which make the reconstructed value unreliable and sometimes unusable at the dams of interest.

ITCOLD established the Working Group on the reconstruction of the maximum annual hydrographs with the shared goal of increasing the database of maximum annual flows with reliable hydrological data, as agreed upon by the operators and the authority. In March 2023, the Working Group presented the results of its work and issued a relevant bulletin that defined criteria for exemption from the obligation to reconstruct the annual maximum hydrological event in cases where there is a practical impossibility to reconstruct reliable hydrological data. The bulletin also provided additional guidance on how to reconstruct the flood hydrograph for the annual maximum.

2 CRITERIA FOR DAM EXEMPTIONS

The hydrologically significant flow values that can be obtained from a hydrograph are:

- maximum flow rate of the hydrograph, flow peak Q_c ;
- maximum average flow rates over different durations, Q_d, \max
- maximum average flow rate over 24 hours, Q_{24} ; and
- maximum daily flow Q_g .

Unfortunately, not all reconstructed hydrographs represent hydrologically reliable data, in fact a flow rate can be considered hydrologically unusable if it has physically unacceptable values. The problem may be due to anomalies in the hydrograph itself, caused by oscillations in the reconstruction due to purely numerical causes. Additionally, if flow values are strongly influenced by assumptions about the components of the balance equation, such as in the case of a basin connected to the reservoir via an unmonitored channel. This problem causes systematic errors in flow rate estimation. Similarly, flow rate values, that are strongly influenced by upstream reservoirs with subterranean basins of significant size compared to the one of interest, are not natural and this causes systematic errors in flow rate estimation.

A flow rate value obtained from a reconstructed hydrograph, while reliable, can be considered hydrologically superfluous if there are other nearby reservoirs in the region or hydrometric sections managed by public authorities that have characteristics of evident similarity to the one of interest. Under these conditions, the flow rates, at the crest and/or of duration d , that can be obtained from the reconstructed hydrographs, are not immediately usable for hydrological analyses.

In order to help dam operators identify situations that could invalidate the validity of flood hydrographs, the authors describe some criteria in the following section, to evaluate possible requests for exemption from the application of Circular No. 3356 of 13.02.2018.

The exemption criteria identified are as follows:

1. Dams with a limited basin: generally, these are dams with a limited catchment area ($<10 \div 20 \text{ km}^2$) and a relatively high ratio between the lake's surface area and the catchment area. In such cases, the reconstruction of hydrographs is generally conditioned by the measurement of the water level, in particular by its tolerance and precision, which can induce oscillations in the hydrograph and make Q_c values unreliable. To overcome this issue, a 24-hour or daily delamination step can be considered for this type of dam.
2. Dams with flood bypasses: if an upstream bypass is not monitored, it does not allow for the natural course of the flood wave in the section of interest to be reconstructed.
3. Several dams for the same reservoir: in cases where reservoirs have more than one dam, hydrograph reconstruction can only be carried out for one of the dams.
4. Dams in series with other dams or adjacent to hydrometric sections of or to other dams already monitored: dams could be defined in series if they are arranged on the same river shaft and the difference between the catchment areas is negligible. Similarly, dams may be exempted if they have upstream official public hydrometrographs relating to catchment areas with small variations in surface area.

5. Dams connected to other dams with large reservoir volumes, a basin extension greater than their own direct basin or with a system conformation that makes reconstruction of the flood wave particularly difficult and unrealistic: often, the connected basins and their contributions are not monitored or are monitored in an approximate manner. In some cases, the flow contribution of these channels is comparable to that of the own basin. Important non-natural contributions can also come from the releases of the upstream dam if it has a high rolling capacity. The common consequence is that the reconstructed hydrographs do not have a natural character and/or the calculated flood flows are very inaccurate.

3 CALCULATION OF MAXIMUM ANNUAL HYDROGRAPHS

The reconstruction of the flood hydrograph starts from the resolution of the balance equation, which in its differential form is as follows:

$$Q_{in} - Q_{out} = dV/dt \quad (1)$$

For a correct resolution of the balance equation it is necessary:

- to identify the plant scheme and the terms that make up the equation;
- to choose the delamination step; and
- to solve the finite difference equation.

3.1 Plant scheme

Figure 1 shows a schematic representation of three watercourses and four dams. The objective is to compute the flood hydrograph for dam A, which is connected to two adjacent dams via pipelines and supplies a hydroelectric power station. The terms that contribute to the balance equations can be classified into input contributions, output contributions, and volume terms.

In the diagram in Figure 1, they can be identified as follows:

Q_{in} = total incoming flow at time t . In Figure 1 the incoming flow rates are represented by:

- $Q_{in,nat}$, the natural flow rate tributary to the reservoir A representing the hydrograph to be determined.
- $Q_{in,i}$, the generic tributary flows from intakes or connected basins that discharge flows into reservoir A.
- $Q_{in-out,der}$, the flow rate pumped (if any) by the downstream hydroelectric plant.

Q_{out} = total outflow at time t . In Figure 1 the outflow rates are represented by:

- $Q_{out,spill}$, the flow rate discharged by the spillways and/or gates;
- $Q_{out,i}$, derived flow towards another reservoir via canal, tunnel or pipeline.
- $Q_{in-out,der}$, derived flow rate. In the case of a pumping system, the flow rate can be considered as outgoing or incoming, depending on the hydraulic direction of the system.

V = volume of the reservoir at time t .

3.2 Finite difference equation resolution

For hydrographs reconstruction (de-lamination) from in-situ measurements, Equation (1) is used in the finite difference form:

$$(\overline{Q_{in,nat}} + \sum \overline{Q_{in}}) - \sum \overline{Q_{out}} = \Delta V / \Delta t \quad (2)$$

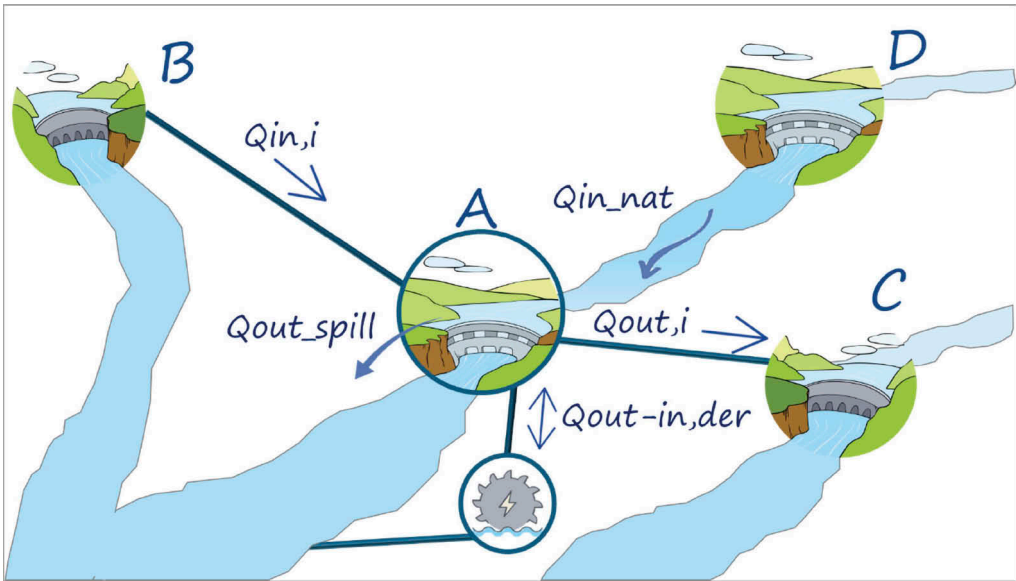


Figure 1. Generic plant scheme for Dam A, with terms of balance equation.

which can be rewritten as follows:

$$\overline{Q_{in,nat}} = \sum \overline{Q_{out}} - \sum \overline{Q_{in}} + \Delta V / \Delta t \tag{3}$$

Where Δt represents the de-lamination step typically varying from a few minutes to a few hours. The de-lamination time can also be assumed to be 24 hours.

The term ΔV is the change in reservoir volume between two consecutive de-lamination steps and the ratio $\Delta V / \Delta t$ is named incremental flow rate during the interval Δt . One source of error in the calculation of ΔV is due to inaccuracies and tolerances in reservoir water levels measurements.

The line above the Q-terms means that the flow rates are average values over the Δt interval and not instantaneous values. So, the terms of incoming and outgoing flow represent the average incoming and outgoing flow rates respectively in the time step Δt and will be calculated by averaging the recorded or calculated flow rates over time.

It is important to emphasise that the flow rate $Q_{e,nat}$, reconstructed using Equation (3) at finite differences, provides the natural hydrograph flowing into reservoir A in Figure 1. No account is taken of the natural flow rates stored in reservoir D, or of those taken or derived from the reservoir D upstream which, if it has large capacity, could render the flow rates reconstructed in A non-natural and therefore hydrologically insignificant. The presence of a large upstream reservoir, that substantially modifies the hydrology of the reservoir of interest, may constitute grounds for exemption from the reconstruction of hydrographs for the downstream reservoir.

3.3 Criteria for choosing de-lamination step Δt

As a guideline, it is suggested to choose a Δt between 15 minutes and 1 hour. For larger reservoirs in relation to the surface area of the catchment basin, regardless of the basin's run-up time, even a Δt of one hour may lead to anomalous oscillations in the reconstructed hydrograph due to inaccuracies and tolerances in the level measurements, which can result in incorrect estimates of the incremental term. To avoid this issue, it is advisable to use de-lamination steps of longer duration, even up to 24 hours. It is important to note that flow rates

reconstructed using a hypothetical Δt of 6 hours, for example, should be considered as “average flow rates of 6 hours duration.” Subsequent hydrological calculations to determine flow values for all other durations of interest (e.g. the peak) can be performed using standard hydrological methodologies that link average flow to duration.

4 EXCEL FILE FOR CALCULATION OF MAXIMUM ANNUAL HYDROGRAPHS

To facilitate the calculation of maximum annual hydrographs, a freely downloadable Excel template has been prepared for event reconstruction. The file enables easy event reconstruction, especially when flow measurements are manual and therefore often have variable acquisition time intervals. It is possible to download this file at <https://www.itcold.it/wpsysfiles/wp-content/uploads/2023/03/PRESENTAZIONI-RAPPORTO-FINALE-Foglio-di-Calcolo-idrogrammi-di-piena.zip>.

5 CONCLUSIONS

The working group, established by ITCOLD to address the issue of reconstructing the maximum annual flood event, brought together representatives from the authority, dam operators, and the university with the goal of achieving a shared outcome. In March, the group presented the results of its work, proposing criteria for assessing the reliability of the hydrograph reconstructed at the dam and providing more precise guidelines for event reconstruction. Additionally, a work file was prepared to assist managers in carrying out this task.

REFERENCES

- Directorate General for Dams and Water and Electricity Infrastructure, 2018 Circular No. 3356. Large dams Sheets of conditions for operation and maintenance - Modification of the procedures relating to hydrological-hydraulic measurements to be carried out in the event of flooding.
- Italian National Committee on Large Dams, 2023. Guidelines for the reconstruction of maximum annual flood hydrograms.

Experiences from inspections and controls on ageing penstocks of hydropower plants

A. Kager & R. Sadei

HYDRO SAFETY Engineering d. Kager Armin

ABSTRACT: In hydropower, the use of steel pipes has proven its worth in the realization of penstocks. Especially at high pressure and large diameters, steel pipes are still unrivalled. However, the longevity of the infrastructure can only be guaranteed if operation is accompanied by periodic checks and professional maintenance. The present technical paper reflects the experience gained during numerous inspections of penstocks over the past 10 years.

1 INTRODUCTION

The use of steel pipes has proven its worth in the realization of penstocks in the Alpine region and beyond. In the construction of hydroelectric power plants, steel pipes have been used in most cases since the beginning of the last century for the laying of numerous and sometimes branched pipeline systems. Even today, steel pipes are used for the realization of penstocks, especially at high pressure and large diameters. These are mostly steel pipes coated on the inside and outside, some of which are buried, but often laid on the surface. Although steel is an ideal material for such pipelines for several reasons, improper installation, maintenance, and operation can result in damage and loss of material due to corrosion - and thus also impair the stability of the pipes in the long term (Figures 1a to c).



Figure 1. (a) Failure of a penstock due to material defect © www.icnnational.com; (b) Failure of a penstock due to pressure surge © www.fateclub.org; (c) Crack caused by ice formation inside © Kager.

In the following, some criticalities and experiences in the field of inspection and evaluation of such pipelines in recent years are pointed out.

2 PIPES

The various types of steel pipes used in the last century and up to the present day are diverse. While fire-welded pipes and riveted joints (Figure 2a) were still used in the first half of the

century, this method was subsequently superseded by the further development of welding. Both the longitudinal joints of the plates and the joints between two adjacent pipes were now made by arc welding or other semi-automated or automated welding processes (MAG, MIG, submerged arc). For smaller diameters, ball & socket joints were often used because they allowed slight angulations along the pipe route during installation (Figure 2b). In recent decades, the longitudinal welds of pipes with diameters of up to 2 m have been displaced, in most cases, by fully automated spiral welds.

After World War II, until the early 1970s, large-diameter and high-pressure pipes, especially in the southern Alpine region, were made with thin-walled steel pipes, which were provided with stiffener rings on the outside (Figure 2c).

The materials used for steel pipelines were aging-resistant, easily weldable, resilient and break-resistant carbon steels, the mechanical properties of which have been steadily improved in the course of the last century.



Figure 2. (a) Pipe with riveted joints; (b) Spiral-welded pipes with ball & socket joints; (c) Pipe reinforced on the outside with stiffener rings and expansion joint © Kager.

3 SHAPE AND SPECIAL PIECES

Along the pipelines, there are usually numerous shaped and special pieces, which have different functions. The most important of these are air valves, safety and shut-off devices, expansion joints, outlets, manholes, connecting flanges, reducer couplings, bends, branches and sensors for flow measurement.

4 CORROSION PROTECTION

Appropriate corrosion protection is key to the longevity of pipes, shapes and special pieces. This must be selected depending on the aggressiveness of the soil and the ambient conditions and carried out professionally.

4.1 *Passive corrosion protection*

As with pipes, there have also been some important further developments in the field of passive corrosion protection (coatings) over the past century. The tar and bitumen coatings used in the beginning, some of which were reinforced with jute and glass fibers, were increasingly replaced by thermoset and thermoplastic coatings. While nowadays, the inside of the pipes is primarily coated with epoxy resins and polyurethanes, the outside is mainly coated with three-layer polyethylene and polypropylene as well as polyurethane.

4.2 *Active corrosion protection*

Active corrosion protection by impressed current and/or sacrificial anodes has so far played a minor role in the field of hydropower and, despite the undisputed effectiveness of active corrosion protection systems, is not discussed in detail in this article.

5 DAMAGES

5.1 Coating damages

Professional care must be taken in the selection and application of coating systems for pressure pipelines. Experience shows that this has not always been done in the past or has not been done for all pipelines. Detachment (Figure 3a), general signs of wear, pores and other defective areas (Figure 3b) usually indicate an incorrect choice of the coating system, inadequate preparation of the surfaces and/or improper application of the individual coatings. Those areas which are coated on-site during or after installation are particularly susceptible (Figure 3c). The coating work there is usually carried out under unfavourable conditions that are difficult to control, and often the specific training and education of the personnel carrying out the work are also inadequate.



Figure 3. (a) Peeling of the coating due to inadequate surface roughness; (b) Punctual damage; (c) Absence of the coating on site-produced welds © Kager.

5.2 Abrasion

Particularly in areas close to the bottom and in areas subject to high hydraulic stress, abrasion phenomena are often observed where the frictional effect of the sediments in the driving water causes wear of the coating, up to its complete dissolution (Figures 4a to b).

5.3 Corrosion

The loss of passive corrosion protection due to the phenomena described in the previous paragraphs is accompanied by the onset or progression of corrosion. While detachment or damage to large surfaces usually causes uniform surface corrosion with relatively little material removal, punctual damage to the coating, such as pores, craters or cracks, often leads to more concentrated anodes, an increased current flow and thus to highly concentrated material losses due to the ensuing electrochemical reactions (Figure 4c). The consequence of such phenomena can be pitting corrosion, which in some cases shows depths of up to one millimeter and more after only a few years. Remediation of such damage is often difficult and expensive. In contrast to the above-mentioned surface corrosion, such areas must be levelled out with suitable stucco compounds before restoration. In the area of abrasively stressed surfaces, the phenomenon of erosion-corrosion often occurs, which causes an acceleration of the inherently existing corrosion effect. Corrosion due to micro-bacterial attack was also observed on some pressure pipelines. Due to the characteristic damage pattern (small, deeply branched holes), this proves to be particularly costly in the rehabilitation of coatings. Phenomena such as bimetallic and crevice corrosion can also be detected on riveted joints and special elements such as the sensors for flow measurement.



Figure 4. (a) Abrasion phenomena at riveted joints close to the ground; (b) Abrasion phenomena in the area of a slope change; (c) Corrosion due to unsuitable coating © Kager.

On the outside, corrosion is more prevalent in those places where permanent moisture occurs, such as in the area of saddle supports, where the penstock enters anchoring blocks, and on stiffener rings. Accumulations of lichens and mosses and the presence of crevices and angled areas also increase the corrosion effect.

In addition, stray current corrosion due to direct currents can occur in the vicinity of built-up areas (e.g., near direct-current railroad installations), and alternating current corrosion can occur on penstocks in the area of influence of medium- and high-voltage power lines. The damaged areas on the outside of the pipes are both pitting-like and crevice-shaped, with sharply defined corrosion holes (Figure 5a). At certain AC densities, corrosion rates of several mm per year can occur.



Figure 5. (a) Corrosion craters due to the action of stray currents; (b) Ovalization due to improper compaction of the pipe trench; Figure (c) Deformation in the area of an anchoring block © Kager.

5.4 *Manufacturing defects*

Pipes, shape species and all the remaining elements of a pressure pipeline can have material defects, which usually result from the manufacture of the elements described and their connection on site.

In the case of as-new pipes made of thin-walled sheets and welded automatically, manufacturing defects on the pipes are rather rare, also because the pipes must pass several inspection stages in the factory before they are finally delivered to the construction site. Welding work on the construction site, on the other hand, is always susceptible and must therefore be adequately controlled.

The situation is different with pipes from the first half of the last century, where quality control had limited resources. Fire-welded pipes, whose longitudinal joints were produced by a combination of thermal and mechanical actions, may have weak points at the joints, which have led to pipe ruptures in the past.

Surface defects such as cracks, pores, flaws or volume defects such as structural defects, blowholes, and non-metallic inclusions could also be detected during inspections on fittings, especially on branches and pipe bends, which were frequently made of cast steel in the past.

5.5 *Damage to pipe connections*

Pipe joints are particularly susceptible to corrosion due to their irregularities and the turbulence they cause. This applies to weld seams, but especially to riveted joints, which are particularly susceptible to corrosion due to the increased abrasion effect. It is not uncommon for rivet heads in the bottom area to be ground flat. In addition, the presence of lead sealing rings, which were frequently used for riveted joints in the first half of the last century, should also be mentioned at this point. At isolated plants, leaks of the lead profiles from the pipe joints could be detected after decades of operation.

5.6 *Deformations*

In buried pipelines, but not only, deformations can occur that are due to improper installation of the pipes. The presence of stones in the bedding or backfilling area and improper compaction of the pipe trench can be identified as causes in most cases (Figure 5b). Occasionally, linear deformations in front of or after rigid anchoring blocks can also be found, which are due to slope movements and the associated settlements or displacements of the fixed points. The corresponding load peaks in the pipe cause deformations, which in some cases exceed the plastic limit of the steel pipes (Figure 5c). In the case of pipes laid on the surface, the pipes may also be damaged by falling trees or stones.

5.7 *Other damage*

In addition to the types of damage mentioned in the previous chapters, which certainly covers the majority of possible damage to a steel pipeline, other damage such as cracks (e.g., due to ice formation in the case of insufficient soil cover), root ingrowth, etc., can also be detected in isolated cases. However, these play a minor role in steel pipelines due to their rarity.

6 INSPECTION AND CONTROL TECHNIQUES

To quantify the damage described in the previous chapters, especially corrosion, and to ensure a fully comprehensive assessment of the infrastructure, the inspector has numerous control and measurement methods at their disposal. The main steps of an assessment of a penstock are as follows:

6.1 *Study of the historical development*

Detailed knowledge of the infrastructure to be inspected before the actual inspection begins is of central importance. The review of planning documents, delivery bills, and reports (e.g., construction diaries, reports on changes during and after construction, reports on rehabilitation and repairs, inspection reports from the past, etc.) enable a targeted focus when carrying out subsequent inspections. Practical experience shows that often too little attention is paid to this point. In some cases, only a few or insufficient as-built documents are available to the inspector, which is often due to the change of generations among the personnel of the operating company and the resulting loss of historical knowledge.

6.2 *Visual controls*

Visual inspection is probably the supreme discipline in the evaluation of pressure pipelines. The pipes should be inspected internally (Figures 6a to b) or employing inspection robots, and externally by trained and experienced personnel (Figure 6c). In the case of buried pipelines, scraping should be carried out at longer intervals to be able to check the condition of the outer coating and the corrosion attack, at least selectively.

Visual inspection essentially involves checking the condition of the passive corrosion protection, the corrosion, the abrasion and the existing joints and special pieces. The latter, if produced by steel casting, are to be inspected for the damage patterns common to the manufacturing process (surface defects such as cracks, pores, flaws or volume defects such as structural defects, blowholes, non-metallic inclusions, etc.).

When inspecting pipelines laid on the surface, the support saddles and anchor blocks must also be checked for damage and anomalies. Attention should be paid to environmental conditions (heavy traffic, medium and high voltage power lines, vegetation, subsidence, landslides, groundwater, etc.).



Figure 6. (a) Inspection activity inside; (b) Exit from a manhole; (c) Inspection activity outside with professional securing © Kager.

When personnel inspect the pipelines, care should be taken to ensure professional planning, the use of qualified and experienced personnel, proper equipment, good ventilation, good lighting conditions, and especially a high level of safety.

6.3 *Non-destructive material testing*

Non-destructive material tests (NDT) are used to inspect pipes for defects, determine their mechanical and geometric properties, and quantify the incidence of corrosion. They can be used in a variety of ways, both in the factory and on pipes that are already buried or exposed.

The most common checks are wall thickness measurements for statistical evaluation of residual wall thicknesses, grid and B-scan measurements to determine corrosion and abrasion, penetrant testing (PT), magnetic particle testing (MT), and ultrasonic testing (UT) to find defects and anomalies on welds and pipe walls, analyses of the coating system (layer thicknesses, buildup with base, intermediate, and top coatings - Figure 8b), tests of the adhesion of the coating to the substrate (during manufacture or after pipe installation by pull-off, X-cut, grid cut), measurements of deformations and ovalizations (laser scan), and hardness tests to estimate the mechanical properties (conditionally non-destructive).

For the determination of corrosion, the high-resolution measurement of the surfaces affected by corrosion using LaserScan has proven to be useful. The inspection provides information on the type of corrosion, the average wall thickness losses and the depths and sharpness of the corrosion craters found (Figures 7a to c and Figure 8a).

The findings obtained are particularly important as a decision-making aid when planning any renovation or repair work: to avoid delays and considerable cost increases, it is necessary to decide at an early stage whether an additional work step, i.e., that of levelling the corrosion craters with stucco compound, is necessary when renewing the passive corrosion protection.

6.4 *Destructive material testing*

Since in many cases, no or only inadequate as-built documentation is available to the inspector, tests often must be carried out on specimens taken from the pipeline to determine the



Figure 7. (a) and (b) Heavily corroded inner pipe surface before and after cleaning; (c) Representation of the results of the surface measurement with laser scan © Kager.

metallurgical characteristics. As a rule, the samples are then subjected to tests in the laboratory to determine the tensile strength in the longitudinal and transverse directions, the flexural strength, the notched impact strength, the hardness, the chemical composition, and the metallurgical structure. Finally, the calculation of the zero or nil-ductility temperature (NDT) is performed by calculation with the previously mentioned input values. Also, tests of welds can be made in the laboratory with appropriate micrographs and X-ray tests (RT).

The findings from the destructive material tests and the checks in the preceding chapters subsequently serve as the basis for the computational assessment of the infrastructure.

6.5 Other controls

Special conditions, such as the effect of slope movements and the associated deformation/stress on a penstock, may necessitate the use of precision extensometers to determine local deformations on the pipe.

Strain gage rosettes can also be attached to the pipe to measure multi-axial strains/stresses. Both measurements should be permanently observed and recorded. If required, they can be combined with an AI-supported alarm system.

6.6 Controls of concrete/reinforced concrete structures

The structures made of concrete/reinforced concrete (support saddle and anchoring blocks) must also be subjected primarily to a visual inspection. In addition, core drillings can be taken from the said structures through the use of core drilling equipment and examined in the laboratory. They are mainly used to determine the compressive strength, the carbonation depth (corrosion protection of the reinforcement), the density, the ultrasonic velocity, the modulus of elasticity and compression, the tensile gap strength and the petrography or chemical analysis of the concrete.

7 CONCLUSION

Steel has proven itself as a material for penstocks in the hydropower sector. It is durable and versatile. Nevertheless, the necessary attention must be paid to steel pipelines, including corrosion protection, and the operation of the infrastructure must be accompanied by periodic inspections and professional maintenance.

The pipes should therefore be inspected at regular intervals so that any necessary repair or rehabilitation measures can be planned and carried out at an early stage. Experienced and skilled personnel should be employed for the inspection of the pipelines; compromises in terms of safety are not acceptable. The measurement and inspection program should be flexibly adapted to the type and condition of the pipeline. All available inspection methods should be discussed in advance and the most suitable ones applied.



Figure 8. (a) Laser scan measurement in the pipe; (b) Analysis of the coating with P.I.G (Paint Inspection Gauge); (c) Checking the coating of a newly laid pipeline for pores © Kager.

During the inspection of pressure pipelines, all existing fittings and special parts, but above all the safety-relevant devices such as emergency shut-off devices, air valves, expansion joints and basic drains must be subjected to a careful visual inspection. The operator must carry out extensive checks to ensure that they are functioning properly.

When constructing new plants or replacing old pipelines with new pipes, experts for active and passive corrosion protection must be consulted in advance and the manufacture of the pipes and their installation must be professionally checked and supervised (Figure 8c). The costs incurred for this represent a fraction of the costs that would be incurred for the rehabilitation work that is often necessary after only a few years.

Last but not least, it should be pointed out that a conscientious collection and storage of documentation and the mapping of all activities, incidents and findings in a geo-information system help the plant operator to pass on important information for subsequent generations, and thus permanently preserve historical knowledge.

REFERENCES

- Horlacher H.B. & Helbig U. 2018 *Rohrleitungen 1 – Grundlagen, Rohrwerkstoffe, Komponenten*. 2nd Edition. Springer Vieweg, Springer Verlag GmbH.
- Horlacher H.B. & Helbig U. 2018. *Rohrleitungen 2 – Einsatz, Verlegung, Berechnung, Rehabilitation*. 2nd Edition. Springer Vieweg, Springer Verlag GmbH.
- Wendler-Kalsch E. & Gräfen H. 2012. *Korrosionsschadenskunde*. 1st Edition. Springer-Verlag Berlin Heidelberg GmbH.
- ASCE, American Society of civil engineers 1995. *Guidelines for evaluating aging penstocks*.
- Brecht M. & Kocks H.J. 2009. *Entwicklung des passiven Korrosionsschutzes von Stahlrohrleitungen*. Specialistic journal *gwf-Gas/Erdgas*, Booklet Anniversary Edition 2009, S. G14–G29.
- Ballatore S. & Frigerio A. 2019. *Penstocks – Historical Notes and Safety Considerations*. Specialistic journal *L'Acqua*, Booklet 4, S. 7–16.

Instable rock cliff at Steinwasser water intake: Immediate and safety measures

A. Koch

IUB Engineering Ltd., Bern, Switzerland

D. Bürki

Kraftwerke Oberhasli Ltd., Innertkirchen, Switzerland

ABSTRACT: The Steinwasser water intake is a 20 m high dam which was endangered by an instable rock cliff located above its left bank. In 2021 the tachymetric monitoring assessed an acceleration of the deformations. The safety of the Steinwasser dam was assessed using an acting force derived from the crash model provided by geologists. The results showed that the structural safety of the dam in case of an uncontrolled rockslide is not fulfilled, thus immediate measures were planned to excavate the material in stages with controlled blasting. The dam was protected by a 1 m thick Rockfall-X mattress and part of the reservoir near the left dam abutment was filled with gravel material to dampen the impact of blasted rocks. The blastings were implemented in such a way that the detached elements (individual boulders) were no bigger than 1 m³ in volume. Vibrations were measured during the construction works in order to ensure the safety of the dam. Regular measurements and the early implementation of appropriate measures are the key components to ensuring a high level of safety while guaranteeing the operation of the Steinwasser water intake.

1 INTRODUCTION

Kraftwerke Oberhasli Ltd. (KWO) is the operator of hydropower plants in the Susten Pass and Grimsel Pass region of Switzerland. With 13 hydropower plants and eight reservoirs, the KWO produces around 2400 gigawatt hours (GWh) of electric energy per year.

The Steinwasser water intake can be found in the Gadmental at the bottom of the Susten Pass at 1,340 metres above sea level. The catchment area encompasses around 30.57 km² and has an inflow of approx. 74.95 million m³/A and an equivalent energy value of 1.5 kWh/m³. Water from the Wendenbach water intake (29.98 million m³/A) from a catchment area measuring 12.08 km² is also channelled via the Steinwasser water intake into the tunnel system of the Hopflauen and Innertkirchen 1 & 1E power plants. The Steinwasser water intake was created in the time period from 1952 to 1954 as a measure to expand the Innertkirchen 1 power plant (235 MW). The dam is approx. 50 m long, 20 m high and mostly hollow inside, as the water intake channel and the flushing gate are integrated inside of the dam. The 18-m broad-crested overflow section on the crest serves as a flood safety protection element.

2 HISTORY

2.1 *Observation*

Located above the left bank of the water intake is a rock cliff, from which 1 to 2 m³ of rocks broke off in June 2016. The boulders—the largest of which measured 0.8 m in length—fell on and damaged the buttress of the dam. The situation was assessed with a geologist, an extensive

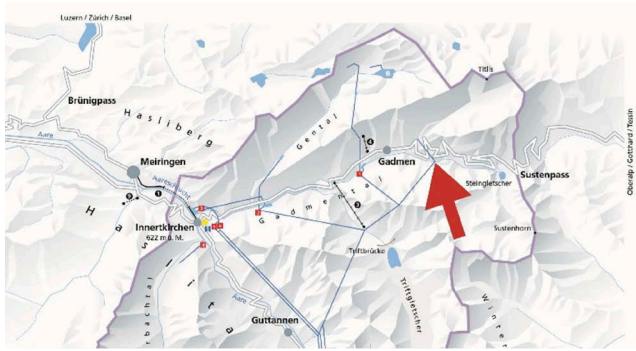


Figure 1. System diagram of the KWO with the location of the Steinwasser water intake.

clean-up operation was carried out in May 2020 and tachymetric monitoring was installed with five reference points and 17 observation points.

The measurements taken in the short series of measurements at the end of 2021 showed an accelerated movement of up to 2.5 mm in two months, primarily in the upper part of the rock cliff. The additional measurement taken after the snowmelt in April 2022 further corroborated this trend. Based on these results, the geologists created a rockslide model, which showed that an uncontrolled rockslide of the cliff could hit the dam, mainly in the area of the left abutment.



Figure 2. Steinwasser water intake and location of the instable rock cliff, April 2022.

2.2 Geology

The slope above the water intake has gradient greater than 45° and is traversed by rock ledges with rock spurs in the cliff settling and layers of loose rock several meters thick. Scree and loose material had accumulated in the leveled out area above the instable rock cliff. The loose material contained numerous boulders of different sizes and has a stable slope with a gradient of $35\text{--}38^\circ$. The location of the bedrock under the loose rock is unknown.

2.3 Safety assessment

The structural safety of the dam was assessed based on different scenarios using the acting force (Ad), which was deduced from the rockslide model provided by the geologist and in accordance with the norm SIA 261/1. The maximum volume of the instable cliff was estimated to be 500 to 600 m^3 . The effects of the equivalent forces on the dam have been assessed using a spatial shell model with the law of conservation of energy.

Table 1. Scenarios for the structural assessment of the water intake in the event of a rockfall.

Scenarios	Rockfall volume	Size of individual boulder	Energy, speed	Equivalent acting force
Scenario 1: Partial rockfall on the west side	2-5 m ³	½ m ³ (approx. 1 * 0.8 * 0.7 m)	240 kJ, 12 m/s	10,600 kN
Scenario 2: Partial rockfall on the east side	10-15 m ³	1 m ³ (approx. 1.3 * 1.0 * 0.8 m)	90 kJ, 11 m/s	4000 kN
Scenario 3: Entire rockfall	500-600 m ³	10 m ³ (approx. 3 * 2.5 * 1.5 m)	2440 kJ, 13 m/s	110,000 kN
Scenario 4: Entire rockfall with subsequent rockslide	1200 m ³	10 m ³ (approx. 1.3 * 1.0 * 0.8 m)	2250 kJ, 12 m/s	110,000 kN

2.3.1 Spatial shell model

Using the AxisVM X6 R1i software, the structure of the water intake was modelled on a simplified basis as a tiled slab made up of multiple layers with shell elements on a 10-metre-long strip. The arch action of the dam was depicted using polygonally successive elements, with the thickness of the elements being approximated as closely as possible to the actual dimension of the trapezium-shaped structure. The intake channel and the inspection walkway were modelled, as they are relevant weak points. The connections between the wall shells and the underlying 2.5-metre thick wall was modelled with an interface element. The support of the model was assumed to be encastred, since the reinforced concrete structure is solid and built on rock. The lateral model limits of the 10-metre-long section are exposed, i.e. modelled without an abutment. The lateral force transmission was disregarded in the model. For equivalent forces F1 and F2, a minimum impact angle of $\alpha = 10^\circ$ and a component of the force acting in the longitudinal direction were taken into consideration. For equivalent force F3, a maximum impact of 60° was taken into consideration.

Table 2. Results from the shell model (AxisVM X6 R1i).

Force application point	Scenario 1	Scenario 2	Scenario 3+4
F1	Local plastification under the impact site	Evidence provided (transverse direction m_y)	Failure, static forces considerably higher than the resistance
F2	Evidence provided (transverse direction m_y)	Evidence provided (transverse direction m_y)	Failure, static forces considerably higher than the resistance
F3	Evidence provided (transverse direction m_y)	Evidence provided (transverse direction m_y)	Failure, static forces considerably higher than the resistance

2.3.2 Law of conservation of energy for scenario 3 and 4

It was assumed that the fall energy would be completely or partially converted into deformation energy on the reinforced concrete structure. In order to calculate the deformations, a mechanism in line with Figure 4 was observed and plastic joint was assumed in each of the nodes. The deformation energy results from the product of the rotation in the node and the plastic moment. It was assumed there would be a uniform 6-metre-wide deformation of the structure. For scenarios 3 and 4 for the individual boulder measuring 10 m³ and a reduced fall energy of 2000 kJ, this resulted in a rotation of 2 degrees at the point (0.0) and a sinking of 15 cm. The deformation is depicted in Figure 4. With this impact, larger gaping cracks must be expected with plastic (irreversible) deformations.

2.3.2 Safety objective and risk assessment

The safety of the water intake as a functioning structure as well as the safety of the maintenance and inspection employees must be guaranteed in the long term and in a sustainable

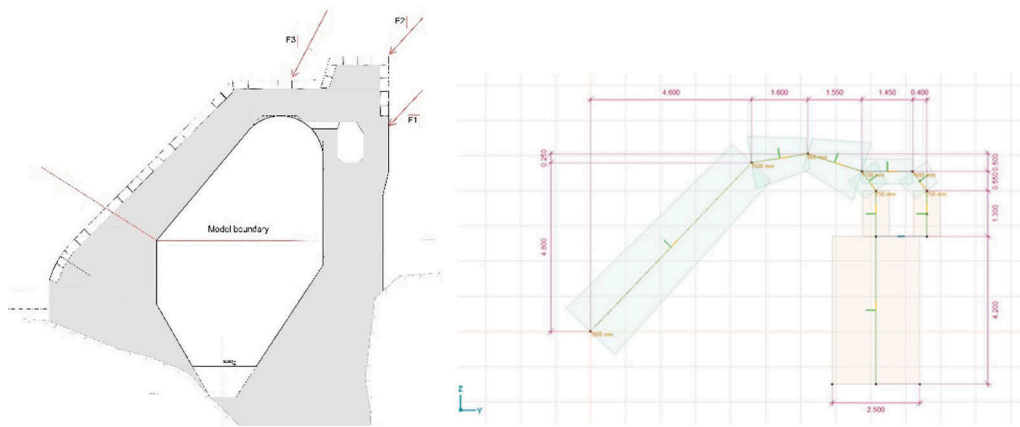


Figure 3. Section of the Steinwasser dam with the force application points and angle of incidence from rockfall scenarios (left), cross-sectional view of the shell model AxisVM X6 R1i (right).

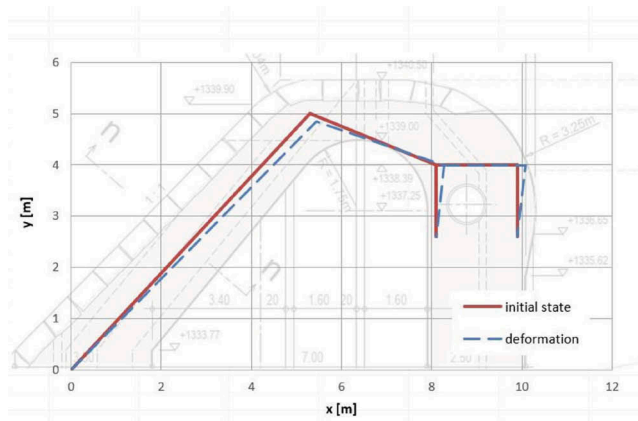


Figure 4. Mechanism for calculating the deformation energy and the resulting deformation for scenarios 3 and 4.

manner. Were there to be an uncontrolled rockfall from the cliff onto the water intake, in isolated events or as an overall event, this could result in major operational restriction being placed on the Steinwasser water intake. Both approaches, the shell model and the law of conservation of energy showed that the structural safety of the dam is not guaranteed in the event of a complete rockslide (Scenarios 3 and 4). In the worst-case scenario (> scenario 4), the destruction of the left bank of the dam cannot be ruled out. The Steinwasser dam could be damaged considerably by the impact of a rockslide and be put out of commission for several months, which would result in a considerable period of production downtime.

2.4 Safety measures and comparison of scenarios

Different scenarios were studied (Table 3). The favorite measure was defined as being a combination of a gradual excavation and securing of the rock cliff with anchors, continuously as work progresses to respond to the geological situation on site (ground risk). This solution ensures that the occupational health and safety of the employees is guaranteed in its implementation and the risk of operating failure due to unpermitted damage to the water intake structure is minimised.

Table 3. Measures assessed as part of a study of different scenarios.

Measures	Assessment
No action	Uncontrolled, water intake may be massively damaged. A large amount of work for occupational health and safety as well as for the maintenance of the water intake.
Blasting of the entire rock cliff	Too much strain for the dam structure.
Gradual excavation	See chapter 3.
Securing of the rock cliff Securing with rockfall safety net approx. > 4500 kJ, level 8	High costs and maintenance works. Water intake is located in an avalanche zone. The grid could suffer from a total loss every 10 to 20 years. No impact in the case of a full or large partial rockfall.

2.5 Procedure

In its capacity as building owner, KWO worked together with the team comprising the planner IUB Engineering Ltd., geologists Kellerhals & Haefeli Ltd. and the specialist company Gasser Felstechnik Ltd. to devise each step of the project in great detail. The time available was estimated to be short, as the rock cliff had to be secured or even removed before the onset of winter. The procedure for excavating the rock cliff was designed as such that the operation of the water intake would not be affected and as little material as possible would need to be deposited upstream of the water intake. To achieve these goals, the following requirements were defined on the basis of the preliminary study:

- The blastings are to be implemented in such a way that the detached elements (individual boulders) are no bigger than 1 m³ in volume. Where possible, the path of travel of the detached elements should be influenced to ensure that the dam is hit by as few boulders as possible.
- The dam is to be protected using Rockfall-X™ mats, which will factor a maximum individual boulder volume of 10 m³ into the dimensions of the protection measures.
- The Rockfall-X mats are to be cleaned sufficiently between each blasting to ensure that the protective effect is also conserved for subsequent blastings.
- Terrain design underneath the belay as a deposition zone with a slope running down into the water.

The approval for all of the measures was issued as a measure for the maintenance of a hydropower plant by the Office for Water and Waste within the Canton of Bern's Office of Construction and Transport on 26 July 2022. The approval was granted due to the circumstances and the overwhelming potential for damage. The specialist departments involved, e.g. the fishery and Senior Engineer Group 1 from the Canton of Bern Civil Engineering Office, were notified in good time so that their requests and concerns could be incorporated into the implementation.

3 IMMEDIATE MEASURES

3.1 Construction site installation and protective measures

As preparation for the removal of the rock cliff, a provisional mobile rockfall safety net was fitted over the belay for occupational safety purposes. The assembly of the mobile installation platform on the slope next to the belay and the transportation of the equipment and construction materials (digger, drill) were carried out by helicopter. The cliff was cleaned and cleared of vegetation (an area of approx. 1375 m²). In order to prevent a major rockslide during the construction work, the belay was provisionally girded with steel cables that were fixed in place with anchors.

The Rockfall-X™ protective mats were positioned on the left bank of the dam. A temporary bridge was built over the existing dam in order to ensure access to the belay and protecting apron at all times, even if the dam were to overflow. Steel palisades were positioned on the upstream side to retain the material displaced as a result of the blastings.

3.2 Excavation and management of the excavation

The excavation of the belay was carried out in several small stages with a maximum volume of approx. 100 m³. The magnitude of each blasting was continually adapted depending on the geometry of the rocks and the local geology. The materials that were blasted and removed in stages were deposited along the left bank of the slope downstream of the water intake. Some of the materials fell in this area during the blastings and the remaining materials were moved here using a crawler excavator.



Figure 5. Time-lapse shot of the excavation.

3.3 Excavation of loose materials and reinforcement of the slope

Loose materials were excavated above the rock cliff in order to form a temporary berm for the construction work. This berm was restored in stages following several blasting operations up to approx. 12 m below the top of the excavation pit. During the construction work, a steel palisade was put up on the berm to offer protection against local rockslides. A temporary barrier made from high performance netting 50/50 was installed along the entire slope and fixed in place temporarily with IBOR32 self-drilling anchors and anchor plates. In addition, vegetation matting was installed under the protective netting on the slope. The stability of this slope against sliding was not guaranteed with the use of other safeguarding measures. The anchors were arranged offset in a 2x1.50 m grid and were designed to be sufficient in length that they could be driven into the rock to at least 1.5 m. Anchors measuring between 3 m and 8 m in length were installed with this process.

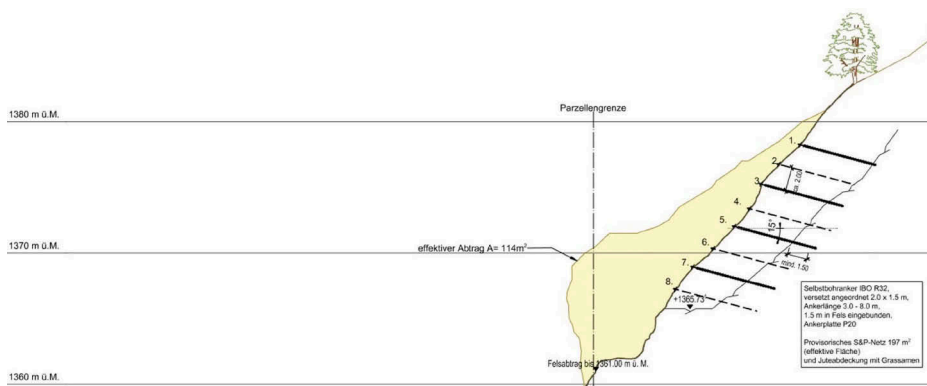


Figure 6. Cross section of the excavation with reinforcement of the slope.



Figure 7. Loading the blast holes, excavation of approx. 100 m³ of materials.

3.4 *Scope of the work*

The belay was excavated in stages to a final height of 1361 meters above sea level. The volume of the remaining main plate was estimated to be around 100 m³. This plate has an approx. 2-metre-wide protecting apron, which can slow down sliding material. The slope up to 4 m above the remaining main plate features heavily weathered rock, boulders and stones, and is not secure. The individual components in this area are not bigger than 1 m³ and will not cause significant damage, were they to fall on the dam. An embankment with a concave protecting apron was created upstream of the dam in order to catch sliding materials and thus prevent materials from being deposited in the reservoir.

Following the construction work, the terrain was surveyed using a drone operated by the Flotron Ltd. surveying office. A 3D area model was created from this survey (point cloud, accuracy to 5 cm). This area model was compared with the existing model (surveys carried out on 28 April 2022, accuracy to 5 cm) in order to calculate the volume of rock that had been removed and deposited. The protecting apron with the embankment on the left side of the reservoir is clearly visible on the images. The total amount of rock excavated was 1624 m³. The material was deposited in the gully downstream of the water intake.

The area around the excavated rock cliff will be reforested. The remaining forest area will be repopulated through natural growth. In the area surrounding the excavated bely, the temporary anchors will remain in the slope and the temporary high performance netting will be removed before the reforesting work is carried out.

4 RISK MANAGEMENT

4.1 *Criteria for triggering immediate action*

In the case of rock movements, the rates of movement are key to determining whether a group of rocks can be safely processed. Holding off taking action can result in extremely high additional costs in connection with the excavation work and operational safety measures and can even result in the implementation being made impossible. For these reasons, it has been decided to implement immediate measures.

4.2 *Operational interruption*

The KWO took statistical values and evaluations with climate models, averaged them and used these figures as the basis for calculating how much an operational interruption would cost. An operational interruption can cost up to CHF 30,000 per day in the months of June to

August (calculated using the net cost price prior to the energy crisis in 2022/23). Theoretically, the costs of an interruption would be several times larger on the market. An operational interruption to the Steinwasser water intake and the neighbouring Wendenbach water intake should be precluded to the greatest extent possible.

4.3 *Meteorology & hydrology, measurement station, construction site safety*

The established natural hazards (flooding, rockfalls and avalanches) have been identified and included in the safety concept. No discharge measurement station is located in the area of the Steinwasser water intake. The flood return periods have been estimated applying factors to a specific discharge rate of $1.40 \text{ m}^3/(\text{s}\cdot\text{km}^2)$ and were defined as $\text{HQ}_{30} = 33 \text{ m}^3/\text{s}$, $\text{HQ}_{100} = 44 \text{ m}^3/\text{s}$, $\text{HQ}_{300} = 54 \text{ m}^3/\text{s}$.

A tailored safety concept plan for rockfalls and flooding has been created to ensure occupational safety during the taking of immediate action on the belay of the Steinwasser water intake. The alert levels provided by the Swiss federal government's natural hazard bulletins (FOEN hazard levels 1–5) served as the basis for this together with threshold values from rain measuring stations and the precipitation radar, as well as measures for activities. To measure the local precipitation, two automatic rain measuring systems were installed during the construction works. The data generated by these systems was able to be viewed online at all times. These measuring stations also triggered an SMS alert.

The construction site installations and protective measures were set up in such a way that the dam could divert floodwater up to HQ_{30} without any damage while the construction work was being carried out. The acting overflow width during the construction work was reduced by 6 m due to the Rockfall-X damping system. With the reduced overflow width, a HQ_{30} with a water level in the water intake of approx. 1'342.0 meters above sea level could be diverted. In addition, a freeboard of 0.5 m under the temporary bridge was included.

4.4 *Vibrations on the dam structure*

The structure has been assessed as being “normally sensitive” in accordance with Swiss standard SN 640 312 and the blastings assessed as being in the “occasional” frequency class. The effects of the blasting on the structure were measured using a vibration monitoring system. The measurement device was installed in the dam. The prescribed threshold values were observed, with alert values 1 (8 mm/s) and 2 (12 mm/s). The trigger level of 2 mm/s was exceeded briefly on isolated occasions. An alert was never initiated during the entire measurement period and the following maximum value was registered (alert value in brackets): 5.03 mm/s (8.0 mm/s). The vibrations generated by the construction work and the blasting did not cause any damage to the Steinwasser dam structure, the sluice gate or the water intake channel.

4.5 *Measurement system and monitoring the movement of the belay during excavation*

Tachymetric measurement devices with the telescope sighted on the belay were installed in May 2020. Measurements were taken selectively during the construction work and the devices were disassembled shortly before the excavation of the rock. The belay was constantly monitored with crackmeters for the duration of the excavation work so that relevant measurements could be measured. In case of unusual movement, manual measuring points were set up as a redundant measurement system at every crackmeter so that the horizontal and vertical movement vectors could be recorded. A rip wire with a siren was also installed during the upper excavation level. The measurements taken after the first blasting stages showed that the risk of the main plate suffering a complete rockslide had not increased.

4.6 Protection of the dam and the reservoir

The dimensioning of the protective measures, namely the Rockfall-X™ damping system, for the dam was carried out in the preliminary project by Geobruigg Ltd. To create a crash zone, a small embankment was formed on the left bank of the water intake using the materials available. A 1-metre-thick layer of Rockfall-X mats (measuring approx. 250 m²) was positioned over the left part of the dam. The mats were fixed to the dam using anchors so that they would remain stable in the event of flooding.

Mobile steel palisades were installed on the embankment as additional protection for the dam and the service gangway. This prevented excavated material from falling in and blocking the water intake. These protective measures were dismantled following the completion of the excavation work. The earth deposited on the left bank was created as an embankment and a concave protecting apron in order to catch sliding materials and thus prevent these materials from being deposited in the reservoir.



Figure 8. Overview of the excavation with the service gangway and the protection of the dam.

5 LESSONS LEARNED AND OUTLOOK

The excavation of the belay was completed successfully and without any accidents. No damage was caused to the Steinwasser dam structure or the safety devices by the construction work and the measured vibrations never exceeded the threshold values. The processed area will undergo annual visual inspections over the next few years. For the time being, measurements will be taken with a tachymeter four times a year. The construction costs for all of the measures incl. planning and monitoring total approx. CHF 731,000. Measurements and monitoring are key to being able to make a well-founded assessment. Manual measurements and level measurements (tachymeter) are frequently used in this respect. These measurement methods have been used for decades to assess the risk of natural hazards in the area of gravitational processes.

The movements of the belay were underestimated. In future, there should be shorter intervals between measurements at the outset. In this instance, a measurement every three-to-four months would have been sufficient. If no significant movements are recorded after one or two years, the measurement intervals could subsequently be adjusted, e.g. annually.

The belay at the Steinwasser water intake was not detected in the satellite-aided displacement measurement (satellite radar) pilot project in the KWO catchment area in 2019, as the perimeter was too small and covered with forest. These new methods will definitely help the owner to identify larger perimeters with a great deal of movement in good time and in so doing improve risk management.

Rock stabilisation work is massively influenced by geology and the ground risk. From the perspective of the owner, the work carried out as part of this project – with the planning

carried out by civil engineers working together with geological consultants as well as the early involvement of an experienced specialist company – proved to be successful. This was key to the successful and accident-free completion of the immediate action. Thanks to the sound and reliable preparation and action planning, the risks were able to be reduced to a minimum (with the exception of ground risk). From today's perspective, there remains an acceptable level of residual risk.

REFERENCES

- Norm SIA 261/1. 2020. *Actions on structures - Supplementary specifications*: section 6. Swiss society of engineers and architects.
- AxisVM X6 R1i, Finite element analysis and design software. Inter-CAD Software Development Company, Budapest, Hungary.
- Geobruigg AG. Handbuch ROCKFALL-X A, damping mats. 31 March 2022. Switzerland.
- Norm SN 640 312. 2013. *Vibrations — Vibrations and impacts on structures*. VSS. Zürich

Emergency preparedness planning in Greek dams

S.L. Lazaridou

Hydroexigiantiki Consulting Engineers, Athens, Greece

G.T. Dounias & S.C. Sakellariou

Edafos SA, Athens, Greece

A.E. Kotsonis, G.P. Kastranta & M.V. Psychogiou

Hellenic Republic Ministry of Infrastructure and Transport, Athens, Greece

ABSTRACT: The paper discusses the main procedures for Emergency Preparedness Planning (EPP) in Greece. The Greek Dam Safety Regulation (DSR) came into force in October 2017, and a Dam Administrative Authority (DAA) was formed to manage its application. One of the main obligations of the dam operators is the preparation of an Emergency Preparedness Plan (EPP). The DAA prepared an EPP Standard, to be followed by Dam Owners and Operators. After discussions with the dam community and the Civil Protection Agency, the Standard was finalized in 2021. All dams within the jurisdiction of the DSR must prepare an updated EPP, following the new Standard. The Standard introduced a hazard potential class analysis, altering the categorization of many dams which was initially based on dam visible height and reservoir capacity. Regional Authorities and Private Companies who act as Dam Operators must comply to the standard's procedures and define responsibilities, resources and equipment for preventive and emergency actions. In some cases, Dam Operators adapting to this more demanding Regulatory framework, must proceed to significant organizational changes. The EPP provides extended information and data to the Civil Protection Agencies involved, to assist them identify downstream risks and conduct evacuation plans. The Dam Owner, the dam Operator and the Civil Protection Agencies need to collaborate and establish a solid and effective communication pathway. The initial experience of the Standard's application is briefly discussed, and some challenges faced by Dam Owners and Operators during the EPP implementation are presented.

1 INTRODUCTION – CASE HISTORY

1.1 *Greek dam safety regulation*

A Greek DSR was issued on the 30th of December 2016, and it became applicable on the 11th of October 2017, along with the establishment of the Dam Administration Authority (DAA). The DAA is operating within the Ministry of Infrastructure, headed by the General Director for Hydraulic Works. According to the ICOLD World Register of Dams, Greece currently has 164 large dams and more than 180 dams are expected to fall within the DSR's jurisdiction.

The DSR consists of 28 Articles for the Dam life cycle and three (3) Annexes, including a Greek dams' inventory. The Emergency planning obligations and procedures of the Dam Owner/Operator are described in Article No 10.

1.2 *Field of application –dam classification*

The Greek DSR applies when the visible dam height is equal or greater than 10 m, or the visible dam height is between 5 m and 10 m and the reservoir equal or greater than 50.000 m³.

Visible dam height is the maximum difference in elevation between the dam crest and its downstream toe as it was formed after dam construction.

According to the first issue of the DSR (12/2016), 149 Greek dams were categorized considering only their visible dam height and the total reservoir capacity. The hazard potential class of the dam was later incorporated in dam classification and the categorization of Greek dams is made as follows:

- Category I: Visible dam height, $H \geq 40$ m or Reservoir volume $> 10.000.000$ m³, irrespective of dam height, or Hazard Potential classified as High
- Category II: Visible dam height $40 \text{ m} > H \geq 20$ m or Reservoir volume $\geq 1.000.000$ m³, irrespective of dam height, or Hazard Potential classified as Medium.
- Category III: Dams that are not classified in categories I and II, or Hazard Potential classified as Low.

The dam is classified to a category when meeting at least one of these criteria (height, reservoir volume, hazard potential).

The Hazard Potential Classes are generally defined as follows:

- Low: No population at risk and minor material damages.
- Medium: Low population at risk (up to 15 people) and several material damages.
- High: Significant population at risk (more than 15 people) and serious material damages.

The analytical criteria set to classify the hazard potential of the dam, as described in the EPP Standard of the DSR and presented in Table 1:

Table 1. Downstream impacted elements, hazard potential classes and consequences (EPP Standard).

Downstream Impacted Elements	Hazard Potential Classes according to the consequences		
	Low	Medium	High
Number of habitats (houses etc)	None	Up to 5	More than 5
Public Gathering Infrastructure*	None	None	Existence
Rural, Industrial etc Transportation Infrastructure	None Rural roads etc	Up to 15 Secondary Provincial (low traffic volume)	More than 15 people National Roads Provincial, highways etc
Organized activities (e.g., recreation)	None	Temporal and restricted	Frequent
Environmental Protection Zones	None	None	Existence
Cultural Protection Zones	None	None	Existence

* Schools, Churches, Theatres, Hospitals etc

2 EPP STANDARD

In the following paragraphs, the main objectives, procedures, and structural layout followed and described in an EPP, are analyzed.

2.1 Objectives of the EPP

According to Article 10 of the Greek Dam Safety Regulation (DSR), an EPP defines the set of actions that must be followed, to minimize the loss of human life and damage to property, mainly in the downstream areas, in case of dam safety emergencies. The EPP also provides to the Emergency Protection Agencies inundation information and mapping of various probable flood events.

2.2 Necessity for an EPP standard

The EPP Standard establishment was considered necessary to provide guidance and a solid framework to dam operators adopting and organizing safety preparedness procedures. The DAA prioritized this action to further activate dam owners to prepare their plans and establish solid collaboration with the Civil Protection Agencies.

2.3 Steps followed for the drafting of the EPP standard

A working group was formed by the Greek Committee on Large Dams (GCOLD) and prepared EPP specifications, followed by a public consultation workshop (02/2018). The working group incorporated the comments provided by the dam community and a final proposal was then submitted to the Dam Administration Authority (DAA). The DAA created a new working group, and an Emergency Preparedness Standard was initially issued on 12/2020 and updated on the 07/2021. The 2nd edition incorporated comments and remarks made by the Hellenic Civil Protection Planning Department of the Ministry for Climate Crisis and Civil Protection.

2.4 EPP application

According to the Standard, EPP's must be implemented for all Greek dams that fall within the DSR jurisdiction, in all categories I-II and III.

2.5 Approval and revision procedures

The EPP is initially implemented during the final dam design study and revised from the Dam Construction Body (DCB), before the first filling of the reservoir. During the operation stage, the Dam Operation Body (DOB), regularly revises the EPP as follows:

Table 2. Required EPP revisions.

Dam Category	Revision*
I	Three (3) to five (5) years.
II	Five (5) to ten (10) years.
III	Eight (8) to fifteen (15) years

* or earlier following organizational changes, legislation revision etc. The Dam Safety Engineer may suggest an emergency revision.

2.6 Classification level, distribution and filing

The EPPs are classified as Confidential, and they are distributed to all stakeholders involved in emergency evacuation and rescue procedures. These are the Civil Protection Agencies, Police and Fire Departments, Municipalities and Regional Authorities. Their representatives receive numbered copies. The Emergency Protection Agencies are responsible for implementing their evacuation plans for water flow releases with downstream consequences and for potential dam failure. At least one copy of the Dam Owner/Operator EPP should be kept in the Emergency Operations Center of the dam.

2.7 Technical and operational characteristics of the dam

The main technical characteristics of the dam are incorporated to a "fill in" Dam Information Standard Table required by the DSR. Additional information is provided, as appropriate, along with specified operational functions of the spillway and bottom outlet such as the reservoir evacuation time estimation. Any system associated with early warning procedures (e.g., sirens) should also be described.

2.8 Incident identification and evaluation procedures

2.8.1 Emergency levels

Three (3) Emergency Levels are defined as follows:

- Level 1 (Internal Alert, Authorities not informed): Unusual event, progressing slowly. A problem has been detected which needs further surveillance for evaluation or remedial measures and actions to be applied.
- Level 2 (General Alert, Authorities are informed): Unusual event, progressing rapidly. The problem gradually deteriorates, it needs constant surveillance or immediate remedial measures and actions since it could lead to dam failure or uncontrolled release of mass water volume. In this level are also included:
 - *Water flow releases during floodgate or outlet works operation, that may have significant downstream consequences.*
 - *Severe flood events.*
- Level 3 (General Alert - Evacuation): Imminent dam failure/dam failure in progress. Dam failure is expected or is in progress.

Each EPP needs to further analyze the abovementioned definitions and predefine potential Incidents and their progression to Emergency Levels. An indicative Incident List considering the dam type and its specific technical and operational features should be developed. This List shouldn't replace the Dam Engineers judgment to assess a dam safety incident.

Civil Protection Agencies are notified at Emergency Levels 2 and 3, according to Standard Notification Charts. The Greek Dam Administration Authority is also notified for all Incidents at Emergency Levels 2 and 3. Notifications are also foreseen for the operation of the spillway and bottom outlet at certain Level 2 alerts.

2.8.2 Indicative incident list

As previously mentioned, an indicative Incident List considering dam type and its specific technical and operational features must be developed. To create the list, the Dam Owner/Operator should consider the dam type, the foundation conditions and permeability reduction measures applied, any past incidents and failures, spillway and bottom outlet operational functions, surveillance system, electromechanical equipment, emergencies such as significant or extreme flooding, earthquakes, sabotage, and vulnerability to cyber-attacks etc.

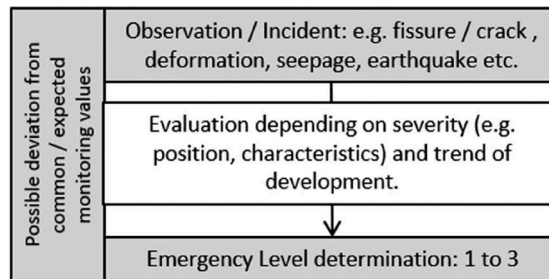


Figure 1. Emergency level determination process.

The list should be accompanied with recommended preventive/corrective actions associated with the appropriate resources and equipment. These actions should include, among others, controlled drawdown of the reservoir level or reservoir emergency evacuation.

2.8.3 Five step response process

A five (5) step response process of the Dam Owner/Operator is illustrated in the following figure:

For the five-step procedure, the Dam Owner/Operator prepares notification charts and standard announcements, for all three (3) emergency levels. The Dam Owner/Operator Director must evaluate and suggest the necessity to evacuate downstream areas. According to the

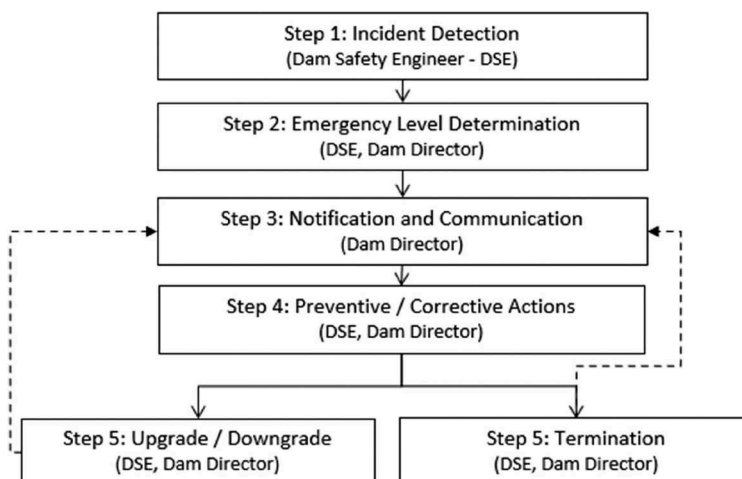


Figure 2. Five (5) step response process.

downstream inundated area boundaries, the final decision is further made either by the Mayor, the Regional Governor, or the Secretary General of the General Secretariat for Civil Protection. The Dam Owner/Operator is also responsible to notify the dam safety staff to evacuate the dam and reservoir area.

Following the termination of an incident, the Dam Owner/Operator prepares an analytical report, considering all aspects of the incident, evaluating the actions taken and suggesting actions for the improvement of the emergency preparedness procedures.

2.8.4 Dam break analysis results, inundation, and other EPP maps

Dam break analysis assumptions and results must be incorporated in the EPP. Information referring to downstream populated areas at risk, critical infrastructure, access roads and bridges, areas of environmental and cultural importance etc. should be noted. The most unfavorable hydrological and non-hydrological scenarios and their inundation maps should be considered.

Significant discharges during operation (gated spillway, bottom outlet) should also be considered since they may impose serious damages and impact downstream areas. If this information and analyses are not available, the Dam Owner/Operator may evaluate and incorporate results and maps from the EC2007/60 Flood Directive.

Additional maps are developed including information from the selected inundation scenarios (such as inundated area boundaries and zones, water flow characteristics: flow depth, flow velocity, depth x velocity, flood wave arrival and peak time), critical infrastructure within the inundated area, proposed warning sign posts and their location, temporary assembly points, prohibited crossings etc.

These maps are produced to assist the Civil Protection Agencies to prepare their evacuation plans and are subject to further update from the responsible agencies.

2.8.5 Notification charts and early warning procedures

The EPP Standard, guides the Dam Owners/Operators in determining the agencies and authorities that must be contacted in case of an emergency (Emergency Levels 2 and 3). A template, Level 2 and 3, notification chart is illustrated in Figure 3.

The Dam Owner/Operator must determine all representatives in charge, record and regularly, usually once a year, update their contact details.

Template notification announcements must be also prepared for the external Emergency Levels 2 and 3 and various probable incidents (e.g., dam break of main dam, dam break of an auxiliary/saddle dam, extreme flood event etc.).

These notifications provide information related to the incident, the unfavorable scenario of reference (hydrological or non – hydrological), corrective and preventive actions applied,

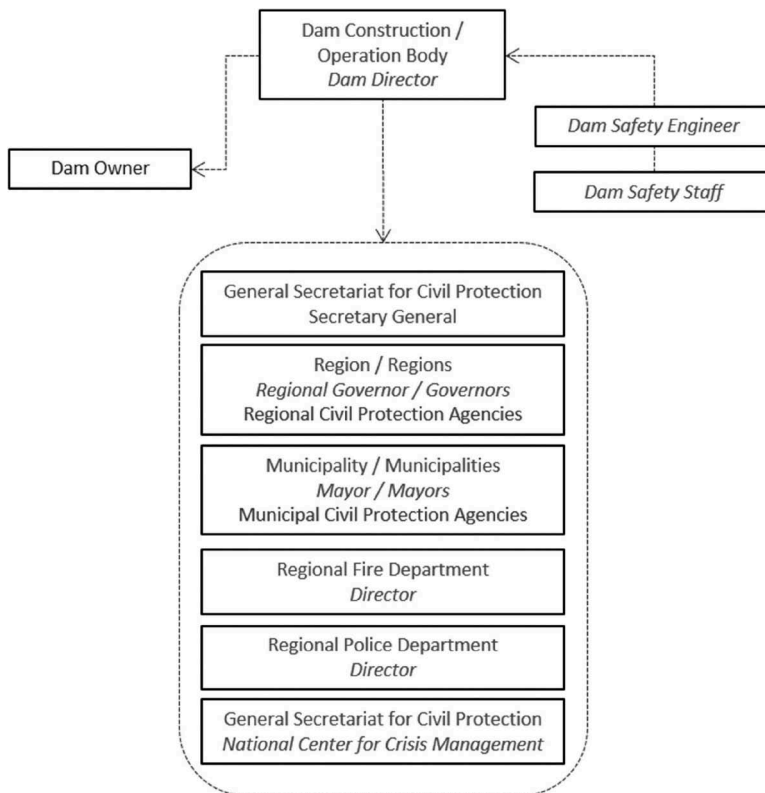


Figure 3. Five (5) step response process.

suggestion to evacuate downstream population at risk, further notifications to be expected, any other useful information.

Templates for public safety warning sign posts is also provided, where appropriate, for the dam and reservoir area, along the riverbanks, at crossings and bridges.

2.8.6 Template forms

Standard, template forms are included in the EPP Standard Annexes. In total, eight (8) template forms are given, and the Dam Owner/Operator may produce many more, if appropriate.

These standard forms mainly refer to:

- Revisions and classification level.
- Contact information of representatives in charge and contacts made during an incident.
- Incident information record, report to the Civil Protection Authority and the DAA.
- Suggestion for the evacuation of downstream population at risk.
- Trainings and preparedness exercises.

3 RESPONSIBILITIES FOR EMERGENCY PREPAREDNESS AND OPERATIONS

3.1 Dam owner organizational structure for dam safety

The DSR and an additional guideline (30/01/2019), both identify minimum staffing requirements, during the construction and operation stages. During the operation, requirements depend on the dam supervision category, which is determined considering several aspects of the project, including downstream population at risk. In all cases, the dam safety staff team comprise of a minimum number of engineers (Civil, Mechanical, Electrical, Mining,

Surveying, Technical), scientists (Geologists), Foremen and Administration Officers. In most cases, Dam Owners/Operators must proceed to significant organizational changes to satisfy the abovementioned requirements.

3.2 Dam owner/operator general responsibilities

According to the DSR, the responsible bodies must conduct all emergency inspections and request, if required, assistance from the Greek Dam Administration Authority (DAA). In this case, the DAA will employ a Dam Safety Review Committee (DSRC) to examine the reported incident.

According to the EPP Standard, the Dam Owner/Operator, must report, all incidents of certain Emergency Level (2 and 3), to the DAA and the Civil Protection General Secretariat.

The Dam Owner/Operator is also responsible:

- To define emergency resources and equipment and make appropriate agreements with local contractors and suppliers.
- To ensure safety and security around the dam and reservoir area.
- To ensure that the communication with all stakeholders and the Civil Protection Agencies, is efficient. The communication means are set with a mutual agreement among all interested parties.
- To ensure that all safety measures, surveillance, and communication procedures are always responsive, including public holidays, weekends etc.

3.3 Dam safety staff responsibilities.

The main responsibilities of the dam safety staff are set as follows:

- The dam safety engineer, monitors and implements EPP procedures, detects the dam safety incidents, suggests their Emergency Level, preventive, and corrective actions.
- The dam director, defines the Emergency Level, implements preventive and corrective actions, activates communication charts, and further suggests at level 3 the necessity to evacuate downstream population at risk.
- The dam safety staff team follow all instructions given by the Dam Safety Engineer and the Dam Owner/Operator Director and participate in regular trainings.

3.4 Dam safety staff emergency response training

The dam safety engineer is responsible for training dam safety staff and must schedule and coordinate periodical internal dam safety exercises. Generalized exercises coordinating multiple stakeholders, are carried out under the responsibility of Civil Protection Agencies. The emergency response exercise framework, is illustrated in the table below:

Table 3. EPP review and emergency response exercise framework.

Dam category	Review	In situ exercise	Generalized exercise.
I	Three (3) to five (5) years*	One (1) to two (2) years*	<i>Coordinated by</i>
II	Five (5) to ten (10) years*	Three (3) to five (5) years*	<i>Civil Protection</i>
III	Eight (8) to fifteen (15) years*	Five (5) to eight (8) years*	<i>Agencies</i>

* or earlier, when specified by the Dam Safety Engineer

The first generalized exercise should be organized before the reservoir first filling. The results should be reviewed and assessed to improve preparedness procedures.

3.5 Civil protection agencies responsibilities

Civil protection Agencies prepare and implement an evacuation plan, for incidents attributed to dam operation (flood events with potential downstream consequences) and probable dam failure. They also coordinate, as mentioned above, generalized emergency preparedness exercises.

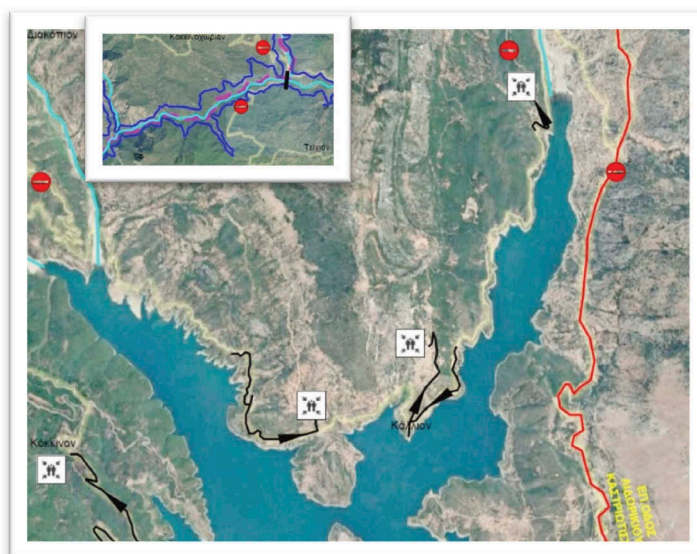


Figure 4. Evacuation routes, assembly locations, warning signs along the reservoir and river crossings.

4 EPP STANDARD APPLICATION - MAIN PROBLEMS AND ACTIONS FOR IMPROVEMENT

4.1 *EPP Standard revision*

The EPP is subjected to further updates, incorporating comments and suggestions provided by Dam Owners/Operators, Civil Protection Agencies and the General Secretariat for Civil Protection.

4.2 *Main problems*

Many Dam Owners/Operators have already prioritized and conducted EPPs. Main issues they have confronted are summarized as follows:

- Lack of early warning systems and appropriate signage around the dam, the reservoir and downstream areas at risk.
- Lack of or very old dam break studies that need to be subjected to update, delaying the EPP implementation.
- Missing studies and design data (e.g., controlled reservoir drawdown) to also assess downstream consequences from the operation of gated spillways and bottom outlets.
- Missing a dam construction folder with as built drawings, installed equipment manuals and organized information about of the dam behavior and history.
- In some cases, Dam Owners have not tested bottom outlets operation, raising concerns about their capability to operate appropriately as designed, in case of an emergency.
- Many Dam Owners still have not complied with minimum staffing demands, haven't implemented their EPPs and lack experience, equipment, and resources to apply them.
- Experience in “in situ” and generalized preparedness and response exercises, is limited.

4.3 *Actions for improvement*

4.3.1 *Education and training*

The Greek Committee on Large Dams conducted, under the auspices of the Greek Dam Administration Authority, three (3) webinars focused on many aspects of the DSR procedures. In the second series, the implementation of an EPP, based on the Standard, was

presented. Approximately 200 participants attended the webinar, mainly Dam Owner representatives (Public and Private), Designers, Consultants, Contractors. Additional training is considered indispensable.

4.3.2 Database management system

A website with an online submission portal for the dam owners is currently being implemented. The online portal is connected to a data management system.

Besides administrative tools, the system includes automatic procedures and guidelines for the Dam Experts and the Dam Safety Review Committee members, including emergency procedures. It will provide online submission forms, to report incidents at Emergency Levels 2 and 3, to the DAA and an incident database. Overall, the database will accelerate emergency procedures associated with the DAA (report of an incident, DSRC staffing, in situ inspection and evaluation, review of corrective actions).

5 CONCLUSIONS

The EPP implementation and application in Greece is not yet complete. The Standard is considered as a sufficient and complete guideline for Dam Owners/Operators. Future updates will incorporate comments and suggestions provided by the Dam Owners/Operators, the Civil Protection Agencies, and all stakeholders. The EPPs provide additional information to assist the Civil Protection Agencies in implementing their evacuation plans. EPPs also provide the appropriate signage for public safety around dams and reservoirs, downstream waterways, and crossings. Several issues have been identified, while conducting EEPs for some major Greek Dam Owners/Operators. Many of these refer to older or missing assessments (dam break studies and other operational scenarios with downstream consequences) and organizational issues such as the lack of early warning systems, dam safety staffing, emergency equipment and resources, trainings and emergency exercises. To assist Dam Owners/Operators in adopting EPPs, the Dam Administration Authority has identified and prioritized several actions, including:

- Providing relevant information (Guidelines, Standards, legislation etc.) for emergency planning via the website and the data management system portal.
- Activation of the dam owner’s submission portal including incident reporting procedures.
- Recording and assessing dam failures and incidents.
- Organization of seminars and workshops on emergency planning and the EPPs.
- International collaboration and exchange expertise with other Dam Safety Authorities.

The abovementioned actions will contribute to establish an effectively responsive communication system between Dam Owners/Operators with the DAA and the Civil Protection Agencies and all stakeholders.

REFERENCES

- DAA 2016. Approval of the Dam Safety Regulation- Dam Administration Authority, *Official Journal of the Government of the Hellenic Republic* (4420 B)
- DAA 2019a. Instructions on the Dam Owner definition for the DSR application, *DAA Decision* (3671/17- 12-2019, Online Publication Number: 6ΦΞΓ465XΘΞ-7ΩΣ)
- DAA 2019b. Guideline on the minimum staffing of the Dam Operation Body for the application of the Dam Safety Regulation, *DAA Decision* (1238/15-04-2019, Online Publication Number: 7XHB465XΘΞ-5H5)
- DAA 2021. Emergency Preparedness Plan Standard - 2nd Edition, *DAA Decision* (340039/29-11-2021, Online Publication Number: ΩΓΩ0465XΘΞ-A53)
- GCOLD 2018. Working Group: Draft Emergency Preparedness Plan Guideline.
- GCOLD 2011. Working Group: Draft presidential decree on dam safety.
- Lazaridou, S.L., Dounias, G.T. Kotsonis, A.E., Kastranta, G.P., Psychogiou, M.V., Experience in the application of the Greek Dam Safety Regulations, Symposium “Management for Safe Dams” - 91st Annual ICOLD Meeting – Gothenburg 13-14 June 2023.

Seismic analysis of old embankment dams: Qualification of the Fr-Jp method

N. Lebrun

EDF-CIH, La Motte-Servolex, France

M. Jellouli

ISL, Paris, France

J.-J. Fry

J-J Fry Consulting, Bassens, France

ABSTRACT: Embankment dams built before 1950 can pose safety problems, as they were built with poorly to moderately compacted materials and without respecting the current state of the art. Inexpensive, easy and reliable tools can be useful for the seismic reassessment of these dams, especially when the owners of the dams have limited financial resources, but these tools have to be sophisticated enough to be able to fit the cyclic pore pressure generation and the dynamic performance of the dam. The current simplified analyses unfortunately do not reproduce the pore pressure generation up to liquefaction and its consequence on dynamic behavior, only take into account the 2D characteristics of dams and ignore the loss of resistances with deformation. Thus, the Fr-Jp method, developed thanks to JCOLD data, sought to fill these gaps by aligning itself with the seismic behavior observed on JDEC recordings on Japanese dams. EDF with the participation of ISL is in the process of putting this method under quality assurance. Software manual, scientific notice, user manual and validation notice are being drafted. This paper describes how the method is designed and justified by its calibration fitting the accelerograms measured on the Japanese dams. A couple of applications are described.

RÉSUMÉ: Les barrages en remblai construits avant 1950 peuvent poser des problèmes de sécurité, car ils ont été construits avec des matériaux peu ou moyennement compactés et ils ne respectent pas l'état de l'art actuel. Des outils peu coûteux, faciles d'emploi et fiables peuvent être adaptés pour la réévaluation sismique de ces barrages, en particulier quand leurs propriétaires ont des moyens financiers limités, mais ces outils doivent être suffisamment sophistiqués pour pouvoir reproduire la génération cyclique de pression interstitielle et le comportement dynamique du barrage. Les analyses simplifiées actuelles ne reproduisent malheureusement pas la génération de pression interstitielle jusqu'à la liquéfaction et ses conséquences sur le comportement dynamique, ne prennent en compte que les caractéristiques 2D des barrages et ignorent la perte de résistance avec la déformation. Aussi, la méthode Fr-Jp, développée grâce aux données de JCOLD, a cherché à combler ces lacunes et à reproduire le comportement sismique enregistré sur les barrages japonais par JDEC. EDF, avec la participation d'ISL, est en train de mettre cette méthode sous assurance qualité. Le manuel du logiciel, l'avis scientifique, le manuel de l'utilisateur et l'avis de validation sont en cours de rédaction. Cet article décrit comment la méthode est conçue et justifiée par son étalonnage en fonction des accélérogrammes mesurés sur les barrages japonais. Deux applications sont décrites.

1 INTRODUCTION

The Great Tohoku Earthquake of March 11, 2011 was the first earthquake to cause human casualties by the failure of a large dam. The failure of Fujinuma dam was initiated by successive

slides of the crest favored by the increase of pore pressure generated by the cycles of seismic shakes. The failed dam was a 19 m high dam for agricultural use, built with limited means at the end of the Second World War. This failure underlines the weakness of small and medium embankments dams built with limited means and shows the urgency to re-evaluate their resistance to earthquakes as a priority. This assessment requires dynamic analyses predicting pore pressure generation. Moreover, there are so many embankment dams that quick and easy methods can be very helpful. In conclusion, a global effective seismic assessment of embankment should firstly rely on simplified dynamic analyses able to simulate pore pressure generation.

2 LIMITS OF CURRENT SIMPLIFIED DYNAMIC ANALYSES

Simplified seismic analyses like Seed & Makdisi (1978), Ambrasey & Menu (1983), Tardieu (1983) and Hyne, Griffith & Franklin (1984) derived from Sarma (1967) are widely used today. In 2014, some of these methods were compared to the observed seismic performance of 2 zoned dams founded on rock, Aratozawa and Takami, shaken under strong motion earthquakes. These comparisons revealed gaps in these methods.

2.1 *Limit 1: 2D modelling cannot capture the 3D vibratory behavior*

The vibratory behavior of a dam is highly influenced by the 3D effects, while current methods are based on 2D assumptions. For instance, the fundamental frequencies, calculated by the transfer function between recorded accelerations in gallery and those recorded on crest of the Aratozawa dam during the 2008 Iwate-Miyagi Nairiku earthquake, are not consistent with 2D modal analysis. These two first observed modes are consistent with 3D modal analysis (Table 1) and not with 2D analytical formulae like those proposed by Makdisi and Seed (1978).

Table 1. Comparison between calculated and measured period factors of the 3 first modes.

Period factor	Formula Makdisi & Seed	Takami dam			Aratozawa dam	
		Modal 2D	Modal 3D	Measured	Modal 3D	Measured
A1	2.6	3.1	2.1	2.1	2.7	2.7
A2	1.1	1.9	1.3	1.25	1.9	1.75
A3	0.7	1.45	1.2	unclear	1.7	unclear

2.2 *Limit 2: The current methods do not compute of the pore pressure generation*

The current simplified methods do not predict the pore pressure generation and its impact on the performance of dams. This gap leads to:

- an overestimation of the dam stability, which could fail during very severe earthquake by pore pressure generation: it was the mode of failure of the Fujinuma dam.
- an overestimation of the dam rigidity: the pore pressure generation was low at Takami and high at Aratozawa (PGA=1g), consequently the measured modulus was correctly predicted at Takami and overestimated at Aratozawa dam.
- an overestimation of the accelerations under strong motion: max permanent displacements or acceleration were overestimated at Aratozawa dam in 2008 (Table 2).

Table 2. Calculated and measured max displacements at Aratozawa dam after the Iwate-Miyagi Nairiku earthquake in 2008.

Comparison	Crest acceleration (g)	Displacement along the most critical circle (cm)		
		Minimum	Medium	Maximum
Measured	0.5	0		4
Makdisi & Seed	1.18	10	26	44
Tardieu	0.54	0	2	7

2.3 Limit 3: The progressive reduction of strength is ignored in simplified methods

Due to the progression of shear bands and unrecoverable shear strains, the strength is reduced during strong shaking. The current methods do not take in account the progressive loss of strength with shear displacement and pore pressure rise.

2.4 Limit 4: The settlements are not estimated in most of simplified methods

Most of simplified methods are focused on shear permanent displacements, however settlements, larger than horizontal displacements, have been reported at Aratozawa and Ishibuchi dams after the Iwate-Miyagi Nairiku earthquake in 2008.

All these drawbacks of the current used simplified dynamic analyses justified the design of a new analysis that does not have the previously mentioned limits.

3 DESCRIPTION OF THE NEW SIMPLIFIED DYNAMIC ANALYSIS

3.1 Main hypotheses

In accordance with the former mentioned limits, the main assumptions of the new method are:

1. The dam is a nonlinear 3D elastic structure.
2. The pore pressure generation and volume strain are calculated with Byrne method (1991).
3. The rigidity and damping are updated at each step based on the average shear strain and the pore pressure generation.
4. The shear resistance depends on pore pressure generation and permanent displacement.
5. The accelerations at crest and in potential sliding mass scalping the crest are calculated in the time domain, by modal projection at the first fundamental modes.
6. The first fundamental modes came from a statistical analysis on 3D parametric survey.
7. The permanent sliding is calculated by double time integration as soon as the inertial force affecting a potential sliding mass is higher than the shear resistance.
8. The max permanent deformations include sliding displacement and soil compressibility.
9. The dam is founded on rock.
10. The accelerogram at the base of the dam is known.

3.2 Input data

The main input data are presented in Table 3.

Table 3. Main input data.

Type	Parameters	Definition	unit
Earthquake data	$a(t)$:	Accelerogram	m/s^2
Dam properties	G_0 :	Initial equivalent shear modulus of the dam	MPa
	ρ :	Wet mass unit of the soil	kg/m^3
	H :	Dam's height	m
	G/G_0 (γ):	Shear modulus reduction curve versus shear strain γ	-
	$\xi(\gamma)$:	Plastic damping curve versus shear strain γ	%
	ξ_r :	Added radiative damping	%
	A_i :	Period factor of mode $n^o i$	-
	FP_i :	Participation factor of mode $n^o i$ at crest	-
	$C1, C2$:	Byrne coefficients for pore pressure generation	-
	M :	Constrained rebound tangent modulus (Byrne)	MPa
Sliding mass data	y/H :	Relative depth of exit of potential sliding mass	-
	$FP_{mass\ i}$:	Participation factor of mode $n^o i$ for sliding mass	-
	k_{c0p}, k_{c0r} :	max and residual critical seismic coefficient at $L_u=0$	-
	k_{c1p}, k_{c1r} :	max and residual k_c values for liquefaction ratio $L_u=1$	-

3.3 Main equations

Fundamental period T_i of mode n^o is given by Equation & and notations of Table 3:

$$T_i = A_i H / [(G/\rho)^{0.5}] \quad (1)$$

Acceleration at crest is a_c depending on $OSC(T_i, \xi)$, the simple oscillator vibration at period T_i and damping ξ associated to the input accelerogram.

$$a_c = \Sigma FP_i \times OSC(T_i, \xi) \quad (2)$$

Volume strain increase $\Delta\varepsilon_v$ versus γ the average shear strain by cycle (Byrne, 1991):

$$\Delta\varepsilon_v = C1.\gamma.\exp(-C2.\varepsilon_v/\gamma) \quad (3)$$

Pore pressure generation Δu with M depending on the compressibility of soil and fluid:

$$\Delta u = M.\Delta\varepsilon_v \quad (4)$$

Shear modulus G update with L_u , the liquefaction ratio, which is equal to the generated pore pressure Δu divided by the initial effective stress σ'_0 :

$$G = G[\gamma](1 - \Delta u/\sigma'_0)^{0.5} \quad (5)$$

where $G[\gamma]$ is the dam shear modulus that depend on distortion γ and the initial shear modulus G_0 (Shear modulus and damping curves).

3.4 Main algorithm steps

The calculations are undergone in explicit numerical scheme. At each time step are calculated:

1. The first fundamental modes and frequencies (Eq. 1),
2. The participation of each mode combined to the acceleration at crest (Eq. 2),
3. The mean shear strain of the dam from displacement at crest,
4. The volume strain and pore pressure increase (Eqs. 3-4),
5. The shear modulus and the damping updating given the pore pressure increase and the mean shear strain at last cycle (Eq. 5),
6. The time step increment and return to step 1.

3.5 Sliding mass equilibrium

In the last step, the average acceleration of the potential sliding mass is compared to its critical value $g.c_c(L_u, d)$, decreasing linearly with the liquefaction ratio L_u and permanent displacement d increases. k_{c0p} , k_{c0r} and k_{c1p} , k_{c1r} are calculated with pseudo-static stability analysis.

The acceleration of the sliding mass is calculated in the same way that the acceleration at crest.

$$a_{mass} = \Sigma FP_{mass-i} \times OSC(T_i, \xi) \quad (6)$$

where $OSC(T_i, \xi)$ is the simple oscillator vibration at period T_i and damping ξ shaken by the input accelerogram.

The only difference with crest acceleration calculation stays in the values of the participation factors which can usually be taken from bibliography or from a finite element modal analysis. This paper discusses an additional method to estimate these factors. In the case of this study,

the same modal analysis gives participation factor for acceleration at crest and for the average acceleration of a sliding mass. It is done with a new post-processing of the same analysis.

3.6 *Permanent displacement assessment*

The total settlement is the sum of three components:

1. Vertical component of the sliding displacement: explained just before.
2. Settlement due to volume strain: calculated as the product of the average volume strain ε_v (equation 3) by the height of the dam.
3. Settlement due to deviatoric strain (spread out of the materials): this task is still in progress, no final approach has been implemented so far (no validation under cyclic tests).

3.7 *Output data*

The calculations described above lead to the time-history results of:

- acceleration at crest $a_c(t)$ and acceleration of the given potential sliding mass, $k_m(t)$
- liquefaction ratio $L_u(t)$,
- damping $\xi(t)$,
- shear modulus $G(t)$ and first fundamental frequencies $f_n(t)$,
- max permanent shear displacement $d_{\max}(t)$ and max settlement $s_{\max}(t)$.

4 DEVELOPMENTS IN 2021 AND 2022

4.1 *Fr-Jp Tool V2.2*

A tool has been developed in 2018 and upgraded progressively. The tool uses the Fr-Jp method with a user interface to make the calculation easier and more efficient than with an excel table. The final validation of the tool should finish in 2023.

4.2 *Easy assessment of 3D period factors and participation factors*

As described before, 3D effects are important, specially in the case of dams in narrow valleys. The period factors (A_i) and participation factors (FP_i) are the main coefficients that reflect the 3D behavior in the Fr-Jp method.

These coefficients can be calculated with a modal elastic analysis. But even if modal elastic analyses are quick and easy, they add one step to the algorithm and then add some complexity to the final user. In 2022, formulas based on 3D modal analysis outputs have been proposed to assess A_i and FP_i in function of dam geometry. The tool can now make all calculation steps with only geometric dam parameters. The user can still provide custom A_i and FP_i if he prefers to run modal analyzes.

4.2.1 *Methodology*

The seven parameters used to define a simplified geometry of the dam are shown in Figure 1.

Several modal analyses have been run with random values for these parameters. A data base with approximately 700 sets of parameters has been build. A digital twin has been then calibrated on this data set. After calibration, the digital twin gives for each set of parameters the best assessment of A_i , FP_i for the first 3 modes and 5 different sliding surfaces.

4.2.2 *Some results and limits*

The calibrations of first mode factors are very good, specially for the period factor. The Figure 2 shows the comparison between digital twin assessments and the target values for A_1 and FP_1 . Standard deviation is less than 1% of the mean value in these two cases.

The calibration for higher modes were more difficult. For instance, the Figure 3 gives the comparison between target values and digital twin assessment for mode 2. Standard deviation is 3.5% of the mean value for A_2 and 25% of the mean value for FP_2 .

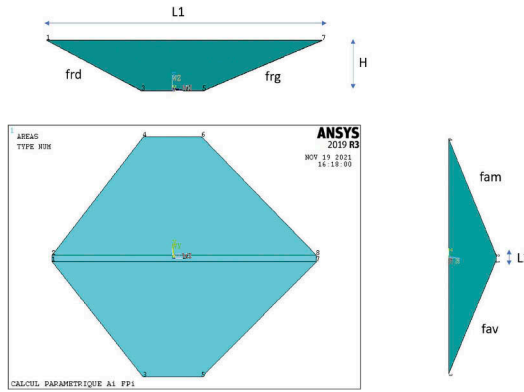


Figure 1. Simplified geometry for analytical assessment of A_i and FP_i .

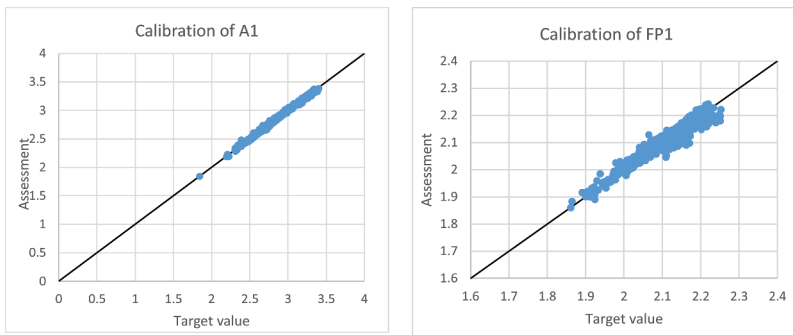


Figure 2. Calibration for $A1$ and $FP1$.

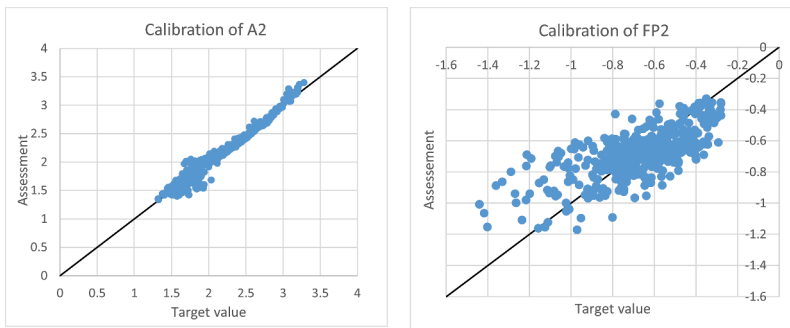


Figure 3. Calibration for $A2$ and $FP2$.

The explanation for these difficulties is that for higher modes, the modes 2, 3 and even higher are sometimes inverted and don't have the same physical pattern (Figure 4).

One possible improvement is to classify the modes by their physical pattern. This work can be done in next years.

Despite the deviation observed for modes 2 and 3, the final results of the Fr-Jp method with analytical formulas for A_i and FP_i are quite accurate because the first mode is by far the dominant mode. This will be shown for some records in the JDEC database.

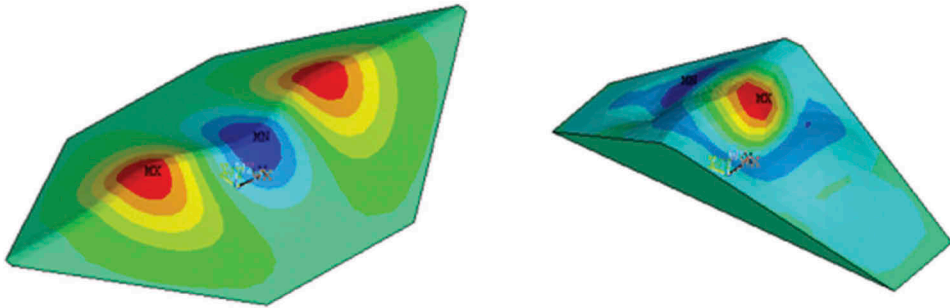


Figure 4. Example of deformations for the second mode.

4.2.3 Effect of the modulus gradient on participation factors

In the JDEC/JCOLD database, we can notice that the amplification of the accelerations between the bottom and the crest is very high in some cases (more than $\times 10$). With the Fr-Jp method we can demonstrate that participation factors for homogenous modulus dam are not high enough to explain these amplifications.

One explanation to these amplifications is the fact that material near the crest have a lower modulus than materials at the bottom and in the core. A comparison has been done between an homogenous modulus dam and a dam with modulus depending on total stress with chevron scheme. With a modal FE analysis, we can demonstrate that participation factors for first mode are approximately 25% higher for stress-dependent modulus dam than participation factors with homogenous modulus dam.

Figure 5 Illustrates the first mode deformation in the two cases.

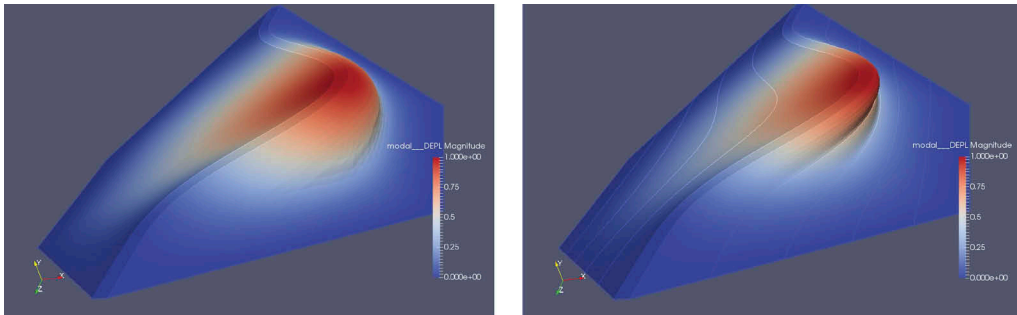


Figure 5. Impact of the modulus gradient to the first mode deformation.

We can see on Figure 6 that amplification at crest is higher in case of modulus depending of confining stress.

5 THE VALIDATION PROCESS

5.1 The required documents

The validation process for the new simplified dynamic analysis includes four documents:

1. a scientific notice
2. a computer notice
3. a user manual
4. a validation notice.

Dam	Mode n°1	Homogenous	Stress-depending	Ratio
ARATOZAWA	FP	2.15	2.68	1.24
INAMURA	FP	2.14	2.65	1.24
IWAYA	FP	2.14	2.71	1.27
KAMIOOSU	FP	2.14	2.66	1.24
KASSA	FP	2.15	2.68	1.25
MIHO	FP	2.15	2.67	1.24
NAGARA	FP	2.10	2.55	1.22
NARAMATA	FP	2.14	2.66	1.24
OOUCHI	FP	2.14	2.66	1.24
SCHISHIKASHUKU	FP	2.16	2.68	1.24
SHIMOYU	FP	2.16	2.67	1.23
TADAMI	FP	2.14	2.63	1.23
TAKAMI	FP	2.15	2.67	1.24
TAKASE	FP	2.18	2.68	1.23
TATARAGI	FP	2.15	2.65	1.23
TEDORIGAWA	FP	2.15	2.70	1.25
TOKACHI	FP	2.16	2.66	1.23
TOKUYAMA	FP	2.16	2.65	1.23
URUSHIZAWA	FP	2.16	2.67	1.24

Figure 6. Impact of the modulus gradient for FPI.

The user manual explains the definition and the choice of the parameters. The parameters were successfully calibrated firstly in 2015 on Aratozawa and Takami earthquakes and secondly on 28 acceleration records given by JCOLD in 2016.

5.2 The justification on JCOLD and JDEC records

The last tool using Fr-Jp method and digital twin assessment for 3 first modes is used.

5.2.1 Criteria of best fitting

The parameters of Anderson (2003), scored from 0 to 10, check the fitting of the computed accelerograms at crest to the observed ones. The parameters are (Figure 7):

C1: Arias Duration	<table border="1"> <thead> <tr> <th>Score</th> <th>Verbal value</th> </tr> </thead> <tbody> <tr> <td>8-10</td> <td>Excellent</td> </tr> <tr> <td>6-8</td> <td>Good</td> </tr> <tr> <td>4-6</td> <td>Fair</td> </tr> <tr> <td><4</td> <td>Poor</td> </tr> </tbody> </table>	Score	Verbal value	8-10	Excellent	6-8	Good	4-6	Fair	<4	Poor
Score		Verbal value									
8-10		Excellent									
6-8		Good									
4-6		Fair									
<4		Poor									
C2: Energy Duration											
C3: Arias Intensity											
C4: Energy Integral											
C5: Peak Acceleration											
C6: Peak Velocity											
C7: Peak Displacement											
C8: Response Spectra ($f < 10\text{Hz}$)											
C9: Fourier Spectra ($f < 10\text{Hz}$)											
C10: Cross Correlation											

Figure 7. Equivalence Score-Verbal value.

The final ranking is quantified by the average score of the ten parameters and qualified (Figure 8) by the verbal scale of Kristekova (2009).

5.2.2 Results of the comparison

The accelerograms at crest, calculated with the digital twin, are compared to the measured ones for 17 records in the JCOLD/JDEC database. As the material properties are unknown, they are determined with a loop.

- In the first step, the method is applied with initial assumed values of material characteristics: elastic shear modulus G_0 and radiative damping ξ .

- In the second step, these values are calibrated to improve the fitting.

The Figure 8 sums up the comparison between calculated and measured accelerograms.

The calibration is from excellent to good (Figures 8-11). It is of matter to notice that the worst comparisons correspond in general to earthquakes with main direction bank to bank or to aftershocks. In some cases, the geometry is also more complex than the simplified one considered in the digital twin.

Nom	PGA (m/s ²)	PCA (m/s ²)	Amplifica	C1	C2	C3	C4	C5	C6	C7	C8	C9	C10	Mean
Inamura1_mr	0.60	2.72	4.51	7.9	7.7	8.8	9.3	8.9	9.8	9.6	8.1	7.8	6.2	8.4
Kassa1_mr	0.22	1.22	5.55	7.8	7.4	10.0	10.0	10.0	10.0	10.0	8.8	7.0	6.0	8.7
Kassa2_mr	0.42	1.76	4.23	7.7	7.7	9.8	9.5	8.7	9.8	10.0	6.8	6.7	5.9	8.2
Kassa3_mr	0.63	2.02	3.21	6.9	7.3	9.9	9.9	8.6	9.9	9.7	6.3	6.7	4.0	7.9
Shichikashuku1_mr	0.35	1.17	3.34	8.6	8.3	9.4	9.7	10.0	9.5	10.0	5.4	7.4	6.2	8.4
Shichikashuku3_mr	0.57	2.89	5.05	8.7	7.9	9.5	10.0	8.0	9.6	9.8	7.3	7.4	5.9	8.4
Shimoyu1_mr	0.40	1.18	2.93	8.0	8.5	10.0	9.1	10.0	9.9	8.9	7.6	7.0	5.4	8.4
Tadami1_mr	0.94	2.13	2.25	5.6	7.1	7.4	9.5	6.5	9.1	9.9	5.7	7.7	3.7	7.2
Tadami2_mr	0.19	0.64	3.42	7.1	8.1	9.9	10.0	8.8	9.2	8.8	6.9	8.9	5.7	8.4
Tadami3_mr	0.60	1.57	2.63	7.6	7.1	9.7	10.0	9.7	9.9	10.0	6.4	8.5	4.4	8.3
Takami1_mr	0.56	3.25	5.80	8.1	7.7	5.9	10.0	8.9	10.0	9.7	5.1	5.7	6.5	7.8
Takami2_mr	0.20	2.47	12.22	8.4	8.2	7.6	9.8	7.2	9.4	9.8	6.2	5.8	7.2	8.0
Tataragi3_mr	0.23	1.28	5.67	8.1	7.8	8.9	9.8	9.8	10.0	9.9	7.0	8.0	5.3	8.5
Tataragi4_mr	0.13	0.97	7.53	7.7	7.4	9.9	9.3	10.0	9.8	9.8	8.8	8.5	4.1	8.5
Tokuyama1_mr	0.22	0.78	3.50	5.2	4.2	6.0	9.9	8.4	7.9	9.4	5.1	4.8	6.0	6.7
Aratozawa1_mr	0.28	1.05	3.73	8.84	9.05	9.83	9.77	9.87	9.99	9.95	8.37	9	7.8	9.25
Aratozawa2_mr	0.33	1.14	3.43	8.37	7.88	9.99	9.85	9.65	9.99	9.64	7.8	8.38	5.9	8.74

Figure 8. Score of the Fr-Jp tool for 17 records in the JDEC/JCOLD database.

Some detailed examples are given below for 3 records going from best score case (Aratozawa_1) to the worst one (Tokuyama_1).

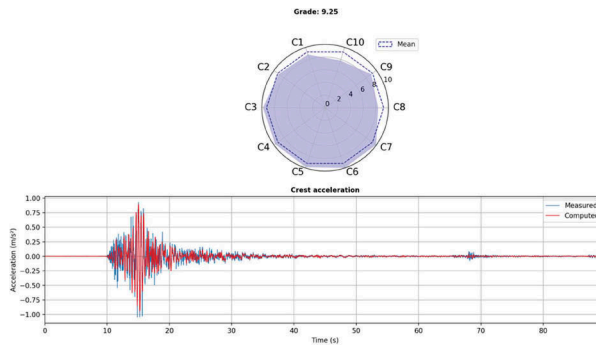


Figure 9. Comparison between recorded and calculated acceleration at crest for Aratozawa_1 record.

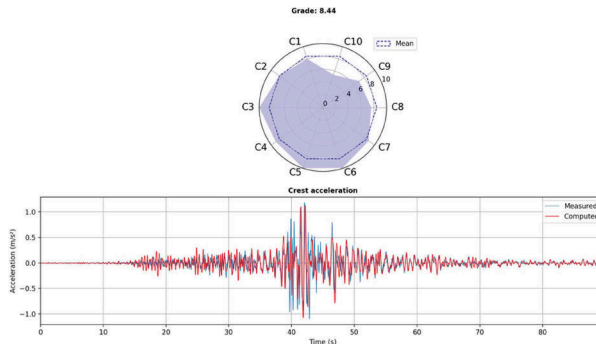


Figure 10. Comparison between recorded and calculated acceleration at crest for Shimoyu_1 record.

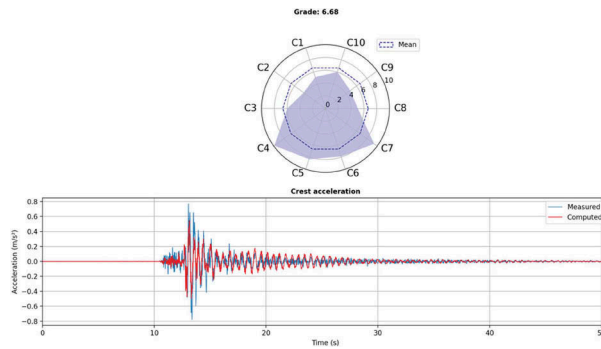


Figure 11. Comparison between recorded and calculated acceleration at crest for Tokuyama_1 record.

6 CONCLUSION AND PERSPECTIVES

The new simplified dynamic analysis has several advantages compared to the former ones: the implementation of damage coupled with pore pressure increase, the loss of strength with shear displacement, the 3D vibration modes and the assessment of max settlement. During the two last years, 2021-2022, the task focused on two objectives:

1. Finalizing the validation of the Fr-Jp tool,
2. Making the Fr-Jp tool easier to use, with only dam geometry, general material characteristics and one accelerogram as input parameters.

The main remaining perspectives that are under progress are:

- Providing a guide for the users to choose material properties and specially Byrne parameters for pressure increase,
- Improving the accuracy of the assessment of higher modes factors.

ACKNOWLEDGMENTS

We thank the Japanese Committee on Large Dam (JCOLD) and JDEC for sharing and making available to the profession the accelerogram records registered on Japanese large dams. We also thank them for the discussions and scientific exchanges on the behavior of large dams subjected to very strong motion earthquakes.

REFERENCES

- Ambraseys, N.N. & Menu, J.M. 1988. Earthquake-induced ground displacements. *Earthquake Engineering and Structural Dynamics* 16 (7), p. 985–1006.
- Bray, J.D. & Travasarou, T. 2007. Simplified procedure for estimating earthquake-induced deviatoric slope displacements. *Journal of Geotechnical and Geoenvironmental Engineering* 133 (4), p. 381–392.
- Hynes-Griffin, M.E. & Franklin, A.G. 1984. Rationalizing the seismic coefficient method. *Misc. Paper GL-84-13*. U.S. Army Waterway Experiment Station, Vicksburg, Miss.
- Makdisi, F.I. & Seed, H.B. 1978. Simplified procedure for estimating dam and embankment earthquake-induced deformations. *Journal of Geotechnical Engineering* 104 (7). p. 849–867.
- Sarma, S.K. 1967. Seismic stability of earth dams and embankments. *Geotechnique* 25. Vol.4. 1975. p. 743–761.
- Tardieu, B., Post G., Lino, M. 1981. Conception parasismique des barrages, *Génie parasismique Davidovici V.*, p.703–748.

Obturation solutions for dry works on underwater installations

M. Leon

Hydrokarst-SDEM, Grenoble, France

ABSTRACT: The obturation of a sluice, bottom outlet or water intake, with subaquatic means, is a way to perform the refurbishment of existing installations and equipment for dams, especially for dry inspections, gate maintenance and reparation/painting of the lining. The obturation avoids the drainage of the full reservoir and all the associated losses: floods management, hydroelectric production, water supply. This can be a solution also if the sluice has no functional maintenance gate or if the refurbishment includes the upstream equipment's (steel lining, trash rack, concreting). The design and construction of these obturators must consider the Civil Works environment (shape and condition), the lack of underwater visibility of the divers, the anchoring system, the sealing and all the logistic for the transportation, handling, erection, drilling and grouting. The efficiency of the watertightness and the transmission of the thrust loads on the existing Civil Works might require the addition of an embedded frame with grouting. Another issue to consider properly is the self-resistance of the sluice against external pressure, directly downstream the obturator. Even if the sluice has a steel liner, its embedding with the concrete structure or its thickness might not be sufficient to avoid a collapse after dewatering the sluice. In this case, stiffener rings or stabilization girders must be added downstream obturation.

RÉSUMÉ: L'obturation des pertuis de barrage par des moyens subaquatiques peut s'avérer nécessaire pour réaliser des travaux de maintenance à sec: inspection, réparation ou remplacement des vannes, travaux de peinture, soudure ou bétonnage. C'est le cas notamment en l'absence de vanne de maintenance fonctionnelle ou si des réparations doivent être menées en amont de celle-ci. Grâce à l'obturation, l'exploitant du barrage peut maintenir la retenue amont à un niveau normal pour éviter les pertes de stockage d'eau, de production hydroélectrique et assurer la continuité de la gestion des crues. La conception et la fabrication de l'obturateur doivent tenir compte d'un ensemble de paramètres dont notamment: la forme et l'état de l'ouvrage béton, le manque de visibilité des scaphandriers pour opérer, les choix techniques pour l'ancrage et l'étanchéité et tous les moyens logistiques pour le transport sur site, la manutention, le montage, le forage des ancrages et si nécessaire, le bétonnage. Pour assurer une bonne étanchéité de l'ensemble d'obturation et transmettre correctement les descentes de charges au génie civil, il peut s'avérer nécessaire d'installer un cadre fixe scellé avec du mortier. Un point à ne pas négliger est la vérification l'auto-résistance du pertuis à la pression extérieure. Même en présence d'un blindage, la stabilité de celui-ci peut être insuffisante car non prévue pour ce cas de charges déséquilibré après la vidange du pertuis. Dans ce cas, des étais ou des renforts devront être installés en aval de l'obturateur.

1 TYPICAL IMPLANTATIONS AND INTEREST

The obturators are usually installed by the divers on the upstream face of the dam wall, over the intake. This implantation is the more convenient for the handling from the surface with external means (crane, winch) and it is safer for the divers to install and manipulate the tools. The hydraulic thrust is directly transmitted to the wall. The main inconvenience is that a great dimension might be necessary due to the bell mouth-shape enlargement usually observed at the intake. The sedimentation in that area can be an issue as well for anchoring and sealing the lower part of the obturator.



Figure 1. Left: Removal of the 4 m-obturator on Idriss I dam (Morocco).

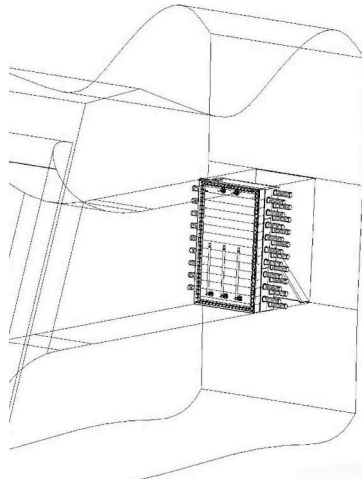


Figure 2. Right: Obturator installed in the bottom outlet sluice on Al Massira dam (Morocco).

This upstream implantation has been used to create a new water intake on Idriss I dam (see Figure 1): the obturator is installed on the plain concrete surface before a massive 2 m diameter boring is performed from downstream to implant a new steel pipe through the dam wall.

An implantation of the obturator inside the sluice can be chosen to reduce its size, to avoid upstream sedimentation or to prevent the upstream part of the sluice from collapsing if it is not self-resistant against external pressure. An example is shown (Figure 2) on the Al Massira dam in Morocco. The inconvenience comes from bringing the obturation elements inside the sluice without the help of a crane or a winch from the surface. In this case, the design of the obturator is systematically in several structural elements that the divers can handle into the sluice. To help the handling, the elements can be designed as waterproof boxes, with ballast system if needed, or attached to air lift bags or rigid buoys, the apparent weight will be lighter or even null.

Obturations can be installed underwater by the divers in any elevation on the dam wall, from the free surface and until 100 m-depth and even more. Once obturated and dewatered, the sluice is accessible for dry works such as welding and painting operations, linear inspection of the sluice with thickness measurement and non-destructive testing, examination of water inflows through concrete, gate refurbishment, etc. The level variations of the reservoir will have no impact on the dry work zone, so the operations of the dam installations can be maintained (spillage, water supply, hydroelectric production) as long as the obturation stays in place.

During the obturation installation and removal, for the safety of the divers, a vigilance on the reservoir level is necessary and inlet flows may be reduced or stopped temporarily in adjacent sluices.

2 TYPES OF OBTURATION

Distinctive designs of obturators can be proposed, depending on the overall dimensions, resistance to pressure, number of elements, areas of the Civil Works that can support the loading.

At first, a classical bulkhead with a reinforced welded steel structure can be proposed, especially for rectangular obturations. It can be simplified with a stoplog design (horizontal steel beams placed on top of each other) to save manufacturing time. These obturators can be designed in several elements (see Figure 5) to match reasonable lifting and transportation capacities. This design is suitable to transfer the loads on the right and left sides of the concrete superstructure. The sill and lintel are not loaded but will complete the sealing perimeter.

An alternative solution to the stoplog with horizontal beams is to use vertical beams instead. In this case, we can use the term of needles. It allows to load the lintel and sill part of the

concrete superstructure instead of the sides. It can be useful also for handling the elements in a vertical shaft or through a small trapdoor above the intake. An example of vertical needles is shown on Figure 3 with the installation of 11 needles per sluice of 40 m-high on Kariba dam spillway, each needle divided in two half and assembled on site with a 25 m-high gantry specially designed. Figure 8 shows another example on the Bou Heurtma dam bottom outlet with a 5 m-high by 3.5 m-width obturation composed of 11 needles.

For low depth obturation in a canal, we can use a sheet pile wall fitted in the sill and sustained by one or several horizontal girders. An example is shown in Figure 4, with a 14 m-high obturation on Laroussia dam (Tunisia).

For circular obturations, it is possible to make lighter design to optimize the subaquatic assembly and handling. The steel structure is based on a semi-elliptical head (or flanged and dished head) commonly seen on pressure vessels (see Figures 1 and 13). If the design needs to divide the obturator in multiple elements, a flat head will be preferred to keep a straight jointing between elements.

Special obturations can be proposed like horizontal tunnel-shape (see Figure 6) or vertical shaft-shape, especially for local refurbishment like gate grooves or sill.

Other designs (not shown here) can be proposed like an hemispherical obturator which can fit in a circular cone-shape convergent or circular bell mouth.



Figure 3. 40 m-high needles installed on two spillway sluices on Kariba dam (Zambia-Zimbabwe).

3 PRELIMINARY INSPECTIONS AND PREPARATION OF THE AREA

To prepare the design of the obturation, a preliminary inspection of the intake is necessary to check the general condition of the concrete and the presence of sedimentation and debris. It will confirm the main dimensions of the intake and compare them to original drawings when given.

The inspection can be completed by divers and/or with a ROV. When possible, an acoustic 3D-scan can be helpful, specially when the underwater visibility is poor. This will help for the design of the obturator, confirm the 3D-dimensions, and save time for the divers from making precise measurements.

On Figure 7, we can see the overall shape of the bottom outlet intake on Bou Heurtma dam in Tunisia superposed with the point cloud issued from the underwater 3D-scanning with the ROV acoustic camera. Several differences in the intake shape can be found and the sedimentation on the sill can be measured. The final design of the obturator can be adapted to the real dimensions of the intake and avoid size adaptation of the obturation elements on site.

Before the intervention for obturation, preliminary works can be done by the divers such as removal of sediments and debris in front of the intake.

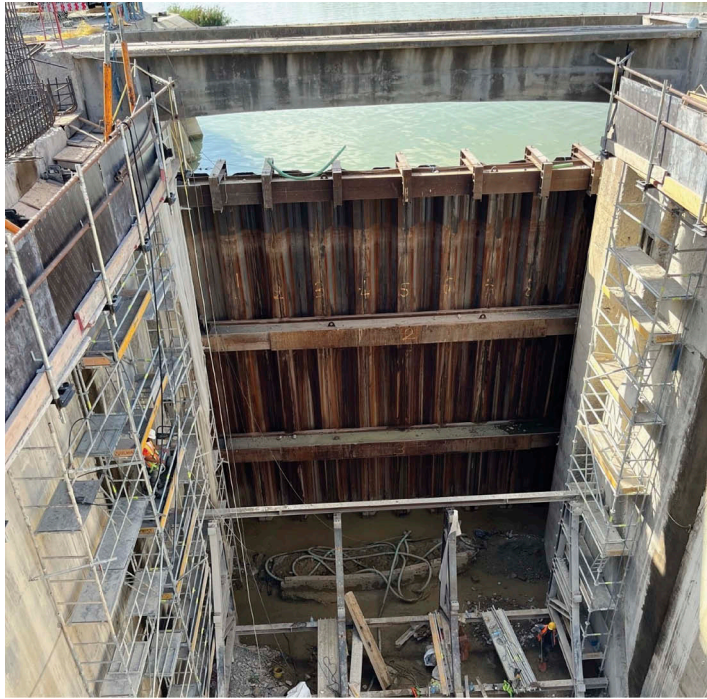


Figure 4. Sheet pile wall on Laroussia dam (Tunisia) in the 14 m-high by 12 m-width spillway sluice.

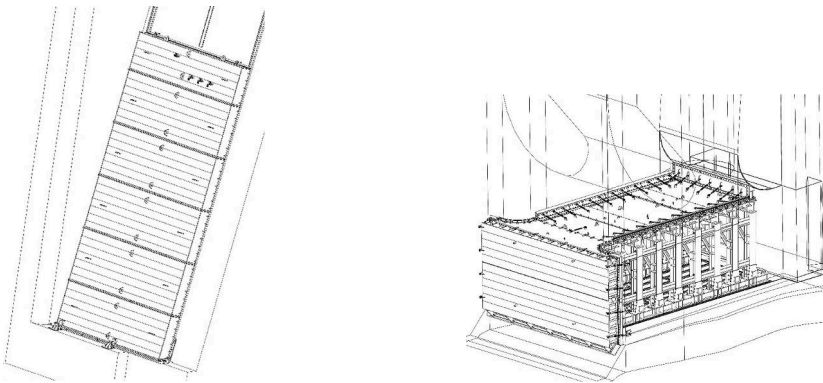


Figure 5. Left: Obturation with a stoplog of 6 elements on Nangbeto dam (Togo). Figure 6. Right: Tunnel-shaped obturation study.

4 ANCHORAGE AND SEALING SOLUTIONS

Upstream obturations must fit on the concrete surface and, if the general condition of the concrete is poor or if the shape to fit is complex, an embedded frame might be necessary. The frame will help also to spread the load on Civil Works. The frame is fixed on the concrete superstructure with chemical anchoring using a drilling or coring machine and a grouting is made between the frame and existing concrete to ensure watertightness.

Upstream obturations do not need heavy anchoring as the hydrostatic thrust is directly transmitted to the concrete surface. Still, the contact pressure on concrete should be checked. For inside-sluice obturations, if a convergent surface is not available, the side anchoring of the obturator might be heavy as it must withstand the thrust sideways in shearing force. Figure 9

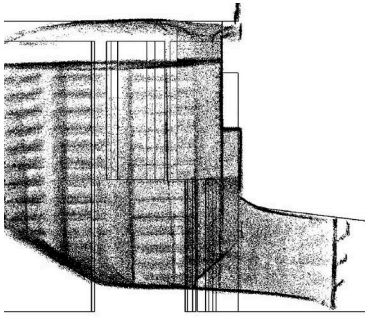


Figure 7. Left: Theoretical shape of the intake superposed with 3D- acoustic scanning (Bou Heurtma).

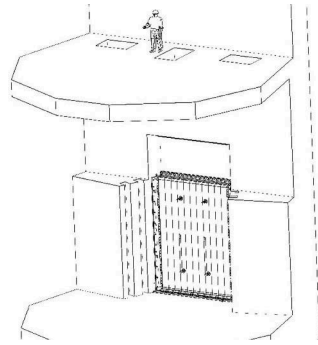


Figure 8. Right: Design of the obturator with vertical needles - Bou Heurtma dam (Tunisia).

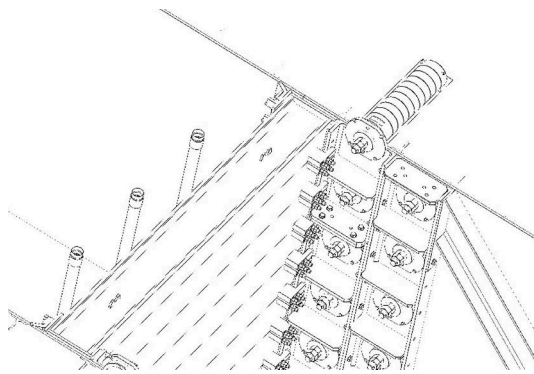


Figure 9. Horizontal cut with anchoring shafts implanted through the steel lining on Al Massira dam.

shows a detail of the Al Massira bottom outlet obturation, with multiple shearing shaft sealed in the concrete through the existing steel lining.

The sealing of the obturation will be adapted depending on the use of an embedded frame or not. For a direct supporting on concrete, the seal will be chosen with large dimensions, like L or D-section rubber seals, to tolerate the rough concrete surface and gain in sealing compression and efficiency. With the support of a steel embedded frame, the sealing can be more compact, with flat or P-section rubber seals. The assembly of both embedded frame and obturator with seals can be tested at the workshop in a blank assembly.

In the case of multi-elements obturators, like stoplogs stacking or needles, the sealing can be done with a rubber sheeting on the full surface. If needed, the sealing will be completed by the divers on site with a malleable resin.

5 DIVING AND NAUTICAL EQUIPMENTS

The diver team needs special equipment's on site like pontoons, life support system, winches for load handling and pontoon translation, generator for pneumatic or hydraulic tools.

The technology of diving is adapted to the configuration of each obturation, which can take one day or several weeks to install depending on the complexity and depth of the underwater works. An economical analysis should be done to choose between the 3 types of diving:

- Surface supplied diving
- Wet bell diving (Figure 10)
- Bell diving, in saturation (Figure 11)



Figure 10. Pontoon fully equipped for wet bell diving.



Figure 11. Pontoon equipped for bell diving in saturation.

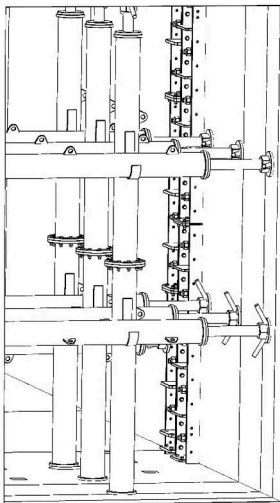


Figure 12. Left: Stabilization girders for rectangular lining sluice on Al Massira bottom outlet.



Figure 13. Right: Truck transporting the obturator on a special frame towards Hongrin dam (Switzerland).

6 SPECIAL ACCESSORIES FOR OBTURATIONS

The obturator must be supplied with accessories such as lifting lugs, centering pins and, to help the divers with low visibility underwater, we provide drilling templates. A blank assembly in workshop is usually necessary before the site assembly.

To run properly the dewatering and rewatering, the obturator is equipped with air vents at the top, and bypass valves at the foot. Air admission is necessary for the dewatering of the sluice, so a flexible hose is connected to the air vent until the free surface of the reservoir. The inlet valves are opened by the diver for rewatering. The inlet pipe is extended upstream above the valve to prevent the diver from being caught by the suction when he opens the valve. One or several two-inches manual valves are generally used.

Downstream of the obturator, after dewatering, the inside pressure in the sluice will no longer equilibrate the external pressure. This part of the sluice, between the trash rack and the maintenance gate, is generally not self-resistant to external pressure in the original design of the dam. The stability of the concrete shaft, with steel lining or not, must be checked. If necessary, the divers will install stabilization girders against the steel lining to prevent it from collapsing after dewatering. Generally, we use tubular beams with a M80 screw to fit correctly in the shaft. The tubes can be divided in several parts with bolted flanges to limit the unit weight and size. To reduce the apparent weight with buoyancy, the tubes can be sealed to keep air inside, or filled with expansive foam. Stabilization girders (4 m-high by 2.5 m-width), used on the bottom outlet steel lining on Al Massira dam, are shown on Figure 12.

Special carrying frame (Figure 13) and a site gantry crane (Figure 14) may be needed also.

7 CONCLUSION

Obturation solutions can be found in most of cases. A technical and economic analysis should be done precisely to confirm the feasibility and several scenarios studied to select the best one.

A preliminary site inspection with divers and/or ROV is necessary before any final design is frozen.

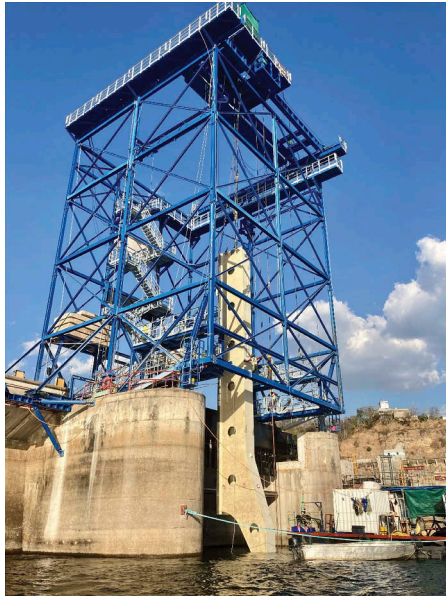


Figure 14. Gantry crane handling a half-needle on Kariba dam spillway (Zambia-Zimbabwe).

The decommissioning of dams in Italy: The state of the art

P. Manni

ITCOLD Decommissioning and downgrade of dams' observatory

G. Mazzà

Vice Chairman of ITCOLD – Italian National Committee on Large Dams

ABSTRACT: Large Dams under state jurisdiction in Italy are 530. The mean age of the Italian dams is approximately 65 years. About 60% of the national dams are predominantly for hydroelectric use, 26% for irrigation and 12% for drinking water; the remaining are dedicated to different uses. The main aspects covered in the paper refers to (i) features of the decommissioned dams; (ii) most frequent reasons that determine the decommissioning; (iii) rules and procedures governing the approval of decommissioning projects; (iv) main decommissioning solutions over the past few years.

The publisher will reduce the camera-ready copy to 75%.

RÉSUMÉ: Les grands barrages sous juridiction étatique en Italie sont au nombre de 530. L'âge moyen des barrages italiens est d'environ 65 ans. Environ 60 % des barrages nationaux sont principalement à usage hydroélectrique, 26 % pour l'irrigation et 12 % pour l'eau potable; les autres sont dédiés à différents usages. Les principaux aspects couverts dans le document concernent: (i) les caractéristiques des barrages déclassés; (ii) les raisons les plus fréquentes qui déterminent le déclassement; (iii) les règles et procédures régissant l'approbation des projets de déclassement; (iv) les principales solutions de déclassement au cours des dernières années.

1 INTRODUCTION

Large Dams under state jurisdiction in Italy are 530.

In 2021 ITCOLD created the Observatory “*Dismissione e Declassamento delle Dighe*” to take stock of situation on the progress about decommissioning and downgrading of large dams in Italy.

The decommissioning of dams was already analyzed by an ITCOLD working Group, which in 2008 issued the Bulletin “*Decommissioning delle Dighe*” (ICOLD, 2018; ITCOLD, 2008).

The Observatory concluded the survey in December 2022 with the issue of a specific Bulletin (ITCOLD, 2022) and the organization of a specific workshop (ITCOLD Workshop, 2022). The main information of the Bulletin about the decommissioning is set out below.

2 LARGE DAMS IN ITALY

Large dams under state jurisdiction are those characterized by height greater than 15 meters and/or total volume greater than 1.000.000 cubic meters. Concrete and masonry dams prevail in the Alps and in the northern-central Apennines; in the southern Regions earth dams prevail, the latter being 169 (over 30% of the overall number).

The mean age of the Italian dams is approximately 65 years, with higher mean values (approximately 75 years) in the Regions of the Alps and in the northern-central Apennines, while in southern Regions the mean age ranges around 50 years.

About 60% of the national dams are predominantly for hydroelectric use, 26% for irrigation and 12% for drinking water; the remaining is dedicated to different uses.

3 FEATURES OF THE DECOMMISSIONED DAMS

The main recent cases of decommissioned dams in Italy are 32; 75% of these dams were built before 1950, 44% of which before 1925; the remaining 25% was built after 1950 (Figure 1). The prevalent localizations of decommissioned dams are in the occidental Alps and in the northern-central Apennines (Figure 2).

The 44% of the decommissioned dams are ordinary gravity dams, predominantly traditional masonry dams; 31% are embankment dams, predominantly homogenous earth dams (Figure 3). These two types of dams are the oldest of the last century.

Decommissioned dams have generally a modest height (66% height between 16-29 meters) and also a limited volume of the reservoir (66% less than 500.000 cubic meters) (Figures 4 and 5). Five dams are regional barrages with height not greater than 15 meters.

The prevalent use of these dams was hydroelectric (53%); irrigation (22%) and then for other usage (Figure 6).

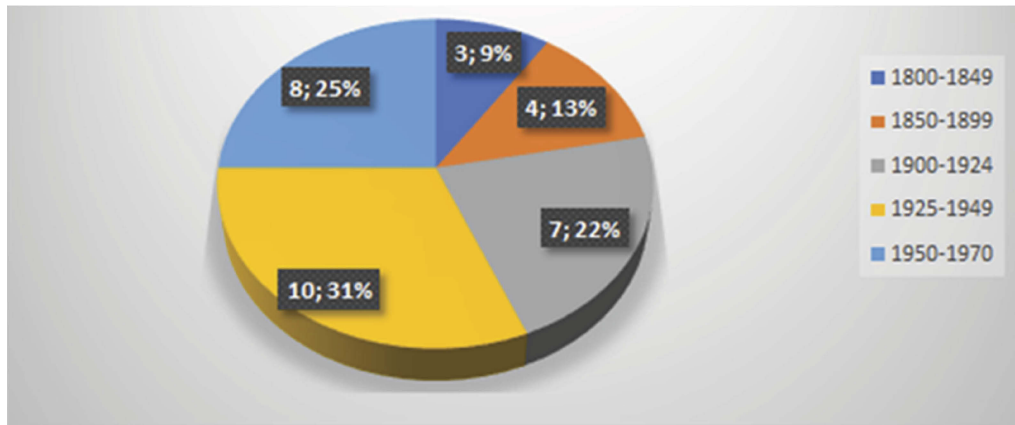


Figure 1. Main recent cases of decommissioned dams in Italy.

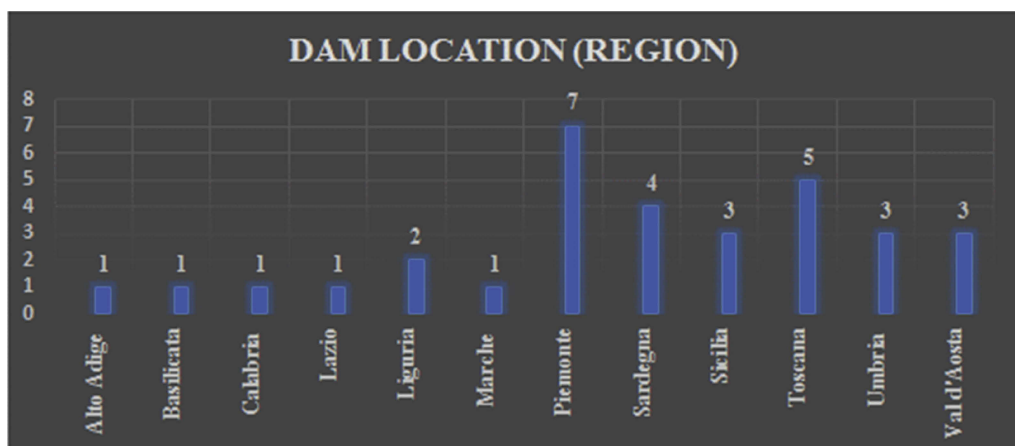


Figure 2. Prevalent localizations of Italian decommissioned dams.

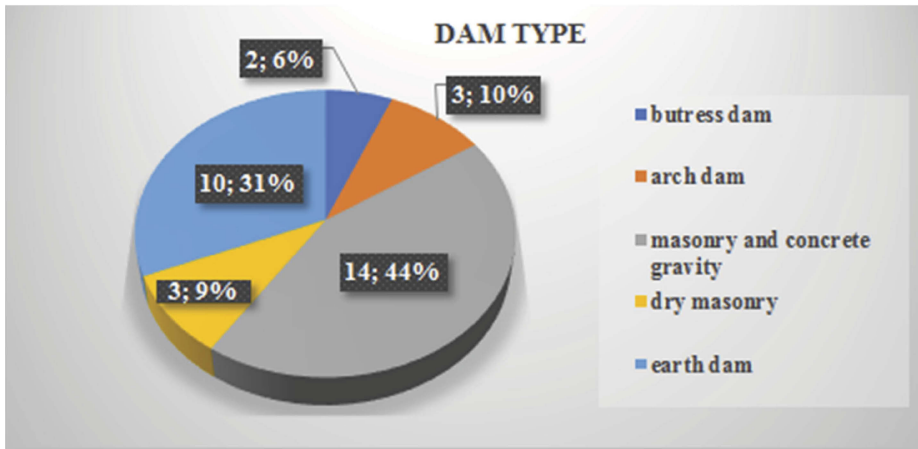


Figure 3. Number and percentage of decommissioned dam according their type.

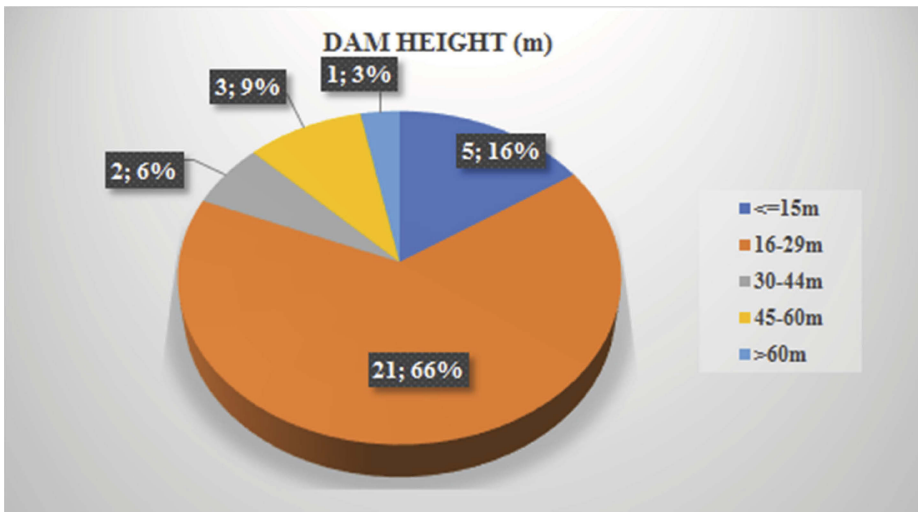


Figure 4. Dam height of decommissioned dams.

4 MOST FREQUENT REASONS THAT DETERMINE THE CHOICE OF DECOMMISSIONING

The choice between decommissioning or rehabilitation of a dam is based on the results of cost-benefit analysis in which several factors are taken into account. If the costs to improve safety and efficiency of the dam are not adequately offset against the benefits associated with continuing to operate the reservoir, the choice of the decommissioning is consequent.

Some of the main reasons which can involve dam decommissioning are indicated below; they are of different nature:

Technical

- Advanced degradation of the structure: decay of material properties due to ageing of the structure.
- Structural or hydraulic insufficiencies with respect to the current acceptance criteria defined by the technical regulations.

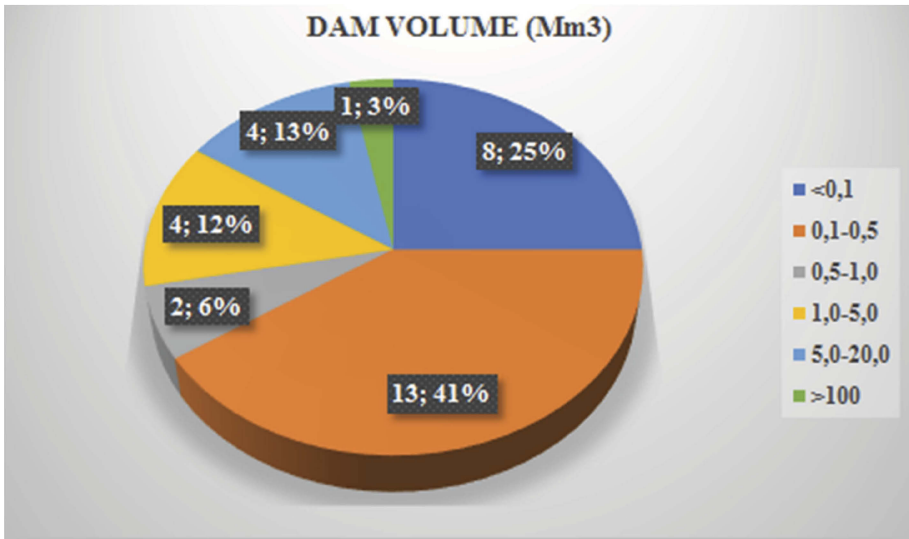


Figure 5. Dam volumes of decommissioned dams.

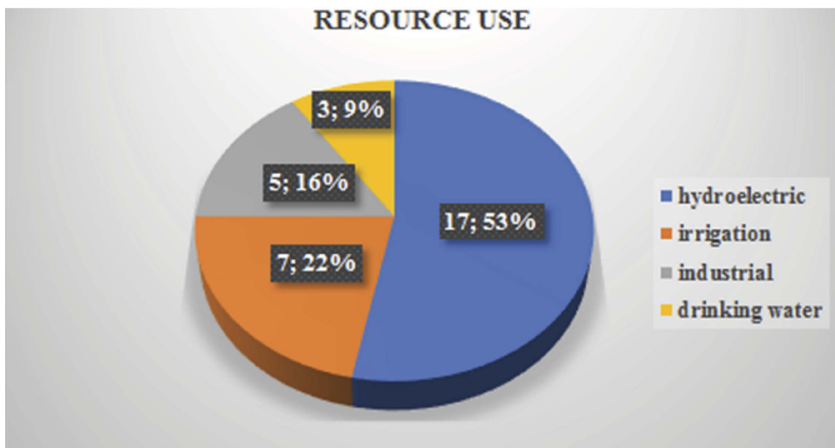


Figure 6. Prevalent use of decommissioned dams.

Economic

- Onerous investments to continue operating safely the dam against insufficient economic return.
- Reduced interest and convenience by the owner to use the water resource for different reasons, such as: need for plant modernization, termination of the production activity, strong silting, operation limitations imposed by the authorities, etc.

Socio-political

- Environmental issues requiring a different management of the river.
- Lack of public interest to continue the exploitation of the water resource.
- Alternative more responsive to new needs, including new retaining works.

5 RULES AND PROCEDURES GOVERNING THE APPROVAL OF THE DECOMMISSIONING PROJECTS

National technical rules, approved by the national Government (Infrastructure and Transport Ministry, 2014), define decommissioning and its objective:

- Decommissioning is the final phase of the life cycle of the infrastructure no longer adequate or functional for the activities for which it was created.
- Decommissioning has the objective of permanently depriving the barrier of its hydraulic retention function to guarantee the safety of the site and of downstream territories.
- Any residual works have to allow safe outflow without backwater. The Hydraulic Authority must indicate the return time of the project flood.

If the decommissioning concerns a large dam, the Ministry of Infrastructures and Transports provides binding technical opinion on the project and the Hydraulic Authority provides the opinion of competence and the approval of the project. At the end of the decommissioning works, the safety supervision of any residual hydraulic works is transferred to the regional Authority.

In Italy, the bottom outlet always open does not correspond to decommissioning. It can rather be an intermediate stage (out of temporary operation), pending the final decision. In this intermediate stage, the owner of the dam must comply with all the provision contained in a specific document (F.C.E.M. “*Foglio condizioni esercizio e manutenzione*” is the contract between the supervisory Authority and the Dam Owner regarding the obligations for the safe management of the dam).

6 THE MOST WIDESPREAD SOLUTIONS REALIZED OVER THE PAST FEW YEARS

Most widespread solution of dam decommissioning, realized in the past few years in Italy consists in opening of breaches or galleries in the dam body with consequent removal of the retention function. For the creation of breaches and openings, cutting with diamond wire is generally used.

The size of the breaches or gates must allow the discharge of the flood flow without significant backwaters. The Hydraulic Authority decides the reference flood flow which must guarantee the good fluvial regime also in extreme flood conditions.

The necessary complementary hydraulic works are carried out to facilitate the outflow; in particular, works of dissipation and restitution of the transiting flows are used.

This solution has been adopted in the last years in Italy in 14 cases (45% of the total decommissioned dams); it has been applied predominantly to masonry and concrete dams but also to earth dams.

For example, in Figure 7 the breach in the small Alpone dam located in the Piemonte Region and also the water flow return channel is shown (ITCOLD, 2022).

Figure 8 Shows the openings performed in the multiple arches dam of Santa Chiara d’Ula located in the Sardinia Region during the emptying of the Omodeo reservoir and the simultaneous filling of the Cantoniera dam on the Tirso river (ITCOLD, 2008 and 2022).

Figure 9 shows the opening performed at the bottom of the flat slab of the Combamala buttress dam in Piemonte Region (ITCOLD, 2022). Later, in 2020-21, conservative maintenance works on the residual structure, deprived of the retention function, were carried out.

Another widespread solution of intervention is the partial demolition of the barrage with consequent cancellation of the retention function and conversion of the dam into a hydraulic work designed to guarantee the flood flow without significant backwaters.

This solution, adopted in 8 cases (26% of the total dams), has been applied predominantly to masonry and concrete dams.

For example, in Figure 10 the final configuration of Rio Salita dam (Tuscany Region) is shown; the dam has been partially demolished and the residual structure transformed in a hydraulic work, i. e., a regulation threshold (ITCOLD, 2022).



Figure 7a. Alpone small dam decommissioning



Figure 7b. Breach in Alpone dam – work in progress in 2010 (left). Return channel downstream the decommissioned Alpone dam (right).



Figure 8. Santa Chiara d'Ula, decommissioned dam in 2002-2003.



Figure 9. Combamala dam: opening at the bottom of the dam in 1997 (left). Particular of the opening in the structure (right).

Moreover, there is another drastic solution, namely the complete demolition of the dam with the implementation of a hydraulic and nature restoration of the site “*ante operam*”; in all the cases examined so far, this solution was applied only for two dams of limited size as the disposal of the demolition materials constitutes a rather major difficulty.

Figure 11 shows the Corongiu I dam, located in Sardinia and built in 1866, before the complete demolition in 1969 (ITCOLD, 2022).

Another case of demolition concerns the earth dam of San Felice di Giano in Umbria (Figure 12); the decommissioning works, currently in progress, provide for the reuse of the earth material obtained from the demolition for the reshaping of the riverbed and banks of the watercourse (ITCOLD, 2022 and ITCOLD workshop, 2022).



Figure 10. Rio Salita dam after decommissioning (2009).



Figure 11. Corongiu I dam before the complete demolition which occurred in 1969.

Last but not the least, the solution was adopted to preserve the integrity of the barrier by depriving its retention function. This option generally includes structures of great architectural or historical value that are considered important to keep track of.

This is the case of Figoi and Galano dams in Liguria Region (ITCOLD, 2022; Pittalunga M., Temporelli G., 2010). At first, the complete demolition of these works was considered, but the final decision was different. It was decided to ensure the hydraulic safety of the two dams and the small work downstream of Galano dam (Figure 13) with the construction of open a breach and a gallery and to maintain the original structures as evidence of their industrial archeological value.

This last option has been undertaken in other cases in Italy.



Figure 12. San Felice di Giano dam: the dam seen from upstream (up-left); reshaping of the riverbed and banks of the watercourse (up-right); the decommissioning works in progress (down).

The current situation about the implementation of the interventions is as follows:

- 24 interventions have been completed, out of a total of 32 (among them, 23 cases of decommissioning and 1 case of rehabilitation),
- 2 interventions are in progress,
- 3 interventions are in the design stage or in the process of being approved by the Authorities, and
- 3 large dams have been made safe and a possible rehabilitation or definitive decommissioning is being studied.

7 SOME CONSIDERATIONS ON THE MOST RECENT INITIATIVES OF THE NATIONAL AUTHORITY TO ENCOURAGE THE REHABILITATION OF DAMS

Almost half (47%) of the decommissioned dams had no owner, as they served disused production activities. In the last 15 years, the safety and/or decommissioning of these dams were guaranteed thanks to public resources and special laws. One of these 15 dams, La Spina earth dam located in Piemonte, has been rehabilitated with hydraulic and structural works; the works were achieved in 2015. Currently the Municipality manages the dam that is used for irrigation (ITCOLD, 2022).

In the last more recent years, significant European and National public funds have been allocated to support investments in the water infrastructures sector (aqueducts, water networks, reservoirs, etc.) and in the hydraulic infrastructures sector (intake and outlet works, dams, etc.).

In particular, the Government has given a significant boost to extraordinary maintenance to increase the safety of the dams with the aim of enhancing the water resource.



Figure 13. The gallery (left) and breach (right) opened respectively in the main and small Galano dams in 2019.

The line “Protection of the Territory and Water Resources” of the “National Recovery and Resilience Plan” (P.N.R.R.) includes 124 interventions for primary water infrastructures, 26 of which concern reservoirs for the supply of drinking water.

Thanks to the “Development and Cohesion Fund” FSC 2014-2020, more than 100 (124) interventions have been undertaken to make existing dams safe, including the completion of the construction of 3 large dams.

In many cases, this has made it possible to avoid the decommissioning of the dams, in line with the transition goals of boosting renewable sources, of which hydropower is the most important and decisive in Italy (40% of the renewable energies production).

The rehabilitation of the dams makes it possible to cope with the increasingly frequent period of drought.

Downgrading is one of the possibilities for rehabilitation.

The downgrading intervention, as defined by the National Technical Regulations for Dams (Infrastructure and Transport Ministry, 2014) - approved by the national Government in 2014 - consists in transforming a dam, under state or regional competence as regards safety supervision, into a work of lower height and/or lower volume of the reservoir. After the downgrading, there is the transfer of competences to another territorial administration.

This solution entails the obligation to carry out improvement or adjustment interventions to achieve the safety levels required by current regulations. In many cases the main purpose of the works is the improvement of hydraulic safety or/and the structural safety of the dam.

On the basis of the cases (18 dams) examined by the ITCOLD Observatory (ITCOLD, 2022) at national level, the downgrading:

- makes it possible the safe operation of the reservoir with lower operating costs (for example: surveillance costs, generally non continuous for small dams);
- responds to needs that are often different from those of the past (for example: different uses of the water resource);
- is often managed by owners (either public or private) other than the previous ones.

REFERENCES

- ICOLD 2018. *Recomandations de la CIGB sur le démantèlement des barrages. ICOLD Dams Decommissioning Guidelines. Bulletin 160.*
- ITCOLD 2008 *Decommissioning delle dighe. Bulletin of the national working Group coordinated by Guido Mazzà.*
- ITCOLD 2022 *Osservatorio Dismissione e Declassamento Dighe. Final Report of the Observatory coordinated by Paola Manni.*
- ITCOLD 2022 *Osservatorio Dismissione e Declassamento Dighe. Seminar proceedings. Published on the ITCOLD website. Sala Convegni ANCE, 25.11.2022, Rome.*
- Infrastructure and Transport Ministry 2014. *Norme tecniche per la progettazione e costruzione degli sbarramenti di ritenuta (dighe e traverse). Decreto 26 giugno 2014.*
- Pittalunga, M. & Temporelli, G. 2010. *Le dighe e i laghi scomparsi di Genova – Borzoli. IA Ingegneria ambientale (vol. XXXIX n.12 dicembre 2010).*

Rehabilitation of the Pàvana Dam in Tuscany (IT) Advantages from the use of building information modelling in the design of a complex hydraulic project

F. Maugliani, A. Piazza, D. Longo, G. Raimondi & R. Sanfilippo
Lombardi Engineering Ltd., Switzerland

A. Parisi
Enel Green Power Italia S.r.l., Italy

ABSTRACT: Located in Italy, at the border between the two municipalities of Castel di Casio (BO) and Sambuca Pistoiese (PT), the buttress dam of Pàvana is a work of historical and architectural value, serving the Suviana hydroelectric cascade.

The dam, built in the 1920s, is managed by Enel Green Power Italia S.r.l., the major Italian energy production company.

The rehabilitation works of the hundred-year-old dam are required due to an alkali-aggregate reaction (AAR) mainly affecting the central portion of the structure.

The rehabilitation project foresees the upgrade of the central dam portion from a buttress dam to a gravity dam, by means of the demolition of the upper section of the three arches and the two buttresses of the central dam body, and the concreting of the volumes between the existing buttresses (including the demolished buttresses themselves). The project is completed by the construction of a new bottom outlet, in order to overcome the actual limits in operation due to sedimentation.

For the detailed design of this complex structural modification, the Building Information Modelling (BIM) method was used, according to a proposal by the designer, well accepted and confirmed by the owner's technicians: a challenging and ambitious activity that allowed for collaborative and efficient work between the various actors involved thanks to its digital sharing tools and the use of a Common Data Environment for the document management, 3D visualization of the various issues, clash detection, and automatic information management.

The model of the existing dam was reconstructed based on the laser scanning survey of the dam and of the previous definitive design made by 2D drawings developed by the dam owner and from a point cloud survey.

The modelling included the complex demolition and construction phases of the individual dam components and a complete overview of the construction sequences (BIM4D).

The BIM model was used not only for the production of the 2D drawings and of the bill of quantities, but also as a basis for the structural and geotechnical FE analysis as well as the three-dimensional geological model, where the results of the geological investigations were integrated.

RÉSUMÉ: Situé en Italie dans la municipalité de Pàvana (PT), le barrage à contreforts du même nom est un ouvrage de valeur historique et architecturale, desservant la cascade hydroélectrique de Suviana et géré par la société italienne de production d'énergie Enel Green Power Italia S.r.l.. Datant des années 1920, les travaux de réhabilitation sont nécessaires en raison d'une réaction alcali-agrégat (RAG) qui affecte principalement la partie centrale de la structure. Le projet de consolidation se concentre sur la conversion de la section centrale du

barrage d'un barrage à contreforts en un barrage-poids et implique la démolition de la partie supérieure des trois arches et des deux contreforts du corps du barrage central, ainsi que le remplissage en béton des espaces entre les contreforts existants (y compris les contreforts démolis eux-mêmes). Le projet comprend également la construction d'une nouvelle décharge de fond, étant donné que la décharge existante est actuellement totalement envasée. Pour la conception exécutive de cette structure plutôt complexe, la méthode Building Information Modeling (BIM) a été choisie: une activité ambitieuse et difficile qui a permis un travail collaboratif et cohérent entre les différents acteurs impliqués grâce à ses outils de partage numérique et à l'utilisation d'un environnement de données commun pour la gestion des documents, la visualisation en 3D des différentes questions et la gestion automatique des informations. Le modèle du barrage existant a été reconstruit sur la base des dessins 2D de la conception finale développés par le propriétaire du barrage et à partir d'un relevé de nuages de points. La modélisation comprenait les phases complexes de démolition et de construction des différents éléments du barrage, ainsi qu'un aperçu complet des séquences de construction (BIM4D). Le modèle BIM a été utilisé non seulement pour la production des dessins 2D et du devis, mais aussi pour l'analyse structurelle et géotechnique par éléments finis ainsi que pour le modèle géologique tridimensionnel, dans lequel les résultats des études géologiques ont été intégrés.

1 INTRODUCTION

The Pàvana Dam, located in Italy on the Limentra di Sambuca river between the municipalities of Castel di Casio (BO) and Sambuca Pistoiese (PT), consists in a mix of arches and buttresses in the central part and lateral gravity sections.

The dam is part of the Suivana-Brasimone hydroelectric scheme operated by Enel Green Power Italia S.r.l. and is an element of the left catchment channel of the system: the reservoir created by the dam directly collects the waters of the Limentra di Sambuca river, and, by means of a headrace tunnel, the waters of the Reno River, coming from the Molino del Pallone dam. A headrace tunnel conveys the waters to the Suviana reservoir, serving Bargi and Suviana hydroelectric pumped storage power plants.

Built in the 1920s, the 54 m high dam consists of a central arched body and lateral gravity sections. In the higher central part, four unreinforced concrete buttresses support three reinforced concrete vaults with 16.50 m spacing. At the upstream dam toe, there is a foundation plinth, and the buttresses are connected by reinforced concrete arches at different levels. The two lateral sections of the dam are lower in front of the central sector: the body on the right bank is of the full gravity type, while the dam body on the left bank is lightweight gravity with internal cavities.

The dam needs structural rehabilitation due to the gradual development of a swelling and cracking phenomenon in the surface of the concrete used for construction, due to the alkali-aggregate reaction (AAR). This affects the main parts of the structure (buttresses, vaults, and arches) with various grades of development, depending on the local quality of the aggregates, the local water exposure and impermeability conditions, and the stress solicitation state.

Moreover, the historical structure does not meet anymore the static requirements of the latest regulations in force in Italy (Technical Standards for Dams NTD14). Therefore, the planned rehabilitation works also include the adaptation of the structure for compliancy to withstand the seismic actions now forecast as design reference for the site.

The project is submitted to the Supervisory Authority General Directorate for Dams and Water Infrastructures of the Ministry of Infrastructures and Transport of Italy.

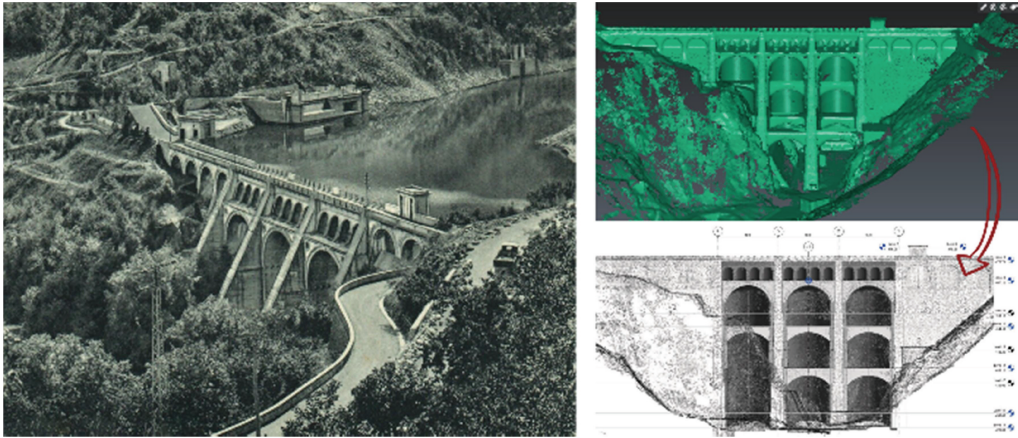


Figure 1. Survey of the existing dam – Point cloud survey and BIM model

2 OBJECT AND SCOPE

The application of a BIM approach to the final design of the consolidation works of a dam is certainly an innovative and challenging case for which there is no precedent in Italy: proposed by the designer the innovative method met the favorable opinion of the client's technical staff, who charged Lombardi SA of the development and follow up of the BIM model.

The job was charged to the BIM Group of Lombardi SA, a specialized technical office Lombardi SA has set up from years to meet the requirements of the clients regarding the implementation and development of the new design method: no change from old design way and mind was required to the other offices of the client and of Lombardi SA.

From the beginning, the design activity with this innovative approach, not contractually required by the client, was considered challenging and ambitious.

Among the results of this experience with the innovative use of the BIM method are:

- Dealing with a type of work that had not previously been addressed with a BIM approach at the corporate level.
- The evaluation of advantages and disadvantages of its application.

The project also provided the opportunity to use and develop business workflows and modeling standards.

3 PROJECT DESCRIPTION

The consolidation project involves converting the middle section of the dam from an arch and buttress dam to a solid gravity dam to ensure the safety performance required by current regulations.

Given the age and poor condition of the existing concrete, the project calls for the demolition of the main body of the structure, with the exception of the lower section of the arches, whose demolition will be avoided to ensure the hydraulic safety of the site areas located immediately downstream.

The minimum reservoir level during the works corresponds to the invert elevation of the intake of the middle level outlet, which also corresponds roughly to the actual height of the sediment deposit in the reservoir. During construction, the lower part of the upstream face of the dam will be maintained to ensure the dam's hydraulic functionality with respect to the design hydrometric levels.

The concreting of the new dam in the lower part precedes the demolition of the buttresses, the concreting of the remaining voids all of which forms a new monolithic foundation for the upper section, where a dam with three independent blocks is constructed (see macro phases of construction). In the monolithic foundation, structural continuity is achieved between the new castings, the downstream faces of the existing arches and the surfaces of the existing lateral buttresses. Structural continuity in the joints between existing structures and new castings is achieved by injections and partially by anchor bars.

4 THE DEVELOPMENT OF THE PROJECT

4.1 *BIM modeling*

The BIM software chosen for the modeling of the Pàvana dam is Autodesk Revit. This software is widely used at the enterprise level, and the choice is related to its versatility in incorporating different disciplines (civil engineering, architecture, plant engineering) and interoperability with other software through the open exchange format .ifc (Industry Foundation Classes).

For a more efficient management of the BIM model, it was divided into sub-models for the different parts of the structure. The design requirements led to the choice of the following MBS (Model Breakdown Structure):

- Digital terrain model (DTM)
- Model of the dam body structure
- Models for specific structures or parts (bottom outlet, retaining walls, tunnels inside the dam body)
- Model of the drawings

The first modeling phase included the reproduction of the model of the dam's actual state, starting from the consistency drawings of the structure made available by Enel Green Power S.p.A. during the detailed design, and from a first point cloud survey dated 2013, enriched in 2020 by a second, more extensive survey that completed the tracing of the upstream area.

With to the aim of using the model to extract quantities for the works BOQ, the central dam body modification model was divided into three blocks, each of which was further subdivided into smaller elements corresponding to the different casting stages, as will be described later.

Demolition is complex because structural safety must be ensured at all stages of the demolition work since the dam remains loaded by the hydrostatic pressure of the reservoir. For this reason, the construction sequence considers performing concreting between the buttresses up to an established intermediate height prior to demolition so that the loads of the arches can be transferred to the new castings without the risk of structural failure, finally allowing to demolish the central buttresses.

Specifically, the BIM model was tailored according to the following construction macro phases:

- Execution of fill castings in the compartments up to the set elevation (monolithic foundation) – Phases 1 to 3;
- Demolition of the existing dam (arches and central buttresses) – Phase 4;
- Demolition of the existing dam (upstream arches and central buttresses until the set elevation) – Phase 5;
- Execution of fill castings in the central buttresses – Phase 6;
- Execution of fill castings in the dam body (in independent blocks and by micro-phases) – Phases 7 to 9. In the final phase will be executed also injection campaigns and drainage drills from the new internal tunnels of the dam.

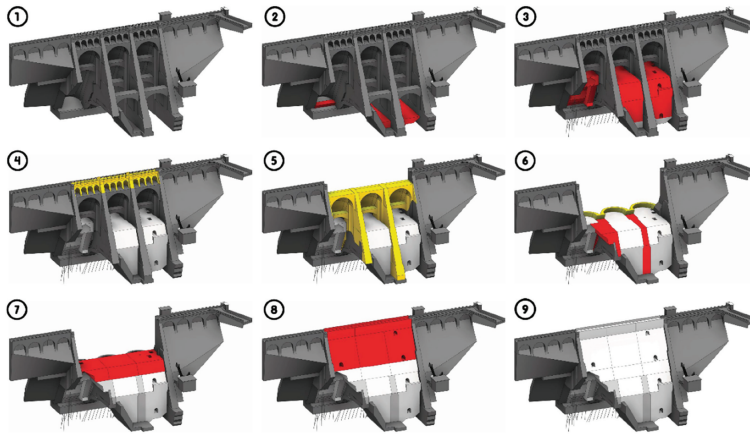


Figure 2. Sequence of construction macro-phases. Legend: Dark gray: existing dam – Light gray: new dam – Yellow: demolition – Red: construction.

Along with the design of the new dam body, a second BIM modeling activity involved the rehabilitation of the bottom outlet, whose inlet located in the deepest part of the reservoir is subject to siltation.

In this light, the project included a second, higher intake, connected to the existing bottom outlet tunnel through an underground shaft. However, the design of the new intake encountered some critical issues: The structure, embedded in a steeply sloping rock on the right bank, required specific measures to stabilize the excavation surfaces in the work area. In this case, BIM modeling provided the tools for a rapid and accurate evaluation of the excavation volumes, supporting geotechnical design.

For the modeling of components with complex geometry, it was necessary to interface Autodesk Revit with Rhinoceros software (Robert McNeel & Associates), such as for the reconstruction of the connection between the intake shaft and the bottom outlet tunnel. In this case, the models created in Rhinoceros were then converted into “Revit families” and integrated into the Autodesk Revit model of the dam.

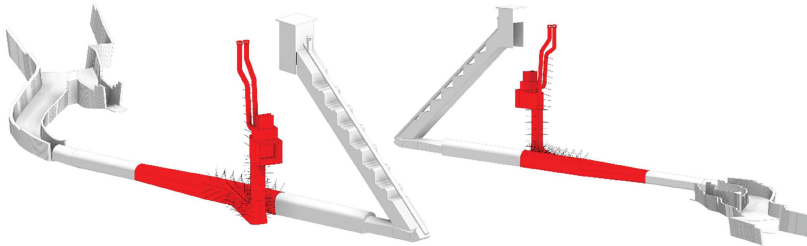


Figure 3. Connection of the new intake structure with the existing bottom outlet tunnel. Legend: Gray: existing objects – Red: construction.

Finally, one major goal of BIM modeling was to extract the 2D drawings of the final design. Some tables that required a particularly high level of detail were created with Autodesk AutoCAD using .dwg views extracted directly from the Autodesk Revit model.

4.2 BIM collaboration

Autodesk’s collaborative cloud platform BIM360 Document Management was chosen for collaboration between BIM specialists and designers. This made it possible to effectively manage both BIM modeling between the various BIM specialists and coordinators and the exchange of information between designers and client through specific access and authorization settings.

This methodical approach facilitated the work of all project participants by ensuring a constantly updated overview of the progress of the modeling and design activities, thus enabling better overall project coordination.

4.3 Quantity take-off

The extraction of quantities was one of the uses of the BIM model that proved to be particularly useful for the final evaluation of the project, as it allowed a more precise definition of the works and, consequently, of the costs generated by this large-scale work. Costs were processed following a tabular extraction of the involved quantities, which required the creation of a BIM model whose geometric and alphanumeric data could follow the same table structure.

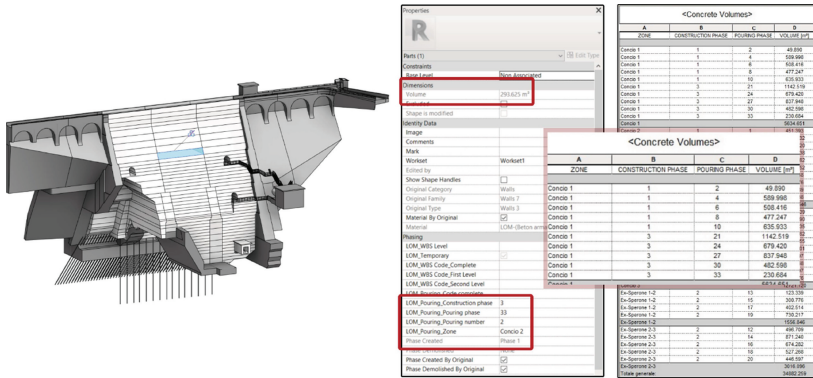


Figure 4. BIM model and data structure for quantity extraction.

Extracting data that could be retrieved and filtered as needed for cost estimating was made possible by careful planning of the project modelling process. For the redesign of the dam in Autodesk Revit, it was first decided to geometrically isolate the central body, which was to be demolished and then rebuilt, so that it could be treated as a single unit. This was in turn divided into three macro blocks, which were used to detail both the different execution phases for the construction of the unit and the number of concrete castings required to complete the works. In order to calculate the quantities of concrete for each casting, the model elements were then geometrically subdivided and computerized in relation to the block of the dam, the construction phase, and the sequential number of the concrete casting.

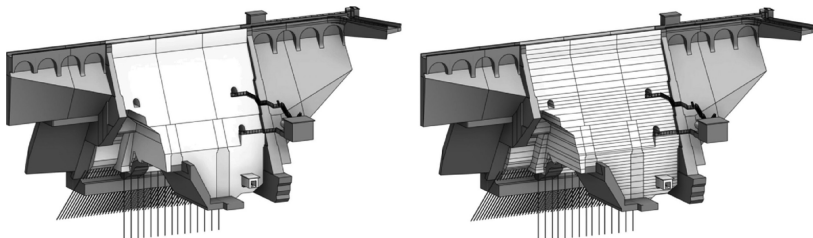


Figure 5. Detail of dam decomposition into blocks and construction phases.

This data structure made it possible to generate dynamic tables capable of constantly reflecting and keeping up to date the quantities of concrete expected in the project and the activities of the work schedule.

In addition to the determination of the concrete volumes, the extraction of quantities also involved a small portion of the excavation volume in an area where the surface is particularly

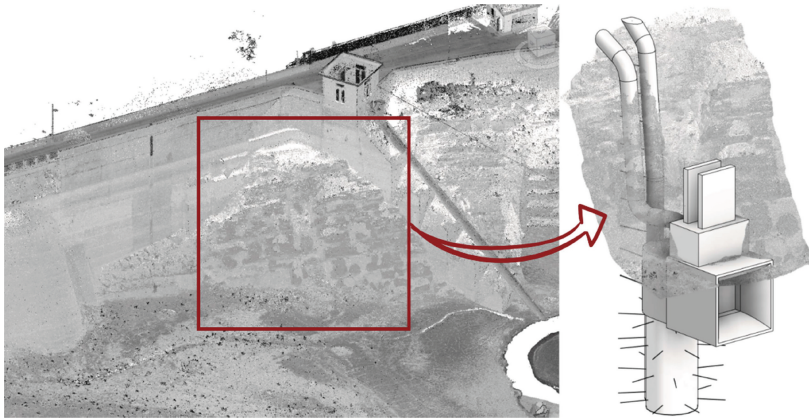


Figure 6. Details of the rock slope and the new intake structure.

irregular, i.e. the new intake structure connected to the bottom outlet, which fits into a steep rock slope and required special attention in the calculation of the excavation volume. For an accurate terrain model of this area, the point cloud obtained by laser scanning survey was used.

In particular, the point cloud survey was used as a database in Dynamo (an application integrated in Autodesk Revit), which, by defining a specific calculation algorithm, allowed the reconstruction of a geometric surface that perfectly matched the rock slope provided by the survey. This surface was invaluable for the reconstruction of the excavation volume required for the construction of the new intake structure.

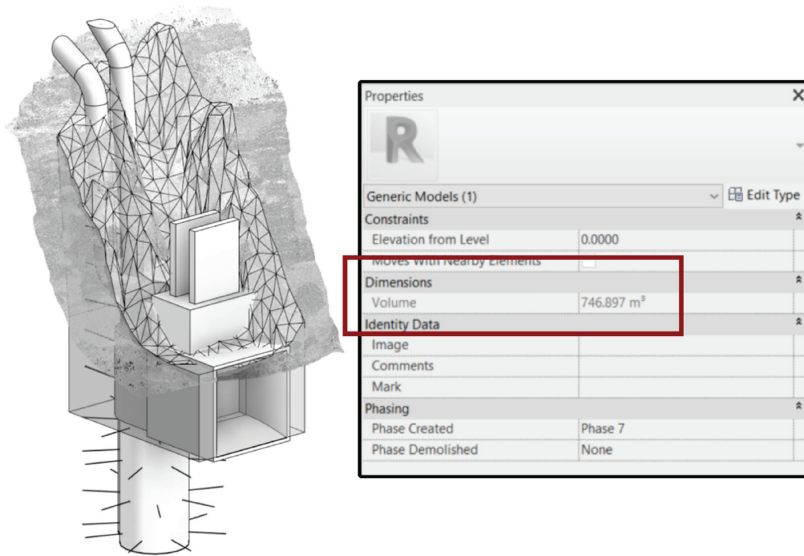


Figure 7. Detail of the excavation geometry of the new intake structure and volume extraction.

4.4 Structural analysis

The BIM model proved to be an excellent basis for the development of structural models. With the help of the Rhino.Inside.Revit and Grasshopper applications, it was possible to transfer the entire dam geometry from the Autodesk Revit environment to the Rhinoceros environment.

Here, the geometries could be optimized so that they were suitable for export into a STEP file, which in turn was imported into FLAC3D and served as the basis for creating the finite element model for the structural and geotechnical calculations.

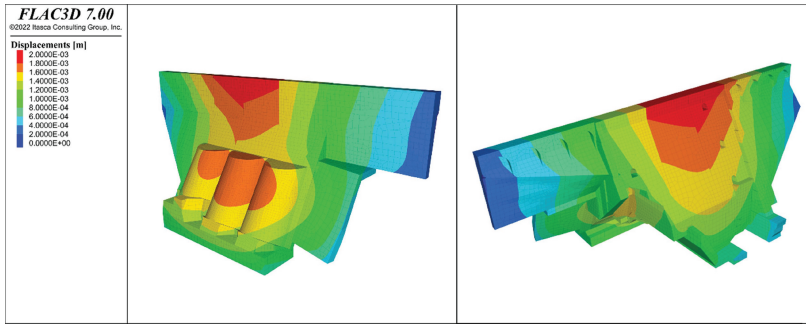


Figure 8. Results of the structural analysis of the dam body.

The BIM model also provided the geometrical basis for the development of a three-dimensional geological model into which the results of the survey campaigns were integrated to provide a particularly meaningful and useful representation for design purposes.

For the moment the geological model was not used for a more detailed representation of the geotechnical characteristics of the dam foundation, by means of local reduction of the geotechnical properties on faults and geological joints with evidence on the foundation layers.

The FLAC 3D model considers the foundation as a continuous media with properties from the geotechnical characterization, i.e., with parameters taking in account of the geological structures and materials, with no explicit modeling of joints and faults: it is however a possible further exploitation for the limits of the BIM method.

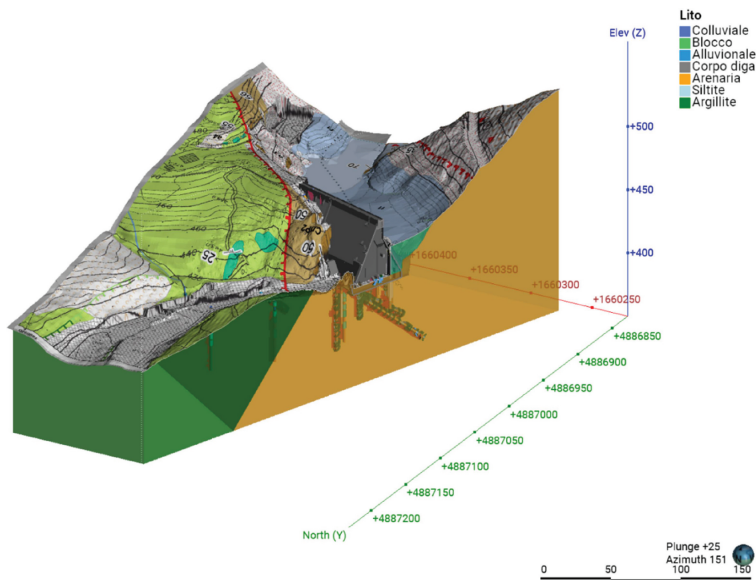


Figure 9. BIM model combined with geological model.

5 CONCLUSIONS

The application of the Building Information Modeling method proved generally effective for the definitive design of the Pàvana dam, an innovative use case of ScantoBIM and design authoring for which there are currently no reports of similar experience, and in any case the first experience with this application for the specific type of work for Lombardi Ltd.

Since this is an existing dam with very distinctive architectural geometries, we had the opportunity to reproduce the exact configuration of the existing geometries in a 3D model, which allowed us to further refine the choice of intervention phases.

The BIM method had an additional advantage over simple 3D modeling: it made it possible to use the model as the single source of information between the designers and the modelers themselves and to improve their collaboration.

If used during the next project phases, this same BIM method will enable the designer and the client to benefit from further advantages as for example the digitalization of the construction process and of the quality checking and the cost estimation on site directly linked to the information included into the model eventually linked to new laser scanning surveys during the construction of the dam. Unfortunately, the adoption of a BIM methodology entailed an increased and more costly design effort in the initial phase, for the reproduction of the real geometry of the dam from the point cloud and for the modelling of the new project layout, but on the other hand, it was immediately apparent how this digital, all-inclusive and collaborative methodology facilitated all the actors involved in understanding the project, exchanging information and evaluating the technical project solutions.

In summary, advantages and disadvantages of the BIM method for this pilot project can be described as follows:

- **DATA CONSISTENCY:** Starting with a point cloud gives the certainty that the geometry of the modeled dam matches its real configuration, which is the basis for the entire design process. Extracting the quantities directly from the model ensures unambiguity of the data regarding the subsequent project phases, where modifications or elaboration could lead to variations of these quantities.
- **UNIQUE SOURCE OF KNOWLEDGE:** The various design aspects were managed centrally in a single model (survey management, layout design, geotechnical and structural design, quantity extraction, construction phases, and preparation of graphic drawings). This feature will be useful when subsequent phases are further developed based on the same BIM model.
- **IMPROVED UNDERSTANDING OF THE STRUCTURE:** A 3D model of the structure, containing all the technical information, allows a better understanding of the design decisions made, thanks to the combination of 3D views and attribute tables associated with each component.
- **FURTHER APPLICATIONS THAT UTILIZE THE BIM MODEL:** The extraction of the 3D solids directly from the BIM model simplified the creation of the calculation mesh for the geotechnical and structural FEM software required for the design. The quantities of volumes and surfaces extracted directly from the model were used to estimate project costs. The work schedule used 3D visualization for a better understanding and presentation of the decisions made to the client.

ACKNOWLEDGEMENTS

The authors would like to acknowledge Enel Green Power Italia S.r.l. for permission to publish the work and all stakeholders involved in this project for the constructive approach during the development of the Pávana Dam BIM Model.

REFERENCES

- ISO 19650 – Organization of information about construction works – Information management using building information modelling – Part 1: Concepts and Principles
- ISO 19650 – Organization of information about construction works – Information management using building information modelling – Part 2: Delivery phase of the assets

Potential Failure Mode Analysis (PFMA) to deal with ageing and climate change affecting dams

Philippe Méan

Ing. Civil EPFL, Ph.D UCD, former Director Energie Ouest Suisse, Switzerland

Thomas Bryant

M. Engineering CEngineering MICE, Senior Dam Engineer, Gruner Stucky SA, Switzerland

ABSTRACT: this article highlights the value of performing a qualitative risk assessment in the form of a *Potential Failure Mode Analysis* (PFMA) to address uncertainties related to Climate Change and Ageing. As they constitute new and overlapping threats with numerous potential dam safety issues, engineers should consider the joint impact of Ageing and Climate Change on dam safety with a specific risk analysis. The dam engineers must here content themselves with a qualitative assessment since the non-stationary processes of Ageing and Climate Change are not easily reducible to statistical analysis. The identification of the potential situations that place the dam at highest risk must be carried out simultaneously and systematically to all dam components. Partial investigations can actually be misleading and result in underestimated risks and missing the potential interdependencies. An explicit method is required to identify globally new dam vulnerabilities potentially induced by Ageing and Climate Change and to verify their influence on the failure modes previously recognized at construction time. An expert's implicit choice of dangerous situations should be avoided as arbitrary. The regular completion of a PFMA on the occasion of a periodic "Comprehensive Safety Inspection" (every 5-year in Switzerland) and the inclusion of its results in the corresponding "Dam Safety Assessment Report" would address uncertainties related to Climate Change and Ageing on dam safety until the next periodic formal Safety Inspection. This would dynamically increase stakeholder's risk awareness and address the best strategy to enhance the dam preparedness and resilience in a holistic framework and potentially contribute to help focus research efforts. It is the authors' belief that *Potential failure mode analysis* (PFMA) could be in practice implemented more widely in Switzerland and in several other EU countries, as a complement to their Standard-based dam regulation, in a period of rapid change and increasing uncertainty calling for regular reviews based on the latest observations.

RESUME: cet article souligne l'importance d'effectuer une évaluation qualitative des risques sous la forme d'une *Analyse des Modes Potentiels de Défaillance* (AMPD) afin de tenir compte des incertitudes liées aux Changement Climatique et au Vieillessement sur la sécurité des barrages. Une méthode explicite est nécessaire pour identifier les nouveaux risques affectant potentiellement les barrages et pour vérifier leur influence conjointe sur les modes de défaillance précédemment reconnus au moment de la construction. On doit ici se contenter d'une évaluation qualitative car les processus non stationnaires du Vieillessement et du Changement Climatique ne se réduisent pas facilement à l'analyse statistique. L'exécution périodique d'une AMPD à l'occasion d'un «Examen périodique approfondi de la sécurité» (tous les 5 ans en Suisse) et l'inclusion des résultats dans le «Rapport d'expertise sur la sécurité du barrage» correspondant permettrait d'adresser les incertitudes liées au Changement Climatique et au Vieillessement jusqu'à la prochaine inspection périodique. Cela permettrait d'accroître de façon dynamique la sensibilisation des intervenants au risque, de mettre en œuvre la meilleure stratégie pour améliorer la résilience des barrages et d'orienter les éventuel efforts de

recherche. Dans une période de changements rapides et d'incertitude croissante qui exigent des analyses régulières fondées sur les dernières observations, les auteurs sont d'avis que *l'Analyse des Modes Potentiels de Défaillance* (AMPD) pourrait être appliquée plus largement en Suisse comme dans plusieurs autres pays de l'UE, en complément de leur réglementation fondée sur les Normes.

1 INTRODUCTION

According to the ICOLD register, there are presently 4898 large dams in the EU27 and Switzerland; these are on average 55 years old (based on Perera et al., 2021). Around half of these large dams are comprised between 55 and 100 years old. This longer than average duration of service compared to other civil infrastructure makes Dam Ageing a major contribution to increased operation risk.

In addition to Ageing, the impact of Climate Change is becoming more and more apparent and is exposing dams to more frequent and more extreme adverse environmental effects that influence and will continue to influence the safety of every dam in the future in various ways.

As the two circumstances constitute new and overlapping threats, engineers must consider their joint impact on dam safety. (Ghimire, 2022).

2 AGEING AND CLIMATE CHANGE

2.1.1 Ageing

Ageing is defined as dam deterioration during its life span associated with time-related change in the properties of the construction materials of the dam structure and its foundation (ICOLD 1994 B93). An extensive review of ageing-induced failures or safety-related case is available in ICOLD 1994 B93. Concrete dams can be affected by long-term processes such alkali aggregate reactions, concrete ageing and irreversible rock mass deformation. Earth dam can suffer in many ways, from settlement filter clogging, core deterioration, pressure building and internal erosion.

The impact of Ageing is not immediately apparent and its detection relies on instrumentation and visual inspections usually followed by investigations. Ageing must actually evolve with time before producing perceptible effects like seepage, pressure modification, displacements, cracking and so on.

As the Ageing process develops, the uncertainty factors increase on material properties and reduce the dam global safety factor prior to being detected. A successful long-term operation does not preclude safety problems arising over the rest of the dam life. A specific risk analysis is necessary to cope with the new conditions potentially affecting the dam, since the future dam behavior cannot be entirely deduced from the past.

2.1.2 Climate change

There are a several references considering directly or indirectly the impact of climate change on dam structures. Future warming of surface air temperature induces change in precipitations (IPCC, 2021). The climatological baseline and the range of climate variability are shifting (USACE 2014). These shifts are anticipated to result in more intense and frequent extreme conditions of rainfall and run-off, as well as altered snowfall volume and melt.

Projected impacts of climate change concern numerous known issues directly or indirectly related to climatology, including catchment precipitation, extreme flood events, glacial lake outburst, permafrost thawing, glacier melting, induced landslides and sedimentation accumulation, long periods of drought/ low flows and increases in extreme heat.

In a comprehensive interdisciplinary review of research, Fluixá-Sanmartín et al. (2018) presented a global review of Climate Change impacts, listed the main expected impacts on different dam safety components and proposed diverse techniques and methods for their assessment in a compartmentalized approach.

Assumptions on the stationary hydrological data are no longer appropriate (USACE, 2018). Hydrology and design criteria may need to be reassessed over the dam lifetime and mitigation measures to be taken. As effects of climate change are subject to considerable uncertainty, update of design criteria remains however unreliable. Empirical statistical analysis cannot help at the present time since historical records are too short. A specific risk analysis of the new threats involved is necessary.

2.1.3 *Tackling the challenge of climate change and ageing*

A holistic approach to dam safety is needed as both effects of Climate Change and Ageing are superimposed on normal loading conditions (Figure 1).

The first step, and probably the most difficult given the prevailing uncertainty, consists in identifying the potential situations and events that place the dam at highest risk.

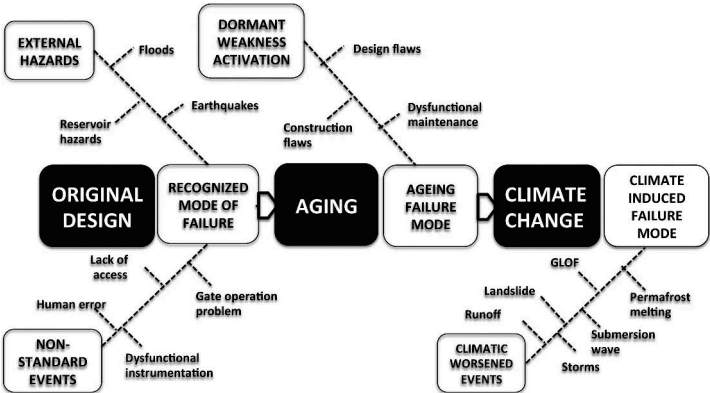


Figure 1. Global risk assessment framework.

As reflecting uncertainty is a major challenge, the identification process should be formalized in a transparent and systematic way. An expert’s implicit choice of dangerous situations should indeed be avoided as arbitrary. An explicit method is instead required to identify globally new dam vulnerabilities potentially induced by Ageing and Climate Change and to verify their influence on the failure modes previously recognized at construction time.

The identification must be carried out simultaneously and systematically to all dam components as partial investigation can actually be misleading and result in underestimated risks by omission of interdependencies.

3 DAM RISK ANALYSIS

Risk analysis for dam safety is a comprehensive concept exhibiting a great number of different tools to deal with potential hazards. During the last 25 years, a proliferation of articles devoted to this subject has been published in the literature. To provide context and clarity, the main approaches are briefly summarized and presented below.

3.1.1 *Standard-based concept*

This traditional approach addresses uncertainty by applying safety coefficients and conservative values for loads and resistance in an indirect manner (ICOLD 2017 B154). It is often called *Standard-based* since the risk management consists in following established rules and proven codes of practice.

To deal with uncertainties, a safety factor expressed as the ratio of resistance divided by load is applied. The failure probability is then proportional to the overlap between the

statistical distribution of resistance and load. As the failure probability of occurrence of the whole dam system is not computed, the global risk cannot be quantified. The consequences are therefore estimated in a second stage, independently of the failure.

Legislation in several countries considers only implicitly dam risk assessment, like Switzerland where dam safety relies on three pillars: intrinsic safe design, meticulous surveillance and emergency planning (Darbre, 1999). Minimization of risks and management of the residual risks are introduced implicitly by a layer of prevention actions and methods (Figure 2).

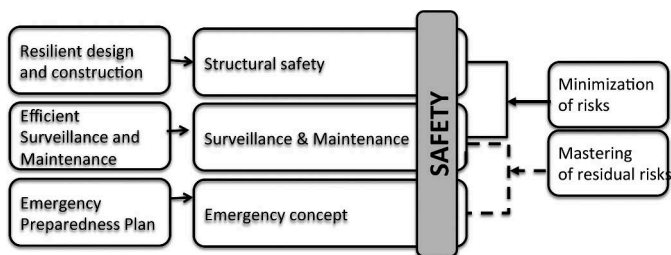


Figure 2. Safety assessment for dams in Switzerland (Adapted from Darbre G., 1999; SFOE, 2015).

3.1.2 Quantitative risk assessment

Quantitative risk assessment is the process of examining and evaluating the tolerability of risk.

In a seminal paper, Bowles, 1998 proposed a overall Risk Assessment framework applied to dams based on the chain-of-event *initiator–response–outcome–consequence* (Figure 3). Producing a value of the risk for the worst loads scenarios and deciding whether this risk value is socially acceptable are the key expected results of the Risk Quantitative assessment.

In 2005, ICOLD provided an extensive review on tools used for explicit risk assessment in dam safety management. ICOLD pointed out inherent limitations of the approach but nevertheless recommended a wider use of the risk-based methods considering that “*the principles of risk assessment are logical and should be considered by all countries as part of the decision-making on dams*” (ICOLD 2005 B130). The publication raised however vigorous discussions in the dam community and was received with skepticism in several ICOLD sections of non English-speaking countries.

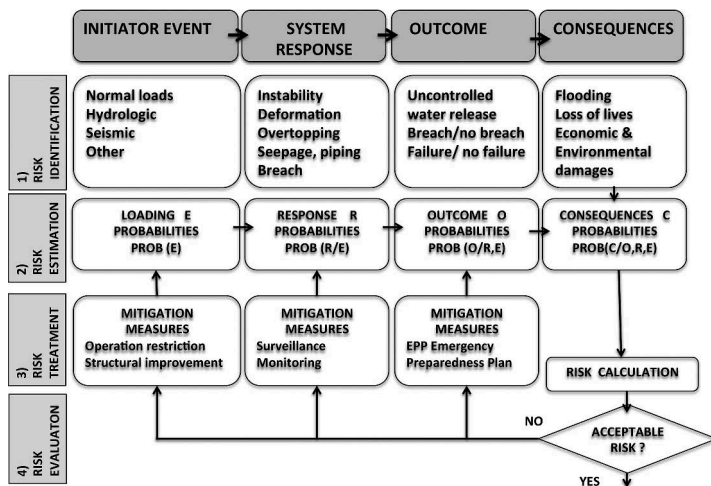


Figure 3. Overall risk quantitative assessment framework (adapted from Bowles, 1998).

The risk assessment methods advocated (ICOLD 2005 B130) were perceived by part of the engineering community as an attack of the traditional method. First, it was argued that

outside the UK and except several English-speaking countries, legislation tends to require absolute levels of safety defined by the safety code standards. Second, the reliability of quantified risk was questioned.

Calculating a representative dam failure risk value remains indeed a formidable challenge as shown hereunder by a short review on the prevailing limitations regarding the chain-of-events identification and probabilities assignment.

Each individual dam in its environment is a special case exhibiting a scarcity of available historical data. This uniqueness prevents the direct estimation of probabilities of the various events potentially leading to dam failure. The problem is even more serious with Ageing and Climate Changes since these non-stationary time processes are not fully captured in historical records.

Forensic investigation of Teton (Iglesia, 2009; ASDSO 1976) and Tom Sauk (Regan, 2010; ADSO 2005) showed that many dam failures do not occur because of simple extreme loadings but are rather caused by numerous adverse interactions of multiple components escalating to total failure by cascading effects (Regan, 2010). Describing failure as the result of a linear chain of events oversimplifies complex failure modes. Finally, the applicability of quantified risk-based techniques to dam safety issues often reduces to qualitative framework for establishing the failure modes associated with the risk of failure (Donnelly et al., 2015).

These complex interactions concern all aspects of the dam considered as a global system including design, construction, maintenance, surveillance as well as the dam owner's management organization (Baecher, 2021). This makes very difficult –if not impossible– to evaluate joint probability of events depending on technical hazards and human factors. Moreover, as the total risk is not simply the sum of individual risks, the correlation between different sources of risks leads actually to greater risks, which create an additional layer of uncertainty of the failure process (Kalinina et al, 2016).

In such a broad spectrum, direct numerical techniques are not available for assigning conditional probabilities for subsequent events following the initiator event. To take in account the multi-dimensionality of risks and their possible interactions, sequential Monte-Carlo models were introduced (Mato et al., 2015). Hampered by the “curse of dimensionality” and their development costs, these models are often focused on academic research (Mignan et al., 2014) and not systematically used in dam engineering practice.

Fully depicting the risks associated with a large dam is highly complex mathematical problem (Matos et al., 2015). For quantifying the probability of occurrence of a dam failure in its multi-dimensionality and complexity, one must finally rely on a variety of soft empirical methods based on engineers' experience and sound judgment (Donnelly et al., 2015). However sophisticated its method of calculation, the quantified result remains, at least in part, a subjective representation of the analyst's experience and judgment.

3.1.3 *Qualitative risk assessment*

In order to avoid intense effort and high costs associated with calculating a representative risk value for a dam failure, Qualitative risk assessment has been proposed. In this approach, the objective is no longer to find a probabilistic quantified value of the dam failure. Instead, the focus is on identifying the scenarios that place the dam at highest risk.

Already in 2002, FERC, a US regulatory federal agency, required that the safety review of all dams of hydroelectric projects comprises an analysis based upon a “failure mode thinking” called *Potential Failure Modes Analysis*, abbreviated “PFMA” (FERC, 2004).

Since then, acceptance of the PFMA has become fairly high in the dam engineering profession, mainly in USA but also in several others non English-speaking countries. Several governmental organizations have already introduced PFMA in their respective legislation for safety of dams or as a good practice: French legislation in 2008 with the compulsory “Etude de danger” for dams, British government in 2021 as part of the dam inspection review.

Comprehensive guidelines to perform a PFMA analysis and to assess required mitigation measures have been recently published (FERC, 2017; World Bank, 2021). For clarity, a brief description of the PFMA method is given hereunder. The interested reader should refer to the previous documents for a full account.

The PFMA is a step-by-step systematic method for identifying all the ways in which a dam and its appurtenant structures could fail under postulated severe loading conditions, decomposed for clarity in distinct sets, comprising normal, hydrologic, seismic and other loads (e.g. Ageing and Climate Change). The PFMA approach consists in breaking down a dam system into its major functions (the so-called “elementary systems”) and detecting the failure mechanisms potentially affecting every component of each elementary system (the event tree).

The PFMA then aims at identifying the cascading consequences on the whole dam system in the event of a failure affecting an elementary system. This approach takes place during a workshop (brainstorming session) with a comprehensive qualified team of individual most familiar with the design, analysis, performance, surveillance and operation of the dam.

In this context, dam failure is only defined as the loss of dam containment function with significant uncontrolled release of water downstream. Other breakdowns of components of the dam system are ignored if they do not lead to a breach.

A simplified ranking of the failure scenarios represents a one-time risk assessment that highlights the main safety priorities. If necessary, failure modes with substantial uncertainties can be further analyzed in a later phase.

Through the identification of the failure scenarios, the PFMA provides efficient means to upgrade dams safety plans by focusing instrumentation and surveillance programs as well as improving the emergency preparedness. The method requires limited resources, is easy to implement and gets straight to the point.

As a successful PFMA will synthesize all useful information available, attendance of the PFMA workshop should include, in addition to dam technical experts, representatives of concerned stakeholders (regulatory authorities, dam owner, dam operator and surveillance warden).

4 PFMA TO DEAL WITH AGEING AND CLIMATE CHANGE

4.1.1 *Holistic approach*

The Standard-based approach implicitly postulates the time persistence of hydrological regime and assumes that the potential change of physical dam properties is contained within the boundaries of given conservative factors of safety. As a result, the traditional Standard-based approach to dam engineering, limited by construction to selected predicted historical hazards, cannot address the new threats of future potential failure modes. Overcoming the non-stationary historical data and the lack of meaningful records requires an explicit consideration of risk.

PFMA is an effective way to complement the Standard-based approach by ensuring that all relevant failure modes are considered. Based on an ex-post analysis of several well-known US dam failures, examples have been given in the literature where modes of failures missed by a strictly Standard-based approach would likely have been detected before the accident, had a PFMA been performed (Regan P.J., 2004, cited in Donnelly C.R., 2005).

As ageing may affect all dam components and as climate change effects generally overlap with those of ageing, the risk assessment of Ageing and Climate Change should be done simultaneously. As PFMA addresses all initiator events, whether normal, hydrologic, seismic or other loads (e.g. Ageing or Climate Change), consistency is ensured.

4.1.2 *Climate preparedness*

Integrating climate change into the flood risk is of major importance. Ongoing research involves scaling down IPCC Global Climate Models (GCM) regionally to obtain local weather data and estimate extreme events through statistical analysis. However, IPCC doesn't give any probabilities to its global warming results since they are dependent on several socio-economic scenarios and on the resulting human emissions (IPCC, 2021). Therefore, reliable statistical projections of climate-induced future rainfalls are not available, let alone flood forecasts. A tough dilemma confronts therefore the dam engineer: flood intensity may well increase but fundamental uncertainty prevails in the predictions.

As an alternative to the lack of reliable hydrologic models, the PFMA is an excellent tool to address pragmatically the climate change uncertainty in a comprehensive framework. The simplified ranking of the failure modes allows focusing on the main risks. The risk mitigation measures already implemented are highlighted or improved, if necessary.

Specifically, PFMA “what if” approach requires an approximate evaluation of the maximum hydrologic loading conditions to set ideas on the order of magnitude of floods. The Probable Maximum Flood (PMF) is usually considered as a proxy for this purpose, as the deterministic upper bound of extreme floods. Before standard-based approaches evolving in formal guidance, the PFMA workshop could address explicitly potential additional mitigation measures, prior to considering increasing the evacuation dam capacity. These potential mitigation measures will be completed by an evaluation of emergency mitigation measures to increase the system resilience.

The best strategy to improve preparedness for Climate Change uncertainty will therefore be adapted periodically for each iteration of the PFMA, whenever new research on impacts is available and as soon as interdependencies are better understood.

4.1.3 Climate and Ageing resilience

It is well known that dam inspection and monitoring play a critical role for dam safety, as failure prevention often relies on early detection of abnormal dam behavior. These preventive actions are generally built in “dam surveillance”, a permanent organizational intervention routinely performed by specialists with different competence levels ranging from basic technical knowledge to broad expertise in dam construction. A three levels surveillance organization is generally recommended (ICOLD B138, 2009; ICOLD B158, 2010). The three levels of surveillance provide an in-depth defence system with three independent layers of protection working in cascade (Méan P., 2019). The process culminates at regular intervals (in Switzerland every 5 year) by a “Comprehensive Dam Surveillance Inspection” and by the production of a formal “Dam Safety Assessment Report”, based on all information available at this time (annual reports, monitoring data and inspection reports). Comparison of successive “Safety Assessment Reports” provides early warning signs to identify abnormal dam behavior.

As Ageing and Climate change are relatively slow evolving phenomena, a PFMA workshop performed on the occasion of the formal “Comprehensive Dam Surveillance Inspection” would allow to overcome Climate Change and Ageing uncertainties in the short term (Figure 4). If needed, special investigations or interim mitigation measures could be ordered. Uncertainties, that are likely to be identified across the dam portfolio, may also help focus specific research (e.g. permafrost monitoring, etc.).

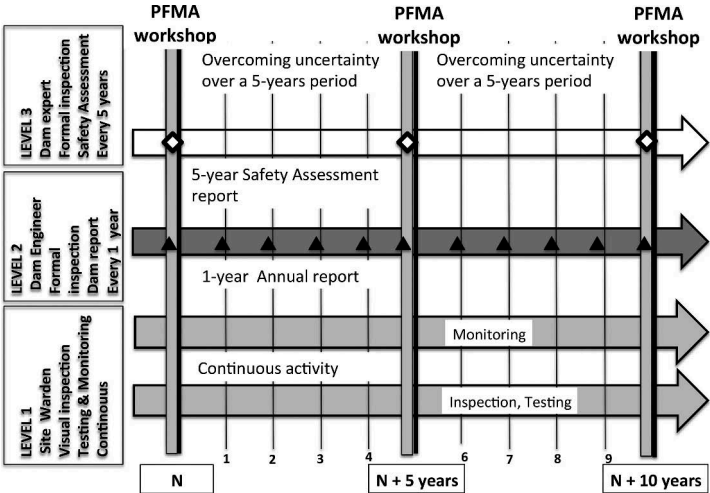


Figure 4. Integration of PFMA in the surveillance activities (modified from ICOLD, 2010).

With such an ongoing assessment of Climate Change and Ageing, recommendations could indeed be issued to ensure continued safe operation during the five-year period between two usual formal Safety Assessments Reports. Without any doubt, including the PFMA process in the dam surveillance routine would improve the dams' climate resilience.

4.1.4 *Risk awareness*

Performing a PFMA is a very efficient way to enhance dam safety. As it allows a dynamic consideration of loading conditions over time, PFMA is, in fact, one of the best cost/benefit risk mitigation measures in itself, providing at lower cost an rare opportunity to detect sources of neglected risks and to evaluate corresponding remedial work, targeted safety inspections and possible improvement of the monitoring system.

4.1.5 *Secondary benefits*

A dam life may typically reach 100 years and more. During this multi-generational period of operational service, the handing-over process from one generation of dam safety/ surveillance specialists to the next entails the transfer of a large amount of information, usually carefully implemented to insure the perfect preservation of all relevant data and reports concerning the dam. Experience is however often difficult to share and there may be unavoidable information losses during the transfer, including elements pertaining to risk management. Participating at a PFMA workshop session would help retain (and leverage) the dam history and working knowledge of key staff. This would increase the risk awareness in a targeted way.

5 CONCLUSIONS

This article aimed to show that performing a qualitative risk assessment in the form of a Potential failure mode analysis (PFMA) is a highly useful initial approach to identify and address pragmatically Climate Change and Ageing uncertainties in a holistic framework in order to enhance dam safety. The authors believe that dam engineers must here content themselves with a qualitative risk assessment and admit that a quantified risk assessment is not yet realistic in present conditions. First, each individual dam in its environment is always a prototype. Second, applicability of quantified risk-based techniques in dam engineering practice often reduces to qualitative framework due to the scarcity of the existing data. Third, the non-stationary processes of Ageing and Climate Change are not easily reducible to statistical analysis.

PFMA is, in fact, one of the best cost/benefit risk mitigation measures in itself, providing at lower cost a rare opportunity to detect sources of neglected risks, to evaluate corresponding remedial works and to identify knowledge gaps, as well as to target safety inspections and possibly to improve the monitoring system. The method requires relatively limited resources, is easy to implement and gets straight to the point.

Performing routinely a PFMA on the occasion of the existing regulatory safety assessment such as the 5-year formal "Comprehensive Dam Surveillance Inspection" in Switzerland and including its results in the corresponding periodic "Dam Safety Assessment Report" would help manage Climate Change and Ageing uncertainties until the next formal Safety Inspection. This approach would dynamically increase stakeholder's risk awareness and address the best strategy to enhance the dam preparedness and resilience in a holistic framework and potentially contribute to help focus research efforts.

It is the authors' belief that *Potential failure mode analysis* (PFMA) could be implemented in practice more widely in Switzerland and in several other EU countries, as a complement to their Standard-based dam regulation, in a period of rapid change and increasing uncertainty calling for regular reviews based on latest observations and understanding.

REFERENCES

- ADSO, Association of State Dam Safety Official, *Lesson learned from dam incidents and failures, Case study Taum Sauk Dam, Missouri 2005, Case study Teton Dam Idaho, 1976.*
- Bowles, S.D. et al, *The practice of dam safety risk assessment and management: its root, its branches and its fruits*, USCOLD 18th Annual meeting, 1998, Buffalo and New York p.8.
- Darbre G.R., *Dam risk analysis, report*, Swiss Federal Office for Water Management, Bienne, 1999.
- Donnelly C.R., 2005, *Assessing the safety and security of dam*, International Conference on Safety & Security of Energy Infrastructures (SEIF-CV) 14-16 November 2005, Brussels.
- Donnelly C.R et al., 2015 *A new quantitative dam safety risk assessment tool for risk-informed decision-making*, Hydrovision, Portland, Oregon.
- FERC 2017, revised edition Engineering Guidelines for the evaluation of hydropower projects, *Dam safety-Performance monitoring program*; Chap 14.3.
- Ghimire S.N. and Schulenberg J.W., 2022, *Impact of climate change (...) and safety threats to earthen dams: post failure case study of two cascading dams in Michigan*, Civil and Environmental Engineering Vol. 18, Issue 2, 551–564.
- Fluixa-Sanmartin J. et al, 2018, Review article, *Climate change impacts on dam safety, Natural hazards and earth system science*, Vol. 18, Iss. 9, pp. 2471–2488.
- Heller V., 2019, *Landslide-generated impulse wave in reservoirs*, ETH Zürich.
- ICOLD, 1994, Bulletin B93, Committee on Dam safety, *Ageing of dams and appurtenant works: review and recommendations.*
- ICOLD, 2005, Bulletin B130, Committee on Dam safety, *Risk assessment in dam safety management: a reconnaissance of benefits, methods and current applications.*
- ICOLD, 2009, Bulletin 138, Committee on Dam safety, *Surveillance: basic elements in a “Dam Safety” process*, p.25, Committee on Dam safety CICB-ICOLD.
- ICOLD, 2010, Bulletin 158, Committee on Dam safety, *Dams surveillance guide*, figure 1.1, Committee on Dam safety CICB-ICOLD.
- ICOLD, 2017, Bulletin 154, Committee on Dam safety, *Dam safety management: operational phase of the dam cycle.*
- Iglesia G., Stadly J., Zhou J., 2009, *Re-analysis of the failure of Teton dam*, 29th Annual USSD Conference Nashville, Tennessee, April 20-24, 2009.
- IPCC, 2012 –*Managing the risks of extreme events and disasters to advance climate change adaptation*, Special report of the Intergovernmental Panel on Climate Change, Cambridge University Press, Cambridge UK, pp25.
- IPCC, 2021, *Technical Summary*, in *Climate Change 2021: The Physical Science Basis. Contribution of Working Group I to the Sixth Assessment Report of the IPCC*, Cambridge University Press, Cambridge, United Kingdom, NY, USA, pp. 33–1.
- Kalinina A., Spada M., Marelli S., Burgherr P., Sudret B., 2016 *Uncertainties in the risk assessment of hydropower dams: state-of-the-art and outlook*, ETH Zurich, Chair of risk, safety and uncertainty quantification.
- Matos J.P. et al., 2015, *Vulnerability of large dams considering hazards interactions: conceptual application of the Generic Multi-Risk framework*, 13th ICOLD Workshop on the numerical analysis of dams, Switzerland, 2015.
- Méan P., Droz. P., 2019, *Improving dam safety with a surveillance self-assessment toolkit*, Hydropower & Dam, Issue 3, pp. 86–96.
- Perera D., Smakhtin V., Williams S., North T., Curry A., 2021, *Ageing water storage infrastructure: an emerging global risk*, UNU-INWEH report, Iss.11 UN Hamilton, Canada.
- Regan, P.J., 2010, *Dams as Systems – A Holistic Approach to Dam Safety*, USSD Dams Annual Conference, 2010, Sacramento, California.
- USACE, 2014, 2018, *Guidance for incorporating climate change Impacts to inland hydrology in civil works studies, designs, and project*, Engineering and construction bulletin no 2018-14.
- SFOE, 2015, *Directives on safety of water retaining facilities*, Part A chap 3, Supervision of Dam Section, Swiss Federal Office of Energy SFOE, DETEC.
- Mignan A., Wiemer S., Giardini D., 2014, *The quantification of low-probability-high-consequences events: part I. Generic multi-risk approach*, Nat. Hazards.
- World Bank, 2021, Good practice note on dam safety – *Technical note 5: Potential Failure Mode Analysis*, World Bank, Washington, DC.

GRIMONIT (GroundRiskMonitor) – an early warning system for difficult measurement conditions

E. Meier & I. Gutiérrez

Edi Meier + Partner AG, Winterthur, Switzerland

M. Büchel

Marc Büchel Media – ocaholic AG, Freienstein, Switzerland

ABSTRACT: In the context of hazard prevention, it is of central importance to continuously monitor deformations on bridges, dams, buildings or in underground mining. Equally challenging is the permanent monitoring of forested landslide areas that pose a risk to railroad tracks or roads. “GRIMONIT” (Ground Risk Monitor) is a fully automated hydrostatic measurement system, which is a further development of the LAS-Meter, developed in cooperation with the ETH. In this paper a measurement with the LAS-Meter is compared with GRIMONIT-measurements. The time span between the two measurements is 11 years. The task was to document the subsidence at the landfill site “Zingel”.

RESUMEN: En el contexto de la prevención de riesgos es de suma importancia la monitorización continuada de deformaciones en puentes, presas, edificios o minería subterránea. Igualmente desafiante es el monitoreo permanente de zonas de deslizamientos boscosas que suponen un riesgo para líneas de ferrocarril o carreteras. GRIMONIT es un sistema de medición hidrostático completamente automatizado, resultante del perfeccionamiento del LAS-Meter y desarrollado en cooperación con la ETH. En este artículo se compara una medición llevada a cabo con el LAS-Meter con otra usando el GRIMONIT, realizada en el mismo lugar 11 años después. El objetivo era documentar una posible subsidencia en la base del vertedero “Zingel”.

1 INTRODUCTION

The development of the GRIMONIT-System has a long history. The idea for the development of GRIMONIT was born at the SNGT Dam Conference in St.Gallen in 2008. The topic at that time was the great danger posed by ageing earth dams at sawmill ponds etc., where, as is well known, no monitoring wells can be drilled and a measuring layout can only be oriented horizontally and not vertically.

The precedent version of GRIMONIT was the LAS-Meter. With this multiple measurement line instrument high resolutions are achieved, e.g., at the base of the Albigna power dam.

The basic physical principles and the implications of possible errors of the LAS-measurement method (Thierbach, 1979; Emter et al, 1989) are described in detail in the article “XII Ingenieurvermessung” in Graz 1996. Since these early days, a lot of experience has been gained in the use of the LAS-Meter (Meier et al, 2010, pp. 97-102). An internal calibration function allowed compensation of the sensor drift, but the maintenance effort was still very high. The reason was the slow response time, which is characteristic for such a system with long extensions. In addition, the impacts caused by fluid losses had to be corrected by means of precise refilling of the system. Long access routes account for a large part of the required service time. Another disadvantage of the LAS-Meter was the small measuring range of only a few centimeters.



Figure 1. Powerdam Albigna, Graubünden, Schweiz (Meier et al, 1996, S. A 8/7).

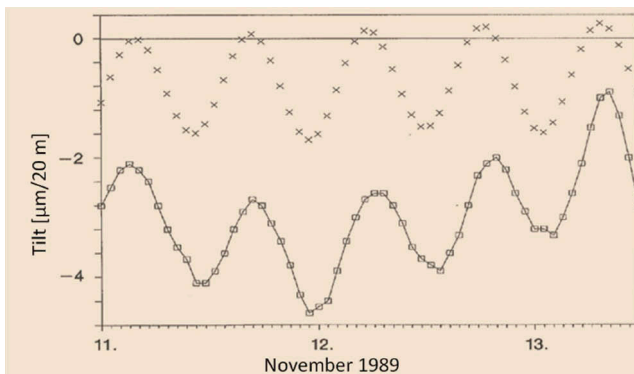


Figure 2. Earthtide record 1989 with LAS-Meter at Albigna power dam (Meier et al, 1996, S. A 8/9).

In contrast to the LAS-Meter, the focus of the current design of GRIMONIT is not on the highest possible resolution, but on the simplest possible handling of the instrument and on a large measuring range.

2 GRIMONIT

The heart of the GRIMONIT-System is composed of one differential and two relative pressure sensors. The measuring probes are connected to this central unit. The measuring probes and tubes are filled with a liquid, making the tubes hydraulically connected.

A differential pressure sensor registers pressure differences, which are converted into height differences. GRIMONIT is able to carry out the necessary filling, rinsing and calibration processes fully automatically, since all venting components are installed in the central unit.

2.1 Measuring method

As with the LAS-Meter, the differential pressure between two measuring probes is determined. Additionally, the relative pressures of these probes are also measured (Figure 4), which significantly increases the measuring range. The accuracy of the relative pressure measurement is lower than that of the differential measurement, but this also has an advantage as the

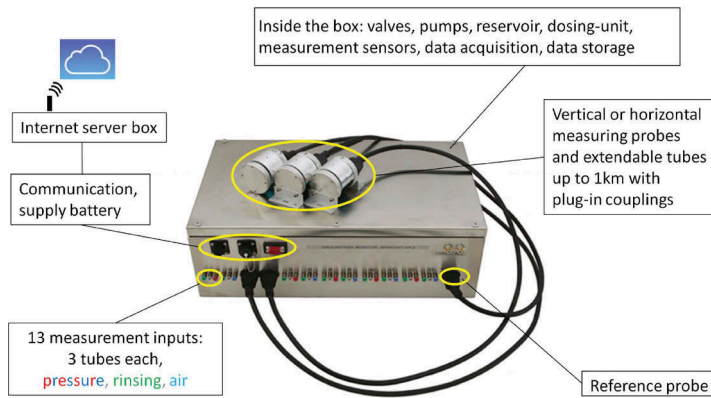


Figure 3. GRIMONIT central unit with two measuring probes and the reference sample connected.

differential pressure signal exceeds the measuring range and thus the progress of the deformation can be recorded for a long time without interruption.

In the current configuration of GRIMONIT, up to 13 measuring probes are set up and are switched sequentially to the pressure sensors. One of these is the reference probe, whose pressure is switched to both sides of the differential pressure diaphragm simultaneously for “zeroing”. The diaphragm prevents the fluid from equalizing, as is the case with a hose scale. The deflection of the diaphragm is converted into an electrical signal, which is a measure for the difference in height between the probes. All measuring probes are switched to the same sensor combination. A measuring cycle, including the zero probe, can be executed in any time interval. In this way, a possible offset drift of the membrane is detected and a possible deviation is corrected with each pass of all measuring positions.

The measuring liquid is pumped from an internal reservoir to the measuring probes (Figure 5). Another tube is used to flush the measuring tube to remove possible air pockets from the liquid. With the LAS-Meter, it has been shown that air bubbles in the tubes of hydrostatic measuring systems are often the cause of incorrect measurements.

Nevertheless, air bubbles can also form inside the GRIMONIT tubes with time. GRIMONIT is therefore equipped with a venting routine that regularly - or manually triggered - vents the measuring tube. The third tube “air” (see Figure 5) connects all measuring probes so that all measuring probes are exposed to the same air pressure. To precisely control how much liquid is transported to the probes, the instrument is equipped with a dosing unit.

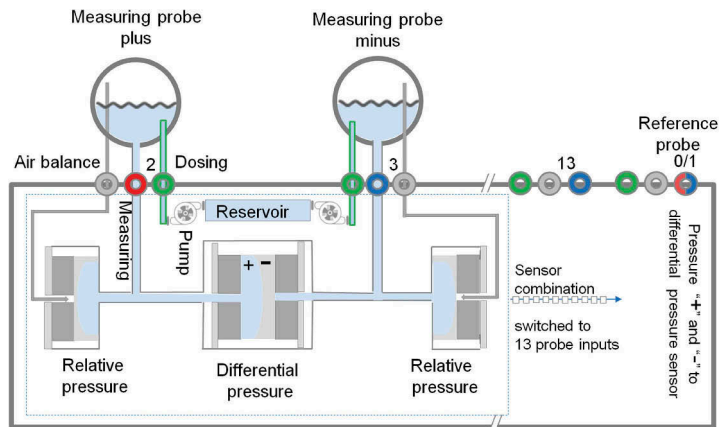


Figure 4. Measuring principle of GRIMONIT: The differential pressure of 2 measuring probes and the relative pressures of each probe are continuously recorded. This combination is switched sequentially to the other measuring inputs with valves. The liquid level in the measuring probes is controlled via the dosing line.

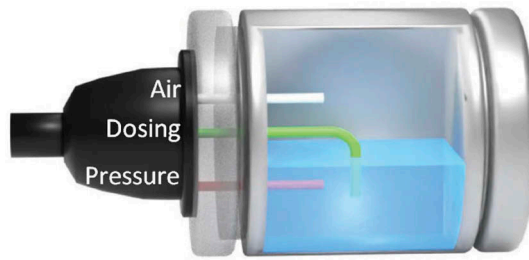


Figure 5. Measuring probe with symbolically drawn connections for pressure, dosing and air compensation. The probe does not contain any electronics and is therefore insensitive to overvoltage.

3 CALIBRATION AND ACCURACY

The most accurate hydrostatic measurements are obtained when an open continuous water surface is available and the distance to the water surface can be measured. This is proven by the results of 192 sensors we installed on a circumference of 300 m in the “Swisslight Source” accelerator at PSI (Paul Scherrer Institute) and that have been operating continuously since 2001. All these so-called HLS sensors register the movement of the base of the accelerator within earth tide resolution, comparable to the record in Figure 2. Optimal measurement conditions were present at the Albigna dam as well as at the accelerator at PSI. For both measurements only a very small measuring range needs to be covered.

While the evaporation of liquid in the HLS measurement at the PSI accelerator has not caused any measurement errors, the loss of liquid in the Albigna measurement with the LAS-Meter caused a significant measurement error over the years.

Basically, GRIMONIT is equipped with the same measuring elements as the LAS-Meter. We can therefore assume that equal results will be achieved under comparable measuring conditions. However, in contrast to the LAS-Meter, the error due to loss of liquid is solved by the recalibration feature of GRIMONIT.

The volume of the measuring liquid increases at high temperatures and causes the level in the measuring probes to rise. The larger the liquid surface area of the measuring probe compared to the cross-section of the measuring tube, the less significant is the temperature-related expansion of the measuring liquid. In the relative pressure range, the expansion of the measuring liquid leads to a measurement error, since this increases the liquid level. However, this can easily be corrected with an additional temperature measurement and a calibration function. In the differential pressure range of the instrument, on the other hand, a change in temperature has no effect, since the liquid surface levels of both measuring probes change by the same amount. In general, the effect of the temperature is minimal for all hydrostatic measuring systems if the measuring probes and the tube delivery are at the same height at the beginning of the measurements.

Other error sources are air bubbles in the liquid. The tube in Figure 6 was filled without bubbles and was immediately connected to the probe. After two days, many air bubbles appeared.

Errors caused by growing air bubbles cannot be easily distinguished from real elevation changes. To eliminate such errors, GRIMONIT flushes the measuring tube before each calibration.

With a test setup in the laboratory, see Figure 7, the possible error influences were investigated. Probe samples of vertical and horizontal layout and different sizes were fixed in pairs on platforms between the floor and the ceiling. The paired probes on each platform could be measured within the range of the differential pressure sensor; the probes between the platforms could only be measured with the relative pressure sensors.

For testing the reaction at distant measuring points, probe 6 was connected to a 100 m tube with a diameter of 2.7 mm. The longer the measuring tube and the smaller the diameter, the slower is the reaction time. The time constant is a measure for defining the reaction time of

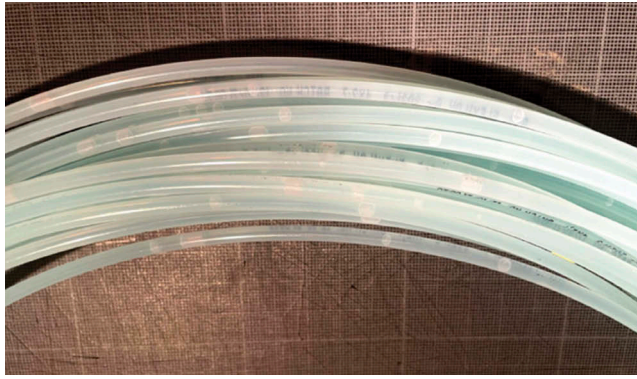


Figure 6. Liquid tube 2 days after first filling. Many bubbles were formed in the liquid during 2 days.

a measurement. It is defined as the elapsed time to reach $1/e = 36.8\%$ of the final value of the step. For the 100 m tube, the measured time constant was 3.8 seconds.

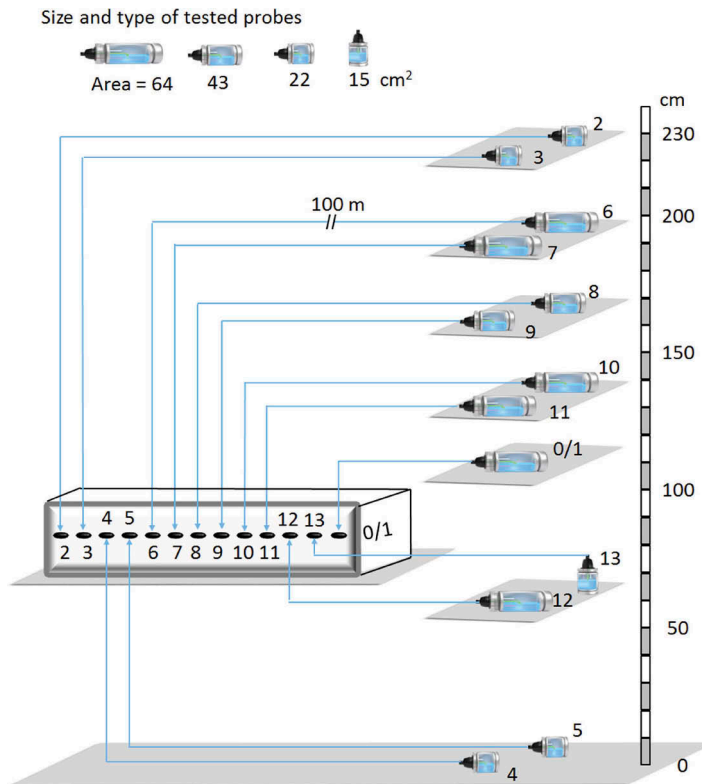


Figure 7. Test setup in the laboratory with probe levels from 0 cm to plus 230 cm.

4 APPLICATIONS

Siliceous limestone is mined in the Zingel quarry, near the town of Schwyz (central Switzerland). As part of the early excavations, a large hole was created that seemed ideally suited as a landfill (Figure 8). In 1997, a project plan for the storage of refuse slag was elaborated. In the rear area of the quarry siliceous limestone would still be mined and the material would be transported through the landfill body via a tunnel on a conveyor belt. The project was approved.



Figure 8. The Zingel quarry. The marked part of the early excavation was to be filled with waste slag, while siliceous limestone is still being mined in the rear part (Lumpert ZKRI, 2000).

As the nature reserve of Lake Lauerz is located in the immediate vicinity, eight inclinometer monitoring tubes were installed to monitor settlements below the landfill sealing. The tubes are accessible from the conveyor tunnel for the measurements. The objective was to record any subsidence of the landfill base due to further replenishment. The aim was to estimate the risk of cracking and leakage of the base barrier.

Since the zero measurements from the year 1996, the landfill has been monitored for over a period of 10 years using commercially available hydrostatic measuring systems and horizontal inclinometers. Due to the contradictory measurement results of the two systems, the person responsible for the landfill started looking for an alternative. He found the solution at the ETH. He decided to use the LAS-Meter.

The first measurements with the LAS-Meter were successfully carried out in 2010. In 2021, another measurement was carried out using GRIMONIT. The measurements with GRIMONIT were significantly less time-consuming as described in chapter three, because the filling and calibration were carried out automatically. GRIMONIT eliminates the maintenance work required with the LAS-Meter and the time-consuming troubleshooting in the event of air inclusions in the system. The control unit, all pumps, valves, and the reservoir are compactly housed in a central unit (chrome steel box Figure 9).



Figure 9. Deformation measurement of the landfill base in the Zingel landfill with GRIMONIT. A sliding rod is used to place the probe into the inclinometer tubes in meter increments. The pressure signal is transmitted via the 50 m long pipe drum. The differential pressure between the probe in the inclinometer tube and the moving reference probe is used to calculate the course of the inclinometer tube.

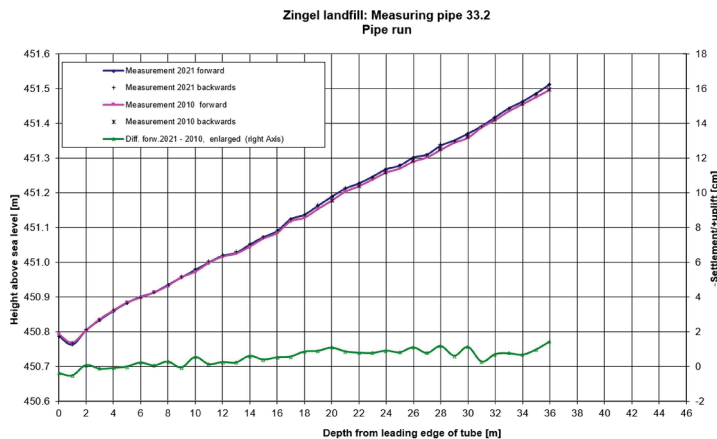


Figure 10. Measurement results from inclinometer tube 33.2, red line: forward and backward measurement 2010, blue line 2021, green line: difference of the two measurements, right scale.

5 CONCLUSION AND OUTLOOK

The 2021 measurement performed with GRIMONIT required a small fraction of the in-situ maintenance time needed in 2010 with the LAS-Meter. With the LAS-Metersystem, all pumps and valves had to be operated manually and it was necessary to wait a long time in the underground until the tubes were clear of air bubbles. However, in 2021, with GRIMONIT the work effort at the quarry was limited to the on-site setup of the system. Time-consuming venting could be conveniently triggered via a remote connection (Internet) at the push of a button.

Similarly, the time required in other fields of applications is shortened. In landslide areas, for example, with several measuring points, only the setting of the measuring probes and the installation of the supply lines are required. All other work steps, such as filling, venting, and calibrating, are performed by GRIMONIT. Once installed, all functions can be controlled and monitored in real time, from the office, via the Internet.

Another advantage of GRIMONIT is the flexibility to use the central measuring unit both continuously and periodically. For an initial hazard assessment, it is usually recommended to leave the GRIMONIT on site and measure continuously. Later on, it can be sufficient to measure after longer time periods as at the Zingel quarry. But inclinometer tubes are not available at every location. It is also possible to install the measuring probes and tubes and leave them permanently at the measuring points, while the GRIMONIT-System is connected later and removed again after performing the measurements.

GRIMONIT succeeds in recording deformations independent of weather conditions; it can also be used in underground mining or in agriculture for estimating soil resilience to compaction due to trafficking with heavy machines. This results in numerous new application possibilities that are waiting to be exploited.

Thanks to financial support from the Federal Office for the Environment (FOEN), cooperation with the University of Applied Sciences Rapperswil and the Swiss Federal Institute of Technology (ETH), and our five industrial partners, GRIMONIT is now available as a versatile and flexible early warning measurement system for vertical movements.

What we are looking to now, is to extend the long-term field experience. The measuring probes tested so far are constructed with Plexiglass, so that the liquid level can be visually checked at any time. In a final, robust version, the probes will be made of metal and the tubes will be appropriately protected to suit the environmental conditions. For this purpose, it makes sense to cooperate with high-voltage cable builders who already have a lot of experience in underground cable installation. In addition, the components installed in GRIMONIT and the control system software can be optimized to reduce energy consumption.

Therefore, interested collaboration partners who are willing to help with practical application and further development are welcome.

REFERENCES

- Emter, D., Zürn, W., Mälzer, H. (1989): Underground Measurements at Tidal Sensitivity with a Long Baseline Differential Fluid Pressure Tiltmeter. Deutsche Geodätische Kommission, Reihe B, 288, 74p.
- Lumpert, R., Zkri (2000) Orthophoto Zingel Steinbruch.
- Meier, E., Ingesand, H., (1996): Ein neuartiges hydrostatisches Messsystem für permanente Deformationsmessungen, XII Internationaler Kurs für Ingenieurvermessung, Graz – Band 1, Verlag Dümmler, Bonn, ISBN 3-427-78101-9.
- Meier, E., Geiger, A., Ingesand, H., Licht, H., Limpach, P., Steiger, A., Zwysig, R., (2010): Hydrostatic levelling systems: Measuring at the system limits. *Journal of Applied Geodesy* 4 (2010), 91–102 de Gruyter 2010. DOI 10.1515/JAG.2010.
- Thierbach, H. (1979): Hydrostatische Messsysteme, Herbert Wichmann Verlag, Karlsruhe.

Arch dams: A new methodology to analyse the sliding stability between the dam and the foundation

X. Molin, C. Jouy, S. Delmas, P. Anthiniac, G. Milesi & C. Noret
Tractebel Engineering, France

ABSTRACT: Arch dams transfer the hydrostatic forces to the foundation, by arch effect. Due to their hyperstaticity, they usually benefit from a significant safety factor. The potential sliding at the dam/foundation contact is a failure mode highlighted by most of the international recommendations. Recent FEM analyses carried out on operational dams confirm that thermal cases can be sensitive conditions, especially in summer. Back analyses require generally to introduce high shear strength on the dam/foundation interface, considered unrealistic, to demonstrate the past good dam behaviour. Tractebel has developed a methodology which takes into account the irreversible displacements which can occur in this area, and the redistribution of internal forces. It has been inspired by the latest CFBR recommendations on arch dams. This methodology was applied to three existing thin arch dams, located in France, in wide valleys. Back-analyses calculations were performed on historical loads. This method provides more realistic shear strength values (friction angle of 55 degrees or less) to justify the observed good behaviour of the dams, while larger values, greater than 70 degrees, were required if no displacement was accepted. Finally, the possibility of accepting irreversible displacements at the dam/foundation interface opens the discussion of the peak and residual shear strengths. Definition of acceptable irreversible displacements is discussed.

RÉSUMÉ: Les barrages voûtes transfèrent les forces hydrostatiques à la fondation par effet voûte. Ils bénéficient généralement d'un facteur de sécurité important. La stabilité au glissement du contact barrage fondation du barrage est un mode de rupture retenu par la plupart des recommandations internationales. Les modèles EF récents réalisés sur d'anciens barrages confirment que les cas thermiques peuvent être des conditions sensibles, surtout en été. Les rétroanalyses nécessitent d'introduire une résistance élevée au cisaillement, considérée comme irréaliste, pour démontrer le bon comportement du barrage observé jusqu'à présent. Tractebel a développé une méthodologie qui prend en compte les déplacements irréversibles qui peuvent se produire dans cette zone, et la redistribution des efforts internes. Il s'inspire des dernières recommandations du CFBR sur les barrages voûtes. Cette méthodologie a été appliquée à trois barrages voûtes minces existants, situés en France, en vallée large. Des calculs de rétro-analyse ont été effectués sur les charges historiques. Cette méthode fournit des valeurs de résistance au cisaillement plus réalistes (angle de frottement de 55 degrés ou moins) pour justifier le bon comportement observé des barrages, tandis que des valeurs plus importantes, supérieures à 70 degrés, sont requises si aucun déplacement n'est accepté. Enfin le principe des déplacements irréversibles ouvre la discussion sur les résistances au cisaillement de pic et résiduelle. La définition des déplacements irréversibles acceptables est discutée.

1 INTRODUCTION

Recommendations have recently been published in France by the CFBR (French Committee for Dams and Reservoirs) for the assessment of existing arch dams behaviour.

During the discussions, it appeared that there were different practices to analyze the loads transmission from the dam to its foundation. Different criteria have been proposed.

This article focuses only on the analysis of shear forces at the interface between dam and foundation. The first paragraph describes the failure mode, as well as the calculation methodology that has been developed.

The second paragraph presents an application on three existing structures.

The last paragraph discusses the impact and acceptability of irreversible displacements.

2 PROPOSED METHODOLOGY FOR VERIFYING THE SLIDING STABILITY AT THE DAM–FOUNDATION INTERFACE

Among the different failure modes of an arch dam, one concerns the sliding stability along the dam and foundation contact. This failure mode is similar to the one analyzed on gravity dams, but with a more complex development due to a non-planar and 3D geometry, and the significant influence of internal forces as thermal loads.

These two specificities allow in theory some adaptations; excessive local shear stresses could be transferred to less loaded areas; and internal forces could be partially dissipated with the allowance of small local irreversible displacements. Consequently, it is recognized that usual design criteria for sliding stability (like the Shear Friction Factor) can be exceeded locally, without compromising the dam stability. However, the methodology and associated design criteria to analyze these adaptations are innovative and thus not fully defined.

2.1 Recommendations

Available recommendations are extracted from USACE (1994), USBR (2006), ANCOLD, Swiss, and CFBR (2021). Most of them give some safety factors, applied to ratio between the strength resistance and the applied shear force, without defining the way to calculate shear forces. This question is not trivial, since the contact of the dam and foundation is not planar: it is possible to consider local shear stresses, or discretize the surface into several smaller areas, more or less planar, and calculate the safety factor on each of them.

Swiss practices give the opportunity if the stresses exceed the admissible values, to demonstrate a redistribution of stresses.

Finally, the French recommendations present a progressive approach, which takes advantage of recent evolutions of numerical models (computer processing power and constitutive laws):

- A first step, with a linear elastic analysis. The dam-foundation interface is divided in several areas, and a common safety factor is calculated for each of them. If low safety factors are found, a second step is proposed, by considering irrecoverable displacements in the model.
- A second step, with the modelling of a joint including allowance for sliding and opening (Coulomb law) in the numerical model (FEM or FDM). The safety factor is not calculated on local forces but on the global equilibrium of the structure through a c and ϕ reduction analysis: the cohesion and friction angle are progressively decreased until reaching the numerical divergence of the model, interpreted as a global rupture. This numerical method is commonly applied to landslides, for which the sliding surface is frequently not planar.

French recommendations are provisionally published, expecting feedback from the Consulting Engineers on this proposed methodology. A main point concerns the acceptability of irreversible displacements, which could decrease the shear strength (from peak to residual) and modify the permeability and uplift pressure distribution.

2.2 Methodology

The proposed methodology is inspired by the French recommendations. It was applied on existing dams, for which usual method based on forces failed to explain the good observed behaviour of the dam, without unrealistic strength values of cohesion or friction angle at the interface between dam and foundation.

Analysis focuses on back analysis in order to compare or validate design criteria and methodology with load conditions already experienced by the dams and for which no damage or abnormal behaviour were observed.

The arch dam is analyzed through finite element method. Dam and foundation are modelled. Numerical joints are introduced:

- Between each vertical block, which allows to simulate a realistic stress distribution during the construction period, before grouting of the contraction joints. Vertical joints are disabled during construction stage, so that each block is independent. Vertical joints are enabled before reservoir impounding.
- Between the dam and the foundation. This joint allows the analysis of shear stresses along this contact, through dedicated post-processing, or non-linear constitutive law, like Coulomb friction, which allows to simulate contact sliding or opening.

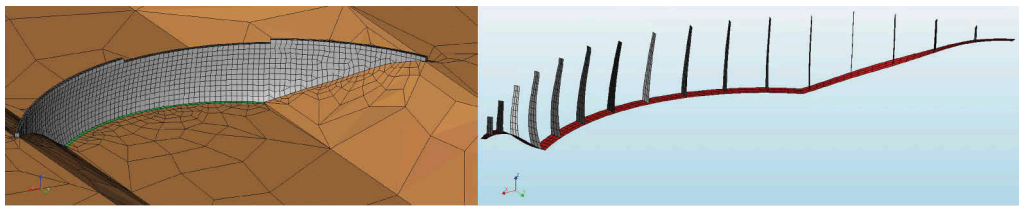


Figure 1. Dam mesh (left), and joints (right) between vertical blocks and dam-foundation interface.

After a first analysis in forces, a c and ϕ reduction analysis is performed at the dam interface contact. However, local conditions/characteristics can be modified with the development of irreversible displacements:

- The apparent shear strength decreases, due to the loss of cohesion and roughness
- The permeability may increase with subsequent change in uplift pressure distribution

Two effects are opposed in this adaptation process: the mobilization of adjacent zones and the reduction of internal forces, which are favorable to stability, and a possible reduction of shear strength and increase of uplift pressures, which are unfavorable. The classical c and ϕ reduction method is not enough to conclude on the behaviour, and a control of the displacements is essential.

Acceptability of irreversible displacements is discussed in the last paragraph of this paper.

The c and ϕ reduction method allows analyzing the increase of the irreversible displacements of different blocks with the shear strength decrease. Such analysis allows to define:

- Shear strength values for which irreversible displacements are considered acceptable
- Shear strength values for which the global equilibrium is reached (numerical convergence), but the magnitude of the irreversible displacements is such that adverse conditions may appear like shear strength decrease toward residual values or change in pore-pressures distribution
- Shear strength values for which the global equilibrium is not reached (numerical divergence)

This methodology has the advantage to separate the analysis of the adaptation process (FEM or FDM) and the discussion of acceptable irreversible displacements.

3 APPLICATION TO DAMS

3.1 Dam 1

Dam 1 is a 23 m high dam built in the 1960s. The ratio between the crest length and maximum height is about 7. The arch dam is therefore located in a wide valley.

The low values of bank slopes generate a high incidence angle of the forces applied by the dam to the foundation.

A back analysis was performed to estimate the apparent shear strength requested to justify the dam stability observed until now. Reservoir level is usually well monitored, and the reading frequency is suitable for a good representativity of the lake level variations. On the other hand, the ambient air temperature data at the dam site are often lacking or are not representative (a single daily temperature measurement is not relevant due to the daily temperature variations and to the dam thermal inertia). Consequently, daily average temperature series have been acquired from official weather service to complete the reservoir level data. Statistical treatment allows to determine annual minimum and maximum mean-daily-temperature for different return periods. Historical representative loadings are easily identifiable on the graph below and used in the back analysis.

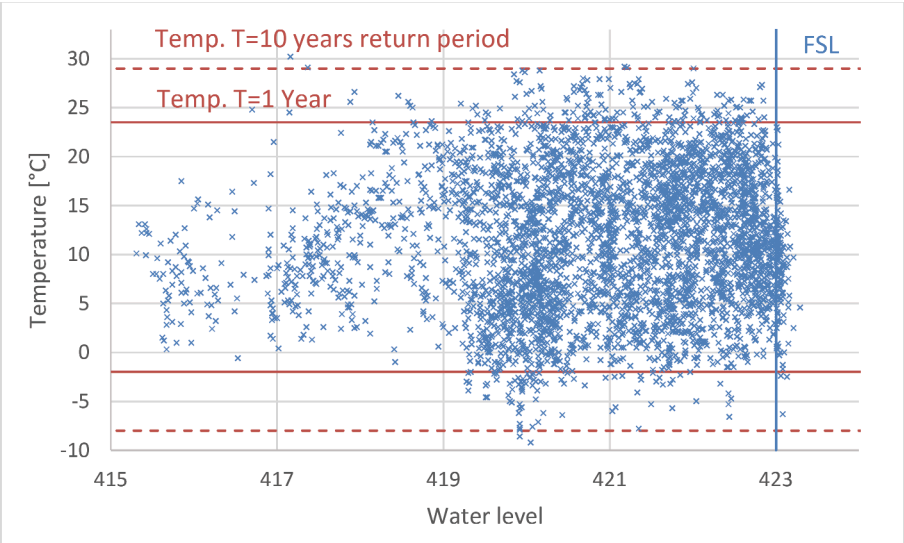


Figure 2. Dam operation, water level vs mean daily temperature.

A first back analysis was performed. The sliding of the dam/foundation contact is not allowed. Shear and normal forces are calculated for each block. Mobilized friction angle varies from 45 degrees at the bottom of banks to 75 degrees in the upper part. If the forces are averaged on each bank, the average friction angle is about 60 degrees.

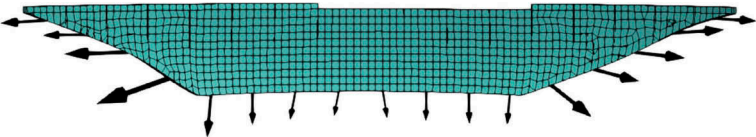


Figure 3. Forces applied by the dam to the foundation for usual summer temperature and normal water level.

A second back analysis considers the possibility of sliding, if the shear stresses exceed the shear strength parameter value in the FEM model. The shear strength is gradually decreased, and the displacement of each vertical block is plotted. In the following Figure 4, the “Plot Q” corresponds to the block at the upper part of the left bank, and the “Plot N” at the lower part of the same bank. Two cases have been considered: with the first one only the friction angle participates to the shear strength and the cohesion is neglected. For the second one, the friction angle remains constant at 45 degrees while the cohesion is adjusted.

For both cases, upper blocks are more loaded and are the first to slide. When all blocks are sliding, numerical divergence occurs. By neglecting the cohesion (left figure) a friction angle greater than 75 degrees is requested for an elastic linear behavior. Between 65 to 75 degrees

irreversible displacements occur but remain moderate. Below 55 degrees, numerical divergence occurs. By considering the cohesion (right figure), very high cohesion value, closed to arch compressive stresses, is requested to avoid irreversible displacements. At 2 MPa, moderate irreversible displacements already occur. Variation are small up to 0,75 MPa, and divergence occurs at 0,5 MPa. The calculated stresses pattern in the dam is not much modified with the sliding if the friction angle remains higher than 50° or if the cohesion (with a 45° friction angle) remains higher than 0,5 MPa. Based on this back-analysis, it is difficult to justify that no irreversible displacement occurred. On the other hand, small adaptation leads to minor change in the stress pattern of arch dam. It is possible that small irreversible displacements occur at the dam-foundation interface, without being easily detected by the monitoring.

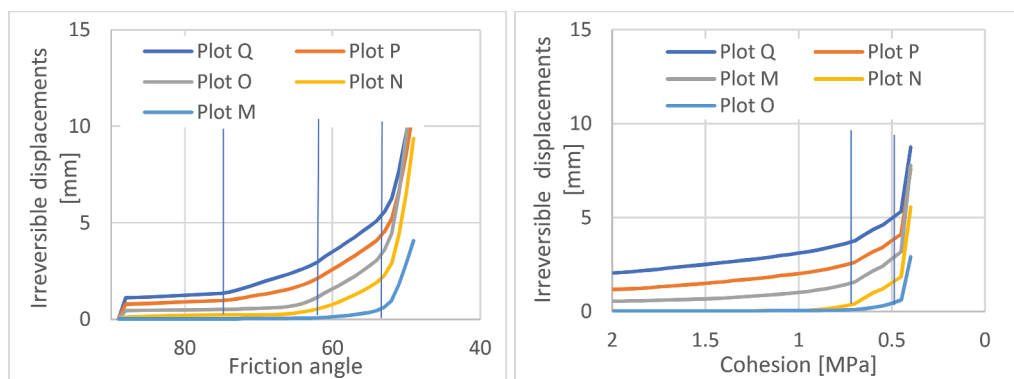


Figure 4. Irreversible displacements according to friction angle, or cohesion (for 45° of friction angle).

3.2 Dam 2

Dam 2 is a 27,6 m high arch dam built in 1945, in a wide valley. The dam is a simple curvature arch dam, with a vertical upstream face and a downstream face inclination of 1/5. Its thickness varies from crest to its base (1.5 m at crest).

Measurements of daily water level and air temperature (from the nearest reliable weather station) over the last 30 years were collected in order to identify the maximum historical loadings experienced by the dam. 3 cases were selected for a back analysis (see chart below):

- R_A3: air temperature close to yearly summer temperature (T1), with upstream level 50 cm above normal reservoir water level (NWL)
- R_A2: upstream level is equal to NWL with air temperature between yearly (T1) and ten-year summer temperature (T10)
- R_A1: air temperature is equal to ten-year temperature (T10) with upstream level 64 cm below NWL

A progressive approach was performed for the back analysis. The analysis focuses only on normal and tangential stresses at the interface between dam and foundation. At first, a linear elastic analysis was carried out.

The good observed behavior of Dam 2 allows us to consider safety factor (regarding sliding along the interface) is at least equal to 1 for these three historical loadings. Thanks to this assumption, minimal strength of dam and foundation interface can be estimated. The Table 1 below gives the results for Dam 2. The contact surface was discretized into several smaller areas, more or less planar, in order to calculate the safety factor on each of them.

The linear elastic analysis shows that a friction angle between 70 (right bank) to 80° (left bank) is required to justify the good observed behavior. The data range is high and above usual strength considered in dams' stability calculations.

As the previous analysis failed to explain the good observed behavior with reasonable strengths, a second step was performed through the simulation of joint sliding and opening

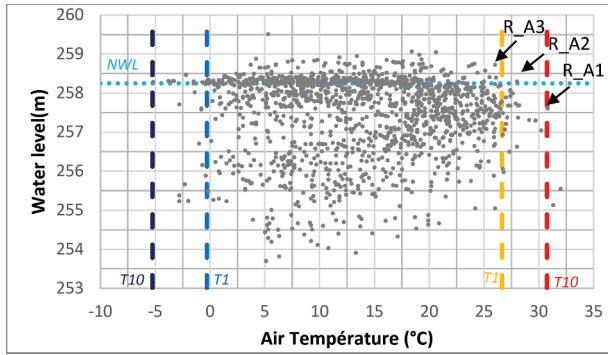


Figure 5. Air temperature vs daily water level.

Table 1. Dam 2 back analysis – average of minimal friction angle.

Case	Parts of the dam	Average of minimal friction angle (with no cohesion)
R_A1	Right bank blocks (incl. abutment)	61°
	Left bank blocks (incl. abutment)	59°
R_A2	Right bank blocks (incl. abutment)	60°
	Left bank blocks (incl. abutment)	64°
R_A3	Right bank blocks (incl. abutment)	60°
	Left bank blocks (incl. abutment)	65°

(Coulomb law) in the numerical model (FEM). A c and ϕ reduction analysis was performed: the cohesion and friction angle were progressively decreased, until the numerical divergence interpreted as a global failure. Results are presented on the chart below.

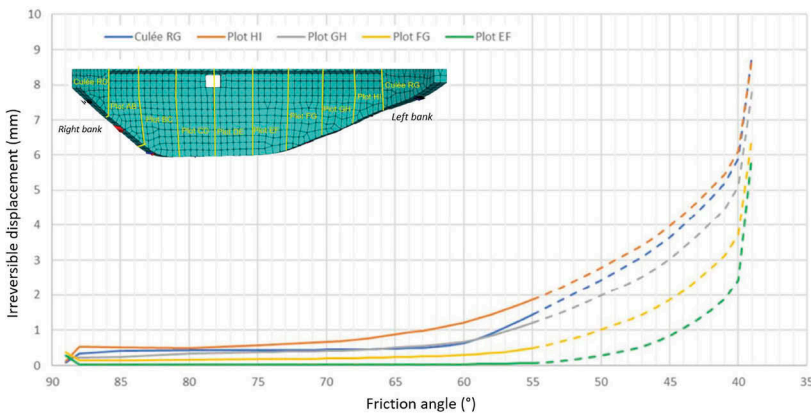


Figure 6. Friction angle vs irreversible displacements.

Because of the hyperstatic behavior of the arch dam, some adaptations can take place. With the progressive decrease of the mechanical characteristics of the dam/foundation interface, the model shows that, as long as friction angle is greater than 40 degrees, Dam 2 is able to find a new stable equilibrium. Irreversible displacements reach 2 to 6 mm (from center of the valley to the left bank).

Numerical divergence appears for friction angle smaller or equal to 40 degrees.

This graph also shows that if an irreversible displacement of 2 mm is deemed acceptable, the friction angle of the dam/foundation contact must be greater than or equal to 55 degrees. This value, lower than the one from the linear elastic analysis, is considered more realistic for numerical friction angle of dam/foundation interface.

The maximum displacement is observed on the left bank of the dam (“plot HI” and « left thrust bloc »).

3.3 Dam 3

Dam 3 was built in the early 1950s and is used to supply drinking water.

Its current height is 38 m and it consists of a thin cylindrical arch dam, with constant thickness of 2 meters in the upper part, thickened by one meter on the downstream side in the lower part. It has been built across a wide valley ($L/H = 3,6 > 3$). On the right bank, the dam is completed with a gravity abutment.

Crest raising works have been done after 20 years of operation in order to increase the capacity of its reservoir (normal water level have been increased by 3,5 m). On this occasion, the right bank abutment have been already reinforced.

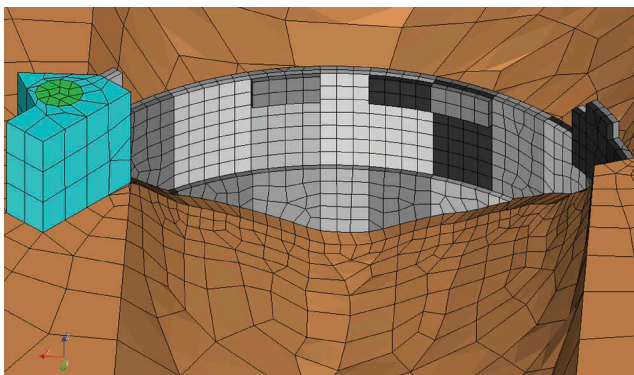


Figure 7. General view of the mesh of Dam 3.

The dam suffered a major flood on 12/01/1988 (maximum flood experienced by the dam), which raised the level of the reservoir at 125.5 m NGF, close to the MWL level (126.5), and well above the NWL level (120.5).

This historical loading is the most unfavorable loading that experienced the structure. The structure did not suffer any damage during this event. The assumptions (contact strength) of the modelling must therefore be consistent with this observation. This historical loading was modelled, and the strength at the contact between the dam and the foundation was calibrated in such a way as to justify the non-sliding of the dam without any safety margin ($SFF = 1$).

This back-analysis was carried out by considering several scenarios, first with the assumption of a linear elastic behavior of the dam/foundation interface, then by allowing the opening of the contact between the dam and the foundation. The forces transferred to the foundation are oriented differently, but the required strength is similar.

Based on this back analysis, the following parameters are required:

- 85 degrees of friction angle at the crown cantilever
- 70 to 40 degrees at bank, from the bottom to the top

The lower part of the dam is more loaded, because the maximum historic loading is related to a hydrostatic loading (flood) instead of thermal loading as in the previous examples.

By considering irreversible displacements, required friction angle is reduced to 55 degrees, which was used to design the dam reinforcement works.

4 DISCUSSION ON THE ACCEPTABILITY OF IRREVERSIBLE DISPLACEMENTS

4.1 *Is a small irreversible displacement credible?*

Through the above given examples, back analysis request very high shear strength (up to 70 degrees of friction angle) to avoid sliding at the dam/foundation contact, which is larger than what is commonly accepted for gravity dams (45 degrees).

For two out of the three analyzed arch dams, the observed behaviour was deemed satisfactory: no drift detected on monitoring instruments, no abnormal readings, no cracking. . .

Allowing small irreversible displacements on numerical modelling allows to find more realistic values for shear strength (50 to 60 degrees of friction angle with a nil cohesion). The question is: do such irreversible displacements really occur or are they related to numerical modelling assumptions?

The use of a joint at the contact of the dam/foundation may be considered as a very strong assumption. Regardless of possible unfavorable orientation of rock discontinuities in the foundation, the contact dam/foundation is a geometrical weakness surface for sliding which may justify the location of a numerical joint. Considering the opening of the joint, this is more disputable because the tensile stresses leading to the opening of the joint may be distributed in the foundation and/or in the concrete.

Regarding the possible occurrence of irrecoverable displacements, several laboratory tests on dam/foundation contact samples obtained from coring have been analyzed and it was observed that the increase of shear stress is progressive, until reaching a peak strength after 1 to 5 mm of shearing, before rapid decrease towards residual strength. The number of analyzed tests is not enough to quantitatively conclude on representative displacement values at peak, but it emphasizes that significant displacements may be mobilized before reaching the peak strength value. The occurrence of such displacement may allow dissipating internal forces caused by thermal loading. . .but should be observed on monitoring instruments, at least as reversible (or partially reversible) displacement.

4.2 *How to define acceptable irreversible displacements*

Irreversible displacements may be acceptable, as long as they do not lead to a loss of shear strength or change in pore-pressure distribution that may endanger the dam foundation. It is simple to write, but hard to clearly define critical values.

For the given examples, back analysis of maximum loading cases allowed a calibration of interface shear strength parameters to fit the simulated behavior to the observed behavior. This allowed a suited design for the strengthening works of the dams (all of them have been or are under rehabilitation in order to improve the load transfer from the dam to the foundation, with prestressed anchors). However uncertainties remain important, and the Authors indicate that for one dam, a specific extreme case was applied, considering residual strength in some areas, to design the dam strengthening works.

The authors recommend to perform shear strength laboratory tests on dam/foundation contact through samples obtained by coring. Tests have to be carried out under high normal stress (1 MPa) with accurate measurement of tangential and normal displacements. The influence of macro-rugosities cannot be assessed by such laboratory tests but the residual strength and the tangential displacement at the peak strength can be considered as representative for simulation purpose.

The authors recommend also to improve the dam monitoring system in the areas where irreversible displacements are numerically found in order to check actual displacements and potential variation of uplift pressures.

REFERENCES

- CFBR, 2021, *Recommendations for the safety assessment of arch dam behavior*.
USACE, 1994 EM 1110-2-2201, *Arch Dam Design*.
FERC, 1999, *Engineering Guidelines for the Evaluation of Hydropower Projects*.

Spitallamm Arch Dam – Challenges faced for replacing the existing Old Dam

E.A. Odermatt & A. Wohnlich
Gruner Stucky Ltd, Renens, Switzerland

ABSTRACT: The 113 m high Spitallamm arch-gravity dam, together with the Seeuferegg gravity dam, form the Grimsel reservoir with a live storage of 94 Million m³ at an altitude between 1'800 and 1'900 masl in the Swiss Alps (Canton of Bern). The dam was erected from 1926 to 1932. It was at that time one of the highest concrete dams in Europe. The dam is set in a narrow gorge cut mainly in Aare granite and granodiorite, both rocks of high strength and low deformability.

After almost one century of operation, the dam has to be replaced, following damages at the upstream dam face. The 113 m high new Spitallamm arch dam is currently being constructed downstream of the old arch-gravity dam. The dam completion and first impounding are scheduled in 2025. The old arch-gravity dam will remain in place and be flooded in the new reservoir.

The paper explains the context for such replacement, addressing first the reasons why the old dam has to be decommissioned, then explaining how it was decided to go for a completely new dam located right downstream of the existing dam, and finally presenting selected interesting technical issues.

1 INTRODUCTION

The existing Spitallamm gravity-dam was built from 1926 to 1932. It is built on the Northern part of the Grimsel pass route on the Aare River and together with Seeuferegg gravity dam built simultaneously, form the 94 Million m³ Grimsel reservoir.

After almost one century of operation by the Kraftwerke Oberhasli (KWO), the existing dam shows increasing signs of ageing, and KWO reasonably decided to replace the dam by the construction of a new double curvature arch dam. Due to topographical constraints, the new dam is being constructed immediately downstream of the old arch-gravity dam and after impounding, this latter will therefore be flooded in the increased reservoir. This layout offers the possibility for KWO to continue operating the Grimsel reservoir during construction and until decommissioning of the old existing dam. In addition, given the proximity of both dams, the environmental impact is strongly limited, which is also an asset to the project. Finally, considering a possible future raising of the reservoir, the arch dam is anticipatedly designed to be heightened.

However, the closeness of both the old and the new dams triggers all sorts of challenges, spanning from specific design checks (such as the impact of the new dam foundation excavation on the old dam behavior) to the construction organization and logistics in such cramped available space.

After a short historical reminder on the existing, almost 100-year-old dam, an overview of the design process is provided below, giving emphasis on some critical issues specific to this project. In particular, the increased monitoring procedure of the existing dam during works and the tailor-made new dam commissioning (impounding of the reservoir) are presented and addressed in this article.

Finally in years 2010, the project had to be postponed and given up mainly due to opposition by environmental NGOs, but also for technical reasons. Namely the existing dam concrete, which is now nearing 100 years of age, was found deteriorating and unsound to accommodate the dam raising. Thereafter, a different solution had to be investigated, especially since the existing dam was slowly coming to a point where it would not meet the safety requirements enforced in Switzerland. KWO then decided to go for a solution of dam replacement. The main advantages of replacing the existing dam vs keeping it and rehabilitate it are mostly three:

- During the entire new dam construction work, it is possible to operate the existing dam (as its safety is not critical) and the Grimsel Reservoir. This is a key economical asset.
- While designing the new dam, the option of potentially raising it in future can be anticipated and considered.
- Replacing the old dam by a new dam located immediately downstream (see Figure 2 below) causes very limited impact on the environment.

On the other hand, the main drawback of such solution is what makes this project so special and challenging, namely the very limited space to build the new dam right at the toe of the existing dam due to topographical and access constraints. The use of 3D modelling and open BIM exchange standards helped considering all project elements and their interferences, cohabitation and possible clashes during the design and construction phases.

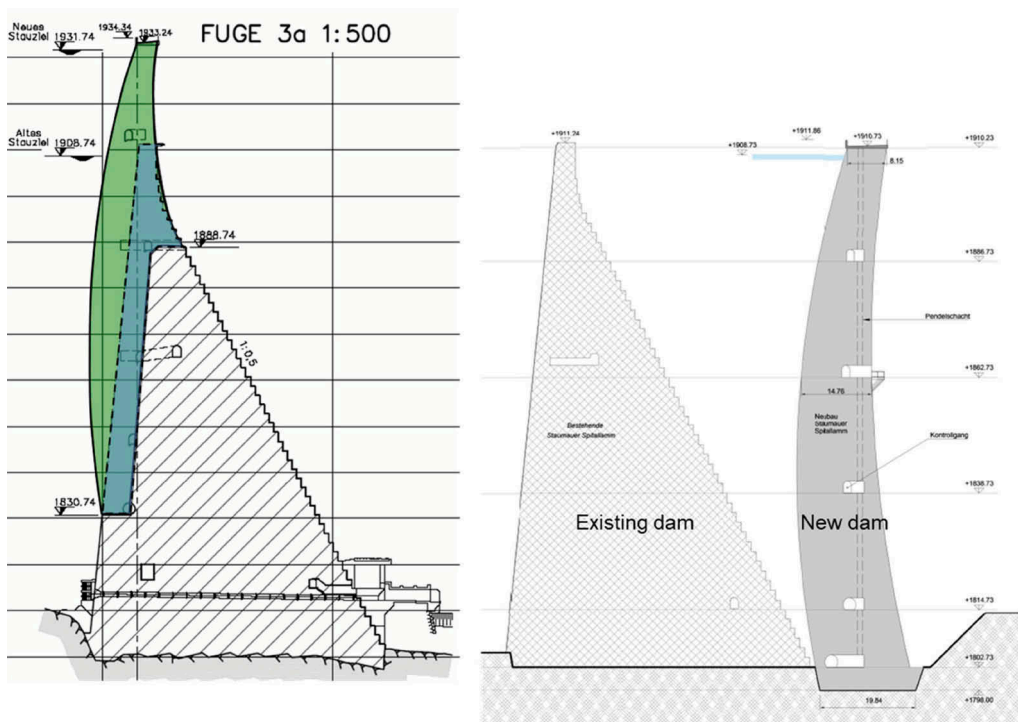


Figure 2. Left: Spittalamm arch dam heightening as designed in the late 1990s. The project was not implemented and given up. Right: Spittalamm arch dam replacement with a new, downstream double curvature arch dam.

3 NEW SPITALLAMM DOUBLE CURVATURE ARCH DAM

The replacement project foresees a new, double curvature arch dam, immediately downstream of the existing dam. The shape was designed based on the actual state-of-the-art of dam engineering, international standards and adjusted with the designer's own database of arch dam

shapes, based on its long experience in dam and arch dam design. The 113 m high dam is designed to be possibly heightened by 23 m in future. The concrete volume of the new arch dam is about 210'000 m³.

The existing dam will be left in place and flooded. This will therefore create two separate reservoirs, the existing *Grimselfsee*, and the new so-called *Zwischensee*, or intermediate reservoir. The existing dam safety is ensured as it is permanently in balance between upstream (US) and downstream (DS) water pressure. To ensure this balance, a “communicating vases” system is built, with connections between the two reservoirs at two different levels. A gallery with a cross section of 5 m² will be blasted through the existing dam after its decommissioning. At another level, the existing galleries system of the dam, with accesses to the downstream face, will be flooded thanks to five boreholes to the upstream face. As the crest levels of both the old and new dams are the same, the old crest will remain unflooded and visible at all times. In case of possible future heightening of the new dam, the old dam will be completely flooded, and will re-appear only with low reservoir levels.

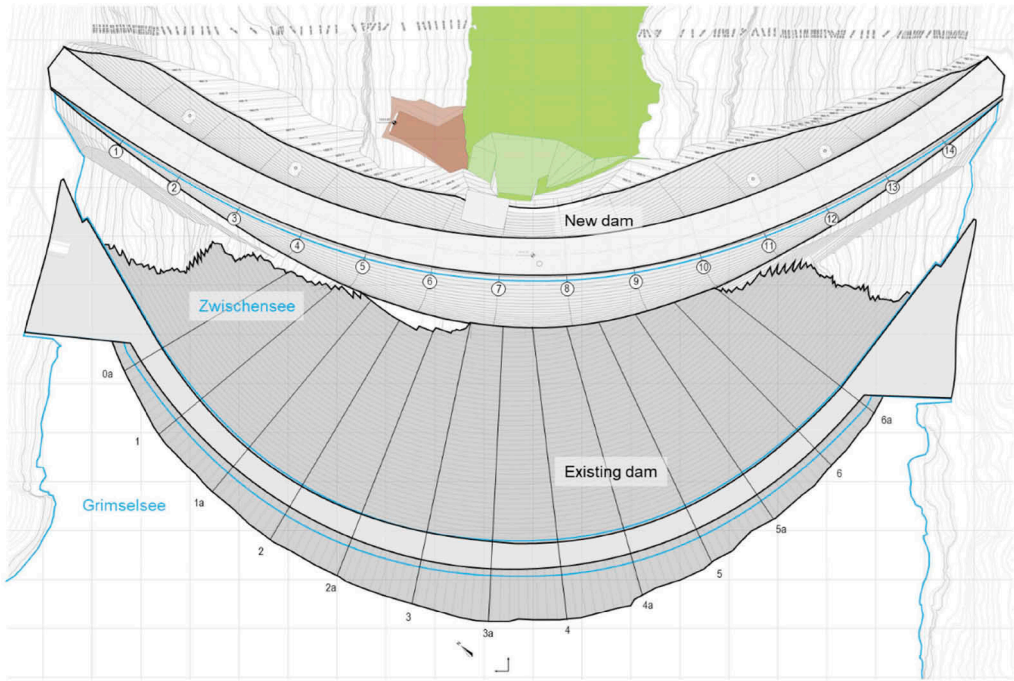


Figure 3. Plan view of old and new Spittalamm dams.

In the new dam, a bottom outlet is designed through the dam body, with a valve chamber downstream of the dam. This bottom outlet is relatively small, as its function is only to empty the relatively small volume comprised between both dams. This water volume is approximately 300'000 m³, whereas the volume of the main reservoir, the *Grimselfsee*, is more than 300 times bigger, about 94 Million m³.

For the main reservoir drawdown and flood spilling, the existing hydraulic system is maintained and extended with a new bottom outlet (also serving as spillway in case of flood), in a tunnel under the left abutment. This is designed to add spilling capacity to comply with the most actual standards, and to anticipate both the possible existing bottom outlet sedimentation and the heightening of the dam.



Figure 4. Leader and follower blocks with climbing formwork (10.06.2022).



Figure 5. Leader and follower blocks at different stages (25.10.2022). From left to right: (1) hard concrete after green cut, (2) fresh concrete, (3) formwork recently lifted with shear keys being placed, (4) lift cleaned and ready for casting with cooling pipes, and (5) lift covered with thermal cover, ready for the Winter break.

The construction is planned in seven building seasons. In fact, at this high altitude in the Swiss Alps, it is impossible to work between November and April due to severe Winter conditions and avalanche risk. Each Winter, it is therefore necessary to stop the construction and prepare the job site for Winter. Each Spring, as soon as the avalanche risk allows it, the site reopening work can begin with snow removal. Two seasons (2019 and 2020) were planned (and stuck to) for the excavation of the dam foundation. Four seasons are planned for the concrete casting of the dam (2021-2024). Side works, such as dam joints grouting, foundation treatment and underground bottom outlet construction take place in parallel. In 2025, the dam crest as well as the last foundation treatment works will be finished, and the impounding procedure will be initiated.

It is interesting to note that Winter 2024-2025 is the only moment when a reservoir drawdown is necessary. This will be used for the breakthrough of the new bottom outlet tunnel and of the connection galleries through the existing dam. The old dam decommissioning will also happen at this time.

Also note that Winter 2020-2021 was of particular interest, as the foundation excavation was completed, especially at the existing dam toe, the gap to accommodate the new dam was not filled with concrete yet, and the reservoir was maintained and operated at full level for winter energy production (see further details and explanations on the interaction between both dams and the stability of the existing dam itself during this period in Section 4).

4 DAM FOUNDATION EXCAVATION AND ABUTMENT STABILITY CONDITIONS

As explained previously, the new dam is built immediately downstream of the existing dam. The rock excavation for the new dam foundation therefore lays in the foundation of the existing dam. This had two main consequences: rock blasting in the immediate vicinity of an existing 90-year-old dam, which could cause damages to the concrete, and removal of rock foundation material in a compressed abutment area of a dam in operation, which could potentially cause deformation and stability issues for the existing dam. The foundation blasting campaign was controlled by implementation of a stringent vibration monitoring process, whereas the consequences of the excavation on the existing dam had to be deeply studied with extensive stability calculations.

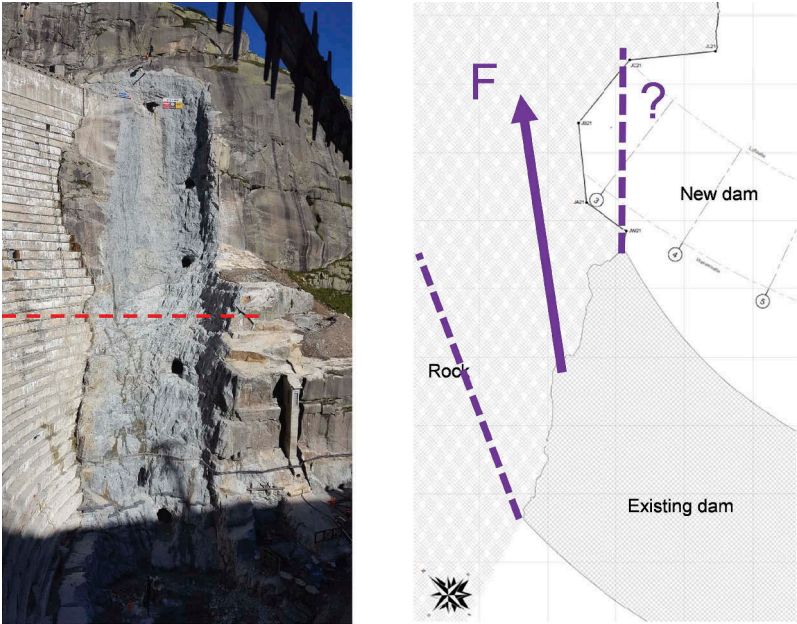


Figure 6. Left abutment excavation. Left: Photography (2020) with approximative situation of section. Right: Horizontal section at 1850 masl with approximative resultant force from existing dam.

4.1 *Monitoring of rock blasting vibrations*

The excavation of the foundation for the new dam was performed with rock blasting in 3-meter-high steps. Due to the rock quality, other methods were excluded for time reasons. In some areas, the excavation is distant only a few meters from the existing dam's concrete. As the blasting vibration could affect the safety of the dam, blasting intensity was limited, and the risk was mitigated and controlled with a near surface vibration monitoring campaign during the entire time of the excavation, as well as during the entirety of the works.

A comprehensive concept on vibration and blasting was developed for this purpose. It specified a vibration measuring network for the registration of working and blasting vibrations at all key points of the KWO scheme before the start of excavation and demolition work. The measurement concept served to ensure safety and to optimize the blasting works. The measurement results were transmitted online and made available to the contractor. In the event that the benchmark values were exceeded, immediate reaction was possible and immediate measures could be instructed quickly and in a targeted manner.

The risk mitigation and monitoring concept was completed with visual inspection of the dam and surroundings, conducted by the operator's dam monitoring personnel and the local site management. These visual inspection routines were conducted according to the intensified dam monitoring concept which is presented further at Section 4.3.

4.2 *Dam stability during construction*

The proximity of the new dam foundation excavation to the existing dam (e.g. Figure 6) raised the question of the existing dam stability. Extensive calculation was performed to ensure the dam safety. This allowed to maintain the dam in full operation during the entire time of the construction. The following sections illustrate the different calculations performed to assess the dam safety.

A 3D finite elements method (FEM) analysis of the dam and a relevant part of its foundation was performed using ZSoil software. Both dam and foundation were modeled as linear-elastic materials. The analysis was conducted in three steps:

- Scenario 0: A first analysis was performed to simulate the pre-existing condition (no excavation downstream of dam) and calibrate the FE model. The load combination is Self-weight and Full reservoir.
- Scenario 1: Following Scenario 0, the new dam foundation excavation was modeled with a trench, by removing a line of elements downstream of the dam. The depth of the modeled trench was 15 m by 15 m.
- Scenario 2: The eventual existence of a potentially unstable rock wedge of 5'400 m³ in the existing dam foundation was considered, and the stability of the dam without this wedge was studied.

The three scenarios were calculated with the basic load combination Self-weight + Full reservoir.

Overall, the influence of the new dam foundation excavation (Scenario 1) on the displacements of the existing dam is very low. The calculated maximum additional displacement is 0.6 mm in the downstream direction. Now that the excavation is over, it is interesting to compare the results of the calculation with the measured displacement of the dam. Of particular interest is the period between Autumn 2020, when the excavation at the dam toe was completed and the reservoir full for the Winter, and Autumn 2021, when the gap at the dam toe was filled with concrete blocks. In the meantime, an irreversible displacement (drift) of 0.4-0.5 mm toward downstream was observed (see Figure 7). This is the same order of magnitude as foreseen by the calculation.

As a conservative scenario, it was also decided to investigate the influence of a potentially unstable rock wedge in the dam foundation (Scenario 2). This fictitious wedge was considered with a big volume (5'400 m³) and located in a critical position, i.e., in the right abutment, at the location of the deepest foundation excavation.

To model a movement of the wedge, some elements were removed from the foundation in the right bank, thus creating a hole in the dam abutment. In that area, the 3D FEM analysis foresees supplementary displacements of 0.1 to 0.4 mm due to the trench downstream of the

dam (Scenario 1). The influence of the wedge (Scenario 2) is very low as well, displacements (in addition to displacements of Scenario 1) of around 1 mm being found. The stress redistribution caused by the new layout is limited as well. The absolute maximum principal stress in concrete around the so-created “hole” is +0.5 MPa, way below concrete’s usual tensile resistance. To check the design parameters sensitivity, other load combinations were also computed (Self-weight + Full reservoir + Winter temperature; Self-weight + Full reservoir + Operating basis earthquake), leading to maximal absolute displacements below 2.0 mm.

Generally, the calculations showed that the order of magnitude of the additional displacements due to the excavation downstream of the dam is very limited in the range of 0.6 mm, and that the equilibrium in the rock mass is not influenced. The comparison between the computation and the measured displacement showed that the FEM analysis was able to correctly foresee the dam behavior in this new layout.

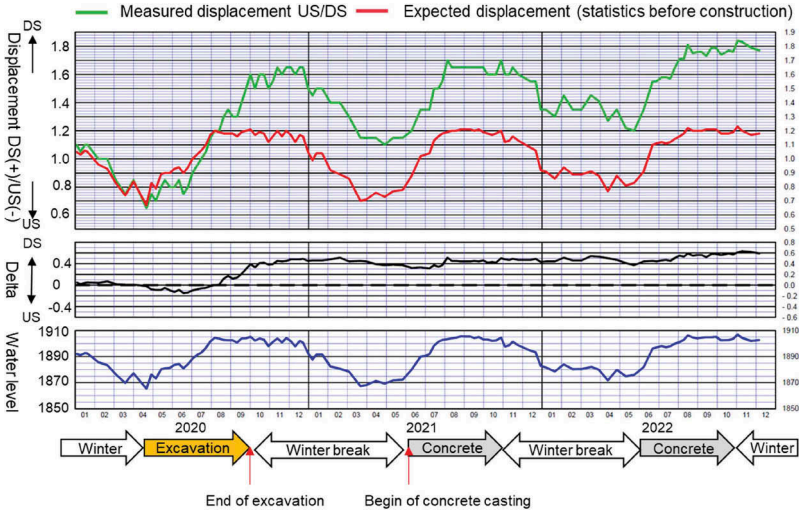


Figure 7. Displacement US-DS of plumb line at dam middle section (©KWO). Divergence between measurement and calculated (based on statistics, before start of works) visible since Winter 2020-2021, irreversible drift in DS direction about 0.4-0.5 mm.

4.3 Dam monitoring during construction

The design calculations presented above show the reduced impact of the construction of the new arch dam on the existing arch-gravity dam, and that its safety is ensured during the entire construction time. To manage the eventual residual risk, the dam is subject to a suitable, reinforced surveillance during the entire construction period. This also assures to operate the reservoir without restriction and to adapt this operation should an unexpected behavior be observed at the existing dam and its foundation e.g., by ordering a reservoir complete or partial drawdown. The set of additional measures comprises more frequent visual inspection and measuring tours, as well as extensive automatic readings of monitoring instruments such as plumb lines, uplift pressures, and seepage discharges. A robotic total station ensures frequent automatic tachymetric surveys of an increased set of measuring points at the downstream face of the existing dam. The entire set of measuring data and visual observations is continuously analyzed by dam safety engineers and summarized in dam safety reports on a regular basis. During the foundation excavation works, a permanent geological survey allowed to check the presence and the conditions of rock mass discontinuities, and to update the geological knowledge of the foundation. All these additional measures will be maintained until the end of the new dam construction and the decommissioning of the existing dam.

5 CONCEPT FOR DAM IMPOUNDING

As previously explained, the construction planning foresees the reservoir impounding for 2025. For this impounding, only the new dam and its abutments are of interest. The banks of the reservoir are not undergoing new conditions, as the new reservoir level corresponds to the old reservoir level (reservoir is unchanged). From a geological point of view, the operation is also considered a refill and not a new impounding. Based on this information, the focus is given on the dam, and an impounding approach based on the total hydrostatic pressure is planned to be used. It is decided to increase every day the load on the dam by 1% of the total hydrostatic pressure. This ensures a constant increase of the load on the dam. The impounding itself should also take 100 days.

In reality, the comprehensive dam commissioning program (Figure 8) follows the habits and rules of Swiss Guidelines, i.e., it foresees a first impounding, followed by a complete drawdown and a second impounding. The first impounding is marked by four breaks (plateaux) at different levels, corresponding to approximately 25%, 50%, 75% respect. 100% of the total hydrostatic pressure. Each plateau is about 10 days, bringing the complete first impounding time to about 140 days. It will begin in Spring and go on over Summer, taking benefit of natural inflows from snow melt.

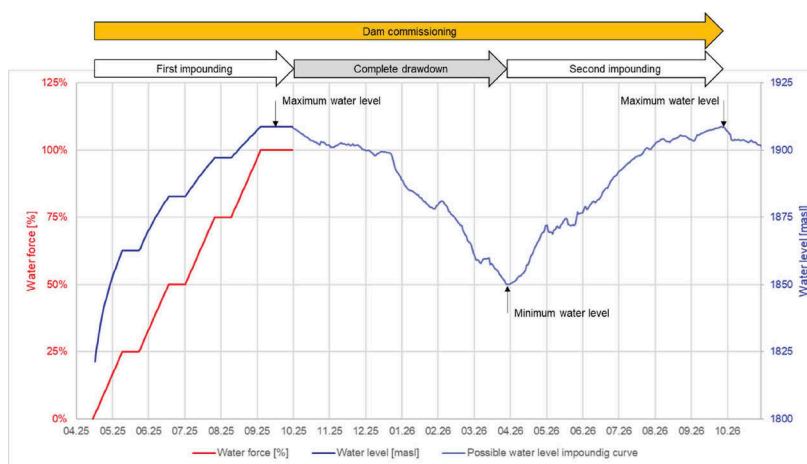


Figure 8. Dam commissioning program, made of a first impounding, followed by a complete drawdown and a second impounding. The first impounding is marked by four breaks (plateaux) at different levels, corresponding to approximately 25%, 50%, 75% respect. 100% of the total hydrostatic pressure.

To comply with the 1% daily increment rule, the existing hydropower scheme will be put to contribution. As a matter of fact, the reservoir is part of the large and complex scheme of KWO. There are several possibilities to control the reservoir level: pumps and turbines connect the *Grimselee* with three other reservoirs, allowing an accurate impounding of the reservoir. The controllable in- and outflows will compensate the uncontrollable natural inflows. The 1% criterion was checked to be technically feasible, considering the average natural inflows, the pump and turbine capacities, as well as the scheme storage capacities.

The situation with the two dams is peculiar. The level between the two dams is of main interest, as it is critical for the impounding of the new dam. In fact, measures will be taken to control the flow between both reservoirs, to precisely control the level against the new dam (*Zwischensee*), whereas some flexibility for energy production can be allowed in the bigger reservoir (*Grimselee*).

During the entire commissioning, intensified dam surveillance is planned. Automatic measurement of several behavior indicators such as uplift pressures, joint opening, rock-meters and seepage discharges, visual inspections, and manual measurements, as well as continuous dam

behavior analysis and plausibility checks of the measurements. The plateaux will be used for a deeper analysis of the dam behavior, combined with geodetical surveys. The dam behavior inferred from the measurements will be compared to a predictive model based on a 3D FEM Analysis. All the stakeholders are involved in this monitoring process: the operator, the designers as well as the authorities.

6 CONCLUSION

The reasons to replace the old Spitallamm dam after almost one century of operation have been presented and discussed, leading to the design and planning of a new double curvature arch dam right at the toe of the old dam. The construction works are scheduled from 2019 to 2025, and at the time of publication of the present article (Spring 2023), the planning is being complied with.

One of the very specific features of this job site is the possibility to keep the old dam in normal operation (no reservoir level restriction). This turns out to be a major asset for the operator KWO.

Such close and cramped layout between the old and the new dam triggers interactions, notably for the safety of the old dam during the new dam foundation excavation. An increased monitoring procedure has been implemented to follow up the behavior of the old dam. The total drift of the dam toward downstream due to the foundation excavation and the works in general is no more than 0.5 mm, in line with the predictive calculations made before works.

The impounding of the reservoir is scheduled for 2025. As a matter of fact, the reservoir itself (*Grimsesee*) is not new and has been operated since 1932. Only the small volume (so-called *Zwischensee*, approx. 300'000 m³, see Figure 3) between both dams will be impounded for the first time. Both volumes upstream and downstream of the old dam will be balanced through galleries to be constructed in Winter 2024-2025.

ACKNOWLEDGEMENTS

We thank the dam and scheme operator Kraftwerke Oberhasli (KWO) for allowing this publication and sharing interesting discussions and information with us.

REFERENCES

Balissat, M. & Filliez, J. & Fankhauser, A. 2022. Decommissioning of an arch-gravity dam and measures taken for its replacement by a double curvature arch dam. Commission Internationale des Grands Barrages, Vingt-septième Congrès des Grands Barrages. Q.104 – R.33: 471–481. Marseille, June 2022.

Concrete dams upgrading using IV-RCC

F. Ortega

RCC dams expert, FOSCE Consulting Engineers, Germany/Spain

ABSTRACT: Immersion Vibrated Roller Compacted Concrete (IV-RCC) is a mass concrete for dam construction. A special mix design has been recently developed for the construction of new concrete dams with the aim of providing best quality to RCC dams, similar or better than the traditional conventional vibrated concrete (CVC). The key advantage of this new type of concrete is that it can be placed and consolidated either like RCC or like traditional CVC. The decision on which methodology should be used for its application can be decided on site, at the point of placement. In this context, we see an opportunity for making good use of this material in the raising, upgrading and renewal works of existing concrete dams in Europe and elsewhere. The paper describes specific characteristics of the materials and mixes required for IV-RCC, as well as some of the specific construction aspects and advantages. The in-situ performance based on existing completed projects is also presented in the paper. Particular attention is paid to specific high-quality mixes as those required, for example, for concrete arch dams.

1 INTRODUCTION

The design and construction of concrete dams worldwide follows two primary approaches: the conventional concrete (CVC) dam and the roller-compacted concrete (RCC) dam. In every new concrete dam project, either option is analysed, and the potential advantages or disadvantages evaluated to a certain extent. Geometrical constraints, high quality and well-proven long-term performance seems to have been the main criteria for the selection of the CVC option in the past, especially in countries with a large tradition in concrete dam construction. However, RCC dam construction has now a history of more than 40 years. The economy of RCC dams is the key to its success against CVC. The potential for cost reduction of RCC dams is based on two main topics: speed of construction and materials optimization. Improvements introduced in the last 15 years in the design and construction of RCC dams have shown that the in-situ quality and concrete properties of RCC can be as good (if not better) than those of dams that have been built with traditional immersion vibrated mixes (CVC).

Experience in construction of CVC and RCC dams has led in the last decade to a combination of both technologies in the same structure, summing up their respective advantages. This is an innovative concept of RCC dam which is called IV-RCC (Immersion Vibrated RCC) dam. There are already some examples of this new technique around the world, with completed dams in operation up to 100 meters in height.

This interesting development has been achieved through optimization of RCC mixes towards a much more workable concrete than the typical dry RCC mixes used in the past. These improvements have been motivated in RCC dams to guarantee bond between layers, to minimize the potential for segregation and to improve the quality of the dam faces.

2 WHAT DOES IVRCC MEAN?

The term Immersion Vibrated Roller-Compacted Concrete (IV-RCC) is a variation of a very workable RCC mix which reaches a consistency like a stiff traditional mass concrete of zero

slump. IV-RCC mixes are produced, transported, and spread as RCC, but the consolidation can be accomplished either by external roller compaction or by internal immersion vibration.

The decision on where to apply in the dam one or the other method of vibration is made on site based on both, design specification and construction practicality. Factors such as the proximity to formed faces or rock abutments, narrow areas of difficult access to large equipment, or especially critical dam zones like embedded instruments, drains or waterstops, are typical places where IV-RCC is immersion vibrated. The rest of the concrete mass is consolidated by roller-compaction.

It must be noted that the main difference from previous RCC dams is that the same concrete mix, without any additional enrichment of grout or mortar, or a different CVC mix, is placed across the entire block. When designed and placed according to certain specifications, IV-RCC will have the same composition and long-term performance in all points of the dam regardless of the method of vibration. As such, the IV-RCC dam will exhibit at the long term many similarities with the traditional concrete dam.

3 SPECIFICATION OF AGGREGATES FOR IV-RCC

The success of the IV-RCC mix lies on the improvement in the quality of the aggregate. The effort and cost of producing a good aggregate shape and an optimised gradation is well justified. A good-quality aggregate will reduce the water demand of the mix for a given level of workability, and consequently the mix can be designed with a lower content of cementitious material to meet the design strength. This implies less heat generated by the mix and lower cost.

3.1 Coarse aggregate

The optimum gradation of the coarse aggregate (particles with nominal size exceeding 5 mm) should be found by combining the various sizes of aggregate to achieve the maximum density and thus minimum voids and the best packing of the particles.

Dust coating the coarse aggregate should be limited to a maximum of 1% (by weight) at the time of entering the mixer. These fine particles should be non-plastic. Excessive coating of coarse aggregate will reduce the tensile strength capacity, as it negatively impacts the paste-aggregate bonding.

Coarse aggregate for IV-RCC should be preferably 100% crushed, i.e., each particle should have at least one fractured face. In addition, a cubical shape of the coarse aggregate particles is required to produce a workable concrete with no segregation. In this regard, the sum of flakiness and elongation indexes is typically limited to 25%.

3.2 Fine aggregate

There are two key-factors in the specification of the fine aggregate for IV-RCC mixes

- Minimum void content of (rodded) compacted fine aggregate below 30%, and
- A high proportion of non-plastic aggregate fines passing 0.075 mm sieve, ideally around 12-14%.

The gradation and void ratio of the fine aggregate are interrelated. As has been shown in some projects (Allende M., et al., 2012), the middle curve of the typical gradation range (Figure 1) produced using a tertiary VSI resulted in the lowest void ratio.

3.3 Combined grading curve

A combined grading curve for IV-RCC mixes has been developed based on experience gained in specific projects where different types of aggregates have been used. This typical gradation (Figure 1) has been assumed by ICOLD for high-workability RCC mixes (ICOLD, 2020). As can be appreciated in the figure, the maximum size of aggregate (MSA) is 50 mm. For natural more rounded aggregate this value should be reduced to 40 mm to control segregation.

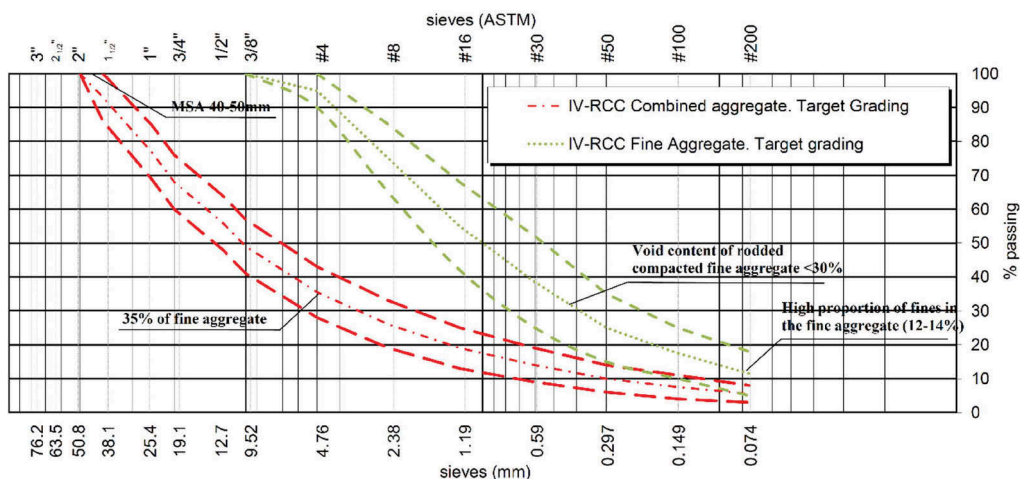


Figure 1. Aggregates for IV-RCC mixes. Combined grading and fine aggregate curves.

4 IV-RCC MIXES. DESIGN AND PERFORMANCE

4.1 Mixture proportions

A typical range of mixture proportions of IV-RCC mixes is included in Table 1. All IV-RCC mixes that have been used or tested at dam projects to date include a high proportion of a supplementary cementitious material (SCM) like fly-ash, natural pozzolan or slag.

Table 1. Typical mixture proportions of IV-RCC.

Material	Kg/m ³
Coarse aggregate (>5mm)	1350-1550
Fine aggregate (<5mm)	700-850
Cement (type I)	50-70
(SCM) Fly-ash/Natural Pozzolan	70-150
Free water	85-130
Admixture	0.5-2.0%

The IV-RCC mix is a super-retarded high-workability RCC mix. The target consistency of the mix as measured in the modified loaded VeBe test (with a total surcharge of 12.5 kg) is between 6 and 12 seconds. In addition, the setting time of these mixes is extended to an initial set of 20 to 24 hours. To that end, a high dosage of a set retarder admixture is an essential component of the mix. The type and dosage of the admixture needs to be carefully studied in preliminary trials at the time of designing the mixes and considering the real outdoor conditions at which the mix will be placed.

4.2 Performance of the IV-RCC mix

The in-situ density of the roller compacted IV-RCC mix is very high, frequently exceeding 99% of the theoretical-air-free density (TAFD). It has been observed a slightly lower density, in the order of 98% of the TAFD, when the same mix is vibrated by immersion.

The main benefit of the IV-RCC mix is its excellent performance at the lift joints due to the high volume of paste that is mobilised to the surface during compaction. The high level of set retardation of this paste allows the effective interpenetration between the new and the old layer achieving a monolithic construction in the vertical direction without joints. Cores drilled from IV-RCC dams show typically a continuous concrete matrix without joints. The only

discernible joints are those that have required some kind of treatment after the time between layers has exceeded the initial set. Figure 2 shows an example of a vertical core taken from an IV-RCC mix with no joints. When testing core samples of IV-RCC for direct tensile strength, the plane of failure is not necessarily located at the position of the joint between two layers. This indicates a similar tensile strength capacity (and cohesion) at the theoretical position of the joint than in the matrix, inside the layer. The weakest points in IV-RCC dams are the joints that have required treatment.



Figure 2. Vertical core of IV-RCC extracted from Enciso dam (Spain) and general view during construction.

The compressive strength of the IV-RCC, although frequently used for the quality control on site due to its simplicity for testing, is not the critical design factor for the dam construction. Thermal and dynamic loads are typically the critical ones in the design of the structure and therefore, tensile strength is the limiting factor when designing IV-RCC mixes. The correlation between in-situ (core) direct tensile strength and cylinder (lab) compressive strength is established in each project at the time of testing the cores extracted from the full-scale trial, that is typically built as part of the mix design investigation process. In IV-RCC mixes the factor between direct tensile strength on vertical cores including joints and compressive strength as measured in cylinders manufactured in the laboratory is ca. 5%.

5 APPLICATION OF IV-RCC IN CONCRETE DAM CONSTRUCTION

5.1 General

While conventional mass concrete (CVC) dams are constructed in separate vertical approximately 15-m wide monoliths, RCC dams are constructed in principle in much larger blocks, ideally placing concrete in horizontal 300-mm thick layers from one abutment to the other. The availability of large construction areas allows that full advantage can be taken of the high-capacity production, delivery and placement equipment and plant. Advanced planning of the construction methodology and logistics for material deliveries is a key element of RCC dams in general, including IV-RCC dams. In addition, the degree of simplicity achieved by designing a dam using IV-RCC plays a major role in its efficiency.

In CVC dams the surface of the lifts are cleaned up to an exposed aggregate finish in every dam block and a mortar is spread as bedding mix ahead of the next lift. This happens systematically every 2.5 or 3.0 meters depending on the height of the forms. However, treatment of lift joints in CVC dams is normally a well-controlled operation as the size of the block and the time available for such activities are usually not critical in the construction programme.

When a joint need to be treated in an RCC dam, the size of the block is much larger, and if not correctly planned, the activity may become critical. This is another important positive

aspect of IV-RCC dams in which the continuous placement and the level of mix retardation reduces to a minimum the creation of such joints.

5.2 *Faces of the IV-RCC dam*

Many ways of forming the faces of an RCC dam have been put into practice throughout the past years. In most cases, a CVC concrete mix, or an RCC with additional grout (GEVR/GERCC) or mortar, has been used against the forms or as interface with the rock abutment, in addition to the RCC mix that was being used in the core of the dam. The use of different mixes and methodologies is against the principle of simplicity that should govern the construction of any RCC dam. However, this was necessary as previous RCC mixes directly placed in these areas would not achieve enough durability and quality surface finish of the dam faces, or a good contact with the rock or other embedded structures.

The introduction of IV-RCC, a concrete mix that is suitable for immersion vibration in a similar way as stiff traditional mass CVC concrete, and that in addition, can be easily roller compacted, is a significant further step in the development of RCC dams. The same mix fits either as CVC interface concrete or as RCC in the rest of the dam. In this way a great homogeneity is achieved in the concrete mass across the dam. The IV-RCC dam can essentially be assumed to behave under operating conditions in a similar manner as a traditional CVC dam but built in a much more efficient way and with much less cementitious content of the mix.

Despite of being built at high placement rates and with a zero-slump mix, the finish achieved by the immersion vibration against the faces is as good as that of the CVC or grout-enriched RCC mixes.



Figure 3. Evaluation of IV-RCC vs. CVC and GEVR facing systems through drilled cores.

Tests on horizontal and vertical cores drilled from the structure shown in Figure 3 have shown that the strength in the interface area between the roller compaction and the immersion vibrated zones is excellent, without planes of separation or discontinuity. Whilst the CVC or the mortar-enriched and the grout-enriched RCC provides a similar good finish at the face as the IV-RCC, it has been found that some discontinuity may occur in the contact between these mixes and the RCC placed in the core, with less workability. This issue is successfully solved with a very workable IV-RCC mix.

5.3 *IV-RCC faces in cold weather*

One of the possibilities that offers IV-RCC is the relatively easy air-entraining of the mix to improve the freeze-thaw resistance of concrete surfaces exposed to cold weather conditions. This is due to the higher level of workability of these mixes compared to RCC or GEVR. In those cases, an additional air-entraining admixture is used in the mix. Consistent air content in IV-RCC between 5 and 7% has been achieved with dosages of the admixture between 0.5 and 0.7% by weight of the cementitious materials.

5.4 Thermal considerations

IV-RCC is a mix with relatively low heat generation but typically placed at high rates, and therefore, with limited possibilities of heat dissipation at early ages of the concrete. Pre- and post-cooling of the mix might be required in certain projects depending on the environmental and structural conditions, in a similar way as has been done in traditional CVC dams.

Pre-cooling methods applied are similar to those used in CVC or RCC dam construction. Post-cooling might be more difficult due to the continuity of the placement in large areas. When building arch dams using IV-RCC it might be required to force the construction to stop at certain levels to install post-cooling piping systems. In this case, the advancing sloped layer placing system (ICOLD, 2020) might be a good option as it would allow time to place the cooling pipes on the top surface of the lifts after joint treatment, but without stopping the continuity of the RCC.

5.5 Impermeability of the IV-RCC dam

The immersion vibration of the IV-RCC done with high-frequency vibrators of at least 75 mm diameter will penetrate down to a depth of ca. 0.5 meters when the 300 mm thick layers are placed in “hot” condition, i.e. within the initial set of the lower layer. Following this procedure, there is an effective redistribution of paste and aggregate particles between the upper and lower layers, that eliminates any plane of discontinuity in the horizontal joint that was the normal case in CVC and GEVR/GERCC facing systems. Such possibility adds additional impermeability to the structure in the upstream face, and at the critical area around water-stops and drains.

In addition, the IV-RCC that is roller compacted is design for impermeability. Results of permeability tests done in vertical holes drilled crossing the joint between layers indicate a coefficient of permeability (10^{-8} to 10^{-12} m/sec) that are similar to those measured in the concrete matrix in laboratory trials.



Figure 4. Enciso IV-RCC dam (105 m high). Downstream view during first spilling of the spillway.

6 APPLICATION OF IV-RCC IN THE UPGRADING OF EXISTING DAMS

Upgrading of existing dams with concrete may involve one of the following design solutions:

- Raising an existing concrete dam,
- Downstream buttressing of an existing concrete, hardfill or embankment dam, or
- Construction of a new dam replacing an existing old one.

IV-RCC as described previously is a material and a construction technique that is applicable to any of the three design options. In an upgrading dam project where roller-compacted concrete is a good solution, the size of some of the concrete blocks might be smaller than desired for a typical RCC construction methodology. This is the case, for example, in a narrow strip at upper levels of the construction, buttressing from downstream an existing concrete (or embankment) dam. In those cases, it could be beneficial to use traditional mass concrete vibrated by immersion rather than RCC, that might be used in wider layers at lower levels in the same structure. The combination of RCC and CVC in different sections of the upgrading project might be an option to consider in the design. However, the long-term properties of both materials will be different, and the time-dependent elastic and thermal properties of both materials need to be carefully considered in the finite element models used in the detailed design, merged with those of the existing dam.

IV-RCC is a material that behaves uniformly, and which application can be adapted to both large and small concrete blocks. The same mix can be used across the new mass concrete structure, and the only difference will be the way it is consolidated depending on the space available and the existence or not of embedded elements that require immersion vibration around them.

Modelling IV-RCC properties in the detailed design phase is simpler than a combination of RCC and CVC mixes, and similar to traditional CVC mass structures. However, it offers the possibility of the cost-effective solution associated with the roller compaction placement method whenever possible within the geometric conditions of the concrete blocks.

It is considered that the use of roller compaction as consolidation method of the 300 mm layers is practicable in concrete blocks with a minimum width of 6 to 8 meters and a block length of more than 60 meters. In these blocks IV-RCC can be consolidated in the core using a 10-to-12-ton vibratory roller and the interfaces vibrated by immersion. The same IV-RCC mix can be used in smaller areas or lifts at upper levels across the entire block and fully consolidated by the traditional method of immersion vibration.

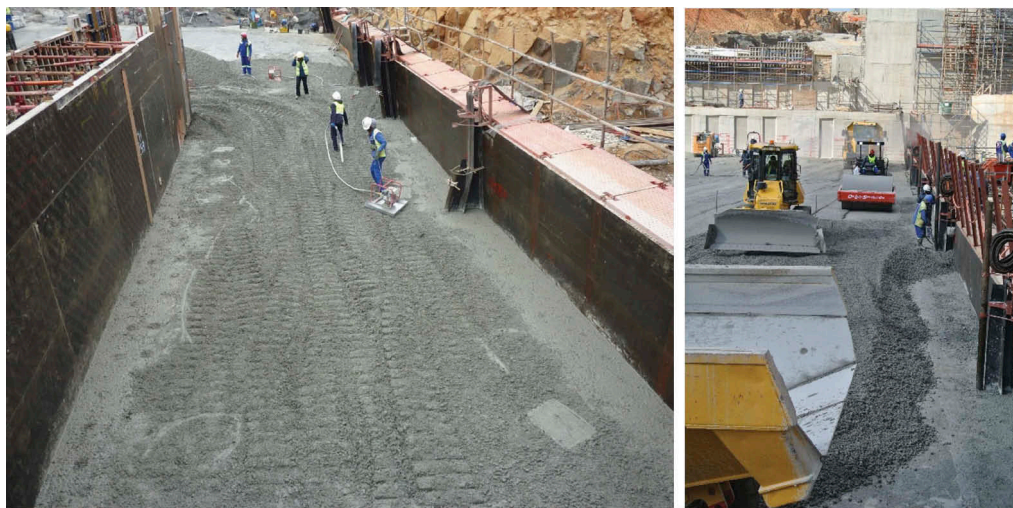


Figure 5. Application of IV-RCC in narrow areas. Note roller compaction in the core of the block and immersion vibration at the faces and around waterstops and drains.

7 CONCLUSIONS

IV-RCC is a relatively modern approach to concrete dam construction that benefits from the advantages of RCC technique but with the possibility of using the same mix as CVC where it is required across the concrete block (faces or narrow areas).

The mix is designed with a lower content of cementitious materials than CVC and with a high proportion of fines in the fine aggregate. The specification of coarse and fine aggregate for IV-RCC focus on improving shape and grading of the particles to reduce voids and water demand. The mix behaves in fresh condition like a zero-slump concrete and is designed as a very workable and super-retarded RCC. The extended initial set of these mixes allow a perfect bonding between placement layers and provide strength to the joint and effective impermeability.

There seems to be a huge potential for using IV-RCC in the construction of new concrete dams or in the upgrading of existing ones. IV-RCC mix is effectively locking the gap between RCC and CVC and offers a cost-effective solution compared to any of the traditional methods.

REFERENCES

Allende, M., Cruz, D. and Ortega, F. “*RCC mix design development for Enciso dam*”. Proceedings of the 6th International Symposium on Roller-compacted concrete dams, Zaragoza, Spain, October 2012. ICOLD, “*Roller-Compacted Concrete Dams*”. Bulletin 177, ICOLD, Paris, 2020.

The driving force of AAR – An in-situ proof

B. Otto & R. Senti

Axpo Power AG, Baden, Switzerland

ABSTRACT: The paper is focused on the AAR behavior of two dams in the Swiss Alps. Instead of measuring and analyzing the crest deformation, numerous strain distributions across the entire dam body were measured by means of extensometers (rocmeters) and sliding micrometers. The measurements were taken periodically during a year cycle and are running since 4 to 5 years. The analysis of the data showed a strong variation of the yearly AAR strain growth over the dam cross section. While the upper crest area swells 200 – 250 $\mu\text{m}/\text{m}/\text{year}$, the dam concrete in 20 m depth from the top of the dam swells only by 50 $\mu\text{m}/\text{m}/\text{year}$. On the upstream side the effect of the cold water is very clearly seen, the swelling rate drops within 5 meters of height by a factor of 5. These strong strain gradients can only be explained by the dominant influence of temperature on the swelling process. This finding is strongly confirmed by the AAR during a year cycle. Swelling occurs only in the warm period, in winter the expansion is ceased completely. The swelling rate is an exponential function of the concrete temperature and unique for each dam depending on the type and size of aggregate.

RÉSUMÉ: L'article se concentre sur le comportement RAG de deux barrages dans les Alpes suisses. Au lieu de mesurer et d'analyser les déformations du couronnement, de nombreuses distributions de tension sur l'ensemble du corps du barrage ont été mesurées à l'aide d'extensomètres (rocmètres) et de micromètres coulissants. Les mesures ont été prises périodiquement au cours d'un cycle annuel depuis 4 à 5 ans. L'analyse des données a montré une forte variation de la croissance annuelle de la déformation RAG sur la section transversale du barrage. Alors que la zone de la crête supérieure se gonfle de 200 à 250 $\mu\text{m}/\text{m}/\text{an}$, le béton du barrage à une profondeur de 20 m à partir du couronnement du barrage ne se gonfle que de 50 $\mu\text{m}/\text{m}/\text{an}$. Du côté amont, l'effet de l'eau froide est très clairement visible, le taux de gonflement diminue d'un facteur 5 à 5 mètres. Ces gradients importants de déformation ne peuvent s'expliquer que par l'influence dominante de la température sur le processus de gonflement. Cette constatation est fortement confirmée par la RAG au cours d'un cycle annuel. Le gonflement ne se produit que pendant la période chaude, en hiver l'expansion est complètement arrêtée. Le taux de gonflement est une fonction exponentielle de la température du béton et est unique pour chaque barrage en fonction du type et de la taille des agrégats.

1 AAR IN CONCRETE DAMS

The alkali-aggregate reaction (AAR) in mass concrete leads to a volume increase, which is a slow process, especially in the colder climate of the Swiss Alps, and causes permanent dam deformations. If movements are restrained, internal differential stresses resulting from the volume increase can cause structural cracks. In the long term, these cracks can diminish the safety of the dam and may force the owner to carry out extensive rehabilitation works or even demolition. One small arch dam in Switzerland, suffering from structural AAR-induced cracking, has already been demolished and reconstructed [Ref. 1].

The presence of AAR in a dam manifests first in the time-dependent permanent displacements of the structure. In publications, the honeycomb cracking is often described as the most typical sign of AAR, but this is only a leaching phenomenon, mainly observed in the crest slab or other slender walls. The swelling mass concrete of dams usually show no signs of honeycomb cracking even after decades of swelling.

By following this logic, the AAR working group of the Swiss Committee on Dams [Ref. 1] assessed the state of the concrete swelling in 147 Swiss dams by analyzing the permanent dam deformations. One of the main objectives of the working group was the identification of an irreversible drift in Swiss concrete dams due to concrete swelling.

Several concrete dams operated by Axpo Power AG show signs of concrete swelling caused primarily by alkali-silica reaction (ASR), the most common type of AAR, except for one dam undergoing volume expansion due to internal sulfate attack (ISA). The two dams presented in this paper are the slender Roggiasca arch dam of in the Southern Alps and the Runcahez gravity dam in central Switzerland (Figure 1).

The Roggiasca dam is a very slender arch dam with a height of 68 m situated at an altitude of 955 m asl and the Runcahez dam is a gravity dam with a height of 30 m situated at an altitude of 1280 m asl (Figure 2). Geologically, both dams are founded on gneiss formations. Figure 1 shows that about 55 to 60% of the Swiss dams located in these geological regions show tendencies of permanent displacements caused by AAR. For the construction of the Roggiasca and Runcahez dams, portland cement with a dosage of 250 to 200 kg/m³ was used.

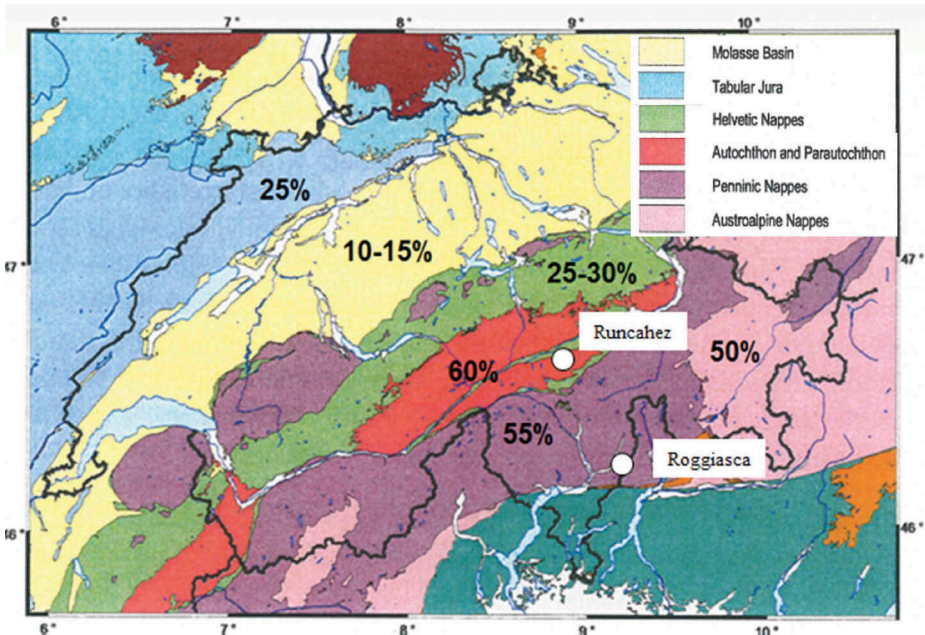


Figure 1. Percentage of dams in Switzerland with tendencies of AAR-induced permanent displacements in various geological regions (Ref. 1).

In Figure 3, the typical long-term upward deformation of the dam crest detected by geodetic monitoring of the Roggiasca and Runcahez dams is shown. This behavior has been observed in a number of Swiss dams experiencing AAR. After the commissioning of the Roggiasca and Runcahez dams in the 1960s, it took about 25 to 35 years until a permanent crest rise was first detected. This AAR “sleeping” period, or initiation time, is typical for dams in Switzerland. The initiation time ranges from about 10 years to 50 years (Ref. 1). The rise of the crest in the following years is progressive over time. The vertical movement reflects mainly the free expansion of the concrete due to AAR.



Figure 2. Roggiasca dam (left) and Runcahez dam (right).

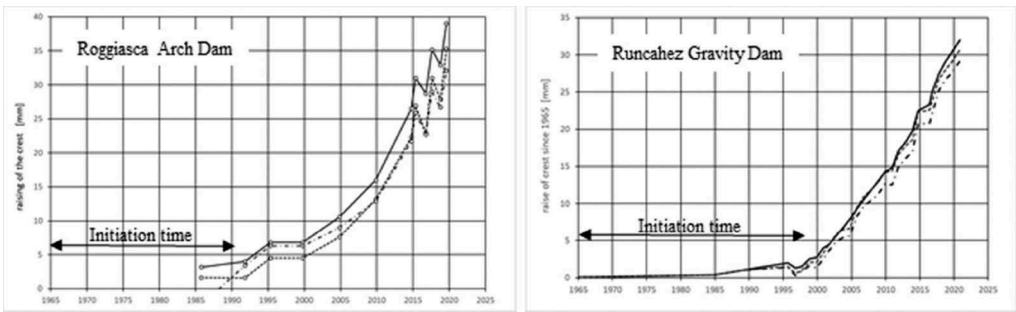


Figure 3. Crest rise due to AAR in the Roggiasca and Runcahez dams since commissioning (as measured at 3 crest points of each dam).

A very similar deformation pattern is observed when analyzing horizontal permanent crest movements from pendulum measurements. The study carried out by the authors in Ref. 1 showed that the start of the permanent horizontal displacements measured by pendulums tends to occur somewhat later than the irreversible vertical deformation. In conclusion, it can be stated that, after an initiation time of several decades, the AAR-induced swelling of concrete leads to irreversible vertical and horizontal deformations, which show no signs of slowing down even after around 60 years since the commissioning of the dams.

The occurrence of AAR in the dam concrete was first investigated by carrying out various laboratory tests for around 10 years. The general outcome of these tests was to confirm AAR in the dam concrete. However, the effects of the cement content and various parameters (e.g. moisture, drying wetting cycles and concrete temperature) on the rate of AAR could not be determined in these tests. Therefore, instead of the laboratory tests, Axpo Power is now focusing on the investigation of the distribution of swelling rates in the dam cross-section based on intensive measurements of the internal strains.

2 DETAILED STRAIN MEASUREMENTS IN DAM CROSS-SECTIONS

Early analysis of the results of geodetic measurements and leveling of the monitored dams indicated that the vertical permanent deformations were not uniform over the height of the dam. In general, the upper part of the dam near the crest showed much larger permanent vertical deformations than the lower part of the dam. The results of triaxial AAR tests in the laboratory show that expansion is lower than the free expansion when the compressive stress exceeds about 2 MPa. At a compressive stress of 4 to 5 MPa, virtually no AAR-induced expansion occurs. The fact that the crest region of a dam suffering from AAR shows

a substantially higher vertical displacement than the lower part closer to the foundation could be partly explained by the distribution of the vertical stresses in a very high dam ($H > 100$ m). However, a similar deformation pattern has been observed even in relatively small dams suffering from AAR.

The existence and speed of AAR can be measured directly by monitoring strains in concrete. During the past 15 years, Axpo Power has been performing detailed strain measurements in a number of dams. The strain measurements were first carried out in the Isola dam (subjected to ISA) and then at the Roggiasca and Runcahez dams.

The main objective of the strain monitoring is to answer the following questions:

- How does the swelling vary over a cross-section of a dam (from the upstream to the downstream side) and from the crest region to the lower part of the dam?
- What is the average rate of AAR-induced swelling in a particular year and how does it change over time?
- Does the swelling show seasonal variations over the course of a year?
- What is the main driving factor behind AAR?

As stated earlier, AAR and the response of the dam to the resulting internal strains are very slow processes. In order to obtain a clear and reliable picture of the spatial variation, the rate and the change of rate of AAR-induced swelling, it can take many years (even more than a decade) of measurements. After 10 to 15 years of measurements, Axpo Power is now finally in a position to answer the above-mentioned questions.

At the Roggiasca dam, extensometers were installed in 3 cross-sections near the upstream face and one sliding micrometer at the middle of a cross-section. The instrumented vertical distance is 15 m (extensometer) and 17 m (sliding micrometer), respectively.

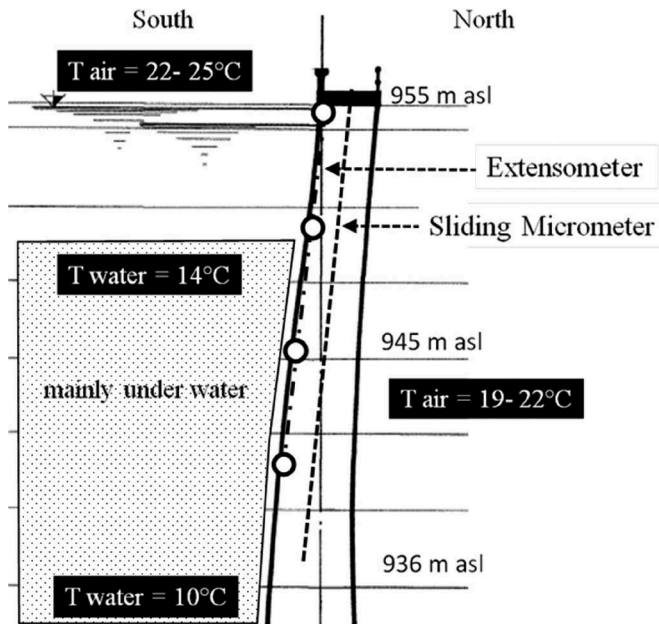


Figure 4. Typical instrumentation of a cross-section of the Roggiasca dam.

Each extensometer consists of 3 sections (5 – 10 – 15 m), which are measured manually. The sliding micrometer has a normal measuring spacing of 1 m.

In Figure 4, the distribution of outside temperatures in summer is also indicated. The lake is normally operated only over the top 4 to 5 m and the upstream face of the dam around 5 m below the crest is most of the time under cold water. The air temperature at an elevation of 950 m asl is around 20 to 25°C in summer. The dam is very slender (designed by the way by the

then young engineer Giovanni Lombardi) with a thickness of only 2.5 to 3.0 m in the uppermost part. Hence, the two measuring lines in Figure 4 have a lateral distance of about 1.5 m.

In Figure 5, the annual strain rates along the measuring lines of the extensometers and the sliding micrometer are depicted. The evaluation is based on 4 years of measurements in the three cross-sections of the dam. The extensometer measurements were performed monthly and the sliding micrometer was measured once a year always on the same date. The annual strain rates were evaluated for each extensometer section (0-5 m, 5-10 m and 10-15 m) in the three dam cross-sections, all of which exhibited a very similar behavior.

In the crest region, the highest annual strain rate of around 220 $\mu\text{m}/\text{m}/\text{year}$ was measured and the entire cross-section was affected.

Below the crest region (the top 5 m of the dam), the behavior changes substantially. The strain rate falls to just 40 $\mu\text{m}/\text{m}/\text{year}$ in the portion of the upstream face located between 5 m and 10 m below the crest, showing a reduction by a factor of around 6 compared to the crest region. At the middle of the cross-section, the reduction of the strain rate with depth is less pronounced. At 14 m below the crest, the strain rate at the middle is about 160 $\mu\text{m}/\text{m}/\text{year}$, reducing to around 70 $\mu\text{m}/\text{m}/\text{year}$ in the lower portion. The large differences of the strain rates must be related to the distribution of the concrete temperature in the dam cross-section, since the aggregates, the cement type and the cement content are identical everywhere. The relatively small vertical stresses cannot be the cause of the large differences of the strain rates. The crest region experiences a much higher strain rate than the lower part of the upstream face most probably due to the fact that it is around 10 °C warmer in summer, indicating a high temperature sensitivity of AAR-induced swelling.

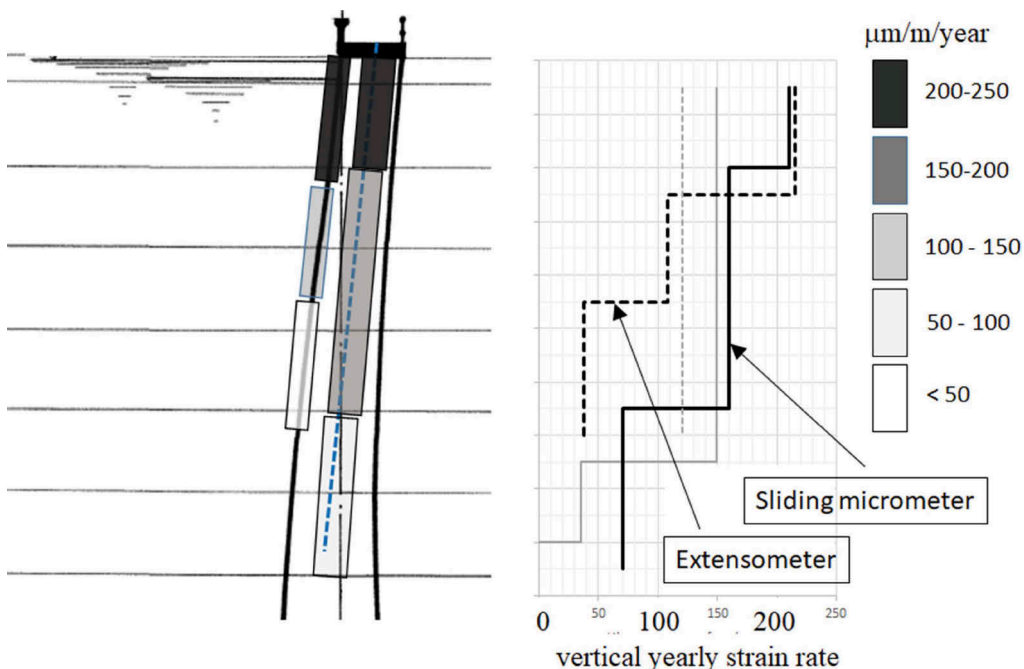


Figure 5. Measured annual strain rates in a monitored cross-section of the Roggiasca dam.

A strong and dominant effect of temperature on AAR-induced swelling, as evident from Figure 5 in the case of the Roggiasca dam, has also been observed in the Runcahez and Isola dams.

3 STRAIN DEVELOPMENT DURING A YEAR

In section 2, the observed distribution of the annual strain rates over the cross-section of a dam was presented. In this section, the change of AAR-induced strain in a dam cross-section over the course of a year is discussed. Since the concrete temperature is the main driving force behind AAR, the strain rates can be expected to be subjected to seasonal variations.

In Figure 6, strains measured in 3 sections of one extensometer are presented for the Rog-giasca dam. In all of these sections, the strains clearly grow in a stepwise manner but with different amplitudes, as expected. Every summer, the top section starts to swell, growing by around 200 $\mu\text{m}/\text{m}$ over a period of around half a year, which is equivalent to a swelling rate of 400 $\mu\text{m}/\text{m}/\text{year}$ during this period.

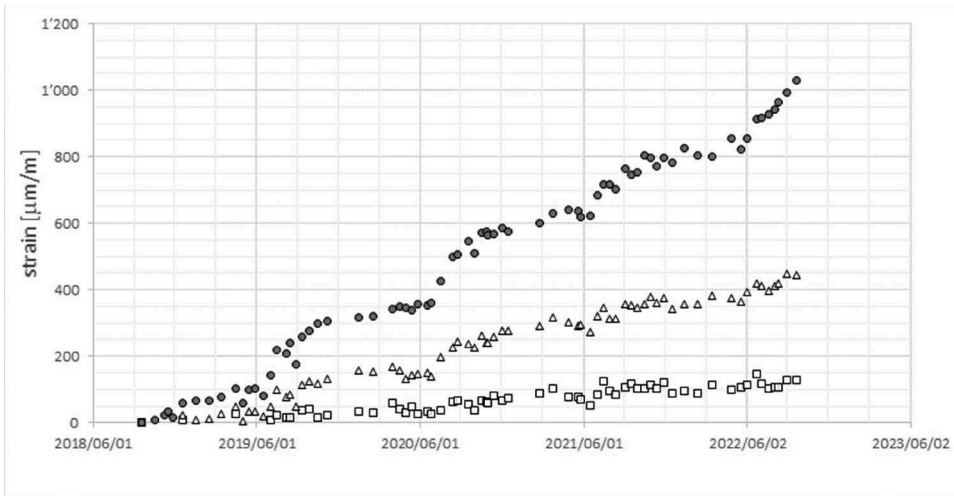


Figure 6. Strain as a function of time in three sections of one extensometer (circles: 0-5 m, triangles: 5-10 m, squares 10-15 m).

The growth of strain measured in the top section of the extensometer during the years 2019 and 2020 is depicted in Figure 7. It is clear that the swelling takes place predominantly in summer, with a minor growth also observed in spring. In winter, there is no sign of any significant increase of the AAR-induced strain.

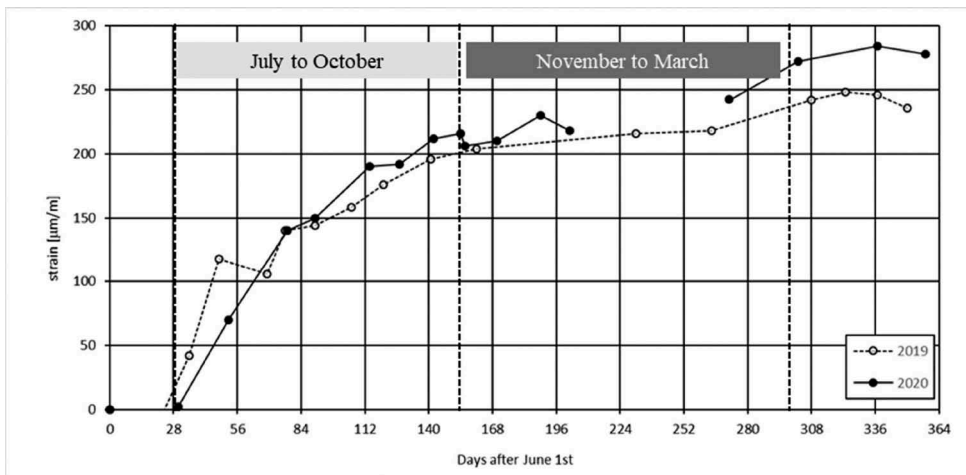


Figure 7. Growth of AAR-induced strain over a period of one year starting from June 1st, 2019 and 2020.

Figure 6 also shows a swelling of 150 $\mu\text{m}/\text{m}$ between day 28 and day 84, which would imply a very high swelling rate of 980 $\mu\text{m}/\text{m}/\text{year}$ during the summer months. One can imagine how severe the AAR-induced swelling would have been if the Roggiasca dam would be located in the warm Mediterranean climate.

A similar pattern of AAR-induced strain growth has been observed in all the extensometers installed in the Roggiasca and Runcahez dams (each equipped with 9 extensometers).

4 CHARACTERISTIC CURVES OF AAR-INDUCED SWELLING IN DAMS

As shown in the previous chapters, the concrete temperature is by far the most important parameter driving free expansion due to AAR. Moisture content, cement type and cement content do not seem to have significant effect on AAR, at least in the dam structures in the northern European climatic condition. The level of compressive stress in concrete (once it exceeds about 2 MPa) and the type of aggregates are the other important factors playing a role in the growth of the AAR-induced strains.

AAR is a chemical reaction, which occurs in the presence of a certain initiation energy or temperature and grows in intensity exponentially with an increase of temperature. Based on this fact, a characteristic curve was developed to represent the AAR-induced swelling of aggregates in the concrete of the Roggiasca and Runcahez dams. The swelling on a certain day of the year depends only on the mean daily concrete temperature at any point in the dam and a characteristic curve (a unique exponential swelling-temperature relationship) governed by the mineralogy and the grain size distribution of the aggregates.

All the available data of the 9 extensometer sections in the Roggiasca and of Runcahez dams were used to calibrate the individual characteristic curves representing the AAR-induced swelling. The only input needed to determine the AAR-induced strains is the measured or calculated concrete temperature field in a dam over the course of a year.

The best-fit analysis of the calculated versus measured strains in the extensometers, after the determination of the initiation (minimum) temperature required to cause AAR, yields a single characteristic curve to represent AAR-induced strains in each dam concrete, as shown in Figure 8. The characteristic curves calibrated for the Roggiasca and Runcahez dams are 2nd order polynomials, which form depends mainly on the type of aggregates.

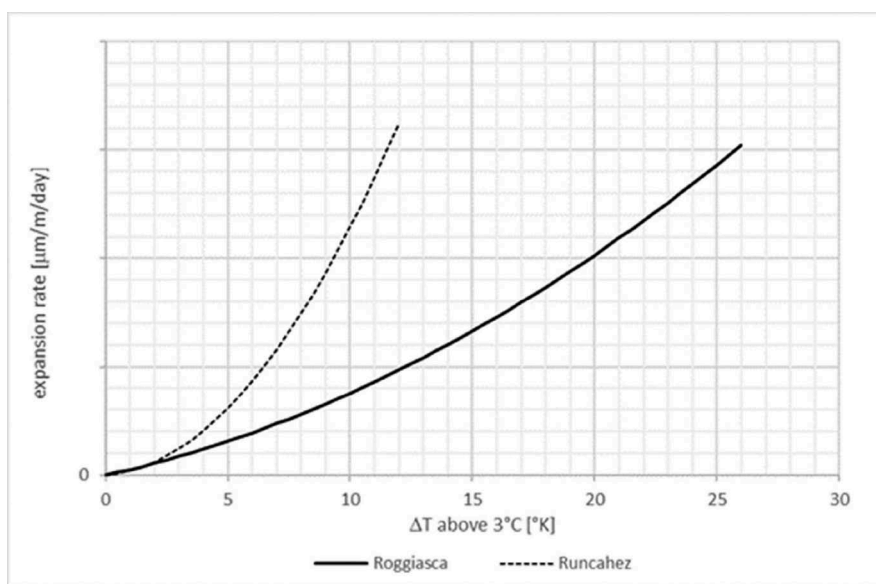


Figure 8. Characteristic curves representing temperature-dependence of AAR-induced swelling of concrete of the Roggiasca and Runcahez dams.

An important finding is the fact that AAR stops completely, or is at least not detectable anymore by measurements, at a temperature below 3 °C in both the dams. In Figure 8, the parameter ΔT is the difference between the actual concrete temperature (> 3 °C) and the initiation temperature of 3 °C.

Figure 8 shows that at a temperature of 15 °C (i.e. $\Delta T = 12$ K), the aggregates of the Runcahez dam swell more than 3 times faster than in the Roggiasca dam. The differences between the characteristic curves are explained by the diversity of the aggregates used in the Swiss dams.

In order to assess the yearly AAR-induced swelling in a dam, one has to know the characteristic curve as well as the seasonal and spatial variation of the concrete temperature. As the swelling rate depends on the concrete temperature, it is not a constant but varies with time. Hence, AAR-induced strains have to be computed using a daily or weekly increments of time.

Figure 9 shows that the measured displacements in the 2 extensometer sections in the Roggiasca dam agree very well with the calculated values obtained using the characteristic curve depicted in Figure 8.

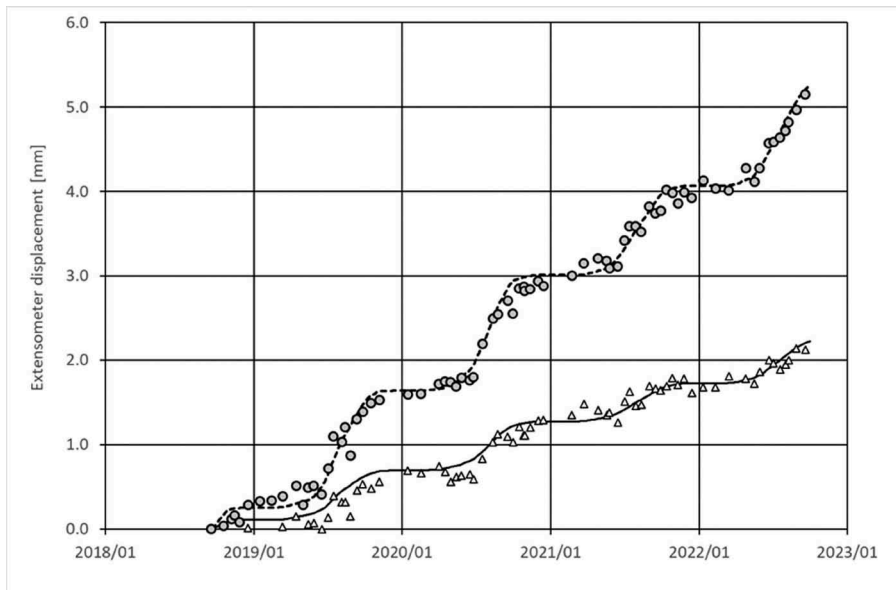


Figure 9. Calculated and measured displacements in 2 extensometer sections in the Roggiasca dam.

5 CONCLUSION

The investigation results presented in this paper have shown that the most important parameter governing AAR is the concrete temperature above the initiation temperature of 3 °C. Below 3 °C, measurements show no significant AAR-induced deformations. Above 3 °C, the swelling rate accelerates rapidly with an increase of concrete temperature. The other factors governing the swelling rate are the type of aggregate and the grain size distribution (sieve line).

The moisture content, the cement type and the cement content do not seem to have any significant effects on the AAR-induced swelling rate observed in these dams. In-situ stresses also play an important role in the distributions of the AAR-induced strains, but only in larger dams with compressive stresses exceeding around 1 to 2 MPa.

The swelling due to AAR can be represented by a characteristic curve, which is unique for each dam, but could change with time. Since the crest rise is progressive over time, this must also be true for the characteristic curve of the AAR-induced swelling. To fit the entire swelling

history and to make any forecast of future deformations, the characteristic curve for each dam will have to be adjusted over time.

Figure 7 illustrates how different expansion rates can be in various dams. Among the dams operated by Axpo Power, the Roggisaca and Runcahez dams have experienced the highest AAR-induced swelling of about 3000 $\Delta m/m$ after 60 years since the commissioning.

REFERENCE

- 1 . Swiss Committee on Dams, Concrete Swelling of Dams in Switzerland, AAR Working Group, May 2017.

Effects of wall roughness on low-level outlet performance

S. Pagliara & B. Hohermuth

Laboratory of Hydraulics, Hydrology and Glaciology (VAW), ETH Zurich, Zurich, Switzerland

S. Felder

Water Research Laboratory, School of Civil and Environmental Engineering, UNSW Sydney, Australia

R.M. Boes

Laboratory of Hydraulics, Hydrology and Glaciology (VAW), ETH Zurich, Zurich, Switzerland

ABSTRACT: Reservoir dams play a key role in modern society, water resources management and economy. Low-level outlets (LLOs) represent important safety structures for regulating the water level in the reservoir, and for its fast drawdown in case of scheduled maintenance or emergency situations. The flow in LLO tunnels is characterized by high velocities and turbulence levels, leading to air entrainment and transport. This results in sub-atmospheric air pressures, which may induce and aggravate serious issues such as gate vibration and cavitation. An adequate flow aeration via an air vent can mitigate these problems and is key to good performance. While many studies focused on the effects of hydraulic parameters, tunnel geometry and air vent design on the air demand of LLOs, the influence of the tunnel wall roughness is still unclear. To this end, physical model tests were carried out to investigate the effects of invert, soffit, and sidewall roughness on the LLO performance, for various combinations of gate opening, energy head at the gate and air vent properties. The roughness modelled in this study represents unlined rock, and it was implemented by attaching expanded aluminum plates to the inner sides of the outlet tunnel. Air velocities in the air vent were measured to estimate the air demand, and pressures along the tunnel were recorded to assess cavitation potential. For rough wall conditions, both the air demand and the cavitation risk were found to increase compared to the smooth tunnel conditions (i.e., acrylic-made invert, walls, and soffit in the model). In conclusion, the study represents a preliminary analysis of the effects of LLO tunnel roughness on air demand and cavitation occurrence, and future research is needed to enable a more quantitative assessment of the differences in air demand between model and real-world prototypes.

1 INTRODUCTION

In modern society and economy, reservoir dams constitute important large water infrastructure, and they fulfil several purposes, including (in order of frequency): irrigation, hydropower production, water supply, flood control, and recreation (Hager et al., 2020). Low-level outlets (LLOs) are primarily designed as safety structures for a fast emergency drawdown of the reservoir, for regulating the water level in case of maintenance works, and for controlling the first impounding of the reservoir. Furthermore, LLOs are used for sediment flushing and for flow conveyance during flood events. Due to their importance for dam safety, LLOs must fulfil a multitude of technical requirements, including (Giesecke, 1982): excellent performance and energy dissipation for all hydraulic conditions, simple and fast operation, no leakages, ease of access for maintenance and longevity. LLOs are typically divided into a pressurized tunnel controlled by a high-head gate, and an outlet tunnel conveying the supercritical

free-surface flow into the atmosphere. The free-surface flow portion is of particular interest in the design due to the occurrence of high-velocity air-water flows (Figure 1).

LLOs of large dams are typically not designed to be operated for long periods of time due to serious issues, including (i) gate vibration due to high-velocity flows, (ii) cavitation due to the development of excessively low pressures, and (iii) hydro-abrasion due to the combination of high sediment loads, where applicable, and significant flow velocities. These also represent the most frequent causes of high-head gates failure (Sagar, 1995). Specifically, cavitation has often been the main cause of damage to spillways and LLOs around the world (ASCE/USCOLD, 1975; Chanson, 1988; Kells & Smith, 1991; Kramer, 2004; Koskinas et al., 2019). Cavitation is defined as the formation of vapor bubbles in a liquid (Falvey, 1990). In hydraulic structures, cavitation is associated to low pressures and very high flow velocities. The cavitation index σ is used to assess the cavitation potential:

$$\sigma = \frac{2 \cdot (p_g + p_{atm} - p_v)}{\rho_w \cdot U_w^2} \quad (1)$$

where p_g is the (relative) gauge pressure, $p_{atm} \approx 101,300$ Pa is the atmospheric pressure (at sea level), p_v is the vapor pressure ($p_v \approx 2,330$ Pa for water at 20°C), ρ_w is the water density, and U_w is the water velocity. Furthermore, the incipient cavitation index σ_i has commonly been used to determine a threshold below which a significant damage to the structure is expected after sufficiently long operation. Notably, a value of $\sigma_i = 0.2$ has often been assumed for smooth spillways following prototype observations (Falvey, 1983). In general, σ_i significantly depends on surface roughness and geometry (Arndt et al., 1979).

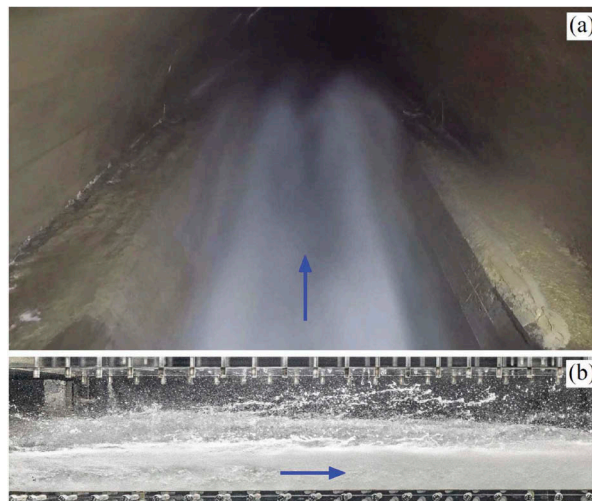


Figure 1. High-speed air-water flows: (a) picture taken inside of the middle outlet of Luzzone Dam, Switzerland; (b) low-level outlet physical model at the Laboratory of Hydraulics, Hydrology and Glaciology (VAW), ETH Zürich. Blue arrows indicate the flow direction.

To mitigate potential issues affecting LLO works, a sufficient air supply to the outlet tunnel via an air vent is crucial. Many empirical design equations are available in literature to predict the relative air demand $\beta = Q_a/Q_w$ of LLOs, i.e., ratio of air discharge through the air vent Q_a over water discharge Q_w , usually expressed as a function of the Froude number at the vena contracta F_c . Among others, Campbell & Guyton (1953) derived a first expression of β based on prototype observations; Wisner (1965) and Sharma (1973) included the effects of air-water flow patterns on β ; Rabben (1984) included the effect of the air vent loss coefficient ζ ; Hohermuth et al. (2020) recently improved the existing design equations by adding the effect of

tunnel slope and length, also comparing model versus real-world prototype data, providing guidance on scale effects. Namely, Hohermuth et al. (2020) derived an empirical equation for β from smooth-tunnel model data, as a function of contraction flow depth (F_c), air-vent cross-sectional area (A_v) and loss coefficient (ζ), LLO tunnel cross-sectional area (A_t), length (L_t), height (h_t), and slope (S):

$$\beta = 0.037 \cdot F_c^{1.3} \cdot \left(\frac{A_v}{A_t \cdot (\zeta + 1)^{0.5}} \right)^{0.8} \cdot \left(\frac{L_t}{h_t} \right)^{0.25} \cdot (1 + S)^{-1.5} \quad (2)$$

Furthermore, Equation (2) was adjusted for prototype data (Hohermuth et al., 2020):

$$\beta = 0.08 \cdot F_c^{1.3} \cdot \left(\frac{A_v}{A_t \cdot (\zeta + 1)^{0.5}} \right)^{0.8} \cdot \left(\frac{L_t}{h_t} \right)^{0.25} \quad (3)$$

Nevertheless, no study has investigated the effect of LLO tunnel wall roughness on the air demand so far. Herein, we provide a preliminary analysis of the effect of tunnel wall roughness on the air demand and cavitation potential of LLOs. This study represents a first attempt of narrowing the gap between air demand data collected in LLO physical models and prototypes, with a view to quantitatively assess the influence of wall roughness on the difference between model and prototype.

2 MATERIALS AND METHODS

2.1 Experimental setup

Experiments were conducted in the low-level outlet (LLO) physical model at the Laboratory of Hydraulics, Hydrology and Glaciology (VAW), ETH Zürich (Figure 1b), which has more recently been used to investigate high-energy air-water flows (e.g., Hohermuth, 2019; Pagliara et al., 2023). The model consists of several key elements: the pressurized tunnel and the gate chamber where the transition from pressurized flow to free-surface flow occurs; the air vent system, providing air supply to the flow; the outlet tunnel, conveying the free-surface flow to the free-outlet. A sketch of the experimental apparatus is presented in Figure 2.

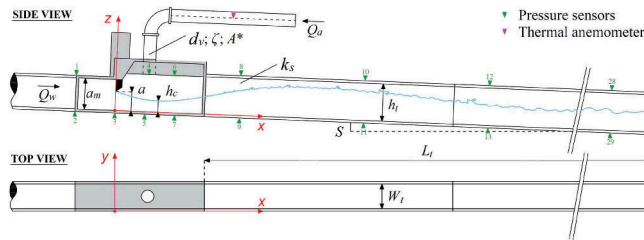


Figure 2. Sketch of the low-level outlet (LLO) physical model along with the main parameters. Note the measurement locations with pressure sensors and thermal anemometer.

Two high-head pumps (Egger EOS 8-300) provided constant water discharges Q_w of up to $0.536 \text{ m}^3/\text{s}$ and energy heads H at the gate of up to 30 m to a rectangular inflow tunnel of 0.20 m width and 0.25 m height, operating under pressure. This inflow tunnel was connected to a gate chamber featuring a sluice gate with a maximum opening $a_{max} = 0.25 \text{ m}$, operated by a stepped motor (SIG Positec-Berger Lahr VRDM, precision = $\pm 0.5 \text{ mm}$), leading to a relative gate opening $A = a/a_{max}$. Downstream of the sluice gate, a steel-made circular air vent was connected to the top of the gate chamber. The air vent pipe had a diameter $d_v = 0.15 \text{ m}$,

corresponding to a cross-sectional area $A_v = \pi \cdot d_v^2/4$. Three different PVC plates with orifice openings 100, 40, and 20% the area A_v were used to vary the air vent loss coefficient $\zeta = 2 \cdot (p_{atm} - p_{a,min})/(\rho_a \cdot v_{a,av}^2)$, with p_{atm} as atmospheric pressure, $p_{a,min}$ as minimum air pressure recorded at the base of the air vent, ρ_a as air density, and $v_{a,av}$ as average air velocity in the air vent. A range of air vent parameters $A^* = A_v/A_t \cdot 1/(\zeta+1)^{0.5}$ was tested, where A_t is the tunnel cross-sectional area (Table 1). The air discharge was estimated as $Q_a = v_{a,av} \cdot A_v$. The outlet tunnel started downstream of the gate chamber with sluice gate. It had a height $h_t = 0.3$ m, a width $W_t = 0.2$ m, a slope $S = 4\%$, and a length of $L_t = 20.6$ m. The origin of the reference system was set at the lower right corner of the sluice gate cross-section (Figure 2). The model allowed to investigate high-velocity air-water flows at a Froude scale of 1:5 to 1:20 for typical high-head LLOs in Switzerland, using W_t as the reference length.

Table 1. List of air vent properties and of the resulting loss coefficient ζ and air vent parameter A^* .

d_v [m]	A_v/A_t [-]	Or. [%]	ζ [-]	A^* [-]
0.15	0.29	100	2	0.18
0.15	0.29	40	10	0.10
0.15	0.29	20	42	0.05

Two inductive flow meters (E+H Promag 50; precision = $\pm 0.5\%$ of the measured value, absolute error = ± 0.4 l/s) were used to measure the water discharge Q_w . Moreover, water and air pressure were measured at several locations, indicated in Figure 2: two pressure sensors (Keller PR-23SY; range = 0 to 3 bar, accuracy = ± 0.008 bar) were used to measure the water pressure in the pressurized tunnel at the invert ($p_{w,i}$) and soffit ($p_{w,s}$); similar pressure sensors (range = -0.1 to 0.1 bar, accuracy = ± 0.001 bar) were used to record air and water pressures along the free-surface tunnel centerline of the invert and soffit. The maximum air flow velocity in the air vent $v_{a,max}$ was measured along the centerline by a thermal anemometer (Höntzsch; precision = $\pm 2.5\%$ of the measured value), and the air flow Q_a in the vent was inferred by assuming a logarithmic velocity profile. This allowed to compute the relative air demand $\beta = Q_a/Q_w$. All measurements were averaged over 180 s to ensure a stable mean value for steady-state conditions, and the system was controlled with LabVIEW software.

The energy head at the gate was calculated as $H = [0.5 \cdot (p_{w,i} + p_{w,s})]/(\rho_w \cdot g) + [Q_w/(W_t \cdot a_m)]^2/(2 \cdot g)$, where ρ_w is the water density, and g the gravitational acceleration. The contraction coefficient C_c was estimated from ortho-rectified images by Hohermuth (2019) for each gate opening a , resulting in values ranging between 0.61 and 0.72. The contraction flow depth was expressed as $h_c = a \cdot C_c$. Finally, the Froude number at the vena contracta was computed as $F_c = Q_w/[(W_t \cdot h_c) \cdot (g \cdot h_c)^{1/2}]$, while the Reynolds number at the vena contracta as $R_c = (Q_w \cdot h_c)/(W_t \cdot h_c \cdot \nu)$, with $\nu \approx 10^{-6}$ m²/s the kinematic viscosity of water at 20°C.

2.2 Wall roughness implementation

The outlet tunnel walls were made of acrylic-glass with a hydraulic roughness of $k_s \approx 3 \cdot 10^{-6}$ to $5 \cdot 10^{-5}$ m (Barr, 1998), herein assumed to be $k_s = 5 \cdot 10^{-5}$ m = 0.05 mm. To modify the wall roughness of the tunnel, expanded aluminum plates were attached to the inner sides (Figure 3).

Three different configurations were tested (Table 2): (1) “full lining”, i.e., the plates covered the tunnel invert, soffit, and sidewalls; (2) “no left sidewall”, i.e., the plates covered the tunnel invert, soffit, and the right sidewall (in flow direction); (3) “invert lining”, the plates covered the tunnel invert only. From a top view (Figure 3a), the plates presented rhomboid openings of dimensions 45 x 20 mm (major x minor diagonal). The aluminum sheets were 1.5 mm thick, and the total thickness of the expanded plate was ≈ 10 mm (Figure 3b). For each of the three configurations, the equivalent sand roughness k_s was estimated by quantifying the head losses resulting from several runs of the LLO tunnel under pressure (see Section 3).

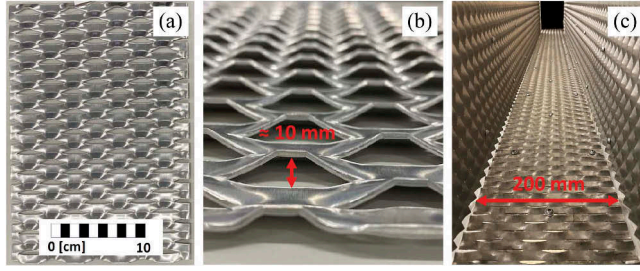


Figure 3. Expanded aluminium plates used to modify the LLO tunnel roughness: (a) top view; (b) side view; (c) view of the tunnel lining.

3 RESULTS AND DISCUSSION

3.1 Estimation of equivalent sand roughness

To quantitatively classify the tunnel roughness, for configurations 1, 2, and 3 (Table 2), the equivalent sand roughness k_s was estimated by running the LLO tunnel under pressure, following the definition of Nikuradse (1933).

Table 2. Roughness plates arrangements in the LLO tunnel. For configuration 4, only pressure data at the tunnel invert were available (used for cavitation assessment).

Configuration n.	Description	f_r [-]	R_c [-]	k_s [mm]
1	Full lining	0.108	$4.9 \cdot 10^5$	13.2
2	No left sidewall	0.069	$5.9 \cdot 10^5$	11.0
3	Invert only	0.024	$8.7 \cdot 10^5$	0.50
4	No lining	0.013	$1.0 \cdot 10^6$	0.05

For each roughness configuration, two different values of water discharge were tested, and pressure measurements at 1000 Hz were performed over a duration of 180 s (Figure 4a). The time-averaged value of the relative pressure at position j along the tunnel invert ($p_{w,i,j}$) and soffit ($p_{w,s,j}$) were used to compute the average value along the tunnel axis, i.e., $p_{av,j} = 0.5 \cdot [p_{w,i,j} + p_{w,s,j}]$, and linear regression was performed to estimate the variation of $p_{av,j}$ along the outlet tunnel (Figure 4b).

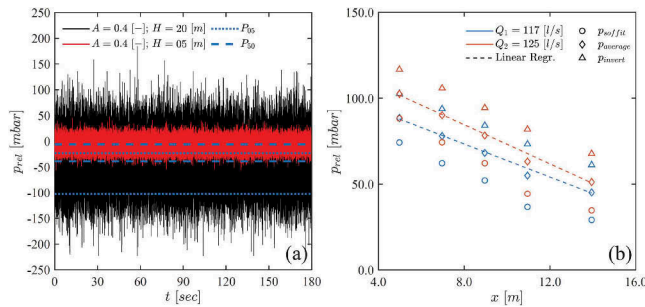


Figure 4. (a) LLO tunnel invert pressure measurements at $x = 1$ m for roughness configuration 3 and two hydraulic conditions, including 50th (P_{50}) and 5th (P_{05}) percentile values; note the increasing pressure fluctuations as the time-averaged value decreases. (b) Head loss along the LLO tunnel used for the estimation of the equivalent sand roughness k_s for the full lined condition (configuration 1).

Finally, the head loss was calculated as $\Delta H_p = \Delta p_{av}/(\rho_w \cdot g) + S \cdot \Delta x$, where Δx is the distance along the outlet tunnel, and Δp_{av} is the pressure drop over Δx . The friction factor f_r was estimated by means of the Darcy-Weisbach equation modified for rectangular channels (Marchi, 1961):

$$f_r = \frac{\Delta H_p \cdot 2g \cdot D_{eq} \cdot A_t^2}{\Delta x \cdot Q_w^2} \quad (4)$$

where $D_{eq} = 4 \cdot A_t / P$ is the equivalent hydraulic radius for rectangular cross sections, with P as wetted perimeter. Finally, the Colebrook-White equation was used to estimate the equivalent sand roughness k_s . The results for f_r and k_s are summarized in Table 2. Notably, the k_s -value for configuration 1 represented a homogeneous value of roughness across all tunnel walls, while the k_s -values for configurations 2 and 3 are to be interpreted as equivalent values, as the roughness was non-homogeneously distributed.

The geometrical features of the LLO physical model were linearly scaled using a Froude similitude with Reynolds numbers ($2 \cdot 10^5 < R_c < 3 \cdot 10^6$), sufficiently large to minimize scale effects, i.e., negligible viscous forces (Heller, 2011). The model k_s -value obtained for the full lined tunnel (i.e., configuration 1) would correspond to unlined blasted rock in a prototype chute with $k_s = 132$ mm for a scale factor $\lambda = 10$. All three rough configurations (i.e., configurations 1, 2, and 3) correspond to a fully rough, turbulent flow regime. The smooth laboratory LLO tunnel (i.e., configuration 4) corresponds to a prototype chute characterized by a very smooth finished concrete (prototype roughness $k_s = 0.5$ mm assuming $\lambda = 10$), falling into the transitionally rough, turbulent regime, i.e., f_r depending on R_c .

3.2 Air demand

This section presents the air demand observations for the three rough wall configurations 1, 2, and 3 (Figure 3; Table 2). The air vent characteristics strongly influenced the air discharge Q_a , and their effects are described by the air vent parameter A^* first introduced by Rabben (1984). In addition, the modified wall roughness significantly affected the hydraulics of the LLO, including the air-water flow conveyed by the outlet tunnel. Different flow patterns of the air-water flow mixture in the outlet tunnel have a pronounced effect on the air demand for smooth walls (Hohermuth, 2019): as the air-water mixture depth increases in the tunnel, the air discharge Q_a through the air vent drops, and so does the air demand $\beta = Q_a / Q_w$. The flow patterns occurring in the present LLO tunnel configurations were visually classified into two main groups, namely spray/free-surface flow (*FSF*) and intermittent/foamy/pressurized flow (*I*). The first group was characterized by a continuous air layer above the air-water flow mixture, while the latter presented either an intermittent air layer (flow pulsations) or a non-distinguishable air layer at all. To this end, it is worth mentioning that the range of combinations of relative gate openings A and hydraulic heads H was heavily restricted by the roughness plates, leading to the complete filling of the LLO tunnel for most of the hydraulic conditions (e.g., fully pressurized outlet tunnel for $A \geq 0.3$, $H \geq 10$ m, and roughness configuration 1).

Figure 5a Presents the relationship between relative air demand β and contraction Froude number F_c in a double-logarithmic plot, with points colored by A^* , shaped by k_s , and filled by the associated flow pattern (i.e., *FSF* or *I*). For tests characterized by *FSF* conditions and the same air vent configuration (i.e., A^*), the air demand can be expressed by a power-law function (Figure 5a). Furthermore, a decrease in A^* (corresponding to an increase in ζ) lead to a decrease in β for a fixed F_c . Notably, a roughly parallel translation of the regression line occurs as A^* decreases (Figure 5a). Wall roughness affects the air demand to a smaller extent (Figure 5b): for a fixed value of ζ and A^* , the air demand β reduces as k_s increases for a fixed value of F_c ; nevertheless, the difference becomes smaller for $F_c < 20$. Notably, the observed trends are completely lost if the tests associated with an *I* flow pattern are introduced in the analysis (transparent points in Figure 5, b).

The air vent system can be thought as a “water aspirator”, where air discharges through the vent Q_a are associated to pressure differences between the two extremities of the air vent (Speerli & Hager, 2000), i.e., p_{atm} and $p_{a,min}$. For a fixed air supply system, i.e., same A/A_t and ζ (thus A^*), the relationship between the minimum relative air pressure at the base of the vent $p_{a,min}$ and the average air velocity $U_{a,av}$ is defined as $p_{a,min} = \rho \cdot U_{a,av}^2 \cdot (\zeta + 1) / 2$ (Figure 6a). An increase of the loss coefficient ζ and/or A/A_t (thus a decrease in A^*) leads to a smaller $p_{a,min}$ for comparable $U_{a,av}$ (i.e., lower negative pressures). For practical applications, this allows to control the air vent operational

point by varying A_v and ζ (for a fixed A_f). Low values of pressure in the gate chamber may aggravate issues such as cavitation and gate vibration, as well as triggering slug flow due to the inverse proportionality between $p_{a,min}$ and the air discharge from the downstream end of the LLO tunnel, as demonstrated by Hohermuth (2019) for smooth tunnels. Particular care should be taken for gate vibration, as the pressure fluctuations are more pronounced as the time-averaged $p_{a,min}$ decreases (Figure 4a). Available guidelines of minimum allowable sub-pressures in the gate chamber suggest values of $p_{a,min}$ of up to -1.5 m of water head (Douma, 1955; USACE, 1980; Speerli & Hager, 2000). As expected, the wall roughness and flow patterns have negligible effect on the relationship between $p_{a,min}$ and $U_{a,av}$ within the tested flow conditions (Figure 6a).

Recently, Hohermuth et al. (2020) derived two empirical equations from smooth-tunnel model data (Equation 2) and prototype data (Equation 3) to predict the relative air demand β . Most β -values predicted by Equation (2) are 50% smaller compared to the one that we observed in physical model tests, suggesting that the modified wall roughness leads to an increase in air demand for otherwise similar flow conditions (Figure 6b). In addition, there seems to be no pattern associated to the k_s -value variations, suggesting that the increase in air demand is mainly driven by the presence of the rough plate along the LLO tunnel invert, common for roughness configurations 1, 2, and 3 (see Table 2). On the contrary, the comparison with the empirical relationship derived by Hohermuth et al. (2020) from prototype data (Equation 3) tends to overestimate the air demand in our model. The significant deviation between model data and predicting equation for prototypes may be due to differences in geometry and scale effects. Furthermore, most of the present data were characterized by a significant formation of spray, which is known to be strongly affected by scale effects (Rabben, 1984; Heller, 2011). Additional flow conditions and wall roughness values should be tested to further investigate these effects.

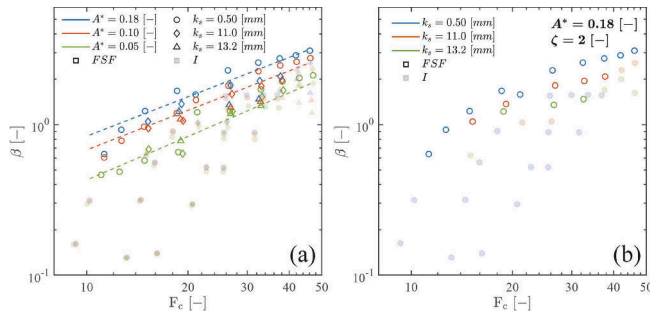


Figure 5. Relative air demand β versus contraction Froude number F_c grouped according to the air vent parameter A^* and equivalent sand roughness k_s , with distinction between free-surface (*FSF*) and intermittent (*I*) flow regimes: (a) all data; (b) dataset for $A^* = 0.18$, corresponding to a loss coefficient $\zeta = 2$.

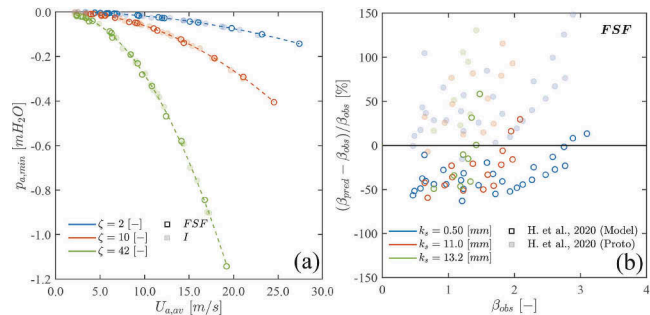


Figure 6. (a) Minimum air pressure at the base of the air vent $p_{a,min}$ versus average air velocity in the air vent $U_{a,av}$, grouped by loss coefficient ζ , with distinction between free-surface (*FSF*) and intermittent (*I*) flow; (b) percentage difference between the air demand for free surface flows (*FSF*) observed in our experimental tests β_{obs} and the one predicted by Hohermuth et al. (2020) β_{pred} from the empirical equations derived for physical model and prototypes.

3.3 Cavitation

Under the assumption that the root-mean-square value of the turbulent velocity fluctuations is used to estimate the cavitation potential of boundary layer flows (Falvey, 1990), the incipient cavitation index σ_i can be expressed as $\sigma_i = 4 \cdot f_r$ (Arndt et al., 1979), where f_r is the Darcy-Weisbach friction factor. The flow depth h_m of the air-water mixture was estimated by high-speed images taken from the side-view of the first block of the LLO tunnel (i.e., from $x = 0.7$ to $x = 3.3$ m), corresponding to the section with minimum invert pressures and maximum velocities. The uncertainty of the estimations was ± 5 cm due to fluctuations of the air-water flow mixture, resulting in an uncertainty in σ_i of less than ± 0.01 . Using the k_s -value estimated in Section 3, i.e., $k_s = 13.2$ mm, the friction factor can be estimated as $f_r = f(k_s/D_h; R_c)$, with $D_h = (W_i h_m)/(2 \cdot h_m + W_i)$ and $R_c = Q_w/(v \cdot W_i)$. For roughness configurations 1, 2, and 3, the range of incipient cavitation index was found within $0.28 \leq \sigma_i \leq 0.33$. In real-world prototypes the air-water mixture flow depth can be estimated from simplified backward calculations (Speerli & Hager, 2000; Hohermuth, 2019), while a more straightforward alternative might be to use the contraction flow depth h_c downstream of the sluice gate (conservative assumption).

The cavitation index σ along the LLO tunnel was computed from Equation (1), with $U_w = U_c$, where U_c is the water velocity at the vena contracta. The minimum values of cavitation index σ were observed within 5 m downstream of the sluice gate. The air-vent loss coefficient ζ had an influence in limiting the cavitation potential (Figure 7a): with increasing ζ for otherwise similar conditions, pressures along the tunnel invert decreased (i.e., increasing sub-pressures), resulting in smaller values of σ and thus increasing the cavitation potential. Figure 7b shows the development of the cavitation index σ along the LLO tunnel invert for two hydraulic conditions (i.e., $A = 0.2$, $H = 20$ m; $A = 0.2$, $H = 30$ m), one air vent configuration ($\zeta = 2$), and the three roughness configurations. Roughness configurations 1 and 2 were characterized by a similar development of σ along the outlet tunnel and by the same σ_i . Configuration 3 showed a similar pattern in the first 5 m downstream of the sluice gate, but it was characterized by a slightly higher incipient cavitation index σ_i , resulting in greater proneness to cavitation. Configuration 4 (smooth conditions) showed the highest values of σ and a very small incipient cavitation index ($\sigma_i = 0.06$). However, for smooth walls and prototype outlet tunnels, a σ_i of 0.20 is typically assumed (Falvey, 1983; 1990). Finally, Figure 7b shows that cavitation might occur only for configuration 3 with $A = 0.2$ and $H = 30$ m, shortly downstream of the gate where $\sigma < \sigma_i$.

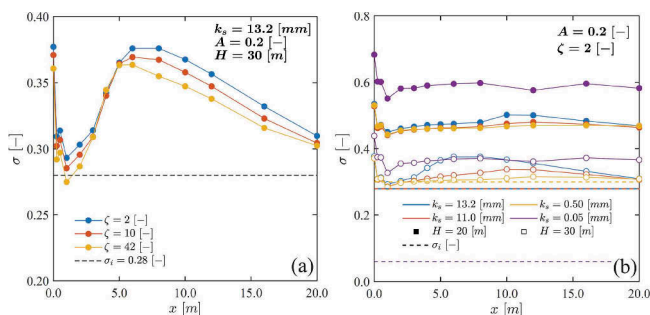


Figure 7. Cavitation index σ versus streamwise position along the LLO tunnel x : (a) effect of the orifice plate opening on σ for the full-lined tunnel ($k_s = 13.2$ mm), $A = 0.2$, and $H = 30$ m; (b) effect of tunnel roughness on σ , including smooth tunnel data, for $A = 0.2$, $H = 20$ m and $A = 0.2$, $H = 30$ m.

4 CONCLUSIONS

Low-level outlets (LLOs) are key safety structures of reservoir dams. The conveyed flow is characterized by high velocities and turbulence levels, resulting in sub-atmospheric air pressures, which may trigger gate vibration and cavitation. Aeration is the key to mitigate such problems, thus the relative air demand (i.e., the ratio of air discharge through the air vent over water discharge) is a fundamental parameter for a safe design of LLOs. This study conducted

a preliminary analysis of the effect of LLO tunnel wall roughness on the air demand and on the cavitation potential of LLOs. Three different roughness configurations were tested by attaching expanded aluminum plates to the acrylic-glass walls of a LLO physical model. The main findings are:

- The relative air demand β was found to increase with the Froude number F_c , and an increase in the air vent loss coefficient ζ (thus a decrease in the air vent parameter A^*) led to a decrease in β for a fixed F_c , confirming previous results for smooth tunnels; a strong dependence of β on the flow pattern was also confirmed. In addition, a slight increase in β with decreasing equivalent sand roughness k_s for $F_c > 20$ and otherwise similar conditions was observed.
- The relationship between the average air velocity inside the air vent $U_{a,av}$ and the minimum pressure in the gate chamber $p_{a,min}$ was shown to be affected neither by the tunnel roughness nor by the flow pattern, confirming observations in smooth tunnels.
- The comparison of present rough wall data with a predicting equation from Hohermuth et al. (2020) developed from physical model data with smooth tunnel showed an average underestimation of β by roughly 50%, suggesting an increase in air demand due to the increased tunnel roughness. The limited influence of the different roughness configurations suggests that the rough invert drives the phenomenon.
- On the other hand, an equation derived by Hohermuth et al. (2020) from prototype data significantly overestimated β compared to rough wall model data. This may be due to the present limited test conditions which were characterised by significant spray formation for most tests, as well as scale effects. Disagreements in tunnel and gate geometries may also partially explain the observed difference.
- An increase of the air vent loss coefficient ζ was shown to aggravate and possibly trigger cavitation. The incipient cavitation index increased when only the LLO tunnel invert was lined (configuration 3) due to the smaller flow depth for otherwise similar conditions compared to the fully and one-sidewall lined tunnel (configuration 1 and 2, respectively).

Overall, this study represents a preliminary assessment of the effects of LLO tunnel roughness on air demand and cavitation occurrence. Future research should expand this study by testing more roughness configurations for a wider range of flow conditions, to enable a more quantitative assessment of scale effects.

ACKNOWLEDGMENTS

The project was supported by the Swiss National Science Foundation (SNSF), grant number 197208 (extra information: www.data.snf.ch/grants/grant/197208).

REFERENCES

- Arndt, R. E. A., Holl, J. W., Bohn, J. C., & Bechtel, W. T. (1979). Influence of surface irregularities on cavitation performance. *Journal of Ship Research*, 23(03), 157–170. <https://doi.org/10.5957/jsr.1979.23.3.157>
- ASCE/USCOLD. (1975). *Lessons from dam incidents, USA*. The Committee on Failures and Accidents to Large Dams. ASCE, New York.
- Barry, D. I. H. (1998). *Tables for the hydraulic design of pipes, sewers and channels* (Vol. 2). Thomas Telford.
- Campbell, F. B., and Guyton, B. (1953). Air demand in gated outlet works. *Proc. 5th IAHR Congress*, Minnesota, USA, 529–533.
- Chanson, H. (1988). *Study of air entrainment and aeration devices on spillway model*. University of Canterbury, Christchurch. <http://dx.doi.org/10.26021/2699>
- Douma, H. (1955). Hydraulic design criteria for reservoir outlets. *Proceeding. 6th International Association for Hydraulic Research, American Society of Civil Engineers (ASCE) Joint, Reston, VA, USA*.
- Falvey, H. T. (1983). Prevention of cavitation in chutes and spillways. *Frontiers in Hydraulic Engineering*, ASCE, New York, 432–437.

- Falvey, H. T. (1990). *Cavitation in chutes and spillways*. Denver, CO, USA: US Department of the Interior, Bureau of Reclamation. <https://luk.staff.ugm.ac.id/USBR/EM42.pdf>
- Giesecke, J. (1982) Verschlüsse in Grundablässen: Funktion und Ausführung (Gates of bottom outlets: performance and design). *Wasserwirtschaft*, 72 (3),97–104(in German).
- Hager, W. H., Schleiss, A. J., Boes, R. M., & Pfister, M. (2020). *Hydraulic engineering of dams*. CRC Press. <https://doi.org/10.1201/9780203771433>
- Heller, V. (2011). Scale effects in physical hydraulic engineering models. *Journal of Hydraulic Research*, 49(3), 293–306. <https://doi.org/10.1080/00221686.2011.578914>
- Hohermuth, B. (2019). *Aeration and two-phase flow characteristics of low-level outlets*. Doctoral dissertation, VAW-Mitteilung Nr. 253, ETH Zurich. <https://doi.org/10.3929/ethz-b-000479079>
- Hohermuth, B., Schmocker, L., & Boes, R. M. (2020). Air demand of low-level outlets for large dams. *Journal of Hydraulic Engineering*, 146(8), 04020055. [https://doi.org/10.1061/\(ASCE\)HY.1943-7900.0001775](https://doi.org/10.1061/(ASCE)HY.1943-7900.0001775)
- Kells, J. A., & Smith, C. D. (1991). Reduction of cavitation on spillways by induced air entrainment. *Canadian journal of civil engineering*, 18(3), 358–377. <https://doi.org/10.1139/191-047>
- Koskinas, A., Tegos, A., Tsira, P., Dimitriadis, P., Iliopoulou, T., Papanicolaou, P., & Williamson, T. (2019). Insights into the Oroville dam 2017 Spillway incident. *Geosciences*, 9(1), 37. <https://doi.org/10.3390/geosciences9010037>
- Kramer, K. (2004). *Development of aerated chute flow*. Doctoral dissertation, VAW-Mitteilung Nr. 183, ETH Zurich. <http://e-collection.ethbib.ethz.ch/show?type=diss&nr=15428>
- Marchi, E. (1961). Il moto uniforme delle correnti liquide nei condotti chiusi e aperti. (Uniform flow in closed and open channels). *L'Energia Elettrica* 38 (4):289–301; 38 (5):393–413 (in Italian).
- Nikuradse, J. (1933). “Strömungsgesetze in rauhen Röhren.” Forschungsheft 361 (Beilage zur ‘Forschung auf dem Gebiet des Ingenieurwesens’, Ausgabe B Band 4, Juli/August 1933), VDI-Verlag GmbH, Berlin, Germany (in German).
- Pagliara, S., Hohermuth, B., & Boes, R. M. (2023). Air-water flow patterns and shockwave formation in low-level outlets. *Journal of Hydraulic Engineering* (in print). <https://doi.org/10.1061/JHEND8/HYENG-13357>
- Rabben, S. L. (1984). *Untersuchung der Belüftung an Tiefschützen unter besonderer Berücksichtigung von Massstabeffekten* (Investigation of aeration of high-head gates with special consideration of scale effects). Mitteilung Nr. 53, Institut für Wasserbau und Wasserwirtschaft, RWTH Aachen (in German).
- Sagar, B. T. A. (1995). ASCE hydrogates task committee design guidelines for high-head gates. *Journal of Hydraulic Engineering*, 121(12), 845–852. [https://doi.org/10.1061/\(ASCE\)0733-9429\(1995\)121:12\(845\)](https://doi.org/10.1061/(ASCE)0733-9429(1995)121:12(845))
- Sharma, H. R. (1973). *Air demand for high head gated conduits*. Doctoral dissertation, University of Trondheim, The Norwegian Institute of Technology, Trondheim.
- Speerli, J., & Hager, W. H. (2000). Air-water flow in bottom outlets. *Canadian Journal of Civil Engineering*, 27, 454–462. <https://doi.org/10.1139/199-087>
- US Army Corps of Engineers (USACE, 1980). Hydraulic Design of Reservoir Outlet Works. *Engineering Manual 1110–2–1602*.
- Wisner, P. (1967). Air entrainment in high speed flows. Proc. 9th ICOLD Congress, Istanbul, 495–507.

Safety of embankment dams in the case of upgrading the existing tailings storage facilities

L. Petkovski, F. Panovska & S. Mitovski

Faculty of Civil Engineering, Ss. Cyril and Methodius University in Skopje, Skopje, North Macedonia

ABSTRACT: The embankments over tailings dams and waste lagoons or the upgrade at the existing tailings storage facilities, from stability aspects of a heterogenic geo environment, has many similarities with the tailings dams with upstream construction method. These earth-fill structures are susceptible to liquefaction during static and dynamic (cyclic) loading and therefore they are civil engineering structures with the highest stability risk. The need to provide an additional volume for depositing tailings material, necessary for the regular operation of mines in conditions of spatial limitation, actualizes the upgrade of the tailings storage facilities. This upgrade is characterized by detailed geotechnical in-situ investigations and sophisticated structural analyses, which are illustrated by the results of the stability analyses (in static and dynamic conditions) of a dry stacking embankment above the tailings storage facility Sasa no. 2, Makedonska Kamenica, Republic of North Macedonia.

1 UPGRADING OF EXISTING WASTE LAGOONS

During the utilization of tailings storage facilities (TSF), flotation tailings with hydro transport (usually gravitational pulp duct) are conducted to the crest on the tailings dam. There, with hydro-cycloning, tailings separate into two fractions. With the coarser, or dry fraction (cycloned sand), the dam body is constructed, and the finer fraction (cyclone mud) is deposited in the waste lagoon. According to the method of advancement or construction of the tailings dams, three methods are used: downstream, central and upstream method, Figure 1.

Previous practice has confirmed that the highest stability of the tailings dam is achieved with the downstream method of advancement. In that case, the crest of the dam is moved downstream and the cycloned sand is deposited in sloping layers along the downstream slope over the tailings sand embankment. The lowest stability of the heterogeneous geoenvironment is obtained by the upstream method of stage advancement. Then, in each subsequent stage, the crest of the sand dam is displaced upstream, that is, the sand dams are founded on top of deposited tailings mud.

Heterogeneous geoenvironment - a tailings dam above a waste lagoon or a tailings dam with upstream construction method is subject to liquefaction under static and dynamic (cyclic) loading. Static liquefaction (Petkovski et al., 2019) is possible: (a) with an additional external load that causes an increase in shear stress, where the state of stress in the (q-p') diagram moves 'up' to an intersection with the failure surface, and/or (b) with an additional water saturation and reduction of the effective normal stresses, where the stress state in the (q-p') diagram moves 'to the left' to the intersection with the failure surface. Dynamic liquefaction (Petkovski et al., 2018) occurs during an earthquake, where cyclic loading causes a continuous increase in pore pressure, which results in decrease in effective stresses, where the state of stress in the (q-p') diagram moves 'to the left' to the intersection with the failure surface. When liquefaction occurs, the structure of the grains is destroyed and the shear strength of the material decreases to steady-state strength. Therefore, tailings dams with upstream construction method are treated as hydraulic structures with highest risk and are not recommended in

seismically active regions. In some countries with high seismicity, for example in Chile and Peru, the construction of tailings dams with upstream progress is prohibited by law.

The upgrading of waste lagoons in existing TSF, from the aspect of the stability of the heterogeneous geoenvironment, has great similarities with tailings dams constructed with the downstream method. The key difference consists in the fact that the period with hydrotransport of the pulp has ended and the waste lagoon of the TSF has been formed up to the final elevation. For the operation of the mine in the future period, if there is no space for a new waste lagoon, that is, there is no hydrotransport of tailings, then, for the pulp from the flotation plant a method with pressing and filtering is applied, which results in 'dry stacking'. If the upper surface of the existing waste lagoon is used as a foundation for dry stacking, due to the existence of excess pore pressure inside the lake of poorly permeable tailings mud, a standard solution is dissipation of pore pressure, Figure 2.

A logical question arises – where does the need come from for the mining companies to initiate solutions with upgrades over the existing waste lagoons? It is obvious that they are embankment constructions with highest risk, and to confirm their stability, detailed geotechnical research and sophisticated structural (static, seepage, dynamic) analyses are necessary, that would result in large financial investments. The explanation, in our opinion, is as follows. On one hand, space for the survival, development and growth of mining companies, which are essential for the existence of the population in certain regions (which rely on the mining industry), due to the imposition of increasingly strict environmental and sociological criteria, is becoming more and more limited. On the other hand, obtaining permission to expand the concession area (or increase the industrial scope) from a huge number of agencies/institutions, in countries that are heavily bureaucratized and, unfortunately, corrupt, for mining companies is prolonged in a long-term exhausting administrative process with uncertain outcome. Therefore, mining companies increasingly decide on solutions for risky hydraulic structures, i.e. embankment structures over existing waste lagoons.

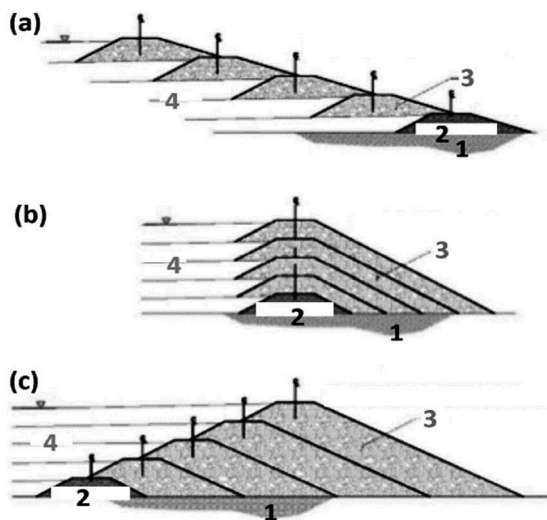


Figure 1. Methods for construction of tailings dams: (a) upstream, (c) central, (c) downstream. 1 – Foundation, 2 – starter dam, 3 – cycloned sand, 4 – cycloned mud.

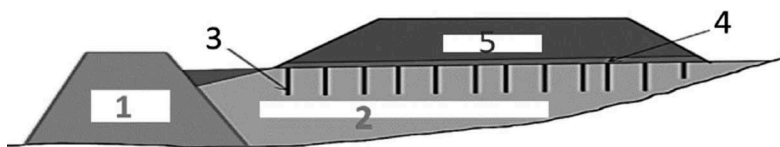


Figure 2. Upgrade to existing waste lagoon with dry stacking. 1 – Existing dam, 2 – existing waste lagoon, 3 – wick drain, 4 – granular bedding, 5 – dry stacking.

2 UPGRADING OF EXISTING WASTE LAGOONS IN RN MACEDONIA

Examples of upgrades on existing waste lagoons (or high-risk hydraulic structures) also exist in RN Macedonia, of which we will single out three, part of mining companies ‘Buchim’ - Radovish, ‘BulMak’ - Probishtip and ‘Sasa’ - M. Kamenica.

Tailings storage facility Topolnica of ‘Buchim’ copper mine, Radovish, has been in use since 1979. In the past period, in TSF Topolnica, more than 130 million m³ of tailings have been deposited, as well as 9 million m³ of stored water. This tailings dam is characterized by construction in phases and a combined construction method, with downstream advancement in first phase and upstream construction during the upgrade in height from the second phase, conducted in two stages (Petkovski et al., 2018). The construction of the sand dam in the initial phase, up to the elevation of 610 masl (1st phase), was carried out in sloped layers, with advancement in downstream direction from the initial dam, with an elevation at the foundation of 518.5 and crest elevation at 558.5 masl. Then, the construction of the sand dam up to the elevation of 630 masl (2nd phase, stage 1), due to the proximity of the village Topolnica to the downstream toe of the dam, was carried out with upstream construction method. In the final stage, the crest elevation is finalized at 654.0 masl (2nd phase, stage 2), with advancement in upstream direction, Figure 3 (Faculty of Civil Engineering, 2018). TSF Topolnica, with height of the tailings dam 2-2 above foundation at the initial dam of $H_0 = 654.0 - 518.5 = 135.5$ m, is one of the highest tailings dams in Europe. The final tailings dam 2-2 height, measured from the crest to the downstream toe, is $H_2 = 654.0 - 512.8 = 141.2$ m, with which this dam represents the highest dam in RN Macedonia (Petkovski et al., 2019.09).

‘Toranica’ mine in the city of Kriva Palanka (BulMak) currently operates with ore production of about 320,000 t/year, and for the needs of the production, the existing TSF is in function. The waste lagoon and tailings dam were formed with construction of an upstream and a downstream dam. The upstream (or retention) dam is conventional dam (earthfill dam with clay facing) with crest at elevation of 977.5 masl. The downstream dam is tailings dam constructed with the downstream construction method, using cycloned sand. The existing TSF Toranica has been upgraded in height twice. The first upgrade was up to crest elevation of 900.0 masl. The retention dam was upgraded with a tailings dam, constructed with central construction method, with crest displaced from the conventional dam, founded on the waste lagoon at position ‘A’. The second upgrade which is in construction phase, was designed up to elevation of 1000 masl, in accordance with the latest technical documentation for the ‘Toranica’ mine tailings dam (Geing KUK, 2018). With this design, the retention dam was planned to be upgraded in height with tailings dam, up to crest elevation of 1000 masl, made of cycloned sand with central construction method, founded on the waste lagoon, at position ‘B’. Alternative solution preparation is ongoing for the upgrade in height up to 1000 masl of the upstream dam (DIPKO, 2022), Figure 4, with location near ‘A’.

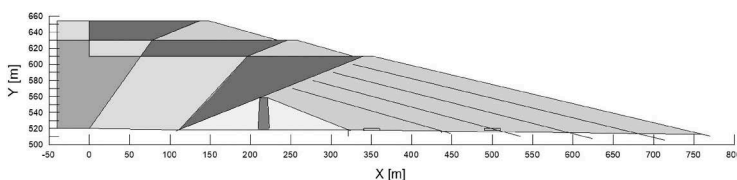


Figure 3. Construction of the tailings dam up to the elevation of 654 masl (2nd phase, stage 2).

In the past service period of TSF of the ‘Sasa’ mine in M. Kamenica, they were intended for disposal of the flotation tailings obtained by the technological process of flotation of lead and zinc minerals. It was transported by hydrotransport to the crests of the tailings dams in a cascade system along the river Kamenichka Reka: 1, 2, 3-1, 3-2 and 4 (during the period when they were active), from where, with the process of hydro - cycloning, it was separated into two fractions. Downstream dams were built with the coarser dry fraction (sand), and the finer liquid fraction was deposited in the waste lagoons.

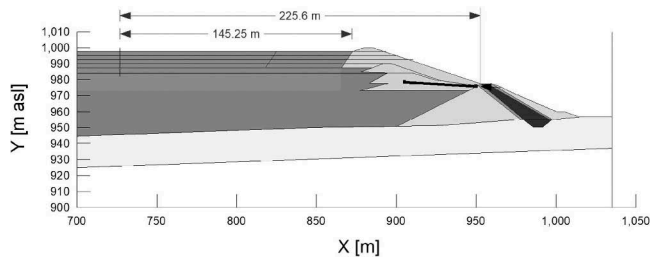


Figure 4. Sketch of the upgrade of the upstream (retention) dam of the tailings dam Toranica, according to Annex 1 of the Detailed Design from 2022 - 08 - 30.

The need to provide additional volume for depositing tailings material, necessary for the regular operation of the ‘Sasa’ mine in the future, was analyzed several times by the expert team of the ‘Sasa’ mine. In July 2019, the first opportunity for disposal of tailings on the existing waste lagoons was reviewed (Faculty of Civil Engineering, 2019). In July 2020, the possibility of dry stacking of tailings, with a volume of at least $2.25 \cdot 10^6 \text{ m}^3$, on the surface of waste lagoons 2 and a part above waste lagoon 1 was updated. Waste lagoon 2 was formed with tailings dam 2, built with a downstream construction method. and with a crest at 1015.0 masl. Upstream from Dam 2, about 3-4 decades ago, a tailings dam 2-2 with a height of 13.0 m was built, which reached the elevation of waste lagoon 2, at 1028.0 masl, upstream of dam 2-2.

The representative longitudinal and cross sections of the geoenvironment are according to the Conceptual design (Faculty of Civil Engineering, 2020), where a dry stacking embankment was adopted in 5.0 m horizontal layers, with 3.0 m berms, a slope of 1:2.5 and a final embankment crest elevation of 1070 masl. (Figure 5).

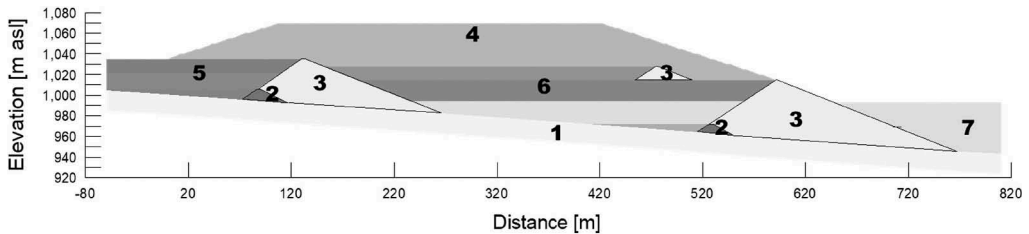


Figure 5. Representative longitudinal section, according to the Conceptual design of 2020.06.26. (1) sand and gravel (alluvium), (2) shale (initial dam), (3) sand - cycloned (dams 1, 2-1, 2-2), (4) dry disposal - embankment, (5) mud 1 - cycloned (lagoon 1), (6) mud 2 - cycloned (lagoon 2), (7) mud 3 - cycloned (lagoon 3-1).

In the further text of this paper, an overview of the key settings and conclusions from the structural analysis of the dry stacking embankment above the existing waste lagoon Sasa 2 is given, i.e. static and seepage analysis (DIPKO, 2021.09.27) and dynamic analysis (DIPKO, 2021.09.28).

3 STRUCTURAL ANALYSIS OF THE DRY DEPOSIT EMBANKMENT ABOVE THE EXISTING WASTE LAGOON ‘SASA 2’

3.1 Basic input data for the structural analysis

The structural (static and dynamic) analysis of the dry stacking above Sasa waste lagoon 2 is made according to the latest recommendations of ICOLD, i.e. with one mathematical model for different phases of the load, where each subsequent phase has an initial stress state determined by the previous stage.

The material in the waste lagoon 1 in the static analysis is modeled with three zones:

- from the ground at 1035 masl (crest of sand dam 1) up to 1021 masl,
- from 1021 masl up to 1,006 masl (crest on initial dam 1),

- from 1006 masl to contact with alluvium (upstream toe on initial dam 1 at elevation of 995.9 masl).

The material in the waste lagoon 2, in the static analysis is modeled with four zones:

- 2-1 from the ground at 1028 masl (crest of sand dam 2-2) up to 1015 masl (crest of sand dam 2-1),
- 2-2 from 1015 masl up to 994 masl,
- 2-3 from 994 masl to 972 masl (crest on initial dam 2),
- 2-4 from 972 masl to contact with alluvium (upstream toe on initial dam 2 at 964.5 masl).

According to the latest geotechnical investigations for tailings 1, 2 and 3-1, as well as for the material from dry disposal, systematized in the following documentation (GEING, 2020), (DIPKO, 2020), (Knight Piésold, 2021), with a larger number of SPT and CPT tests, at selected locations, the following key data was obtained:

1. Pore pressure in waste lagoons 1 and 2 is about 50% of the hydrostatic pressure.
2. Values of the coefficient of consolidated undrained shear strength $S(\text{liq})/\sigma'v0$, obtained by CPT are:
 - For waste lagoon 2, at the surface it is 0.21, at a depth of 30 m it is 0.24 and at a depth of 45 m it is 0.26.
 - For waste lagoon 1, it is 0.21 on the surface and 0.23 at a depth of 30 m.
3. Under liquefaction conditions, the values for the coefficient $Su(\text{liq})/\sigma'v0$, obtained by CPT are:
 - For waste lagoon 2, on the surface it is 0.04, at a depth of 30 m it is 0.12.
 - For waste lagoon 1, on the surface it is 0.10, at a depth of 20 m it is 0.05.

Under liquefaction conditions, the parameters for determining the residual shear strength coefficients $Sr/\sigma'v0$, obtained by SPT are systematized in Table 3.1.

5. For the maximum compaction (highest strength) of the embankment from dry stacking, according to data from the laboratory of the Faculty of Civil Engineering in Skopje, systematized on 27.4.2021, the optimal humidity is 10.9%, which gives a maximum dry volume weight of 21.5 kN/m³.

Table 3.1. Parameters for determination on the coefficients on the residual strength on shear in conditions on liquefaction.

	BH1, TSF-1		BH2, TSF-2		BH3, TSF-2	
h [m blg]	7.0	21.0	6.4	23.4	12.0	25.6
FC, passing 0.075 mm [%]	48	65	65.0	91.0	23.0	35.0
NI(60-sr)	14	20	13	19	15.5	27

3.2 Measures to improve the stability and adopted form of the geoenvironment

The criterion for optimizing the shape of dry stacking embankment is maximization of the volume by satisfying the criteria for temporary and permanent static stability and acceptable seismic resistance of the heterogeneous geoenvironment. In the modeling, in order to fulfill the optimization criterion, stability improvement measures were gradually applied and verified.

The first measure to improve the stability of the geoenvironment is the installation of drainage carpets at the contact of the embankment of dry stacking with the existing waste lagoon 1 and 2 (at an elevation of 1035 masl upstream of dam 1, at elevation of 1028 masl upstream of dam 2-2 and at elevation of 1015 masl upstream of dam 2-1), and inside the new embankment of dry stacking – at elevation of 1050 masl. With this measure, the pore overpressure in the embankment of dry stacking during construction is practically eliminated and it is reduced in the waste lagoons. This measure has the most significant impact in improving stability and has been retained in all further variants.

A second measure to improve the stability of the geoenvironment that was considered was construction of concrete piles in the critical zones of under-toe slope instability, with the following

parameters: distance between two centroids $L = 1.0$ m, diameter $d = 0.6$ m, depth $H = 25$ m, modulus of elasticity $E = 20.0$ GPa, cross section $F = 0.471$ m², moment of inertia $I = 0.0064$ m⁴. As expected, since the piles are not anchored in a rigid environment, no improvement in stability is obtained. With the model, it was confirmed that such a measure for the geoenvironment in question has a negligible impact and was therefore not considered in the further variants.

A third measure to improve the stability of the geoenvironment that was considered was taking into account the tensile strength of the geotextile covering the drainage blanket. By applying joint elements, a geocomposite (geotextile connected to a geogrid) was modeled with the following parameters: thickness $d = 4$ mm, modulus of elasticity $E = 1.0$ GPa, cross section $F = 0.008$ m² (for two layers of geocomposite). As expected, the geocomposite can provide more uniform settlements (irrelevant for the dry stacking embankment), however, it cannot improve the overall under-toe slope stability. The model confirmed that such a measure for the subjected geoenvironment has a negligible impact on stability and was therefore not considered in further variants.

The fourth measure to improve the stability of the geoenvironment that was considered was the reduction of the load in the active zone of the critical slip surfaces. This can only be achieved by increasing the berms in the individual stages during the construction of the embankment from dry stacking, which will inevitably cause a decrease in the volume of dry stacking. This measure was considered in a larger number of variants, with a gradual increase in the widths of the berms, but also with a simultaneous check of the static stability and the seismic resistance (of the longitudinal and cross section models), in order to determine the maximum volume of the dry stacking embankment that meets the criteria for structural stability. In this way, the shape of the embankment with dry stacking was adopted (Figures 6, 7 and 8), for which the results of structural stability analysis are presented in the following text.

3.3 Results of the static analysis

The initial state of stresses before the start of dry stacking is determined by approximating the pore pressure distribution (Figure 9), with the 'In situ' type of analysis, thus simulating the initial state of total stresses (initial state for the next stage of loading) and effective stresses.

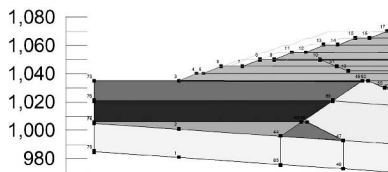


Figure 6. Upstream slope of the embankment from dry stacking (at the longitudinal section).

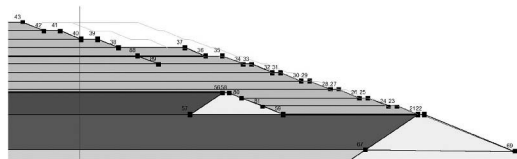


Figure 7. Downstream slope of the dry embankment tailings (at the longitudinal section).

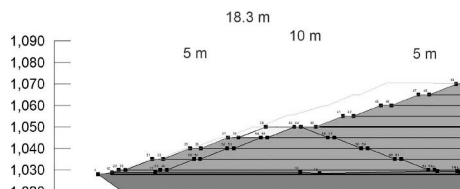


Figure 8. Left slope of the embankment of dry stacking (at the cross section).

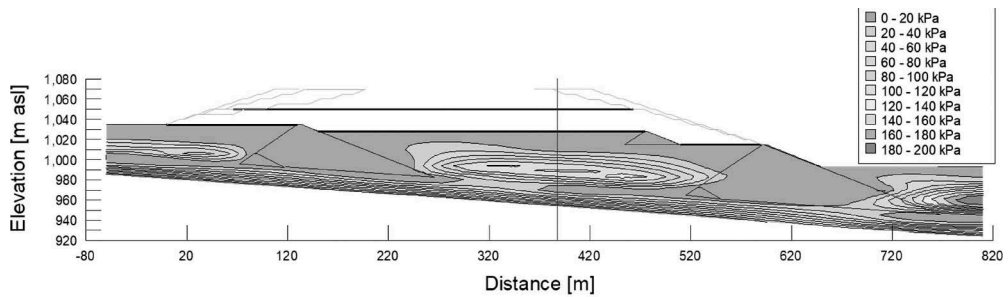


Figure 9. Approximate initial condition for the pore pressure in tailings storage facilities 1, 2 and 3-1.

The construction of the dry stacking embankment in phase 1-1 with a duration of 2.05 years is modeled in 7 stages (or load increments) with a duration of 9,226,341 sec, simulated with 10 calculation steps with an exponential time increment. This analysis was done by applying consolidation analysis of coupled mechanical and seepage response in time domain, i.e. ‘Coupled Stress/PWP’ type of analysis.

Finally, for phase 1-1, the stability of the upstream and downstream slope of the embankment with dry stacking was checked, using the finite element method (FEM), that is, with realized stresses from the analysis of the state of stresses and deformations. The increase in stability with pore pressure dissipation in the final stage of stage 1-1 is as follows: for downstream slope from 1.429 to 1.437, and for upstream slope from 1.341 to 1.414.

After simulating the construction of phase 1-1, phase 1-2 with a duration of 0.59 years, and phase 2 with a duration of 3.49 years are modeled, which are not visible in the model for the longitudinal section. The construction of the dry stacking embankment in phase 3 with a duration of 3.87 years is modeled in 6 stages (or load increments) with a duration of 20,336,977 sec, simulated with 10 calculation steps with an exponential time increment. At the end of this phase, the cumulative values of horizontal and vertical displacements, pore pressure and effective normal vertical stresses were determined (Figure 10). The increase in stability (expressed by the slope stability factor) with the dissipation of pore pressure in the last stage of stage 3 is as follows: for the downstream slope from 1.379 to 1.383, and for the upstream slope from 1.323 to 1.330.

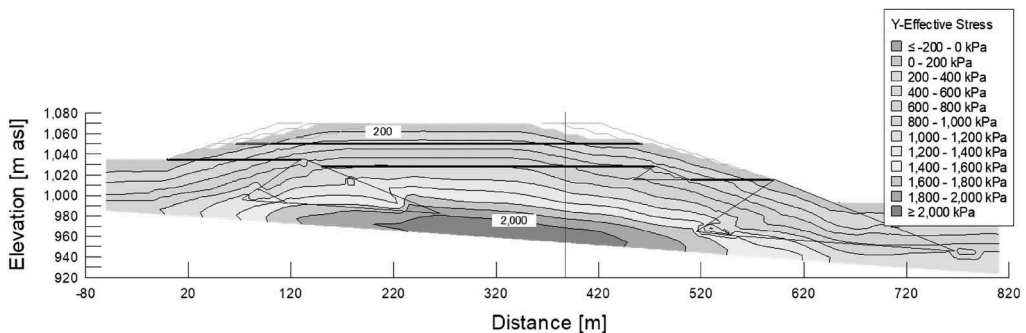


Figure 10. Effective normal vertical stresses at the end of phase 3, in tailings storage facilities 1, 2 and 3-1.

3.4 Results of the dynamic analysis

The selection of the parameters of the design earthquakes and the adoption of the dynamic parameters are taken from a suitable seismological data base (IZIIS - Skopje, 2020.10). The usual procedure for analyzing the dynamic response of embankment dams with reservoirs is to conduct it with at least three different accelerograms, for two levels of seismic excitation: (1) operating basis earthquake - OBE and (2) safety evaluation earthquake - SEE. In the subject analysis of a dry stacking embankment where there is no danger of sudden and uncontrolled reservoir emptying caused by potential crest damage, a simplified procedure was

adopted, with one synthetic accelerogram for three levels of excitations, whereas in the analyses, a basic design earthquake is also added - DBE (Design Basis Earthquake), with a repetition period of $T= 475$ years, which is used for paramount constructions that do not cause a potential danger to the environment.

The dynamic response of the geoenvironment, during SEE with PGA 0.36 g and $PGAy = 0.25$ g, duration of $t =20$ s, with synthetic accelerogram $T=10,000_1$, is given in Figures 11, 12, 13 and 14. A visual check that the dynamic response is correct is the diagram of the relative horizontal displacements. The permanent vertical displacement, caused by the inertial forces during the uplift which is relevant for the assessment of the seismic resistance of the dam 2-1 with crest at elevation at 1015 masl, is the crest settlement of 22 cm.

During the earthquake, there is an increase in the pore pressure, which creates a liquefaction zone after the earthquake (Figure 15). The occurrence of liquefaction will cause a redistribution of effective stresses, which will result in post-earthquake displacements in the geoenvironment. In the following text, Figure 16 shows the critical slip surface for the downstream slope in the post-earthquake phase.

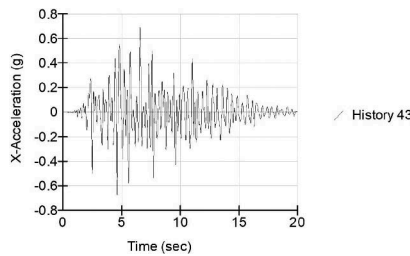


Figure 11. Absolute accelerations $a[g] \div t[s]$ in horizontal direction, downstream crest of dry stacking embankment.

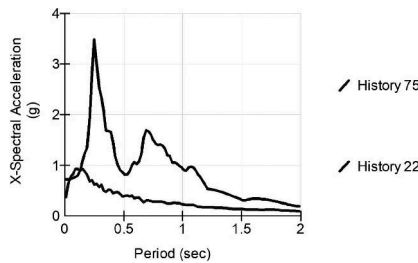


Figure 12. Response spectrum of accelerations $Sa [g] \div T [s]$ for $DR = 0.05$, in the bedrock (excitation) and in the crest of dam 2-1 (response).

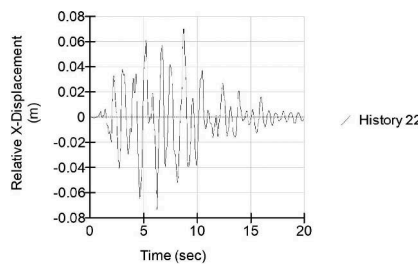


Figure 13. Relative displacements, horizontal $x[m] \div t[s]$, in the dam crest 2-1.

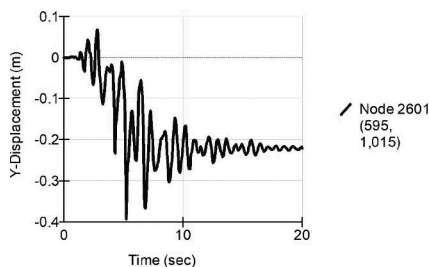


Figure 14. Permanent vertical displacements, by dynamic deformation method, $Y[m] \div t[s]$, in dam crest 2-1.

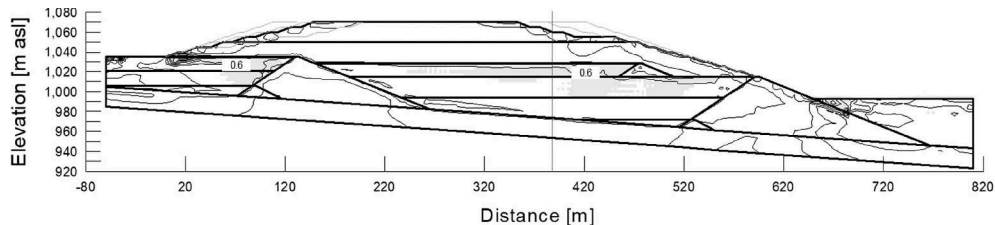


Figure 15. Distribution of the coefficient q/p' [-] with a liquefied zone, for the state of stresses at the end of the earthquake action.

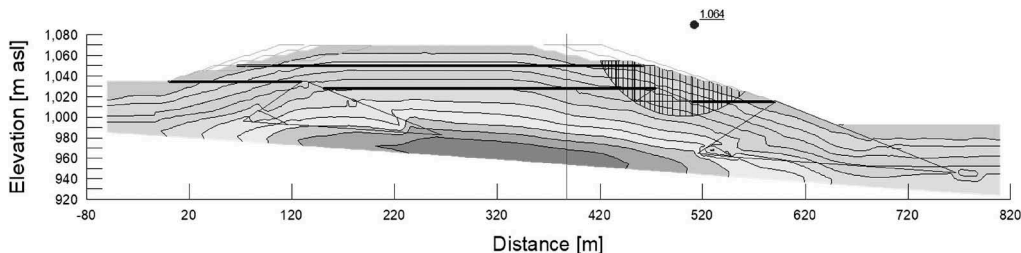


Figure 16. Critical slip surface for the downstream slope, in the post-earthquake phase.

4 CONCLUSIONS

After reviewing the results, we can conclude that the static and dynamic stability of the dry stacking embankment with the defined shape (berm sizes at the appropriate elevations) are satisfied, and we highlight the following conclusions:

1. The construction of two sub-phases 1-1 and 1-2 must be realized in one phase 1, with filling in horizontal layers, because a separate construction of phase 1-1 does not have satisfactory temporary stability of the left slope.
2. If during the construction of the combined phases 1-1 and 1-2 (that is, phase 1) temporary instability towards the right slope is noticed, then phases 1 and 2 should be filled simultaneously.
3. Pseudostatic stability under the action of a strong earthquake is not satisfied for any slope (downstream, upstream and left) of the dry stacking embankment. Therefore, the seismic resistance of the geoenvironment must be investigated and verified by dynamic time domain analysis taking into account the liquefaction phenomenon.
4. Maximum acceleration in the crest at 1015 masl of dam 2-1 (determined by longitudinal section analysis) is 0.23 g (for OBE), 0.41 g (for DBE), and 0.70 g (for SEE).
5. Maximum acceleration in the crest at 1070 masl of the dry stacking embankment (determined by cross-sectional analysis) is 0.22 g (for OBE), 0.40 g (for DBE) and 0.45 g (for SEE).
6. Permanent vertical displacement, caused by the inertial forces during the excitation, which is relevant for the assessment of the seismic resistance of the dam 2-1 with a crest at 1015

- masl (determined by longitudinal section analysis) is the crest settlement, and is 0 cm (for OBE), 0 cm (for DBE) and 22 cm (for SEE),
7. With the dynamic response of the representative sections (longitudinal and cross section), for a level of seismic excitation OBE with $PGA = 0.07$ g with a repetition period $T = 145$ years, liquefaction occurs in the waste lagoons Sasa 1 and Sasa 2.
 8. Minimum values of the safety coefficient in the post-earthquake phase (determined by analysis of the longitudinal section) are $F_s = 1.064 \leq F = 1.1$ (for the downstream slope) and $F_s = 1.237 > F = 1.1$ (for the upstream slope) for OBE, DBE and SEE.

REFERENCES

- DIPKO – Skopje, 2021.09.27, Detailed design for dry disposal above TSF 2 and TSF 1 of the mine Sasa, M. Kamenica, Book 2. Static analysis of dry disposal above TSF 2, L. Petkovski (responsible designer) et al.
- DIPKO – Skopje, 2021.09.28, Detailed design for dry disposal above TSF 2 and TSF 1 of the mine Sasa, M. Kamenica, Book 3. Dynamic analysis of dry disposal above TSF 2, L. Petkovski (responsible designer) et al.
- DIPKO - Skopje, 2022.08.30, Design for upgrading the retention dam from elevation 993.5 to elevation 1000.0 masl at TSF Toranica, K. Palanka (Annex no. 1 of the Detailed design for upgrading the retention and tailings dam from 986.5 to 1000 m above sea level on TSF Toranica), L. Petkovski (responsible designer) et al.
- DIPKO, Skopje, 2020-11-25, Geotechnical Investigation Report from SPT and CPTu performed at Sasa tailings dams, Jovan B. Papic (responsible researcher)
- Faculty of Civil Engineering - Skopje, 2018.09, Innovative seismic resistance analysis of TSF Topolnica, for variable height of operating level in the waste lagoon from 649.0 to 652.0 masl, with an estimate of maximum tailings storage in the waste lagoon (Annex no. 4 of the Construction design of TSF Topolnica, Buchim, with crest at 654.0 masl), L. Petkovski (responsible designer), et al.
- Faculty of Civil Engineering - Skopje, 2019.07.23, Technical solution for dry disposal of tailings above waste lagoons, with a preliminary assessment of the stability of the tailings dams of the mine Sasa, M. Kamenica, L. Petkovski (responsible designer), et al.
- Faculty of Civil Engineering - Skopje, 2020.06.26, Conceptual design for additional volume for dry stacking disposal at TSF 2 and 3-2 of the mine Sasa, M. Kamenica, L. Petkovski, (responsible designer), et al.
- Geing - Skopje, 2018-09-12, Detailed design for upgrading the retention and sand dam from 986.5 m above sea level to 1000 m above sea level at TSF Toranica - K. Palanka, Natalija A. Bozhinovska (responsible designer)
- Geing KuK - Skopje, 2020.09.29, Elaboration of additional geotechnical investigation works and laboratory investigations of TSF 2 – SASA Mine, S. Georgievski (responsible researcher)
- IZIIS - Skopje, 2020.10, Seismic hazard study for the SASA-2 profile, Report 2020-59, D. Dojchinoski (responsible researcher) et al.
- Knight Piésold, London, 2021-05-12, File No.: LO501-00057/05-03, CPT ground investigation on TSF 1 and TSF 2 at the Sasa Lead and Zinc Mine in North Macedonia, Joel Slater (responsible researcher)
- Petkovski L., Mitovski S., 2018.04 ‘Numerical analysis if displacements in the post-exploitation period of tailings dams with a combined construction method’, Topic - Tailings Dams, USSD 38th Annual Meeting and Conference, A balancing Act: Dams, Levees and Ecosystems, April 3- May 4, 2018, Miami, Florida, USA, CD Proceedings
- Petkovski L., Mitovski S., 2018.07, ‘Assessment of seismic resistance of combined tailings dams’, 26. Congress on Large Dams, ICOLD, 1–7 July 2018, Vienna, Austria, CD Proceedings Q.101-R.58, p.978–991
- Petkovski L., Mitovski S., 2019.05, ‘Application of SPT Results On Liquefaction Phenomenon Modeling Of Tailings Dam’, 3-rd International Symposium on Dams and Earthquakes, organized by WGDE-EC-ICOLD and PCOLD, ISBN: 978-972-49-2308-6 Proceedings, p.209–220, (6-8).05.2019, Lisbon, Portugal
- Petkovski L., Mitovski S., 2019.09 ‘An analysis of the waste lagoon water level influence on the liquefaction resistance of the tailings dams’, 11th ICOLD European Club Symposium, ‘The future of Dams (in Europe): Prospects and Challenges in a changing Environment’, CD Proceedings - Session 8: Advances in dam engineering: modelling, 2-4 October 2019, Chania, Crete, Greece

First rehabilitation measures of the Biópio dam, Angola

C.J. Ponte

CAB, Luanda, Angola

P. Afonso

PRODEL, EP, Luanda, Angola

ABSTRACT: The Biópio dam is a 19 m high structure, concluded in 1956 on the Catumbela river, about 50 km from the town of Lobito (Angola), being its main purpose the production of energy. The dam is essentially composed by the bottom discharge, on the left bank, and seven spill weir blocks with thin piers, supporting 15 m high automatic tilt gates and a roadway deck, with a total length of 156 m. Inspections carried out in 2007 and 2009 revealed, besides a large deterioration of the dam, appurtenant works and respective equipment, the development of large cavities in some piers, near the support of the gates, which allow the reservoir water to enter into and put under pressure the drainage gallery. As a first step for the full rehabilitation and upgrading of the dam, the owner (the National Energy Enterprise of Angola- ENE EP), with the support of the Energies of Portugal – EDP International, considered of interest the first repair of the above referred to cavities. This paper reports on the major aspects of these works.

1 INTRODUCTION

The Biópio dam, constructed in Angola near the town of Lobito, has been in operation since 1956, with the main purpose of energy production. The powerhouse, located about 700 m from the dam, has four groups with 18 MW of capacity.

The safety control of the works, made essentially through visual inspections, showed some abnormal aspects of the behaviour, after a few years of operation, namely the permanent deformations of the piers supporting the equipment of the bottom outlet, and the tilt gates. In the seventies, several interventions were made as well as repair works.

However, the problems continued, and during almost eight years, it was not possible to open the Stone type gate of the bottom discharge. So, a large volume of sediments accumulated in the reservoir near the dam, and it became impossible to inspect the channels between the piers, particularly near the bolts which fix the bearings of the axis of the tilt gates, even during the dry period (usually from the middle of May to September).

When the opening of the bottom discharge became possible, after some mechanical interventions, the reservoir was emptied, and a thorough visual inspection was performed, which revealed the existence of large cavities in some piers, besides other deteriorations.

The rapid increase of those deteriorations called for the implementation of first rehabilitation measures, to ensure adequate dam safety conditions, before a more extensive intervention, aiming at the rehabilitation and updating of all the components of the project, would be performed. The main aspects of these first rehabilitation measures are described hereafter.

2 DETECTION AND EVALUATION OF THE DAM DETERIORATION

The reformulation and updating of the monitoring scheme in 2006, made a more adequate surveillance of the works possible. So, even before the opening of the bottom discharge, during a visual inspection of the dam drainage gallery, it was detected that water was flowing directly to the gallery from one of the aeration tubes. This flow was increasing with time and, about one year after this occurrence, another aeration tube began to drain.

Initially, it was thought that this water came to the tubes due to a deterioration of the copper water stops located upstream in the joint separating the two half piers. However, the inspection of the dam after the emptying of the reservoir revealed the development of the cavities above referred to, as well as an important erosion of the spillway channels and bucket basins.

In fact, as stated in the original project, when the gates open, a small functional gap exists between them and the surface of the adjacent piers, allowing water to flow through this gap. This water, transporting sediments of different grain sizes, some of which reaching at least coarse sand dimensions, caused the above-mentioned large erosions. It is considered that the accumulation of a large volume of sediments near the upstream face of the dam, as shown on Figure 1, together with the long period of operation without opening the bottom discharge, contributed to increase that erosion process.



Figure 1. Sediments accumulated near the upstream face of the dam, after opening a 3 m high trench.

This erosion process originates very large cavities into and near some piers as shown on Figure 2, affecting the concrete which supports the bolts of the bearings of the gate axis, especially those bolts located near the cavities, as well as the steel reinforcements of the piers. On the other hand, the erosion process attacked the concrete and the steel reinforcements of the spillway channels and bucket basins (see Figure 3).

Besides, large pieces of wood transported by the water prevented the gates to close, when the water level in the reservoir decreases as illustrated on Figure 4. This originated the deformation of the upstream face of the gates, and also increased the flow of water and sediments, worsening the erosions.

Among the effects of the above indicated erosion process, and taking into account the rapid increase of the cavities in the piers, particular concern was attributed to the existence of a direct communication between the reservoir and the drainage gallery, owing the effects of the water pressure in the concrete fissures, and on the monitoring equipment installed in the gallery, to the erosion of the concrete blocks supporting the bolts of the bearings of the gate axis and to the extensive erosion of the surface concrete and steel reinforcements of the spillway channels and buckets.

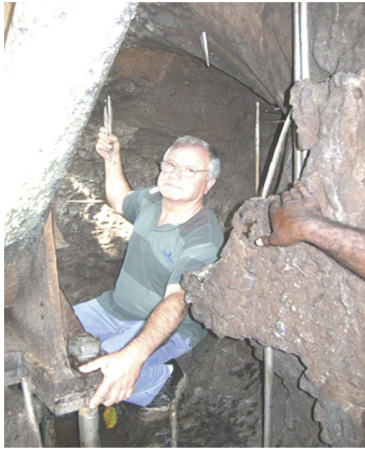


Figure 2. Cavity on the right face of pier 6, illustrating its large dimensions, as well as the cut and damaged steel reinforcements, and the bolt of the gate axis.



Figure 3. Spillway channel with damaged and pulled out surface steel reinforcements.



Figure 4. Large piece of a tree stuck trapped between the gate and the pier surface.

3 FIRST REHABILITATION MEASURES

A general rehabilitation and updating of the Biópio scheme is being envisaged. However, it was considered of interest to implement first rehabilitation measures, in order to prevent the inflow of the reservoir water into the drainage gallery and the progress of the erosion process.

These measures, planned in 2009, were implemented in the dry season of 2011, and essentially included the filling of the cavities developed into and near the piers. These works included: the cleaning of the surface of the cavities, by air and water jets; the installation of new steel reinforcements, adequately fixed to the existing concrete; the filling of the cavities with a shrinkage compensating concrete, then with grout, in order to ensure that no voids will remain, and an appropriate link is obtained between the new and the existing concrete.

For a better connection between concrete, an epoxy binder (Ikosit K101N) was applied to allow a better connection between new concrete and old concrete. The same procedure was adopted when filling the cavities (see Figure 5).



Figure 5. Application of epoxy binder.

A barrier was made with Sika Monotop 618 in the areas of the sills that were concreted with cement-based one-component repair mortar with synthetic resins, silica fume and reinforced with fibers, in order to obtain a more homogeneous and resistant surface.

These kinds of works were carried out for the blocks which support the bolts of the bearings of the gate axis, and for the surface of the spillway channels and buckets (see Figures 6 and 7).

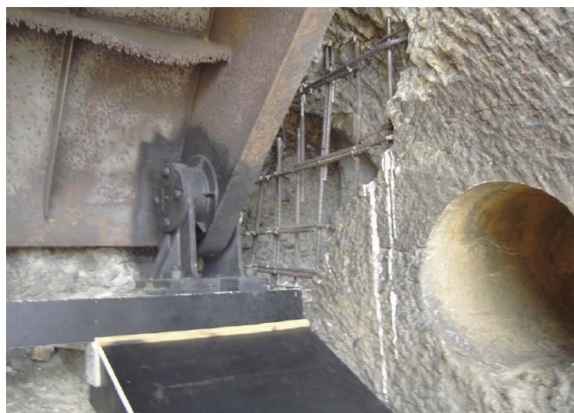


Figure 6. Repair of the cavities, into and near the piers surface.



Figure 7. Repair of the spillway channel surface.

The reinforcement of the boundary zones of the gates with steel plates, and repair of the bearings of the gate axis with sand blasting and corrosion protection, were also included in the first rehabilitation measures. Furthermore, the gap between the gates and the adjacent surface of piers, was limited to about 10 mm.

In order to limit the accumulation of sediments near the upstream face of the dam and near the entrance of the water intake (to prevent deterioration of the power plant hydraulic equipment), the opening of the bottom outlet, at least twice a year and during large floods, was included in the operation rules.

4 CONCLUSION

The case of the Biópio dam illustrates the need of an appropriate design and operation, as well as a proper maintenance and monitoring of these works.

The bottom outlet is important to empty the reservoir, and when the reservoir sedimentation is an issue, the example of Biópio dam demonstrates the necessity to operate it regularly to control the accumulation of sediments near the dam as well as close to the water intake. Emptying of the reservoir may also be required to allow the inspection of structural elements usually underwater.

Periodic visual inspections of all components of the works are particularly relevant for detecting first signs of an abnormal behaviour.

ACKNOWLEDGEMENTS

Acknowledgements are due to the dam owner (ENE-EP), and to EDP International, namely to Eng. Santos, H.- Head of the Angola delegation, for permitting and supporting this paper.

A special reference should be made to LNEC Research Officer, Ribeiro, A. B. for his advice on the concrete specifications. A mention is also made to the collaboration of Mr. Amante, J. technician specialist in monitoring activities.

REFERENCES

Gomes, A. S. & Pedro, J. O., Emilio, F. T. & Batista, A. L. 2009. – First rehabilitation measures to be implemented in the dry season of 2009; Gathering and analysis of bibliographic elements; Analysis and interpretation of the major pathologies - corrective measures; Contributions to the tender for the rehabilitation and updating. *EDP International, 2009. Reports to the National Electricity Company July and September, 2010 May, and 2011 March, Lisbon, Portugal.*

Dams in Angola, reconstruction of the Matala dam

C.J.C. Pontes & P. Portugal

CAB-Angolan Committee of Dams, Luanda, Angola

ABSTRACT: Since 2008, after signing the peace agreements in 2002, Angola has been carrying out several dam constructions and rehabilitation projects, with the aim of developing the country's economy and serving its population better, in agricultural irrigation, potable water supply and power generation. Most Angolan dams were affected, directly or indirectly, during the armed conflict that took place for about 30 years. Some suffered from sabotage actions, or from the absence of adequate maintenance and/or rehabilitation actions for long periods. Further, in the case of the Matala dam, the concrete has developed alkalis reactions that boosted concrete degradation.

RÉSUMÉ: Depuis 2008, après la signature des accords de paix en 2002, l'Angola a mené à bien plusieurs projets de construction et de réhabilitation de barrages dans le but de développer l'économie du pays et de mieux servir sa population, dans les domaines de l'irrigation agricole, de l'approvisionnement en eau potable et de la sécurité alimentaire, ainsi que la production d'électricité. La plupart des barrages angolais ont été touchés, directement ou indirectement, par le conflit armé qui a duré environ 30 ans. Certains ont souffert d'actions de sabotage ou du manque d'entretien et/ou de réhabilitation adéquates pendant longues périodes. Pour ce qui concerne le cas particulier du barrage de Matala, le béton a développé des réactions alcali-agrégats qui ont accéléré la dégradation du béton.

1 DAMS IN ANGOLA

More than 30 dams constructed.

More than 20 projects have been identified and are under study.

HPP Laúca; at present one of Africa's largest dam-projects, in operation.

HPP Cambambe II (700 MW) inaugurated in June 2017.

Table 1. Some of the main Angolan dams.

Name	Capanda	Cambambe	Laúca	Gove	Caculo-Cabaça**
TYPE	RCC	Concrete	RCC	Earth/Rockfill	RCC
Height	110m	88m	132	58m	105m
River	Kwanza	Kwanza	Kwanza	Cunene	Kwanza
Storage	4795 hm ³	20 hm ³	5 482 hm ³	2 574 hm ³	463 hm ³
Function	Reg;Irrig;Pw	HydroPower	HydroPower	Reg;Irrig;Pw	HydroPower

** Under construction

In 2021, the total installed capacity for electricity generation was 5.9 GW, split into 63% hydropower and 37% thermal. The country has a diversified theoretical energy spectrum that makes up a total of 80.6 GW, with solar energy being the most abundant energy source (55 GW), followed by hydro (18 GW), wind (3.9 GW), and biomass (3.7 GW) – see web sites in References.

2 RECONSTRUCTION OF THE MATALA DAM

2.1 *Characterization (before)*

Built in 1950s, Concrete Dam, Type: Gravity, Height: 16 m maximum height above foundation; Crest length: 1035 m, 6 Free Concrete Spillways, 29 Spillways with gates (sluice gates), Bottom Outlet; 3x13,6 MW Kaplan Turbines, 2 auxiliary Francis units with horizontal axis turbines, with a power of 440 kW. Irrigation canal - capacity of 5 m³/s.

2.2 *Main pathologies*

The concrete structures at the Matala Dam were affected by AAR (Alkali-Aggregate Reaction). The presence of this phenomenon was confirmed by the deformations observed on many of the concrete structures, notably at the spillway pier joints (Figure 1) and the pedestals supports for the flap gate lever arms. It was observed that the deformation of the concrete reduced the operating capacity of the gates (Figure 2). The openings at the top of the joints reached values greater than 130 mm. These movements have affected the concrete road bridge to the point where the roller bearings have undergone large rotations. The bottom outlet had been inoperative since 1981.



Figure 1. Longitudinal joints of the abutments.



Figure 2. Swinging tower of sluice gates.

2.3 Laboratory tests & previous studies

The activities carried out included the extraction of 22 concrete core samples and the execution of the following tests: a) petrography: ASTM C856; b) compressive strength: CSA A23.2-14C; c) modulus of elasticity: ASTM C469; d) density and absorption: ASTM C642; d) chemical analysis of the original concrete; and e) residual expansion tests.

Tests conducted by others, according to ASTM C1260, resulted in a relatively low expansion value of 0.08% at 16 days (Chongjiang Du 2010). However, one-year test results performed according to ASTM C1293, showed a much higher expansion in the order of 0.22% and 0.36%, with the threshold value being 0.04% (Chongjiang Du 2010).

The average concrete compressive strength based on 14 specimens was 32.3 MPa, with a standard deviation of 5.1 MPa. The original construction drawings show a compressive strength of 30 MPa for the concrete bridge structure. Upon examination of the cores, the presence of polygonal micro-cracking, coatings on the aggregates and veinlets of alkaline-silica gel was confirmed.

The test for the potential expansivity of aggregates, based on CSA A23.2-14A and using a fly ash content of 25%, resulted in an expansion of 0.001% at 52 weeks and of 0.011% at 104 weeks (Terratech 2007). This is considerably lower than the 0.04% limit. However, given the nature of the concrete structure being constructed (i.e. a spillway equipped with radial gates); a fly ash content of 35% was eventually selected. Although some of the test results were not entirely conclusive, the presence of AAR at the Matala Dam was confirmed by the concrete deformations and other observations. The results provided guidance for mitigating in the expected expansion due to AAR.

2.4 Intervention in the structure of the Dam

Rehabilitation works were carried out to maintain the spillway discharge capacity and to restore the integrity of the structures. Works included construction of a new gated spillway (with the application of 8 new radial gates spillways, between piers 7 to 15), pier pinning, bridge roller support rehab and concrete repairs. Aggregates from the original quarry were used and fly ash was added to the concrete mix.



Figure 3. View of the 8 new radial gates.

2.5 Installation of a dam safety system

For the piers not incorporated in the new spillway, a total of 11 anchors were provided along two rows. One row is near the top of the piers and the second row is at mid-height. The installation of these anchors in the piers was preceded by the cleaning of the joint, followed by its complete grouting. An internal drainage system was provided to prevent any seepage to migrate downstream along the pier joint and additional piezometers were installed (Figure 3).

Other measure implemented to mitigate the effects of the AAR was to: a) seal large cracks present on the original ogee sections; and b) apply a partially-flexible polymerized cementitious

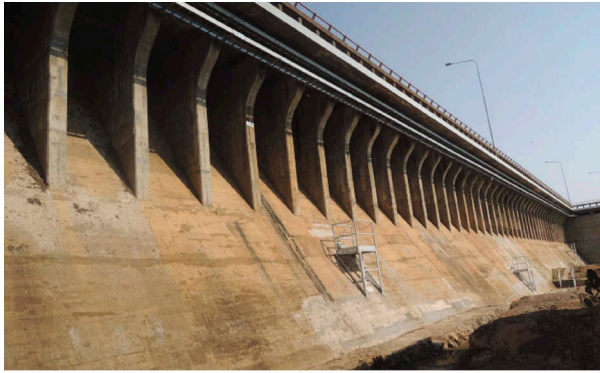


Figure 4. Gravity section and new piezometers.

coating on the crest of the ogees. The same coating was also applied on the concrete surfaces of the pier walls and tops of the pier bases, where large cracks were present. Also, the cracks present on the original stilling basins and gravity sections were sealed Figure 5.



Figure 5. Sealing works along the free overflow spillways.

3 CONCLUSION

Rehabilitation works need to focus on the root cause of the deformations in order to implement appropriate corrective measures to ensure the integrity and functionality of the structure.

The execution of detailed and focused site inspections is essential for a proper diagnostic and understanding of the mechanisms and deformations associated with AAR in order to:

- ensure the safety of the dam
- eliminate the imminent risk of collapse
- ensure the evacuation capacity as well as retention
- ease maintenance work.

REFERENCES

<http://www.inrh.gv.ao/portal/snrha>

<http://www.prodel.co.ao/index.php/pt/producao-hidrica/produca-hidrica-sub>

<http://www.angolaenergia2025.com/pt-pt/conteudo/novas-grandes-hidricas>

Chongjiang Du (2010). Dealing with Alkali Aggregate Reaction in Hydraulic Structures. *Lahmeyer International GmbH, August 18, 2010.*

Estimation of settlement in earth and rockfill dams using artificial intelligence technique

Mohammad Rashidi

Stantec, Civil Engineer, Denver, USA

Kwestan Salimi

Stantec, Geotechnical Engineer, Denver, USA

Sam Abbaszadeh

Stantec, Senior Civil Engineer, Denver, USA

ABSTRACT: The impermissible settlement is one of the most important reasons for the failures of earth and rockfill dams. An appropriate estimation of settlement after construction is required to evaluate the performance of the dam and to inform dam design engineers of any possible problem. This study was designed to apply artificial intelligent methods to predict settlement after constructing central core rockfill dams. Attempts were made in this research to prepare models for predicting settlement of these dams using the information of 50 different central core earth and rockfill dams all over the world using Genetic Programming (GP) methods. The results indicated that prediction of settlement based on the single parameter of dam height cannot be accurate and other parameters such as stiffness and shear strength properties of materials are effective in dam settlement. Based on the sensitivity analysis, parameters such as height of dam, modulus of elasticity and unit weight of core, and modulus of elasticity and internal friction angle of rockfill materials have the highest influence on the settlement of the dams and were considered as the input parameters. The results obtained from comparing the artificial intelligent method and empirical relationships showed that GP results were more appropriate tools to solve the problems with complex mechanisms and several effective factors, such as prediction of settlement of dams. The new developed models in this study are ready to be applied as a robust predictor tool for monitoring and safety evaluation of earth and rockfill dams in Europe.

1 INTRODUCTION

Earth and rockfill dams as the most important geo-structures have been playing a fundamental role in providing water required for human societies. These important geo-structures are usually constructing with the optimum use of local materials. Lack of high-quality local aggregates and soils for construction of these large geo-structures, along with weak compaction frequently result in uncontrolled settlement and excessive deformations. This impermissible deformation in the rockfill dam usually leads to load transfer from core with soft materials to the shell with relatively high stiffness aggregates (Cooke,1984). This phenomenon is called arching in earth dams. As a result of the arching, pore water pressure can become more than total stress within core and this excessive water pressure may lead to longitudinal tension cracks as shown in **Fehler! Verweisquelle konnte nicht gefunden werden.** These cracks lead to an increase in flow rate in drains in the heel of the dam and generally will cause heel instability and ultimately dam failure. Therefore, an appropriate estimation of settlement during and after construction is required to supervise the performance of the dam and to warn design engineers of any possible problem.

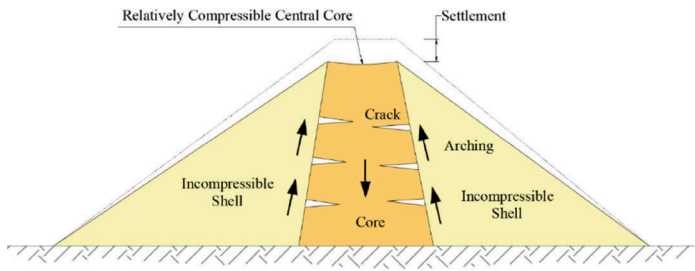


Figure 1. Settlement and cracking in core for earth and rockfill dams.

There are two most used empirical relationships in the dam industry offered by Clements (1984) and Hunter & Fell (2003) to predict to the settlement of earth and rockfill dams. Clements studied the settlement of 68 rockfill dams and proposed equation 1 based on his findings:

$$S = \beta H^\delta \quad (1)$$

where S is settlement in meters, H is the dam height in meters, β and δ are the constant values based on the type of the dam (For earth dams with central clay core, β and δ should be 0.2 and 1.1, respectively).

Similarly, Hunter and Fell (2003) developed correlations between core settlement and earth dam height during construction. The author evaluated the settlement of 42 earth dams with clay cores and 25 earth dams with gravelly cores and proposed equations 2 and 3:

$$S = 0.152H^2 + 12.6H \text{ (Earth dams with clay cores)} \quad (2)$$

$$S = 0.183H^2 + 7.26H \text{ (Earth dams with sandy and gravelly cores)} \quad (3)$$

Despite the simplicity, the common weak point of these relationships is their dependency on the single parameter of dam height. While many parameters are involved in dam settlement such as stiffness and shear strength parameters of materials that have not been considered in these formulae. In order to overcome these limitations, and to propose a more accurate and simple method, artificial intelligence techniques can be utilized. These techniques have no limitation in applying further effective parameters. In this study, the novel and intelligent method, Genetic Expression Programming (GEP), which are highly applicable for solving such problems, are used to estimate the settlement in earth and rockfill dams.

2 STUDY OF DATABASE

The present paper uses the information of 50 central core earth and rockfill dams. The information related to 35 of these dams have only two parameters namely height and settlement which was collected from earlier studies among the available documents as shown in Table 1 (Habibagahi, 2002). Rest of field records of measured settlement of rockfill dams (15 dams) are reported along with full specification of these dams as indicated in the Table 2 (Cetin et al., 2000; Alonso et al., 2005; Karbor-e-shyadeh and Soroush, 2008; Gikas et al., 2008; Siyahi et al., 2008; Latifi et al., 2012; Rezaee, 2015; Rashidi et al., 2017; Rashidi and Haeri, 2017; Rashidi et al. 2018). As shown in Table 2, several parameters, such as height of dam, dry unit weight, initial friction angle, cohesion, elasticity modulus, Poisson ratio, dilation angle, and hydraulic conductivity, are considered to be influential in settlement of earth and rockfill dams. In the first part of this study, one input parameter (dam height) was traditionally used for predicting settlement after constructing central core rockfill dams, and then the developed relationship was evaluated by comparison with validation data sets. Multi-Input GEP models were also developed for the prediction of rockfill dam settlement and then the results were compared to well-known empirical relationships outlined in the literature.

Table 1. Specifications of some central core rockfill dams used in this study.

No.	Dam Name	Height (m)	Total Settlement (m)
1	Akosombo	113	0.65
2	Ambuklao	129	0.81
3	Beas	133	0.41
4	Cherry Valley	101	0.14
5	Dhunn Valley	35	0.07
6	El Infiernillo	148	0.46
7	Estreito	97	0.05
8	Gepatsch	153	1.24
9	Messaure	101	0.01
10	Mud Mountain	122	0.58
11	Notteley	56	0.18
12	Preuca	60	0.26
13	Presidente Aleman	75	0.13
14	South Holston	87	0.61
15	Tooma	68	0.06
16	Watauga	97	0.47
17	Outardes 4 dam 1	122	0.17
18	Outardes 4 dam 3	25	0.02
19	LG2 Main Dam	168	0.42
20	LG2 Dyke D5	66	0.09
21	LG2 Dyke D7	55	0.04
22	LG2 Dyke D8	30	0.02
23	LG3 North Dam	93	0.09
24	Caiapiscou KA3	54	0.03
25	Caiapiscou KA5	47	0.03
26	Laurel	90	0.09
27	LG3 South Dam	93	0.13
28	Netzhualcoyotl	138	0.43
29	Kajakai	100	0.04
30	Cupatizio	72	0.09
31	High Aswan	111	0.12
32	Llyn Brianne	91	0.15
33	Outardes 4 dam	110	0.10
34	Hyttejuvet	93	0.18
35	Muddy Run	76	0.27

3 GENETIC EXPRESSION PROGRAMMING

Genetic Expression Programming was employed in this study to develop prediction model for estimating the settlement in earth and rockfill dams. Genetic Expression Programming is a branch of artificial intelligence and a generalization of genetic algorithms (GAs) (Goldberg 1989). GEP starts with an initial population of randomly generated computer programs composed of functions and terminals appropriate to the input domain. The functions may be standard arithmetic operations, standard programming operations, standard mathematical functions, logical functions, or domain-specific functions. Then via a supervised trial and error process, the initially generated functions and terminals are adjusted to get appropriate functions and terminals that can accurately estimate the output.

In GEP, programs are usually expressed as syntax trees rather than as lines of code. For example, Figure 2 shows the tree representation of the program $\max(x + y, x - 6)$. Where x and y as the independent variables and 6 as constant are leaves of the tree. In GEP leaves of the tree are called terminals, while the arithmetic operations (+, -, and max) are internal nodes called functions. The sets of allowed functions and terminals together form the primitive set of a GEP system. Like other evolutionary algorithms, in

Table 2. Specifications of some central core rockfill dams used in this study.

No.	Dame Name	Part	γ_{dry} kN/m ²	ϕ	C kN/m ²	E Mpa	ν	ψ	K m/s	H m	S cm
1	Gavoshan	Core	17.5	27	50	26	0.3	0	1.00E-08	128	270
		Shell	22.5	40	0	124	0.24	8	1.00E+00		
		Filter	20	35	0	64	0.28	4	1.00E-04		
2	Siah-Sang	Core	16	30	15	5	0.4	0	1.00E-09	33	23
		Shell	18	34	1	15	0.35	13	8.00E-08		
		Filter	18	36	3.5	10	0.3	7	2.00E-04		
3	Taham	Core	17.5	27	50	35	0.35	2	2.00E-07	123	90
		Shell	23.5	40	0	70	0.3	8	3.00E-06		
		Filter	21.1	36	0	50	0.3	6	5.00E-01		
4	Shirin Dare	Core	16	33	160	10	0.38	0	1.00E-10	66	175
		Shell	20	41	0	90	0.31	11	5.00E-01		
		Filter	19.5	36	0	45	0.36	6	2.00E-01		
5	Darab's Roodbal	Core	18	20	17	15	0.38	1	1.00E-08	71	92
		Shell	19	38	0	33	0.37	1	1.00E-01		
		Filter	18.5	31	0	24	0.35	6	1.00E-04		
6	Vanyar	Core	20	21	15	16	0.35	0	5.00E-08	91	85
		Shell	20.3	38	0	45	0.3	8	1.00E-04		
		Filter	18.5	33	0	22	0.3	6	1.00E-05		
7	Gorgass	Core	17.5	30	50	16	0.33	0	1.00E-08	123	235
		Shell	22.5	43	0	72	0.2	8	1.00E+00		
		Filter	20	36	0	35	0.26	5	1.00E-04		
8	Bidvaz	Core	17.6	18	47	17	0.35	0	1.00E-09	67	77
		Shell	21	40	0	34.5	0.3	10	1.00E+00		
		Filter	19	35	0	24	0.27	5	1.00E+00		
9	Mornos	Core	18.5	26	24	75	0.3	0	1.00E-07	126	47
		Shell	22	40	1	150	0.3	11	1.00E-05		
		Filter	20	37	0	100	0.3	6	1.00E-03		
10	Ataturk	Core	16.1	15	100	15	0.35	0	6.00E-07	184	285
		Shell	20.9	43	0	32	0.3	8	1.00E-01		
		Filter	-	-	-	-	-	-	-		
11	Beliche	Core	15	14	120	10	0.4	0	1.00E-08	55	105
		Shell	20	36	0	15	0.3	8	1.00E-01		
		Filter	-	-	-	-	-	-	-		
12	Ghoocham	Core	16.5	29	41	15	0.35	0	4.00E-07	45	45
		Shell	19	38	0	30	0.25	6	1.00E-03		
		Filter	21.5	43	0	32	0.25	6	1.00E-05		
13	Alborz	Core	16.6	18	20	15	0.3	0	1.00E-08	78	135
		Shell	17.2	32	0	30	0.28	6	1.00E-01		
		Filter	20	34	0	28	0.29	6	1.00E-02		
14	Dachan	Core	16.5	18	10	19	0.36	0	1.00E-08	82	110
		Shell	17.2	32	0	34	0.3	6	1.00E-01		
		Filter	17.2	32	0	33	0.28	6	1.00E-01		
15	Nara Dam	Core	20.8	22	35	17	0.4	0	4.00E-07	40	38
		Shell	19.7	33	0	32	0.3	8	1.00E-01		
		Filter	-	-	-	-	-	-	-		

GEP the individuals in the initial population are typically randomly generated. There are a number of different approaches to generate this random initial population, such as the full and grow methods (the most simple and earliest) and a widely used combination of the two known as ramped half and half (Ksoza 1992). Genetic operators of GEP are applied to individuals that are probabilistically selected based on fitness (objective function).

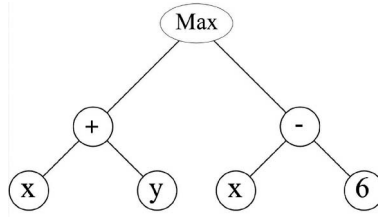


Figure 2. Representation of an Expression Tree in GEP (“Max” represents the Maximum function).

The advantage of GEP over other soft computing techniques (such as artificial neural networks and adaptive neuro fuzzy inference systems) is that GEP is not a black box and outputs are in form of semi-complex mathematical solutions, which could be applicable to the actual problems. The GEP approach is relatively new in the field of geotechnical engineering although some studies have been dedicated to their application recently (Noorzad et al, 2014; Onyelowe et al, 2021, Yong et al, 2021).

In this study the data set was divided into training (70%), and validation (30%) subsets to prevent overfitting. The performance of the testing set is very critical because it determines the accuracy and generalization capability of the model.

Two statistical evaluation criteria were used to assess the performance of the intelligent methods. These criteria are Root Mean Square Error (RMSE) and determination coefficient (R^2), respectively, given by Equations 4 and 5.

$$RMSE = \sqrt{\left(\frac{1}{n}\right) \sum_{i=1}^n (a_i - p_i)^2} \quad (4)$$

$$R^2 = \left(\frac{\sum_{i=1}^n (p_i - \bar{p})(a_i - \bar{a})}{\sqrt{\sum_{i=1}^n (p_i - \bar{p})^2 (a_i - \bar{a})^2}}\right)^2 \quad (5)$$

where a is the actual value and p is the predicted value, \bar{a} and \bar{p} are the mean of actual and predicted values, respectively. Evidently, a model with good performance (ie. RMSE close to 0 or R^2 close to 1) will be the best model among several candidates.

4 PREDICTION OF SETTLEMENT USING GEP

Genetic Expression Programming was employed in this study to develop prediction model for settlement of core rockfill dams and find the most appropriate model. In the first subsection, the Genetic Expression Programming model was developed based on one input parameter (dam height), and then this model was evaluated by comparison with validation data sets. In the second subsection, GEP prediction model was generated based on the multi input parameters and then the results were compared to well-known empirical relationships such as Clements (1984) and Hunter & Fell (2003).

4.1 Prediction of settlement based on one input parameter

First, 3 equations were offered through the GEP method using 35 data sets according to one input parameters called H (Height). Equations 6 to 8 were developed for predicting settlement of central core rockfill dams.

$$S = 9.91 + 0.00645H^2 + \frac{-0.164}{\cos(-0.164H^2)} - 0.471H - 0.0000168H^3 \sin(-0.0565H^2) \quad (6)$$

$$S = 10.5 + 0.00658H^2 + \frac{-0.165}{\cos(0.994H)} - 0.48H - 0.000017H^3 \sin(-0.0565H^2) \quad (7)$$

$$S = 102 + 0.00653H^2 - 0.473H - 0.0000168H^3 \sin(-0.0565H^2) \quad (9)$$

Table 3 demonstrates the results of the studies carried out for all equations to predict settlement of rockfill dams. The criteria to measure and compare the obtained equations were RMSE and determination coefficient (R^2) values. According to this table and with respect to RMSE and R^2 values, Equation 7 is the most appropriate and at the same time, the simplest equation. Figure 3 shows the coefficient of determination of this equation for all equations.

Table 3. GEP results to predict settlement of rockfill dams.

Equation	R^2	RMSE
6	0.8602	0.01014
7	0.8677	0.00960
8	0.7680	0.01683

As previously outlined, out of the 50 sets of data, 35 sets of data (70%) were considered for training and the remaining 15 sets of the data (30%) were considered for validation. The training and validation data sets were not selected randomly and selected from two sets of databases as presented in Tables 1 and 2.

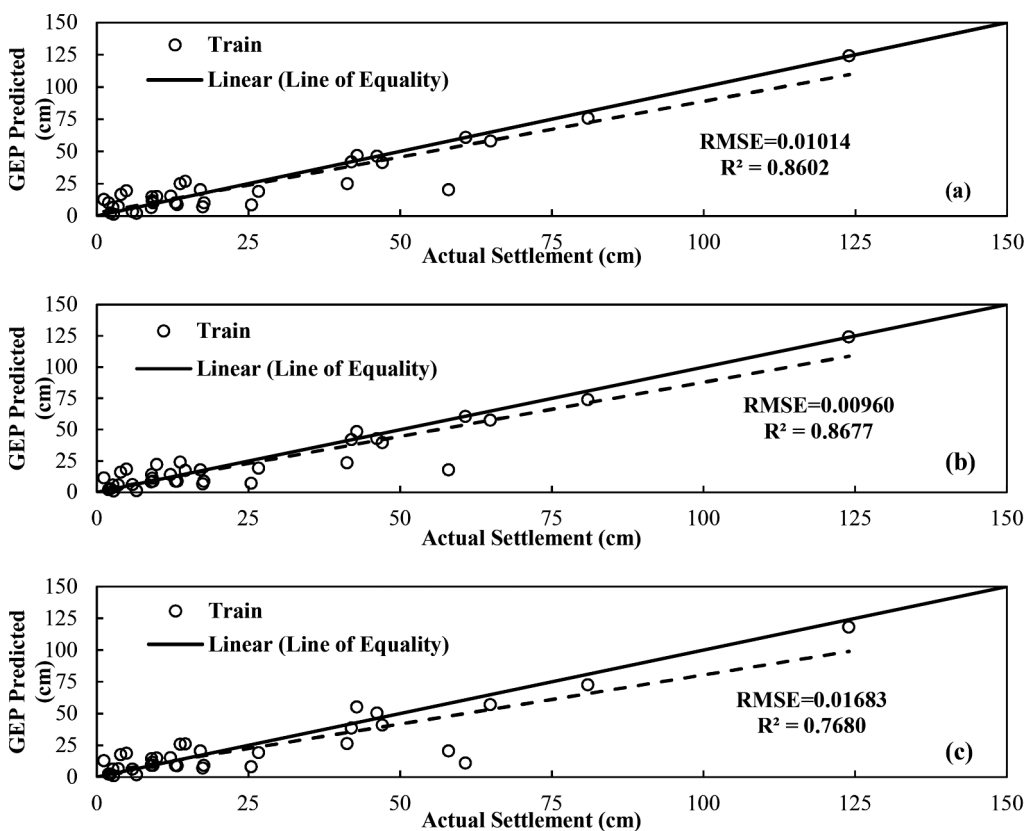


Figure 3. Coefficient of determination between actual settlement and predictions of GEP for Equations (a) 5, (b) 6, and (c) 7.

The prediction power of the selected model is further evaluated in Figure 4. The correlation coefficient and root mean squared error were selected to evaluate the model performance in each of the training and validation datasets. As observed from Figure 5, the generalization of the model in prediction of settlement is not reasonable. The plot demonstrates how the proposed GEP-based solution does not fit the second sets of experimental data. In other words, prediction of settlement based on the single parameter of dam height indicated lower accuracy. To overcome this issue, other input parameters such as stiffness and strength properties of earth dam materials need to be included in the GEP to develop more robust and accurate prediction models.

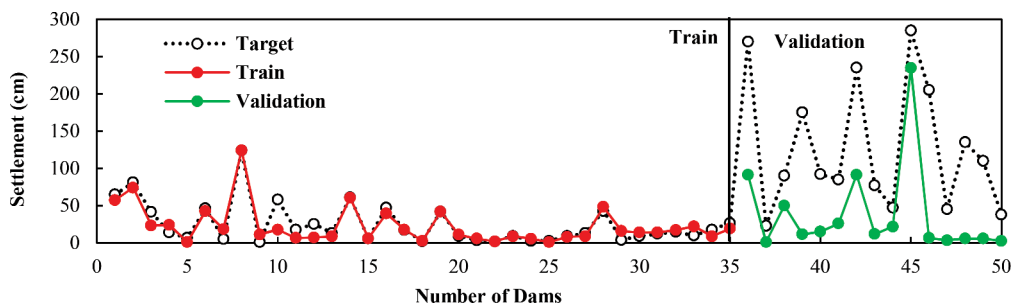


Figure 4. Performance of the GEP Model in two data sets (Train and Validation Phases).

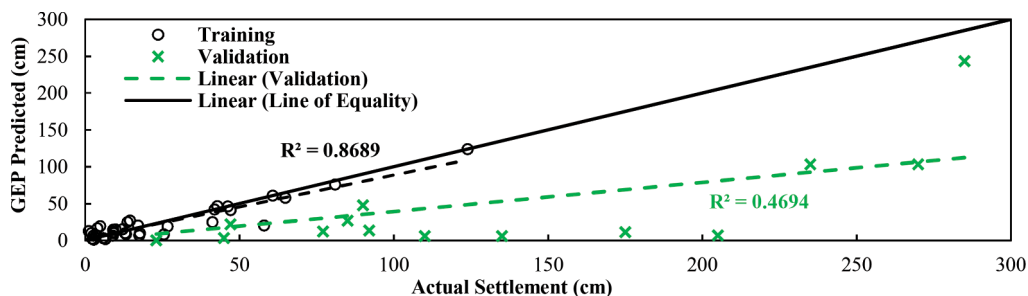


Figure 5. Comparing the training and validations sets.

4.2 Prediction of settlement based on multi input parameters

It was shown in the previous section that the deficiency of presented relationships obtained by GEP was their dependency on the single parameter of dam height. Thus, other important parameters such as dry unit weight, initial friction angle, cohesion, elasticity modulus, Poisson ratio, dilation angle, and hydraulic conductivity which are presented in Figure 6 should be included into GEP model to improve the accuracy of prediction settlement model. As an initial step for developing multi-input GEP model for the prediction of rockfill dam settlement, sensitivity analysis was performed to select to most influential parameters for inclusion in the model.

Figure 7 shows the results for the sensitivity analysis of the GEP model developed in this study. Lower magnitude of the sensitivity number is an indication of the insensitivity of the output layer (settlement) to the parameter varied. Conversely, a higher value of the sensitivity number denotes a greater impact of this parameter on the output of the model.

Based on the sensitivity analysis results presented in Figure 7, the modulus of elasticity of the core and shell materials were identified to have the highest influence on the settlement of the earth and rockfill dams. The height of dam was found to have the largest influence on the settlement. Dry density of the core materials and internal friction angle of shell aggregates were ranked after modulus of elasticity and height as the most influential parameters to impact the dam settlement.

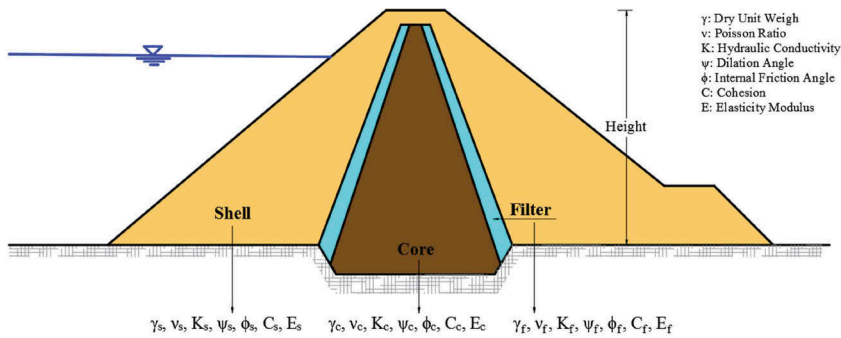


Figure 6. Input parameters for predicting settlement.

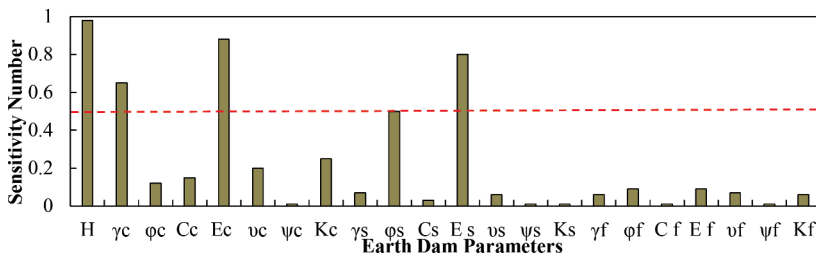


Figure 7. Sensitivity of the settlements to the earth dam features.

After selection of the four input parameters including height of dam (H), the elasticity modulus of core (E_c) and shell materials (E_s), dry density of the core materials (γ_c), three equations were developed through the GEP method using 15 data sets accordingly. Equations 9 to 11 were developed for predicting settlement of central core rockfill dams

$$S = 19.2 + 3.47H + 1.28 E_s + 34.7 \sin(179H) + \frac{-0.394}{\sin(179H)} - 4.65E_c - 0.118H\gamma_c - 15.9\cos(E_s)^2 \quad (9)$$

$$S = 10.9 + 1.6H + 1.22 E_s + 35.2 \sin(179H) - 5.09E_c \quad (10)$$

$$S = 1.72H + 1.27 E_s + 4.8E_c \quad (11)$$

For prediction of settlement based on multi-input parameters, out of the 15 sets of data, 12 sets of data (80%) were considered for training and the remaining 3 sets of the data (20%) were considered for validation. The training and validation data sets were selected randomly from the database. Figure 8 shows the relationship between actual settlement and predictions of GEP for Equations 9, 10, and 11.

After developing the GEP prediction model based on the multi-input parameters, the results were compared to well-known empirical relationships including Clements (1984) and Hunter & Fell (2003) to examine the level of accuracy of new developed models compared to the traditional equations. This comparative evaluation was performed based on the new database for 15 earth and rockfill dams with central core presented in Table 2.

Table 4 and Figure 9 summarize the statistical results of new developed GEP models based on the multi-input parameters in comparison with empirical relationships. As illustrated in the table, determination coefficient (R^2) of empirical relationships including Clements (1984) and Hunter & Fell (2003) are 0.52 and 0.49, respectively, while the simplest GEP model (equation 11) showed the R^2 of 0.91. This indicates the low accuracy of existing empirical relationships and non-applicability of them for prediction of settlement in earth and rockfill dams.

Poor prediction of these traditional equations is due to their dependency on the single factor of height. In order to achieve the applied and reliable equations, it is better to consider

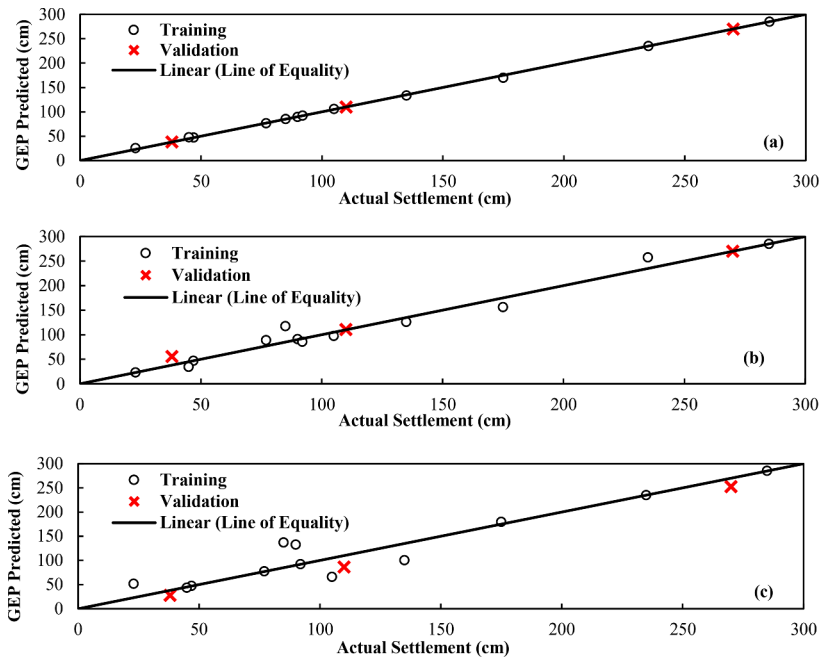


Figure 8. Relationship between actual settlement and predictions of GEP for Equations (a) 9, (b) 10, and (c) 11.

Table 4. GEP results to predict settlement of rockfill dams.

Equation	R^2	RMSE
9	0.9996	2.8880
10	0.9731	13.3658
11	0.9078	23.5717
Hunter & Fell (2003)	0.4887	62.6694
Clements (1984)	0.5217	46.6350

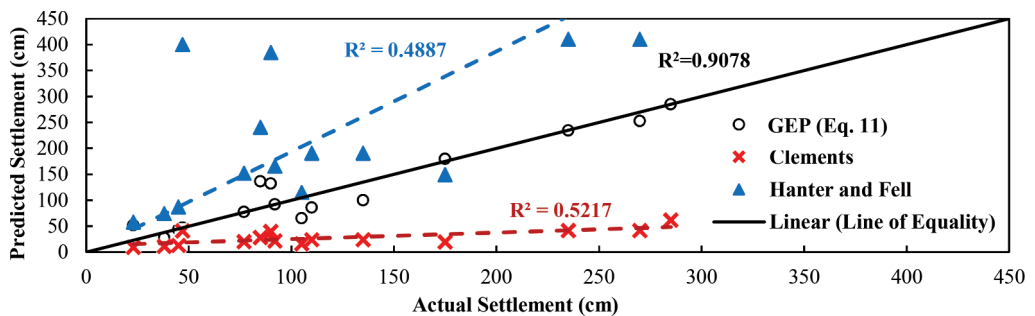


Figure 9. Coefficient of determination between the actual dam settlement and predictions of GEP models (Eq. 10) and experimental relationships (Clements (Eq. 1) and Hunter and Fell (Eq. 2)).

further effective parameters. The new GEP models revealed that including parameters such as dry unit weight, cohesion, elasticity modulus as the input parameters increased the intelligence of the resulting relation.

5 CONCLUSIONS

The focus of this research effort was to develop the models using artificial intelligence technique to predict the settlement of earth and rockfill dams with central core. In this research effort, the novel and intelligent GEP method was used to estimate the settlement based on the information of 50 different dams in the world. Parameters such as height of dam, modulus of elasticity, dry density were considered as the input parameters. The results indicated that prediction of settlement based on the single parameter of dam height cannot be reliable and aforementioned input parameters are effective in the dam settlement. In addition, the results obtained from comparing the artificial intelligent method and empirical relationships showed that GEP results were more appropriate tools to solve the problems with complex mechanisms and several effective factors, such as prediction of settlement of dams. The new developed models in this study are ready to be applied as a robust predictor tool for monitoring and safety evaluation of earth and rockfill dams in Europe¹.

REFERENCES

- Alonso, E. E., Olivella, S., & Pinyol, N. M. 2005. A review of Beliche Dam. *Géotechnique*, 55(4),267–285.
- Cetin, H., Laman, M., & Ertunc, A. 2000. Settlement and slaking problems in the world's fourth largest rock-fill dam, the Ataturk Dam in Turkey. *Engineering Geology*, 56(3-4), 225–242.
- Clements RP. (1984) Post-construction deformation of rockfill dams. *J Geotech Eng Div* 1984;110 (7):821–40.
- Cooke, J. B. (1984). Progress in rockfill dams. *Journal of Geotechnical Engineering*, 110(10), 1381–1414.
- Gikas, V., & Sakellariou, M. 2008. Settlement analysis of the Mornos earth dam (Greece): Evidence from numerical modeling and geodetic monitoring. *Engineering Structures*, 30(11), 3074–3081.
- Goldberg, D. E. 1989. Genetic algorithms in search, optimization and machine learning, Addison-Wesley Longman Publishing, Boston, MA.
- Habibagahi G. 2002. Post-construction settlement of rockfill dams analyzed via adaptive network-based fuzzy inference systems. *Sci World J* 2002;29 (3):211–33.
- Hunter, G., & Fell, R. 2003. The deformation behaviour of embankment dams. *University of New South Wales*, School of Civil and Environmental Engineering.
- Karbor-e-shyadeh, A. H., & Soroush, A. 2008. A comparison between seismic behaviors of earth dams with inclined and vertical clay cores-a numerical analysis approach. *In Proc. of 14th World Conference on Earthquake Engineering*, Paper(No. 457).
- Koza, J. R. 1992. Genetic Expression Programming on the programming of computers by means of natural selection, MIT Press, Cambridge, MA.
- Latifi, N., Marto, A., & Khari, M. 2012. Monitoring results of Alborz earth dam during construction. *Electronic Journal of Geotechnical Engineering*, 17, 2474–2484.
- Noorzad, A., Behnia, D., Moeinossadat, S. R., & Ahangari, K. 2014. Prediction of Crest Settlement of Concrete-Faced Rockfill Dams Using a New Approach.
- Onyelowe, K.C., Ebid, A.M., Nwobia, L. and Dao-Phuc, L., 2021. Prediction and performance analysis of compression index of multiple-binder-treated soil by Genetic Expression Programming approach. *Nanotechnology for Environmental Engineering*, 6(2), pp.1–17.
- Rashidi, M, Azizyan, G. and Heidari, M. 2017. Numerical Analysis and Monitoring of an Embankment Dam During Construction and First Impounding (Case Study: Siah Sang Dam). *Scientia Iranica*
- Rashidi, M. and Haeri, S. M. 2017. Evaluation of The Behavior of Earth and Rockfill Dams During Construction and First Impounding Using Instrumentation Data and Numerical modeling. *Journal of Rock Mechanic and Geotechnical Engineering*, Volume 9, Issue 4, Pages 709–725
- Rezaee, H. 2017. Evaluation of Long-term Settlement of Ghoocham Dam By Numerical Analysis, Proceedings of the 4th International Conference, Published by *Verlag der Technischen Universität Graz*, Graz University of Technology
- Siyahi, B., & Arslan, H. 2008. Nonlinear dynamic finite element simulation of Alibey earth dam. *Environmental geology*, 54(1), 77–85.
- Yong, W., Zhou, J., Jahed Armaghani, D., Tahir, M.M., Tarinejad, R., Pham, B.T. and Van Huynh, V., 2021. A new hybrid simulated annealing-based Genetic Expression Programming technique to predict the ultimate bearing capacity of piles. *Engineering with Computers*, 37(3), pp.2111–2127.

1.

Structural health monitoring of large dams using GNSS and HSCT-FE models. Swelling effect detection

M. Rodrigues, J.N. Lima & S. Oliveira
Laboratório Nacional de Engenharia Civil, Lisbon, Portugal

J. Proença
CERIS - Instituto Superior Técnico IST-ID, Lisbon, Portugal

ABSTRACT: The use of Global Navigation Satellite System (GNSS) displacement monitoring technology enables permanent and remote monitoring of large dams. The validation of GNSS displacements monitoring system installed in Cabril dam since 2016 has been accomplished by comparing the GNSS measurements not only with triangulation and plumb line methods, but also with Finite Element Models (FEM) and Hydrostatic-Seasonal-Creep-other Time effects (HSCT) models for effects separation. Analysis of a 7-year monitoring period has demonstrated the precise and reliable nature of this method, as it successfully detected the development of pathological behaviour trends associated with concrete swelling reactions.

1 INTRODUCTION

Structural health monitoring of large dams is essential to ensure their continuous and safe operation. The monitoring process involves the quantitative and qualitative evaluation of the structural response to various loads, including long-term and short-term effects. Among these loads, the swelling effect is an important long-term variable that can significantly affect the dam's structural integrity. Therefore, it is necessary to develop a robust and reliable monitoring system to detect such effects and continuously validate the dam's structural health.

To achieve this goal, structural health monitoring systems require the continuous observation of the dam's response using various monitoring techniques, namely capable of measuring displacements (Brownjohn, 2007). In particular, the observation results must be compared with numerical models, such as FEM, to obtain more in-depth insights into the dam's behaviour. However, developing such a monitoring system poses many challenges, including system reliability, data storage, overhead, environmental conditions, data mining, processing, and display of results. To overcome these challenges, various techniques and methods have been proposed, such as using GNSS and models for effects separation of the type Hydrostatic-Seasonal-Time combined with FE results.

In this research paper, we show an example for detection of swelling effects in a large arch dam - the Cabril dam - using GNSS and models for effects separation of the type Hydrostatic-Seasonal-Creep-Time combined with FE results. The proposed method using GNSS antennas allows for the continuous monitoring of the dam's displacements and the detection of structural deterioration, leading to improved safety and reliability.

2 GNSS

Monitoring systems with GNSS make it possible to measure long and short-term displacements. Comparing with other monitoring techniques, GNSS has the following advantages (Shen et al., 2019): (a) does not require intervisibility between points to be observed; (b) allows real-time

monitoring; (c) not dependent on weather conditions; (d) allows dynamic monitoring of deformation; (e) allows monitoring of long-term deformation; (f) benefit from the automatic management and processing of observations; and (g) no hardware maintenance required.

Due to these advantages, this positioning system has been widely used in monitoring the structural behaviour of large civil engineering works around the world.

The year 2016 was a milestone in the geodetic monitoring of Portuguese dams, since a GNSS monitoring program started in four large dams: Baixo Sabor, Cabril, Feiticeiro and Foz Tua.

In a study of long time series of observation with GNSS on a short base materialized at LNEC campus, it is shown that increasing the duration of the observation session decreases the level of uncertainty of measuring displacements with GNSS. For example, the average uncertainty level for one-hour and 24-hour observation sessions is 2 mm and 0.4 mm, respectively (Lima & Casaca, 2018). That is, GNSS measurements manage to reach sub-millimetre precision, but, for that, they need several hours of continuous observation. The accuracy of this type of measurement decreases with the decrease in the observation interval, which may compromise the effectiveness of GNSS in measuring vibrations with millimetre amplitudes. However, the careful application of filters to the GNSS time series or the fusion of GNSS observations with observations from other equipment (e.g., accelerometers) greatly improves the performance of GNSS in dynamic monitoring.

The application of GNSS in monitoring the structural behaviour of large dams requires the observation to be continuous and, consequently, its processing to be automatic. As displacements of large dams are, in general, in the order of several millimetres and at rates of several millimetres per year, it is necessary to use a highly accurate relative positioning to measure such displacements. For this, GNSS antennas must be installed in places with a clear horizon, where it is recommended the target point antennas to be installed at the crest. It is also recommended the reference point antennas to be installed in places close to the dam, in stable areas of the rocky massifs outside the dam's influence zone. The observation session minimum duration should be 1 hour with low pass filters application to reduce noise, such as moving averages (Section 3).

Unlike conventional monitoring, current monitoring trends are characterized by continuous and automated observation. The information provided by this type of monitoring makes notable points behaviour known (and, consequently, structural integrity is also known) continuously and almost in real time. Yet, the measuring instruments must remain continuously on site, which could translate into a large investment if top-of-the-range instruments are chosen. Alternatively, low-cost equipment can be used without compromising the required high level of precision.

3 MOVING AVERAGES AS A LINEAR FILTER

The data observed by the GNSS monitoring system should be smoothed before being analysed. One approach that has led to satisfactory results involves applying a moving average filter (MAF) to raw GNSS monitoring data.

To understand these filters application, one should consider the linear combination of the terms of a time series x_0, x_1, \dots, x_n :

$$y_k = \sum_{j=-q}^r w_j x_{k+j} \quad (k = q + 1, \dots, n - r) \quad (1)$$

where the coefficients w_j are the weights and are in number $m (= q + r + 1)$. This linear combination is said to be of order m . If $q = r$ and $w_j = w - j$, the filter is said to be symmetric. If the sum of the weights equals 1, the filter is called a weighted moving average. If the weights are all equal and their sum is equal to 1, the filter is called a simple moving average (Haykin, 2002).

Applying a filter to a time series x_0, x_1, \dots, x_n , called the input time series, will generate a new time series y_0, y_1, \dots, y_n , called the output time series. The spectral characteristics of the output time series are related to the spectral characteristics of the input time series through the filter transfer function. The transfer function is a complex function with frequency domain arguments. The magnitude of the transfer function is called the filter gain (Priestley, 1981). If the filter gain, for a given angular frequency ω , is greater than 1, the filter amplifies the input

time series at frequency ω . On the other hand, if the filter gain, for angular frequency ω , is less than 1, the filter reduces the input time series at that frequency.

Furthermore, the variation in the amplitude of the filter can also introduce an offset (delay) in the output time series as a function of frequency. While symmetric filters do not introduce significant lags, asymmetric filters, on the contrary, can introduce considerable lags.

The estimated uncertainty for the hourly solutions of the horizontal components is about five times greater than the estimated uncertainty for the daily solutions of the same components. However, the time series of the hourly solutions have a higher temporal resolution than those of the daily solutions. The application of symmetric moving averages to the time series of the hourly solutions significantly reduces the uncertainty without compromising the temporal resolution. Moving averages work as low-pass filters and are very easy to implement in time series.

4 HSCT MODELS

The main purpose of the separation of effects models is to isolate each load's effect, which facilitates the study about the influence of each load on the observed displacement histories (Rocha, 1956). The Hydrostatic, Seasonal, Creep and other Time effects (HSCT) models are a specific type of separation of effects models which consider the creep effects and, consequently are capable of detecting anomalous or pathological components on observed displacements time series (Rodrigues et al., 2021, 2022).

Among the pathologies dams can develop over time, swelling is becoming more relevant, arousing interest in its evolution and subsequent study of its effects. Many concrete dams have registered problems related to swelling due to chemical reactions occurring between cement components and the aggregate (Silva, 1993; Gomes, 2007; Esposito et al., 2016; Abd-Elssamd, 2020). The swelling reactions occur with relatively high humidity and temperature, producing a gel that fills the concrete internal microstructure pores. This process eventually generates cracking, the consequent concrete damage, and a global volume increase (swelling). Many dams have problems due to swelling reactions, the most serious cases in Portugal are Santa Luzia, Pracana and Alto Ceira. The case of Alto Ceira dam was an extreme example of concrete swelling pathological effect consequences, which led to the dam decommissioning.

For performing the quantitative interpretation of the monitoring data, a HSCT-FE model was implemented on a software named *DamSafe4.0*. In the analysis of the observed displacement histories, the used HSCT models (multiple linear regression models) are based on the following regression equation (see Table 1).

$$u(h, T_{\text{air}}, t) = u_e^{\text{HP}}(h) + u_e^{\text{T}}(T_{\text{air}}) + u_C^{\text{HP}}(h, t) + u_C^{\text{SW}}(t) + u_{\text{swelling}}(t) + k \quad (2)$$

This HSCT model is capable of making the time effect separation into one creep component related to the Hydrostatic Pressure (HP), $u_C^{\text{HP}}(h, t)$, one creep component associated with the Self-Weight (SW), $u_C^{\text{SW}}(t)$, and one other time effects component, for example, swelling, $u_{\text{swelling}}(t)$. To estimate the creep effect, it is important to distinguish SW creep from HP creep: for this purpose, it is useful to estimate the elastic response component for both loads. This procedure can be executed using the FEM, especially for the SW effect.

The functions used to represent each separated effect correspondent to each term of the regression equation (Equation 1) are presented in Table 1.

Table 1 displays the use of exponential functions to represent the HP elastic effect, where a is the regression coefficient, h is the reservoir water level and c_f is a shape coefficient for the exponential function.

The HP creep effect is obtained as a superposition response to a sequence of constant load "steps" (obtained as a discretization of the water level variation in constant intervals): creep coefficients are applied to the elastic displacement values calculated for each constant water level step. The viscoelastic response is equal to the superposition of the creep effect computed for each step (j). The creep effect estimation for the water level variation is given by the following equation

$$u_C^{HP}(h, t) = a \times \sum_{j=1}^p \phi(t, t'_j) \left(e^{h_j/c_r} - e^{h_{j-1}/c_r} \right) \quad (3)$$

where p is the total number of water level steps in the considered discretization (from $j=1$ to p), and $\phi(t, t'_j)$ is the creep coefficient at time t for the hydrostatic load step at time instant t'_j .

The temperature effect can be simulated with the air temperature values registered at the site (it is usual to apply a phase shift of approximately 20 to 30 days, which is roughly the dam response time to an air temperature variation) or by harmonic functions with annual and/or half annual periods (Willm & Beaujoint, 1966). Where b or b_1 and b_2 are the regression coefficients, T_{air} is the air temperature at the site, and \bar{t} is the date of the year, in days after Jan1st.

The SW creep effect is considered as taking into account that SW corresponds to a constant load (gravity's direction), applied to the whole structure. The creep effect can be estimated using the elastic displacements computed by FEM for the SW and considering the appropriate creep coefficients (estimated by the creep function), taking into account the structure concrete mean age (mean date of the construction period).

Table 1. Adjustment functions used in each term of the regression equation.

Term	Effect	Adjustment function
$u_e^{HP}(h)$	Hydrostatic pressure elastic effect	$a(e^{h/c_r} - 1)$, $15 \lesssim c_r \lesssim 35$ (alternatively, the a value can be determined by the FEM)
$u_e^T(T_{air})$	Temperature effect	bT_{air} or $b_1 \cos(\frac{2\pi\bar{t}}{365.25}) + b_2 \sin(\frac{2\pi\bar{t}}{365.25})$, ($0 < \bar{t} < 365.25$ days) (Willm & Beaujoint, 1966)
$u_C^{HP}(h, t)$	Hydrostatic pressure creep effect	$\sum_{j=1}^p \phi(t, t'_j) \Delta u_{e,j}^{HP}$, $\Delta u_{e,j}^{HP} = a(e^{h_j/c_r} - e^{h_{j-1}/c_r})$
$u_C^{SW}(t)$	Self-weight creep effect	$\phi(t)u_e^{SW}$
$u_{swelling}(t)$	Swelling	$c \times (1 - e^{-t/\beta})$ where $\beta = t_{hs}^n \times n/(n-1)$, $n = 3.258$ and $t_{hs}^n \simeq 8000$ days (hs - half swelling)
k	Independent term	-

The adjustment functions associated with the displacements created by the swelling effect are presented in Table 1. In the presented formulation c or c_1 , c_2 and c_3 are the regression coefficients. Usually, the result is a sigmoid-type curve, which slowly increases over time until half of its total displacement, where, at that point, changes from convex to concave (inflection point), moving then towards stabilization. The referred swelling curve inflection point is also known as half-swelling point. Alternatively, the swelling effect can be represented by polynomial functions.

The independent term, k , is included in the model so it can consider the initial observation (the first campaign of the analysed period).

With this formulation, a HSCT model curve adjusted to the observation values is obtained by applying the Least Squares Method (LSM).

In HSCT models use, it is important to emphasize the following: (i) before applying the LSM, the SW creep component can be removed from the observed values and corrected observed values are obtained for HSCT separation of effects analyses; (ii) the choice between the proposed adjustment functions for a given effect depends on the one that better adjusts itself to the observed data; and (iii) to acquire reliable results for the HSCT-FEM outputs, it is convenient to have observations in quantity, preferably obtained with assured quality and well distributed over time, where observed values are present at each year's weather seasons and at water levels representative of all the reservoir filling levels.

5 CABRIL DAM

Cabrill dam is located on the Zêzere river and has been in operation since 1954. This dam has a maximum height of 132 m and its crest stands at 297 m of elevation with a length of about

290 m. Cabril dam is a double curvature arch dam with the geometry presented in Figure 1. A GNSS system, financed by FCT, was installed in Cabril dam by LNEC and EDP in 2016, to enable the continuous automatic measurement of the three displacement components at the top of the central section (Oliveira et al., 2014), with a sampling frequency of 20 Hz. This system includes a GNSS receiver located outside the dam (about 200 meters afar from it), which is being used as reference, and another GNSS receiver that was installed at the crest centre, the object point (Figure 1). The location of the reference receiver favours error reduction because it has been installed in a stable location, with a free horizon, at the left bank. This system has been in operation since July 2016, continuously providing data, 24 values per day, for a better evaluation of Cabril dam's behaviour.

The Cabril dam GNSS observations used in this study corresponded to the daily averages measured. This solution presents a much lower noise than, for example, the hourly averages solution, because the daily displacement variation of the pillar that supports the reference antenna, caused by the daily thermal variation, is eliminated when using the daily averages.

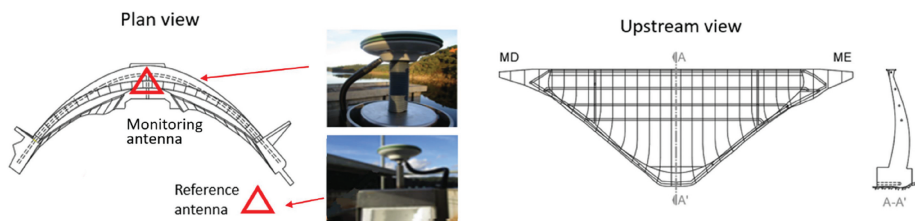


Figure 1. Cabril dam. GNSS system installed to measure displacements at the top of central section.

6 FEM

A 3D finite element model was developed for Cabril dam's structural behaviour analysis, using hexaedral finite elements (isoparametric, with 20 nodes) to represent the dam and the foundation (Figure 2). A discretization with three elements along the thickness was assumed for the dam body, which was automatically generated using the program *Dam3DMesh1.0*. This discretization considered that the existing horizontal cracking on the dam upper zone could be simulated using horizontal interface elements, as represented in Figure 2 by the red line. This crack is considered closed on the upstream face and completely open in the entire thickness up to the downstream face. Figure 2 shows the 3D mesh geometry and the material properties considered.

It is relevant to note that this model geometry and its material definition is a result of continuous improvement by systematic comparison with observed data.

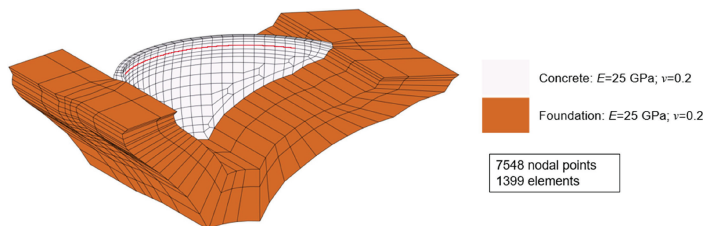


Figure 2. Cabril dam FE model with a horizontal discontinuity (crack band simulation).

At Cabril, there are no plumb lines installed in the central section, they have only been installed in two blocks approximately midway between the central section and the abutments. The GNSS observed displacements validation on the central section was achieved through a numerical 3D model with finite elements previously validated with the displacements observed by the plumb lines installed in blocks closer to the abutments (Rodrigues et al., 2021).

7 FE MODEL RESULTS

The FE model analysis considered the combination of the following actions: Hydrostatic Pressure (HP), Temperature (T) and Swelling (Swe) effect. The results are presented in Figure 3. In the top, it is presented the comparison between GNSS observations (grey lines) and the FE model simulation (red line). In the middle and in the bottom are presented the temperature and HP load variations used in the model, respectively. The swelling load adopted is equivalent to the one validated in previous work about this dam that involved the swelling reactions effect (Rodrigues et al., 2022). The swelling load was defined in the numerical model by imposing a strain field compatible to the one observed in the isolated strainmeters scattered throughout the dam body. Generically, the imposed strains increase exponentially from bottom to top, where values of about 20×10^{-6} were imposed at the base and values of about 400×10^{-6} were imposed at the crest.

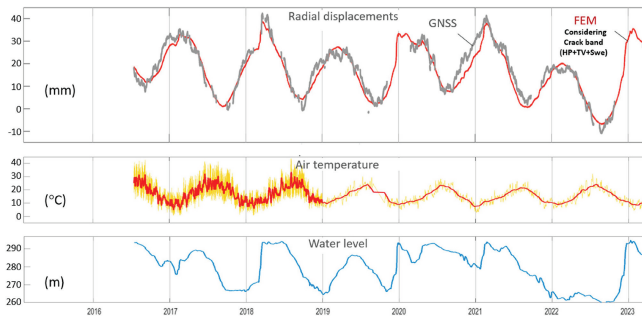


Figure 3. Cabril dam. Comparison between GNSS measured radial displacements at the top of central section (positive values towards downstream) and the correspondent FEM simulation results due to the main loads variation: air temperature, water level and swelling.

From the analysis of the results presented in Figure 3 it is possible to verify that the FE model results adjust themselves very closely to the GNSS observations which is indicative of the numerical model validity. Additionally, it is important to mention that without the swelling effect, the FE model results would have deviated from the observation results. In previous works (Rodrigues et al., 2021), for less extended GNSS observation periods, it was indifferent to consider or not the swelling effect since it did not have significant time to develop to a noticeable degree.

8 HSCT MODEL RESULTS

Following numerous tests of various HSCT and hybrid HSCT-FE model configurations, the HSCT-based model that achieved the most effective global adjustment to the GNSS data presents the following features: (i) for the HP elastic effect estimation, it was considered one exponential function with a c_f value of 25; (ii) the temperature effect is estimated as proportional to the observed daily average air temperature, considering an 18 days delay to simulate the heat wave propagation throughout the concrete; (iii) the HP creep effect is simulated by the creep coefficients application to the elastic response, for the monthly water level history discretization in constant intervals, and considering a concrete material with a Bazant and Panula creep law in which: $E_0 = 25$ GPa, $\phi_1 = 2.64$, $\beta = 0.042$, $m = 0.441$ and $n = 0.168$, matching a concrete moderately damaged by swelling (there is evidence of swelling reaction occurrence by visible gel exudations at the upper inspection gallery); (iv) the SW creep effect is estimated with the same creep coefficient application to the elastic displacements determined by the FE model, for the SW action; (v) the time effect related to swelling is given by a 3 terms polynomial, t^3+t^2+t . This model is equivalent to the one applied in a previous work that involved this dam and GNSS monitoring (Rodrigues et al., 2021). The resulting regression equation has the following form.

$$u - \phi(t, t_0)u_{c,FEM}^{SW} = a_1 \cdot (e^{h/20} - 1) + a_1 \cdot \sum \phi(t)u_{e,a_1}^{HP} + a_2 \cdot (e^{h/25} - 1) + a_2 \cdot \sum \phi(t)u_{e,a_2}^{HP} + b \cdot T_{air} + c_1 \cdot t^3 + c_2 \cdot t^2 + c_3 \cdot t + k \quad (4)$$

$$\sum \phi(t)u_{e,a_1}^{HP} = \sum_{j=1}^p \phi(t, t_j) (e^{h_j/20} - e^{h_{j-1}/20}) \quad (5)$$

$$\sum \phi(t)u_{e,a_2}^{HP} = \sum_{j=1}^p \phi(t, t_j) (e^{h_j/25} - e^{h_{j-1}/25}) \quad (6)$$

As mentioned, to apply HSCT-FE hybrid models, FEM results are necessary. As it is possible to verify, FEM results are used for the estimation of the SW displacement component. Additionally, FEM results, like the HP elastic effect and the temperature effect, are also used to verify the agreement between HSCT and FE models, as the following figures display.

Figure 4 shows the HSCT separation of effects results for the analysed GNSS monitoring data.

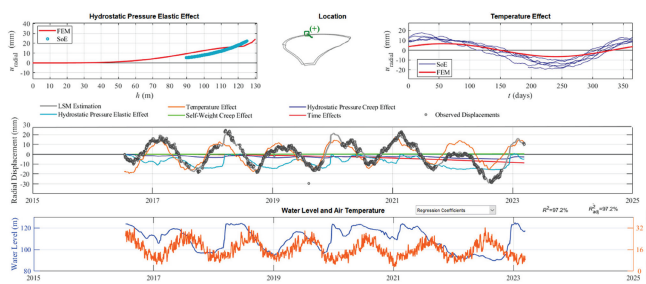


Figure 4. Cabril dam. HSCT model results (2016-2023) for the GNSS antenna located on top of the central cantilever. Identification of upstream displacements component due to swelling.

Figure 4 is organized according to the following format: on top, at the centre, it is presented the following information: the dam geometry in a 3D representation, the location of the GNSS antenna, and the indication of the positive axis direction; on top, the left graph presents the HP influence line, where the blue dots are results from the statistical method whereas the red line is computed with the FE model; on top, the right graph presents the temperature effect variation throughout the year, where the blue curves represent each year's thermal wave resulting from the statistical method, whereas the red line is the FE model calculated thermal wave; the middle graph is the main separation of effects graph, in this graph is displayed each separate effect evolution over time, where the grey dots represent observations of the analysed GNSS radial displacement, the grey curve represents the HSCT solution (LS method), the light blue curve represents the HP elastic response, the orange curve represents the temperature effect, the dark blue curve represents the HP viscoelastic effect, the green curves represents the SW viscoelastic effect and the red curve represents the swelling reaction effect (Swe). In this figure, the coefficient of determination (R^2) and the correspondent adjusted values (R_{adj}^2) are presented as quantitative indicators of the adjustment quality. The bottom graph presents the air temperature and the water level time evolution.

The results presented in Figure 4 allow for several key conclusions to be drawn: i) the HSCT model temperature and HP elastic effects are highly consistent with the FEM results, indicating a strong level of accuracy in the model; ii) the HSCT model curve aligns perfectly with the GNSS observations, suggesting that the model has been adjusted effectively; iii) the swelling effect has an accumulated impact of approximately 9 mm towards upstream, equating to roughly 1 mm per year; iv) there is a strong correlation between the radial displacements observed by the GNSS (downstream - upstream) and the weekly moving average of the air

temperature; v) the time lag between the peak radial displacements due to thermal wave and the peak values of the air temperature wave is approximately 18 days, which can be attributed to the dam's thermal inertia as previously outlined in the HSCT model definition.

9 CONCLUSIONS

In conclusion, this study showed that the use of GNSS displacement monitoring technology enables accurate and reliable monitoring of large dams. Through a 7-year monitoring period of Cabril dam, the results show that GNSS can achieve sub millimetric accuracy to detect the development of small pathological structural behaviour trends such as the concrete swelling effect. These findings are consistent with previous studies on this subject. GNSS's continuous monitoring capabilities provide high-quality data, enabling statistical models that show a high level of agreement with observations. Compared to conventional monitoring systems, GNSS is robust and requires no maintenance or calibration. Its automatic monitoring design makes it an efficient alternative for dam structural health monitoring. This study also demonstrates the effectiveness of GNSS displacement measurements for detecting the swelling effect in large dams, namely when HSCT-FE models are used for GNSS data analysis. The validation of GNSS measurements through comparisons with triangulation and plumb line methods, as well as Finite Element Models (FEM) and Hydrostatic-Seasonal-Creep-other Time effects (HSCT) models for effects separation, further strengthens the study's conclusions. Overall, the results of this study highlight the potential of GNSS technology for remote and permanent monitoring of large dams.

ACKNOWLEDGMENTS

The authors thank Energias de Portugal (EDP) for their support in the installation and maintenance of the GNSS monitoring system installed in Cabril dam, and for allowing the use of its data. This research was funded by the Foundation for Science and Technology (FCT) in the framework of the project PTDC/ECI-EGC/5332/2020 - Seismic Monitoring and Structural Health of Large Concrete Dams (SSHM4Dams), involving LNEC, ISEL-IPL and IST-ID, and within the scope of the project UIDB/04625/2020, which is under development at the Civil Engineering Research and Innovation for Sustainability (CERIS) centre.

REFERENCES

- Abd-Elssamd, A.; Ma, Z. J.; Le Pape, Y.; Hayes, N. W.; Guimaraes, M. (2020). Effect of Alkali-Silica Reaction Expansion Rate and Confinement on Concrete Degradation. *ACI Materials Journal* 117 (1): pp. 265:278.
- Brownjohn, J.M. (2007). Structural health monitoring of civil infrastructure. In *Phil. Trans. R. Soc. A*, 365, 589–622.
- Esposito, R.; Anaç, C.; Hendriks, M.; Çopuroğlu, O. (2016). Influence of the Alkali-Silica Reaction on Mechanical Degradation of Concrete. *Journal of Materials in Civil Engineering* 28(6).
- Gomes J. P. (2007). *Modelação do comportamento estrutural de barragens de betão sujeitas a reações expansivas*, Ph.D. Thesis, FCT-UNL.
- Haykin, S. (2002). *Adaptive Filter Theory*. Prentice Hall, New Jersey, USA.
- Lima, J.N.; Casaca, J. (2018). Monitoring dam displacements with GNSS: strategy, accuracy and benefits. *Dam World 2018, Proceedings of Third International Dam World Conference*, Foz do Iguaçu, Brazil.
- Oliveira, S.; Lima, J. N.; Henriques, M. J. (2014). A Integração do GNSS no Controlo de Segurança de Grandes Estruturas. In: *Jornadas Portuguesas de Engenharia de Estruturas (V)*. November 26 to the 28th. Lisbon.
- Priestley, M. B. (1981). *Spectral Analysis and Time Series*. Academic Press, London, UK.
- Rocha, M. (1956). Nota sobre a interpretação dos resultados da observação de barragens. LNEC. Report 1126/56.
- Rodrigues, M., Oliveira, S., Lima, J. N., & Proença, J. (2021). Displacement monitoring in Cabril dam using GNSS. *Dam Engineering*, 31(3), 149–165.

- Rodrigues, M., Oliveira, S., & Proença, J. (2022). Modelos híbridos de separação de efeitos do tipo HSCT-FE para o estudo do comportamento de barragens abóboda sob ações expansivas. *Portuguese Journal of Structural Engineering*, 3(18), 73–80.
- Shen, N.; Chen, L.; Liu, J.; Wang, L.; Tao, T.; Wu, D. e Chen, R. (2019). A Review of Global Navigation Satellite System (GNSS)-based Dynamic Monitoring Technologies for Structural Health Monitoring. *Remote Sens.*, 11, 1001.
- Silva, H. S. (1993). Estudo do envelhecimento das barragens de betão e de alvenaria. Alteração físico-química dos materiais, Specialist Thesis, LNEC.
- Willm, G.; Beaujoint, N. (1967). Les méthodes de surveillance des barrages au service de la Production Hydraulique d'Electricité de France; Problèmes anciens e solutions nouvelles. In: IX ICOLD Congress, R.30, Q.34. Istanbul.

Dynamic behavior of exposed geomembrane systems in pressure waterways

S. Vorlet, R.P. Seixas & G. De Cesare

Platform of Hydraulic Constructions (PL-LCH), Ecole Polytechnique Fédérale de Lausanne (EPFL), Lausanne, Switzerland

ABSTRACT: Geomembrane systems have been used in dams and reservoirs as rehabilitation technology since several decades and are now used worldwide. They act as impervious layer to prevent and mitigate water leakage and damage to structures. They meet the needs of many challenges faced by aging dams by improving their performance and lifespan, enhancing their resilience and sustainability. More recently, their application was extended to pressure waterways and surge shafts. A Finite Element model is developed to investigate the dynamic behavior of a framed hyperelastic geomembrane specimen for enhanced application in pressure waterways accounting for the dynamic behavior of the geomembrane system and fluid-structure interactions in the frequency domain. The nonlinear constitutive behavior of the geomembrane is modeled by the Mooney-Rivlin equation. The effect of water is considered by the added mass approach for the modal characteristics of the geomembrane. The damping is included as Rayleigh damping. Results show that the modal characteristics of the geomembrane are strongly influenced by the material nonlinear constitutive behavior. The first natural frequencies of the hyperelastic geomembrane specimen are found at low frequencies in vacuum. The natural frequencies also strongly increase with the increase of pre-tension in vacuum. In the presence of water, the variation of the natural frequency with pre-tension is highly reduced. The increase in hydrostatic pressure tends to moderately increase the natural frequencies of the specimen. Finally, the damping ratio has almost no influence on the natural frequencies.

1 INTRODUCTION

The growth in demand for renewable energy at a global scale implies the increase in reliance on renewable energy sources, leading to new challenges in terms of environmental, technological, and socio-economic development. Hydropower is poised to have a major role in the upcoming decades due to its historical importance and storage capacity, which allows for operation adaptability, reliability and compliance to complex grid requirements. The increase in renewable energy demand is a challenge for hydropower, both in terms of maintenance and expansion of hydropower plants. Because new hydropower projects are expensive and can carry a significant environmental cost, the most effective way to overcome this challenge is to increase the efficiency of existing hydropower plants (Nogueira et al., 2016; Quaranta et al., 2021; Zarfl et al., 2015). This is particularly the case for developed countries in which, unlike the rest of the world, hydropower development has been relatively minimal in the last two decades (Quaranta et al., 2021). With nearly half of hydropower plants commissioned worldwide before the 1980s, many are now approaching a critical stage of aging, causing challenges related to their maintenance, retrofitting, upgrading and expansion, mostly in North America and western Europe (Quaranta et al., 2021). With aging, hydropower plants are likely to develop weaknesses in their structural integrity, eventually leading to water leakage, head losses, and consequently reduction of their operational capacity. In the case of pressure waterways, where the mainly energy losses occur (Nogueira et al., 2016), both the pressure tunnel and pressure shaft tend to experience a reduction in their performance over their lifetime due to erosion, corrosion, and sediment deposits. Therefore, the hydropower sector is at

a critical point and the transformation and adaptation of existing structures is a challenge. In addition, existing schemes will be increasingly stressed in the coming years due to the growing demand for renewable energy production. The modification and flexibilization of hydropower operations is a major challenge. Innovative dependable solutions are required to rehabilitate hydropower plants and in particular pressure waterways, ensuring safe and optimized operations.

Geomembrane systems (GS) are used in civil engineering applications as impervious barriers. In hydropower, they have been applied since several decades as rehabilitation technology for aging structures. They act as impervious layer and are employed in hydraulic canals, reservoirs, dams, and hydraulic tunnels. GS are a superposition of geosynthetic materials, usually a nonlinear hyperelastic geocomposite formed by a geomembrane and a geotextile. There are several configurations of GS (homogeneous, multi-layered, scrim-reinforced, and backing-reinforced). The geomembrane is usually made of polymeric material and plasticized polyvinyl chloride (PVC-P) are the most widely used geomembranes for applications in hydropower (Cazzuffi & Gioffrè, 2020; Hsuan & Koerner, 2008; Marence et al., 2020; Scuro & Vaschetti, 2017a; Scuro, Alberto et al., 2017).



Figure 1. Examples of GS applications in hydropower: (a) reservoir of Pico da Urze pumped storage plant, Portugal, (b) hydraulic canal of Larona hydropower plant, Indonesia, (c) upstream pumped face of Paradelada dam, Portugal. Images: courtesy of Carpitech.

Later, their application has been extended to pressure waterways (pressure tunnels and shafts) and surge shafts (Cazzuffi et al., 2012; Scuro & Vaschetti, 2017b, 2021). In pressure waterways, both the pressure tunnel and pressure shaft tend to experience a reduction in their performance over their lifetime due to erosion, corrosion and sediment deposits (Koerner & Koerner, 1996; Nogueira et al., 2016; Quaranta et al., 2021), and GS reduce water leakage, bridge potential cracks, and prevent the existing lining from further deterioration. In addition, they improve the energy efficiency and durability of the scheme by reducing friction losses in pressure waterways, where most of the energy is dissipated (Nogueira et al., 2016). Backing-reinforced geomembrane systems with a PVC-P geomembrane and a backing geotextile, usually made of polypropylene (PP), are the most widely used in pressure waterways. The current application technique consists of fixing the GS to the existing lining with perimeter seals, followed by the successive application of the fastening lines longitudinally, inducing prestress in the GS (Cazzuffi et al., 2012). As a result, the geomembrane is divided into smaller rectangular specimens fixed on the edges and free to move in the center.

Although the application of geomembrane liners in pressure waterways is very promising and is poised to gain importance in the next years and decades, research and development are still needed to integrate in the design the concepts of fluid-structure interactions and the resulting flow-induced vibrations of the hyperelastic geomembrane system. If not addressed properly, the nonlinear dynamic behavior induced by the hyperelastic material constitutive relation and by the interaction with the flow might potentially lead to the failure of the system. In addition, the use of renewable energies, such solar, wind or biomass, leads to transient flow and pressure conditions (e.g. in grid regulating pumped storage plants), resulting in higher stress in the geomembranes than in the past, hence the urgent need for research on these systems. The precise knowledge of the dynamic characteristics is essential for an application with enhanced performances and structural integrity in pressure waterways.

Finite Elements (FE) models to describe the dynamic behavior of geomembrane systems in the frequency domain are at an early stage of development. The nonlinear hyperelastic material constitutive behavior, the nonlinear interactions with the flow and the lack of experimental data currently restrict the FE models development. This paper presents the FE model



Figure 2. Application of an exposed geomembrane system in pressure waterways; illustration of the Helms penstock access tunnel, USA; geomembrane system with fastening system and perimeter seals. Image: courtesy of Carpi Tech.

developed to assess the modal characteristics of geomembrane systems in pressure waterways for various prestrain levels and accounting for fluid-structure interactions, where the effect of hydrodynamic load is not yet considered. The effect of the pre-tension, the hydrostatic pressure and the damping ratios on the modal characteristics are assessed and presented.

2 SETUP AND PROCEDURE

2.1 Numerical setup

The FE model is developed to assess the free vibrations characteristics of prestrained geomembrane systems in pressure waterways using the FE analysis software ANSYS 20.2. The FE model considers a framed geomembrane of dimensions $c = 0.3$ m and $s = 1$ m with clamped boundary conditions on the edges. The thickness and density of the geomembrane are estimated to $h = 5$ mm and $\rho_s = 1400$ kg/m³. The mesh is built with SOLID186 type of element (20-node quadratic solid element), and SOLID187 type of element (10-node quadratic tetrahedron element) supporting large deflections, hyperelasticity and suitable for incompressible hyperelastic materials. The numerical approach first considers a static analysis to account for nonlinear deformations due to gravity effects (self-weight and hydrostatic pressure) and prestrain, followed by a modal analysis. The prestrain level of the geomembrane ε , the hydrostatic pressure ΔP , corresponding to the difference in hydrostatic pressure below and above the geomembrane, and the damping ratio ζ are investigated and are given as input parameter in the FE model. The prestrain is applied in the y -direction only. The hydrostatic pressure is acting uniformly on the membrane along the z -axis along with gravity if $\Delta P = p^+ - p^- > 0$.

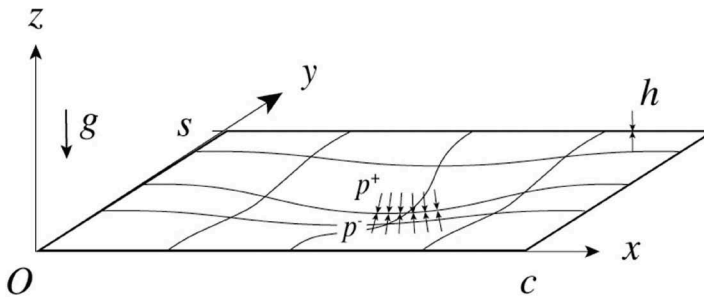


Figure 3. Schematic of the computational domain of the rectangular geomembrane specimen with dimensions c , s , h , and the hydrostatic pressure above the geomembrane p^+ and below the geomembrane p^- .

2.2 Hyperelastic material model

For hyperelastic materials, linear stress-strain relations are not suitable to characterize the hyperelastic mechanical behavior with large nonlinear deformations (Chakravarty & Albertani, 2011a, 2011b). Hooke's law is only valid at very small strains, after which it overestimates the stress level for a certain strain (Stanford et al., 2008) and a nonlinear constitutive relation is needed. Several formulations and models for the strain energy density function have been developed for isotropic and incompressible hyperelastic materials ($\nu = 0.5$). In this paper, the Mooney-Rivlin formulation is used to fully describe the constitutive behavior of the hyperelastic geocomposite. The Mooney-Rivlin material model is an extended formulation of the Neo-Hookean model and is considered one of the most accurate in the description of the state of hyperelastic material under large deformations, up to 150% strains (Stanford et al., 2008). The five-parameters formulation of the Mooney-Rivlin material model is used and the parameters are derived from uniaxial tensile experimental data, provided by CarpiTech for a 3 mm thick PVC-P geomembrane heat-bonded to a 500 g/m² non-woven geotextile (SIBELON[®]), and are $C_{10} = -3.2E7$ Pa, $C_{01} = 3.7E7$ Pa, $C_{11} = -1.1E8$ Pa, $C_{20} = 3.2E7$ Pa and $C_{02} = 1.2E8$ Pa.

2.3 Added mass

The added mass of the surrounding fluid is considered in the FE model to consider the fluid-structure interactions. The surrounding fluid exerts resistance when the specimen vibrates in fluid. The added mass is the additional inertia resulting from the specimen movement opposition by the fluid when the specimen is accelerated relative to the fluid. Hence, the angular natural frequencies of the specimen decrease because of added mass (Chakravarty, 2013; Kaneko et al., 2014). The added mass relies on the geometry and dimensions of the specimen and the density of the fluid ρ_s and is given for the rectangular specimen vibrating in water by the following equation (Kaneko et al., 2014):

$$m_a = \rho_f \pi \left(\frac{c}{2}\right)^2 \left(\frac{s}{2}\right) K \quad (1)$$

where K is constant and depends on the ratio c/s . The added density is then obtained dividing the added mass by the volume of the geomembrane:

$$\rho_a = \rho_f \pi \left(\frac{c}{8h}\right) K \quad (2)$$

Finally, the effective density of the geomembrane is $\rho_e = \rho_s + \rho_a$ (Chakravarty & Albertani, 2011b).

2.4 Damping

The added damping induced by the surrounding fluid is implemented in the FE model as Rayleigh damping. The Rayleigh damping model expresses the damping $[c]$ by the linear combination of a mass proportional part and a stiffness proportional part (Nakamura, 2016) by the coefficients α_m and β_k (Chakravarty & Albertani, 2012):

$$[c] = \alpha_m [m] + \beta_k [k] \quad (3)$$

where the coefficients are frequency-dependent and ω_n is the n th-mode natural circular frequency in vacuum and ξ_n is the damping ratio of the n th-mode natural circular frequency (Nakamura, 2016):

$$\alpha_m = \frac{2\omega_1\omega_2(\xi_1\omega_2 - \xi_2\omega_1)}{\omega_2^2 - \omega_1^2} \quad (4)$$

$$\beta_k = \frac{2(\xi_2\omega_2 - \xi_1\omega_1)}{\omega_2^2 - \omega_1^2} \quad (5)$$

The n th-natural frequencies of the geomembrane are determined using the FE model in vacuum. In this paper, the damping ratio is assumed to be constant ($\zeta_1 = \zeta_2$). Several levels of damping ratios are investigated.

2.5 Model convergence

The mesh-independency of the solution is ascertained by assessing the convergence of the maximal out-of-plane displacement at the center of the geomembrane at static loading and the convergence of the natural frequencies of the first six modes for various degrees of freedom (DOF). The slack geomembrane is considered ($\varepsilon = 0$) and undamped, and in vacuum. It is found that the convergence is achieved for $DOF = 122'265$ for both the maximal out-of-plane displacement and the natural frequencies.

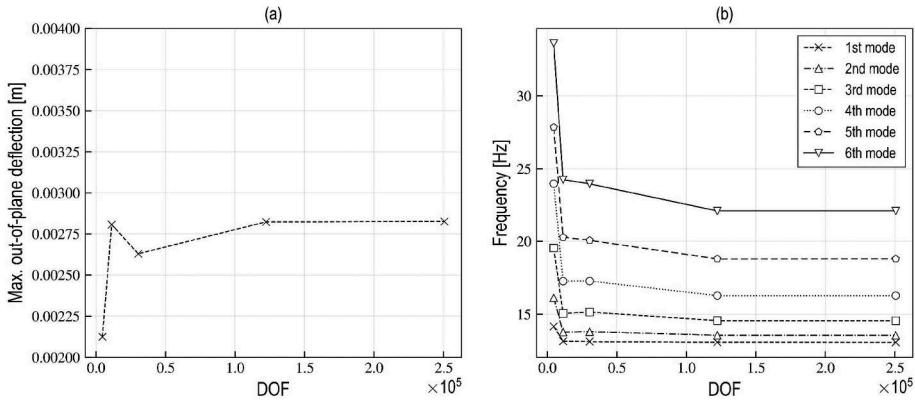


Figure 4. Mesh-sensitivity study: convergence of the maximal out-of-plane deflection at static loading (a) and convergence of the natural frequencies (b); slack undamped geomembrane in vacuum.

3 RESULTS

3.1 Deformation at static loading

Hyperelastic materials are characterized by large amplitude of deformations at quasi-static loading. The deformation behavior of the nonlinear hyperelastic geomembrane is first investigated at static loading under the effect of gravity for various prestrain levels in vacuum and for various hydrostatic pressure levels. The maximal out-of-plane deformation of the prestrained

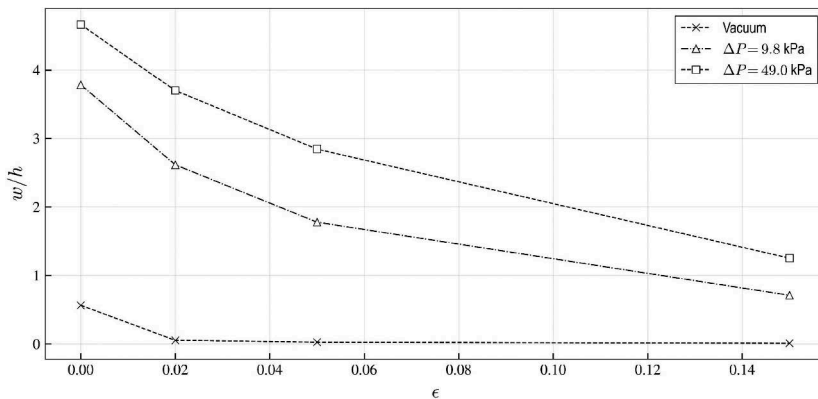


Figure 5. Static maximal out-of-plane deflection of the geomembrane for various prestrain and hydrostatic pressure levels accounting for the nonlinear constitutive relation of the geomembrane.

geomembrane is shown in Figure 5. The maximal out-of-plane deformation occurs at the center of the geomembrane. It increases with the effect of gravity and the presence of water. But the deformation decreases with the increase of the prestrain level of the geomembrane.

3.2 Modal characteristics in vacuum

The first six mode shapes of the slack geomembrane from the FE model in vacuum are presented in Figure 6, in which the effect of the pre-tension is not considered (slack specimen). Results present typical mode shapes for rectangular geometries, with the number of nodal lines increasing with the frequency. The first natural frequencies are observed at very low frequencies, due to the hyperelastic constitutive behavior of the material and the low bending rigidity of the geomembrane. In addition, results highlight that the natural frequencies are close to each other.

The variation of the natural frequencies of the geomembrane with pre-tension in vacuum is shown in Figure 7. The natural frequencies of the geomembrane are strongly increased due to the increase in the prestrain level in the geomembrane for all six first modes. Natural frequencies are also observed to be closer to each other with the increase in the prestrain level between the various modes.

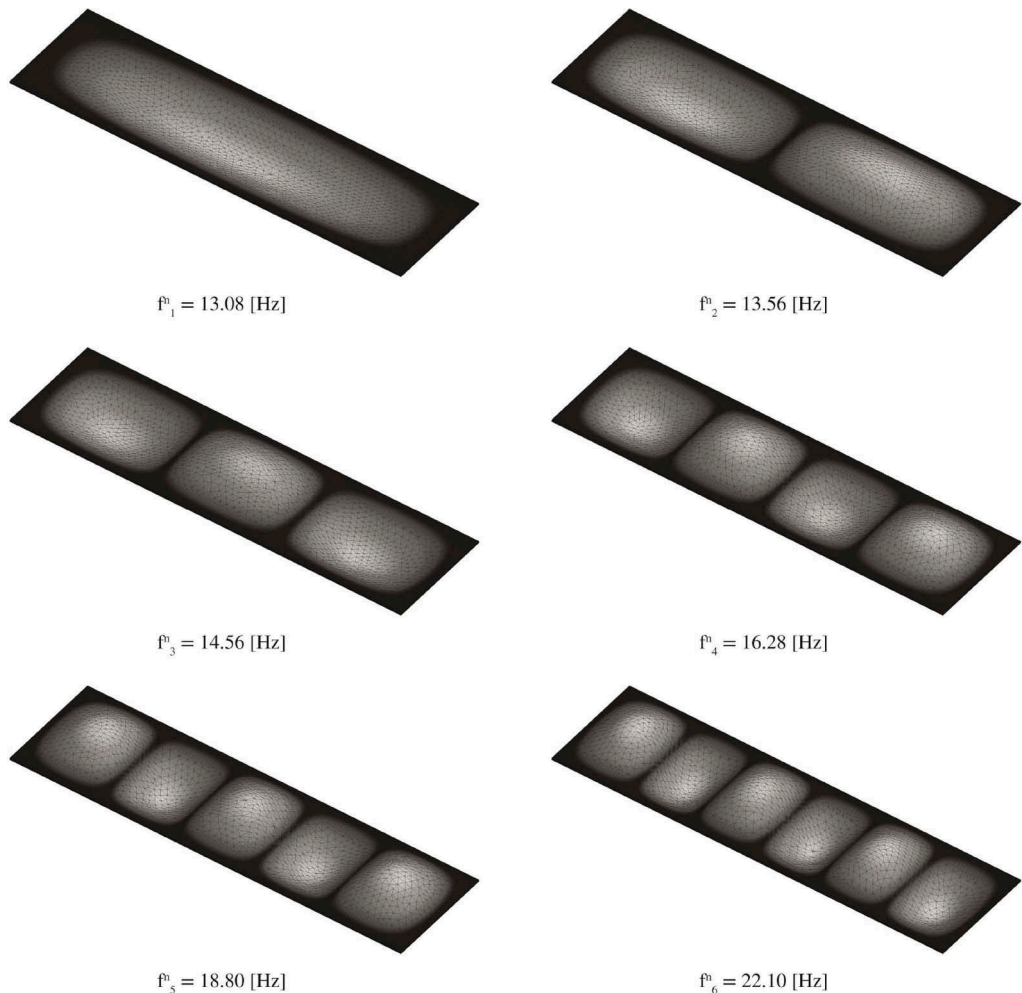


Figure 6. Mode shapes for the slack geomembrane specimen ($\epsilon = 0$) from the FE model in vacuum.

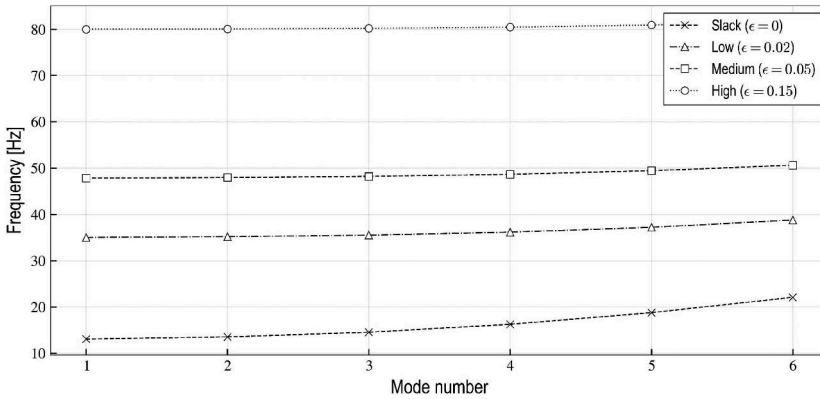


Figure 7. Natural frequencies of the first 6 modes for various prestrain levels in vacuum.

3.3 Modal characteristics in water

The effect of water is investigated with the added mass approach. The variation of the first natural frequency for various prestrain and hydrostatic pressure levels is shown in Figure 8. When in vacuum, the prestrain clearly impacts the first natural frequency of the geomembrane, in accordance with the previous case. When the effect of water is considered, the variation of the first natural frequency with prestrain is extensively decreased and the first natural frequency remains approximately constant. The increase in the hydrostatic pressure level has no major effect on the variation of the first natural frequency of the prestrain geomembrane.

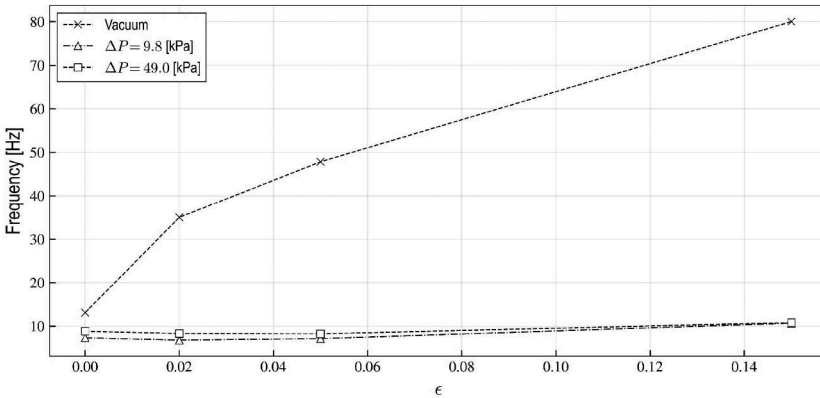


Figure 8. First natural frequency for various prestrain and hydrostatic pressure levels.

The evolution of the first six natural frequencies of the prestrained geomembrane with various prestrain levels for different hydrostatic pressure levels is shown in Figure 9. The natural frequencies remain at low levels in presence of water, even in case of high prestrain. In addition, the natural frequencies slightly increase with the increase in hydrostatic pressure, as water is considered incompressible, in which case the added mass remain constant with the increase of hydrostatic pressure. This effect is however limited with the increase of pre-tension. Indeed, the natural frequencies of the highly prestrain geomembrane specimen remain approximately constant with the increase in hydrostatic pressure.

3.4 Influence of damping ratio

The influence of the damping ratio on the evolution of the natural frequencies of the highly prestrained geomembrane specimen in vacuum and in presence of water is assessed. The damping

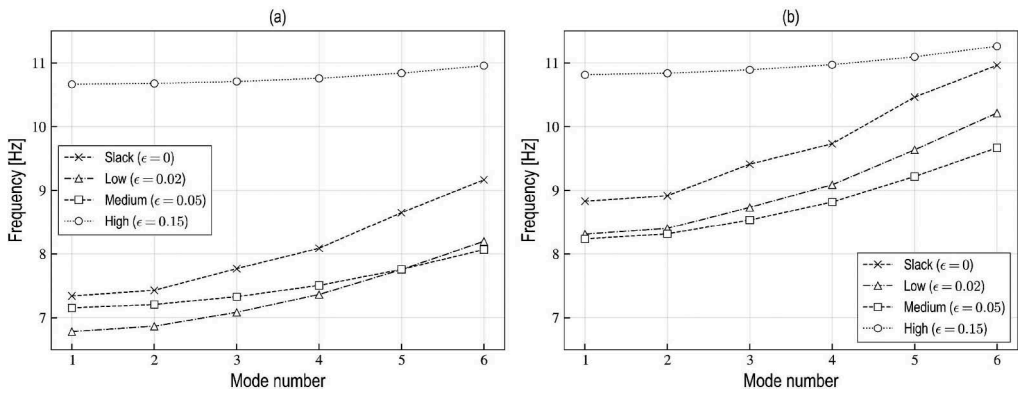


Figure 9. Natural frequencies of the first 6 modes for various prestrain levels of the geomembrane specimen immersed for various hydrostatic levels; $\Delta P = 9.8$ kPa (a), $\Delta P = 49.0$ kPa (b).

is implemented as Rayleigh damping. The variation of the natural frequencies of the first six modes is shown in Figure 10. It is shown that the damping ratio has no effect in the variation of the natural frequencies of the geomembrane specimen for all six modes in vacuum, and that the effect is very limited when in presence of water, as the natural frequency remains approximately constant. However, the damping ratio reduce the amplitude of the deformation.

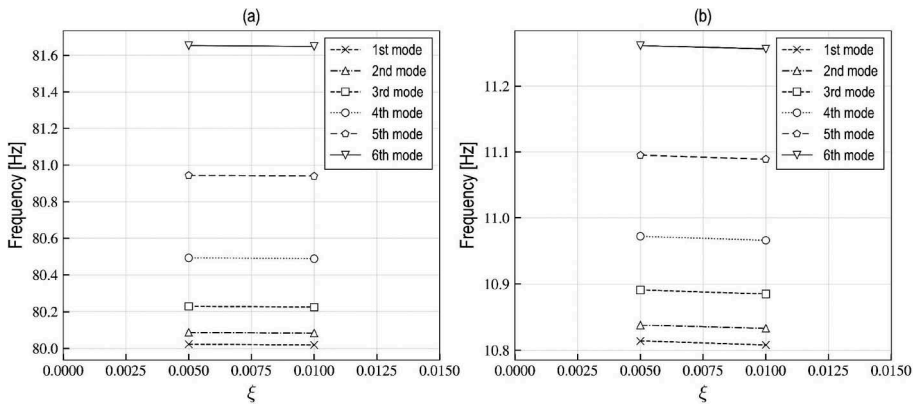


Figure 10. Effect of damping ratios on the natural frequencies of the first six modes with highly prestrained geomembrane specimen ($\epsilon = 0.15$); in vacuum (a) and with hydrostatic pressure $\Delta P = 49.0$ kPa (b).

4 CONCLUSION

In this paper, the modal characteristics of a geomembrane specimen are presented for potential enhanced application in pressure waterways. A Finite Element model is developed to investigate the modal characteristics of the hyperelastic geomembrane specimen. The nonlinear constitutive behavior of the geomembrane is modeled by the Mooney-Rivlin formulation. The effect of water is considered by the added mass approach for the modal characteristics of the geomembrane. The damping is included as Rayleigh damping. The independency of the solution is assessed with a mesh-sensitivity analysis.

It is found that the maximal out-of-plane deformation at static loading increase in the presence of water but decrease with the increase of prestrain level in the geomembrane. The modal characteristics of the geomembrane are strongly influenced by the material nonlinear constitutive behavior. The first natural frequencies of the hyperelastic geomembrane specimen are found at low frequencies in vacuum. The natural frequencies also strongly increase with the

increase of pre-tension in vacuum. In the presence of water, the variation of the natural frequency with pre-tension is highly reduced. The increase in hydrostatic pressure tends to moderately increase the natural frequencies of the specimen. Finally, the damping ratio has almost no influence on the natural frequencies. Although promising, the results presented in this paper still need to be confirmed with experimental data.

ACKNOWLEDGEMENTS

The authors wish to acknowledge CarpiTech for making experimental data and photographs available. This project is supported by the Platform of Hydraulic Constructions (PL-LCH, former Laboratory of Hydraulic Constructions) of EPFL, Switzerland, and by the Research Fund of the Swiss Committee on Dams.

REFERENCES

- Cazzuffi, D., & Giofrè, D. (2020). Lifetime assessment of exposed PVC-P geomembranes installed on Italian dams. *Geotextiles and Geomembranes*, 48(2), 130–136. <https://doi.org/10.1016/j.geotexmem.2019.11.015>
- Cazzuffi, D., Scuro, A. M., & Vaschetti, G. L. (2012). Chapter 15—Hydraulic tunnels. In S. K. Shukla (Ed.), *Handbook of geosynthetic engineering: Geosynthetics and their applications* (2nd ed). ICE.
- Chakravarty, U. K. (2013). Analytical and Finite Element Modal Analysis of a Hyperelastic Membrane for Micro Air Vehicle Wings. *Journal of Vibration and Acoustics*, 135(5). <https://doi.org/10.1115/1.4024213>
- Chakravarty, U. K., & Albertani, R. (2011a). Energy Absorption Behavior of a Hyperelastic Membrane for Micro Air Vehicle Wings: Experimental and Finite Element Approaches. *International Journal of Micro Air Vehicles*, 3(1), 13–23. <https://doi.org/10.1260/1756-8293.3.1.13>
- Chakravarty, U. K., & Albertani, R. (2011b). Modal Analysis of a Flexible Membrane Wing of Micro Air Vehicles. *Journal of Aircraft*, 48(6), 1960–1967. <https://doi.org/10.2514/1.C031393>
- Chakravarty, U. K., & Albertani, R. (2012). Experimental and Finite Element Modal Analysis of a Pliant Elastic Membrane for Micro Air Vehicles Applications. *Journal of Applied Mechanics*, 79(2). <https://doi.org/10.1115/1.4005569>
- Hsuan, Y. G., & Koerner, R. M. (2008). Aging of Geomembranes Used in Hydraulic Structures. *Proceedings of Geosynthetics Research and Development in Progress*, 1–7. [https://doi.org/10.1061/40782\(161\)40](https://doi.org/10.1061/40782(161)40)
- Kaneko, S., Nakamura, T., Inada, F., Kato, M., Ishihara, K., Nishihara, T., & Langthjem, M. A. (Eds.). (2014). Chapter 8—Vibrations in Fluid–Structure Interaction Systems. In *Flow-induced Vibrations (Second Edition)* (pp. 359–401). Academic Press. <https://doi.org/10.1016/B978-0-08-098347-9.00008-4>
- Koerner, G. R., & Koerner, R. M. (1996). Geosynthetic use in trenchless pipe remediation and rehabilitation. *Geotextiles and Geomembranes*, 14(3), 223–237. [https://doi.org/10.1016/0266-1144\(96\)00012-X](https://doi.org/10.1016/0266-1144(96)00012-X)
- Marence, M., Lilliu, G., & Lemke, S. (2020). Composite membrane lining in pressure tunnels and shafts: Design practice and new possibilities. *Proceedings of Hydro 2020*, 9.
- Nakamura, N. (2016). Extended Rayleigh Damping Model. *Frontiers in Built Environment*, 2. <https://www.frontiersin.org/articles/10.3389/fbuil.2016.00014>
- Nogueira, H. I. S., Pfister, M., & Schleiss, A. J. (2016). Approaches to Reduce Friction Losses in Headrace Waterways of Hydropower Plants. *Journal of Hydraulic Engineering*, 142(5), 02516001. [https://doi.org/10.1061/\(ASCE\)HY.1943-7900.0001123](https://doi.org/10.1061/(ASCE)HY.1943-7900.0001123)
- Quaranta, E., Aggidis, G., Boes, R. M., Comoglio, C., De Michele, C., Ritesh Patro, E., Georgievskaiia, E., Harby, A., Kougiyas, I., Muntean, S., Pérez-Díaz, J., Romero-Gomez, P., Rosa-Clot, M., Schleiss, A. J., Vagnoni, E., Wirth, M., & Pistocchi, A. (2021). Assessing the energy potential of modernizing the European hydropower fleet. *Energy Conversion and Management*, 246, 114655. <https://doi.org/10.1016/j.enconman.2021.114655>
- Scuro, A., & Vaschetti, G. (2017a). Geomembrane sealing systems for dams: ICOLD Bulletin 135. *Innovative Infrastructure Solutions*, 2(29). <https://doi.org/10.1007/s41062-017-0089-0>
- Scuro, A., & Vaschetti, G. (2017b). Geomembrane sealing systems for dams: ICOLD Bulletin 135. *Innovative Infrastructure Solutions*, 2(29). <https://doi.org/10.1007/s41062-017-0089-0>
- Scuro, A., & Vaschetti, G. (2021). Geomembranes to Line Surge Shafts. In H. Shehata & M. Badr (Eds.), *Advancements in Geotechnical Engineering* (pp. 106–120). Springer International Publishing. https://doi.org/10.1007/978-3-030-62908-3_8

- Scuero, Alberto, Vaschetti, Gabriella, & Bacchelli, Marco. (2017). *The Use of Geomembranes in Dams*. 506–514. <https://doi.org/10.3217/978-3-85125-564-5-067>
- Stanford, B., Ifju, P., Albertani, R., & Shyy, W. (2008). Fixed membrane wings for micro air vehicles: Experimental characterization, numerical modeling, and tailoring. *Progress in Aerospace Sciences*, 44(4), 258–294. <https://doi.org/10.1016/j.paerosci.2008.03.001>
- Zarfl, C., Lumsdon, A. E., Berlekamp, J., Tydecks, L., & Tockner, K. (2015). A global boom in hydro-power dam construction. *Aquatic Sciences*, 77(1), 161–170. <https://doi.org/10.1007/s00027-014-0377-0>.

The Rigoso project. Two old masonry dams to be recovered

L. Serra

Waterways, Rome, Italy

G. Gatto & F. Bisci

Studio Speri, Rome, Italy

M. Rebuschi

Frosio Next, Brescia, Italy

F. Fornari & L. Dal Canto

Enel Green Power, Rome, Italy

ABSTRACT: The Rigoso project includes two dams (Lake Verde and Lake Ballano), built in 1907-8 for hydroelectric purposes, in stone masonry and based on morainic debris. Over the years, interventions have been made to strengthen the dam sections, necessary for the water losses of the foundation. Currently the two works are in disuse due to drastic reservoir limitations imposed by the Italian agency for large dams. The need to fix them definitively and to partially recover their hydroelectric use prompted the Operator, Enel Green Power, to plan their substantial restructuring, which involves reducing the height, making the structures safe with interventions to consolidate facing and foundations, the creation of an adequate drainage system. As a result of the reduction in height, the project is configured as a partial decommissioning. The design had to face not insignificant challenges, given that the constraint of implanting a new project over a century old works, based on permeable loose soils, requires greater accuracy than those required in the design of new works. A further challenge is added to the technical requirements, in fact the two works are located in a Regional Park, and therefore any demolished material must be classified and recovered in the works.

1 INTRODUCTION

Dams are among the main tools that every organized society is equipped with to manage water resources, to drink, to irrigate and to produce energy. The oldest known were built 5,000 years ago, but storing water has certainly been practiced since the beginning of agricultural societies, immediately after the last Ice Age.

The modest resources available to carry out the large movements of materials have limited these infrastructures to locations suffering of limited water availability. But, with the introduction of motorized equipment and with the evolution of cement production techniques, at the end of the 19th century, initiatives have raised for the construction of small hydroelectric plants

In Italy, between the late 1800s and early 1900s, flourished the construction of hydroelectric plants to make energy available for nascent modern industries.

Once these works began to take shape, a field of expertise was going to be formed in Italy with a process of trial and error. A well-recognized core of Design Standard was not already developed and some technical uncertainties were not correctly appointed.

The dams of Lake Verde and Lake Ballano, now 115 years old, are examples of these pioneering experiences. Made of masonry with mortar, these dams are sized to withstand only the thrust of the water. They are equipped with spillways and organs for bottom outlet and intakes, and belong to quite sophisticated hydroelectric production equipment, with conveyance tunnels and penstocks.

The problems with these, as with similar works of the period, were the limited technical knowledge related to the foundations such as bearing capacity and permeability, the accuracy of the hydrological analyses, the environmental sensitivity and the seismic loads.

For our team of designers the possibility of participating in the recovery of these plants, that have been in the territory for over a century, true industrial archaeology, is a motivation to do a good job.

2 THE RIGOSO PROJECT

The Rigoso plant is in Emilia Romagna, in the province of Parma, near the Apennine watershed between Emilia and Tuscany.

The hydroelectric project exploits the two reservoirs for water derivation and for a modest accumulation. Hydroelectric production takes place at the terminal head which feeds the Rigoso plant (Figure 1).

Both lakes are set on depressions and morphological steps formed within glacial cirques due to differential erosion, in which small bodies of water had naturally formed, the capacity of which is increased by the dams (Figure 2). These are based on permeable moraine deposits, which has always been a problem that over time attempts have been made to remedy with cuts.

The works are located in the context of the northern Apennine chain, the result of various collision phases involving the Apula and Europa plates, starting from the Cretaceous and still ongoing today.

The area is dominated by the Macigno Formation, belonging to the Tuscan Domain, and in part on heterogeneous and heterometric deposits, mainly sandstone, attributable to deposits of undifferentiated Quaternary till. From a lithological point of view, the Macigno Formation, dated to the Upper Oligocene – Lower Miocene, is made up of arenaceous and arenaceous turbidites – gray pelitic with medium to medium – fine grain size in the less thick layers and coarse to very coarse in the thick and very thick. The entire unit has a thickness ranging from hundreds of meters up to 2000 meters.

The two reservoirs are located in an area of environmental and landscape value. The projects were therefore set up for absolute respect for the natural environment and for landscape enhancements and for tourist use.

The environmental protection interventions concern rigorous specifications for the conduct of the construction, recovery of demolition materials in the work, modeling of the banks to ensure consistency with the natural shapes, revegetation of the area and of the construction site, new trails with furnished rest areas.

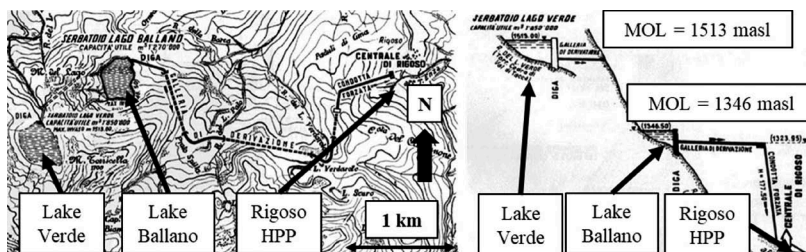


Figure 1. Plan and profile of Rigoso hydropower plant.

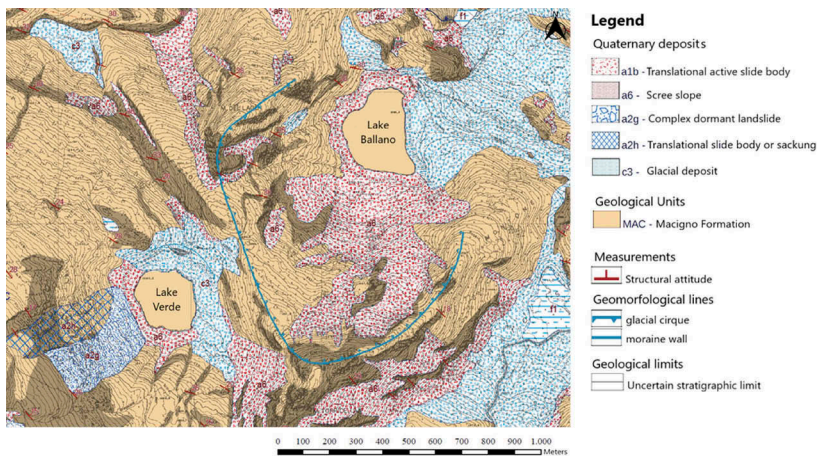


Figure 2. Geological plan of the Rigoso hydropower plant area.

3 LAKE BALLANO DAM

3.1 General

Lake Ballano today is reduced to only the original portion of the natural lake given that a limitation of the reservoir has been imposed for safety reasons and the dam is completely isolated from the current reservoir (Figure 3).

New design reduces the height of the dam, strengthen it especially in the foundation to ensure its safety, equipping it with completely refurbished grout curtain and drainage systems and advanced monitoring system for remote control. This ensures a partial recovery of the reservoir and the restoration of the functionality of the plant.

The original dam was 20 m high and the reservoir volume 1.27 Mm³. After the completion of the works the height of the dam will be 9.70 m and the reservoir 0.60 Mm³.



Figure 3. Actual state of Lake Ballano.

3.2 Present

The foundation of the dam appears to be composed of a superficial detrital deposit of gravitational origin and glacial moraine, under which there is an arenaceous base formation. The dam rests partially on surface deposit and partially on base formation.

The original dam body is in stone masonry with hydraulic lime mortar, entirely founded on the morainic deposit.

Subsequently, a stone masonry body with cement mortar was placed upstream of the original barrier (1928-1929) (Figure 4). The two bodies appear to be integrated by means of grips. The dam is not equipped with contraction joints.

The drainage system of the dam body consists of vertical holes with a length of 4.00 m which lead into a limited drainage gallery.

The hydraulic seal of the dam is provided for by coating the upstream face with cement plaster, quite damaged (Figure 5).

The hydraulic seal of the foundation is entrusted to additional concrete structures, built in a subsequent phase (1950). This element basically forms the new upstream footing of the dam and extends down to the basic sandstone rock formation. During the construction of this structure, waterproofing injections were also carried out on the base rock. There is a further injection screen in the foundation rock, built in an even later phase (1980). There is no drainage system in the foundation.

The barrier is completed by the secondary embankment on the right made of stone masonry with hydraulic lime mortar.

Spillways are foreseen on the right shoulder. Bottom outlet and intake are inserted in a tunnel that crosses the dam body up to near the upstream face and are isolated by locally operable butterfly valves.

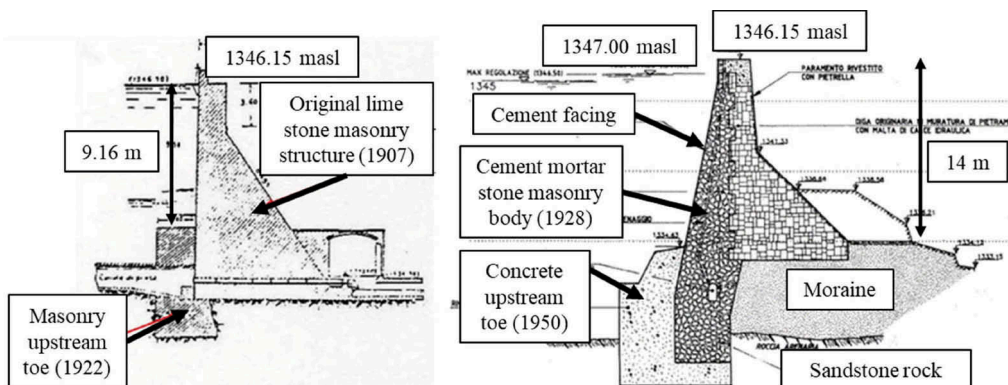


Figure 4. Original section (on the left side) and present section (on the right side) of Lake Ballano dam.



Figure 5. Actual state of Lake Ballano's upstream facing.

3.3 Future

The main intervention envisaged for the dam body is its partial demolition, in order to reduce the height of the dam to match with safety parameters under seismic events (Figure 6).

A concrete slab will be built on the lowered crest of the dam to prevent the percolation of rainwater inside the wall mass.

The resulting material from the demolition of the dam will be used to produce the concrete necessary for the construction of the new upstream face. This facing will ensure the hydraulic seal of the dam body, which historically has always been problematic. The new concrete upstream face will be created following the demolition of the current deteriorated shotcrete seal of the upstream face.

The construction of contraction joints with a distance between centers of approximately 6.0 m is envisaged. The hydraulic seal of the joints will be guaranteed by a waterstop.

The new upstream facing will abut on the new concrete upstream footing. This will be built at the foot of the upstream new dam body, to attain the foundation rock. For the new upstream foot, similarly to the new facing, contraction joints at a distance of 6 m with waterstop is envisaged. Underneath a grout curtain will be injected.

A drainage screen is foreseen, both in the dam body and in the foundation. The drainage system is provided by means of draining pipes with a distance of 2 m and a diameter of 120 mm in the dam body and 200 mm in the foundation. The drainage pipes in the foundation are pushed to a depth such as to involve every possible sliding surface, reasonably contained in the medium fractured rock layer, for at least 6.0 m.

An inspectable tunnel is envisaged in the new upstream toe of the dam. The size of this tunnel also allows it to fulfill the possible future need to make new injections into the foundation.

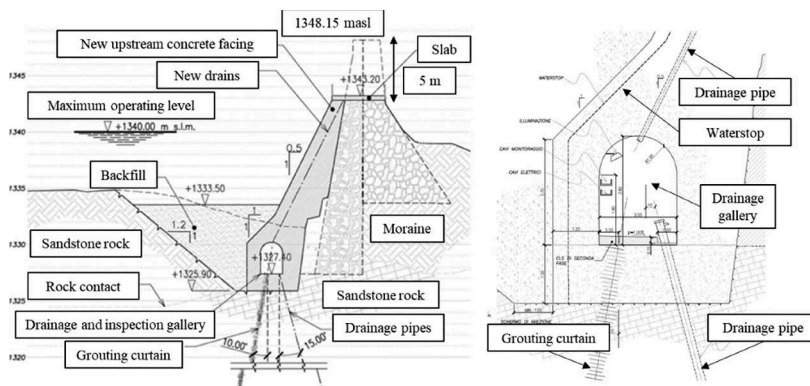


Figure 6. New section of Lake Ballano da (left side) and new upstream toe detail(right side).

4 LAKE VERDE DAM

4.1 General

The Lake Verde dam is at a higher altitude than that of Ballano (about 1,500 m above sea level). At the dam there are only the water intakes to divert the flow to the Ballano Lake (Figure 7).

The Lake Verde dam has been substantially out of service since 1964, due to the geological and structural problems of the dam.

The project purpose is the maximum recovery of the volume of water resources that can be accumulated in the reservoir, ensuring compatibility with the characteristics of the territory (geology, seismicity and environmental value) and respecting the latest technical safety regulations (structural and hydraulic).

The reservoir will be increased of 0.46 Mm^3 reaching a total of 0.72 Mm^3 . The lake surface level will be stable, thus determining the conditions for an environment favorable to the creation of a humid ecosystem and favoring the wildlife of the park and a controlled tourist use.

The works are scheduled only in the summer seasons outside of the spring breeding periods. Access tracks are designed to have characteristics strictly compatible with the environment, and the construction site spaces have been delimited and regulated, providing for the final recovery by removing all work residues and revegetating the construction site areas. In addition, paths around the lake have been designed, with equipped rest areas, and the dam itself is shaped in steps to create equipped panoramic terraces from which the paths of the park depart.

The work is protected but there are no guard posts, which are performed by the Ballano station which is just a few minutes away, also with the help of automatic control and video surveillance systems.



Figure 7. Actual state of Lake Verde.

4.2 Present

The Lake Verde dam is located on the upper side of a lying fold, with north-eastern vergence (Apennines), which mostly involved the turbiditic formation of Macigno (Oligocene-Miocene) (Figure 2). The geological survey carried out leads to the conclusion that the litho-stratigraphic sequence, including both the impoundment area of the existing dam and the basin behind it, is made up of detrital soils of glacial and gravitational origin to which locally, sediments of lacustrine origin overlap.

The substratum is entirely represented by an arenaceous formation in flysch facies which emerges in the upper portion of the slopes and plunges below the dam, which instead is entirely founded on morainic soils.

The section of the dam has undergone numerous transformations. From the original section (Figure 8), further upstream bodies and a cut-off have been added.

However, the section is not tested for the seismic loads, and suffers water loss in the foundation, not serious but with substantial risk of internal erosion and subsidence of the foundation, and with the presence of under pressure which make the work not verified.

The condition of the materials making up the dam, the various types of masonry with mortar and concrete for the surface coating of the upstream face, is mediocre and needs to be totally revised (Figure 9).

The spillway, on the left abutment, must be demolished, given that the level of the reservoir (original, today the reservoir does not reach the dam) must be lowered.

The bottom outlet is served by an overhead structure incompatible with seismic loads, so the bottom outlet must be redone.

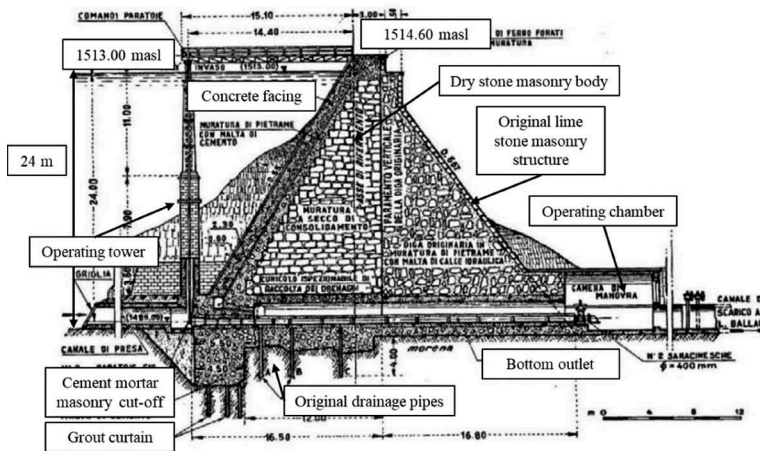


Figure 8. Existing section of Lake Verde dam.



Figure 9. Upstream (left side) and downstream (right side) face of Lake Verde dam.

4.3 Future

The dam is demolished at different levels, which include the terraces (1,505 m. level), accesses between the upstream and downstream of the dam and to the bottom outlet access tower (which are basically the new dam crest) and the spillway (at 1,498 m. level) (Figure 10). The terraces are equipped for touristic fruition. The bottom of the excavations above the terraces is shaped and revegetated with the same essences as the surrounding slopes.

The upstream facing will be demolished and totally rebuilt.

A cofferdam will be erected, utilizing materials coming from the demolitions with an impervious blanket upstream, allowing the excavation of the foundation of the bottom outlet tower and the grouting operations, also allowing the passage of vehicles to the left shoulder of the dam.

The materials coming from the demolitions are totally reused on site as aggregates of part of the concretes (the massive structures and the retaining walls) and for fillings, reshaping and stone works.

The foundation basement of the tower also forms a waterproofing cut in the most depressed point upstream of the dam. From this foundation the realization of waterproofing and consolidation injections is foreseen.

Drainage pipes for under pressure relief are provided along the transversal axis of the dam. These pipes discharge into the tunnel in which the pipeline of the bottom outlet runs, filled with drainage material.

The new bottom outlet completely replaces the previous one, which is demolished.

New control devices are positioned upstream, with access from a new well-sized and solidly founded turret, and from regulating bodies located downstream of the dam.

The downstream water conveyance is ensured by a pipeline positioned in the old access tunnel, which is widened for the positioning of the pipeline and then filled with draining material.

The original spillway will be demolished and replaced by a large threshold with a discharge channel downstream and a terminal stilling basin.

The path around the lake the lake creates a loop on the shore, with equipped areas in flat and panoramic points. It constitutes an ideal nature trail, at high altitude, in the green, by the water's edge. The dam, as it is structured, becomes part of this eco-compatible fruition circuit. The terraces, equipped in safety, are accessible via a system of freely accessible stone ladders (the reserved areas are fenced and video controlled). This nature circuit is accessible via a steep track in the woods, which starts from Ballano, passable on foot or by four-wheel drive control and maintenance vehicles with limited access.

The Ballano station will allow the park authority to monitor and provide assistance in the event of abuse or accidents. From this trail system branch off other paths that lead to the mountain ridge, and to lakes and refuges in the surrounding area of the park.

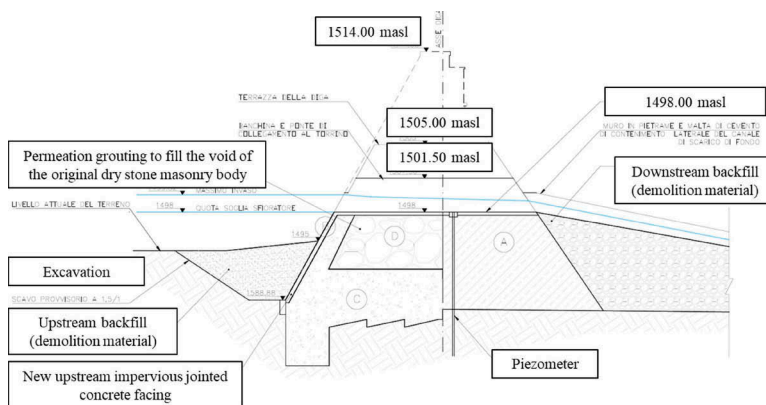


Figure 10. New designed section of Lake Verde dam.



Figure 11. Rendering of Lake Verde dam project.

Numerical modelling of the Pian Telessio dam affected by AAR

R. Stucchi & E. Catalano

Lombardi Engineering Ltd., Giubiasco, Ticino, Switzerland

ABSTRACT: The Pian Telessio dam, an 80 m high arch-gravity dam located in Northern Italy, is suffering from the effects of an alkali-aggregate reaction (AAR) since the second half of the 70s. The concrete expansion due to the AAR causes an upstream drift that reached approximately 60 mm in 2008. In 2008 rehabilitation works by means of vertical slot cuttings in the upper half of the dam were performed to reduce the effects of the concrete expansion. The rehabilitation works allowed a minor recovery of the upstream drift in the order of 5-10 mm, lower than expected.

The structural safety of the dam has been re-evaluated by means of a 3D numerical model, including the effect of the AAR expansion. The implemented AAR model, specifically developed for this analysis, accounts for several aspects affecting the swelling reaction: reaction kinetics, state of stress and temperature. The results of the calibration were remarkably satisfactory showing an agreement with several field measurements: displacements, joints opening, crack pattern and state of stress.

1 INTRODUCTION

The Pian Telessio dam is an arch gravity dam completed in 1955 in the Orco Valley (Piedmont, northern Italy). With a height of 80 m and a crest length of 515 m the dam impounds a reservoir with a capacity of 24 mio. m³ at a normal operating level of 1917 m asl. The dam thickness ranges from 5.7 m at the crest to a maximum of 35 m at its base.

Figure 1 Shows the typical dam section. As it is often designed according to Italian practice, the dam body is separated from the foundation slab (*pulvino*) by means of a peripheral joint, which prevents the occurrence of tensile stresses at the dam-rock interface. One drainage gallery runs along the peripheral joint, while two horizontal inspection galleries are located within the dam body at higher elevations (1863 and 1883 m asl).

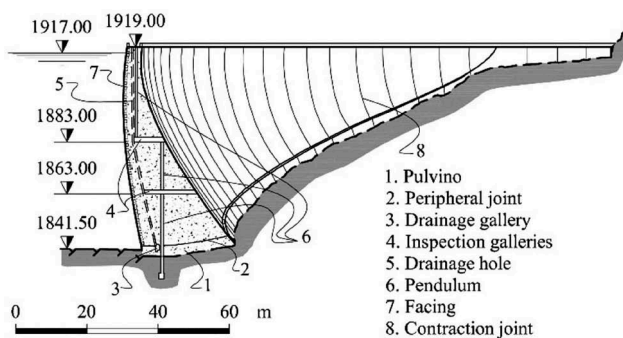


Figure 1. Typical dam section.

Besides other measuring instruments, four sections of the dam are equipped with pendulums for the measurement of the displacement of the dam body. After approximately 20 years of regular and reversible behavior, since the second half of the 70s the dam started showing an

upstream drift in radial direction, reaching 80 mm at the central pendulum in 2020. In addition to this, horizontal cracks appeared in the upper inspection gallery, which are not visible on either the upstream or downstream face.

After excluding other causes, such for example movements of the valley flanks, it was assessed that the permanent displacements are caused by the concrete expansion due to an ongoing alkali-aggregate reaction (AAR).

The studies performed in the 2000s, indicated that under certain unusual operating conditions, i.e. low reservoir levels with high summer temperatures, the safety margins required for this type of structures are not guaranteed. Although the most critical condition occurs when there is no risk of an uncontrolled release of water, the high vertical compressive stress at the dam heel, indicated by the structural analyses, represented a potential risk to the integrity of the dam and was therefore considered unacceptable.

It is worth recalling that the AAR model adopted in the analyses carried out as part of the rehabilitation works only considered the effect of the compressive stress on the expansion rate, according to Charlwood et al. (1992). In particular, it was assumed that the expansion rate decreases as the compressive stress increases, according to an experimental law proposed by Hobbs (1990). This model will be named as “Charlwood” in the following.

The short-term countermeasure introduced in 2003 was the limitation of the minimum reservoir level in the summer months. This operational limitation was not acceptable in the long term. Therefore, rehabilitation works were proposed, designed and finally carried out in the 2008. The works consisted of the execution of 16 vertical slots using diamond wire (Amberg et al. 2009) with a height between 21 and 39 m.

On a conceptual level, the scope of the intervention was to temporarily transform the dam into a structure consisting of independent blocks, similar as the original situation during the construction of the dam. In this configuration, the vertical compressive stress at the base of the dam is only due to the dead load and is therefore compatible with the stress levels prescribed by the standards. After the slots were executed, the arch effect required to support the hydrostatic pressure due to the full reservoir was restored by grouting of the slots.

Structural analyses conducted as part of the rehabilitation works with the “Charlwood” model had indicated that the effect of the slots would be a recovery of the upstream drift of approximately one third of the total upstream drift at the time of the intervention (approximately 60 mm).

The upstream drift recovery recorded by the monitoring system during the works was only 5-10 mm. This raised the doubt that the intervention was less effective than assumed. An updated structural analysis was required to assess the stress state within the structure and its structural safety.

Preliminary analyses (Amberg et al. 2013) performed adopting the same structural model used in the analyses carried out as part of the rehabilitation works (*Trial Load Method*), but with a different distribution of the AAR-induced concrete expansion, satisfactorily reproduced the behavior of the dam before, during and after the rehabilitation works. The obtained stress distribution was compatible with the standard requirements, confirming that the execution of the slots is a guarantee that the stress distribution within the part of the dam affected by the cuts depends only on the dead load, regardless of the amount of the drift recovery. The dam has therefore been in normal operating conditions since the rehabilitation works was carried out.

More detailed analyses were performed by adopting a 3D numerical model and a complex but practical AAR model, specifically developed for these analyses. The details of the analyses will be presented later in the paper.

2 AAR MODEL

2.1 *Model description*

The chemical reactions that cause concrete expansion are complex and not yet fully understood. However, the main factors affecting the magnitude and spatial distribution of expansion due to the alkali-aggregate reaction can be identified in sufficient detail to be used in engineering (Amberg et al. 2019).

The AAR model considered in the new 3D structural analyses considers the following aspects affecting the swelling reaction: reaction kinetics, state of stress and temperature. Humidity is not considered as a factor influencing the AAR for this specific case study, assuming that the water content in the concrete is sufficient for the development of the chemical reaction, not limiting its progress.

2.2 Reaction kinetics

The AAR expansion model adopted is based on the work of Capra & Bournazel (1998). This model assumes that AAR follows a first-order kinetic law, described by:

$$\frac{dA}{dt} = k \cdot (1 - A) \quad (1)$$

where A represents the percentage of alkali that have reacted and measures the advancement of the reaction varying between 0 and 1; k is the kinetic constant, i.e., the reaction velocity at time $t=0$ (hence $A=0$).

In addition, the model assumes that the chemical reaction and the concrete expansion are dissociated: the concrete expansion starts occurring only when the cracks, which are initially generated within the aggregates, also propagate in the cement paste. To dissociate the reaction and the expansion, a parameter A_0 is defined. When the reaction advance exceeds A_0 , the macroscopically observable expansive phenomenon begins.

This assumption leads to an abrupt change of expansion rate at the end of the latency period, which is not in agreement with real observations, characterized by an initial gradual increase in the expansion rate. To overcome this problem, the original model was slightly modified by introducing a circular connection between the two linear stretches of the relationship between expansion (ε_{AAR}) and reaction advance (A). Mathematically, this results in the equations shown in Figure 2. The parameter c is the only additional parameter introduced to consider the circular connection.

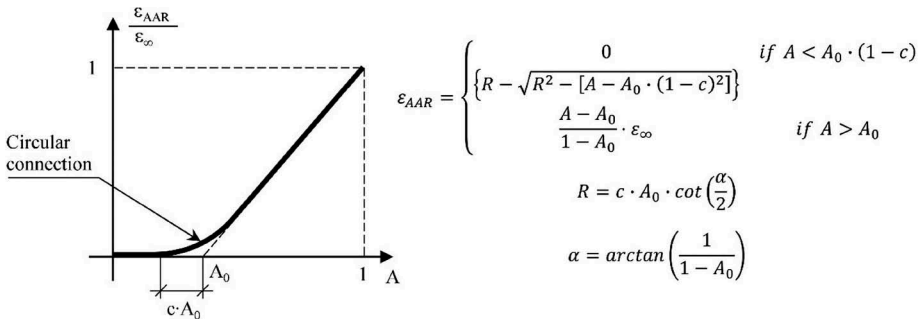


Figure 2. Relationship between normalized expansion ($\varepsilon_{AAR}/\varepsilon_{\infty}$) and reaction advancement (A).

2.3 Temperature

Temperature affects AAR, as for all chemical reaction, changing the reaction velocity. In the adopted model, the relationship between the temperature and the kinetic constant (k) of the chemical reaction follows the Arrhenius equation:

$$k = k_0 \cdot e^{\frac{E_a}{R} \left(\frac{1}{\theta_0} - \frac{1}{\theta} \right)} \quad (2)$$

where k_0 = reaction rate at the reference temperature θ_0 ; E_a = activation energy; R = gas constant (8.31 J/mol/K); θ = temperature (temperatures are in Kelvin degrees).

2.4 Stress state

The AAR-induced expansion obtained with the above defined equations must be intended as “free” expansion. It is known that the stress state has an influence on the evolution of expansion. In particular, a compressive state of stress limits the expansion.

The adopted AAR model simulates the effect of the stress state according to Saouma & Perotti (2006). This formulation assumes that the AAR-induced expansion ε_{AAR} is volumetric and to determine the amount of expansion in each of the three principal directions ($\varepsilon_{AAR,i}$) weights W_i varying between 0 and 1 are applied:

$$\varepsilon_{AAR,i} = \varepsilon_{AAR} \cdot W_i \quad (3)$$

The greater the compression in one direction, the lower is the weight assigned to that direction. When the compression reaches the value σ_u , the expansion in that direction is totally inhibited ($W_i=0$). In all possible combinations, the sum of the weights in the three principal directions is always equal to 1, which means that the expansion is redistributed in the three principal directions while keeping the volumetric expansion constant, as shown in experimental studies by Multon & Toulemonde (2006).

3 NUMERICAL MODEL

3.1 Model description

For the structural analyses of the Pian Telesio dam a three-dimensional calculation model was used. The finite-difference code FLAC3D (version 7.0, Itasca 2019) was adopted.

The model reproduces the geometry of the dam, as defined in the original project documentation, and the foundation rock covering an area of 500x600 m. The minimum distance between the model boundaries and the dam is 90 m in the horizontal direction and 140 m in the vertical direction. In Figure 3 a 3D view of the numerical model is presented.

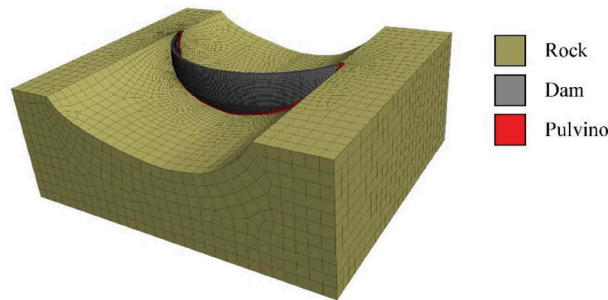


Figure 3. 3D view of the numerical model.

The peripheral joint and the contraction joints are modelled with interfaces with a nil tensile strength, allowing the opening of the joints in areas where there would otherwise be tensile stress in the direction perpendicular to the joints.

Concrete and rock elastic modulus are defined in such a way that the displacement obtained with the model correspond with those recorded by the pendulum installed in the dam, considering a period before the effects of the AAR became evident. An elastic modulus of 28 GPa for both the concrete and the rock is assumed.

The following phases are considered in the numerical analysis: i) dam construction and filling of the reservoir in the year 1953; ii) dam behavior in the period 1953-2008; iii) rehabilitation works in the year 2008; iv) dam behavior in the period 2008-2050.

The considered hydrostatic load, which has been kept constant throughout the duration of the analysis (97 years), corresponds to a characteristic water level, lower than the full supply level that

induces an average stress state in the dam during the annual cycle. This assumption is necessary to correctly simulate the evolution of the AAR expansion, which depends on the stress state.

The analysis would require the thermal state within the dam for the whole period of analysis. Since only the temperatures recorded by the 6 thermometers located near both faces are available from 2001 onwards, a characteristic sinusoidal trend of the temperatures recorded by the thermometers was determined. The trend thus determined was assumed valid for the entire period analyzed with the numerical model. The temperature field inside the dam is then calculated using an algorithm based on the Laplace transform (Lombardi et al. 2008).

During the analysis the equilibrium of the dam is recalculated monthly to update the stress state of the dam, which affects the AAR induced expansion as per Equation 3. The assumed time step is considered appropriate for the slow development of the AAR.

3.2 Calibration and model parameters

Based on the results of long-term laboratory tests on concrete specimens performed in 2011 by the Ecole Polytechnique Fédérale de Lausanne (EPFL) and applying the correlations proposed by Bérubé et al (2002), it was possible to estimate the average expansion rate in the structure (17-25 $\mu\text{m}/\text{m}/\text{year}$) and the volumetric expansion at infinite time (7000-10,000 $\mu\text{m}/\text{m}$). These values are taken as reference for the definition of the input parameters of the adopted AAR model.

With the calibration process, the parameters of the AAR model are appropriately calibrated to minimize the deviation between the displacements detected by the monitoring system and those obtained from the three-dimensional numerical model, at different elevations and at different locations in the dam body, over the entire calibration period (1953-2017).

During the calibration process, a parametric analysis has been conducted on the value of the activation energy. In addition to the typical value of 45 kJ/mol (Grimal et al. 2010, Morenon et al. 2021), two higher values were considered: 90 kJ/mol and 135 kJ/mol. With all three activation energy values, and by properly adjusting the other model parameters, the measured displacements of the pendulums are accurately reproduced by the model (Figure 4). The figure shows also the displacements obtained with the “Charlwood” model used in the analyses for the rehabilitation works.

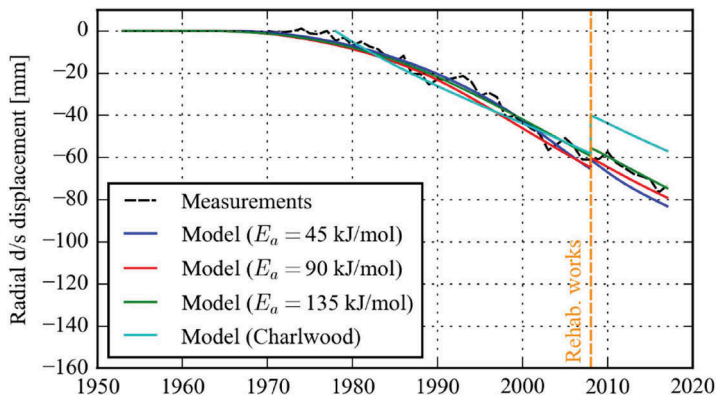


Figure 4. Comparison between the measured displacements (annual average) and those predicted by the AAR models (central part of the dam, 1919 m asl). Charlwood model refers to the model used in the analyses for the rehabilitation works.

It is interesting to note that different assumptions for the AAR model produce the same displacements of the dam up to 2008, but with different expansion distributions and different stress states (Figure 5). The AAR models accounting for the effect of the temperature had obtained greater expansions at the downstream face, lower compressions in the upper arches (0-1 MPa in 2008), smaller openings of the peripheral joint (60% of the dam thickness in 2008) and lower vertical compressions at the dam heel (7 MPa in 2008). Instead, the “Charlwood” model had obtained a practically uniform AAR induced expansion over the thickness but concentrated in

the upper arches, higher compressions in the upper arches (2-3 MPa in 2008), a greater opening of the peripheral joint (80% of the dam thickness) and thus a greater vertical compression at the dam heel, exceeding 10 MPa in 2008, which had suggested the implementation of the rehabilitation works by means of slot cutting. Differences are visible also for the drift recovery. The “Charlwood” model predicted that the intervention would reduce the drift by about 20 mm, which is 3-4 times more than the value predicted by the AAR models that account for the effect of the temperature reproducing the recorded value with good accuracy (Figure 4).

Only the behavior of the dam during the rehabilitation works, which made the upper part of the structure isostatic by means of the slot cuts, made it possible to establish which expansion distribution was closer to reality and which AAR model better reproduces the actual dam behavior and its internal stress state. To date, there is no doubt that the expansion distribution obtained accounting for the temperature effect best approximates the actual expansion distribution in the structure.

According to the results of the numerical model, for the AAR models accounting for the effect of the temperature the upstream drift is caused mainly by a differential expansion between the downstream and the upstream face (higher at the downstream face). On the other hand, according to the “Charlwood” model the drift is mainly caused by the uniform expansion of the upper arches. Since vertical slot cuttings would only eliminate the effects of arch expansion, it would have a limited effect on the drift in the former case and a more pronounced effect in the latter case, as shown by the results of the analyses.

It is also worth making some observations regarding the effect of the activation energy. Differences in the distribution of the AAR induced expansion along the thickness of the dam and, consequently, in the distribution of internal stresses are obtained changing the activation energy (Figure 5). Only for the model with an activation energy of 135 kJ/mol the presence of a tensile stress in the central part of the dam, with the faces compressed vertically, can be clearly observed. This result is compatible with the presence of a horizontal crack in the inspection gallery at elevation 1883 m asl, but not visible to the faces. The model with activation energy 45 kJ/mol results in an almost linear swelling distribution which does not allow the creation of a tensile zone in the central part of the dam.

In fact, the activation energy controls the relationship between the reaction rate and the temperature. With an activation energy of 45 kJ/mol the reaction rate doubles every 10°C, while with 135 kJ/mol it increases 8-fold for the same variation of temperature.

In conclusion, it was decided to adopt the highest value of the activation energy. Although this value deviates from the literature, it was found to be the one that best reproduces both global (displacement) and local (stress state) aspects of dam behavior. Furthermore, the non-linear distribution of the expansion along the thickness of the dam is confirmed by the multi-base extensometers installed in the dam in order to directly measure the AAR induced expansion. The full set of the AAR model parameters obtained with the calibration process are listed in the Table 1.

3.3 Model results

With the set of calibrated parameters, the model is able to accurately reproduce the behavior of the dam before the rehabilitation works in 2008, including an initial period of about 20-25 years with no permanent displacements, the limited drift recovery produced by the intervention, and the fact that the drift continues at the same rate after 2008, as shown in Figure 6.

With regard to the safety conditions of the structure, compressions in the arches do not represent for this case the greatest criticality since the dam has a high thickness. On the other hand, due to the shape of the dam section the vertical compression at the dam heel might exceed the admissible values under certain particular operating conditions (empty reservoir, summer temperatures) because of the opening of the peripheral joint which concentrates the vertical stress in a reduced contact area. For the condition of empty reservoir and in absence of AAR the vertical compression at the dam heel was 4.1 MPa and reached, according to the model, 7.1 MPa in 2008, with an increase of 1 MPa every 20 year. The peripheral joint is open, downstream, for 30% of its thickness in absence of AAR and 60% in 2008, according to the model. It is pointed out that the instrumentation for monitoring the openings of the peripheral joints and the stress variations at the dam heel confirmed the results of the model.

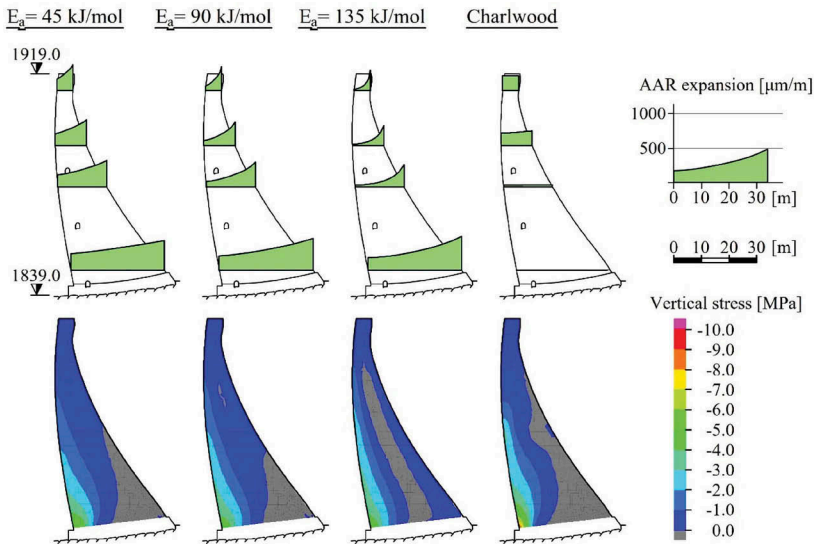


Figure 5. AAR expansion (upper part) and vertical stress (lower part, compressive stresses are negative) distribution in the central section of the dam in 2008 with empty reservoir for different AAR models.

Table 1. AAR model parameters.

Parameter	Value
Volumetric expansion at infinite time, ϵ_{∞} [$\mu\text{m}/\text{m}$]	10,000
Reaction rate at the reference temperature, k_0 [1/days]	3.9E-4
Reference temperature, θ_0 [$^{\circ}\text{C}$]	38
Activation energy, E_a [kJ/mol]	135
Reaction advance parameter, A_0 [-]	2.68E-2
Circular connection parameter, c [-]	0.6
Compressive stress that inhibits expansion, σ_u [MPa]	10

The AAR model could also be used for having some indications for the near future. The chemical reaction is expected to continue at an essentially constant rate in the future. It is worth noting that the expansions estimated by the model are well below the expansion at infinite time. In fact, the reaction progress (A) does not exceed about 0.05 in the model, indicating that the reaction is still at an early stage.

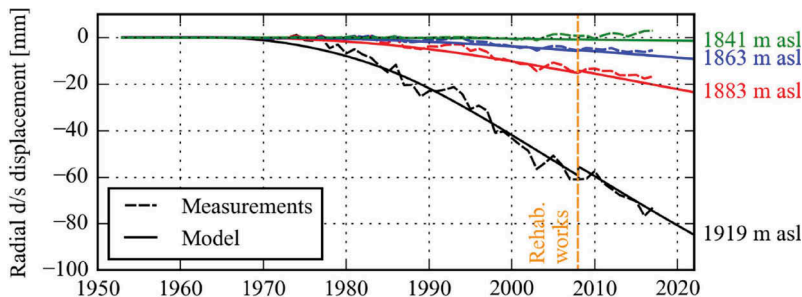


Figure 6. Measured displacements (annual average) at the central section of the dam.

4 CONCLUSIONS

Reproducing the behavior of an AAR-affected structure is very challenging due to the many factors influencing AAR induced expansion. For a dam, this is made even more complicated

by the fact that in a hyperstatic structure there is no direct relationship between displacement and stress state. In fact, the performed studies showed that the same displacement pattern can be obtained with different distributions of AAR expansion, and therefore different stress state in the structure. This highlights the limitations of assessing the structural safety of an hyperstatic structure such as an arch dam based only on its displacements.

The safety assessment of the dam is conducted with the aid of a three-dimensional numerical model and an AAR model, developed specifically for this analysis, which considers the following aspects affecting the swelling reaction: reaction kinetics, state of stress and temperature.

The results are very satisfactory. In addition to the good correspondence between measured and predicted displacements, the model satisfactorily reproduces several other monitored aspects of the dam behavior: stress state as deduced by the crack pattern, openings of the peripheral joint, stress variation at the dam heel, expansion distribution along the dam thickness. It is emphasized that in order to better reproduce both the displacements of the dam and its internal tension state, deduced from the distribution of cracks, an activation energy value of 135 kJ/mol was adopted, which is higher than that indicated in the literature. This could reproduce the effect of some factors not directly included in the swelling model.

The model also showed that an intervention with vertical slot cuts can lead to limited drift recovery if the drift is caused by a larger expansion at the downstream face.

According to the numerical model, the vertical compression at the dam heel for the empty reservoir condition, which was the aspect for which it was decided to intervene with the rehabilitation works, increases slightly (1 MPa in 20 years) remaining below the admissible level in the medium term. This highlights that a dam might exhibit permanent upstream displacement due to AAR expansion without a relevant change in the stress state.

The AAR is expected to continue at an essentially constant rate in the future for this case, requiring constant monitoring of dam behavior and periodic safety assessment.

REFERENCES

- Amberg, F., Bremen, R., Brizzo, N. 2009. Rehabilitation of the Pian Telesio dam (IT) affected by AAR-reaction. *23rd Congress on large dams*, Brasilia, Q. 90, ICOLD.
- Amberg, F., Stucchi, R., Brizzo, N. 2013. The effect of temperature on the development of the Alkali Aggregate Reaction at the Pian Telesio Dam. *9th ICOLD European Club Symposium*, Venice.
- Amberg, F., Stucchi, R., Charlwood, R., Salamon, J., Curtis, D. 2019. Management of Expansive Chemical Reactions in Concrete Dams & Hydroelectric Projects - Part 2: Physical effects and structural analysis of behaviour. *HYDRO 2019*, Porto.
- Bérubé, M-A., Frenette, J., Pedneault, A., Rivest, M., 2002. Laboratory Assessment of the Potential Rate of ASR Expansion of Field Concrete. *Cement, Concrete, and Aggregates, CCAGDP*, Vol. 24, No.1, 2002, pp. 13–19.
- Capra, B., Bournazel, J.P. 1998. Modeling of induced mechanical effects of alkali-aggregate reactions. *Cement and concrete Research*, 2251–260.
- Charlwood, R.G., Solymar, S.V., Curtis, D.D. 1992. A review on Alkali Aggregate Reactions in Hydroelectric Plants and Dams. *International Conference on concrete Alkali-Aggregate Reactions in Hydroelectric Plants and Dams*, Canadian Electrical Association, Fredericton.
- Grimal, E., Sellier, A., Multon, S., La Pape, Y., Bourdarot, E. 2010. Concrete Concrete modelling for exper-tise of structures affected by alkali aggregate reaction. *Cement and Concrete Research*, 502–507.
- Hobbs, D.W. 1990. Cracking and expansion due to the Alkali-Silica reaction. *Struct Eng Rev* 2:65–79.
- Itasca Consulting Group, Inc. 2019 FLAC3D — Fast Lagrangian Analysis of Continua in Three-Dimensions, Ver. 7.0. Minneapolis: Itasca.
- Lombardi, G., Amberg, F., Darbre, G.R. 2008. Algorithm for the prediction of functional delays in the behaviour of concrete dams. *International Journal on Hydropower and Dams*, Vol. 15, Issue 3, pp. 111–116.
- Moreno, P., Sellier, A., Multon, S., Grimal, E., Kolmayer, P. 2021. Benchmark Study Results: EdF/LMDC. In: Saouma V.E. (eds) *Diagnosis & Prognosis of AAR Affected Structures. RILEM State-of-the-Art Reports*, vol 31. Springer.
- Multon, S., Toutlemonde, F. 2006. Effect of applied stresses on alkali-silica reaction-induced expansions. *Cement and Concrete Research* 36 912–920.
- Saouma, V., Perotti, L. 2006. Constitutive Model for Alkali-Aggregate Reactions. *ACI Materials Journal* 103(3) 194–202.

Flood protection levees – from an existing portfolio of old structures to safe and reliable protection systems

Rémy Tourment
INRAE, France

Adrian Rushworth
Environment Agency, UK

Jonathan Simm
HR Wallingford, UK

Robert Slomp
Rijkswaterstaat, The Netherlands

Malcolm Barker
GHD, Australia

David Bouma
Tonkin + Taylor Ltd., New Zealand

Noah Vroman
US Army Corps of Engineers Levee Safety Center – USA

ABSTRACT: In many countries, levees and flood defences raise (or have raised until recently) different issues associated to their ageing and often too to a lack of proper management during long periods of time. This leads to uncertain safety and performance, and sometimes catastrophic consequences. In this paper, based on an international confrontation of experience and lessons learned, we present the most important of these issues and a framework to better organize the management of these structures: identification of existing portfolios of structures, organizing them into consistent systems, the need for a high-level policy, for a proper local management and for technical guidance.

RÉSUMÉ: Dans de nombreux pays, les digues et autres ouvrages de protection contre les inondations soulèvent (ou ont soulevé jusqu'à récemment) différents problèmes liés à leur vieillissement et souvent aussi à un manque de gestion appropriée pendant de longues périodes. Cela conduit à une sécurité et des performances incertaines, et parfois des conséquences catastrophiques. Dans cet article, basé sur une confrontation internationale de retours d'expérience, nous présentons les plus importants de ces problèmes et un cadre pour mieux organiser la gestion de ces ouvrages: le recensement des structures existantes, les organiser en systèmes cohérents, la nécessité d'une politique de haut niveau, d'une bonne gestion locale et d'un corpus technique de référence.

1 INTRODUCTION

There are many issues associated with levees and other types flood defences, as they can sometimes be overlooked, even forgotten, particularly in places that have not suffered from a major flood event in a long period of time. This can lead to ageing, deteriorated portfolios

of structures that will have a poor performance when the next major flood event happens, eventually causing paradoxically more damage than the same natural flood without defences.

Levees and flood defences have an important role in mitigating flood risk. Floods can have important or even catastrophic consequences on human life, the economy, the environment and cultural heritage, while an efficient flood protection system will be able to avoid all damage up to a certain intensity of event and lower the consequence above this level. The performance of flood protection systems is gaining importance in our modern world, as there is more at stake in the protected areas, where development is constantly increasing, while the natural hazards are also increasing due to climate change.

Many countries have important portfolios of levees and flood defences. Often, these structures are old or even very old, they were built sequentially, raised, repaired. . . , sometimes built locally by riparian owners without the global view of a hydraulically consistent system. This has led to a number of issues including:

- heterogeneity in the structures
- a lack of information;
- reduction or loss of awareness of the existence of the levees over time;
- uncertain performance both in terms of protection level and in terms of mechanical resistance due to a lack of continuous and proper management and maintenance.

In the recent decades, in different countries, the importance of safe and performant levee systems has been recognised after a catastrophic flood event.

Based on the authors' experience in their respective countries and the information exchanged with members of the ICOLD Technical Committee on Levees (ICOLD TC LE) and the EUCOLD Working Group on Levees and Flood Defences (EUCOLD LFD WG), in this paper presents common denominators, examples and specific approaches on how to restore an existing portfolio of flood defences and to ensure its lasting efficiency. More detailed information about ICOLD TC LE member countries information on their own issues and approach can be found in (EUCOLD Working Group on Levees and Flood Defenses, 2018) and (CIGB ICOLD, 2023).

2 REDISCOVERING LEVEES

In many countries, a major flood or storm event leading to catastrophic consequences was needed for the community to rediscover levees at a local or national scale, see Table 1.

During the Rhone River floods of the winter 1993-1994, which were the first important ones since 1856, breaches in the levees caused the flooding of the Camargue delta island, almost entirely included in the territory of the City of Arles. When they were informed, the technical services of the City of Arles were deeply surprised as they were not aware of the existence of levees, although all of the Rhone River in Arles is surrounded by levees. This example illustrates the level of forgetfulness about the existence and usefulness of levees, even locally, when floods do not occur for a long time. At a larger scale, in countries where flood prone areas are not the most heavily populated areas national governments have often considered floods a local issue.

It is often difficult to obtain adequate funding over time, particularly for the management and maintenance of levees. Financing in most countries has been intermittent and often follows large flood events. There are generally two options that are used for taking action after a catastrophic flood event:

- A first option is to repair the levees, even sometimes by rebuilding them stronger and higher than before and let things go back to the way they were before, without initiating a long-term policy for efficient flood risk management. This option usually results in a slow deterioration of the structures and the potential for a failure and flooding during a subsequent flood event.
- The second option, that some countries have chosen following a major or catastrophic event is to initiate a long-term policy for an efficient flood risk management and the safety and performance of flood protection structures and systems. Examples of this option are

Table 1. Some recent catastrophic floods involving levees, from (Tourment, 2018).

Country	Event	Consequences
Belgium, England, Netherlands	1953 Storm Surge	> 2500 casualties
Germany	1962 North Sea storm	340 casualties
Switzerland	1987 summer floods	8 casualties 1.2 billion CHF damages
Czech Republic, Germany, Poland	1997 Oder and Morava floods	114 fatalities 3.8 billion euro damage
France	1999 Aude river	25 casualties
Central Europe	2002 Danube, Elbe, Vltava floods	21 casualties > 12 billion euro damages
France	Three floods in 2002 and 2003 downstream Rhone river	14 casualties 2 billion euro damages
USA	2005 Hurricane Katrina	1836 casualties 125 billion dollar damages
UK	Summer 2007 floods	13 fatalities 3 billion £ damages
Italy	2010 Veneto flood	3 casualties 0.5 billion euro damages
France	2010 Xynthia storm	59 casualties, 1-3 billion euro damages
Japan	2011 Tohoku Tsunami	10-20,000 casualties, nuclear accidents (incl. Fukushima), 360 billion dollar damages
Germany	2013 Elbe, Saale, Danube floods	7 casualties > 4 billion euro damage

the Netherlands after the 1953 storm, England after the 1998 Easter floods (Bye, P., Horner, M., 1998), the USA after the 2005 hurricane Katrina, or after a series of events, like France after the 1993-1994, 1999, 2002 and 2003 floods and the 2010 Xynthia storm. This option usually takes time, years, maybe decades, and different steps before the policy can be in place and its effects reached and sustained.

3 GENERIC ISSUES WITH LEVEES

Beyond specific issues with individual levees or levee systems, at a large scale of a regional, national, or federal portfolio, in the absence of high-level policy¹ measures to ensure long term safety and efficiency of flood protection structures and systems some generic issues can be identified, in terms of governance or in terms of technical guidelines.

3.1 Governance and funding

When there is no high-level policy measure for the management of levees, it is common that levees built in the past become “orphan levees”, with no management structure. This results in unawareness of the existence of the levees, their function, not to mention their safety and performance. When, in the absence of a general framework for levee management, there is an actual management for some levees, it is often fragmented and inconsistent at the system scale. This can lead to the performance and safety being reduced to the lower of all segments of the levee system. What makes this worse is that ownership of the land the levees are built on is necessarily fragmented in long levee systems. In absence of a distinct attribution of

1. In this paper we call “high-level” measures the ones that are taken at a federal, national, regional or large catchment scale. We cannot be more specific given the variety of situations in the different countries.

responsibility to a levee management structure, the responsibility of the levee management, therefore, falls into the land owners who usually don't have the skills nor the financial ability to properly and consistently maintain the levees.

Although legislation or regulations regarding flood risk management may be in place, however, this is often non-existent for the levees and flood protection structures. A surprising example is the EU Flood Directive which does not explicitly cover levees in its framework related to flood risk management, not even mentioning them.

Finally, funding the management of flood protection structures in the long term is very difficult. In most countries, funding has been intermittent and often follows large flood events and is devoted to repairing or building defence infrastructure. Furthermore, it is often difficult to obtain adequate funding over time for the management and maintenance of levees in spite of the fact that both of these aspects are crucial for the effective protection when a rare event happens. Levees, and more generally flood protection structures like flood control dams, have a public interest and their management and operation are more likely to be funded by public organisations. Funding for these organisations is usually generated by taxation of the public and there is a risk that if the public organisation's main objective is not flood risk management, funding for levees will not be guaranteed in the long term.

3.2 *Lack of technical guidelines*

Until recently, no commonly agreed levee specific guidelines/guidance existed which could be used in all countries in the world. This differs significantly from large dams, which benefit from a large body of technical guidance documents written at the international level thanks to the work of ICOLD, the World Bank and other international organisations and institutions. The first international initiative to draft a technical document covering levee issues has been the International Levee Handbook (ILH), started in 2008 and published in 2013 (Ciria, 2013) (Tourment et al., 2017).

Nonetheless some countries, like the Netherlands since the 1990's, have published their own specific technical guidelines in English, but these had no international status. National technical guidance devoted to levees is generally scarce since there is generally little or no interest in the levee issues, apart from the occurrence of catastrophic flood events. This is evidenced by the Netherlands where guidelines started ahead of other countries, after the 1953 storm surge. France had a wake-up call after the Rhone floods of 1993-94, which led to Cemagref initiating a series of technical and scientific publications on levees issues, for example (Mériaux, P. Royet, P., Folton, C., 2007) first published in French in 2001, followed by other institutions.

4 HIGH LEVEL POLICY MEASURES

Flood risk management relies on many different complementary and consistent measures, that can be structural or non-structural. Dams and levees are clear examples of structural measures while non-structural measures and instruments include for example activities related to emergency management and raising risk awareness, as well as financial and regulatory instruments. Flood protection structures, when pre-sent, are essential to flood risk management, but it is paramount to complement and be consistent with the other measures for the efficiency of a flood risk management policy. Hence, development of a policy regarding flood protection structures is necessary, but needs to be done consistently with the other flood risk management policies.

4.1 *Inventories*

At the Country, State, or catchment scale, considering national legislation, the first necessary step is to gather data on the existing portfolio: the existing structures, their location, the protected areas and assets situated in these areas; if not already existing, the identification and mapping of flood prone areas (with different flood levels/probabilities) has to be undertaken in association with this "census" of levees. This information on the structures has to be

sufficient in details and precision to enable a high-level assessment of their nature, safety and performance in terms of flood risk reduction, but also to assess residual risk, based on a quick, first level analysis.

A balance between risk and resources has to be found, both at the local and at the high-levels of management. It is necessary, therefore, to complete the inventory in order to form a base for all future high level policy measures, as the extent of the portfolio of structures and their performance in risk reduction is required to inform policy decision making.

4.2 *Legislation and regulation*

4.2.1 *Governance*

Governance of protection systems has then to be clearly organised, in terms of roles, responsibilities and also funding, in relation to already existing generic or specific regulations. As examples of generic regulations, there are those regarding the general ownership and management frameworks, while specific ones can deal with flood risk, water management, environmental issues, etc.

One of the main goals of the governance policy framework has to be the definition of the tasks and responsibilities of the organisation (or organisations) in charge of levees management, in order to solve the issue of “orphan levees”, and to clearly define what has to be done by this (or these) organisation(s). Ideally levee management has to be performed at the scale of a hydraulically consistent levee system, or when not possible it has at least to be organised so that a form of coordination is organised at this scale. There are two main options to assign the responsibility of levees as follows:

- using dedicated organisations like in The Netherlands, where “WaterBoards” (regional water authorities) were created to tackle both flood risk and water management,
- by adding tasks to existing organizations like in France with groups of municipalities.

In both these options, the related legal frameworks are extensive covering both the organisations and the tasks separately (Flood Defences act 1996, NL and GEMAPI, 2014, France).

The second and equally important goal of the governance policy is to set up a sustainable funding mechanism for the organisation(s) responsible for levee management so they can properly conduct their tasks. This funding mechanisms has to be reliable and guarantee the levee manager’s permanent ability to maintain the levee safety and performance. Usually, a more or less local funding source is the right scale, as it allows spending and benefits to be linked.

The governance policy can also deal with the issue of funding for large construction works like the construction of new defences, improvement of existing ones or important repairs after a major event. As this is an occasional task it can be based on a different mechanism as the one for regular management, and can involve national/regional solidarity.

4.2.2 *Risk*

Levees can be associated in a regulation framework to (flood) risk in two different ways: either as a risk factor (potential failure) or as a mitigating factor (protection performance). Some regulations are orientated to one or the other. For instance, in France the first regulation on hydraulic structures (dams and levees) from 2007 was centred on the failure of the levees and the associated risk, while the more recent 2015 regulation provides more emphasis on the protection provided by levee systems and flood retention structures (Tourment, R. et al., 2020). The reality is that flood protection structures change the flood risk, hopefully reducing it significantly, but they do not eliminate risk. Regulation should acknowledge both aspects to properly deal with these risk aspects.

The purpose of a flood protection policy framework should be in terms of risk to acknowledge the flood risk then to assess it and to manage it so it is acceptable (or tolerable) for society, which are actually the purposes of risk management in general. Using structures like levees or dams as flood management tools make it necessary to assess the natural flood risk (without protection structures), the risk associated to the structures (both in terms of reduction but also in case of failure) and consequently the residual risk, combination of both natural risk and risk associated to the structure.

A question is raised on the issue of tolerable or acceptable flood risk. Different countries use different approaches on the way to determine this tolerable risk, either at a national level or at a local community level. Consequently, determining the performance of the levees in terms of protection level, or failure probability or residual risk also can be done at a high level or left to a local level.

In any case, a risk approach is now the generally accepted way to deal with the issues related to floods and flood protection and, therefore, has to be as clearly as possible integrated in the policy frameworks.

4.2.3 *Management tasks*

The policy framework has to define what basic management operations have to be done in terms of management, and if different organisations are designated to share these management tasks what each one has to perform.

The management of levees has the objective to ensure that the levees will be able to perform as required during the flood event, ensuring the defined protection and not aggravating the flooding of the protected area by a breach (structural failure) or by another type of (functional) failure. The management organisations are among the first ones in the chain of decision when an important change has to be made in the system.

Section 5 describes in more detail the roles related to local management.

4.2.4 *Control*

The high-level framework needs to be implemented to be actually efficient. To be sure that it is correctly applied the national/ regional/federal level may want to organize a control organisation in charge of checking the way local levee managers properly fulfil their responsibilities. It is important that this control level should be separate from the operational level, as some flood examples have shown that if a single organisation is not reporting to any other one it may fail to assume its tasks and responsibilities.

5 LOCAL MANAGEMENT

In order to ensure that the levees will be able to perform as required during the flood event, levee management organisations have to have a proper and constantly updated knowledge of their portfolio, but also ensure proper routine inspection and maintenance in normal times (routine), during floods and after floods. They also need to decide and define changes in the levee system, all by themselves or in association with other organisations (funding agencies, government, local authorities, ...), as in the end they will have to manage the updated system.

5.1 *Choosing the protection systems and structures to incorporate in a management portfolio*

In the situation of a “new” levee management structure “inheriting” existing structures when a high-level policy is put into place and creates the responsibility of levees management, as described in section 4.2.1, one of the first decisions to make is to decide which of these existing structures will be integrated in the levee management structure’s portfolio. Maintaining and sometimes retrofitting or improving the different structures has a cost and has to be compared to the benefits in terms of damage reduction.

To inform this decision it is necessary to have a clear idea about the structures, their actual hydraulic role during a flood and their performance in terms of resistance to the different failure modes. Hydraulically consistent flood protection systems, associated with their related protected areas and stakes and protection level have to be assessed in this step. It may be decided to abandon certain systems and areas, but it is also necessary to ensure that abandoned structures will not cause harm in the event of a flood or structure failure. This may eventually lead to total or at least partial deconstruction of structures and levees.

5.2 *Regular (continuous) management*

In their permanent tasks, levee managers have to:

- clearly define their organisation, both internal and in relation with other organisations,
- conduct regular (routine) inspections,
- have regular safety assessments and risk analysis of the levees,
- as necessary, following a safety assessment, a risk analysis or a flood event, decide and conduct follow-up actions, like levee reinforcements or even system modifications,
- properly store and organise all knowledge about levees and all related information, both historical and new,
- prepare for emergency situations, in order to be able to conduct inspections before, during and after a flood and initiate emergency maintenance and operation,
- organise information of authorities in charge of early warning systems and evacuation plans, be able to rely on qualified help, in terms of specialised engineering and of construction.

Safety assessments and risk analyses are among the more powerful and useful tools to inform decision making. They allow managers to identify potential failure modes, the most probable failure locations and their consequences, as well as either structural or organisational remediation measures.

5.3 *Occasional improvements of existing structures and system*

Design, construction and management measures to restore or improve the safety and performance of flood protection systems have to be implemented at a system or structure scale. When determining what should be done, based on either a safety assessment and/or a risk analysis, it is important to decide who will carry out the work and whether it should be carried out at national, regional or local level. This may vary in a country over time according to the level of urgency and major repairs after a flood event are often taken up by national organisations e.g. NL 1953 (storm surge) and USA 2005 (Hurricane Katrina).

6 TECHNICAL GUIDANCE

At the technical level, there is a strong need for guidance, first because as stated earlier levee guidance has only begun to be developed recently, but also because science, techniques and practice are making continual progress. Guidance has become available in some countries at a national level, and to a lesser extent internationally. There is a strong need for national and international sharing of knowledge and good practices.

There is a danger that technical rules for engineering tasks, like design, assessment, risk analysis can be frameworks or detailed models to be followed faithfully, leaving less place to the engineer's mind or to innovations.

6.1 *Guidance providers*

Nationally and internationally, professional and scientific associations, learned societies are among the main providers of recognised guidance. For levees and other hydraulic structures, this includes ICOLD, ISSMGE, IAHR and their national chapters. Some research institutions are also providing guidance related information or useful basic science, either by themselves or by participation in collective research projects, like for instance the EU FP7 research project FloodProBE (<http://floodprobe.eu>).

The need for an international Community of Practice (CoP) on Flood Risk Management (FRM) and also one focused on levees has been recognised in the final workshop common to the FloodProBE and the ILH projects. The interest of a CoP involving all types of actors and the links between these types is shown in Figure 1. Development of valid and usable guidance needs to involve all these types of actors.

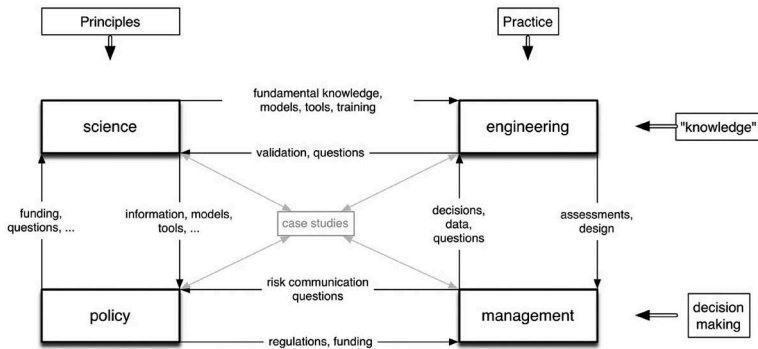


Figure 1. The FRM-CoP actors and interactions (© R. Tourment).

At the moment a permanent host organisation for a FRM-CoP has not been found, but ICOLD can now be seen as the international host for a levee CoP, as detailed in the next section.

6.2 ICOLD and national dam committees

Levees are now a clear part of the ICOLD activities. Since the creation of the working group on Levees and Flood Defences (<https://lfd-eurcold.inrae.fr>) of the European Club of ICOLD in 2015, the creation of the ICOLD Technical Committee on Levees in 2017, the fact that “Small Dams and Levees” were one of the four central topics in the Vienna ICOLD Congress in 2018 and the many activities related to levees in the Marseille ICOLD Congress in 2022 (see <https://lfd-eurcold.inrae.fr/index.php/2022/07/20/levees-in-icold-and-highlights-of-levees-in-the-marseille-icold-congress/>) there is no doubt levees are as much a natural part of ICOLD activities as dams. Over time, more and more National Committees have included levees in their scope. In the ICOLD newsletter issued for the 2022 Marseille congress, Michael Rogers, then President of ICOLD, has called for “*all ICOLD National Committees and Technical Committees to continue the embracement of levees into the technical approach and scope of their individual ICOLD organizations*”.

Design and construction of new levees or retrofitting of existing ones can be adapted from dam guidance, but needs specific development. In the near future, the bulletins produced by the ICOLD TC on Levees (TC LE) will support this development of levee guidance, as well as, hopefully, the bulletins developed by other Technical Committees taking into account the similarities and differences identified by TC LE in its deliverables.

6.3 Important issues needing guidance

Among the many technical issues needing more scientific and practical guidance, new or development of existing ones, the following issues have been identified, while not being an exhaustive listing:

- risk issues: understanding risks, levee systems risk analysis methods, consequence assessment (Tourment, R. et al., 2016),
- failure modes, failure scenarios (Simm, J. et al., 2012) (Van M.A. et al., 2022),
- spillways or spillway sections on levees, allowing safe overtopping for resilient levee systems (Degoutte G., Tourment, R., 2021).

Research is obviously also needed in many scientific domains, mainly geomechanics and hydrology/hydraulics, but that may not only be directly related to levees. A more comprehensive overview of data needs, research needs and guidance needs can be found in (EUCOLD Working Group on Levees and Flood Defenses, 2018).

7 CONCLUSION

Levee failures in recent decades leading to catastrophic inundations in many countries, in Europe and other parts of the world, have made the authorities and the citizens aware that existing structures, often old, sometimes forgotten as they are only occasionally loaded, have to be properly managed and maintained. On the other hand, many countries are still not aware of the possible hazard of orphan levees and still need to initiate a national policy for levee safety and performance, hopefully before a catastrophic event occurs. We hope that ICOLD involvement, international exchange of information and, humbly, this paper that is a call for action in all countries, will help promote better levees and levee management for a better world.

ACKNOWLEDGEMENTS

The authors want to acknowledge the work conducted in the EUCOLD LFD WG and in the ICOLD TC LE, and thank all their members, particularly Marcel Bottema from NETH-COLD who coordinated the work on (EUCOLD Working Group on Levees and Flood Defenses, 2018) and (CIGB ICOLD, 2023). We also thank the ICOLD officials, both in the ICOLD Board and the National Committees boards who supported the creation of the EUCOLD LFD WG and ICOLD TC LE.

REFERENCES

- Bye, P., Horner, M., 1998. *1998 Easter Floods – Final assessment by the independent review team. Volume 1 & Volume 2.* <https://www.gov.uk/government/publications/easter-1998-floods-review>
- CIGB Icold, 2023. *Levees and flood defences across the world, Characteristics, Risks and Governance.* Paris: CIGB ICOLD.
- Ciria, 2013. *The International Levee Handbook.* London: Ciria.
- Degoutte G., Tourment, R., 2021. Spillways on river levees. DOI: 10.35690/978-2-7592-3285-7
- EUCOLD Working Group on Levees and Flood Defenses, 2018. *European and US Levees and Flood Defences - Characteristics, Risks and Governance.* La Motte Servolex: CFBR
- Mériaux, P., Royet, P., Folton, C., 2007. *Surveillance, maintenance and diagnosis of flood protection dikes.* Versailles: QUAE.
- Simm, J. et al., 2012. *The significance of failure modes in the design and management of levees – a perspective from the International Levee Handbook team.* In the Proceedings of the 2nd European Conference on Flood Risk Management, FLOODrisk2012, Rotterdam, The Netherlands, 19-23 November 2012
- Tourment, R. et al., 2016. The risk analysis of levee systems: a comparison of international best practices. In *E3S Web Conf. Volume 7, 2016; 3rd European Conference on Flood Risk Management (FLOODrisk 2016)* DOI: <https://doi.org/10.1051/e3sconf/20160703009>
- Tourment R. et al, 2017. Levees and flood defences: an international community and recent advances. In *85th annual meeting of International Commission on Large Dams*, Jul 2017, Prague, Czech Republic. pp.11. (hal-02606396)
- Tourment, R. 2018. Small Dams and Levees – General Report for Question 103. In *Twenty-Sixth International Congress on Large Dams/Vingt-Sixième Congrès International des Grands Barrages, 4th - 6th July 2018, Vienna, Austria.* Paris: CIGB ICOLD.
- Tourment, R. et al., 2020. *The new French regulation on flood protection structures: consequences on risk management.* In Science and practice for an uncertain future - FLOODrisk 2020-4th European Conference on Flood Risk Management. Budapest: Budapest University of Technology and Economics.
- Van, M.A., Rosenbrand, E., Tourment, R., Smith, P. and Zwanenburg, C., 2022. *Failure paths for levees.* International Society of Soil mechanics and Geotechnical Engineering (ISSMGE) – Technical Committee TC201 ‘Geotechnical aspects of dikes and levees’, February 2022. Download <https://doi.org/10.53243/R0006>

Software tool for progressive dam breach outflow estimation

D.F. Vetsch, M.C. Halso, L. Seidelmann & R.M. Boes

Laboratory of Hydraulics, Hydrology and Glaciology, ETH Zurich, Zurich, Switzerland

ABSTRACT: Hazard assessment due to a dam failure is an important task in risk management. Assessment of the related hazard potential is based on a dam break analysis, a multi-step workflow in which the first step includes the analysis of possible dam failure and estimation of the outflow hydrograph. For that purpose, various approaches with different level of details with regard to modelled physical processes are available. Among the simplest approaches are parameter models, which are often used due to their straightforward and efficient application. The open-source software BASEbreach provides a suite of parameter models, developed particularly for the estimation of the outflow discharge resulting from progressive dam failure. We illustrate the software capabilities by comparing different approaches for instantaneous and progressive dam failure. Further, we show that the maximum breach discharge may be overestimated or underestimated depending on the approach and the situation. Estimation of the maximum breach discharge is always associated with great uncertainties. Hence, the BASEbreach software provides access to relevant parameters for local sensitivity analysis. Also, Monte-Carlo simulations in combination with the Peter parameter models are available for uncertainty quantification. The software is a valuable tool for engineers and practitioners to estimate the potential breach outflow from progressive embankment dam failure.

1 INTRODUCTION

Homogeneous embankment dams without sealing element are a common hydraulic infrastructure for flood protection, hydropower, and water supply, e.g. for milling or breweries. Some of these facilities are no longer used today, but still exist due to an ecological function or because deconstruction is too costly. Due to their function, these dams are often located near settlements. Such dams may fail, and they therefore pose a potential hazard, particularly during floods. Assessment of the related hazard potential is based on a workflow consisting of the (i) analysis of possible dam failure and estimation of the outflow hydrograph, (ii) calculation of the flood wave propagation, and (iii) quantification of the resulting flooding intensities and hazard. A common dam failure mechanism is a progressive breach development due to overtopping. The related breach outflow due to such a failure can be estimated by parameter models, which consider reservoir and dam characteristics, and assume a breach geometry varying in time in combination with an erosion model.

2 MATERIALS AND METHODS

2.1 *Software*

The BASEbreach software (<https://gitlab.ethz.ch/vaw/public/basebreach>) provides a suite of dam breach parameter models for the simulation of time-varying breach outflow due to progressive failure of an embankment dam. The model setup and evaluation of model results are

supported by an intuitive graphical user interface (Figure 1), which allows for direct comparison of the different approaches. For some models, relevant parameters can be specified and changed by the user. The model results include all major variables as time series such as breach discharge [m^3/s], flow velocity [m/s], hydraulic radius [m], unit transport rate [m^2/s], sediment discharge [m^3/s], and breach width [m]. All configuration data and model results can be saved for reuse or further evaluation, respectively. The software is open source and released under the GNU public license 3 (GPLv3).

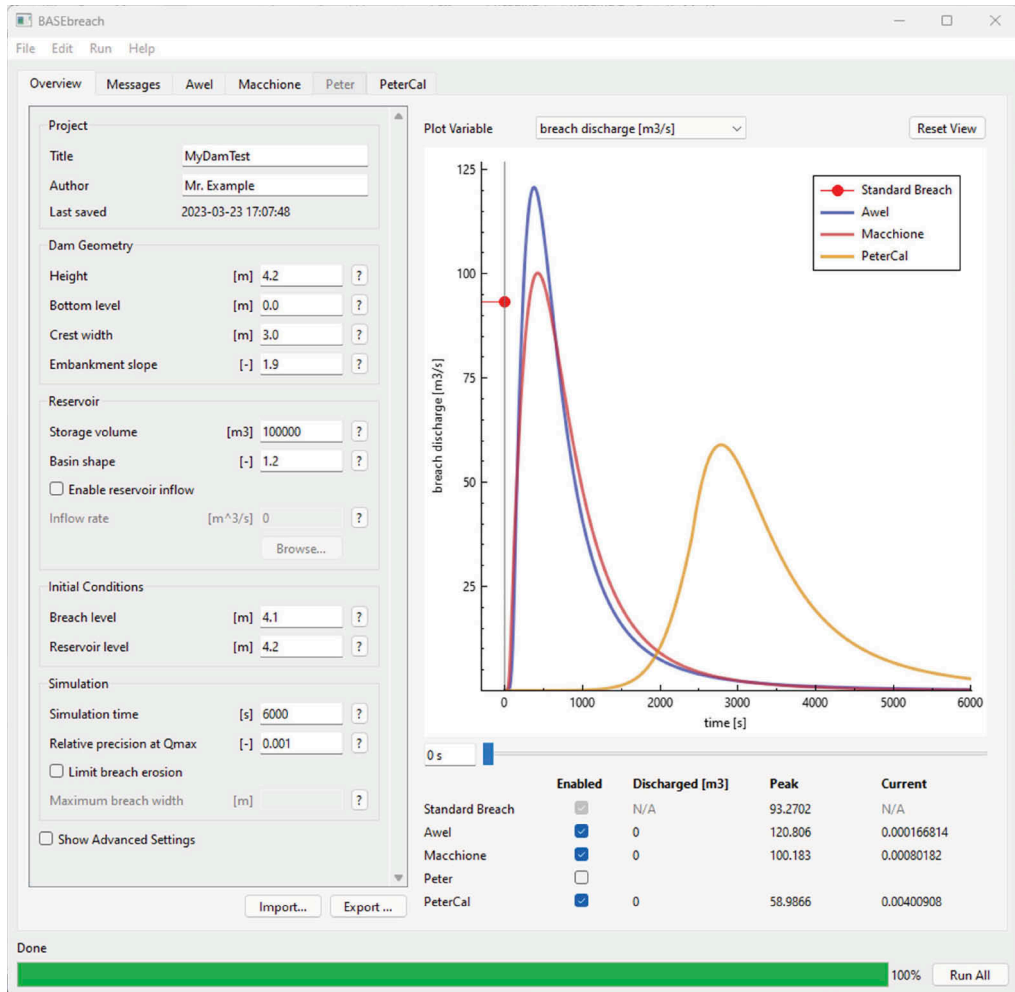


Figure 1. Graphical user interface of the BASEbreach software.

2.2 Dam breach models

2.2.1 General parameters

The general parameters (Figure 2) define the basic simulation setup. The dam geometry is described by the dam height H_D (which is the difference between the minimum dam crest level z_C and the reservoir bottom level at the upstream dam toe z_T), the width of the dam crest W_C , and the embankment slope m_D (H:1) of the upstream and downstream dam faces. In case m_D differs for these, a mean value should be selected. The geometry of the breach is characterized by the breach side angle β against the horizontal (Figure 2a). Further, the maximum breach

width may be specified to account for lateral constraints such as non-erodible valley flanks. As initial conditions, the reservoir level H_W and the breach level H_B at the beginning of the simulation must be specified, where $H_W > H_B$. The initial water and breach level may be defined reasonably lower than for full supply conditions to consider the case of dam failure due to an overtopping flow subsequent to piping.

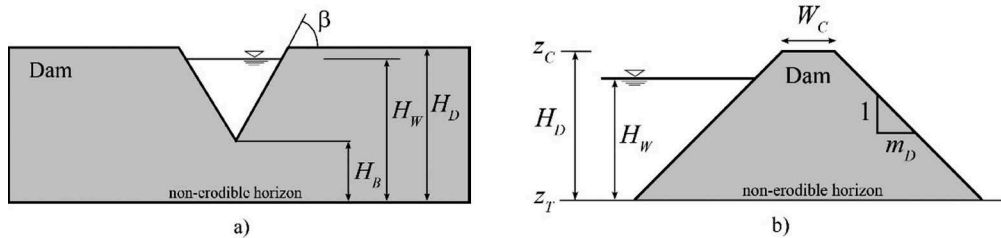


Figure 2. a) Cross-sectional view and b) side view of schematic dam.

Additionally, the initial reservoir capacity $V_{W,0}$, which corresponds to the storage capacity at full supply level unless otherwise specified, and the reservoir shape coefficient α_0 must be defined. During the simulation, the actual reservoir capacity $V_W(t)$ is computed as (Kühne, 1978):

$$V_W(t) = V_{W,0} \left(\frac{H_W(t)}{H_{W,0}} \right)^{\alpha_0} \quad (1)$$

where $H_{W,0}$ = initial water level, and $H_W(t)$ = time-varying water level. The coefficient α_0 describes the shape of the reservoir and thus the vertical distribution of the reservoir volume. The coefficient usually varies between 1 and 4. The larger α_0 , the more water volume is in the upper segment of the reservoir. A cuboid-shaped reservoir has an α_0 value of 1. To describe a V-shaped reservoir, an α_0 value in the range of 3 to 4 is assumed.

Usually, the simulation is considered as an initial value problem. However, to account for increased reservoir volume during flood events, inflow to the reservoir can be specified as a constant or with a hydrograph.

2.2.2 Standard breach model

The standard breach model allows for the estimation of peak discharge for a partial and instantaneous failure of small embankment dams, i.e. no progressive failure is considered. It is used for classical risk assessment of small earthen embankment dams in Switzerland (Müller, 2003) and serves as a reference value. The breach geometry is an isosceles trapezoid with height H_W , bottom width $2H_W$, and top width $4H_W$. The maximum breach discharge $Q_{B,max}$ can be estimated with H_W representing the water depth at full water supply level as:

$$Q_{B,max} = 2.58 H_W^{2.5} \quad (2)$$

2.2.3 Macchione model

The *Macchione* model (Macchione, 2008, Macchione and Rino, 2008) is a simplified physically-based model for simulation of progressive failure of homogenous earthen embankment dams with an emphasis on a small set of correlated parameters. The cross section of the breach is assumed to develop at first in vertical direction with a triangular shape until the non-erodible horizon, i.e. typically the base of the dam, is reached (Figure 2). Subsequently, the breach expands laterally due to erosion of the breach slopes.

The temporal evolution of the breach shape is described as a function of the breach hydraulics, the breach erosion and the reservoir drawdown. The governing equations of the

model are two ordinary differential equations, one describing the depletion of the reservoir level over time and one describing the enlargement of the breach over time. The propagation of breach erosion is proportional to the calibration parameter v_e , referred to as the characteristic velocity. Macchione (2008) applied a deterministic calibration based on historical dam failures and obtained a mean value of $v_e = 0.07$ m/s with $\tan(90^\circ - \beta) = 0.2$, i.e. $\beta = 78.69^\circ$ to the horizontal (Figure 2a). In particular, this value should be used when cases of dams similar to those examined in Peter (2017) are considered.

2.2.4 AWEL model

The AWEL model (Vonwiller et al., 2015, Boes et al., 2015) was developed at VAW for the investigation of the progressive failure of small embankment dams. The development was commissioned by the Office of Waste, Water, Energy and Air (AWEL) of the Canton of Zurich, Switzerland, hence the name. The model is based on the Macchione model, where the erosion velocity was calibrated using a series of 2D numerical model experiments of progressive dam failure with the software BASEMENT (Vetsch et al., 2020). The dam geometries and reservoir volumes used for the model experiments were taken from 90 small embankment dams in the Canton of Zurich. Consequently, the model was calibrated within the following limits: $500 \leq V_{W,0} \leq 200'000$ m³, $1 \leq H_W \leq 10$ m, $0.5 \leq W_C \leq 12$ m, $1 \leq m_D \leq 4$.

2.2.5 Peter model

The Peter model (Peter, 2017) is a physics-based model for simulation of progressive failure of homogenous earthen embankment dams, with an emphasis on a small set of correlated parameters. The breach geometry is defined by a parabola with side angle β against the horizontal at the dam crest. The cross section of the breach is assumed to develop at first mainly in a vertical direction with a parabolic shape until the non-erodible horizon (typically the dam base) is reached (Figure 3). Further development of the breach leads to an enlargement of the breach owing to erosion of the breach slopes.

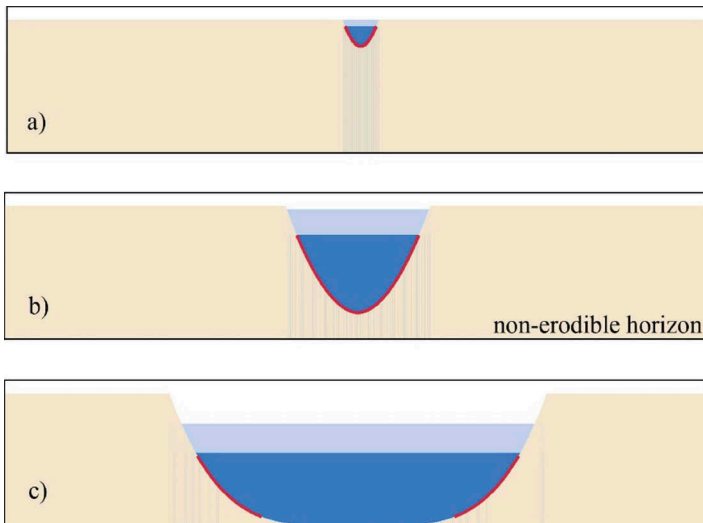


Figure 3. Example of breach progression with the Peter model: a) initial breach, b) vertical and lateral breach erosion (breach height is smaller than dam height), c) only lateral breach progression after reaching a non-erodible horizon.

The temporal evolution of the breach shape is described similar to the Macchione model and is based on two ordinary differential equations. However, the transport rate which controls breach erosion is computed as a function of breach flow velocity u and hydraulic radius r :

$$q_s = \gamma u^{\nu} r^{\eta} \quad (3)$$

where $\nu = 2c_1 + c_2$ and $\eta = c_1(1 - 2c_4) + c_3$. The erosion scaling coefficient γ is a global scaling coefficient that acts as a tuning factor to accelerate or hinder the erosion process. The two exponents ν and η combine the empirical formulation of transport and friction laws (Peter, 2017). For instance, choosing the Meyer-Peter Müller transport formula ($c_1 = 1.5$ and $c_2 = c_3 = 0$) and Strickler's friction law ($c_4 = 2/3$) yields $\nu = 3$ and $\eta = -0.5$. The two exponents are physically interpreted as:

- the larger $\nu > 0$ is, the stronger will be the influence of hydraulics on sediment transport (high flow velocity leads to more intense sediment transport),
- the smaller $\eta < 0$ is, the smaller will be the influence of breach geometry on sediment transport.

2.2.6 Peter 'calibrated' model

The Peter 'calibrated' model (Peter et al., 2018a) is similar to the Peter model but was probabilistically calibrated for 15 historical dam breach events. The derived parameters are $\gamma = 0.00025$, $\nu = 4.15$ and $\eta = -0.65$. Comparing this formulation with the theoretical values from the transport law by Meyer-Peter and Müller and the friction law by Manning ($\nu = 3.0$ and $\eta = -0.5$), the transport within the breach can be considered more total sediment-load like, i.e. bed and suspended load ($\nu = 4.15 > 3.0$) and less sensitive to the cross-sectional geometry ($\eta = -0.65 < -0.5$).

2.3 Consideration of uncertainties

Some of the input parameters of the above models are well-defined for a given situation. For example, the geometry of the dam and the reservoir are usually available at good accuracy. However, some parameters are not so simple to determine. For prototype embankment dams the composition and grain size distribution of embankment material is often unknown, e.g. for embankments made of moraine material with a widely-graded grain size distribution and cohesive properties. Consequently, a calibration of relevant values is necessary. The AWEL model has already been calibrated for small embankment dams in Canton Zurich, Switzerland (c.f. range of parameters of considered dams). Also, the Macchione and Peter 'calibrated' models were calibrated based on data from various embankment dams (Peter, 2017).

For the Peter and Macchione models, certain parameters can be varied to control the progress of breach erosion. For instance, the progress of vertical erosion is controlled in the Macchione model by the characteristic velocity v_e , and in the Peter model by the erosion scaling coefficient γ . In both models, the breach side angle may be adjusted, to account for steep breach slopes due to cohesive effects.

The variation of single parameters allows for an assessment of the model sensitivity. With the BASEbreach software, the Peter model can be used in combination with Monte Carlo simulation (Peter et al., 2018b). In doing so, the relevant parameters are not specified by fixed values, but by a probability distribution (e.g. log-normal distribution). While running a Monte Carlo experiment, the variables are sampled automatically from the defined probability distribution. The results are many hundreds or thousands of outflow hydrographs showing the result of variation of the relevant parameters.

3 APPLICATION OF BASEBREACH

3.1 Comparison of models for progressive failure

The performance of the different dam breach models for progressive failure introduced in section 2 is illustrated for three realistic cases of small homogenous embankment dams. Reservoir properties and dam geometry are summarized in Table 1. The reservoir shape coefficient is $\alpha_0 = 1.5$ for all cases.

Simulation of the three cases shows that the maximum breach discharge clearly differs among the models (Table 1). Despite the AWEL (AW) and Macchione (MA) models sharing the same modelling approach, the simulations resulted in distinctly different maximum breach discharge $Q_{B,max}$ for the case D1, which had the smallest reservoir capacity $V_{W,0}$. With increasing reservoir capacity the difference decreases, and for case D3, which has the largest $V_{W,0}$, the results are similar. This can be attributed to the fundamentally different calibration procedure of the two models. For both approaches, breach erosion starts soon after initial overtopping and subsequently proceeds rapidly, resulting in a breach outflow hydrograph as depicted (for case D2) in Figure 4. In contrast, breach erosion in the Peter ‘calibrated’ (PC) model progresses much slower at the beginning and thus the discharge hydrograph occurs later during the simulation. The reasons for this are the different approach for the breach geometry and the calibration of the sediment transport model, i.e. the erosion scaling coefficient. For similar properties for the MA and the PC models, i.e. the Meyer-Peter and Müller transport law ($\nu = 3.0$), friction law by Manning ($\eta = -0.5$) and $\gamma = g^{-1.5} v_e = 0.0023$ (where g is acceleration due to gravity and $v_e = 0.07$ m/s), the resulting breach outflow hydrograph and the maximum breach discharge are similar. Furthermore, both the MA and PC models respond similarly to variation of the parameter controlling erosion, i.e. characteristic erosion velocity v_e (MA) and erosion scaling coefficient γ (PC) (Table 2).

Table 1. Test cases for illustration of model performance and resulting maximum breach discharge $Q_{B,max}$ (SB = standard breach, MA = Macchione, AW = AWEL, PC = Peter calibrated).

Case	$V_{W,0}$ m ³	H_W m	W_C m	m_D -	$Q_{B,max,SB}$ m ³ /s	$Q_{B,max,MA}$ m ³ /s	$Q_{B,max,AW}$ m ³ /s	$Q_{B,max,PC}$ m ³ /s
D1	22'700	7.8	1.5	2.0	438.4	95.8	56.8	8.9
D2	100'000	4.2	3.0	1.9	93.3	109.6	120.8	67.0
D3	140'000	3.1	2.5	1.5	43.7	105.9	107.0	75.7

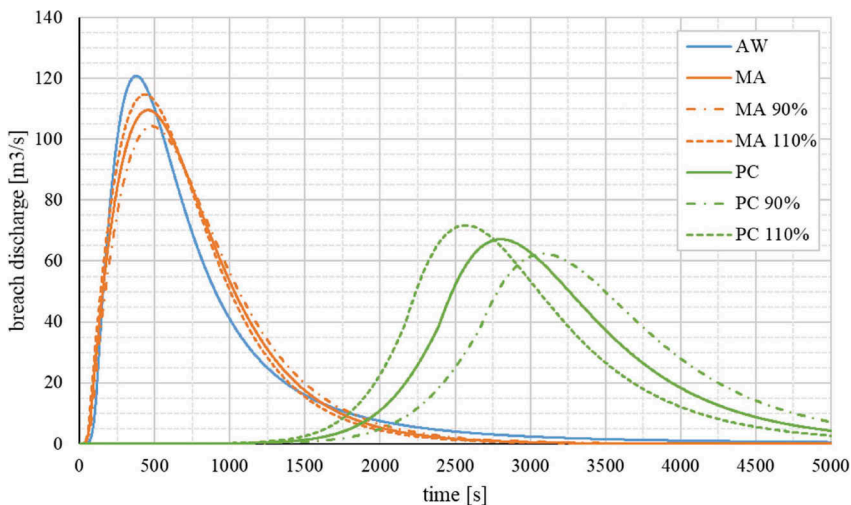


Figure 4. Simulated breach discharge hydrographs for case D2 with Macchione (MA), AWEL (AW) and Peter ‘calibrated’ (PC) models, and sensitivity ($\pm 10\%$) of the MA and PC models with regard to parameters characteristic velocity v_e (MA) and erosion scaling coefficient γ (PC).

3.2 Instantaneous versus progressive failure

The standard breach (SB) approach assumes an instantaneous failure of the dam with simplified trapezoidal breach geometry. For estimation of the maximum breach discharge only the

Table 2. Resulting maximum breach discharge $Q_{B,max}$ for case D2 with Macchione (MA) and Peter ‘calibrated’ (PC) models, and sensitivity ($\pm 10\%$) with regard to parameters characteristic velocity v_e (MA) and erosion scaling coefficient γ (PC).

Case	v_e m/s	$Q_{B,max,MA}$		γ -	$Q_{B,max,PC}$	
		m ³ /s	%		m ³ /s	%
90%	0.063	104.3	95	0.000225	62.4	93
100%	0.070	109.6	100	0.000250	67.0	100
110%	0.077	114.6	105	0.000275	71.8	107

height of the dam is considered and other factors, such as the dam and reservoir volume, are not considered. The standard breach model does not take the total reservoir volume into account.

Comparison of the SB model with the MA or AW models, which consider a progressive failure process, shows that the maximum breach discharge $Q_{B,max}$ for small reservoirs can be either overestimated or underestimated, depending on the situation (Table 1). An overestimation tends to occur for larger dam heights and small reservoir volumes, whereas underestimation is observed for larger reservoir volumes and smaller dam heights. Consequently, the hazard assessment based on the standard breach approach is not always on the safe side.

4 CONCLUSIONS AND OUTLOOK

The software BASEbreach presented herein allows the calculation of the maximum breach discharge for homogeneous embankment dams with different parameter models. The primary goal is to represent the dam failure process progressively and thus more realistically. In the parameter models AWEL, Macchione, and Peter, the breach discharge is calculated in a simplified way, while also considering the dynamic change of the storage volume and the breach geometry. Consequently, the reservoir shape and the erosion rate are the most important calibration parameters and have a significant influence on the shape of the breach outflow hydrograph, including the maximum breach discharge.

The uncertainties in dam breach modelling and thus in predicting the maximum breach discharge are generally large and from multiple sources. The origin of the existing uncertainties lies in the still incomplete understanding of the processes taking place during dam breaching. For example, there are large uncertainties in the erosion rate, especially in the case of cohesive dam materials. Also, there are model uncertainties due to assumptions and simplifications regarding the model equations. In addition, there are uncertainties in the input variables due to partly missing or incorrect information. In the case of small dams, this may include the dam structure or the stage-volume relationship. As part of the ongoing research at VAW on dam breaching, we review the calibration of the parameter models available in BASEbreach, and develop an enhanced model which allows to also consider the breaching process of zoned dams.

ACKNOWLEDGEMENTS

The development of the BASEbreach software was financially supported by the Office of Waste, Water, Energy and Air (AWEL) of the Canton of Zurich, Switzerland, and the Swiss Federal Office of Energy (BFE).

REFERENCES

- Boes, R., Vonwiller, L. & Vetsch, D. F. (2015) Breaching of small embankment dams: Tool for cost-effective determination of peak breach outflow. *36th IAHR World Congress: Deltas of the Future and what happens upstream, The Hague, The Netherlands, June 28 - July 3, 2015*. IAHR.
- Kühne, A. (1978) Charakteristische Kenngrößen Schweizerischer Speicherseen. *Geographica Helvetica*, 33, 191–199 (in German).
- Macchione, F. (2008) Model for Predicting Floods due to Earthen Dam Breaching. I: Formulation and Evaluation. *Journal of Hydraulic Engineering-Asce*, 134, 1688–1696.
- Macchione, F. & Rino, A. (2008) Model for Predicting Floods due to Earthen Dam Breaching. II: Comparison with Other Methods and Predictive Use. *Journal of Hydraulic Engineering-Asce*, 134, 1697–1707.
- Müller, R. W. (2003) Die Beurteilung der besonderen Gefahr mit vereinfachten Flutwellenberechnungen. Workshop kleine Talsperren. Bundesamt für Wasser und Geologie (in German).
- Peter, S., Siviglia, A., Nagel, J. B., Marelli, S., Boes, R., Vetsch, D. F. & Sudret, B. (2018a) Development of Probabilistic Dam Breach Model Using Bayesian Inference. *Water Resources Research*, 54, 4400.
- Peter, S. J. (2017) Dam break analysis under uncertainty. *VAW-Mitteilung* 241 (R. Boes, ed.), Laboratory of Hydraulics, Hydrology and Glaciology, ETH Zurich, Switzerland.
- Peter, S. J., Vetsch, D. F., Siviglia, A. & Boes, R. (2018b) Probabilistische Dambruchanalyse. *Wasser Energie Luft*, 2018, 185 (in German).
- Vetsch, D. F., Bürgler, M., Gerke, E., Kammerer, S., Vanzo, D. & Boes, R. (2020) BASEMENT – Softwareumgebung zur numerischen Modellierung der Hydro- und Morphodynamik in Fließgewässern. *Oesterreich Wasser- und Abfallwirtschaft*, 72, 290 (in German).
- Vonwiller, L., Vetsch, D. F., Peter, S. & Boes, R. (2015) Methode zur Beurteilung des maximalen Breschenabflusses bei progressivem Bruch homogener Erdschüttdämme an kleinen Stauhaltungen. *Wasser Energie Luft*, 107, 37–43 (in German).

Ageing and life-span of dams

M. Wieland

ICOLD Committee on Seismic Aspects of Dam Design, Honorary Member of ICOLD, Dam Consultant, Dietikon and AFRY Switzerland, Zurich, Switzerland

ABSTRACT: Ageing is the main factor governing the life-span of any engineering structure. In the context of this paper the term ageing is used to describe the decrease in safety of the dam body with time. The factors to be considered include all time-dependent physical processes and changes in safety criteria that govern the safety assessment of dams. Long life-spans can only be reached, if the dam satisfies all safety criteria during its long life, which implies that the owner or operator provides take care of a dam and provide adequate maintenance.

1 INTRODUCTION

The economic life of a dam ends when (i) a dam has been damaged or failed, (ii) the safety of a dam does not satisfy current safety criteria, (iii) the reservoir can no longer be used, and (iv) if a dam is no longer needed and can be decommissioned. The present paper is concerned with item (ii), which depends on different types of ageing processes, time-dependent natural and man-made hazards and changes in dam safety criteria during the long life of a dam.

Therefore, in a wider perspective ageing may be considered a process of deteriorating dam safety, which also includes time-dependent hazards and changes in safety criteria and not only physical and chemical deterioration of dam and foundation materials or of hydro-mechanical and electro-mechanical components. Technological progress must also be considered as an ageing issue, which mainly includes software and electronic hardware as well as telecommunication systems, etc. To delay these different types of ageing processes requires different strategies.

First, it must be determined if a dam satisfies the current safety criteria, which has to be checked periodically, as, for example, in Switzerland every five years. Dam safety means not only structural safety, but also includes dam safety monitoring, operational safety and maintenance, and emergency planning. All these safety factors must be considered in the periodic safety reviews.

Ageing of the dam body includes chemical deterioration like swelling of mass concrete, the effect of seepage in embankment dams and the foundation rock, and physical damage due to repeated frost cycles in concrete dams or cracking in concrete dams, due to thermal effects, shrinkage, creep, foundation settlements or various hazards from the natural and man-made environments. Gated spillways may be damaged due to rockfalls and low-level outlets may be blocked by sediments or other types of accumulated debris. Ageing involves the safety deterioration of a dam and ultimately governs its life-span.

This paper is an extension of a previous paper by the author (Wieland, 2010).

2 NEED FOR THE SAFETY EVALUATION OF DAMS

It is a basic requirement that people living downstream of a dam, whether new or old, must feel equally safe, which means that all dams must always satisfy the same minimum safety criteria specified in dam safety guidelines or laws. As the knowledge on hazards will change with

time and safety guidelines may be changed, etc. safety evaluations have to be carried out repeatedly during the long life-span of dams. The belief that a dam designed for a life-span of 100 years will remain safe for the full 100 years is a misconception. Likewise, if people believe that a dam, which has survived say 50 years, is safe, is also a misconception, as there are rare events such as strong earthquakes that may not have occurred within this period. A typical case is the castle in Gaziantep built during the 2nd and 3rd centuries in the southeast of Turkey, which remained intact for about 1800 years until it was damaged by the magnitude 7.8 earthquake on February 6, 2023. Therefore, one must be careful not to jump to premature conclusions regarding dam safety.

The main reasons for the safety evaluation of storage dams are given below for the most important natural hazards, i.e. flood and earthquake hazard.

The earthquake safety of a dam should be checked in the following cases:

- New information on (i) seismic hazard, which includes ground shaking, movements along faults or other discontinuities in the footprint of the dam or the reservoir and mass movements, and/or (ii) seismotectonics is available;
- A dam has been subjected to strong earthquake shaking;
- New seismic design criteria are introduced;
- New seismic performance and safety criteria are introduced for different design earthquakes;
- New dynamic analysis methods are employed, such as nonlinear dynamic analysis;
- The seismic vulnerability of a dam has increased due to dam modifications, ageing, etc.,
- The risk classification of dams has changed, which may depend on the reservoir volume, the dam height, dam type, age of dams and the consequences of dam failure, and
- The seismic risk has increased, e.g., due to the increased number of people living downstream of a dam and/or due to economic developments, etc.

Similarly, the flood safety of a dam should be checked in the following cases:

- New information on flood hazard is available (e.g., effect of climate change, changes in land use in the catchment region, effect of construction of dams upstream of a dam, etc.);
- A dam has been subjected to an extreme flood or the spillway was in operation for a long period of time;
- New flood design criteria are introduced for different dam types;
- New flood performance and safety criteria are introduced for different dam types (e.g. n-1 rule for discharge of safety flood of embankment dams or composite dams formed concrete and embankment dams);
- New analysis methods for flood routing and/or for estimating extreme floods are introduced;
- The flood vulnerability of a dam has increased due to dam modifications, ageing, etc.,
- The risk classification of dams has changed, which may depend on the reservoir volume, the dam height, dam type, age of dams and the consequences of dam failure, and
- The flood risk has increased, e.g., due to the increased number of people living downstream of a dam and/or due to economic development, etc.

For other types of natural and/or man-made hazards, other reasons for the safety evaluations may apply.

It is recommended that the different factors listed above are reviewed periodically, e.g., every five years. Based on the result of this review, a safety evaluation for specific hazards is recommended. The outcome of such safety re-evaluations will be a set of recommendations, which may include structural improvements, i.e. improvement of flood or earthquake safety, early warning systems for floods and restrictions on the reservoir level, e.g., lowering of the reservoir level before the rainy season, etc. Note, earthquake early warning systems have hardly any safety benefits as the warning times are only a few seconds. For other hazards, other safety measures may be required.

It is expected that such safety re-evaluations may be required at intervals of about 20 to 40 years. It would not be practical to carry out safety reviews as soon as new information on the

seismic or flood hazards become available. For example, there are many seismologists working in the field of seismic hazard analysis and, therefore, new analysis methods and new results are published almost monthly by different researchers and analysts. This would imply that the seismic safety of existing dams would have to be re-checked almost “daily”. This is also a problem for the design of new dams as the seismic design criteria will change when different seismic hazard studies by different experts are being carried out. Therefore, in practice, the design values must be “frozen” for some time unless during construction faults or unstable slopes, etc. are detected with an important impact on the dam’s safety.

In order to avoid frequent seismic re-analyses of dams, it is recommended to check its seismic safety reserves, by increasing the seismic hazard by factors of say 1.3, 1.5 or 2.0. In this case, the effects of changes in results of seismic hazard analyses can easily be assessed without requiring a re-analysis. Unfortunately, up to now the analysis of seismic reserves is not carried out, although the author has made such recommendations already several years ago.

In general, it is better to spend the money on the safe design of a dam than spending the same amount of money on sophisticated seismic hazard analyses. Unfortunately, this is not the case today for the seismic hazard and climate change effects. However, this observation may not apply to the case of other hazards.

3 LIFE-SPAN OF DAM

The main factors having an impact on the life-span and which may call for the upgrading of a dam are the following (Wieland, 2010):

- Changes in the design criteria (hydrology and seismic hazard) for different dam types based on new information obtained since the initial design of the dam.
- Changes in methods of analysis and new safety concepts (for example, n-1 rule for discharge facilities of embankment dams for the safety flood).
- Results of risk assessments (new risks and change in risk acceptance criteria) requiring higher safety standards.
- Ageing of construction and foundation materials and components.

As these four factors are time-dependent, the life-span of a dam is also time-dependent. Usually, the life-span will shorten if no action is taken - mainly maintenance – and/or when the different components of a dam project do not have any safety reserves. Because of the high safety factors used, e.g., for the lifting devices of gates in old run-of-river power plants, these ropes and chains are still safe today, in spite of the fact that new and generally more severe load combinations must be considered compared to those at the time of construction.

Similarly, the seismic safety of most dams is still adequate today, despite the fact that the seismic loads may be much higher today than at the time of the dam construction. The main reason is that the seismic load combination used in the past did not determine the design of the dam or is no longer considered relevant today. This is the case for the old load combination of rapid reservoir drawdown combined with seismic action, as this scenario with an empty reservoir is not important for the safety of people living downstream of the dam. Therefore these dams had some extra seismic safety reserves. Thus, as today different seismic safety criteria and methods of dynamic analysis are used, the increased seismic loads did not have any negative impact on the safety of most dams, whose seismic safety was re-assessed, and thus on their life-span.

The situation is different for dams or components, which were fully optimized at the time of the design and therefore do not have any significant safety reserves. They may have to be strengthened or the reservoir level has to be lowered to comply with the current safety criteria. Increasing the height of such dams is also difficult, which today is an option for increasing the energy production or for extending the life-span of reservoirs threatened by siltation.

If a dam remains safe, which means that it must have been well-maintained, it can easily be used for more than 100 years. For example, the Maigrauge gravity dam in Switzerland - the first concrete dam in Europe - was built in 1872 and is still in operation today. Its life-span

may exceed 200 years, if it will be well-maintained in the future as in the past. However, some safety modifications were required regarding flood safety (new spillway) and seismic safety (installation of rock anchors in the dam body to increase sliding stability) (Mivelaz et al., 2006). In addition a shotcrete protection had to be provided at the dam faces as the old concrete was not frost resistant.

4 AGEING PROCESSES

4.1 Introduction

In the context of this paper the term ageing is used to describe the decrease in safety of the dam body with time, as safety is the main factor governing the life-span of a dam.

Sedimentation is usually not a major factor for the structural safety of the dam body of large storage dams but may be a major factor for small dams or run-of-river power plants in mountainous regions, whose reservoirs can be filled completely with debris during a severe flood. If such projects are planned in such regions, they should either not be built or modified to account for large debris flows resulting, e.g., from large mass movements in the catchment area, the failure of landslide dams or glacial lake outburst floods (GLOF) as in the Himalayas. Sedimentation of the reservoir, however, has an impact on the utilization of the water in the reservoir and with increasing sedimentation and changes in the use of the water the reservoir rule curves may have to be changed, but this is in general not a dam safety issue. Sediment flushing can cause serious erosion in irrigation and sediment flushing outlets.

Dam safety includes not only the safety of the dam body, but also the proper functioning of the spillway and low-level outlets during and after extreme events. Intakes of spillways or low-level outlets may be blocked by sediments or debris from mass movements into the reservoir and related equipment may be damaged by rockfalls, earthquakes, etc. Of course, the safety of the dam body could also be affected by these natural hazards and many others as discussed by Wieland (2023). In the subsequent discussion, it is assumed that the safety deterioration is the result of physical deterioration of construction materials and components, and changes in performance and safety criteria.

4.2 Physical ageing processes

Physical ageing processes develop relatively slowly with time, but the rate of deterioration may increase more quickly with increased deterioration. The ageing of the concrete and of the foundation rock includes the following processes:

- Chemical processes (swelling of mass concrete due to alkali aggregate reactivity (AAR), sulphate attack, leaching, etc.).
- Physical and mechanical processes (thawing-freezing and drying-wetting cycles; cracking due to temperature effects, shrinkage, creep and non-uniform foundation movements; abrasion due to operation of spillways and/or low-level outlets, etc.).
- Biological processes (growth of plants in cracks or joints, mussels at intakes and grillages, etc.).
- Seepage in the foundation and the dam body (disintegration of grout curtain, degradation of foundation materials like gypsum-anhydrite, weakening of matrix of conglomerate rock, change in uplift of the dam due to increased permeability of concrete and the foundation rock resulting in changes in the stability of the dam and abutment, etc.).

In reinforced concrete structures (spillways, low-level outlets) and face slabs of concrete-faced rockfill dams, corrosion of the reinforcement will eventually take place. Concrete dams, except for run-of-river power plants and some dams with thin structural elements like Ambursen dams, which are no longer built today, are unreinforced concrete structures. There are some modern arch dams where steel reinforcement was provided to cope with thermal stresses, large seismic stresses or at locations where cracks developed during construction, and there

are special cases where a seismic belt is provided at the crest of arch dams. Therefore, concrete dams, which do not have any steel reinforcement, have a much longer service life than reinforced concrete structures exposed to weather.

The ageing processes have to be checked by periodic visual inspections, tests and by monitoring of the dam (mainly dam deformations, growth of cracks, joint movements, seepage, chemical analyses of seepage water, uplift pressure distribution, etc.), but not everything is visible or measurable.

Dense frost-resistant concrete should have a very long service life. Under ideal environmental conditions (moderate temperature variations, low humidity, etc.) the life-span of a concrete dam can be very long. But it can also be very short if some of the safety-critical elements are no longer functioning properly.

Due to the many factors affecting the operational condition and environment of a dam, it is not possible to be specific about the remaining service life of existing dams. This has to be assessed periodically on a case-by-case basis. Quite a few concrete dams may, however, require major rehabilitation, especially those showing signs of abnormal behaviour or AAR.

Embankment dams are engineered structures using mostly natural materials, part of which may be processed (e.g. filters). The foundation is as essential for the life-span of the dam structure as the structure itself. Maintenance of a foundation is achieved by providing it with supplementary treatment, e.g., by reinforcing or extending the grout curtain or by replacing it with a cutoff, by installing relief wells or any other means of drainage depending on the actual situation and its requirements.

Properly designed and constructed embankment dams can remain structurally stable and safe for centuries as long as they are not subjected to erosion processes. However, embankment dams are most vulnerable to floods and internal erosion. A well-designed and maintained embankment dam is a very resilient structure and can also sustain extreme loading conditions.

4.3 *Ageing due to technological development*

Dam safety criteria and methods of analysis needed to verify the performance and safety criteria are changing with time. Especially the different analysis methods of hazards and the analysis of dams subjected to these hazards as well as the definition of hazard scenarios (i.e. load combinations) are changing. These changes have to be taken care of. For example, design codes for different types of structure are updated at intervals of about 4 years such as the frequently used IBC (International Building Code, latest version 2021) and ACI 318 (Building Code Requirements for Structural Concrete, latest revision 2022). Although the ICOLD guidelines for different aspects of dam design and dam safety are updated less frequently than those for building structures, bridges, etc., it is obvious that due to the technological developments during the long life of dams, the performance and safety criteria will change. This means that even under the assumption that the design loads and actions remain unchanged, which is not the case, the safety of the dam may not satisfy the latest safety criteria. This development can be considered as a type of ageing process.

Therefore, it is required to re-assess the safety of a dam when new changes in safety criteria are introduced, as dams are among the structures that must satisfy the current safety criteria. This is not necessarily the case for other types of structures.

5 SAFETY, LIFE-SPAN AND SUSTAINABILITY OF DAMS

Today, the term sustainability is used for “everything” and the UN has published 17 sustainable development goals. Not all of them are relevant for dams or other infrastructure projects and most of them are related to non-technical aspects.

To obtain sustainable dams, a distinction must be made between technical and non-technical aspects. The technical aspects are mainly dam safety and long life-span, whereas non-technical aspects are related to the environment and social aspects. Basically, the most important aspect of any structure is “safety first”. This not only applies to people involved in

construction and maintenance works but also to the safety of the completed dam project, i.e. it must be able to safely withstand all types of hazards from the natural and man-made environment. Therefore, safety is the pre-requisite of any dam project and it must take precedence over all non-technical aspects. This fact is not clearly visible in the UN development goals.

Basically, any dam project can only be sustainable if it is safe and has a long life-span. The average age of Swiss dams is about 75 years and they are safe and well-maintained, which means that they are sustainable, as otherwise they would have already been decommissioned or the old technology of dam construction would have been abandoned, if this technology were unsafe. That some dams are still in operation for 1000 years or more also show that they are able to provide economic benefits, which is another key factor for sustainable dams.

Although the design life of different elements of a dam project is specified, this does not mean that it is equal to the life-span of a project, as nobody can predict the future. For example, the 272 m high Enguri arch dam in Georgia, completed only a few years before the dissolution of the Soviet Union, became unsafe during the civil unrest in Georgia after independence as vital equipment and dam monitoring instruments were looted, so it was no longer possible to declare the dam safe. Thus, within a short period of time, in effect a safe dam became unsafe. The same is true, when no proper maintenance is provided.

It must be the objective of any dam owner and operator to ensure that the dam is safe and that the life-span is extended as much as technically possible. The importance of these two interconnected goals may not be fully realized at the time of construction of a new dam, especially when private developers have concessions for 25 to 40 years only.

In terms of the CO₂ footprint, an embankment dam is superior to a concrete dam that may require about 200 kg of cementitious material per m³ of mass concrete. Moreover, the life-span of embankment dams made of locally available materials of good quality may be considerably longer than that of concrete dams. Masonry dams could reach similar life-spans to embankment dams.

Finally, it should be mentioned that most large dam projects are multi-purpose projects and that the main purpose of the water stored may also change with time. In the Swiss Alps the main purpose is power production, but in future reservoirs may play an increasing role for water supply and flood protection, etc. Therefore, to assign the whole CO₂ footprint of dam construction to the energy production in a multi-purpose project with basically an “unknown” life-span is in general considerably overestimated.

In terms of safety, life-span each large dam project is a prototype subjected to many different hazards, some of them are site and project-specific, therefore a comparison of the safety, life-span and also the sustainability with other projects is very difficult, if not impossible.

6 EFFECT OF CLIMATE CHANGE ON SAFETY AND LIFE-SPAN OF DAMS

Climate change has an effect on all weather-related hazards of a dam project, which from the dam safety point of view is mainly the flood hazard. There exist all kinds of scientific predictions for the next 25 to 75 years. However, the time-dependence of hazards and the emergence of new types of hazard is nothing new for dam engineers. The best way of dealing with such time-dependent hazards, which includes climate change related hazards, is by a “participatory approach”, i.e. that all hazards and their safety implications are reviewed periodically, e.g. every five years in the case of Switzerland. This review will show if a safety re-evaluation is necessary. If the safety re-evaluation shows that a dam is no longer safe then different structural and non-structural options must be evaluated. As mentioned earlier, in this context it is useful to determine the safety reserves of dams against different time-dependent hazards. By doing this, a re-analysis of the dam safety is only required if the hazard exceeds the maximum hazard a dam can withstand safely.

By following this well-established procedure, the effect of climate change on dam safety and the life-span of a dam can be evaluated. No new dam safety concepts are required specifically for climate change.

However, with increasing flood hazard and higher frequency of floods, the sediment transport into the reservoir will increase, which means that the life-span of the reservoir may be

shortened or that modifications in the reservoir rule curves will be required more frequently. Furthermore, sediments and/or turbidity currents may block intakes of safety-critical low-level outlets or spillways. The removal of such sediments will require increased maintenance if no other measures are taken to protect these intakes.

7 CONCLUSIONS

The main conclusions from the discussion of the effects of ageing on the life-span of dams are as follows:

1. The life-span of a dam is as long as it satisfies current safety criteria, i.e. this implies that proper maintenance must be provided.
2. Ageing of dams includes both physical ageing processes and ageing due to ongoing technological developments, which requires periodic updates of design and safety guidelines for dams. Climate change may increase the rate of some physical deterioration processes, mainly in concrete, and, thus, may shorten the life-span of concrete dams, if no adequate maintenance actions are taken.
3. The pre-requisites for a sustainable dam are structural safety of the dam body and the safety-critical elements like spillways and low-level outlets and a long life-span. Environmental and social aspects are subsidiary.
4. New and old dams must satisfy the same safety criteria at all times.
5. Most hazards affecting dam safety, including hazards due to climate change, are time-dependent.
6. The implications of time-dependent hazards on dam safety can be dealt with by having periodic reviews of the hazards and their effect on dam safety.
7. The assessment of the effect of climate change hazards on dam safety does not require any new safety concepts.
8. Well-designed, well-constructed and well-maintained dams can have life-spans exceeding 100 years, but the use of the reservoir will be affected by sedimentation.
9. The life-span of embankment dams is generally longer than that of concrete dams.
10. Rule curves for reservoir operation may have to be modified to account for reservoir sedimentation and changes in the future use of the reservoir, etc.
11. Accelerated sedimentation due to climate change has no effect on dam safety as it is taken into account in the design.
12. As dams have been built everywhere in the world with different climate conditions, there exists extensive experience, which can be used to assess possible effects of more extreme weather conditions.

DISCLAIMER

The opinions expressed in this paper are those of the author.

REFERENCES

- Mivelaz, L., Favez, B. & Lazaro, P. 2006. Upgrading the Maigrauge Dam. Proc. 22nd Int. Congress on Large Dams, ICOLD, Barcelona, Spain, June 2006.
- Wieland, M. 2010. Life-span of storage dams, Int. Journal Water Power and Dam Construction, Jan. 2010.
- Wieland, M. 2023. How to deal with the many hazards affecting dam safety? Proc. 2nd Int. Conf. on Dam Safety Management and Engineering (ICDSME 2023), Kuala Lumpur, Malaysia, 16-17.3.2023.

Hongrin arch dams – Rehabilitation works of the central artificial gravity abutment

A. Wohnlich

Gruner Stucky Ltd, Renens, Switzerland

R. Leroy

Alpiq Ltd, Lausanne, Switzerland

ABSTRACT: The Hongrin hydroelectric pumped storage scheme is located in Switzerland (Canton of Vaud); it was constructed at the end of the 1960s and presents two concrete arch dams 123 m high (northern dam) and 90 m high (southern dam). Both arch dams are connected by means of an artificial gravity abutment located on the central hill dividing both valleys.

The scheme is now more than 50 years old and over the decades, damages have materialized on the central artificial gravity abutment; namely, marked concrete cracking appeared along some horizontal construction joints, probably caused by insufficient concrete curing at the time of the construction (thermal cracking due to heat hydration). Over the years, such cracking pattern caused slow irreversible downstream displacements of the artificial gravity abutment in the range of 8 to 10 mm, which tend to increase over time.

The paper presents and discusses how the case was handled, starting for the monitored behaviour of both dams, the observation of damages in the artificial gravity abutment especially after the 2015 heatwave, the engineering studies considering a 3D model of both dams and the simulation of 15 years of operation, leading to the strengthening project consisting in the implementation of a total of approx. 50'000 kN vertical prestressed anchors in the artificial gravity abutment. The rehabilitation works took place in 2018. As a result, favorable results in terms of structural behavior are being observed.

1 INTRODUCTION

This paper discusses the case of the damaging of the central artificial gravity abutment connecting both Hongrin arch dams. Such damages to the massive buttress structure occurred slowly over decades in the form of increasing cracking which mostly took place on horizontal construction joints between successive concrete lifts, and thus an increasing irreversible displacement toward downstream. The occurrence of the progressing damage was identified as of 1990s, which allowed the operator Forces Motrices Hongrin-Léman (FMHL) to adapt a monitoring process and give a specific attention to the behavior of this part of the structure. Collaboration between experienced engineers (Alpiq), dam experts and engineers for the project design (Gruner Stucky), and FMHL was enforced on the critical issue and a close follow-up of the artificial gravity abutment conditions was ensured.

After the occurrence of 2015 heatwave and the confirmation of through-cracks along construction joints, dedicated studies were launched to identify the most suitable strengthening works to fix the problem. The implementation of prestressed anchors through the structure in 2018 is presented, as well as the outcome of the works in the following years and in terms of structural behavior of the artificial gravity abutment, whose displacements are now back in the elastic domain with no more drift observed.

2 DESCRIPTION OF THE SCHEME

Hongrin arch dams form the 52 Mio m³ Hongrin reservoir, which is the upper reservoir of the pumped-storage scheme Hongrin-Léman operated by FMHL. After the construction of the new underground powerplant in 2015, the scheme has a 480 MW installed capacity (initially 240 MW) between the upper Hongrin reservoir (elevation 1255 masl) and the lower Lake Geneva (elevation 372 masl). The underground scheme is located at Veytaux, near Montreux.

Hongrin arch dams present a unique layout, see Figure 1. Two double curvature arch dams were built in years 1966-1971. They close two valleys, namely Grand-Hongrin and Petit-Hongrin valleys, and they connect on a common artificial gravity abutment located on the central hill (La Jointe) dividing both valleys.



Figure 1. Hongrin arch dams, view from downstream, right bank.

The North dam is the highest at 125 m, for a 325 m crest length. On the other hand, the South dam is 97 m high for a 270 m long crest. Both dams have a crest length to height ratio in the range of 2.6-2.8. The concrete volume of the North dam is 230'000 m³, whilst it is almost half (114'000 m³) for the South dam. Both arch dams are only 2.7 m thick at the crest. Their slenderness only allowed to accommodate an inspection gallery near the rock foundation, from where the rock treatment (grout curtain, drainage) was carried out.

The artificial gravity abutment is 30 m high. Its crest accommodates a technical area with a stair access and a shaft into the inspection gallery. An access is also provided from the downstream (DS) face of the abutment into the inspection gallery, see Figure 2.

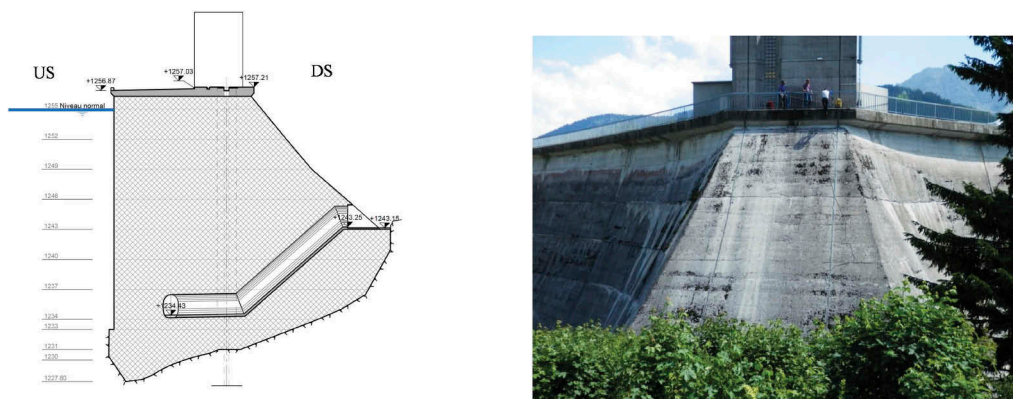


Figure 2. Artificial gravity abutment connecting both arch dams. Left: cross-section. Right: Picture from DS.

3 BEHAVIOR OF BOTH DAMS ALONG THE YEARS

3.1 *General behavior*

Generally, the main observable feature for both North and South arch dams is an irreversible drift toward upstream (US). Both dams behave in a similar way. Over the past 37 years and for both dams, the upper arch near the crest is showing the largest drift toward US between 0.2 mm/year and 0.4 mm/year. The largest drift is observed in the upper part of the dams, mostly due to the thermal effect which is stronger there than the water pressure acting on the US face. This is mostly due to the slenderness of the dams near the crest and the effect of the air temperature and direct exposure to solar radiation which is stronger at the top than at the bottom of both dams.

Namely over the decades a steady increase of air, water and therefore dam concrete temperatures is noted. In detail:

- *Air temperature:* An increase of around 0.10°C/year is measured over the last decades, with a tendency to even stronger increase in the recent years. This can only be explained by the ongoing environmental global warming.
- *Water temperature:* An average increase of 0.12 to 0.13 °C/year is measured in Hongrin reservoir over the decades. Firstly, this is a consequence of the increasing air temperature as explained in the above bullet point. But it is also due to a change in the operation rules of FMHL pumped-storage plant in Veytaux, following the commissioning in 2016 of the second powerhouse in parallel to the first one (built in the end of the 1960s). More water from Lake Geneva is now being pumped up to Hongrin reservoir. Obviously, this water taken at elevation 370 masl is warmer than the hydrological water flowing from the catchment area into the Hongrin reservoir at elevation 1250 masl and higher. The annual total volume of warm water being pumped from Lake Geneva has become relatively larger than the annual total volume of hydrological water drained in the catchment area at Hongrin dams (3 to 1 until 2015; 5 to 1 from 2016).
- *Dam concrete temperature:* Both dams are equipped with total 33 concrete thermometers. Because of the average temperature increase of both air and water, the concrete temperature also shows steady increase over the years, ranging from approx. 0.06°C/year in the core of the section, to 0.08°C/year near the DS dam face, to 0.10°C/year near the US face. This trend even tends to increase over the last years.

A raising of the dam crest is also observed by means of levelling measurement. This occurs for the same reasons as explained above for the US drift. However, the order of magnitude is much less remarkable.

In terms of leakage through the dam concrete and into the rock galleries (drainage), the situation is stable, if not trending lower; total average values are smaller than 10 l/min for each dam.

3.2 *Specific behavior of the central artificial gravity abutment*

An irreversible trend of the central artificial gravity abutment toward DS was detected as of decade 1980-1990. The annual range is of 3-4 mm. The trend increased more and more over the years 2000-2015, as shown in Figure 3 below. Interestingly one notes that the drift toward DS is only read at crest level; near the foundation level (el. 1235 masl) the behavior is regular and stable, showing elastic displacement in the range of approx. 1 mm.

Figure 4 shows the same monitoring data in a different way. Displacements are shown according to the reservoir level. The increasing trend toward DS is clearly observable, especially after year 2011. Furthermore, the graph clearly shows the combined effect of the heat-wave that struck Switzerland in July 2015 together with the very low reservoir level. For operational reasons, the reservoir level was deeply lowered (-40 m) in July 2015, at a time when it is usually full or nearly full. The exceptional heat and hot weather prevailing then struck directly on the US dam face which is usually under water. This resulted in the upper dam arches heating and moving toward US, leaning strongly on the artificial gravity abutment which gave way in an almost 3 mm sudden move toward DS.

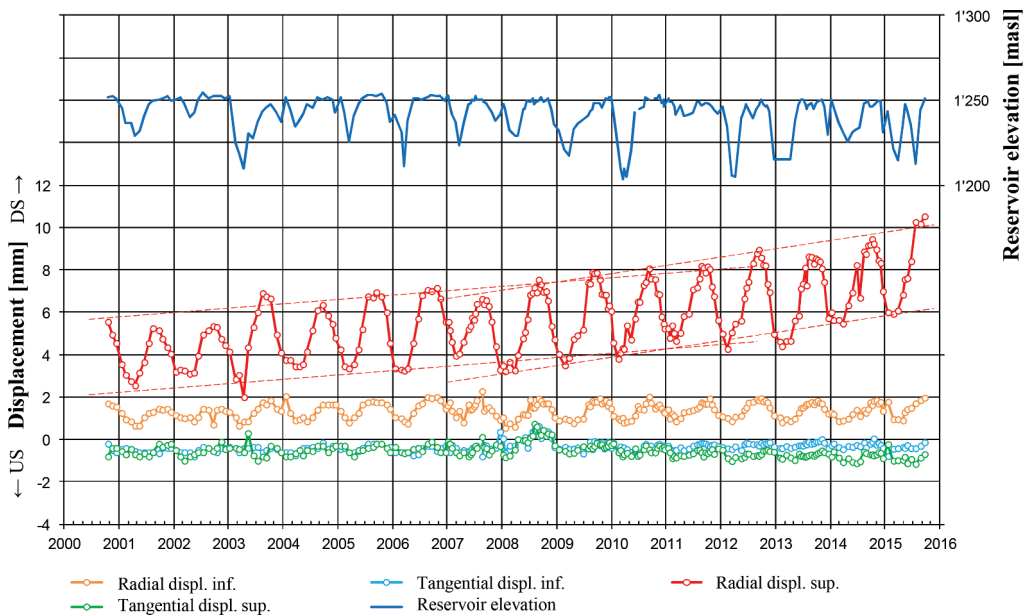


Figure 3. Artificial gravity abutment, radial (US/DS) and tangential (left bank-right bank) displacements monitored with inverted pendulum over years 2000-2015 at crest level (el. 1257 masl – sup.) and in inspection gallery (el. 1235 masl – inf.). The increasing trend toward DS is highlighted (-----).

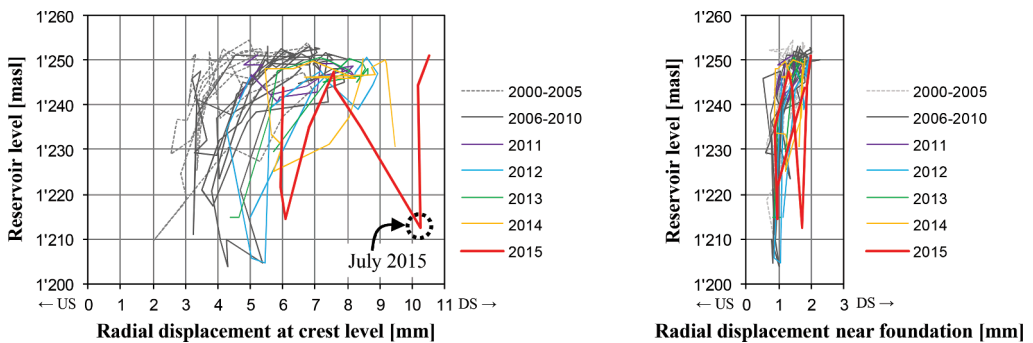


Figure 4. Artificial gravity abutment, radial (US/DS) displacements envelopes plotted against reservoir level. To be noted the abnormal behavior occurred in July 2015 (heatwave). To be noted as well the absence of trend and very small reversible displacement (in the range of 1 mm) at inspection gallery (near foundation).

A detailed survey of the artificial gravity abutment revealed the existence of a crack network, amongst which the most persistent were identified on horizontal construction joints at elevation 1256.1, 1252 and 1246 masl, see Figure 5. Such through-cracks were pre-existing the heatwave of July 2015. A specific thermo-mechanical study on the construction of the artificial gravity abutment, replicating the construction stages and corresponding dates, showed the existence of vertical tensile stresses from thermal origin at the interface between two successive concrete lifts. Therefore, it is plausible that such horizontal cracks were triggered by a lack of concrete cure during construction of the massive buttress structure.

In particular, after the heatwave event occurred in July 2015 and the subsequent 3 mm or so move toward DS, a deflection of the same magnitude is observed along the upper through-crack, right below the crest slab (el. 1256.1 masl). The other two through-cracks show less deflection (el. 1252 and 1246 masl).

Other subvertical cracks were also identified on the US face but they were less persistent and marked than the three abovementioned horizontal through-cracks.

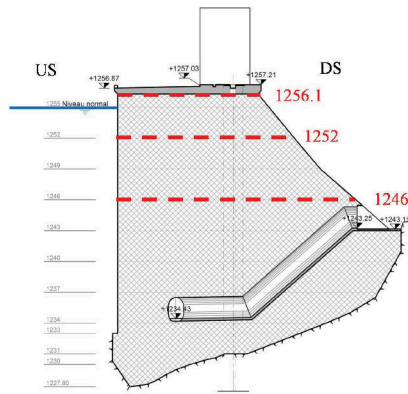


Figure 5. Artificial gravity abutment, survey of its condition. In red are shown the three most persistent through-cracks which developed on horizontal construction joints between successive concrete lifts.

Following the 2015 heatwave event, the increasing displacement monitored toward DS and the developing damage along horizontal through-cracks, FMHL decided to launch specific studies in view of the artificial gravity abutment rehabilitation. This rehabilitation was also conditioned by the commissioning of the new pumped storage powerplant in Veytaux. Until the implementation of rehabilitation works, the monitoring and surveillance of the massive buttress structure was increased during the summer season.

4 ENGINEERING STUDIES FOR THE STRENGTHENING PROJECT

4.1 Finite element analysis

To replicate the displacements measured in the dams, a 3D Finite Element model of both dams and the central artificial gravity abutment was built, using software DIANA. The mesh was made of approx. 14'500 elements and 17'500 nodes.

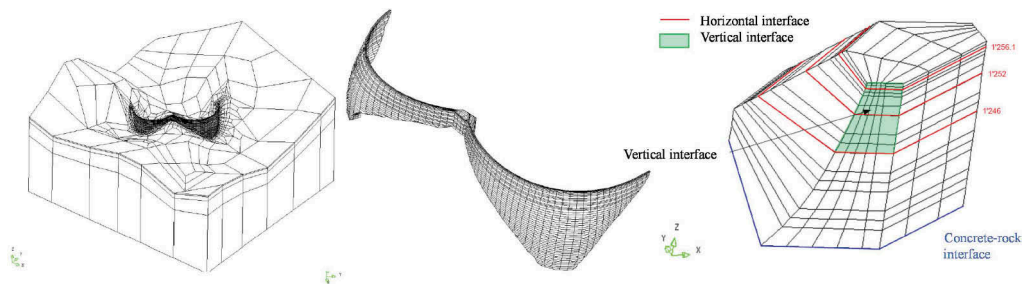


Figure 6. 3D Finite Element model. On the left, view of the whole model. In the middle, closer view from US to dams. On the right, modelling details on the artificial gravity abutment with definition of horizontal (through-cracks), vertical (interface arch dam with artificial gravity abutment) and inclined (interface with rock foundation) contact elements.

The thermo-mechanical calculation was run over a period of 15 years with a monthly time step, simulating the air and water temperatures as well as the reservoir level over years 2000-2015 until occurrence of July 2015 heatwave.

Contact elements were used to model the surface behavior of the three horizontal cracks and the vertical support of both arch dam against the artificial gravity abutment. Contact elements were also used for the dam foundation on the rock mass. The friction behavior of the contact surfaces is modelled according to Mohr-Coulomb criterion, with the cohesion parameter c imposed to zero ($c = 0$) and the friction angle ϕ different for each contact surface.

The calibration of the model was a critical part of the study, because of the many parameters to be adjusted. First the calibration is thermal, thanks to the concrete temperature data monitored in both dams. Then the calibration is mechanical based on the monitored dams' displacements. The calibration process is even more sensitive due to the nonlinear behavior of the artificial gravity abutment and its discontinuity planes. No less than 33 thermometers and 18 geodetic targets were used to calibrate the model. Finally, it was possible to adjust a good match of monitored and computed temperatures and displacements, as shown below in Figure 7 (examples from South dam temperature and displacement).

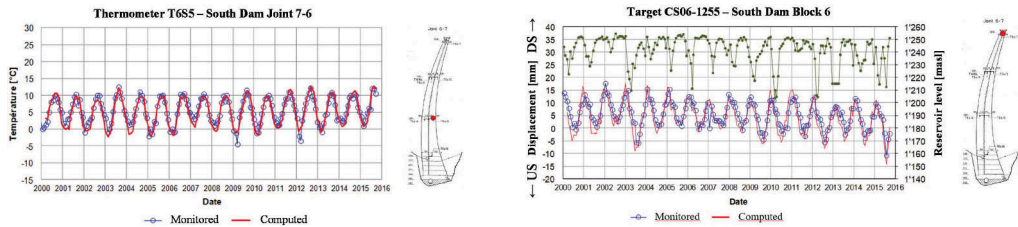


Figure 7. Calibration of Finite Element Model with monitored data, selected examples of the South arch dam. On the left, thermometer. On the right, target at the crest elevation.

Of particular interest is obviously the comparison of monitored vs computed displacements at the crest level of the artificial gravity abutment (Figure 8). As can be seen, the match “monitored vs computed” is reasonably satisfying for the many points of measurement of the structures.

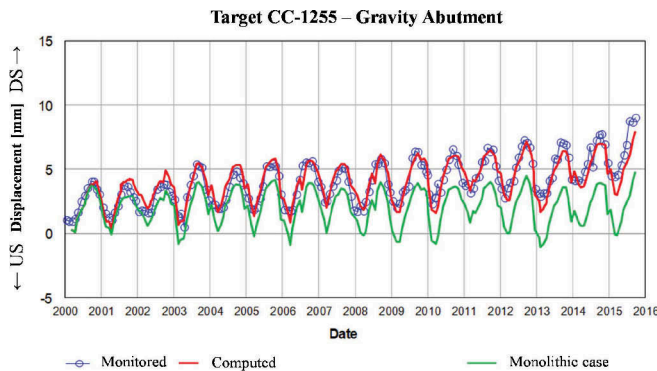


Figure 8. Calibration of Finite Element Model with monitored data, case of the artificial gravity abutment at crest level. In green line, the monolithic case computed without contact surface (discontinuities) in the massive structure.

On the basis of the calibrated model, the project for the rehabilitation of the damaged artificial gravity abutment could be carried out.

4.2 Rehabilitation Project

A comprehensive alternative study was performed to assess which rehabilitation solution was the most interesting from a long term technical and economical perspective. Many solutions were studied, including removal and reconstruction of the artificial gravity abutment, concrete cracks grouting, installation of passive anchors (steel bars) through the cracks, installation of active anchors (prestressed anchors), and others. Finally, FMHL selected the use of vertical prestressed anchors installed in the crest slab. Figure 9 shows views of the retained solution.

The rehabilitation project considers all standard cases of a design: stability checks against sliding, tilting and upheaval. The last two are not critical in the present case where the issue is about sliding on a horizontal crack surface.

Load cases and partial factors of safety are selected in accordance with the Guidelines issued by SFOE (Swiss Federal Office for Energy). In addition to thermal and static load cases, a dynamic load case (10⁷000-year return period earthquake) is also considered.

In order to take into account the ongoing climate change effect, the air and water temperatures acting on the structures are increased by an additional 2°C in the design calculations.

The project considers the use of 23 prestressed anchors (type 19-06), plus 3 trial prestressed anchors (same type), plus 3 unequipped drilling holes for potential replacement or addition of prestressed anchors if needed in future. Total 29 prestressed anchors. All anchors are designed in accordance with Swiss Norm SIA 267.

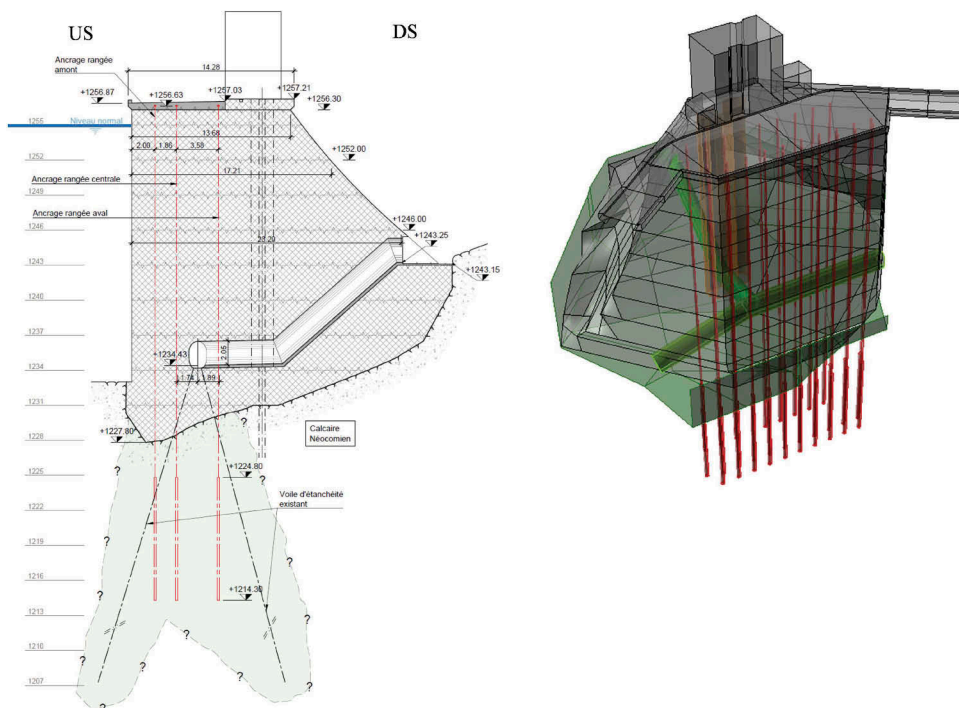


Figure 9. Solution implemented for the rehabilitation of the artificial gravity abutment: 29 vertical prestressed anchors for a total load of 50'000 kN. On the left, US-DS cross-section. On the right, perspective view of the artificial gravity abutment.

Six prestressed anchors are equipped with measuring cells, which allow the regular monitoring of the effort in the anchors. The project requires the destruction and removal of the existing crest slab, before construction of the new heavily reinforced concrete slab accommodating all 29 prestressed anchor heads.

5 REHABILITATION WORKS OCCURRED IN 2018

5.1 Concrete works

The rehabilitation works of the artificial gravity abutment were carried out in 2018. They started in June with the removal of the existing crest slab. The slab was about 70 cm thick and had to be sawed in pieces to be removed with a crane. Following this, the concrete surface had to be prepared to accommodate the anchor heads and the reinforcement. To ensure proper bonding between the existing concrete surface and the new slab, the surface was hydro demolished (July). Then two layers of reinforcement were installed (August), before concreting of the new slab in September (total concrete volume 154 m³). Figure 10 shows the main work stages.



Figure 10. Concrete works. Top left, existing slab sawing and removal in pieces. Top right, hydro demolished surface of concrete ready to accommodate reinforcement and anchor heads. Bottom left, reinforcement being placed. Bottom right, concreting of new slab.

5.2 Installation of Prestressed Anchors

Installing the prestressed anchors started in late September with the three trial anchors. Those serve to test the whole system (vertical drilling, placing the anchor and its head, etc.) and how the grouting procedure works within the rock foundation conditions. Following this and some adjustments, the remaining 23 anchors were installed and tensioned until mid-December 2018.

Finishing works such as laying of the asphalt pavement were performed after Wintertime in April 2019. Figures 11 and 12 show some details of these works.

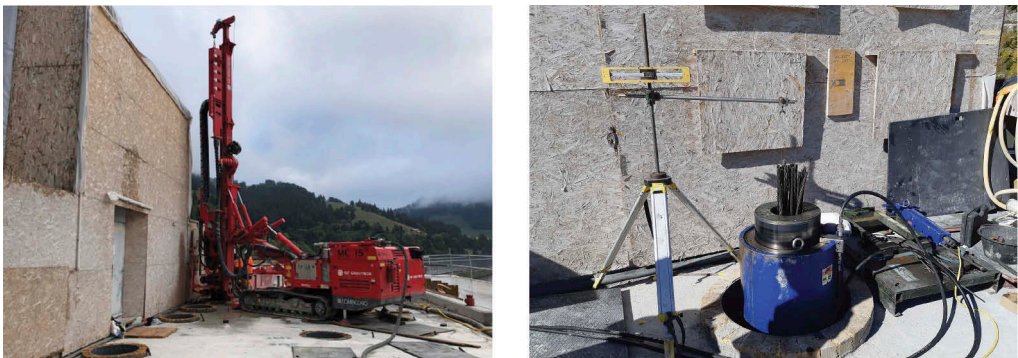


Figure 11. Left, drilling machine. Right, tensioning of a prestressed anchor.



Figure 12. Left, strands excess length cutting. Right, final state of the artificial gravity abutment.

6 LESSONS LEARNT AND CONCLUSIONS

The steady drift of the artificial gravity abutment was identified as of decade 1980s; it was very slow by then. From decade 2000s, the trend became somewhat more marked, and it increased even more in the 2010s. A critical time was the heatwave occurred in July 2015, which unfortunately coincided with a low reservoir level. This triggered a sudden 3 mm move toward DS along preexisting through-cracks on horizontal construction joints between two concrete lifts.

Following this event, final studies were launched to prepare a rehabilitation/strengthening project of the artificial gravity abutment. Works, consisting in implementation of approx. 50'000 kN vertical prestressed anchors, were executed in 2018.

Figure 13 shows the positive effect of the strengthening works. Although it is still early to look back on the 2018 works, it is noticeable that the trend toward DS has stopped after 2018.

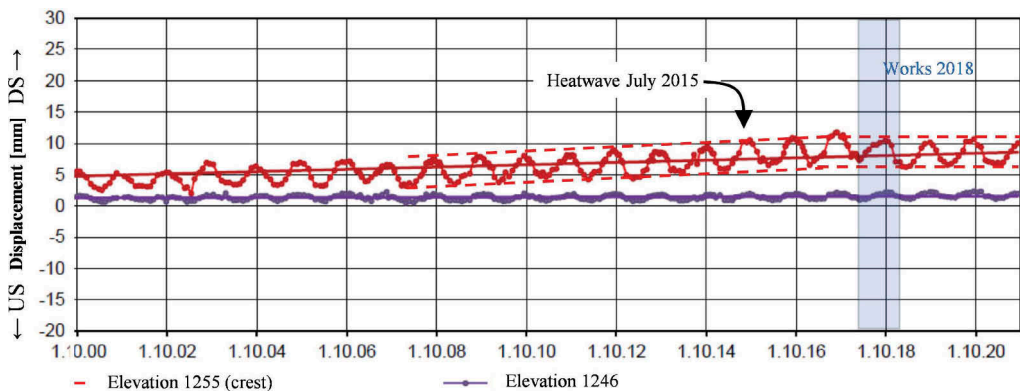


Figure 13. Artificial gravity abutment, optical survey monitoring data over years 2000-2021. The increasing drift toward DS of the top of the buttress structure is clearly observable, as is the stabilization of the displacement following rehabilitation works of 2018.

Hongrin dams' artificial gravity abutment case demonstrates that a close follow-up of the dam behavior and regular collaboration between the operator and its experienced engineers and experts allowed the early detection of the irreversible drift of the damaged artificial gravity abutment. The misbehavior of the structure was managed and followed up with relevant monitoring over the years. Eventually the heatwave 2015 was only the trigger for rehabilitation works for a problem which was long known. The rehabilitation project and works occurred in 2018 were tailored and appropriate, bringing the expected results in terms of structural behavior and integrated asset risk management.

Dealing with aging dams on the Drava River in Slovenia

P. Žvanut

Slovenian National Building and Civil Engineering Institute, Ljubljana, Slovenia

ABSTRACT: There are eight hydropower plants (HPPs) on the Slovenian part of the Drava River. Six HPPs (Dravograd, Vuzenica, Vuhred, Ožbalt, Fala and Mariborski otok) are situated directly in the river course, while the other two HPPs (Zlatoličje and Formin) are located in derivation channels of the river. For this purpose, ten concrete gravity dams were built between 1918 and 1978 with a structural height between 17 and 54 m. Due to the great age of these dams, it is necessary to monitor the condition of the dam structures and their surroundings even more carefully, which enables appropriate action in the case of identified deficiencies. These activities are carried out through regular annual technical observations, which include the monitoring of the deformations of the dams and the filtration of groundwater in the wider area of these structures, as well as regular accurate visual inspections. In order to gain a better insight into the condition of dams, some measurements (mainly hydrostatic and partly hydrodynamic) have already been automated. Recently, drones have also been included in the monitoring of dams, which allow insight into the condition of dam structures and their areas of influence, even in hard-to-reach or inaccessible places. Data obtained through technical observation of dams are also used for numerical analyses of dams, namely for the calibration of numerical models for calculating the static and the dynamic safety of dams. The results of the surveillance of these dams showed that, mainly due to the aging of the dam structures and also due to extraordinary events (i.e. flood and equipment failure), the renovations of the dams were necessary. Due to the aging of the dams, the renovation of the oldest dam on the Drava River in Slovenia (Fala Dam) began as early as 1987, which was followed by the renovation of seven more dams (Dravograd, Vuzenica, Vuhred, Ožbalt, Mariborski otok, Melje and Zlatoličje) in the following years. The remaining two dams (Markovci and Formin) still need to be renovated; the renovation of the Markovci Dam is currently underway (it should be completed in 2026), while the start of renovation of the youngest dam on the Drava River in Slovenia (Formin Dam) is scheduled for 2024. The renovation included the revitalization of the mechanical, electrical and structural parts of the dams. After the complete renovations of the dams, the surveillance systems of the dams were updated. Two dams were also renovated due to extraordinary events. The rehabilitation of the Formin Dam - due to damage after floods - was performed between 2013 and 2014, while the rehabilitation of the Mariborski otok Dam - due to damage following equipment failure - was carried out between 2018 and 2020. These dams needed to be properly renovated so that they continue to serve their purpose well in the coming decades.

1 INTRODUCTION

On the Slovenian section of the Drava River eight hydropower plants are located. Six HPPs (Dravograd, Vuzenica, Vuhred, Ožbalt, Fala and Mariborski otok) are situated directly in the river course, while the other two HPPs (Zlatoličje and Formin) are located in derivation channels of the river. For this purpose, ten concrete gravity dams were built between 1918 and 1978 with a structural height between 17 and 54 m (Figures 1-2; SLOCOLD 2023).

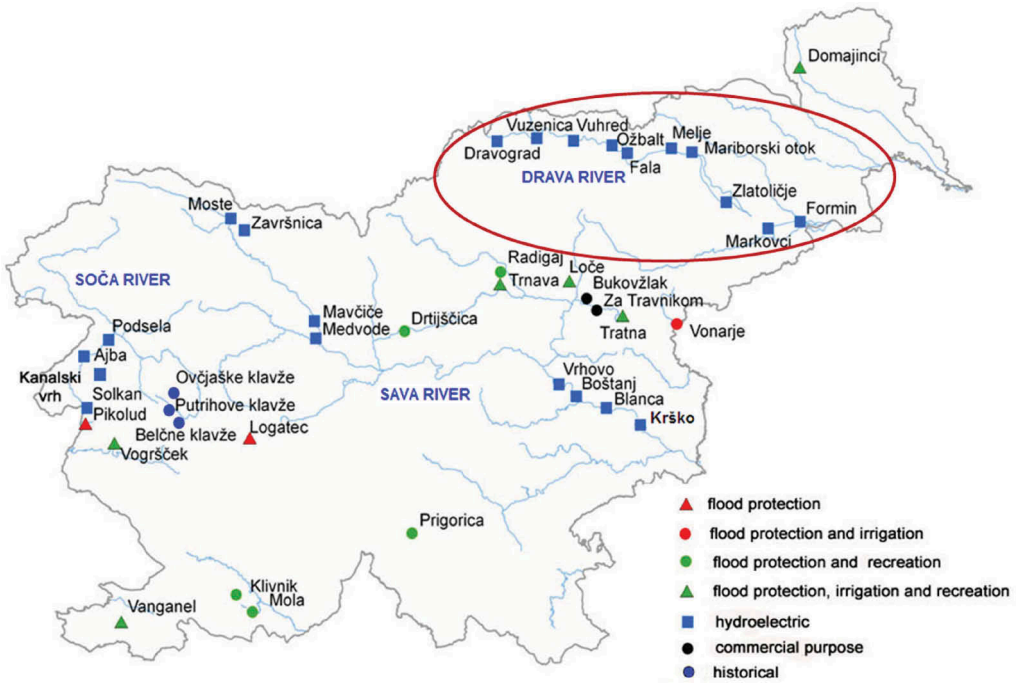


Figure 1. Locations of large dams on the Drava River in Slovenia.



Figure 2. Detailed locations of HPPs on the Drava River in Slovenia.

These dams created eight multipurpose reservoirs. In addition to their priority use for electricity production, the reservoirs are also used for floods mitigation, irrigation, industrial water use and recreation (DEM 2023).

2 SURVEILLANCE OF DAMS

Due to the great age of these dams, it is necessary to monitor the condition of the dam structures and their surroundings even more carefully, which enables appropriate action in the case of identified deficiencies. These activities are carried out through regular annual

technical observations which include: deformation measurements (vertical displacements, horizontal displacements, relative displacements and inclinations), detailed visual inspections (structural, geotechnical), groundwater measurements (piezometric levels, uplift pressures, temperatures, electrical conductivities and outflows) and measurements of external loads on the dams (Figure 3). In order to gain a better insight into the condition of dams, some measurements (mainly hydrostatic and partly hydrodynamic) have already been automated (Žvanut 2023).

Recently, drones have also been included in the monitoring of dams, which allow insight into the condition of dam structures and their areas of influence, even in hard-to-reach or inaccessible places (Figure 4).

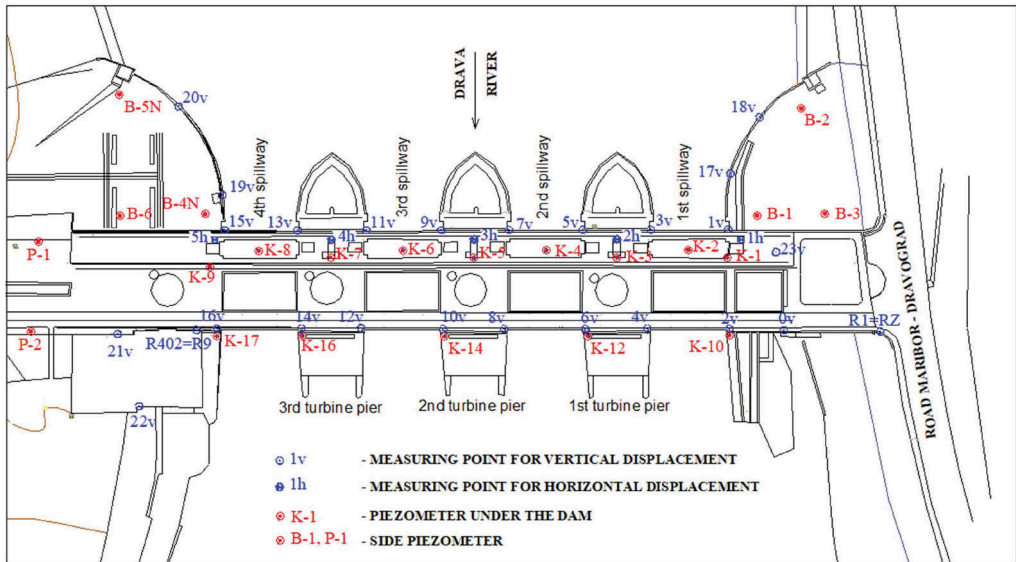


Figure 3. Monitoring system for deformation and groundwater measurements.



Figure 4. Drone for monitoring of dams.

Figures 5 and 6 show damaged places on the dam, which were registered during the periodic visual and thermographic inspection of the condition of the concrete surfaces of the Ožbalt Dam (Brunčič & Tomše 2023), while Figure 7 shows the damage found after an extraordinary visual inspection of the Mariborski otok Dam, followed by an extraordinary event (Žvanut 2021).

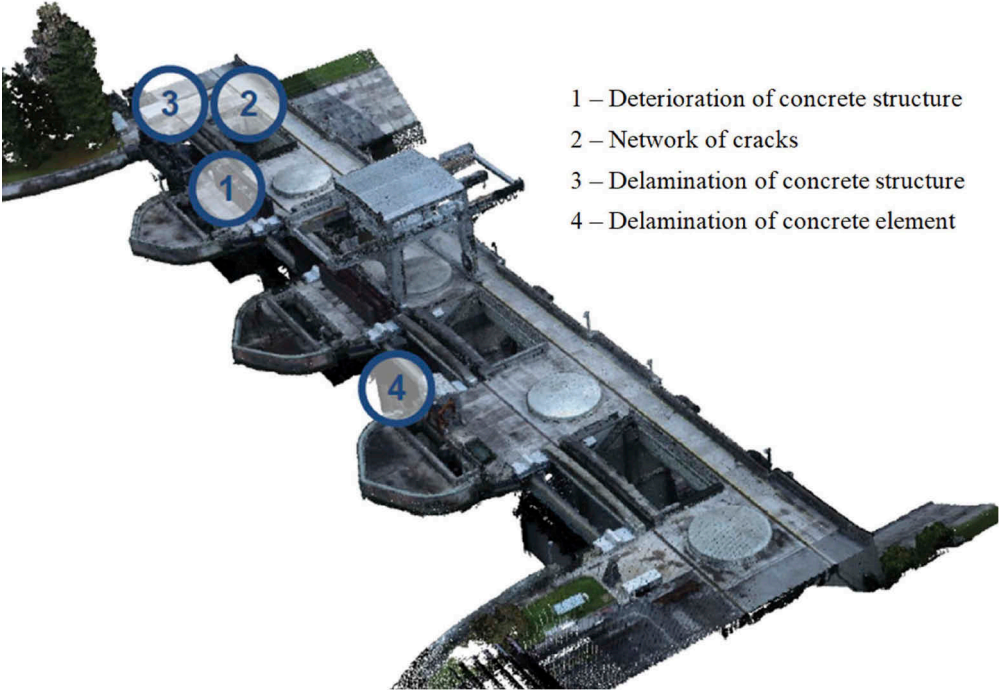


Figure 5. Numbered damaged places on the upstream side of the Ožbalt Dam.

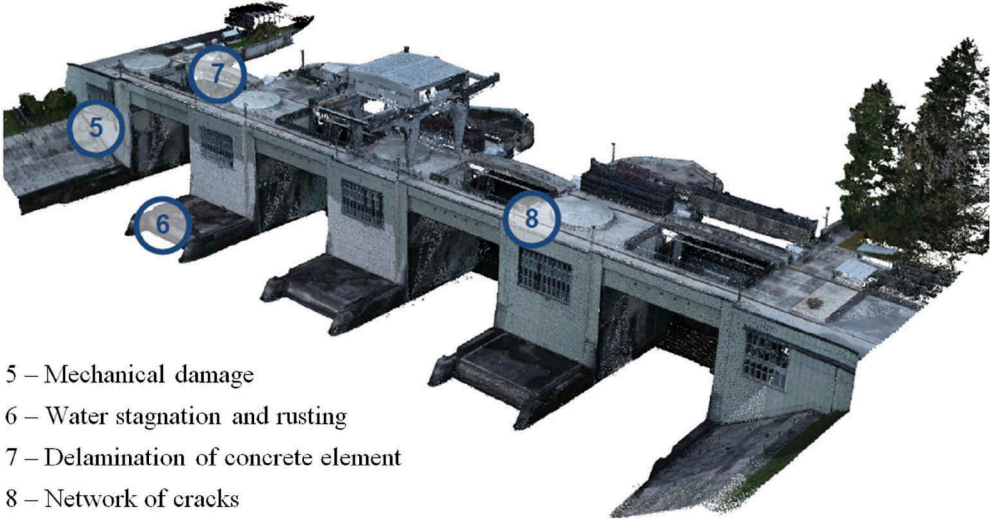


Figure 6. Numbered damaged places on the downstream side of the Ožbalt Dam.



Figure 7. Damaged concrete beam and damaged upper spillway gate on the Mariborski otok Dam.

Data obtained through technical observation of dams are also used for numerical analyses of dams, namely for the calibration of numerical models for calculating the static and the dynamic safety of dams.

3 RENOVATION OF DAMS

The results of the surveillance of these dams showed that, mainly due to the aging of the dam structures and also due to extraordinary events (i.e. flood and equipment failure), the renovations of the dams were necessary (Figure 8).

Due to the aging of the dams, the renovation of the oldest dam on the Drava River in Slovenia (Fala Dam) began as early as 1987, which was followed by the renovation of seven more dams (Dravograd, Vuzenica, Vuhred, Ožbalt, Mariborski otok, Melje and Zlatoličje) in the following years. The remaining two dams (Markovci and Formin) still need to be renovated; the renovation of the Markovci Dam is currently underway (it should be completed in 2026), while the start of renovation of the youngest dam on the Drava River in Slovenia (Formin Dam) is scheduled for 2024 (Table 1). The renovation included the revitalization of the mechanical, electrical and structural parts of the dams. After the complete renovations of the dams, the surveillance systems of the dams were updated.

Two dams were also renovated due to extraordinary events. The rehabilitation of the Formin Dam - due to damage after floods - was carried out between 2013 and 2014 (Žvanut 2022), while the rehabilitation of the Mariborski otok Dam - due to damage following equipment failure - was performed between 2018 and 2020 (Žvanut 2021).



Figure 8. Rehabilitation works on the Mariborski otok Dam.

Table 1. Overview of dams and periods of their renovation.

Dam	Built	Renovated
	year	years
Dravograd	1944	1994-2000
Vuzenica	1957	1994-2000
Vuhred	1958	2000-2005
Ožbalt	1960	2000-2005
Fala	1918	1987-1995
Mariborski otok	1960	1994-2000 2018-2020*
Melje	1968	2006-2009
Zlatoličje	1969	2007-2013
Markovci	1968	since 2019
Formin	1978	2013-2014* start in 2024

* Due to extraordinary events.

4 CONCLUSION

An appropriate system for surveillance of the condition of aging dam structures is necessary. These include regular observation of deformations of the dams and the filtration of groundwater in the wider area of structures, as well as regular detailed visual inspections. For a better insight into the condition of the dams, some measurements have already been automated. Recently, drones have also been included in the monitoring of dams, which allow insight into the condition of dam structures and their areas of influence, even in hard-to-reach or inaccessible places. More and more sophisticated numerical tools (e.g. based on the finite element method) are of great help in the static and dynamic analysis of these structures.

The results of the surveillance of the dams showed that, mainly due to the aging of the dam structures and also due to extraordinary events, the renovations of the dams were necessary. These dams needed to be properly renovated so that they continue to serve their purpose well in the coming decades.

REFERENCES

- Brunčič, A. & Tomše, T. 2023. Visual and thermographic inspection of the condition of the concrete surfaces of the Ožbalt Dam. *Periodic report*. Slovenian National Building and Civil Engineering Institute, Ljubljana, Slovenia.
- DEM. 2023. *Hydroelectric Power Generation Company Ltd website*. <http://www.dem.si>. Maribor, Slovenia.
- SLOCOLD. 2023. *Slovenian National Committee on Large Dams website*. <http://www.slocold.si/>.
- Žvanut, P. 2021. An extraordinary event at the Mariborski otok Dam. *Proc. ICOLD Symp. on Sustainable Development of Dams and River Basins, New Delhi*, 24-27 February 2021.
- Žvanut, P. 2022. Surveillance of the banks of reservoirs on the Drava River in Slovenia after extensive floods. *Proc. ICOLD & CFBR Symp. - Sharing Water: Multi-Purpose of Reservoirs and Innovations, Marseille*, 30 May 2022. E3S Web of conferences, vol. 346.
- Žvanut, P. et al. 2023. Technical monitoring of ten concrete dams on the Drava River in Slovenia. *Annual reports 1996-2023*. Slovenian National Building and Civil Engineering Institute, Ljubljana, Slovenia.

Author index

- Abati, A. 745
Abbaszadeh, S. 927
Abbate, A. 267
Abdulamit, A. 409
Adam, N.J. 613
Aelbrecht, D. 294, 590
Afonso, P. 918
Agresti, P. 632
Albayrak, I. 469, 540
Allkja, S. 622
Alós Shepherd, D. 641
Amini, A. 526, 600
Andrian, F. 632
Anthiniac, P. 863
Askarinejad, A. 209
- Balestra, A. 3, 100, 161, 367
Barbier, T. 431
Barker, M. 972
Bartosova, A. 511
Basson, G.R. 450
Baumann, R. 347
Beckhaus, K. 641
Berthod, R. 745
Besseghini, F. 651
Bianco, P. 558
Bisci, F. 956
Blanck, C. 440
Boavida, I. 574
Boes, R.M. 3, 150, 303, 469,
687, 768, 898, 981
Bollaert, E.F.R. 659
Bonafè, A. 778
Bosman, A. 450
Bouma, D. 972
Bourgey, P. 669
Brath, A. 778
Bresciani, M. 511
Bretz, N.-V. 177
Brousse, G. 460
Bryant, T. 846
Büchel, M. 855
Bühlmann, M. 678
Bürgler, M. 687
Bürki, D. 791
- Bussard, T. 89
- Canale, L. 338
Carrel, M. 277
Carstensen, D. 129, 418
Catalano, E. 696, 964
Centa, M. 402
Chanudet, V. 590
Cheresova, E. 703
Claps, P. 778
Colombo, M. 753
Costa, M.J. 574
Costantini, E. 582
Côté, M. 713, 745
- Dahal, S. 469
Dal Canto, L. 956
Dašić, T. 286
De Cesare, G. 440, 479, 526,
532, 548, 600, 946
Decaix, J. 294
Degen, V. 558
Delmas, S. 863
Detering, M. 113
Dounias, G.T. 724, 801
Drommi, J.-L. 294, 590
Droz, P. 60
Dubuis, R. 479
- Efstratiadis, A. 187
Ersoy, B. 322
Escuder-Bueno, I. 312
Evers, F.M. 150, 469, 768
- Faggiani, G. 734
Fankhauser, A. 48
Fauriel, J. 303, 613, 745
Favero, V. 107
Felder, S. 898
Felix, D. 303
Feliziani, D. 778
Fern, I. 72
Feuz, B. 48
Filliez, J. 303, 613
Fischer, C. 418
- Fluixa-Sanmartin, J. 177,
312
Folchi, R. 199
Fornari, F. 956
Fournié, Y. 632
Friedli, B. 209
Frigerio, A. 753
Fry, J.-J. 386, 810
- Gabbud, C. 558
Gander, B. 763
Gassner, J. 277
Gatto, G. 582, 956
Gehrmann, L. 113
Geisseler, B. 338
Gianora, C. 651
Giraud, S. 338
Godinho, F.N. 574
Gronsfeld, R. 418
Gross, T. 113
Guilloteau, T. 377, 669
Gunn, R.M. 713
Gustafsson, D. 511
Gutiérrez, I. 855
- Hager, W.H. 32
Halso, M.C. 768, 981
Haselsteiner, R. 322
Heizmann, A. 121
Heß, M. 129
Hirt, Ch. 220
Ho Ta Khanh, M. 329
Hohermuth, B. 150, 687,
898
Hribar, A. 494
- Jacobsen, T. 487
Jellouli, M. 810
Jobard, Y. 357
Joly, B. 294
Jonneret, A. 89
Jouy, C. 863
Jovani, A. 137, 141
- Kacurri, E. 141

Kager, A. 783
 Kahl, A. 150
 Kantoush, S.A. 518
 Kastranta, G.P. 801
 Katterbach, M. 651
 Kavčič, I. 402
 Kayser, J. 641
 Kisliakov, D.S. 229
 Kleist, F. 641
 Klopries, E. 418
 Klun, M. 494
 Koch, A. 791
 Kodre, N. 402
 Korell, A. 161
 Koshiha, T. 503
 Kotsonis, A.E. 801
 Kryżanowski, A. 494

 Lambert, D. 540
 Landry, C. 294
 Lauener, G. 540
 Laugier, F. 329
 Launay, M. 511
 Lazaridou, S.L. 724, 801
 Lebrun, N. 810
 Lecuna, S. 431
 Leite, R. 574
 Leite Ribeiro, M. 511
 Leon, M. 820
 Leroy, R. 39, 996
 Lilliu, G. 121
 Lima, J.N. 937
 Lin, J. 518
 Lino, M. 338
 Longo, D. 837

 Maddahi, M.R. 469
 Maddalena, G. 150
 Maestri, M. 778
 Maggetti, D. 100, 161, 367
 Maier, J. 347
 Malaj, A. 622
 Malla, S. 678
 Mancusi, L. 267
 Manni, P. 827
 Manzini, N. 357
 Marshall, M. 526, 600
 Martel, S. 532
 Masarati, P. 734
 Massignani, S. 258
 Matta, E. 511
 Maugliani, F. 161, 837
 Mazzà, G. 753, 827

 Méan, P. 846
 Meier, E. 855
 Mellal, A. 240
 Menouillard, T. 347, 713
 Mészáros, T. 703
 Meunier, P. 431
 Meyer, Ch. 169
 Mico, A. 177
 Milesi, G. 863
 Mitovski, S. 908
 Moldenhauer-Roth, A. 540
 Molin, X. 863
 Morales-Torres, A. 312
 Morris, M. 386
 Mörtl, C. 548
 Mrva, M. 703
 Müller, B. 220
 Müller, M. 540
 Munari, S. 183
 Münch, C. 294
 Murakami, K. 503

 Nahrath, S. 394
 Nicolet, C. 294
 Noret, C. 863
 Ntemiroglou, C. 187

 Oberender, P.W. 209
 Odermatt, E.A. 871
 Oliveira, S. 937
 Ortega, F. 881
 Otto, B. 889

 Pachoud, A.J. 209
 Pagliara, S. 898
 Palmieri, A. 367
 Panovska, F. 908
 Papachatzaki, Z.R. 724
 Parisi, A. 837
 Perona, P. 532
 Perroud, M. 558
 Petkovski, L. 908
 Petriti, K. 622
 Pfister, L. 209
 Pianigiani, F. 778
 Piazza, A. 837
 Pinheiro, A.N. 574
 Piras, F. 778
 Pontes, C.J.C. 918, 923
 Portela, M.M. 574
 Portugal, P. 923
 Pougatsch, H. 18, 72

 Proença, J. 937
 Psychogiou, M.V. 801

 Qosja, E. 141
 Quarg-Vonscheidt, J. 641

 Raimondi, G. 837
 Rashidi, M. 927
 Rebuschi, M. 956
 Reynard, E. 394
 Richter, W. 566
 Robbe, E. 377
 Rodrigues, M. 937
 Rogledi, F. 753
 Rombaldoni, J. 558
 Romero, B. 220
 Rossetti, E. 100
 Ruffato, P. 199
 Ruggeri, L. 778
 Rushworth, A. 972
 Rusjan, S. 494

 Sadei, R. 783
 Saharei, P. 532
 Sainati, F. 778
 Sakellariou, S.C. 801
 Sakki, G.-K. 187
 Salimi, K. 927
 Sanfilippo, R. 837
 Santoro, F. 778
 Santos, J.M. 574
 Sarrasin, O. 177
 Sausse, J. 669
 Scarella, M. 250
 Schaeren, G. 89
 Schenk, K. 511
 Schleiss, A.J. 18, 386
 Schröder, X. 394
 Schroff, R. 440
 Schüttrumpf, H. 418
 Schwager, M.V. 209, 229
 Seidelmann, L. 981
 Seixas, R.P. 946
 Senti, R. 678, 889
 Serra, L. 582, 956
 Shaha, F. 137
 Sievers, B. 80
 Simm, J. 972
 Simon, A. 377
 Slomp, R. 972
 Smolar-Žvanut, N. 402
 Stahl, H. 220, 347
 Stähly, S. 277

Stematiu, D. 409
Stern, L. 469
Stucchi, R. 651,
696, 964
Suchier, L. 377
Sumi, T. 503, 518

Takata, S. 503
Taylor, R.M. 590
Terret, A. 753
Thermann, K. 169
Thevenet, R. 460
Tourment, R. 972
Tzenkov, A.D. 229, 240

Ulrich, N. 632

Valero, D. 687
Vallotton, O. 240
Van Gorp, S. 357
Vaschetti, G. 250
Verdho, E. 141
Vermeille, A. 460
Vermeulen, J. 329
Vetsch, D.F. 469, 687, 768,
981
Vidmar, A. 494
von Trentini, F. 511
Vorlet, S. 107, 600, 946

Vroman, N. 972

Wahlen, S. 277
Walser, F. 80
Werner, L. 322
Wieland, M. 989
Wiget, A. 80
Wohnlich, A. 48,
871, 996
Wolf, S. 418

Zanoli, R. 258
Zenz, G. 566
Žvanut, P. 1005



Taylor & Francis

Taylor & Francis Group

<http://taylorandfrancis.com>